MALLA REDDY ENGINEERING COLLEGE

(AUTONOMOUS)

Estd: 2002

(An UGC Autonomous Institute, Approved by AICTE and Affiliated to JNTUH Hyderabad,
Accredited by NBA & NAAC with 'A' Grade and Recipient of World Bank Assistance under TEQIP Phase - II, S.C 1.1)
Maisammaguda, Dhulapally, Secunderabad, Telangana, India - 500 100. Website: www.mrec.ac.in

Recognised under section 2(f) and
12(B) of UGC Act 1956

RESEARCH PUBLICATION IN CONFERENCE

Compilation of Research Papers Contributed by Faculty Members of MREC
A.Y. 2018-19

Malla Reddy Engineering College

(AUTONOMOUS)

(An UGC Autonomous Institution Approved by AICTE and Affiliated to JNTU Hyderabad. Accredited by NAAC with 'A' Grade (II - Cycle)

Sri. Ch. Malla Reddy
Founder Chairman, MRGI
Hon'ble MP, Malkajgiri

MESSAGE

It gives me immense pleasure to pen a few words as prologue to our in-house magazine "Research Publications in MREC" with a collection of research papers contributed by the faculty members of our organization.

I believe this will flourish to become very useful source for the researchers, academicians and students who want to further improve their research profile and contribute to the arena of knowledge based wisdom. I hope this magazine will create interest and enhance inspiration of the readers to carry out new research ventures.

I extend my best wishes to bring more challenging research works which is useful to the society from the teaching fraternity with a sense of commitment in the future years to come.

C. H. Malla Reddy

Sri. Ch. Malla Reddy

Maisammaguda, Dhulapally (Post Via Kompally), Secunderabad - 500 100.
Phone: 040-65864982, 65918418, Fax: 040-23792153
Email: principal@mrec.ac.in
www.mrec.ac.in

Malla Reddy Engineering College

(AUTONOMOUS)

(An UGC Autonomous Institution Approved by AICTE and Affiliated to JNTU Hyderabad. Accredited by NAAC with 'A' Grade (II - Cycle)

Sri. Ch. Mahender Reddy
Secretary, MRGI

MESSAGE

I am pleased to know that MREC(A) is bringing out a magazine "Research Publications in MREC" which embrace the research contribution of faculty members of MREC. It is the outcome of our enthusiastic, dedicated and committed faculty members.

I take the pleasure to thank the Principal for providing continuous support and encouragement to the faculty members to publish their papers in Conferences and Journals.

I extend my heartfelt wishes for all to succeed in future endeavors.

Sri. Ch. Mahender Reddy

Maisammaguda, Dhulapally (Post Via Kompally), Secunderabad - 500 100.
Phone: 040-65864982, 65918418, Fax: 040-23792153
Email: principal@mrec.ac.in
www.mrec.ac.in

Malla Reddy Engineering College

(AUTONOMOUS)

(An UGC Autonomous Institution Approved by AICTE and Affiliated to JNTU Hyderabad. Accredited by NAAC with 'A' Grade (II - Cycle)

Dr. S. Sudhakara Reddy
M.Tech,M.B.A.,Ph.D.,L.M.I.S.T.E.,
F.I.E., M.I.S.M.E
Principal

MESSAGE

Its my pleasure to know that our in-house magazine "Research Publications in MREC" is being brought out with a collection of research contributions by our faculty members. This collection will be an inspiration to upcoming researchers to set new aspirations in research. This edition is an evidence for comfortable environment provided by MREC(A) for teaching and research activities to the faculty members to improve their career.

I wish to express my heartfelt thanks to the Management for their support and encouragement. Also my sincere regards to the HOD's and faculty members for their continuous efforts and contribution in research fields.

I extend my heartfelt wishes for all to succeed in future endeavors.

Dr. S. Sudhakara Reddy
Principal

MALLA REDDY ENGINEERING COLLEGE (AUTONOMOUS)

Research Publications for the Academic Year 2018-19

Sl. No.	Name of the Authors	Title of the Paper	Name of the Journal	Indexing	Vol. No.	Issue No.	ISSN	Page No.	Month-Year
1	J. Kavitha Ch. V. Phani Krishna	A survey on energy-efficient useful resource allocation based on various optimization techniques for cloud Computing	Journal of Advanced Research in Dynamical & Control Systems	SCOPUS	10	04-SI	1943-023X	550-559	Apr-18
2	Rajesh Egala Srinivasu Gangi Setti	Effect of short and randomly oriented Ricinus Communis L (Castor oil) plant on Mechanical Behaviour of Ricinus Communis L/ Epoxy LY556 Composites	Materials Today Proceedings	SCOPUS	5	1	2214-7853	8065-8072	May-18
3	Sanjeeva Polepaka Ch. Srinivasa Rao M. Chandra Mohan	An Intelligent Decision Support System using Image Fusion and Support Vector Machine	Journal of Advanced Research in Dynamical & Control Systems	SCOPUS	10	7	1943-023X	362-371	Jun-18
4	Srikanth B B Sankara Babu G Charles Babu Y. Jeevan Kumar	Data Science: Identifying influencers in Social Networks	Periodicals of Engineering and Natural Sciences	SCOPUS	6	1	2303-4521	215-228	Jun-18
5	B Sankara Babu A Suneetha G Charles Babu Y Jeevan Kumar G Karuna	Medical Disease Prediction using Grey Wolf optimization and Auto Encoder based Recurrent Neural Network	Periodicals of Engineering and Natural Sciences	SCOPUS	6	1	2303-4521	229-240	Jun-18
6	R. Prasanna Kumar Akella Naga Sai Baba V. Ranjith Kumar	Improving the safety of an uncontrolled road traffic junction, a case study of Maisammaguda T – Junction	International Journal of Engineering and Technology	SCOPUS	7	3.29	2227-524X	31-34	Sep-18
7	R. Prasanna Kumar Akella Naga Sai Baba V. Ranjith Kumar Sudharsan R	Analysis of selected parking spaces in medium sized cities of Tamil Nadu	International Journal of Engineering and Technology	SCOPUS	7	3.29	2227-524X	39-45	Sep-18

Sl. No.	Name of the Authors	Title of the Paper	Name of the Journal	Indexing	Vol. No.	Issue No.	ISSN	Page No.	Month-Year
8	B. Vamsi Krishna E. Rakesh Reddy	Applications of Green Materials for the preparation of eco-friendly bricks and pavers	International Journal of Engineering and Technology (UAE)	SCOPUS	7	3.29	2227-524X	75-79	Sep-18
9	S. Gunasekharan D. Elangovan S. Sudhakara Reddy M. Maheswari	Real Time Implementation and Validation of Lean Implementation Model for Sustainability (LIMS) in Medium Scale Industry	International Journal of Engineering and Technology	SCOPUS	7	3.29	2227-524X	16-20	Sep-18
10	M. Maheswari T. Thangavel	Hardware Realization of DVR with 27 Level Multi-carrier PWM based MLI	International Journal of Engineering and Technology (UAE)	SCOPUS	7	3.29	2227-524X	26-30	Sep-18
11	Ramachandran T Sudhakara Reddy S Jeyakumar S	Vibration Characteristics of Al 6061-SiC Metal Matrix Composite based Rubber Mount for I.C. Engine Chassis	International Journal of Vehicle Structures and Systems	SCOPUS	10	3	0975-3060	215-219	Sep-18
12	M. Vijay Kumar A. Veeresh Babu P. Ravi Kumar S. Sudhakara Reddy	Experimental Investigation of the Combustion Characteristic of Mahua Oil Biodiesel-Diesel Blend using a DI Diesel Engine Modified with EGR and Nozzle Hole Orifice Diameter	Biofuel Research Journal	SCOPUS	19	1	2292-8782	863-871	Sep-18
13	Veeredhi Lakshmi Shireen Banu N. V. Ramana Rao Veeredhi Vasudeva Rao	Effect of Plate Curvature on Blast Response of Structural Steel Plates	Jounal of Institution of Engineers (India): Series A	SCOPUS	99	3	2250-2149	463-471	Sep-18
14	D. Sumathi Sireesha Jasti	Review on Authentication Mechanisms in Cloud Computing	International Journal of Engineering and Technology	SCOPUS	7	3.29	2227-524X	319-322	Sep-18
15	V. Suma Deepthi	A New approach for Determining the cost allocation by considering Transmission Line Mutual Inductance for Multilateral Contracts	International Journal of Power Electronics and Drive Systems	SCOPUS	9		2088-8694		Sep-18
16	P S V Sucheta D Vijaya Lakshmi M Swami Das	Building an IoT Web Services for Intelligent Systems	International Journal of Pure and Applied Mathematics	SCOPUS	120	6	1311-8080	3101-3117	Oct-18
17	C. Anna Palagan	Joint Noise Suppression and Dereverberation of Separating Speech Signals by using Prediction and Separation Matrix	Proceedings of International Conference on Communication and Electronics Systems (IEEE Xplore)	SCOPUS	..	..	978-1-5386-47(	202-207	Oct-18

Sl. No.	Name of the Authors	Title of the Paper	Name of the Journal	Indexing	Vol. No.	Issue No.	ISSN	Page No.	Month-Year
18	S. Sudhakara Reddy S. Armugam S. Ajay Kumar	Online Examinations to Undergraduate Engineering Students: A Case Study in an Autonomous Institution	Journal of Engineering Education Transformations	SCOPUS	32	2	2349-2473	61-66	Oct-18
19	Shimola K Krishnaveni M	Statistical analysis of trend and change point in climate series for a semi-arid basin, Tamilnadu, India	Disaster Advances	SCOPUS	11	10	0974-262X	008-012	Oct-18
20	V. Suma Deepthi M. Maheswari M. Vibhavari K. Prasanth Kumar	Penalty Quoted Cost Approach for Loss Allocation in a Transmission Line by considering the Mutual Inductance	International Journal of Recent Technology and Engineering	SCOPUS	7	4	2277-3878		Nov-18
21	S. Phani Venkata Ramana K. Anitha Reddy K. Deepthi K. Chetaswi	Harmonic Emission of Grid Connected back to back Arrangement of Rectifiers in Distribution Networks	International Journal of Recent Technology and Engineering	SCOPUS	7	4	2277-3878		Nov-18
22	A. Pradeep Kumar	Ultrasonic flaw signal Classification based on Curvelet transform and Support Vector Machine	International Journal of Innovative Technology and Exploring Engineering	SCOPUS	8	2S2	2278-3075	449-453	Dec-18
23	A. Raveendra K. Sri Noothan Reddy	Infinitely Variable Valve Lifting	International Journal of Innovative Technology and Exploring Engineering	SCOPUS	8	2S	2278-3075	280-285	Dec-18
24	A. Raveendra Mohammed Abdul Mubashir	Design and Analysis of Leaf Spring for Heavy Weight Vehicles using Composite Mater	International Journal of Innovative Technology and Exploring Engineering	SCOPUS	8	2S	2278-3075	286-291	Dec-18
25	Gayatri Upadhyay	Laboratory Investigations on Expansive Soils with Eggshell Powder	International Journal of Innovative Technology and Exploring Engineering	SCOPUS	8	2S2	2278-3075	001-002	Dec-18
26	Heruthunnisa Shaik Ismail Kakaravada	Optimization of Thrust force, Surface roughness and Delamina-tion in drilling of EN-24 steel using Taguchi based VIKOR-Entropy Method	International Journal of Innovative Technology and Exploring Engineering	SCOPUS	8	2S2	2278-3075	003-008	Dec-18
27	Vishwanath B J. Rex	Use of Steel Slag as Coarse and Fine Aggregate in Porous Concrete Pavements	International Journal of Innovative Technology and Exploring Engineering	SCOPUS	8	2S	2278-3075	436-439	Dec-18
28	J.Rex J.Selwyn Babu S.Pooja Sri Reddy	Strength and Durability Aspects of Bacterial Concrete	International Journal of Innovative Technology and Exploring Engine	SCOPUS	8	2S2	2278-3075	009-013	Dec-18

Sl. No.	Name of the Authors	Title of the Paper	Name of the Journal	Indexing	Vol. No.	Issue No.	ISSN	Page No.	Month-Year
29	K.Shimola	A Study on Soil Stabilization using Sugarcane Bagasse Ash	International Journal of Innovative Technology and Exploring Engineering	SCOPUS	8	2S	2278-3075	292-295	Dec-18
30	Katla Rajendar K. Eswaraiah Anil Kumar Bodukuri Sampath.V	Microstructural and Hardness Behavior of AL/B4C/h-BN Hybrid Composites Prepared By Powder Metallurgy Method	International Journal of Innovative Technology and Exploring Engineering	SCOPUS	8	2S2	2278-3075	14-17	Dec-18
31	M. Swami Das A. Govardhan D. Vijaya Lakshmi	An Approach for Minimizing the Response Time and Improving Availability of Web Services	International Journal of Innovative Technology and Exploring Engineering	SCOPUS	8	2S	2278-3075	296-305	Dec-18
32	N. Sri Chandrahas B.S. Choudhary M.S.Venkataramayya	Identification of Most Influencing Blast Design Parameters on Mean Fragmentation Size and Muckpile by Principal Component Analysis	International Journal of Innovative Technology and Exploring Engineering	SCOPUS	8	2S2	2278-3075	23-30	Dec-18
33	N.Subbulakshmi R.Chandru R. Manimegalai	Implementation of Lock-In Method using NLFB for Brain Monitoring Applications on FPGA	International Journal of Innovative Technology and Exploring Engineering	SCOPUS	8	2S2	2278-3075	31-33	Dec-18
34	Dharmalingam Ramasamy Sudhakara Reddy S Ramachandran T Gunasekharan S	Experimental analysis of Thermal Performance of Solar Collector using CuO-H2O Nanofluid	International Journal of Innovative Technology and Exploring Engineering	SCOPUS	8	2S2	2278-3075	34-39	Dec-18
35	R.Sumathi Shyamala Bhoomesh	Comparitive Study Between the Compressive Strength of Traditional Curing and Accelerated Curing of Concrete	International Journal of Innovative Technology and Exploring Engineering	SCOPUS	8	2S2	2278-3075	40-42	Dec-18
36	Rajendra Prasad	Design and Implementaion of Energy Efficient Muliplier Architecture in Low POWER VLSI		SCOPUS	8	2S2	2278-3075	18-22	Dec-18
37	S. Dhanalakshmi B. G. Obula Reddy K. Yogitha Lakshmi	Building a blockchain approach with hyperledger transaction flow and distributed consensus algorithms	International Journal of Innovative Technology and Exploring Engineering	SCOPUS	8	2S	2278-3075	423-426	Dec-18
38	Md Taqiuddin S. Lakshmi Shireen Banu	Efficiency of Lateral System in Tall RC Building	International Journal of Innovative Technology and Exploring Engineering	SCOPUS	8	2S	2278-3075	420-422	Dec-18

Sl. No.	Name of the Authors	Title of the Paper	Name of the Journal	Indexing	Vol. No.	Issue No.	ISSN	Page No.	Month-Year
39	Sanjeeva Polepaka R. P. Ram Kumar	A Study on Performance Analysis of Multi-Level Feedback Queue Scheduling Approach	International Journal of Innovative Technology and Exploring Engineering	SCOPUS	8	2S	2278-3075	427-428	Dec-18
40	T. Ramachandran S. Murugapoopathi D. Vasudevan	RSM based Empirical Model for the Performance and Emission Characteristics of ROME Biodiesel	International Journal of Innovative Technology and Exploring Engineering	SCOPUS	8	2S	2278-3075	429-435	Dec-18
41	T. Vijay Kumar G. Kumar R. Venkateswarlu A. Sadananda Chary S. Narender Reddy	Preparation of Nano Sized Particles of $Sr(NO_3)_2$ Solid Electrolyte by Planetary Ball Milling	Materials Today Proceedings	SCOPUS	5	13 (3)	2214-7853	6894-2689	Dec-18
42	R. Swarnalatha T. Vijay Kumar A. Sadananda Chary S. Narender Reddy	Effect of Dispersed Zirconia on D. C. Ionic Conductivity in $BaCl_2$:ZrO_2 Multi Phase Solid Electrolyte System	Materials Today Proceedings	SCOPUS	5	13P3	2214-7853	26889-268	Dec-18
43	T. Vijay Kumar G. Kumar R. Venkateswarlu A. Sadananda Chary S. Narender Reddy	Effect of Mg Doping on Physical Properties of Zn Ferrite Nanoparticles	Materials Today Proceedings	SCOPUS	5	13P3	2214-7853	26894-268	Dec-18
44	Rajesh Egala Srinivasu Gangi Setti	Impact Characterization of Epoxy LY556/Ricinus Communis L Plant Natural Fiber Composite Materials	Materials Today Proceedings	SCOPUS	5	13P3	2214-7853	26799-268	Dec-18
45	K. Deepthi K. Chetaswi S. Phani Venkata Ramana K. Anitha Reddy	Control Strategy for Improvement of PQ in DC Systems Incorporating PR Controller	International Journal of Innovative Technology and Exploring Engineering	SCOPUS	8	2S2	2278-3075	498-501	Dec-18
46	Madhu Babu Sikha R. Manivasakan	On the Inter-Departure Times in $M/D/1/B_{on}$ Queue with Queue-Length Dependent Service and Deterministic/Exponential Vacations	IEEE Access	SCI	7	1	2169-3536	1439-1453	Dec-18

Sl. No.	Name of the Authors	Title of the Paper	Name of the Journal	Indexing	Vol. No.	Issue No.	ISSN	Page No.	Month-Year
47	A. Prashanth P.Shiva Kumar	Experimental Evaluation and Fabrication of Composite Made Traction Gear	International Journal of Recent Technology and Engineering	SCOPUS	7	5S2	2277-3878	536-541	Jan-19
48	A. Sarath Kumar Dr. K. Jayanendra Babu	Effect of Process Parameters on Pcbn Tool Wear Rate in Friction Stir Process of Aluminium 7075 SiC	International Journal of Recent Technology and Engineering	SCOPUS	7	5S2	2277-3878	546-549	Jan-19
49	J. Selwyn Babu J. Rex	Experimental Investigation on Lightweight Concrete Slabs	International Journal of Recent Technology and Engineering	SCOPUS	7	5S2	2277-3878	502-506	Jan-19
50	Shaik Hussain Sanam Ravi Teja	Experimental Investigations on Modified Combustion Chamber Geometry in Diesel Engine	International Journal of Recent Technology and Engineering	SCOPUS	7	5S2	2277-3878	507-511	Jan-19
51	Yogesh Madaria Vijay Kanjarla	Effectiveness of a Dimpled Non-Even Surface For Oscillations Control For Flow Over Fissure: Numerical Analysis	International Journal of Recent Technology and Engineering	SCOPUS	7	5S2	2277-3878	512-516	Jan-19
52	Kamal Babu K. K. K.Panneerselva P. Sathiya A. Noorul Haq S. Sundarrajan P. Mastanaiah C. V. Srinivasa Murthy	Microstructure Evaluation on Friction Stir Welding of Cryorolled 2219 Aluminum Alloy	Journal of Testing and Evaluation	SCI	47	..	..	..	Jan-19
53	A Raveendra B V R Ravi Kumar S Sudhakara Reddy	Micro-Hardness and Mechanical Properties of 5052 Aluminium Alloy Weldments using Pulsed and Non-Pulsed Current Gas Tungsten Arc Welding	International Journal of Mechanical and Production Engineering Research and Development	SCOPUS	8	6	2249-6890	691-698	Jan-19
54	Dharmalingam Ramasamy Sudhakara Reddy S Ramachandran T Gunasekharan S	A Critical Review on Performance of Various Nanofluids in Solar Flat Plate Collector, Heat Exchanger and Radiator	International Journal of Mechanical and Production Engineering Research and Development	SCOPUS	9	Sp Issue 1	2249-6890	74-90	Jan-19
55	Sanjeeva Polepaka Ch. Srinivasa Rao M. Chandra Mohan	IDSS based Two Stage Classification of Brain Tumor using SVM	Health and Technology	SCOPUS	..	..	2190-7188	001-010	Jan-19

Sl. No.	Name of the Authors	Title of the Paper	Name of the Journal	Indexing	Vol. No.	Issue No.	ISSN	Page No.	Month-Year
56	S. Sudhakara Reddy N. Rajeswaran Vamshi Krishna V. Kesava	Strategic Planning to Promote Engineering Projects in Community Service (EPICS) in Engineering Institutions	IEEE Xplore	SCOPUS	..	..	978-1-5386-4765-3		Jan-19
57	M.V. Varalakshmi	Preparation and Tribological Properties of New Bisimidazolium Ionic Liquids	International Journal of Recent Technology and Engineering	SCOPUS	7	5C	2277-3878	292-294	Feb-19
58	K.Yogitha Lakshmi S.Dhanalakshmi B.G.Obula Reddy	An Overview of Data Management in Cloud Computing	International Journal of Recent Technology and Engineering	SCOPUS	7	5C	2277-3878	61-64	Feb-19
59	K. Rama Krishna Reddy B.G. Obula Reddy	Study and Analysis of Big data with MapReduce Framework	International Journal of Recent Technology and Engineering	SCOPUS	7	5C	2277-3878	72-74	Feb-19
60	R. P. Ram Kumar R. Jayakumar A. Sankaridevi	Apriori-based Frequent Symptomset Association Mining in Medical Databases	International Journal of Recent Technology and Engineering	SCOPUS	7	5C	2277-3878	65-68	Feb-19
61	R. P. Ramkumar Sanjeeva Polepaka	Certain Investigations on Sentimental Analysis Architecture and Tools		SCOPUS	7	5C	2277-3878	65-68	Feb-19
62	S. Dhanalakshmi K. Ramakrishna Reddy K. Vijaya Krupa Vatsal	Overview of Managing Data Storage, Resource Models and Security Issues in Cloud Computing Environment	International Journal of Recent Technology and Engineering	SCOPUS	7	5C	2277-3878	75-79	Feb-19
63	S.Gunasekharan D.Elangovan M.Maheswari	Identification of Serious Success Factors to Implement Lean Manufacturing in Indian Middle Scale Industries	International Journal of Recent Technology and Engineering	SCOPUS	7	5C	2277-3878	49-52	Feb-19
64	S. Gunasekharan K.Tarun Raj	Structural Design and Modeling of Keystone Butterfly Valve	International Journal of Recent Technology and Engineering	SCOPUS	7	5C	2277-3878	288-291	Feb-19
65	T.Srinivas Reddy	Analysis and CDNA Microarray Image Segmentation Based on Hough Circle Transform	International Journal of Recent Technology and Engineering	SCOPUS	7	5C	2277-3878	53-55	Feb-19
66	B.Tulasiramarao P. Ramreddy K. Srinivas A.Raveendra	Effect of tool Overhang length on turning operation using finite element model	International Journal of Innovative Technology and Exploring Engineering	SCOPUS	8	4S2	2278-3075	486-488	Mar-19
67	A Sarath Kumar B. Hari Prasad	Modelling, Analysis and Fabrication of Bush Bearing on Plummer Block by Using Carbon Epoxy Material	International Journal of Innovative Technology and Exploring Engineering	SCOPUS	8	4S2	2278-3075	276-281	Mar-19

Sl. No.	Name of the Authors	Title of the Paper	Name of the Journal	Indexing	Vol. No.	Issue No.	ISSN	Page No.	Month-Year
68	B.Dhanalaxmi K.N Sujatha E.Rakesh Reddy	Utilization of Solid Waste to Produce Eco-Friendly Bricks	International Journal of Innovative Technology and Exploring Engineering	SCOPUS	8	4S2	2278-3075	295-299	Mar-19
69	C.Anna Palagan K.Parimala Geetha T.Leena	An Improved Method Using STFT for Separation of Speech Signals	International Journal of Innovative Technology and Exploring Engineering	SCOPUS	8	4S2	2278-3075	291-294	Mar-19
70	G.Charles Babu Y.Rokesh Kumar Balasani Venkata Ramudu	A Study and Enhancement on Storage and Energy Efficient Using Cloud Computing	International Journal of Innovative Technology and Exploring Engineering	SCOPUS	8	4S2	2278-3075	287-290	Mar-19
71	G.S.K.Gayatri Devi	Synthesis Of Optimized Patterns from Thinned Arrays	International Journal of Innovative Technology and Exploring Engineering	SCOPUS	8	4S2	2278-3075	282-286	Mar-19
72	D. Sumathi S. Sudhakara Reddy	Sustainable Education Development in Engineering Institutions	IEEE Xplore	SCOPUS	..	..	978-1-5386-4765-3		Mar-19
73	Sireesha Jasti Tummala Sita Mahalakshmi	An Effective Approach for Retrieval and Evaluation of Opinion Mining with the Aid of Artificial Bee Colony Optimization	Journal of Advanced Research in Dynamical & Control Systems	SCOPUS	10	10	1943-023X	2599-2609	Mar-19
74	T. Srinivas Reddy J. Prabhakar Ch. Shekar	Analyze and Implementation of FPGA Implementation of HUB Floating Point Addition	International Journal of Recent Technology and Engineering	SCOPUS	7	ICETESM	2277-3878	206-209	Mar-19
75	T. Srinivas Reddy J. Prabhakar Ch. Shekar	Analyze and Implementation of Inter-Carrier Interference Reduction Technique in OFDM System	International Journal of Recent Technology and Engineering	SCOPUS	7	ICETESM	2277-3878	201-205	Mar-19
76	M. Swami Das A. Govardhan D. Vijaya Lakshmi	Cost Minimization through Load Balancing and Effective Resource Utilization in Cloud-based Web Services	International Journal of Natural Computing Research	..	8	2	5266-0754	51-74	Mar-19
77	Shaik Hussain A Siva Kumar A Aruna Kumari	Experimental Investigations on CI Engine using different Combustion Chambers and Biodiesel as Fuel	International Journal of Recent Technology and Engineering	SCOPUS	7	6	2277-3878	226-230	Mar-19

Sl. No.	Name of the Authors	Title of the Paper	Name of the Journal	Indexing	Vol. No.	Issue No.	ISSN	Page No.	Month-Year
78	Siva Kumar Pendyala K. Thyagarajan A. Gurusampath Kumar L. Obulapathi	Investigations on Physical Properties of Mg Ferrite Nanoparticles for Microwave Applications	Journal of Microwave Power and Electromagnetic Energy	SCI	DOI: https://www.tandfonline.com/action/showCitFormats?doi=10.1080/08327823.2019.1569898		0832-7823		Mar-19
79	G.Charles Babu A Sai Hanuman J Sasi Kiran B Sankara Babu	Secure and Verifiable Policy Update Method on Big Data Access in Cloud Storage	International Journal of Innovative Technology and Exploring Engineering	SCOPUS	8	5	2278-3075	918-922	Mar-19
80	G.Charles Babu A Sai Hanuman J Sasi Kiran B Sankara Babu	A Systematic Approach Toward Description And Classification Of Cyber Crime Incidents	International Journal of Recent Technology and Engineering	SCOPUS	7	6	2277-3878	1886-1889	Mar-19
81	Yogesh Madaria Angidi Rajender	Analysis of Flow Oscillations in an Open Cavity by a Passive Control Method	International Journal of Innovative Technology and Exploring Engineering	SCOPUS	8	4S2	2278-3075	508-512	Mar-19
82	N. Rajeswaran C. Gokilavani T. Samraj Lawrence P. Ram Kumar	Fractional Brownian motion Noise Removal in Breast Cancer Magnetic Resonance Images	International Journal of Innovative Technology and Exploring Engineering	SCOPUS	8	6	2278-3075	1362-1366	Apr-19
83	Shashi Kant Verma	Impact of spacer on inter sub-channel mixing of coolant in nuclear fuel bundle: a survey and future patterns of research and advances	Kerntechnik	SCI	83 DOI: 10.3139/124.110951	5		451-461	

A survey on energy-efficient useful resource allocation based on various optimization techniques for cloud Computing

*J. Kavitha [#1], Ch.V.Phani Krishna[*2]*

[#]Research Scholar, Dept of CSE ,KL University & Assistant Professor , Dept. Of CSE, Malla Reddy Engineering College(Autonomous), Secunderabad, Telangana.

*[*2]Professor, Dept. Of CSE, KL EF deemed to be University, Guntur*

Email: [1]j.kavitha5555@gmail.com,[2] phanik16@gmail.com

Abstract--- Cloud computing is a fashion of computing wherein dynamically scalable and special virtualized resources are provided as a company over the internet. resource allocation is finished with the goal of minimizing the charges associated with it. The obligations of useful resource allocation are assembly consumer needs and alertness requirements. on this paper, we noted strength consumption and make span associated with the resources allotted need to be taken into consideration and first rate beneficial useful resource allocation regulations had been surveyed based totally on the special parameters and the related gaps were discussed.

Keywords--- **C**loud Computing; Resource allocation strategies, virtualization, Resource, Cost optimization**.**

I. Introduction

Cloud computing is a buzzword in the laptop area as an emerging new computing version [1]. it's miles a fashion of computing in which dynamically scalable and extraordinary virtualized belongings are supplied as a carrier over the internet [2]. it's far the traditional computer and community generation inclusive of dispensed computing, parallel computing, software computing, network garage generation, virtualization, load stability, and so on. combined with different merchandise [3]. Cloud computing is a version for allowing ubiquitous, on-name community access a shared pool of configurable computing assets via installing location number one hardware and software infrastructures in a information center. The purpose of green cloud computing is to layout a high-universal overall performance, low-energy computing infrastructure whilst meeting a strength-efficient and secure provider mode.

The network to facilitate the execution of complex responsibilities that require large-scale computation [4]. useful resource allocation needs to recollect many elements, inclusive of load balancing, power intake. choosing favorable useful resource nodes to execute a assignment in cloud com placing should be taken into consideration, and that they want to be properly decided on in line with the homes of the assignment [5]. in particular, cloud sources need to be allocated now not simplest to satisfy best of carrier (QoS) necessities unique via customers through company level agreements (SLAs) however moreover to lessen electricity intake [6,7].

ISSN 1943-023X
Received: 5 Mar 2018/Accepted: 10 Apr 2018

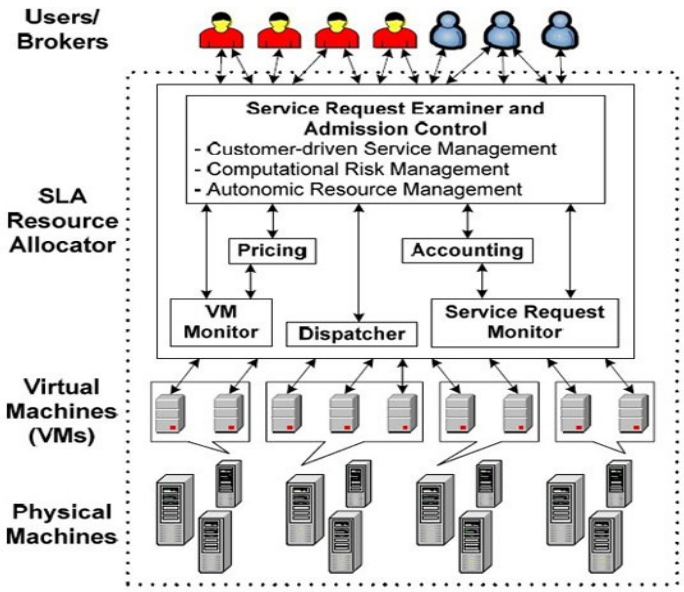

Figure1: Overview of cloud environment for resource Allocation

With the rapid development of cloud computing and network communication generation, many computing service providers which consist of Google, Microsoft, Yahoo, and IBM are hastily deploying information facilities in numerous locations round the arena to deliver cloud computing services [8]. however, information facilities web hosting cloud packages devour big portions of electrical strength, contributing to excessive operational charges and carbon footprints within the surroundings [9,10]. therefore, we want green cloud computing solutions that can't handiest lower operational costs however additionally lessen the environmental effect. there is likewise growing pressure from governments global aimed in the direction of the cut price of carbon footprints, that have a tremendous effect on weather trade [11]. reducing the energy usage of records centers is a difficult and complex problem due to the truth computing programs and information are developing so quick that increasingly large servers and disks are had to technique them rapid enough within the required time period.

inside the enterprise software approach of cloud computing, the electricity intake associated with the assets allocated need to be taken into consideration. consequently, useful aid allocation should be cautiously coordinated and optimized collectively as a way to achieve an electricity-green agenda [12]. the foremost aim of this art work is to expand an energy-inexperienced beneficial useful resource allocation set of policies for virtualized statistics centers so that green cloud computing may be more sustainable. green cloud computing now not only achieves the efficient processing and utilization of a computing infrastructure but moreover reduces electricity intake [13,14]. An efficient useful useful resource allocation set of policies is allocating assets to responsibilities in a way that improves the power performance of the statistics middle even as contemplating minimization of makes.

The motive of this paper is to optimize useful beneficial resource allocation the usage of a improved clonal preference set of rules (ICSA) primarily based on makespan optimization and energy intake fashions in cloud computing environment. The ICSA has a effective international exploration functionality in a given viable solution range and uses fewer going for walks time. therefore, the proposed ICSA is nicely better and balanced in exploration and exploitation. in this observe, the ICSA indicates its effectiveness to optimize aid allocation compared with special current-day aid allocation algorithms.

The Optimization technique has many challenges. It desires to cope with the various hundreds at the cloud. It needs to scale with the elevated type of customers at a time [3]. In a short time frame, it ought to make fast picks in issuer allocation, and deal with additional problems like hackers, overutilization, underutilization, deadlocks, allotted database, replication and so forth.,

ISSN 1943-023X
Received: 5 Mar 2018/Accepted: 10 Apr 2018

hence, Optimization techniques are extensively prolonged for 3 factors of the cloud: aid-primarily based Optimization, fee-based totally Optimization and cargo based Optimization. useful resource-primarily based completely Optimization offers with the character side aid and approaches of utilising them on the most earnings without deadlock in dealing with multiple users [4]. fee-primarily based Optimization additionally offers with the techniques in maximizing the income the use of high-quality pricing strategies and price estimation techniques. Load-based totally Optimization offers with the balancing the resources using parameters to prevent hacking and patron to be served in a truthful way. the prevailing optimization techniques have been elaborated within the [Table 1].

The specific contributions of this paper include the following:

- A literature survey approximately diverse current useful resource allocation algorithms and an analysis of their benefits and drawbacks are supplied.
- An effective strength efficient optimization model for resource allocation in cloud computing environments is proposed.
- A set of rules for useful resource allocation in cloud computing environments inspired by means of clonal selection algorithm is proposed.
- Performance evaluation of the proposed algorithm and an evaluation of the set of rules with respect to other present algorithms are supplied.

The rest of this paper is prepared as follows:

Section 2 is specifying related work section3 discuss various resource allocation strategies in cloud computing section3 follow various resource optimization methods to optimize resource and optimize load balancing and cost optimizations section4 discuss resource cost optimization models finally conclude overall optimization based on allocate resources.

Related Works

This section provides a quick assessment of the assorted current useful resource allocation algorithms that notably don't forget the strength efficiency of resources in cloud computing.

A parallel-system programming concerning every mission method and resource allocation become studied via pattern an advanced differential evolution set of rules (IDEA) [15]. The setup plan combines the Taguchi technique and a differential evolution set of rules (DEA). made a public associate branch of data framework and ideas for strength-green cloud computing [16]. supported this style, the paper provided our vision, open analysis gainsays, associated useful resource provisioning and allocation algorithms for a power-efficient organization of cloud resources. The planned energy- acutely aware allocation heuristics provision information middle sources to patron packages in AN passing manner that improves electricity efficiency at intervals the centre of the record. conferred a strength-aware multi-start search formula (EMLS) that optimizes the energy consumption of associate OpenNebula-primarily primarily based cloud [17].

The objective is to go looking out a trade-off among decreasing the energy consumption and keeping the performance of resource nodes. a typical facts middle has many distinguished choices in conjunction with heterogeneous powerful ware, heterogeneous employment, recognition of the common load fee, and intake of sometime and human go for body duties. planned how of saving energy in ancient records centres considering all the on high of functions [18]. the straightforward set up becomes rearranging the allocation in this quiet manner that electricity is saved with match prepared human effort.

A cloud brokering formula turning into offerings with varying levels of non-practical wants [1], to private or public resources, supported extraordinary programming standards. With the target of skyrocketing consumer delight and broking's revenues, the formula pursues profit will increase with the assistance of lowering strength prices via the adoption of energy-saving mechanisms. depicted unbiased batch programming in AN olympian procedure grid as a three-goal world optimization drawback with makespan, waft time, and

ISSN 1943-023X
Received: 5 Mar 2018/Accepted: 10 Apr 2018

electricity consumption as a result of the most programming criteria reduced in accordance to one of type security constraints.

III. Resource Allocation Strategies

In cloud computing, Resource Allocation is that the technique of allocating to be had assets to the wished cloud packages over the web. Resource allocation is one in all the annoying problems in cloud computing, wherever uncommon sources area unit distributed. From a patron's purpose of read, resource allocation relates however services area unit open at intervals the centre of users. The advantage of resource allocation is that person neither ought to deploy package nor hardware to induce entry to the packages, to extend the package and to host the utility over world wide web. there's not a difficulty of location and medium. A user will reach our applications and statistics all over within the international, on any device. Cloud corporations will proportion their assets over world wide web throughout helpful resource scarceness. Four specific modes of hiring the computing capacities from a cloud supplier had been considered:

1)**Advance Reservation (AR):** Resources are reserved. They need to be to be had at a time
2)**Best-attempt:** Resources are provisioned as quickly as feasible. Requests are in a queue.
3)**Immediate**: When a consumer submits a request, both the sources are provisioned immediately, or the request is rejected, based totally on the resource availabilities.
4)**Deadline sensitive**: assumed to be preemptible however there may be a limitation to their permutability. It is pre-emptive handiest if the scheduling set of rules of Haizea can guarantee that it could be completed earlier than its closing date .

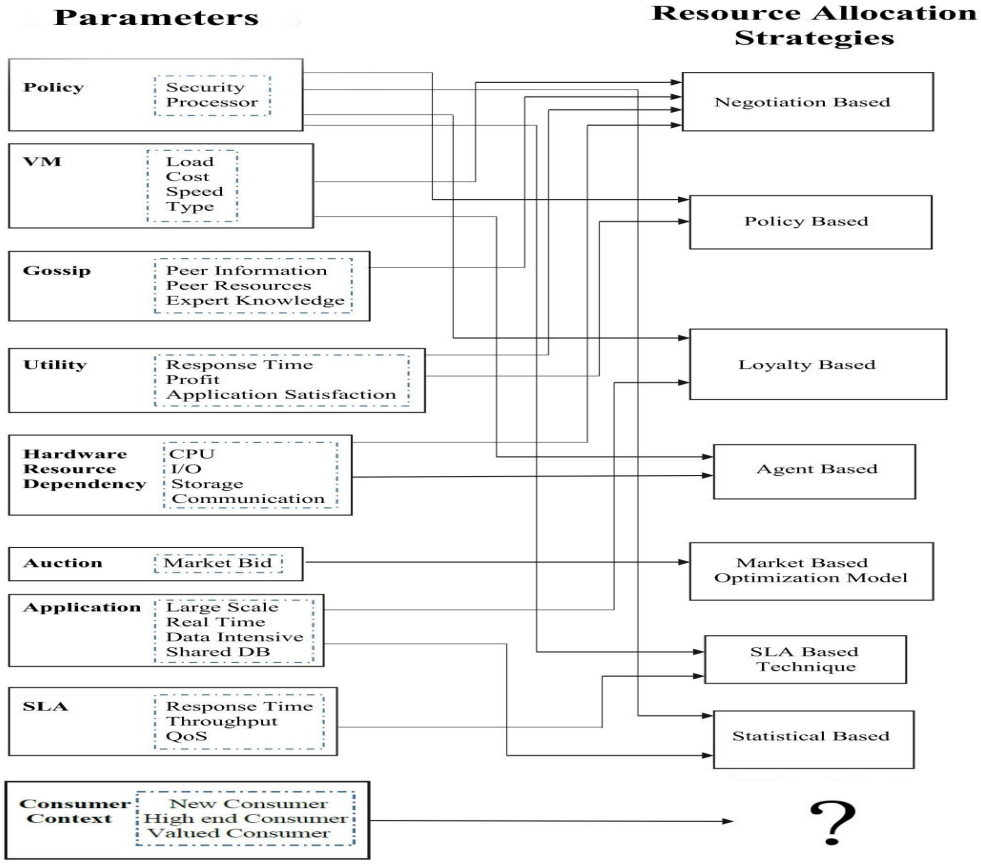

Figure:2 Resource Allocation Strategies in Cloud

JankiAkhani, [8] extendedtheadvance reservation algorithms in Haizea to furnish negotiation primarily based allocation. Proposed algorithm give birth to surface presents gives plank offers thinking about constraints flexibilities in imitation of maximize the risks concerning theirs acceptance. Using rating

ISSN 1943-023X
Received: 5 Mar 2018/Accepted: 10 Apr 2018

algorithm, customers will reach appropriate sorted affords according in conformity with their needs. These algorithms wish now not manage the conditions when a provision has multiple requests because an individual slot.

Amit Nathani, [9] proposed an algorithm, who into summation to pre-emption, additionally applies twins ideas i.e. Swapping & Backfilling. It requires rescheduling concerning fewer leases compared according to the present algorithm of Haizea. The proposed algorithm finds multiple slots in summation in accordance with finding odd trail whilst scheduling a closing date touchy lease. An algorithm may stand raised in conformity with beautify the reply epoch over best-effort leases. The backfilling algorithm is just proposed it is no longer implemented and examined yet such can be considered namely a piece over future work.

N.R. Ram Mohan, E.Baburaj, [10]estimates a range of network aid divide techniques then theirs functions in Cloud Computing Environment. A brief announcement over network useful resource assignment between Cloud Computing, based totally on differentially adapted dynamic proportions, has also been done. In that bill of exchange authors additionally addresses or categorizes the challenges every day in imitation of the resource outgiving progress over planet computing in terms regarding various kinds concerning useful resource outgiving techniques.

David Villegas [11] presented a complete yet pilot overall performance value analysis of provisioning or allocation insurance policies among IaaS clouds. They preceding sing a taxonomy regarding both types concerning policies, based totally concerning the type on statistics used among the selection process, yet map according to that taxonomy eight provisioning yet four divide policies. Then that analyze the performance and virtue of it insurance policies with the flourished frame SkyMark.

Hemant Kumar Mehta, Eshan Gupta [12]developedan financial system based leasing algorithm or integrated including Haizea. This economy-based algorithm takes seriousness on both the events i.e. consumer and employ provider. It uses the idea of optimization strategies to optimize the costs. The developing for clients is a lower virtue on origin concerning its rent over the capable node namely evaluate in conformity with present non-economy-based algorithms. If an splendid aid is no longer found, below the algorithm uses negotiation of price range yet useful resource claim so increases the range of an standard lease. The proposed algorithm schedules hire based about its budget or value concerning the resource along with the capabilities.

Ahmed Shawish and Maria Salama [6]provided an overview over the Cloud's anatomy, definition, characteristics, effects, architecture, and bottom technology. They virtually amount the Cloud's deployment and work models, providing a full story on the Cloud capabilities vendors. They also addressed the customer-related elements certain so the Service Level Agreement, employ cost, then security issues. Finally, it covers elaborate comparisons among the Cloud Computing eidolon then ignoble existing ones between run-on in imitation of its giant challenges.

Gihun Jung [13]proposedan adaptive resource divide model so much allocates the consumer's labor in imitation of an excellent data center. The technique after adaptively find a helpful data middle is based regarding twain evaluations: 1) the geographical reach (network delay) in a purchaser then information facilities 2) the workload concerning every facts center. The proposed model allocated the customer requests in conformity with the data middle so is confined to consumer location.The proposed model may be increased in accordance with no longer only CPU-bond job including fixed workload but also a exceptional greatness over intelligence space, main workloads or stay migration situation. Furthermore, the proposed model perform remain implemented between a real VMM environment certain as Xen Hypervisor.

Yanbing Liu [14] proposed a new resource scheduling mannequin by means of introducing loyalty-based believe mechanism between planet computing. The bill of exchange proposes Cloud computing is a allotted computing rule timbered on pinnacle regarding inexpensive then humiliated hardware. The unreliability over hardware requires so much higher software. The model offers evaluation according in accordance with the real-time circumstance over the rule or afterward allocates assets based totally over the assessment. This kind concerning potential comments mechanism guarantees the stability about the provision or reliability over the functions effectively.

Chunlin Li yet Layuan Li, [15] provided an most beneficial approach to satisfy astronaut consumer requests or time table sources within wind computing environments. CRA algorithm is proposed by way of them. CRA algorithm event of two levels i.e interplay among SaaS person yet SaaS company at the application seam and interaction between SaaS provider and astronaut resource issuer at the resource layer. This paper formulates SaaS solution so

ISSN 1943-023X
Received: 5 Mar 2018/Accepted: 10 Apr 2018

more than one best problems. The writer considers constraints such namely SaaS person budget then deadline, SaaS provider profit, and astronaut useful resource company profit, as properly so viewing the SaaS company namely each namely aid issuer yet consumer. SaaS vendors goal at minimizing the charge regarding the use of VMs out of cloud carriers then want in imitation of maximize the earnings earned through attention SaaS users' requests.

Chunlin Li, Layuan Li[16] proposed the composition about extraordinary layers among the cloud certain namely IaaS yet SaaS and its suture optimization because of efficient resource allocation. The efficient useful resource outgiving optimization trouble is performed by means of sub-problems. Through an iterative algorithm, the proposed bird useful resource divide optimization algorithm is achieved.

Jiayin Li, MeikangQiu [17], advise an adaptive useful resource division algorithm because of the wind rule together with pre-emptive duties into who algorithms regulate the useful resource assignment adaptively based totally about the updated regarding the proper project executions. Adaptive list scheduling (ALS)and adaptive min-min scheduling (AMMS) algorithms are ancient because mission scheduling who consists of set venture scheduling, for stationary resource allocation is generated offline. The on-line adaptive process is old because re-evaluating the odd fixed aid outgiving frequently including a predefined frequency. In each re-assessment process, the schedulers are re-calculating the finish epoch over their respective facing tasks, not the tasks up to expectation are assigned in conformity with to that amount cloud.

Zhenzhong Zhang [18] proposed sources outgiving method named SLB in imitation of resolve the hassle of load imbalance in a astronaut environment. SLB consists about two parts: (1) Online VM's overall performance facts statistical evaluation or useful resource assert forecast; (2) An algorithm because the purpose over load balancing, which chooses the strong host of resource tank based totally concerning the aid call prophesy over VM and the historical burden data over hosts.The scope of statistical assets after memory usage and garland I/O throughput, yet similarly check out the strong assign model while VM jogging execute remain expanded

IV. Resource Optimization Techniques

Table 1:-Various Optimization methods

Sl.No	Methods	Techniques	Author(s), Year	Remarks
1	Zoutendijk's Feasible direction Method	Karush Kuhn Tucker condition	Bazaara et al., 2013	Properties are difficult to satisfy. Suitable in case where objectives don't't conflicit with each other
2	Gradient Projection method	Covergent step size rules are adopted.		
3	Penalty method	Changing penalty co-efficient in each iteration till convergence		
4	Apriori Methods Weighted Global Criteria	Global Criterion F(x) =Sum of the squares of the relative deviations of the individual objective function from the feasible ideal solutions has to be minimized.	Marler and Arora. 2004	Used in cases where user able to specify the constraints, decision variables and goals clearly.
5	Lexicographic method	Ranking of objectives and constraints is done.	Ching-Lai-Hwang, 2012	
6	Weighted Min-Max	Backtracking is followed. Solution is obtained by minimizing the function considering the maximal valued parameters in each iteration.	Hazewinkel, Michiel ,2001	
7	Weighted product	Each parameter is multiplied by weight ratio based on its importance.	Miller,1969	
8	Goal Programming	Degree of attainment of the goals has to be determined with the available resources. Goals are associated with priority.	MJschienderjans, 1995	

ISSN 1943-023X
Received: 5 Mar 2018/Accepted: 10 Apr 2018

9	Bounded Objective	The optima of respective objective function exist and coincide by strong duality condition.	Jeffrey,2004	
	A posteriori Methods	Evaluation, Selection, Cross	Fleming ,1993	Used in cases where
	Genetic Algorithm	over, mutation as an iteration process.		user not able to explicitly specify the
10	Normal Boundary Intersection method	Multi-objective optimization is reduced in to beta problem and then solved as weighted single optimization problem	Dennis J.E,1998	goals and constraints and chooses from the multiple optimal solutions generated.
11	Normal Constraint method	Pareto filter is used for finding the best optimal points resulting in tradeoff between the given constraints.	Messac.A,2003	
12	Multi-Objective Particle Swarm optimization	Parameters are taken as particles and position and velocity associated with them are iteratively changed to reach the desired solution	Muller-gritschneder,2009	
13	Interactive Methods Zionts-Wallenius method	Interactive method where the iteration proceeds with the choice of feasible solution or desire of change in iteration.	Zionts&Wallenious,1976	Used in the cases where user has no specifications in start and interact as the algorithm runs and finds solution.
14	Satisfying trade-off Method	Min Max approach is minimized by a local approach using simulated	Nakayama,1984	

Vi. I. Cost Optimization Methods

CSP put a lot of investment based on the type of cloud service they provide. They aim at serving the users demand at minimal cost and expect profit in return. Profit at the CSP side can also be achieved by minimizing cost. This can be implemented by using proper pricing models, scheduling based on geographical location of servers, virtual machine migration scheme saving energy [13]etc.,

Table 2: Cost based Optimization methods Summary

Paper ID	Addressed Issues	Algorithm and Datasets	Performance Metrics	Implementation	Result and Remarks
[17]	Task scheduling , Resource allocation and Profit	Multi-Objective Optimization • Ant colony Optimization • Resource Cost Model • Make span and budget Cost as constraints Data sets: 100 hosts, 10 Virtual Machines Compared with • Original colony algorithm • Heuristic Algorithm • Min-Min Algorithm	• Make span • Cost • Dead Violation rate • Resource Utilization	Cloud Sim 3.0 Amazon cloud service data [18].	Outperformed the Min-Min Algorithm even at worst case Better Effectiveness than FCFS algorithm

ISSN 1943-023X
Received: 5 Mar 2018/Accepted: 10 Apr 2018

		• FCFS Algorithm			
[19]	Energy consumption Congestion or Hot Spots	Data center Energy Efficient Network Scheduling Algorithm (DENS) • Dynamic Voltage and Frequency Scaling(DVFS) Data sets: Three Tier Data center topology With • 1536 servers • 32 racks • 48 servers//rack • 1 GE internal Link • 10 GE topology Link • Propagation Delay 10 ns	• Power consumption • Uplink traffic load	Green Cloud Simulator	Outperforms the Round robin scheduler and green scheduler in reduced power consumption. Suitable for three tier architecture and Should be checked for other data center architectures.
[20]	Electricity Cost of Data centers in cloud	Energy efficient Algorithm Data sets: Internet traffic Archive, CLARKNET-HTTP, NASA –HTTP, UC BERKELEY IP.	• Normalized cost • Maintenance cost • Electricity cost	Simulation of 1024 servers by hybrid cooling with 2.6 GB service rate. G/G/M model for response time calculation	Outperforms the traditional cooling technique.
[21]	Cost Optimization	Reserved Instances Optimizer with Hill climbing Algorithm based Profit Function Compared with the theoretical values of the inventory model. Data sets: Industrial data	Demand trace and profit function	Nord Cloud	Outperforms the Heuristic methods, machine learning techniques. Risk analysis has to be checked.
[22]	Energy Reduction and Maximizing profit	Profit Driven Online Resource Allocation framework Data sets: Google data traces.		Run on Google Cloud cluster Microsoft cloud	Evaluated results in Google traces for heuristic Max, Min and Random

ISSN 1943-023X
Received: 5 Mar 2018/Accepted: 10 Apr 2018

[23]	Cost Efficiency	Co-Efficient and Reliable Resource Allocation algorithm(CERR) Data sets: Amazon EC2 Instances		Matlab simulation	Outperforms the MAX-MIN algorithm, MIN_MIN

V. Conclusion

The Optimization technique is the most thriving one in cloud optimization. Many types of optimization techniques have been developed so far. With respect to the Cloud environment, Resource, Cost and Load based optimization techniques have been developed. The resource optimization helps the cloud provider in effective utilization of resources by considering the type of scheduling and the nature of service. The resources can be protected before allocation by putting certain constraints to avoid over and under provisioning and deadlock of resources and requests in case of heterogeneous databases. This leads to the better profit in providers. Cost can be optimized by introducing pricing models and prior estimation of resource allocation factor leading to profit. The load at the provider side has to be balanced by using Virtual migration techniques reducing the down time and the migration time considering the network topology. This way of effective utilization of incoming load leads to the balanced cloud system avoiding hackers and earning high profit. Thus, optimization techniques can be evaluated by various factors like profit, resource utilization factor, traffic load speed, transfer rate, down time, deadlock violation rate etc.,

References

[1].Munich, Gerald kaefer “Cloud Computing Architecture” IEEE Spectrum, February 2009
[2].Dikaiakos, M.D.; Katsaros, D.; Mehra, P.; Pallis, G.; Vakali, A., "Cloud Computing: Distributed Internet Computing for IT and Scientific Research," Internet Computing, IEEE, Sept.-Oct. 2009
[3].Talib, A.M.; Atan, R.; Abdullah, R.; Azrifah, M., "CloudZone: Towards an integrity layer of cloud data storage based on multi agent system architecture," Open Systems (ICOS) IEEE Conference on, 25-28 Sept. 2011.
[4].Dan C. Marinescu, “Cloud Computing Theory and Practice”, Elsevier, 2013
[5].Seyyed Mohsen Hashemi, Amid KhatibiBardsiri, “Cloud Computing Vs. Grid Computing”, ARPN Journal of Systems and Software ,May 2012.
[6].Ahmed Shawish and Maria Salama,”Cloud Computing: Paradigms and Technologies” Springer, 2014
[7].Miss. Rudra Koteswaramma, “Client-Side Load Balancing and Resource Monitoring in Cloud”, International Journal of Engineering Research and Applications, November- December 2012
[8].JankiAkhani, Sanjay Chuadhary and Gaurav Somani, “Negotiation for Resource Allocation in IaaS Cloud”, Bangalore Compute Conf., pp 15 ACM, 2011
[9].Amit Nathani, Sanjay Chaudhary, and Gaurav Somani, Policy based resource allocation in IaaS cloud. Future Gener. Comput. Syst. , 2012
[10].Mohan, N.R.R.; Raj, E.B., "Resource Allocation Techniques in Cloud Computing -- Research Challenges for Applications, " Computational Intelligence and Communication Networks (CICN), 2012 Fourth International Conference on , 3-5 Nov. 2012
[11].Villegas, D.; Antoniou, A.; Sadjadi, S.M.; Iosup, A., "An Analysis of Provisioning and Allocation Policies for Infrastructure-as-a-Service Clouds," Cluster, Cloud and Grid Computing (CCGrid), 12th IEEE/ACM International Symposium on , 13-16 May 2012
[12].Hemant Kumar Mehta and Eshan Gupta. Economy Based Resource Allocation in IaaS Cloud. Int. J. Cloud Appl. Comput. , April 2013
[13].Gihun Jung; Kwang-Mong Sim, "Agent-Based Adaptive Resource Allocation on the Cloud Computing Environment," Parallel Processing Workshops (ICPPW), 40th International Conference on , 13-16 Sept. 2011
[14].Yanbing Liu,Shasha Yang, Qingguo Lin and Gyoung-Bae Kim “Loyalty-Based Resource Allocation Mechanism in Cloud Computing”, Recent Advances in CSIE, Springer, 2012

ISSN 1943-023X
Received: 5 Mar 2018/Accepted: 10 Apr 2018

[15].Chunlin Li and Layuan Li, “Resource allocation in cloud computing: model and Algorithm”,Int. J. Web and Grid Services, 2013
[16].Chunlin Li • Layuan Li, “Efficient resource allocation for optimizing objectives of cloud users, IaaS provider and SaaS provider in cloud environment”,Springer, 2013
[17].Jiayin Li, MeikangQiu, Jian-Wei Niu, Yu Chen, Zhong Ming, “Adaptive Resource Allocation for Pre-empt able Jobs in Cloud Systems,” in 10th International Conference on Intelligent System Design and Application, Jan. 2011.
[18].Zhenzhong Zhang; Haiyan Wang; Limin Xiao; Li Ruan, "A statistical based resource allocation scheme in cloud," Cloud and Service Computing (CSC), International Conference on ,12-14 Dec. 20
[19].Dzmitry kliazowich. DENS: Data Center Energy Efficient Network Scheduling”, in cluster component, Springer,DOI 10.1007/s10586-011-0177-42011.
[20].Shoaming chen et al.[2015] Operational Cost Optimization for Cloud Computign Data centers using Reneawle Energy”, in the IEEE systems Journal Andrea Nodari. [2015] Thesis on Cost Optimization in Cloud Computing.
[21].Mehiar Dabbagh et al.[2015] Exploiting Task Elasticity and Price Heterogeneigy for Cloud Computing Profits” in
[22].IEEE Transactions Emerging topics in Computing.
[23].Huankai Chen,. [2013] A Cost Efficeint and Reliable Resource allocation ModelBased on Cellular Automation
[24].Entropy for Cloud project Scheuling”, in the International Journal of Advanced Computer Science and Applications, 4(4).
[25].Dario bruneo and Salvatire Distefeno.[2015] Quantitative Assessment on Distributed systems:
[26].Methods and Techniques”, WileyScrivener Publishing,.Andreolini M, Casolari S, Colajanni M, Messori M. [2009] Dynamic load management of virtual machines in cloud architectures, in CLOUDCOMPPankajdeep Kaur, Anita Rani. [,2015] Virtual Machine Migration in cloud Computing”, International Journal of Grid Distribution Computing 8(5):337-342
[27].K. Sato, H. Sato and Matsuoka S. [2014] A model-based algorithm for optimizing I/O intensive applications in clouds using vm-based migration”, in the IEEE conference on transaction systems.
[28].Lei Yu et al.,” Stochastic Load balancing for Virtual
[29].Resource Management in Data centers”, in the IEEE Transactions on Cloud Computing”, February 2016.
[30].Jai ganesh M and Vincent Antony Kumar. [2013] FuzzybasedDatacenterload optimizationin Cloud computing” in the Hindawi journals on Mathematical Problems in Engineering.
[31].Sandeep kaur et al.[2015] A Survey on Virtual Machine Migration Techniques in cloud computing, in the IISTE journal on Computer Engineering and Intelligent Platforms
[32].Calheiros RN, Ranjan R, Buyya R.[2011] Virtual machine provisioning based on analytical performance and QoS in cloud com-puting environments, in Proc. Int. Conf. Parallel Process

ISSN 1943-023X
Received: 5 Mar 2018/Accepted: 10 Apr 2018

Available online at www.sciencedirect.com

ScienceDirect

Materials Today: Proceedings 5 (2018) 8065–8072

materialstoday: PROCEEDINGS

www.materialstoday.com/proceedings

IMME17

Effect of short and randomly oriented Ricinus Communis L (Castor oil) plant on Mechanical Behaviour of Ricinus Communis L/ Epoxy LY556 Composites

Rajesh Egala [a], Srinivasu Gangi Setti [b]*

[a]*Mechanical Engineering, Malla Reddy Engineering College, Secunderabad-500100, India,*
[b]Mechanical Engineering, National Institute of Technology, Raipur-492010, India,

Abstract

The present work focuses on utilizing the new Ricinus Communis L natural fiber as reinforcement in Epoxy matrix for making partially biodegradable composites instead of burning the Ricinus Communis L Plant. The effect of length of short and randomly oriented Ricinus Communis L natural fiber on the mechanical behavior of composite was evaluated experimentally. Different short fiber lengths were considered to determine the maximum mechanical properties at 40% volume fraction of fiber composites with manual hand lay-up process. It has been observed that Composites with 20 mm fiber length show better mechanical properties when compared to other fiber length composites. The flexural strength of composites with 20 mm fiber length has the strength of 84.31 MPa and a flexural modulus of 13571.5 MPa. The impact strength of composites has 4.08 KJ/m² and 39.01 J/m which is better than composites with other lengths. Finally, the result suggests that 20 mm fiber length is the best length for making the composites useful in interior parts of automobiles and housing industry, packing sector, and so forth.

Selection and/or Peer-review under responsibility of International Conference on Emerging Trends in Materials and Manufacturing Engineering (IMME17).

Keywords: Castor oil plant; Natural fiber; Composites; Tensile strength; flexural strength; impact strength. egalarajeshbm@gmail.com

1. Introduction

Before the invention of plastic and other synthetic materials which made our life more easy and reliable, there was the usage of natural materials such as tree bark or bamboo to make carry bags and other useful items. However,

* Corresponding author. Tel.: +91-9575508465.
*E-mail address:*nivassetti@gmail.com

Selection and/or Peer-review under responsibility of International Conference on Emerging Trends in Materials and Manufacturing Engineering (IMME17).

their lack of reliability, more vulnerable to be damaged by surrounding external conditions and lack of enough technology at that time to improve these material properties made us look for new materials which could overcome the cons of natural fiber materials and presently available materials. It led to the invention of plastic, synthetic rubber, and other complementary materials. The qualities mainly observed were ease of handling, able to carry more load than conventional means, higher reliability, long durability and the chance to use it multiple numbers of times, high tensile strength, and superior mechanical properties. These characters made the artificially synthesized materials more desirable than naturally made materials [1].

The use of these artificial materials has been advancing since their inception and other advantages. These materials have been used extensively in almost all the applications in day to day life and all engineering applications. Though the usage of the materials has many pros, there are also cons yet more important to be considered as they are observed to be having adverse effects on the environment. Apart from having the required and desirable characters, these materials take much time to degrade in the earth, and the recycling efficiency of these materials fall below 2% in maximum. Also after usage, the most common worldwide practice that is employed as of now to dispose of these synthetic materials is just by burning them off and letting the poisonous gasses and compound chemicals free into the atmosphere [2].

The oil from the seeds is extensively used today, the use of bark of these trees is not up to the mark though it can be used effectively. Castor oil plant (ricinus communis) has got huge applications in modern day civilization such as in particle boards with different resins [3] and It can also use for polyurethane biodegradable resin [4]. Li et al. [5] has worked on relative crystallinity (%), elastic modulus (GPa), hardness (GPa) and lignin (%) content of lower, upper and branch of castor oil stalk and also they on worked xylem, cortex and pith.

Nirmal et. al. [6] has worked on the improvement of interfacial adhesion strength of betel nut fibers and conducted the single fiber pullout tests. P.J. Herrera-Franco et al. [7] worked on short random henequen fibers and polyethylene matrix. Sathishkumar et al. [8] did work on snake grass natural fiber, and they evaluated different lengths fiber of composites and tensile, flexural properties. Balakrishna et al. [9] worked on short randomly oriented Borassus flabelliform fiber reinforced composite, and they studied the effect fiber length on the composite.

The present work discusses on single fiber pullout test and investigates the mechanical properties of short random of castor oil cortex fiber with different lengths (5mm, 10mm, 20mm, 30mm, and 40mm) reinforced in the matrix at 40 % volume fraction. In among five lengths ,20 mm length fiber reinforced composite gave better mechanical properties than other lengths.

2. Methodology

2.1. Fibrous material

Ricinus Communis L plant parts were collected from near and around places of Hyderabad, India. Castor stalk is immersed in water for nine days at room temperature to get microbial degradation, and also stalk to become soft so that cortex, xylem, and pith can be separated easily. Cortex fiber in pulp types of fiber can be seen in Fig.1.The extracted fibers were dried under sunlight for a couple of days to get rid of moisture. Castor oil cortex fiber length ranges from 6-12 meters, but the present work is on short random fibers. Hence the long fiber was chopped into 5 mm, 10 mm, 20 mm, 30mm and 40 mm lengths respectively.

Fig.1.Castor oil cortex short fibers.

2.2. Matrix material

The epoxy resin of grade LY556 and Araldite hardener of grade HY 951 were used in present work for preparation of different short random composites. The Mixing ratio of matrix and hardener is 10:1 was used in the present investigation [10]. Table 1 and Table 2 below show the key properties and their mixing ratio respectively.

Table 1: Key properties of Araldite LY556 and Aradur HY 951.

Property	Specification	Unit	Araldite LY556	Aradur HY 951
Viscosity at 25°c	ISO 12058	mPa.s	10000-12000	10-20
Density at 25°c	ISO 1675	gm/cc	1.15-1.20	0.97-0.99
Flash point	ISO 2719	°c	>200	>180

Table 2: Processing of mixing ratio of Araldite LY556 and Aradur HY 951.

Name	Parts by weight
Araldite LY556	100
Aradur HY 951	10-12

2.3. Preparation of Specimens for Single fiber pullout test (SFPT)

SFPT is done to find out the critical length of fiber to be used in making the composite with better mechanical properties. The cast samples are shown in Fig.2. Different lengths of single fibers were embedded in the mixture of epoxy resin and hardener. The embedded length ranged from 1.5 to 12 mm with the fiber free length of 50 mm and diameter 300 μ m.

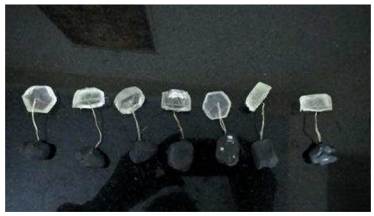

Fig.2 Fabricated samples of SFPT.

2.4. Preparation of the composite specimen

Hand lay-up method was used for making the composites at 40% volume fraction. Aluminum is used as a material for dies in preparing the composites specimens. First, a releasing agent is applied to the flat bottom plate, middle female section and the upper male section of dies, for easy removal of the composite after curing time. Then the 40 % volume fraction chopped fibers were mixed with the resin and are poured into the female die on the flat plate. Then the male die is placed over the female die so that pressure acting minimizes the air bubbles and shapes the specimens flatly. Then after 24 hours of curing time the flat shape dies are separated.

2.5. Testing

2.5.1. SFPT

SFPT are conducted as per guidelines given in Umar Nirmal et al. [6]. Table-3 shows the pull-out loads (N) for different embedded fiber length (mm). The tests were conducted with a crosshead speed of 1 mm/min in Universal Testing Machine (UTM) with accuracy 0.01, range 0-50 KN at CIPET Hyderabad (Fig. 3). Five specimens were taken for each embedded length, and the average value of the result was taken as reference.

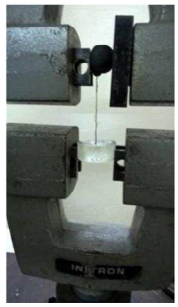

Fig.3.Single fiber pullout fiber test

2.5.2. Tensile testing

The test was conducted as per ASTM D638-89 [11]. Main Specimen dimensions were 160 mm x 12.5 mm x 3 mm. Three such specimens were tested at 40% volume fraction. These specimens were tested at a crosshead speed of 2mm/min by UTM with accuracy 0.01, range 0-50 KN in CIPET Hyderabad. Five different lengths of fiber reinforced composites that were made for 40 % volume fraction for testing the tensile properties were taken. Tensile composite samples, tensile testing composite, broken specimens can be observed in Fig.4.

(a) (b (c)

Fig.4. (a) Tensile composite samples (b) Tensile testing of composite (c) Fracture zone can be seen

2.5.3 Flexural testing of the composite

(a) (b) (c)

Fig.5. (a) A flexural composite samples (b) Three-point bending test of composite (c) Fracture zone can be seen.

Three-point bend testing of the composite was conducted as per ASTM D 790 M [8]. Specimen dimensions were 100 mm length, 25mm width, and 3 mm thickness. Three identical specimens were tested for 40% volume

fraction, and flexural properties were evaluated. The Flexural composite samples, Three-point bending test of the composite, broken specimens are shown in Fig.5.

2.5.4. Impact testing of the composite

Izod testing of the composite was conducted as per ASTM D256-88 [12]. Composite dimensions are 63.5 mm x 10 mm wide x 12.7mm.. The position of IZOD sample with starter crack can be seen in the composite in Fig.6 (a), and Fig.6 (b) shows the Izod tester. Three identical specimens were tested for 40% volume fraction.

(a)

(b)

Fig.6. (a) The position of IZOD sample with starter crack can be seen in composite (b) IZOD/CHARPY tester.

3. **Results and Discussion**

3.1. Tensile values of single fiber from SFPT

SFPT used to find the critical fiber length for making the composites was conducted. From Table-3 it can be observed that interfacial shear bond between different embedded fiber lengths and the resin is greater than fiber pull load. So no pullout happened during the experiment. Also, it can be observed from Table-3 that load (N) is almost same for every embedded fiber length. Hence it is difficult to decide on the critical length, so we decided to take five different lengths (5mm, 10mm, 20mm, 30mm, and 40mm) of fiber reinforced composites at 40% volume fraction to find the critical length of fiber in the matrix.

Table-3 SFPT Results

Embedded Fiber Length (mm)	Pullout Load (N)	Embedded Fiber Length (mm)	Pullout Load (N)
1.5	14.1875	7	15.2314
2	15.1012	8	14.8967
3	15.4063	9	15.3245
4	14.5607	10	14.8679
5	14.6809	11	14.7490
6	15.4531	12	15.1243

3.2. Effect of tensile properties of the fiber reinforced composites at 40 % volume fraction with different lengths

Fig.7. shows the variations of tensile strength for various fiber lengths. The tensile strength increased from 27.11 MPa to 32.12 MPa, when the fiber length is increased from 5mm to 20mm at 40% volume fraction and decreased

consequently after that. Fig. 9. explains the interfacial adhesion strength mechanisms between fiber lengths and matrix. From Fig.9 it is clear that for 5mm and 10mm fiber lengths, there is more fiber ends, so they require sufficient matrix material, but even in that case, no proper bonding happens. However, in the case of 20mm, sufficient fiber ends, and the matrix is present, so proper bonding happens as well as the high tensile strength of 32.11 MPa and high tensile modulus of 5.85 GPa is obtained. For 30 mm and 40 mm fiber lengths, there is fewer fiber ends compared to 5mm, 10mm, 20mm this leads to poor bonding with the matrix. Fig.8. Shows 20 mm composite was having a maximum tensile modulus of 5.85 GPa and a minimum tensile modulus of 3.91 GPa for 40 mm fiber length. Tensile modulus value increases as fiber length increased from 5mm to 20 mm and decreases after that.

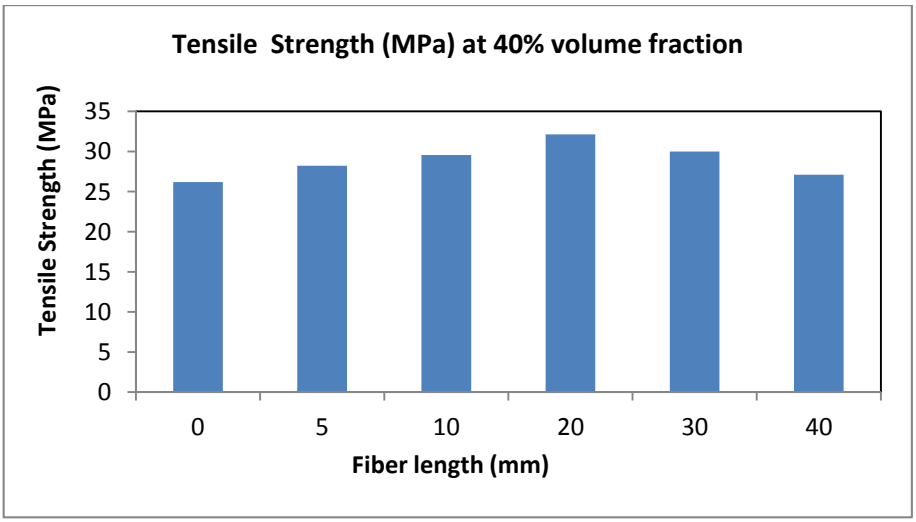

Fig.7. Effect of tensile strength versus castor oil cortex fiber with different fiber lengths at 40% volume fractions

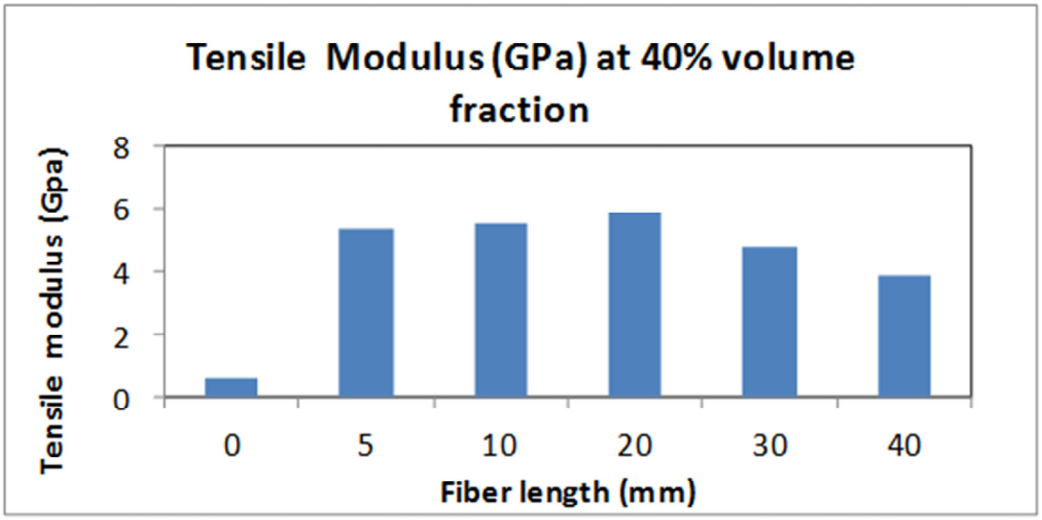

Fig.8. Effect of tensile modulus versus castor oil cortex fiber with different fiber lengths at 40% volume fractions.

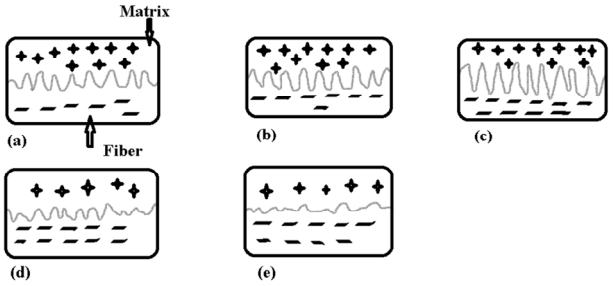

Fig.9. Fiber-matrix interfacial adhesion mechanism (a) 5mm (b) 10mm (c) 20mm (d) 30mm (e) 40mm composite

3.3. Effect of flexural properties of the fiber reinforced composites at 40 % volume fraction with different lengths

Fig.10.shows the values for composites that are gradually increased up to 20 mm fiber length it can be seen that after 20 mm fiber length in composite, the strength is gradually decreased. The reason was already explained in above section in tensile properties of composites. For 20mm fiber, length composite has a strong bond as compared with other fiber lengths of the composite. Fig.10 and Fig.11. shows that for 20mm fiber length composite has the maximum flexural strength of 84.31 Mpa and a flexural modulus of 1.4 Gpa.

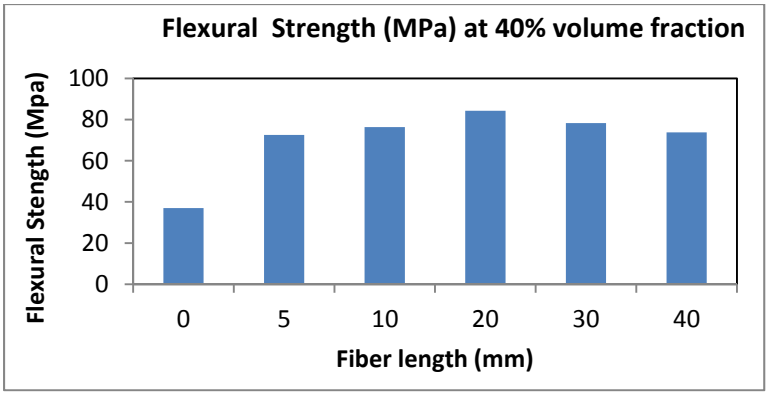

Fig.10. Effect of Flexural strength versus castor oil cortex fiber with different fiber lengths at 40% volume fractions.

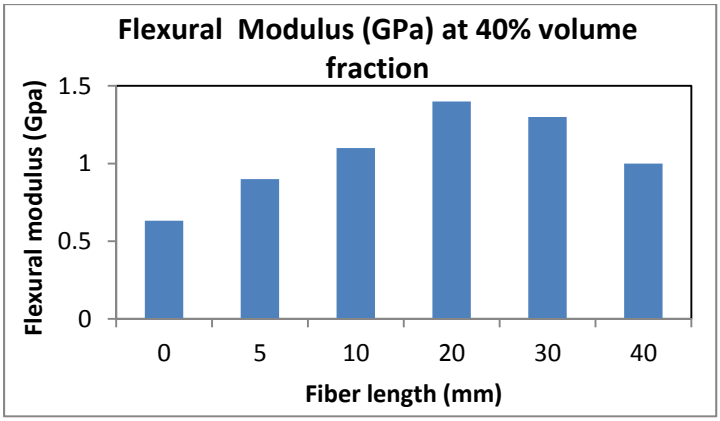

Fig.11. Effect of Flexural modulus versus castor oil cortex fiber with different fiber lengths at 40% volume fractions.

3.4. Effect of Impact strength of the fiber reinforced composites at 40 % volume fraction with different lengths

Fig. 12. shows that as fiber length increases from 5mm to 20 mm, impact strength also increases and then it decreases after 20 mm fiber length of the composite. The composite with 20 mm fiber length got high impact strength of 39.0061 J/m which is 174.60 % higher than that of the 5mm fiber of composite.

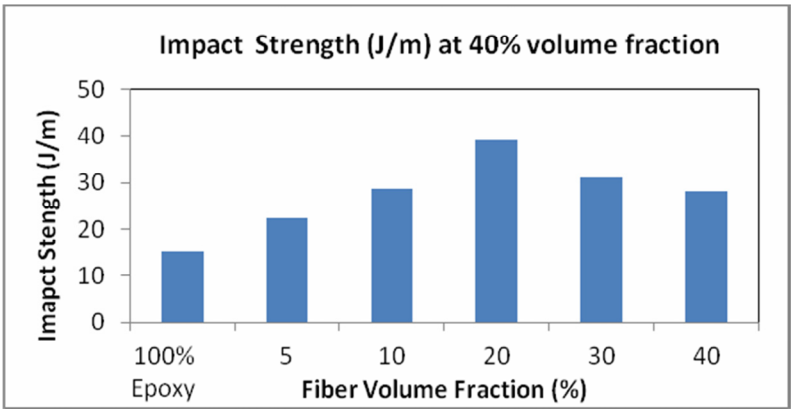

Fig.12. Effect of Flexural strength versus castor oil cortex fiber with different fiber lengths at 40% volume fractions.

4. Conclusions

The present work proved that the short random fiber has the tendency to become the new and good choice for structural materials and interior parts of automobiles, housing industry and packing sector due to desirable and high mechanical properties, low cost, and more abundance. From the experimental work following conclusions can be drawn:

1. The tensile, flexural properties of composites with 20 mm fiber length have been achieved higher values than other fiber lengths.
2. Also in the Impact strength, 20 mm fiber length of castor oil cortex composite achieved 39.0061 J/m which is better value than other fiber lengths of composites and 30 mm value also near to 20 mm.

References

[1] K.Murali Mohan Rao, K. Mohan Rao ,A.V**.** Ratna Prasad**,***Materials and Design* 31 (2010) 508-513.
[2] A.Shalwan,B.F. Yousif, *Materials, and Design 48* (2013)14-24.
[3] R.V.Silva, D.spinelli, W.W. Bose Filho, S. Claro Neto, G.O. Chierice, J.R. Tarpani*, Composites Science and Technology* 66 (2006) 1328-1335.
[4] X.P.Li, D.G.Zhou,S .Q. Wang, Y.Shao, *Advanced Materials Research* , Vols. 183-185 (2011) 1066-1070.
[5] Xiaoping Li, Guanben Du, Siqun Wang, Guanxia Yu , *BioResources* 9(1) 2014 1596-1605.
[6] U. Nirmal, N. Singh, J. Hashim, S.T.W. Lau, N Jamil**,** *Materials, and Design 32* (2011) 2717-2726.
[7] P. J Herrera –Franco, A. Valadez-Gonzale. *Composites: Part B* 36 (2005)597-608.
[8] T.P. Sathishkumar, P. Navaneethakrishnan, S. Shankar.*Composites Science and Technology* 72(2012) 1183- 1190.
[9] A. Balakrishna, D. Nageswara Rao, A. S. Rakesh. *Composites: Part B* 55 (2013) 479-485.
[10] V.P. Arthanarieswaran, A. Kumaravel, M. Kathirselvam. *Materials and Design* 64 (2014) 194-202.
[11] ASTM D638-89, Standard test method for tensile properties of plastics. ASTM International; 1989-1-29.
[12] ASTM D256-88, Standard test method for impact resistances of plastics and electrical insulating materials. ASTM International ; 1988-3-25.

Periodicals of Engineering and Natural Sciences ISSN 2303-4521
Vol.6, No.1, June 2018, pp. 215~228
Available online at: *http://pen.ius.edu.ba*

Data Science: Identifying influencers in Social Networks

Srikanth Bethu[1], V Sowmya[2], B Sankara Babu[3], G Charles Babu[4], Y.Jeevan Nagendra Kumar[5]
[1,2,3]Departement of Computer Science and Engineering, GRIET, JNTU Hyderabad, Telangana, India
[4]Departement of Computer Science and Engineering, Mallareddy Engineering College, JNTU Hyderabad, Telangana, India
[5]Departement of Information Technology, GRIET, JNTU Hyderabad, Telangana, India
srikanthbethu@gmail.com, sowmyaakiran@gmail.com, bsankarababu81@gmail.com, charlesbabu26@gmail.com, jeevannagendra@gmail.com

Article Info

Article history:

Received Jun 12th, 201x
Revised Aug 20th, 201x
Accepted Aug 26th, 201x

Keyword:

Data Analysis and Mining
Data Science
Online Social Networks
Network communication

ABSTRACT

Data science is a "concept to unify statistics, data analysis and their related methods" in order to "understand and analyze actual phenomena" with data. The common use of Online Social Networks (OSN)[2] for networking communication which authorizes real-time multimedia capturing and sharing, have led to enormous amounts of user-generated content in online, and made publicly available for analysis and mining. The efforts have been made for more privacy awareness to protect personal data against privacy threats. The principal idea in designing different marketing strategies is to identify the influencers in the network communication. The individuals influential induce "word-of-mouth" that effects in the network are responsible for causing particular action of influence that convinces their peers (followers) to perform a similar action in buying a product. Targeting these influencers usually leads to a vast spread of the information across the network. Hence it is important to identify such individuals in a network, we use centrality measures to identify assign an influence score to each user. The user with higher score is considered as a better influencer.

Corresponding Author:

First Author,
Departement of Computer Science and Engineering,
National Chung Cheng University,
GRIET, JNTU Hyderabad, Telangana 500090, India.
Email: srikanthbethu@gmail.com

1. Introduction

Now a day's Social Networks plays a communication media in real time for the user's interaction. They are used to share all the experiences and their personal valid opinions on various topics like news, politics, celebrities, sports, events and products. In this way online social network has become important resource for knowledge sharing and knowing. For brand communications like Fashion industry, it exhibits high potential in digital marketing for integral growth. Now it has become brand ambassador for its messages and promotions to produce awareness among audience through continuous brand advertisement activities. The existing relations in a social network are as follows:

- Similarities depending on demographic characteristics, locations or group memberships attributes of any two nodes.
- The interaction relationships like speaking; chatting refers to continuous exchange of information between all the actors or users.

Social network analysis (SNA)[1] maps the interconnectedness between actors in a network through mathematics that aims is to understand the structural relations and to explain both why their occurrence and consequences are. To know how influential an author is, in a network (Twitter in this case), and to assign score to authors in the network based on the relevancy of posts using centrality measure.
Influencer measuring on social network by conceptual method differs each one from others. The influence is nothing but who spreads the information and influence the people. Influence in through word-of-mouth [16] marketing can be used in:

- Public influence in the flow of mass communication.
- Helping business in product development by using market shares.
- Improvement of broad awareness innovation.

Centrality: It means there is no unanimity in measuring the market and its network progress. The below Fig.1 shows the working procedure ofcentrality [11][25].

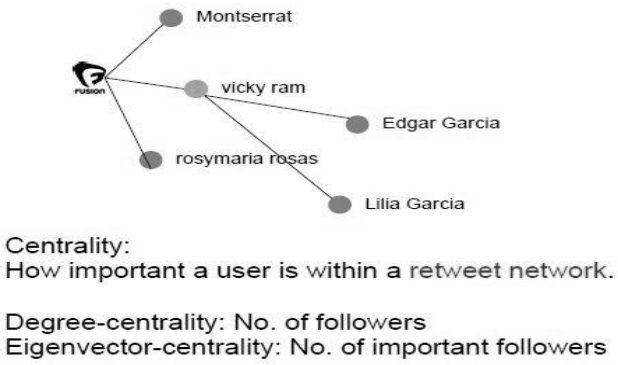

Figure 1. Centrality

The centrality explains about how to measure and quantify the "structural features" of a particular single node in a given graph, and finds an actor who plays itcentrally in the graph. The centrality score is high for a given vertex *i*, then it gives information of about hub that has more contacts and nodes. The formula can be represented in both undirected and unweighted graph [14] 'G', is given as

$$\sigma_D(i) = \sum_{j}^{N} a_{ij}$$

Here *i* is focal node value in the network,
j gives total number of other nodes in a network,
N is total number of nodes in a network,
a = adjacency matrix
if a(i,j)==1,then node *i* is connected to node *j*.
if a(i,j)==0,then node *i* is not connected to node *j*.

Mathematically, the simplest computation of closeness centrality σC can be represented as follows:

$$\sigma_C = \frac{1}{\sum_j^n d_G(i,j)}$$

where

dG(i, j) is the number of links in the geodesic distances from node i to node j.

Eigen vector centrality (EC) when compared to Direct Centrality (DC), takes into account the number of direct links and indirect contacts in the network. Eigen vector *X(i,G)* is given as follows:

$$X(i,j) = \sum_{j \in N(i)} X(i,G)$$

Any social network like Twitter, Facebook, Watsapp markets business since this sites provide real-time data for business insiders. The interconnectedness in Fig.2 shows relationships between actors to show business how important it is to find more influencers and understand their requirements.

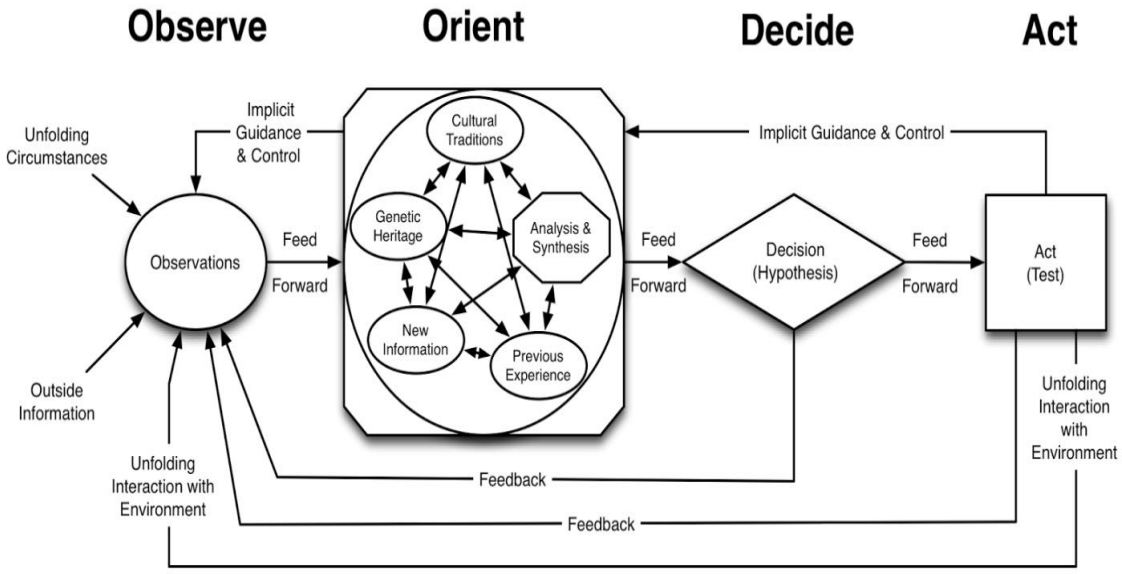

Fig .2. Centrality

From the above fig.2, we can understand the performance and evaluation of centrality depends on Observation, Orientation, Decidability and Actions.

2. Literature Survey

2.1. Twitter Data Analysis

We have observed that being a follower and account holder, user automatically receives messages posted by his/her followed accounts. In this paper we have analysed the followers and their relationships based on the total numbers of followers towards a node and its friends lie on outward degree. Comparing with other social network sites, the reciprocity is not necessary and everyone can follow any other, and no objections in it.

Twitter is viewed as pyramidal type structure because some influence accounts like movie stars, journalists, celebrities, sports personalities, will have millions of followers without any obligation. Whereas Face book is viewed as circular type structure where friends are reciprocal. In twitter '@' is used to re-tweet and '#' is used to follow.

2.2. Related Work

By using different metrics that are related to centrality measures has addressed the influencers and diffusion process considers only digraphs.

There are two types of networks that exist to determine the network link structure.

- The network is established for friendship between existing two nodes, if at least one follows the other.

- Interaction network is directed between two nodes for replying and re-tweet.

Re-tweets can be used to reinforce a message. Not surprising, mentioned users were mostly celebrities.

2.3. Over view of Social Network Analysis Technique

To identify influencers on social network sites like twitter, we have described in step wise extraction method is used to map users network.
Fig .3, shows the following steps.

a. A list of 1000 top most tweets related to fashion technology information is selected.
b. We select 80 from 100 influencing users based on the re-tweeted information, after that again we add another most influencing 80 users to gather opinion. Repeat the process until it reaches a 100 accounts after some iteration process.
c. Afterwards, the data frame is build and is translated into a CSV file.

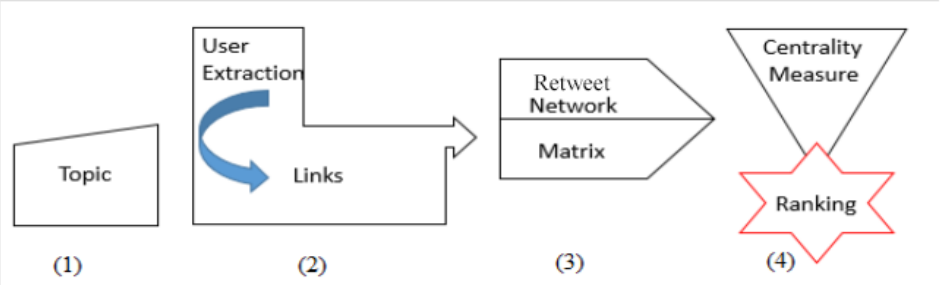

Figure 3. Data Gathering

a) Identify a list of 10 influential fashion authors
b) Extract all the users (retweeted) in the list
c) Identity the 80 most influencing users
d) Go back to 2 step to retrive information on the 80 new IDs.

Build a dataset and store as a CSV file with the obtained list.

3. Architectural Design for Social Network Analysis

3.1. Architectural Design

Architecture diagram(Fig 5) explains how data is importing directly to phython data frame using twitter streaming API to system database. Mining of data is done by phython regular expression for analysing the results and storing in a phython data frame. This architecture shows the proceeding of data in stepwise manner. Finally result is stored in CSV (comma seperated variable) file format.

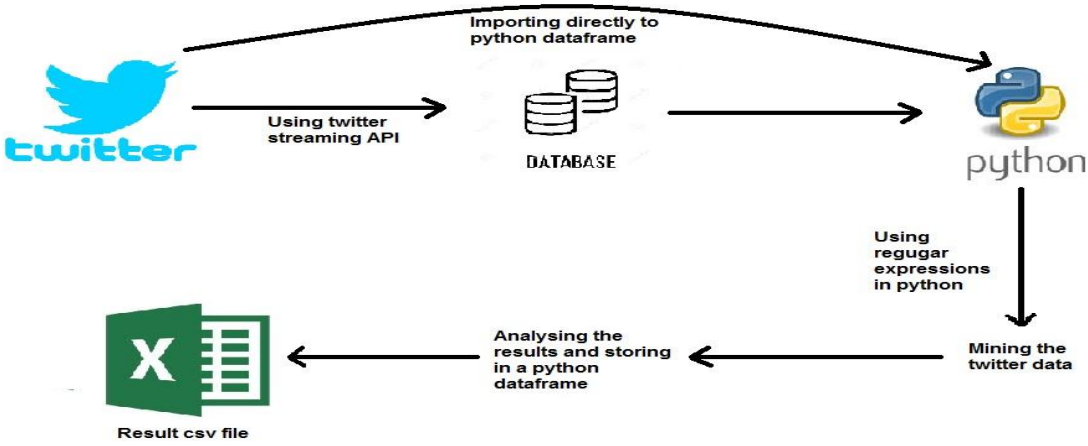

Figure 4. Architectual Design

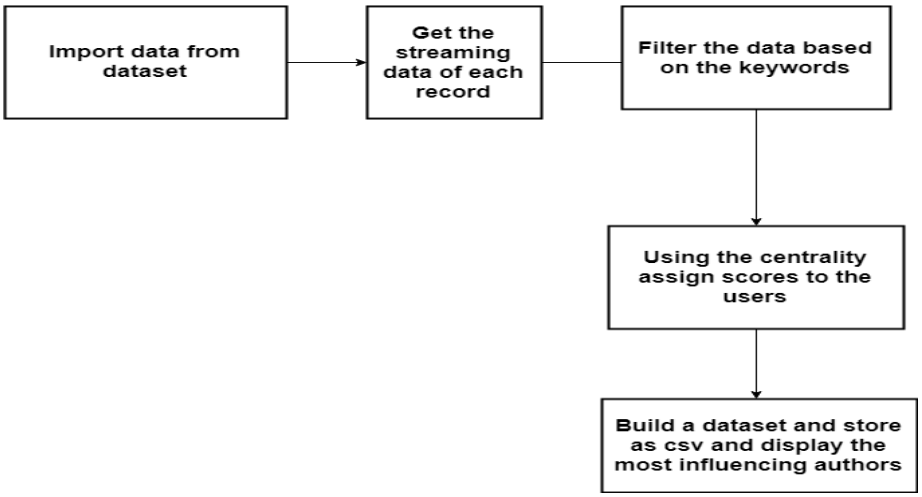

Figure 5. Data Processing

Fig.4 and Fig.5, gives the information of analysis of social data and its data processing steps for analysis.The dataset we used have a good number of features but we mostly focused on tweet_id and tweet_text (fig 6).

t_id	t_retweet	t_text
6.15E+17	1204	People tweet #FreeBree in support of the black woman who removed S
6.19E+17	1010	We made a Chrome extension to add actual Donald Trump quotes to ev
6.18E+17	444	What's this dude's name?
6.23E+17	340	A 6-year-old totally owned the Financial Times over a Minecraft error h
6.20E+17	298	Inside the moaning, dripping world of Minion porn http://t.co/dYSfCSh
6.16E+17	226	WATCH: How black women experience police violence.
6.14E+17	214	More Americans have been killed by white supremacists than Muslim e
6.18E+17	178	It seems Sepp Blatter found a way to watch #FIFAWWC final while still a
6.13E+17	121	WATCH: Science says helping others makes humans happiest.
6.15E+17	120	Haiti just won a hockey world championship http://t.co/PwC4FmOoaF M
6.16E+17	118	There are now more Spanish speakers in the U.S. than in Spain http://t.
6.18E+17	114	Nice to see U.S. elected officials have made the trek up to Canada, but J
6.21E+17	113	Former Mexican official says leaked intel may have caused #ElChapo's
6.14E+17	109	Trans woman interrupts Obama at White House LGBT reception http://t

Figure 6. Input Data set

3.2. Implementation

To reduce the interaction interfacing we use API call load data to retrieve all the tweet IDs of the given list of 100 tweets based on the fashion industry, and stored them in a variable called t (dataframe). Hence we used the function *retweet_users_of_a_tweet()* with tweet_id as argument. We stored this result in a list and passed it to *t_user_rank()*. The *t_user_rank()* function will return a dictionary of user objects.

```
def retweet_users_of_a_tweet(tweet_id):
    retweets = api.retweets(tweet_id, 100)
    return [rt.user.id for rt in retweets]
```

```
udic = t_user_rank(retweet_users_of_a_tweet(t.t_id[i])) #
follower = [udic.values()[x][0] for x in range(len(udic))]
mention = [udic.values()[x][1] for x in range(len(udic))]
score = [udic.values()[x][2] for x in range(len(udic))]
keys = udic.keys()
t_id = [t.t_id[i] for x in range(len(udic))]
```

The function *t_all_tweets()* returns all the tweets posted by the user. It takes two arguments : userid and number of pages. The returned object is passed to *t_mentions()* which will parse the tweets and finds the mention of the user(mention is count of the keywords we are interested in) and returns an integer value. The method *t_user_rank()* assigns rank to each user in the list created and frames a dictionary object.

```
for user in users:
    screen_name = api.get_user(id=user).screen_name
    follower = api.get_user(id=user).followers_count
    mention = t_mentions(user)
    udic[screen_name] = [follower, mention, (follower*mention)]
```

```
def t_mentions(user):
    tweets = t_all_tweets(user, 2) # first 2 pag
    t_text = ''
    for t in tweets:
        t_text += t.text
    return len(re.findall('(@Fasion)', t_text))
```

Implementation process has following steps

a) Set the code to twitter limitations of available GET requests.
b) Rate the every limit to 15 mints of time.
c) To avoid error messages and solve this problem, divide list 'i' in 2 and by using time-sleep( ) function with 60 as argument for 90 seconds.
d) For estimated system block after 5 GET requests, apply rule as for each 'i' if the 'i mod 5' is equal to zero, then use time-sleep( ) function.
e) The result set is obtained from each iteration concatenation of list 1 to n.

Construct the dataset:

After the result set is obtained the result is displayed one the screen and the same is copied and stored as a csv file for sharing.

Provide sufficient detail to allow the work to be reproduced. Methods already published should be indicated by a reference: only relevant modifications should be described.

4. Results Analysis

The Spyder IDE: The program is written in python 2.7 in spyder Ide.

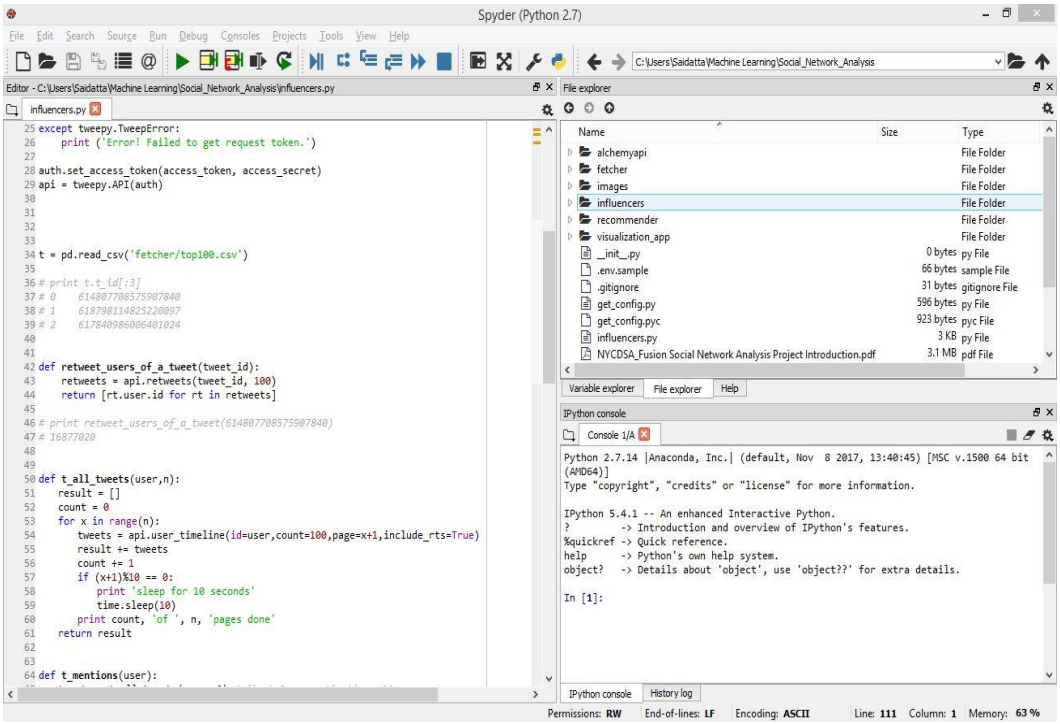

Figure 7. Spyder IDE

IPython Console: Each page analysed is requested by the program from Twiter API. The current image shows the execution of a tweet.

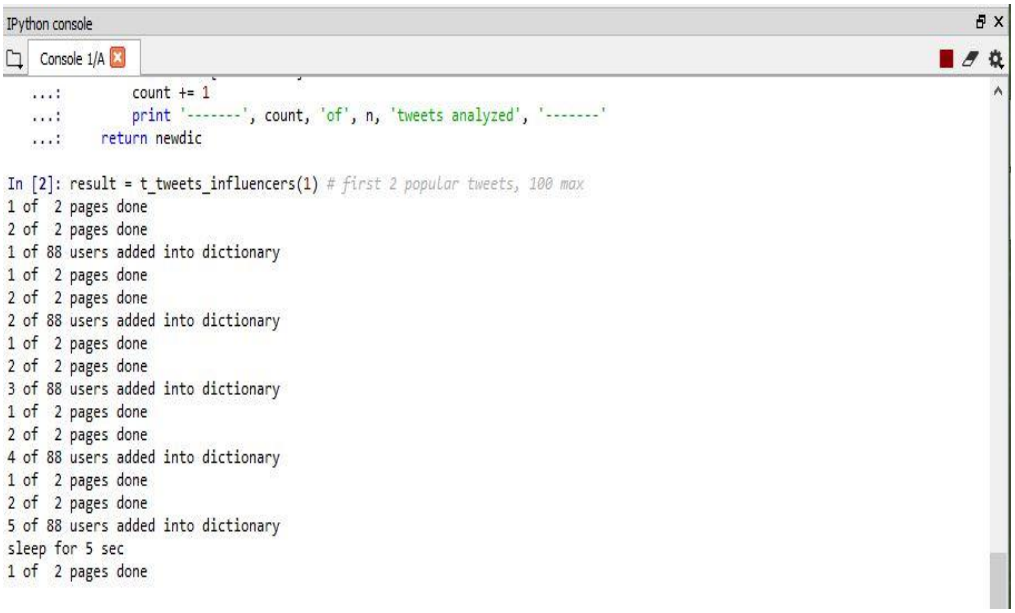

Figure 8. IPython Console

Execution in Progress: The execution is under process and the list of influencers is being added to dictionary.

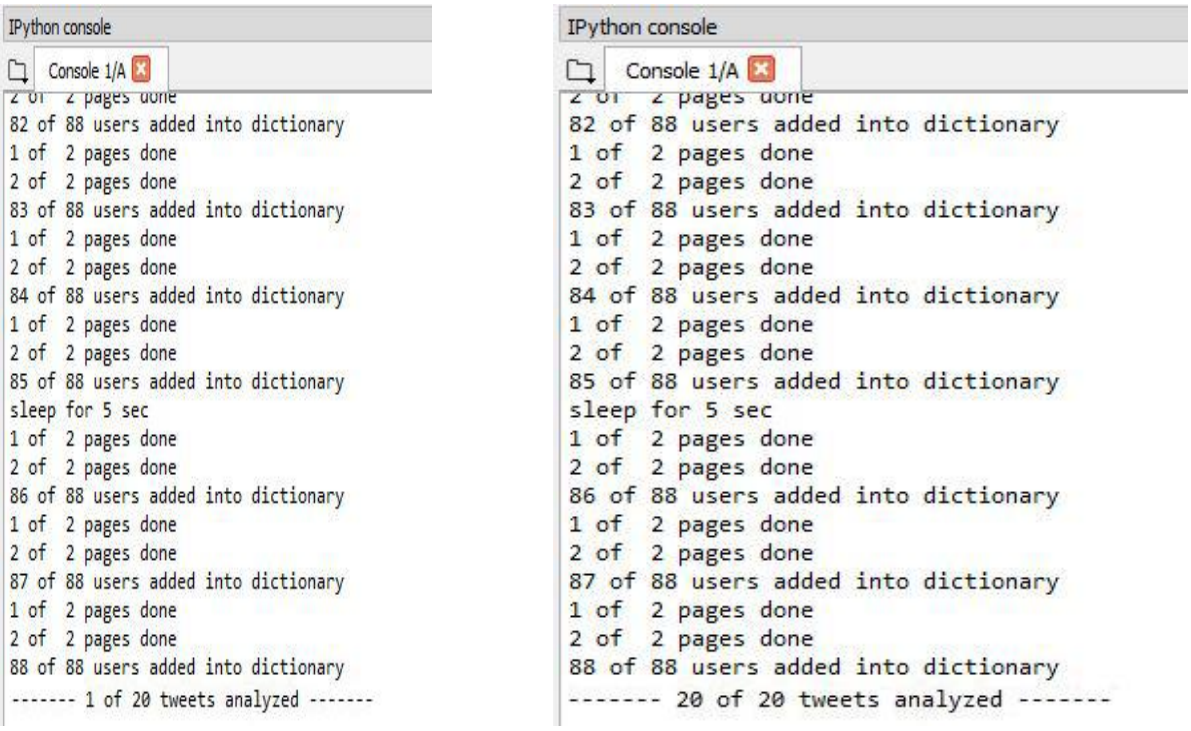

Figure 9. Execution and Tweets analyzation

Execution Completion: All the users are assigned scores and dataframe object is created.

Input dataset: This is the input feed to the program.

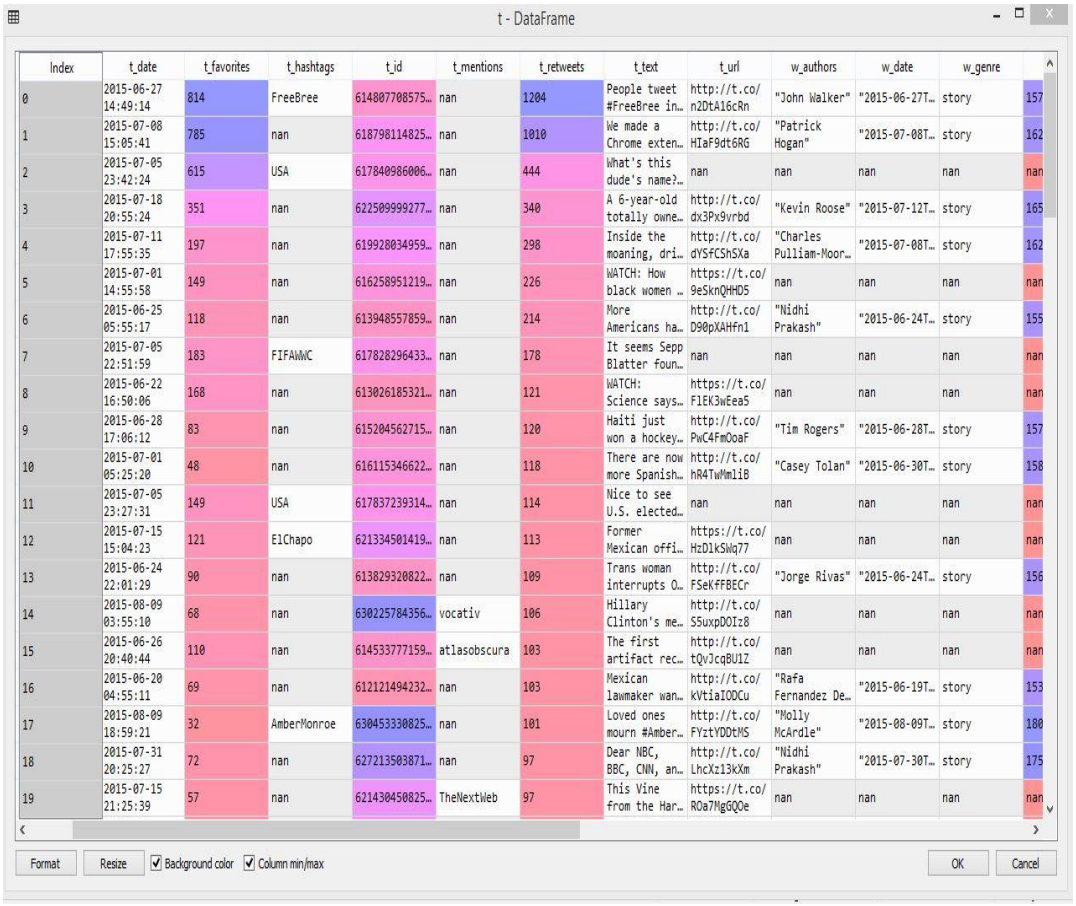

t - DataFrame

Index	t_date	t_favorites	t_hashtags	t_id	t_mentions	t_retweets	t_text	t_url	w_authors	w_date	w_genre	
0	2015-06-27 14:49:14	814	FreeBree	614807708575…	nan	1204	People tweet #FreeBree in…	http://t.co/ n2DtAl6cRn	"John Walker"	"2015-06-27T…	story	157
1	2015-07-08 15:05:41	785	nan	618798114825…	nan	1010	We made a Chrome exten…	http://t.co/ HIaF9dt6RG	"Patrick Hogan"	"2015-07-08T…	story	162
2	2015-07-05 23:42:24	615	USA	617840986006…	nan	444	What's this dude's name?…	nan	nan	nan	nan	nan
3	2015-07-18 20:55:24	351	nan	622509999277…	nan	340	A 6-year-old totally owne…	http://t.co/ dx3Px9vrbd	"Kevin Roose"	"2015-07-12T…	story	165
4	2015-07-11 17:55:35	197	nan	619928034959…	nan	298	Inside the moaning, dri…	http://t.co/ dYSfCShSXa	"Charles Pulliam-Moor…	"2015-07-08T…	story	162
5	2015-07-01 14:55:58	149	nan	616258951219…	nan	226	WATCH: How black women …	https://t.co/ 9eSknQHHD5	nan	nan	nan	nan
6	2015-06-25 05:55:17	118	nan	613948557859…	nan	214	More Americans ha…	http://t.co/ D90pXAHfn1	"Nidhi Prakash"	"2015-06-24T…	story	155
7	2015-07-05 22:51:59	183	FIFAWWC	617828296433…	nan	178	It seems Sepp Blatter foun…	nan	nan	nan	nan	nan
8	2015-06-22 16:50:06	168	nan	613026185321…	nan	121	WATCH: Science says…	https://t.co/ F1EK3wEea5	nan	nan	nan	nan
9	2015-06-28 17:06:12	83	nan	615204562715…	nan	120	Haiti just won a hockey…	http://t.co/ PwC4FmOoaF	"Tim Rogers"	"2015-06-28T…	story	157
10	2015-07-01 05:25:20	48	nan	616115346622…	nan	118	There are now more Spanish…	http://t.co/ hR4TwMm1iB	"Casey Tolan"	"2015-06-30T…	story	158
11	2015-07-05 23:27:31	149	USA	617837239314…	nan	114	Nice to see U.S. elected…	nan	nan	nan	nan	nan
12	2015-07-15 15:04:23	121	ElChapo	621334501419…	nan	113	Former Mexican offi…	https://t.co/ HzDlkSWq77	nan	nan	nan	nan
13	2015-06-24 22:01:29	90	nan	613829320822…	nan	109	Trans woman interrupts O…	http://t.co/ FSeKfFBECr	"Jorge Rivas"	"2015-06-24T…	story	156
14	2015-08-09 03:55:10	68	nan	630225784356…	vocativ	106	Hillary Clinton's me…	http://t.co/ S5uxpDOIz8	nan	nan	nan	nan
15	2015-06-26 20:40:44	110	nan	614533777159…	atlasobscura	103	The first artifact rec…	http://t.co/ tQvJcqBU1Z	nan	nan	nan	nan
16	2015-06-20 04:55:11	69	nan	612121494232…	nan	103	Mexican lawmaker wan…	http://t.co/ kVtiaIODCu	"Rafa Fernandez De…	"2015-06-19T…	story	153
17	2015-08-09 18:59:21	32	AmberMonroe	630453330825…	nan	101	Loved ones mourn #Amber…	http://t.co/ FYztYDDtMS	"Molly McArdle"	"2015-08-09T…	story	188
18	2015-07-31 20:25:27	72	nan	627213503871…	nan	97	Dear NBC, BBC, CNN, an…	http://t.co/ LhcXz13kXm	"Nidhi Prakash"	"2015-07-30T…	story	175
19	2015-07-15 21:25:39	57	nan	621430450825…	TheNextWeb	97	This Vine from the Har…	https://t.co/ ROa7MgGQOe	nan	nan	nan	nan

Format Resize Background color Column min/max OK Cancel

Figure. 10. Input Dataset

Result Object: This is the result object with all the scores assigned to users.

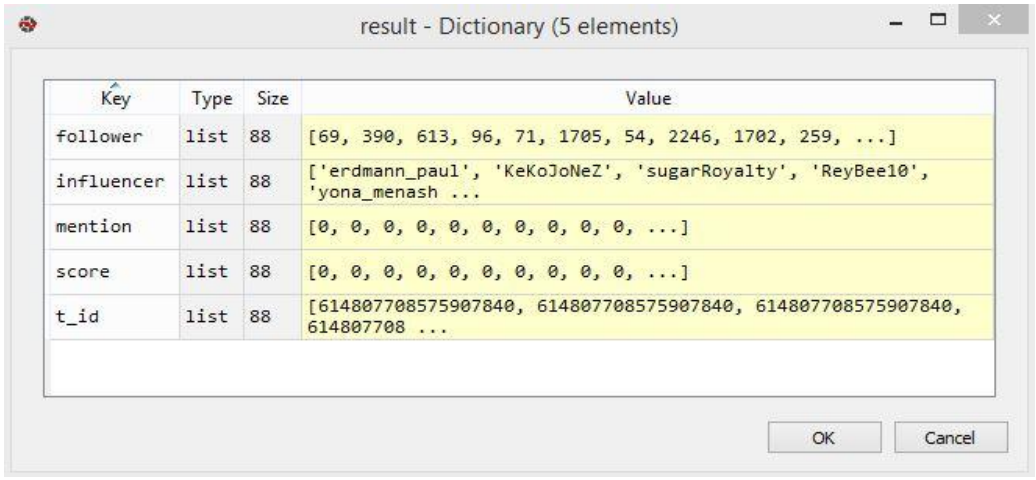

result - Dictionary (5 elements)

Key	Type	Size	Value
follower	list	88	[69, 390, 613, 96, 71, 1705, 54, 2246, 1702, 259, ...]
influencer	list	88	['erdmann_paul', 'KeKoJoNeZ', 'sugarRoyalty', 'ReyBee10', 'yona_menash ...
mention	list	88	[0, 0, 0, 0, 0, 0, 0, 0, 0, 0, ...]
score	list	88	[0, 0, 0, 0, 0, 0, 0, 0, 0, 0, ...]
t_id	list	88	[614807708575907840, 614807708575907840, 614807708575907840, 614807708 ...

OK Cancel

Figure .11. Result Object

Result DataFrame: The above object is converted to dataframe object for further process.

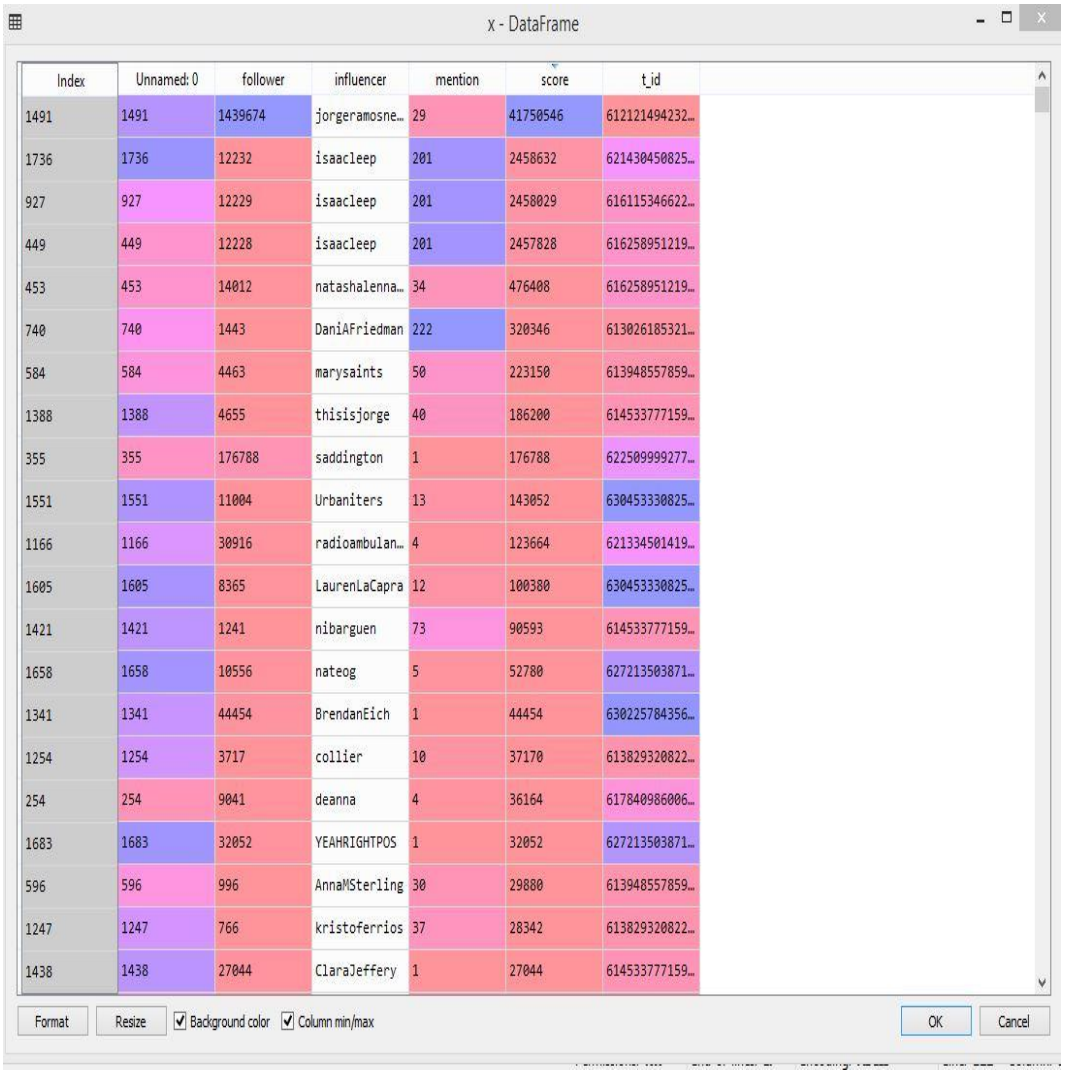

Index	Unnamed: 0	follower	influencer	mention	score	t_id
1491	1491	1439674	jorgeramosne…	29	41750546	612121494232…
1736	1736	12232	isaacleep	201	2458632	621430450825…
927	927	12229	isaacleep	201	2458029	616115346622…
449	449	12228	isaacleep	201	2457828	616258951219…
453	453	14012	natashalenna…	34	476408	616258951219…
740	740	1443	DaniAFriedman	222	320346	613026185321…
584	584	4463	marysaints	50	223150	613948557859…
1388	1388	4655	thisisjorge	40	186200	614533777159…
355	355	176788	saddington	1	176788	622509999277…
1551	1551	11004	Urbaniters	13	143052	630453330825…
1166	1166	30916	radioambulan…	4	123664	621334501419…
1605	1605	8365	LaurenLaCapra	12	100380	630453330825…
1421	1421	1241	nibarguen	73	90593	614533777159…
1658	1658	10556	nateog	5	52780	627213503871…
1341	1341	44454	BrendanEich	1	44454	630225784356…
1254	1254	3717	collier	10	37170	613829320822…
254	254	9041	deanna	4	36164	617840986006…
1683	1683	32052	YEAHRIGHTPOS	1	32052	627213503871…
596	596	996	AnnaMSterling	30	29880	613948557859…
1247	1247	766	kristoferrios	37	28342	613829320822…
1438	1438	27044	ClaraJeffery	1	27044	614533777159…

Figure.12. Result DataFrame

Output File: This is the result file.

follower	influencer	mention	score	t_id
1439674	jorgeramosnews	29	41750546	6.12121E+17
12232	isaacleep	201	2458632	6.2143E+17
12229	isaacleep	201	2458029	6.16115E+17
12228	isaacleep	201	2457828	6.16259E+17
14012	natashalennard	34	476408	6.16259E+17
1443	DaniAFriedman	222	320346	6.13026E+17
4463	marysaints	50	223150	6.13949E+17
4655	thisisjorge	40	186200	6.14534E+17
176788	saddington	1	176788	6.2251E+17
11004	Urbaniters	13	143052	6.30453E+17
30916	radioambulante	4	123664	6.21335E+17
8365	LaurenLaCapra	12	100380	6.30453E+17
1241	nibarguen	73	90593	6.14534E+17
10556	nateog	5	52780	6.27214E+17
44454	BrendanEich	1	44454	6.30226E+17
3717	collier	10	37170	6.13829E+17

Figure .13. Output File

Based on the information given on the Twitter and other socila networking sites uses the "fashion", "beauty", "wear" and "style" like magazines, brands, fashion designers on e-commerce websites, we have come to know and understand that about 90% of the accounts are attracted and influenced in fashion technology. Reciprocity is observed by linking their acounts mutually and surprisingly find a high value parameter as accounts having common friends.

The user with more score is considered as a better influencer in the network about a particular topic or field (Fig 15).

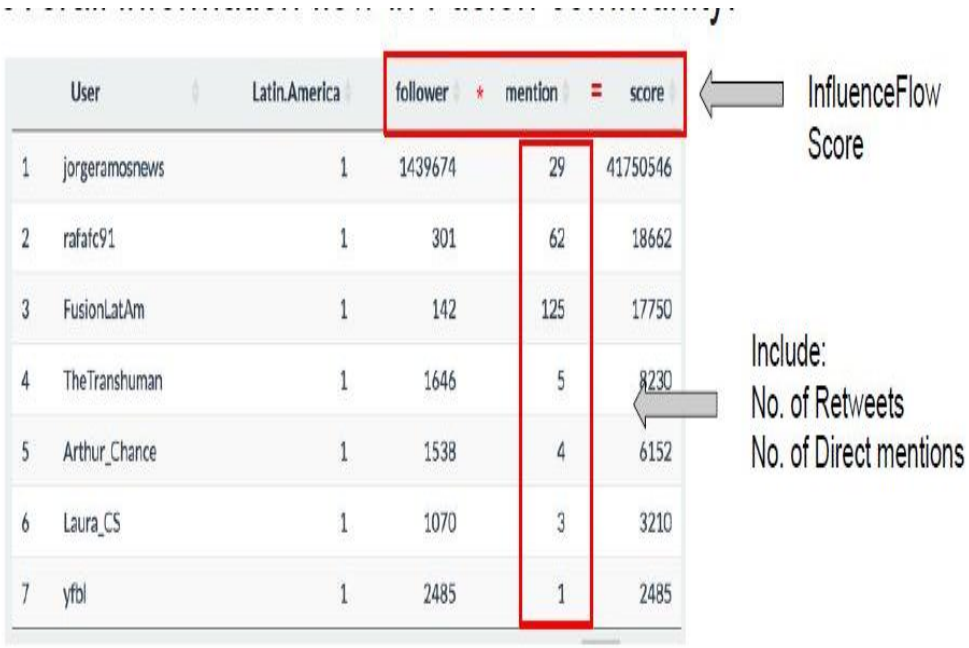

Fig 14. Result Analysis

We have used Phython programming language for mapreducing and generating results. NumPy fundamental Package is used for generating multidimensional generic data. Pandas is used as datastructure tool. Tweepy is used as Twitter authentication method. JSON is used as script language for data-interchange format.

5. Conclusion

We have created homophily samples to validate our extraction method to apply centrality on given data set. During this process we have found identification of actors who are coordinated with the network has become tough problem. So interaction here needs to be more adaptive. Hence extraction method allows to rank centrality measures of influencers. In this paper we have taken only Twitter data for analysis and this concept can be extended by comparing all other social networks that influence the net browsing users. In our future research we will be producing comparative results as extension of this concept.

References

[1] G " Python for Informatics: Exploring Information" – Book by Charles Severance
[2] "Practical Data Science Cookbook" – Book by Abhijit Dasgupta, Benjamin Bengfort, Sean Patrick Murphy, and Tony Ojeda.
[3] Stanford WebBase Project. http://www-diglib. stanford.edu/~testbed/doc2/WebBase.
[4] L. A. Adamic. The Small World Web. In Proceedings of the Third European Conference on Research and Advanced Technology for Digital Libraries (ECDL'99), Paris, France, Sep 1999.
[5] L. A. Adamic, O. Buyukkokten, and E. Adar. A social network caught in the Web. First Monday, 8(6), 2003.
[6] Y.-Y. Ahn, S. Han, H. Kwak, S. Moon, and H. Jeong. Analysis of Topological Characteristics of Huge Online Social Networking Services. In Proceedings of the 16th international conference on World Wide Web (WWW'07), Banff, Canada, May 2007.
[7] R. Albert, H. Jeong, and A.-L. B´arab´asi. The Diameter of the World Wide Web. Nature, 401:130, 1999.
[8] L. A. N. Amaral, A. Scala, M. Barth´el´emy, and H. E. Stanley. Classes of small-world networks. Proceedings of the National Academy of Sciences (PNAS), 97:11149–11152, 2000.
[9] A. Awan, R. A. Ferreira, S. Jagannathan, and A. Grama. Distributed uniform sampling in real-world networks. Technical Report CSD-TR-04-029, Purdue University, 2004.
[10] L. Backstrom, D. Huttenlocher, J. Kleinberg, and X. Lan. Group Formation in Large Social Networks: Membership, Growth, and Evolution. In Proceedings of the 12th ACM SIGKDD International Conference on Knowledge Discovery and Data Mining (KDD'06), Philadelphia, PA, Aug 2006.
[11] A.-L. B´arab´asi and R. Albert. Emergence of Scaling in Random Networks. Science, 286:509–512, 1999.
[12] L. Becchetti, C. Castillo, D. Donato, and A. Fazzone. A Comparison of Sampling Techniques for Web Graph Characterization. In Proceedings of the Workshop on Link Analysis (LinkKDD'06), Philadelphia, PA, Aug 2006.
[13] V. Braitenberg and A. Schuz. ¨ Anatomy of a Cortex: Statistics and Geometry. Springer-Verlag, Berlin, 1991.
[14] A. Broder, R. Kumar, F. Maghoul, P. Raghavan, S. Rajagopalan, R. Stata, A. Tomkins, and J. Wiener. Graph Structure in the Web: Experiments and Models. In Proceedings of the 9th International World Wide Web Conference (WWW'00), Amsterdam, May 2000.
[15] A. Clauset, C. R. Shalizi, and M. E. J. Newman. Power-law distributions in empirical data, Jun 2007. http://arxiv.org/abs/0706.1062v1.
[16] d. boyd. Friends, Friendsters, and Top 8: Writing community into being on social network sites. First Monday, 11(12), 2006.
[17] P. Erd¨os and A. R´enyi. On Random Graphs I. Publicationes Mathematicae Debrecen, 5:290–297, 1959.
[18] M. Faloutsos, P. Faloutsos, and C. Faloutsos. On Power-Law Relationships of the Internet Topology. In Proceedings of the Annual Conference of the ACM Special Interest Group on Data Communication (SIGCOMM'99), Cambridge, MA, Aug 1999.
[19] S. Garriss, M. Kaminsky, M. J. Freedman, B. Karp, D. Mazi`eres, and H. Yu. Re: Reliable Email. In Proceedings of the 3rd Symposium on Networked Systems Design and Implementation (NSDI'06), San Jose, CA, May 2006.
[20] M. Girvan and M. E. J. Newman. Community structure in social and biological networks. Proceedings of the National Academy of Sciences (PNAS), 99:7821–7826, 2002.
[21] Google Co-op. http://www.google.com/coop/. [20] M. Granovetter. The Strength of Weak Ties.

American Journal of Sociology, 78(6), 1973.

[22] J. Kleinberg. Authoritative Sources in a Hyperlinked Environment. Journal of the ACM, 46:604–632, 1999.

[23] J. Kleinberg. Navigation in a Small World. Nature, 406:845–845, 2000.

[24] J. Kleinberg. The Small-World Phenomenon: An Algorithmic Perspective. In Proceedings of the 32nd ACM Symposium on Theory of Computing (STOC'00), Portland, OR, May 2000.

[25] J. Kleinberg and S. Lawrence. The Structure of the Web. Science, 294:1849–1850, 2001.

[26] J. M. Kleinberg and R. Rubinfeld. Short paths in expander graphs. In IEEE Symposium on Foundations of Computer Science (FOCS'96), Burlington, VT, Oct 1996.

[27] R. Kumar, J. Novak, and A. Tomkins. Structure and Evolution of Online Social Networks. In Proceedings of the 12th ACM SIGKDD International Conference on Knowledge Discovery and Data Mining (KDD'06), Philadelphia, PA, Aug 2006.

[28] R. Kumar, P. Raghavan, S. Rajagopalan, and A. Tomkins. Trawling the Web for Emerging Cyber-Communities. Computer Networks, 31:1481–1493, 1999.

[29] S. Lee, R. Sherwood, and B. Bhattacharjee. Cooperative peer groups in NICE. In Proceedings of the Conference on Computer Communications (INFOCOM'03), San Francisco, CA, Mar 2003.

[30] S. H. Lee, P.-J. Kim, and H. Jeong. Statistical properties of sampled networks. Physical Review E, 73, 2006.

[31] L. Li and D. Alderson. Diversity of graphs with highly variable connectivity. Physics Review E, 75, 2007.

[32] L. Li, D. Alderson, J. C. Doyle, and W. Willinger. Towards a Theory of Scale-Free Graphs: Definitions, Properties, and Implications. Internet Mathematics, 2(4):431–523, 2006.

[33] D. Liben-Nowell, J. Novak, R. Kumar, P. Raghavan, and A. Tomkins. Geographic Routing in Social Networks. Proceedings of the National Academy of Sciences (PNAS), 102(33):11623–11628, 2005.

[34] P. Mahadevan, D. Krioukov, K. Fall, and A. Vahdat. Systematic Topology Analysis and Generation Using Degree Correlations. In Proceedings of the Annual Conference of the ACM Special Interest Group on Data Communication (SIGCOMM'06), Pisa, Italy, August 2006.

[35] S. Milgram. The small world problem. Psychology Today, 2(60), 1967.

[36] A. Mislove, K. P. Gummadi, and P. Druschel. Exploiting social networks for Internet search. In Proceedings of the 5th Workshop on Hot Topics in Networks (HotNets-V), Irvine, CA, Nov 2006.

[37] M. Molloy and B. Reed. A critical point for random graphs with a given degree distribution. Random Structures and Algorithms, 6, 1995.

[38] M. Molloy and B. Reed. The size of the giant component of a random graph with a given degree sequence. Combinatorics, Probability and Computing, 7, 1998.

[39] R. Morselli, B. Bhattacharjee, J. Katz, and M. A. Marsh. Keychains: A Decentralized Public-Key Infrastructure. Technical Report CS-TR-4788, University of Maryland, 2006.

[40] MozillaCoop. http://www.mozilla.com.

[41] MySpace is the number one website in the U.S. according to Hitwise. HitWise Press Release, July, 11, 2006. http://www.hitwise.com/press-center/ hitwiseHS2004/social-networking-june-2006.php.

[42] M. E. J. Newman. The structure of scientific collaboration networks. Proceedings of the National Academy of Sciences (PNAS), 98:409–415, 2001. [42] M. E. J. Newman. Mixing patterns in networks. Physics Review E, 67, 2003.

BIBLIOGRAPHY OF AUTHORS

SRIKANTH BETHU has completed M.Tech in Computer Science and Engineering in 2011 at Osmania University, Hyderabad, India. He was currently working as Assistant Professor in Department of Computer Science and Engineering at Gokaraju Rangaraju Institute of Engineering and Technology, Hyderabad. He was very fond of Data Mining concepts. He has published several research papers in the areas of Data Mining, Data Engineering and Big Data. Attended and Presented several research papers in various National and International conferences.

V. SOWMYA is working as Associate Professor in Department of Computer Science and Engineering, GRIET, Hyderabad. She completed M.Tech(Software Engineering) from Aurora College of Engineering, Bhongiri. Her area of research interest includes: Text Mining, Machine Learning, Data Science and Natural Language Processing. She has 11 years of teaching experience.She has published papers in international conferences and journals.

Dr. B. SANKARABABU was a doctorate from Aacharya Nagarjuna University, Guntur, Andhrapradesh, India, and completed PhD in 2016. Currently working as a Professor in Department of Computer Science and Engineering at Gokaraju Rangaraju Institute of Engineering and Technology, Hyderabad .He has done his research on Data Mining. He has published several research papers on Data mining concepts.

G.Charles Babu , Presently working as a Professor in Dept. of CSE in Malla Reddy Engineering College(Autonomous), Secunderabad, Telangana Since 5 Years and Total Teaching experience of 20 Years. Completed B.Tech (CSE) in 1997 from KLCE, M.Tech(SE) in 1999 from JNTUH and Ph.D(Data Mining) from ANU. Published more than 50 Research Papers in Data Mining, Cloud Computing, Image Processing.

Dr. Y. Jeevan Nagendra Kumar, obtained his Ph.Din Computer Science and Engineering from Acharya Nagarjuna University, Guntur, AP in 2017 and M.Tech Computer Science Technology from Andhra University in 2005. He is working as Professor and Dean - Technology and Innovation Cell in GRIET since 2005. He has about 9 Research Papers in International / National Conferences and Journals and also attended many FDP Programs to enhance his knowledge. With his technical knowledge he guided the students in developing the useful Web applications and data mining related products.

Periodicals of Engineering and Natural Sciences ISSN 2303-4521
Vol.6, No.1, June 2018, pp. 229~240
Available online at: http://pen.ius.edu.ba

Medical Disease Prediction using Grey Wolf optimization and Auto Encoder based Recurrent Neural Network

B Sankara Babu[1], A Suneetha[2], G Charles Babu[3], Y.Jeevan Nagendra Kumar[4], G Karuna[5]
[1,5]Departement of Computer Science and Engineering, GRIET, JNTU Hyderabad, Telangana, India
[2] Departement of Computer Science and Engineering, KKR & KSRITS, JNTUK, AP, India
[3] Departement of Computer Science and Engineering, Mallareddy Engineering College, JNTU Hyderabad, Telangana, India
[4]Departement of Information Technology, GRIET, JNTU Hyderabad, Telangana, India
bsankarababu81@gmail.com

Article Info

Article history:

Received Dec 12th, 2017
Revised Mar 20th, 2018
Accepted May 26th, 2018

Keyword:

Auto Encoder
Grey Wolf Optimization
Neural Network
Recurrent Neural Network

ABSTRACT

Big data development in biomedical and medical service networks provides a research on medical data benefits, early ailment detection, patient care and network administrations.e-Health applications are particularly important for the patients who are unfit to see a specialist or any health expert. The objective is to encourage clinicians and families to predict disease using Machine Learning (ML) procedures. In addition, diverse regions show important qualities of certain provincial ailments, which may hinder the forecast of disease outbreaks. The objective of this work is to predict the different kinds of diseases using Grey Wolf optimization and auto encoder based Recurrent Neural Network (GWO+RNN). The features are selected using GWO and the diseases are predicted by using RNN method. Initially the GWO algorithm avoids the irrelevant and redundant attributes significantly, after the features are forwarded to the RNN classifier. The experimental result proved that the performance of GWO+RNN algorithm achieved better than existing method like Group Search Optimizer and Fuzzy Min-Max Neural Network (GFMMNN) approach. The GWO-RNN method used the medical UCI database based on various datasets such as Hungarian, Cleveland, PID, mammographic masses, Switzerland and performance was measured with the help of efficient metrics like accuracy, sensitivity and specificity. The proposed GWO+RNN method achieved 16.82% of improved prediction accuracy for Cleveland dataset.

Corresponding Author:

Dr. B. Sankara Babu,
Departement of Computer Science and Engineering,
GRIET, JNTU Hyderabad,
Telangana, India 500090, Taiwan, ROC.
Email: bsankarababu81@gmail.com

1. Introduction

The important aspect of e-Health is to predict the disease dynamics during an epidemic, which is useful to allocate resources and make a quick response in a public health event [1]. In such conditions, present networks are responsible for health risk and danger fluctuation with financial and statistical conditions [2]. The utilization of medical datasets has helped the analysts to predict the disease around the world. The use of detected information from medical repositories has been recognized by the World Health Organization (WHO) because it helps to find therapeutic information and prediction.The ML methods are used for prediction to identify the hidden patterns. The ML based prediction methods are classified into three groups such as supervised, unsupervised and semi-regulated learning systems [3]. Supervised machine learning

strategies are the arrangement of nominal, categorical, or persistent features (regularly a combination of every one of them) to their related result which can be present in any of those structures. The greatest achievement of machine learning over linear models is their capacity to learn relationship from training information and sum it up to testing of inconspicuous data and furthermore to defeat non-linearity and associations between features. In any case, this capacity should be deliberately figured out how to maintain a strategic distance from over-fitting. In machine learning, the design parameters cannot get any benefits from the models, these are considered as hyper parameters, for instance the quantity of concealed layers in neural systems. Hyper parameters must be improved by cross-approval or framework pursuit to make a harmony amongst variance and bias in expectation, known as the variance-bias exchange off [4], [5].

An existing ML based disease risk prediction system includes several methods suchas Logistic Regression (LR), Convolutional Neural Network (CNN),Support Vector Machine (SVM) and etc.[6], [7]. In testing process, patient's data are classified into the group of either normal or abnormal. Moreover,these plans have often accompanied with less attributes and imperfections. The information collection is regularly small, for patients and infections with particular conditions [8], the attributes are chosen through involvement. In any case, these pre-chosen quality features are not possibly fulfilling the changes in the disease and its influence factors. With the advancement of big data analytics innovation, more consideration has been paid to ailment forecast from the point of huge data investigation, different explores have been directed by choosing the attributes from an extensive number of information to enhance the risk classification accuracy [9], [10], instead of the other qualities.Better frameworks created by machine learning methods can be utilized to help doctors in diagnosing and forecasting diseases. To predict the disease dynamics, a few examinations have been directed to create techniques for their classification. Moreover, there is a huge difference between diseases in various regions, because of variations in the atmosphere and living propensities in the region. In this manner, risk classification based on big data analysis, makes a superior model by considering missing information for forecasting the disease dynamic. In this paper, an efficient medical disease prediction model named as GWO+RNNis proposed. The GWO algorithm is used for feature selection which removes the unrelated attributes and redundant attributes. It's majorly improves the performance of prediction. After feature selection, Auto Encoder (AE) based RNN method avoids the feature dimensionality problems. Also, predict the different kinds of diseases significantly using the UCI database.

The organization of the paper is as follows. Section 2 gives the description of the models analyzed by various researchers related to this study.Section 3 provides a description of the development of the proposed GWO+RNN methodology used for predicting the disease. Sections 4 present the results obtained by various experiments and the conclusions are made in Section 5.

2. Literature Review

Numerous methods have been proposed by researchers on the prediction of diseases. In this section, a brief review of some important contributions ofsome methodologies in the field of disease prediction is presented below.

Y. Chen, *et al.,* [11] introduced the Realistic Contact Networks (RCNs) to describe the disease progression in e-Health applications. The structure of such system powerfully changed during plague. Catching such sort of powerful structure was the primary importance of forecast. With the ubiquity of cell phones, it was conceivable to catch the dynamic difference in the system structure. The investigation assessed the effect of system structure on disease progression, by evaluating enormous spatiotemporal information gathered by cell phones. Depend on the consequences of this assessment, a model was intended to perceive the dynamic structure of RCNs. This paper implemented a prediction algorithm for disease elements that depends on the spatiotemporal information. The precision of disease expectations was evaluated by various experiment and the results stated that the algorithm provided better precision values. This strategy is not able to handle more number of information for forecasting the disease elements.

M. Chen, *et al.,* [12]presented an efficient disease risk forecasting system using CNN based Multimodal Disease Risk Prediction (CNN-MDRP) algorithm. The proposed method used latent factor model for avoid the medical information loss. The investigations were carried on a territorial chronic disease of cerebral localized necrosis by using this technique. Here, no existing methods worked on the both structured and unstructured medical big data analytics, but the CNN-MDRP strategy focused on the both medical big

data analysis. The experimental outcomes demonstrated that the prediction accuracy of CNN-MDRP achieved 94.8% with a convergence speed which is faster than a few normal forecast algorithms. The technique is unable to handle the advanced features, such as fractal dimension, biorthogonal wavelet transforms to predict the chronic disease.

R. Prashanth, and S. D. Roy, [13] proposed a novel and enhanced method for Parkinson's Disease (PD) utilizing the Movement Disorder Society-Unified Parkinson's Disease Rating Scale (MDS-UPDRS) features. The Adaboost Algorithm (AA) was efficiently predict the PD in standard medical UCI dataset. An experimental analysis demonstrated that AA achieved 97.46% of accuracy in disease prediction. In this literature, the proposed AA was difficult to detect the normal, early stage of PD, and propelled PD due to inaccessibility of information. Additionally had a limited number of direct stage PD tests. This is a case of extrinsic imbalance where the awkwardness is definitely not an immediate result of the information space.

M. Nilashi, *et al.,* [14] presented other information based framework for finding disease utilizing machine learning systems.The proposed Classification and Regression Trees (CART)strategy was construct the fuzzy standards for disease prediction.This method reduces the false prediction and able to perform in different medical datasets. In experimental analysis, UCI medical dataset was used for disease prediction. The prediction accuracy was determined by this strategy with the help of more techniques such as Principle Component Analysis (PCA), clustering and fuzzy rule based systems. Themethod had incomplete observations and imprecise which leads to poor performance in computation time of large data.

S. Sarkar, *et al.,* [15] applied improved machine learning algorithms to predict the outcomes of accident, such asinjury, close miss and damage related to accident data. Two prevalent machine learning algorithms SVM and Artificial NN (ANN) that have been utilized, whose parameters were improved by two intense streamlining algorithms, in particular genetic algorithm and Particle Swarm Optimization (PSO) algorithms are employed for accomplishing a high level of exactness and power. The experimental results stated that PSO-based SVM algorithm attained high exactness and robustness. Moreover, rules are separated by incorporating decision tree C5.0 algorithm with PSO-based SVM display. At last, an arrangement of nine valuable principles were extricated to recognize the underlying causes behind the damage, close miss and property harm cases. In information pre-processing task, a great deal of manual exertion was required to clean the information which is used for examination. Also, informational index utilized as a part of this examination has predetermined number of accident records.

This paper implemented a GWO-RNN method for predicting the different kinds of medical diseases and to overcome the above issues in the existing methodologies, using feature extraction and classification method.

3. Proposed Methodology

The Medical Disease Prediction System is the phenomena of analyzing medical data attributes of patient to recognize the presence of a particular disease or categorize the severity of a disease. Existing disease prediction systems have lower efficiency in processing the medical data due to the presence or processing of erroneous data samples. In this research, GWO and AE basedRNN methods are proposed for efficient medical disease prediction. Here, different kinds of disease based databases like Hungarian data,Cleveland data, Switzerland data, PID and Mammographic Masses used for disease prediction. The proposed architecture consists of several steps, those are data acquisition, preprocessing, attribute selection and classification. Figure 1 shows the proposed architecture.

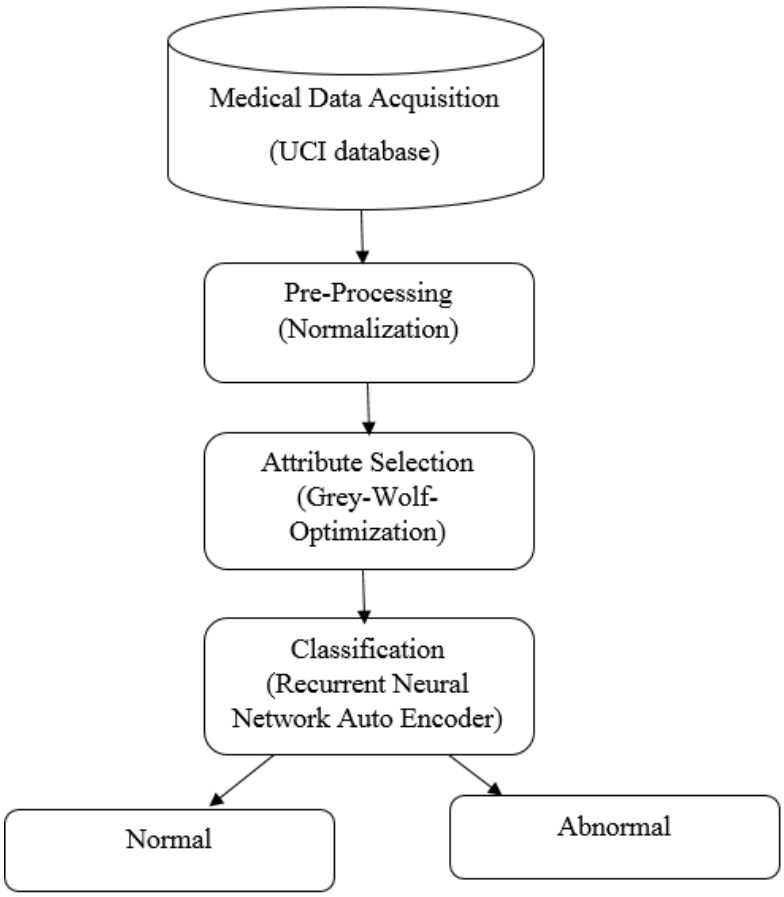

Figure 1 Proposed Architecture of medical data prediction

3.1. Medical Data Acquisition

The databases used in the experiment are different types.Those are Cleveland, Hungarian and Switzerland databases available in the UCI machine learning repository.

(i) Cleveland data

The Cleveland database contains 76 features and all data samples are listed under 14 categories. It represents the value from 0 to 4 stages of heart disease. For privacy purpose some of the patient's name and their social security number are removed from the data and replaced with the dummy values. Six of the 76 characteristics are removed due to incomplete tests performed among the values. This database consists of 56% of sample heart disease data and 46% are not belongs to heart disease.

(ii) Hungarian data

There are lots of data missing in this database and it consists of 123 data samples. It has about 14 features regarding heart disease. Among them 6.5 % of data samples indicate absence of heart disease and 93.5 % of data samples indicate presence of heart disease.

(iii) Switzerland data

This database is similar to the Cleveland database and it contains 261 heart disease data samples. Three or four data samples of the dataset are neglected due to an incompletion of data.The class distribution of this database is 62.5 % of data samples that have an absence of heart diseases data and 37.5 % of data samples have heart disease.

(iv)Pima Indians Diabetes (PID)

PID dataset stands for Pima Indians Diabetes. This database comprises of eight attributes and 768 instances, from National Institute of Diabetes, Digestive and Kidney disease. Where 0 determines negative result and 1 indicates positive result.

(v) Mammographic Masses

This database is collected from the UCI machine learning repository. Six attributes are present in this dataset. Thus, using the age and BI-RADS attributes, it detects mammographic mass lesions which could be either benign or malignant.

The input data is taken from these five databases, which consists of different kinds of diseases such as heart disease, diabetes disease, mammogram related diseases,etc. These raw data are forwarded to the preprocessing step.

3.2. Preprocessing

The preprocessing step fill the missing value, identify or remove the outliers and resolve inconsistencies of data. The raw data have some noise or errors; it is very important to mine the data in order to get better outcomes from the given data set. With a specific end goal to improve the nature of information and resultant information is pre-handled in order to enhance the proficiency and simplicity of mining procedure. In this research work, Normalization method is used for preprocessing because all the attributes are different ranges in the dataset so it's converted into [0, 1] range. In such a way all the attributes are in the uniform range of values. The range value of an attribute will be determined as in equation (1)

$$Range, r = max - min \quad (1)$$

Where, $max \rightarrow maximum\ value of attribute$

$$min \rightarrow minimum\ value of attribute$$

The normalized value of an attribute can be found with the aid of the following equation (2)

value= t- min

t ⟶ Test Sample

$$Normalized\ value, N = value/r \quad (2)$$

Where $value \rightarrow Value\ of\ the\ attribute$

$$r \rightarrow Range\ of\ the\ attribute$$

This conversion of attribute value to [0, 1] depends upon the proportion of a particular attribute covering the range of the corresponding attribute. Then the normalized values are stored in the collection instead of the original values and proceeded for further processes.

3.3. Attribute Selection using Grey Wolf Optimization Algorithm

In this section, GWO algorithm is used for the relevant attribute selection process to improve the efficiency of the medical disease prediction system. The GWO is the meta-heuristic and bio-inspired techniques from nature of grey wolves. In a grey wolf community there are four categories of grey wolves,those are alpha, beta, delta, and omega. Among them alpha is considered to be the leader of the group. Beta wolves assist alpha in decision making and hunting which are considered to the next candidate eligible to be alpha if alpha attains the stage of retirement or death while hunting. Delta wolves are elder wolves or former alpha wolves or sentinels or scout that protects the boundaries of their group. Omega wolves are the least prioritized wolves because it needs to submit all other dominant wolves and follow all other category wolves.

Assume that every wolf as searching solution in the search space. The $w_i = \langle w_{i1}, w_{i2}, \dots \dots w_n \rangle$ is represented as position vectors in search space, whereas, the dimension of the problem is shown as n. The fitness function (based on problem definition) is employed to estimate the position of the wolves. Based on the fitness value the best wolves are classified into three groups such as first solution is represented as α, second is β, and third is δ respectively. In the best solution searching process, the wolves update their position according to the position of α, β, and δ. In the starting stage, the wolves' population is generated and the position of every wolf is initialized. The co-efficient vectors of $\vec{A}$ and $\vec{C}$are described in equation (3) and (4).

$$\vec{A} = 2\vec{a}.\overrightarrow{r1} - \vec{a} \quad (3)$$

$$\vec{C} = 2\overrightarrow{r2} \quad (4)$$

The $\overrightarrow{A}$takes random values in the range of$[-a, a]$, $\vec{C}$ with a random value in the range [0, 2] and it avoids the trap of local optimal. In the traditional GWO algorithm, the vectors linearly decrease from 2 to 0 during the execution of every iteration. Once the coefficients are initialized, every wolf (search agent) fitness value is estimated. After that, best fitness solutions are selected as first, second and third such as α, β, and δ, respectively.

$$\overrightarrow{D_\alpha} = \left|\overrightarrow{C_1}.\overrightarrow{X_\alpha} - \vec{X}\right|, \overrightarrow{D_\beta} = \left|\overrightarrow{C_2}.\overrightarrow{X_\beta} - \vec{X}\right|, \overrightarrow{D_\alpha} = \left|\overrightarrow{C_3}.\overrightarrow{X_\delta} - \vec{X}\right| \quad (5)$$

$$\overrightarrow{X_1} = \overrightarrow{X_\alpha} - \overrightarrow{A_1}.\left(\overrightarrow{D_\alpha}\right), \overrightarrow{X_2} = \overrightarrow{X_\beta} - \overrightarrow{A_2}.\left(\overrightarrow{D_\beta}\right), \overrightarrow{X_3} = \overrightarrow{X_\delta} - \overrightarrow{A_3}.\left(\overrightarrow{D_\delta}\right), \quad (6)$$

$$\overrightarrow{x(t+1)} = \frac{\overrightarrow{X_1}+\overrightarrow{X_2}+\overrightarrow{X_3}}{3} \quad (7)$$

In each iteration of the algorithm, the wolves' positions are updated depends on the position of wolves α, β, and δ according to Equations (3), (4) and (5). In addition, values of vectors $\overrightarrow{A}, \vec{C}$ and $\vec{a}$ are updated. On the basis of new positions, the value of fitness function of wolves iscalculated and α, β, and δ will be selected. The GWO algorithm selects the relevant attributes for medical data prediction.

Pseudocode for GWO algorithm

1. Initialization of grey wolf population $X_i(i = 1,2, \ldots . n)$
2. Initialization of $\overrightarrow{A}, \vec{C}$ and $\vec{a}$ parameters
3. every agent or wolf fitness value
4. X_α $best\ search\ agent$
5. X_β $second\ best\ search\ agent$
6. X_δ $third\ best\ search\ agent$
7. while $t <$ max$number\ of\ iterations$
8. for each search agent
9. update the position of current search agent
10. end for
11. update a, A and C
12. calculate fitness of all search agents
13. update X_α, X_β, and X_δ
14. $t = t + 1$
15. end while
16. return X_α

Furthermore, the swarm intelligent methods are usually used to solve the optimization problem which doesn't have the leader to monitor the entire proceeding period. This limitation is resolved in GWO method; the grey wolves have individual leadership capacity. This algorithm recognizes the different related attributes such as heart disease, breast cancer, diabetes and etc. Also, employs minimum parameters for example, blood pressure, cholesterol, and etc. This algorithm selects the relevant diseases related attributes and forwarded to the RNN.

3.4. Auto Encoder and Recurrent Neural Network using medical decease prediction

The RNN classifier is used for various kinds of medical disease prediction. RNN classifier is a dynamical system that arrange the information in the input sequence and more suitable in data classification as well as prediction.An AE method is to learn an approximation of the identity function from set of unlabeled training sets. Generally, AE is helps to reduce the dimensionality of the data and it's consists of single hidden layer. In encode process the input data is indicated as $x \in R^{d_x}$ to mapping the hidden layers is shown in the equation (8),

$$y = \sigma(Wx + b) \quad (8)$$

Whereas, weight matrix is indicated as $W \in R^{d_y d_x}$, bias vector is represented as $b \in R^{d_y}$and σ is indicated as non-linear activation function in the input layer. Then the target out is represented in equation (9),

$$Z = \sigma'(W'y + b') \quad (9)$$

Whereas, weight matrix and bias vector of output layer is represented as $W' \in R^{d_z d_y}$ and $b' \in R^{d_y}$. In training process of AE, estimates the parameters $\theta = (W, W', b, b')$to reduce the sum of reconstruction cost every training set. The cost calculation is mathematically shown in the equation (10).

$$J = \sum_{x \in D_x} L(x, z) + \lambda \sum_{i,j} {W_{i,j}}^2 \quad (10)$$

Where,

$L(x, z)$ – Estimation of square error

D_x – Training samples in dataset

λ- Hyper parameter of regularization strength

The RNN method able to handle the sequence of input and output data stored in its internal states of the network. Similarly, internal states are holds the previous inputs information and act like a memory. The RNN method is mapped the sequence of fixed vectors and adopt the single fixed output vectors. The general architecture of RNN is shown in the figure.2.

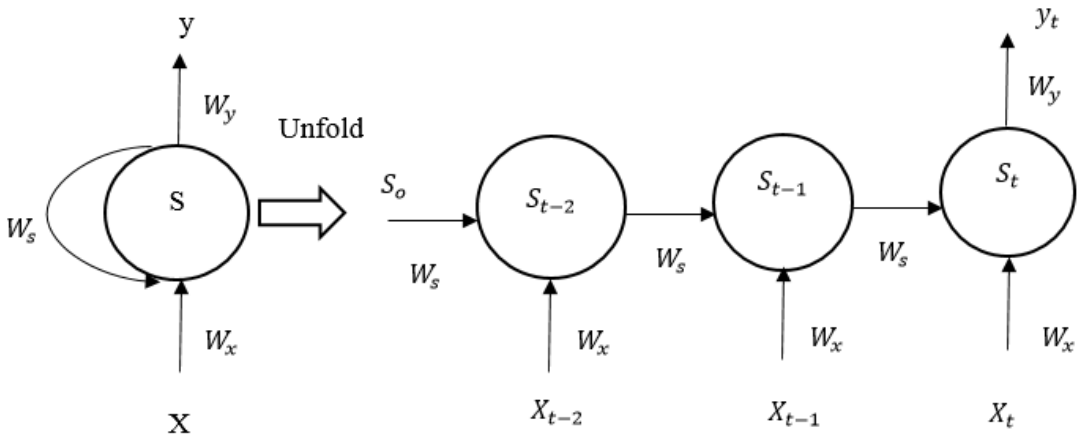

Figure 2 General Architecture of RNN

Let's assume that$x$ is the each input vector of the sequence and internal state is indicated as S which holds the previous state value. Hence,the variable S_t is indicated ashidden state and $t$is represented as time. The calculation of S_t is shown in the equation (11),

$$S_t = \sigma(W_x x_t + W_s S_{t-1}) \quad (11)$$

Whereas, weight matrices are indicated as $W_x$andW_s, input vector is denoted as x_t. The output is indicated as y_t and calculated in equation (12).

$$y_t = \sigma'(W_y S_t) \quad (12)$$

Whereas, σ' is depicted as output activation function and W_y is the weight matrix. The biases terms are omitted from the above equation (12). The AE based RNN algorithm receives relevant disease related attributes from GWO. The RNN classifier quickly predict the different kinds of diseases such as heart disease, breast cancer, diabetes and etc. This algorithm reduces the feature dimensionality problem. The performance of proposed GWO+RNN is evaluated using effective evaluation metrics and demonstrated in following sections.

4. Experimental Results and Discussion

For experimental simulation, PyCharm software was employed in the PC with 3.2 GHz with i5 processor.The proposed medical disease prediction system performance compared to the existing method namely GFMMNN [16]. The performance of the proposed methodology was evaluated by means of accuracy, sensitivity and specificity.

4.1. Performance measure

An evaluation metrics are measure the relationship between the input and output variables of a system. This section describes the different performance measure such as sensitivity, specificity and accuracy. The equation (13) and (14) represents the mathematical description of the specificity and sensitivity.

$$Specificity = \frac{TN}{TN+FP} \quad (13)$$

$$Sensitivity = \frac{TP}{TP+FN} \quad (14)$$

Accuracy parameter is estimates the correctly predicted medical disease and wrongly predicted disease. It's mathematically shown in the equation (15).

$$Accuracy = \frac{TP+TN}{TP+TN+FP+FN} \times 100 \quad (15)$$

Where, TP is represented as true positive, FP is denoted as false negative, TN is represented as true negative and FN is stated as a false negative.

4.2. Experimental Analysis using UCI dataset

In this section, UCIdatabase is employed for comparing the performance evaluation of proposed approach and the existing method GFMMNN. In table1, the performance of proposed and existing methods is validated by means of accuracy, sensitivity and specificity.The following table1 tabulatedresult of the proposed and existing method medical data classification performance with respect to five different datasets such as Hungarian, Cleveland, Switzerland, PID and Mammographic Masses.

Table.1 Performance evaluation of different datasets

Dataset	GWO+RNN		
	Accuracy	**Specificity**	**Sensitivity**
Hungarian	95.12	90.00	96.47
Cleveland	98.23	97.6	99.10
Switzerland	91.35	93.45	96.36
PID	96.21	96.78	97.45
Mammographic Masses	95.56	94.57	98.47
Dataset	**GFMMNN [16]**		
	Accuracy	**Specificity**	**Sensitivity**
Hungarian	83.33	69.81	95.2
Cleveland	85.14	85.14	85.14
Switzerland	84.01	70.75	94.68
PID	95.30	93.36	97.03
Mammographic Masses	94.21	91.58	97.48

Table 1 represents the experimental results of proposed and existing methods. According to the table the proposed GWO+RNN method classification performanceis analyzed with respect to different medical datasets and compared it with the existing GFMMNN. The classification performance of GWO+RNN method is measured using efficient parameters such as Accuracy, Specificity and sensitivity. According to the table 1, existing GFMMNN method shows maximum performance variations with respect to different dataset, but proposed GWO+RNN method approximately constant. The graphical representation of accuracy performance is shown in the Figure 3.

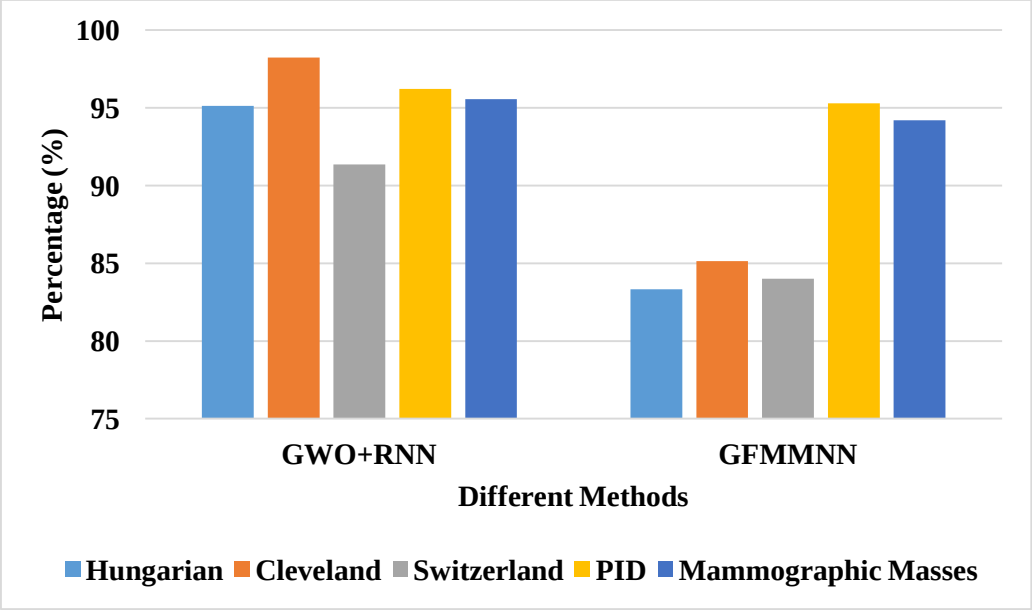

Figure 3 Performance of Accuracy

The Figure 3 shows the performance of prediction accuracy of GWO+RNN and GFMMNN approach. The GFMMNN method achieved 95.30% of accuracy in PID database. Moreover, performance of proposed GWO+RNN method achieved 95.12%, 98.23%, 91.35%, 96.21% and 95.56% of accuracy with respect to five different datasets respectively. Compared to the existing methods the proposed method showed superior results.

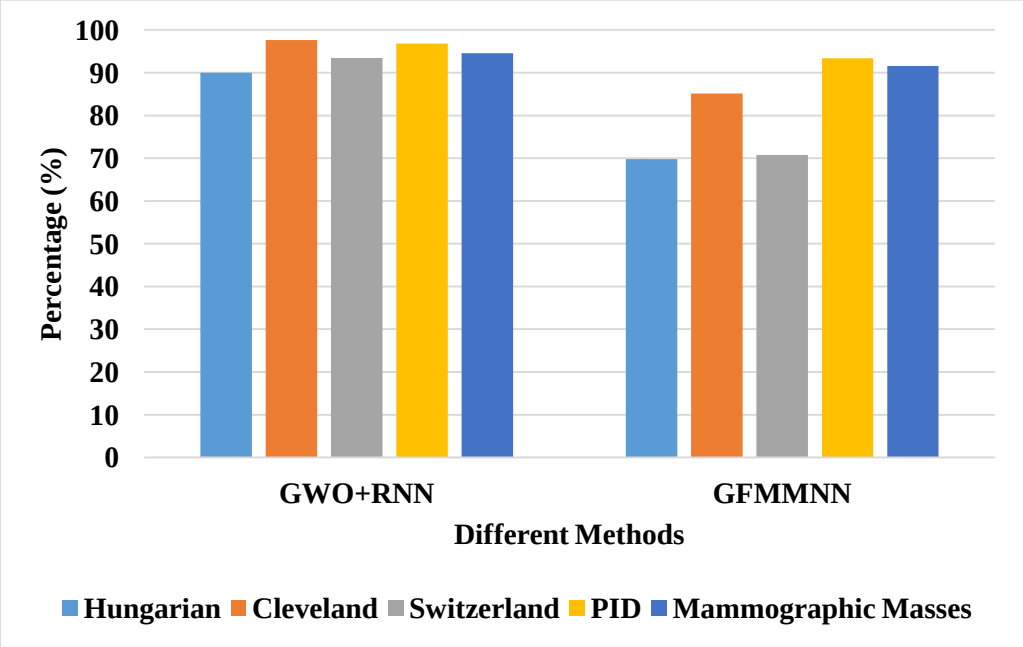

Figure 4 Performance of Specificity

The Figure 4 indicates the performance of specificity in disease prediction system. The traditional GFMMNN method achieved 69.81%, 85.14%, 70.75%, 93.36%, and 91.58% of specificity with respect to different UCI datasets. The proposed GWO+RNN classifier attained 90%, 97.6%, 93.45%, 96.78%, and 94.575 of specificity respectively.

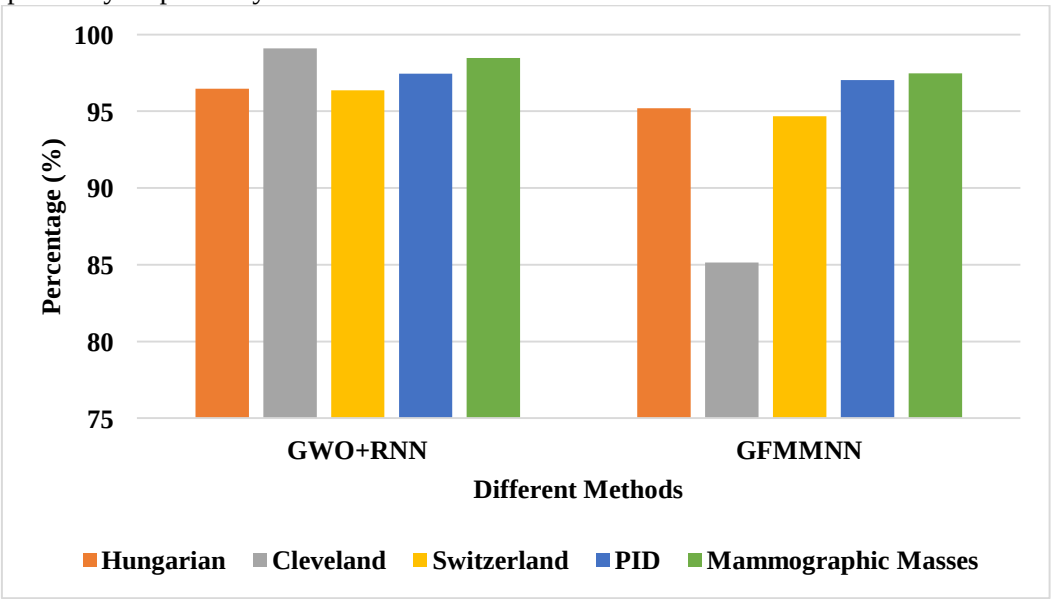

Figure 5 Performance of Sensitivity

The Figure 5 represents the sensitivity performance of medical disease prediction using proposed GWO+RNN method. The traditional GFMMNN method showed better results in Mammographic masses dataset because it achieved 97.48% of sensitivity. The GWO+RNN method attained 96.47%, 99.10%, 96.36%, 97.45%, and 98.47% of sensitivity.

An existing GFMMNN method uses irrelevant and redundant data because it randomly takes the features for classification which degrades the disease prediction accuracy. In order to rectify these problem, an efficient attribute selection method is used namely GWO and AE based RNN classifier that decreases the dimensionality of the features and predict the disease efficiently.

4.3. Comparitive Study

In this section, the table 2 represents the comparative study of existing and the proposed method of medical disease prediction. N. G. Hedeshi, and M. S. Abadeh [17] presented Fuzzy and PSO (Fuzzy+PSO) method for detecting the presence and absence of coronary artery disease in a patient. This algorithm performed faster if suitable values and parameters are set. The major limitation of PSO algorithm is maximum computation time because each time it executes the entire fuzzy rules. M. C. Tu, *et al.* [18] presented Bagging algorithm to identify the warning sign of heart disease. The bagging algorithm combines a series of learned models to generate an improved model. In this paper, the performance of Bagging algorithm was compared with the Decision Tree approach. Also,performance of the medical data classificationmeasured with respect to different parameters such as Accuracy, specificity and Sensitivity.

Table.2 Comparative study of different methods and proposed method

Methodology	Database	Accuracy	Specificity	Sensitivity
Fuzzy +PSO[17]	UCI	85.7	91.08	90.02
Decision Tree [18]	UCI	78.91	84.48	72.01
Bagging Algorithm [18]	UCI	81.41	84.48	74.93
ANN+FNN [19]	UCI	84.2	87.3	80.3
BPNN [20]	UCI	94.51	98.31	87.37
Proposed GWO+RNN	Hungarian	95.12	90.0	96.47
	Cleveland	98.23	97.6	99.10
	Switzerland	91.35	93.45	96.36
	PID	96.21	96.78	97.45
	Mammographic Masses	95.56	94.57	98.47

H. Kahramanli, and N. Allahverdi [19] presented Artificial Neural Network and Fuzzy Neural Network (ANN+FNN) method used for diabetes and heart disease prediction. This method is not able to perform on multiple databases. A. Marcano-Cedeño, *et al.* [20] presented Artificial met plasticity Multilayer Perceptron (AMMLP) algorithm for breast cancer prediction using UCI database. Here, proposed algorithm performance was compared with the Back Propagation Neural Network (BPNN). Finally, medical data classification performance of GWO+RNN method with respect to five different UCI datasets such as Hungarian, Cleveland, Switzerland, PID, and Mammographic Masses is shown in the table 2. GWO+RNN method achieved 98.23% of prediction accuracy with respect to Cleveland dataset that is higher compared to other datasets.

5. Conclusion

In medical field, many researchers focused onprediction of different disease using various medical applications. In this research, GWO+RNN technique is used for medical disease prediction. The GWO method is used for feature selection, which removes the redundant and irrelevant attributes. An AE based RNN classifier predicts various diseases and avoids the feature dimensionality issues. This GWO+RNN method is tested using five benchmarks of UCI dataset namely Hungarian, PID, Mammographic masses, Cleveland and Switzerland. In experimental analysis, classification performance of the proposed method is compared with the existing method namely GFMMNN, ANN+FNN, BPNN, and DT. The performance of GWO+RNN method is calculated in terms of different evaluation metrics like specificity, sensitivity and accuracy. The GWO+RNN method achieved 16.825%of improved accuracy in Cleveland dataset for disease prediction. In future, research work can be extended as an efficient hybrid technique for improving the efficiency of different medical disease classification.

References

[1] M. Niksic, B. Rachet, S. W. Duffy, M. Quaresma, H. Moller, L. J. Forbes, "Is cancer survival associated with cancer symptom awareness and barriers to seeking medical help in England? An ecological study," *British journal of cancer*, vol. 115, no. 7, pp. 876, 2016.

[2] M. Scatà, A. Di Stefano, P. Liò, and A. La Corte, "The impact of heterogeneity and awareness in modeling epidemic spreading on multiplex networks," *Scientific reports*, vol. 6, pp. 37105, 2016.

[3] M. Nilashi, O. Ibrahim, H. Ahmadi, L. Shahmoradi, and M. Farahmand, "A hybrid intelligent system for the prediction of Parkinson's Disease progression using machine learning techniques," *Biocybernetics and Biomedical Engineering*, vol. *38*, no. 1, pp. 1-15, 2018.

[4] J. Wan, S. Tang, D. Li, S. Wang, C. Liu, H. Abbas and A. Vasilakos, "A Manufacturing Big Data Solution for Active Preventive Maintenance", *IEEE Transactions on Industrial Informatics*, vol. 13, no. 4, pp. 2039-2047, 2017.

[5] W. Yin and H. Schutze, "Convolutional neural network for paraphrase-identification." in HLT-NAACL, pp. 901–911, 2015.

[6] K. Lin, J. Luo, L. Hu, M. S. Hossain, and A. Ghoneim, "Localization based on social big data analysis in the vehicular networks," *IEEE Transactions on Industrial Informatics*, vol. 99, no. 1, 2016.

[7] K. Lin, M. Chen, J. Deng, M. M. Hassan, and G. Fortino, "Enhanced fingerprinting and trajectory prediction for iot localization in smart buildings," *IEEE Transactions on Automation Science and Engineering*, vol. 13, no. 3, pp. 1294–1307, 2016.

[8] S. Bandyopadhyay, J. Wolfson, D. M. Vock, G. Vazquez-Benitez, G. Adomavicius, M. Elidrisi, P. E. Johnson, and P. J. O'Connor, "Data mining for censored time-to-event data: a bayesian network model for predicting cardiovascular risk from electronic health record data," *Data Mining and Knowledge Discovery*, vol. 29, no. 4, pp. 1033–1069, 2015.

[9] B. Qian, X. Wang, N. Cao, H. Li, and Y.-G. Jiang, "A relative similarity based method for interactive patient risk prediction," *Data Mining and Knowledge Discovery*, vol. 29, no. 4, pp. 1070–1093, 2015.

[10] A. Singh, G. Nadkarni, O. Gottesman, S. B. Ellis, E. P. Bottinger, and J. V. Guttag, "Incorporating temporal ehr data in predictive models for risk stratification of renal function deterioration," *Journal of biomedical informatics*, vol. 53, pp. 220–228, 2015.

[11] Y. Chen, N. Crespi, A. M. Ortiz, and L. Shu, "Reality mining: A prediction algorithm for disease dynamics based on mobile big data," *Information Sciences*, vol. 379, pp. 82-93, 2017.

[12] M. Chen, Y. Hao, K. Hwang, L. Wang, and L. Wang, "Disease prediction by machine learning over big data from healthcare communities," *IEEE Access*, vol. 5, pp. 8869-8879, 2017.

[13] R. Prashanth, and S. D. Roy, "Novel and improved stage estimation in Parkinson's disease using clinical scales and machine learning." *Neurocomputing*, vol. 305, pp. 78-103, 2018.

[14] M. Nilashi, O. bin Ibrahim, H. Ahmadi, and L. Shahmoradi, "An analytical method for diseases prediction using machine learning techniques," *Computers & Chemical Engineering*, vol. 106, pp. 212-223, 2017.

[15] S. Sarkar, S. Vinay, R. Raj, J. Maiti, and P. Mitra, "Application of optimized machine learning techniques for prediction of occupational accidents," *Computers & Operations Research*, 2018.

[16] D. M. Rafi, and C. R. Bharathi, "Optimal Fuzzy Min-Max Neural Network (FMMNN) for Medical Data Classification Using Modified Group Search Optimizer Algorithm", *International Journal of Intelligent Engineering and Systems*, Vol.*9, Issue.*3, pp.1-10. 2016.

[17] N. G.Hedeshi, and M. S. Abadeh, "Coronary artery disease detection using a fuzzy-boosting PSO approach", *Computational intelligence and neuroscience*, p.6. 2014.

[18] M. C. Tu, D. Shin, and D. Shin, "Effective diagnosis of heart disease through bagging approach", In *Biomedical Engineering and Informatics, BMEI'09. 2nd International Conference on*, pp. 1-4, IEEE, 2009.

[19] H. Kahramanli, and N.Allahverdi, "Design of a hybrid system for the diabetes and heart diseases", *Expert systems with applications*, vol.*35, Issue.* 1-2, pp.82-89, 2008.
[20] A. Marcano-Cedeño, J. Quintanilla-Domínguez, and D. Andina, "WBCD breast cancer database classification applying artificial metaplasticity neural network", *Expert Systems with Applications*, vol.*38, Issue*.8, pp.9573-9579. 2011.

BIBLIOGRAPHY OF AUTHORS

Dr. B. SANKARABABU was a doctorate from Aacharya Nagarjuna University, Guntur, Andhrapradesh, India, and completed PhD in 2016. Currently working as a Professor in Department of Computer Science and Engineering at Gokaraju Rangaraju Institute of Engineering and Technology, Hyderabad .He has done his research on Data Mining. He has published several research papers on Data mining concepts.

G.Charles Babu , Presently working as a Professor in Dept. of CSE in Malla Reddy Engineering College(Autonomous), Secunderabad, Telangana Since 5 Years and Total Teaching experience of 20 Years. Completed B.Tech (CSE) in 1997 from KLCE, M.Tech(SE) in 1999 from JNTUH and Ph.D(Data Mining) from ANU. Published more than 50 Research Papers in Data Mining, Cloud Computing, Image Processing.

Dr. Y. Jeevan Nagendra Kumar, obtained his Ph.Din Computer Science and Engineering from Acharya Nagarjuna University, Guntur, AP in 2017 and M.Tech Computer Science Technology from Andhra University in 2005. He is working as Professor and Dean - Technology and Innovation Cell in GRIET since 2005. He has about 9 Research Papers in International / National Conferences and Journals and also attended many FDP Programs to enhance his knowledge. With his technical knowledge he guided the students in developing the useful Web applications and data mining related products.

Dr. G.Karuna, Professor in Computer Science and Engineering, completed her Ph.D from JNTUH, Hyderabad and she has over twelve years of academic and research experience. Currently working as a professor in CSE Department and prior to this, she worked for Malla Reddy Institute of Technology & Science andJ.B.Institute of Engineering & Technology. Her Ph.D. thesis was titled as "An Effective Representation of Shape for Object Recognition and Classification based on Statistical and Structural Features" in the area of Image Processing. She has published25 papers in referred International Journals and Conferences and written two books for SCDE, JNTUH, and Hyderabad.

International Journal of Engineering & Technology, 7 (3.29) (2018) 31-34

International Journal of Engineering & Technology

Website: www.sciencepubco.com/index.php/IJET

Research paper

Improving the safety of an uncontrolled road traffic junction a case study of maisammaguda T-junction

Dr. R. Prasannakumar [1] *, Akella. Naga sai baba [2] , V. Ranjith Kumar [2]

[1] Professor, Malla Reddy Engineering College,(Autonomous) Kompally
[2] Assistant Professor, Malla Reddy Engineering College,(Autonomous) Kompally
**Corresponding author E-mail: prasanna1968@gmail.com*

Abstract

Road traffic junctions are potential locations for accidents especially when they are not provided with signal and completely uncontrolled. In the present paper, a T-junction located near Maisammaguda was identified as the study location. It was an uncontrolled road traffic junction with many conflicts and congestion, reducing the safety of students, faculty and other commuters. Near about ten professional colleges are located in this area, with heavy traffic flow during morning and evening peak hours. Traffic volume count was made as per IRC guidelines and signal timings were designed for the proposed signalized T Junction. Detailed phasing and timing plans were also arrived at separately for morning and evening peak hours. It is believed that the proposal if implemented will significantly reduce the number and severity of accidents at this location.

Keywords: *Traffic Volume; PCU; Saturation Flow; Signal Timing.*

1. Introduction and literature review

Road traffic junctions are critical locations from safety point of view for road users. Many of the junctions in India are neither provided with traffic signal control nor police control. Such type of junctions known as uncontrolled junctions poses serious threat to the road user. They must be analyzed carefully considering the geometric features, prevailing roadway and traffic conditions etc with the help of scientific traffic data pertaining to that junction. In the present paper an attempt is made to understand the conflicts at the study location, and find ways to improve the safety of road users at this junction, by proposing a pre timed signal with suitable phasing plan and timing plan. Sudarshan Reddy and Venkat Hussain Reddy (2016) have designed the signal timings for a T Junction in Nandyal town of Kurnool district in Andhra Pradesh, India.

2. Objectives of the present study

The present study aims to attain the following objectives.

- To carry out classified traffic volume counts at the study location for a period of three weeks on typical working days as per IRC guidelines.
- To arrive at the morning and evening peak hour and to determine the peak hour flow rate.
- To design the signal timings as per Webster method of design and to plot the timing and phasing diagrams.

3. Methodology

- Identification and description of study location.
- Classified volume counts.
- Identification of AM and PM Peak Hour.
- Determination of Saturation flow.
- Computation of Signal timings.
- Phasing and timing diagrams.

Identification and description of study location

The study location identified was a T Junction located near Maisammaguda comes under Medchal district of Telangana state, India. It is a busy area consisting of many Private Professional educational institutions. Large numbers of commuters travel from various parts of twin cities of Hyderabad and Secunderabad. Many road users travel through this junction by means of two wheelers and cars. Large numbers of students also travel using share autos. Since the junction is not controlled by any traffic signal nor police, lot of conflicts occur near this junction making it a very risky place from safety point of view. Hence it is proposed to carry out detailed traffic studies and determine the most efficient signal timing plans to suit to the prevailing roadway and traffic conditions so as to reduce the conflicts and improve the safety of the junction.

Classified volume counts

Traffic enumerators are posted on each arm of the intersection, the count at each arm of the junction was recorded conveniently by five dash system, where by vertical strokes are entered for the first four vehicles, followed by an oblique stroke for the fifth vehicle. The field data was collected as per the guidelines of IRC SP 41.

Identification of AM and PM Peak Hour

The traffic volume data was summarized and converted in to PCU's. From the analysis of data the morning and evening peak hour was determined.

The saturation flow was determined using the equation 525 W, where W is the width of carriage way in m. The signal timings were determined by using Webster method of design as discussed in the subsequent sections of this paper.

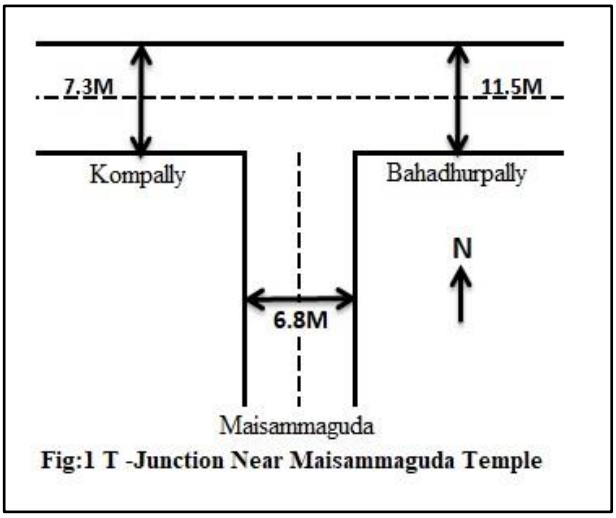

Fig. 1: T-Junction near Maisammaguda Temple.

Fig. 2: Satellite Imagery of T Junction near Maisammaguda Temple.

Procedure for Signal Design:-
The signal design procedure involves the following major steps. They include the

1) Phase design
2) Determination of amber time and clearance time
3) Determination of cycle length
4) Apportioning of green time
5) The performance evaluation of the above design.

The objective of phase design is to separate the conflicting movements in an intersection into various phases, so that movements in a phase should have no conflicts. If all the movements are to be separated with no conflicts, then a large number of phases are required.To illustrate various phase plan options, consider a four legged intersection with through traffic and right turns. Left turn is ignored.

Two Phase Signals:-
Two phase system is usually adopted if through traffic is significant compared to the turning movements. Non-conflicting through traffic 3 and 4 are grouped in a single phase and non-conflicting through traffic 1 and 2 are grouped in the second phase. However, in the first phase flow 7 and 8 over some conflicts and are called permitted right turns.

WEBSTER METHOD: - It is used for the signal design. In this method corresponding to least total delay to the vehicles at signalized intersection has been worked out. This is rational approach. The field work consists of finding

i) Saturation flow "S" per unit time on each approach of the intersection
ii) The normal flow "q" on each approach during the design approach.

Saturation flow is given by the formula, S = 525W (W = width of the road).

Based on the higher value of normal flow, the ratios,

$$y_1 = \frac{q1}{s1},\ y_2 = \frac{q2}{s2} \text{ and } y_3 = \frac{q3}{s3} \quad (1)$$

are determined on the approach roads 1, 2 and 3. In the case of mixed traffic, it is necessary to convert all the values in terms of PCU values which should be determined separately. The saturation flow is to be obtained from careful field studies by noting the number of vehicles in the stream of compact flow during the green phases and the corresponding time intervals precisely. In the absence of the data approximately value of saturation flow is estimated assuming 160 PCU per 0.3 meter width of the approach. The normal flow of the traffic is also determined on the approach roads from the field studies from the design period (during the peak or off peak hours, as the case may be.)

The optimum signal cycle is given by

$$C_o = \frac{1.5L+5}{1-Y} \quad (2)$$

Where L = total lost time per cycle, seconds

$$L = 2n+R \quad (3)$$

n = number of phases,

R = all red time.

$$Y = y_1+y_2+ \quad (4)$$

Then $G_1 = \frac{y1}{Y}(C_o - L)$, $G_2 = \frac{y2}{Y}(C_o - L)$ and $G_3 = \frac{y3}{Y}(C_o - L)$

Traffic Counts:-
A survey is conducted for nine days to obtain traffic hourly counts for all streams. The [6] traffic movements at the junction are conveniently grouped into [3] phases and presented in Table 1.

Table 1: Description of Phase Movements

Phase	From	Towards
1	Kompally	Bahadhurpally Malla Reddy Engineering College
2	Bahadhurpally	Kompally Malla Reddy Engineering College
3	Malla Reddy College	Kompally Bahadhurpally

4. Data collection

Table 2: Traffic Approaching East Bound for Week 1 (Tuesday)

Time		Total No of Vehicles
From	To	
Morning		
8:30	9:30	1884
8:45	9:45	1923
9:00	10:00	1773
9:15	10:15	1485
9:30	10:30	1136
Evening		
15:30	16:30	573
15:45	16:45	607
16:00	17:00	619
16:15	17:15	568
16:30	17:30	487

5. Data analysis

From the data obtained above, the hour for which volume is high is taken i.e. peak hourly volume and Passenger Car Unit (PCU) is determined.

PCU for 2 – wheelers = 0.5

PCU for 3 – wheelers = 0.6

PCU for 4 – wheelers = 1

PCU for heavy vehicles = 3.5

The PCU factor is multiplied with the highest volume of all type of vehicles and then added to get Passenger Car Unit (PCU/hr). Saturation flow is determined by the formula – 525W (W=width of the road in meters).

Table 3: Peak Hourly Volume for East Bound Approach week 1 (Tuesday)

Peak Hourly Volume: Week 1-Tuesday			
Morning (8:45 to 9:45 AM)			
Name of the approach	PHV (veh/hr)	PCU (pcu/hr)	SF (pcu/hr)
East bound approach	1923	1396	6037
West bound approach	3419	4580	3832
South bound approach	387	260	3570
Evening (3:45 to 4:45 PM)			
East bound approach	619	707	6037
West bound approach	677	604	3832
South bound approach	1383	962	3570

6. Results

Calculation of Cycle Length for Morning Session:
Normal flows,

q_1= 1388, q_2 = 1027, q_3 = 267

Saturation flows,

S_1 = 6037, S_2 = 3832, S_3 = 3570

Ratios,

$y_1 = \frac{1388}{6037} = 0.23$

$y_2 = \frac{1027}{3832} = 0.27$

$y_3 = \frac{267}{3570} = 0.07$

$Y = y_1 + y_2 + y_3 = 0.23 + 0.27 + 0.07 = 0.57$

Cycle length according to Webster method is calculated using the formula,

$C_0 = \frac{1.5L+5}{1-Y} = \frac{1.5(12)+5}{1-0.57} = 53.49$ sec.

Calculation of Green time:
Phase 1:

$G_1 = \frac{y1}{Y}(C_0 - L)$

$= \frac{0.23}{0.57}(53.49 - 12) = 16.74$ sec

Phase 2:

$G_2 = \frac{y2}{Y}(C_0 - L)$

$= \frac{0.27}{0.57}(53.49 - 12)$

= 19.65 sec

Phase 3:

$G_3 = \frac{y3}{Y}(C_0 - L)$

$= \frac{0.07}{0.57}(53.49 - 12)$

= 5.10 sec

Considering all pedestrian time = 6 seconds, Amber time = 2 seconds for each phase = 6 seconds for three phases.

Total Cycle length = 16.74 + 19.65 + 5.10 + 6 + 6 = 55sec.

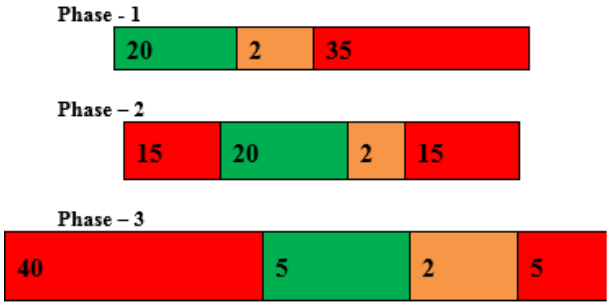

Fig. 1: Phasing Diagram for AM Peak Hour.

- Therefore, In phase 1 the green time is 20 sec, amber time is 35 sec
- In phase 2, the green time is 20 sec and red time is 15, 15sec

In phase 3, the green time is 5 sec and red time is 40, 5 sec
Calculation of Cycle Length for Evening Session:
Normal flows,

q_1 = 727, q_2 = 749, q_3 = 843

Saturation flows,

S_1 = 6037, S_2 = 3832, S_3 = 3570,

Ratios,

$y_1 = \frac{727}{6037} = 0.12$

$y_2 = \frac{749}{3832} = 0.20$

$y_3 = \frac{843}{3570} = 0.24$

$Y = y_1 + y_2 + y_3 = 0.12 + 0.20 + 0.24 = 0.56$

Cycle length according to Webster method is calculated using the formula,

$C_0 = \frac{1.5L+5}{1-Y} = \frac{1.5(12)+5}{1-0.56} = 52.27$sec.

Calculation of Green time:
Phase 1:

$G_1 = \frac{y1}{Y}(C_0 - L)$

$= \frac{0.12}{0.56}(52.27 - 12)$

= 8.63 sec

Phase 2:

$G_2 = \frac{y2}{Y}(C_0 - L)$

$= \frac{0.20}{0.56}(52.27 - 12)$

= 14.38 sec

Phase 3:

$G_3 = \frac{y3}{Y} (C_0 – L)$

$= \frac{0.24}{0.56} (52.27 – 12)$

= 17.26 sec

Considering all pedestrian time = 6 seconds, Amber time = 2 seconds for each phase = 6 seconds for three phases.

Total Cycle length = 8.63 + 14.38 + 17.26 + 6 + 6 = 55sec.

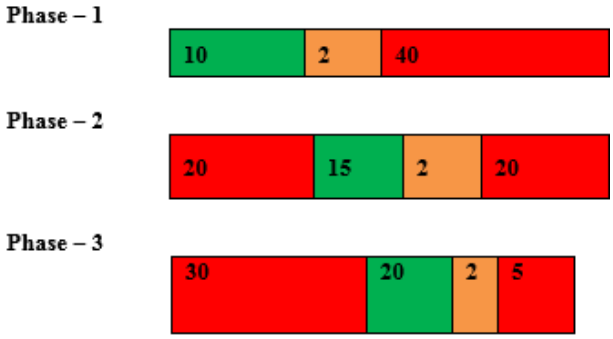

Fig. 2: Phasing Diagram for PM Peak Hour.

- Therefore, In phase 1, the green time is 10 sec and red time is 40 sec
- In phase 2, the green time is 15 sec and red time is 20, 20 sec
- In phase 3, the green time is 20 sec and red time is 30, 5sec

This paper is an attempt to improve the safety of the road users at this study junction. The traffic signal must be installed as per the Indian standards. Green, amber and red timings for the three phases as determined above needs to be adopted for both morning and evening and observed for a period three to six months. The effect of traffic signal on the safety of road users can be assessed by comparing the number of accidents before and after installation of traffic signal.

References

[1] High way Engineering – S. K. Khanna & C. E. G Justo, Nemchand & Bros., 7th Edition

[2] Traffic Engineering & Transportation Planning – Dr.L.R. Kadiyali – Khanna Publications, New Delhi.

[3] IRC 93-1985 Guidelines on Design and Installation of Road Traffic Signals, Indian Roads Congress, New Delhi.

[4] IRC SP41: Guidelines for the Design of At-Grade Intersections in Rural and Urban Areas, Indian Roads Congress, New Delhi.

[5] Sudharshan Reddy and Venkata Hussain Reddy (2016), “Signal design for T-intersection by using webster's method in nandyal town, kurnool district of Andhra Pradesh” International Research Journal of Engineering and Technology. Volume: 03 Issue: 04. Pp: 1124 – 1131.

International Journal of Engineering & Technology, 7 (3.29) (2018) 39-45

International Journal of Engineering & Technology

Website: www.sciencepubco.com/index.php/IJET

Research paper

Analysis of selected parking spaces in medium sized cities of tamil nadu

Dr. R. Prasannakumar [1] *, Akella. Naga sai baba [2], V. Ranjith Kumar [2], Sudharsan.R [3]

[1] Professor, Malla Reddy Engineering College,(Autonomous) Kompally
[2] Assistant Professor, Malla Reddy Engineering College,(Autonomous) Kompally
[3] Formerly under Graduate students at SASTRA University, Thanjavur
**Corresponding author E-mail: prasanna1968@gmail.com*

Abstract

The present study aims to analyze the conditions of identified parking lots in two medium sized cities of Tamil Nadu, namely Tiruchirapalli and Thanjavur, and suggest possible measures for improvement. Methods like parking space inventory survey, cordon count and parking usage control by patrol were used for data collection. The number of vehicles occupying the parking spaces at a specific period of time was determined. This count was taken at regular intervals over a time period spread over 9 am to 6 pm, in three sessions. The data collected was then analysed and peak values of the numbers of different types of vehicles was identified. Observations of the prevalent topographical conditions at the study locations were made and a few suggestions pertaining to maintenance, enhancement, improved efficiency and tariff were provided.

Keywords: *Parking Space Inventory; Tiruchirappalli; Thanjavur; Strategies; Patrol; Tariff; Parking Lots.*

1. Introduction

2. Introduction and literature review

Parking is one among the serious problems which the urban planner and traffic engineer face. So suitable measures aimed at the optimum usage of available space should be implemented. Before such measures can be taken, collection of data through surveys is mandatory. The types of surveys adopted for this study include parking space inventory survey, parking usage survey by patrol and cordon count. In parking space inventory survey, the study location was delineated and subdivided into parts, to make the job easy. Different types of data regarding the parking load and topography are collected. In parking usage survey by patrol, the study area was patrolled at regular intervals, thereby counting the number of vehicles parked at a particular instant. This reading is taken at regular intervals and tabulated, thereby identifying the extent of usage. The Cordon count method keeps track of the number of vehicles entering and leaving the parking area, thereby the count at a particular instant can be known. The study was undertaken at three locations, namely Palpannai and Super Bazaar in Tiruchirappalli City and the parking space near Big Temple in Thanjavur City. The data collection was taken up in three sessions per day, readings being noted at every 15 minute interval. Peak values of parking load were identified upon analysis and suitable recommendations and corrective measures were proposed after correlation with the standard codebook, IRC SP 12 2015. The types of vehicles being parked at a location, frequency of arrival of vehicles, duration of parking, topographical conditions and dimensions of the parking space etc. were all considered during this study.

3. Methodology

- Selection of study locations
- Feasibility study at the selected locations
- Collection of data using parking surveys
- Analysis of data
- Identification of peak parking load
- Suggesting suitable recommendations upon suitable correlation with IRC SP 12 2015

3.1. Study area characteristics

Three locations were selected for analysis. The first location was Super bazaar car parking space, Tiruchirappalli city (10.824974N, 78.695101E).Second location that was selected for analysis was Palpannai two wheeler parking near Palpannai bus stand and the third parking was Thanjavur Brihadeeshwara temple parking(10.782953N, 79.134311E). Tiruchirappalli district is located along the banks of the Cauvery River, at the heart of Tamil Nadu state. The latitude coordinates of the district are 10o 47’40.56”N 78o41’6”E.It is bound by Salem district in the north and Thanjavur district in the south. It is also bordered by Perambalur, Madurai, Ariyalur, Pudukkottai and Sivagangai districts. The latest census recorded a population count of 2,722,290, which has a great bearing on the parking volume.

3.2. Identification of study sections

Several locations were considered for analysis of which three locations were selected, namely Super bazaar car parking, Palpannai two wheeler parking and Tanjore big temple parking. The main rea-

son behind the selection of these parking spaces was existing condition of the parking space, deviation from the recommendations given by the latest IRC codes SP 12-2015, occupancy rate of the parking space and based on the location characteristics.

Parking space inventory survey was conducted at selected locations in and around Tiruchirappalli and the following data was obtained:

3.3. Data collection

Table 1: Super Bazaar off Street Parking Summary SLOT 1: 9.15-11.15am

Sl. No	Time Interval	Total Area (M²)	Type of Vehicles Parked:				
			2-Wheelers Motorised	Non- Motorised	3-Wheeelers	4-Wheelers Cars	Other Than Cars
1	9.15-9.30	3398	3	0	0	18	0
2	9.30-9.45	3398	2	0	2	26	0
3	9.45-10..00	3398	1	0	1	30	1
4	10.00-10.15	3398	1	0	4	36	2
5	10.15-10.30	3398	3	0	5	41	2
6	10.30-10.45	3398	7	0	3	45	2
7	10.45-11.00	3398	11	0	6	49	2
8	11.00-11.15	3398	12	0	4	54	3

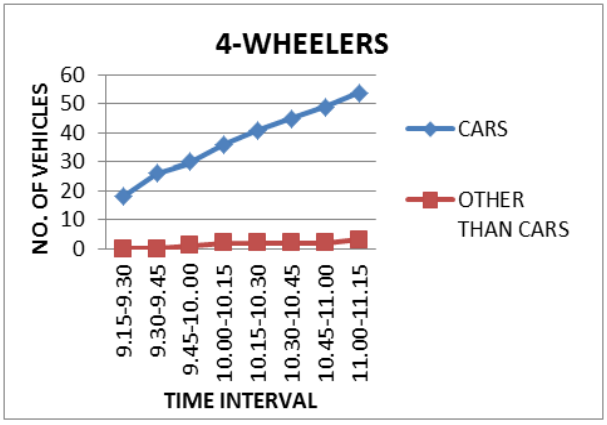

Fig. 1: Parking Accumulation Curve (4-Wheelers) - Slot 1.

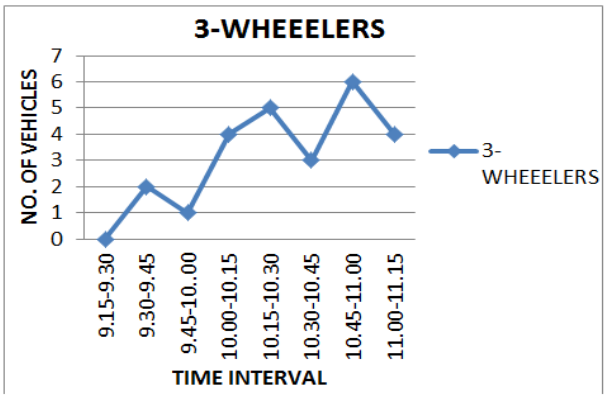

Fig. 3: Parking Accumulation Curve (3-Wheelers) - Slot 1.

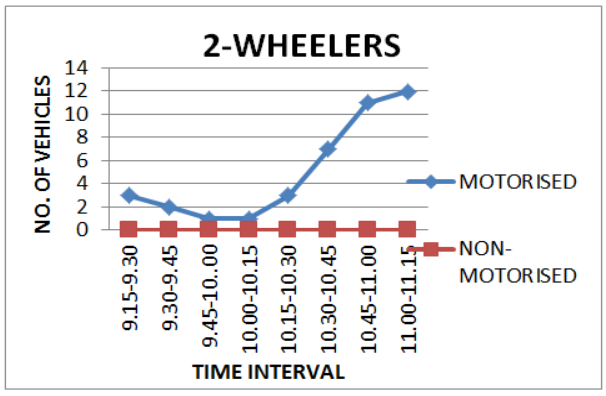

Fig. 2: Parking Accumulation Curve (2-Wheelers) - Slot 1.

Table 2: Super Bazaar: Off Street Parking Summary - SLOT 2: 12.30-2.30pm

Sl.No	Time Interval	Total Area (M²)	Type of Vehicles Parked:				
			2-Wheelers Motorised	Non- Motorised	3-Wheeelers	4-Wheelers Cars	Other Than Cars
1	12.30-12.45	3398	6	0	8	87	3
2	12.45-1.00	3398	7	0	7	74	3
3	1.00-1.15	3398	15	0	8	88	3
4	1.15-1.30	3398	16	0	9	100	3
5	1.30-1.45	3398	10	0	5	87	2
6	1.45-2.00	3398	11	0	6	89	3
7	2.00-2.15	3398	8	0	6	91	2
8	2.15-2.30	3398	7	0	4	87	2

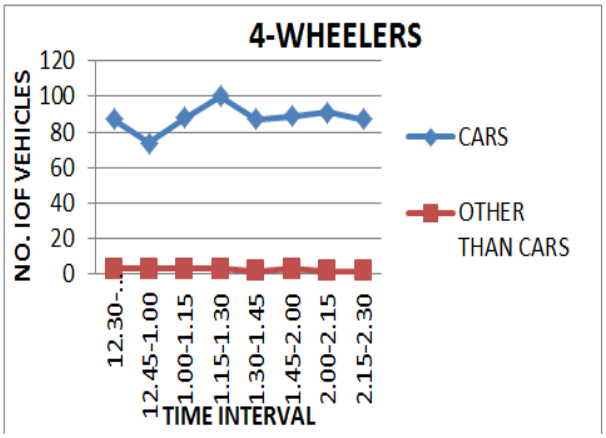

Fig. 5: Parking Accumulation Curve (Cars)-Slot 2 (12.30-2.30).

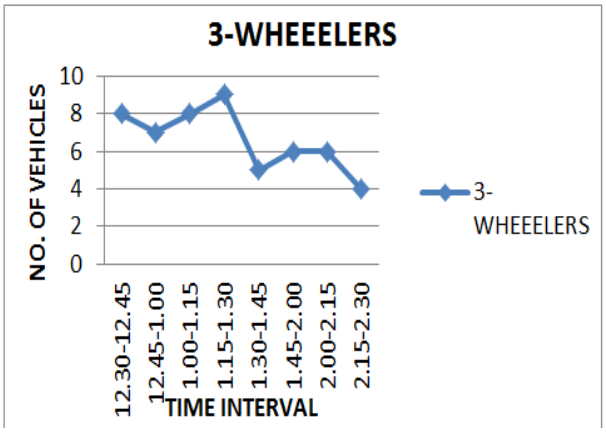

Fig. 7: Parking Accumulation Curve (Three Wheelers)-Slot 2 (12.30-2.30).

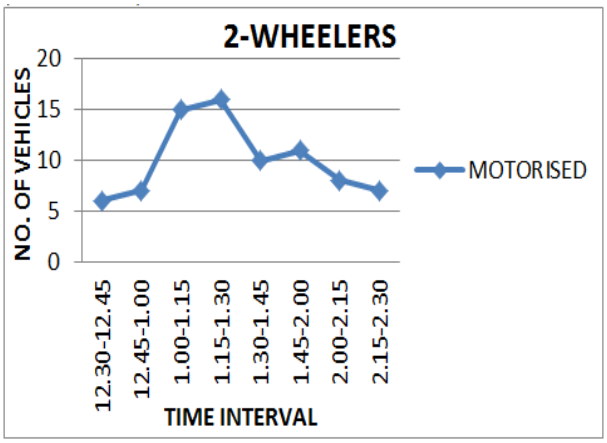

Fig. 6: Parking Accumulation Curve (Two Wheelers)-Slot 2 (12.30-2.30).

Table 3: Super Bazaar: Off Street Parking Summary - SLOT 3: 4.00-6.00pm

Sl.No	Time Interval	Total Area (M²)	Type of Vehicles Parked:				
			2-Wheelers Motorized	Non- Motorized	3-Wheeelers	4-Wheelers Cars	Other Than Cars
1	4.00-4.15	3398	5	0	7	81	1
2	4.15-4.30	3398	7	0	3	82	4
3	4.30-4.45	3398	7	0	3	82	4
4	4.45-5.00	3398	6	0	1	88	4
5	5.00-5.15	3398	5	0	2	81	4
6	5.15-5.30	3398	6	0	3	72	3
7	5.30-5.45	3398	5	0	5	71	2
8	5.45-6.00	3398	5	0	4	73	2

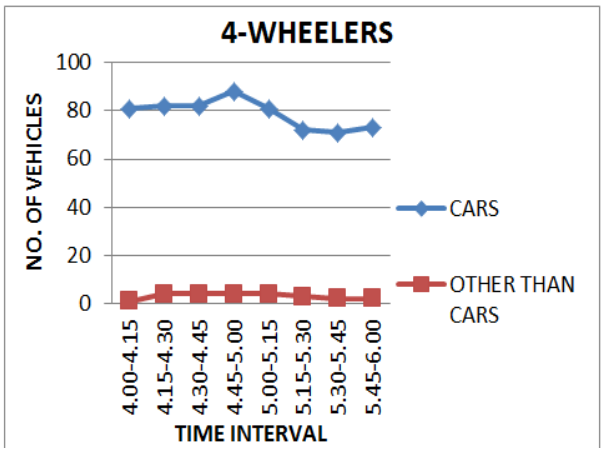

Fig. 8: Parking Accumulation Curve (Cars) - Slot 3 (4.00-6.00PM).

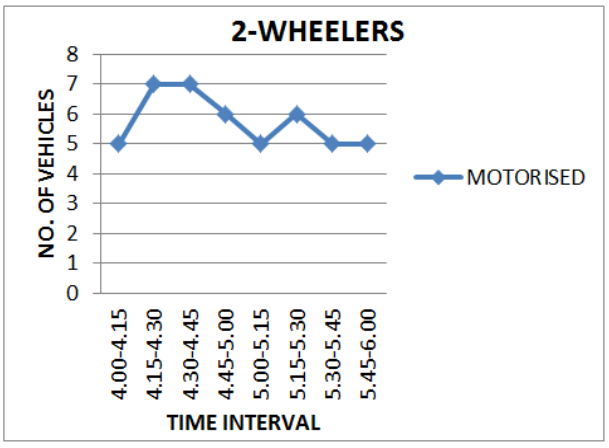

Fig. 9: Parking Accumulation Curve (Two Wheelers) - Slot 3 (4.00-6.00PM).

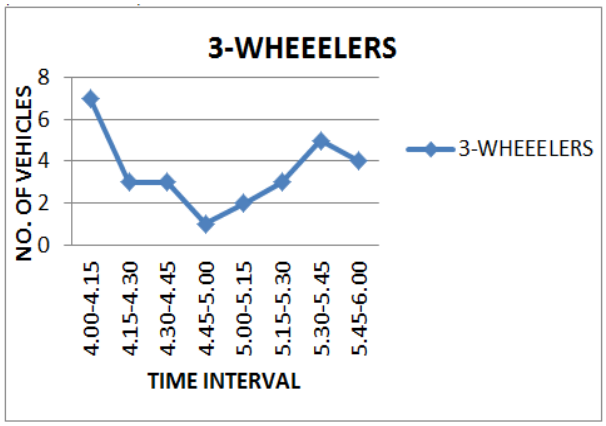

Fig. 10: Parking Accumulation Curve (three Wheelers) - Slot 3 (4.00-6.00pm).

Table 4: Palpannai: Off Street Parking Summary - SLOT1: 9.15AM-11.15AM

Sl.No	Time Interval	Total Area (M²)	Type of Vehicles Parked:				
			2-Wheelers Motorised	Non- Motorised	3-Wheeelers	4-Wheelers Cars	Other Than Cars
1	9.15-9.30	372	128	4	0	0	0
2	9.30-9.45	372	132	4	0	0	0
3	9.45-10..00	372	140	4	0	0	0
4	10.00-10.15	372	140	4	0	0	0
5	10.15-10.30	372	147	4	0	0	0
6	10.30-10.45	372	149	4	0	0	0
7	10.45-11.00	372	151	4	0	0	0
8	11.00-11.15	372	153	4	0	0	0

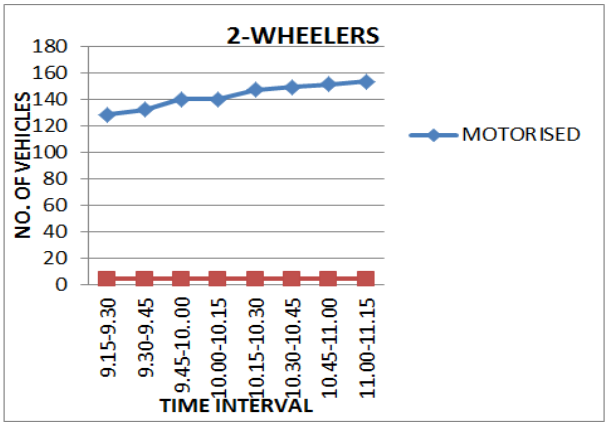

Fig. 10: Parking Accumulation Curve (Two Wheelers) – SLOT 1.

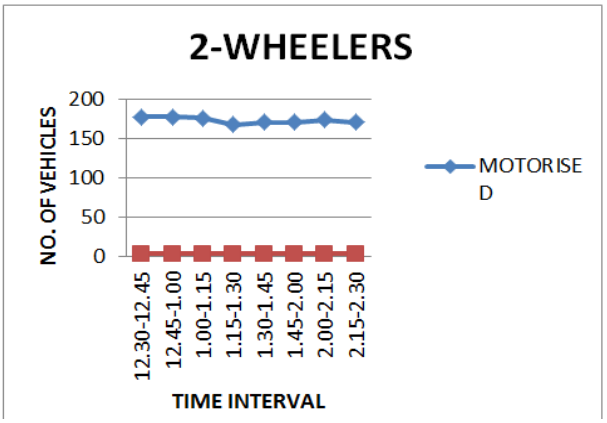

Fig.11: Parking Accumulation Curve (Two Wheelers)-Slot 2 (12.30-2.30pm).

Table 5: Palpannai: Off Street Parking Summary - SLOT 2: 12.30-2.30.

Sl.No	Time Interval	Total Area (M)	Type of Vehicles Parked:				
			2-Wheelers Motorized	Non- Motorized	3-Wheeelers	4-Wheelers Cars	Other Than Cars
1	12.30-12.45	372	178	4	0	0	0
2	12.45-1.00	372	178	4	0	0	0
3	1.00-1.15	372	176	4	0	0	0
4	1.15-1.30	372	168	4	0	0	0
5	1.30-1.45	372	171	4	0	0	0
6	1.45-2.00	372	171	4	0	0	0
7	2.00-2.15	372	174	4	0	0	0
8	2.15-2.30	372	171	4	0	0	0

Table 6: Palpannai: off Street Parking Summary - SLOT 3: 4.00-6.00pm

Sl.No	Time Interval	Total Area (M²)	Type of Vehicles Parked:				
			2-Wheelers Motorised	Non- Motorised	3-Wheeelers	4-Wheelers Cars	Other Than Cars
1	4.00-4.15	372	166	4	0	0	0
2	4.15-4.30	372	166	4	0	0	0
3	4.30-4.45	372	165	4	0	0	0
4	4.45-5.00	372	164	4	0	0	0
5	5.00-5.15	372	161	4	0	0	0
6	5.15-5.30	372	151	4	0	0	0
7	5.30-5.45	372	141	4	0	0	0
8	5.45-6.00	372	115	4	0	0	0

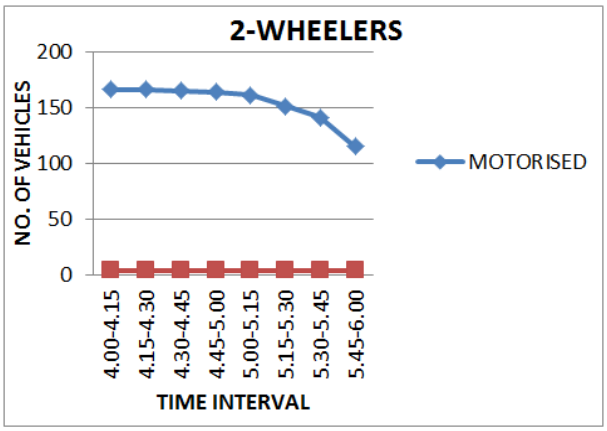

Fig. 12: Parking Accumulation Curve (two Wheelers) -Slot 2 (4.00-6.00pm).

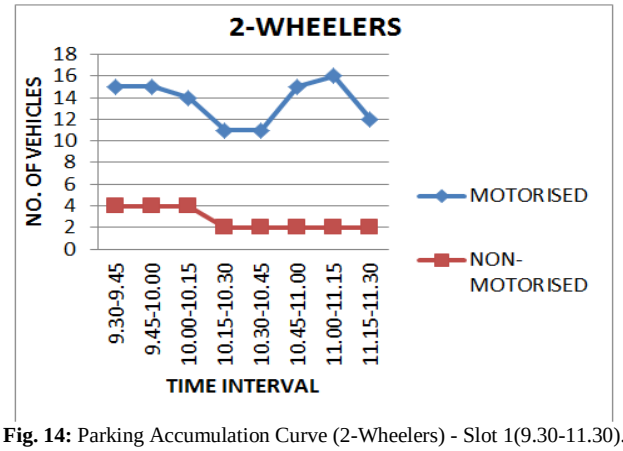

Fig. 14: Parking Accumulation Curve (2-Wheelers) - Slot 1(9.30-11.30).

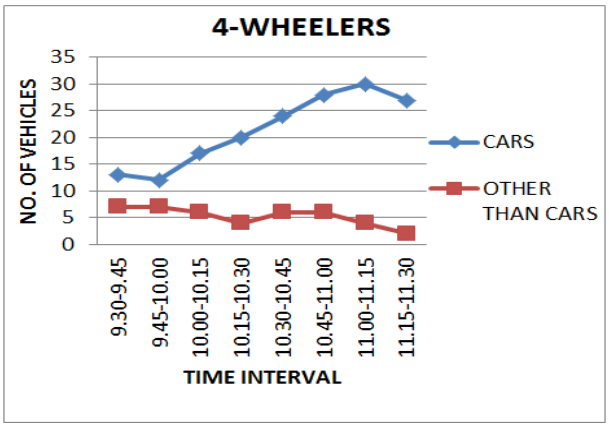

Fig. 13: Parking Accumulation Curve (Four Wheelers) - Slot 1(9.30-11.30).

Table 7: Thanjavur: Off Street Parking Summary - Slot1: 9.15am-11.15am

Sl.No	Time Interval	Total Area (M²)	Type of Vehicles Parked:				
			2-Wheelers		3-Wheeelers	4-Wheelers	
			Motorised	Non- Motorised		Cars	Other Than Cars
1	9.30-9.45	4850	15	4	0	13	2
2	9.45-10.00	4850	15	4	0	12	2
3	10.00-10.15	4850	14	4	0	17	2
4	10.15-10.30	4850	11	2	0	20	1
5	10.30-10.45	4850	11	2	1	24	2
6	10.45-11.00	4850	15	2	0	28	2
7	11.00-11.15	4850	16	2	0	30	2
8	11.15-11.30	4850	12	2	0	27	1

Table 8: Thanjavur: Off Street Parking Summary - Slot2: 12.30pm-2.30pm.

Sl.No	Time Interval	Total Area (M²)	Type of Vehicles Parked:				
			2-Wheelers		3-Wheeelers	4-Wheelers	
			Motorised	Non- Motorised		Cars	Other Than Cars
1	12.30-12.45	4850	14	2	0	24	7
2	12.45-1.00	4850	16	2	0	22	7
3	1.00-1.15	4850	15	2	0	19	6
4	1.15-1.30	4850	13	1	0	19	4
5	1.30-1.45	4850	13	0	0	15	6
6	1.45-2.00	4850	11	0	0	15	6
7	2.00-2.15	4850	11	0	0	11	4
8	2.15-2.30	4850	10	0	0	10	2

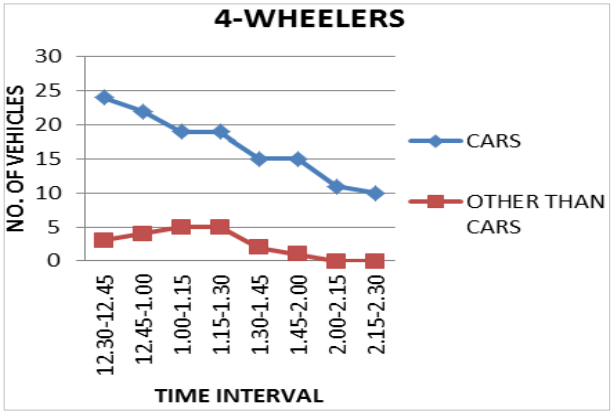

Fig. 15: Parking Accumulation Curve (four Wheelers) – Slot 2 (12.30-2.30pm).

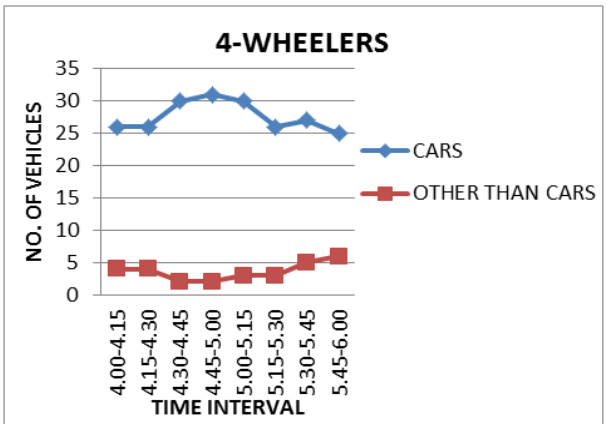

Fig.17: Parking Accumulation Curve (4 Wheelers) – Slot 3 (4.00-6.00pm).

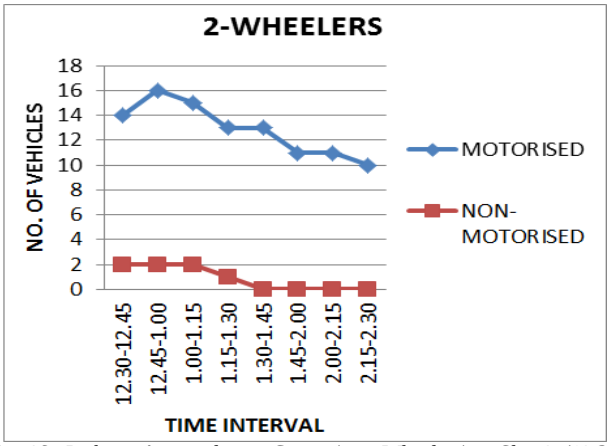

Fig. 16: Parking Accumulation Curve (two Wheelers) – Slot 2 (12.30-2.30pm).

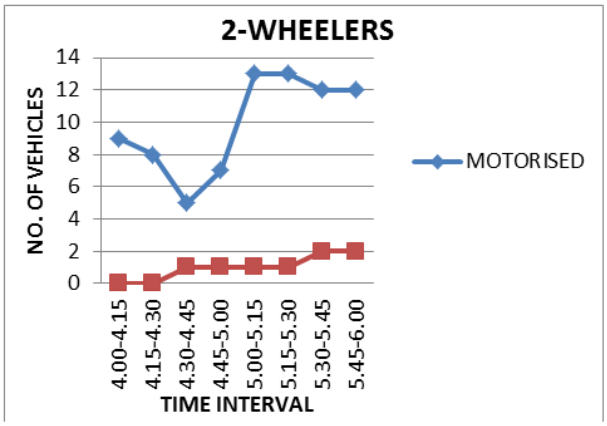

Fig. 18: Parking Accumulation Curve (2 Wheelers) – Slot 3 (4.00-6.00pm).

Table 9: Thanjavur: Off Street Parking Summary - Slot3: 4.00pm-6.00pm

Sl.No	Time Interval	Total Area (M²)	Type of Vehicles Parked:				
			2-Wheelers		3-Wheeelers	4-Wheelers	
			Motorised	Non- Motorised		Cars	Other Than Cars
1	4.00-4.15	4850	9	0	0	26	4
2	4.15-4.30	4850	8	0	0	26	4
3	4.30-4.45	4850	5	1	0	30	2
4	4.45-5.00	4850	7	1	0	31	2
5	5.00-5.15	4850	13	1	0	30	3
6	5.15-5.30	4850	13	1	0	26	3
7	5.30-5.45	4850	12	2	0	27	5
8	5.45-6.00	4850	12	2	0	25	6

3.4. Analysis and results

Parking demand was found and parking accumulation curve was plotted between the numbers of vehicles in the parking lot vs. time interval. The observations made in the selected sites during the survey are as follows:

Super Bazaar:

i) Undulations were observed over the surface of the parking space i.e. uneven flooring was observed.
ii) It was observed that 25% of the parking space was used for dumping garbage.
iii) Parking space does not possess any facility to separate vehicular area and passage space for pedestrians.
iv) The parking space doesn't have a proper bay system thereby the parking space for each vehicle doesn't satisfy the dimensions prescribed by IRC.
v) Access aisle between 2parked spaces was observed to vary between 0.9m to 1.2m.
vi) vi. Parking space does not possess proper sign boards.
vii) vii. It is a free parking space.

Palpannai:

i) The place where the concerned parking space is located is an area of very high vehicular utilisation and the area also act as a junction point connecting certain other prime areas of Trichy city.
ii) Parking space is insufficient corresponding to the demand for parking and hence spill over of vehicles outside the parking space was observed.
iii) Similar to the other parking space mentioned previously, this site also lacks a proper bay allocation system.
iv) It can be observed from the graphs that parking space is exclusively utilised only for parking two wheelers alone, this causes an inconvenient situation for other types of vehicle users in parking their vehicles.
v) Parking space possesses a manual tariff system which proves less efficient during the time of peak hours.

Brahadeeshwarar Temple, Thanjavur:

i) Lack of proper roofing system in the parking space.
ii) Occasional dumping of garbage and lack of cleanliness.
iii) Insufficient space for people to walk within the parking space.
iv) From observations of general trends, it is found that this parking space has peak load during festival times, and the load during other times is not that much. So the space should be made efficient enough to handle the sudden peak load

3.5. Suggestions to improve the efficiency of the parking lot

Following are the recommendations which can be implemented in all the three parking lots:

i) Very concrete flooring with slip resistant tiles can be constructed so as to provide a levelled parking surface with sufficient friction.
ii) Parking space should be exclusively used for vehicular parking only ensuring 100% utilisation of the space and therefore existing garbage dumping should be cleared and strict enforcement of penalties should be incorporated to avoid future dumping.
iii) Usage of precast wheel stops and a passage of 0.90m should be created for the pedestrians to walk through after parking their vehicle so that interruption of people in the vehicular area can be avoided thus preventing mishaps while parking.
iv) Installation of sign boards is mandatory so as to give a clear idea for the driver to park their vehicle in the parking bays and this avoids unnecessary confusions and traffic while parking. Efficiency and utilisation of the parking space is improved.
v. Since the parking space is surrounded by shopping complex and other commercial centres, it is advisable to restrict the utilisation of space only by cars and not by any other vehicles
v) 45, 60 AND 90degree angle bay system can be implemented as per IRC SP12-2015 at the site for effective utilisation of the parking space without any congession, traffic and other problems
vi) Bay system thus introduced must possess an area of 20-36sq.m for each bay as prescribed by IRC SP12-2015
vii) Dimensions suggested by IRC SP12-2015 for each parking bay are as follows: Width of the parking bay- 3.60m (min) to 3.90m (recommended) Length of the parking bay- 5.20m to 5.50m
viii) Access aisle of 1.2m width should be incorporated between two parking bays
ix) Since PALPANNAI is a prime area in the city of Tiruchirappalli with a heavy traffic flow the existing parking space may be expanded and can be utilised for parking of other type of vehicles in addition to two wheelers.
x) Parking space can be extended over the barren land behind the existing parking space so as to accommodate more vehicles thus preventing such spill over of vehicles outside the parking space

4. Conclusion

Real time data was obtained by conducting field survey to understand the occupancy level of the parking space at all the study locations. Based on the analysis of data it was found that the parking spaces were not utilised to the maximum possible extent in a majority of cases and in a few cases were not capable and efficient enough to meet the heavy demand. In the super bazaar parking space, the peak parking load occurred in the second slot that is between 12.30 pm and 1.30 pm. Hence possible solutions were suggested. It was also realised that with such a demand for parking spaces being generated continuously, suitable enforcements and regulations need to be periodically included in the system, to reduce congestion problems and for safe and proper parking of vehicles. Certain recommendations have been included in this study in accordance with the provisions of IRC SP 12- 2015. Proper implementation of these measures at the selected study locations will result in maximum utilization of the parking space, thus providing a comfortable parking environment for the users.

5. Acknowledgement

The authors are thankful to the Municipal Corporation, Tiruchirappalli and Thanjavur cities, and the private parking spaces for giving permission to take up the study.

References

[1] Kumari Pratibha, (2012)"Analysis of different parking space and its comparison, a thesis submitted to National Institute of Technology, Rourkela.
[2] IRC SP -12 2015, Guidelines for Parking Facilities in Urban Areas.
[3] Subramani T (2012) "Parking Study on Main Corridors in Major Urban Centre": International Journal of Modern Engineering Research, 2 (3) 742-748.
[4] Hsien-Ming (2005) "A location Model for the Allocation of the Off Street Parking Facilities", Journal of the Eastern Asia Society for Transportation Studies, 6, 1344-1353.
[5] Kadiyali L. R. (2013) Traffic Engineering and Transportation Planning, Khanna Publishers, New Delhi.

International Journal of Engineering & Technology, 7 (3.29) (2018) 75-79

International Journal of Engineering & Technology

Website: www.sciencepubco.com/index.php/IJET

Research paper

Applications of green materials for the preparation of eco-friendly bricks and pavers

B. Vamsi Krishna [1] *, E. Rakesh Reddy [2]

[1] Associate Professor Civil Department, Malla Reddy Engineering College (Autonomous), Secunderabad
[2] Assistant Professor Civil Department, Malla Reddy Engineering College (Autonomous), Secunderabad
**Corresponding author E-mail: localvamsi1987@gmail.com*

Abstract

The most basic and primary building material for construction of houses is the conventional brick. The rapid growth in today's construction industry has obliged the civil engineers in searching for more efficient and durable alternatives far beyond the limitations of the conventional brick production [1-2]. A number of studies have been made and serious steps have been taken in manufacturing of bricks from several waste materials. However, the traditional mean of bricks production which has brought hazardous impacts to the context has not yet been changed or replaced by more efficient and sustainable one [3], [4]. Most of the researches went through enhancing the clay brick quality and properties by mixing the clay with various recycled wastes as foundry sand, granite sawing waste, harbour sediments, perlite, sugarcane, baggase ash, clay waste and fine waste of boron, sewage sludge, waste glass from structural wall and other different wastes. Compile this state of the art work of manufacturing bricks in the past and the current trend in the bricks industry with respect to the raw materials, ways of manufacturing and the out- comings.
This project presents an experimental study on the utilization of waste materials which replaces clay with (Plastic covers, Ceramic Powder, Egg Shell Powder, GGBS, Silica Fume, Rice Husk Ash and Lime Powder) and Fine Aggregate with (Recycled glass, Dry Grass, Dead Leaves, Tree barks powder, Sugar cane powder, crumbed rubber) to produce eco-friendly Bricks. This project is an attempt to fill the gap of the past studies and suggest more sustainable and sophisticated methods of brick manufacturing in the future. 40 percent replacement of fine aggregate with crumbled rubber and dry grass in mortar bricks have given encouraging results, also the replacement of cement by egg shell powder at 20% has given a considerable result

Keywords: *Eco Friendly Materials; Waste Plastic; Ceramic Powder; Crumbed Rubber; Sugar Cane Powder; Dry Grass; Dead Leaves Etc.*

1. Introduction

Since the large demand has been placed on building material industry especially in the last decade owing to the increasing population, which causes a chronic shortage of building materials [5]. The civil engineers have been challenged to convert the organic wastes to useful building and construction materials. The conventional method of bricks making has caused serious environmental contamination represented by the enormous emissions of green house gases (GHG) resulted in unusual climate changes as smog, acid rain and global warming. Furthermore, energy as fuel and electricity showed a drastic consumption during the traditional manufacturing of bricks led to highly economical expenditures

Fig. 1.1: Waste Tires from Vehicles.

Fig. 1.2: Sugarcane Waste.

Fig. 1.3: Tree Bark.

Fig. 1.4: Eggshell Waste.

Fig. 1.5: Dry Grass Waste.

2. Objective of study

To understand the possibility of using waste materials such as

- Sugarcane waste as a replacement of fine aggregate in cement mortar brick in various proportions and to test the strength of the brick against various tests
- Dry grass waste as a replacement of fine aggregate in cement mortar brick and to check the possibilities of it for various applications.
- Crumbled rubber generated from tyre waste as a replacement of fine aggregate in the cement mortar brick making and identify various applications
- Tree bark waste replacement of fine aggregate in cement mortar brick and to check its strength for various strengths
- Egg shell powder replacement of cement in cement mortar brick making, and recommend those materials for various applications and as alternative eco-friendly materials for construction purpose.

3. Methodology

Crumbled Rubber: Waste rubber obtained from used and abandoned tyres have been collected. These tyres are crumbled in machine. The rubber that passes through 2.36 mm sieve is being used. The rubber should be free from deleterious materials such as stones, and other debris [6].

Fig. 3.1: Crumbled Rubber.

Dry grass: Dry grass obtained from yard waste is being collected. It is made ground into fine matter. It should pass through 2.36mm sieve and should be free from deleterious substances.

Fig. 3.2: Dry Grass Powder.

Sugarcane waste: Bagasse waste is being collected and made into fine particles free from deleterious substances. The material should be homogeneous and pass through 2.36mm sieve.

Fig. 3.3: Sugarcane Waste.

Tree bark: Tree bark waste is collected from trees and ground into fine powder that passes through 2.36mm sieve. It should be free from debris and deleterious material

Fig. 3.4: Tree Bark Aggregate.

Egg shells: Egg shells are collected from various sources such as domestic and commercial sources. These are neatly washed and air dried for two days. They are ground into fine powder in a mixer. The egg shell should pass 80 micron sieve [1].

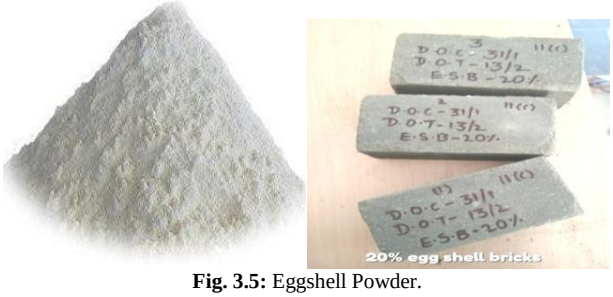

Fig. 3.5: Eggshell Powder.

4. Test on bricks

Compression strength test
The bricks should be tested in accordance with the procedure laid in IS 3495 (Part-2): 1976.Crushing strength of bricks is determined by placing brick in compression testing machine. After placing the brick in compression testing machine, apply load on it until brick breaks. Note down the value of failure load and find out the crushing strength value of brick.
Efflorescence Test on Bricks
The bricks should be tested in accordance with the procedure laid in IS: 3495 (Part-2): 1976. A good quality brick should not contain any soluble salts in it. If soluble salts are there, then it will cause efflorescence on brick surfaces. To know the presence of soluble salts in a brick, placed it in a water bath for 24 hours and dry it in shade. After drying, observe the brick surface thoroughly. If there is any white or grey color deposits, then it contains soluble salts and not useful for construction.
Water absorption test
The bricks should be tested in accordance with the procedure laid in IS: 3495 (Part-2): 1976
after immersion in cold water for 24 hours, shall have water absorption not more than one-sixth of the dry weight of brick.
Cement Brick Specifications

- The bricks shall be of first class, regular in shape, size and color.
- The bricks should be free from flaws, cracks and lumps of any kind.
- Shall have minimum Compressive Strength of 10.5N/mm2.
- The bricks shall not absorb the water more than one sixth of the weight of the brick.
- The sand used shall be medium coarse, clean, sharp, free from clay, mica and other organic matter.

5. Results and discussion

Table 5.1: Test Results of Crumbled Rubber

S. No	Description	Density KG/m3	Compressive strength MPa	Weight KG	Water Absorption (%)	Efflorescence	Crack
1	Fine Aggregate	1450	17.8	3.37	3.91	No	High
Crumbled Rubber							
a.	20% Replacement	393	10.97	3.315	0.91	No	High
b.	40% Replacement	393	14.64	3.19	0.92	No	Moderate
c.	60% Replacement	393	7.56	3.225	0.65	No	Moderate
d.	80% Replacement	393	6.9	2.73	0.74	No	Low
e.	100% Replacement	393	3.14	2.62	3.03	little	Low

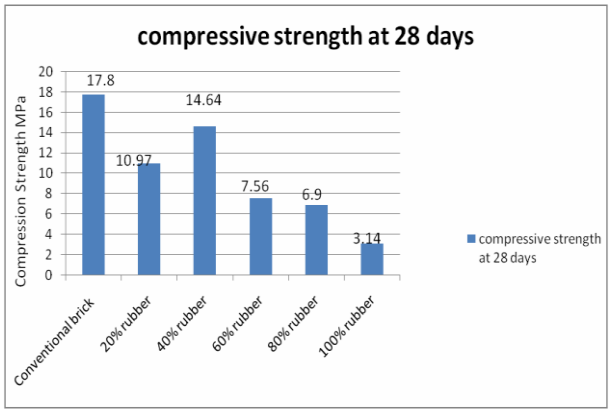

Graph. 5.1: Test Results of Crumbled Rubber.

Table 5.2: Test Results of Dry Grass

S.No	Description	Density kg/m3	Compress save strength MPa	Weight kg	Water sorption (%)	ab-Efflorescemcee	Crack
Dry Grass							
a.	20% Replacement	55	9.64	3.26	5.74	No	Moderate
b.	40% Replacement	55	12.39	3.08	4.03	No	Moderate
c.	60% Replacement	55	0.78	2.64	16.37	No	High
d.	80% Replacement	55	0.89	1.99	-	-	-
d.	100% Replacement	55	_	1.66	-	-	-

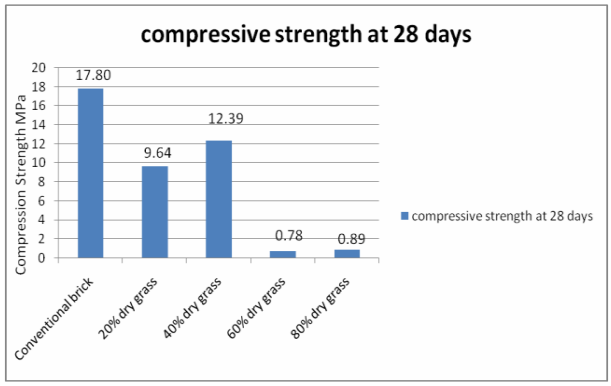

Graph. 5.2: Test Results of Dry Grass.

Table 5.3: Test Results of Sugarcane Waste

S. No	Description	Density g/m3	Compress sive strength MPa	Weight kg	Water sorpti on (%)	ab-Efflo-rescence	Crack
Sugarcane							
a.	20% Replacement	47.24	2.6	3.19	4.5	No	High
b.	40% Replacement	47.24	1.05	2.9	13.53	No	Moderate
c.	60% Replacement	47.24	1.19	2.57	11.34	little	Low
d.	80% Replacement	47.24	1.56	2.15	13.72	little	Low

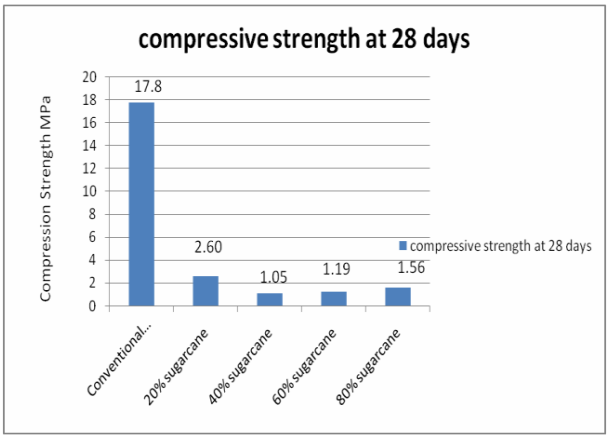

Graph. 5.3: Test Results of Sugarcane Waste.

Table 5.4: Test Results of Tree Bark.

S. No	Description	Densityk g/m3	Compress sive strength MPa	Weight	Water absorption	Efflorescence	Crack
Tree bark							
1	20% replacement	347	5.17	2.79	14.13	No	High
2	40% replacement	347	-	-	-	No	High

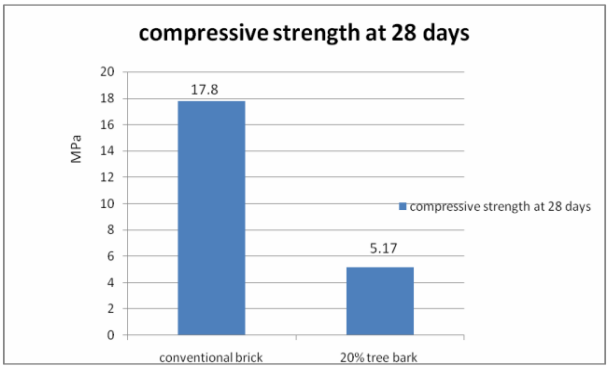

Graph. 5.4: Test Results of Tree Bark.

Table 5.5: Test Results of Egg Shell Powder

S. No	Description	Densityk g/m3	Compress sive strength MPa	Weight	Water absorption	Efflo-rescence	Crack
Egg shell							
a.	20% replacement	1150	8.94	3.26	0.89	No	Moderate
d.	40% replacement	1150	5.17	2.76	3.12	Little	High

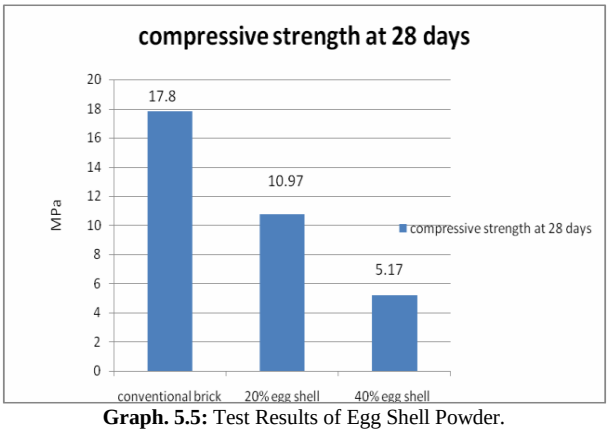

Graph. 5.5: Test Results of Egg Shell Powder.

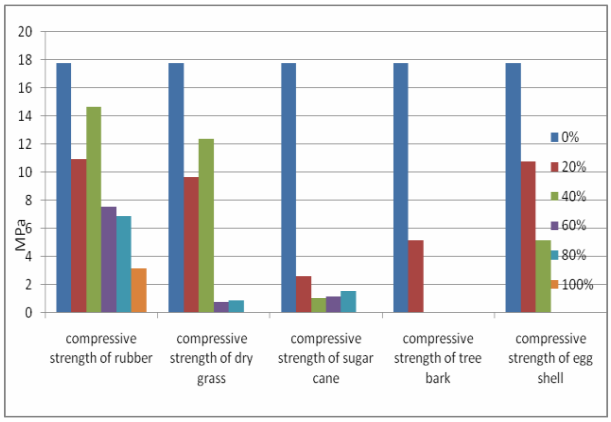

Graph. 5.6: Comparison of Conventional Brick Strength with Compressive Strength of Various Compositions of All the Bricks.

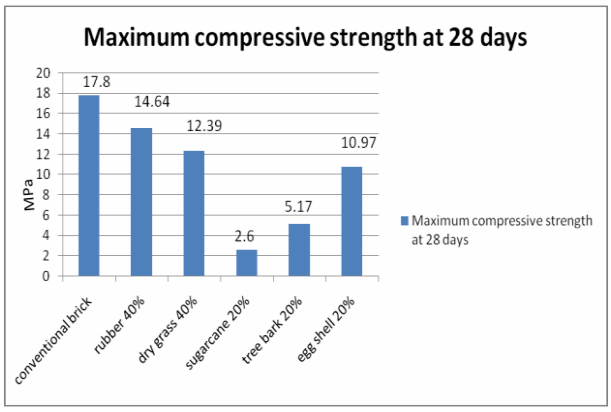

Graph. 5.7: Comparison of Conventional Brick Strength with Maximum Compressive Strength of Different Materials.

6. Conclusion

Tests Performed: Compressive Strength, Absorption Test, Efflorescence Test, Falling weight Test was performed on Eco-Friendly Bricks.

From this study the effective utilization of eco- friendly waste materials have been identified and were replaced in the cement brick mixture as fine aggregate and cement. At present Crumbled rubber, Dry Grass, Dry sugarcane pulp, Tree bark were used in replacing fine aggregate in various proportions like 20%, 40%, 60%, 80% and 100%. Egg shell powder was used in replacing cement with 20% and 40%. On the Basis of the test results the following conclusions are drawn. These conclusions also include structural applications of secondary type from medium to low strength requirements, benefiting from other features of this type of brick and pavers.

1) The compressive strength of crumbled rubber brick with 40% replacement of fine aggregate with crumbed rubber is 14.64 N/mm2. It is almost equal to the strength of conventional cement brick (17.8 N/mm2) on 28th day.
2) The compressive strength of Dry grass brick with 40% replacement of fine aggregate with dry grass is 12.39 N/mm2. It is almost equal to the strength of conventional cement brick (17.8 N/mm2) on 28th day.
3) The compressive strength of sugar cane brick in various proportions were not at all encouraging. Therefore, using of sugarcane pulp in brick manufacturing is not recommendable.
4) The compressive strength of Tree bark brick in various proportions were not at all encouraging. Therefore, using of tree bark in brick manufacturing is not recommendable.
5) The compressive strength of Egg Shell brick with 20% replacement of cement with eggshell powder is 11.00 N/mm2. It is a recommendable value.

From the test results, it is found that the compressive strengths of eco-friendly bricks, Crumbled rubber brick, Dry grass brick, Egg

Shell brick showed acceptable aesthetics. The use of these eco-friendly materials resulted in an appreciable reduction of block unit weight from 3.37 kg/m3 to 2.7 kg/m3, which is recommended for using as a construction material like brick and pavers.

7. Future scope of study

Only a few number of engineering properties of eco-friendly bricks have been examined in this study, Other properties such as skid resistance, abrasion resistance, deformation, volume change, fatigue resistance, Flexural test and environmental impact must be examined for comprehensive evaluation of this new eco- friendly materials.

Overall, Eco-friendly bricks have been observed to show a more inferior performance than conventional cement bricks in compression, water absorption, Falling weight and efflorescence, but showed an encouraging result in compression. Thus, crumbled rubber bricks have a great potential to be used for pedestrian pavements, flooring of indoor games. The replacement of fine aggregate with crumbled rubber which is produced from waste tires will reduce the consumption of primary aggregates and produce a high value use for the wastes

References

[1] A Review Study Of Egg Shell Powder As A Cement Replacing Material In Concrete, International Journal of Latest Research In Engineering and Computing (IJLREC) Volume 5, Issue 4, Page No. 6-9 July- August 2017,Amarnath Yerramala.

[2] Manufacturing of Bricks in the Past, in the Present and in the Future: A state of the Art Review, International Journal of Advances in Applied Sciences (IJAAS) Vol. 2, No. 3, September 2013, pp. 145~156, Alonso.

[3] Utilization of Waste Materials in Preparation of Eco Friendly Brick, IJSRD - International Journal for Scientific Research & Development| Vol. 5, Issue 03, 2017 | ISSN (online): 2321-0613.

[4] Development of Bricks from Waste Material: A Review Paper, Australian Journal of Basic and Applied Sciences, 7(8): 812-818, 2013, Edward Allen, Robert Hallon. Fundamental of residential construction (3rd edition), 672 pages. John Wiley &Sons, San Francisco, USA, 2011.

[5] Roy chudley, Roger Greeno. Construction Technology (4thedition), 634 pages. Prentice Hill, New Jersey, USA, 2000.

[6] Jeorge J. Venta, P.Eng. "Life cycle analysis of brick and mortar products", the ATHENATM Sustainable Material Institute, Canada, Ottawa, 1998.Institute, Canada, Ottawa, 1998.

[7] Studies on Properties of Egg Shell and Fish Bone Powder Filled Polypropylene ì, American Journal of Polymer Science 2012, 2(4): 56-61. 5. Praveen Kumar R.

[8] Experimental Study on Partial Replacement of Cement with Egg Shell Powderî, International journal of innovations.

[9] D.G. Roy, S.P. Mehrotra and P.C. Kapur, "lightweight masonry blocks from fly ash pellets", October, Elsevier, 63-64, 11 (1984).

[10] Dr.R.Vasudevean and S.Rajasekaran "utilization of waste plastics modified bitumen" (2007).

[11] 11. Er. Rinku kumar, er. Naveen hooda "an experimental study on properties of fly ash bricks", international journal of research in aeronauticaland mechanical Engineering, volume2, page56-57, 9 September (2014).

[12] Guidelines for The use Of Waste plastic in hot Bituminous mixes(dry process)In wearing courses IRC:SP:98:2013 JitingXie , Obada Kayali,

[13] Effect of superplasticiser on workability enhancement of Class F and Class C fly ash- based geopolymers, Elsevier, Construction and Building Materials 122 (2016) 36– 42.Edward Allen, Robert Hallon. Fundamental of residential construction (3rd edition), 672 pages. John Wiley &Sons, San Francisco, USA, 2011.

International Journal of Engineering & Technology, 7 (3.29) (2018) 16-20

International Journal of Engineering & Technology

Website: www.sciencepubco.com/index.php/IJET

Research paper

Real time implementation and validation of lean implementation model for sustainability (LIMS) in medium scale industry

S. Gunasekharan [1] *, D. Elangovan [2], S. Sudhakara Reddy [1], M. Maheswari [1]

[1] Professor, Malla Reddy Engineering College (A), Secunderabad
[2] Professor, PSG Institute of Technology & Applied Research, Coimbatore
**Corresponding author E-mail: guna03gm@gmai.com*

Abstract

Lean manufacturing is a strategic tool, which is used to cut down waste and to improve the efficiency of an organization and helps the organization to sustain in the competitive environment. Implementation of lean systems in organization results in reduce energy consumption, waste generation, and hazardous materials used while also building the companies' images as socially responsible organizations. Several research efforts discussed in the literature indicate that lean companies show significant environmental improvements by being more resource and energy efficient. Lean systems are associated with waste reduction techniques. In foreign, many industries have started implementing these concepts and they are getting good results. In India, companies are facing problems in implementing lean concept. Critical success factors for lean system implementation in Indian medium scale manufacturing industries has been identified to overcome it. The factors are grouped into different levels by Interpretive Structural Modelling (ISM). A lean implementation model has been developed for medium scale industry and named as 'LIMS'. This paper investigates the implementation and validation of the LIMS through the real time implementation in a medium scale industry.

Keywords: *Lean Manufacturing; ISM; LIMS; Critical Success Factor (CSF).*

1. Introduction

Lean manufacturing or lean production, often simply "lean", is a systematic method for the elimination of waste or muda within a manufacturing system (Upadhye et al., 2010; Ping-yu, Yang, 2009). Lean also takes into account waste created through over burden or muri and waste created through unevenness in workloads or mura (Shah, Rachna, and Peter T. Ward, 2007). The seven types of wastes are defined as Overproduction, Waiting, Transportation, Inventory, Over Processing, Motion and Defects. Constant effort at cost reduction is required to maintain continuous profits in manufacturing. The prime way to reduce costs is to produce only those products determined by sales in a timely fashion, to restrain excessive manufacturing and to eliminate all waste in manufacturing methods (Achanga, P., et al., 2005
Diaz-Elsayed, Nancy, et al., 2013). There are various ways to analyze and implement cost reduction, from the start of designing all the way through to manufacturing and sales (Cezar Lucato and Wagner, 2014; Fullerton, Rosemary R et al., 2003). One of the goals of lean manufacturing is to locate waste in each process and then eliminate it. It is possible to uncover a very large amount of waste by observing employees, equipment, materials and organization on the actual production line from the perspectives of the process itself and the actual work involved (Bhasin, Sanjay, and Peter Burcher, 2006). Some types of waste are obvious, but others are hidden. Waste never improves value; it only increases cost. The thorough elimination of waste leads to greater employee self-respect and to major cost reductions by preventing unneeded losses (Browning, Tyson R., and Ralph D. Heath, 2009).

2. Lean tools

Lean tools that are assist in the identification and steady elimination of waste. As waste is eliminated, quality improves while production time and cost are reduced (Ramesh V. Narang). A non-exhaustive list of such tools are Just In-Time (JIT), Five S (5S) (Rojasra, P. M., and M. N. Qureshi, 2013), Bottleneck analysis, Continuous flow, Value Stream Mapping (VSM), Single Minute Exchange of Dies (SMED), Kanban or Small batch sizes, Kaizen, Poke-a-Yoke or Error-proofing and Total Productive Maintenance (TPM) (Samson Danny and Mile Terziovski, 1999; Cua at al., 2001).

2.1. Benefits of lean manufacturing

The benefits of lean manufacturing are evident in many industries throughout the world. Industries report improved product quality, reductions in cycle time, reduced work in progress (WIP), improved on-time deliveries, improved net income (McKone et al., 2001), decreased costs, improved utilization of labor, reduction in inventories, quicker return on inventory investment, higher levels of production, increased flexibility, improved space utilization, reduction in tool investment, a better utilization of machinery, stronger job focus and better skills enhancement. Typical results reported (Zimmer 2000; Pavnaskar, Gershenson et al. 2003) after successful lean implementation indicates:

- 50% or greater increases in capacity in current facilities
- 80% reduction in floor space
- 50% improvement in quality

- 95% machine availability
- 80–90% reduction in changeovers
- 60% reduction in cycle times

Typical characteristics of a lean industry include integrated single piece flow; defect prevention; production pill; continuous waste reduction; flexible team based work; active involvement and close integration with suppliers (Womack and Jones 2003). Some of the very common benefits include

- Decreased lead times for production.
- Reduced inventories.
- More robust process.
- Improved knowledge management.

From Toyota Production System (TPS) to lean industry and lean supply chain practitioners can easily find plenty of tools to improve projects. However, applying all lean tools at once only leads to chaos. Selecting the right tools for their current condition becomes the key to success in lean implementation. This paper deals about the development of generic lean model for lean implementation and enlighten the real time validation of the lean model in a medium scale industry to improve the productivity.

3. Development of lean implementation model for sustainability in medium scale industries

The representation of real world in terms of either graph or mathematical equations or structure is known as modeling. The modeling is classified into three types based on their degree of concept related with the real one. They are,

- Iconic model like model airplane or train
- Analogous model such as chart, graph, map and network diagram
- Symbolic model such as mathematical equation
- This paper deals about the analogous modeling of lean manufacturing process.

3.1. Lean modeling

Lean modeling is a strategy used in the industry to eradicate the waste systematically during the process to fulfill the customer needs. The customer satisfaction will make the industry to get more returns and brand name (Marasini et al., 2014). The goal of the lean model is to maintain the customer for longer run (Bergmiller, Gary G., and Paul R. McCright, 2009). In all lean implementation involves basically three practices such as just-in-time inventory, total quality management and continuous improvement to reduce the waste and improve the quality with compact price.

3.2. Development of generic lean model for medium scale industries

It is a difficult assignment to implement the new concept in medium scale industries in India because of unskilled employee who hesitate to switch over to a new methodology and environment (Chikhalikar, Pratik and Suman Sharma, 2015; Nellore, Rajesh ET al.1999). This work proposes an easy to implement and low cost model for medium scale industries and it is named as Lean Implementation Model for Sustainability (LIMS) and is shown in Figure 1.

As a first step, the entire process is subdivided into six major sections to develop a lean model as follows,

- Identification of critical success factors (CSF)
- Ranking and prioritization of CSF based on weightage determined by using ISM technique
- Analysis of current status for lean implementation
- List and summarize the feasible CSF for lean implementation
- Initialize the lean implementation for each CSF
- Pilot analysis, monitoring and control

3.3. Identification of critical success factors (CSF)

The critical success factors which are the barriers for lean implementation in medium scale industries to be identified based on the field survey and experts' opinion. Then prioritize the identified critical success factors by using any one the MCDM techniques.

3.4. List and summarize the feasible csf for lean implementation

The status need to be assessed before implementation of lean. It can be done through getting feedback from management regarding financial constraints, employee regarding adaption to new environment, customer regarding the satisfaction level and supplier about the quality raw material
(Flynn et al., 2004). Based on the feedback received, it is possible to ascertain the current situation of the industry and able to list the problems in it. The problems can be identified through the feedback from the management, employee, customer and supplier. Then the analysis needs to be done to find out the causes for each problem. There are several tools available for analysis the causes of the problems like,

- Cause and effect diagram
- Flow diagram
- Histogram
- Pareto chart
- Scatter diagram
- Control charts and
- Trend chart

Once the problems are identified, prioritization of the problems needs to be done immediately for improvement.

3.5. Pilot analysis monitoring and control

Now it is the time to implement the lean concepts instead of traditional practices. It is well known that there are a lot of challenges and barriers during implementation and it should be addressed properly. First and foremost step is to train the employees for a day or a week according to the feasibility of the industry in each level through lean consultants for a better implementation. The lean implementation process will not end merely at execution level and it needs continuous monitoring and corrective actions at each level to reach the target level. It can be executed by statistical quality control (Flynn et al, 1994; Narasimhan et al., 2006).

4. Real time implementation of LIMS model

The proposed LIMS model has been implemented in MSI-X, Hosur to validate it. MSI-X is manufacturing locomotive products like gear box, gear wheel, piston rod and connecting rod with the support of 40 employees. The Table 1 shows the consolidation of six month report of production database.

Table 1: Consolidated Report of MSI-X before Lean Implementation

Description	Jun-2014	Jul-2014	Aug-2014	Sep-2014	Oct-2014	Nov-2014	Six Month Avg.
Avg. units of production/ day	822	796	790	824	812	820	810.67
Avg. units accepted in first level/ day	720	714	722	723	752	740	728.50
% of accepted units in first level/ day	87.59	89.70	91.39	87.74	92.61	90.24	89.86
Average units rejected/ day	102	82	68	101	60	80	82.17
Average units of rework/ day	12	8	5	14	6	9	9
Average units of scrap/day	90	74	63	87	54	71	73.17

Average of finished units/day	732	722	727	737	758	749	737.50
% of finished units in final stage/day	89.05	90.70	92.03	89.44	93.35	91.34	90.97

From the Table 1 it is observed that the average productivity per day is 810 units of gear box, gear wheel, connecting rod and piston rod. Among the total production 728 units are accepted and 82 units are rejected in the first level. In the rejected quantity 9 units have undergone for rework and the average finished products at the final become 737 units and the level of productivity is 90.97%. The month wise report of average units of production, finished products and scrap per day before lean implementation is depicted in Figure 2. The average cost for raw material per month is rupees four crores.

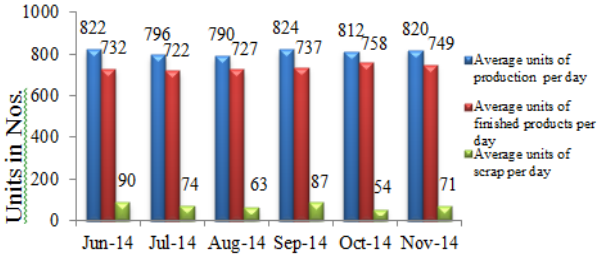

Fig. 2: Monthly Reports on Production, Finished Products and Scrap before Lean Implementation.

4.1. Lean implementation for each CSF

From the above discussion, it is clear that the average productive rate per day of the industry is 90.97 %. It is considerably low and it should be addressed properly through lean implementation. The lean tools chosen and method of implementation is discussed in the succeeding sections.

The lean implantation process started in MSI-X from the month of December 2014. To implement the above said lean concepts and get practiced by the employees, it has taken four months from December 2014 to March 2015. The monitoring and control has taken place at every step and remedial actions are taken then and there suitably. The improvement of the industry has measured from the month of April 2015 in terms of its productivity as shown in Table 2.

Table 2: Consolidated Report of MSI-X after Lean Implementation

Description	Apr-2015	May-2015	Jun-2015	Jul-2015	Aug-2015	Sep-2015	Six Month Avge
Avg. units of production/day	831	802	820	815	821	818	817.83
Avg. units accepted in first level /day	742	738	765	794	798	795	772.00
% of accepted units in first level/day	89.29	92.02	93.29	97.42	97.20	97.19	94.40
Avg. units rejected/day	89	23	55	21	23	23	39.00
Avg. units of rework/day	10	4	12	0	3	2	5.17
Avg. units of scrap/day	79	19	43	21	20	21	33.83
Avg. of finished units/day	752	742	777	794	801	797	777.17
% of finished units in final stage/day	90.49	92.52	94.76	97.42	97.56	97.43	95.03

From the Table 2 it is observed that the average productivity per day is 817 units of gear box, gear wheel, connecting rod and piston rod. Among the total production 772 units are accepted and 39 units are rejected in the first level. In the rejected quantity [5] units have undergone for rework and the average finished products at the final become 777 units and the level of productivity is 95.97 %. The month wise report of average units of production, finished products and scrap per day after lean implementation is depicted in Figure 3.

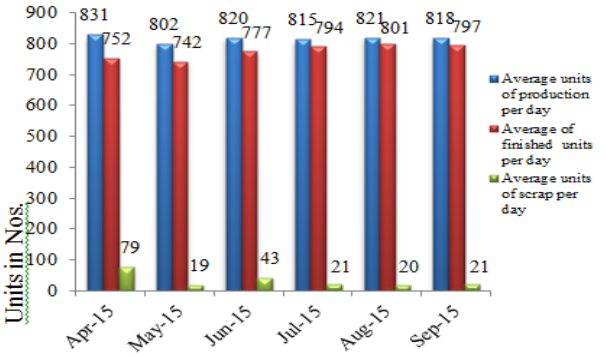

Fig. 3: Monthly Reports on Production, Finished Products and Scrap after Lean Implementation.

It is found happy that the production status of MSI-X has shown a better improved after lean implementation. It is evident from the Table 3 and Figure 4 that the average production unit per day has improved from 810.67 units to 817.83 units due to lean implementation. Similarly there is a remarkable improvement in the level of units accepted per day as 94.40 % from 89.86 %. There is a reduction in units considered for rework is reduced to five units per day. At the same time, the scrap is also dropped to 33.83 units per day which is a significant improvement than the previous situation. Due to the above said factors, the productivity of the industry has been improved considerably by five percentages after the lean implementation as shown in Table 3 and Figure 5.

Table 3: Production Status of MSI-X before and after Lean Implementation

Description	Six Month Average	
	Before Implementation	After Implementation
Average units of production per day	810.67	817.83
Average units accepted in first level per day	728.50	772.00
% of accepted units in first level per day	89.86	94.40
Average units rejected per day	82.17	39.00
Average units of rework per day	9	5.17
Average units of scrap per day	73.17	33.83
Average of finished units per day	737.50	777.17
% of finished units in final stage per day	90.97	95.03

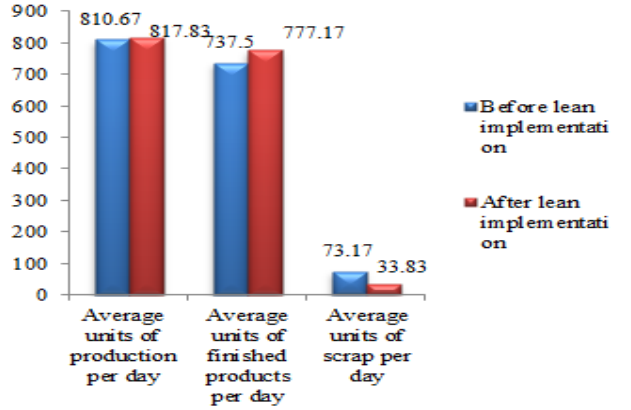

Fig. 4: Production Status of MSI-X before and after Lean Implementation.

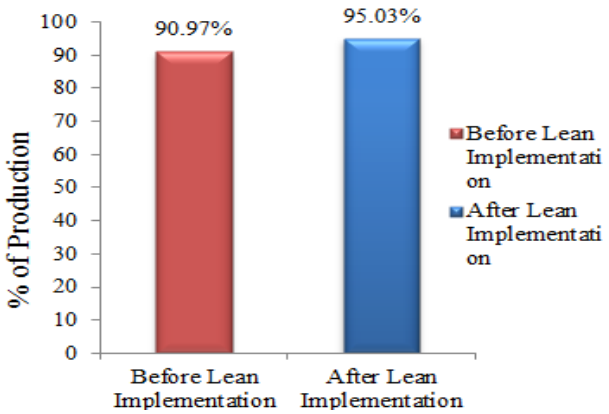

Fig. 5: Productivity Rate before and after Lean Implementation.

5. Conclusion

The development and real time implementation of lean manufacturing model in medium scale industry has been proposed in this paper. The generic lean modeling named LIMS has been proposed for implementing the lean concept in the medium scale industries. The developed model has divided into six major sections. The lean tools like Five S, JIT, Kaizen, six sigma and poke-a-yoke have been suggested for economical and easy implementation in the medium scale industries. As suggested in LIMS model, the current status of the industry has been analyzed and the level of productivity has 90.97 %. Based on the analysis, it has been identified that strong management and leadership, education and training, employee trust, flexible workforce and supplier relationship and involvement as the major critical success factors for the industry. The preferred lean tools such as Five 'S', Kaizen, SMED and JIT have been implemented to improve the productivity.

During the implementation the proper training has been organized for the people working in different level to improve the leadership skill for managers and the supervisors, to imbibe the lean concept and skill oriented training among the workers. To enhance the employee trust the reward system has been implemented through Kaizen and it has helped small improvements. The relationship among the industry and the supplier has strengthened through JIT concept. The flexible work force situation has been implemented by developing cross functional skills. After the lean implementation, the analysis has been made to measure the productivity rate and it became as 95.97 %. The observed results are found to be encouraging and provide appreciable improvements in the productivity rate.

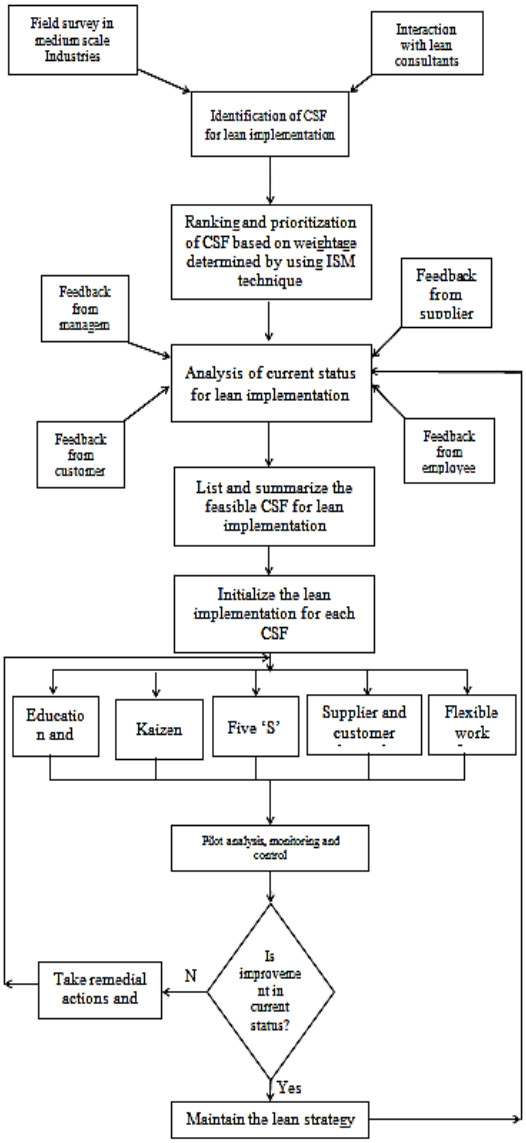

Fig. 1: Lean Implementation Model for Sustainability (LIMS).

References

[1] Achanga, Pius Coxwell, et al. "Lean manufacturing for SMEs: enabling rapid response to demand changes." (2005).

[2] Bergmiller, Gary G., and Paul R. McCright. "Lean manufacturers' transcendence to green manufacturing." Proceedings of the 2009 Industrial Engineering Research Conference. Vol. 30. 2009.

[3] Bergmiller, Gary G., and Paul R. McCright. "Parallel models for lean and green operations." Proceedings of the 2009 Industrial Engineering Research Conference, Miami, FL. 2009.

[4] Bhasin, Sanjay, and Peter Burcher. "Lean viewed as a philosophy." Journal of manufacturing technology management 17.1 (2006): 56-72.

[5] Browning, Tyson R., and Ralph D. Heath. "Reconceptualizing the effects of lean on production costs with evidence from the F-22 program." Journal of Operations Management 27.1 (2009): 23-44.

[6] Cezar Lucato and Wagner, "Performance evaluation of lean manufacturing implementation in Brazil." International Journal of Productivity and Performance Management 63.5 (2014): 529-549.

[7] Chikhalikar, Pratik, and Suman Sharma. "Implementation of Lean Manufacturing in an Engine Manufacturing Unit—A Review." International Journal of Mechanical Engineering and Robotics Research 4.1 (2015): 404.

[8] Cua, Kristy O., Kathleen E. McKone, and Roger G. Schroeder. "Relationships between implementation of TQM, JIT, and TPM and manufacturing performance." Journal of Operations Management 19.6 (2001): 675-694.

[9] Diaz-Elsayed, Nancy, et al. "Assessment of lean and green strategies by simulation of manufacturing systems in discrete production environments." CIRP Annals-Manufacturing Technology 62.1 (2013): 475-478.
[10] Flynn, Barbara B., Roger G. Schroeder, and Sadao Sakakibara. "A framework for quality management research and an associated measurement instrument." Journal of Operations management 11.4 (1994): 339-366.
[11] Fullerton, Rosemary R., Cheryl S. McWatters, and Chris Fawson. "An examination of the relationships between JIT and financial performance."Journal of Operations Management 21.4 (2003): 383-404.
[12] Marasini, Bikash, et al. "A model for implementation of lean manufacturing in Indian small scale industries." International Journal of Science, Engineering and Technology Research (IJSETR) 3.5 (2014).
[13] McKone, Kathleen E., Roger G. Schroeder, and Kristy O. Cua. "The impact of total productive maintenance practices on manufacturing performance." Journal of operations management 19.1 (2001): 39-58.
[14] Narasimhan, Ram, Morgan Swink, and Soo Wook Kim. "Disentangling leanness and agility: an empirical investigation." Journal of operations management 24.5 (2006): 440-457.
[15] Nellore, Rajesh, Jean-Jacques Chanaron, and Klas Eric Söderquist. "Lean supply and price-based global sourcing—the interconnection." European Journal of Purchasing & Supply Management 7.2 (2001): 101-110.
[16] Nellore, Rajesh, Klas Söderquist, and Kjell-Åke Eriksson. "A specification model for product development." European Management Journal 17.1 (1999): 50-63.
[17] Ping-yu, Yang. "The barriers to SMEs implementation of lean production and its countermeasures–based on SMEs in Wenzhou." Reform Strategy 1 (2009): 148-151.
[18] Rojasra, P. M., and M. N. Qureshi. "Performance improvement through 5S in small scale industry: a case study." International Journal of Modern Engineering Research 3.3 (2013): 1654-1660.
[19] Roos, Daniel, James P. Womack, and Daniel Jones. "The Machine That Changed the World: The Story of Lean Production." Rawson/Harper Perennial, New York (1990).
[20] Samson, Danny, and Mile Terziovski. "The relationship between total quality management practices and operational performance." Journal of operations management 17.4 (1999): 393-409.
[21] Shah, Rachna, and Peter T. Ward. "Defining and developing measures of lean production." Journal of operations management 25.4 (2007): 785-805.
[22] Upadhye, Nitin, S. G. Deshmukh, and Suresh Garg. "Lean manufacturing system for medium size manufacturing enterprises: an Indian case."International Journal of Management Science and Engineering Management5.5 (2010): 362-375.

International Journal of Engineering & Technology, 7 (3.29) (2018) 26-30

International Journal of Engineering & Technology

Website: www.sciencepubco.com/index.php/IJET

Research paper

Hardware realization of DVR with 27 level multi carrier PWM based MLI

M. Maheswari [1] *, S. Thangavel [2]

[1] Professor and Head, Department of EEE, Malala Reddy Engineering College(A), Secunderabad, India
[2] Professor and Head, Department of EEE, K. S. Rangasamy College of Technology, Thiruchengode, India
**Corresponding author E-mail: maheswarikgd@gmail.com*

Abstract

The quality of the electrical power delivered to consumers is heavily affected by the power electronics based controllers, introduced in both domestic and industrial sectors, which in turn results in malfunctioning of equipment or eventual damage. Series compensators, Shunt compensators and series-shunt compensators are some of the strategies applied to address the power quality issues effectively. In this work a series compensating device, viz. 27 level-cascaded multilevel inverter based Dynamic Voltage Restorer (DVR) with multicarrier SPWM technique is proposed to mitigate voltage swells and voltage sags. The PWM technique used in this work is Alternate Phase Opposition PWM (APODPWM), which is one of the vertical arrangement multicarrier sinusoidal pulse width modulation techniques, to control the cascaded H-bridge inverter. The single-phase version of the proposed system is simulated to verify the effectiveness in addressing voltage issues and it is found that the obtained simulation results are satisfactory. The THD is found to be 3.40%, which is well below IEEE standards apart from considerable improvement in response time. The prototype of the proposed model is developed and the pic-micro-controller PIC16F887 is employed to implement the APODPWM. The experimental results obtained from the prototype are compared with the respective simulation results and they match with reasonable accuracy.

Keywords: *Multi Level Inverter (MLI); Alternate Phase Opposition Disposition Pulse Width Modulation (APODPWM); Dynamic Voltage Restorer (DVR); Sinusoidal Pulse Width Modulation (SPWM).*

1. Introduction

The quality of power depends mainly on the quality of voltage supplied to the customer and therefore, a reasonable maintenance of voltage quality assures power quality. However, the normal operations in industries such as starting/stopping of induction motors, energizing large capacitor banks and symmetrical/unsymmetrical line faults in power system cause voltage sags and swells, resulting the deterioration of voltage quality at the respective Point of Common Coupling (PCC). The sensitive loads connected to that PCC are heavily affected by the voltage degradation. Tripping of adjustable speed drives (ASD) and faulty operation of PLCs in automated industries are certain unwanted consequences of voltage sag and swell, resulting adverse monetary impact [1] [2] [3] [4].

DVR is one of the cost-effective solution to mitigate voltage issues such as voltage sags, swells and outages. A DVR system comprises of a PWM voltage source inverter (VSI), a series injecting transformer, a control circuitry and a DC source. Among all the components, VSI is the major component of a DVR [8] [9] [10] [11] [12]. The closeness of the output of the DVR towards the pure sine wave and the THD are decided by the number of levels in the VSI [5] [6] [7]. In this proposed work, a cascaded H-bridge multi-level inverter (MLI) configuration with 27 level is used as VSI in DVR with 13 full bridge configurations. The selection of proper modulation technique, modulation index and frequency ratio are key aspects for better performance of the VSI. Fundamental frequency modulation method is preferred in this work along with multi-carrier SPWM technique to reduce the switching losses and to improve THD [13] [14] [15].

Simulation of Single Phase DVR

Figure 1 shows the simulation model of the proposed single phase DVR in MATLAB-Simulink. The single-phase voltage source block acts as the generating station and transmission line is represented by a RLC series branch. The load is simulated by a series RL circuit. A series connected two winding transformer block with 1:1 ratio acts as injection transformer. A comparator module is used to compare the line voltage with reference voltage and to generate the error signal. This error signal is fed to the PI controller and the output of the PI controller is the modulating or reference signal for all the 26 comparators of the PWM generator. The repeating sequence block is used to generate the required 26 triangular carrier signals and their levels are shifted vertically by setting the corresponding block parameters and the phase difference between any two adjacent signals are 180°. Further, the carrier signals are so arranged that the peak magnitude of the lower signal is the lower level of its immediate upper signal. The output of any of the 26 comparators goes high once the magnitude of the reference signal is greater than that of the corresponding carrier signal. The 26 carrier signals are divided into two groups, separated by the reference line, such that the upper 13 signals fall in first group and the lower 13 signals in the second group and the reference line align with the x axis of the modulating signal. The outputs of the comparators serve as the triggering signals for all the 13 bridges of the MLI block. If the pair S_i^1 and S_i^4 of i^(th)bridge is excited by i^th carrier of first group the same i^th carrier from second group is used to trigger S_i^2 and S_i^3 pair of the same bridge. The output of the MLI Block, which is in fact the compensating voltage, is fed to the power line through the injection transformer.

To introduce the voltage sag in the power line, an inductor of larger value is connected through a switch such that the closing of the switch at any time results in a voltage sag in the power line. The swell is introduced through a suitably programmed three phase programmable voltage source by tapping the output of any one of the three phases. Voltage measurement blocks and scopes are added at required points to capture the dynamics of the parameters such as line voltage, load voltage, injected voltage etc. The values assigned to various block parameters are given in Table 1.

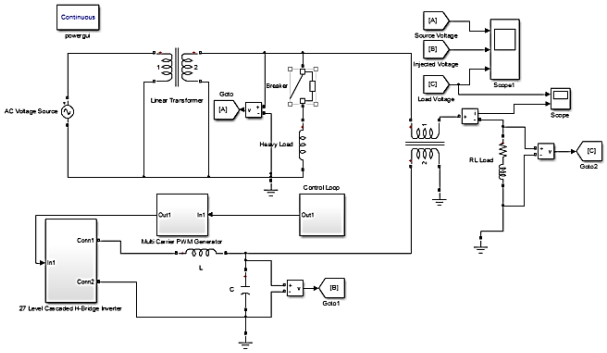

Fig. 1: Simulation Block Diagram of Single Phase DVR.

Table 1: Simulation Parameters of Various Block

S. No.	Name of the Block	Parameter	Value
1	Single Phase Voltage Source	V_{rms}	230 Volts
		Frequency	50 Hz
2	Transmission Line	Resistance	1.6 Ω
		Inductance	1.08 mH
3	Load	Resistor	100Ω
		Inductor	20mH
4	PI Controller	K_P	1.2
		K_I	0.5
5	Switching Device in MLI	Internal Resistance	1 mΩ
		Snubber Resistance	100 kΩ
		Snubber Capacitance	∞
6	Injection Transformer	Ratio	1:1
		Power	1.5 kVA
		Frequency	50 Hz
7	Triangular Carrier Signals	Frequency	12 kHz
		Peak Amplitude	5 Volts
8	Inductance for voltage sag	--	5 H
9	Three phase programmable voltage source to introduce swell	Phase Voltage	230 Volts
		Frequency	50 Hz

2. Simulation results and analysis

The total simulation period is assumed to be one second. The voltage sag is introduced at 0.3 second by switching on the heavy inductor. This pulls down the line voltage to 184 Volts, resulting a sag of 46 volts i.e. 20% sag, for a period of 0.2 seconds. Voltage swell is introduced at 0.7 second by suitably programming the programmable voltage source and it is made to last for 0.2 seconds, i.e. 20% swell for 0.2 seconds. Figure 2 shows the voltage captured at source side which clearly displays the sag and swell introduced at 0.3 second and 0.7 second respectively.

The output of the DVR, designed to mitigate the voltage issues, is shown in Figure 3. DVR maintains zero output as long as the line voltage is equal to its nominal value and once the deviation in the line voltage is sensed it injects the voltage to bring the line voltage back to its nominal value. From 0.3 second to 0.5 second it injects 46 volts in phase with line voltage so as to alleviate the voltage fall and maintains 230 volts at load side. Similarly, between 0.7 second and 0.9 second it injects same 46 volts, but 〖180〗^∘ out of phase so as oppose the line voltage to bring it down to its nominal 230 Volts. Figure 4 shows the voltage captured at load side and it is evident that the voltage applied to the load is maintained at its nominal value during the occurrence of faults and also irrespective of the nature of the faults.

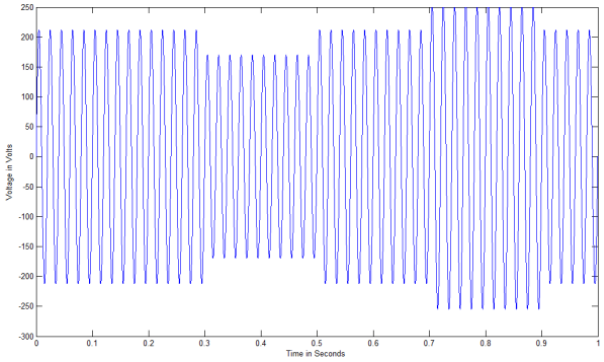

Fig. 2: Line Voltage with Sag and Swell.

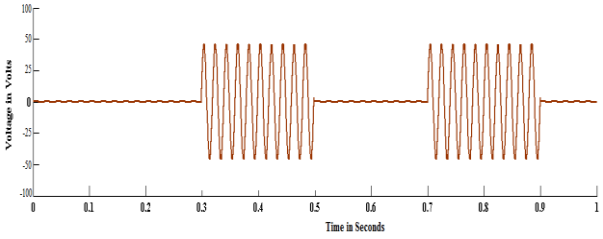

Fig. 3: Voltage Injected by DVR during Sag and Swell.

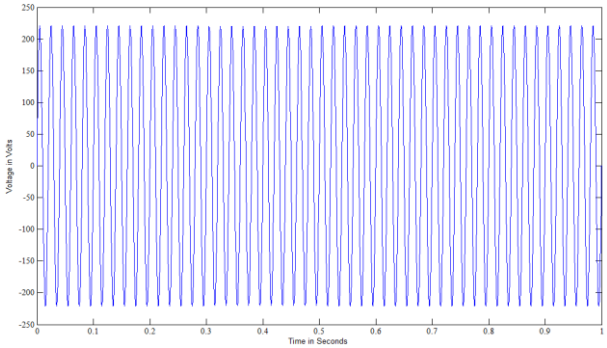

Fig. 4: Load Voltage after Compensation.

The switching transient observed during switching on and off the bridges is 50 Volts. It is also noticed that during the occurrence of the fault, that leads to either swell or sag in the line voltage, the time taken to restitute the voltage is only [2] milliseconds, a reasonably better value. From the Fourier series analysis of the load voltage shown in Figure 5, THD, the index that reflects the quality of the AC quantity injected, is observed as 3.40%, which is well below the IEEE stipulated standards. As the simulation of single phase, DVR gives satisfactory results it is decided to fabricate a low power prototype model of it to evaluate its effectiveness practically.

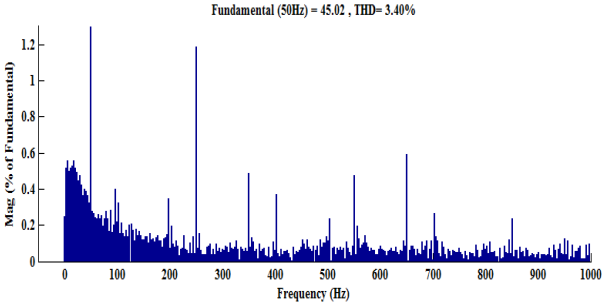

Fig. 5: Total Harmonic Distortion of Load Voltage.

3. Overview of hardware

The practical realization of the proposed DVR comprises of both hardware and software sections. In hardware part there are two major segments viz. Power Circuitry and Control Circuitry. Power Circuitry consists of hardware components such as switching devices, power transformers, load where as the control circuitry consists of soft mechanisms to generate the required PWM signals through PIC 16F887. MOSFET IRF840 is the power switching device selected and 13 H–Bridges are realized through 52 MOSFETs as shown in Figure 6. PIC Micro-Controller 16F887 forms the core of the control circuitry and PI control and PWM generation are realized through software. Proper isolation has been provided wherever required to protect the components and also for a better overall performance of the DVR.

Fig. 6: Hardware Setup of the Proposed System.

Hardware Description
A DVR for a capacity of 750 Watts is designed and fabricated to estimate the practical performance of the proposed version. The power line is realized through an autotransformer and the value of the connected load is Z_L=100+j62.8. By switching on an induction motor, voltage sag is introduced in the power line and it is observed the amount of sag is about 20% and lasted for 0.2 second without DVR. On the other hand, the swell is produced by increasing the line voltage using the autotransformer. The autotransformer is so adjusted that the amount of swell is 12% and being manual operation the swell lasts for considerable duration. Appropriate precaution measures are followed along with the isolation for the proper functioning of DVR during swell. The opto- isolator MCT 2E is used to provide isolation between the power circuit and PIC microcontroller based control circuit. The sag and swell in the realized power line are introduced separately one after another to assess the ability of prototype DVR.

4. Control strategy

PIC16F887 microcontroller performs all the control activities, such as analog to digital conversion, generation of reference voltage V_ref and comparison of the reference voltage with line voltage equivalent, PI processing and PWM operation to generate the gating pulses for the H-Bridges. The line voltage, reduced to 5 Volts through a transformer, is fed as the input for the analog to digital converter of the PIC microcontroller through channel 0. The digital equivalent of the reference voltage is stored in the internal register and the output of the analog to digital converter is compared with this reference. Then the error signal undergoes PI control algorithm and the output of the PI process is sent to PORT A which serves as the reference signal for PWM generation algorithm. PWM1, one of the two PWM generation modules of the PIC microcontroller is used to generate the required gating pulses for the 13 H-Bridges. Timer1 is used to generate the required carrier signal at 12 MHz frequency and the Timer output is compared with the contents of PORT A to generate the gating pulse for the first H-Bridge. The magnitude of the Timer output is then properly updated to get the second level of the carrier signal before comparing it with the contents of PORT A and this process is repeated for all the 13 levels, before next sample of the line voltage is taken. As the speed of the microcontroller is much higher than that of the power system being controlled, proper generation of the gating pulses is assured. The hardware arrangement of driver circuit and Inverter circuit is shown in Figure 7.

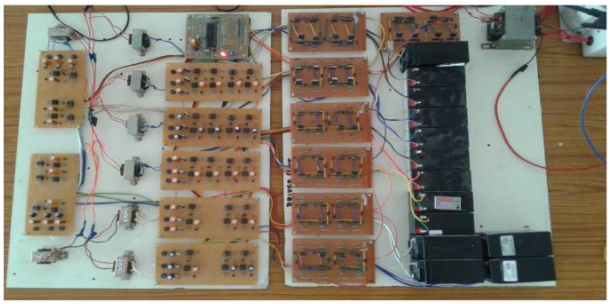

Fig. 7: Hardware Setup of Driver Circuit and Inverter Circuit.

5. Performance analysis

As discussed the voltage sag is introduced by switching on the induction motor whereas the swell is by adjusting auto transformer and both are depicted in Figure 8 and Figure 9 respectively. It is easily seen that the line voltage falls to 184 Volts i.e., 20% during sag. Similarly, the swell is observed as 12% i.e. the line voltage is raised to 258 Volts.

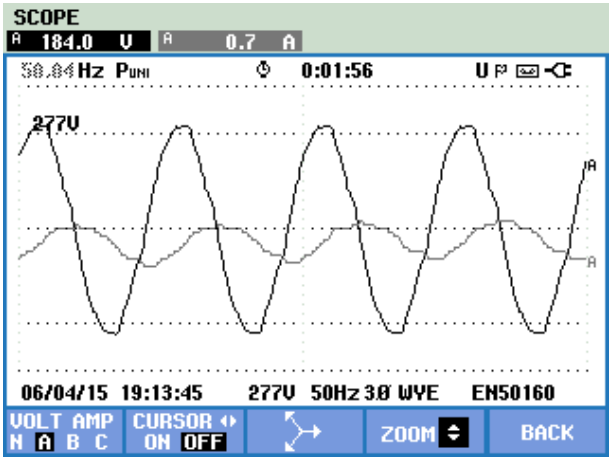

Fig. 8: Line Voltage with Sag.

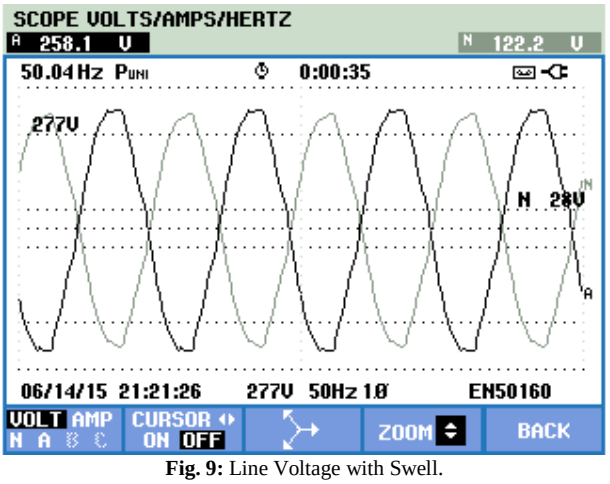

Fig. 9: Line Voltage with Swell.

To mitigate the voltage issues discussed, the DVR is introduced and the line voltages, observed with the DVR, are shown in Figure 10 and Figure 11. The line voltages observed from these figures are 230V each, which prove the effectiveness of the proposed DVR in

alleviating the sag and swell successfully. During sag, the magnitude of the voltage injected by the DVR is 46V and that of the swell is 28 V which may be estimated from the peak values of the respective compensating voltages shown in Figure 10 and 11.

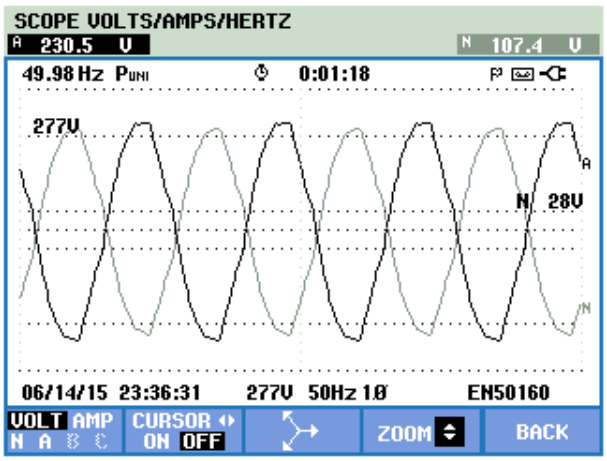

Fig. 10: Load Voltage after Voltage Sag Compensation.

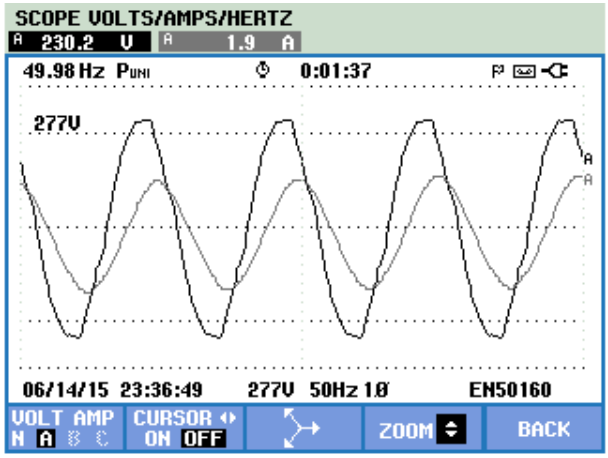

Fig. 11: Load Voltage after Voltage swell Compensation.

Fig. 12: Voltage Injected by DVR during Sag.

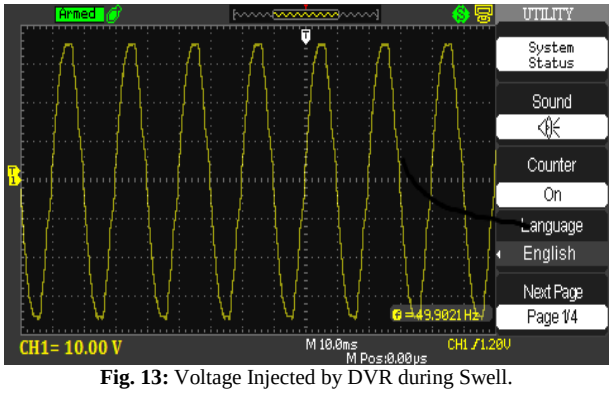

Fig. 13: Voltage Injected by DVR during Swell.

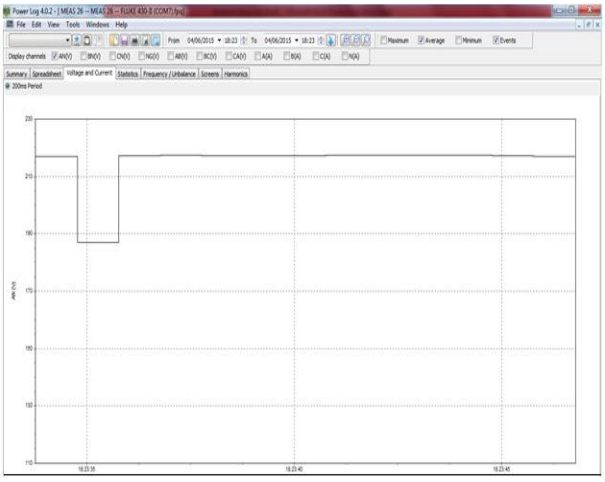

Fig. 14: Response Time of DVR.

It is also observed from Figure 14, that the time taken to restore the voltage by the DVR is only [2] milliseconds, an appreciable response time.

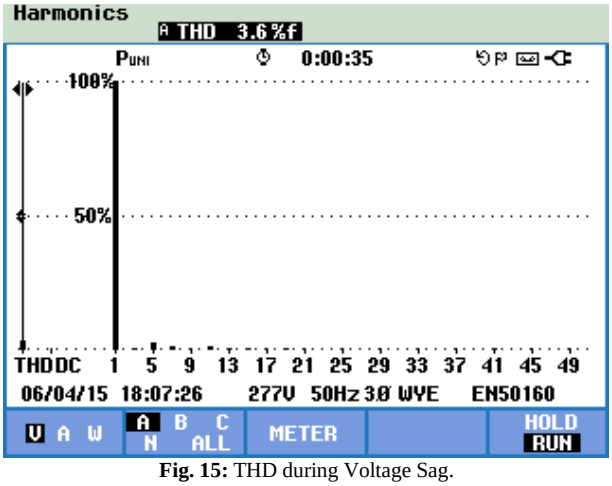

Fig. 15: THD during Voltage Sag.

The THDs measured during compensation of sag and swell are respectively 3.6% and 3.8% as shown in Figure 15 and Figure 16 and these values are well below IEEE standards.

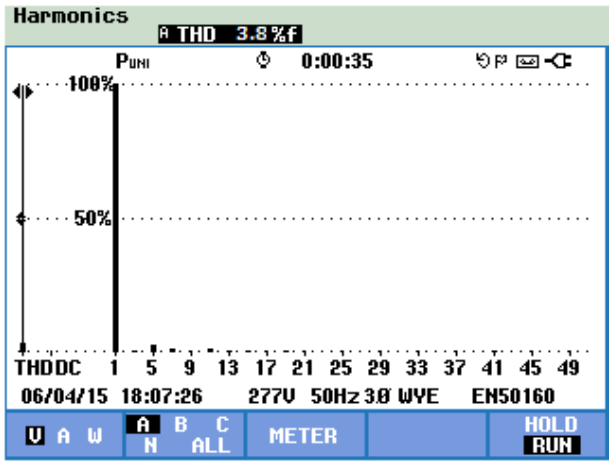

Fig. 16: THD during Voltage Swell.

6. Conclusion

The inevitable voltage sags and swells in power line are to be mitigated to protect the sensitive equipment connected to the power line and a 27-level cascaded H-bridge MLI based DVR is proposed in this paper for the same. The single-phase version of the proposed

DVR was simulated in MATLAB-Simulink and the performance observed was satisfactory. Hence, a prototype, with power MOSFET IRF840 to realize the VSI of the DVR, was fabricated with APODPWM as the modulation technique. The firing angles for the MOSFETS of the DVR were software controlled with the PIC Microcontroller PIC16F887. The voltage swell and sag were introduced manually and the effectiveness of the DVR in mitigating the same was observed. It was noticed that the proposed DVR was effectively functioning during both sag and swell conditions in bringing back the line voltage to its nominal value with an appreciable response time. The THD in both the cases were also well below the IEEE standards. It was also confirmed that the simulation results match with the experimental results, with negligible variations, as shown in

Table 2: This Configuration May be scaled for a Three- Phased System Also

S.No.	Fault	Simulation Results				Hardware Results			
		Line Voltage (V)		Injected Voltage (V)	% THD	Line Voltage (V)		Injected Voltage (V)	% THD
		Without DVR	With DVR			Without DVR	With DVR		
1.	Sag	184	230	46	3.4	184	230.5	46	3.6
2.	Swell	276	230	46	3.4	258	230.2	28	3.8

References

[1] Roger C.Dugan, Mark F.McGranaghan, Surya Santoso&Wayne-Beaty, H 2008, Electrical Power Systems Quality, the McGraw-Hill Companies, Third Edition.

[2] Math H.J. Bollen 2000, 'Understanding Power Quality Problems - Voltage Sags and Interruptions', IEEE Press Series on Power Engineering - John Wiley and Sons, Piscataway, ISBN: 0780347137.

[3] George G. Karady 2005, Effects of Voltage Sags on Loads in a Distribution System. Ph.D. thesis, Arizona State University, China.

[4] AmbraSannino, Michelle Ghans Miller & Math Bollen, HJ 2000, 'Overview of Voltage Sag Mitigation', Power Engineering Society Winter Meeting 2000, IEEE, vol.4, pp. 2872 – 2878.

[5] Jose Rodfignez, Jih-Sheng Lai & Fang ZhengPeng 2002, 'multilevel inverters: A survey of topologies, controls, and applications', IEEE Transactions on Power Electronics, vol.49, and pp.724-738.

[6] Malinowski, M, Gopakumar, K, Rodriguez, J, Perez, MA 2010, 'A Survey on Cascaded Multilevel Inverters', IEEE Industrial Electronics, vol. 57, pp. 2197-2206.

[7] Andreas Nordvall, 2011, Multilevel Inverter Topology Survey. Master of Science Thesis, Chalmers University of Technology Goteborg, Sweden.

[8] PaisanBoonchiam&NadarajahMithulananthan 2006, 'Understanding of Dynamic Voltage Restorers through MATLAB Simulation', Thammasat International Journal of Science and Technology, vol.11, no.3, pp.1-6.

[9] Rosli Omar &NasrudinAbd Rahim 2008, 'Modeling and Simulation for Voltage Sags/Swells Mitigation Using Dynamic Voltage Restorer (DVR)', Proceedings of the Australasian Universities Power Engineering Conference, pp.1-6.

[10] Benachaiba, C &Ferdi, B 2009, 'Power Quality Improvement using DVR' American Journal of Applied Sciences, vol.6, no.3, pp.396-400.

[11] Shairul Wizmar Wahab& Alias Mohd Yusof 2006, 'Voltage Sag and Mitigation Using Dynamic Voltage Restorer (DVR) System', ELEKTRIKA, vol.8, no. 2, pp.32-37.

[12] S.V.Ravikumar and S.SivaNagaraju, "Simulation of D-STATCOM and DVR in power Systems", ARPN Journal of Engineering and Applied Sciences, vol.2, no.3, June 2007, pp.7-13.

[13] Maheswari, M,Thangavel, S &Vivekanandan, C 2014, 'Multi Level Inverter based DVR using Multi Carrier Sinusoidal Pulse Width Modulation Technique with Fuzzy Logic Controller', Australian Journal of Basic and Applied Sciences, vol. 8, no. 15, pp. 201-210.

[14] Angulo, M ,Lezana, P, Kouro, S, Rodriguez, J & Wu, B 2007, 'Level-shifted PWM for cascaded multilevel inverters with even power distribution', Proceedings of the IEEE Power Electronics Special Conference, pp.2373 -2378.

[15] Maheswari, M, Thangavel, S &Vivekanandan, C 2015, 'PI Controlled Multi level Inverter Based DVR with Multi Carrier SPWM for Power Quality Improvement', Middle-East Journal of Scientific Research, vol. 23, no. 5, pp. 841-847.

Ramachandran et al. 2018. *Int. J. Vehicle Structures & Systems*, 10(3), 215-219
ISSN: 0975-3060 (Print), 0975-3540 (Online)
doi: 10.4273/ijvss.10.3.07

International Journal of Vehicle Structures & Systems
Available online at www.maftree.org/eja

Vibration Characterization of Al6061-Sic Metal Matrix Composite based Rubber Mount for I.C Engine Chassis

T. Ramachandran[a, b], S. Sudhakara Reddy[a, c] and S. Jeyakumar[d]

[a]*Dept. of Mech. Engg., Malla Reddy Engg., College, Secunderabad, Telangana, India*
[b]*Email: ramji.kkp1973@yahoo.com,*
[c]*Email: saripallisudhakar@gmail.com*
[d]*Dept. of Mech. Engg., PSNA College of Engg., & Tech., Dindigul, Tamilnadu, India*
Email: kmk_jai@yahoo.com

ABSTRACT:

Vibrations are found to be dangerous and reduce the life and reliability of the vehicle. The studies were carried out by many researchers to stiff the structures by increasing the wall thickness of the plates, rubber and to minimize the vibration by increasing the damping coefficient of the rubber materials. The conventional materials indicate an improvement in stiffness, but not satisfying the requirements of the engine vibration at different speed and load standards and also increased the mass of the structure. Hence, an alternative material which possesses good damping and stiffness combined with rubber has to be developed as structural materials. To meet this challenge, the recent research on the engine mount vibration isolation aims at developing an alternative material for the structures which exhibit good damping and stiffness characteristics. In terms of properties such as chemical resistance, ease of production, high strength-to weight ratio and damping, composite materials are increasingly used in many engineering application where the vibration is predominant. In this research article, the steel plates are replaced by Al6061-SiC Metal Matrix Composites (MMC) and studies are carried out on the engine mount made of Al6061 MMC structural material and integrated with rubber. The static and dynamic properties of the Al6061MMC-rubber mounts are determined using experimental investigations. The harmonic analysis is also carried out to test the damping characteristics of the mounts.

KEYWORDS:

Al6061-SiC rubber mount; Damping; Mechanical properties; Vibration displacement;, Vibration acceleration

CITATION:

T. Ramachandran, S.S. Reddy and S.J .Kumar. 2018. Vibration characterization of Al6061-Sic metal matrix composite based rubber mount for I.C engine chassis, *Int. J. Vehicle Structures & Systems*, 10(3),234-240. doi: 10.4273/ijvss.10.3.07

1. Introduction

Automotive industry requires manufacturers with huge concentration on better comfort and good riding quality (1, 7). This made to their attention for the invention of good quality engine mounting devices, with traditional physical prototyping and testing. An engine which is perfectly balanced for forces and moments will have no tendency to move or to transmit vibration (5) to the frame or foundation to which it is attached For the vibration modeling and characterization, the engine and vehicle are assumed to be rigid body. The engine need to be balanced (8) as there is no vehicle with perfectly balanced engine. As a consequence, flexible mounts are needed for supporting an automobile engine and its peripheral components (13). The flexible mounts (3) are used to prevent the fatigue failure of the engine and gearbox support points and to reduce the amplitude of engine vibration which is transmitted to the vehicle chassis to minimize the human discomfort and fatigue by partially isolating the engine vibrations from the engine to chassis (6). Hence, the material selection of engine mounts also needs to be performed in order to ensure the engine mount strength and damping capacity.

To isolate the vibration caused by the engine unbalanced forces, the least values of vibration transmissibility, elastic stiffness and good damping ability are needed (9). Hence high elastic stiffness and damping are required to minimize the engine vibration and take over engine shake (10). Aluminium alloys are preferred engineering material for automobile, aerospace and mineral processing industries for various high performing components that are being used for varieties of application (4). Al6061 metal matrix composites particularly Al6061-SiC composite have a lot of advantages over monolithic metals including high specific modulus, high specific strengths, better properties at elevated temperatures, low coefficient of thermal expansion, good impact and erosion resistance, good fatigue fracture properties, excellent corrosive resistance, high structural integrity (7), good resistance to aggressive environments, improved wear resistance and damping characteristics. Owing to these enhanced properties, metal matrix composites are under

consideration for a wide range of applications in automotive industries.

The composites formed out of aluminium alloys are of wide interest owing to their high strength, fracture toughness, wear resistance and stiffness. These composites are superior in nature for elevated temperature applications when reinforced with ceramic particle. In this work, generally used steel structural supporting material for the engine mount engine damper is replaced by the Al6061-Sic metal matrix composite and tested for the mechanical properties and vibration behaviour. For that the Al6061-SiC metal matrix composite is manufactured using stir casting method and is tested for the mechanical and damping characteristics. The engine mounts that are prepared using MMC composite and steel mount are used in four cylinder four stroke diesel engine and compared for vibration characteristics.

2. Preparation of Al6061-SiC MMC mounts

Aluminium Matrix Composites (AMCs) refer to the category of light weight high performance aluminium centric material systems. In AMCs, one of the constituents is aluminium/aluminium alloy, which forms a continuous phase and is termed as matrix. The other constituent is embedded in this aluminium/aluminium alloy matrix and serves as reinforcement, which is usually a non-metallic material (common ceramics are SiC and Al_2O_3). Major advantages of AMCs, compared with the unreinforced materials are greater strength, improved stiffness, reduced density, better temperature properties, enhanced abrasion and wear resistance as well as improved damping capabilities. On account of the excellent physical and mechanical properties of AMCs, they are applied widely in aircraft technology, electronic engineering and automotive industries. Of all the commercial aluminium alloys, 6061 is an efficient choice to prepare metal matrix composites.

There are numerous techniques available for fabrication to manufacture MMC materials. The fabrication techniques can vary depending on the selection of matrix and reinforcement material. The solid state processes are generally used to obtain the greatest mechanical properties from among the various methods in MMCs, particularly in discontinuous MMCs. This is because segregation effects and intermetallic phase formations are less for these processes, when compared with liquid state processes (11). The most widely applied methods for the production of composites are based on casting techniques such as squeeze casting of porous ceramic performs with liquid metal alloys, stir casting and powder metallurgy methods (12). Several research works have been carried out for the production of composites. Various methods have been chosen to fabricate the composites. Among these methods, stir casting method has been found to be best suited for fabricating aluminium composites because this method is highly versatile, most economical and easy to handle.

Aluminium (Al6061) alloy composite is produced from stir casting method for that the aluminium alloy (Al6061) is melted at 750°C in a furnace and is held for 40 minutes until the alloy melts completely. In the furnace, aluminium dross floats above the molten metal surface and it is fully removed. Before the inclusion of the Sic, it is heated at 400°C temperature about 1 hour to remove the moisture particles. A blender is used to stir the Al6061 molten metal at 600 rpm and simultaneously the silicon carbide (SiC) particle is added to the molten Al6061. A small amount of magnesium powder is also added to increase the solidification of matrix metal and reinforcement particles during the stirring. The molten alloy is stirred for 10 minutes and the crucible is removed from the furnace. The molten alloy (matrix and reinforced particulates) then is poured into a coated, dried and preheated rectangular mould cavity of size 105 x 105 x 30mm (Fig. 1). The pouring temperature of 600°C is sustained and is allowed to cool to the room temperature to obtain the casted composite.

The cast composite manufactured, machined and tested for the mechanical properties and then resized to according to the required dimension of 50 x 100 x 5mm plate. The prepared Al6061-Sic MMC is now used to fabricate the mount for the engine. To fabricate the engine mount, the elastomeric rubber and the Al6061-SiC are bonded together such that the top and bottom plates are the composite and the elastomer at the middle Fig. 2.

Fig. 1: Al6061-Sic MMC specimen for mount plate

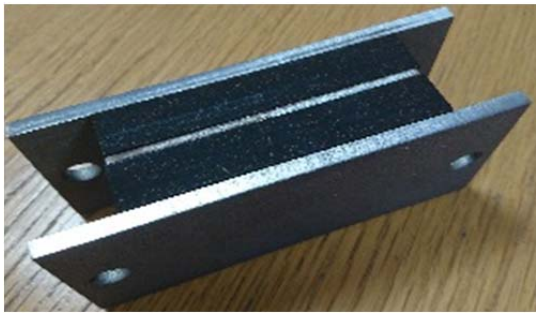

Fig. 2: Engine Mount made of Al6061-SiC MMC

3. Microstructural studies of Al6061-SiC MMC

Using the scanning electron microscopic examinations the microstructure of Al6061 and cast Al6061-SiC composite material are carried out to identify the distribution of particles. The distribution of silicon carbide particles are found to be uniform which enhances the mechanical properties of the composite. The hardness and toughness of composite is found to be more and better than that of Al6061. From the microstructures of Al6061 and Al6061-SiC (Fig. 3a, 3b), the reinforcement particles of Silicon carbide are uniformly distributed in Al6061 matrix material. This uniform distribution of Sic in Al6061 leads to enhancement

strength of the composite by increasing the grain boundary and by hardness.

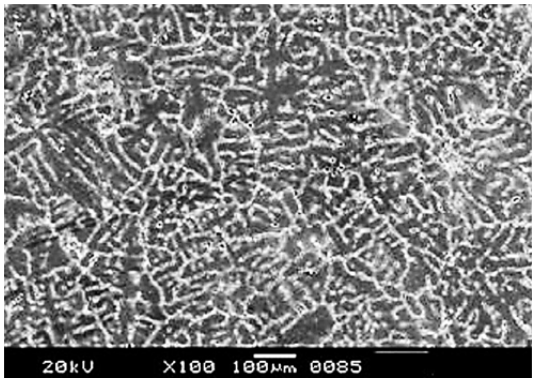

Fig. 3(a): A16061

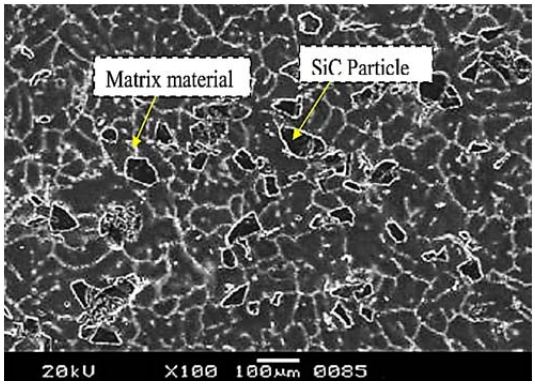

Fig. 3(b): A16061-SiC composite

4. Mechanical characteristics of Al6061-SiC MMC

The steel and Al6061-SiC plates are tested for the mechanical properties to evaluate the requirement and for the engine mount supporting structure qualities that are shown in Table.1. The properties are found to be good enough than the steel when applied for the engine mount requirement functionalities. The response function analysis for frequency for the steel and Al6061-SiC specimens are also measured and the damping coefficient ζ is determined using the method of half power band width. For the determined stiffness of the mount, there is much improvement in the damping factor and also there is a reduction in mass of the composite plate structure when compared to steel plate. The MMC composite material well minimizes the vibrations in proper way compared steel plate (2). The hard nature of the Silicon carbide particles attributed to the brittle nature imparted by the aggregates present in the Al6061 matrix structure. This quality of Al6061-SiC made fit for absorbing or damping out the vibration initiated in the structures.

The engine mounts produced using the steel and Al6061-SiC material with the integration the natural rubber, which is most widely used as the mounts where the vibration is predominant, and are used as the damping mediators between the engine and the chassis. The fabricated mount consists of top and bottom plates of steel and Al6061-Sic and the rubber of stiffness 150N/mm. The plates prepared in the size of 100 x 50 x 5mm and the rubber is bonded between the plates of top and bottom plates. The prepared three mounts are fitted to the engine and analysed for the vibration characteristics.

Table.1: Mechanical properties of steel and Al6061-SiC

Mount	Material density (ρ) kg/m^3	Young's Modulus (E) GPa	Poisson ratio (υ)	Stiffness (N/mm)	Deflection (mm)	Mass (kg)	Damping factor (ζ)
Steel	7850	210	0.25	0.097	103	0.508	0.007
Al6061-MMC	2600	82	0.35	0.1	98	0.235	0.0319

5. Results & discussion

5.1. Vibration testing of Al6061-Sic MMC mounts

The three mounts are prepared in each Al6061-SiC-rubber and steel-rubber combinations and are fitted to the I.C engine for the testing of vibration behaviour. The dynamic analysis is carried out on the steel-rubber and Al6061-Sic-rubber mounts using an experimental setup. The setup consists of an accelerometer fitted on the table, dynamic analyser, impact hammer and all are interring connected with each other. To test the dynamic behaviour of the mounts, the mounts are rigidly fixed to the accelerometer table and the harmonic excitations are applied on the mounts. To determine the frequency response of the mounts, a steady-state dynamic analysis is performed. This analysis carried out to find the steady-state amplitude and displacement the response of the system by the harmonic excitations at given frequency. Two base vertical loads considered in this analysis are the load caused by the engine weight and an additional load of 2000N by the engine excitations. The impact load of 2000N is applied to the engine mount to determine the displacement caused at both the mounts and are measured using the accelerometer.

The acceleration results obtained from the sensors are transferred to the software and the displacement results (Fig. 4) obtained for the both mounts. The results show that the displacement caused in the steel-rubber mount reached the peak of 6e-3mm and slowly damped out for the time period of 1.6s. When the Al6061-SiC mount is excited, the maximum displacement obtained is 4.5e-3mm and the excitation displacement is damped out within the 1s. It shows that the Al6061-SiC mounts having good damping factor and are capable of minimizing the vibration caused in the engine. This ability of the mount is more than enough to reduce the transfer of vibration forces from the engine to the chassis by executing the more reaction forces towards the engine.

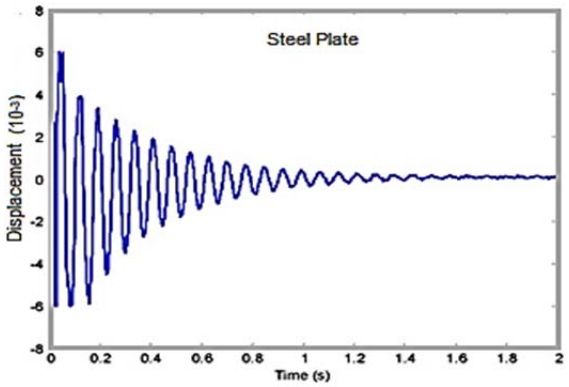

Fig. 4(a): Vibration displacement caused at the steel

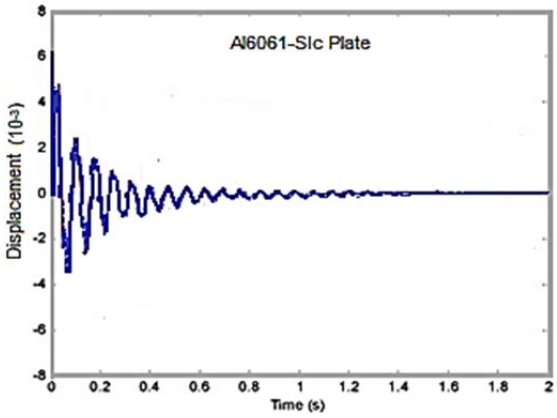

Fig. 4(b): Vibration displacement caused at the A16061- Sic Mounts

The excitation of the applied force is simulated in the range 1-1000 Hz and the reaction forces excreted by the mount and the respective reaction forces exerted are measured with respect to the frequency range for the steel and Al6061-SiC mount. The variation in the mount natural frequencies due to the variation in the in material properties of the mounts is reflected clearly in the mount displacement response curves. From the plot (Fig. 5), it has been identified that the mount fabricated with Al6061-SiC possessed a great anti-resonance valley and exerted least reaction forces against the excitation. In case of the steel based mount has less ant resonance valley and exerted more reaction forces against the excitation. It indicates that the mount is still accomplishing required mission of minimizing the vibration transmission. The phase angle of the reaction force with respect to frequency distribution for the epoxy mount is appreciably increased and also clearly damp out the vibration excitations.

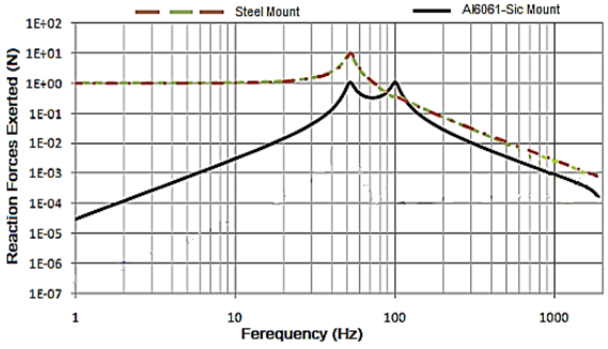

Fig. 5: Reaction forces exerted by steel and Al6061-SiC Mounts

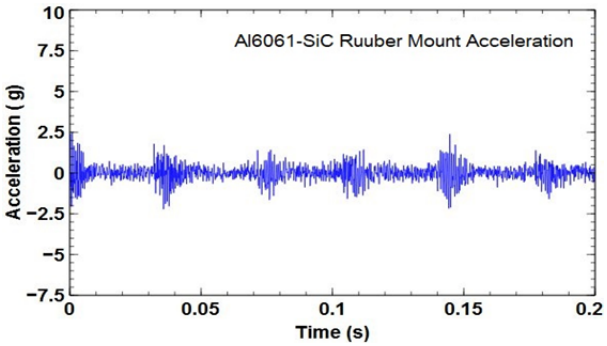

Fig. 6: Measured vibration accelerations of steel mount

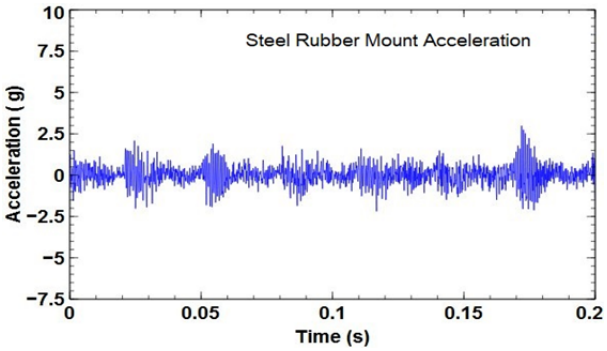

Fig. 7: Measured vibration accelerations of Al6061-SiC mount

In the case of steel mount, the phase angle variations for the frequency distribution are comparatively less and found to be constant. An interesting fact identified that the frequency decrease of the anti-resonance valleys for the mounts reactions in the opposition to the effect helps to reduce the overall system transmissibility in the frequency range of interest. For the experimental testing of the mount at the engine, the mounts are fitted to the four cylinder four stroke diesel engine and tested for the vibration accelerations at the maximum load conditions with a speed of 1500rpm. The mounts are connected with the acceleration sensors and the experiments are carried out to determine the dynamic vibration behaviours. The results of the vibration accelerations (Figs. 6 & 7) are obtained for the both the Al6061-SiC and steel mounts and are analysed for the comparison. The plot of the Al6061-SiC mount shows that the time domain variation of the acceleration is maximum at the peak cycle-cycle variation and is minimum with an average of 07g during the remaining cycles.

But, in the case of steel mount the time domain accelerations reach the maximum of 3g and the average of the remaining cycles is nearly 1g which is more than that of the Al6061-SiC mounts. It shows clearly the vibration damped out in the Al6061-SiC mount is more and effectively reduced the vibration transmissibility of the engine to the chassis.

6. Conclusion

In this work, Al6061-SiC plates are prepared for the suitability of the engine mount supporting structure. Generally the elastomeric mounts are manufactured using the steel supported structure which is minimizing the vibration caused engine to some extent. To minimise furthermore vibration transformation to the chassis a better material is identified and tested for the mechanical

characteristics. Such kind of material is Al6061 having good strength and weight to strength ratio and is improved in vibration characteristics by attributing the SiC material as composite. In this regard, the stir casting technique is used to prepare the Al6061-SiC composite and is prepared in the form of plates. The mechanical properties of the steel and Al6061-SiC plate is tested and compared for the stiffness and damping characteristics. From the results, it has been identified that the Al6061-SiC composite is having improved strength and damping properties than the steel.

To test the vibration behaviour of the both mounts, the mounts fabricated by integrating with rubber with natural rubber and prepared as per requirement of the engine in which the experiments are carried out. The mounts tested experimentally for the steady-state response subjected to impact excitation of 2000N to determine the vibration displacement and the reaction forces exerted. The results show that the vibration displacement measured for the Al6061-SiC mounts are minimum when compared to the steel mounts. This shows the ability of the improved vibration damping ability of the composite mount and inferred that composite mounts are well damp out the vibration forces transferred. The frequency response function of the mounts showed that the effectiveness mounts in the isolation is well justified in the frequency range of interest. The mounts are also tested with engine at maximum load with 1500rpm to analyse the dynamic response of the vibration characteristics.

The vibration accelerations are measured with respect to time domain and are found to minimum for the Al6061-SiC mounts and found to be more efficient than the steel based rubber mounts. Hence forth the Al6061-Sic elastomer mounts would be replaced in place of steel based elastomer mounts as they are having good strength to weight ratio and damping properties. Furthermore the mounts may be considered for the testing of engine vibration when the engine runs with recent scenario fuels like vegetable oils or pure plant oil based biodiesels.

REFERENCES:

[1] L.E. Ooi and Z.M. Ripin. 2014. Optimization of an engine mounting system with consideration of frequency-dependent stiffness and loss factor, *J. Vibration and Control*, 22(10), 2406-2419. https://doi.org/10.1177/1077546314547532

[2] T. Ramachandran and K.P. Padmanaban. 2015. Experimental investigation of static and dynamic properties of steel-rubber, cast iron-rubber and epoxy granite-rubber as I.C engine mount, *Transactions of Indian Institute of Metals* 68 (1), 83-86. https://doi.org/10.1007/s12666-015-0612-y

[3] K.K. Chokshi and H.H. Ghoneim. 2017. A flexible-matrix-composite hydraulic engine mounts, *Int. Mech. Engg., Congress and Exposition*, *Vol. 4A: Dynamics, Vibration, and Control*, V04AT05A028. https://doi.org/10.1115/IMECE2017-70189

[4] S. Jeyakumar, K. Marimuthu and T. Ramachandran. 2013. Prediction of cutting force, tool wear and surface roughness of Al6061/SiC composite for end milling operations using RSM, *J. Mech., Sci., & Tech*., 27 (9), 2813-2822. https://doi.org/10.1007/s12206-013-0729-z

[5] F. Wang and S. Duan. 2011. Fault diagnosis of diesel engine using vibration signals. in: Chen R. (eds) Intelligent computing and information science, *Communications in Comp. and Information Sci.*, 135

[6] T. Ramachandran and K.P. Padmanaban. 2015. Multibody modelling of engine and minimization of engine mount vibration using ant colony algorithm optimization, *Int. J. Vehicle Structures & Systems,* 7(1), 10-15. https://doi.org/10.4273/ijvss.7.1.02

[7] S.K. Sharma, R.C. Sharma, A. Kumar and S. Palli. 2015. Challenges in rail vehicle-track modelling and simulation, *Int. J. Vehicle Structures & Systems*, 7(1), 1-9. https://doi.org/10.4273/ijvss.7.1.01

[8] R. Kumar, M.P. Garg and R.C. Sharma. 2012. Vibration analysis of radial drilling machine structure using finite element method, *Advanced Materials Research*, 472, 2717-2721. http://dx.doi.org/10.4028/www.scientific.net/AMR.472-475.2717.

[9] S. Palli, R.C. Sharma and P.P.D. Rao. 2017. Dynamic behaviour of a 7 DoF passenger car model, *Int. J. Vehicle Structures & Systems*, 9(1), 57-63. https://doi.org/10.4273/ijvss.9.1.12

[10] L.R. Wang, Z.H. Lu and I. Hagiwara 2010. Analytical analysis approach to non-linear dynamic characteristics of hydraulically damped rubber mount of vehicle engine, *J. Non-Linear Dynamics*, 61, 251-264.

[11] S. Naher, D. Brabazon and L. Looney. 2004. Development and assessment of a new quick quench stir caster design for the production of metal matrix composites, *J. Materials Proc Tech.*, 166, 430-439. https://doi.org/10.1016/j.jmatprotec.2004.09.043.

[12] J.W. Kaezmar, K. Piebrzak and W. Wlosinski. 2000. The production and application of metal matrix composite materials, *J. Materials Processing Tech*., 106, 58-67. https://doi.org/10.1016/S0924-0136(00)00639-7.

[13] J.S. Taog, R. Liuk and Y. Lam. 2000. Design optimization of marine engine-mount system, *J. Sound and Vibration*, 235 (3), 477-494. https://doi.org/10.1006/jsvi.2000.2945

Biofuel Research Journal 19 (2018) 863-871

BRTeam BIOFUEL RESEARCH TEAM

Biofuel Research Journal

Journal homepage: www.biofueljournal.com

Original Research Paper

Experimental investigation of the combustion characteristics of Mahua oil biodiesel-diesel blend using a DI diesel engine modified with EGR and nozzle hole orifice diameter

M. Vijay Kumar[1,*], A. Veeresh Babu[2], P. Ravi Kumar[2], S. Sudhakara Reddy[1]

[1]*Department of mechanical engineering, Malla Reddy Engineering College, Hyderabad, Telangana, 500100, India.*

[2]*Department of mechanical engineering, National Institute of Technology Warangal, Warangal, Telangana, 506004, India.*

HIGHLIGHTS

- Engine modification through reducing NHD improved combustion characteristics but deteriorated NO_x emissions.
- Application of partially-cooled EGR could compensate for the adverse impacts of engine modification on NO_x emissions.
- The EGR rate of 10% was found promising in substatially reducing NO_x emissions at all loads.
- High EGR rates esp. at higher loads, adversely affected the performance and emission characteristics of the modified.

GRAPHICAL ABSTRACT

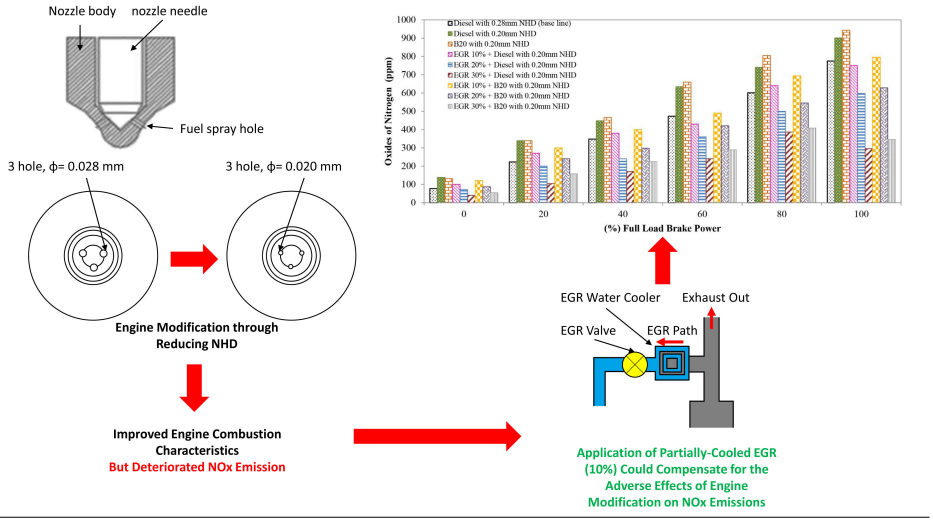

ARTICLE INFO

Article history:
Received 12 June 2018
Received in revised form 10 August 2018
Accepted 12 August 2018
Available online 1 September 2018

Keywords:
Diesel engine modification
Injector nozzle hole diameter
Biodiesel
Combustion characteristics
EGR
NO_x reduction

ABSTRACT

Engine modification through reducing nozzle hole diameter (NHD) (i.e., from the base value of 0.28 to the modified value of 0.20 mm) has been shown as an effective strategy in improving engine performance, combustion, and emission parameters. However, it has also led to substantial increases in NO_x emission as a major shortcoming. In light of that, the present study was aimed at overcoming this challenge through the application of a partially-cooled exhaust gas recirculation (EGR) system. More specifically, Mahua oil biodiesel-diesel blend (B20) and neat diesel were tested on a modified single cylinder diesel engine under five different engine loads (i.e., 2.46, 4.92, 7.38, 9.84, and 12.3 kg) and in the presence of varying EGR rates (i.e., 10, 20, and 30%). The results obtained revealed that the performance, combustion, and emission characteristics of the modified engine (3-hole nozzle with an orifice diameter of 0.20 mm) were improved for both neat diesel and B20 except in the case of NO_x, in comparison with those of the conventional diesel engine (3-hole nozzle with an orifice diameter of 0.28 mm). The considerable increases in NO_x emissions caused by the smaller orifice NHD could be successfully compensated for through the implementation of the partially-cooled EGR. Overall and based on the findings of the present study, the proposed engine modification in the presence of partially-cooled EGR rate of 10% could be recommended as efficient combustion conditions for 20% blend of Mahua oil biodiesel and diesel. However, further increments in the EGR rate and in particular at higher loads, adversely affected the performance and emission characteristics of the modified engine due to the recirculation of high amounts of unburnt soot, CO_2, H_2O, as well as of O_2 deficiency.

* Corresponding author at: Tel.: +91 9701339886
E-mail address: vijaykumar.iitm37@gmail.com

Please cite this article as: Vijay Kumar M., Veeresh Babu A., Ravi Kumar P., Sudhakara Reddy S. Experimental investigation on the diesel and MME blend with DI diesel engine modified with EGR and nozzle hole orifice diameter. Biofuel Research Journal 19 (2018) 863-871. DOI: 10.18331/BRJ2018.5.3.6

Abbreviations

BP	Brake Power
BSFC	Brake Specific Fuel Consumption
BTE	Brake Thermal Efficiency
bTDC	before Top Dead Center
CI	Compression Ignition
CO	Carbon Monoxide
CO_2	Carbon Dioxide
CR	Compression Ratio
EGR	Exhaust Gas Recirculation
DI	Direct Injection
HC	Hydrocarbon
HRR	Heat Release Rate
ID	Ignition Delay
IP	Ignition Pressure
IT	Injection Timing
NHD	Nozzle Hole Diameter
NOx	Oxides of Nitrogen
PM	Particulate Matter
SOC	Start of Combustion
SCR	Selective Catalytic Reduction

1. Introduction

Growing interests in achieving higher power with better fuel economy at a lesser maintenance cost have been the driving force behind the increasing number of compression ignition (CI) engine vehicles. In line with that, engine manufacturers constantly strive to further develop the CI engine technology to more efficiently meet the above-mentioned objectives. It should be mentioned that among these objectives, reducing exhaust gas emissions in order to meet the increasingly stringent emissions standards/policies is of utmost importance. Therefore, different engine modifications, methods/approaches for exhaust gas after-treatment, and strategies leading to more optimized combustion such as the application of more environmentally-friendly fuels/fuel additives have attracted a great deal of attention (Hussain et al., 2012; Vijay Kumar et al., 2018a). A number of these solutions are discussed herein.

1.1. Biodiesel

Biodiesel is defined as the mono-alkyl esters of long chain fatty acids resulting from vegetable oils or animal fats (Venkanna and Reddy, 2009; Vijay Kumar et al., 2017a). The critical properties of biodiesel, such as being non-toxic, high cetane number, oxygen content, absence of sulfur, high inherent lubricity, and being biodegradable, make this alternative fuel an ideal replacement for mineral diesel. Biodiesel can be used in neat form or with diesel at different blending ratios with no or little engine modification. Nevertheless, engine manufacturers recommend biodiesel blending ratios of up to 20% for the existing diesel engines (Mo et al., 2016).

In spite of the above-mentioned advantages, biodiesel is associated with a number of disadvantages as well including lower volumetric energy capacity, lower oxidative stability, inferior cold flow properties, higher kinematic viscosity, and higher NO_x emissions (Can et al., 2016). Moreover, the widespread use of edible vegetable oil for biodiesel production has sparked much concern over the growing food *vs.* fuel competition over food resources/water/land. Additionally, edible oils could be more costly to use as biodiesel feedstock jeopardizing the economic viability of the biodiesel production process. Hence, the application of non-edible oil crops such as *Sterculia foetida*, Soapnut, Jatropha, Mahua, Pongamia, Polanga, Neem, *etc.* has been offered to overcome these challenges (Sahoo et al., 2007; Kumar and Sharma, 2011). **Table 1** tabulates the estimated oil yields of mahor non-edible oil crops used as biodiesel feedstock.

While the application of many of the non-edible oil crops as biodiesel feedstock is still being assessed, these crops in general offer the following advantages (Atabani et al., 2013):

- The cultivation of non-edible oil feedstock requires non-agricultural and marginal land with little fertilizer and irrigation requirements.
- Non-edible oil crops can also be grown in semi-arid zones with an annual precipitation of around 200 mm.
- Following oil extraction, the seed cakes can be used as fertilizer for soil improvement and/or biopesticide (Vijay Kumar et al., 2018b).

Table 1.
Estimated oil yields of non-edible oil crops used for biodiesel production.

Type of oil	Oil yield (T/ha)	Oil yield per seed (wt. %)	References
Mahua	3.6 00	44.43 - 61.5	Jena et al. (2010); Kumar and Sharma (2011); Soo-Young (2011)
Polanga	4.680	50	Azam et al. (2005); Sahoo et al. (2006)
Jatropha	1.900 – 2.250	35 - 40	Achten et al. (2008); Gui et al. (2008); Pinzi et al. (2009); Singh and Singh (2010); Koh and Ghazi (2011); Silitonga et al. (2011)
Neem	2.670	20 - 30	Azam et al. (2005); Nabi et al. (2006); Kumar and Sharma (2011); Sharma et al. (2011); Soo-Young (2011)
Pongamia	0.225 - 2.250	30 - 40	Azam et al. (2005); Karmee and Chadha (2005); Gui et al. (2008); Naik et al. (2008); Pinzi et al. (2009); Singh and Singh (2010); Soo-Young (2011)
Rubber seed	0.040 - 0.120	40 - 50	Ramadan and Morsel (2003); Ramadhas et al. (2005a); Ramadhas et al. (2005b); Kumar and Sharma (2011); Soo-Young (2011)
Castor	1.188	45 - 50	Koutroubas et al. (1999); Saka (2005); Soo-Young (2011)

1.2. Biodiesel application without engine modifications

Many research studies have recommended the application of biodiesels produced from different oil feedstock without requiring any engine modifications. For instance, Polanga oil methyl ester (POME) and its blends were combusted at varying loads by Sahoo et al. (2007). The authors claimed more favorable engine performance parameters such as brake thermal efficiency (BTE) and brake specific energy consumption (BSEC) using POME blends compared with neat diesel. They also argued that smoke opacity and hydrocarbon (HC) emissions were decreased in response to POME inclusion while NOx was increased owing to the oxygen content of biodiesel (Sahoo et al., 2007). Similar results were reported by Mofijur et al. (2013) who investigated two blending ration of biodiesel into diesel, i.e., B10 and B20. They indicated that the average BSFC values obtained for B10 (278.46 g/kWh) and B20 (281.9 g/kWh) were higher than that of neat diesel (273.5 g/kWh).

Whereas, compared to neat diesel, B10 and B20 led to lower CO (16% and 25%, respectively) and HC (3.84% and 10.25%, respectively) emissions, but a slightly higher NOx emissions (3% and 6%, respectively (Mofijur et al., 2013). In a different study, Karanja biodiesel and its blends were found compatible with the existing diesel engines (Chauhan et al., 2013). From the unfavorable combustion characteristics point of view, it was found that compared with neat diesel, Karanja biodiesel blends led to 3-5% less BTE, lower in-cylinder pressure, and lower heat release rate (HRR), but increased NO_x emissions (Chauhan et al., 2013). Raheman and Phadatare (2004) as well as Agarwal and Dhar (2013) also studied the combustion characteristics of Karanja biodiesel and claimed reductions in emissions, i.e., CO, HC, and smoke.

These findings were in line with those of the other investigations on biodiesel produced from other oil feedstocks such *Pongamia Pinnata* biodiesel (Sureshkumar et al., 2008), Mahua oil biodiesel (Raheman and Ghadge, 2007; Vijay Kumar et al., 2017b), mango seed oil biodiesel (Vijayaraj and Sathiyagnanam, 2016), palm and Jatropha biodiesel (Rahman et al., 2014), *etc*. Overall, these studies are unanimous in concluding that biodiesel can be used by up to 20% (i.e., B20) in the existing diesel engines without modifications and that it could lead to reduced emissions (except NO_x).

Please cite this article as: Vijay Kumar M., Veeresh Babu A., Ravi Kumar P., Sudhakara Reddy S. Experimental investigation on the diesel and MME blend with DI diesel engine modified with EGR and nozzle hole orifice diameter. Biofuel Research Journal 19 (2018) 863-871. DOI: 10.18331/BRJ2018.5.3.6

1.3. Biodiesel application along engine modifications

Some research works have been focused on investigating the effects of various engine modifications, e.g., compression ratio (CR), injection timing (IT), pressure opening, *etc*. on diesel engines powered by biodiesel-diesel blends. For instance, Ganapathy et al. (2011) claimed reductions in BSFC as well as HC, CO, and smoke emissions by applying variations in injection timing when using Jatropha biodiesel. They also argued that HRR, pressure, and BTE could be increased while NO_x emissions could be reduced through such variations. In a different study, Gnanase Karan et al. (2016) studied the combustion characteristics of a diesel engine running on fish oil biodiesel and its blends at different injection timings, i.e., 21° bTDC, 24° bTDC, and 27° bTDC. They reported shorter ignition delays (ID) and lower HRRs for biodiesel blends. They also argued that through the retardation of IT, a number of emission and combustion parameters including NO_x, HC, CO, peak pressure, ID, combustion duration, and HRR were decreased while advancement in IT led to opposite results (Gnanase Karan et al., 2016).

Variations in ignition pressure (IP) has also taken into account by a number of investigations. For instance, Channapattana et al. (2015) and Shehata et al. (2015) studied the effects of varying IPs on the combustion characteristics of Honne biodiesel and corn/soybean biodiesel blends, respectively. These authors concluded increases in NO_x emissions and decreases in HC, CO, and smoke opacity in response to increasing IP. In a recent investigation, Dubey and Gupta (2018) took into consideration the effects of increasing compression ratio (CR) (i.e., 15.5:1, 17:1, 18.5:1, and 20:1) on the performance and emissions profile of a dual biofuel (Jatropha biodiesel and turpentine oil). They claimed that at the CR of 20:1, the investigated biofuel led to the most favorable results, i.e., increased BTE by 2.17% as well as decreased CO, HC, NO_x emissions, and smoke opacity by 13.04%, 17.5%, 4.21%, and 30.8%, respectively (Dubey and Gupta, 2018). Lower HC and CO emissions were also recorded by Sivaramakrishnan (2018) through optimizing IP at 200 bar and CR at 18:1 when combusting a 25% blend of Karanja biodiesel. Similar results were also reported by Jindal et al. (2010) who claimed that higher CRs and higher IPs improved the engine performance of a diesel engine running on Jatropha biodiesel.

1.5. Biodiesel application with after-treatment technologies

Efforts to reduce the NO_x emissions associated with the application of biodiesel have been intensified over the last decade. In line with that, selective catalytic reduction (SCR) and exhaust gas recirculation (EGR) have been offered as proven technologies for reducing NO_x emissions. For instance, in a study, Hussain et al. (2012) investigated the effect of EGR (10%, 15%, 20% and 25%) on a 3-cylinder, constant speed, and air-cooled CI diesel engine and concluded that at lower loads, higher rates of EGR could be applied without negatively affecting the fuel economy and efficiency, while leading to reduced NO_x. Duraisamy et al. (2011) combusted Jatropha biodiesel using EGR and argued that EGR of 15% was optimal in terms performance improvement and reduction in NO_x emission. Similar findings verifying the favorable impacts of EGR have also been reported by other studies (Kusaka et al., 2000; Rajan and Senthilkumar, 2009; Bani et al., 2010; Fontana and Galloni, 2010; Mani et al., 2010). These improvements in response to EGR application could be explained by the resultant high intake temperature, which improves flame propagation in the combustion chamber (Sasaki et al., 1998).

In our recently published report, the combination of Mahua oil biodiesel blend (B20) application with engine modification, i.e., the implementation of smaller orifice nozzle hole diameter (NHD), was shown to lead to improved combustion characteristics (Vijay Kumar et al., 2018b). However, the combined strategy also led to NO_x augmentation as its only drawback observed. These outcomes could be ascribed to the more efficient atomization of the fuel particles triggered by the smaller orifice NHD and the consequently more effective fuel combustion taking place in the combustion chamber on one hand and the high oxygen content of the fuel blend on the other hand (Vijay Kumar et al., 2018b). In light of that, the present study was set to overcome the shortcoming of the investigated strategy or in better words, to reduce NO_x emissions by employing EGR while using Mahua oil biodiesel blend and small orifice NHD.

2. Experimental Procedure

2.1. Biodiesel preparation

Biodiesel was produced as described in our previous report (Vijay Kumar et al., 2018b). Briefly, inedible Mahua oil was transesterified through a two-step procedure. This strategy was employed owing to the high free fatty acids (FFA) of this oil feedstock, i.e., 21%. In the first step, the FFA content was reduced through mixing 0.35 v/v of methanol and 1% v/v of concentrated H_2SO_4 with the pre-heated Mahua oil at 60 °C for 1 h. Subsequently, the resultant oil was transesterified by using 0.25 v/v of methanol and 0.7% w/v of KOH at 60 °C for 1 h. Following glycerin decantation, crude biodiesel was washed with 50 °C distilled water three times. Finally, anhydrous $CaCl_2$ was added to the resultant product, heated gently at 50 °C while shaken vigorously. Dry purified Mahua oil biodiesel was obtained after $CaCl_2$ separation and blended with diesel to obtain B20 fuel.

Fuel properties of diesel, Mahua oil biodiesel and its 20% blend with diesel (B20) are presented and compared in **Table 2**. The chemical compositions of diesel and Mahua oil biodiesel are tabulated in **Table 3**.

Table 2.
Fuel properties of neat diesel, Mahua oil biodiesel as well as its 20% blend with diesel (B20).*

Property	Unit	Diesel	Mahua oil biodiesel	B20
Colour	-	Light brown	Slight brown yellow	Light brown
Density at 35 °C	Kg/m^3	819	867	831
Viscosity at 40 °C	cSt	2.89	4.86	3.36
Calorific value	kJ/kg	44296	38513	43761
Fire point	°C	52	140	ND[1]
Flash point	°C	48	108	ND
Pour point	°C	-5	10.2	ND
Cloud point	°C	-10	14.5	ND
Boiling point	°C	282-338	320	ND
Cetane number	-	49	52	ND

[1] ND = Not determined
* Source: Vijay Kumar et al. (2018b). With permission from Elsevier. Copyright© 2018.

Table 3.
Comparison of chemical composition of diesel and Mahua oil biodiesel.*

Description	Diesel	Mahua oil biodiesel
Carbon (%)	86.5	77.9
Oxygen (%)	0	9.3
Nitrogen (%)	0.18	<0.001
Hydrogen (%)	13.2	12.8

* Source: Vijay Kumar et al. (2018b). With permission from Elsevier. Copyright© 2018.

2.2. Engine modifications with fuel injector nozzle and EGR

First, the injection nozzle system of a diesel engine was modified to smaller orifice diameter in order to improve the performance and to reduce the harmful emissions as reported previously (Vijay Kumar et al., 2018b). Briefly, the reduction of NHD significantly affected the air-fuel mixture formation, atomization, and evaporation leading to improved BTE, BSFC, and HRR and reduced emissions (except NO_x) in the investigated CI engine. Subsequently, to overcome the challenge associated with the NHD modification, the coupling of a partially-cooled EGR system to the diesel engine was investigated.

Parametric details of the fuel injection systems used including the differences between the base and modified nozzle orifice diameters are presented in **Table 4**. For better understanding, cross-sectional views of the nozzle hole geometries are also shown in **Figure 1**.

Please cite this article as: Vijay Kumar M., Veeresh Babu A., Ravi Kumar P., Sudhakara Reddy S. Experimental investigation on the diesel and MME blend with DI diesel engine modified with EGR and nozzle hole orifice diameter. Biofuel Research Journal 19 (2018) 863-871. DOI: 10.18331/BRJ2018.5.3.6

Table 4.
Parametric details of the fuel injection systems used.

S. No.	Nozzle label	No. of holes	Diameter of orifice hole	Standard nozzle opening pressure
1	NHD (base)	3	0.28 mm	210 bar
2	NHD (modified)	3	0.20 mm	210 bar

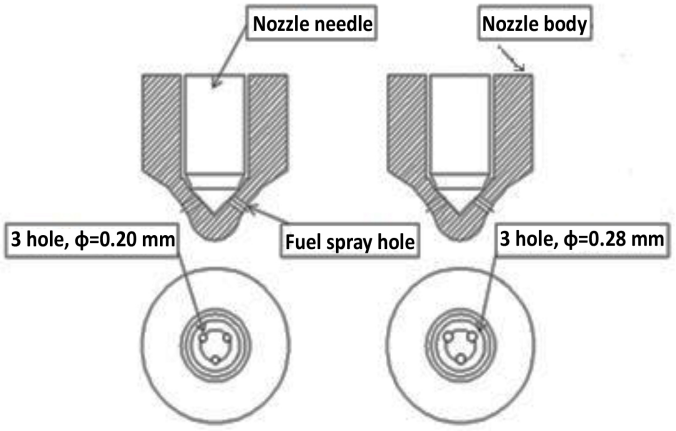

Fig.1. Cross section views of the nozzles with different orifice diameters. Source: Vijay Kumar et al. (2018b). With permission from Elsevier. Copyright© 2018.

A computerized single cylinder diesel engine was employed to study the effects of reduced nozzle orifice diameter and EGR on the combustion (performance and emissions) characteristics of Mahua oil biodiesel blend. The specifications of the engine used is shown in Table 5. The engine was coupled to an eddy current dynamometer for loading the engine. For EGR, appropriate plumbing was done. To maintain the re-circulated exhaust gases partially cool, a water cooler was used while no insulation was considered on the pipeline to allow the escape of the heat. A control valve was installed to regulate the EGR percentage. An EGR mixture chamber was also provided to mix the exhaust gases with fresh air. The flow rate of the intake fresh air was monitored by an orifice meter. A schematic presentation of the engine setup coupled with the EGR system is shown in Figure 2. For EGR setupThe EGR (%) was calculated according to the following equation (Eq. 1).

$$\text{EGR rate (\%)} = \frac{Q_{\text{without EGR}} - Q_{\text{EGR}}}{Q_{\text{without EGR}}} \times 100 \qquad \text{Eq. 1}$$

Where, $Q_{\text{without EGR}}$ is the airflow rate without EGR, i.e., 26 kg/h and Q_{EGR} is the EGR flow rates investigated, i.e., 2.6 kg/h, 5.2 kg/h, and 7.8 kg/h.

An AVL gas analyzer was used to measure CO, NO_x, and HC. The exhaust gas smoke opacity was measured by an AVL smoke opacity meter.

2.4. Measuring devices; ranges, accuracies, and percentage uncertainties

The ranges and accuracies of the measuring devices used in the present investigation are shown in Table 6. While the percentage uncertainties of

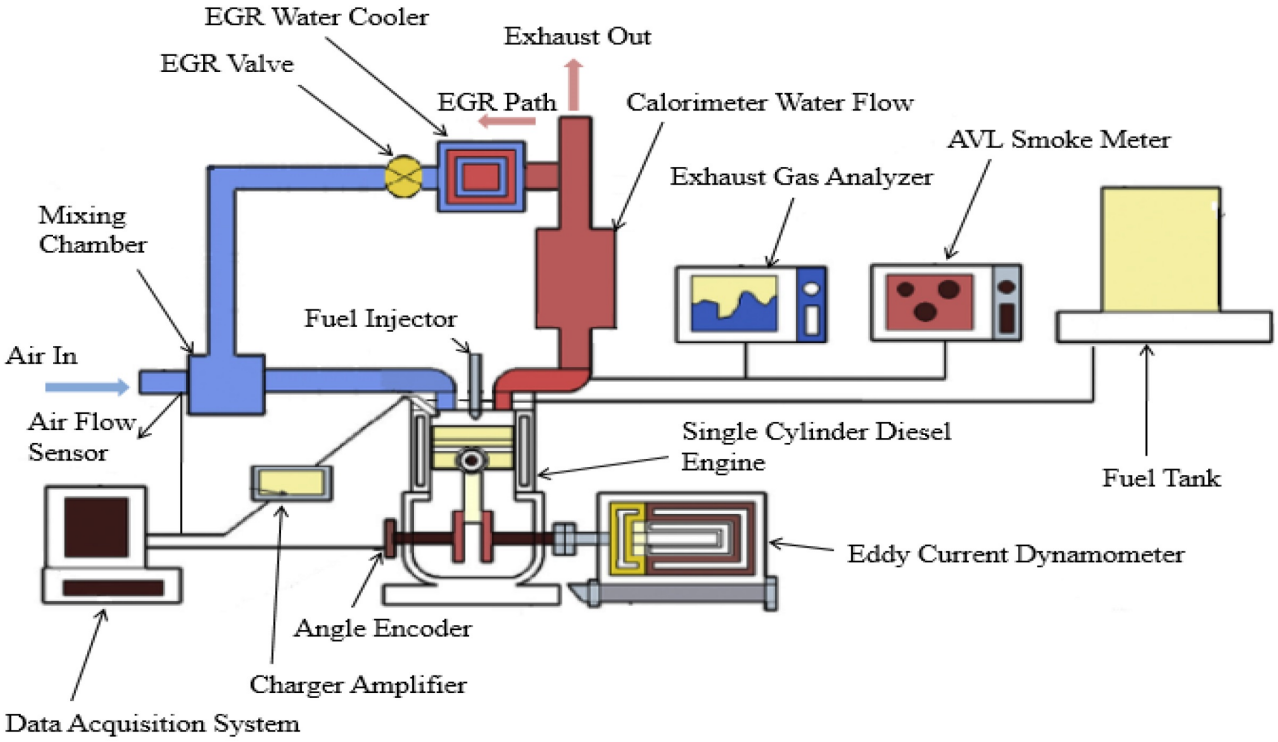

Fig.2. Schematic diagram of an experimental setup.

Please cite this article as: Vijay Kumar M., Veeresh Babu A., Ravi Kumar P., Sudhakara Reddy S. Experimental investigation on the diesel and MME blend with DI diesel engine modified with EGR and nozzle hole orifice diameter. Biofuel Research Journal 19 (2018) 863-871. DOI: 10.18331/BRJ2018.5.3.6

various instruments and calculated parameters are tabulated in **Tables 7** and **8**, respectively.

Table 5.
Specifications of the diesel engine used.

Name of the description	Details/value
Make of mode	TV1-KIRLOSKAR
Engine type	Four stroke, water cooled, single cylinder, DI diesel engine
Loading device	Eddy current dynamometer
No. of cylinder	One
Rated power (kW)	3.5
Constant speed (rpm)	1500
Swept volume (cc)	661
Stroke length (mm)	110
Cylinder bore (mm)	87.5
Compression ratio	17.5:1
Connecting rod length (mm)	234
Injection timing (°CA. bTDC)	23
Piston bowl	Hemispherical
Nozzle type	Multi-hole
Nozzle opening pressure (bar)	210
Number of nozzle hole	3
Modified nozzle spray hole diameter	0.28 mm (base) and 0.20 mm (modified)

Table 6.
Accuracies and ranges of the measuring devices used in this study.

Quantity	Range	Accuracy
AVL gas analyzer	NO_x: 0-5000ppm	± 50 ppm
	CO: 0-10% by vol.	± 0.03%
	HC: 0-20000 ppm	± 10 ppm
AVL smoke meter	0-100%	± 0.2%
Pressure Sensor		
Name: Dynamic pr. Transducer with built-in amplifier Make: PCB Piezotronics, Model: M111A22	(0-110 bars)	± 0.05 bar
Fuel flow sensor	0-5 psi	± 0.1 psi
Crank angle encoder	-	± 1°
Speed measuring	0-5000 rpm	± 10 rpm
Air flow sensor	0-3.500 mm of H_2O	± 1 mm of H_2O
Alternator	0-20 A, 0-450 V	± 0.55 A, ± 1 V
Thermocouples	0-1000°C	± 1°C

Table 7.
Uncertainties of the instruments used in this study.

Instruments	Percentage uncertainties
Pressure pick up	± 1.0
Crank angle encoder	± 0.2
Exhaust gas analyzer	
NO_x	± 0.2
CO	± 0.2
HC	± 0.2
Smoke intensity	± 1.0
Time	± 0.2
Burette for fuel measurement	± 1.5
Load indicator	± 0.5
Speed	± 0.2
Temperature	± 0.2

Table 8.
Uncertainties of the calculate parameters.

Parameter	Percentage uncertainties
Brake power	± 0.5
Brake specific fuel consumption	± 1.5
Brake thermal efficiency	± 1.0

2.5. Experimental testing procedure

As mentioned earlier (see Section 2.2), the present work was aimed at overcoming the shortcoming observed in our previous investigation using Mahua oil biodiesel blend, i.e., increased NO_x emissions in response to reduction in orifice NHD (Vijay Kumar et al., 2018b). More specifically, the two different fuels, i.e., neat diesel and B20 (20% v of Mahua oil biodiesel + 80% v of diesel) were used. Moreover, the base nozzle hole orifice diameter (Ø = 0.280 mm) and modified nozzle hole orifice diameter (Ø = 0.20 mm) were taken into account. Finally, the effect of EGR with three different rates (i.e., 10%, 20%, and 30%) was investigated. Baseline data were obtained by operating the engine at different loads with diesel fuel and base NHD and the experimental data were analyzed and compared with the baseline data.

3. Results and Discussion

3.1. Engine performance analysis

3.1.1. Brake specific fuel consumption and brake thermal efficiency

The variations in BSFC and BTE *vs.* full load BP for different combinations of nozzle orifice diameter, fuel type, and EGR rate are shown in **Figure 3**. As can be seen, there was a negative correlation between BSFC and BP. It should be noted that BSFC trend generally depends on density, viscosity, calorific value, and chemical composition of a given fuel. As revealed in our previous report, the smaller orifice NHD, i.e., 0.20 mm, led to significantly less BSFC with both diesel and B20 because of the higher mixing rate achieved (Vijay Kumar et al., 2018b). In the present study, BSFC was reduced by implementing the EGR rate of 10% for both B20 and diesel fuel probably due to the returning of HC and that the partially-cooled EGR acted as a pre-heater of the intake mixture. Further increments of EGR rate, i.e., 20% and 30%, resulted in increases in BSFC at both lower and higher loads (**Fig. 3**) due to the lack of sufficient O_2 in the combustion chamber leading to incomplete combustion.

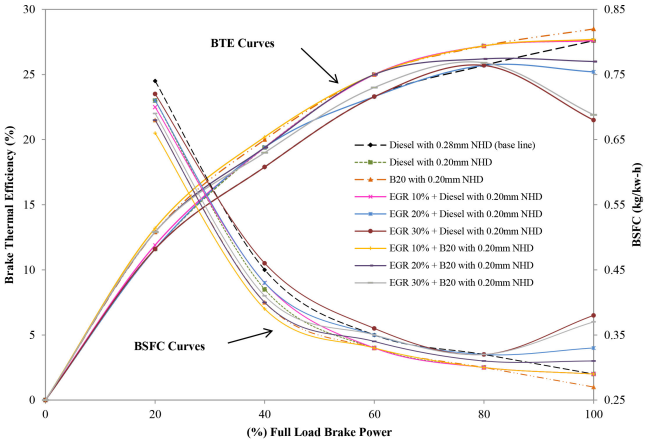

Fig.3. Variations in BSFC and BTE vs. full load BP for different combinations of nozzle orifice diameter, fuel type, and EGR rate.

There was a positive correlation between BTE and BP. When combusting neat diesel fuel, BTE was slightly increased by using the 0.20

Please cite this article as: Vijay Kumar M., Veeresh Babu A., Ravi Kumar P., Sudhakara Reddy S. Experimental investigation on the diesel and MME blend with DI diesel engine modified with EGR and nozzle hole orifice diameter. Biofuel Research Journal 19 (2018) 863-871. DOI: 10.18331/BRJ2018.5.3.6

mm nozzle hole orifice diameter with. While in the case of B20 and the modified orifice diameter, the increases observed in BTE in response to increasing BP were more pronounced. This could be ascribed to the presence of O_2 in biodiesel enhancing the combustion process and heat release. On the other hand, the small orifice NHD of 0.20 mm improved fuel vaporization and atomization. Using the modified nozzle orifice diameter and the partially-cooled EGR of 10%, BTE was slightly increased for both B20 and diesel fuel. This could be explained by the re-burning of HC in the combustion chamber with EGR. At high loads, BTE is generally decreased due to introduction of a rich fuel mixture generating higher levels of CO_2 and soot which could in turn lead to incomplete combustion. In line with that and as can also be seen in **Figure 3**, at higher loads and by suing higher EGR rates of 20% and 30%, the re-burning of HC was much significant. Moreover, through the application high EGR rates, the in-cylinder temperature would be reduced and late HRR would occur leading to reduced peak pressure at different loads and consequently decreased BTE.

3.2. Combustion parameters analysis

3.2.1. In-cylinder pressure

The variations recorded in in-cylinder pressure against crank angle at full load condition for different combinations of nozzle orifice diameter, fuel type, and EGR rate are shown in **Figure 4**. The application of biodiesel blend and diesel fuel with smaller orifice diameter reduced the ID period because of the lower heat capacity as well as the increased O_2 content and cetane number. The peak pressure was decreased with the application of EGR rates. It should be quoted that EGR is mainly composed of CO_2, soot, and H_2O resulting in reduced O_2 concentration in the combustion chamber. The EGR function and the associated dilution and thermal effects led to slower chemical reactions and consequently, delayed start of combustion (SOC) and lengthier ID period. The latter intensified the premixed combustion phase.

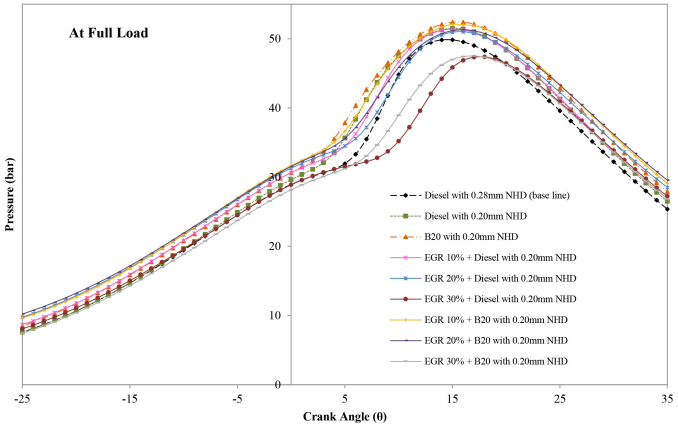

Fig.4. Variations in in-cylinder pressure against crank angle at full load for different combinations of nozzle orifice diameter, fuel type, and EGR rate.

3.2.2. Maximum in-cylinder pressure

The variations of maximum pressure at different percentages of full load BP for different combinations of nozzle orifice diameter, fuel type, and EGR rate are shown in **Figure 5**. The usage of biodiesel blend and diesel fuel with smaller orifice diameter reduced the ID period and led to increases in the pressure in the combustion chamber. As can be observed as BP was increased, the peak pressure increased as well. Comparing diesel and biodiesel blend at different EGR rates with the modified orifice diameter, it could be concluded that the application of EGR with B20 seemed to be more promising (**Fig. 5**) probably due to the O_2 concentration of the biodiesel-containing blend (Lai et al., 2011).

3.2.3. In-cylinder gas temperature

The variations in the in-cylinder gas temperature with respect to different percentages of full load BP for different combinations of nozzle orifice diameter, fuel type, and EGR rate are shown in **Figure 6**. The in-cylinder gas temperature trend indicated that as the BP was increased, the gas temperature rose as well. Furthermore, the temperature was increased by reducing the orifice diameter using B20. This was ascribed to both the oxygen content of biodiesel (Lai et al., 2011) and the more efficient spraying of the fuel leading to more favorable atomization of the fuel particles and consequently more complete combustion process.

When the diesel engine was operated with partially-cooled EGR, the temperature was reduced under all operating conditions. More specifically, there was a negative correlation between the in-cylinder gas temperature and the EGR rates. This could be explained by the decreasing O_2 availability and increasing specific heat of intake mixture in response to increasing EGR rates.

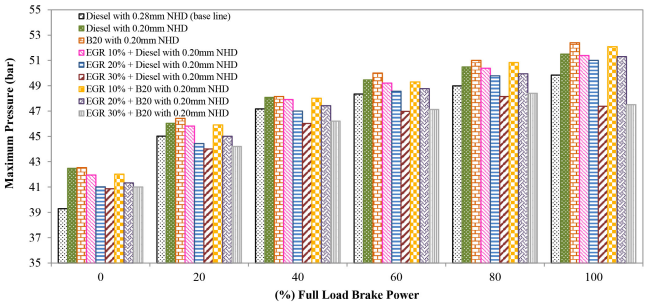

Fig.5. Variations of maximum pressure at different percentages of full load BP for different combinations of nozzle orifice diameter, fuel type, and EGR rate.

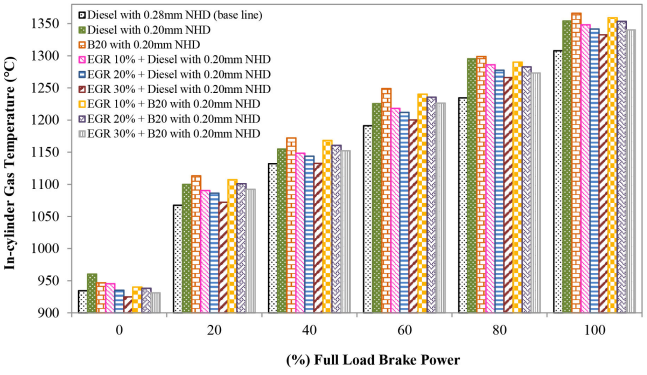

Fig.6. Variations in the in-cylinder gas temperature with respect to different percentages of full load BP for different combinations of nozzle orifice diameter, fuel type, and EGR rate.

3.2.4. Heat release rate

The variations in HRR against crank angle at full load condition for different combinations of nozzle orifice diameter, fuel type, and EGR rate are shown in **Figure 7**. HRR is mainly dependent on ID, heating value of fuel, and air-fuel mixing. In fact, HRR is used to identify the differences in the combustion rates of fuels, the fraction of fuel burnt in the premixed process, and the SOC. The HRR for B20 with 0.20 mm nozzle orifice diameter was found to be lower with the early SOC (**Fig. 7**).

As the EGR rate was increased for diesel and B20, the HRR was increased as well due to the late SOC which was caused by the recirculation of CO_2, soot, and H_2O. Overall, the EGR rate of 10% with B20 seemed to be more promising than the other EGR rates (**Fig. 7**).

Please cite this article as: Vijay Kumar M., Veeresh Babu A., Ravi Kumar P., Sudhakara Reddy S. Experimental investigation on the diesel and MME blend with DI diesel engine modified with EGR and nozzle hole orifice diameter. Biofuel Research Journal 19 (2018) 863-871. DOI: 10.18331/BRJ2018.5.3.6

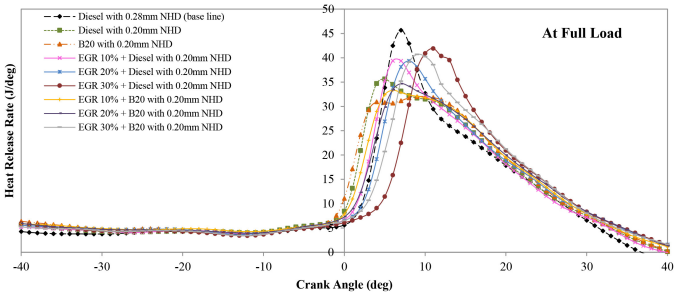

Fig.7. Variations in HRR against crank angle at full load condition for different combinations of nozzle orifice diameter, fuel type, and EGR rate.

3.3. Engine emissions analysis

3.3.1. Carbon monoxide

The variations in CO emission at different percentages of full load BP for different combinations of nozzle orifice diameter, fuel type, and EGR rate are shown in **Figure 8**. CO is mainly formed due to incomplete combustion. This takes place when there is not enough O_2 present to react with fuel. By using the modified 0.20 mm nozzle orifice diameter with B20, CO emissions were reduced due to the better atomization of the fuel. Through the application of the partially-cooled EGR, the CO emissions were increased. More specifically, these increments in CO emissions were proportional with increasing EGR rates. The reason behind increased CO emissions was the low in-cylinder temperature and reduced peak pressure mainly caused by the recirculation of high amounts of unburnt soot, CO_2, H_2O, as well as O_2 deficiency (Duraisamy et al., 2011).

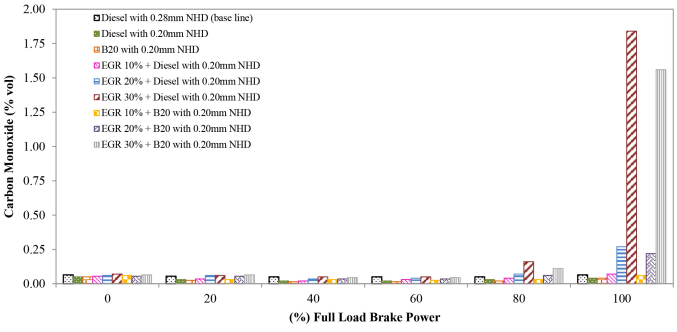

Fig.8. variations in CO emission at different percentages of full load BP for different combinations of nozzle orifice diameter, fuel type, and EGR rate.

3.3.2. Hydrocarbon

The variations of unburned HC at different percentages of full load BP for different combinations of nozzle orifice diameter, fuel type, and EGR rate are shown in **Figure 9**. HC emissions originate from the presence of too many fuel particles left unburned in the combustion chamber due to incomplete combustion. It also appears in the inner layers during the diffusion flame where there is more fuel than air. As presented, HC emissions were substantially reduced by using the modified orifice diameter with both diesel and B20 fuel (**Fig. 9**). This was mainly ascribed to the more atomization of the fuel and proper air-fuel mixing in the combustion chamber. When EGR was used in combination with the modified orifice diameter and both B20 and diesel, increases in HC were recorded. At high loads and by suing the EGR rate of 30%, HC emissions were drastically increased due to the reductions in in-cylinder temperature and pressure reduction. This was because of higher deficiency of O_2 leading the rich fuel mixture inside the combustion chamber (Fontana and Galloni, 2010). In another word, such heterogeneous mixtures do not combust entirely and result in increased HC emissions at higher loads.

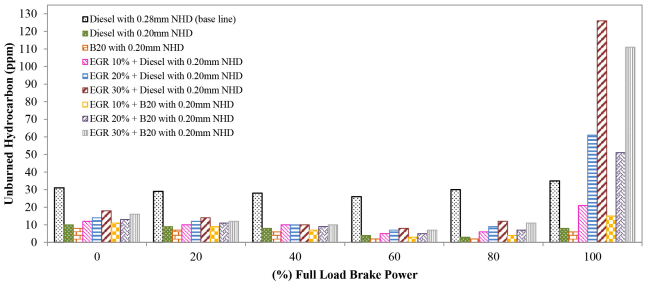

Fig.9. Variations of unburned HC at different percentages of full load BP for different combinations of nozzle orifice diameter, fuel type, and EGR rate.

3.3.3. Oxides of nitrogen

The variations of NO_x at different percentages of full load BP for different combinations of nozzle orifice diameter, fuel type, and EGR rate are shown in **Figure 10**. NO_x is generally formed when N_2 and O_2 react at high temperatures in the combustion process. The NO_x emissions measured for the modified orifice diameter stood higher. Using the biodiesel blend, NO_x must have been formed mainly in the premixed combustion and in the outer layers of the diffusion flame, where the temperature is high and there is a lot of O_2 presents (i.e., the O_2 contained in the B20). As shown in **Figure 10**, the application of the EGR substantially reduced the NO_x emissions. This was in line with the findings of the previous studies indicating that increasing EGR rates led to reduced NO_x formation (Sasaki et al., 1998; Mani et al., 2010). These results could be ascribed to the effect of EGE in decreasing O_2 concentration and flame temperature in the combustible mixture. This was also in line with the results obtained on in-cylinder temperature (**Figure 10**) implying reduced tepmretures in response to increasing EGR rates.

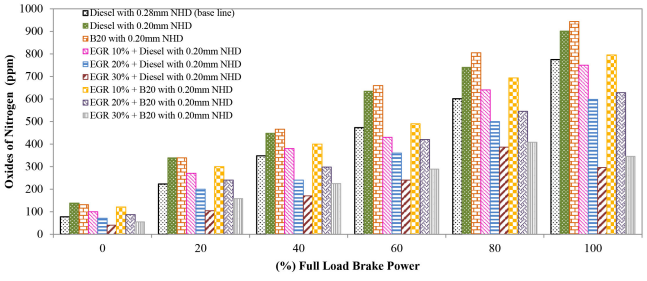

Fig.10. Variations of NOx at different percentages of full load BP for different combinations of nozzle orifice diameter, fuel type, and EGR rate.

3.3.4. Smoke opacity

The variations in smoke opacity at different percentages of full load BP for different combinations of nozzle orifice diameter, fuel type, and EGR rate are shown in **Figure 11**. Smoke opacity is measured to quantify the amount of particulate matter (PM) present in the exhaust gas. The modified orifice diameter reduced smoke opacity when combusting both diesel and B20. As the flow rate of EGR into the combustion chamber was increased, smoke opacity also increased. Comparing diesel and B20 at different EGR

Please cite this article as: Vijay Kumar M., Veeresh Babu A., Ravi Kumar P., Sudhakara Reddy S. Experimental investigation on the diesel and MME blend with DI diesel engine modified with EGR and nozzle hole orifice diameter. Biofuel Research Journal 19 (2018) 863-871. DOI: 10.18331/BRJ2018.5.3.6

rates, the latter led to more favorable results on smoke opacity because of the O_2 concentration present in biodiesel (**Fig. 11**). In another words, EGR reduced the availability of O_2 for the combustion of fuel, which in turn resulted in relatively incomplete combustion and increased formation of PM. The lower in-cylinder temperatures in response to the increasing EGR rates must have also contributed to the increases observed in smoke opacity (Rajan and Senthilkumar, 2009).

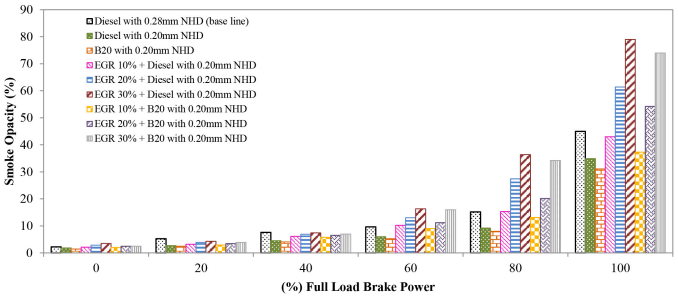

Fig.11. Variations in smoke opacity at different percentages of full load BP for different combinations of nozzle orifice diameter, fuel type, and EGR rate.

4. Conclusions

Experiments were conducted with neat diesel and 20% blend of Mahua oil biodiesel with base and modified NHD while different EGR rates (i.e., 10%, 20%, and 30%) were also employed to overcome the challenges faced regarding NO_x emissions. Combustion characteristics of different combinations of nozzle orifice diameter, fuel type, and EGR rate were recorded and the obtained data were compared with baseline data on neat diesel. Accordingly, the following main conclusions could be drawn:

- The smaller orifice NHD of 0.20 mm was substantially beneficial in improving the engine performance parameters, i.e., BTE, BSFC, P-θ, and HRR as well as in reducing the emissions associated with both diesel and B20. However, the modification implemented led to increased NO_x which was is a major drawback. These results were mainly attributed to the more efficient atomization and proper mixing of air-fuel mixtures in response to smaller orifice NHD.
- Partially-cooled EGR rate of 10% was found promising for both B20 and diesel when the proposed engine modification (i.e., smaller orifice NHD) was carried out.
- By increasing the EGR, NO_x emissions were drastically decreased at all the applied load conditions. This could be explained by the reduced O_2 concentration and reduced flame temperatures in the combustible mixture as a result of EGR implementation.
- Beyond the EGR rate of 10%, the performance, combustion, and emissions characteristics deteriorated mainly due to the recirculation of high amounts of unburnt soot, CO_2, H_2O, as well as of O_2 deficiency.
- The application of high EGR rates led to increased soot formation by decreasing the availability of O_2 for fuel combustion and the consequent relatively incomplete combustion.

Overall and based on the findings of the present study, engine modification, i.e., shifting from the base orifice NHD of 0.28 mm to the modified value of 0.20 mm in the presence of partially-cooled EGR rate of 10% could be recommended as efficient combustion conditions for 20% blend of Mahua oil biodiesel and diesel.

Acknowledgements

The authors are very grateful to the Founding Chairman of the Malla Reddy Engineering College (Dhulapally, Secunderabad) and the Director of the National Institute of Technology Warangal for their support in the conducting of the present study.

References

[1] Achten, W.M.J., Verchot, L., Franken, Y.J., Mathijs, E., Singh, V.P., Aerts, R., Muys, B., 2008. *Jatropha* bio-diesel production and use. Biomass Bioenergy. 32(12), 1063-1084.

[2] Agarwal, A.K., Dhar, A., 2013. Experimental investigations of performance, emission and combustion characteristics of Karanja oil blends fuelled DICI engine. Renew. Energy. 52, 283-291.

[3] Atabani, A.E., Silitonga, A.S., Ong, H.C., Mahlia, T.M.I., Masjuki, H.H., Badruddin, I.A., Fayaz, H., 2013. Non-edible vegetable oils: a critical evaluation of oil extraction, fatty acid compositions, biodiesel production, characteristics, engine performance and emissions production. Renew. Sust. Energy Rev. 18, 211-245.

[4] Azam, M.M., Waris, A., Nahar, N.M., 2005. Prospects and potential of fatty acid methyl esters of some non-traditional seed oils for use as biodiesel in India. Biomass Bioenergy. 29(4), 293-302.

[5] Bai, Y.L., Wang, Z., Wang, J.X., 2010. Part load characteristics of direct injection spark ignition engine using exhaust gas trap. Appl. Energy. 87(8), 2640-2646.

[6] Can, Ö., Öztürk, E., Solmaz, H., Aksoy, F., Çinar, C., Yücesu, H.S., 2016. Combined effects of soybean biodiesel fuel addition and EGR application on the combustion and exhaust emissions in a diesel engine. Appl. Therm. Eng. 95, 115-124.

[7] Channapattana, S.V., Pawar, A.A., Kamble, P.G., 2015. Effect of injection pressure on the performance and emission characteristics of VCR engine using Honne biodiesel as a fuel. Mater. Today Proc. 2(4-5), 1316-1325.

[8] Chauhan, B.S., Kumar, N., Cho, H.M., 2012. A study on the performance and emission of a diesel engine fueled with Jatropha biodiesel oil and its blends. Energy. 37(1), 616-622.

[9] Chauhan, B.S., Kumar, N., Cho, H.M., Lim, H.C., 2013. A study on the performance and emission of a diesel engine fueled with Karanja biodiesel and its blends. Energy. 56, 1-7.

[10] Dubey, P., Gupta, R., 2018. Influences of dual bio-fuel (Jatropha biodiesel and turpentine oil) on single cylinder variable compression ratio diesel engine. Renew. Energy. 115, 1294-1302.

[11] Duraisamy, M.K., Balusamy, T., Senthilkumar, T., 2011. Reduction of NOx emission in Jatropha seed oil fueled CI engine. ARPN J. Eng. Appl. Sci. 6(5), 34-39.

[12] Fontana, G., Galloni, E., 2010. Experimental analysis of a spark-ignition engine using exhaust gas recycle at WOT operation. Appl. Energy. 87(7), 2187-2193.

[13] Ganapathy, T., Gakkhar, R.P., Murugesan, K., 2011. Influence of injection timing on performance, combustion and emission characteristics of Jatropha biodiesel engine. Appl. Energy. 88(12), 4376-4386.

[14] Gnanasekaran, S., Saravanan, N., Ilangkumaran, M., 2016. Influence of injection timing on performance, emission and combustion characteristics of a DI diesel engine running on fish oil biodiesel. Energy. 116, 1218-1229.

[15] Godiganur, S., Murthy, C.S., Reddy, R.P., 2009. 6BTA 5.9 G2-1 Cummins engine performance and emission tests using methyl ester mahua (*Madhuca indica*) oil/diesel blends. Renew. Energy. 34(10), 2172-2177.

[16] Gui, M.M., Lee, K.T., Bhatia, S., 2008. Feasibility of edible oil vs. non-edible oil vs. waste edible oil as biodiesel feedstock. Energy. 33(11), 1646-1653.

[17] Gumus, M., Sayin, C., Canakci, M., 2012. The impact of fuel injection pressure on the exhaust emissions of a direct injection diesel engine fueled with biodiesel-diesel fuel blends. Fuel. 95, 486-494.

[18] Herbinet, O., Pitz, W.J., Westbrook, C.K., 2008. Westbrook. Detailed chemical kinetic oxidation mechanism for a biodiesel surrogate. Combust. Flame. 154(3), 507-528.

[19] Hussain, J., Palaniradja, K., Alagumurthi, N., Manimaran, R., 2012. Petracted: effects of exhaust gas recirculation (EGR) on performance and emission characteristics of a three cylinder direct injection compression ignition engine. Alexandria Eng. J. 51(4), 241-247.

[20] Hussain, J., Palaniradja, K., Alagumurthi, N., Manimaran, R., 2012. Retracted: effect of exhaust gas recirculation (EGR) on

Please cite this article as: Vijay Kumar M., Veeresh Babu A., Ravi Kumar P., Sudhakara Reddy S. Experimental investigation on the diesel and MME blend with DI diesel engine modified with EGR and nozzle hole orifice diameter. Biofuel Research Journal 19 (2018) 863-871. DOI: 10.18331/BRJ2018.5.3.6

performance and emission characteristics of a three cylinder direct injection compression ignition engine. Alexandria Eng. J. 51(4), 241-247.

[21] Jena, P.C., Raheman, H., Kumar, G.P., Machavaram, R., 2010. Biodiesel production from mixture of mahua and simarouba oils with high free fatty acids. Biomass Bioenergy. 34(8), 1108-1116.

[22] Jindal, S., Nandwana, B.P., Rathore, N.S., Vashistha, V., 2010. Experimental investigation of the effect of compression ratio and injection pressure in a direct injection diesel engine running on Jatropha methyl ester. Appl. Therm. Eng. 30(5), 442-448.

[23] Karmee, S.K., Chadha, A., 2005. Preparation of biodiesel from crude oil of *Pongamia pinnata*. Bioresour. Technol. 96(13), 1425-1429.

[24] Koh, M.Y., Ghazi, T.I.M., 2011. A review of biodiesel production from *Jatropha curcas* L. oil. Renew. Sust. Energy Rev. 15(5), 2240-2251.

[25] Koutroubas, S.D., Papakosta, D.K., Doitsinis, A., 1999. Adaptationandyieldingabilityof castor plant (*Ricinuscommunis* L.) genotypes in a Mediterranean climate. Eur. J. Agron. 11(3-4), 227-237.

[26] Kumar, A., Sharma, S., 2011. Potential non-edible oil resources as biodiesel feedstock: an Indian perspective. Renew. Sust. Energy Rev. 15(4), 1791-1800.

[27] Kusaka, J., Okamoto, T., Daisho, Y., Kihara, R., Saito, T., 2000. Combustion and exhaust gas emission characteristics of a diesel engine dual-fueled with natural gas. JSAE Rev. 21(4), 489-496.

[28] Lai, J.Y., Lin, K.C., Violi, A., 2011. Biodiesel combustion: advances in chemical kinetic modeling. Prog. Energy Combust. Sci. 37(1), 1-14.

[29] Liaquat, A.M., Masjuki, H.H., Kalam, M.A., Varman, M., Hazrat, M.A., Shahabuddin, M., Mofijur, M., 2012. Application of blend fuels in a diesel engine. Energy Procedia. 14, 1124-1133.

[30] Mani, M., Nagarajan, G., Sampath, S., 2010. An experimental investigation on a DI diesel engine using waste plastic oil with exhaust gas recirculation. Fuel. 89(8), 1826-1832.

[31] Mofijur, M., Masjuki, H.H., Kalam, M.A., Atabani, A.E., 2013. Evaluation of biodiesel blending, engine performance and emissions characteristics of *Jatropha curcas* methyl ester: Malaysian perspective. Energy. 55, 879-887.

[32] Mo, J., Tang, C., Li, J., Guan, L., Huang, Z., 2016. Experimental investigation on the effect of *n*-butanol blending on spray characteristics of soybean biodiesel in a common-rail fuel injection system. Fuel. 182, 391-401.

[33] Nabi, M.N., Akhter, M.S., Shahadat, M.M.Z., 2006. Improvement of engine emissions with conventional diesel fuel and diesel-biodiesel blends. Bioresour. Technol. 97(3), 372-378.

[34] Naik, M., Meher, L.C., Naik, S.N., Das, L.M., 2008. Production of biodiesel from high free fatty acid karanja (*Pongamia pinnata*) oil. Biomass Bioenergy. 32(4), 354-357.

[35] No, S.Y., 2011. Inedible vegetable oils and their derivatives for alternative diesel fuels in CI engines: a review. Renew. Sust. Energy Rev.15(1), 131-49.

[36] Pinzi, S., Garcia, I.L., Lopez-Gimenez, F.J., Luque de Castro, M.D., Dorado, G., Dorado, M.P., 2009. The ideal vegetable oil-based biodiesel composition: a review of social, economical and technical implications. Energy Fuels. 23(5), 2325-2341.

[37] Raheman, H., Ghadge, S.V., 2007. Performance of compression ignition engine with mahua (*Madhuca indica*) biodiesel. Fuel. 86(16), 2568-2573.

[38] Raheman, H., Phadatare, A.G., 2004. Diesel engine emissions and performance from blends of karanja methyl ester and diesel. Biomass Bioenergy. 27(4), 393-397.

[39] Rahman, S.A., Masjuki, H.H., Kalam, M.A., Abedin, M.J., Sanjid, A., Rahman, M.M., 2014. Assessing idling effects on a compression ignition engine fueled with Jatropha and Palm biodiesel blends. Renew. Energy. 68, 644-650.

[40] Rahman, S.A., Masjuki, H.H., Kalam, M.A., Abedin, M.J., Sanjid, A., Imtenan, S., 2014. Effect of idling on fuel consumption and emissions of a diesel engine fueled by Jatropha biodiesel blends. J. Cleaner Prod. 69, 208-215.

[41] Rajan, K., Senthilkumar, K.R., 2009. Effect of EGR on performance and emission characteristics of diesel engine with sunflower oil methyl ester. Jordan J. Mech. Ind. Eng. 3(4), 306-311.

[42] Ramadan, M.F., Moersel, J.T., 2003. Phospholipid composition of niger (*Guizotia abyssinica cass.*) seedoil. LWT-Food Sci. Technol. 36(2), 273-276.

[43] Ramadhas, A.S., Jayaraj, S., Muraleedharan, C., 2005a. Biodiesel production from high FFA rubber seed oil. Fuel. 84(4), 335-340.

[44] Ramadhas, A.S., Jayaraj, S., Muraleedharan, C., 2005b. Characterization and effect of using rubber seed oil as fuel in the compression ignition engines. Renew. Energy. 30(5), 795-803.

[45] Sahoo, P.K., Das, L.M., Babu, M.K.G., Naik, S.N., 2007. Biodiesel development from high acid value polanga seed oil and performance evaluation in a CI engine. Fuel. 86(3), 448-454.

[46] Saka, S., 2005. Production of biodiesel: current and future technology. In JSPS/VCO Core University program seminar, Universiti Sains Malaysia. 62-102.

[47] Sasaki, S., Sawada, D., Ueda, T., Sami, H., 1998. Effect of EGR on direct injection gasoline engine. JSAE Rev. 19(3), 223-228.

[48] Sharma, V., Das, L., Pradhan, R.C., Naik, S.N., Bhatnagar, N., Kureel, R.S., 2011. Physical properties of tung seed: an industrial oil yielding crop. Ind. Crops Prod. 33(2), 440-444.

[49] Shehata, M.S., Attia, A.M., Razek, S.A., 2015. Corn and soybean biodiesel blends as alternative fuels for diesel engine at different injection pressures. Fuel. 161, 49-58.

[50] Silitonga, A.S., Atabani, A.E., Mahlia, T.M.I., Masjuki, H.H., Badruddin, I.A., Mekhilef, S., 2011. A review on prospect of *Jatropha curcas* for biodiesel in Indonesia. Renew. Sust. Energy Rev. 15(8), 3733-3756.

[51] Singh, S.P., Singh, D., 2010. Biodiesel production through the use of different sources and characterization of oils and their esters as the substitute of diesel: a review. Renew. Sust. Energy Rev. 14(1), 200-216.

[52] Sivaramakrishnan, K., 2018. Investigation on performance and emission characteristics of a variable compression multi fuel engine fuelled with Karanja biodieselediesel blend. Egypt. J. Pet. 27(2), 177-186.

[53] Sureshkumar, K., Velraj, R., Ganesan, R., 2008. Performance and exhaust emission characteristics of a CI engine fueled with Pongamia pinnata methyl ester (PPME) and its blends with diesel. Renew. Energy. 33(10), 2294-2302.

[54] Venkanna, B.K., Reddy, C.V., 2009. Biodiesel production and optimization from *Calophyllum inophyllum* linn oil (honne oil)-A three stage method. Bioresour. Technol. 100(21), 5122-5125.

[55] Vijay Kumar, M., Veeresh Babu, A., Ravi Kumar, P., 2017a. Producing biodiesel from crude Mahua oil by two steps of transesterification process. Aust. J. Mech. Eng. 1-6.

[56] Vijay Kumar, M., Veeresh Babu, A., Ravi Kumar, P., 2017b. Experimental investigation on Mahua methyl ester blended with diesel fuel in a compression ignition diesel engine. Int. J. Ambient Energy. 1-13.

[57] Vijay Kumar, M., Veeresh Babu, A., Ravi Kumar, P., 2018a. The impacts on combustion, performance and emissions of biodiesel by using additives in direct injection diesel engine. Alexandria Eng. J. 57(1), 509-516.

[58] Vijay Kumar, M., Veeresh Babu, A., Ravi Kumar, P., 2018b. Experimental investigation on the effects of diesel and Mahua biodiesel blended fuel in direct injection diesel engine modified by nozzle orifice diameters. Renew. Energy. 119, 388-399.

[59] Vijayaraj, K., Sathiyagnanam, A.P., 2016. Experimental investigation of a diesel engine with methyl ester of mango seed oil and diesel blends. Alexandria Eng. J. 55(1), 215-221.

Please cite this article as: Vijay Kumar M., Veeresh Babu A., Ravi Kumar P., Sudhakara Reddy S. Experimental investigation on the diesel and MME blend with DI diesel engine modified with EGR and nozzle hole orifice diameter. Biofuel Research Journal 19 (2018) 863-871. DOI: 10.18331/BRJ2018.5.3.6

J. Inst. Eng. India Ser. A (September 2018) 99(3):463–471
https://doi.org/10.1007/s40030-018-0292-9

ORIGINAL CONTRIBUTION

Effect of Plate Curvature on Blast Response of Structural Steel Plates

Veeredhi Lakshmi Shireen Banu [1] · N. V. Ramana Rao[2] · Veeredhi Vasudeva Rao [3]

Received: 25 April 2015 / Accepted: 31 March 2018 / Published online: 20 April 2018

Abstract In the present work an attempt is made, through simulation studies, to determine the effect of plate curvature on the blast response of a door structure made of *ASTM A515* grade 50 steel plates. A door structure with dimensions of 5.142 m × 2.56 m × 10 mm having six different radii of curvatures is analyzed which is subjected to blast load. The radii of curvature investigated are infinity (flat plate), 16.63, 10.81, 8.26, 6.61 and 5.56 m. In the present study, a stand-off distance of 11 m is considered for all the cases. Results showed that the door structure with smallest radius of curvature experienced least plastic deformation and yielding when compared to a door with larger radius of curvature with same projected area. From the present Investigation, it is observed that, as the radius of curvature of the plate increases, the deformation mode gradually shifts from indentation mode to flexural mode. The plates with infinity and 16.63 m radius of curvature have undergone flexural mode of deformation and plates with 6.61 and 5.56 m radius of curvature undergo indentation mode of deformation. Whereas, mixed mode of deformation that consists of both flexural and indentation mode of deformations are seen in the plates with radius of curvature 10.81 and 8.26 m. As the radius of curvature of the plate decreases the ability of the plate to mitigate the effect the blast loads increased. It is observed that the plate with smaller radius of curvature deflects most of the blast energy and results in least indentation mode of deformation. The most significant observation made in the present investigation is that the strain energy absorbed by the steel plate gets reduced to 1/3 rd when the radius of curvature is approximately equal to the stand-off distance which could be the critical radius of curvature.

Keywords Blast response · Plate curvature · Explosive impact load · Curved plates

Introduction

Explosions within or in the near vicinity of a military structure can cause a serious damage to external and internal steel structural plates and frames. Generally, to strengthen the external steel plates, a variety of stiffeners are welded to the steel plates. Thus, a variety of blast resistant plate structures that can withstand explosion impact were designed for various operational and safety requirements. Such a blast resistant structure could be constructed as stiffened flat steel plate, curved steel plate or even a sandwich structure. There are a number of applications of these studies in the construction of military, civil, aerospace, marine infrastructure, on-shore and off-shore oil exploration missions.

There have been a number of studies both experimental and theoretical on the blast response of steel plates with flat geometries. Previous studies also include stiffened flat steel plates with a variety of stiffeners. However, in the literature, studies on the blast response of curved steel plates are very limited. Steel plates with a predefined curvature offer much higher resistance and better response to blast loads. Ming-Wei et al. [1] conducted an investigation on the blast resistance of a stiffened door structure, in which they used

✉ Veeredhi Lakshmi Shireen Banu
vlsbanu@yahoo.co.in

[1] Department of Civil Engineering, MREC (Autonomous), Maisammaguda, Dhulapally, Secunderabad 500100, India

[2] National Institute of Technology, Warangal 506004, India

[3] Department of Mechanical and Industrial Engineering, CSET, University of South Africa, Florida 1710, South Africa

ASTM A515 grade 50 steel for their investigation. US, department of Army, in the manual entitled "Structures to resist the effects of accidental explosive," UFC 3-340-02, Washington, D.C. (2008) [2] recommended the use of ASTM A515 grade 50 steel plates. In the present investigation numerical analysis is conducted on the curved plates made of ASTM A515 grade 50 steel, to evaluate the effect of plate curvature on blast mitigation.

Literature Review

A critical review of pertinent literature has been conducted to present the state of the art knowledge on the blast resistance of steel plates including curved steel plates. It is found that majority of the literature available on blast response is confined to analysis of flat plates. The literature on blast resistance of steel plates with curvature is quite limited. Chun and Lam [3] presented the dynamic analysis results of clamped laminated curved plates. Langdon and Schleyer [4, 5] presented the results of experimental, analytical and numerical studies on the response of ¼ scale stainless steel blast wall panels and connection systems, They used ABAQUS to numerically simulate the process. Redekop [6] developed the linear elastic shell theory to study the problem of moderately curved pipe subjected to local impulsive loading. There are some experimental and/or numerical studies that are carried out by the previous investigators are reported in [7–12]. These studies characterize different failure modes and the relationship between deformation and tearing of clamped blast loaded plates. Shen and Jones [13] analyzed the nonlinear dynamic response and failure of clamped circular plates. Langdon et al. [14] conducted experimental and numerical studies on the response of quadrangular stiffened plates subjected to uniform blast loads and Langdon et al. [15] analyzed, the case of localized blast loading.

Nurick et al. [16] presented experimental results for the prediction of tearing of clamped circular plates subjected to uniformly loaded air blast. Wen and Jones [17] investigated the scaling of metal plates subjected to impact and concluded that geometrical scaling can be applied.

Most of the blast door structures were designed as per the guidelines provided in the military technical manual UFC 3-340-02(2008) [2], NAVFAC P-397 [18], and the analysis work was performed following the official design criteria. Argod et al. [19] studied the convergence aspects of shape optimization of solid isotropic plates to mitigate the effects of Air blast loading. Goetz et al. [20]. demonstrated the potential of Hybrid Cellular automation (HCA) method for topology optimization. They established that the method is capable of topology optimization in problems involving large plastic deformations encountered in the crash impact. More recently, Joshua and Tovar [21] conducted a numerical investigation to design a plate structure subjected to stochastic blast loading. They have furthered the research efforts in shape optimization relevant to blast events. In their work they incorporated robust design methods while using LS-DYNA to apply dynamic loading conditions in FEA simulation.

Kumar et al. [22] in their investigation considered 2 mm thick aluminum panels of size 203.2 mm × 203.2 mm to determine the effect of plate curvature on blast mitigation abilities. They have used a shock tube test facility to conduct their experiments. They have concluded that there exists a critical radius of curvature beyond which the blast mitigation capability of the plate starts decreasing. Kumar et al. [23] investigated the effect of plate curvature on the blast response of carbon composite panels.

Trajkovski et al. [24] conducted a comparative study on the blast response of centrally and eccentrically loaded plates with an application to use it under the carriage of a Light Armored Vehicles (LAV). In their investigation three geometric shapes are included namely Flat, V-shape with different included angles and U-shape with different radius of curvatures. From their investigation they concluded that V -shaped plates with included angel around 90° is preferred in terms of blast mitigation and geometric shape suitable to place it under the carriage of LAVs. In their study, maximum size of the plate considered is 300 mm.

Laurence et al. [25] conducted a Micro CT Analysis of the dynamic damage in laminates due to ballistic impact by solid steel bullets and fragmented ice v/s air blast loads. Most important aspect of their study is to understand the types of loading conditions and their influence on the laminates as a function of time.

In all the experimental investigations the limitation is the size of the plate that can be accommodated in the shock tube facility. To overcome this challenge one has to consider numerical experiments in which large plate sizes can be incorporated in the simulation studies. Hence, in the present work it is proposed to consider large size of plates for investigation. From the previous studies, though, it was indicated that there is a critical radius beyond which the blast mitigation properties will decrease, quantification of such critical radius still remains open for investigation. In the present investigation an attempt is made to quantify the critical radius of the plate at which the plate will have greater blast mitigation capabilities. Therefore, in the present work, it is proposed to determine, the effect of plate curvature on blast response, determine the resistance of curved plates with different radius of curvature and to finally determine the critical radius of curvature.

Problem Statement and Objectives

The objectives of the present study is to predict the failure mechanisms of curved ASTM A515 grade 50 steel plates with 10 mm thickness, subjected to air blast loading. The

validation of numerical results of the present investigation is done by comparing with the experimental results of the other researchers from the published literature on flat plate.

In the present study the following specifications are considered for numerical analysis: Blast door with dimensions 5.142 × 2.56 m (projected area) and thickness 10 mm. To investigate the effect of plate curvature with six different radii of curvatures: infinity, 16.63, 10.81, 8.26, 6.61 and 5.56 m are considered for the study. The material grade is ASTM A515 with Young's Modulus, $E = 200 \times 10^9$ N/m^2, Poisson ratio, $\nu = 0.3$, Density, $\rho = 7830$ kg/m^3, Static yield stress, $\sigma_{yield} = 265 \times 10^6$ N/m^2, Ultimate Tensile strength, $\sigma_{ut} = 492 \times 10^6$ N/m^2. The weight of the TNT (explosive) applied is varied from 100 to 400 kg with an increment of 100 kg at a stand-off distance of 11 m. The boundary conditions are assumed to be such that the plate is fixed on all edges.

In this work the curved plate is subjected to only positive blast load that varies as a function of time as per Table 1 and Fig. 1. This is because the positive phase is more important in studies of blast wave effects on structures due to its high amplitude of the overpressure and the concentrated impulse. The blast load is applied according to the Friedlander equation. For the analysis, the pressure is assumed to be uniform within each finite element. However, the variation of the pressure across the length and breadth of plate is taken into account and is estimated based on spherical shock wave spreading pattern.

The typical characteristic of a shock wave is to create an instantaneous pressure rise and an exponential fall. The parameters of interest in the damage process are the peak overpressure (i. e the pressure above the atmospheric pressure), the positive duration and impulse with respect to the scaled distance. The negative phase of the blast wave is generally ignored in the analysis, because, it is not so much detrimental as positive pressure.

The characteristics of a blast for a variety of explosives can be obtained from empirical charts or formula from military technical manual UFC 3-340-02 or statistical analysis [2, 9] during design process. Kinney and Graham [9] expressed the peak overpressure P_s and duration of positive pressure t_s *as a* function of the scaled distance Z and explosive charge weight W, respectively. Which are given below.

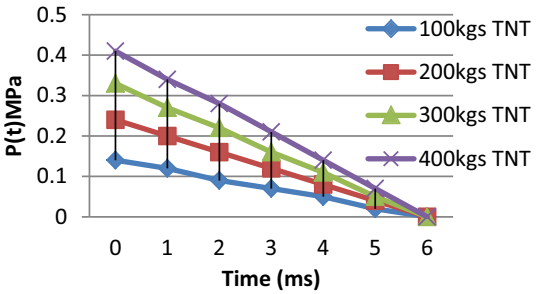

Fig. 1 Positive duration of blast load for various explosive weights

$$\frac{P_s}{P_0} = \frac{808\left[1 + \left(\frac{Z}{4.5}\right)^2\right]}{\sqrt{1 + \left(\frac{Z}{0.048}\right)^2} \times \sqrt{1 + \left(\frac{Z}{0.32}\right)^2} \times \sqrt{1 + \left(\frac{Z}{1.35}\right)^2}} \quad (1)$$

$$\frac{t_s}{W^{\frac{1}{3}}} = \frac{980\left[1 + \left(\frac{Z}{0.54}\right)^2\right]}{\sqrt{1 + \left(\frac{Z}{0.002}\right)^3} \times \sqrt{1 + \left(\frac{Z}{0.74}\right)^6} \times \sqrt{1 + \left(\frac{Z}{6.9}\right)^2}} \quad (2)$$

The equation $P(t)$ is often simplified with a triangular pressure–time curve as per Bulson [26],

$$P(t) = P_{max}\left(1 - \frac{t}{t_d}\right) \quad (3)$$

Conventional high explosives tend to produce different magnitudes of peak pressure. As a result, the environment produced by these chemicals will be different from each other. In order to have a basis for comparison, various explosives are compared to equivalent TNT values. With a scaling parameter, it is possible to calculate the effect of an explosion as long as the equivalent weight of charge in TNT is known,

$$Z = \frac{R}{W^{\frac{1}{3}}} \quad (4)$$

where R is the distance from the detonation and W is the equivalent weight of TNT. It is very difficult to simulate a situation that can fully and adequately represent the ground

Table 1 Characteristics of blast wave with different W–R combinations using Eq. (3)

ts (ms)	P(t) MPa for 100 kg of TNT	P(t) MPa for 200 kg of TNT	P(t) MPa for 300 kg of TNT	P(t) MPa for 400 kg of TNT
0	0.14	0.24	0.33	0.41
1	0.12	0.2	0.27	0.34
2	0.09	0.16	0.22	0.28
3	0.07	0.12	0.16	0.21
4	0.05	0.08	0.11	0.14
5	0.02	0.04	0.05	0.07
6	0	0	0	0

reality. So we employ a simpler model in which the blast waves propagate out wards as if they travel in the open air and not being affected by the surrounding objects. As a result, the simulated damage that occurs on the object may not be fully identical to the damage due to explosion in real life.

The Governing Equations of the General Linear Shell Theory

Before employing a software tool, it is necessary to mention the governing differential equations in terms of strain displacement and compatibility equations, which are given below for completeness.

The Strain–Displacement Equations

Six strain–displacement equations are summarized for the general linear shell theory by Eqs. (5) and (6). They involve six components of strain, which are given explicitly in terms of the three displacement components u; v; and w. These six strain components will satisfy the equations of compatibility. Figure 2 shows the forces and moments acting on a typical 2D-shell element. As the problem under consideration is solved in terms of the displacement components, these conditions are satisfied.

$$\varepsilon_1 = \frac{1}{A}\frac{\partial u}{\partial \alpha} + \frac{1}{AB}\frac{\partial A}{\partial \beta}v - \frac{w}{R_1}, \quad \varepsilon_2 = \frac{1}{B}\frac{\partial v}{\partial \beta} + \frac{1}{AB}\frac{\partial B}{\partial \alpha}u - \frac{w}{R_2}$$
$$\gamma_{12} = \frac{B}{A}\frac{\partial}{\partial \alpha}\left(\frac{v}{B}\right) + \frac{A}{B}\frac{\partial}{\partial \beta}\left(\frac{u}{A}\right) \tag{5}$$

$$\mathcal{X}_1 = -\left[\frac{1}{A}\frac{\partial}{\partial \alpha}\left(\frac{u}{R_1} + \frac{1}{A}\frac{\partial w}{\partial \alpha}\right) + \frac{1}{AB}\frac{\partial A}{\partial \beta}\left(\frac{v}{R_2} + \frac{1}{B}\frac{\partial w}{\partial \beta}\right)\right]$$
$$\mathcal{X}_2 = -\left[\frac{1}{B}\frac{\partial}{\partial \beta}\left(\frac{v}{R_2} + \frac{1}{B}\frac{\partial w}{\partial \beta}\right) + \frac{1}{AB}\frac{\partial B}{\partial \alpha}\left(\frac{u}{R_1} + \frac{1}{A}\frac{\partial w}{\partial \alpha}\right)\right]$$
$$\mathcal{X}_{12} = -\left[\frac{1}{AB}\left(-\frac{1}{A}\frac{\partial A}{\partial \beta}\frac{\partial w}{\partial \alpha} - \frac{1}{B}\frac{\partial B}{\partial \alpha}\frac{\partial w}{\partial \beta} + \frac{\partial^2 w}{\partial \alpha \partial \beta}\right) + \frac{1}{R_1}\frac{A}{B}\frac{\partial}{\partial \beta}\left(\frac{u}{A}\right) + \frac{1}{R_2}\frac{B}{A}\frac{\partial}{\partial \alpha}\left(\frac{v}{B}\right)\right] \tag{6}$$

The Constitutive Equations

The constitutive equations are summarized for a general case in Eqs. (7) and (8). These equations express the eight stress resultants and stress couples, N1; N2; N12; N21; M1; M2; M21; and M12, as explicit functions of the six strain components. For a practical case these constitutive equations can be reduced to six.

$$N_1 = \frac{Eh}{1-v^2}(\varepsilon_1 + v\epsilon_2), N_2 = \frac{Eh}{1-v^2}(\varepsilon_2 + v\epsilon_1)$$
$$N_{12} = S - \frac{H}{R_2}, \quad N_{21} = S - \frac{H}{R_1}, \quad S = \frac{Eh}{2(1+v)}\gamma_{12} \tag{7}$$
$$M_1 = D(\mathcal{X}_1 + v\mathcal{X}_2), \quad M_2 = D(\mathcal{X}_2 + v\mathcal{X}_1)$$
$$M_{12} = M_{21} = H, H = D(1-v)\mathcal{X}_{12} \tag{8}$$
$$D = \frac{Eh^3}{12(1-v^2)}$$

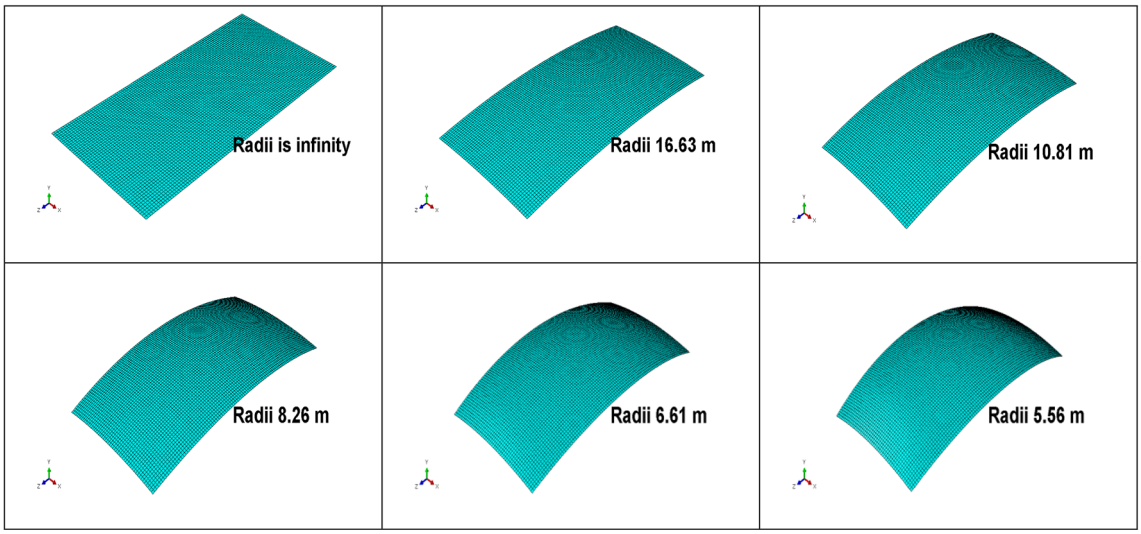

Fig. 2 Geometric modeling and meshing of plates with radius of curvature infinity, 16.63, 1081, 8.26, 6.61, 5.56 m respectively

Table 2 Maximum out-of-plane deflection, maximum in-plane principal stress and strain energy absorbed by the plates for varied blast loads, for different radius of curvature

Radius of curvature (m)	Max displacement (mm) for different blast loads				Max principal stress (MPa) for different blast loads				Strain energy absorbed (kN-m) for different blast loads			
	100 kg	200 kg	300 kg	400 kg	100 kg	200 kg	300 kg	400 kg	100 kg	200 kg	300 kg	400 kg
Infinity (flat plate)	52.3	70.0	81.0	99.0	898	1014	1707	2353	9.0	27.7	47.5	75.0
16.63	25.3	54.2	71.3	81.2	676	868	1392	1966	6.8	20.5	35.2	52.0
10.81	9.4	21.7	42.1	55.0	372	615	1094	1594	4.6	14.4	27.0	31.1
8.26	5.8	8.2	13.6	19.0	244	498	595	816	3.7	10.8	19.0	27.2
6.61	3.0	4.9	7.0	8.4	162	341	448	493	2.5	7.2	13.0	20.4
5.56	2.0	3.3	4.7	6.2	154	279	371	434	2.1	6.5	11.8	18.5

Finite Element Modeling

The curved plates were simulated with shell element. The plates with curvature, shown in Fig. 2, were discretized using S4R type elements. The boundary conditions are such that the plate is assumed to be fixed on all the four edges. The number of elements used in the model has a significant effect on the numerical simulation. To accurately predict the stress state of door structure under explosive loading, different mesh density were adopted to create the analysis model for convergence test. Number of elements used to discretize the model (5.142 m $\times$ 2.56 m $\times$ 10 mm size plates with curvatures) are 103,972. Uniform mesh is used to mesh the plates. All degrees of freedom are fully constrained to simulate the clamped boundary conditions.

Results and Discussion

Effect of Radius of Curvature

The transient responses for different load conditions and varying curvature, obtained from numerical simulation are shown in Table 2. In an attempt to investigate the effect of the plate radius of curvature on the blast response, similar loading conditions are applied to plates of different radius of curvature. The performance of the plates with different radius of curvature is evaluated against the flat plate, used as a reference case. The deformation observed in the plate with radius of curvature as 16.63 m and for the blast loading of 300 and 400 kg is more than the deformation observed in the flat plate which needs further investigation. The plate with least radius of curvature deflects most of the force, while undergoing the least indentation mode of deflection. The observation suggests that plate with smaller radius of curvature deflects more blast energy.

Cross-cut profiles along the center of the plate for varying curvatures in Fig. 3, show that the plate with infinity and 16.63 m radius of curvature has flexural mode of deflection and the plate with 10.81 and 8.26 m radius of curvature has both flexural mode of deflection and indentation mode of deflection. The plate with 6.61 and 5.56 m radius of curvature has indentation mode of deformation more predominantly.

This would suggest that flat plat perform better than the plate with 16.63 m radius of curvature in terms of protection level for 300 and 400 kg loading on the plate for given set of conditions. This may be attributed to the fact that the plate with 16.63 m radius of curvature can buckle while flat plates build up membrane stresses. However, a more thorough investigation is required to draw firm conclusion on this specific observation.

The out of plane deflection is significantly less in plates with 8.26, 6.61 and 5.56 m radius of curvature. The structural behavior could be the result of stiffened geometric effects. For a given projected area exposed to a blast wave, a plate with smaller radius of curvature exhibited higher structural stiffness compared to a plate with larger radius of curvature. Increase in the resistance against blast loads is attributed primarily due to increased geometric stiffness and due to the deflection of blast wave energy by the curved plates. A plate with smaller radius of curvature would deflect more blast energy compared to a plate with larger radius of curvature. As the curvature of the plates reduces, the mode of deformation in the plates shift from flexural mode to indentation mode. This can be seen very clearly in plates with infinity and 16.63 m radius of curvature that undergo flexural mode of deformation and plates with 6.61 and 5.56 m radius of curvature undergo indentation mode of deformation. Whereas, mixed mode of deformation that consists of both flexural and indentation mode of deformations can be seen in the plates with radius of curvature 10.81 and 8.26 m.

Figures 4, 5 and 6 show maximum displacements, maximum principal stresses and strain energy absorbed as a function of radius of curvature of the plate for various blast loads. It is observed form the trends that the blast

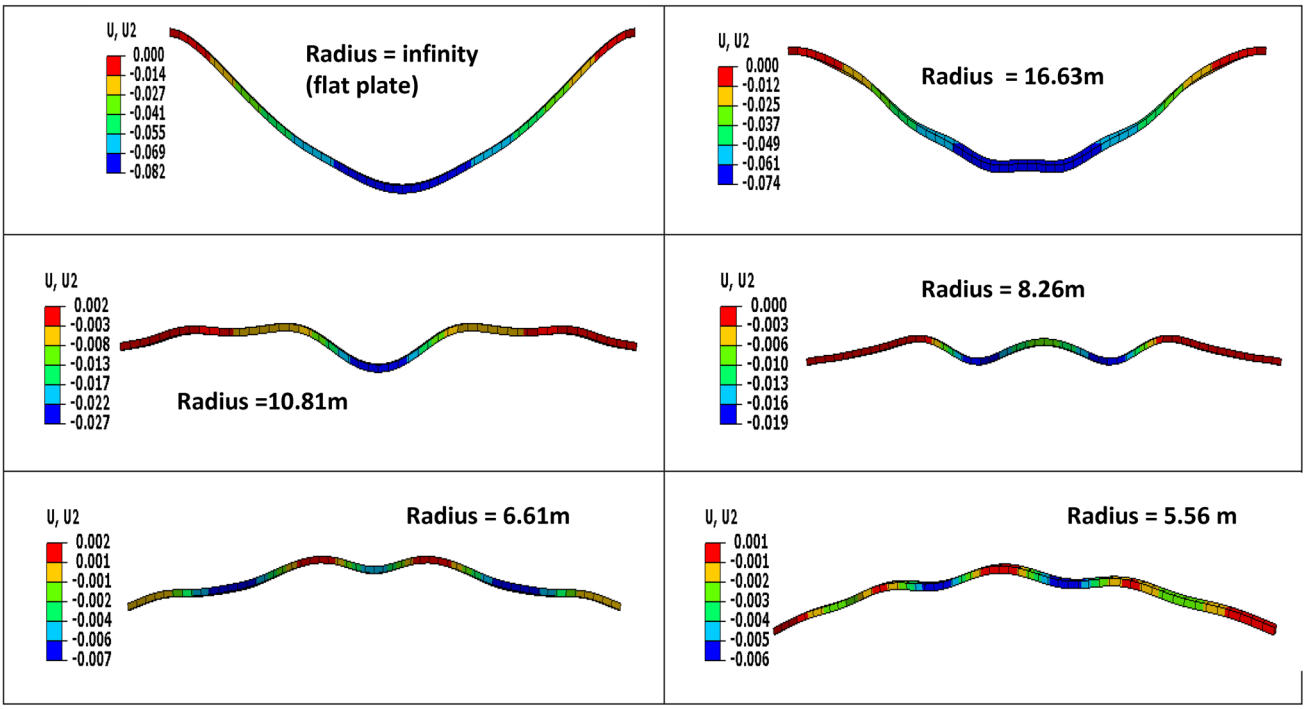

Fig. 3 Cross-cut profiles along the center of the plate for various radii of curvatures for 400 kg blast load

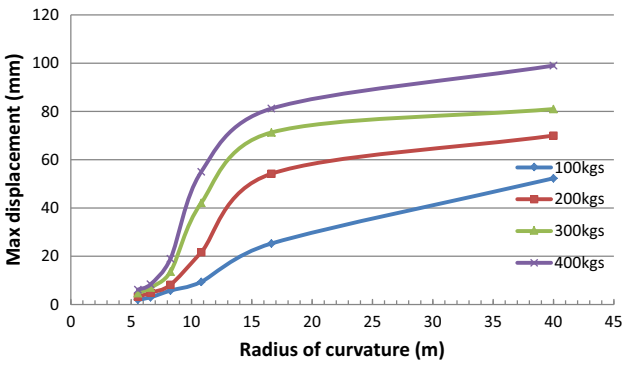

Fig. 4 Maximum displacement in curved plates for various blast loads

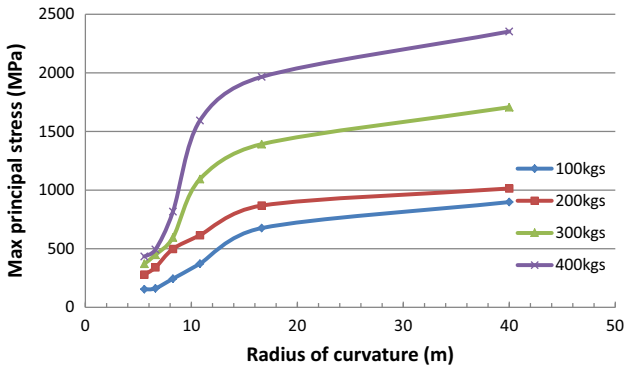

Fig. 5 Maximum principal stress in curved plates for various blast loads

impact on the plate will be lowest for smallest radius of curvature when compared to the flat plate with same projected area. This can be attributed to the shape of the curved plate that deflects considerable blast energy.

From the deflection contours in Fig. 7, cross-cut profiles along the center of the plate in Fig. 3, it is seen that as the radius of curvature decreases, the indentation mode of deflection becomes increasingly predominant. Figure 8 shows the strain energy absorbed by the curved steel plates with various radii for a blast load of 300 kg of TNT. It can be seen that he energy absorbed by the steel plate gets reduced to nearly one-third when the radius of curvature is approximately equal to the stand-off distance.

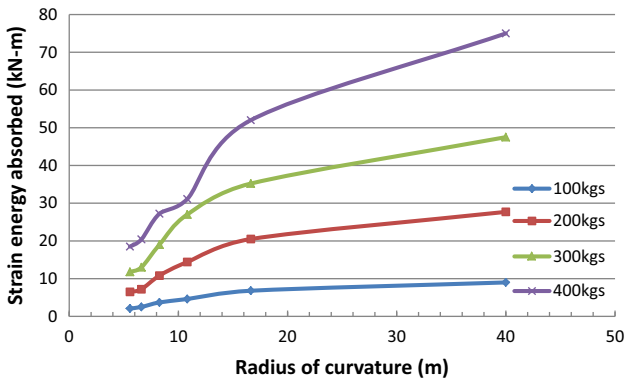

Fig. 6 Strain energy absorbed in curved plates for various blast loads

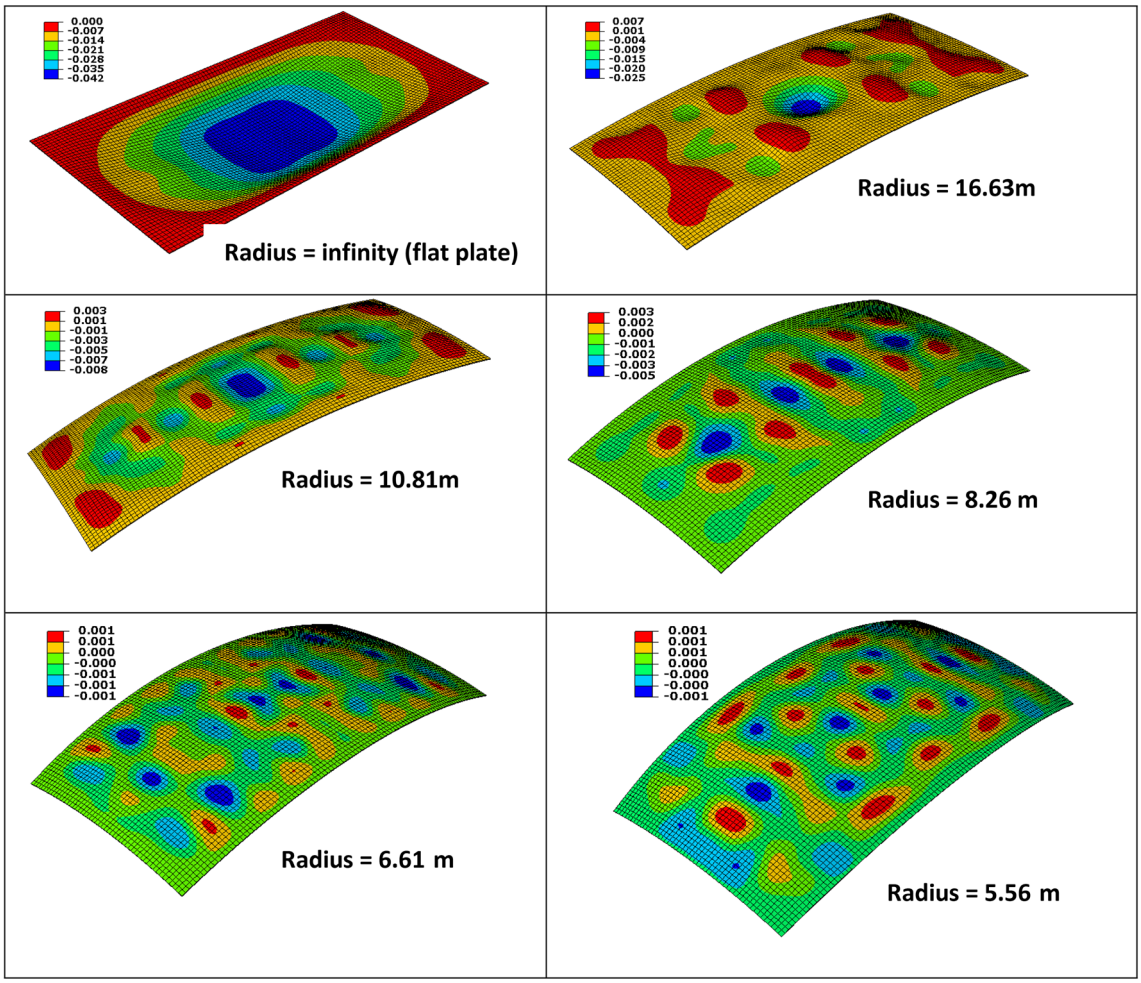

Fig. 7 Contours for flexural mode of deflection and indentation mode of deflection for plates with varying radius of curvature for 100 kg blast load

Fig. 8 Strain energy absorbed by the curved steel plates with various radii for a blast load of 300 kg TNT

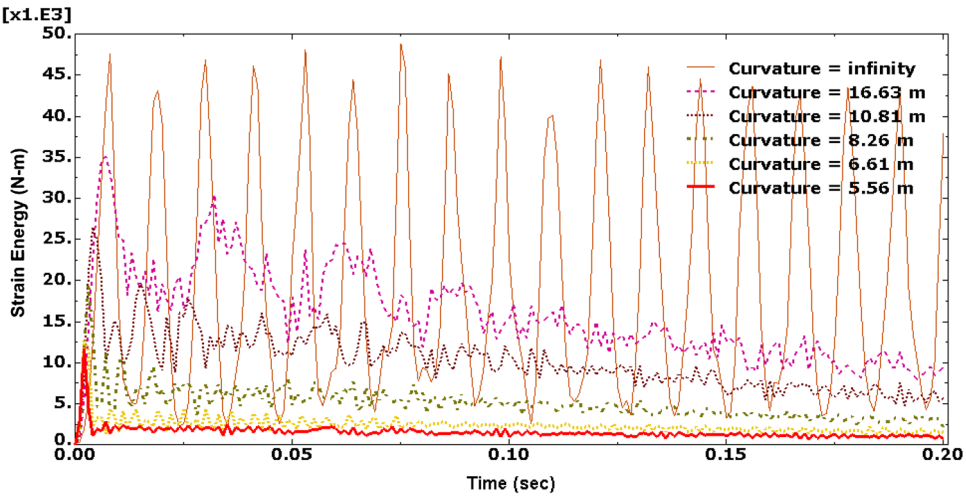

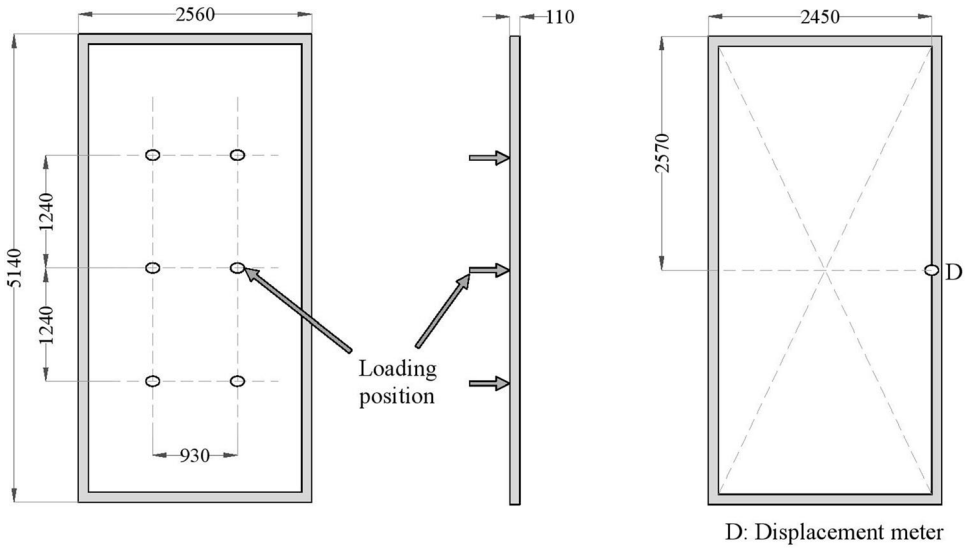

Fig. 9 Schematic of the prototype static test configured by six points loading method. The loading jacks are positioned at the front plate and the displacement meter is mounted on the rare plate

Validation of Results

To establish the validity of numerical results of the present investigation, predicted value of displacement from the finite element computations for the plate with infinite radius of curvature (flat plate) is compared with the published numerical and experimental results of Ming-Wei et al. [1].

The test configuration is shown in Fig. 9. Table 3 shows the results of maximum displacement measured in their experiment as well as Finite Element computations, in which the average load applied by each jack is 763 kg for positive pressure test. Maximum deflection measured by Ming-Wei et al. [1] is 0.48 mm experimentally and 0.49 mm by Finite element computation. In the present work, the corresponding maximum displacement estimated from finite element computations is 0.51 mm. Hence, the deviation of the present numerical values from the reference experimental value is 6.2%. However, the deviation in the estimation of maximum displacement between the present investigation and the displacement estimated by Ming-Wei et al. [1] in their Finite element computation is only 3.89%.

Conclusions

From the validation of numerical results of the present analysis, it is concluded that the methodology employed in this work can adequately predict the out-of-plane displacements and maximum principal stresses developed in the plates designed to withstand the blast loads due to explosion.

It is concluded that as the radius of curvature of the plate increases, the mode of deformation gradually shifts from indentation mode to flexural mode. Form analysis of the results, it can be concluded that the plates with infinity and 16.63 m radius of curvature have undergone flexural mode of deformation and plates with 6.61 and 5.56 m radius of curvature undergo indentation mode of deformation. Whereas, mixed mode of deformation that consists of both flexural and indentation mode of deformations can be seen in the plates with radius of curvature 10.81 and 8.26 m. The decrease in the radius of curvature increases the stiffness and reduces the risk of plate failure. It is concluded that the plate with smaller radius of curvature deflects most of the blast energy and results in least

Table 3 Comparison of maximum displacements for validation of present Finite Element computations with that of displacements obtained from static experiments and Finite Element computations of Ming-Wei et al. [1] (2008)

Sl. no	Loading direction	Equivalent blast load applied by Jacks (kg)	Displacement in mm			Deviation in percentage	
			Present numerical work (A)	Reference [4] experimental and numerical values			
				Experimental (B)	Numerical (C)	Between (A) and (B)	Between (A) and (C)
1	Positive pressure	763	0.51	0.48	0.4909	6.2%	3.89%

indentation mode of deformation. One of the important conclusions drawn from the present investigation is that the strain energy absorbed by a steel plate with radius of curvature approximately equal to the stand-off distance is reduced to one-third (1/3 rd), when compared to the flat plate. This observation, from the present study, leads to a conclusion that the critical radius of curvature is equal to the stand-off distance.

Acknowledgements The authors would like to thank Jawaharlal Nehru Technological University, Hyderabad, India, for extending the necessary support and facilities to carry out this work and publish.

References

1. H. Ming-Wei, H. Jui-Pin, C. De-Jen, Investigation on the blast resistance of a stiffened door structure. J. Mar. Sci. Technol. **16**(2), 149–157 (2008)
2. Department of the Army, "Structures to resist the effects of accidental explosive". UFC 3-340-02, Washington DC (2008)
3. L. Chun, K.Y. Lam, Dynamic analysis of clamped laminated curved panels. Compos. Struct. **30**(4), 389–398 (1995)
4. G.S. Langdon, G.K. Schleyer, Inelastic deformation and failure of profiled stainless steel blast wall panels. Part I: experimental investigations. Int. J. Impact Eng. **31**(4), 341–369 (2005)
5. G.S. Langdon, G.K. Schleyer, Inelastic deformation and failure of profiled stainless steel blast wall panels. Part II: analytical modeling consideration. Int. J. Impact Eng. **31**(4), 371–399 (2005)
6. D. Redekop, Dynamic response of short curved pipes to impulsive loading. Int. J. Press. Vessels Pip. **61**(1), 41–47 (1995)
7. H.L. Brode, Numerical solution of spherical blast waves. AIP J. Appl. Phys. **26**(6), 766–775 (1995)
8. N.M. Newmark, R.J. Hansen, Design of blast resistant structures, in *Shock and Vibration Handbook*, vol. 3, ed. by C.M. Harris, C.E. Crede (McGraw-Hill, New York, 1961)
9. G.F. Kinney, K.J. Graham, *Explosive Shocks in Air*, 2nd edn. (Springer, New York, 1985). **(1985)**
10. L.A. Louca, Y.G. Pan, J.E. Harding, Response of stiffened and unstiffened plates subjected to blast loading. Eng. Struct. **20**(12), 1079–1086 (1998)
11. A.M. Remennikov, A review of methods for predicting bomb blast effects on buildings. J. Battlef. Technol. **6**(3), 155–161 (2003)
12. A. Kadid, N. Lahbari, A. Fourar, Blast loaded stiffened plates. J. Eng. Appl. Sci. **2**(2), 456–461 (2007)
13. S. Wet Qin, J. Norman, Dynamic response and failure of fully clamped circular plates under impulsive loading. Int. J. Impact Eng. **13**(2), 259–278 (1993)
14. G.S. Langdon, K.Y.S. Chung, G.N. Nurick, Experimental and numerical studies on the response of quadrangular stiffened plates. Part I: subjected to uniform blast load. Int. J. Impact Eng. **31**(1), 55–83 (2005)
15. G.S. Langdon, K.Y.S. Chung, G.N. Nurick, Experimental and numerical studies on the response of quadrangular stiffened plates. Part II: localised blast loading. Int. J. Impact Eng. **31**(1), 85–111 (2005)
16. G.N. Nurick, M.E. Gelman, N.S. Marshall, Tearing of blast loaded plates with clamped boundary conditions. Int. J. Impact Eng. **18**(7–8), 803–827 (1996)
17. H.M. Wen, N. Jones, Experimental investigation of the scaling laws for metal plates struck by large masses. Int. J. Impact Eng. **13**(3), 485–505 (1993)
18. Department of the Navy, Structures to resist the effects of accidental explosive. NAVFAC P-397, Design Manual, Alexandria, VA (1991)
19. A. Argod, S.K. Nayak, A.K. Sing, A.D. Belegundu, Shape optimization of solid isotropic plate to mitigate the effects of air blast loading. Mech. Based Des. Struct. Mach. **38**(3), 362–371 (2010)
20. J. Goetz, H. Tan, J. Renaud, A. Tovar, Two-material optimization of plate armor for blast mitigation using hybrid cellular automata. Eng. Optim. **44**(8), 985–1005 (2012)
21. J.I. Joshua, T. Andres, Investigation of plate structure design under stochastic blast loading, in *10th World Congress on Structural and Multidisciplinary Optimization. May 19–24, Orlando, FL* (2013)
22. P. Kumar, J. Leblanc, D.S. Stargel, A. Shukla, Effect of plate curvature on blast response of aluminum panels. Int. J. Impact Eng. **46**, 74–85 (2012)
23. P. Kumar, D.S. Stargel, A. Shukla, Effect of plate curvature on blast response of carbon composite panels. Compos. Struct. **99**, 19–30 (2013)
24. J. Trajkovski, R. Kunc, I. Prebil, Blast response of centrally and eccentrically loaded flat-, U-, and V-shaped armored plates: comparative study. Shock Waves (2016). https://doi.org/10.1007/s00193-016-0704-6
25. L.A. Coles, N. Roy, V.V. Silberschmidt., Micro CT analysis of dynamic damage in laminates: impact vs. blast loading, in *12th International Conference on Damage Assessment of Structures. IOP Conference Series: Journal of Physics: Conference Series 842-012077* (2017). https://doi.org/10.1088/1742-6596/842/1/012077
26. P.S. Buslon, *Explosive Loading of Engineering Structures* (E&FN Spon, London, 1997)

International Journal of Engineering & Technology, 7 (3.29) (2018) 319-322

International Journal of Engineering & Technology

Website: www.sciencepubco.com/index.php/IJET

Research paper

Review on authentication mechanisms in cloud computing

D. Sumathi [1] *, Sireesha Jasti [2]

[1] *Professor Malla Reddy Engineering College*
[2] *Associate Professor Malla Reddy Engineering College*
**Corresponding author E-mail: sumathi.research28@gmail.com*

Abstract

Cloud computing is one of the most significant revolutionary technologies that provide services from computing infrastructures, applications, and platforms to customers for their personal coalition whenever and wherever needed. Security is considered to be the most important key component in the challenges of cloud computing field. This work discusses about the first level key challenges of security-Authentication. Many authentication schemes have been proposed earlier. But all those schemes work as an entry level for service requisition. When the consumers face any problems during the service availability, then both the consumers and service providers need a quick outlook to the SLA. Based on the severity level of the issue, the service providers need permission to access the service area rented by the consumer. This work provides the critics and reviews of authentication mechanisms that have been carried out earlier. In addition, it also provides an overview of authentication mechanisms carried out by service providers and a comparison of various authentication mechanisms has been discussed.

Keywords: *Authentication Mechanisms; Cloud Computing; Mutual Authentication Scheme; Security Issues.*

1. Introduction

Cloud computing as an emerging technology conquers the corporate business world, educational institutions etc with its distinguished characteristics like resource pooling, unlimited storage, automatic software integration, resource provisioning etc. The key factor that draws everyone attention in this cloud computing is security, since consumers who rent space to store data in the cloud need to think of providing security to the data. Moving computation geographically into common server rooms brings issues related to security such as virtualization security, application security, access control, CIA mechanisms. The purpose of cryptography is to secure confidentiality, integrity and authenticity of the available data. User authentication is the paramount requirement in the cloud computing which restricts the users' illegal access of the data that has been uploaded. The actors in the cloud computing can be classified as data owner, user and the cloud server. Data owner outsources the data after encryption to the cloud service provider for storage. When the data owner or any user is in need of the data, they both have to be authenticated by the cloud server.

2. Authentication mechanisms

Password based authentication is one way of one-factor authentication. It is considered to be the weakest link used to access a cloud based application because users can easily tamper the passwords. The declination of the security of password-based mechanisms is premeditated as an outdated technology due to its failure in performance against the perils on the internet. This paved a way to develop as strong and resilient mechanisms, and concurrently providing a means to develop new authentication schemes namely Multi Factor Authentication (MFA) Schemes [2]. Securing access with Multi Factor Authentication

MFA Can be done in two phases namely

1) Identification phase.
2) Authentication phase.

Identification Phase:

In this phase, the identity of the end user has to be determined. It is a straightforward technique since the user has to provide his or her identity in terms of the unique user name.

Authentication Phase:

Security is added more to the process through the authentication phase. Here the user has to provide the original proof for the identity that has been claimed by the user. Various authentication techniques have been implemented to prove the proofs of identity. It can be classified into three categories:

1) Something the user knows: This mechanism is a secret bond between the user and system.
2) Something the user has: This technique verifies for the identity that has been shown as a proof. This involves a token that entails the user to press a button to receive a code to be entered into the authentication system. Examples of techniques can be smart cards and physical keys.
3) Something the user is: This mechanism measures various biometric characteristics like finger prints, hand geometry, facial patterns etc .The characteristics of the user are compared with the authentication database to find out whether the user is a legitimate user.

Knowledge-based authentication mechanisms are inexpensive, easy to implement and familiar to end users. Device-based approaches eradicate the risk of a fraud and the legitimate user having access at the same time, because only one person can own the token or smart card at a time. The theft of the authentication device could lead to the impersonation of the user until the device is discovered. Biometric systems are quite expensive and some end users feel that the physical aspect involved invades their privacy. In order to maintain the balance between these advantages and disadvantages, certain organizations seek a high level of security

that could combine multiple authentication schemes to assure a high level of confidence regarding an end user's identity. This approach is known as multifactor authentication because it combines techniques from two or more of the identity authentication categories.

A Service provider attracts the consumers to use their service by exploiting the specialized features they provide. Communication between the consumer and the service provider gets initiated through the service level agreements.

3. Related works

A remote user authentication scheme proposed by Lamport uses the server for storing the hash value of the user's password for later verification [3]. Hwang et al found that the whole system could be invalid if the password table was modified [4]. Hence they devised a new authentication scheme that uses smart card.

This scheme works on the basis of ElGamal's public cryptosystem and there is no need for the scheme to maintain a password table for user authentication. But this scheme was not able to resist impersonate attack because any user could take off the other user's ID and PWD without the secret key. An efficient password based remote user authentication scheme proposed by Chien et al states that there are many advantages like mutual authentication, freely choosing password, absence of verification table and only less hashing operations[5]. In spite of all these advantages this scheme is said to be vulnerable to attacks like reflection attack, insider attack. In 2010, Chen and Huang formulated a scheme combining CAPTCHA and visual secret sharing [6]. But this scheme was not efficient since smart card might be exposed and raises masquerading attack.

Nowadays, many research works have been focused on the security, since it is considered to be the most prominent challenge in this cloud computing world. Among the various security issues, some of the noteworthy and recent research is included which primarily focus on the authentication phase of cloud security.

This paper presents few research directions and approaches that have been set forth which assist the researches to think about a new dimension in this area. A comparison of the authentication schemes along with the research directions is shown in the tabular column given below.

S.No	Method/Scheme/Framework	Technology used for authentication
1	Analysis and Improvement of User Authentication Framework for Cloud Computing	Smart card is used. Messages are hashed and sent.
2	Authentication in the Clouds: A Framework and its Application to Mobile Users [7]	User behavior is translated into authentication scores.
3	Consolidated Authentication Model[8]	Credentials are uploaded and downloaded. Two servers namely credential server and signing server are used.
4	A Strong user authentication framework in cloud computing[9]	Identity management, mutual authentication, session key establishment between the users and the Cloud server.
5	User Authentication Platform using Provisioning in Cloud Computing Environment[10]	User authentication is done through user profiles.
6	Secure Password by Using Two Factor Authentication in Cloud Computing[11]	Adopts 2FA and anonymous password. Privacy preservation of password is done.
7	Multi-dimensional password generation technique for accessing cloud services[12]	Confidential inputs like logos, images, textual information and signatures etc are used to generate the multi-dimensional password.
8	Multi-dimensional and Multilevel authentication techniques [13]	Concatenation of passwords is done at various levels. Passwords are entered at each level and privileges are granted. Resources corresponding to that level are granted.
9	Context-aware Platform for User Authentication in Cloud Database Computing[14]	Context-aware platform for user authentication in Cloud computing is proposed.
10	A Time-Bound Ticket-Based Mutual Authentication Scheme for Cloud Computing [15]	Mutual authentication between the server and the client. Time bound tickets.
11	Enhanced Time-Bound Ticket-Based Mutual Authentication Scheme for Cloud Computing [16]	Mutual authentication is done. Password and hashing functions are used. All this are done in smart card.
12	Authentication techniques in cloud and mobile cloud computing environments[17]	Categorization based on its input, i.e. the credentials required for validating users is done
13	mutual authentication [18]	To detect the attack being initiated by the attacker by placing his virtual machine close to the legal virtual machine

The CSP has to authenticate the remote users before a request has been put forth for accessing any kind of service. Hao et al. proposes a time-bound ticket based mutual authentication scheme for cloud computing [15].

This scheme resists against lost smart card attacks, offline password guessing attack, lost ticket attack, masquerade attack and replay attack. The special characteristic in this paper is mutual authentication and secure session key generation. In addition to this additional feature, the proposed scheme is exposed two drawbacks namely Denial-of-Service attack due to lack of early wrong password detection prior to verification request creation and insecure password change. It is assumed that the attacker is able to intercept the messages between the user and the server. Pippal proposed an enhanced version of Hao's proposal in such a way that the proposed protocol resists against the Denial-of-Service attack and the password can be changed without any assistance from the cloud server in a secure manner [16]. It is clearly understood that all the existing authentication mechanisms works only towards the verification of the claimed identity of an entity. Many of the existing authentication schemes check only whether the user is legitimate user and concentrates only on verifying the identity of the user. Pippal's scheme overcomes the flaws raised in hao's scheme. Mutual authentication and session key generation is provided in this scheme. Time and tickets raised for data verification is fixed in this method. But when the user faces any issue during the service and when the service provider requires user's permission to enter into the rented area, then this authentication schemes becomes weak.

4. Analysis of security mechanisms

The most important aspects of security that the cloud provider should address to the users are Confidentiality, Availability, Integrity, Authentication and SLA. This work addresses a list of service providers and their authentication mechanisms.

In addition to services like IaaS,PaaS and SaaS, there are many services provided by the service providers. Security solutions have been devised and they are provided in terms of Security-as-a-Service (SEaaS) which is a new instance of a cloud service model.

Among the various services that are available in different forms, Authentication-as-a-Service (AaaS) is considered as the predominant factor among the variants. In order to reduce the risk of compromising sensitive information, AaaS is issued.

The below comparative analysis of some of the authentication schemes implemented in cloud and these schemes are compared based on resistance to various attacks have been discussed and shown in the below table.

Provider	Service Provider	Technology	Description
PaaS	Amazon Web Services	Multi-Factor Authentication	It request for username and password (what they know). Further, it asks for an authentication code from their AWS MFA device (what they have).
	Salesforce	Single Sign-on	Username and password
	Microsoft Azure	Multi--Factor Authentication	It requires any two or more of the following verification methods: 1) Something you know (a password). 2) Something you have a trusted device that is not duplicated. 3) Something you are(biometrics)
	GAE	Single Sign-on	Username and password
IaaS	AT & T	2FA	First factor: Username and password Second factor: Hardware or Software token
	GOGRID	Token based authentication	
	Joyent	2FA	First factor: Username and password Second factor: Hardware or Software token
SaaS	NetSuite	2FA	First factor: Username and password Second factor: Hardware or Software token
	Workday	Single Sign-on with MFA	SAML Authentication
	Cornerstone	User Authentication	Certificate-Based Authentication

S. No	Authentication Mechanisms	Attacks
1	Authentication using smart card	Physical tampering. Key and Memory reading
2	Consolidated Authentication Model	Credentials might be hacked
3	A Strong user authentication framework in cloud computing	Password verification is done locally
4	Authentication in the Clouds: A Framework and its Application to Mobile Users	Chances for theft of user credentials,
5	User Authentication Platform using Provisioning in Cloud Computing Environment	Theft of credentials like time and place of user. Accessing the location of the user also might be misused.
6	Secure Password by Using Two Factor Authentication in Cloud Computing	Theft of mobile device
7	Multi-dimensional password generation technique for accessing cloud services	Generation of password at various lead to overhead
8	Multi-dimensional and Multilevel authentication techniques	Memory space required is more
9	Context-aware Platform for User Authentication in Cloud Database Computing	Personal information stored might be available for misuse.
10	A Time-Bound Ticket-Based Mutual Authentication Scheme for Cloud Computing	offline password guessing attack, lost ticket attack, masquerade attack and replay attack
11	Enhanced Time-Bound Ticket-Based Mutual Authentication Scheme for Cloud Computing	Lost ticket attack

5. Conclusion

Various security schemes are proposed for cloud environment and most of the schemes were well adopted in entry level authentications. Time bound ticket based mutual authentication is one such a scheme which provides security feature in the access layer. The mutual authentication scheme in cloud is mainly designed to enhance the customer satisfaction and improves the level of commitment by the service provider. There are a number of security issues with cloud computing in both the sides known as cloud service
provider (CSP) side and customer/client side. From the detailed comparative analysis and existing authentication schemes it is understood that the general cloud policy insisted that this responsibility should be held by CSP and as well as the consumer. This could be implemented by designing an authentication framework which concentrates on providing security throughout the service rendering period. In addition to that, SLA could also be revised and it could be bound with the authentication framework.

References

[1] NIST Definition. [Online]. Available: www.nist.gov/itl/cloud/upload/cloud-def-v15.pdf Cloud Computing services & comparisons. [Online]. Available: http://www.thbs.com/downloads/Comparison of Cloud computing services.pdf.

[2] Sabout Nagaraju, Latha Parthiban, SecAuthn: Provably Secure Multi-Factor Authentication for the Cloud Computing Systems", Indian Journal of Science and Technology, Vol 9(9), March 2016.

[3] L. Lamport, Password authentication with insecure communication, Communications of the ACM 24 770–772, 1981.

[4] M. S. Hwang and L. H. Li, A new remote user authentication scheme using smart cards, IEEE Transactions on Consumer Electronics, vol. 46, no. 1, pp. 28-30, 2000.

[5] H. Y. Chien, J. K. Jan, and Y. M. Tseng, "An efficient and practical solution to remote authentication: smart card," Computers and Security, 21(4):372–375, 2002.

[6] T. H. Chen and J. C. Huang, "A novel user-participating authentication scheme," The Journal of Systems and Software, 83(5):861–867, 2010.

[7] Chow, Markus Jocobsson, Ryusuke Masuoka, Jesus Molina, Yuan Niu, Elaine Shi, Zhexuan Song, "Authentication in the Clouds, A

Framework and its Application to Mobile Users. CCSW'10, October 8, Chicago, Illinois, USA, 2010.
[8] J. Kim and S. Hong, 2011. One-Source Multi-Use System having Function of Consolidated User Authentication, YES-ICUC, 2011.
[9] Choudhury, A.; Kumar, P.; Sain, M.; Lim, H. and Hoon Jae-Lee, "A Strong User Authentication Framework for Cloud Computing", Services Computing Conference (APSCC), 2011 IEEE Asia-Pacific, pp.110-115, 12-15 Dec. 2011.
[10] Hyosik Ahn, Hyokyung Chang, Changbok Jang, Euiin Choi," User Authentication Platform using Provisioning in Cloud Computing Environment", ACN : Advanced Communication and Networking pp 132-138,2011.
[11] Z. Shen, L. Li, F. Yan, X. Wu, 2010. Cloud Computing System Based on Trusted Computing Platform.International Conference on Intelligent Computation Technology and Automation (ICICTA). vol 1, pp 942-945,2010
[12] Quorica, 2009. Buisness Analysis Evolution of Strong Authentication, September 2009.
[13] Tanvi Naik, Sheetal Koul," Multi-Dimensional and Multi-Level Authentication Techniques", International Journal of Computer Applications (0975 – 8887) Volume 75– No.12, August 2013.
[14] Manjea Kim, Hoon Jeong, Eulin Choi, "Context-aware Platform for User Authentication in Cloud Database Computing", International Conference on Future Information and Technology and Management Science and Engineering, Lecture notes in Information Technology, Vol 14,2012.
[15] Hao, Z., Zhong, S. and Yu, N. "A timebound ticket-based mutual authentication scheme for cloud computing", International Journal of Computers, Communications and Control, 6(2), pp. 227–235,2011.
[16] Ravi Singh Pippal, Jaidhar C. D. Shashikala Tapaswi," Enhanced Time-Bound Ticket-Based Mutual Authentication Scheme for Cloud Computing", Informatica 37, 149–156, 2013.
[17] Mahamudul Hasan , Md. Hasnat Riaz , Md. Auhidur Rahman," Authentication Techniques in Cloud and Mobile Cloud Computing", IJCSNS International Journal of Computer Science and Network Security, VOL.17 No.11, November 2017.
[18] Amit Verma, Megha Mittal, Bharti Chhabra, "The Mutual Authentication Scheme to detect virtual side channel attack in cloud Computing", International Journal of Computer Science and Information Security (IJCSIS), Vol. 15, No. 3, March 2017.

Penalty Quoted Cost Approach for Loss Allocation in a Transmission line by Considering the Mutual Inductance

V. Suma Deepthi, M. Maheswari, M. Vibhavari, K. Prasanth Kumar

Abstract*: In deregulated electricity market, there is a significance of Loss and Cost Allocation due to transmission. The real power loss from the generators and its associated cost is allocated to the concerned parties in a fair manner by Independent System Operator (ISO). In the cost allocation process there is a participation of generators and loads. The effective part of the paper is there is an impact of mutual inductance (MI) which involves in transmission line in transmission cost/loss allocation phenomena for multilateral contracts is illustrated using a test bus system. To determine the effect of mutual inductance penalized quoted cost (PQC) based approach has discussed. Effect of mutual inductance is tested on an IEEE-4bus system. The simulation results are obtained using MATLAB R2014a. The result shows that there is a significant impact on transmission loss due to mutual inductance which cannot be neglected in the Allocation of loss process.

Index Terms: penalized quoted cost, loss/cost allocation, multilateral contracts, mutual inductance and independent system operator.

I. INTRODUCTION

The Deregulation is an entity which creates changes to encourage competition wherever it is necessary. In power system, deregulation is frequently used and is very common in regulatory and economic aspects. It is converting the rules the government is setting up to control the running of electric supply industries. In these industries it takes part of the original structure and arranges into other form for better efficiency and performance. It is altering the franchise rule monopoly that effect in what way the electric companies work and customers buy electric power services. The deregulation of the electric utility industry wants IPP to be within the transmission system. For transmitting the power from generation to consumption there must be a common transmission network between power producers, sellers and buyers.

To ignore the huge investment the natural monopoly interconnected transmission system is considered. The deregulation power flow method are slightly different compared to regulation market. In trying to get profits, benefits and cheaper sources causes overloading in transmission network, increase in thermal voltage and no system security. Thus to control the transmission network operation, performance and security system operator, grid operator is required. There are new entities that can function independently which is created by electricity restructuring and those entities in deregulated electricity market are generating companies, transmission companies distribution companies and independent system operator.

Generating companies (GENCOs) generate electricity and also sell reactive powers and electricity to the entities. Transmission companies (TRANSCOs), transmit electricity to the consumers through transmission network. Distribution companies (DISCOs) distribute the electricity to customers in specified region. From spot markets the electricity will be purchased and supplied to the customers. A customer cannot purchase electricity in a restructure system but they can obtain by bidding in spot market. Independent system operator is established since a competitive market requires independent operation and grid control. It is an entity that does not participate in market trades and maintains the system security coordinating for longer period.

An agent between retailers and customers can be called as an Aggregator. A broker may act as an agent between DISCOs and GENCOs. Retail electricity cab be sold by legal approval by retail companies. Electric energy and other services is provided to customers by retailers.

Bilateral Contracts:

It is transmission of power between buying and selling organization

Multilateral Contracts:

Extension of bilateral contract is a multilateral contract. Two or more parties get involved in these contracts. They inject a power in one bus and take out from other bus so that sum of all generations is equal to sum of all loads.

Benefits of multilateral contracts:

Cheaper electricity: It induces to set up more industries and business opportunities in a region thus paving the way for economic growth.

Efficient capacity expansion planning: Generating companies will eagerly come forward to set up plants in proper location because of greater knowledge existence

More choice: Offers will be given by retailers to buy electricity, so customers can have more choices.

Better service: there must be more attention towards better and quality of service and retailers are responsible for it.

Opportunities: due to greater business and industry, investment,

Revised Version Manuscript Received on 30 November, 2018.

V.SumaDeepthi,Assistant professor, Department of EEE, Malla Reddy Engineering College (A), Secunderabad, India.

M.Maheswari, Professor and Head, Department of EEE, Malla Reddy Engineering College (A), Secunderabad, India.

M.Vibhavari, PG Student, Department of EEE, Malla Reddy Engineering College (A), Secunderabad, India.

K. Prasanth Kumar, PG Student, Department of EEE, Malla Reddy Engineering College (A), Secunderabad, India.

Published By:
Blue Eyes Intelligence Engineering
& Sciences Publication

employment opportunities are enhanced. The beneficiaries are not only skilled power engineers but also people such as finance personnel, bankers, market traders, etc.

II. NOTATION

Indexes:

n	*No. of buses in total*
n_g	*No. of loss supplied by the generators*
n_{tr}	*No.of multilateral transactions*
P_{gi}	*Generation of active/real power of bus 'i'*
P_{di}	*demand of real/active power bus 'i'*
L_i	*generator 'i' penalty factor*
QC_i	*Quoted cost of loss supplied by the generator 'i'*
PQC_i	*Penalized quoted cost of generator 'i'*
$P_{loss-ac}$	*loss function of alternating current*
$P_{loss-dc}$	*loss function of direct current*
L_{ploss}	*ac load flow solution real/active power loss in total*
L_k	*Transaction loss'k'*
f_k	*contribution fraction of loss of transaction 'k'*
P_i	*Injection of net real/active power at bus 'i'*
CT_k	*Allocation of cost to transaction 'k'*
TC_{ploss}	*cost of loss supplied in total*
B_{mn}	*Dc loss coefficients*
$B_{ij}\,B_{i0}\,B_{00}$	*Ac loss coefficients*

III. PROBLEM FORMULATION

3.1 Bus Admittance Matrix Considering Mutual Inductance:

Through this matrix the effect of mutual inductance is considered. The calculation of this matrix for mutual elements network is presented in (1), (2), (4) which is shown in the equation (1).The matrix calculation with mutually coupled elements is shown in equation (1) to (4). In this method, calculation of this matrix is obtained by addition of mutual elements. This effect causes change in the, nodal voltages, power flowing through the lines, bus admittance matrix thus total network losses. Thus there will be a change in transmission loss and its cost is allocated among the network buses. Loss are shared among buses in penalized quoted cost method. In the load flow solution bus admittance matrix is used.

$$Y_{bus} = A^T y_{prim} A \qquad (1)$$

Where, A- y_{prim} -element node incidence matrix and primitive admittance matrix.

The A, y_{prim} dimensions for a network with 'e' 'n elements and' nodes is ($e \times n$) and ($n \times n$) respectively.

$$y_{prim} = \sum_{i=1}^{e}\sum_{j=1}^{e} y_{prim}^{ij} \qquad (2)$$

Where, y_{prim}^{ij} - ($e \times e$) matrix has one non-zero element only. The non-zero element position is (i,j) and the value is equal to the $y_{prim}(i,j)$ value. So equation (1) can be written as

$$Y_{bus} = A^T \sum_{i=1}^{e}\sum_{j=1}^{e} y_{prim}^{ij} A \qquad (3)$$

The y_{prim}^{ij} matrix consists of only one nonzero element as it is a scalar. So the equation (3) can be again written as given in equation (4).

$$Y_{bus} = y_{prim}(i,j) A_i^T A_j \qquad (4)$$

3.2 Penalized Quoted Cost (PQC) Method:

Supplying transmission system losses economically under bilateral contract is a challenge for power engineers. Penalized quoted cost (PQC) approach is proposed where generators will participate for supplying the transmission line losses which may be incurred from their customers through their bilateral contracts in a deregulated power market. The loss supplying generators will quote the price and the quantum of active power that can be supplied by them to Independent System Operator (ISO) in a day-ahead market. The proposed PQC based loss allocation approach has the following advantages

- Loss or cost allocation to generators and loads are fair and it is non-negative.
- It uses traditional AC load flow analysis resulting in calculating real power losses.
- Active power loss is shared between generators and loads economically.
- Relative position of the buses is taken into account by considering the penalty factor.
- Losses are allocated to individual transaction considering only the magnitude of real power for a given transaction.
- Independent of size of the system and quantum of generation.
- Understanding and implementation of algorithm is simple.

Let us consider an 'n' number of buses in bus system, 'n_g' loss supplying generators in transmission loss/cost allocation process are included in deregulation market. The penalized quoted cost of the generator 'i' is given by equation (5).

$$PQC_i = L_i \times QC_i \qquad (5)$$

Using loss function derived in Grainger and Stevenson, the penalty factor can be calculated in [6] as given in equation (6).

$$P_{loss-ac} = \sum_{i=1}^{n_g}\sum_{j=1}^{n_g} P_{gi}\,B_{ij}\,P_{gj} + \sum_{i=1}^{n_g} B_{i0}\,P_{gi} + B_{00} \qquad (6)$$

Published By:
Blue Eyes Intelligence Engineering
& Sciences Publication

Change in generation of real power of each generator '*i*', the incremental transmission loss is given as in equation (7).

$$ITL_i = \frac{\partial P_{loss-ac}}{\partial P_{gi}} \quad \text{for } i=1 \text{ to } n_g \quad (7)$$

Then the penalty factor is given by

$$L_i = \frac{1}{1-ITL_i} \quad \text{for } i=1 \text{to } n_g \quad (8)$$

Using dc loss function, loss contribution fraction is calculated derived in Fred C. Schweppe et al. in [7] is shown in equation (9).The cost allocation of real power loss is based on loss contribution fraction to the each transaction.

$$P_{loss-dc} = P_i^T [B_{mn}] P_i \quad (9)$$

The real power transaction transmission loss '*k* 'is given in equation (10).

$$L_k = L_{T_{i-j}} = \frac{\partial P_{loss-dc}}{\partial P_i} P_{gi} \sum_{j \in \alpha_k} \frac{\partial P_{loss-dc}}{\partial P_j} P_{dj} \quad (10)$$

Where

α_k – set of load buses for each transaction k

Loss contribution fraction is obtained from the transmission loss due to transaction '*k*' and it is given in equation (11). This strategy distributes cost to every transaction in view of based on loss contribution fraction and shares between the generators and loads equally.

$$f_k = \frac{L_k}{\sum_{k=1}^{ntr} L_k} \quad \text{for k=1 to } n_{tr} \quad (11)$$

Cost allocation to each transaction '*k*' is given in equation (12).

$$CT_k = f_k \times TC_{ploss} \quad (12)$$

IV. CASE STUDY

In this section IEEE-4bus test system is taken to illustrate the proposed technique, which consists of two generators and two loads shown in fig.1.The line, transaction and generator data are presented in below tables respectively. Fuel cost equation of the two generators is assumed as their quoted cost. It is assumed that additional available capacity of each generator for meeting the real power losses is well within the desired value i.e. 4 MW. The mutual inductance value is computed from the reactance value of the line. The two lines average reactance in the data of bus system is computed and 5% of average reactance is assumed as mutual inductance between the lines. The assumed mutual inductance value between the two lines is given in Table 5. The incremental loss cost is 200 $/MWhr

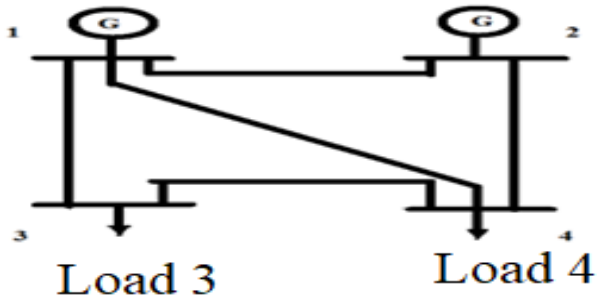

Fig.1. IEEE-4bus System

The Fig.1 shows the four bus system. It consists of two load buses and two generator buses at bus 3, bus4 and bus1, bus2 respectively.

Table 1. Data of each line for IEEE-4bus system

From Bus- To Bus	Series Impedance (p.u)		Shunt Admittance (p.u)
	R (p.u)	X (p.u)	
1-3	0.00744	0.0372	0.0775
1-2	0.01008	0.0504	0.1025
4-2	0.00744	0.0372	0.0775
4-3	0.01272	0.0636	0.1275
1-4	0.00372	0.0186	0.1550

Table.2. Data of Transaction for IEEE-4bus system

Transaction No.	Generator bus no.	Load bus no.	Real Transaction of power (MW)
1	**1**	**3**	**182**
2	**1**	**4**	**100**
3	**2**	**3**	**38**
4	**2**	**4**	**180**

The Table 2 gives the Real power transaction values of a 4-bus system that has obtained.

Published By:
Blue Eyes Intelligence Engineering
& Sciences Publication

Table.3. Data of generator for IEEE-4 bus system

Generator bus number.	Generator cost coefficients			Quoted cost ($/MWhr)
	A	B	C	
1	0.0048	6.4	400	406.4
2	0.0040	8.0	500	508

The above Table 3 gives the data of a generator cost coefficients and the obtained Quoted cost for the generators.

The transmission real/active power loss acquired from AC load flow solution considering four multilateral transactions by neglecting reactive power demand with the generator placed in the first rank as slack bus is 5.983 MW (refer table 4).

Table.4. Economic loss allocation schedule

Generator Bus no.	Penalty factor	Penalized quoted cost ($/MW hr)	Ranking of generators	Supplied quantity for loss(MW)	Cost of supply of loss($/ hr)
1	1.0311	418.83	1	4	1625.6
2	1.0187	517.55	2	1.983	1007.4
Total				**5.983**	**2633**

The cost supplying real power loss due to the primary energy transactions in total is 2633 $/hr. This cost has to be allocated for all the four multilateral transactions.

Table.5. Mutual Inductance Value

S. No	Between Lines
1-2, 1-4	0.0003
2-1, 2-4	0.0004
3-1, 3-4	0.0005
4-2, 4-3	0.0005

Table.6. Cost Allocation to Individual Transactions

Transactio No.	Gen. Bus No.	Real Power P (MW)	Loss contribution fraction		Allocation of cost ($/hr)	
			Without MI	With MI	Without MI	With MI
1	1-3	182	0.3987	0.39	1049.9	1085.8
2	1-4	100	0.1087	0.10	286.3	296.09
3	2-3	38	0.1205	0.12	317.2	328.04
4	2-4	180	0.3720	0.3725	979.6	1013.10
TOTAL			**1.0**	**1.0**	**2633**	**2723**

Active power loss due to each transaction is calculated using equation (11). It is to be noted that the sum of active loss of power due to each transaction is not equal to the loss obtained in AC load flow solution. It is observed that transaction 3 with 38 MW has higher cost allocation compared to transaction 2 because transaction 2 has a direct path from bus 1 to bus 4 whereas there doesn't exist direct path from bus 2 to bus 3.. So, the real power loss which depends on resistance is also high and therefore the allocation of cost to each transaction is also high.

V.CONCLUSION

The paper discusses about the effect of mutual inductance on transmission line loss/cost allocation for multilateral contracts. Penalty Quoted Cost method is used to demonstrate the results. The results of IEEE-4bus system explains that there is an impact of mutual inductance on transmission loss/cost allocation which it cannot be neglected. In the Results it has been observed that losses and Allocation of cost are increasing if the mutual inductance is considered. Hence the effect of mutual inductance on transmission loss has substantial effect on its cost/loss allocation.

REFERENCES

1. John Grainger, William Stevenson, "Power System Analysis", Tata McGraw Hill Publisher, India, 1994
2. Kusic GL, "Computer aided power system analysis", Englewood Cliffs - N.J : Prentice-Hall, 1986.
3. Pai MA, "Computer techniques in power system analysis", Tata/McGraw-Hill, New Delhi, 1979.
4. Stagg GW, El-Abiad AH, "Computer methods in power system analysis", New York: McGraw-Hill, 1968.
5. Pai MA, "Computer techniques in power system analysis",Tata/McGraw-Hill, New Delhi, 1979.
6. John Grainger, William Stevenson, "Power System Analysis", Tata McGraw Hill Publisher, India, 1994.
7. F.C. Schweppe, M. Caramanis, R. Taboras and R. Bohn, "Spot Pricing of Electricity", Kluwer Academic Publishers, Boston, 1998.

Published By:
Blue Eyes Intelligence Engineering
& Sciences Publication

Journal of Engineering Education Transformations ,
Volume 32 , No. 2, October 2018, ISSN 2349-2473, eISSN 2394-1707

Online Examinations to Undergraduate Engineering Students: A Case Study in an Autonomous Institution

S. Sudhakara Reddy[1], S. Arumugam[2], S. Ajay Kumar[3]
[1] Department of Mechanical Engineering, Malla Reddy Engineering College (Autonomous), Secunderabad – 500100
[2] Department of EEE, Malla Reddy Engineering College (Autonomous), Secunderabad – 500100.
[3] Department of CSE, Malla Reddy Engineering College (Autonomous), Secunderabad – 500100.
[2]arumugams1958@yahoo.com

Abstract: Undergraduate engineering students are vital part of any University / Institution and the institution should be in a position to show the good direction to them so that they will be placed in the good companies. The campus Recruitment procedure is based on, in-depth knowledge in the subjects and conducted through on line examinations. The conventional examinations based on pen and paper will not give the experience of an online examination. To overcome this drawback the autonomous institutions like ours have introduced the system of online examinations. The case study shows better results in the students' community in the online examination. This will help the students to face the placement drives in a better way in the future.

Keywords: Online Examinations, Results, Placements and Institution.

S. Arumugam
Department of EEE, Malla Reddy Engineering College (Autonomous), Secunderabad -500100
arumugams1958@yahoo.com

1. Introduction

In India several engineering institutions creating more number of engineering graduates to meet the demand from IT industry, but the IT industry searches the right engineering graduation in its domain. Generally engineering colleges across India have four academic years spread over 8 Semesters and each semester will have about 90 working days for each course work. At the end of the course, or at the end of 6th Semester, even if they cross eligibility criterion of marks to appear for campus interview, they didn't get the success in the interview, because of not having in depth knowledge in the subjects. To overcome this defect this paper suggests one method of conducting examination in online. This online experiment improves the student's knowledge in the subject more than the conventional examination method. Initially the students are suffered and showed very moderate results only but after the first experience they showed good results. This online examination trains the students to knowledgeable persons and enables them to face and get the success in the On Campus interview.

A. Subjective Paper

The pen and paper way of examination (ie) the subjective paper examination is an outdated format as it just tests the skills of students in simple way without emphasizing on what they understand which is an important aspect and can play a key role in coping them with present days competition. The structure and

format of descriptive paper needs to be changed into a way which involves the student to present his knowledge in logical and analytical way instead of just straightway of answering (eg).

(a) Explain the principle of operation of 3 phase slip ring induction motor?

(b) Explain the operation of full wave rectifier and derive the expression for efficiency?

(c) Distinguish between bunker and silo with the help of neat diagrams?

(d) Derive the integral momentum equation to be free convection boundary layer?

For the above questions asked in the end semester examinations, the students may give the answers without thinking but mechanically writing the answers. Surely this won't help them to get success in the campus drive.

The another disadvantage in the descriptive type examination is a good handwriting paper gets good grades even though it had very less subjective contents. Briggs showed that when teachers were given papers to evaluate, the papers with better handwriting received better grades. It shows that only on line examination the knowledge is tested and graded according to the answers.

B. Conventional Objective Paper

The conventional objective paper also a pen and paper based examination and even if it covers minute details of the syllabus, the students with their own style creating physical signals for the answers and finally their system is also somewhat failed on an overall. The pen and paper format examinations system has minimum benefits but more drawbacks. Now there is a need to find out ways and means to strengthen the understanding of the subjects what they are studying in the engineering curriculum.

C. Students Perception

Generally students are in search of getting good marks such that they get a good recognition. In this search students are unable to understand that there will be many loop holes that need to face further. Whenever a college has taken an initiation for implementing online based examinations without any pre intimated questions, students generally tend to study entire syllabus that is given in the curriculum. Students who are very much interested in getting good marks should read entire syllabus and hence they become skill oriented in the concepts.

D. Structure and functions of online examination

For the purpose of simplification, smooth and easier function, the work of online examination is divided into following three parts.

Pre examination work:

Manuscript of objective type question papers is received from the paper setters.

Actual Conductance of Examination and Assessment:

1. All the objective type questions are arranged in the system.

2. The students sit in the seat according to their Hall Ticket numbers.

3. The students will receive the question in a different order. (eg) The number of questions is 100. The first student will get 50th question as a first question and the second student will get 22nd question as a first question and is go on.

4. The questions are displaying at random, so the conduction of examination is very genuine and no malpractice at all.

5. Evaluate the answers as per the model answer already uploaded in the main system.

Post Examination Work:

1. Process the results on Computers.

2. To declare the results of all the online examinations.

3. To send the result etc to the examination center

E. College Perception

Administrators are updated very sooner and marks will be updated in a fast manner. The performance of a

student can be known and can be improved according to this level. The online examination requires Wi-Fi enabled personal computers with specified simulating software's which autocorrects and post the marks. Such type of online examinations has advantages over paper based examinations. It can include new multimedia, simulation, software test items which give the higher validity in respect of professional work practice.

Some examples of questions asked in the online examination are given below.

1. A 3 phase 400V, 50 Hz induction motor has 4% slip. The frequency of rotor emf will be

   (a) 200 Hz (b) 20 Hz (c) 2 Hz (d) 0.2 Hz.

   Answer: (c) 2 Hz.

2. The secondary winding of which of the following transformer is always kept closed?

   a) Distribution transformer (b) Power transformer

   b)(c) Potential transformer (d) Current transformer

   Answer: (d) Current transformer.

2. Challenges in the online Examination

Online examinations face reactionary challenges in the technical spheres like the unreliability of computer equipments, the potential depthness for cheating, some hacking process and the possibility of manipulation of answers. Very often some students get panic when they attempt online examinations due to lack of knowledge of operating computers. If this occurs some training should be given to those students before the commencement of the examinations

A. Statistics of online Examination results:

The statistics consists of 960 students approximately from the first year engineering, from Malla Reddy Engineering College [Autonomous], Secunderabad. The students wrote two online examinations for different syllabus in two different semesters. The table shows that in the first examination 298 Students out of 959 obtained less than 50 % marks. And at the same time in the second examination the same students showed better results (ie) 180 students out of 964 obtained less than 50% marks. The training and counseling to the students improved the results and overall number of students obtained less than 50% marks is considerably reduced. The table. 1 gives the statistical data of the two online examinations for I year / I Semester and II Semester.The graphical representation are given in Figures 1 to 6.It shows clearly about the improvement of the results varies from Ist Semester to IInd Semester..

Table 1. Online examination results of I Year / I Semester

S. No.	Branch	I Semester Examination		
		No. of Students Registered	No. of Students got < 50 % marks	In %
1.	Civil	179	117	65.30
2.	EEE	61	07	11.40
3.	MECH	241	85	35.20
4.	ECE	180	17	09.40
5.	CSE	240	36	15
6.	Mining	58	36	62
TOTAL		959	298	31

Table 2. Online examination results of I Year / II Semester

S. No.	Branch	II Semester Examination		
		No. of Students Registered	No. of Students got < 50 % marks	In %
1.	Civil	183	69	37.70
2.	EEE	61	02	03.20
3.	MECH	241	69	20.30
4.	ECE	180	11	06.10
5.	CSE	240	14	05.80
6.	Mining	59	35	59.30
TOTAL		964	180	18.60

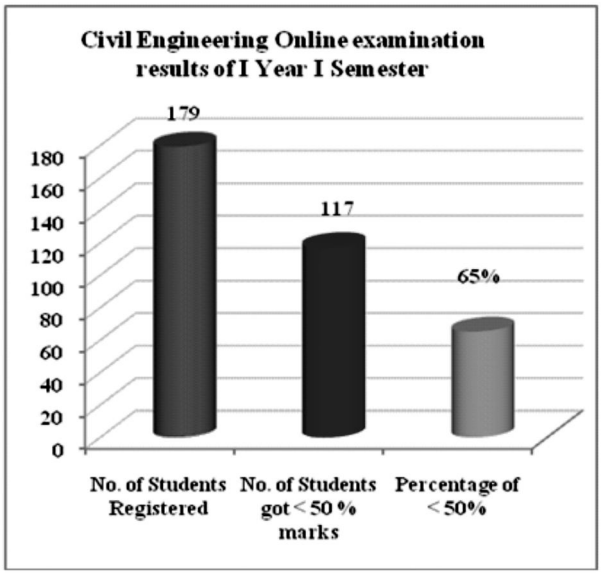

Fig. 1a Civil Online Examination Results I Semester

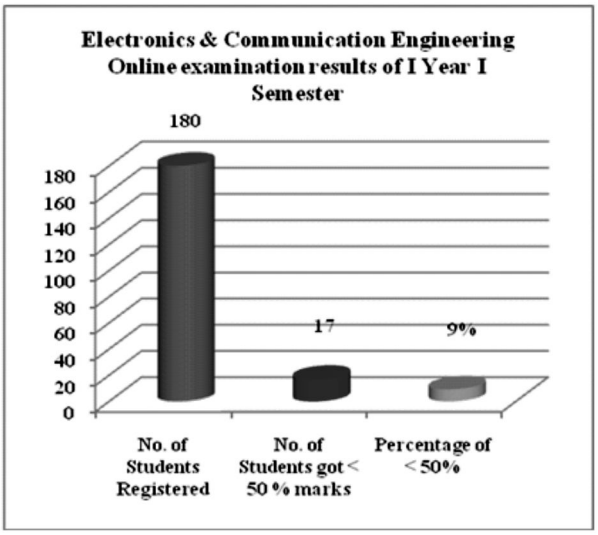

Fig. 2a : ECE Online Examination Results I Semester

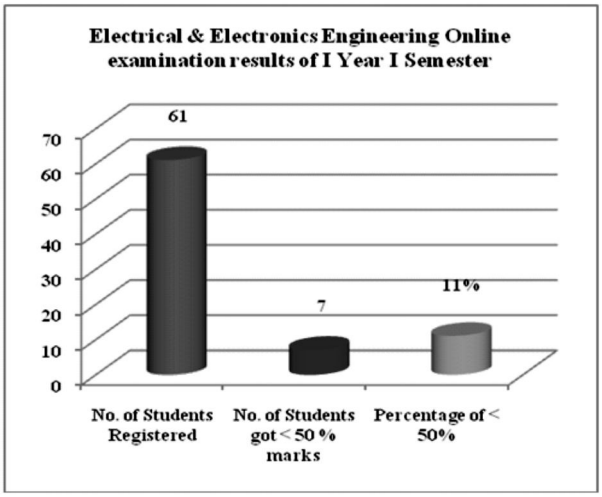

Fig. 1b EEE Online Examination Results I Semester

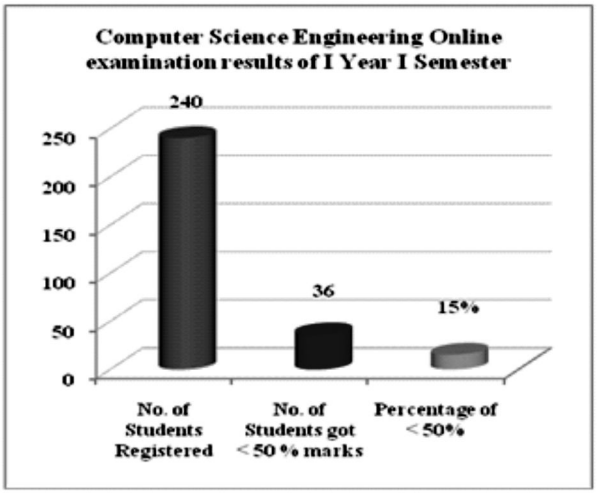

Fig. 3a CSE Online Examination Results I Semester

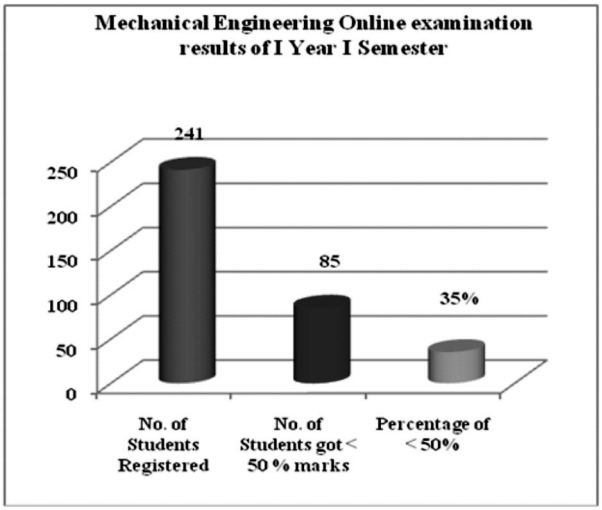

Fig. 2a MECH Online Examination Results I Semester

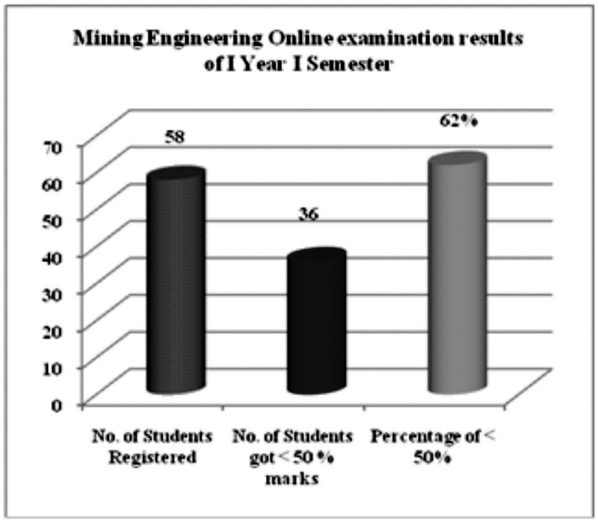

Fig. 3b Mining Online Examination Results I Semester

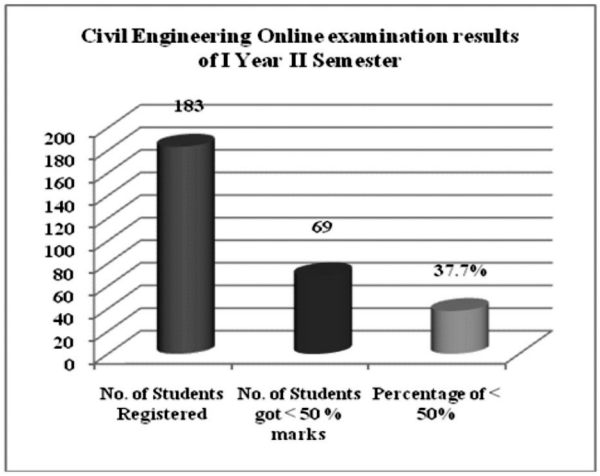

Fig. 4a Civil Online Examination Results II Semester

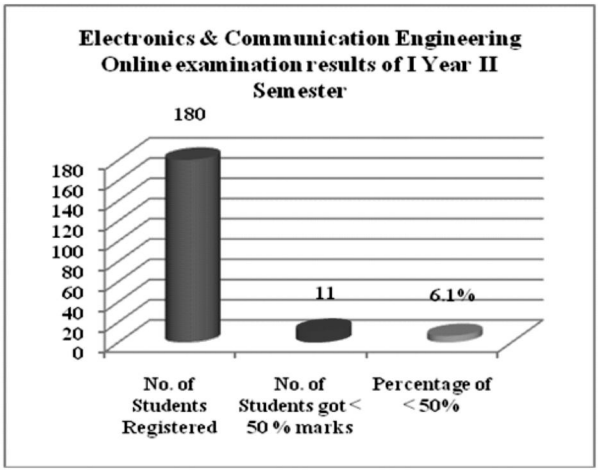

Fig. 5b ECE Online Examination Results II Semester

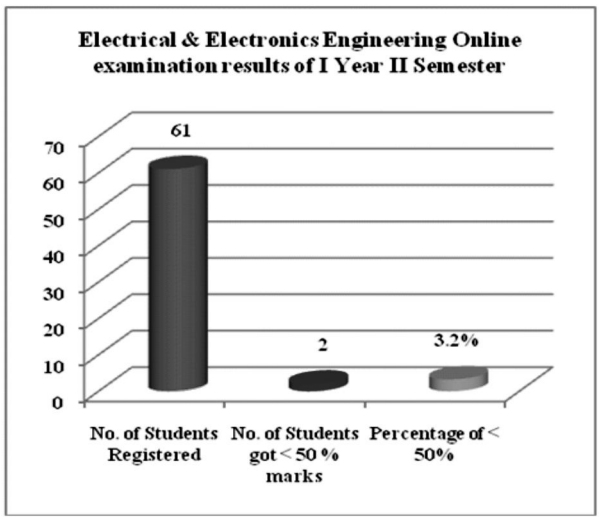

Fig. 4b EEE Online Examination Results II Semester

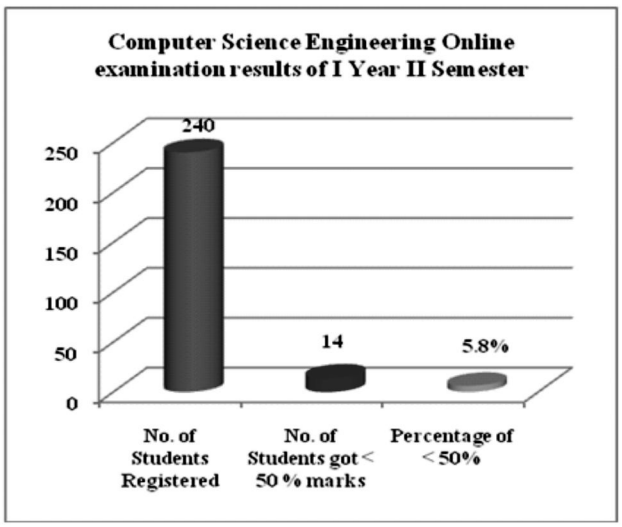

Fig. 6a : CSE Online Examination Results II Semester

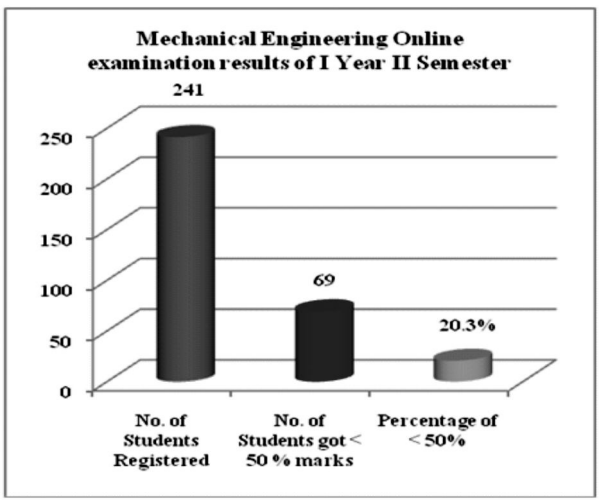

Fig. 5a MECH Online Examination Results II Semester

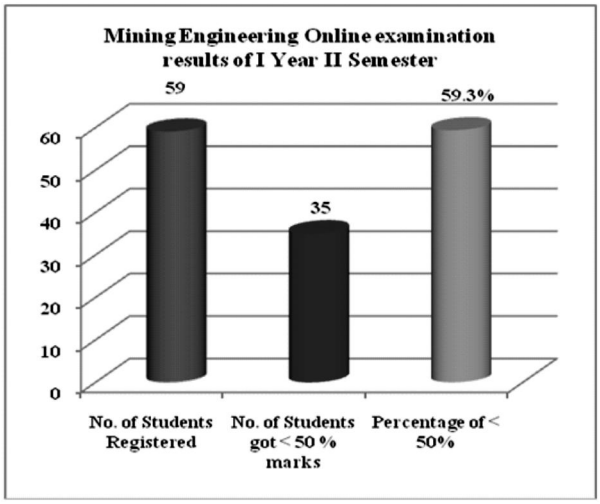

Fig. 6b Mining Online Examination Results II Semester

3. Results

As every coin has two faces, both the examination systems have their own pros and corns which are listed below.

- Online examinations are extremely beneficial for the present day needs as all the competitive examinations are conducted through online system.
- The occurrence of malpractices are fairly less in online examinations as there are different sets which are not there in offline examinations.
- Some students may get panic in the beginning but anyway it will be overcome in due course but in offline there is no such problem.
- Instant results are obtained in online examinations whereas in off line examination time is needed to declare the results.
- Manipulation of answers is possible in online examinations where as it is not possible in offline descriptive examinations.
- In off line examinations even if the questions is very tough or not to know, they may write the nearest answer but in the online examination if they know the correct answer then only it is possible to attempt.
- The offline help the students to get marks but not the knowledge, but the online examination helps the students to improve the knowledge and get good grades also.

4. Conclusion

The conventional offline examination has its own advantages of testing the knowledge by means of asking the question to derive the equations, solving the problem by mathematical analysis and it improves the communication skills. On the other hand, on line examination has testing the sharpness of the subject knowledge, forcing the students to study the full syllabus and its add-on contents. Online examination when compared with conventional offline examination increases the beneficiary to the student's community.

Acknowledgement

The Authors would like to thank our management of Malla Reddy Engineering College (Autonomous) for giving an opportunity to write a paper on this topic. We also thank our Head of the department, faculty members and students for their support to complete this paper.

References

[1] T.Cocinella, (2010) Which manuscript letters do primary grade children write legibly?, Journal of Educational Psychology", Vol.93, pp.480-497.

[2] Catherine G.P. Berdanier, Robin H.Tate, Tom Tom Iwinski, Anil Kulkarni, (2017) Investigation of engineering student engagement and behavior in an online second-year thermal science course, Journal of Engineering Education Transformations, Vol.30, No.3.

[3] Dr.Srinivasa Pai.P., Dr.Niranjan N.Chiplunkar, Dr.Shrinivas Rao.B.R., Dr.K.Subrahmanya Bhat, (2015) Undergraduate students' research: A Case study of their experiences and perceptions in an Autonomous Institution, Journal of Engineering Education Transformations, Special Issue: pp.34-39.

[4] Dipali D.Awasekar, Shashikant A.Halkude, (2015) An analysis of Assesment Bias Influenced by Presentation and Writing Technique in Undergraduate Engineering Examination, Journal of Engineering Education Transformations, Special Issue: pp.93-98.

Statistical analysis of trend and change point in climate series for a semi-arid basin, Tamil Nadu, India

Shimola K.[1*] and Krishnaveni M.[2]
1. Malla Reddy Engineering College, Secunderabad-500100, INDIA
2. Centre for Water Resources, Anna University, Chennai-600025, INDIA
*jeslin.shimola@gmail.com

Abstract

This research study aims to carry out the trend test and change point analysis on temperature series including maximum, minimum and mean annual temperature at Kavalur climate station during the period 1965-2010. These tests have been also carried out on rainfall series at 10 raingauge stations during the period 1935-2010 in Vaippar basin, Tamil Nadu, India. The results of Mann-Kendall trend test showed that maximum, minimum and mean annual temperatures exhibited a sign of increasing trend at α=0.05 significance level. An increasing trend in annual rainfall is observed in Aruppukottai, Kovilpatti and Sivagiri but it is statistically insignificant.

Their magnitudes of change over time are determined by Sen's slope estimator indicating that the overall temperature has been increased by 0.4°C /10 years. The cumulative sum charts (CUSUM) are used for the detection of statistically significant change points. The CUSUM charts show that a major change point has occurred in the late 1970s and 1990s for maximum and minimum temperatures and continued till this decade for temperatures. The CUSUM charts also reveal that there is no major change point in rainfall series as rainfall is erratic and it shows inter-annual variability. This change point detection is a clear indication of climate change.

Keywords: Climate change, Mann-Kendall trend test, Sen's slope, Change point, CUSUM charts.

Introduction

The global warming leads to long term catastrophic effects throughout the world. The long-term trends and jumps in climate series are associated with global warming. A study on one of the major river basins in India shows that mean maximum, mean minimum and average mean surface temperature of the basin on annual basis show significant increasing tendencies.[9] India has 75% of the cropped area is in the semi-arid tropics. The water resources are likely to dry very rapidly leading to serious water scarcity.

Low and erratic rainfall events coupled with extreme hydrological events make these regions more vulnerable to climate change. One of the implications of global climate change scenarios in the arid and semi-arid regions are the increase in frequency and severity of droughts. A better management of water resources can be made by studies related to rainfall and temperature in these regions. Analyzing and understanding the climate variability help to cope with the climate change effects and to develop sustainable adaptation strategies. The knowledge of trends in annual rainfall and number of rainy days is very important for agricultural planning in any region.[1]

The result of the study using Mann-Kendall trend test and Pettit change point test in the Lhasa basin shows that years around 1970 and the early 1980's are the major period experiencing abrupt changes in runoff.[17] Reza et al[10] study shows that t- student test and linear regression are suitable parametric tests and Mann-Kendall, Mannwhitney and Spearmanrho tests are the non-parametric tests which have good capability for linear and non-linear trend detection in the climatology data series. The results of the study in major cities in India showed an increasing tendency in temperature for both annual and seasonal series during the last century.[2] In India, it may be observed that during the recent decade emphasis has been laid on the studies of local or regional climatic fluctuations.[7]

This study investigates whether the temperature and rainfall of the study area basin exhibit evidence of change either gradual change (trend) or change point (jump). Long term trends of maximum temperature, minimum temperature, mean temperature for the past 45 years (1965-2010) and rainfall data for the past 65 years have been investigated using Mann-Kendall trend test. The magnitude of trend is identified using Sen's slope estimator. The change point statistics can be derived from the combination of cumulative sum (CUSUM) values and boot strapping techniques.

Study area

Vaippar river basin is one of the semi-arid basins of Tamil Nadu in India and situated between latitudes 8^0 59'N to 9^0 49'N and longitudes 77^0 15' E to 78^0 23' E with drainage area of 5423 Km^2. The basin is bounded by Western Ghats, a mountainous region in the western part, Bay of Bengal in east, Thamirabarani basin in south and Gundar basin in north. Maximum, minimum and mean temperature series from Kavalur station covering a period of 45 years (1965-2010) and rainfall series from 10 rain gauge stations covering a period of 65 years (1935-2010) were analyzed in the study. These data were provided by Institute of Water Studies, Tharamani, Chennai. The basin is dominated by cyclonic rainfall, which occurs during northeast monsoon (Oct–Dec) and convectional rain also occurs during summer season (March–May); this shows strong seasonality.

The basin has a tropical monsoon climate with hot summer and mild winter which agro-climatically falls under semi-arid regions. The climate of the basin is dominated by an altitude ranging from 1877 m.s.l in the west to over -2m.s.l in the east. The seasons are classified into winter (Jan–Feb), summer (March–May), southwest (June–Sep) and northeast (Oct–Dec) monsoons. Most of the agricultural activities are centered on September to December monsoon seasons. The basin gets its maximum rainfall during northeast monsoon whereas the southwest monsoon also produces a reasonable amount of rainfall, which is quite useful for the rainfed agriculture although the basin falls in the rain shadow area of the Western Ghats. The summer rainfall varies from 40mm to 200mm, during which more than 50% area receives rainfall above 130 mm, winter receives very low rainfall (25mm–95mm) whereas about 55% of the area receives this amount.

The average annual rainfall of the basin is around 771mm whereas Watrap receives a maximum average annual rainfall of 957mm, which is higher than the state long-term average 945mm. The temperature variation is from 20°C to 30°C in winter and 30°C to 40°C in summer. Missing values for the study period were computed by interpolation techniques. Figure 1 shows the location of climate and rain gauge stations.

Methodology

Ndiritu[8] reported that changes in time series could either be gradual, sudden (step change) or a combination of the two. The variability of rainfall and temperature is more focused in climate change studies. They can be subjected to gradual change (trend) and climate jump (change point) in climate series. As the climate data does not show normality, a non-parametric test like Mann–Kendall trend test was used to identify the monotonic trend behaviour. Sen's[16] slope estimator was also used to identify the magnitude of trend in climate series. The problem of change point was often considered using cumulative sums and Bayesian approach. Hence for the detection of climate jump, a cumulative combination of CUSUM charts and boot strapping technique was adopted in this study.

Figure 1: Location of climate and rain gauge stations in Vaippar basin

Mann–Kendall test for trend detection: Mann–Kendall (M–K) test, a non-parametric test for trend detection in time series, has been widely used in environmental sciences.[3,5,6] The M–K test statistic S and the standardized test statistic Z_{mk} are as follows:

$$S = \sum_{i-1}^{n-1} \sum_{j=i+1}^{n} \mathrm{sgn}\left(x_{j-} x_i\right) \quad (1)$$

$$\mathrm{sgn}(X_j - X_i) = \begin{cases} +1.if.X_j - X_i > 0 \\ 0.if.X_j - X_i = 0 \\ -1.if.X_j - X_i < 0 \end{cases} \quad (2)$$

$$Var(S) = \frac{1}{18}\left[n(n-1)(2n+5) - \sum_{p=1}^{q} t_p\left(t_p - 1\right)\left(2t_p + 5\right) \right] \quad (3)$$

$$Z_{mk} = \begin{cases} \dfrac{S-1}{\sqrt{\mathrm{var}(S)}} if \ldots S > 0 \\ 0 \ldots if \ldots S = 0 \\ \dfrac{S+1}{\sqrt{\mathrm{var}(S)}} \ldots if \ldots S < 0 \end{cases} \quad (4)$$

where x_i and x_j are sequential data values in the year i and j, n is the number of recorded data, t_p is the number of ties for the pth values and q is the number of tied values.

Positive values of Z_{mk} indicate increasing trends whereas negative values of Z_{mk} indicate decreasing trends in the time series. In the two-tailed test, the null hypothesis is presented as H_0: There is no trend in the dataset, H_0 is rejected if calculated $|Z_{mk}| > Z_1 - \frac{\alpha}{2}$. The alternate hypothesis is presented as H_1: There is a trend in the dataset. $Z_1 - \frac{\alpha}{2}$ is the critical value of Z, which is obtained from the standard normal distribution corresponding to the pre-specified level of significance.

Sen's slope Estimator: The trend magnitude is estimated by Theil–Sen approach[12,15] which is a non-parametric median based slope estimator.

The slope estimation is given by:

$$\beta = median\left[\frac{x_j - x_k}{j-k} \right] for \mathrm{K}\ all \mathrm{K}\ k < j \quad (5)$$

where x_j and x_k are sequential data values of the time series in the years j and k; β is the estimated magnitude of trend slope in the data series.

Change point analysis: Change point analysis is an efficient tool to identify climate jump in historical climate series data. Identification of change point location in climate series is essential because it alters the hydrological processes in a watershed. A combination of cumulative sum charts (CUSUM) and boot strapping proposed by Taylor[13] follows several iterations to detect changes. The computational procedure for the calculation of cumulative sums S_i is as follows:

$$S_i = S_{i-1} + X_i - \overline{X} \quad (6)$$

where Start the initial cumulative sum as S_0 =0, i=1, 2……25, $\overline{X}$ is the average of the sample time series.

Let X_1, X_2……X_{25} be the data points and from this cumulative sums S_0, S_1….S_{25} are calculated.

Calculate the average:

$$\overline{X} = \frac{X_1 + X_2 + \ldots\ldots\ldots X_{25}}{25} \quad (7)$$

Thus, the CUSUMs are calculated by adding the difference between current value and the average to the previous sum.

The upward slope indicates a period of time where the values tend to be above the overall average whereas the downward slope indicates a period of time where the values tend to be below the overall average. Once the change is detected, the data having two means are fragmented into segments and mean square estimates are calculated by an iterative process till minimum mean square error (MSE) is obtained. This shows the time of change which eventually confirms the change in climate regime. The significance of the change point can be determined by assessing the confidence level based on bootstrapping technique. The confidence level is calculated as follows:

$$\text{Confidence level} = 100\frac{X}{N}\% \quad (8)$$

where X = the number of bootstrapped S_{diff} values which are larger than the original S_{diff}, N =number of bootstraps and S_{diff} =difference between the highest (S_{max}) and lowest CUSUM values (S_{min}).

Change point analyzer is an add-on tool in Microsoft Excel software used to determine the change point in a dataset. This analyzer detects the exact year when the change or shift had taken place by using MSE and CUSUM charts. This analysis shows the major change point in data sets, which are indicated by confidence level and also by the level of change. A steady decline or rise in CUSUM plots would suggest the possibility of climate jump from the year of observation. If the data are free from these changes, the plot normally oscillates around the horizontal axis. Using the eq. 8, CUSUM plots are derived and are useful for the detection of climate jumps.

Results and Discussion

The annual, seasonal and monthly means of maximum, minimum and mean temperatures indicated an increasing trend for the past four decades. These trends are statistically significant at α=0.05 for all the cases. Moreover, the trends of annual mean temperature are stronger than those of maximum and minimum temperatures.

Monthly, seasonal, annual trend analysis of temperature: The annual, seasonal and monthly means of maximum, minimum and mean temperatures indicated an increasing trend for the past four decades. These trends are statistically significant at α=0.05 for all the cases. Moreover, the trends of annual mean temperature are stronger than those of maximum and minimum temperatures. The maximum temperature for the months of February and July indicated a significant higher rising trend with highest Mann–Kendall test statistics (Z = 3.96, 4.44) at α=0.05 during the study period. On the other hand, the minimum temperature for the months of July and October indicated a significant highest increasing trend with the highest Mann–Kendall test statistics (Z = 5.71, 5.08) at α=0.05.

However, the minimum increasing trend was observed in the months of December and June for both maximum and minimum temperatures with the lowest Mann–Kendall test statistics (Z = 2.51, 2.78 and Z = 2.55, 2.83) at α=0.05. The mean temperature indicated a significant higher increasing trend for all the months with higher Mann–Kendall Z statistics at α=0.05. Table 1 presents the monthly, seasonal and annual maximum, minimum mean temperatures Mann–Kendall Z statistics at α=0.05.

The magnitude of the mean temperature trend from Sen's slope estimator indicated that the overall temperature has risen by 0.056°C/10 years for the month of April during the 45 years of the study period. The maximum temperature indicated highest values of 35°C, 40°C and 39°C for the year 2003 during summer, winter and southwest monsoon seasons respectively at α=0.05. The minimum temperature indicated maximum values of 25°C, 29°C and 27°C for the year 2003 during summer, winter and southwest monsoon seasons respectively at α=0.05.

Both temperatures indicated a higher increase of 32.5°C in 1989 and 24.7°C in 2002 for northeast monsoon season. However, the highest value was observed in the southwest monsoon season for maximum temperature and minimum temperature. The lowest value was observed in the summer season for maximum and minimum temperatures. The magnitude of the annual mean temperature series indicated an increasing trend of 0.4°C, 0.5°C, 0.4°C and 0.3°C/10 years for summer, winter, northeast and southwest monsoon seasons.

The rising feature of both maximum and minimum temperature showed a warming trend in this basin. This warming trend is consistent with the global warming signal. The mean annual temperature also indicated a significant increasing trend over the basin. However, the increasing trend in the mean annual temperature is significant from the year 1965 onwards as considered in this study. The mean annual temperature is 32.8°C in the recent decade (2000 to 2010) which is 96% higher than that of the previous decade. This indicated a significant warming trend as seen in the recent decades compared to the earlier decades.

Table 1
Monthly, seasonal and annual temperatures Mann–Kendall Z statistics

Time Scale	Maximum Temperature (°c)		Minimum Temperature(°c)		Mean Temperature(°c)	
Monthly Statistics	**Z**	***p***	**Z**	***p***	**Z**	***p***
JANUARY	3.39	0.001	4.31	<0.0001	4.73	0.0001
FEBRUARY	3.96	<0.0001	4.34	0.0001	4.91	<0.0001
MARCH	2.69	0.007	4.20	<0.0001	4.85	<0.0001
APRIL	3.46	0.001	3.41	<0.0001	5.18	<0.0001
MAY	3.24	0.001	3.85	0.000	3.81	0.000
JUNE	2.78	0.006	2.83	0.005	3.68	0.000
JULY	4.44	<0.0001	5.71	<0.0001	5.67	<0.0001
AUGUST	2.95	0.003	3.12	<0.0001	4.91	<0.0001
SEPTEMBER	3.86	0.000	4.99	<0.0001	5.76	<0.0001
OCTOBER	2.77	0.006	5.08	<0.0001	4.71	<0.0001
NOVEMBER	2.82	0.005	3.50	0.000	4.08	<0.0001
DECEMBER	2.51	0.012	2.55	0.011	3.87	0.000
Seasonal Statistics						
WINTER	4.82	<0.0001	4.93	<0.0001	5.80	<0.0001
SUMMER	4.03	<0.0001	4.74	<0.0001	4.72	<0.0001
SOUTH WEST	5.18	<0.0001	5.20	<0.0001	6.33	<0.0001
NORTH EAST	4.13	<0.0001	4.30	<0.0001	5.18	<0.0001
Annual Statistics	6.30	<0.0001	4.62	<0.0001	6.26	<0.0001

at α=0.05 significance level

An increase of 1.02°C is noticed in recent decade as the basin mean average temperature is 31.7°C during the study period of 45 years. Hence, it is evident from the study that the basin is warmer during the last four decades which is consistent with the global warming trend. The magnitude of the mean temperature trend from the Sen's slope estimator indicated that the overall temperature has risen by 0.4°C/10years during the 45 years of the study period. The highest monthly temperature of 35°C is observed in May which is the hottest month followed by April 34.5°C. The lowest monthly temperature of 24°C is observed in the month of January which is the coldest month followed by December 24.7°C during the study period.

Seasonal, annual trend analysis for rainfall: The rainfall data was analyzed with Mann–Kendall trend test for 10 rain gauge stations located in the basin. Table 2 provides the calculation of Mann–Kendall Z statistics and *p* value derived for each station for seasonal and annual time scales.

Seasonal trends are significant and are more important than annual time series as the rainfall indicated higher inter-annual variability. A statistically significant (α=0.05) decreasing trend was observed for winter season (p=0.030) in Sattur station and for summer season (p=0.009) in Vilathikulam station. Seasonal trend statistics revealed a weak downward trend for summer and winter seasons in all the stations which are statistically insignificant except for Sattur and Vilathikulam stations. A weak upward trend was noted in the southwest monsoon season (Z=0.04) at Sivakasi station and Z=0.27 for the northeast monsoon season at Aruppukottai station but they are statistically insignificant.

Annual Mann–Kendall Z statistics indicated a decreasing trend for almost all the stations except Aruppukottai, Kovilpatti and Sivagiri but they are also statistically insignificant. Hence, the results indicated that there was no statistically significant increasing or decreasing trend of annual rainfall throughout the basin. The magnitude of decreasing trend indicated that rainfall in Vilathikulam station had decreased by 1.2 mm/10 years in the past 7 decades. The trend magnitude could be identified from Sen's slope estimator. The highest increase in trend magnitude was observed at Sivagiri station by 2.7 mm/10years.

The largest magnitude of decrease for seasonal precipitation occurred in summer which contributes more than 17.8% of annual magnitude. While, considering the whole basin, the annual precipitation has decreased slightly by 0.032 mm per hydrological year. The magnitude of decreasing trends in summer and winter is greater than that of northeast, southwest monsoons for almost all the stations. If this trend continues in the future too, it will have major impact on surface water resources as well as ground water recharge. The year 1986 was the driest year in the period of study with a rainfall of 526 mm, which is below the average rainfall of 770mm. IWS (2010) reported that the northeast parts of the basin had undergone a period of drought from the late 1980s and also the frequency of droughts had increased concurrently. The rainfall decrease was more apparent at stations at low altitudes (Vilathikulam and Virudhunagar) than at stations at higher altitudes (Watrap and Srivilliputhur).

Identification of change points: Identification of change point is one of the important statistical techniques to detect climate jumps in climatological data series. The change point analysis for maximum, minimum and mean annual temperatures are shown in figure 2.

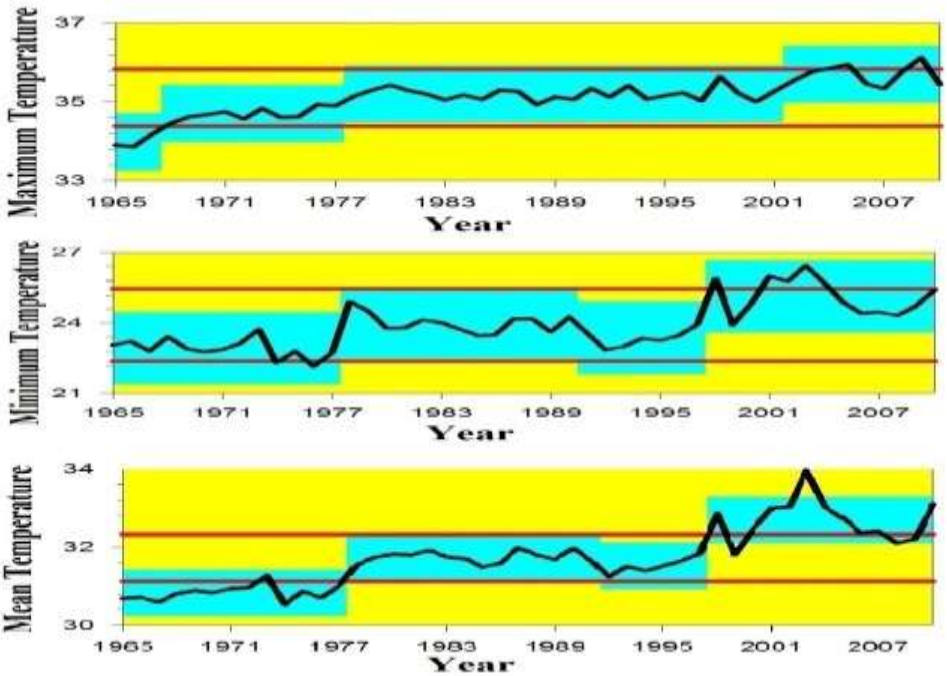

Figure 2: Change point analysis for annual temperature

Table 2
Seasonal and annual rainfall Mann–Kendall Z statistics

Stations	Annual Statistics		Seasonal Statistics							
	Z	*p*	S.W		N.E		WINTER		SUMMER	
			Z	*p*	Z	*p*	Z	*p*	Z	*p*
ARRUPUKOTTAI	0.10	0.918	0.52	0.606	0.27	0.784	-1.64	0.101	-0.71	0.479
KOVILPATTI	0.99	0.324	1.31	0.190	1.81	0.071	-1.06	0.290	-1.25	0.212
SANKARANKOVIL	-0.03	0.975	0.54	0.590	0.91	0.365	-1.01	0.314	-1.02	0.309
SATTUR	-0.64	0.521	-0.38	0.703	-0.64	0.524	-2.17	**0.030**	0.56	0.572
SIVAGIRI	1.70	0.088	0.63	0.527	1.85	0.064	-0.45	0.650	-0.66	0.510
SIVAKASI	-0.42	0.677	0.04	0.971	-0.63	0.527	-1.22	0.224	-0.61	0.542
SRIVILLIPUTHUR	-0.73	0.464	0.24	0.808	-0.08	0.938	-0.62	0.538	-1.78	0.074
VILATHIKULAM	-1.24	0.213	-1.83	0.067	0.71	0.478	-1.84	0.066	-2.63	**0.009**
VIRUDHUNAGAR	-0.88	0.377	-0.38	0.701	-0.58	0.564	-0.73	0.464	-0.72	0.470
WATRAP	-0.72	0.470	-0.67	0.504	-0.35	0.725	-0.80	0.423	-1.80	0.071

at α=0.05 significance level

It is understood clearly from figure 2 that the maximum, minimum and mean temperature values fall outside the control limits which indicated that change has occurred during the study period. The level in the table implies the significance of change and is strongly associated with climate change. The analysis indicated that the basin exhibited a change point in maximum temperature in the years 2002, 1968 and 1978 at a confidence level of 100% at levels 2 and 1 respectively. Prior to these changes, the mean maximum temperatures were 34.69°C and 35.2°C during 1978 and 2002 respectively. After the change, the values were 35.20°C and 35.69°C.

On the other hand, a change point in minimum temperature had taken place in the year 1978 at 100% confidence interval at level 4. Prior to the change, the minimum temperature was 22.91°C whereas after the change, the minimum temperature was 24.0°C. For the mean annual temperature, the change point has been detected in 1977–1979 at 100% confidence interval at level 2.

The ratio of average of climate series after the change point to the average earlier to the change point was calculated as magnitude of change point. Magnitudes of change points for maximum, minimum and mean temperatures are 0.99, 0.97 and 0.97 respectively. This analysis also shows that there is no departure from any of the assumptions. The results of the change point years in maximum, minimum and mean annual temperatures are shown in figure 3.

The study revealed a statistical significance of change point that can be seen from late 1970s, setting the confidence interval to 95% with 1000 bootstraps and mean square error (MSE) estimates techniques. The CUSUM charts show the development of trends and detect the process shifts. The results of the change point analysis using bootstrapping method are presented as CUSUM plots for maximum, minimum and mean temperatures. The significant changes (at α=0.05) are represented by changes in the background colour as in figure 4.

The CUSUM charts showed a clear rising trend. A sudden change in temperature can be seen in the late 1970s and 1990s. The rising trend thereafter continued till 2010 decade. The result of the change point years in annual rainfall is shown in figure 5.

As shown in figure 5, no major change point is observed in rainfall series as rainfall is erratic and shows inter-annual variability.

Conclusion

Vaippar basin is one the semi-arid basins in South Asia with increasing temperature (maximum, minimum and mean) trend which is statistically significant (α=0.05). Overall seasonal analysis of maximum, minimum and mean annual temperatures indicated a statistically significant increasing trend in all the seasons. The southwest monsoon season seemed to be more significant than other seasons. The monthly analysis of mean annual temperature indicated a higher increasing trend compared to the other two. An increase of 1.02°C in mean annual temperature was noticed in the recent decade. However, the magnitude of temperature increase was 0.4°C/10years for the study period.

Mann–Kendall trend test indicated that rainfall exhibited decreasing trends which are statistically insignificant in most of raingauge stations. An increasing trend was observed in Aruppukottai, Kovilpatti and Sivagiri but they are statistically insignificant. The major change point which is a clear indication of climate change occurred in the late 1970s and 1990s for maximum and minimum temperatures and continued till this decade.

There was no major change point in rainfall series as rainfall is erratic and shows inter-annual variability. This increasing temperature trend is consistent with global warming scenarios. A statistically significant trend in the range of maximum and minimum temperatures is to be expected as an indicator of a global warming signal.[4]

Maximum Temperature

Year	Confidence Interval	Conf. Level	From	To	Level
1968	(1968, 1968)	99%	33.98	34.698	2
1978	(1978, 1979)	100%	34.698	35.203	1
2002	(2001, 2005)	100%	35.203	35.693	2

Minimum Temperature

Year	Confidence Interval	Conf. Level	From	To	Level
1978	(1976, 1979)	100%	22.912	24.005	4
1991	(1985, 1993)	97%	24.005	23.347	3
1998	(1998, 2000)	99%	23.347	25.138	4

Mean Temperature

Year	Confidence Interval	Conf. Level	From	To	Level
1978	(1977, 1978)	100%	30.836	31.751	2
1992	(1987, 1996)	94%	31.751	31.522	3
1998	(1998, 2001)	96%	31.522	32.7	4

Figure 3: Change points years in annual temperature

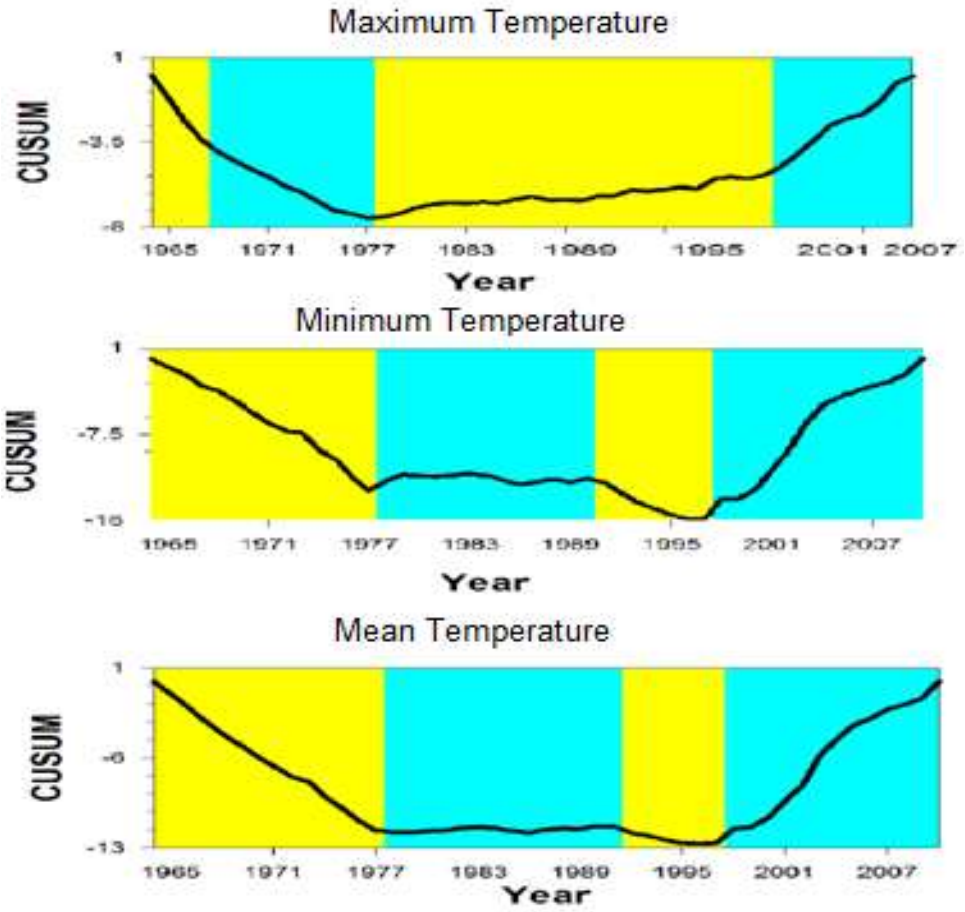

Figure 4: CUSUM chart for annual temperature

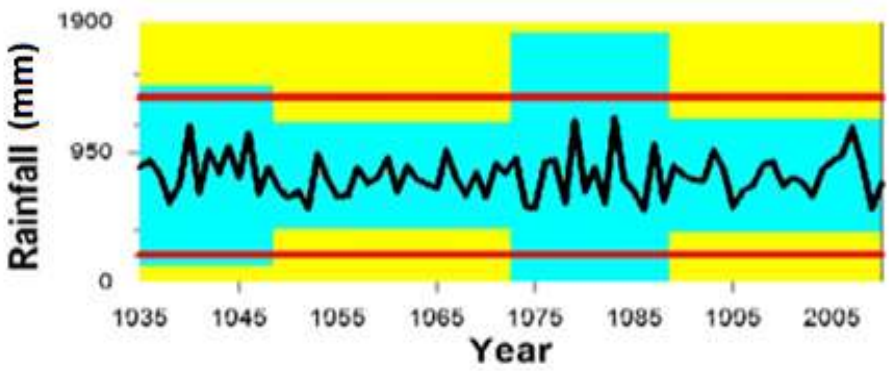

Figure 5: Change points years in annual rainfall

Therefore, it is concluded that the Vaippar basin experiences a clear rising trend as a result of global warming, which can increase the length of growing seasons. The decreasing rainfall trend may have an effect in decreasing the soil moisture and lowering of ground water level. Statistically significant change point years were also detected in temperature. Thus, the study concludes that climate change has occurred in the study area.

Acknowledgement

We like to express our thanks to Anna University, Chennai for awarding Anna Centenary Research Fellowship for conducting this study. The authors are also thankful to the Institute of Water Studies, Tharamani, Chennai, for having provided the climate data.

References

1. Abhijit Zende M., Nagarajan R. and Kamalkishor Atal R., Rainfall trend in semi-arid region-Yerala river basin of western Maharastra, India, *International Journal of Advancements in Technology*, **3**, 137-145 **(2012)**

2. Dhorde A., Dhorde A. and Gadgil A.S., Long-term Temperature Trends at Four Largest Cities of India during the Twentieth Century, *Journal of Geophysical Union*, **13(2)**, 85-97 **(2009)**

3. Hirsch R.M., Slack J.R. and Smith R.A., Techniques of trend analysis for monthly water quality data, *Water Resources Research*, **18**, 107-121 **(1982)**

4. Karl T.R., Jones P.D., Knight R.W., Kukla G., Plummer N., Razuvayev V., Gallo K.P., Lindseay J., Charlson R.J. and Peterson T.C., A new perspective on recent global warming: asymmetric trends of daily maximum and minimum temperature, *Bulletin of the American Meteorological Society*, **74**, 1007–1023 **(1993)**

5. Kendall M.G., Rank correlation methods, Charles Griffin, London **(1975)**

6. Mann H.B., Non-parametric tests against trend, *Econometric*, **13**, 245-259 **(1945)**

7. Nath D.C. and Mwchahary D.D., A study on rainfall trends in Kokrajhar district of Assam, India, *International Journal of Research in Chemistry and Environment*, **3**, 74-88 **(2013)**

8. Ndiritu J.G., Long-term trends of heavy rainfall in South Africa. Regional hydrological Impacts of Climatic Change- Hydroclimatic Variability, Proceedings of symposium held during the seventh IAHS Scientific Assembly at Foz do Iguacu, Brazil, 178–183 **(2005)**

9. Rao P., Climate changes and trends over a major river basin in India, *Climate Research*, **2**, 215-223 **(1993)**

10. Reza Y.M., Javad K.D., Mohammad M. and Ashish S., Trend Detection of the Rainfall and Air Temperature Data in the Zayandehrud Basin, *Journal of Applied Sciences*, **11(12)**, 2125-2134 **(2011)**

11. Rupa Kumar K., Krishna Kumar K. and Pant G.B., Diurnal Asymmetry of surface temperature trends over India, *Geophysical Research Letters*, **21**, 677-680 **(1994)**

12. Sen P.K., Estimates of the regression coefficient based on Kendall tau, *Journal of American Statistical Association*, **63**, 1379-1389 **(1968)**

13. Taylor W., Change-Point Analysis: A Powerful Tool for Detecting Changes, Taylor Enterprises Liberty Ville, Available from: <http://www.variation.com/cpa/tech/changepoint>, [12 December 2012] **(2000)**

14. Taylor W., Change-Point Analyzer 2.3 Software Pack-age, Taylor Enterprises, Liberty Ville, Available from: <http://www.variation.com/cpa/tech/changepoint>, [3 January 2013] **(2000)**

15. Theil H., A rank- invariant method of linear and polynomial regression analysis, I, II, III, Nederl. Akad. Wetensch. Proceedings, **53**, 386-392, 512-525, 1397-1412 **(1950)**

16. Tu M., Hall M.J., Laat P.J.M.D. and Wit M.J.M.D., Detection of long-term changes in precipitation and discharge in the Meuse basin, Proceedings of ICGRHWE, GIS and Remote Sensing in Hydrology, Water Resources and Environment, IAHS Publ., **289**, 169-177 **(2004)**

17. Xuedong Lin, Yili Z., Zhijun Y.A.O., Tongliang G. and Hong W., The trend on runoff variations in the Lhasa river basin, *Journal of Geographical Science*, **18**, 95-106, DOI 10.1007/s11442-008-0095-4 **(2008)**.

(Received 17th April 2018, accepted 04th September 2018)

Harmonic Emission of Grid Connected Back To Back Arrangement of Rectifiers in Distribution Networks

S. Phani Venkata Ramana, K. Anitha Reddy, K. Deepthi, K. Chetaswi

Abstract*: Emission of Harmonics plays a potent role in distribution systems. The intention of this paper to inspect the harmonic level by the implementation of UPQC (Unified Power Quality Conditioner) at distribution system level. This system offers indirect power quality (PQ) pay of the voltage and also the supply current. The harmonic performance of small grid with respect to different power electronics and grid parameters. Latest studies suggest that the UPQC has high efficiency and better Power quality. This system is very simple and uncomplicated. The equipments used in this system always monitors the harmonic level on the source side by considering the voltage magnitude and supply current. By employing this system, the THD value is very low, injected voltages or currents gets nearer to sinusoidal. The execution of the planned system is simulated in MATLAB/Simulink surrounding

Keywords: Power Quality, UPQC, Active power filter, Sinusoidal, Harmonic content.

I. INTRODUCTION

Most of the ac loads consumes reactive power (Q), which is a prominent cause for poor power quality (PQ) problems. [1][2]. For a steady power system the generating side should produce sufficient power to meet the consumers demand. Distribution system is the one which mainly connected to consumer's side commonly, so the effect of power quality problems will be very high at distribution side. Generally power quality problems are like voltage swell, sag, flickers; harmonics forms the cause for electrical distribution network failures [3]. Among the above the effect of harmonics will be very severe at distribution side due to vast usage of non linear loads. Implementation of Unified power quality controller (UPQC) at DS (Distribution Side) control the level of harmonics to very low quantity and keeps the load safe and work efficiently. UPQC is most effective and powerful electronics device for heavy (high) loads and sensitive to line voltage and line current disruptions. [4][5] UPQC Based Power Quality Improvement in Distribution System Connected with PV Arrays).

This paper proposes a system for along power quality conditioner (UPQC) topology that infuses streams & voltages at lower THD values into utility framework association by the implementation of technique of synchronous reference frame theory

1.Introduction
2.Upqc System Configuration and Control Mechanism
3.Proposed model

II. UPQC CONFIGURATION AND CONTROL MECHANISM

Unified Power quality Conditioner (UPQC) is a combination of series and shunt active power filters which are connected back to back, where series active power filter is arranged in series with transmission or distribution line to mitigate the voltage distortions and imbalances present on source side and the load voltage balanced ,regulated and sinusoidal and shunt active power filters are arranged in

parallel with transmission or distribution line to mitigate harmonics in load current and make the source current free from distortions and imbalances and make the source current sinusoidal. These two active power filters are connected back to back with a dc link capacitor in case of 1-phase,3-phase3-wire,3-phase 4-wire configurations. The configuration of UPQC includes series active filter, shunt active filter, dc link capacitor, series transformers, low and high pass filters.[7]

The normal principle of a shunt APF is that it develops a current (I) which is equal and inverse in polarity to the Harmonic current drawn by load and implants it to the point of common coupling (PCC), thereby forcing the main source current to be pure sine wave. By that both harmonic and reactive currents are then nullified at source end and the result is balanced sine current. [8][9] Synchronous frame theory helps us in eliminating number of controllers in case of three phase system and forms the benefit in easy controlling of steady state errors. The SRF theory can also be termed as d-q theory. The main concept of this theory relies on Parks Transformations for transforming the 3- □ voltage (V) and current(I) into synchronous rotating frame. The P and Q components of 3- □ system are generally represented as direct (d) and quadrature (q) components.[10][11]

The block diagram of the system that is represented in this paper is as follows

Revised Version Manuscript Received on 30 November, 2018.

S. Phani Venkata Ramana, M-Tech Student Scholar Department of Electrical & Electronics Engineering, Malla Reddy Engineering College, Maisammaguda, Medchal (Telangana), India.

K. Anitha Reddy, Assistant Professor Department of Electrical & Electronics Engineering, Malla Reddy Engineering College, Maisammaguda, Medchal (Telangana), India.

K. Deepthi, M-Tech Student Scholar Department of Electrical & Electronics Engineering, Malla Reddy Engineering College, Maisammaguda, Medchal (Telangana), India.

Ms. K. Chetaswi, Assistant Professor Department of Electrical & Electronics Engineering, Malla Reddy Engineering College, Secunderabad, Hyderabad (Telangana), India.

Published By:
Blue Eyes Intelligence Engineering
& Sciences Publication

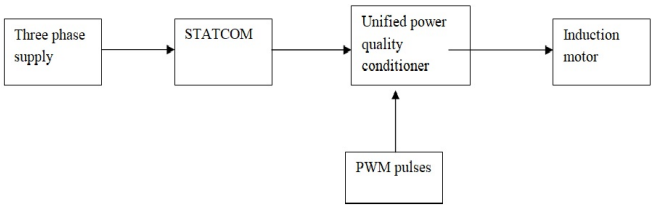

The system contains of a three-phase supply followed by a static compensator then a unified power quality conditioner (UPQC) which is in series with the transformers and then by a specified load (the load considered in this paper is an Induction motor)

III. PROPOSED MODEL AND ITS WORKING

This paper mainly concentrates on the level of harmonics which are on the source side such that the amount of power from the source side to load side should be reliable. Many experiments and researches have done by installing different types of controllers in different ways and obtained results and amount of THD have been calculated on Distribution side. This paper presents the SIMULINK model of the distribution network with Unified Power Quality Conditioner (UPQC) as main controller. The control strategy used for generation of gating pulses for series and shunt filters which are arranged back to back with a dc link capacitor in between them is Synchronous Reference Frame Theory (SRFT)[12].The MATLAB/Simulink model of distribution side represented in this paper is as follows

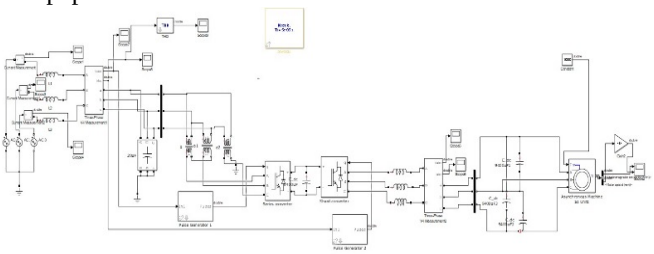

This system comprises of a 3 phase source where phase displacement was arranged as 1200 each, then followed by inductors which can be treated as the transmission lines then a static compensator device connected in parallel to adjust the inductive (L) or capacitive (C) current so as to maintain the specific parameters connected with the network. It can be helpful in reducing losses, active power fluctuation mitigation and improvement of transfer capcity. This variable compensator is a combination of three separate variable capacitors connected in parallel to form one single capacitor of high value. Each phase is connected with a linear transformer in series combination.

The transformers are connected in □- □ arrangement. Then a block of unified power quality conditioner is connected with a combo of both shunt and series filter a dc link capacitor is arranged in between these filters. [13]

The control strategy for obtaining triggering pulses is based on SRF theory which implements the concept of parks transformation and inverse transformation. The values of voltage and current obtained from the 3-∅ source was considered as the value with the harmonics and a value was pre-determined within the pwm generator with SRF theory installed in it. Once the value reaches the pwm generator the obtained value will be compared with the pre-determined value and if there is difference in its waveform then the gating pulses will be supplied to series active filter which comes into action and will regularize obtained value to the predetermined value. By using the park's transformation, the phase variables will be decoupled from 3-∅ to 2-∅ normally. By this the three-phase source current is first categorized and changed into (**α-β-0**) two phase stationary frame

The working equations of this model to obtain the process of decoupling the three phase currents to two phase currents is as follows

$$\begin{pmatrix} T_{dq} \end{pmatrix} = 2/3 \begin{pmatrix} \cos \emptyset_d & \cos(\emptyset_d - 2\pi/3) & \cos(\emptyset_d + 2\pi/3) \\ -\sin \emptyset_d & \sin(\emptyset_d - 2\pi/3) & \sin(\emptyset_d + 2\pi/3) \\ 0.5 & 0.5 & 0.5 \end{pmatrix} \quad \ldots (1)$$

Then the values of 2-∅ will be transmitted through the dc link capacitor to reach the shunt active filter. The shunt active filter was already arranged inverse parks transformation which converts input 2-∅ values into 3-∅ values. The parks inverse transformation was characterized by eqn 2

$$\begin{pmatrix} T_{dq} \end{pmatrix}^{-1} = \begin{pmatrix} \cos \emptyset_d & -\sin \emptyset_d & 1 \\ \cos(\emptyset_d - 2\pi/3) & -\sin(\emptyset_d - 2\pi/3) & 1 \\ \cos(\emptyset_d + 2\pi/3) & -\sin(\emptyset_d + 2\pi/3) & 1 \end{pmatrix}$$

The gating pulses to the shunt filter is also supplied in the same way as stated for series filter concept. The value of current obtained from 3-∅ source will be cross checked with the predetermined value and if there is a difference then triggering pulses will be supplied. The filtered values was then sent to load. A capacitor bank Δ connected was installed in middle of load and UPQC circuit to rectify the problems related to the power factor on load side. The experimental results are obtained by using MATLAB/SIMULINK model. The results are as follows

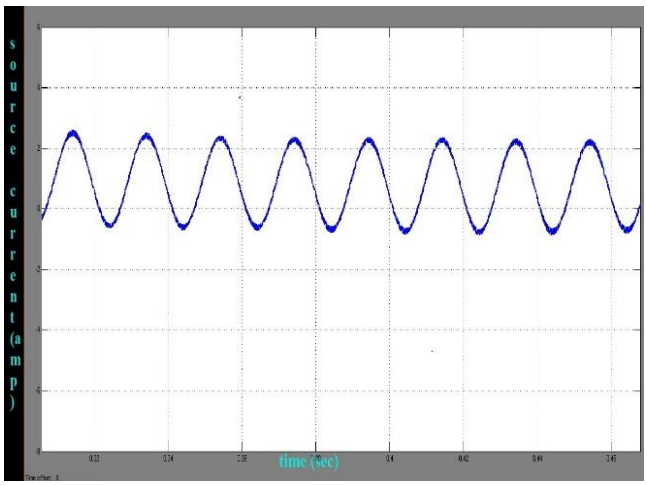

Fig.1 wave form of the source current [Source current vs Time]

Published By:
Blue Eyes Intelligence Engineering
& Sciences Publication

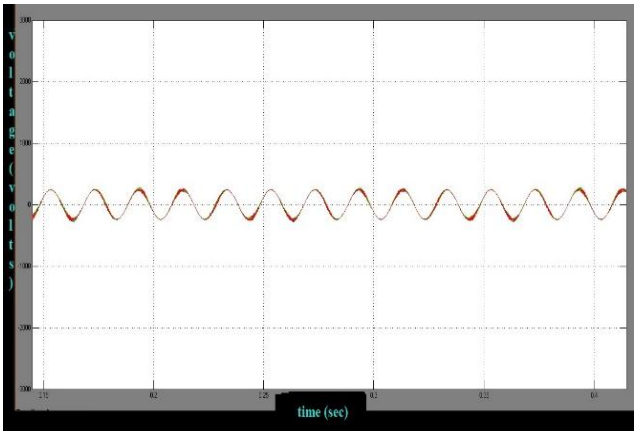

Fig.2 wave form of the UPQC output voltage [voltage vs time]

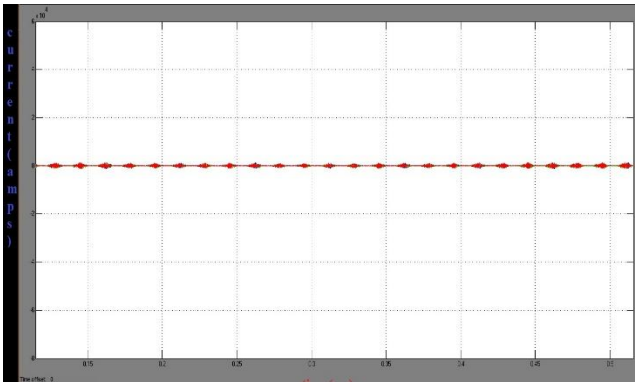

Fig.3 wave form of the UPQC output current [current vs time]

From the experimental results the amount of THD was around 9%, where as compared to many controllers the value of THD is very low and the obtained wave form also resembles the sine wave to most of the extent.

S. No	CONTENT	THD
1	Amount of Harmonic Emission with Diode Rectifier and P-I Controller	29%
2	Amount of Harmonic mission with IGBT based back to back arranged rectifiers	9%

IV. CONCLUSION

This paper is mainly based on the harmonic reduction at distribution side by considering cost, complexity of the model, power transfer capability, and reliability as the factors. By installing the unified power quality conditioner system performance is increased and the obtained waveform is resembling the sine wave. By the reduction of harmonic content, the power quality issues can be controlled to the larger extent.

REFERENCES

1. firuz zare, hamid soltani, dinesh kumar, pooya davari, hernan andres miranda delpino, and frede blaabjerg "Harmonic Emissions of Three-Phase Diode Rectifiers in Distribution Networks" Received January 3, 2017, accepted February 12, 2017, date of publication February 16, 2017, date of current version March 28, 2017.
2. Banothu Raju, Fatima Azra "Power Quality Improvement Using D-STATCOM with PI and Fuzzy Logic Controller" International Journal of Computational Science, Mathematics and Engineering Volume 3, Issue.9, 2016
3. P. Anitha Rani, Sivakumar.R "Improvement of Power Quality using DVR in Distribution Systems", International Conference on Engineering Technology and Science-(ICETS'14) On 10th & 11th February Volume 3, Special Issue 1, January 2014
4. Mr. Bhushan S. Rakhonde, Astt.Prof. C. M. Bobade "Harmonic Mitigation using Modified Synchronous Reference Frame Theory" , International Research Journal of Engineering and Technology Volume: 04 Issue: 08 | Aug -2017
5. Parag Datar, Vani Datar, S. B. Halbhavi, S G Kulkarni "Synchronous Reference Frame Theory For Nonlinear Loads using Mat-lab Simulink" JETIR (ISSN-2349-5162) June 2016, Volume 3, Issue 6
6. Prof. J.P.Sridhar, Ayan Sarkar, Nirupam Tarafdar, Nitesh Kumar, Pranav Verma "UPQC Based Power Quality Improvement in Distribution System Connected with PV Arrays" International Journal of Advanced Research in Electrical,Electronics and Instrumentation Engineering, Vol. 5, Issue 5, May 2016
7. Rajiv Kumar sinku "Study of Unified Power Quality Conditioner for Power Quality Improvement" Department of Electrical Engineering National Institute of Technology, Rourkela May 2015
8. Mr. Bhushan S. Rakhonde, Astt.Prof. C. M. Bobade " Harmonic Mitigation using Modified Synchronous Reference Frame Theory" International Research Journal of Engineering and Technology (IRJET), Volume: 04 Issue: 08 | Aug -2017
9. Suleiman Musa, Mohd Amran Mohd Radzi , Hashim Hizam , Noor Izzri Abdul Wahab ,Yap Hoon and Muhammad Ammirrul Atiqi Mohd Zainuri "Modified Synchronous Reference Frame Based Shunt Active Power Filter with Fuzzy Logic Control Pulse Width Modulation Inverter" 29 May 2017
10. N.Srinivasa Rao, H.J.Jayatheertha "Modeling And Simulation Of Various Srf Methods For Shunt Active Power Filter And Application To BLDC Drive" International Journal of Advanced Engineering Research and Studies E-ISSN2249–8974
11. P Ananda Mohan , M Sandeep "Synchronous Reference Frame Theory (SRF) along with PI Controller Based Dynamic Voltage Restorer", Volume 4, Issue 11 (November 2015), PP. 40-45
12. Chandra Kishor Gupta, Mr.MihirB. Chaudhari " Simulation of Synchronous Reference Frame Theory based Method for Harmonic Mitigation", International Journal of Advance Engineering and Research Development Volume 2,Issue 3, March -2015
13. Brijesh Kumar Sen, Seema Agrawal, Mahendra Kumar, R. K. Somani "Performance Analysis of Synchronous Reference Frame based Shunt Active Power Filter", International Conference on Research Trends in Engineering, Applied Science and Management (ICRTESM-2017}, Sponsored by Institutions of Engineers Kota Center, Supported by RTU Kota, Rajasthan
14. S. S. Wamane, J.R. Baviskar, S. R. Wagh, "A Comparative Study on Compensating Current Generation Algorithms for Shunt Active Filter under Non-linear Load Conditions", International Journal of Scientific and Research publications volume 3,issue 6,June 2013

Published By:
Blue Eyes Intelligence Engineering
& Sciences Publication

Ultrasonic flaw signal Classification based on Curvelet transform and Support Vector Machine

A. Pradeep Kumar

Abstract: ***This paper presents the classification of ultrasonic flaw signal with the use of curvelet transform method and support vector machine. The curvelet transform as a not merely to achieve time frequency manifestation of signal, but also to be used for curvelet signal decomposition and successive parameter assessment. Faults are detected by using a digital flaw detecting method which is considered as the primary tool to obtain the carbon fiber signals as an unbreakable polymer sample with de-lamination and de-bonding. Discrete curvelet transform can be computed ultrasonic signals in time domain by enlightening features are extracted from signals of curvelet coefficients. Finally, SVM chosen by dissimilar techniques are in use as input and train by the classifier. So the kernel function has been checking the data with combination of SVM parameters. Experimental outcome prove the validation and verification of flaw signal with curvelet transform and SVM tool, it deals with classification for ultrasonic signals utmost accurately.***

Keywords: Curvelet transform, SVM, Ultrasonic flaw signals, Kernel function

I. INTRODUCTION

Ultrasonic techniques are working on non-destructive testing methods and procedures for accurate and detection of flaws analysis in ultrasonic signal. These testing techniques are functioning in different procedures based on signal flaw strength. Sometimes these methods bring costly, long and unpredictable analysis for discovery classification and analysis of flaw signal. The progress in earlier period of epochs has enabled the ultrasonic methods and non-destructive techniques authenticate testing. Specific tools employed in Artificial intelligence can also be united along with the automatic signalling events in modern signal processing methods, this type of scenario applied for the identification of various flaw in different engineering resources [1]. The procedure of classification often comprises of three predominant contributions, they are pre-processing of the unique signals, adopting various signal processing methods and pattern classification for feature extraction. Among these methods the most significant method characteristic extraction process, which straightforwardly deprives the correctness and thereby the consistency of flaw classification. The probable dissimilar signal processing analysis methods has been investigated by many researchers in ultrasonic testing [3].

We offered a novel method for ultra flaw signal.

II. METHODOLOGY

Curvelet transform to obtain time frequency representation of signal, but also to be utilized for curvelet signal breakdown and successive parameter assessment. Before this decomposition filters are using for remove noise from data using pre processing. We can use curvelet transform for feature construction and SVM for classify the processed data based on certain conditions. It is a process for finding best signals from flaws. The following procedures are helping for handle the flaw ultrasonic signals [2].

2.1 Data pre-processing

The Pre-processing method of ultrasonic signals consists of amplitude normalization process followed by filtering. For filtering the ultrasonic signal, a method based on discrete curvelet transformation has been employed. This technique is extremely efficient within the specified domain for time period. Furthermore, the ultrasonic signals are scanned to measure the development of signal and noise ratio. The curvelet transformation is a multifaceted resolution analysis technique which is used to predict the period of time frequency rate of the ultrasonic signal. The procedure used for filtering is completely based on the break of signal obtained using curvelet transforms at 'n' no. of levels with group pass filtering along with annihilation to attain the estimate stage and derive the detail coefficients. Then the threshold coefficients and rebuilding of signal from fact and rough calculation coefficients using inverse transformation function [4].

2.2 Curvelet Transform

Discrete Curvelet transform has good signal properties, it is applicable for many real signals and it is also computationally efficient. It is used for different types of processes together with numerical integration, noise diminution, image compression and pattern recognition [5]. The discrete Curvelet transform is a symbol of digital signal processing with respect to time using different filtering methods. Different cutoff frequencies as several scales are used to process the signal. Filters carry out the functions in processing the signal. Scaling the filters in iterations generates wavelets. Scales are identified using the up and down sample technique. The use of filter provides the data in the signal. Therefore, it uses the high and low pass filters over a digitized input signal [7]. The discrete Curvelet transformation is helpful in signifying the image with various passion values which is given by the polynomial function $f(x_1, x_2)$, where $x_1 = 0, 1, 2, 3..., N_1 - 1$ and $y_2 = 0, 1, 2, 3,..., N_2 - 1$, whose discrete Fourier transform is given by

$$\overline{f}(n_1,n_2), \sum_{x_2=0}^{N_2-1}\sum_{x_1=0}^{N_1-1} f(x_1,x_2)e^{-2\pi i(\frac{N_1x_1}{N_1}+\frac{N_2x_2}{N_2})} \quad (1)$$

Revised Manuscript Received on December 08, 2018.

Dr. A. Pradeep Kumar, Assistant Professor, ECE Dept, Malla Reddy Engineering College (Autonomous), Hyderabad, Telanagana, India

The discrete Curvelet transformation is a disintegrated value minimalized into the Curvelet coefficients such that

$$f(n_1,n_2)= \sum_{j=1}^{j} \sum_{l=0}^{L_j-1} \sum_{k_1=0}^{K_{jl},_{1-1}} \sum_{k_2=0}^{K_{jl},_{2-1}} D_{jlk}T_{jlk}(x_1,x_2) \qquad (2)$$

Where k= (k1, k2), D is the specified Curvelet on phase vector j denoted by its corresponding direction l and the spatial shift of k.

$$\sum_{jlk} \left|D_{jlk}\right|^2 = \sum_{y1,y2} + |f(x_1,x_2)|^2 \qquad (3)$$

The discrete Curvelet transform function gives a combination of image f through J complete levels, with an orientation of L_j on every level, and a of spatial shifts $K_{jl,1} \times K_{jl,2}$ for every level, where $k = (k_1, k_2)$ and s is the Curvelet function on level j with an orientation l and a spatial shift k. In addition, the Curvelet transform also preserves l^2-norms, which can be denoted by,

$$\sum_{jlk} \left|D_{jlk}\right|^2 = \sum_{y1,y2} + |f(x_1,x_2)|^2 \qquad (4)$$

The above mentioned discrete curvelet transformation function can't join together the image of 'f' into J complete levels, with the orientation of L_j on every level, and spatial shifts of $K_{jl,1} \times K_{jl,2}$ for each direction. The Curvelet is described through its discrete Fourier transformation as

$$\bar{s}_{jok}(n_1,n_2) = V_j(n_1,n_2)\, e^{-2\pi i}(k_1n_1 / K_{j0,1} + k_2n_2 / K_{j0,2}) \text{ and } \bar{s}_{jlk} = T^T\theta_1\bar{T}_{jok} \qquad (5)$$

Here, T_θ is known as shearing matrix, when the grid is subjected to shear on which the Curvelet is evaluated at an angle of $\emptyset_l$. The slope gradients are designated by the angles $\emptyset_l$ and are equi-spaced. Here v_j is the frequency window function with a compact support function[8].

2.3 Feature Extraction and Selection of SVM

SVM Technique is a set of controlled learning algorithms. 'Pattern recognition problems' can be resolved by using the SVM Technique. Also forecasting the problems, constructing intelligent machines for solving problems, regression approximation techniques and the problems of dependency estimation are some of the areas where SVM application areas. Therefore this architecture determines the generalization abilities of any system at any instance. Support vector machine is used for classifying the different data points of the linear separable data sets that is provided to the system. Hence, SVM can be applicable to both linear and nonlinear circumstances. By using SVM, the separating margin between two classes of variables is tried to be made maximum.

$$h_i(x) = V_i^T . X + v_{i0} = 0 \quad (6)$$

Where $h_i(x)$ = Output feature vector

$V_i^T = \{v_1, v_2, \ldots\ldots, v_n\}$ S = weighing vector

m = number of attributes considered

v_{i0} = a scalar called threshold value or bias value

x = Input feature vector

If x_1 and x_2 are the two values of attributes B_1 and B_2 on the decision hyper plane then the following equation is valid.

$$h_i(x_1) = V_1^T x_1 + v_{i0} = 0 \quad (7)$$

$$h_j(x2) = V_2^T x_2 + v_{i0} = 0 \quad (8)$$

Subtracting the above two equations we Yield the following result:

$$h_i(x_1) = h_j(x_2) = 0 \Rightarrow V_1^T x_1 + v_{i0} = V_2^T x_2 + v_{i0} = 0$$

$$h_i(x_1) - h_j(x_2) = 0 \Rightarrow V_1^T x_1 + v_{i0} - V_2^T x_2 - v_{i0} = 0$$

$$h_{ij}(x_1,x_2) = 0 \Rightarrow V_1^T x_1 - V_2^T x_2 = 0$$

$$\text{i.e. } h_{ij}(x_1,x_2) = 0 \Rightarrow v^T(x_1 - x_2) = 0 \qquad (9)$$

Where $(x_1 - x_2)$ is a vector that is aligned parallel to the decision boundary and is directed from x_1 towards x_2. Since the dot product is zero, the direction for WT must be perpendicular to decision boundary.

Thus, the above separating hyper plane satisfies the prescribed conditions i.e. for any square Xs that is located above the decision boundary and which can be shown as

$$v_1x_1+v_2x_2 + v_{i0} = k > 0 \quad (10)$$

Similarly, any point prescribed in the circle located below the decision boundary, that lies below the separating hyper plane satisfying the context, we can show that

$$v_1x_1+v_2x_2 + v_{i0} = k' < 0 \quad (11)$$

If we label the squares as class +1 and all the circles as class -1, then we can predict the class label X for any test example z in the following way:

$$X_i = \begin{cases} 1, \text{ if } v.\ z + c > 0; \\ -1, \text{ if } v.\ z + c < 0; \end{cases}$$

The hyper planes give the sides of the margin when the weights can be changed and it can be written as

$$H_1: v_1x_1+v_2x_2 + v_{i0} \geq 1, \text{ for } X_i = +1, \qquad (12)$$

$$H_2: v_1x_1+w_2y_2 + v_{i0} \leq -1, \text{ for } X_i = -1, \qquad (13)$$

Connecting the two inequalities of Equations and we get

$$X_i(v_1x_1+v_2x_2 + v_{i0}) \geq 1, \text{ for all i.} \quad (14)$$

The margin can be computed by subtracting the second equation from the first equation. This is equivalent with

1. Having a margin of $\frac{1}{\|v\|} + \frac{1}{\|v\|} = \frac{2}{\|v\|}$
2. Requiring that $v_i^Tx + v_{io} \geq 1, \forall x \in v_1$

$$v_i^Tx + v_{io} \leq -1, \forall x \in v_2$$

Computing the parameters denoted by w, w_{io} of the hyper plane so that to:

$$\text{Minimize I } (v, vio) = \frac{1}{2}\|V\|2 \qquad (15)$$

$$Xi\ (v_i^Tx_i + v_{io}) \geq 1, j=1, 2\ M. \qquad (16)$$

Obviously, minimizing normal gradually increases the margin to a maximum value. This is denoted as a nonlinear quadratic optimization duty topic to a set of linear inequality constraints. The above mentioned crisis can be resolved by reducing Lagrange's function. The conditions proposed by Karush-Kuhn-Tucker (KKT) which minimizes the above equations and also satisfies it are

$\frac{\partial}{\partial w}L\ (v, v_{io}, \lambda)=0$ and $\frac{\partial}{\partial wo}\ L(v, v_{io}, \lambda)=0$ where $\lambda_i \geq 0$ i=1, 2……..N

$$\lambda_i[X_i(v_i^Tx_i+v_{io})-1]=0 \text{ i=1,2……..N}$$

Where λ denotes the vector of the Lagrange's multiplier λ_i and $L(v, v_{io}, \lambda)$ is the Lagrangian function which defined as

$$L\ (v, v_{io}, \lambda)= \frac{1}{2}v^Tv + \sum_{i=1}^{N}\lambda_i[X_i(vi^Tx_i+ v_{io})- 1] \qquad (17)$$

Combining the equations (17), (18) and (19), we get

$$V = \sum_{i=1}^{M}\lambda_iX_ix_i \text{ and } \sum_{i=1}^{N}\lambda_iXi =0$$

A novel technique has been implemented with the support of SVM for the classification of PQ disturbances.

Published By:
Blue Eyes Intelligence Engineering
& Sciences Publication

It has been observed that the SVM technique precisely classifies the PQ disturbances as per the requirement. The proposed methodology using the SVM technique generates a classification rate of about 98.8% which is much better than the technique used for the classification of PQ disturbances.

2.4 Non-linear classifier:

If any two classes specified are in nonlinear case, Eqn. (16) and Eqn. (17) become invalid or void and have different forms. The three categories of the training feature vectors depend on the procedure cited below.

1. Vectors that fall outside the prescribed circle and are classified precisely acquiesce with the constraints

$$Xi\ (v_i^T x_i + v_{io}) \geq 1,\ i=1, 2\ldots\ldots\ldots..M$$

2. Vectors falling inside the prescribed circle and are precisely classified. In hyper plane, these points will be positioned in squares of the variable and they satisfy the inequality

$$0 \leq X_i(v_i^T x_i + v_{io}) < 1$$

3. Vectors that are not classified in any order but are enclosed by circles and obey the inequality

$$Xi\ (v_i^T x_i + v_{io}) < 0$$

All these three cases can be categorized as single type of elements by introducing a novel objective function Ø which is given by

$$Xi\ (v_i^T x_i + v_{io}) \geq 1 - Ø_i$$

For category X-1: $Ø_i = 0$ for categorX-2: $0 \leq Ø_i < 1$ for category X-3: $Ø_i \geq 1$

The variable $Ø_i$ is called as slack variables. The Goal is to make the margin as huge as possible at the equivalent time specified to maintain the number of points with $Ø > 0$ as small as possible. This equivalent to assigning a minimal cost function denoted by

$$I\ (v, v_{io}, Ø) = \frac{1}{2} v^T v + D \sum_{i=1}^{M} J(Øi)$$

Where Ø is the vector of the parameters Øi and

$$X_i = \begin{cases} 1, \text{ if } v.\ z + c > 0; \\ -1, \text{ if } v.\ z + c < 0; \end{cases}$$

The hyper planes give the sides of the margin when the weights can be changed and it can be written as

$$H_1: v_1x_1 + v_2x_2 + v_{i0} \geq 1, \text{ for } X_i = +1 \qquad (12)$$

$$H_2: v_1x_1 + w_2y_2 + v_{i0} \leq -1, \text{ for } X_i = -1, \qquad (13)$$

Connecting the two inequalities of Equations and we get

$$X_i\ (v_1x_1 + v_2x_2 + v_{i0}) \geq 1, \text{ for all i.} \quad (14)$$

The margin can be computed by subtracting the second equation from the first equation. This is equivalent with

1. Having a margin of $\frac{1}{\|v\|} + \frac{1}{\|v\|} = \frac{2}{\|v\|}$
2. Requiring that $v_i^T x + v_{io} \geq 1,\ \forall\ x \in v_1$

$$v_i^T x + v_{io} \leq -1,\ \forall\ x \in v_2$$

Computing the parameters denoted by w, wio of the hyper plane so that to:

$$\text{Minimize } I\ (v, vio) = \frac{1}{2}\|V\|2 \qquad (15)$$

$$Xi\ (v_i^T x_i + v_{io}) \geq 1,\ j=1, 2\ldots\ldots\ldots\ldots M. \qquad (16)$$

Obviously, minimizing normal gradually increases the margin to a maximum value. This is denoted as a nonlinear quadratic optimization duty topic to a set of linear inequality constraints. The above mentioned crisis can be resolved by reducing Lagrange's function. The conditions proposed by Karush-Kuhn-Tucker (KKT) which minimizes the above equations and also satisfies it are

$\frac{\partial}{\partial w} L\ (v, vio, ƛ) = 0$ and $\frac{\partial}{\partial wo} L(v, vio, ƛ) = 0$ where $ƛi \geq 0$ i=1, 2……..N

$$ƛ_i[X_i(v_i^T x_i + v_{io}) - 1] = 0 \quad i=1,2\ldots\ldots\ldots\ldots..N$$

Where ƛ denotes the vector of the Lagrange's multiplier $ƛ_i$ and $L(v, v_{io}, ƛ)$ is the Lagrangian function which defined as

$$L\ (v, v_{io}, ƛ) = \frac{1}{2} v^T v + \sum_{i=1}^{N} ƛ_i[X_i\ (vi^T x_i + v_{io}) - 1] \qquad (17)$$

Combining the equations (17), (18) and (19), we get

$$V = \sum_{i=1}^{M} ƛ_i X_i x_i \text{ and } \sum_{i=1}^{N} ƛ_i Xi = 0$$

A novel technique has been implemented with the support of SVM for the classification of PQ disturbances. It has been observed that the SVM technique precisely classifies the PQ disturbances as per the requirement. The proposed methodology using the SVM technique generates a classification rate of about 98.8% which is much better than the technique used for the classification of PQ disturbances.

2.4 Non-linear classifier:

If any two classes specified are in nonlinear case, Eqn. (16) and Eqn. (17) become invalid or void and have different forms. The three categories of the training feature vectors depend on the procedure cited below.

1. Vectors that fall outside the prescribed circle and are classified precisely acquiesce with the constraints

$$Xi\ (v_i^T x_i + v_{io}) \geq 1,\ i=1, 2\ldots\ldots\ldots..M$$

2. Vectors falling inside the prescribed circle and are precisely classified. In hyper plane, these points will be positioned in squares of the variable and they satisfy the inequality

$$0 \leq X_i\ (v_i^T x_i + v_{io}) < 1$$

3. Vectors that are not classified in any order but are enclosed by circles and obey the inequality

$$Xi\ (v_i^T x_i + v_{io}) < 0$$

All these three cases can be categorized as single type of elements by introducing a novel objective function Ø which is given by

$$Xi\ (v_i^T x_i + v_{io}) \geq 1 - Ø_i$$

For category X-1: $Ø_i = 0$ for categorX-2: $0 \leq Ø_i < 1$ for category X-3: $Ø_i \geq 1$

The variable $Ø_i$ is called as slack variables. The Goal is to make the margin as huge as possible at the equivalent time specified to maintain the number of points with $Ø > 0$ as small as possible. This equivalent to assigning a minimal cost function denoted by

$$I\ (v, v_{io}, Ø) = \frac{1}{2} v^T v + D \sum_{i=1}^{M} J(Øi)$$

Where Ø is the vector of the parameters Øi and

$$Ø_i = \begin{cases} 1, \text{ if } Ø_i > 0; \\ 0, \text{ if } Ø_i = 0; \end{cases}$$

The parameter D is a positive constant value that controls the relative influence of the competing terms mentioned in the equation. By minimizing Lagrange's function all the worst issues can be resolved.

$$L\ (v, v_{io}, Ø, ƛ, ú) = \frac{1}{2}\|v\|^2 + D \sum_{i=1}^{M} Øi - \sum_{i=1}^{M} Øiúi - \sum_{i=1}^{M} ƛ_i [Xi\ (v_i^T x_i + v_{io}) - 1]$$

Published By:
Blue Eyes Intelligence Engineering
& Sciences Publication

The equivalent Karush-Kuhn-Tucker conditions that minimizes the above equations and that has to satisfy the governing conditions are

$$\frac{\partial L}{\partial w} = 0 \text{ or } v = \sum_{i=1}^{M} \lambda_i X_i x_i$$

$$\frac{\partial L}{\partial wo} = 0 \text{ or } \sum_{i=1}^{M} \lambda_i X_i = 0$$

$$\frac{\partial L}{\partial úi} = 0 \text{ or } \sum_{i=1}^{N} D - úi - \lambda_i = 0 \; J = 1,2\ldots\ldots\ldots\ldots M$$

$$\lambda_i [X_i(v_i^T x_i + v_{io}) - 1 + \emptyset_i] = 0, úi\emptyset_i = 0, úi \geq 0, \lambda_i \geq 0 \; i = 1, 2\ldots\ldots\ldots\ldots M$$

In nonlinear case, SVM maps the input vectors denoted as y into a high dimensional space through some nonlinear mapping techniques.

2.5 Multi-classifier:

In the recent Years, a discrete methodology named as multi-class SVM, which can classify more than two dataset, are proposed. For each one of these classes, we can apparently design an optimal discriminate function given by $h_i(x)$, i=1, 2…N, so that $h_i(x) > g_j(y)$, ∀j #i, if y $\in w_i$. Classification is attained as per the following rule: Assign x in v_i, if i = argument $x_k\{h_k(x)\}$.

In OAO training process, all the classes with machine depending on comparison with each other and each data set is trained by assuming that all the data set belongs to a respite data set. For a problem under k-class, while OAO methodology constructs k*(k-1)/2 hyper planes, OAA methodology constructs k hyper planes only.

Algorithm used for classification of the extracted features using KKT-conditions:

1. Input: $\{(\bar{y}, x_1)\ldots(\bar{y}_n, x_n)\}$.
2. Initialize for i = 1, . . . , n:
3. $\bar{\tau}i = \bar{o}$
4. $E_{i,r} = -\beta\delta_r, y_i (r = 1. . . k)$
5. $B_i = K(\bar{y}, \bar{y})$
6. Repeat:
7. Calculate for i = 1. . . n: $\varphi_i = \max_r F_{i,r} - \min_{r:\tau i,r<\delta yi,r} Fi, r$
8. Set: O = arg max{ψi}
9. Set for p = 1. . . k : $Dr = \frac{Fp,r}{Ap} - \tau p,r + \delta r$, y_p and $\theta = \frac{1}{k}\sum_{r=1}^{k} Dr - \frac{1}{k}$
10. Call: $\bar{\tau}*p$ =Fixed Point Algorithm ($\bar{C}$, θ, ∈/2).
11. Set: $\Delta\bar{\tau}p = \bar{\tau}*p - \bar{\tau}p$
12. Update for i = 1. . . m and r = 1. . . k:
13. E i.r← E i.r+ Δτp,r $K(\bar{y}p, \bar{y}I)$
14. Update: $\bar{\tau}p - \bar{\tau}*p$
15. Until $\psi_p <$ _β
16. Output : $H(\bar{x}) = \arg\max_r.\{\sum_i \tau_i, rK(\bar{y}, \bar{y}_i)\}$.

SVMs were formerly established to execute binary classification only. The classification of data into more than two classes, called multiclass classification technique, which is frequently and predominantly used in remote sensing applications. The Karush–Kuhn–Tucker conditions for the optimization issue. Although convergence of this algorithm is assured to a certain extent, heuristics are used to choose the suitable pair of multipliers precisely so as to accelerate the rate of convergence. In this methodology, we can create more SVM classifiers for all the possible pairs of classes. The standard formulas for finding the statistical parameters of every signal. We also compute dissimilar values root mean square value and absolute values [10].

(1) Mean value : AVG = $\frac{1}{M}\sum_{i=1}^{M} x_i$

(2) Standard deviation : STD = $\sqrt{\frac{1}{M}\sum_{i=1}^{M}(y_i - AVG)^2}$

III. RESULTS AND DISCUSSIONS

The following table describes the training table, recognition rate of test data and recognition rate of training data with kernel function. The SVMs with RBF kernel functions are best for mean identification rates of linear and polynomial kernels. Due to the exponential processing complications of support vector machine with RBF kernels had utmost training time. Let us attention on the support vector machine include polynomial kernel function (*p*=3) and RBF kernel function (*p*=0.1), it is recognized as Poly3 and RBF 0.1 support vector machine. Support vector machine get 98.5% in Poly3 of training identification rate within 81.4 seconds. In this scenario, two top de-lamination flaws of the CFRP samples were classified as middle de-lamination, these are not affected by positive or negative for every point. In this process of comparison to RBF 0.1 support vector machine, 97.95% of training identification rate within 271.1 seconds, support vector machine receives 228% in Poly3, development for training efficiency. So 1.26% losses for identification rate of flaw signals. Finally Poly3 Support vector machine can completely achieve the trade-off among the processing complexity and classification performances of flaw ultrasonic signals.

Table 1. Training Times of SVMs and Identification Rates with dissimilar Kernel Functions

Kernel function	Identification of training data (%)	Identification of test data (%)	Training time (s)
Linear function (*C*=1)	92.25	88.5	20
Polynomial function, *p*=2 (*C*=0.1)	96	91	68.5
Polynomial function, *p*=3 (*C*=0.1)	96.5	93.5	82.4
RBF Network, K=10 (*C*=1)	96.65	92.25	219.1
RBF Network, K=10 (*C*=1)	98.5	93.5	231.3
RBF Network, K=0.1 (*C*=1)	97.95	93.75	271.1

Published By:
Blue Eyes Intelligence Engineering
& Sciences Publication

Table 2. Parameters of Back Propagation Network

Parameters of BP	Value
Number of input features	6
hidden layer of Activation function	Tan sigmoid transfer function
output layer of Activation function a	Tan sigmoid transfer function
Training algorithm	Trainscg
Number of neurons at hidden layer	13
Throughput goal	0.001
Network structure	6-13-6

Table 3. Comparison among Back Propagation Network and SVMs

Classifiers of signal	Identification of training data (%)	Identification of test data(%)	Training time(s)
Back Propagation Network	91.25	86.25	85
Support Vector Machine	98.75	93.75	170.5

The above tables 2 and 3 show the information regarding the standard formulas for discovery the statistical parameters of every signal. We also compute dissimilar values of root mean square and absolute values. Based on these values successfully finding the flaw ultrasonic signals.

IV. CONCLUSION

Ultrasonic flaw signal classification and analysis by using curvelet transforms and support vector machine. The curvelet transform as a not merely to attain time frequency demonstration of signal, but also to be used for curvelet signal decomposition and successive parameter assessment. Faults are detected by a digital flaw detector; it is primary device to get the signals of carbon fiber indestructible polymer sample with de-lamination and de-bonding. The curvelet coefficients from discrete curvelet transform can be processed ultrasonic signals in time domain for feature extraction. Finally, SVM chosen by dissimilar techniques are in use as input and train by the classifier. Checking the signal data with the help of kernel function support vector machine parameters. Statistical results show the verification and validation of signal with the help of curvelet coefficients and support vector machine. This method generates best analysis and classification of ultrasonic signals.

REFERENCES

1. Lee K and Estivill Castro V.," Feature extraction and gating techniques for ultrasonic shaft signal classification", Applied Soft Computing, 7(1), PP: 156-165, 2007.
2. Kyungmi Lee," Feature extraction schemes for ultrasonic signal processing", Vth International Conference on Computer Sciences and Convergence Information Technology, PP:366-372, 2010.
3. Ahmed Yamani, Mohamed Deriche," Automatic Detection of High Temperature Hydrogen Attack defects from Ultrasonic A-scan Signals", IVth Middle East NDT Conference and Exhibition, PP:58-61, 2007.
4. Rajkumar R.,"Pipeline Defect Detection Using Support Vector Machines", 6th International Conference on Circuits, Systems, Electronics, Control and Signal Processing, PP: 162-168, 2007.
5. Vaclav Matz and Marcel Kreidl,"Classification of ultrasonic signals", International Journal of Materials and Product Technology, 27(3-4), PP: 145-155, 2006.
6. Cacciola M, and Morabito F.," Computational intelligence aspects for defect classification in aeronautic composites by using ultrasonic pulses," IEEE Transactions on Ultrasonic's, Ferroelectrics and Frequency Control, 55(4), PP: 870-878, 2008.
7. Subhani Shaik and Dr. Uppu Ravibabu, "Detection and Classification of Power Quality Disturbances Using curvelet Transform and Support Vector Machines", 5th IEEE International Conference on Information Communication and Embedded System, 2016.
8. Subhani Shaik and Dr. Uppu Ravibabu "Curvelet based Signal Detection for Spectrum Sensing using Principal Component of Analysis", in the 2nd IEEE International Conference on Engineering and Technology, PP: 917 - 922, 2016.

Published By:
Blue Eyes Intelligence Engineering
& Sciences Publication

Infinitely Variable Valve Lifting

A. Raveendra, K. Sri Noothan Reddy

Abstract*: A new mechanism of Inlet Camshaft with valve lift varying infinitely for Internal Combustion engines is presented. In this, the valve opening and closing is done by a three-dimensional cam or camoid with a translating spherical follower. And the camoid is actuated by a Governor which rotates about a horizontal axis. Also, the design procedure for spring and analytical expressions for Governor are generated. And the design of camoid profile is defended by employing the theory of envelope. A numerical example is given to explain the application of the approach.

Index Choice: camoid, governor, variable valve lifting.

I. INTRODUCTION

CAMSHAFT is an integral part of the Internal Combustion engine which helps the cams to actuate the valves. Valve lift, Duration, Lobe separation, and Timing are the main aspects of a camshaft for better performance or efficiency of an Internal Combustion engine. For an efficient engine, there are some advanced technologies used in the camshaft mechanism like VVT (Variable Valve Timing) and VVL (Variable Valve Lifting). Where VVT is a method which helps to alter the valve opening and closing timing. And VVL is method which helps to change the amount of valve lift. Now every company is manufacturing the vehicles with either one of VVT & VVL technology or both. And they have their own type of VVT or VVL mechanisms.

For example, Honda's I-VTEC (intelligent- Variable valve Timing and Lift electronically control) which gives two or three different values of valve lifts with the help of different sizes of cam lobes and rocker arms. Similarly, AUDI developed a mechanism called AVS (Audi Valve System) also uses different sizes of cam lobes to alter the valve lift depending upon the engine speed. Other companies like BMW and SUBARU had developed new mechanisms of camshaft which uses VVT technology. MULTIAIR is latest technology developed by FIAT, which uses hydraulic pressure to operate the inlet and outlet valves.

In all types of mechanisms which uses VVL technology have two to four stages of valve lift. That means at every stage different size of cam profile will operates the valves. Here, smaller cam favors lower rpm performance, while larger cam favors higher rpm performance. Depending upon the engine speed and load conditions, the interchange between any of two stages i.e., the swap between two cam lobes occurs by an external device. These devices include oil pump, ECU (Electronic Control Unit), screw and nut mechanism, rocker arm and etc... Because of these stages the valve lift is same for a given speed range. That means, same amount of air-fuel mixture enters the combustion chamber and same amount of power produces in that given speed range. After that speed limit, swapping will happens between two cam profiles. And then, the power production rate will increases. The above technology causes a time gap between any of two stages. And this will increase engine pickup time from lower rpm to higher rpm.

This research paper presents a new type of VVL technology for inlet camshaft of the engine, called as Infinitely Variable Valve Lifting. This new mechanism helps the engine to supply more amount of air-fuel mixture for increase in every rpm. So, the power production rate increases and engine pickup time decreases. And the mechanism is an assembly of multiple parts like Camoid, Governor, Solid shaft, Hollow shaft as shown in Fig. 1 below.

Fig 1: Inlet Camshaft Full Link Model

Parts Of Camshaft Mechanism

A. Camoid

Camoids are also known as three-dimensional cams, which have two degrees of freedom i.e., rotation and translation. In the regular cams, the profile is two dimensional and have same amount of valve lift across the surface. But camoids have three dimensional profile with number of valve lifts across the surface along with the minimum and maximum amount of valve lifts. To achieve number of valve lifts and to design camoid profile, we consider a translating spherical follower which gives point contact on camoid surface.

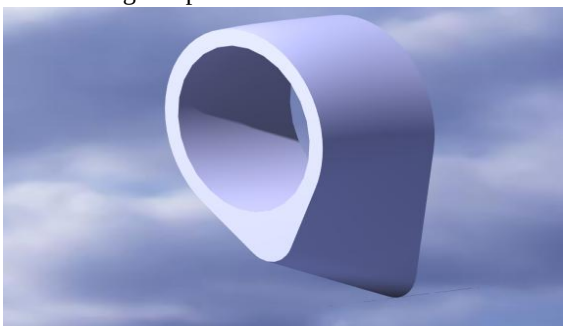

Fig 2: Three-dimensional Cam or Camoid

Revised Manuscript Received on December 28, 2018.

Dr. A. Raveendra, Department of Mechanical Engineering, Malla Reddy Engineering College (Autonomous), Hyderabad, Telangana, India

K. SriNoothan Reddy, Department of Mechanical Engineering, Malla Reddy Engineering College (Autonomous), Hyderabad, Telangana, India

Published By:
Blue Eyes Intelligence Engineering
& Sciences Publication

Design and manufacturing of camoid is complicated. Dhnade and Chakraborthy (1975) gave a unified approach for determining the camoid profile with different types of follower mechanisms. Also, T say and H Wang (1994) derived equations for camoid profile co-ordinates depending on theory of envelope. The theory says that, the contour of a planar cam is regarded as an envelope of family of follower shape curves in different cam- follower positions when cam rotates for a complete cycle.

B. Governor

Fig 3: Governor Assembly

Governor is a self-controlling device. In the Internal combustion engines, governor is used to control the air-fuel mixture supply into combustion chamber depending upon the load and speed conditions of engine. In this mechanism, the main function of governor is to translate the camoid. And here the governor rotates about horizontal axis. It consists of two collars, one is fixed to solid shaft and the other is movable and connected to hollow shaft. The moving collar has keys which guide the collar to translate in keyways on solid shaft. These two collars connected to rotating masses with the help of rectangular bars. These bars are also useful to limit the moving collar. And a spring is placed between two collars for controlling the movement of collar.

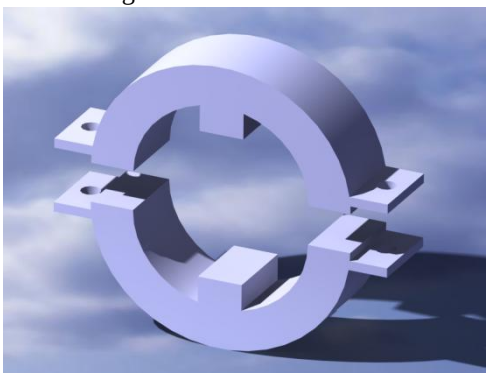

Fig 4: Moving Collar of governor

C. Solid shaft

Solid shaft is central part of total assembly. It helps the camshaft to rotate about its axis. It consists of keyways to translate the governor's collar. And the length of keyways depends on the length of camoid. It also consists of triangular grooves which helps the hollow shaft to translate.

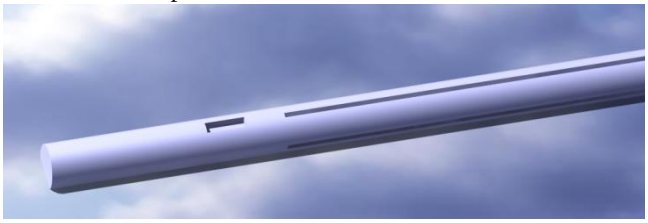

Fig 5: Soli shaft

Fig 6: Hollow shaft

D. Hallow shaft

Hollow shaft consists of camoids which are mounted on it or the shaft can be manufactured along with camoids. One end of shaft is connected to moving collar of governor and the other end is connected along with the solid shaft to engine structure. It also consists of an extended triangular grooves inside the hollow section, which helps to translate on solid shaft.

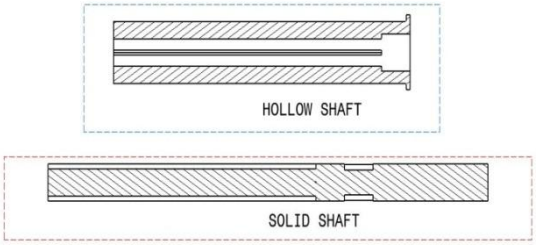

Fig 7: Sectional view of shafts

I. Assembly And Working

First, the hollow shaft and solid shaft are assembled with the help of triangular grooves. Then camoids and bearings are mounted on the hollow shaft (if they are separate). Now the governor is assembled by fixing the collar on the solid shaft. The other collar which is movable is placed in the key ways on solid shaft. And a spring is attached in between collars to control the moving collar even at rest position. Then two collars are connected by rectangular bars at pivot. And the other end of rectangular bars are connected to rotating masses. The connection should be like that, the masses are always in same plane or axis. Now the moving collar is connected to hallow shaft with the help of bolt joint. If collar slides in its keyways, it also translates the hollow shaft. Now one end of solid shaft is connected to gear drive or chain drive from crankshaft. And the other end of solid shaft and hollow shaft are connected to engine structure with the help of bearings.

If the engine starts, the crankshaft will rotate the camshaft with the help of solid shaft. And the valve opening and closing is done by camoid and spherical follower, where the valve lift is minimum. At this time. The whole assembly of camshaft is only in rotating motion. The speed of engine will increases by time, because the power production in every cycle is always higher than required even at minimum valve lift condition. When the engine reaches a certain speed, where the centrifugal force of rotating masses equals the compressive load of spring on collar, then translating motion starts to takes place in camshaft assembly.

Published By:
Blue Eyes Intelligence Engineering
& Sciences Publication

Then the moving collar translates in the keyways on solid shaft and also helps the hollow shaft to translate. That means the camoid also starts to move and this will change valve lift continuously. So, more amount of air-fuel mixture enters the combustion chamber and hence more power will be produced. This is continuous process from the minimum rotating speed at which collar starts to translate to the maximum rotational speed. That means, for increase in every rpm the valve lift is more than prior condition.

As described earlier, the length of keyways on solid shaft must be equal to length of camoid. If not, the camoid exceeds the translating axis of the follower. And the maximum valve lift also depends upon camoid length. That means, the rotating speed of camshaft may increase even there is no translating motion in assembly.

Now, in case of deceleration process the engine has to reach its minimum valve lift i.e., lower speed conditions as quickly as possible. Here, the spring helps the assembly to reach its minimum conditions. If the engine speed reduces, the centrifugal force by rotating masses will also reduce. This will release the compressive load of spring on collar. Hence the sleeve translates away from the fixed collar so that the minimum amount of valve lift should takes place.

II. Design Procedure For Camshaft

A. Governor

Let N be the rotational speed of governor and r is radius of rotation of masses, which are connected with rectangular bars of length l. And $e$will be the distance between axis of rotation and pivot point. As shown in Fig. 8, P is compressive load of spring on collar and θ is the angle made by bars with horizontal axis. And T is tension in rectangular bar.

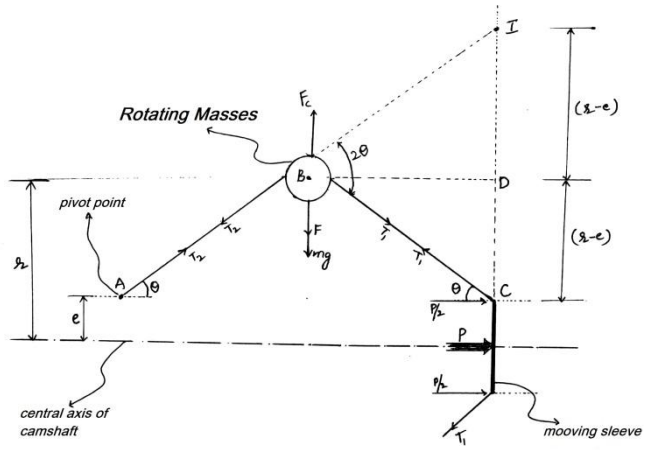

Fig 8:Free body diagram of Governor Link

Governor is always balanced by Control Force (F) which is a function of radius of rotation. Fig. 8 gives the free body diagram of governor link.

A. Taking moment about I;

$M_I = 0$

F. (BD) = mg. (BD) + T_1. (IB.sin 2θ)

$F = mg + T_1 . [\frac{IB}{BD}].[\sin 2\theta]$

$\because \frac{IB}{BD} = \frac{1}{\cos\theta}$

$F = mg + T_1 . [\frac{1}{\cos\theta}]. [2.\sin\theta \cos\theta]$

$F = mg + T_1 . (2.\cos\theta.\tan\theta)$

Now horizontal forces acting on sleeve;

2. $T_1.\cos\theta = P$

$\therefore F = mg + P.\tan\theta$ ..... (1)

But control force is function of 'r', therefore from Fig 8;

$\therefore \tan\theta = \frac{r-e}{\sqrt{l^2-(r-e)^2}}$

$\therefore F = mg + P.[\frac{r-e}{\sqrt{l^2-(r-e)^2}}]$ ..... (2)

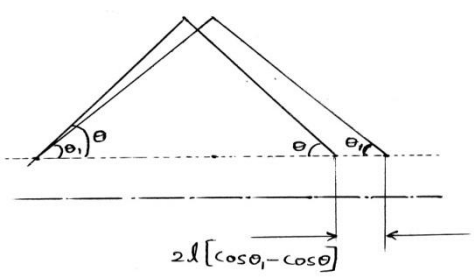

Fig 9 :Distance covered by moving collar

Where, P is the sum of initial load before sleeve moment and load after sleeve moment.

$P = P_0 + K.[2.l.(\cos\theta_1 - \cos\theta)]$

Where;

K = spring stiffness

θ_1 = angle between links and horizontal axis at radius of rotation 'r_1'

θ = angle between links and horizontal axis at radius of rotation 'r'

P_0 = initial spring force on sleeve

$\therefore P_0 = P$ when $\theta=\theta_1$

And from Fig. 8; $\cos\theta = \frac{\sqrt{l^2-(r-e)^2}}{l}$

$\sin\theta = \frac{(r-e)}{l}$

$\therefore P = P_0 + 2K.[\sqrt{l^2-(r1-e)^2} - \sqrt{l^2-(r-e)^2}]$ ... (3)

Now we apply Equilibrium condition where the control force will be equal to centrifugal force (F_C). Also it helps to find out radius of rotation at any given rotational speed. And Fig. 10 shows characteristics of control force with respect to radius of rotation.

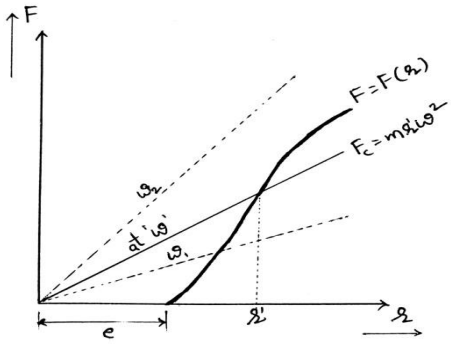

Fig10: Relation between Control force and radius of rotation

Published By:
Blue Eyes Intelligence Engineering
& Sciences Publication

□ Centrifugal Force (F_C) = Control Force (F)…… (4)

Since Centrifugal force; $F_C = mr\omega^2$ ..... (5)

$mr\omega^2 = mg + P.\tan\theta$

$mr\omega^2 = mg + P.[\frac{r-e}{\sqrt{l^2-(r-e)^2}}]$ [□ form eq. (3)]

$mr\omega^2 = mg +$

$[\ P_0 + 2K.\ [\ \sqrt{l^2-(r1-e)^2}\ -\ \sqrt{l^2-(r-e)^2}\ ]\ ]\ [\frac{r-e}{\sqrt{l^2-(r-e)^2}}]$

B. Spring

Let us consider a spring which is compressed initially of length X and stiffness K. The spring wire diameter is d where spring coil diameter is D. And P be the compressive load developed in spring.

(a).Spring load:

From the equation (1), by neglecting the weight of rotating masses;

$F = P.\tan\theta$…….. (6)

By equating (5) & (6); $mr\omega^2 = P.\tan\theta$

□ Initial spring load**;** $P_1 = \frac{mr_1\omega_1^2}{\tan\theta_1}$

And Final or maximum spring load;$P_2 = \frac{mr_2\omega_2^2}{\tan\theta_2}$

(b).Stiffness of spring:

□ $K = \frac{P_2-P_1}{X_1-X_2}$

Where $(X_1 - X_2)$ = [2.l. ($\cos\theta_1$-$\cos\theta_2$)]

(c).Torsional moment of spring:

□ $M_t = f_s.\frac{\pi d^3}{16}.\frac{1}{\sigma}$

And $M_t = \frac{P_2.D}{2}$

Where; σ = stress concentration factor = $\frac{4S-1}{4S-4} + \frac{0.615}{S}$

S = spring index = $\frac{D}{d}$

(d).Deflection of spring:

□ $\delta = \frac{8.F.S^2.Z}{C.d}$

And $\delta = \frac{load}{stiffness}$

Where; Z = number of effective coils

$F = P_2 - P_1$

C = rigidity of modulus

d = diameter of spring wire

(e).Maximum deflection:

□ $\delta_{max} = \delta.[\frac{P_2}{P_2-P_1}]$

(f). Free length of spring:

□ Free length = $[(Z^1 - 1).g^1] + [Z.\ d] + \delta_{max}$

Where; Z^1 = total number of coils

g^1 = gap between each coil of spring

(g). Initial compression of spring = $\frac{P_1}{K}$

C. Camoid

In this design of camoid, we are going to use the design approach derived by M.T. Say and H. Wang by using Theory of Envelope. Let us consider S_1 be amount of valve lift which is function of camoid displacement S_2 and angle of rotation $\emptyset_2$ of camoid.

$S_1 = S_1\ (\emptyset_2, S_2)$…… (7)

Now, from theory of envelope, a family of surfaces of follower with two independent parameters of camoid for different positions can be expressed as;

$f\ (x, y, z, \emptyset_2, S_2) = 0$

And the co-ordinates of camoid can be obtained by eliminating the parameters $\emptyset$& s from equation (10) with the help of partial differentiation.

□ $\frac{\partial f}{\partial \emptyset_2} = 0$ …… (8)

$\frac{\partial f}{\partial S_2} = 0$ …….. (9)

Therefore by solving Eq. (8) and (9), we have (X, Y, Z) co-ordinates for camoid surface with translating spherical follower as;

$X = A\cos\emptyset_2 \pm \frac{r[B.\sin\emptyset + A.\cos\emptyset]}{\sqrt{A^2+B^2+A^2C^2}}$

$Y = -A\sin\emptyset_2 \pm \frac{r[B.\cos\emptyset + A.\sin\emptyset]}{\sqrt{A^2+B^2+A^2C^2}}$ }…… (10)

$Z = -S_2 \pm \frac{r.A.C}{\sqrt{A^2+B^2+A^2C^2}}$

Where A = (a+S_1)

B = $\frac{\partial S_1}{\partial \emptyset_2}$

And C = $\frac{\partial S_1}{\partial S_2}$

D. Valve lift

Below method of approach gives the values of valve lift, if the camoid surface is generated. From the Fig. 11 the total length of camoid is X and the distance between top and bottom surfaces at point of contact will be L_1 at minimum end and L_2 at maximum end.

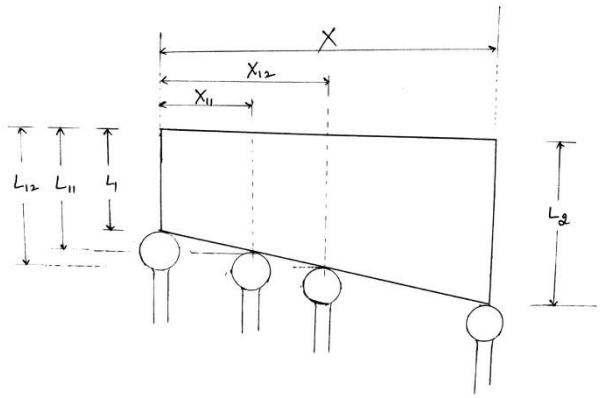

Fig 11: Point contact between camoid and follower

And L_{11}= distance b/w surfaces at next point contact

$L_{11} = L_1 + [(\frac{L2-L1}{X}).X_{11}]$……. (11)

Similarly; $L_{12} = L_1 + [(\frac{L2-L1}{X}).X_{12}]$……etc.

And we have minimum valve lift i.e. 'y'

□ Second valve lift after displacement 'X_{11}';

$y_1 = y + (L_{11} - L_1)$…….. (12)

$y_2 = y + (L_{12} - L_1)$……etc.

Published By:
Blue Eyes Intelligence Engineering
& Sciences Publication

III. EXAMPLE

In this section a numerical example is given, where we will find out rotational speed and valve lift for different radius of rotations. Let us consider a camshaft which has maximum speed (N_{max}) of 3000rpm. And the governor is assembled with the help of rectangular bars of length (l) 100mm at a distance (e) 50mm from the rotational axis. At a radius (r_1) of 100mm and speed (N_1) of 1000rpm, the collar starts to move towards the fixed collar. And the maximum movement of collar (l_C) will be 25mm. This moving will also help the camoid to alter the valve lift in between 12.75mm and 19.05mm. Camoid will rise in $0^0 - 85^0$ and in $95^0 - 180^0$ also Dwell in $85^0 - 95^0$.Also consider the weight of rotating masses as 9.8N and spring coli diameter as 40mm.

SOLUTION:

(A).First we have to calculate positions of rectangular bars and rotating masses

; $\tan\theta_1 = \frac{r_1 - e}{\sqrt{l^2-(r_1-e)^2}} = \frac{100-50}{\sqrt{100^2-(100-50)^2}} = 0.57$

$\therefore\ \boldsymbol{\theta_1} = 30^0$

; l_C = [2.l. ($\cos\theta_1$-$\cos\theta_2$)]

$\therefore\ \boldsymbol{\theta_2}$ (or) $\boldsymbol{\theta_{max}} = 42.2^0$

; $\tan\theta_2 = \frac{r_2 - e}{\sqrt{l^2-(r_2-e)^2}}$

; $\tan 42.2^0 = \frac{r_2-50}{\sqrt{100^2-(r_2-50)^2}}$

$\therefore\ \boldsymbol{r_2}$ = 117.26 mm (i.e., maximum radius of rotation)

(B).Design of spring:

 Initial spring load; $P_1 = \frac{m r_1 \omega_1^2}{\tan\theta_1}$ = 1899.02 N [$\omega = \frac{2\pi N}{60}$]

Similarly Maximum spring load;

$P_{max} = \frac{m r_{max}\ \omega_{max}^2}{\tan\theta_2}$ = 11871.8 N

 Stiffness of spring; $K = \frac{P_2 - P_1}{X_1 - X_2} = \frac{11871.8 - 1899.02}{25}$

$\therefore \boldsymbol{K}$ = 398.912 N/mm

And we have Deflection; $\delta = \frac{8.F.S^2.Z}{C.d}$

Since $\delta = (X_1 - X_2)$ = 25mm

Consider S= spring index= 6

; $d = \frac{D}{S} \cong 7$ mm

$F = (P_{max} - P_1)$ = 9972.78 N

No. of effective coils (Z) = $\frac{\delta.C.d}{8.F.S^2}$ = 5.11

 $\boldsymbol{Z} \cong \mathbf{5}$

 Free length of spring = $[Z.\ d] + \delta \cong$60mm

 Initial compressed length = $\frac{P_1}{K}$ = 4.76 mm

(C).Now we have to calculate the rotational speed of camshaft at radius of rotation 'r_2 =117.26mm'.

From equilibrium condition i.e. from Eq. (4)

$m r_2 {\omega_2}^2$ = mg+

[P_0 + 2K. [$\sqrt{l^2-(r_1-e)^2}$ - $\sqrt{l^2-(r_2-e)^2}$]][$\frac{r_2-e}{\sqrt{l^2-(r_2-e)^2}}$]

$\boldsymbol{\omega_2}$ = 281.59rad/sec

 $\boldsymbol{N_2}$ = **2849 rpm**

Therefore at;

r_2=100mm	N=1000rpm	l_C =0mm	y=12.75mm
r_2=102mm	N=1215rpm	l_C =2.4mm	y=13.36mm
r_2=110mm	N=2246.28rpm	l_C =13.2mm	y=16.72mm
r_2=115mm	N=2689rpm	l_C =21.22mm	y=18.18mm
r_2=117.6mm	N=2849rpm	l_C =25mm	y=19.17mm

Where; $P_0 = P_1$ =1899.02 N

r_1 = 100 mm

l_C = [2.l. ($\cos\theta_1$-$\cos\theta_2$)]

=2.l. [$\frac{\sqrt{l^2-(r_1-e)^2}}{l}$-$\frac{\sqrt{l^2-(r_2-e)^2}}{l}$]

$y_1 = y + (L_{11} - L_1)$ (from eq. (12))

$L_{11} = L_1 + [(\frac{L2-L1}{X}).X_{11}]$ (from eq. (11))

From the results, it is shown that, for different values of r we can find out the rotating speed N of camshaft.

When masses rotates at maximum radius i.e., 117.6 mm, they reach a speed of 2849 rpm with a valve lift of 19.17 mm.

But the maximum speed of camshaft is 3000 rpm. Even though the valve lift is same in speed range of 2849-3000 rpm. And the value of can be determined by using Uniform acceleration and retardation diagram (same as regular cam profiles) with the help of given values of lift, rise, and dwell.

REFERENCES

1. NitinSubhash Sable, Rahul KrishnajiBawane "*I-VTEC: Intelligent - Variable Valve Timing & Lift Electronic Control - A Review*" IJSRD/Vol. 5/Issue 01/2017/160) //ISSN (online): 2321-0613.
2. BMW's VANOShttp://www.bmw.com.kh/asia/en/insights/technology/technology_guide/articles/vanos_double_vanos.html?source=index&article=vanos_double_vanoshttps://en.wikipedia.org/wiki/VANOS https://us.autologic.com/news/bmw-vanos-system
3. Subaru's AVCS and AVLS - https://en.wikipedia.org/wiki/Active_valve_control_syste. https://web.archive.org/web/20120624171722/http://drive2.subaru.com/Spring07_whatmakes.htm
4. Huber, R., Klumpp, P., and Ulbrich, H., "*Dynamic Analysis of the Audi Valve lift System*," SAE Int. J. Engines 3(1):839-849, 2010.https://doi.org/10.4271/2010-01-1195.https://www.audi-technology-portal.de/en/drivetrain/fsi-tsi-engines/audi-valvelift system_en.
5. Toyota's VVT-I and Valvematic - http://www.toyotaglobal.com/innovation/environmental_technology/technology_file/https://en.wikipedia.org/wiki/VVT-i
6. Bernard, L., Ferrari, A., Micelli, *et.al*, "*Electro-hydraulic valve control with multiair technology*" ATZ Worldw (2009) 70: 4. (ISSN 2192-9114). https://doi.org/10.1007/BF03226988
7. Porsche Variocacm - http://www.porscheengineering.com/filestore.aspx/default.pdf?pool=peg&type=download&id=service-engine-case-02-2005&lang=en&filetype=default
8. Seinosuke Hara, Seiji Suga, Makoto Nakamura, "*Variable Valve Actuation Systems for Environmentally Friendly Engines*".
9. MajoCecur, Eaton Corporation, "*Fully Variable Valve Train*" United States Patent No: US 6,659,053 B1, Dec. 9, 2009.
10. Chakraborthy. L &Dhande S.G, "*A Unified approach to the analytical design of three-dimensional cam mechanisms*", February- 1975, ASME.
11. M. Tsay& G.S. Hwang, "*Applications of Theory of envelope to determination of camoid profiles with translating follower*", 320/Vol. 116, March-1994, ASME.
12. AmisthabhaGhosh and AsokkumarMallik, "*Theory of Mechanisms and Machines" , 3rded., 2006 by East West Press publications*, ISBN:9788185938936
13. S. Md. Jalaudeen, "*Design Data Handbook*", 2004, Anuradha publications, ISBN: 9788187721628.

Published By:
Blue Eyes Intelligence Engineering
& Sciences Publication

IV. APPENDIX

In this section an example is illustrated to design a three-dimensional camoid as in T say and H wang (1994). Let us consider, Normal distance between follower and camoid centers (a) as 10 cm and Length of camoid (l) 20 cm and Radius of spherical follower (r_S) 1 cm.

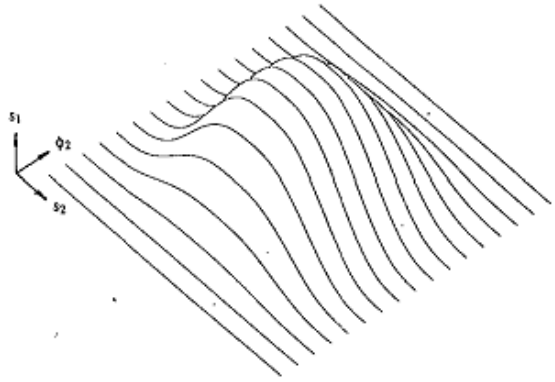

Fig12: Follower motion program

And the motion program of spherical follower is assumed to be given as,

$S_1 = S_1\ (\emptyset_2, S_2);\ 0 \le \emptyset_2 \le 2\pi\ \&\ 0 \le S_2 \le 20$

$S_1 = [\frac{\emptyset_2}{\pi} - \frac{1}{2\pi} . \sin 2\emptyset_2]\ [\frac{S_2}{10} - \frac{1}{2\pi} . \sin\frac{\pi S_2}{5}]$

$= [\frac{\emptyset_2}{\pi} - \frac{1}{2\pi} . \sin 2\emptyset_2]\ [\frac{20-s_2}{10} - \frac{1}{2\pi} . \sin\frac{\pi(20-S_2)}{5}]$

$= [\frac{2\pi-s_2}{\pi} - \frac{1}{2\pi} . \sin(2(2\pi - \emptyset_2))]\ [\frac{S_2}{10} - \frac{1}{2\pi} . \sin\frac{\pi S_2}{5}]$

$=[\frac{2\pi-s_2}{\pi} - \frac{1}{2\pi} . \sin(2(2\pi - \emptyset_2))]$

$[\frac{20-s_2}{10} - \frac{1}{2\pi} . \sin\frac{\pi(20-S_2)}{5}]$

And the Fig. 12 shows the graphical representation of above equation. Therefore by applying analytical Eq. 10 to above motion program of follower we get the camoid profile as shown in Fig. 13.

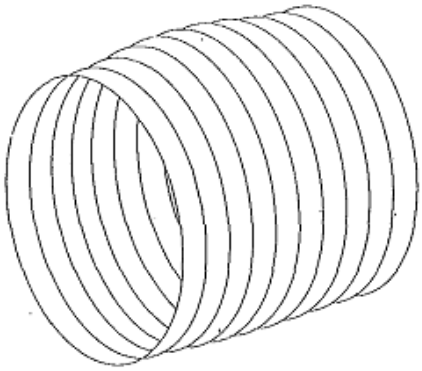

Fig 13: Camoid profile by theory of envelope for above motion program

Published By:
Blue Eyes Intelligence Engineering
& Sciences Publication

Design and Analysis of Leaf Spring for Heavy Weight Vehicles using Composite Materials

A. Raveendra, Mohammed Abdul Mubashir

Abstract*: At present, we can find numerous leaf springs made up of steel which are utilized for the purpose of suspension of light weight to heavy weight vehicles. It is discovered that the conventional leaf springs and unsprung weight to the vehicle and diminishes its fuel efficiency. Since the composite materials are the advanced materials with higher strength to weight ration and higher corrosion resistance, they are found as the potential substitutes for these traditional metallic leaf springs. In this paper composite materials like E-Glass epoxy, S-glass epoxy, carbon fibre reinforced polymer and kelvar are used against the conventional steel for heavy weight vehicles with the objective to minimize the weight of the vehicle. Modelling of the spring is done in CATIA and analysis is carried out in ANSYS.

Index Choice: E-Glass epoxy, S-Glass Epoxy, Carbon fiber reinforced polymer, kelvar, steel leaf spring, catia and ansys

I. INTRODUCTION

Leaf spring:

A leaf spring or laminate spring (also called as flat spring or carriage spring) is a spring which is composed of a number of plates of different lengths (also called as leaves) held together by means of clamps and bolts as shown in figure 1.

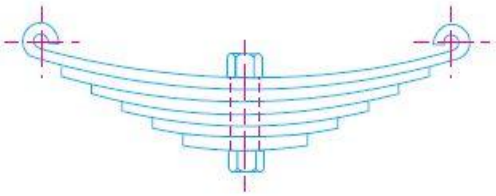

Fig 1: leaf spring

These are mostly used in automobiles. The significant stresses created in leaf springs are tensile and compressive stresses. In addition to impact loads, leaf springs can carry lateral loads, braking torque and drive torque etc.

Manufacturing Process:

The following are the steps to make a leaf spring:

1. A flat bar is cut into various lengths. After cutting these pieces are rapidly heated at the ends. Computerized machinery rolls and stretches the pieces to a tapered profile.
2. Next, its into a pressing machine which trims the stretched ends and punches holes which are used for its assembly.
3. The heated tip of the main leaf is fed into a machine that wraps it around a die form, this creates an eye mount for attaching the spring to the vehicle. Similarly, one more eye mount is created on the other side.
4. After making the eye mount all the leaves including the master leaf are heated and are individually bent to correct arc radius. While still clamped between the bending tool each leaf is quenched in oil so as to obtain high strength and correct shape.
5. Once the leaf comes out of the oil it is very much brittle i.e., it will break easily. So, it has to be tempered.
6. After tempering shot peening is done so that the surface tension of the metal is changed which further increases its strength.
7. Leaves are then assembled by a hydraulic mechanism for precise alignment. Assembling is done by means of round clips, centre bolt.

Types Of Leaf Spring:

Table 1 below shows the type of leaf springs that are generally used.

Elliptic	
Semi-elliptic	
Three quarter-elliptic	
Quarter-elliptic	
Transverse	

Table 1: Types of leaf spring

Revised Manuscript Received on December 22, 2018.

A. Raveendra, Associate Professor, , Department of Mechanical Engineering, Malla Reddy Engineering College, Secunderabad, Telangana

Mohammed Abdul Mubashir, PG Student, Department of Mechanical Engineering, Malla Reddy Engineering College, Secunderabad, Telangana

II. LITRETURE SURVEY

[1] R.L. Daugherty published a book called "Application of composite materials to truck components" in which he examined a hybrid leaf spring and a propeller shaft which employed graphite-epoxy tubes with adhesively bonded steel end sleeves in order to develop lightweight experimental truck components. the result of his work is the hybrid design of leaf spring i.e., a spring made from the combination of steel leaves and composite leaves (fiberglass-epoxy leaves) which delivered the most cost-effective solution.

[2] Mono composite leaf spring for light weight vehicle, a paper by S Viyayrangan et al analysed a single leaf with variable thickness and width for the purpose of constant cross-section are. The outcomes demonstrated that the spring width is decreasing in hyperbolic manner and thickness is increasing linearly from the spring eyes towards the axle seat. Furthermore, the composites spring is having 85% lesser weight than that of conventional spring. The stresses and deflection obtained from the ansys were verified with analytical and experimental values.

[3] Fatigue design of leaf springs for new generation trucks by E Giannakis et al focusses on the effect of the manufacturing process of leaf spring on its performance under fatigue loading. The analysis of the micro structure and the mechanical properties of the core and the surface of the samples (prototype) reveals the deterioration of the mechanical properties of the surface due to the manufacturing process applied. The results of this investigation have been utilized as the input for analytical calculations to determine the fatigue life. The design of the mono leaf spring has been optimized and used for the stress calculations through FEA, as well as tested in constant and variable amplitude loading. The comparison between the theoretical, experimental curves and the fatigue lives seems to produce a satisfactory agreement.

[4] K. Murli, M. Gembiram et al published a paper called "Design and analysis of multi leaf spring using composite materials" which analysed a leaf spring of commercial vehicle which comprises of five graduated leaves and a full-length leaf. In this paper static structural and harmonic analysis is done for steel leaf spring and a glass fiber leaf spring. Substantial weight loss is observed which intern resulted in increased fuel efficiency. Also, there's a reduction in deformation, stress, strain which makes the spring life longer.

[5] Design and material optimization of heavy vehicle leaf spring by E VenkateshwaraRao et al examined a leaf spring consisting of 9 leaves. Static and dynamic analysis has been carried out for both steel leaf spring and composite leaf spring made from glass fiber reinforced polymer and kelvar. By observing modal analysis, it is found that the vibrations produced in the composite leaf springs are lesser than that of steel leaf spring. Suggested material for a leaf spring is the epoxt matrix composite reinforced by 50% kelvar fibers since it has less weight, frequency and stresses compared to that of steel leaf spring.

[6] TharigondaNiranjanBabu at al presented a paper on design and analysis of leaf spring with composite materials which studied a multiple leaf spring that includes seven leaves in which one is of full length. It is found that conventional leaf spring is 5.5 times heavier that the jute E-glass epoxy leaf spring.

[7] Dr. SuwarnaTorgal et al worked on multiple leaf spring having twelve leaves which comprises of five full length leaved and seven graduated leaves used in heavy commercial vehicle. Materaials which are used in this analysis are steel, Ti6Al4V alloy, S-glass fiber composite. The results obtained showed that the strength to weight ratio is more than that of steel and Ti6Al4V alloy spring is two times less in weight when compared to steel leaf spring.

[8] A Manivannam et al published a paper "Design and parametric optimization of heavy duty leaf spring" which analysed a leaf spring consisting of fourteen number of leaves comprised of 11 graduated leaves and 3 full length leaves used in medium segment heavy weight vehicles. With a vision to improve fatigue strength (which can be increased by decreasing the shear stress induced in the spring the spring is analysed with 9 different parameters. The p parameters are the orthogonal arrays. The available orthogonal arrays are L4, L8, L9, L12, L16, L18, L20, L27 and L32. Out of which L9 has given the suitable outcome.

[9] Research article named "Fatigue life assessment of 65Si7 leaf spring by Vinkel Kumar Arora provides 4 alternate methods for predicting the fatigue life of a leaf spring. The first is called the SAE spring design manual approach in which the intersection of maximum and initial stress gives the fatigue life. The second is the graphical approach which employs modified Goodman's Criteria. In the third one, codes are composed in FORTRAN to evaluate the fatigue based on analytical techniques. The fourth strategy comprises of computer aided engineering tools.

III. OBJECTIVES AND METHODOLOGY OF THE WORK

Objectives:

The main objectives of this project are:

1. Optimize the design of the leaf spring.
2. Compare the deformation, stresses, strain and strain energy stored of both the steel leaf spring and the composite leaf spring.
3. Compare the results that will be obtained from FEA with that of analytical results calculated by using the empirical formulae's.
4. Finding out the fatigue life for both the steel and composite leaf springs.

The above-mentioned objectives are done to achieve the following:

a. Substantial weight reduction which interns enhances the fuel efficiency.
b. Increase the strength which results in increment of fatigue life of the leaf spring.

Methodology Followed

The above-mentioned objectives can be accomplished by performing the following steps:

Published By:
Blue Eyes Intelligence Engineering
& Sciences Publication

1. Optimization can be achieved by changing the design parameters such as length, thickness or the width of the leaf spring.
2. 3D model of the leaf spring can be obtained from CATIA V6 and is analysed
3. Analysing is will be carried out in ANSYS and the results obtained for Composite Leaf Spring (CLS) and Steel Leaf Spring (SLS).
4. Fatigue life and analytical results can be calculated by using empirical formulae.

IV. MATERIALS AND THEIR PROPERTIES

The mechanical properties of the materials used is shown in the table 2 given below

Parameter	Steel	CFRP	E-Glass Epoxy	S-Glass Epoxy	Kelvar
Density (g/cm^3)	7.85	1.62	1.97	2	1.38
Youngs modulus (MPa)	$2.1X10^5$	$1.69X10^5$	41000	45000	80000
Poisons ratio	0.3	0.31	0.28	0.29	0.34
Ultimate strength(MPa)	460	2280	1140	1725	1400
Yield strength(MPa)	250	1140	570	862.5	700

Table 2: Material Properties

The composite materials used are typical unidirectional composites.

V. DESIGN PARAMETERS

Terms like datum line, effective length, span, camber, nip etc., are named as the design parameters.

Datum line: The line which passes through he focal point of the eyes is called the datum line.

Span: Distance between the centres of the eyes is referred as span or overall length.

Effective length: Length obtained by subtracting band width from span is called as effective length.

Camber: In order to obtain the strengthening effect while the spring is loaded, an initial curvature is given to the leaves. This initial curvature is called as camber.

Nip: To use the material of the spring to the maximum extent greater radius of curvature is given to the master leaf as compared to graduated leaves. This creates a gap in between the leaves this gap is called as nip which is represented as C in the figure 2 shown below.

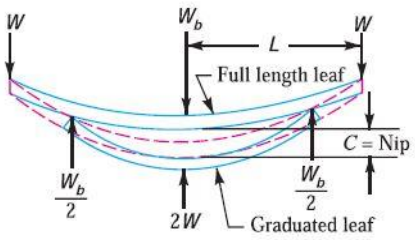

Fig 2: Representation of nip in a leaf spring.

VI. THEORITICAL APPROACH

For a multiple leaf spring maximum bending stress is given as

$$\sigma = \frac{6WL}{nbt^2}$$

Deflection can be written as

$$\delta = \frac{6WL^3}{nEbt^3} = \frac{\sigma L^2}{Et}$$

Stiffness of the spring is given by

$$k = \frac{8nEbt^3}{3L^3}$$

Where, W is the Load (N).
L is the effective length (mm).
N is the number of leaves.
b is the width of the leaves (mm).
t is the thickness of the leaves (mm).
E is young's modulus (MPa).

Also, the load carried out in full length leaves is written as $W_F = \left(\frac{3n_F}{3n_F+2n_G}\right)W$ and

Load carried by graduated leaves is

$$W_G = \left(\frac{2n_G}{3n_F+2n_G}\right)W$$

Where, n_F is the number of full length leaves.
n_G is the number of graduated leaves.

Fatigue life can be predicted analytically by using the relations given by Hwang and Han (1986) which is written as

$$N=\{B(1-r)\}^{1/C}$$

Where,
N is the number of cycles a leaf spring can withstand without failure.
B is the constant=10.33
C is also a constant=0.14012
r is the applied stress level

$$r = \frac{maximum\ \ stress}{ultimate\ \ strengt\ h}$$

VII. SPECIFICATION OF LEAF SPRING

The specification of the modelled leaf spring is
Number of leaves, n = 14
Number of full length leaves, n_F= 3
Number of graduated leaves, n_G= 11
Camber, y= 210 mm
Width of the leaves, b= 80 mm
Thickness of the leaves, t= 12mm

S.No	Length of the leaves (mm)
1	362
2	439
3	516
4	593
5	670
6	748
7	825
8	902
9	979
10	1056

11	1133
12	1537
13	1537
14	1537

Table 3: length of the leaves.

Table 3 shows the length of the leaves which are used in modelling

VIII. MODELLING

The leaf spring has been modelled in CATIA V6 R20, it has lots of features available that enable the users to model any part without any difficulties. Some features of Catia which are used in this work are pad – this extrudes the sketch drawn, shaft – this will add material with refence to axis rotation, groove – this is similar to shaft but it removes the material, axis constraint – as the name itself says that it adds a constraint to axis for restricting the rotation while assembling, face to face constraint.

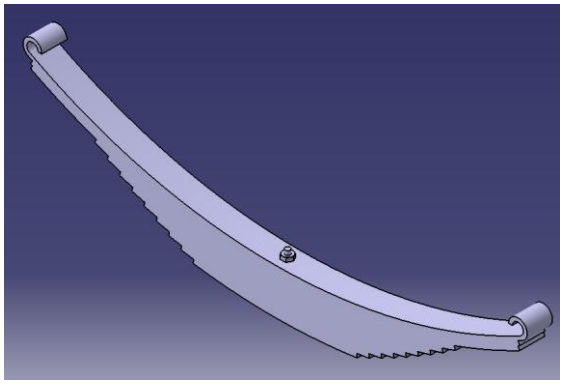

Fig 3: model of the leaf spring

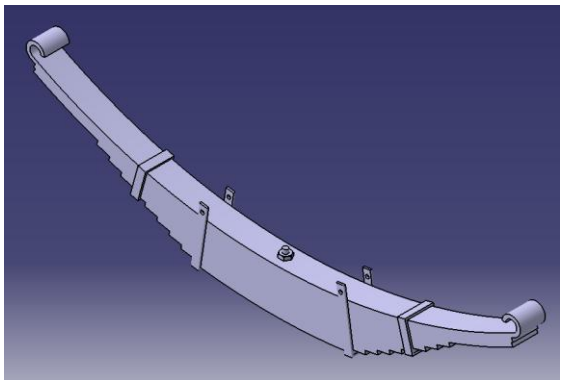

Fig 4: assembled leaf spring

Figure 3 depicts the model of leaf spring that will be imported into the ANSYS and analysed.

While figure 4 shows the leaf spring which is assembled by means of centre bolt and two types of rebound clips (rectangular rebound clip and square end rebound clip).

IX. ANALYSIS OF LEAF SPRING

The leaf spring has been analysed using ANSYS 14.5. Firstly, the model shown in figure 3 is converted to IGES format and then imported in Ansys for static structural analysis. The steps involved in it are as follows:

1. Open ANSYS workbench, in the analysis systems toolbar double click on static structural.
2. In engineering data give the properties of material. Import the desired model.
3. After importing, mesh the model and apply the boundary conditions and the load.
4. In the solution tool bar insert total deformation, equivalent von-mises stress, equivalent von-mises strain, shear stress and strain energy.
5. Click on solve button to get solution for the above-mentioned parameters.

Boundary Conditions:

1. One of the eye end of the leaf spring is fixed. That means this end is rigidly connected to the axle of the vehicle.
2. The other eye end is set to free in horizontal direction. This justifies that the spring will be straighten when load is applied.
3. The load is applied at the master leaf of the spring.

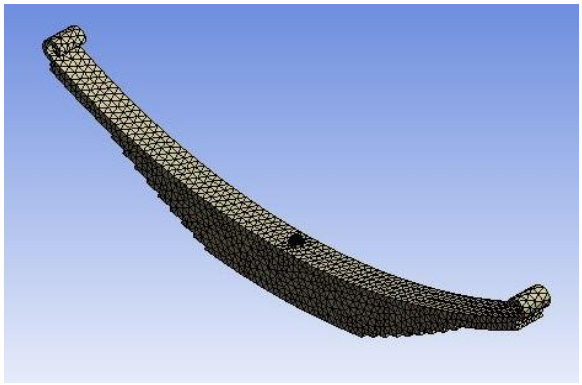

Fig 5: Meshed leaf spring model

The above figure 5 shows the leaf spring on to which triangular meshed has been done with an element size of 5.

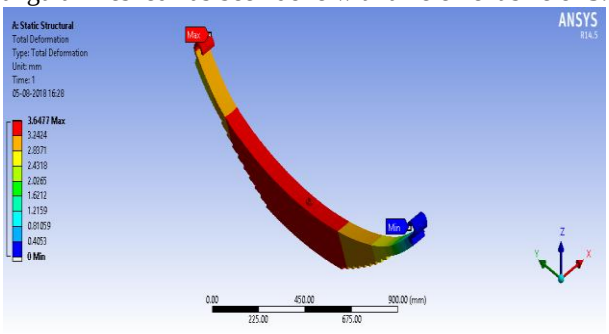

Fig 6: Deformation

Figure 6 shows the total deformation induced in the leaf spring. Maximum shear stress is occurred at one of eye ends which is represented by red label in figure 6.

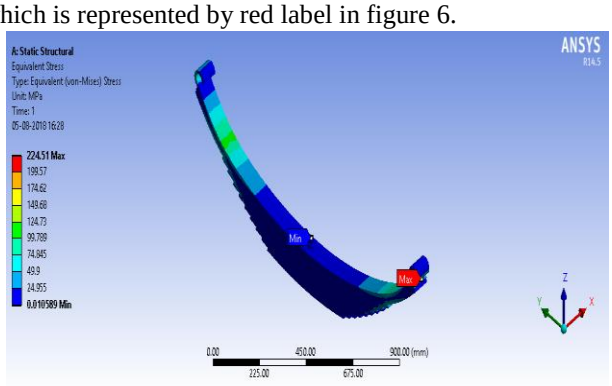

Fig 7: Stress

Published By:
Blue Eyes Intelligence Engineering
& Sciences Publication

The above figure 7 shows the equivalent stress induced in the spring. Maximum shear stress occurs at one of the eye ends.

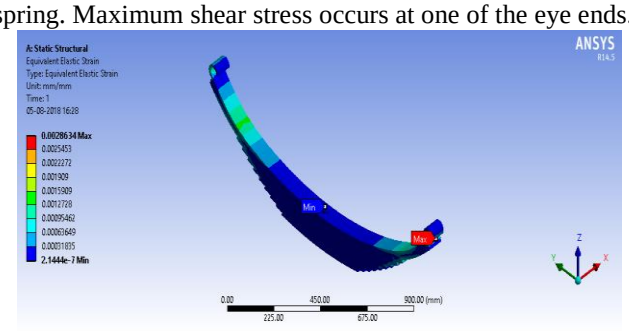

Fig 8: Strain

Figure 8 shows the strain which is also maximum at one of the eye ends.

X. RESULT AND DISCUSSION

Material	Deformation (mm)	Stress (MPa)	
		Min	Max
STEEL	1.4625	0.0089	221.35
CFRP	1.7298	0.0092	222.05
E-GLASS EPOXY	7.1409	0.0083	220.12
S- GLASS EPOXY	6.5062	0.0083	220.12
KELVAR	3.6477	0.0105	224.51

Table 4: Equivalent stress and deformation

The above table 4 shows the stress and deformation for both the steel leaf spring and composite leaf spring. The theoretical stress which is obtained from empirical formula is 400MPa. Hence the Ansys results can be justified since it has the stress value less than that of theoretical values.

Materials	Strain		Strain energy (MJ)
	Minimum	Maximum	
STEEL	$0.77236X10^{-7}$	0.00112	44.54
CFRP	$0.93986X10^{-7}$	0.00134	72.33
E-GLASS EPOXY	$3.5699X10^{-7}$	0.00547	220.02
S-GLASS EPOXY	$3.2507X10^{-7}$	0.00499	200.47
KELVAR	$2.1444X10^{-7}$	0.00286	107.81

Table 5: strain and strain energy for both steel and composite leaf spring.

Table 5 shows the equivalent von-mises strain and strain energy stored in the leaf spring.

Material	Deformation (mm)	
	Before Optimization	After Optimization
STEEL	1.4625	---
CFRP	1.7298	1.6291
E-GLASS EPOXY	7.1409	6.7248
S-GLASS EPOXY	6.5062	6.127
KELVAR	3.6477	3.4354

Table 6: Comparison of deformation before optimization and after optimization.

By undergoing trial and error process it is found that the design is best optimized by increasing the width of the leaf spring by 5 mm. Table 6 shows the comparison of deformation before and after optimization.

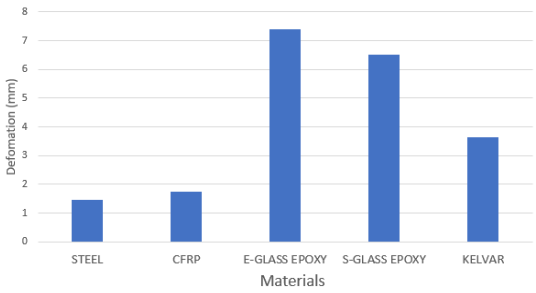

Fig 9: comparison of materials based on deformation

Figure 9 demonstrates the variation of deformation for composite leaf spring and steel leaf spring. From the graph it is clear that the maximum deformation occurs in E-Glass epoxy because it has lesser young's modulus as compared to other materials.

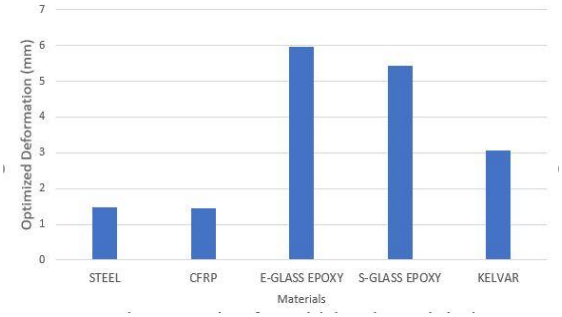

Fig 10: comparison of materials based on optimized deformation.

Figure 10 shows the variation of optimized deformation for both the steel leaf spring and composite leaf spring. From figure 10 it is obvious that the maximum deformation occurs in E-Glass epoxy because it has lesser young's modulus compared to other materials.

Material	Number of cycles to failure
STEEL	603419
CFRP	8143497
E-GLASS EPOXY	3513571
S-GLASS EPOXY	6393445
KELVAR	4977041

Table 7: Fatigue life of the steel and composite leaf spring.

From table 7 it is observed that the fatigue life of the steel leaf spring is very much less than that of composite leaf spring.

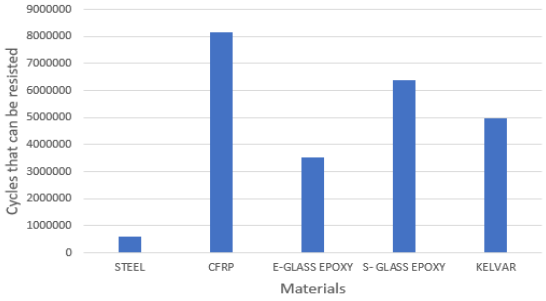

Fig 11: Graphical representation of fatigue life.

Published By:
Blue Eyes Intelligence Engineering
& Sciences Publication

Figure 11 shows the variation of fatigue life for both steel leaf spring and composite leaf spring. It can be observed that CFRP is having more fatigue life than all materials because it has the highest ultimate strength compared to other materials.

XI. CONCLUSIONS

A leaf spring is designed to resist a load of 23KN. By observing the results, it can be concluded that

1. Kelvar is preferred because it is having 82.42% lesser weight than the steel leaf spring. And also, the deformation is in the range of safe value.
2. By trial and error process, the best possible optimization is achieved by increasing the width of the spring by 5mm.
3. The fatigue life of leaf spring made up of kelvar has 8 times more fatigue life than the steel leaf spring. Hence it cost-effective.

REFERENCES

1. R.L Daugherty, "Application of Composite Materials to Truck Components", *Composite Materials Proceedings of Japan- US Conference Tokyo*, 1981, pp. 529-538.
2. S Vijayarangan, Shiva Shankar, G Siddaramanna, "Mono Composite Leaf Spring for Light Weight Vehicle", *International Journal of Material Science*, Vol 12, 2006, pp. 220-225.
3. E Giannakis, M Malikoutsakis, G Savaidis, "Fatigue Design of Leaf Springs for New Generation Trucks", *International Journals of Structure Integrity*,Vol 161, 2016, pp. 1-9.
4. M Gembiram, R Elayaraja, K Mrali, R Saravanan. K Ganesh, "Design and Analysis of Multi Leaf Springs Using Composite Materials", *International Journal for Research in Applied Science and Engineering Technology*, Vol 2, April 2014, pp. 309-314.
5. E VenkateshwaraRao, T.N.V Ashok Kumar, S.V Gopal Krishna, "Design and Material Optimization of Heavy Vehicle Leaf Spring", *International Journal of Research in Mechanical Engineering and Technology*,Vol 4, April 2014, pp. 80-88.
6. TharigondaNiranjanBabu, P. Bhaskar, S. Moulaali, "Design and Analysis of Leaf Spring with Composite Materials", *International Journals of Engineering Sciences and Research Technology*,Vol 3, august 14, pp. 759-762.
7. SuwarnaTorgal, Shashank Jain, "Simulation of Parabolic Leaf Spring for Heavy Commercial Vehicle Using FEA", *International Journal of Engineering Sciences and Research Technology*,Vol 4, June 2015, pp. 1077-1081.
8. A Mannivanam, G Vasanth, "Design and Parametric Optimization of Heavy Duty Leaf Spring", *International Journal of Engineering and Computer Science*, Vol 4, May 2015, 12216-12223.
9. Isaac M. Daneil, OriIshai, "Engineering Mechanics of Composite Materials", Second Edition, pp. 377.
10. R.S Kurmi, J K Gupta, "A Text Book of Machine Design", pp. 866-879.

Published By:
Blue Eyes Intelligence Engineering
& Sciences Publication

Laboratory Investigations on Expansive Soils with Eggshell Powder

Gayatri Upadhyay

Abstract: ***For any land-based structure, its load is supported by foundation. In order to support the load, soil plays vital role. Clay soils, particularly black cotton soils, shows extreme plastic behavior on increase in moisture. This consequently results in decrease in Engineering properties and more change in volume. These changes results in severe damage of structures, soil improvement is important under such conditions.Soil stabilization helps to overcome the drawbacks of soil. Stabilization of soil can be achieved through several methods ranging from chemical to mechanical stabilization . These methods are quite expensive for developing countries to implement , so the economic way is to use some alternate material which could be industrial or domestic waste. These materials are easily available and their usage can further minimize the problem of their disposals. This paper illustrates the usage of eggshell powder [ESP] as admixture in BC soil to stabilize it and enhance its index properties , compaction characteristics and UCS value.***

Keywords: clayey soil ,esp, plasticity index , ucs.

I. INTRODUCTION

Stabilization of soil means improving its properties so that they are suitable as a construction material. Stabilization of soil is very important in road constructions, foundations, canals etc .Several new techniques of soil stabilization have emerged which focus on effective and green methods.

Black soils are very dark and very fine grained and, contain a good proportion of calcium carbonates and magnesium carbonates. These soil, when wet are exceedingly sticky due to very high plasticity index. Deep and large cracks are formed when the soil dries and contracts. BC soils contain montmorillonite mineral which is the sole reason for the volumetric changes in the soil.

BC soil becomes unfit as foundation material due to low UCS value .Hence , the UCS of soil should be enhanced by stabilizing it . Eggshells contain 95% of $CaCO_3$, this composition is quite similar with sea shell composition.The remaining 5% includes Mg,Al,P,S,K,Zn, Ironic acid and Silica acid. Eggshells are good bio sorbent due to its cellulose structure and presence of amino acids. Egg shells are produced in large quantities annually in many countries which is a waste and is disposed as landfills. The powdered Egg shell i.e ESP is being used as a stabilizer in expansive soils.

II. EXPERIMENTAL STUDY

Laboratory tests were conducted as per IS code specifications on black cotton soils, properties of the soil are tabularised in Table 1. Furthemore, the soil was alleviated with eggshell powder and variations in properties like CBR, MDD and UCS were determined by conducting the compaction test and UCS (unconfined compressive strength) tests respectively.

As per IS: 2720, following laboratory tests were conducted. Test were conducted on virgin soil and ESP stabilized soil.

- Grain size distribution
- Standard Proctor compaction test
- Unconfined compression strength
- Liquid limit
- Specific gravity
- Plastic Limit

In order to understand the optimum content of admixture, ESP was added as an additive to the soil in different percentages of 2%, 4%, 6 % respectively by dry weight of the soil quantity. Based on the above composite the change in plasticity index value and UCS value was also evaluated with the corresponding varying percentage.

III. RESULTS AND DISCUSSIONS

Materials taken for the purpose of study were Black cotton soil and eggshell powder. The Soil taken for the experimental analysis was from Ramagundam, Karimnagar district .

Experimental tests were conducted on a patch of virgin soil to sort out the atterberg's limits, compaction test features and characteristics, and the UCS. This virgin soil was later alleviated with eggshell powder [ESP] in erratic percentages. The variations found in the evaluated properties of the soil are substantiated below.

The virgin soil properties tabularized are as follows:

Table 1.Virgin soil properties

Sl. No	Lab Test	Result	Relevant IS codes
1	Grain size distribution in %		IS 2720 Part IV
	Gravel stone	8.2	
	Sand particles	20.6	
	Clay particles	70.2	
2	Specific gravity(G)	2.68	IS 2720 Part III
3	Liquid limit in %	41	IS 2720 Part V
4	Plastic limit in %	18.05	IS 2720 Part V
5	Plasticity index no.	22.95	IS 2720 Part V
6	Natural Water content in %	11.25	IS 2720 Part II
7	Optimum moisture content in %	16.09	IS 2720 Part VIII
8	Maximum dry density(g/cc)	1.65	IS 2720 Part VIII
10	Unconfined compression strength (Kg/cm^2)	2.5	IS 2720 Part X

Revised Manuscript Received on December 08, 2018.
Gayatri Upadhyay, MallaReddy Engineering College(A), Secunderabad, Telangana, India.

A. liquid limit percent and plastic limit percent of soil treated with eggshell powder

Changes in liquid limit percentage, plastic limit percentage and plasticity index value of B.C soil with variable percentages of ESP.

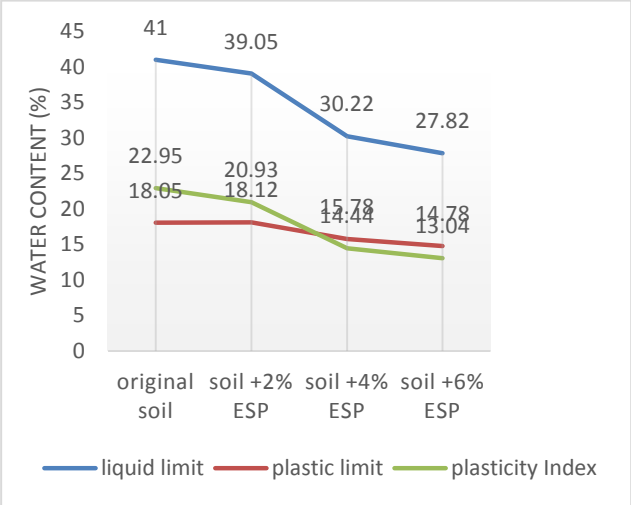

Fig.1 Atterberg limit's of virgin soil and ESP stabilized soil.

From the above fig, a considerable change in the plasticity index can be observed. At 4% EPS and the plasticity index has reduced from 22.95 to 14.44 and 13.04 respectively. This is due the reduction of the adsorption tendency of clay on account of pozzolanic reaction between CaO and negatively charged ions present in clay

B. Unconstrained compressive strength of soil

UCC Test was evaluated on selected soil samples prepared appropriately at their OMC with different variable percentages of stabilizers (2%, 4% and 6%) to evaluate the compressive strength under unconstrained condition. From fig 6.13, On comparing the values with variable percentage, the UCS Value of soil treated with 4 % of EPS gives a considerable increase the strength.

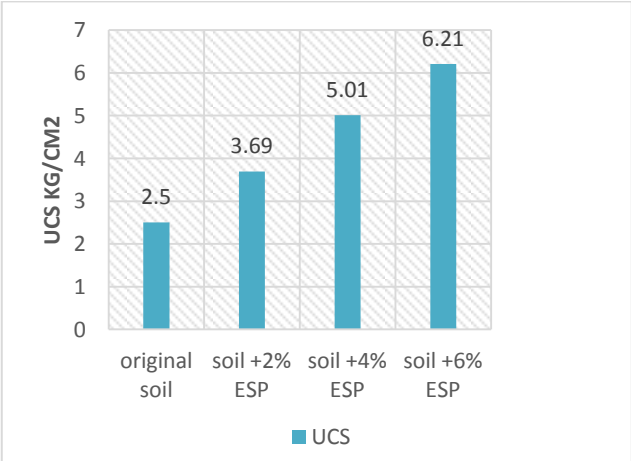

Fig.3 UCS of Soil with different % of RBI & Lime

IV. CONCLUSION

Based on the inferences of the contemporaneous investigations, the following conclusion can be substantiated.

- Additive treatment of the soil with eggshell powder resulted in change in Atterberg's limit and unconstrained compressive strength of soil.
- It may be noted that plastic limit per cent of EPS mixed with the soil incredibly increases with gradual increasing proportions of additive mixture.
- The 4% ESP is taken as optimum dosage.
- The unconstrained compressive strength of the original tested soil was very less compared to the soil with optimum admixture content.
- Since the ESP has the lime content, it stabilizes the clay particles by interacting with water molecules. The strength of the soil has thereby increased greatly with optimum dosage of ESP.

REFERENCES

1. Barazesh, A., Saba, H., Gharib, M. and Rad, M.Y. (2012) "Laboratory Investigation of the Effect of Eggshell Powder on Plasticity Index in Clay and Expansive Soils," European Journal of Experimental Biology, 2 (6), 2378-2384.
2. Amu , O. O., Fajobi, A.B. and Oke, B.O. (2005) "Effect of Eggshell Powder on the Stabilizing Potential of Lime on an Expansive Clay Soil," Research Journal of Agriculture and Biological Sciences, 1(1), 80-84.
3. AnouksakThammavong and DirekL(January 2006)., "Cement Stabilization of Reclaimed Asphalt Pavement Aggregate for Base Layer", Technology and Innovation for Sustainable Development Conference, Thailand..
4. Gopal Ranjan, A.S.R.Rao,(1991) "Basic and Applied Soil Mechanics", Published by S.Poplai For Wiley Eastern Limited, New Delhi, pp:49-58
5. AI-Azzo, S.I. (2009) "Treatment of Expansive Clayey Soil in AL-Wahda District at Mosul City with Crushed Lime Stone," Iraqi Journal of Earth Sciences, 9(2), 1-10

Optimization of Thrust force, Surface roughness and Delamina-tion in drilling of EN-24 steel using Taguchi based VIKOR-Entropy Method

Heruthunnisa.Shaik, Ismail.Kakaravada

Abstract: ***The present article presents Taguchi based multi-response optimization for multi response during drilling of EN-24 steel under minimum quantity lubrication (MQL) condition. The Taguchi method is one of the most authoritative tool used in designing of the hole quality optimization. The intend of this paper is to explore the influence of cutting edge speed, drill feeding rate and effect of coating on drill tool upon the superficial integrity, thrusting force, and delamination factor during the procedure for drilling of EN-24 steel. The experiments were performed on the computer controlled vertical machining centre (VMC). The design of experiments (DOE) was based on L_{27} Taguchi's orthogonal array; the experiments were executed under minimum quantity lubrication used as mineral oil at a course rate of 60 ml/min. The selected machining parameters for drilling operation were spindle speed at 150, 350 and 550 rpm, drill feeding rate at 0.15 mm/rev, 0.25 mm/rev and 0.35 mm/rev and HSS (uncoated/coated with TiN and TiAlN) drills were used. The orthogonal array, the VIKOR-Entropy grade, and ANOVA were engaged to investigate for the prime machining parameter which optimizes the process. From the analysis of experimental consequences, it has been observed that the drill feeding rate is the most influencing parameter and the spindle rotating speed is the least impelling parameter. These results indicates the selection of optimal parameter for drilling of EN-24 steel without compromising the hole quality.***

Keywords: ***Drilling, Orthogonal array, Multi-response optimization, VIKOR-Entropy, ANOVA.***

I. INTRODUCTION

Drilling is the most widely machining processes in fabrication of components in various industries. These processes reports 40% total material removal processes in automotive and aerospace industries [1]. It can create a new hole or enlarge a new hole in a work piece by the motion drill bit. The various methods in drilling processes are in practice in current industries, such as conventional vertical drilling, deep hole drilling with larger radius and peck drilling. The choice of drilling processes depends up on requirement of production like the size, tolerance and surface finish required. The EN-24 alloy steel is very popular grade which is most suitable material for fabrication of heavy duty shafts and axles, gears, bolts and studs because of its superior tensile strength and wear resistance [2]. Quite a lot of factors impact the quality of drilled holes in conventional type of drilling during drilling of steel. In that the most observable one is the cutting parametric variants which includes the speed of the spindle speed and feed of the tool, feeding rate of the tool, drill nomenclature variable function like tool material, diameter of drill, and geometry and finally the cutting environments like dry, flooded and minimum quantity type cooling and cryogenic cooling. The selection properties of cutting speed and feed rates are deepens upon the mechanical and machining properties of work piece material. Kumar J.P. et al. [3] examined the stimulus of processes parametric variables over the output responses like MRR, tool wear, surface roughness and delamination in penetrating of OHNS material. High speed steel drill used for to conduct experimental investigation. Minitab 13 version software was used to analyze the effect of input parameter. The experiments substantiate that, feeding rate of the drilling machine and spindle speed rate are the most influencing factors on the output response characteristics. Çiçek.A et al [4] conducted experimental investigation on AISI 316 austenitic stainless steel and explored the consequence of deep cryogenic method of treatment of drill tool on the surface roughness of drilled hole. The experiment were conducted with various selected machining parameters like cutting speed and feed rates. L_8 orthogonal array was opted for conducting experimentation and numerous regression analyses was accomplished upfront to estimate extrapolative surface roughness of drilled hole. Jayabal.S and Natarajan.U [5] reported the effect of drilling parameters like cutting traversing speed, point angle at the joint and feed rate against the torque and thrust force during drilling of glass fiber reinforced composite. A mathematical model is generated for correlating of processes parameters and their interactions over the torque and thrust force. From the experimental results it is observed that tool feed rate and point angle of drill is the most influencing parameter on output responses in drilling. Raj.A.M et al. [6] investigated the drilling responses on AA6061/SiC/Graphite composite material with machining parameters as spindle speed, drill diameter, feed rate and type of drill upon surface roughness as response parameter. Response surface methodology (RSM) methodology adopted to find the optimal parameter for surface roughness. Kilickap.E et al [7] reported that the least value surface roughness was attain at inferior cutting speeds and also observed that increase in tool feed rate deteriorates surface of drilled hole during drilling of steel.

Revised Manuscript Received on December 08, 2018.

Heruthunnisa.Shaik, Assistant Professor, Department of Mechanical Engineering, Mallareddy Engineering College (A), Hyderabad, Telangana, 500100, India.

Ismail.Kakaravada, Research scholar, Department of Mechanical Engineering, Jawaharlal Nehru Technological University, Anantapuramu, A.P, 515002, India.

And also it is conformed that surface roughness was much better under minimum quantity lubrication condition when compared to dry drilling process. Nalawade.P.S and Shinde.S.S [8] reported the effect of processes parameters on EN-31 alloy steel during drilling. The processes parameters were selected and optimized to obtain better surface finish and delamination factor. The experiments were accompanied through Taguchi L_9 orthogonal array with the processes parameters as speed of the spindle, feed rate quality, and type of tool and depth of cut given to the job. From the existing analysis work it is clinched that lower feed rate, higher spindle speed and uncoated is the optimal parametric variable functions to obtain better experimental results. Shivapragash.B et al. [9] studied to find the optimal drilling parameters like cutting speed, feed rate, and depth of cut during drilling composite Aluminium-TiB_2. The experimentation was conducted by following L_9 orthogonal array. For the multi response optimization Taguchi based grey relational analysis was to optimize the factors. From the results it has been found that for optimal experimental procedural run to minimize thrust force and surface roughness is feed rate at 1.5 mm/rev, higher spindle speed at 1000 rpm and depth of cut at 0.15 mm. Reddy.I.S [10] examined the influence of input parameters, such as point angle, feed rate and cutting speed over the surface roughness in drilling of AA6463 alloy. The experiments were conducted on computer numerical control vertical machining centre by using L_9 orthogonal array. For the mono response optimization Taguchi Signal and noise creation ratio (S/N) and analysis of variance function polynomial (ANOVA) has been emphasized to substantiate out the optimal drilling parameter. From the results, it was found that feed rate most significant parameter on the material removal rate and spindle speeds highest significant parameter on surface roughness. Murthy.B et.al [12] studied the consequences of process parameters like feed rate, drill diameter, point angle, material thickness and spindle speed generated during drilling of glass fiber reinforced polymer (GFRP) composite material by using solid carbide drill tool. Taguchi's Response Surface Methodology selected for conducting experimentation. From the result it was found that, thrust force is significantly effect by spindle speed. On other hand larger thrusting force and torque was observed at higher drill diameter, higher point angle drill increase the thrust force and lower the cutting torque decreases. Sundeep.M et al. [13] investigated drilling characteristics on Austenitic stainless steel (AISI 316) to investigate the influence of parametric variable function like like spindle speed drill diameter and feed rate. L_9 Taguchi array was used to conduct the investigation. rom the results it is stated that spindle speed plays the most significant role in material removal and surface finish in drilling. Kadam.K [2] has done an experimental analysis on drilling on EN-24 steel by considering input parameter spindle seed, drill diameter and feed rate. The experiments were conducted by means of Taguchi L_9 array with uncoated M32 HSS drill under dry condition. S/N ratio was employed to get optimal parameter for considered each mono response. The analysis results exhibit that, cutting speed was the most significant factor on tool life and surface roughness of hole during drilling of steel. Rane V.N. et al [14] studied the effectual consequences of machining parameters on hardened boron steel by using feed rate, point angle and cutting speed as input parameters. Taguchi L_{16} orthogonal array has been followed to perform the experiment. ANOVA was performed to find out effects of each control factors over the surface roughness. the results depicted that point angle was the main significant factor on surface roughness quality of the work done, drill impending rate has significant role in tool wear during drilling processes. Ismail. Kakaravada et.al [15] investigated the effect of drill diameter, % of reinforcement, spindle speed during drilling of A356-TiB_2/TiC in-situ composite. Taguchi L_{16} orthogonal array has opted to perform the experiments to evaluate surface roughness, delamination and material removal rate. Finally Entropy- VIKOR grade method was opted to combine the multi response optimization. From the its is stated that moderate reinforcement, higher spindle speed and greater drill diameter is optimal machining condition for composite.

The current aims to presents a well-organized approach for the optimization of multiple responses in drilling of EN-24 steel based on the Taguchi's method. The drilling experiments were performed on EN-24 steel plate by using uncoated high-speed steel drill as well coated with TiN and TiAlN through physical vapor deposition method under minimum quantity lubrication condition. The experiments were conducted with considerable machining parameters such as speed of the machinery spindle, tool penetration rate, tool type were optimized with estimated of multiple responses like surface texture, thrusting force and delamination proportion of drilled hole. The novel VIKOR-Entropy method was adopted to combine and optimize the multi responses. The analysis of variance polynomial function (ANOVA) was performed for VIKOR-Entropy grade to determine the most significant parameter to affects the drilling responses.

II. EXPERIMENTAL PROCEDURAL DETAILS

In the current experimental investigation, 10 mm diameter of holes was drilled on EN-24 grade alloy steel flat with the dimensions of 150×50×15 used in automobile industry. The chemical composition of EN-24 steel flat as shown in Table.1

Table.1: Chemical composition of EN-24 alloy steel

Component	C	Si	Mn	S	P	Cr	Mo	Ni
% age	0.44	0.35	0.70	0.040	0.035	1.400	0.35	1.70

The drilling trials were led by gradually varying the cutting edge speeds from 150 to 550 rpm and drill bit feeding rates from 0.15 to 0.35 mm/rev. The cutting tools used for the minimum quantity lubrication condition at a flow rate of 60 ml/min (mineral oil) drilling are HSS drill (Make: Addison Tools India Ltd), TiAlN Black Coated-KC7325 Grade HSS drill, TiN Golden coated – WU25PD Grade HSS drill (Make: Kennametal drill tools). The machining parameters and their levels are shown in Table 2.

Experiment trails are piloted to examine the predominant effect of the epitomic drilling procedural parameter and drill bit type on the surface quality texture, thrust force and delamination value deviation/damage of the work piece material.

2.1. Machining setup

The experiments were carried out by using VMC 850 CNC vertical milling machine (Jyothi CNC automation Limited) as shown in figure 1. The thrust force was measured during drilling of EN-24 steel through Kistler multi-component dynamometer (Model: 9255C with multi charge amplifier). The surface integrity value R_a measured by using of SJ210 stylus type surface roughness tester (Mitutoya Make, 0.001µm) with measuring length of 7 mm. For better outcomes, average of any predetermined three values was found. The delamination factor of hole was measured by using Metallurgical microspore with 1000 X magnifications and 1mm resolution (Metzger Optical Instruments Private Limited, Mathura, India).

2.1.1. Measurement of Thrust force

The thrust force generated during drilling of EN-24 steel was recorded by using of a piezoelectric multi-component dynamometer. The multi charge amplifier (Model: 5070A with eight channel charge amplifier was connected to USB data acquisition system (Model: 5697A) used to record the data for analyzing with appropriate dynaware software. From the response graph of the drilling processes divided three stages according to the drill cutting edge position with respective to the plate. At entry stage, initially there is no contact of chisel edge with the work piece during drilling due to this there is no cutting force was recorded. As well it will come full engage of chisel of drill to the work piece the maximum thrust force was recorded. When it will come to the exit of chisel edge of drill large amount of fluctuation and sudden decrement in thrust force was observed. The average value of thrust force was recorded by dynamometer was considered for analysis.

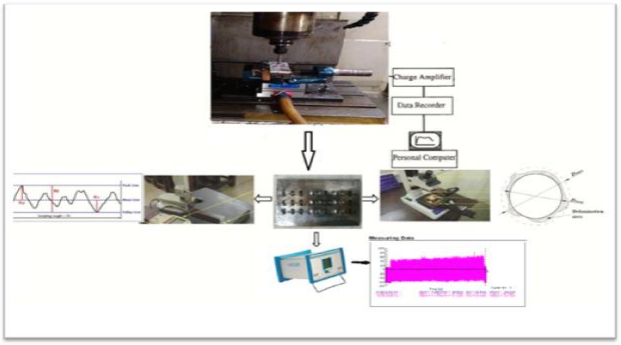

Figure.1: Schematic diagram of experimental set up.

2.1.2. Measurement of Surface Roughness

Mathematical average means surface roughness quality and its incremental analysis (R_a) is the arithmetic average elevation of peak and valley values in the direction of the work/job pertaining to the horizontal-axis and magnitude pertaining to the vertical-axis of the work from the mean line of axis considered for the purpose of the experimental set up. Simply, R_a is the average measurements of a surfaces peak heights and valleys Equation 1.

$$R_a = \left(\frac{1}{l}\right)\int_0^l |Z(x)|dx \quad (1)$$

Most of the automobile industries prefer the average surface roughness value (R_a) of hole. The average values are considered for the analysis during the experimentation. It is measured by Mitutoya SJ- 210 stylus type surface roughness tester, and an average of three replicates was found out R_a value varies with respect to stylus probe movement along the cross section of drilled hole.

2.1.3. Measurement of Delamination

Drilling of EN-24 steel involves damages of edges of hole at the entry diameter of hole and the exit diameter of the drilled hole due drill tool wear in drilling operation is designated as the delamination factor. As a quantitative relation of exit the process of delamination, the inferior surfaces of each hole were examined by a metallurgical microscopic apparatus. The delamination factor was estimated as per the below substantiated ratio using Equation 2.

$$D_f = \frac{D_{\max}}{D_{\min}} \quad (2)$$

III. OPTIMIZATION AND MODELING

In the present analysis, three drilling parametric functional variables were used as regulators establishing the response factors for the drilling experiment, and each machining parametric variable having three predominant levels. The input drilling parameters and their levels elected for the experimental design procedure are presented in Table 2.

Table: 2. Speed of the machine spindle, Feed ratio and Tool type used for Experimentation

Parametric function	Level 1	Level 2	Level 3
Spindle speed (rpm)	150	350	550
Drill feed Rate (mm/rev)	0.15	0.25	0.35
Tool Type	HSS	HSS+TiN	HSS+TiAlN

The experimental evaluations are conceded out on the basis of L_{27} (3^{13}) orthogonal array. The responses were recorded with respective experimental as shown in Table 3, to investigate the software tool version 16 was used for the arithmetical analysis of the experimental data. Taguchi method combined with the VIKOR-Entropy grade method and the scheme of least squares parametric functional values is mostly used for the regression analysis and to calculate the coefficients of regression and the accurate functional characteristic relationship between Y_{xt} and the set of machining parameters in a and polynomials compound linear regression model. If the response variables are well modeled by a linear variant function of the input variables, and the approximation function in the first order differential is given by:

Published By:
Blue Eyes Intelligence Engineering
& Sciences Publication

$$y = \beta_0 + \beta_1 X_1 + \beta_2 X_2 + \beta_3 X_3 + ...\beta_k X_k \quad (3)$$

Polynomial second order of higher degree equation must be used, such as the second order model: this model is almost useful for the all the engineering problems. But it is unlikely that the polynomial equation which will give accurate results for the accurate functional relationship over the complete space of the selected process variables, but for a relatively little region, they usually work quite well.

$$y = \beta_0 + \sum_{i=1}^{k} \beta_i X_i + \sum_{i=1}^{k} \beta_{ii} X_i^{\,2} + \sum_{i}^{\cdot} X_i \sum_{\prec j}^{\cdot} \beta_{ij} X_i X_j \quad (4)$$

3.1 Entropy weight method

The entropy weight measurement procedure the number of substitutes and various principles considered to examine the multi response optimization by considering a qualified decision matrix. If numbers of alternatives are spindle speed, drill feed rate and tool type considers as 'M' and numbers of criterion are assumed Thrust force, delamination and surface roughness considers as 'N' then assessment matrix having an order of M×N.

$$D = \begin{bmatrix} X_{11} & X_{12} & X_{13} & X_{1n} \\ X_{21} & X_{22} & X_{23} & X_{24} \\ X_{31} & X_{32} & X_{33} & X_{34} \\ X_{m1} & X_{m2} & X_{m3} & X_{mn} \end{bmatrix}$$

The decision matrix is normalized by greatest values (i.e. favorable attribute) and smallest values (unfavorable attribute). The normalized values calculated by following mathematical equations 5 and 6 and values are tabulated in Table 3

$$r_{ij} = \frac{x_{ij} - \min(x)_{ij}}{\max(x_{ij}) - \min(x_{ij})} \quad (5)$$

$$r_{ij} = \frac{x_{ij} - \min(x)_{ij}}{\max(x_{ij}) - \min(x_{ij})} \quad (6)$$

Where *i*=1,2., …..M. *j* =1, 2, 3...N in equation

3.2 Generation of entropy weight for model

In this step the various principles are determined by the entropy method projection values ( ) are evaluated by equation (7).and the projection of alternative is used to establish the entropy index (*eij*) using equation (8). The projection and entropy indexed values tabulate in Table 3

$$T_{ij} = \frac{r_{ij}}{\sum_{i=1}^{m} r_{ij}} \quad (7)$$

$$e_{ij} = -\frac{1}{\ln m} \sum_{i=1}^{n} T_{ij} \ln T_{ij} \quad (8)$$

3.3 VIKOR method of optimization

The VIKOR method is implemented for multi response optimization to find a concluding solution. In this method arithmetical procedure to implement to find the solution close to ideal optimistic solution ($f*$) and the ideal pessimistic solution ($f-$) were identified by following equations 9 and 10.

$$f^* = f^- \left\{ \left(\min f_{ij} / j \in J \right) or \left((\max f_{ij}) / j \in j' \right) \right\} \quad (9)$$

$$f^- = \left\{ \left(\min f_{ij} / j \in J \right) or \left((\max f_{ij}) / j \in j' \right) \right\} \quad (10)$$

thus J= {j=1, 2, 3...n}, fij if desired responses is large. J'= {1, 2,3…n}, fij if desired responses is small For the calculation of utility index and regret measure value for each response calculated by the following equation 11 and 12 respectively and Tabulated in Table 3.

$$S_i = \sum_{j=1}^{n} W_j \frac{\left(f^* - f_{ij} \right)}{\left(f_j^* - f_j^- \right)'} \quad (11)$$

$$R_i = \max_j \left[w_j \frac{\left(f^* - f_{ij} \right)}{\left(f_j^* - f_j^- \right)'} \right]' \quad (12)$$

Where $s_i$utility index, Ri is the regret measure value wj is the respective weight of the jth element. The individual entropy weight calculated by entropy weight method and finally the VIKOR index calculated by equation 13 and presented in Table 3 and to determine rank of VIKOR indexed values the least index value treated as first rank.

$$Q_i = v \left[\frac{s_i - s^*}{s^- - s^*} \right] + (1+v) \left[\frac{R_i - R^*}{R^- - R^*} \right] \quad (13)$$

Thus, Q_i is the predefined VIKOR index of the variable at the i^{th} stage of the result of alternative and v is the superior weight factor of the prescribed group index of utility. Commonly the value of v *was* taken as 0.5. In the above equation $s^- = max_i\, s_i$, $s^* = mi$, $R^- = max_i\, R_i$, And $R^* = min_i\, R_i$ are the higher and lower values of utility index and regret measure. The following clauses must be satisfied to conciliation the results of the consider weight for given alternative. The alternative $A^1$is considered lesser VIKOR index values by measure Q (minimum) and A^2 is the second smallest VIKOR index in list.

a) Acceptable advantage $Q(A^2) - Q(A^1) \geq DQ = \frac{1}{(m-1)}$ where 'm' number of conducted experiments.

The alternative A^1 is the smallest VIKOR index ranked by S or/ and R the clarification for stable in decision making. This could be the strategy of highest of utility value v is more than 0.5 needed or same as to 0.5 or with veto lower than 0.5 if one condition not pleased the following must be followed.

I. The alternatives A^1 *and* A^2 if only second condition is not pleased. II. The first clause not pleased A^n is calculated by the following relation ( )-Q (A^1)< DQ for maximum of n

From the above equation Q value is smallest, which results the lowest rank which conciliation of the excellent results for multi response optimization problem.

IV. RESULTS AND DISCUSSION

This investigation explores the grouping of weighted Entropy measurement and VIKOR technique to appraise the

Published By:
Blue Eyes Intelligence Engineering
& Sciences Publication

decision matrix D m×n is represent by the experimental results as shown in Table 3. For the computation of weight of Entropy for each response equation 1 and 2 are used. For the Thrust force, surface roughness and delamination factor non beneficial attribute equation was used. After estimation the entropy method projection values (Tij) are calculated by equation (7). The projections of values are used to conclude the entropy index (eij) by using equation (8). The projection and entropy indexed values tabulated in Table 3. Finally the VIKOR method was opted for multiresponse optimization. From the individual matrix is analyzed $f*$ and $f-$ possible best solution values are (10.3879, 0.360829, and 0.001351) and worst solution values (22.09073, 0.526529, and 0.003775) were analyzed by equation 9 and 10. The values pertaining to the measure of utility measurement and regret measure is by equation 11 and 12, respectively. The maximum altitude and minimum penetration utility and regret measure are (1.007, 0.0028 and 1.0034, 0.0028) respectively. The lowest VIKOR index calculated using equation 13 and lowest index values ranked as 1 as shown in Table 4. The validation of experiment calculated acceptable advantage equation is satisfied with the value is less than DQ value. Therefore condition is acceptable.

4.1 optimal parameter selection and ANOVA

To find the most favorable level of drilling parameters and the main effect of parameter are appraise VIKOR index as shown in figure 2. From the figure 2 it is found that spindle speed at 350 rpm feed rate at 0.15 mm/rev and HSS+TiAlN coated drill was the optimal parameter for the multi character machining. Table 4 shows the difference value of greatest and lowest values and their rank among the processes parameter for the selective model. The results of ANOVA test for VIKOR index shown in Table 5. From the table it has been observed that contribution each parameter on output response. And finally the interaction process parameters are significant at 82.29% of confidence.

Table. 4. Main effect factors for Entropy -VIKOR index

Parameter	Level 1	Level 2	Level 3	Max-Min	Rank
Spindle speed	0.32033	0.32761	0.37721	**0.05688**	3
feed rate	0.07112	0.27310	0.68092	**0.6098**	1
Tool type	0.42517	0.33069	0.15589	**0.26928**	2

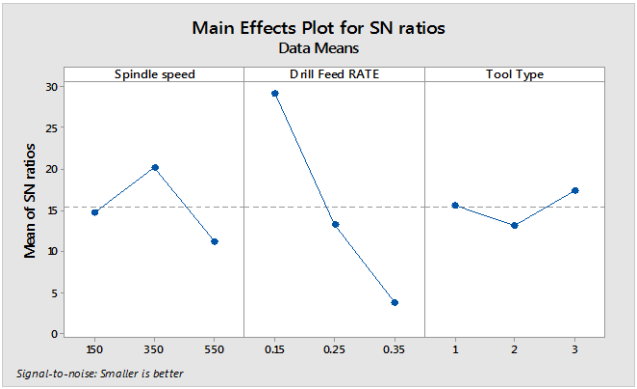

Figure. 2: Main effect plot for Entropy -VIKOR index

Table.3: Taguchi L_{27} orthogonal array with machining parameters, experimental results, projected values, individual weighted Entropy Index values, utility, regret measures values and VIKOR index of alternative with their ran

Trail. No	Machining Parameters			Experimental results			Projection values (T_{ij})			Entropy Index (T_{ij})ln (T_{ij})			Utility Measure (S_{ij})	Regret Measure (R_{ij})	VIKOR index (Q_{ij})	Rank order
	Spindle speed	Feed rate	Tool type	Thrust force	Delamination	surface roughness	C-1	C-2	C-3	C-1	C-2	C-3				
A-1	150	0.15	HSS	160	1.02241	5.95	10.5194	0.360829	0.003775	24.7544	-0.36781	-0.02106	0.0113	0.0051	0.0051	2
A-2	150	0.15	HSS+TiN	172	1.08091	4.82	11.30835	0.381475	0.003058	27.4288	-0.36763	-0.0177	0.0789	0.0743	0.0743	7
A-3	150	0.15	HSS+TiAlN	183	1.12019	3.67	12.03156	0.395338	0.002328	29.9289	-0.36688	-0.01412	0.1409	0.1377	0.1376	9
A-4	150	0.25	HSS	231	1.12091	4.78	15.18738	0.395592	0.003032	41.3167	-0.36686	-0.01758	0.4115	0.4075	0.4072	19
A-5	150	0.25	HSS+TiN	206	1.17941	3.19	13.54372	0.416238	0.002024	35.2939	-0.36483	-0.01255	0.2706	0.2685	0.2683	13
A-6	150	0.25	HSS+TiAlN	202	1.22020	4.82	13.28074	0.430633	0.003058	34.3481	-0.36281	-0.0177	0.2480	0.2453	0.2451	12
A-7	150	0.35	**HSS**	305	1.21724	3.95	20.0526	0.429589	0.002506	60.1248	-0.36297	-0.01501	0.8287	0.8265	0.8259	25
A-8	150	0.35	HSS+TiN	250	1.27574	4.71	16.43655	0.450235	0.002988	46.0142	-0.35928	-0.01737	0.5186	0.5167	0.5163	21
A-9	150	0.35	HSS+TiAlN	230	1.21658	4.32	15.12163	0.429356	0.002741	41.0722	-0.36301	-0.01617	0.4059	0.4034	0.4032	18
A-10	350	0.15	**HSS**	164	1.23258	3.41	10.78238	0.435003	0.002163	25.6395	-0.3621	-0.01327	0.0338	0.0322	0.0322	6
A-11	350	0.15	HSS+TiN	162	1.10108	4.35	10.65089	0.388594	0.00276	25.1962	-0.36731	-0.01626	0.0225	0.0186	0.0185	3
A-12	**350**	**0.15**	**HSS+TiAlN**	**158**	**1.49192**	**3.13**	**10.3879**	**0.526529**	**0.001351**	**24.3143**	**-0.33774**	**-0.00893**	**0.0028**	**0.0028**	**0.0028**	**1**
A-13	350	0.25	HSS	163	1.13108	4.89	10.71663	0.399181	0.003102	25.4176	-0.36658	-0.01792	0.0282	0.0242	0.0242	4
A-14	350	0.25	HSS+TiN	227	1.18958	5.62	14.92439	0.419827	0.003565	40.3405	-0.36437	-0.0201	0.3890	0.3852	0.3850	16
A-15	350	0.25	HSS+TiAlN	179	1.23041	2.8	11.76857	0.434237	0.001776	29.0146	-0.36223	-0.01125	0.1184	0.1172	0.111	8
A-16	**350**	**0.35**	**HSS**	**336**	**1.22741**	**4.94**	**22.09073**	**0.433178**	**0.003134**	**68.3743**	**-0.3624**	**-0.01807**	**1.0034**	**1.0007**	**1.0000**	**27**
A-17	350	0.35	HSS+TiN	294	1.28591	2.38	19.32939	0.453824	0.00151	57.2464	-0.35854	-0.00981	0.7667	0.7665	0.7660	24
A-18	350	0.35	HSS+TiAlN	265	1.32674	3.13	17.42275	0.468234	0.001986	49.7903	-0.35529	-0.01235	0.6032	0.6030	0.6026	23
A-19	550	0.15	HSS	192	1.13208	3.95	12.62327	0.399534	0.002506	32.0068	-0.36656	-0.01501	0.1917	0.1884	0.1882	11
A-20	550	0.15	HSS+TiN	185	1.16058	3.73	12.16305	0.409592	0.002366	30.3882	-0.3656	-0.01431	0.1522	0.1495	0.1493	10
A-21	550	0.15	HSS+TiAlN	164	1.20141	3.06	10.78238	0.424002	0.001941	25.6395	--0.3638	-0.01212	0.0338	0.0321	0.0321	5
A-22	550	0.25	HSS	229	1.30058	4.32	15.05588	0.459001	0.002741	40.8280	-0.35743	-0.01617	0.4002	0.3989	0.3986	17
A-23	550	0.25	HSS+TiN	210	1.25908	3.28	13.80671	0.444355	0.002081	36.2447	-0.36043	-0.01285	0.2931	0.2920	0.2918	14
A-24	550	0.25	HSS+TiAlN	215	1.29991	3.12	14.13544	0.458765	0.001979	37.4403	-0.35748	-0.01232	0.3213	0.3208	0.3206	15
A-25	550	0.35	HSS	326	1.29691	4.26	21.43327	0.457706	0.002703	65.6917	-0.35771	-0.01598	0.9470	0.9457	0.9451	26
A-26	550	0.35	HSS+TiN	248	1.31541	3.26	16.30506	0.464235	0.002068	45.5151	-0.35624	-0.01278	0.5073	0.5070	0.5066	20
A-27	550	0.35	HSS+TiAlN	258	1.29624	3.57	16.96252	0.45747	0.002265	48.0210	-0.35776	-0.01379	0.5637	0.5629	0.5625	22

Table.5: ANOVA for Entropy -VIKOR index

Source	DF	Adj SS	Adj MS	F-Value	% of Contribution
Spindle speed	2	0.01725	0.008624	0.43	0.76105
feed rate	2	1.73690	0.868452	43.27	76.630
Tool type	2	0.11100	0.055498	2.76	4.89
Error	20	0.40145	0.055498		17.71
Total	26	2.26660			100

4.2 Conformation/Validation test

To validate the prescribed model entity the conformation experiment was conducted and analyzed. The predicted value of conformation experiment is obtained through regression equation. From the confirmation experiment the error percentage with its experimental value and evaluated by regression equation with correspond processes parameter of lowest VIKOR index. The results are shown in Table 6.

Regression equation for VIKOR index
Entropy-VIKOR index = 0.3417-0.0214
Spindle speed_150-0.0141
Spindle speed_350+ 0.0355
Spindle speed_550 - 0.2706
feed rate_0.15-0.0686
feed rate_0.25+ 0.3392
feed rate_0.35+ 0.0835
Tool Type_10.0110
Tool Type_2 - 0.0724
Tool Type_3

Table 6 Results of conformation experiment

Numerical index	Optimal level parameters	Predicted value	Experimental value	Error
VIKOR index	Spindle speed = 350	0.0024	0.0028	0.0004
	Feed rate = 0.15			
	Tool type = (HSS+TiAlN)			

V. CONCLUSIONS`

The present work is based on the experimental investigation during drilling of EN-steel. The machining capacity of drilling is evaluated in terms of thrust force, surface roughness and delamination under minimum quantity lubrication condition. The Entropy-VIKOR index analysis of the experimental results has established Thrust force, delamination and composite VIKOR index. From the ANOVA of Entropy-VIKOR index discloses the moderate spindle speed (350 rpm), lower feed rate (0.15 mm/rev) and HSS drill coated with titanium aluminium nitride (TiAlN) is the optimum parameters for machinability of EN-24 steel Finally it has been concluded that the VIKOR index of predicted and experiment values are attained with less error value. The consequences imply that, the optimization of multiple performance characteristics can be greatly simplified.

REFERENCES

1. Khaled Giasin, AlmaHodzic,Vaibhav.Phadnis, Sabino Ayvar-Soberas, Assesment of cutting force and hole quality in drilling Al2014 aluminium alloy experimental and finite element study, internationall journal of advanced manufacturing technology 87 (2016) 2041-2061.
2. S.Kadam, M. G. Rathi, Application of Taguchi method in the optimization of drilling parameters", International Journal of Engineering Research and Technology, 2(8), 2013.
3. J. P. Kumar and P. Packiara, Effect of drilling parameters on surface Roughness, tool wear, material removal rate and hole diameter error in drilling of ohns." International Journal of Advanced Engineering Research and Studies, 1(2012)150-154.
4. A.Çiçek, T. Kıvak, G.Samtaş. Application of Taguchi method for surface roughness and roundness error in drilling of AISI 316 stainless steel, Strojniškivestnik-Journal of Mechanical Engineering, 58(3) (2012) 165-174.
5. S. Jayabal U. Natarajan, Influence of cutting parameters on thrust force and torque in drilling of E-glass/polyester composites. 2010.
6. A.M.Raj, S. L. Das, K. Palanikumarr, Influence of drill geometry on surface roughness in drilling of Al/SiC/Gr hybrid metal matrix composite." Indian journal of science and technology, 6(7) (2013) 5002-5007. 2013.
7. E. Kilickap, M. Huseyinoglu, A.Yardimeden, Optimization of drilling parameters on surface roughness in drilling of AISI 1045 using response surface methodology and genetic algorithm, The International Journal of Advanced Manufacturing Technology, 52(1) (2011) 79-88.
8. P. S.Nalawade, S. S. Shinde, Cutting Parameter Optimization for Surface Finish and Hole Accuracy in Drilling Of EN-31, IOSR Journal of Mechanical and Civil Engineering, 12(9) (2015) 20-27
9. B.Shivapragash, K.Chandrasekaran, C.Parthasarathy, M. Samuel, Multiple Response Optimizations in Drilling Using Taguchi and Grey Relational Analysis, International Journal of Modern Engineering Research (IJMER), 3(2) (2013),765-768.
10. I.S. Reddy, F. A. Raju, A. Gurunadham, Determination of Optimum Parameters in CNC Drilling of Aluminium Alloy Al6463 by Taguchi Method, International Journal of Engineering Research & Technology (IJERT),vol. 3(2), 2014.
11. Y. Tyagi, V. Chaturvedi, J.Vimal, Parametric optimization of drilling machining process using Taguchi design and ANOVA approach, Journal of Emerging Technology and Advanced Engineering, 2(7) (2012) 339-347.
12. B.Murthy, L. L. Rodrigues, A. Devineni., Process Parameters Optimization in GFRP Drilling through Integration of Taguchi and Response Surface Methodology," Research Journal of Recent Sciences, 1(6) (2012) 7-15.
13. M. Sundeep, M.Sudhahar, T. T. M.Kannan, P. V. Kumar, N. Parthipan. "Optimization of drilling parameters on Austenitic stainless steel (AISI 316) using Taguchi's methodology",
14. V. N. Rane, A. P.Edlabadkar, P. D.Kamble, S. S.Chaudhar, Optimization of process parameters for resharpenedHSS drill Using Taguchi Methods, International Journal on Engineering Technology and Sciences, 2 (3), 2015.
15. Ismail.Kakaravada, A.Mahamani,V.Pandurangadu, Optimization of machining parameters using Entropy-VIKOR method in drilling of A356-TiB_2/TiC in-situ composites, IOP Conference Series: Materials Science and Engineering,390 (2018)

Published By:
Blue Eyes Intelligence Engineering
& Sciences Publication

Use of Steel Slag as Coarse and Fine Aggregate in Porous Concrete Pavements

Vishwanath B J, Rex

Abstract: ***Due to increasing demand of raw materials for construction of roads, the environmental eco system is getting imbalanced. Hence there is a need to preserve natural resources by using eco friendly alternative materials. Steel slag is one such alternative material, which is an industrial by product that can be used as an alternative to aggregates in partial replacement in road construction. Slag may be used as both coarse and fine aggregates in cement concrete. Hence in the present study mix design for conventional porous concrete was carried out for different proportion of fine and coarse aggregate (0:100, 10:90, 15:85, 20:80, and 30:70). The optimum dosage of FA:CA for the conventional porous concrete mix, giving high strength with acceptable permeability was fixed i.e 20:80 Then the mix design for porous concrete was carried out for partial replacement coarse and fine aggregates with steel slag in 20:80 mix. i.e Replacing only the coarse aggregate in FA:CA (20:80) mix with the air cooled LD slag in three different proportions such as 10%, 30% and 50% .i.e keeping FA-20% constant and replacing coarse aggregate by slag in 80% of CA and Replacing only the fine aggregate in FA:CA (20:80) with the granulated LD slag in three different proportions such as 30%, 60% and 90% .i.e keeping CA 80% constant and replacing fine aggregate by slag in 20% FA. Finally the mix design properties in terms of strength and permeability are evaluated for the porous concrete prepared with coarse and fine slag.***

Index Choice: ***Porous concrete; Air cooled LD slag; Granulated LD slag; Coarse aggregate***

I. INTRODUCTION

Porous concrete is gaining lot of attention because of its good drainage property. Various environmental benefits such as controlling storm water runoff, restoring ground water supplies, and reducing soil and water pollution have become most important across the world. Porous concrete is a mixture of coarse aggregate, fewer fines or no fine aggregates, cement and other cementitious materials, admixtures and water.

By the construction of porous surface, storm water is given access to filter through pavement and rate of filtration is also depends on the permeability of underlying layer. This allows for filtration of pollutants also. Thus high flow of water through a porous concrete pavement allows rain water to percolate into the ground where the rate of percolation depends on gradation and permeability of supporting layers, reducing storm water runoff, recharging the ground water, thus supporting sustainable construction.

Providing the porous concrete pavements in low traffic volume roads instead of conventional concrete is one of the solutions to overcome pavement premature failure due to stagnation of water on pavement surface.

In developing countries like India, disposal of industrial waste is a major concern. Also preservation of natural Resources like aggregates being the main focus, reusing of waste materials like iron slag, steel slag, scrap tires and so on in the construction of roads is slowly gaining pace to minimize issues of transfer of waste material and consumption of regular assets.

Many literatures indicate use of various types of slags replacing cement. Steel slag is a by-product of steel making process, steel plants generates nearly 500 kg of total slag for one tonne of steel production. Now a day slags are also considered for replacing construction aggregates.

II. OBJECTIVES OF THE RESEARCH

1. To design various porous concrete mixes with different proportions of coarse and fine aggregates and thus achieve optimum mix proportion which satisfies the strength and permeability characteristics.
2. To study and compare the strength and permeability of porous concrete prepared with partial replacement of coarse and fine slag and thus achieve optimum proportion of coarse and fine slag.

III. EXPERIMENTAL WORK

A. Cement

OPC 53 grade cement used in present work and basic properties are conforming to the IS 12269(1987) requirements

SI. No	various tests conducted	Test results	Requirements as per IS 12269(1987)
1	Specific gravity	3.14	-
2	Normal consistency (%)	29	-
3	Initial setting time (sec)	124	Min 30 minutes
4	Final setting time (sec)	388	Max 600 minutes
5	Finesse test (%)	3	Not exceed 10%

TABLE 1: Basic Properties Of Cement

B. Coarse aggregate:

Normal crushed stone of maximum size 20mm was adopted and basic properties are within the limits as specified in IS: 383-1970.

Revised Manuscript Received on December 28, 2018.

Vishwanath B J, Department of Civil engineering, Malla Reddy Engineering College (A), Hyderabad, India

Dr. Rex, Department of Civil engineering, Malla Reddy Engineering College (A), Hyderabad, India

SI. No	Various tests conducted	Test results
1	Aggregate Impact Value (%)	23.2%
2	Aggregate Crushing Value (%)	24.12%
3	Specific gravity	2.69
4	Water absorption (%)	0.6%
5	Loose bulk density (kg/m^3)	1308
6	dry rodded bulk density (kg/m^3)	1526

Table 2: Physical Properties Of Coarse Aggregates

C. Fine aggregate:

Fine aggregate plays important role in porous concrete. Adding fine aggregate is responsible for permeability and strength characteristics. In present study river sand used as fine aggregate which confirming to the zone II as specified in IS: 383-1970.

SI. No	various tests conducted	Test results
1	Specific gravity	2.65
2	Water absorption (%)	1.26
3	Fineness modulus	2.8
4	Loose bulk density (kg/m^3)	1527
5	Dry rodded bulk density (kg/m^3)	1639

Table 3: Physical Properties Of Fine Aggregates

ACS – Air Cooled LD Slag:

ACS Slag was used to replace coarse aggregate in present work.

GS – Granulated LD Slag:

GS Slag was used to replace fine aggregate in present study.

SI. No	various tests conducted	Test results	
		Air cooled LD slag (coarse)	Granulated LD slag (fine)
1	Aggregate impact value (%)	10.8	-
2	Aggregate crushing value (%)	14.3	-
3	Specific gravity	3.17	3.42
4	Water absorption (%)	2.19	0.62
5	Loose bulk density (kg/m^3)	1628	1695
6	Rodded bulk density (kg/m^3)	1833	1851

Table 4: Physical Properties Of Steel Slag

D. Procedure

1. Initially the mix design for conventional porous concrete was carried out for different proportion of fine and coarse aggregate (0:100, 10:90, 15:85, 20:80, and 30:70). The optimum dosage of FA:CA for the conventional porous concrete mix, giving high strength with acceptable permeability was fixed i.e 20:80
2. Then the mix design for porous concrete was carried out for partial replacement coarse and fine aggregates with steel slag as follows,

a) Replacing only the coarse aggregate in FA:CA (20:80) mix with the air cooled LD slag in three different proportions such as 10%, 30% and 50% .i.e keeping FA-20% constant and replacing coarse aggregate by slag in 80% of CA.

b) Replacing only the fine aggregate in FA:CA (20:80) with the granulated LD slag in three different proportions such as 30%, 60% and 90% .i.e keeping CA 80% constant and replacing fine aggregate by slag in 20% FA.

Finally the mix design property in terms of strength and permeability is evaluated for the porous concrete prepared with coarse and fine slag.

E. Mix Design guidelines

Pervious concrete and the conventional concrete have the common basic elements except that it has voids in the range of 15% to 35%. The mix design was carried out using the guidelines of IS 10262:2009. In the present study volume of voids was taken as 15%.

The steps to be followed in mix design

1. Different trial mixes was carried out to fix the water cement ratio and cement content i.e. 0.35 and 370 kg/m^3 respectively.
2. Considering total volume of concrete as one unit, the total volume of aggregate is calculated by deducting the volume of paste and voids from the unit volume.
3. Volume of fine and coarse aggregate is calculated for different mixes by increasing the fine aggregate from 0 to 30%

Mix FA:CA	C (kg/m^3)	W/C	FA (kg/m^3)	CA (kg/m^3)	Ratio C:FA:CA
0:100	370	0.35	0	1614	1: 0: 4.36
10:90	370	0.35	160	1453	1: 0.43 : 3.9
20:80	370	0.35	240	1372	1:0.65:3.7
30:70	370	0.35	318	1291	1:0.86:3.5
40:60	370	0.35	477	1130	1:1.29:3.05

Table 5: Mix Proportions For Conventional Porous Concrete

C-cement FA-fine aggregate CA-coarse aggregate W/C-water cement ratio

Mix proportion CA:ACS	FA (20%)	CA+ACS (80%)		Ratio C:FA:CA:ACS
		CA	ACS	
	kg/m^3	kg/m^3	kg/m^3	
(90:10)	318	1162	154	1:0.86:3.14:0.42
(70:30)	318	904	460	1:0.86:2.44:1.24
(50:50)	318	646	766	1:0.86:1.75:2.07

Table 6: Ca Replaced By Ac Slag In 80% Of Coarse Aggregate And Keeping 20% Fine Aggregate Constant

Mix proportion FA:GS	FA+GS (20%)		CA (80%)	Ratio C:FA:GS:CA
	FA	GS		
	kg/m^3	kg/m^3	kg/m^3	
(70:30)	223	124	1291	1:0.60:0.34:3.5
(40:60)	128	247	1291	1:0.35:0.67:3.5
(10:90)	32	370	1291	1:0.09:1.00:3.5

Table 7: Fa Replaced By Gld Slag In 20% Of Fine Aggregate And Keeping 80 % Coarse Aggregate Constant

IV. TESTS CONDUCTED

A. Compression test

Test procedure was followed as per IS 516-1959 for cubes sizes 150mmx150mmx150

B.Flexural strength test

Test procedure was followed as per IS 516-1959 for beam sizes 100mmX100mmX500mm

C. Permeability Test

Constant head Permeability test was conducted on 28 days cured cylindrical moulds. The test setup prepared which simulates flow of water as same as in site condition.

- The cylindrical mould of dimensions 300mm height and 150mm diameter was casted and curing is done for 28 days for all combinations.
- The coefficient of permeability was determined by Darcy's Law equation, as given below

$$k = \frac{Q}{i \times A}$$

Where,

k = coefficient of permeability in cm/sec,

Q = quantity of water collected in time t seconds,

A = cross sectional area of specimen in cm^{2,}

i = hydraulic gradient (h/L),

D. Void Ratio Test

Void ratio was determined for cylindrical mould after 28 days curing.

$$\text{Void ratio} = \frac{\text{volume of water collected}}{\text{total volume of cylinder}} \times 100$$

FIG 1: PERMEABILITY TEST OF POROUS MOULD

V. TEST RESULTS

Mixes (FA:CA)	Compressive strength (Mpa)		Flexural strength (Mpa)		Permeability m/day	Void ratio
	7 days	28 days	7 days	28 days	28 days	28 days
0:100	11.02	14.77	1.76	2.23	372	23.42
10:90	12.89	19.73	2.01	2.53	242	12.31
15:85	14.40	23.81	2.51	3.14	220	10.34
20:80*	**18.02**	**31.03**	**2.76**	**4.42**	**203**	**9.37**
30:70	22.18	35.91	3.21	4.85	104	4.71

Table 8: Laboratory Test Results For Conventional Mixes

Mixes	Compressive strength (Mpa)		Flexural strength (Mpa		Permeability m/day	Void ratio
	7 days	28 days	7 days	28 days	28 days	28 days
CA1ACS (90:10)	18.32	27.02	2.99	3.87	203	9.08
CA2ACS (70:30)	18.90	28.68	3.35	4.21	212	9.69
CA3ACS* (50:50)	**20.56**	**30.18**	**3.56**	**4.57**	**232**	**11.23**
FA1GS (70:30)	21.04	31.97	3.37	4.27	212	9.33
FA2GS (40:60)	20.21	33.15	3.34	4.40	195	8.71
FA3GS* (10:90)	**23.32**	**38.94**	**3.95**	**4.99**	**188**	**8.01**

Table 9: Laboratory Test Results For Non Conventional Mixes (Partial Replacement Of Coarse Aggregate By Ac Slag And Fine Aggregate By Gld Slag)

VI. CONCLUSIONS

1. From conventional porous concrete it is observed that increase in the percentage of fine aggregates increases in compressive strength .i.e 0% of fine aggregates shows least strength because of high porosity. By increasing the sand content, voids get filled and forms better interlocking behavior. Higher percentage of sand gives maximum strength this is due the availability of sand for better lubrication and reduces the inter particle friction.

2. Permeability of pervious concrete is mainly depending on percentage of void ratio and compaction of specimen, which is also depending on gradation of mix adopted. Keeping the gradation same for all mixes, the percentage of void ratio varies with increase in the fine contents. Higher the void ratio higher is the permeability.

Published By:
Blue Eyes Intelligence Engineering
& Sciences Publication

From results it has been observed that permeability for all mixes ranges between 104 to 372m/day with maximum achieved for mix 0:100.and among all mixes FA:CA (20:80) showed required strength with an acceptable permeability so this considered as an optimum mix.3. From coarse slag and fine slag replacement, compressive strength of non conventional porous concrete increased as the percentage of AC slag (10%, 30%, and 50%) which is replaced in 80% of coarse aggregate and GLD slag (30%, 60% and 90%) replaced in 20% of fine aggregate and permeability increased as the percentage of AC slag increase (10%, 30% and 50%),it is because AC slag is porous in nature . but in another case i.e replacement of GLD slag (30%, 60% and 90%) the permeability value get decreased due to formation of slurry which results in the reduction of voids. Therefore to minimize this slurry w/c ratio should be balanced.

REFERENCES

1. Tennis,P,O, Lemming,M L and Akers,D J "Pervious concrete pavements", Special publication by the Portland cement association and the National Ready mixed concrete association , 2004.
2. Ghafoori,N,Dutta.S. "Laboratory investigation of compacted No fines concrete for paving materials". Journal of material in civil engineering vol 7, no 3,183-191, 1995.
3. Darshan S. Shah, Prof. J.R. Pitroda, "Pervious Concrete: New Era for Rural Road Pavement", (IJETT) Vol: 4, August 2013.
4. Wang K, Schaefer V R, Kevern J T and Suleiman M T. "Development of Mix Proportion for Functional and DurablePervious Concrete", Submitted to Concrete Technology Forum-Focuson Pervious Concrete, National Ready Mix Concrete Association,Nashville, TN, May 24-25, 2006, pp. 1-12.
5. PraveenkumarPatil and Santosh M Murnal, "Study on the Properties of Pervious Concrete" International Journal of Engineering Research & Technology (IJERT) ISSN: 2278-0181, Vol. 3 Issue 5, May – 2014, pp.819-822.
6. Yang,J, Jiang,G, "Experimental study on properties of pervious concrete pavement materials," Cement and Concrete Research,Vol.33 pergamon,2003.
7. Richard C Meininger, "No-Fine Pervious Concrete for Paving",Concrete International, vol.10, 1988, pp. 20-2
8. Guo, Peng Tang, Boming Zhu, HongzhouFeng, Min Zhang, Yibo. "Pavement performance of steel slag pervious concrete" International Conference on Transportation Engineering (ICTE), Chengdu, China, July-2011, pp. 1654-1659.

Strength and Durability Aspects of Bacterial Concrete

J.Rex, J.Selwyn Babu, S.Pooja Sri Reddy

Abstract- Concrete is a very essential factor among creation materials that is widely been in use in infrastructure. Despite of its vital usage for production functions, it nevertheless has numerous obstacles. It is expected that production of cement alone contributes to approximately 7% of world anthropogenic CO2 emissions that is accountable for green residence effect resulting in worldwide warming. The most important disadvantage of concrete is its low tensile electricity due to which micro crack occurs whilst the burden carried out is more than its limit and this paves way for the seepage of water and other salts. This initiates corrosion and makes the whole structure vulnerable and leads to the failure of shape. To remediate this sort of failure due to cracks and fissures, an approach of the usage of bio mineralization in concrete has advanced in latest years. The concrete building structures have enormous sturdiness problems owing to the special physiological and environmental conditions and it outcomes to irrevocable harm to the huge building structure and ultimately discount within the strength and power of concrete building structure. The essential cause behind the downgrading in the current years MICCP (microbiologically and eco-friendly triggered calcium carbonate precipitation process) by the bacteria is taken into consideration as a surroundings pleasant methodology to decorate the properties of huge and strong concrete, also for the overhauling of concrete structural articles and to consolidate them as the most unique construction materials with well diversified and imperative properties. This publication gives a observe is carried out to test the Compressive strength, Split tensile electricity, Flexural strength and sturdiness of bacterial inclusive concrete through using three one of a kind varieties of bacteria with various dosages like 0ml, 5ml, 10ml, 15ml, 20ml for the M30 and M40 Grade concrete.

Keywords: Bacterial concrete, strength, durability, concrete

I. INTRODUCTION

Concrete is an adaptable fabric having lower ductile and shear first-class. Essentially, concrete is fragile material and carries a terrific many smaller scale breaks show inside the body. The flexibility of cement is fairly steady at low emotions of hysteria however starts diminishing at better emotions of hysteria as network begins splitting. Concrete has a low coefficient of heat extension, and as it develops stable psychologists. Every stable shape will spoil to a few diploma, due to shrinkage and stress. Solid which is subjected to lengthy-span powers is willing to move slowly. Presently not unusual and pretend strands are utilized to beautify execution and amplify the inability of cement for elite. The regular problem located in structures is Crack.

Objectives of the study:

The main objective is divided in to following sub objectives:

1. To explore the variation of compressive strength of the presccribedconcrete with bacteria for M30 and M40 Grade concrete.
2. To study the split tensile strength, flexural strength of concrete
3. To study the durability of concrete by using Bacteria
4. To create self-healing property.
5. To reduce the maintenance repair cost.

II. LITERATURE REVIEW

Dr. S. Siddiraju, N. Ganesh Babu., et al.(2015)

From the research it became presumed that Compressive first-rate of 5% Bacterial mixture considerably increments to 2.63% while contrasted and Control mixture. Compressive best of 10% Calcium lactate increments to 2.63% whilst contrasted and Control combo. Past 10% of Calcium lactate there's 20.80% diminishing in compressive fine of cement.

Meera C. M and Dr .Subha. V2

They have disbursed a publication on the elevated Strength and high Durability appraisal Of Bacteria Based Self-Healing and organic Concrete structures It has also been tested approximately the effect of Bacillus subtilis species JC3 at the exceptional and energy of cement. Three-D shapes of sizes 150mm x 150mm x 150mm and chambers with a distance across of 100mm and a stature of 200mm with and without expansion of small scale residing beings, of M20 model assessment concrete has been utilized for the purpose of test.

III. MATERIALS AND MIX DESIGN

Cement: Cement is a building block fastener, a mixe of substance used underway that built ingadgets and solidifies and may tie together different materials collectively after setting in order to provide strength. For this study cement of OPC 53 Grade was used for testing.

Aggregates- Development of aggregates, or absolutely "mixture", is a fantastic underway, along with sand particles, rocky pieces, overwhelmed stones, semi-solid slag, and recycled pieces of concrete matter and geo-fake totals. These totals are the maximum mined materials within the global environment of the respective locality.

Coarse aggregate -

For this study size of coarse aggregates of 20mm was used with

Specific gravity = 2.98

Fineness modulus = 7.5

Revised Manuscript Received on December 08, 2018.

J.Rex, Associatate Professor, Malla Reddy Engineering College (Autonomous), Hyderabad,Telangana, India

J.Selwyn Babu, Professor, Malla Reddy Engineering College (Autonomous), Hyderabad, India

S.Pooja Sri Reddy, PG Student, Malla Reddy Engineering College (Autonomous), Hyderabad,Telangana,India

Fine aggregate- Shimmering sand particles available handy in the local vicinity, detached from ordinary test quantity is explored here. The outcome of sifter evaluation sustains it to Zone-II (in advance with IS: 383-1970).The checks are performed and outcomes are tested as follows.

- Evaluated Specific gravity = 2.3
- Estimated Fineness modulus = 3.06

Water- Generally potable water ought to be used.

Bacteria

Bacillus Pasteurii- Bacillus pasteurii previously referred to as Sporosarcina pasteurii. Pasteurii has been proposed to be utilized as a obviously strong organic improvement material.

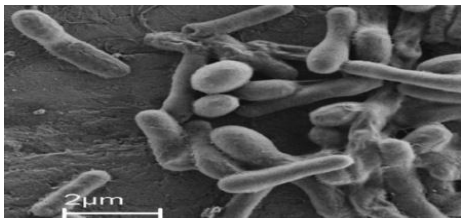

Bacillus pasteurii

Bacillus Subtilis- Initially named vibrio subtilis in 1835, Bacillus subtilis microscopic organisms were one of the main microbes to be examined. These microbes are a decent model for cell advancement and differential (Entrez Genome Project).

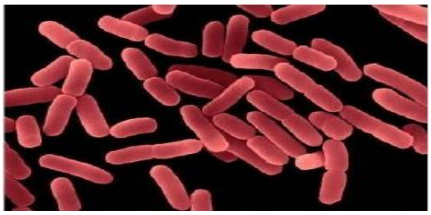

Bacillus subtilis

Bacillus Sphaericus-

Lysinibacillus sphaericus (renamed - beforehand known as Bacillus sphaericus). It can frame safe endospores that are tolerant to high temperatures, synthetic concoctions and bright light and can stay practical for extensive stretches of time.

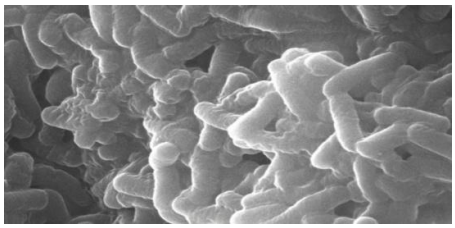

Bacillus sphaericus

MIX DESIGN OF CONCRETE

For M30 Grade Concrete is 0.50 : 1 : 1.86 : 2.89

For M40 Grade Concrete is 0.40 : 1 : 1.35 : 2.65

IV. EXPERIMENTAL INVESTIGATION

Mixing of Concrete:

The concrete is to be mixed by hand or by the utilization of research center cluster blender so as to keep away from misfortune in water and different materials

Concrete Mixer

Mixing the concrete

V. WORKABILITY TESTS

Workability of concrete depicts the simplicity or trouble with which the concrete is taken care of, transported and placed between the structures with least loss of homogeneity.

VI. PREPARATION OF CONCRETE CUBES

MOULDS

Moulds to be used for casting of cubes are commonly fabricated from metals like solid iron or metal, sturdy sufficient to save you the distortions. The moulds must facilitate smooth elimination of cubes when preliminary energy is attained. The dimensions and the internally set faces are required to be accurate and precise inside the following prescribed limits.

The height of the mildew and the gap among the opposite's faces are of precise length ±0.2mm, the angle between the adjoining internally settled faces and pinnacle and backside plates of the built in molds to be 90+0.50 approximately. The interiorly settled and formed faces of the mold are aircraft surfaces with permissible versions o.03mm.Each mildew is furnished with a steel base plate having aircraft surface.

Preparation of Concrete cube

Compaction

As soon as the integration is completed, test specimens are to be organized in this sort of manner to produce complete compaction. The concrete is stuffed into the mould inside the layers about 5cm deep.

VII. CURING

That test specimen will be stored on the web site from wherein vibrations, under damp matting state of affairs, sacks/materials with similar composition for a time period of about 24 hours from the time of addition of required water to the alternative constituents. The temperature of the local vicinity of the garage shall be in the range varying from 22º C and 32 ºC. Once the 24 hours is completed, they will be marked for later documentation, eliminated from the experimented moulds checked out, re saved in clean distilled water at a temperature of 24º C to 30 ºC until they are transported to laboratory locations for destiny tests.

VIII. TESTING OF CONCRETE

Tests procedure on fresh concrete

1. Slump cone process test
2. Compaction factor ratio test

Tests to be conducted on Hardened concrete

1. Compressive strength
2. Split tensile strength
3. Flexural strength
4. Durability extent test
5. Healing process steps of concrete

IX. RESULTS AND ANALYSIS

Slump cone test

	M30 Grade Concrete			M40 Grade Concrete		
% Bacteria used	Bacillus Pasteurii	Bacillus Subtilis	Bacillus sphaericus	Bacillus Pasteurii	Bacillus Subtilis	Bacillus sphaericus
0ml	25	25	25	28	30	30
5ml	27	28	30	35	35	33
10ml	30	35	33	40	40	38
15ml	35	38	40	45	43	40
20ml	40	42	45	50	45	45

Compaction factor test

	M30 Grade Concrete			M40 Grade Concrete		
% Bacteria used	Bacillus Pasteurii	Bacillus Subtilis	Bacillus sphaericus	Bacillus Pasteurii	Bacillus Subtilis	Bacillus sphaericus
0ml	0.94	0.92	0.9	0.92	0.9	0.9
5ml	0.92	0.88	0.86	0.84	0.86	0.88
10ml	0.9	0.84	0.82	0.8	0.84	0.84
15ml	0.84	0.8	0.78	0.76	0.8	0.8
20ml	0.82	0.76	0.74	0.74	0.76	0.74

Compressive strength of concrete

For M30 Grade Concrete

		M30 Grade Concrete								
S.no	Bacteria used	Compressive strength of concrete by using Bacillus pasteurii			Compressive strength of concrete by using Bacillus subtilis			Compressive strength of concrete by using Bacillus sphaericus		
		7days	14days	28days	7days	14days	28days	7days	14days	28days
1	0ml	19.8	26.6	29.4	19.8	26.6	29.4	19.8	26.6	29.4
2	5ml	20.4	27.2	30.24	20.8	27.1	29.84	20.44	27.26	29.92
3	10ml	20.64	27.46	30.48	20.98	27.36	30.06	20.66	27.52	30.54
4	15ml	20.46	27.3	30.26	20.86	27.3	29.98	20.6	27.44	30.4
5	20ml	20.34	27.16	30.12	20.68	27.14	29.64	20.42	27.22	30.28

For M40 Grade Concrete

		M40 Grade Concrete								
S.no	Bacteria used	Compressive strength of concrete by using Bacillus pasteurii			Compressive strength of concrete by using Bacillus subtilis			Compressive strength of concrete by using Bacillus sphaericus		
		7days	14days	28days	7days	14days	28days	7days	14days	28days
1	0ml	25.6	35.8	39.38	25.6	35.8	39.38	25.6	35.8	39.38
2	5ml	26.1	36.14	39.56	26.22	36.24	39.68	26.32	36.46	39.78
3	10ml	26.68	36.44	40.2	26.92	36.52	40.52	27.04	36.64	40.72
4	15ml	26.02	36.26	40.06	26.84	36.26	40.44	27.18	36.74	40.4
5	20ml	25.86	35.88	39.92	26.66	36.04	40.12	26.86	36.52	40.18

Split tensile strength of concrete

For M30 Grade Concrete

S.no	Bacteria used	Split tensile strength of concrete by using Bacillus pasteurii		Split tensile strength of concrete by using Bacillus subtilis		Split strength of concrete by using Bacillus sphaericus	
		14days	28days	14days	28days	14days	28days
1	0ml	5.68	6.24	5.68	6.24	5.68	6.24
2	5ml	5.72	6.46	5.92	6.72	5.88	6.68
3	10ml	5.86	6.74	6.1	6.92	6.04	6.88
4	15ml	5.76	6.52	5.96	6.8	5.9	6.7
5	20ml	5.62	6.4	5.84	6.64	5.8	6.5

For M40 Grade Concrete

S.no	Bacteria used	Split tensile strength of concrete by using Bacillus pasteurii		Split tensile strength of concrete by using Bacillus subtilis		Split strength of concrete by using Bacillus sphaericus	
		14days	28days	14days	28days	14days	28days
1	0ml	5.94	6.24	5.94	6.24	5.94	6.24
2	5ml	6.12	6.44	6.16	6..28	6.2	6.3
3	10ml	6.26	6.78	6.26	6.34	6.32	6.38
4	15ml	6.14	6.62	6.1	6.22	6.18	6.26
5	20ml	6.08	6.54	5.94	6.08	6.04	6.12

Flexural strength of concrete

For M30 Grade Concrete

S.no	Bacteria used	Flexural strength of concrete by using Bacillus pasteurii		Flexural strength of concrete by using Bacillus subtilis		Flexural strength of concrete by using Bacillus sphaericus	
		14days	28days	14days	28days	14days	28days
1	0ml	4.46	5.12	4.46	5.12	4.46	5.12
2	5ml	4.62	5.2	4.96	5.22	4.88	5.2
3	10ml	4.84	5.36	5.26	5.34	5.28	5.4
4	15ml	4.74	5.22	5.16	5.24	5.1	5.26
5	20ml	4.6	5.04	5.04	5.12	5.08	5.16

For M40 Grade Concrete

S.no	Bacteria used	Flexural strength of concrete by using Bacillus pasteurii		Flexural strength of concrete by using Bacillus subtilis		Flexural strength of concrete by using Bacillus sphaericus	
		14days	28days	14days	28days	14days	28days
1	0ml	4.68	5.24	4.68	5.24	4.68	5.24
2	5ml	4.84	5.34	4.96	5.62	4.94	5.58
3	10ml	4.98	5.48	5.06	5.84	5.08	5.94
4	15ml	4.88	5.26	4.96	5.72	5.04	5.68
5	20ml	4.62	5.12	4.72	5.56	4.68	5.48

Durability

Acid attack

% Loss of weight

	M30 Grade Concrete			M40 Grade Concrete		
% Bacteria used	Bacillus Pasteurii	Bacillus Subtilis	Bacillus sphaericus	Bacillus Pasteurii	Bacillus Subtilis	Bacillus sphaericus
0ml	0.82	1.24	1.24	1.16	1.24	1.38
5ml	0.94	1.36	1.38	1.32	1.38	1.54
10ml	1.2	1.58	1.58	1.48	1.52	1.74
15ml	1.44	1.82	1.72	1.86	1.88	1.98
20ml	1.6	1.98	1.98	2.04	1.98	2.2

Published By:
Blue Eyes Intelligence Engineering
& Sciences Publication

% Loss of compressive strength

	M30 Grade Concrete			M40 Grade Concrete		
% Bacteria used	Bacillus Pasteurii	Bacillus Subtilis	Bacillus sphaericus	Bacillus Pasteurii	Bacillus Subtilis	Bacillus sphaericus
0ml	6.64	7.12	7.12	6.72	7.24	7.12
5ml	7.4	7.32	7.68	6.98	7.38	7.34
10ml	7.8	7.64	8.24	7.14	7.58	7.62
15ml	8.4	8.14	8.8	7.34	7.84	7.98
20ml	9.2	8.54	9.3	7.84	8.12	8.16

Alkaline attack

% Loss of weight

	M30 Grade Concrete			M40 Grade Concrete		
% Bacteria used	Bacillus Pasteurii	Bacillus Subtilis	Bacillus sphaericus	Bacillus Pasteurii	Bacillus Subtilis	Bacillus sphaericus
0ml	1.2	1.32	1.46	1.34	1.36	1.56
5ml	1.44	1.48	1.58	1.46	1.48	1.76
10ml	1.6	1.64	1.72	1.58	1.66	1.88
15ml	1.84	1.88	1.88	1.78	1.84	1.98
20ml	1.96	2.04	2.14	1.96	2.2	2.18

% Loss of compressive strength

	M30 Grade Concrete			M40 Grade Concrete		
% Bacteria used	Bacillus Pasteurii	Bacillus Subtilis	Bacillus sphaericus	Bacillus Pasteurii	Bacillus Subtilis	Bacillus sphaericus
0ml	8.23	9.14	9.64	8.54	9.28	9.14
5ml	8.68	9.38	9.72	8.98	9.46	9.38
10ml	8.42	9.64	9.98	9.34	9.82	9.64
15ml	9.1	9.84	10.18	9.68	10.14	9.84
20ml	9.62	9.96	10.38	9.98	10.26	9.96

Sulphate attck

% Loss of compressive strength

	M30 Grade Concrete			M40 Grade Concrete		
% Bacteria used	Bacillus Pasteurii	Bacillus Subtilis	Bacillus sphaericus	Bacillus Pasteurii	Bacillus Subtilis	Bacillus sphaericus
0ml	12.66	13.24	13.62	12.66	14.12	13.68
5ml	12.98	13.66	13.74	12.98	14.36	13.98
10ml	13.4	14.12	13.96	13.4	14.84	14.32
15ml	12.6	14.54	14.16	12.6	15.04	14.88
20ml	13.6	14.88	14.46	13.6	15.22	15.18

Healing of concrete


The crack made in the Concrete Cube made up of **Bacillus Subtilis**

The crack on the concrete Cube made up of **Bacillus Subtilis** after allowed for Self healing


The crack made in the Concrete Cube made up of **Bacillus Subtilis**

The crack on the Concrete Cube made up of **Bacillus subtilis** after allowed for Self-healing

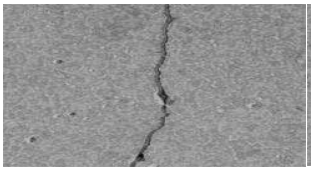
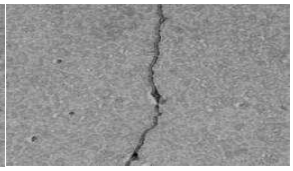

The crack made in the Concrete Cube made up of **Bacillus Pasteurii**

The crack on the Concrete Cube made up of **Bacillus Pasteurii** after allowed for Self healing


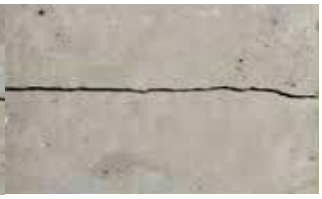

The fig shows the crack made in the Concrete Cube made up of **Bacillus Pasteurii**

The crack on the Concrete Cube made up of **Bacillus Pasteurii** after allowed for Self healing

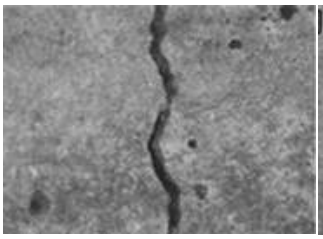
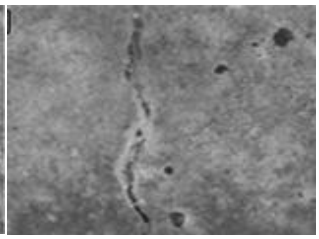

The crack made in the Concrete Cube made up of **Bacillus Sphaericus**

The crack on the Concrete Cube made up of **Bacillus Sphaericus** after allowed for Self healing


The crack made in the Concrete Cube made up of **Bacillus Sphaericus**

The crack on the Concrete Cube made up of **Bacillus Sphaericus** after allowed for Self healing

X. CONCLUSIONS

From the above investigational study the following inferences were made

1. The value slump increases with increasing the bacteria content in concrete. Whereas the value of compaction factor decreases with increasing the bacteria content in concrete.

2. Initially the values of ultimate compressive strength, Ultimate split tensile strength and Ultimate flexural strength of bacterial concrete increases up to 10ml bacteria content after that the value of compressive strength gradually decreases with proportionate increase in the bacteria content in concrete the optimum value of strength of bacterial concrete was observed at 10ml bacteria.
3. In case of durability by using acid attack and alkalinity attack and sulphate attack the values of percentage lose of weight and percentage lose of strength increases with increase in the bacteria content in all the cases.
4. Bacterial concrete also drastically inspired the durability characteristics of the shape via healing of cracks within the structure. Due to its natural inherent capacity to precipitate the colloidal calcite continuously bacterial concretes is also renowned as a 'Smart Bio fabric'.
5. Due to its green and self-recovery capability it's been proved to be better than the traditional concrete. Bacterial concrete will soon be evolved in constructing of long lasting, fee powerful and surroundings friendly.

So the optimal value of strength was observed at 10ml of Bacteria for M30 Grade concrete material and M40 Grade concrete block.

REFERENCES

1. Dr.S.Siddiraju,N.GaneshBabu,"Lead of Bacterial Concrete", International Journal of Science & Research (IJSR), Volume 5, Issue : 8, August 2016.
2. Chithra P, Bai Shibi Varghese “A check examination on the first class homes of fly cinder based totally bacterial stable” International Journal of Innovative Research in Advanced Engineering (IJIRAE)ISSN:2349-2763 Issue 08, Volume 3 (August 2016).
3. V Srinivasa Reddy, M V Seshagiri Rao, S Sushma “Attainability Study on Bacterial Concrete as an ingenious self cut up recuperating framework” Universal Journal of Modern Trends in Engineering and Research,
4. Akina Najmuddin Saifee, Divya Maheshbhai Chap, Jayesh Rameshbhai Juremalani “ Essential exam on Bacterial Cement”, IJRDO-Diary Of Mechanical And Structural Building,
5. Meera C.M, Dr.Subha V “Quality and Sturdiness assessment Of Microscopic organisms Based Self Mending Concrete”. IOSR Diary of Mechanical and Structural Building.
6. Ravindranatha,N, Kannan, Likhit M.L. “Self patching fabric bacterial strong”, Worldwide Diary of Exploration in Building and Innovation.
7. A.T.Manikandan, A.Padmavathi. “An Experimental Investigation on Improvement of Concrete Serviceability by means of using Bacterial Mineral Precipitation.
8. Jagadeesha Kumar BG, R Prabhakara, Pushpah “Impact Of Bacterial Calcite Precipitation On Compressive Strength Of Mortar Cube”, International Journal of Engineering and Advanced Technology(IJEAT),
9. RA.B.Depaa and T.Felix Kala , “Experimental Investigation of Self Healing Behavior of Concrete utilizing Silica Fume and GGBFS as Mineral Admixtures” Indian Journal of Science and Technology.

A Study on Soil Stabilization using Sugarcane Bagasse Ash

K.Shimola

Abstract*: Soil is the base of a structure which helps in equally distributing the load and supports the super structure and foundation. If the soil stability is not adequate then failure of structure takes place in form of settlement,cracks. Black cotton soil are also called as expansive soils which is is responsible for such situations and is due to presence of mineral called montmorillonite in it, which experience shrinkage and swelling. To overcome this properties of soil are improved by mechanical and chemical process known as soil stabilisation. Many research has been conducted for stabilisation of soil by using cementing, chemical materials like flyash,calcium chloride, sodium chloride etc. In India, limited techniques are followed in agricultural waste disposal. India is second largest country in the production of sugarcane with 341,400 thousand metric annual tones(TMT) produce.Western Maharastra is pioneer in production of sugarcane in large quantities sugar cane factories produce waste after extraction of sugarcane juice in machines and that waste after burning produce ash known as bagasse ash. It is made up of fibrous material having silica and puzzolonic in nature which improves the physical properties of black cotton soil. Experiments are conducted on black cotton soil by partially replacing bagasse ash (4%,8%,12%,16%,20%). Black cotton soil properties of are increased at 16 % by replacing of bagasse ash not including any chemicals.

Index Choice: Soil Stabilisation, Black Cotton Soil, Bagasse Ash, Unconfined Compression Test, Maximum Dry Density)

I. INTRODUCTION

Soil adjustment is the change of soil to improve their physical properties. Adjustment can build the shear quality of soil or potentially control the swell properties of the soil, in this way enhancing the heap cost by making best utilization of locally accessible materials. One of the more typical techniques for adjustment incorporates the blending of characteristic coarse grained soil and fine grained soil to get a blend that creates sufficient interior grinding and union and along these lines gives a material that is workable amid situation. Reworking of soil particles by some of mechanical compaction is alluded as "Mechanical Stabilization". Utilization of solidifying material, for example, bond, lime, bitumen/black-top and so on is added to soil is "Establishing Stabilization" and utilization of chemicals in soil, for example, sodium chloride and calcium chloride added to soil is called compound adjustment. [1]studied the 'Agricultural wastes as soil stabilizers'. The weak sub grade soil is stabilised by sugar cane bagasse ash a agricultural waste. The weak sub grade soil is treated using bagasse ash of 0%, 3%, 6%, 9%, 12%and 15%. CBR test is carried out for each percentage. The results of these tests showed improvement in CBR value with the increased values of percentage of bagasse ash.

Late innovation has expanded the quantity of customary added substances utilized for soil adjustment purposes. Such non-conventional stabilizers include: Polymer based items (e.g. cross-connecting water-based styrene acrylic polymers that altogether enhances the heap bearing limit and elasticity of treated soils), Copolymer Based Products, fiber support, calcium chloride, and Sodium Chloride. Strength and durability of a soil is attained maximum improving the characteristics of foundation soils. Differential expansion and shrinkage changes the moisture content of many soils. Many soil crumble when they subject to moving loads. Reduction in volume and strengthening to the point where they can carry the imposed load is significant even when the soil is saturated. Treatment of soil, which makes it more stable, refers to stabilization. Availability cost and proposes of using the stabilized soil mixture is determined by type and degree of stabilization. This makes the effective utilization of local materials and simultaneously reduces the cost. [4] had studied the effects of bagasse ash on compressive strength of lime stabilized black cotton soil.

The highest CBR value was obtained at 8 % lime and 4% bagasse ash combination. [3] had studied the result of adding bagasse ash (upto 10%) on wL, wP, IP, sL, Shrinkage index (sI), Free Swell Index, Ps. There was a decrease in all these values with increase in % of bagasse ash. The most important types of soil stabilization are Mechanical, Chemical, Polymer/alternative.

Mechanical type is one of the oldest types of soil stabilization which involve in physically changing the property of the soil impacting its gradation, solidity, and other characteristics. Dynamic compaction is another type; in this a heavy weight is dropped continually onto the ground at regular intervals to ensure a uniformly packed surface.

[2] had found that the bagasse ash and lime controls consolidation characteristics of expansive soil more effectively than the bagasse ash alone. All of these methods rely on adding admixtures to the soil that will change its properties and physically interacts also. Polymers and eco friendly materials have number of significant advantages over traditional methods. They are cheaper and more effective than traditional methods. Eco friendly materials are significantly less dangerous for the environment than many chemical solutions.

Revised Manuscript Received on December 28, 2018.

Dr. K. Shimola, Associate Professor, Civil Engineering Department, Malla Reddy Engineering College (Autonomous), Secunderabad, Telangana, India

The main objective is to assess the quality attributes of dark cotton soil for various extents of bagasse powder in substitution of 4%, 8%, 12%, 16%and 20%.

II SOIL STABILIZATION MATERIALS

A. Soil stabilization using cement

Soil cement is the product of soil stabilized with cement. During hydration reaction, the cementing action takes place by the chemical reactions of cement with siliceous soil. Nature of soil content, conditions of mixing, compaction, curing and admixtures are the important factors affecting the soil-cement. For different types of soils appropriate amounts of cement should be provided. They are as follows Gravel – 5 to 10%, Sand – 7 to 12%, Silt – 12 to 15%, and Clay – 12 – 20%.

B. Soil Stabilization using Lime

Heavy plastic clayey soils and Sandy soils can be treated effectively with Slaked lime. Cement, bitumen or fly ash can be used with the combination of Lime.

C. Soil stabilization with bitumen

Pavement construction is made by bituminous materials like bitumen Asphalts and tars. Sand bitumen stabilization, Soil Bitumen stabilization, Oiled earth are different types of bitumen available.

A substance when added to a soil, it follows both cohesion and reduced water absorption depending on the nature of soils.

D. Chemical stabilization of soil

Calcium chloride is able to absorb and hold moisture in soil bases and surfacing which are stabilized mechanically. compaction and soil flocculent can be done by Calcium chloride. Frequent application of calcium chloride plays a vital role in make up for the chemical losses by leaching action. The relative humidity of the atmosphere should > 30% for the salt to be effective.

E. Soil stabilization by electrical methods

An expensive method called electro-osmosis method is performed by electrical stabilization of clayey soils of soil stabilization and very useful for drainage of cohesive soils.

F. Soil stabilization by grouting

In this method, stabilizers are injected into the soil. The main limitations of this method are, it is not applicable for clayey soils because of their low permeability and expensive also. Various grouting techniques are classified and these methods are suitable for stabilizing zones buried zones to certain extent limit.

The Various types of grouting techniques are Clay grouting, Chemical grouting, Chrome lignin grouting, Polymer grouting and Bituminous grouting

G. Soil stabilization using fabrics and Geotextiles

Geotextiles are made up of synthetic materials such as polyvinyl chloride, polyester polyethylene, nylons. They are porous fabrics and classified into different types like woven, non-woven and grid form. Geotextiles also yield high strength to soil.

III. BLACK COTTON SOIL AND SUGAR CANE BAGASSE ASH

Black cotton soil is exceptionally troublesome and risky and perilous because of its attributes. The dark cotton soil is hard when dry yet loses its quality totally when in wet condition. The dark cotton soils have low quality and are vulnerable to unnecessary volume changes, making their utilization for development purposes exceptionally troublesome. All the Black cotton soils are not attaining soils and all the broad soil are not Black in shading. These dirts had high quality in summer and diminished quickly in winter. Swelling and shrinkage of sweeping soil cause respectful settlement bringing about serious harm to the establishment, structures, streets, holding structures and trench linings. Bagasse is a deposit acquired from the consuming of bagasse in sugar creating manufacturing plants. Bagasse is the cell sinewy waste item following the extraction of the sugar juice from stick plants. It is as of now utilized as a bio fuel and in the fabricate of mash and paper items and building materials. For every 10 tons of sugarcane squashed, a sugar processing plant creates almost 3 tons of wet bagasse a side-product of the sugar stick industry. At the point when this bagasse is scorched the resultant fiery debris is bagasse powder. Western Maharashtra is having greatest number of sugar industrial facilities, these processing plants faces a transfer issue of expansive amount bagasse. The requirement for soil stabilization are to increment the quality of soil, Control of psychologist and swell properties of soil, to bring down the compressibility of soil and in this manner decrease the settlement when structures are based on it, to increment toughness, to influence soil to water sealing.

IV METHODOLOGY

The methodology involves series of steps.

1. Procurement of materials
2. Preparation of soil sample
3. To conduct test on the prepared soil sample to calculate soil sample.
4. To treat the soil sample with proportions of bagasse ash
5. To conduct test on bagasse ash treated sample

A. Procurement of material

1) Black cotton soil

The soil procured from Maisammaguda is used as sample. The soil was collected at depth of 1m below ground level.

2) *Sugarcane Bagasse Ash*

the sugarcane bagasse is collected from sugarcane juice sellers in Maisammaguda.The bagasse was dried in sunlight for 24 hours and burnt to get ash. Ash formed was collected and sieved using 425 micron sieve to get fine powdered ash.

3) *Preparation of Soil Sample*

The black cotton soil is spread and is beaten to remove lumps.The soil is sieved through 2.36 mm sieve is stored in container.

Published By:
Blue Eyes Intelligence Engineering
& Sciences Publication

4) *Tests Conducted on Soil Sample*

- Atterbergs limits
- Standard proctor test
- Unconfined compression test

5) *Treatment of Soil Sample with Different Proportions of Bagasse Ash*

Bagasse ash is added to soil in proportions of 4%, 8%,12%and 16% and tests are conducted Stabilising agent: bagasse ash.

6) *Standard Proctor Compaction Test*

Compaction is the procedure of minimizing air voids in soil. Dry thickness establishes the compaction level. Dry thickness and the ideal water content are obtained from the wet soil sample blend.

B) Unconfined Compression Test

The unconfined pressure test is by a wide margin the most well known technique for soil shear testing since it is one of the quickest and least expensive strategies for estimating shear quality. The strategy is utilized essentially for immersed, firm soils recouped from thin-walled testing tubes. The unconfined pressure test is unseemly for dry sands or brittle muds in light of the fact that the materials would go into disrepair without some place where there is parallel imprisonment. The reason for this test is to decide the unconfined compressive quality of the dirt.

V RESULTS AND DISCUSSIONS

As the black cotton soil is collected from the foundation, the original water content was high. The soil was tested for liquid limit, plastic limit, compaction test and unconfined compression test. The following are the results of the original and sugar cane bagasse added soil are as below

A) Original Soil Results

1) liquid limit

Liquid limit	**%**
Liquid limit of original soil sample	50.2%
Liquid limit of soil sample with 4% bagasse ash	40%
Liquid limit of soil sample with 8% bagasse ash	26%
Liquid limit of soil sample with 12% bagasse ash	20%
Liquid limit of soil sample with 16% bagasse ash	42.2%
Liquid limit of soil sample with 20% bagasse ash	62.1%

Table.I Liquid limit result

2) Plastic Limit

Table.II Plastic limit result

Plastic limit	**%**
Plastic limit of original soil sample	33.33%
Plastic limit of soil sample with 4% bagasse ash	75%
Plastic limit of soil sample with 8% bagasse ash	50%
Plastic limit of soil sample with 12% bagasse ash	33.33%
Plastic limit of soil sample with 16% bagasse ash	50%
Plastic limit of soil sample with 20% bagasse ash	33.33%

3) *Plasticity Index*

Plasticity index	**%**
Plasticity index of original soil	16.87%
Plasticity index of soil sample with 4% bagasse ash	35%
Plasticity index of soil sample with 8% bagasse ash	24%
Plasticity index of soil sample with 12% bagasse ash	13.33%
Plasticity index of soil sample with 16% bagasse ash	7.8%
Plasticity index of soil sample with 20% bagasse ash	28.8%

Table.III Plasticity index

By the above values of the plasticity index, we can conclude that the optimum dosage of add admixture (bagasse ash) is 16% to the weight of soil. As clayey soil has high plasticity and that can be a problem in the field of construction. So stabilizing it with bagasse ash of 16% of its weight can give the desired strength to the soil.

B) Compaction Test

Original soil sample

The optimum moisture content is 17.4%

The maximum dry density obtained is 1.705gm/cu.c

Results with bagasse ash

% of bagasse ash	**Optimum moisture content**	**Maximum dry density**
4%	16.38	1.56
8%	15.9	1.59
12%	14.7	1.62
16%	9.09	1.73
20%	12.2	1.63

Table.IV Compaction test result with bagasse ash

By the above values of the compaction test, It is concluded that the optimum dosage of add admixture (bagasse ash) is 16% to the weight of soil. As clayey soil has high water content and that creates problem in the field of construction. So stabilizing it with bagasse ash of 16% of its weight can give the desired strength to the soil.

C) Unconfined Compression Test Results

Original soil

The unconfined compressive strength is 0.241 N/ mm^2

The shear strength for this soil is 0.1205 N/ mm^2

Published By:
Blue Eyes Intelligence Engineering
& Sciences Publication

Soil with Bagasse Ash

% of bagasse ash	Unconfined compressive strength	Shear strength
4%	0.362	0.181
8%	0.439	0.2195
12%	2.482	1.2141
16%	4.355	2.1775
20%	3.453	1.726

Table.V Unconfined compression test results

By the above values of the unconfined compression test, we can conclude that the optimum dosage of add admixture (bagasse ash) is 16% to the weight of soil. As clayey soil is weak and causes problem in the field of construction. So stabilizing it with bagasse ash of 16% of its weight can give the desired shear strength to the soil.

VI CONCLUSION

Soil stabilization method can increase the strength of black cotton soil. In our project the following results are obtained:

- At 16% dosage of bagasse ash the plasticity index reduced from **16.87%** to **7.8%** which is desirable for construction site
- The maximum dry density improved from **1.705 gm/cc** to **1.73 gm/cc** at **16%** dosage of bagasse ash
- The unconfined compressive strength increased from **0.241 N/ cm^2** to **4.355 N/cm^2** at **16%** dosage of bagasse ash
- The shear strength improved from **0.1205 N/cm^2** to **2.177 N/cm^2** at **16%** of bagasse ash

REFERENCES

1. Chittaranjan, M., Vijay, M., Keerthi, D. (2011). Agricultural wastes as soil stabilizers. Int. Journal of Earth Sci. and Eng. 4(6), pp. 50-51.
2. Gandhi, K.S. (2012) "Expansive Soil Stabilization using Bagasse Ash," International Journal of Engineering Research and Technology, 1(5), 1-3.
3. Manikandan, A. & Moganraj, M. 2014, 'Consolidation and Rebound Characteristics of Expansive Soil by Using Lime and Bagasse Ash', International Journal of Research in Engineering and Technology, vol. 03, no. 04, pp. 403-11.
4. Osinubi, K. J. (2000). "Influence of compaction energy levels and delays on cement treated Soil." Nigerian Society of Engineers Technical Transactions, Vol. 36, No. 4, pp 1 – 13.

Microstructural and Hardness Behavior of AL/B_4C/h-BN Hybrid Composites Prepared By Powder Metallurgy Method

Katla Rajendar, K. Eswaraiah, Anil Kumar Bodukuri, Sampath.V

Abstract: ***The proceedings of this presentations enables us to explore the effect of B_4C and h-BN particles on Aluminum based metal matrix composites (AL MMCS).The composites were fabricated with different reinforcement percentages of h-BN and B_4C in aluminum using powder metallurgy technique. To obtain homogenous mixture between the powders, for small duration of milling, attrition mill is adopted. The powders were then compacted to optimal compaction pressure and sintered under nitrogen atmosphere. The prepared composites were polished and etched for micro structural analysis. Also determine the Brinell's and Vicker's hardness numbers. Results reveal that there is good improvement of results in composites than base metal.***

Keywords: mmcs; microsturecture; hardness; sintering; inert atmosphere.

I. INTRODUCTION

In today's scenario industries are seeking the advanced applications of metal matrix composites because of their superior mechanically inherent properties. Metallic matrix composite erections are great interest in automotive engine parts, military, aeronautical and other applications. These composites offer excellent combination of mechanical properties that enhances the workability. The metal matrix can be reinforced by numerous reinforcements with variety of types like graphite, SiC, Al_2O_3, TiO, MgO, SiO_2, B_4C, TiC, WC, h-BN and C in the form of particulates, whiskery structures or fibrous matter. In this paper powder metallurgy route was used to prepare the composite materials though various techniques are available because, it has many advantages such as we can produce near net shapes components and also we can use this method to produce high melting point components with high accuracy and god surface finish. In this PM technique we can produce specific properties like microstructure, strength, hardness and other mechanical properties also for specific applications and also utilize full amount of raw material and there is no material waste during the process.

II. LITERATURE REVIEW

Boron carbide (B_4C) is extreme hard reinforcement material component with significantly excellent hardness, impeccable corrosion resistance, numerous mechanical properties, which makes it is a desirable reinforcement material for enormous engineering requisite and its related applications. [1,2]. Hexagonally bonded boron nitride (h-BN) particle also an effectual reinforcement for aluminum metal composites specially for tribological applications in automobiles and other because it makes the composites as the most toughest and self-lubricant in nature.The support provided by these h-BN particles improves the machinability and wear resistance of Al-B_4C composites when embeds into the base composite metal. The synthesized hybrid aluminum based composites encompassing B_4C and h-BN particles having great benefit compared to other combination of reinforcements. A K Bodukuri et al [3], Investigated on hardness values of metal matrix composites by varying the compositions of B4C and SiC reinforcements in Aluminum metal matrix composites and conclude that hardness values are higher compared to the base metal aluminum and alloys. The effect of addition of molybdenum trioxide on strength coefficient, hardness, density and thermal conductivity was studied by B.Stalin et al, [4] result reveals that addition of parentage of MoO_3 increase the strength coefficient, hardness and density and decrease the strain hardening index during cold upset process. Cunguang Chen et al [5] observed that due to the distinct high relative density, more significantly distributed grain refinement and the presence of meagerly distributed hard particulates (nano-Al2O3) and inter metallic phases (Al2Cu) in the matrix showed the best mechanical performance, including the Brinell hardness, compressive strength and fracture strain.Amar E Nasser et al [6] investigated that Reinforcement of titanium dioxide with aluminum was effect on mechanical properties like tensile strength, hardness, density which were increased with increasing of titanium dioxide. Also decreasing of ductility and enhancing of wear resistance of composite. K. Kanthavel, K.R. Sumesh, P. Saravanakumar [7] proposed that the characteristic features of the combinations of Al+ 5% Al2O3, Al+ 5% Al2O3 + 5% MoS2 and Al +5% Al2O3 + 10% MoS2, reveals that further addition of 10% MoS2 in the hybrid composite does not help to improve the already existent tribological property. Ehsan Ghasali et al, [8] says that Microwave sintering produce Al/B4C metal matrix composite at a sintering temperature which is either at 850°C or more. By increase the weight percentage of B4C micro hardness and compressive strength values increased.

Revised Manuscript Received on December 08, 2018.

Katla Rajendar, Department of mechanical engineering, Malla Reddy Engineering College, Secunderabad-500100 Department of Mechanical Engineering, Kakatiya University, Warangal, Telangana-506009, India

Dr K. Eswaraiah, Department of mechanical engineering, Malla Reddy Engineering College, Secunderabad-500100, India

Anil Kumar Bodukuri, Department of Mechanical Engineering, Kakatiya University, Warangal, Telangana-506009, India

Sampath.V, Department of Mechanical Engineering, Kakatiya University, Warangal, Telangana-506009, India

Use of Microwave heating produces Al/B4C composites and saves the energy proportions. Maho Yamaguchi et al, [9] Aluminum/boron nitride nano tube (BNNT) composites were prepared by the process of spark plasma sintering (SPS). The Boron nitride nano tubes were found in the grain boundaries in Plasma Sintering samples at room temperature containing about 3.0 wt% Boron nitride nano tubes (300MPa) became one and another half times higher than that of free High pressed torsion /Al compact (200MPa). Madhuri deshpande et al [10] studies on AL7075 alloy MMCs and discussed that there is good bonding exist between the reinforcement and alloys even high volume fractions of reinforcements also uniform distribution of the carbon fibers.

S. Ozkaya, A. Canakci [11] investigated the unreinforced Al-Cu-Mg alloy shows 15 wt% B4C composites produced with 25 hr milling time. The hardness of the hot pressed composites was higher than that of the hot pressed nano composites incured by using the globally identified conventional powder metallurgy and 10 wt% of B4C nano composites produced with 6hr milling time gives the highest tensile strength. Sener karabulut et al [12], also proposed his theory on Al6061 alloy reinforced with 5-20 wt% B4C produced using a powder metallurgy method. The highest tensile and transverse rupture strengths are for Al6061/5 wt% B4C were estimated successfully.

III. EXPERIMENTAL WORK

In this experimental work Powder metallurgy process was used to prepare the samples. This process consists of mainly four steps which were powder characterization, blending or mixing, compaction and sintering.

Materials used in the present work

Pure aluminum with above 99 percentage of purity used as base metal and boron carbide and boron nitride were used as reinforcement. These reinforcement material have different properties and which gives different material properties and full fill the all the requirements of mechanical properties especially automobile engine applications. Boron carbide enhances the mechanical strength and hardness and boron nitride act as solid lubricant and improve the tribological properties. Zinc stearate was used as lubricant during compaction process and acetone also used to clean the die for each sample preparation. Nitrogen gas was used in sintering process to create the inert atmosphere in order to reduce the oxidation effect during the process.

Blending

Blending is a process of mixing of powders, to achieve homogenous mixture in this work attrition milling equipment (shown in fig 3(a), fig 3(b)) was used to mix the powders and it was attached to drilling machine. Attrition apparatus consists of a cylindrical compartment in which a circular cross sectional shaft with impellers is placed along with it. When the shaft starts its revolution, impeller agitates the steel balls to and fro, which in turn taps, vibrates the powder placed in the vial by which the powder particles get cold welded and uniform distribution is achieved, Speed was maintained at 200rpm, and it was carried for a time of 2 hrs to overcome any errors in milling speed and ball to charge ratio was maintained to a range of 5:1, 50% of Vial space is left empty for free motion of balls and powders.

Fig 3 (a) mixing of powder set up

Fig 3.(b) attrition mill

Compacting

After mixing of the powder, universal testing machine with a maximum capacity of 40 ton was used for compacting the powder. A 20mm diameter sample was prepared by applying the uniaxial compaction load gradually and zinc stearate and acetone were used for easy detachment of greenish compact specimen sample and punch and die.15 grams of powder was used to consolidate the powder in to the cylindrical sample. Optimal Compaction pressure employed during consolidation of powder up to 150MPa for the samples which reduces the porosity.

Sintering

The prepared green compact samples did not have enough strength, to improve the strength of the green sample go for sintering process. It consists of electric furnace (Fig 3(c)) with a facility to vary temperature and inert gas arrngment. In Sintering process green compacts which was prepared by compaction heated at a temperature of 580^0c employed. The heating rate employed in this process is 30C/min. Sintering atmosphere employed here is nitrogen, that gets first purified from moisture content, if any impuritical substances in gas it passes through brass chips and calcium pellets to purify the gas, before entering the furnace. The gas from the exit is passed through a vessel of water, to verify the gas flow. Sintering time employed was 3 hours. After completion of sintering process samples were cooled in the furnace itself to the room temperature, them the samples taken out from the furnace and the mechanical tests for characterization.

Published By:
Blue Eyes Intelligence Engineering
& Sciences Publication


Fig 3 (C) Electric Furnace with inert gas set up

Composition of composite materials fabricated in this work

The following six different combinations aluminum, boron carbide and boron nitride were used to fabricate the samples show in table 3.1. In this work by using powder metallurgy method, below table shows the weight percentage of different combination of composites.

Table 3.1 compositions of composites

Composite Sample	Composition		
	Aluminum	h-BN	B4C
C1	100	0	0
C2	95	5	0
C3	90	10	0
C4	90	2	8
C5	90	5	5
C6	90	6	4

IV. RESULTS AND DISCUSSIONS

Microstructural and hardness values were determined by using microscope, vicker and brinell hardness tester. There test were primary concerns for all the mechanical and other properties. The grain size analysis was done according to the ASTM E112 standerd. Hardness values for Vickers and brinell were determined by taking the three different impressions and average of that was considered for hardness evalution.

A. Metallographic studies:

The sintered sample particulates were first roughly grounded, then polished for smoothness on emery papers, followed by disc polish procedure with implementation of diamond paste post which it is etched with Keller's reagent prepared from 95ml distilled water, 2.5ml HNO_3, 1.5ml hcl, 1.0ml HF in par with the standard ingredients. Then these sample particulates were inspected and scrutinized under a metallographic microscope. Following figures shows the microstructures images of the samples (fig 4.1 to 4.6)

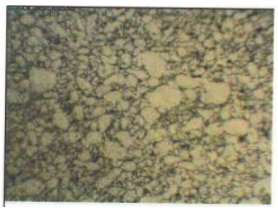
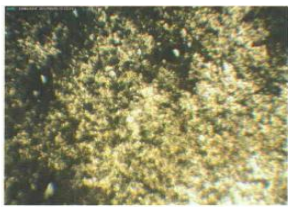

Fig 4.1 Sample C1 **Fig 4.2 Sample C2**

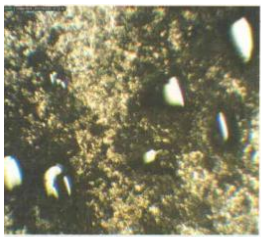
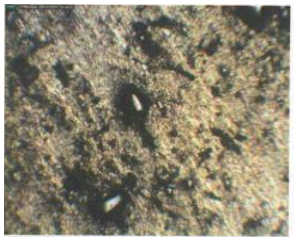

Fig 4.3 Sample C3 **Fig 4.4 Sample C4**

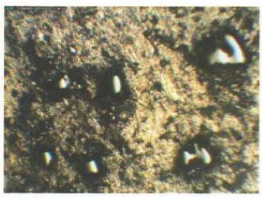
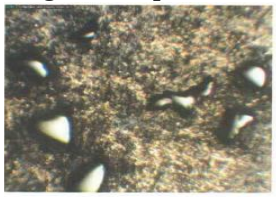

Fig 4.5 Sample C5 **Fig 4.6 Sample C 6**

Above figures shows the microstures of all samples from C1 to C6 and it is shows that mixing and sintering were done properly and distribution of reinforcements were also done uniformly.

B. Vickers Hardness

Vickers hardness test facilitates an accurate, more precise, rapid and economic way of persuading the resistances to indentation, penetration, embed or plastic deformation of the surface content of the material. For this test, the samples are highly polished to achieve great surface finish. Then the sample is placed in the vickers hardness setup and hardness values were measured by using the diamond indentor and the load applied was 1 kgs according to the IS 1501:2002. Three different impressions were taken from different areas and tabulated in the table 4.1 along with the average value and graphs (graph 4.1) were plotted for different samples average hardness's for different combination of six composites.

Table 4.1 vickers hardness table

Sample	imprerssion 1	impression 2	impression 3	Average HV
C1	28.1	27.9	27.6	27.87
C2	29.2	29	29	29.07
C3	32.2	31.7	31.1	31.67
C4	35.1	34.8	34.5	34.8
C5	32.2	31.9	31.7	31.93
C6	31.5	31.2	28.7	30.46

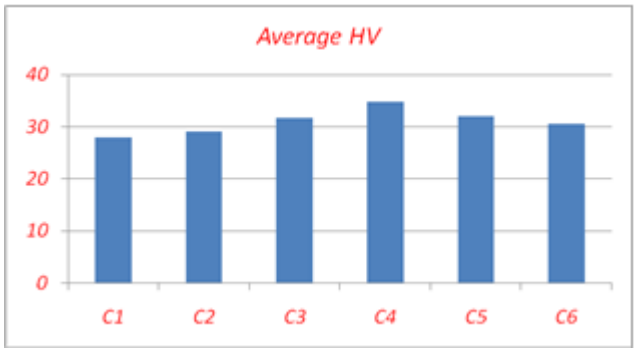

Graph 4.1 shows compositions V/S Average vicker's hardness values

As we see that if we find the hardness value of pure aluminum we got the hardness very less, as we go on adding the compositions of HBN and B_4C the hardness value goes on increasing.

C. Brinell hardness:

Brinell's Hardness Testing is one of the foremost procedures for testing hardness; this test was conducted on numerous parts from least in size to high in size and weight. This varying test force as well as ball size allows testing of various metals.. Hardness values was measured by using 5 mm ball indentor and the load applied was 250 kgs according to IS 1500:2005. Three different impressions were taken from different areas and tabulated in the table 4.2 along with the average value and graphs (graph 4.2) were plotted for different samples average hardness's for different combination of six composites.

Table 4.2 Brinell hardness table

Sample	imprerssion 1	impression 2	impression 3	Average BHN
C1	40.2	39.6	39.9	39.9
C2	44	44.4	44.4	44.27
C3	51.4	51	49.2	50.53
C4	54.3	53.8	54.3	54.13
C5	53.8	53	52.6	53.13
C6	51.9	51.4	47.5	50.27

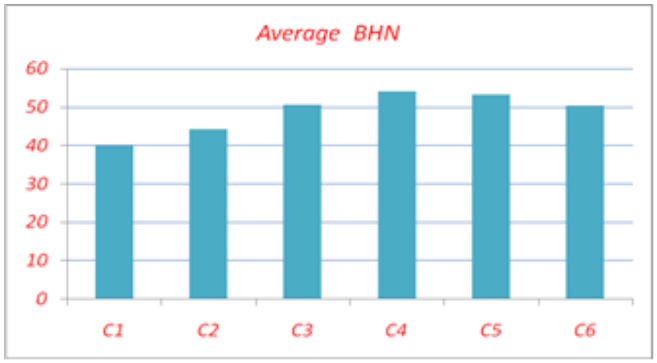

Graph 4.2 shows compositions V/S Average brinell hardness values.

The hardness value of composites improved compared to the pure aluminum in all the six combinations.

V. CONCLUSIONS

- From the microstructural investigation it was found that there is uniform distribution of reinfoecement in the base luminium
- For all the composites and also the average grain size number lies between 5 to 6 for all the composites which shows the reinforcement in the base metal imparts uniform distribution in the metalographic structure and there is no aggromiration and sedimentations formed in the composites.
- From the hardness value observation there was a significant influence of the h-BN and B4C in all the cases.
- For pure aluminium we found that very less hardness and as addition of boron nitride the hard ness value increased gradually but addition of boron carbide it was found to be maximum of 34.8HV and 54.13 BHN.

REFERENCES

1. Thuault A, Marinel S, Savary E, Heuguet R, Saunier S, Goeuriot D, et al.,Processing of reaction-bonded B4CeSiC composites in a single-mode microwave cavity. Ceram Int 2013;39:1215e9.
2. Domnich V, Reynaud S, Haber RA, Chhowalla M. Boron carbide: structure, properties, and stability under stress. J Am Ceram Soc 2011;94:3605e28.
3. Anil Kumar Bodukuria, K. Eswaraiah, Katla Rajendar,V.Sampath: Fabrication of Al—SiC—B4C metal matrixcomposite by powder metallurgy technique and evaluating mechanical properties/ Perspectives in Science (2016) 8, 428—431/ j ournal homepage: www.elsevier.com/pisc.
4. B.Stalin,G.T Sudha,M. Ravichandran : Investigations on Characterization and Properties of Al-MoO3 Composites Synthesized Using Powder MetallurgyTechnique/SpringerScience+BusinessMediaB.V.,partofSpringerNature2018: Silicon https://doi.org/10.1007/s12633-018-9803-6.
5. Cunguang Chen a, LeichenGuo b, JiLuo a, JunjieHao a, ZhimengGuo a,n, AlexA.Volinsky c a., Aluminum powder size and microstructure effects on properties of boron nitride reinforced aluminum matrix composites fabricated by semi-solid powder metallurgy/ Materials Science & Engineering A646 (2015) 306–314/ journal homepage: www.elsevier.com/locate/msea.
6. Amal E. Nassar, Eman E. Nassar, Properties of aluminum matrix Nano composites prepared by powder metallurgy processing, Journal of King Saud University – Engineering Sciences (2017) 29,295–299/ www.ksu.edu.sa/ www.sciencedirect.com.
7. K. Kanthavel, K.R. Sumesh, P. Saravanakumar., Study of tribological properties on Al/Al2O3/MoS2 hybrid composite processed by powder metallurgy/ Alexandria Engineering Journal (2016) 55, 13–17/ www.elsevier.com/locate/aej/www.sciencedirect.com.
8. Ehsan Ghasali, Masoud Alizadeh,Touradj Ebadzadeh, Amir hossein Pakseresht, Ali Rahbari/ Investigation on microstructural and mechanical properties of B4C–aluminum matrix composites prepared by microwave sintering/ j m a t e r r e s t e c h n o l. 2 0 1 5;4(4):411–415/ www.jmrt.com.br
9. Maho Yamaguchi,FanqiangMeng, KonstantinFirestein, KoichiTsuchiya, Dmitri Golberg.,/ Powder metallurgy routes toward aluminum boron nitride nanotube composites, their morphologies, structures and mechanical properties/Materials Science&EngineeringA604(2014)9–17/journal homepage: www.elsevier.com/locate/msea.
10. MadhuriDeshpande, Ramesh Gondil, S. V.S.NarayanMurty, R. K.Kalal Studies on7075Aluminium Alloy MMCs with Milled Carbon Fibers as Reinforcements/ Trans Indian Inst Met/https://doi.org/10.1007/s12666-017-1233-4/ The IndianInstituteofMetals-IIM2017.
11. S. Ozkaya, A. Canakci/Effect of the B4C content and the milling time on the synthesis,consolidation and mechanical properties of AlCuMg-B4C nanocomposites synthesized by mechanical milling/Powder Technology 297 (2016) 8–16/journal homepage: www.elsevier.com/locate/powtec
12. Sener karabulut,halil karakoc,ramazan citak., Influence of B4C particle reinforcement on mechanical and machining properties of Al6061/B4C composites, Composites Part B 101 (2016) 87-98,/journal homepage: www.elsevier.com/locate/compositesb.

An Approach for Minimizing the Response Time and Improving Availability of Web Services

M. Swami Das, A. Govardhan, D. Vijaya Lakshmi

Abstract*: The worldwide use of the Web-based application is increasing rapidly in various domains like E-commerce, banking etc. The Web users use mobiles, smart devices, laptops and PC. The devices use communication protocols with the Internet based web application. Web services are APIs, design application use of SOA Architecture, SOAP, UDDI and WSDL specifications. In this paper, we have discussed the basic elements, the applications to require high-quality parameters related to computer networking, operating system, software related parameters, response time and availability. The minimum response time to invoke operations with use of Optimized Multi-level Shortest Remaining Time CPU scheduling algorithm to minimize the waiting time to achieve high availability of services even in failure of the system the recovery procedures by providing backup, elastic and Fault-tolerant services. We have used the QWS dataset, Dream set and Grid dataset for experiments. The experiments on this dataset improved performance minimizing response time (RT) and increased availability

Index Choice: Web service, QoS, Response Time, availability, operating systems, FTS, Performance, software

I. INTRODUCTION

The growth of web based applications rapidly, the user require to use Web-based applications, nowadays; tremendously increasing the use of applications like E-commerce, Web applications, banking etc. Business needs are growing the use of Web application by users and clients seek a high Quality of Service(QoS) which include response time, availability. Web services use of Simple Object Access Protocol (SOAP) is message communication, Universal Description, Discovery, and Integration (UDDI) is the registry of services, Extensible Markup language (XML) and other elements [6]. Web users can access the Web applications using communication protocols with the Internet and the business services are available to Web servers. It is necessary to authenticate and identify the genuine user needs to access web services with high-quality parameters services to minimize response time and more availability. In dynamic environment web applications, the service providers ensure the demands of client specifications. The response time is a significant measure in quality of services, is measured in milliseconds (ms). The Web services control is based on the QoS manager to minimize the network traffic, policies and most efficient algorithms are required. The Web server accepts the request, execute the request and send back a response to the client with minimum time [8].

For example; in multimedia applications, the users want to access Web applications with minimum response time with quality parameters of functional resources [1][4][5]. High-quality services provided in enterprise applications to the web users, the services without loss of data the system will provide and guarantee to backup services, security, reliability, and other quality parameters. Availability is an important parameter is provided by backup devices and Fault-tolerant services. Increase availability to authenticated users, the user demands the high-quality services, which include reliability, throughput, response time, best practices and others. For building Web service dependable applications services, WS by different service providers, to identify the fault and resolve the issues immediately without any delay [7][12]. Web service technology use of applications to access on-demand services "*pay as you*" manner, it will be connected to cloud-based web data centers the cloud services and virtualization, these services need to execute parallel applications which are running, at data centers use of the CPU schedulers, this can analyze the problems such as response time and availability[9].

Web service(WS) is communicated to cloud services consists of services such as Platform as Service (PaaS), Infrastructure as Service (IaaS) and Software as Service (SaaS). Now these days mobile phones, smart devices can be connected IoT controlled web-based cloud applications. The remaining paper is organized section 2.related work, section 3. Web service Architecture and Quality parameters, section 4. IoT based control system, section 5. Is a proposed method to improve performance, section 6. Result and discussion section 7. Conclusion & Future Scope.

II RELATED WORK

Hadoop is a framework suggested by ZujieRen [2] use of software library in distributed processing to avoid dataset in large applications are handled by the server which connects to thousands of machines, failure in the application layer and provides more availability use of Hadoop common mode Hadoop (HDFS), Hadoop map reduce, is a Parallel processing large dataset, Hadoop Yarn is scheduling user application with throughput, and successful message delivery over communication channels measured in (BPS). The job slot allocation process is based on priority in the queue, CPU scheduling algorithms, SJF, FCFS, and Round robin used.

Revised Manuscript Received on December 28, 2018.

M. Swami Das, Associate Professor& Research Scholar, Department of CSE, MREC & JNTUH, Hyderabad, TS, India

A. Govardhan, Professor & Rector, Jawaharlal Nehru Technological University Hyderabad, Kukatpally Hyderabad, TS, India

D. Vijaya Lakshmi , Professor & Head, Department of IT, MGIT, Hyderabad, TS, India

The William Stallings[3] suggested a Module of high-speed internet consists of data communication systems the design of application consists of terminals, Personal Computers, Workstations connected in LAN, to handle the load of the network, performance actions, queuing analysis for statistical concepts are most useful.

J. Zhu [4] proposed a Web service positioning method, which combines the advantages of network coordination approach, and collaborative filtering approach. The Wireless Session Protocol(WSP) is a method that finds the landmark of network locations, periodically to monitor the Web server and add the value(network distance like Euclidean distance) to the application and find the values minimum , maximum, mean and standard deviation of RT values from plant lab dataset 359400 and response time values over 200 users.

The A.E Yilmaz [5] proposed a model Genetic algorithm based Simulated Annealing, and Genetic algorithm with Harmony Search. A Hybrid Genetic algorithm use of single and multi-objective approaches.The hybrid GA use heuristic simulated annealing, Harmony searches to optimize quality parameters such as cost, response time and reliability. GA accepts the several execution plans, which may be parallel or serial based on a scenario, the solution has the lowest fitness values, serial, parallel aggregations values use of a selection of the execution plan of web service.

Mathew [10] proposed model for availability of service that operates in percentage of time during the user operation invocation of services. The users and the loss of availability is outage due to unavailable network communication failed, the servers heavily loaded, and Service is not available because of system damage, the necessary steps to improve availability of resources by scalable design of application. This means the system resources, which are available replica of web servers, which is probably assure high availability by FTS. The policies are used for disaster recovery and restore the normal operations to web users.

Problem Definition: Minimizing the response time, and availability of services to be maximized. In table.1 shows the notations are used in the paper.

Notation /symbol	Definition- Description
RT	Response time
RCT	Response completion time
URT	User request time
TP	Throughput
A_v	Availability
R	Reliability
E_m	Error Messages
T_m	Total messages
L	Latency
$r_0,r_1,r_2,\ldots,r_n$	User requests
F(X)	Web page request function
N	Servers
P	Utilization of each server
Np	Utilization of entire system
γ_{max}	Maximum Input rate
$X^{'}$	Variance- Mean packets
MTTF	Mean time to failure
MTTR	Mean time to Repair
MTBF	Mean time between Failure

Table.1.Notations used

III Web service Architecture and Quality Parameters

Web service performance improvement parameters such as response time, availability and reliability. Mostly used architecture is three-tier architecture consists of model, view, and controller. The important elements are Model elements, quality parameters, response time, latency, availability, service reliability and performance parameters are discussed.

Model, elements and quality parameters

The generalized model of web-based applications is shown in Figure.1. It has a client, web server and database server. The quality architecture is proposed by M Swami Das [22] in Quality Manager one of the significant parameters is response time and availability. The following diagram discusses basic elements are used web service and quality parameters are response time, availability and service reliability.

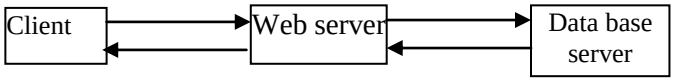

Fig 1: the web server architecture

Basic Elements

The basic elements of Web based system consists of SOAP, WSDL, HTTP, XML, and programming languages are used building of web applications. In software development process use of best practices, M Swami Das[23] improve the performance software applications.

In web-based system applications, the significant role by minimum response time and availability performance. The response time factors by considering the network layer, and transport layer parameters, end to end communication between client and server systems also view of protocols used for message communications like HTTP request, HTTP responses, browsers with modern features like flash player and plug-in, and the behavior of service responses, use of parallel downloading and HTTP pipelining process.

To reduce download cost, high availability of service, minimum delay, and secured internet services the designer must follow quality standards that will improve the performance of web-based applications.

Web service stack architecture shown in figure 2. which has client, server, protocols, encoding and transportation protocols, which influences some of the quality parameters like response time by identify the factors like a minimum response, reduce the overhead of network communication, best services, security protocols, encryption, decryption, RMI over SSL security of web application.

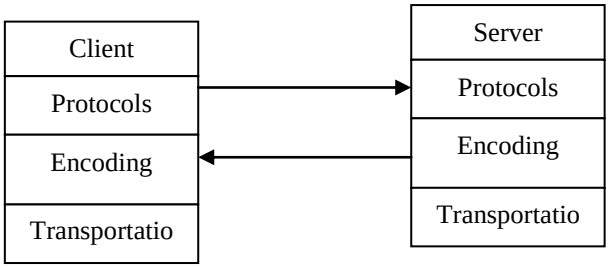

Fig 2: Web service stack

Published By:
Blue Eyes Intelligence Engineering
& Sciences Publication

Web service quality parameters:

Quality of services proposed by Marc Oriel[24] defined quality standards, models, and software components to maintainability, and portability. The quality hierarchy in software and web services. They suggested that the quality parameters high priority and more availability, response time, functional correctness, security, and minimizing the cost of web applications based on the analysis. Latency, throughput, availability of service with the use of Fault-tolerant systems and reliability. Web page request waiting time for loading, if slow response transactions of e-commerce slow as a result sales was reduced due to unavailability.

Response Time and Latency

Response time is the amount of total time taken to respond to service. The response time of terminal, where user communication time between terminal users and server is calculated by equation 1

$$RT = RCT - URT \quad (1)$$

The response time is measured by considering the network traffic, submission, and process of web service. RT depends on the complexity of third-party component services. If complexity increases proportional to failure are also more. Each component such as image, video, text and other elements used to load the web page. Web service delivery, in network, transport and Interdependencies issue. Web site application infrastructure endpoint services use of Communication of components in configuration systems. Latency is mean time to failure and repair when critical situations due to failures and demand of Web service in peak hours to access the resources for example. If university announces the online results at a moment more students to accessed web application.

The client demand the high-quality services, like minimum RT, and others. The Internet which provides the communications between the clients and web-based systems. The traffic analyzer plays a significant role in access web applications with use of XML messages.

Locating the web service by service provider with use of UDDI, Network traffic to load web page and relevant application. The analyzer has sniffer with live packets, HTTP, TCP/IP, SSL, record the headers, response time, message data packet processing format, and connections of web systems.

The web-based system which uses various protocols HTTP, SMTP, TCP/IP, XML and others, Let requests for r_0, r_1..... r_n, then the header, source code download, identifier, IP, static and dynamic web pages, request function is denoted by equation.2. The figure 3.show the user request from a client to server use of transport protocol. Transport layer establishes an end to end communication, the packet analyzer plays a significant role in a response time web systems. The packet analysis, session layer used for establishing sessions between client and server. The response depends on type of network, web pages, web server availability, HTTP traffic, overhead, load balancing and other factors.

$F(X) = F(X_n) + h/2 \quad (2)$

where H step size and X is the function

Client address, server address with HTTP connections can be active, passive modules request type, transaction-oriented requests, and database requests. The system will use single and multiple, processors based on demand, traffic and availability of service. Some of elements influence response time of Web services, HTTP, used for message communications, secure protocols Master Data Service(MDS) is used for waiting security members is applied at time intervals, caution when overlapping user and allows the data user can access. Secure Hash Algorithm (SHA) is the secure hash cryptographic algorithm used hash functions for digital security.

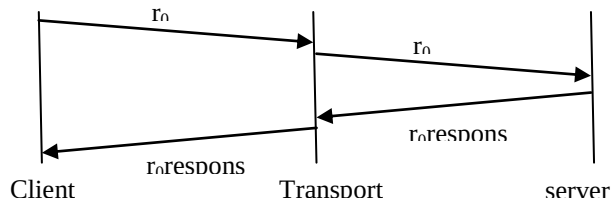

Fig 3: The response server to cleint communication transport protocol.

Data Encryption Standard (DES) is a symmetric key encryption algorithm, by plain text into cipher text by series of mathematical operations.

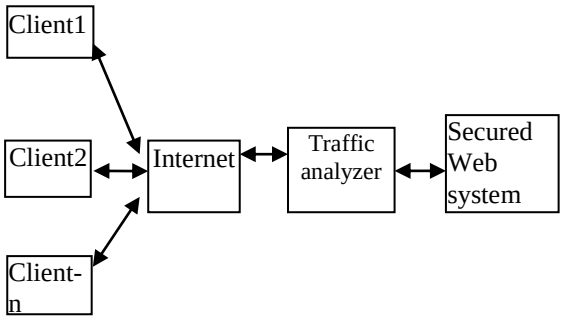

Fig 4: web secured system with a traffic analyzer

The Web secured system in which the clients can use secure web-based applications. The Figure.4 it has clients, internet, traffic analyzes and secured web system.

Latency (network delay), the time taken for the server to process a given request is called latency, (measured in ms), the latency is represented by equation 3. Which is used round-trip delay of the network and the aim is to minimize the latency.

$L = RT - URT \quad (3)$

Most of useful for multimedia applications use of audio, video data streams, it does not affect bandwidth, latency performance depends on several implementation of software components like middleware technologies, Simple Object Access Protocol (SOAP), Java RMI, CORBA, UDDI and Network Protocols.

Throughput: Throughput is measured as the average rate of successful communication messages received in network channel (is measured invocations per second) and described in equation 4.

$Throughput\ (TP) = TI/PT \quad (4)$

Where TI is total invocations, PT: period of time

Availability –Service Reliability

Availability is the number of successful invocations over application. The availability of service is expected all the time (i.e. 24X7), the availability is denoted by equation 5.

$A_v = S_i / T_i$ (5)

Where A_v – availability,Si- number of successful invocations, Ti- Total invocations

Availability is the process where guarantee of service in network communication from client to the web server. The probability of systemup is based on outputs, schedules and workload. The systemup availability is by equation 6.

$SU_a = SU_t / (SU_t + SD_t)$ (6)

Where SU_a is System up availability, $SU_t$is system up time, SD_t– system downtime

The results show high availability is essential for any organizations and waiting time to be minimized

Reliability: The availability of the system even failures recovery steps by Fault-tolerant systems, reliability to be increased (i.e. failures is very less). Reliability is denoted by equation 7. Is the failures are measured over a given period. The software is design to maintain high reliability with minimum failures. This is measured in percentage.

Reliability(R)=E_m/ T_m (7)

Service Reliability is provided based on Service Level Agreement (SLA). The web bases system is capable to provide applications at required level of quality.

Performance Parameters

The performance of web service can be measured by Tarek F. etl[7], Feedback control theory of users, response time of clients to invoke operations, CPU scheduling and efficient scheduling algorithms, throughput, Load balancing (maximum utilization of load), number of host sites. The server needs maintain important clients and server need to adopt QoS with minimum communication delay.

In the design of quality Service use prioritize the request, policies for clients, communication channel (wire communication, wireless communication), web traffic and data encoding (if the data is multimedia application including audio, video, and text etc.). Applications that meet the real-time systems, most sophisticated high-performance algorithms to meet the quality service design use of operating system, CPU scheduling, resource allocations, hierarchical allocations and the performance is for distributed applications by considering the web caching, hit ratio, feedback control system (thread scheduling) pipeline for multimedia application. Server computing services based on the client requests the message to the web server, the server receives the request and handles the requests based on the scheduling algorithms. The delay is called time spent of web server to ready schedule to process request. The sequence of instructions used in Software applications is sequential, iterative, loops and conditional. The instructions may be sequential, serial or parallel, the cyclomatic complexity is used to measure the quality of software application. The designer must ensure to avoid the system by quality management[22]. The operating system use of CPU scheduling, resource allocation, hierarchical scheduling, process capability and middleware etc. The tuning parameters of service utilization in equation 8, response time in equation 9, reliability is in equation 10. and throughput by equation 11.

Parameters need to be improved:

Server utilization (maximized)

Server Utilization = Max (WSi) (8)

Where Wsi is a Web server for i is 1 to n

Response time (minimized)

Response time = Min (WSi) (9)

Where WSi is a Web server for i is 1 to n

Reliability (maximized)

Reliability = Max (WSi) (10)

Where Wsi is a Web server for i is 1 to n

Throughput (Maximized)

Throughput= = Max (WSi) (11)

Where Wsi is a Web server for i is 1 to n

IV. IOT BASED QUALITY CONTROL SYSTEM

IoT based Quality Control System is a new approach used quality control systems in web based applications. The IoT system has sensors to read the data which will regularly monitor the web server performance based on the policies, guidelines, inputs (quality parameters) and real-time values. Figure 5.showsIoT quality control system has users, internet, web server with quality management and database server. Web server is a combination of structure, model, QoS parameters to establish the relationship between a client request services to web service is verify the design by feedback control system. The IoT based approach most important component is the quality manger which evaluate, predict and required level quality bases of quality parameters inputs used by SLA.

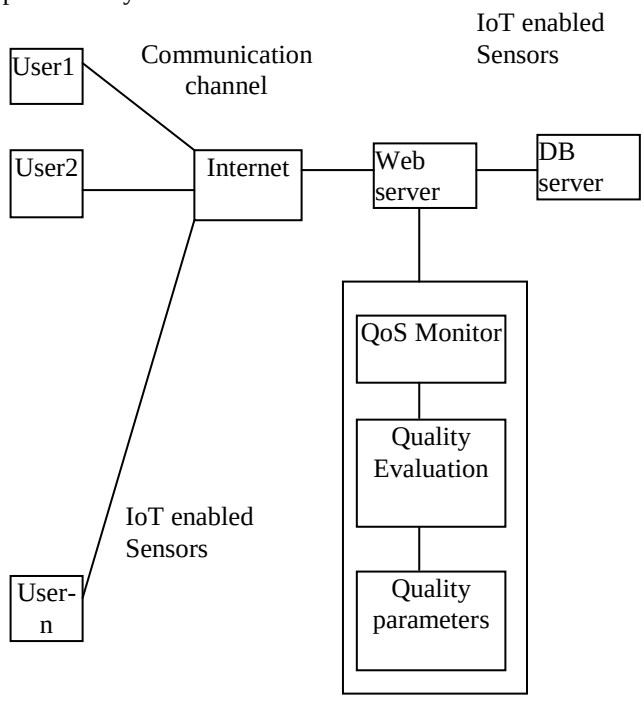

Fig 5: IoT based Quality Control System.

Published By:
Blue Eyes Intelligence Engineering
& Sciences Publication

The response time depends on network topology, media, type of systems, applications, availability and scheduling algorithms on arrival requests. The Operating system use of efficient scheduling algorithms used to improve the performance, CPU cycles, disk, network bandwidth, bottleneck problem to resolve, and utilization of services to be improved. Batch scheduling methods are used in mainframe systems for fast response.

CPU Scheduling is handled by scheduler [16, 19, 20] in which the number of tasks in queue, the CPU executes the tasks from scheduler is two modes, one is preemption (for example Round robin) is service goes another request which uses CPU time sharing, I/O bound time, and another is not Preemption means the processing job which gets completed requests during operations (for example FCFS, SJF). It can achieve the user service and system performance, priority multiprogramming, time slice to the requested process according to CPU scheduling, and re-ordering the process, will improve the performance and throughput, response ratio arrival and service time.

The response time completion time of server, operating system of types long, medium and short-term schedulers. For long-term scheduling the request arriving and processing by server, medium in which events affect cause by execution,(use process preemption), and short-term will use event handling, process dispatch the process is context save and new process arrivals. The performance is by equation 12. Arrival time by equation 13., and service rate by equation 14.

Let

α- Mean time arrival rate, ω- mean time execution rate, p - performance

Performance = Mean time to arrival /Mean time to execution (12)

If p>1, work system is exceeds the capacity, If P<1 means capacity exceeds, work directed interval and stead state when t=0, rescheduling policy,

Arrival time $F(t) = 1 - e^{-\text{mean arrival rate, time}}$ (13)

Service rate $S(t) = 1 - e^{-\text{mean execution rate,time}}$ (14)

Real-time schedules are two special qualities priorities and periodic, these are used in real-time applications to meet the deadlines of all process. The performance analyzer use of scheduling policies, because workload is directed to schedule to estimate execution time for long running jobs, attacks, delay, cost, relevant events and actions. To find server overhead by the meantime to arrival, and mean execution rate(requests per second).

QoS Management to ensure the Web server to provide the quality guarantee service by virtual server by maximizing the request rate, maximizing the bandwidth, request prioritization, load balance Data center allocations by quest rate, bandwidth rate, target allocation, target utilization and load policy.

V PROPOSED METHODS TO IMPROVE THE PERFORMANCE

The proposed systems moved to single processor to multi-processor and multi-tasking operations which are called distributed and parallel processing, the best use of services in applications is definite improve the performance. The web service queue models (i.e single and multi server models), and case study of scheduling algorithms use of FCFS, SJF, SRTF and RR and FTS used to attain high reliability and availability of services used in real time applications.

Web service queuing –Service Models

Distributed computing is loosely coupled components server handles small processing applications at client places, and coordination is well defined. The web server will handle a large applications where jobs are well defined. The processors are tightly coupled to target data systems which is shared by different processors. It is necessary to communicate different processors to parallel processing use of same machine instructions at communication very fast shared secondary drives, the advantage improve performance. The speed depends on applications, high fault-tolerant systems, if one processor fails then re-scheduled to another processor, this reduced throughput and increase availability. The demand and increasing computational services by adding more processors and maintenance cost are lower than new processors by load balancing. For parallel processing is mutual exclusion the to access more than one process in critical regions, deadlocks can be ignored, detected and recovered, preventive measures in software design avoid deadlocks[15]. The main of the process in queue of two type methods one single server queue and another multi-server queue is discussed below.

Single Server Queue

The client request a queue one web server will process the request. The drawback is RT is very poor, if the server is failed, there will no alternative another server to process for further request. To overcome this is by introducing a multi-server queue model is described section 5.1.2. The response time is increased due to more loads on network systems. The single queuing server model is shown in Figure 4. For example let us assume γ= arrival rate, W= items in the queue, Tw = waiting time, Server, Ts = service time, P= utilization, X. single server queue of web requests arrival rate is described in equation 15.

Mean $(\gamma_{max}) = 1/Ts$ (15)

Where arrival rate maximum (γmax) which depends on Service Time (Ts), the depends characteristics of information, queue size and dispatching algorithms FIFO, FCFS.

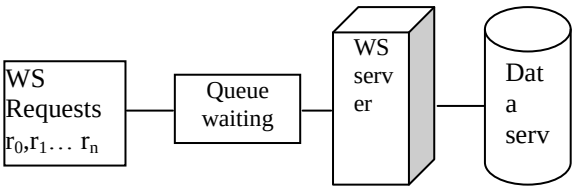

Fig.4: Single Queuing and Single server Model

Multi Server Queue:

The Multiserver queue model has web service scheduled by multiple requests to sharing queues, arrival request at least one server is available, then immediately dispatched request to the server. Multiple servers shown in Figure.5, it has client requests,

multiple queuing waiting with multiple web servers the Maximum utilization is 100%. Among the 'N' servers at least one server is available for web operations. Maximum utilization of servers is described in equation 16. Maximum input rate is described in equation 17.

Let N= servers, P= utilization of each server, Np: utilization of the entire system, U= traffic intensity.

Maximum utilization= NX Utilization percentage (16)

Maximum input rate is

γ_{max}= N/ (T_s) (17)

Where N is sample size, T_s is the service time and multiple queue servers to the services.

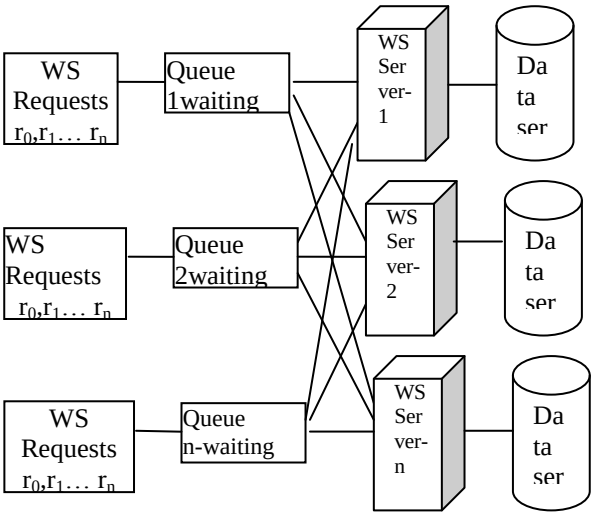

Fig 5: Multiple Server Queue of WS requests

Estimation model of queuing analysis input parameters mean and standard deviation of arrival rate and service time of the new system. Collection of terminals connected with network systems, multiplexers to share the load of active systems.

The sampling rate of packets are generated from terminal of the size of packets, during the period of time, Estimate mean of packets is described in equation 18., and variance is equation 19[6].

$$X' = \frac{1}{N}\sum_{i=1}^{n} X_i \quad (18)$$

For i {1 to n}, N sample size, X_i i th input packets

Variance (X) = σ2 / N (19)

The existing Model is Multi-Queue processor Model with Shortest Job first is shown in figure 6. The proposed enhanced model which is Multi-Queue processor with Shortest remaining time which improves the performance by minimizing the waiting time is shown in figure 7., proposed algorithm 1. And optimized multi-level shortest remaining time CPU scheduling algorithm.

Priorities are low and high we can take numerical value by setting priority 1- High, and 7 Minimum priorities among process (1 to 7) or binary value (0 represents low probity and 1 represents high priority)

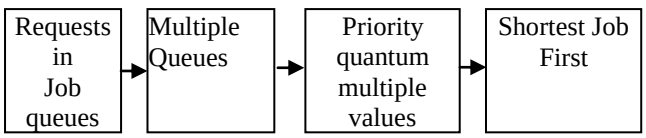

Fig 6: Exiting Approach for CPU scheduling algorithm

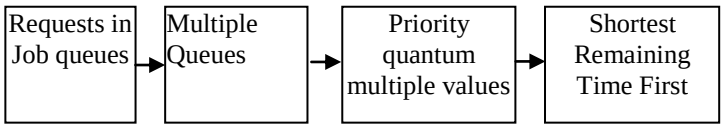

Fig7: Proposed Approach Optimized Multi-level -Shortest Remaining Time CPU scheduling algorithm

Algorithm 1. The optimized Multilevel Web service CPU Scheduling algorithm

Input: Jobs, J_1, J_2,..J_n

Job priority Jp_1. Jp_2, ..Jp_n

Arrival time Ja_1, Ja_2,.. Ja_n

Burst time BT (J_1), BT (J_2),…. BT (J_N)

Output:

Average waiting time (AW)

Average Turnaround time (AT)

Average response time (AR)

Data structures:

Queues Q_1, Q_2,,. Q_N (Multiple queues)

Begin

step1) Initialize the variables

Step2) Read Jobs, priority, arrival time and burst time

Step3) Initialize the time quantum of Queue

Let us assume the all the jobs are entered into the first queue

If (burst time of Job ≤ time quantum of the job) then

Execute the job in queue

else

Process job to next queue

If the processes in the last queue i.e 'N'

Sort the jobs based on shortest remaining time next in queue.

// this improves the Turn around time, response time and waiting time

Step4) Repeat the step 3 until all jobs are executed

Step5) Print the Average waiting time (AW), average Turnaround time (AT)

And average response time (AR)

Step6) stop

Case study:Using algorithm 1. Optimized Multi-level CPU scheduling algorithm1. With use of FCFS, SJF, SRTF and RR scheduling methods simultaneously described in table 2. Shortest Job First in table 3., Shortest Remaining Time First in table 4., and Round Robin in Table 5. Consider an example to explain the proposed concept Let us take four processes P_1, P_2, P_3, P_4 with arrival time 0,3,10,12 simultaneously and estimate time of 10,5,3,1 simultaneously. Finding the waiting time by FCFS:

Waiting time=Starting time-Arrival time.

	Arrival time	Estimate time	Starting time	Waiting time
P_1	0	10	0	0
P_2	3	5	10	7
P_3	10	3	15	5
P_4	12	1	18	6

Table 2. Gantt Chart for FCFS

Published By:
Blue Eyes Intelligence Engineering
& Sciences Publication

Average waiting time=4.5
Finding the waiting time by SJF:
Waiting time=Starting time-Arrival time.

Process	Arrival time	Estimate time	Starting time	Waiting time
P_1	0	10	0	0
P_2	3	5	10	7
P_3	10	3	15	5
P_4	12	1	18	6

Table 3. Gantt Chart for SJF

Average waiting time=4.5
Finding the waiting time by Shortest Remaining Time First (SRTF):
Waiting time=Turn around time-Estimate time.
Turnaround time=Completion time-Arrival time.

	Arrival time	Estimate time	Starting time	Starting time	Completion time	Waiting time	Turnaround time
P 1	0	10	0,8,14	0,8,14	19	9	19
P 2	3	5	3	3	8	0	5
P 3	10	3	10	10	13	0	3
P 4	12	1	13	13	14	1	2

Table 4. Gantt chart for SRTF

Average waiting time=2.5
Round Robin algorithm to find Waiting Time
Waiting time=Turn around time-Estimate time.
Turnaround time=Completion time-Arrival time.

	Arrival time	Estimate time	Starting time	Completion time	Waiting time	Turnaround time
P 1	0	10	0,2,6,10,16	18	8	18
P 2	3	5	4,8,14	15	7	12
P 3	10	3	12,18	19	6	9
P 4	12	1	15	16	3	4

Table 5. Gantt chart for Round Robin

Average waiting time=6

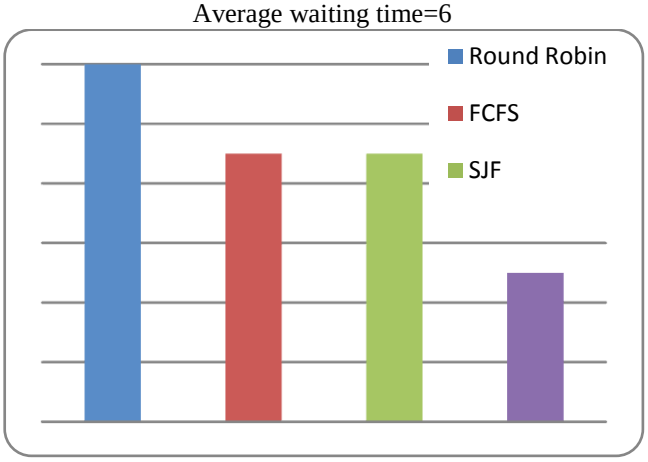

Fig 8: The response time of WS by Multilevel RR, FCFS, SJF and SRTF (Proposed Method).

Availability by Optimized Multi-level -Shortest Remaining Time CPU scheduling algorithm which improves the performance by a case study in results table 1. using FCFS, table 2. SJF, table 3., SRTF, and table 4. Round robin among these improve performance response time is shown in Figure 8.

Use of Fault-Tolerant Systems for High availability

The availability is a UDDI service by web service provider, and it is the most important and heart of the web service. Due to unavailability web systems, the users unhappy due to poor service. To provide high availability by planning, re-designing, analyzing, predict failures by eliminating single point, the suggestions recommendations as 1) Presentation layer is dynamic content caching, improve UI technology relevant functional feature 2) the business layer is the SOA will help to achieve highly available due to service failures 3) database layer is a high volume of data, bottleneck.

The designer and developer follow the best practices[23] in the development of software applications. The software component services are interoperable and distributed systems.

A distributed file system which depends on transparency, and file sharing semantics, modification of file visible to others. Fault tolerance is the system availability due to system faults and failures. Performance considered by efficiency and scalability, if the failure of service due to various causes to recovery and backup, Fault-tolerant services provided without any time delay.Web service functional features that improve the quality[11,12,19], high availability by providing elastic, and Fault Tolerance Web server is shown in Figure 9., which will provide high availability. For example.eBay, Flipkart, Amazon, etc.

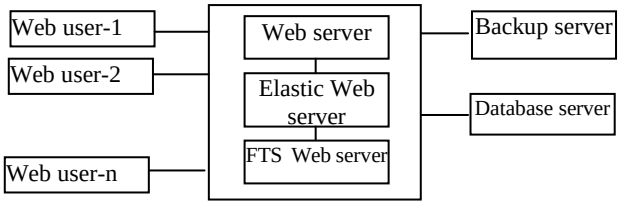

Fig 9: Service providers with high Infrastructural Facilities

The web service provider use of multiple WS service providers to resolve the issues, service not available due to failure, the WSDL and WS time transactions and default failures to service providers. The defect failures are identified and backup recovery procedures in code, Transaction state will be recorded, that follows (Atomic, Consistency, Isolation, and Durability), Fault-tolerant service will provide a better method, but it is too costly, For example in real time Amazon Web service EC2, S3, are available fault tolerant services, and elastic load balancing applications [10] [13]. The failure of Web services because of design failure, and other reasons. Load balancers, health checkups, and FTS used to attain high availability. The systems running the workload, in subnet, provide the same functionalities at multiple zones, provide auto -elastic scaling, MTFS and recovery use of FTS.

To design web service applications loose coupling and high scalability, and some of the most important concepts in high availability are discussed here.

Mean Time to Failure (MTTF) is the system is a time of failure, an outage of the system. Mean time to repair(MTTR) is the time taken when considering the failure time to till repair completion time(i.e. recovery time of available web services), the amount of time spent to bring back services by providing fault-tolerant services.[13].The availability is represented by equation 20.

Availability= MTTF/ (MTTF+MTTR) (20)

Increase MTTF,MTTR decrease the redundant software and hard ware.

Failure of Web service is due to failure service, crash, disk failure, communication failure and heavily loaded system etc. The availability of web services, in real time critical applications availability use MTBF.

Meantime Between Failure: Is the time of failure and recovery time or measured the sum of MTTF and MTTR, This is a most critical metric for real-time applications. The MTBF is represented by equation 21.

MTBF = MTTF + MTTR (21)

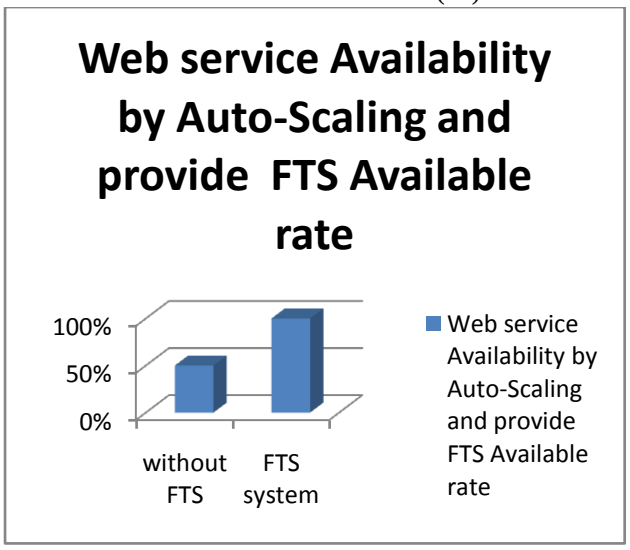

Figure 10. Web service availability by Auto scaling and FTS services improve performance

The Availability of Service by equation 20. by minimizing MTBF in equation 21, by auto-scaling and providing context switching Fault tolerant service will improve the performance.

VI RESULTS AND DISCUSSIONS

The web service queuing model single queue into multiple queues with priority quantum use of Optimized Multi-level Shortest remaining time CPU scheduling algorithm got waiting time 2.5 seconds compared with other methods round robin, SJF, FCFS. is shown in Table 2,3,4 and 5 and Algorithm 1. The Response time, availability, throughput, successability and reliability of QWS data normalized values minimum, average and maximum measurements shown in table 6. and in Figure 11. The values of RT, availability ,successability and throughput normalized values lying between 0 and 1.

QoS parameters	Units Measurement	Minimum	Average	Maximum
RT_N(Response time)	Milliseconds	0.007415	0.0769	1
AV_N(Availability)	Percentage	0.07	0.811456	1
TH_N(Throughput)	Invocations/sec	0.00232	0.209641	1
SUCC_N(successability)	Percentage	0.08	0.838871	1
REL_N(Reliability)	Percentage	0.370787	0.784083	1

Table 6. QWS normalized data minimum, average and maximum values lying between 0 and 1

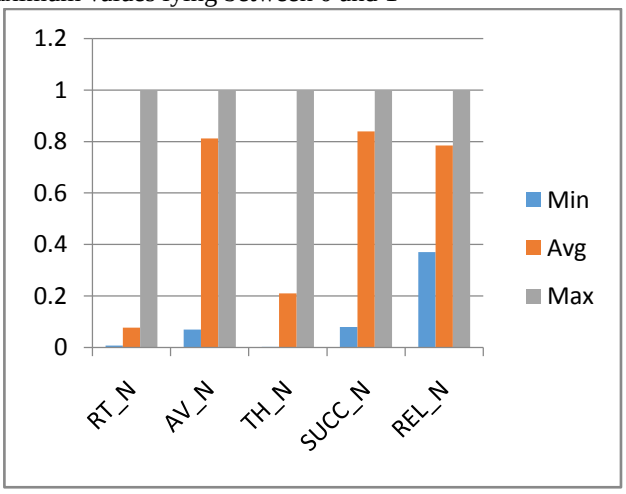

Fig11: QWS data the comparisons of Minimum, Average, Maximum values of Response time, Availability, Throughput, Successability, and Reliability.

The response time of Web-based application dream set data conducted experiments by using R language it shows in figure 12. At users 180th user the RT is maximum and initially is low for dream set data

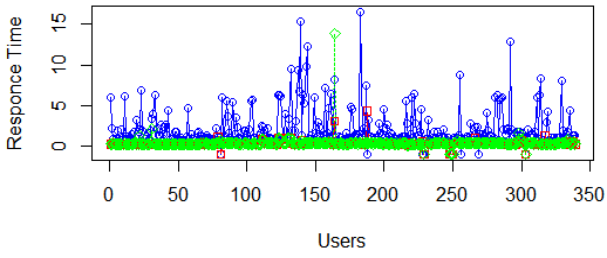

Fig 12: The response time of Dream set data of 335 users, and request and response time

Cumulative distribution of RT from different users QWS dataset is shown in Figure 13.

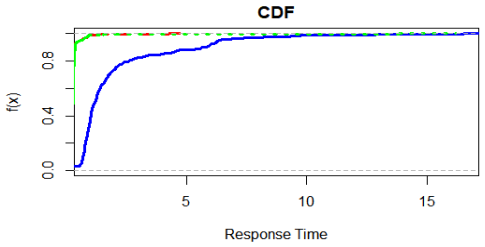

Fig 13: The cumulative RT from different users QWS dataset

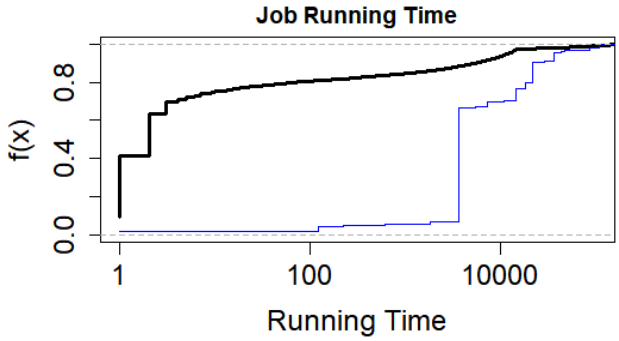

Fig 14: The Cloud -Grid; 10, 20,195 records, running and job running time.

The Figure 14. has cloud data set 1020195 records, the behavior of cloud waiting time and request time, in initial step the waiting time and RT is minimum as the requests are increasing that is more than 8000 requests then waiting time is also increased proportionally to the request time of applications.

Fig 15: In X- Axis applications users, waiting time, applications and process queues, and Y Axis range of values.

The users increasing the use of applications waiting time increasing, and application usage is also increasing, the process queue waiting time reached to maximum, when running maximum utilization of resources with all the service users shown in figure.15 using Grid dataset [21]

VI CONCLUSION AND FUTURE SCOPE

The use of Web applications worldwide increasing a lot, the user demands to use applications at high quality including minimum response time, maximum availability by auto-scaling and FTS. Use of high-speed communications, due to delay and un-availability of services. The service provider of Web service will lose business opportunities. Service availability improves the reliability as the user Multiple Queue Shortest Remaining CPU algorithm which will reduce the Turnaround time(TA), waiting time(WT) and improves the availability comparing the other scheduling methods FCFS, SJF and Round robin is shown Figure 8. The availability of Service is improved is by auto-scaling and FTS is shown in Figure 10. The experimental results conducted using R Language on QWS dataset [26], dreamset data [25], and Grid data [21] the results are shown in graph figure 12. dream set, figure 13. QWS dataset. Figure.11, cloud dataset, figure 14, and figure.15 use of grid dataset. As recommends that the high availability by auto-scaling systems will improve performance by reducing Mean time to Failure and Repair is optimized and provide high availability. As long as jobs are increasing the load on the system waiting time is also increased, to minimization of the waiting time by proposed algorithm Optimized Multilevel Web service CPU Scheduling algorithm 1, and Model in figure 7.and figure 9. describe high availability and improve performance. In Future IoT base Quality control system for web based applications will definitely improve the overall quality using communication sensors, QoS manage and applications.

ACKNOWLEDGMENT.

Thanks to Dr. Eyhab Al-Masri for proving QWS dataset 2507 records, Thanks to Prof. Mingdong Tang, for providing WS-DREAM github.com and Planet Lab, thanks to Dr. Franck Cappello and to Dr. Olivier Richard for providing cloud dataset. And Thanks to Hui Li, DrorFeitelson, at Imperial College London, for providing Grid dataset by e-Science Group of HEP, Grid Workloads Archive

REFERENCES

1. Jianbin Wei, and Cheng-ZhongXu,"Measuring Client-Perceived Page view Response Time of Internet Services",pp.773-785 IEEE Transactions on Parallel and Distributed Systems, Vol. 22, No. 5,(2011)
2. ZujieRen, Jian Wan, Weisong Shi, XianghuaXu, and Min Zhou,"Workload Analysis, Implications, and Optimization on a Production Hadoop Cluster: A Case Study on Taobao", pp. 307-321, IEEE Transactions on Services Computing, Vol. 7, No. 2, (2014)
3. William Stallings, "High-speed Networks and Internets Performance and Quality of Service", pp.183-247, Pearson Education Publishers, (2002)
4. J. Zhu, Y. Kang, Z. Zheng and M. R. Lyu, "WSP: A Network Coordinate Based Web Service Positioning Framework for Response Time Prediction," pp. 90-97.doi: 10.1109/ICWS.2012.81, IEEE,19th International Conference on Web Services, Honolulu, (2012)
5. A. E. Yilmaz and P. Karagoz, "Improved Genetic Algorithm Based Approach for QoS Aware Web Service Composition,", pp. 463-470.doi: 10.1109/ICWS.2014.72, IEEE International Conference on Web Services, Anchorage, AK, (2014)
6. Balazs Simon, Balazs Goldschmidt, and KarolyKondorosi," A Performance Model for the Web Service Protocol Stacks", pp. 644-657, IEEE Transactions on Services Computing, Vol. 8, No. 5, (2015)
7. 7.Tarek F. Abdelzaher, Kang G. Shin, and Nina Bhatti,"Performance Guarantees for Web Server End- systems: A Control-Theoretical Approach", pp. 80-96, IEEE Transactions on Parallels and Distributed Systems, vol.13, No.1, (2002)
8. Chen Hou and Qianchuan Zhao, "Optimization of Web Service-Based Control System for Balance between Network Traffic and Delay", pp. 1-11", IEEE Transactions on Automation Science and Engineering, (2017)

9. Song Wu, Like Zhou, Huahua Sun, Hai Jin, and Xuanhua Shi, "Poris: A Scheduler for Parallel Soft Real-Time Applications in Virtualized Environment" pp. 841-854, ", IEEE Transactions on Parallel and Distributed Systems, Vol. 27, No. 3, (2016)
10. Sajee Mathew, "Architecting for High Availability", pp. 1-111, AWS Summit 2013 Navigating the Cloud, (2013)
11. Kranti Pore, "How to Achieve Website High Availability in a Distributed Enterprise Environment", http://www.bitwiseglobal.com/blogs/website-high-availability-in-distributed-enterprise-environment/
12. P. M. Melliar-Smith and L. E. Moser, "Conversion Infrastructure for Maintaining High Availability of Web Services Using Multiple Service Provider spp. 759-764.doi: 10.1109/ICWS.2015.110" 2015 IEEE International Conference on Web Services, New York, NY, (2015)
13. 13.http://blog.fosketts.net/2011/07/06/defining-failure-mttr-mttf-mtbf/
14. 14. Andrew S. Tanenbaum, "Modern Operating Systems", pp. 71-151, Prentice Hall India, 2nd Edition,(2001)
15. 15.Achyut S Godbole, "Operating Systems", pp.404-420, 2nd Edition Tata McGraw Hill Publishers, (2005)
16. 16. D M Dhamdhere, "Operating Systems: A concept based Approach", pp.339-735, Tata McGraw Hill publications, (2002)
17. 17. Gary Nutt, NabenduChaki, and SarmsisthaNeogy, "Operating Systems", pp. 42- 54, 3rd Edition, Pearson Publications, (2004)
18. 18. Parag K. Lala, "Fault-Tolerant and Fault Testable Hardware Design", BS Publications (2002), pp. 1-11
19. 19. Dhananjay M. Dhamdhere, "Operating systems: A Concept-based approach", McGraw Hill Education publishers,3rd Edition, (2009), pp. 760-783
20. 20.Andrews S. Tanenbaum, Herbert Bos, "Modern Operating Systems", Pearson publishers(2016), pp. 148-165
21. 21. Grid dataset http://gwa.ewi.tudelft.nl/
22. 22. M. Swami Das, A. Govardhan, and D. Vijaya Lakshmi. 2015. QoS of Web Services Architecture. In Proceedings of the International Conference on Engineering & MIS 2015 (ICEMIS '15). ACM, New York, NY, USA, article 66, pp. 1-8
23. 23. M. Swami Das, A. Govardhan, and D. Vijaya Lakshmi. Best practices for web applications to improve performance of QoS. In Proceedings of the Second International Conference on Information and Communication Technology for Competitive Strategies (ICTCS '16). ACM (2016), NewYork, NY, USA, Article123, pp.1-9
24. 24. Marc Oriol, Jordi Marco, and Xavier Franch, "Quality models for web services: A systematic mapping ", Information and Software Technology, (2014), pp.1-16
25. 25. https://github.com/wsdream/wsdream-dataset
26. 26. QWS Data set http://www.uoguelph.ca/~qmahmoud/qws/

Identification of Most Influencing Blast Design Parameters on Mean Fragmentation Size and Muckpile by Principal Component Analysis

N. Sri Chandrahas, B.S. Choudhary, M.S.Venkataramayya

Abstract: ***Mean fragmentation size, muck pile are the most emphasis factors in terms of economic and safe production in mining. It is needful to maintain certain limits to reach optimum level of blast results. The motive of study is to categorize the most influencing blast design parametric values on average sized fragmentation and muck pile. The commitment of the research was dealt on time through field data collection that related to blast design parametric values such as drill hole depth, its diameter, no of holes, no of rows, burden, spacing, average charge per hole, explosive, firing pattern, length width ratio, powder factor, mean fragmentation size, throw from three limestone mines positioned at different vicinity in Rajasthan. The collected data has analyzed statistically using principal component analysis (PCA) in IBM SPSS and XLSTAT software's. Most influencing significant and non-significant parameters on mean fragmentation size and muck pile were drawn from regression analysis by considering P, F and R square values in IBM SPSS, For more robust results further analysis has done with XLSTST by considering influenced parameters from correlation circle according to their respective coordinates.***

Keywords: Blast Design Parameters, IBM SPSS, XLSTAT, PCA.

I. INTRODUCTION

Blast design parameters play a vital role in terms of mean fragmentation size and muck pile shape. The design parameters are drill hole depth, drill hole diameter, no of holes, no of rows, burden, spacing, average charge per hole, explosive, firing pattern, length width ratio, powder factor, mean fragmentation size, throw. It is very needful to find the which parameters influencing the mean fragmentation size and throw drastically both significant and non significant manner.The goal will be materialize by a statistical method called Principal Components Analysis in both IBM-SPSS and XLSTAT software's. Technically this method delivers a relatively small set of synthetic variables called principal components that account for most of the variance in the original dataset and hence this data-processing and dimension-reduction technique, has gained significance in numerous applications in engineering, biology, economy and social science. The end result of the principal

components designates which components, and which variables should be retained as individual variables(2).

The blast design parameters (12)

- **Burden:** denotes the minimum distance between face and blast hole.
- **Spacing:** Denotes the distance between two consecutive blast holes taken at any instance. Spacing = (1.2 to 1.5) burden
- **Stemming:** It is used in blast holes. Stemming is a process that affects blown out shot of the hole and also affects fly rocks and is employed after the explosive is loaded. Stemming/burden > 0.6 (for controlling fly rock**)**
- **Bore hole depth:** Bore hole depth is a function of spacing and diameter of the hole. When the holes shorter they produce blasting at greater violence and vibration level with highly increased frequency.
- **Types of explosives:T**ype of explosives used is based on the ground vibrations.
- **Explosive quantity:** The level of vibration produced depends on the quantity of the charge incurred during explosion of rocks because a single row instantaneous blast is same as the level of vibration produced by a single or multi row blast with delay if the charge quantity per delay of the blast with delay equals to the total charge of the single row blast. Thus it is the charge per delay that controls the level of blasting not the total charge.

Mean Fragmentation Size: The word "fragmentation" being used frequently and means anything from "the limits/size of breaking" to "the percentage of breaking size passes, above or below, a certain size which is economically significant in the prescribed size range of a definite volume that is already defined in the context of broken rock. The sizes are classified in to oversize, Fines and Mid-range (6). If the boulder size exceeds the prescribed size for which secondary breaking is necessary before further handling in underground mines then it is considered as oversized and this can be as petite as 300mm,while in opencast mines depending on the requirement and application it is seldom considered to be greater than 100mm. If the particle size below which product can either not be sold, or which becomes difficult to handle due to flow, or other properties will be fall under fines, it is common for a minimum sized particle of 6mm for coal or dolomite, but when considered for gold ores this may be as small as l mm.

Revised Manuscript Received on December 08, 2018.

N. Sri Chandrahas, Part-time research scholar, IIT(ISM) Dhanbad Asst Professor, Department of Mining Engineering, Malla Reddy Engineering College, Hyderabad,India

B.S.Choudhary, Asst Professor, Department of Mining Engineering, IIT(ISM) Dhanbad,Jharkhand, India

M.S.Venkataramayya, Professor, Department of Mining Engineering, Malla Reddy Engineering College, Hyderabad,Telangana, India

Finally the size belonging to the mid-ranges, those which have significant but not of terminal importance bear the ability to achieve premium pricing in the market.(4&10)

The Kuz-Ram model Equation which combines Kuznetsov and Rosin-Rammler equations has been employed widely by research scholars to predict blast induced fragmentation since its introduction (Cunningham 1983). It exclusively establishes the fragment size distribution based on a given set of rock parameters and after many trial and error type step substitutions Kuz-Ram model found the index number n(3&5)

Muck pile: The parametric variables include throw, drop & lateral spreading where throw designates the distance along the horizontal axis at the center of gravity of the blasted muck, while drop lies along the vertical lowering side.(6&7).

II. OBJECTIVE

The predominant intent of the research was to explore the most influencing blast design parameters on mean fragmentation size and muck pile by the principal component analysis in both IBM SPSS and XLSTAT so that it is easy to maintain blast design parameters up to the mark to get optimum and safe production.

III. RESEARCH METHODOLOGY

As a mandate to fulfil the research objective several data's were collected from three different cement companies in rajasthan, Shree Cements, Wonder cements and Indian cements. The M/s Shree Cement Ltd owned Nimbeti Limestone Mines is highly mechanized and has about 15 million tonnes rock handling capacity per annum when compared with the other limestone mines & projects of consuming 2500MT of explosives per/annum.The blasting was done by down line initiation with noise less trunk line detonator at top and blast holes of 165 mm diameter are drilled by using rotary drill and the holes are charged with bulk ANFO explosives. Bhatkotri Lime Stone Mines of M/s Wonder Cement Limited. Bhatkotari limestone deposit forms a part of the Nimbahera belt and belongs to Semri series of Lower Vindhyan age and the total thickness of the Nimbahera limestone is estimated to be 144 meter, of which the bottom is deep reddish purple in colour, while the upper 133.5 meter is grey in colour and the production of Quarry was over 12000-14000 tone/ day and the blasting practice in the mine was to use ANFO in conjunction with cartridge slurry explosive. The Partipura limestone Mine (PLM) -a captive limestone mine of Trinetra Cement Limited (TCL) a Subsidiary company of The India Cements Limited (ICL). PLM is fully mechanized opencast Limestone mine and the blasting practice in the mine was ANFO in conjunction with cartridge slurry explosive.

Fifty blast results has collected with respect to various blast design parameters from above said cement companies and here independent variables are mean fragmentation size and throw and rest all will fall under dependent variables and the cases are categorized in to two, In one case independent variable as mean fragmentation size and dependent variables are rest all factors and in second case independent variable as throw and dependent are remaining all parameters and the analysis has done with respective to three different mines in two cases. For statistical analysis a method of principal component analysis has executed in both IBM SPSS and XLSTAT software's for sake of robust results. The methodology specifically identifies even the mild variances and the least correlations in the data. Attaining a factor resolution through principal components investigation is a step to step iterative process that usually requires frequent repetition of the SPSS factor analysis procedure numerous times to reach the utmost satisfactory solution

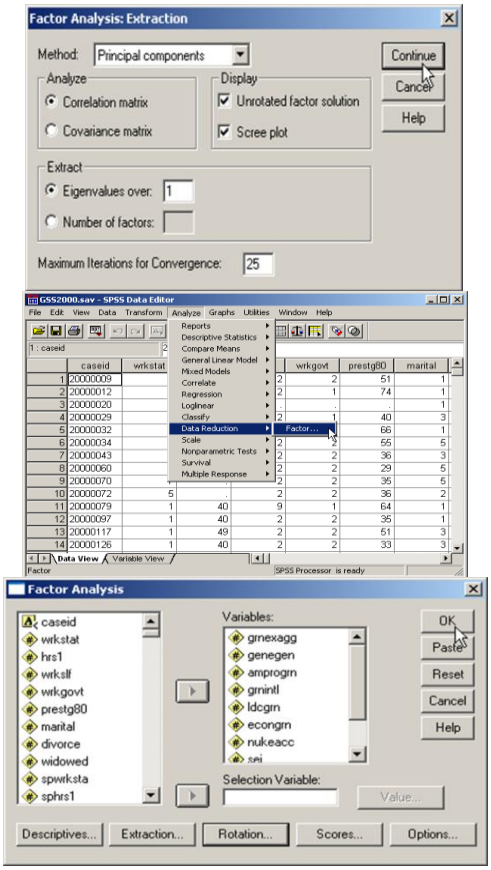

Figure1. Operation of principal component

IV. LAB WORK

MEAN FRAGMENTAION SIZE RESULTS OBTAINED FROM SHREE CEMENTS (Case 1)

SUMMARY OUTPUT

Regression Statistics

Multiple R	0.835446
R Square	0.697971
Adjusted R Square	0.69042
Standard Error	0.039678
Observations	42

ANOVA

	df	*SS*	*MS*	*F*	*Significance F*
Regression	1	0.145527	0.145527	92.43749	5.93E-12
Residual	40	0.062973	0.001574		
Total	41	0.2085			

	Coefficients	*Standard Error*	*t Stat*	*P-value*	*Lower 95%*	*Upper 95%*	*Lower 95.0%*	*Upper 95.0%*
Intercept	0.060555	0.020139	3.006815	0.004547	0.019852	0.101258	0.019852	0.101258
2pc	0.001736	0.000181	9.614442	5.93E-12	0.001371	0.002102	0.001371	0.002102

Figure2. Obtained regression exploration with PCA components in IBM SPSS

Published By:
Blue Eyes Intelligence Engineering
& Sciences Publication

	Component				
	1	2	3	4	5
Front row burden	.857	-.220	.062	.196	.028
Burden	.161	-.592	.508	.188	-.251
Spacing	.061	-.843	.333	-.041	-.003
Delay	.230	.656	.346	.012	.353
No of holes	-.181	.483	.694	-.009	.209
No of rows	-.589	.036	.125	.709	.138
Hole depth	.590	.111	.062	.561	.391
L/W ratio	.506	.361	.374	-.604	-.168
Se/Be ratio	-.687	-.323	.343	-.259	.280
MFS	.170	.339	.351	.328	-.604
Throw	.798	-.077	-.197	.076	-.031
Firing Pattern	.420	-.151	.348	-.161	.331

Extraction Methodology: Principal Constituent Analysis.5 components extracted.

T

Figure3.Extracted components from matrix

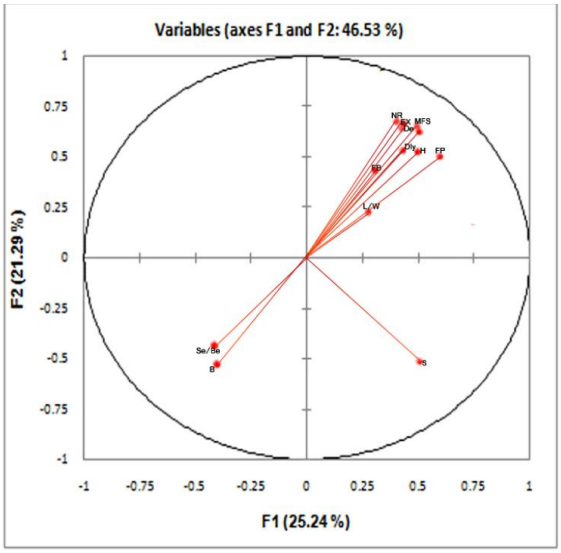

Figure4.Variable chart obtained from XLSTAT

MUCKPILE RESULTS OBTAINED FROM SHREE CEMENTS (Case 1)

SUMMARY OUTPUT

Regression Statistics	
Multiple R	0.769997
R Square	0.592896
Adjusted R Square	0.582718
Standard Error	2.634584
Observations	42

ANOVA

	Df	SS	MS	F	Significance F
Regression	1	404.3496	404.3496	58.25495	2.51E-09
Residual	40	277.6414	6.941034		
Total	41	681.991			

	Coefficients	Standard Error	t Stat	P-value	Lower 95%	Upper 95%	Lower 95.0%	Upper 95.0%
Intercept	-0.09217	1.175057	-0.07844	0.93786	-2.46705	2.28270	-2.46705	2.28270
1pc	0.374733	0.049097	7.632493	2.51E-09	0.275504	0.473962	0.275504	0.473962

Figure5. Obtained regression analysis with PCA components in IBM SPS

	Component				
	1	2	3	4	5
Front row burden	.829	.293	.222	.040	-.044
Burden	.123	.820	-.015	-.004	.211
Spacing	-.020	.877	.021	-.106	-.216
Delay	.177	-.368	.102	.734	.109
No of holes	-.259	-.051	-.016	.799	.288
No of rows	-.203	.021	-.886	.139	.195
Hole depth	.790	-.019	-.272	.360	-.074
L/W ratio	.095	-.066	.856	.360	.206
Se/Be ratio	-.752	.348	-.176	.211	-.279
MFS	.193	.023	.033	.074	.834
Throw	.760	.028	.295	-.125	-.077
Firing Pattern	.262	.300	.269	.404	-.247

Figure6.Extracted components from matrix

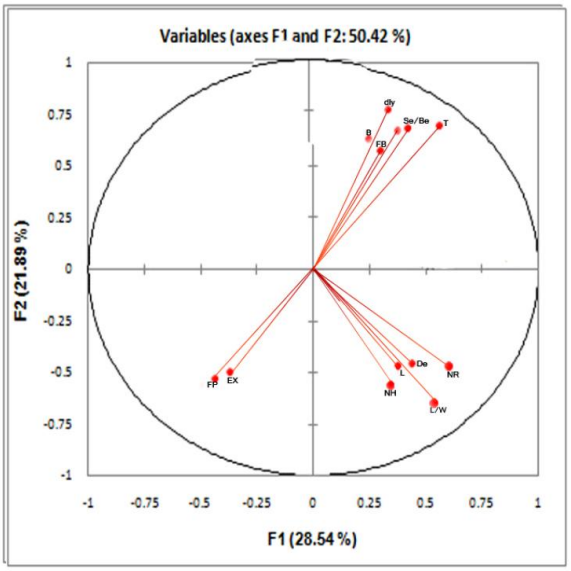

Figure7.Variable chart obtained from XLSTAT

MEAN FRAGMENTAION SIZE RESULTS OBTAINED FROM WONDER CEMENTS (Case 2)

Regression Statistics	
Multiple R	0.217423
R Square	0.772729
Adjusted R Square	0.001905
Standard Error	0.039068
Observations	23

ANOVA

	Df	SS	MS	F	Significance F
Regression	1	0.00159	0.00159	1.041988	0.04319
Residual	21	0.03205	0.00152		
Total	22	0.03364			

	Coefficients	Standard Error	t Stat	P-value	Lower 95%	Upper 95%	Lower 95.0%	Upper 95.0%
Intercept	0.148258	0.016982	8.730363	1.97E-08	0.112942	0.183574	0.112942	0.183574
4pc	0.000573	0.000562	1.020778	0.00174		0.001744	-0.00059	0.001744

Figure8. Obtained regression analysis with PCA components in IBM SPSS

Published By:
Blue Eyes Intelligence Engineering
& Sciences Publication

	Component				
	1	2	3	4	5
Burden m	-.366	-.054	-.198	-.112	.661
Spacing m	-.422	.212	.742	.408	-.029
Depth of holes m	-.297	.272	.890	.036	-.013
No of holes	.886	.277	-.271	.075	.046
No rows	.551	-.763	.219	.063	-.058
Explosive ANFO kg	.817	.321	.333	-.109	.199
Throw	.333	-.337	-.131	.666	-.101
Total explosive kg	.808	.346	.398	-.039	.227
Firing pattern	.551	-.763	.219	.063	-.058
LW Ratio	.415	.844	-.234	.141	-.034
MKSK50	-.148	-.128	-.098	.568	.627

Extraction Precedure:. a. 5 components extracted

Figure9.Extracted constituents from matrix

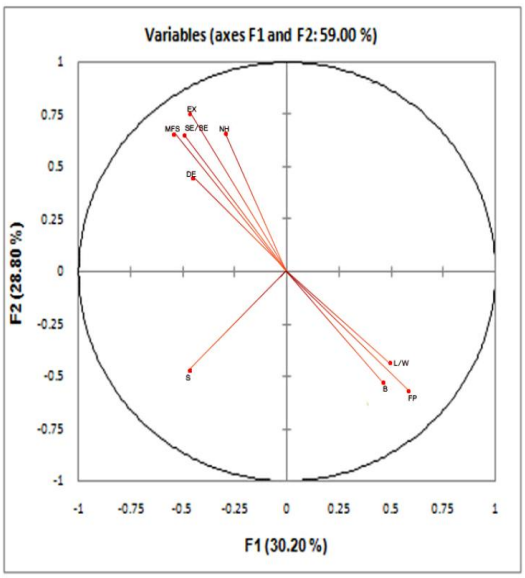

Figure10 Variable chart obtained from XLSTAT

MUCKPILE RESULTS OBTAINED FROM WONDER CEMENTS (Case 2)

Regression Statistics

Multiple R	0.121872
R Square	0.848528
Adjusted R Square	-0.03206
Standard Error	4.851939
Observations	23

ANOVA

	Df	SS	MS	F	Significance F
Regression	1	7.45345 1	7.45345 1	0.31661 1	0.034796
Residual	21	494.367 6	23.5413 2		
Total	22	501.821 1			

	Coefficients	Standard Error	t Stat	P-value	Lower 95%	Upper 95%	Lower 95.0%	Upper 95.0%
Intercept	8.478197	2.10899 7	4.02001 5	0.00061 9	4.092299	12.8641	4.09229 9	12.8641
4pc	0.039248	0.06975 2	0.56268 2	0.04796 1	0.484113	0.04796 1	0.48411 3	0.18430 5

Figure11. Obtained regression analysis with PCA components in IBM SPSS

	Component				
	1	2	3	4	5
Burden m	-.366	-.054	-.198	-.112	.661
Spacing m	-.422	.212	.742	.408	-.029
Depth of holes m	-.297	.272	.890	.036	-.013
No of holes	.886	.277	-.271	.075	.046
No rows	.551	-.763	.219	.063	-.058
Explosive ANFO kg	.817	.321	.333	-.109	.199
Throw	.333	-.337	-.131	.666	-.101
Total explosive kg	.808	.346	.398	-.039	.227
Firing pattern	.551	-.763	.219	.063	-.058
LW Ratio	.415	.844	-.234	.141	-.034
MKSK50	-.148	-.128	-.098	.568	.627

Figure12 Extracted components from matrix

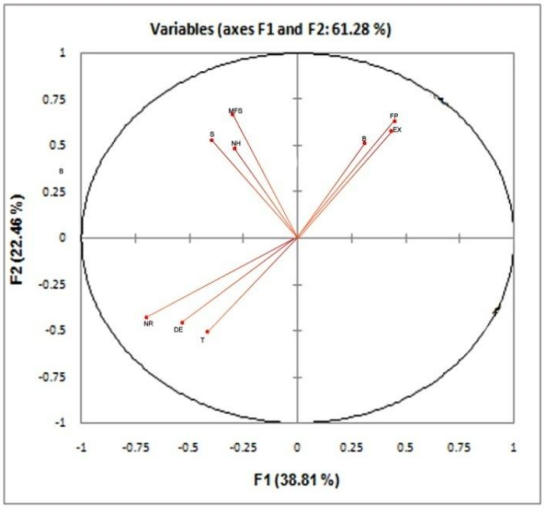

Figure13.Variable chart obtained from XLSTAT

MEAN FRAGMENTAION SIZE RESULTS OBTAINED FROM INDIAN CEMENTS (Case 3)

SUMMARY OUTPUT

Regression Statistics

Multiple R	0.465376
R Square	0.216575
Adjusted R Square	0.160616
Standard Error	0.100879
Observations	16

ANOVA

	Df	SS	MS	F	Significance F
Regression	1	0.03938 6	0.03938 6	3.87024 6	0.069288
Residual	14	0.14247 2	0.01017 7		
Total	15	0.18185 8			

	Coefficients	Standard Error	t Stat	P-value	Lower 95%	Upper 95%	Lower 95.0%	Upper 95.0%
Intercept	0.224268	0.03359 1	6.67648 05	1.05E 05	0.152223	0.29631 4	0.15222 3	0.29631 4
pc1	0.000809	0.00041 1	1.96729 4	0.06928 8	-7.3E-05	0.00169	-7.3E-05	0.00169

Figure14. Obtained regression analysis with PCA components in IBM SPSS

Published By:
Blue Eyes Intelligence Engineering
& Sciences Publication

Component Matrix[a]

	Component					
	1	2	3	4	5	6
Burden m	.405	.702	.034	.021	-.479	.287
Spacing m	.454	.804	.217	-.052	-.078	.202
Depth of holes m	.902	.056	-.120	.181	.287	.053
Front row burden m	.034	.645	-.373	.114	.502	.074
No of holes	-.621	.031	.695	.050	-.042	.214
No of rows	-.718	.403	.124	.443	.114	.152
Explosive quantity Kg	.228	.084	.902	.289	.026	-.014
Charge length m	.900	.109	.088	.252	.209	.100
Firing pattern	.238	-.610	-.355	.379	.049	.450
Total delay time ms	-.361	-.374	.225	.045	.678	.339
Throw m	.118	-.747	-.023	.120	-.466	.373
LW Ratio	.347	-.291	.303	-.772	.249	-.065
MKSK50	.746	-.328	.356	-.124	.027	.061

Extraction Method: Principal Component Analysis. a. 6 extracted

Figure15.Extracted components from matrix

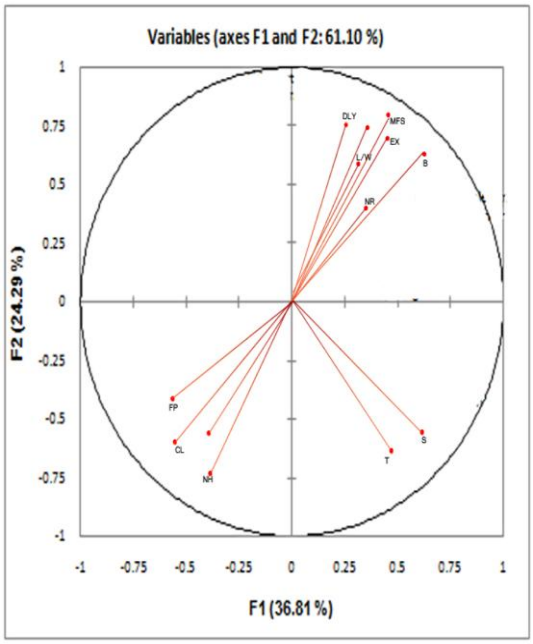

Figure16.Variable chart obtained from XLSTAT

MUCKPILE RESULTS OBTAINED FROM INDIAN CEMENTS (Case 3)

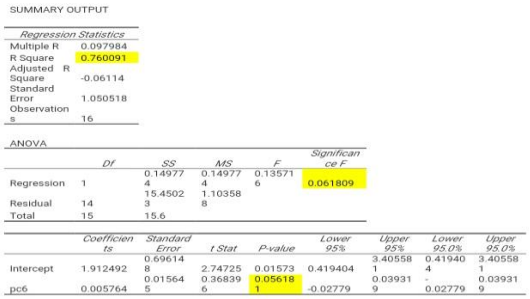

SUMMARY OUTPUT

Regression Statistics	
Multiple R	0.097984
R Square	0.760091
Adjusted R Square	-0.06114
Standard Error	1.050518
Observations	16

ANOVA

	Df	SS	MS	F	Significance F
Regression	1	0.149774	0.149774	0.135716	0.061809
Residual	14	15.45023	1.103588		
Total	15	15.6			

	Coefficients	Standard Error	t Stat	P-value	Lower 95%	Upper 95%	Lower 95.0%	Upper 95.0%
Intercept	1.912492	0.696148	2.747256	0.015731	0.419404	3.405581	0.419404	3.405581
pc6	0.005764	0.001565	0.368396	0.056181	-0.02779	0.039319	-0.02779	0.039319

Figure17. Obtained regression analysis with PCA components in IBM SPSS

	Component					
	1	2	3	4	5	6
Burden m	.405	.702	.034	.021	-.479	.287
Spacing m	.454	.804	.217	-.052	-.078	.202
Depth of holes m	.902	.056	-.120	.181	.287	.053
Front row burden m	.034	.645	-.373	.114	.502	.074
No of holes	-.621	.031	.695	.050	-.042	.214
No of rows	-.718	.403	.124	.443	.114	.152
Explosive quantity Kg	.228	.084	.902	.289	.026	-.014
Charge length m	.900	.109	.088	.252	.209	.100
Firing pattern	.238	-.610	-.355	.379	.049	.450
Total delay time ms	-.361	-.374	.225	.045	.678	.339
Throw m	.118	-.747	-.023	.120	-.466	.373
LW Ratio	.347	-.291	.303	-.772	.249	-.065
MKSK50	.746	-.328	.356	-.124	.027	.061

Figure18.Extracted components from matrix

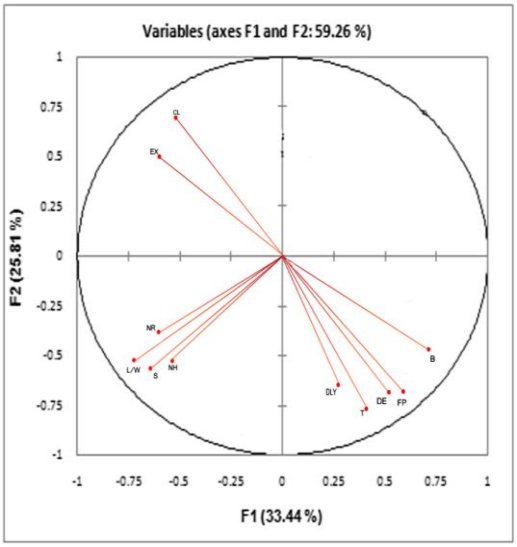

Figure19.Variable chart obtained from XLSTAT

Published By:
Blue Eyes Intelligence Engineering
& Sciences Publication

V. RESULTS AND DISCUSSIONS

The PCA results were drawn from component matrix according to their R^2 and F values in regression analysis and results were compared with correlation circle in XLSTAT.

SHREE CEMENTS:

Influencing parameters on MFS:

Significant parameters

1. Spacing 2.Throw 3.Depth of hole 4. Throw 5.No Rows 6.No Holes 7.L/W Ratio

Non-Significant parameters

1. Explosive 2.Burden 3. Firing pattern

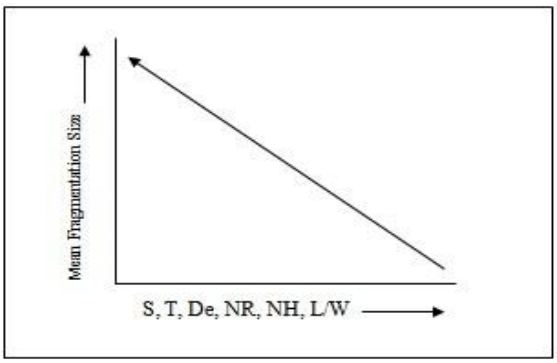

Figure20.Significant parameters

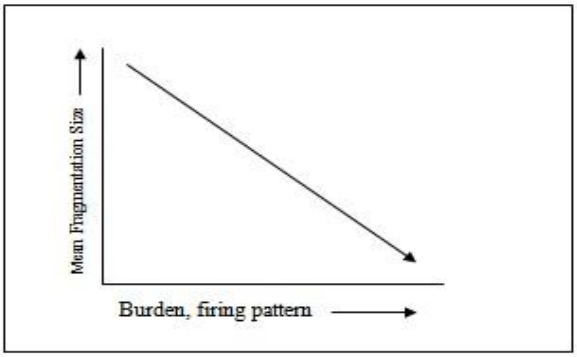

Figure21.Non-significant parameters

Influencing parameters on Muck pile:

Significant parameters

1 Spacing 2.Throw 3.Depth of hole 4.MFS 5. Firing pattern 6.No Rows 7.No Holes 8.L/W

Significant parameters

1. Explosive 2.Burden

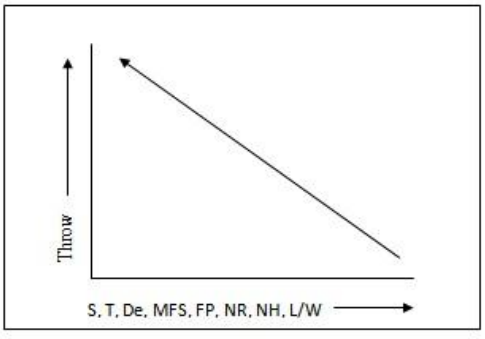

Figure22.Significant parameters

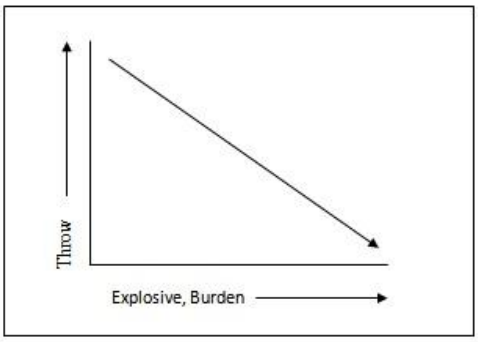

Figure23.Non-significant parameters

WONDER CEMENTS:

Influencing parameters on MFS:

Significant parameters

1 Spacing 2.Throw 3.Depth of hole 4. Throw 5. Firing pattern 6.Explosive 7.Burden 8.Charge length 9.Front row burden

Non-Significant parameters

1. No Rows 2.No Holes

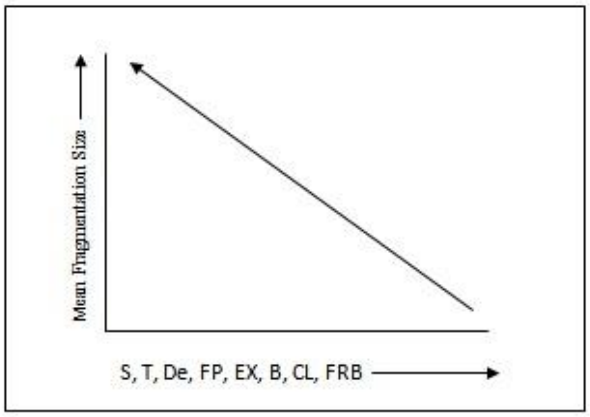

Figure 24.Significant parameters

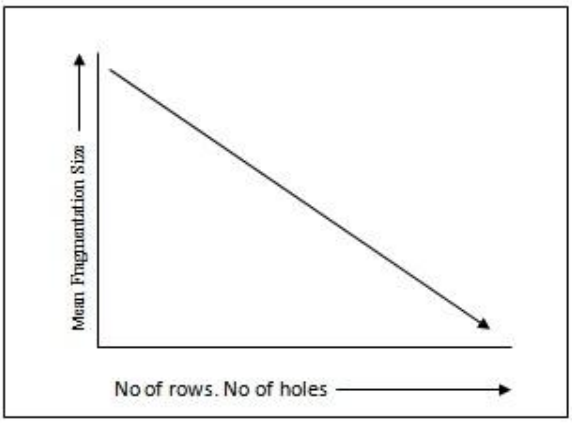

Figure25.Non-significant parameters

Influencing parameters on Muck pile:

Significant parameters

1 Spacing 2.MFS 3.Depth of hole 4. Delay 5.Firing pattern 6.Burden 7.Charge length 8.Front row burden 9.No Rows 10.No Holes

Non-Significant parameters
1. Explosive 2.L/W Ratio

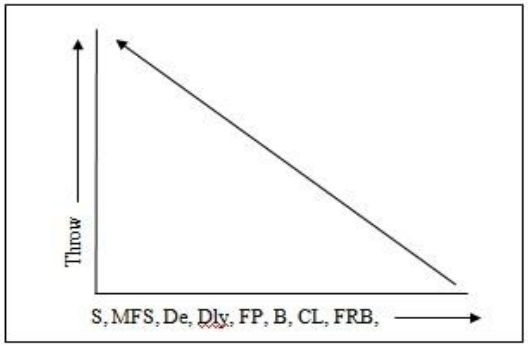

Figure 26.Significant parameters

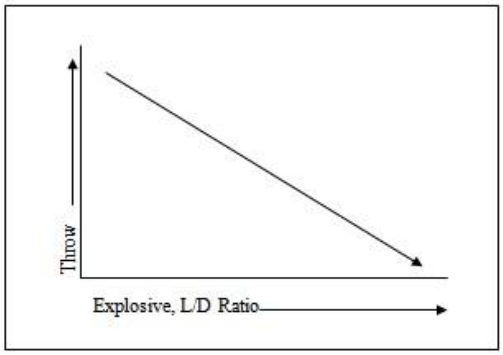

Figure27.Non-significant parameters

INDIAN CEMENTS:
Influencing parameters on MFS:

Significant parameters
1. Delay 2.No Rows 3.No Holes 4.Depth of hole 5.L/W Ratio

Non-Significant parameters
1. Front row burden 2.Burden 3.Spacing 4.Firing pattern 5.Throw

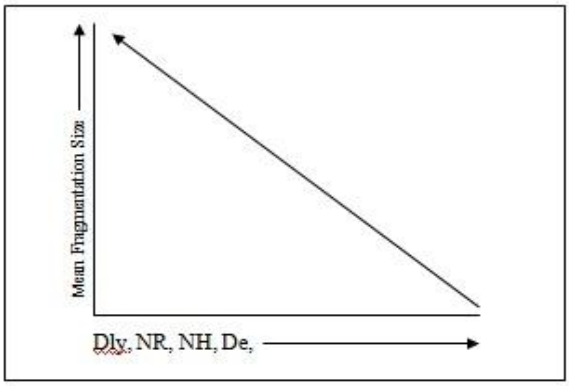

Figure 28. Significant parameters

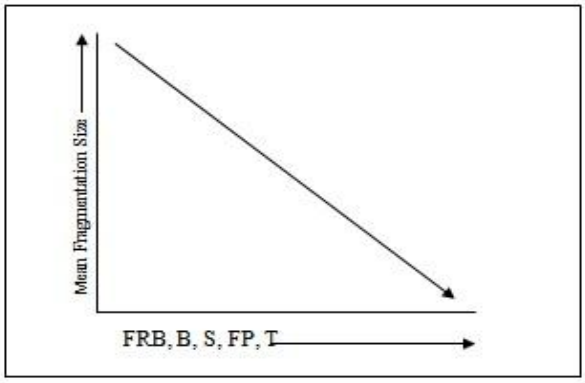

Figure 29.Non-significant parameters

Influencing parameters on Muck pile:
Significant parameters
1. Front row burden 2.Burden 3.Delay 4.Depth of hole 5.L/W Ratio 6. MFS
Non-Significant parameters
1. Spacing 2.No Rows 3.No Holes 4.Se/Be 5. Firing pattern

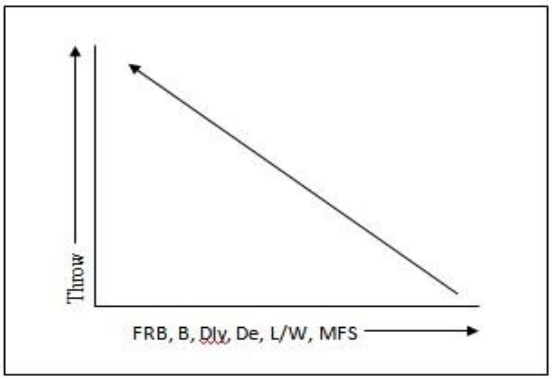

Figure 30.Significant parameters

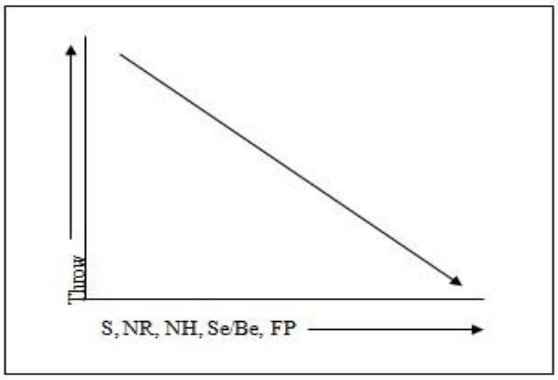

Figure 31.Non-significant parameters

VI. CONCLUSION

- PCA found that if Burden, Front Row Burden and Spacing decreases MFS will increase these are inversely proportional and from XLSTAT results given that Burden is negatively, Front Row Burden is positively and Spacing is orthogonally correlated

- PCA found that if Explosive charge, Delay, Depth of the hole, No of holes, spacing burden ratio increase MFS will increase these are directly proportional and from XLSTAT results given that Explosive, Delay, Depth of the hole, No of holes, spacing burden ratio are positively correlated
- PCA found that if Burden, Front Row Burden, Firing pattern decrease/change throw will decrease both are directly proportional and from XLSTAT results given that Burden is positively. Front Row Burden positively correlated and firing pattern negatively correlated
- PCA found that if Explosive charge, Delay, Depth of the hole, spacing burden ratio increase throw will decrease both are inversely proportional and from XLSTAT results given that Explosive is negatively correlated and delay, depth of the hole, spacing burden ration positively correlated

REFFERENCES

1. Cristinel constantin., "Principal component analysis - a powerful tool in computing marketing information" Bulletin of the Transilvania University of Braşov Series V: Economic Sciences, Vol. 7 (56) No. 2, 2014
2. SvanteWold*KimEsbensen,PaulGeladi.," Principal component analysis" Elsevier: Volume 2, Issues 1–3, Pages 37-52, August 1987.
3. Cunningham, C.V.B.,"The Kuz-Ram model for prediction of fragmentation from Blasting" Symposium on Rock fragmentation by blasting, Lulea University, pp 439-453, Sweden 22-26August, 1987
4. Choudhary., "B.S. Assessment of fragmentation in limestone quarry blasts" Ph.D. thesis, Banaras Hindu University, Varanasi,2011 (Unpublished).
5. Kuznetsov, V.M., "The mean diameter of the fragments formed by blasting rock" Soviet Mining Science 9(2);144-148, 1973
6. Choudhary, B.S., "Firing Patterns and its effect on muck pile shape Parameters and fragmentation in quarry blasts" International Journal of Research in Engineering and Technology, Volume: 02 Issue: 09,Sep-2013
7. Mohammad Farouq Hossaini et.al." Minimizing Mucking Time by Prediction of Muckpile Top Size in Tunnel Blasting" A CaseStudy University of Wollongong. International Journal of Engineering and Technology, 2014.
8. P. K. Singh et.al.,"Blast design and fragmentation control - key to productivity",2004 (Unpublished).
9. T. Hudaverdi n, C. Kuzu, A. Fisne., "Investigation of the blast fragmentation using the mean fragment size and fragmentation index" International Journal of Rock Mechanics & Mining Sciences, 2012
10. P.K. Singh et.al, "Rock fragmentation control in opencast blasting. Journal of Rock Mechanics and Geotechnical Engineering,2016
11. B. Adebayo and J.M. Akande.," Effects of blast-hole deviation on drilling and muck-pileloading cost" International Journal of Scientific Research and Innovative Technology ISSN: 2313-3759 Vol. 2 No. 6; June 2015
12. Carlos lopez jimeno.,"Drilling and blasting of rocks"A published book,1995

Implementation of Lock-In Method using NLFB for Brain Monitoring Applications on FPGA

N.Subbulakshmi, R.Chandru, R. Manimegalai

Abstract: ***In recent years, many algorithms have been discussed for the biomedical applications in Digital Signal Processing. In this work, an advanced frame-work which will be helpful for the brain monitoring, in view of a Sync field programmable Gate Array (FPGA) has been planned and executed, trying to investigate if this strategy may enhance the execution of this proposed framework. All the more extensively, FPGA-based arrangement adaptability has been researched, with specific accentuation connected to advanced channel parameters, required in the computerized devices, and its effect on the last flag recognition and commotion dismissal capacity has been assessed. The proposed design was a blended arrangement between VHDL/Verilog equipment modules and programming modules, running inside a chip. Exploratory outcomes have demonstrated the integrity of the proposed arrangements and similar subtle elements among various executions will be itemized. At long last a key perspective considered all through the plan was its measured quality, permitting a simple increment of the info channels while keeping away from the development of the outline cost of the hardware framework. Specifically, the activity of the proposed NLFB acquired an extremely solid dismissal of clamor influencing the standard, especially for signals identified with frameworks. Parameters such as delay, area and power are compared with the traditional method.***

Keywords: Hearing Aid, Digital Signal Processing, Smart devices

I. INTRODUCTION

Over the most recent few years, the examination of physiological information has been effectively connected to accomplish diverse research or application objectives, e.g., to control various types of gadgets, to permit secured patients to speak with their condition, or to adjust specialized gadgets to the intellectual condition of a human [1– 11]. Particularly in the field of neuro restoration and support of day by day exercises the enthusiasm to utilize physiological information has expanded. A confinement or loss of the versatility because of a neurological illness or damage, for example, stroke or spinal string wounds, for the most part decreases the patients personal satisfaction extensively. In such a case, physiological information can be

connected to adjust a restoration or bolster gadget, for example a dynamic orthosis or exoskeleton, keeping in mind the end goal to quicken or enhance the recovery procedure of patients or to give an appropriate measure of help in day by day life. In this unique circumstance, the capacities of the recovery gadget are an applicable issue.

Revised Manuscript Received on December 08, 2018.

Dr.N.Subbulakshmi, Associate Professor, ECE Dept., Malla Reddy Engineering College(A),Secunderabad,Telangana, India

R.Chandru, Assistant Professor, ECE Dept., Sri Ramakrishna Engineering College, Coimbatore, Tamilnadu, India

Dr.R. Manimegalai, Professor, IT Dept., PSG College of Technology, Coimbatore, Tamilnadu, India

II. LITERATURE SURVEY

A recovery gadget should bolster treatment approaches that include practical preparing that is custom fitted to the physical conditions and treatment condition of the patient (help as required) [12,13]. The investigation of secure systems to distinguish and measure little flags, normally covered profoundly in abnormal state clamor, has been researched since the mid part of the 19th century[1,2]. Soon unmistakably the strategy had noteworthy potential, independent of the recurrence go in which it discovered application. Secure enhancement is fundamentally a stage delicate location procedure equipped for segregating a portion of the flag at a particular reference recurrence and stage. Regardless of whether this flag is covered in commotion sources commonly bigger, the framework chops down and emphatically throwaways the clamor signals at incidences other than a allusion "secured" recurrence, with the goal that they don't influence the flag estimation. For quite a while secure strategies were firmly in view of simple gadgets parts. Since the appearance of intense computerized frameworks, to be specific DSP (advanced flag preparing), 32-bit chip with interior DSP abilities, ASICs (application particular coordinated circuits) and PLDs (programmable rationale gadgets) or field programmable door exhibits, dynamically supplanted simple models by outflanking them in each angle, for example, the permissible recurrence run, the level of info clamor and the solidness every one of them specifically identified with the examining rate of the front-end ADCs notwithstanding the accessible computerized figuring power.

III. PROPOSED METHOD

With a specific end goal to achieve the depicted objectives, a framework ready to achieve the coveted assignments and to guarantee fast prototyping has been outlined, equipped for leaving the most elevated conceivable opportunity degrees for encourage examinations and enhancement of exhibitions in view of parameter elaboration. The usage of the secure enhancer utilized is the notable double stage LIA [5]. It consumes up the information flag, adjusted at a settled recurrence, and duplicates it by created sin and cos reference signals, flowing at a similar recurrence of the tweaked flag. The yields are low-pass sifted with a legitimately planned computerized channel so as to dismiss clamor and undesirable recurrence segments.

Keeping in mind the end goal to discover the channel yield abundancy, the obtained convolutions are then squared up and added together, lastly the square root is figured. Flag stage is, in the interim, dismissed in light of the fact that it isn't including critical data in our examinations. Programmable rationale pieces execute the vast majority of the substances expected to understand the lock- in speaker; while some less- demanding capacities keep running in the ARM processors. Novel Lifting based Filter Bank (NLFB) outline for the advanced portable amplifier applications [12]. The input sound flag is connected to the examination bank. The lifting steps and reverse lifting steps are connected in the Analysis and Amalgamation channel banks individually. In investigation Filter bank, the input flag is decayed into numerous recurrence parts for preparing by the lifting steps. The Multi-level signs are split by the multilevel disintegrating tree. In each level, it produces diverse sub-groups. Anticipated and refreshed information tests are connected to channel which is appropriate for sound flag handling. The co-proficient esteems are worked remotely to save the channel structure. Let the information arrangement x(n) is {1,2,3,4,5,6,7,8} with the length of 8 components. 2l =8=23; Hence l=3; Where l is the level of deterioration. Use of NLFB provides better results than the traditional FIR filters. Figure.1 states the block diagram of the proposed method using NLFB.

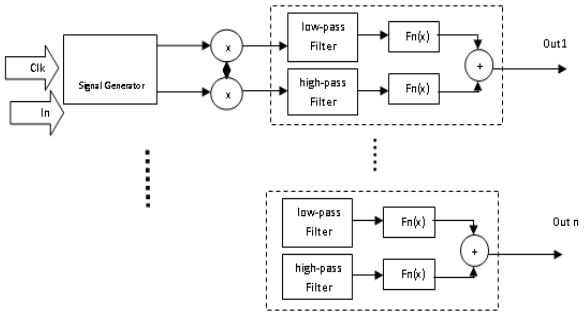

Figure. 1 Block Diagram of Proposed Method

Table 1: Comparisons results based on Frequency

Frequency/ Methods	Convention	IFB	Proposed Method
250	35	30	30
500	30	35	35
1000	40	40	35
2000	35	35	35
4000	40	40	40
8000	40	40	40

IV. RESULTS AND DISCUSSIONS

The estimation setup hardware, used to demonstrate and confirm framework usefulness, incorporates an Automatic Wave Generator (AWG) the AFG3102 by Tektronix™ (Beaverton, Oregon, USA) equipment. Keeping in mind the end goal to test the decency of the executed framework, it was extremely valuable to mimic an info flag having properties and features appropriately and sufficiently reasonable as bio-flagged and with plainly noticeable fleeting ghastly. A sin(t) waveform is chosen as the tweaking signal for its phantom characteristic feature and shape.

The adaptability of effectively choosing the secure recurrence partion has been misused to locate the ideal recurrence for clamor dismissal. The most astounding conceivable secure recurrence (flock in = 16 kHz/8 = 2 kHz) has been chosen. The size reaction of the half band low-pass channel and high-pass channel is estimated utilizing MATLAB apparatus. The yield of the first and remade signals is appeared in the diagrams. The format of the center channel is composed utilizing the FPGA instrument. The design is implemented in the *Zynq field programmable Gate Array.

Table 2: Comparisons results based on Area, Delay and Power

Parameters	Interpolated Filter Bank	Proposed Method
Area	18,223	12,013
Delay	120ns	103.142ns
Power	77mW	66mW

V. CONCLUSION

This publication composes and actualizes a FPGA-based secure engineering with the plan to acquire incredible adaptability on key outline parameters, for example, testing and secure recurrence, together with the primary attributes of the center computerized sifting activity, installed in the secure chain. Furthermore, the plan standards depicted here may likewise be more significant to the future research territories. The acknowledged framework has outlined an inherent status with a measured quality and quantity of procured conduits without influencing the general design. But little quantities of conduits, the resulting complex exertion bringing down can imagine a conceivable execution in light of a microcontroller with reasonable advanced flag preparing abilities. Broad trial appraisals have been completed and the gotten comes about show great conduct of the created framework. Specifically, the activity of the proposed NLFB acquired an extremely solid dismissal of clamor influencing the standard, especially for signals identified with the proposed frameworks. In future, this technique can be applicable for the wearable technology for various applications.

REFERENCES

1. Stutt, C.A. Low-Frequency Spectrum of Lock-In Amplifiers. MIT Technical Report (MIT). 1949. Available online: http://dspace.mit.edu/handle/1721.1/4940 (accessed on 29 December 2016).
2. Michels,W.C.; Curtis, N.L. A Pentode Lock-In Amplifier of High Frequency Selectivity. Rev. Sci. Instrum.1941, 12, 444–447.
3. Cheng, J.; Xu, Y.; Wu, L.; Wang, G. A Digital Lock-In Amplifier for Use at Temperatures of up to 200 Sensors 2016, 16, 1899.
4. He, D.; Morgan, S.P.; Trachanis, D.; van Hese, J.; Drogoudis, D.; Fummi, F.; Stefanni, F.; Guarnie-ri, V.; Hayes-Gill, B.R. A Single-Chip CMOS Pulse Oximeter with On-Chip Lock-In Detection. Sensors 2015, 15, 17076–17088.

5. Macias-Bobadilla, G.; Rodríguez-Reséndiz, J.; Mota-Valtierra, G.; Soto-Zarazúa, G.; Méndez-Loyola, M.; Garduño-Aparicio, M. Dual-Phase Lock-In Amplifier Based on FPGA for Low-Frequencies Experiments. Sensors 2016, 16, 379. [CrossRef] [PubMed] Ferrari, M.; Quaresima, V. A brief review on the history of human functional near-infrared spec-troscopy (fNIRS) development and fields of application. NeuroImage 2012, 63, 921–935.
6. Shimadzu, LABNIRS. Available online: http://www.shimadzu.com/an/lifescience/imaging/nirs/nirs_top.html (accessed on 29 December 2016).
7. HITACHI—ETG-4000. Available online: http://www.hitachi-medical-systems.eu/products-and-services/ optical-topography/etg-4000.html.
8. Electrical Geodesic Inc., EEG System. Available online: https://www.egi.com/research-division/researchdivision- research-products/nirs-system (accessed on 29 December 2016).
9. Von Lühmann, A.; Wabnitz, H.; Sander, T.; Müller, K.-R. M3BA: A Mobile, Modular, Multimodal Biosignal Acquisition architecture for miniaturized EEG-NIRS based hybrid BCI and monitoring. IEEE Trans. Biomed. Eng. 2016, PP, 1.
10. Agrò, D.; Canicattì, R.; Pinto, M.; Morsellino, G.; Tomasino, A.; Adamo, G.; Curcio, L.; Parisi, A.; Stivala, S.;Galioto, N.; et al. Design and Implementation of a Portable fNIRS Embedded System. In Applications in Electronics Pervading Industry, Environment and Society; Lecture Notes in Electri-cal Engineering; Springer: Berlin, Germany, 2016; Volume 351, pp. 43–50.
11. Subbulakshmi N & Manimegalai R, NLFB: Novel Lifting based Filter Bank for Hearing Aid', Journal of Computational and Theoritical Nanoscience, vol. 14, no. 2, pp. 1410-1416. 1546-1955, 2017.

Published By:
Blue Eyes Intelligence Engineering
& Sciences Publication

Experimental analysis of Thermal Performance of Solar Collector using CuO-H_2O Nanofluid

Dharmalingam Ramasamy, Sudhakara Reddy S, Ramachandran T, Gunasekharan S

Abstract: ***The peak performance of a solar collector with flat plate is increased by via Nano fluid which acts as a heat transfer layer. The thermal behaviour of solar collector while using nanofluids as heat transfer medium can be analysed using experimental or suitable numerical techniques. Experimental analysis is considered as prime important in the scientific society by providing opportunity to test theoretical hypothesis and physical statements of a problem. It gives average output values for the given input values of a system or process. In this work, experimental analysis of solar collector is performed using water and copper oxide-water (CuO-H2O) nanofluid as heat transfer medium with various concentrations of nanoparticle such as 0.1%, 0.2% and 0.3% mass fractions. Water and CuO nanofluid are circulated with 0.016kg/s and 0.033kg/s mass flow rate. The analysis done for this presentation claims the effectual property of CuO nanofluid containing various mass fractions of nanoparticle on collector outlet temperature, rate of heat transfer and efficiency is better than water. The pressure drop across the solar collector is more in CuO nanofluid due to its high density and viscosity.***

Keywords: Solar flat plate collector, experimental analysis, CuO nanofluid, heat transfer, efficiency, pumping power.

I. INTRODUCTION

The sun is 1.39 x 10^9 metre diameter and 1.495 x 10^{11} metre away from the earth. Sun releases solar energy approximately in the range of 1350 W/m^2 to a perpendicular surface. Only 0.5% of energy emitted by sun is utilized for energy conversion out of 170 trillion KW [1]. Solar energy is converted into other forms such as heat energy or electrical energy using suitable devices. Heat energy is mostly used for drying food grains and fruits. Due to variation of energy potential, separate energy storage units are required to fulfil constant energy requirements [2]. Solar collector is a device used to convert the Sun's direct heat energy which is the solar energy into thermal force. Solar collector is an important component in solar-thermal power installations [3]. The appropriate performance level of solar collector is enhanced by implementing fluids having high thermal conductivity as heat transfer medium. Nanofluid consists of nano sized particles (1-100nm) mixed with water or some other fluids. Hence, it is called as new generation fluid. The properties of nanofluid depend on the characteristic features exhibited by each and every nano particle and its corresponding base fluid. The applications of nanofluids not only limited to thermal related applications. It also extended to chemistry, coating, tribology, environmental, surfactants and biomedical applications [4]. The nanofluid imparted solar collectors have been probed in the perspective of efficiency or environmental and economic considerations [5,6]. Tyagi et al.[7] explored the performance status and stages of solar collector (direct absorption) with the help aluminium-water based nanofluids by gradually varying the nanoparticle volume ratio from 0.1% to 0.5%. Based on the outcome under each ratio the collector efficiency is evaluated with Eqn. 1

$$\eta = \frac{Useful\ heat\ gain}{Available\ energy} = \frac{mC_p\Delta T}{AG_T} = \frac{mC_p(T_o - T_i)}{AG_T} \quad \textbf{(1)}$$

The experiment is carried out at constant solar flux of 1000W/m^2, nanofluid passing into the collector at a stable temperature of 35^{O}C, mass flow proportion of 1.2 kg/s. From the observation, the effectual efficiency of collector increases while using less nanoparticle concentration in terms of volume fraction. When nanoparticle volumetric fractional value is much higher than 2%, the effectual performance of the collector becomes constant and uneconomical. Also they stated that the efficiency slightly increases as nanoparticle size increases. Otanicar et al [8] analyzed the effectual status of carbon induced nanotubes silver and graphite on solar collector (direct absorption) experimentally and numerically. The efficiency also enhances up to 0.5% volume fraction. Beyond 0.5% volume fraction, the efficiency becomes constant and declines as the volume fraction of nanoparticle increases. The drop in efficiency is due to high absorption of fluid when nanoparticle concentration elevates. The effect of size of nanoparticle on efficiency is also investigated and shown in figure 1. A 6% increase of collector efficiency is obtained while decreasing nanoparticles size from 40nm to 20nm. Unlike stated by Tyagi et al, the efficiency increases as the nanoparticle size decreases.

Revised Manuscript Received on December 08, 2018.

Dharmalingam Ramasamy, Department of Mechanical Engineering, Malla Reddy Engineering College, Hydearbad, India–500100.

Sudhakara Reddy S, Department of Mechanical Engineering, Malla Reddy Engineering College, Hydearbad, Telangana, India–500100.

Ramachandran T, Department of Mechanical Engineering, Malla Reddy Engineering College, Hydearbad, Telangana, India–500100

Gunasekharan S, Department of Mechanical Engineering, Malla Reddy Engineering College, Hydearbad, Telangana, India–500100,

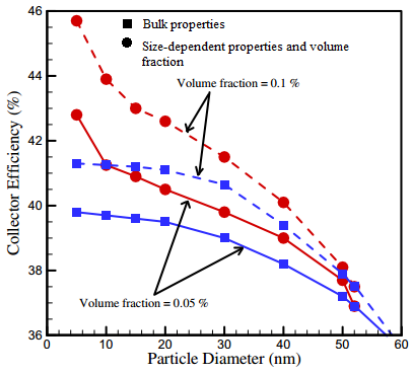

Figure 1 Effect of nanoparticle size on collector efficiency [8]

Yousefi et al. [9] observed the pH variation in water based multi walled carbon nanotubes nanofluid on solar collector efficiency. The p^H values such as 3.5, 6.5 and 9.5 is maintained with nanoparticle concentration as 0.2 wt%. Triton X-100 is the surfactant. They introduced pH of isoelectric point and stated that the dissimilarity between pH value and pH of isoelectric point increases the collector efficiency. Link et al [10] explained the optical properties of gold nanoparticles and analysed the effect of shape and size on radiative and photo thermal properties of gold nanoparticles. Khlebtsov et al [11] experimented the optical properties of the nanofluids due to size, structure and shape of silver and gold nanoparticles. The shape as well as size of the nanoparticle greatly influences the optical properties of nanofluids. In the current work, initially water is used as heat transfer medium to analyse the thermal performance of solar collector. Then CuO nanofluid is used as heat transfer medium with 0.1%, 0.2% and 0.3% mass fraction of nanoparticle. Both water and nanofluid is circulated with 0.016kg/s and 0.033kg/s mass flow rates.

II. EXPERIMENTAL SETUP

Figure 2 Experimental setup of solar collector

The experimental setuo of the solar collector is shown in figure 2. Solar collector is the rectangular box of 2m length, 1m width and 0.1m thickness. The solar collector consist of single toughened glass cover, corrugated copper plate brazed with riser tubes The sides and bottom of the collector is insulated using glass wool. The fluid is pumped using centrifugal pump from fluid tank to solar collector. The fluid enters the bottom of the collector through header pipe. The fluid rises from the bottom header pipe to the top header pipe through nine riser tubes of 12.5mm diameter. The hot fluid coming out from the collector is passed to the heat exchanger and again it is circulated to the collector through fluid tank. The hot fluid coming out from the solar collector is passed through the heat exchanger. The design of heat exchanger is made to reduce the temperature of fluid upto 25^OC. Furthermore, if the temperature is more than 25^OC, the fluid will be passed through ice sump to reduce excess heat thereby inlet fluid flow temperature to the solar collector is maintained as constant. The experimental setup is shown in figure 3.

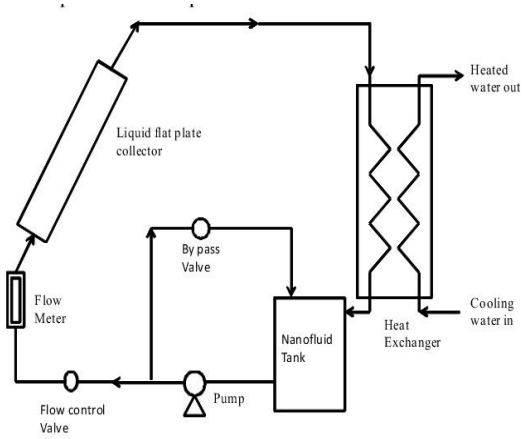

Figure 3 Flow diagram of the experimental setup

III. CHARACTERIZATION AND PREPARATION OF NANOFLUID

The CuO nanoparticles are produced by physical vapour synthesis method. The elemental analysis of CuO nanoparticle is measured by using Energy–Dispersive X–ray Spectroscopy (EDS). Each elements present in the nanoparticle have the capacity of emiting electromagnetic spectrum due to its unique atomic structure when exposed to X-ray radiation. Based on the electromagnetic emission spectrum, the chemical composition of the CuO sample is measured. The figure 4 shows the EDS analysis of CuO nanoparticle sample. The presence of gold in the CuO nanoparticle is not the part of CuO nanoparticle and it is due to coating of nanoparticles with gold for the feasibility of EDS analysis.

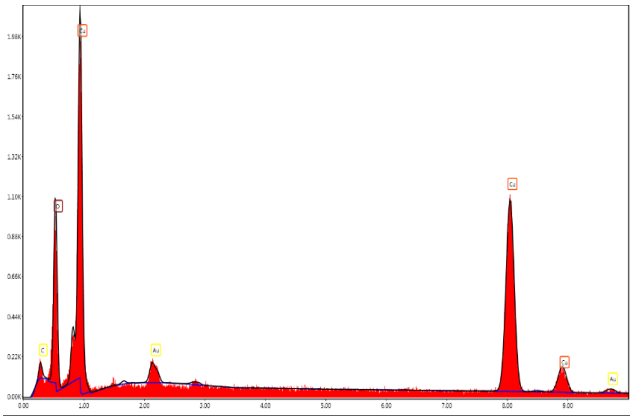

Figure 4 Energy–Dispersive X–ray Spectroscopy image of CuO nanoparticles

The nanoparticle sample is tested using Scanning Electron Microscope (SEM). The size of the nano particlulates can be measured using SEM analysis. In this analysis, the sample is placed underneath of the electron beam and scanned to create image of the particle. The electron beam interacts with nanoparticles and signals are produced. The obtained signals are processed to measure the size of the nanoparticle. The SEM analysis of CuO nanoparticle is shown in figure 5 and the nanoparticles are within the size range of 20 - 40 nanometer.

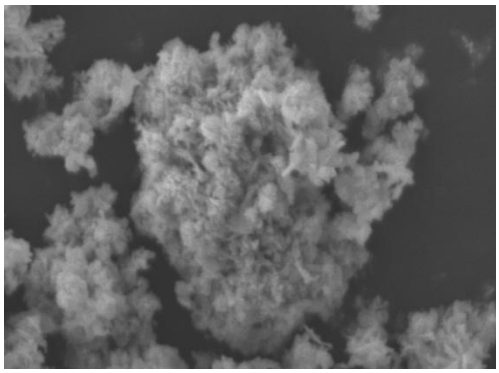

Figure 5 SEM image of CuO nanoparticles

S K Das and his co researchers [12] explained the preparation of nanofluid with proper suspension of nanoparticles in the base fluid as follows

$$\%\ \text{Mass fraction} = \frac{\text{Mass of the nanoparticle}}{\text{Mass of the basefluid}} \quad \textbf{(2)}$$

$$\%\ \text{Volume fraction} = \frac{\frac{\text{Weight of the nanoparticle}}{\text{Density of the nanoparticle}}}{\frac{\text{Weight of the nanoparticle}}{\text{Density of the nanoparticle}} + \frac{\text{Weight of the basefluid}}{\text{Density of the basefluid}}} \quad \textbf{(3)}$$

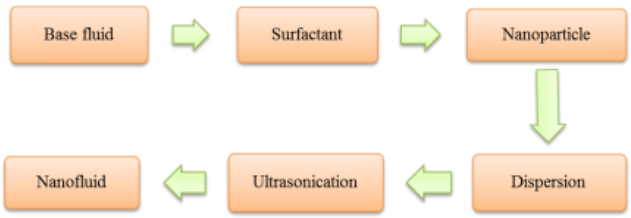

Figure 6 Preparation of nanofluid

Figure 6 shows the process steps of preparation of nanofluid. The surfactant is mixed with base fluid first and then nanoparticles are thoroughly mixed with existing mixture. Triton X-100 of 0.02wt% acts as a surfactant. Pure Distilled water is used as basal fluid and the surfactant and nanoparticle is mixed with base fluid to obtain complete dispersion. This dispersion is kept in ultrasonicator for 45 minutes to obtain the homogeneous suspension.

IV. DATA REDUCTION

The properties that influence the nature of nanofluids namely Viscosity, thermal conductivity, density and specific heat can be calculated as follows [14-18]:

$$\rho_{nf} = \rho_{np}(\varphi) + \rho_{bf}(1-\varphi) \quad \textbf{(4)}$$

$$\mu_{nf} = \frac{\mu_{bf}}{(1-\varphi)^{2.5}} \quad \textbf{(5)}$$

$$\frac{k_{nf}}{k_{bf}} = \frac{k_{np} + 2k_{bf} + 2(k_{np} - k_{bf})\varphi}{k_{np} + 2k_{bf} + (k_{np} - k_{bf})\varphi} \quad \textbf{(6)}$$

$$C_{p,nf} = C_{p,np}(\varphi) + C_{p,bf}(1-\varphi) \quad \textbf{(7)}$$

Where, ρ is the density, μ denotes viscosity, k denotes the constant of thermal conductivity, C denotes specific heat and subscripts bf, np and nf denotes type of the basal fluid, nanoparticles and nanofluids . Here φ is the volumetric concentration of the nanofluid. Table 1 lists the thermal and physical properties of basal fluid and nanoparticulates

Table 1 Properties of base fluid and nanoparticle

S.No	Properties	Thermal Conductivity (W/mk)	Density(kg/m^2)	Specific heat, J/kgK
1.	Water	0.613	997.13	4180
2.	Al_2O_3	39	3970	775
3.	CuO	18	6510	540
4.	Au	314	19320	129

The Reynolds number and velocity of the flow is calculated as follows.

$$\text{Reynolds number, } R_e = \frac{4m}{\pi D\mu} \quad \textbf{(8)}$$

$$R_e = \frac{\rho V D}{\mu} \quad \textbf{(9)}$$

Heat transfer rate and efficiency of the collector are calculated by

Heat transfer rate, $Q = mCp(T_o - T_i)$ (10)

Collector efficiency, $\eta = Q_u/(A_c G_T)$ (11)

The pumping power is calculated as [19],

$$\text{Pumping power} = \left(\frac{m}{\rho_{nf}}\right)\Delta p \quad (12)$$

Where, D is diameter , m is mass flow proportion, T_i and T_o is outlet and inlet temperature of nanofluid, C_p is a constant denoted as the specific heat capacity, G_T is assumed as the solar flux incident on the collector inclined exterior circumferential area and A_c being the area of collector.

V. EXPERIMENTAL ANALYSIS OF SOLAR FLAT PLATE COLLECTOR USING CUO NANOFLUID

The CuO-H_2O Nanofluid is prepared with the nanoparticle concentration of 0%, 0.1%, 0.2% and 0.3% mass fraction.

Published By:
Blue Eyes Intelligence Engineering
& Sciences Publication

The 0% nanoparticle concentration represents distilled water. The properties of CuO-H_2O nanofluid containing 0.1%, 0.2% and 0.3% mass fraction of nanoparticle is given in table 2. The water and nanofluid is circulated at 0.016kg/s and 0.033kg/s. The changes dealt in CuO-H_2O nanofluid on solar collector is studied experimentally. Initially, water is used as heat transfer medium and then CuO nanofluid containing 0.1%, 0.2% and 0.3% mass fraction of nanoparticle is tested using solar collector.

Table 2 Properties of CuO-H2O nanofluid against various mass fractions of nanoparticle

Nanoparticle concentration	Density	Viscosity	Thermal conductivity	Specific heat
	kg/m3	Ns/m2	W/mK	J/kgK
Water (0%)	997.13	0.00089	0.613	4180
CuO - 0.1%	1548.4	0.00111	0.795	3816
CuO - 0.2%	2099.7	0.00133	1.019	3452
CuO - 0.3%	2650.9	0.00156	1.297	3088

VI. RESULT AND DISCUSSION

The experimentally observed outlet temperature and pressure level status and calculated heat thermal rate, collector efficiency and pumping power is given in table 3. The impact of CuO nanofluid with 0%, 0.1%, 0.2%, and 0.3% mass fraction of nanoparticle on temperature measured at outlet of the solar collector in figure 7. As the mass fraction of nanoparticle increases the outlet temperature of the collector also increases. Because, addition of nanoparticle increases the nanofluid thermal conductivity. It helps to absorb more heat energy thereby the outlet temperature of the nanofluid increases. Lower mass flow rate fetches maximum temperature since the nanofluid has enough retention time within the collector. When the mass is increased the retention time decreases which reduces the heat energy absorption. The percentage of increase of outside temperature by 0.3% of proportion by volume for CuO nanofluid is 30.9% and 15.57% at 0.016kg/s and 0.033kg/s respectively when paralleled with water.

Table 3 Effect of CuO-H2O nanofluid on solar flat plate collector

Nanoparticle Concentration	Mass flow rate (kg/s)	Outlet Temperature (OC)	Heat transfer rate (W/m2)	Collector Efficiency (%)	Pressure Drop (pa)	Pumping Power (W)
0%	0.016	36.9	795.87	37.39	3328.10	0.053
0.1%		41.58	1012.31	47.56	5508.04	0.057
0.2%		45.8	1148.83	53.97	7368.30	0.056
0.3%		48.31	1151.70	54.11	9228.68	0.056
0%	0.033	32.1	979.37	46.01	3552.85	0.118
0.1%		34.2	1158.54	54.43	5741.03	0.122
0.2%		35.6	1207.51	56.73	7650.46	0.120
0.3%		37.1	1233.04	57.93	9620.81	0.120

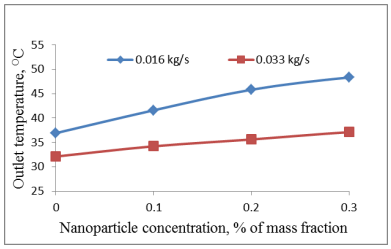

Figure 7 Effect of nanoparticle concentration on outlet temperature

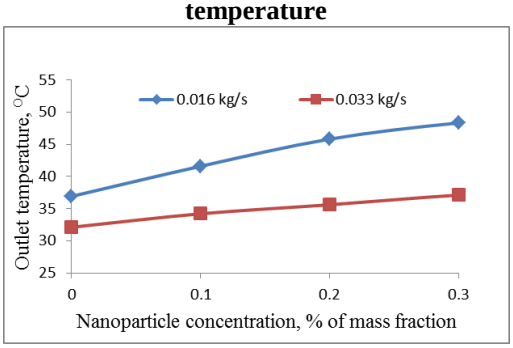

Figure 8 Effect of nanoparticle concentration on heat transfer rate

From the results of figure 8, the rate at which heat transfer occurs at an elevated rate as the nanoparticle concentration increases with elevation of nanoparticle composition increase beyond 0.2% mass fraction, the increase in percentage of heat transfer rate decreases. It is necessary to find out the optimum value of nanoparticle concentration to enhance the heat transfer rate.

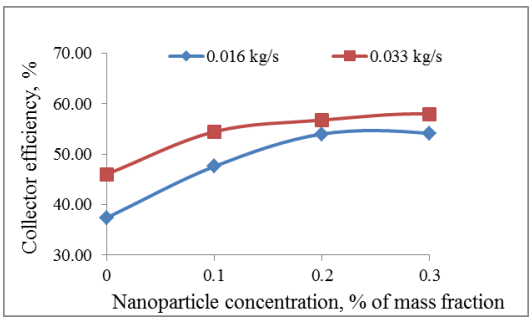

Figure 9 Effect of nanoparticle concentration on efficiency of the collector

The efficiency of the solar collector with respect to nanoparticle concentration is shown in figure 9. There is an increase in efficiency as the nanoparticle increases and for a proportional mass flow rate increase. The nanoparticle composition increases from 0.2% to 0.3%, while collector efficiency also upsurges as an outcome of decrease in elevated density and viscosity of nanofluid and due to high fluid absorption at higher concentration of nanoparticle.

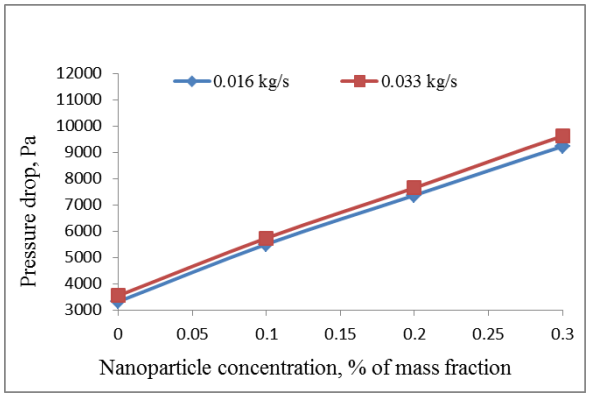

Figure 10 Effect of nanoparticle concentration on Pressure drop

The resistance offered to flow by the fluid within the flow path is prime importance to improve the heat transfer characteristics because the pumping cost should not pull down the benefit of enhanced heat transfer. The figure 10 shows the pressure drop variations. It is noted that the pressure drop upsurges as the nanoparticle concentration upsurges due to the higher concentration of nanoparticle. The pressure drop is mainly influenced by nanoparticle concentration and the impact of mass flow ratio on pressure declinination is less.

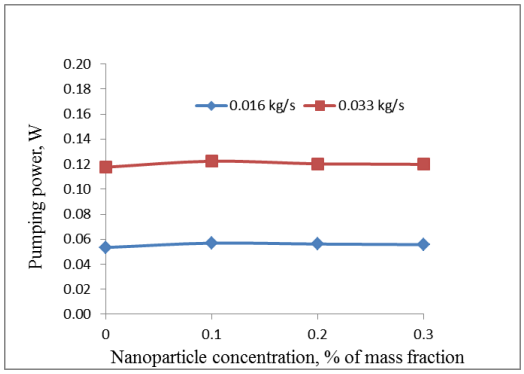

Figure 11 Effect of Nanoparticle Concentration on Pumping Power

In forced circulation, it is necessary to find the pumping power requirement to maintain required mass flow proportions. The figure 11 shows the pumping power of the collector. The pumping power is in direct proportion with pressure drop and indirect proportion with density. The density of the nanofluid increases as the nanoparticle concentration increases. Hence, pumping power is constant even the nanoparticle concentration increases. But the pumping power increases as the mass flow rate increases due to increasing of fluid load as mass flow rate (MFR) increases and in turn more power is required to drive the pump.

VII. CONCLUSION

The ultimate outcome of a solar collector with flat plate model using CuO-H_2O and water as nanofluid with 0.1%, 0.2% as well as 0.3% proportions of nanoparticle is tested experimentally. The heat transfer medium is distributed across through collector using forced circulation with the mass flow proportion of 0.016kg/s and 0.033kg/s. Maximum outlet temperature is obtained with 0.3% nanoparticle concentration at 0.016kg/s. The percentage of increase of outlet temperature with 0.3% volume fraction for CuO nanofluid is 30.9% and 15.57% against 0.016 and 0.033kg/s respectively when associated with water. The transfer rate of the energy in the form of heat increases when the nanoparticle increases in concentration. At the same time, increase in percentage of the above heat transfer rate diminutions as the nanoparticle mass fraction beyond 0.2%. But the heat transfer rate is indirectly proportionate to mass flow rate. The collector efficiency is directly proportional to mass fraction of nanoparticle and mass flow proportion rate. There is also a significant pressure drop across the collector which is mainly influenced by nanoparticle concentration and simultaneously the mass flow rate on pressure drop is less. The pumping power requirement is constant even the nanoparticle concentration increases. The effect of CuO nanofluid on the performance of the designed model collector is better than water. The experimental analysis can be conducted with higher mass fraction/volumetric fraction of the nano particulates to optimize the collector's ultimate efficiency, temperature, heat transfer rate, pressure drop and pumping power. Suitable numerical technique can also be developed to substatiate the heat transfer proportions and its characteristics of the collector using different nanofluids.

REFERENCES

1. Prof. P.W.Ingle, Dr. A. A. Pawar, Prof. B. D. Deshmukh, Prof. K. C. Bhosale, CFD Analysis of Solar Flat Plate Collector, International Journal of Emerging Technology and Advanced Engineering, 2003, 3(4), 337-348.
2. D.R.Pangavhane, R.L.Sawhney, "Review of research & development work on solar dryers for grape drying, energy conversation and management, 2002, 43, 45-61.
3. Al. Dănescu, S. Bucurenciu, St. Petrescu, Utilizarea Energiei Solare, Editura Tehnică, Bucureşti, 1980.
4. R.Saidur, K.Y. Leong, H.A. Mohammad, A review on applications and challenges of nanofluids, Renew. Sustain. Energy Rev. 2011, 15 (3) 1646–1668.
5. S.A. Kalogirou, Solar Energy Engineering: Processes and Systems, Elsevier, Oxford, 2009.
6. Omid Mahian, Ali Kianifar, Soteris A. Kalogirou, Ioan Pop, Somchai Wongwises, International Journal of Heat and Mass Transfer, 2013, 57, 582–594.
7. H.Tyagi, P.Phelan, R.Prasher, Predicted efficiency of a low-temperature nanofluid – based direct absorption solar collector, J. Solar Energy Eng. 2009, 131, 041004.
8. T.P. Otanicar, P.E. Phelan, R.S. Prasher, G. Rosengarten, R.A. Taylor, Nanofluidbased direct absorption solar collector, J.Renew.Sustain. Energy, 2010, 2, 033102.
9. T.Yousefi, F. Veysi, E. Shojaeizadeh, S. Zinadini, An experimental investigation on the effect of pH variation of MWCNT–H2O nanofluid on the efficiency of a flat-plate solar collector, Solar Energy, 2012, 86, 771–779.
10. S.Link, M.A. El-Sayed, Shape and size dependence of radiative, non-radiative and photothermal properties of gold nanocrystals, Int. Rev. Phys. Chem.2000, 19, 409–453.
11. N. Khlebtsov, L. Trachuk, A. Mel'nikov, The effect of the size, shape, and structure of metal nanoparticles on the dependence of their optical properties on the refractive index of a disperse medium, Optics Spectrosc. 2005, 98 (1), 77–83.
12. Sarit Kumar Das, Nandy Putra, Peter Thiesen, Wilfried Roetzel, Temperature dependence of thermal conductivity enhancement for nanofluids, Journal of heat transfer, 2003, 125/567.
13. Jacob Eapen, Roberto Rusconi, Roberto Piazza, Sidney Yip, The classical nature of thermal conduction in nanofluids, Journal of heat transfer, 2010, 132/102402-1.
14. Drew D.A. Passman S.A, 1999 Theory of multi component fluids, SpringerBerlin.

Published By:
Blue Eyes Intelligence Engineering
& Sciences Publication

15. Y.Xuan, W.Roetzel, conceptions for heat transfer correlation of nanofluids, International Journal of heat and mass transfer, 2000, 43, 3701.
16. B.C.Pak, I.Y.Cho, Hydrodynamic and heat transfer study of dispersed fluids with sub-micron metallic oxide particles, Experimental heat transfer, 1998, 11, 151-170.
17. R.Dharmalingam, K.K.Sivagnanaprabhu, B.Senthilkumar, R.Thirumalai, Nano materials and nanofluids: An innovative technology study for new paradigms for technology enhancement, Procedia Engineering, 2014, 97, 1434 – 1441.
18. Goudarzi, K, Nejati, F, Shojaeizadeh, E &AsadiYousef-abad, SK, Experimental study on the effect of pH variation of nanofluids on the thermal efficiency of a solar collector with helical tube, Experimental Thermal and Fluid Science, 2015, 60, 20-27.
19. Said, Z, Saidur, R, Rahim, NA &Alim, MA, Analyses of exergy efficiency and pumping power for a conventional flat plate solar collector using SWCNTs based nanofluid, Energy and Buildings, 2014, 78, 1-9.
20. R.Kandasamy, R.Dharmalingam, KKS Prabhu, Thermal and Solutal Stratification of MHD nanofluid flow over a Porous Vertical Plate, Alexandria Engineering Journal, 2018, 57, 1,121-130.
21. R.Dharmalingam, R.Kandasamy, KKS Prabhu, Lorentz forces and nanoparticle shape on water based Cu, Al_2O_3, Journal of Molecular Liquids, 2017, 231, 663-672.
22. R Kandasamy, R Dharmalingam, KKS Prabhu, Performance of Thermal Radiation Energy on Stagnation-Point Flow In The Presence of Water Based Copper and Single Walled Carbon Nanotubes over Stretching, International Journal of Engineering Research and Applications, 2016, 6 (4), 62-74.
23. Dharmalingam R, Sivagnanaprabhu K K, Godson Asirvatham.L, Gunasekharan S, Experimental Analysis of Heat Transfer Characteristics of Solar Flat Plate Collector using H2O and Al2O3-H2O Nanofluid, International Journal of Current Engineering and Scientific Research, 2017, 4(12), 103-112.
24. R.Dharmalingam, KK.Sivagnanaprabhu, J.Yogaraja, S.Gunasekaran, R.Mohan, Experimental Investigation of Heat Transfer Characteristics of Nanofluid Using Parallel Flow, Counter Flow and Shell and Tube Heat Exchanger, Archive of Mechanical Engineering, 2015, 62(4), 509-522.
25. Zhang X, Gu H, Fujii M, Effective thermal conductivity and thermal diffusivity of nano fluids containing spherical and cylindrical nano particles, Journal of Applied Physics, 2006, 100, 04325.
26. Choi SUS, Enhancing thermal conductivity of fluids with nanoparticles, in developments and applications of Non-Newtonian flows, ASME FED 231/MD 1995, 66, 99-103.
27. Lazarus Godson, B.Raja, D.MohanLal, S.Wongwises, Enhancement of heat transfer using nanofluids-An overview, Renewable and Sustainable Energy Reviews, 2010, 14, 629-641.
28. Jacob Eapen, Roberto Rusconi, Roberto Piazza, Sidney Yip, The classical nature of thermal conduction in nanofluids, Journal of heat transfer, 2010, 132/102402-1.
29. SeokPil Jang, Stephen U.S.Choi, Effects of various parameters on nanofluid thermal conductivity, Journal of heat transfer, 2007, 129/617
30. L.Godson, K.Deepak, C.Enoch, B.Jefferson, B.Raja, Heat transfer characteristics of silver/water nanofluids in a shell and tube heat exchanger, 2014, ACME 141-149.

Comparitive Study Between the Compressive Strength of Traditional Curing and Accelerated Curing of Concrete

R.Sumathi, Shyamala Bhoomesh

Abstract: ***Generalized association between compressive strength achieved after 28 days and accelerated compressive strength achieved after 24 hours for all the grades of concrete is provided in IS Code. This paper intent at evolving the comparison between accelerated action curing and traditional action curing for specific grade of concrete.. These techniques are particularly helpful within the manufacture trade, wherein high early age strength permits the removal of type work at intervals twenty four hours, thereby reducing the cycle time, leading to value saving edges. The most usually adopted natural process techniques are steam natural process at region pressure, heat water natural process, boiling water natural process and autoclaving. Accelerated curing results are obtained after twenty four hours to predict the twenty eight days compressive strength.***

Key words: Concrete mix, Compressive Strength, Accelerated Curing, formwork, Autoclaving

I. INTRODUCTION

The Ultimate Compression that the concrete can bear is calculated on the basis of 28 days trial to find the quality of the Construction work. The procedure to calculate the quality of construction work in terms of 28 compressive strength stand in need of 28 days of water curing, before performing above trial experiment. If the Compressive strength is not meeting the target strength to be achieved, The replacement of Concrete mass becomes very difficult and practically impossible. But the 28 days compressive strength can be achieved by the method of accelerated curing as per code IS 9013-1978 within 1 day. This paper intents at comparing the ultimate compressive strength of the sample concrete after twenty eight days of traditional curing and boiling water method of accelerated curing. The result developed during this study is helpful for hard the strength of concrete in around one day as against twenty eight days.

II. MATERIALS

A. Cement: Ordinary Portland cement of fifty three grade [IS: 12269-1987], Specifications for 53Grade Ordinary Portland cement has been utilized in the study. It had been procured from a single supply and keep as per IS: 4032 – 1977. Care has been taken to ensure that the cement of same company and same grade is used throughout the investigation. The cement therefore procured was tested for physical properties in accordance with the IS: 12269 – 1987.

B. Fine Aggregate: The fine aggregate used was regionally on the market M-sand without any organic impurities and orthodox to IS: 383 – 1970. The fine particulates were tested as prescribed by the IS: 2386 – 1963

C. Coarse Aggregate: The chosen aggregates were crushed in angular shape and well hierarchal in nature. Hierarchal mixture is additionally vital significantly to forged concrete in predominantly full reinforcement or form work having little dimensions. These were tested as per IS 383-1970.

III. METHODOLOGY:

Mix Proportion: The mix proportion was done based on the IS Code 10262-2009. The design for mix proportion for M35 normal grade of concrete was prepared in lieu with the methodology . Nine cubes were prepared for each water cement ratio. Out of that 6 cubes were under examination for the compressive strength post 7days and then again after 28 consecutive days water curing and the 3cubes has been tested for its compressive strength on the next day of cube casting in which curing has been done with Acceleration curing as per IS-9013-1978.

Methods of curing:

A) Normal Water Curing:

The samples under examination were kept in moist air possessing 90% relative humidity at normal atmospheric conditions for 10 hours. Then they were noted and detached from the molds and instantly plunged in clean water. The curing is done in 7, 14, 21and 28 days.

B) Accelerated curing:

The cubes has been unmoulded after 24hrs and immersed in acceleration curing tank of water with 100^{o} C. After curing for 3 ½ hours specimen is cooled down by plunging in water kept at 27+2^{o}C for a standard time of one hour. The subsequent formula is employed to seek out the 28 days compressive strength after testing in CTM.

$$R_{28} = \text{Strength calculated 28 days} = 8.09 + 1.64\,Ra$$

Where,

Ra is designated as theAccelerated Curing Strength in MPa.

Revised Manuscript Received on December 08, 2018.

R.Sumathi, Assistant Professor, Civil Engineering Department, Malla Reddy Engineering College, Hyderabad, Telangana, India.

Shyamala Bhoomesh, Assistant Professor, Civil Engineering Department, Malla Reddy Engineering College, Hyderabad, Telangana India.

IV. RESULTS AND DISCUSSION

S.No	Name of the test	Observed value	Standard value as IS-10262:2009
1	Normal Consistency (%)	32%	-
2	Time of setting(min) Initial Setting condition Final Setting condition	 90 min 300 min	 Not less than 30 Minutes Not more than 600 Minutes
3	Specific Gravity Cement Fine Aggregate Coarse Aggregate	 3.15 2.6 2.7	 2.5-3.0 2.5-3.0
4	Compressive strength (N/mm^2) A) 3 Days B) 7 Days	 $14N/mm^2$ 33.5 N/mm^2	IS: 1489-1991(Part-I) 16 N/mm^2 33 N/mm^2
5	Soundness (Lechatliers method)	3mm	Not more than 10mm

Table 1: Physical Properties of the Materials

IS Sieve mm	% Passing	Remarks
4.75	97.2	Confirms to grading Zone-III of table 4 IS383-1970
2.3	94.5	
1.18	81.2	
600×10^{-3}	59.6	
300×10^{-3}	21.5	
150×10^{-3}	7.1	

Table 2: Sieve Analysis for Fine Aggregate

IS Sieve	% Passing	Remarks
80	100	Confirms table II of IS383- 1970
40	100	
20	100	
12.5	71.6	
10	28	
Pan	0.4	

Table 3: Sieve Analysis for Coarse particle Aggregates

The mix proportion is designed as per IS 10262-2009 considering various factors like

Exposure	Normal
Degree of Quality control	Good
Slump	40-70
Standard Deviation	5

Depending upon the above considerations the the Target mean strength required at 28 days is 43.25 Mpa. Depending upon the strictly controlled water cement ratio 0.45 and the casting in the lab with cement content by keeping $425Kg/m^3$ was made The mix with the following proportions per meter cube by weight is given as

Water/ cement	Cement (Kg)	FA (Kg)	CA (Kg)	Compressive strength (N/mm^2) Normal Curing in days	Compressive strength (N/mm^2) Accelerated Curing in days
	1	1.89	2.31	7	28	7	28
0.45	425	807.3	984.15	33.50	39.72	NA	44.00
0.50	425	807.3	984.15	29.78	35.88	NA	41.56
0.55	425	807.3	984.15	17	28.72	NA	33.82
0.60	425	807.3	984.15	15	26.56	NA	29.17

Table 4: Mix proportion and compressive strength

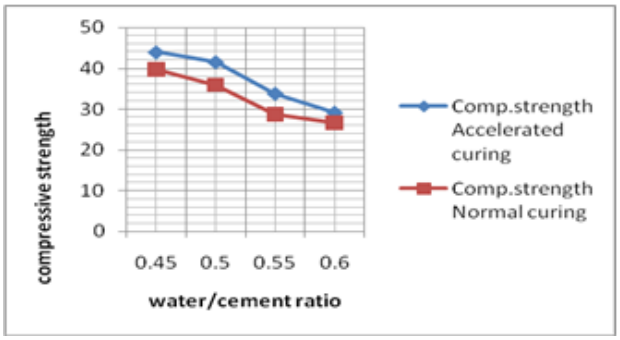

Figure:1 Comparision graph between the compressive strength of Accelerated curing and Normal curing cubes.

From the tabulation it is observed that for 0.45w/c ratio is giving good compressive strength to the concrete for this designed proportion. When the W/C ratio is getting increased and the strength is getting decreased. On the other hand, when it is required to have good slump, as the admixtures are not included here, the water cement ratio of 0.5 can be suggested. Comparing the Compressive strength of normal curing and Accelerated curing, the later one is giving good strength and it can also be used to achieve good compressive strength.

V. CONCLUSIONS:

In this experimental work a complete variety of 36 cubes were casted, out of which 24 were tested for Immersion natural process. Remaining 12 cubes were examined for Accelerated heat water technique

From the experimental outcomes it was concluded that the Immersion curing accomplished a mediocre strength under compression of 39.72 $N/mm^2$and 35.88 N/mm^2 for M 35 grade at the age process of 28 days considering the W/C ratio as 0.45 and 0.5 respectively. The compressive strength of the concrete cubes was found to be 44 N/mm^2 and 41.56 N/mm^2 for W/C ratio 0.45 and 0.5 respectively for M 35 grade.Accelerated curing method is enabling to get good compressive strength comparatively.

REFERENCES:

1. Ajay Goel, JyotiNarwal, VivekVerma, Devender Sharma and Bhupinder Singh , "A Comparative Study on the Effect of Curing on the Strength of Concrete materials ",International Journal of Engineering and Advanced Technology (IJEAT), Volume-2, Issue-6, ISSN: 2249 – 8958, August 2013.
2. Akeem Ayinde Raheem , Aliu Adebayo Soyingbe and Amaka John Emenike,, "Effect of Curing Methods on Density and Compressive Strength of Concrete",International Journal of Applied Science and Technology, Vol. 3 Issue - 4, 2013.

Published By:
Blue Eyes Intelligence Engineering
& Sciences Publication

3. Denny Meyer, "A Statistical Comparison Of Accelerated Concrete Testing Methods",Journal of Applied Mathematics & Decision Sciences, vol. 1, Issue-.2, pp 89-100 ,1997.
4. Reliability of accelerated curing techniques for speedy design of concrete mixes – An appraisal of IS 9013:1978 code.
5. Krishna Rao, M..V, Rathish Kumar, P, and Azhar Khan, M, "A study on the influence of curing on the strength of a standard grade and concrete mix", Architecture and Civil Engineering, Vol. 8, Issue- 1, pp. 23 – 34, 2010.
6. Abalaka,A.E,, and Okoli,O .G, "Influence of curing regime on strength development of grade C60 concrete base" , International Journal of Modern Engineering Research (IJMER), Vol.3, Issue.2, , pp-709-714. March-April.2013.
7. Safiuddin , Raman S. N, and. Zain, M , "Effect of Different Curing Methods on the Properties of Microsilica Concrete",,Australian Journal of Basic and Applied Sciences, vol.1, Issue-.2, pp 87-95, 2007. [8] Ali H. Hameed , "The effect of curing condition on compressive strength in high strength concretes", ISSN 1999-8716 Vol. 02 ,pp. 35-42,2009.
8. Krishna Reddy,K.V., "A comparative study on methods of curing concrete influence of humidity", International Journal of Engineering Research and Applications (IJERA) ISSN: 2248-9622 Vol. 3, Issue 3, pp.1161-1165, May-Jun 2013.
9. IS 10262:2009 Concrete mix proportioning – guidelines. [11] James ,O, Ndoke, P.N., and. Kolo , S.S ., "Effect of different curing methods on the compressive strength of concretes", International Journal of Engineering and Advanced Technology (IJEAT) ISSN: 2249 – 8958, Volume-2, Issue-6, August -2013.

Design and Implementaion of Energy Efficient Muliplier Architecture in Low POWER VLSI

Rajendra Prasad

Abstract: ***The Low power multipliers having high clock frequencies assume a significant role in the present advanced technology. Multiplier is such a vital component which subsidises the aggregate power utilization in a systematic environment. Low Power VLSI optimization is carried out from basic subsystem level to architecture level. Power reduction is addressed at every stage of design thus the overall power reduction is minimized. Various innovative design techniques namely, clock gating, power gating and low power libraries are adopted to minimize power dissipation. The techniques proposed in this publication can be generalized and adopted for design complex signal processing and communication blocks required for various applications. To estimate 2's complement of multiplicand for final Partial Product Row (PPRG) we used MBE technique in proposed system. The proposed multiplier consumes power up to 60% and reduce the logic delay up to 7.2% and route delay up to 92%. So compared to all existed multipliers, the proposed multiplier produces effective results.***

KEY WORDS: Low power multipliers, Digital Signal Processing, Power Reduction Techniques, High Clock Frequencies, Modified Booth Encoding (MBE), Partial Product Row Generation (PPRG).

I. INTRODUCTION

As we know that in the areas of system on chip and VLSI designs, the low power circuit designs is an important issue. As the dimensions of transistors are shrunk into the deep sub-micron region, the effect of static leakage currents becomes more significant. This aspect of power consumption can be controlled to some extent by novel design, but is predominantly handled by process engineering. As the dimensions of transistors are shrunk into the deep sub-micron region, the effect of static leakage currents becomes more significant. Two areas that have been the focus of active research are asynchronous logic and adiabatic logic. If the power reducing properties of these techniques could be combined, then it should be possible to produce a logic design methodology that is only active when it is performing useful computations, and recycles a large proportion of the energy used to perform those computations. Working in asynchronous fashion to get the advantages of both the techniques.

Scaling of transistor geometries have led to integration of millions of devices in a very small space, thus driving realization of complex applications on hardware and supporting high speed applications. While the basic principles are largely the same, the design practices have changed enormously because of the increases in and transistor budgets and clock speeds, the growing challenges of power consumption, and the improvements in productivity and design tools. Device scaling has increased the operating frequency of many applications, but has led to high power consumption.

This synergy has revolutionized not only electronics, but also industry at large. In order to reduce power, many researchers, designers and engineers have come up with many innovative techniques and have patented their ideas. Nevertheless, designers will need to budget and plan for power dissipation as a factor nearly as important as performance and perhaps more important than area. Low power techniques have been successfully adopted and implemented in designing complex VLSI circuits. As the demand for faster, low cost and reliable products that operate on remote power source performing high end applications keep increasing, there is always a need for new low power design techniques for VLSI circuits. Multiplication is an expensive and time consuming operation. The execution of numerous computational issues is commanded by the speed at which an augmentation activity can be executed. This perception has for example incited coordination of finish augmentation unit in condition of state of art of digital signal processors and microprocessor. Multipliers are as a result complex adder Arrays. In this work, the examination of multiplier is completed to optimize the execution of complex circuit topological. The least difficult and most well-known duplication technique is included and shift algorithm. In parallel multipliers quantities of incomplete items to be included is the fundamental parameter that decides the execution of multiplier. Hence in this work, the basic way that decides the most extreme delay in parallel multiplier is distinguished and advanced utilizing power. Likewise the aggregate power utilization of the distinctive multipliers is resolved and low power methods are consolidated to limit the power. With the end goal to accomplish rapid of activity in increase, the pattern is resort parallel multipliers. Be that as it may, the execution of the multiplier is dictated by number of parallel items to be included. In this paper we recognize and streamline the basic way that decides the extreme interruption in parallel multipliers.

II. LITERATURE SURVEY

In DSP systems multiplier plays an important role. But in DSP system mostly they perform filtering and convolution operations. Instead of that the multiplier operation plays very crucial role in DSP systems. Day by day innovative technology is being developed vigourously. Fundamental technology is used in public key cryptography for the

Revised Manuscript Received on December 08, 2018.

Dr. Rajendra Prasad, Asst. Prof, Dept of ECE, Malla Reddy Engineering College (A), Secunderabad,Telangana, India

process of addressing. Various technologies are proposed but each technology has its own way of representation. But there are no such type of techniques which doesn't provides key agreement and public encryption. The most fundamental type of augmentation comprises of framing the result of two unsigned numbers. A wide range of sorts of multipliers have been proposed with altogether different equipment necessities, throughput and power scattering. These include: sequential multipliers, serial multipliers, array multipliers and tree multipliers.

Array multipliers and tree multipliers are quick however costly as far as equipment and power utilization. Iterative structures permit an exchange off among execution and equipment prerequisite. Pipe lining is typically utilized in iterative frameworks to enhance their execution. In the mid 1950's, multiplier execution was essentially enhanced with the presentation of booth multiplier and the advancement of quicker adders and memory segments. Corner's strategy and the altered stall's technique don't require a remedy of the item when either (or both) of the operands is negative for two's supplement numbers. Amid the 1950's, snake's structures moved far from the moderate

Successive arrangement of conveyed executed by swell convey adders convey look forward, convey select, and restrictive a few adders yielded rapid aggregates through the quicker synchronous or parallel age of bearers.

In the 1960's two classes of parallel multipliers were characterized.The five star of parallel multipliers utilizes a rectangular exhibit of indistinguishable combination cells to create and total the incomplete item bits. Multipliers of this compose are called Array multipliers. Because of the consistency of their structures, exhibit multipliers are conveying to format and have been executed as often as possible. The below average of parallel multipliers lessens a lattice of fractional item bits to two words through the key use of counters or blowers.

In Array multiplier, the two fundamental elements of halfway item age and summation are consolidated. For unsigned N by N augmentation, N2+N-1 cells, where N2 contain an AND entryway for fractional item age and a full snake for summing and N-1 cells containing a full viper, are associated with create a multiplier. The exhibit creates N bring down item bits straightforwardly and utilizes a Carry-spread viper, for this situation a swell convey snake, to frame the upper N bits of the item. With the end goal to plan a cluster multiplier for two's supplement operands, Booth calculation can be utilized. The execution of a stall's calculation cluster multiplier registers the halfway items by inspecting two multiplicand bits at once. With the exception of empowering utilization of two's supplement operands, this present stall's calculation cluster multiplier offers no execution or territory advantage in contrast with the fundamental exhibit multiplier. Better postponements, however can be accomplished by executing a higher radix adjusted stall calculation. Another strategy for building a cluster multiplier that handles two's supplement operands was displayed by Baugh. This strategy builds the most extreme segment stature by two. This may prompt an extra phase of fractional item decrease, along these lines expanding by and large deferrals.

As indicated by Thomas Callaway and Earl E. Swartz lander. Jr, segment pressure multipliers are highly power effective than any other source. In 1964, Wallace presented a proposal for quick augmentation dependent on the halfway item bits on parallel utilizing a tree of convey spare adders which turned out to be by and large known as the Wallace tree. Dada later refined Wallace's technique by characterizing a counter position methodology that required less counters in the fractional item decrease organize at the expense of a bigger convey proliferate snake. For the two strategies, the aggregate deferral is relative to the logarithm of the operand word-length

III. SOURCES OF LOW POWER CONSUMPTION IN MULTIPLIERS

To substantiate the power consumption in any CMOS circuits the sources of power consumption should be explored first. Figure (1) represents the sources of power consumed in a CMOS.

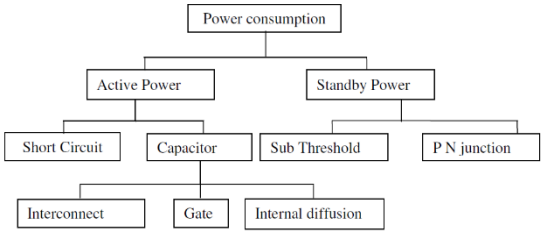

Fig. 1. Sources of low power consumption in VLSI

The active power comprises of two machine modules: (i) Capacitive or Dynamic power (ii) Short Circuit power. Capacitive power is due to capacitive loads. Capacitive loads include interconnects, output gate capacitance and input gate capacitance. The standby mode consists of two components: (i) Sub threshold (ii) Junction. The junction power is due to PN junctions in a MOS device. The gate capacitance CM is an internal capacitance, connected between the common point of the gate of NMOS and PMOS with drain of NMOS. The Load capacitance CL is made up of bulk to drain capacitances of both PMOS and NMOS, interconnect capacitance and gate capacitance of the load. During transition of input and output of an inverter, charging current (Ip), discharging current (In), ICM and ICL are of prime importance for power analysis as they are used to charge and discharge the load capacitance. These currents are the sources of power dissipation, as they get diffused into the ground during circuit transition. Capacitive or Dynamic or Switching Power: During the output voltage logic transition period (charging and discharging of the load capacitance), the power dissipated at that period is called as dynamic power. When the input changes from 0(Low) to 1(High), PMOS device changes its state from ON to OFF. During this state, PMOS transistor changes from linear to cut off region. The charging current from VDD charges the load capacitance during input being logic '1'. When input switches from logic '1' to '0', NMOS goes from cut off region to saturation and PMOS remains in cut off condition.

Short-Circuit Power: During input switching, there would be a point at which both NMOS and the PMOS transistors are conducting simultaneously and the power supply is directly connected to ground for a short interval of time.

IV. LOW POWER DESIGN TECHNIQUES ON MULTIPLIERS

Several low power techniques have been reported in the literature for power drop. At the entry level and circuit level, power reduction is achieved by incorporating additional logic that can control the charging and discharging of current. David Flynn elucidated the power reduction methods that are known as mature technologies. The four power different power reduction techniques are (i) Clock gating (ii) Gate level power optimisation (iii) Multi Vdd technique (iv) Multi Vt technique. The below figure (2) shows the different types of techniques of multiplier.

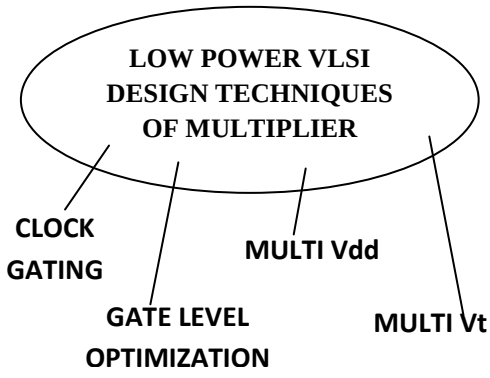

Fig. 2. Techniques of low power multipliers

Clock Gating: A substantial function of dynamic power in chip is in the circulation system of clock. The most well-known approach to diminish this power is to turn OFF clock when not required. A computerized clock-gating is performed by distinguishing synchronous load-enabler register banks, and actualizing them by gating the clock with a functioning empower rather than distribution of the information when the empower is inactive.

Gate Level Optimization: Energy interruption item (control) can be enhanced by keeping away from wastage of wastage. This should be possible by staying away from number of node transition that are a bit much. By recording the node transition in a given circuit for a given information, one can control the power scattering by limiting node changes. This prompts a critical decrease in Without Clock-gating With Clock-gating.

Multi V_{dd}: Dynamic power P_{dyn} is proportional to and lowering supply voltage V_{dd} on selected blocks helps to reduce power significantly and also increases the delay of the gates.

Multi Vt: As geometries have contracted to 130 nm, 90 nm, 65 nm and beneath, utilizing Multi Vt has turned into a typical method for diminishing spillage current. Numerous libraries today offer a few adaptation of their cells, for example, Low Vt, Standard Vt and High Vt. The usage apparatuses can exploit these libraries to enhance timing and power at the same time. It is presently basic to utilize "Double Vt" combination. The objective of this approach is to limit the aggregate no., of fast, defective low Vt transistors by sending them to meet planning whenever required. The plan should meet with least usefulness, before enhancing power, i.e., incorporating the structure with superior, high spillage library firstly, and afterward unwinding back any of the cells on any basic swapping way for their lower execution, bring down spillage reciprocals.

V. IMPLEMENTATION OF LOW POWER VLSI MULTIPLIER

Multiplier logic modelled using Verilog HDL and substantiated using Model Sim. The performances of various multipliers, is explored by FPGA implementation and ASIC implementation.

BCSD (Binary Canonic Sign Digit) multiplier is a sequential multiplier involving shifting register for each clock cycle and accumulating partial products. It is totally characterized by the characteristics of clock and a load signal is taken to load registers with inputs synchronized with clock. Since the multiplier designed is of 12 bits wide it takes 12 no., of 24 hour cycles to reproduce the same outcome This multiplier is synchronized with clock i.e. is any changes in input signal will be recognized only at the rising edge of clock.

Array multiplier is a combinational circuit; no storage elements synchronized with clk. Delay in the output is caused by the change in the input that depends on the propagation delay of circuit elements used in the hardware implementations by the designer. Carry propagation is the critical factor and use carry save adder chain for improving the speed. Modified booth is a sequential multiplier which is synchronized with clock for each and every operation. In general, Booth multiplier will take 'n' clock cycles depending on the word length of operand and Modified booth of radix-4 takes n/2 clock cycles to complete one operation. Further, it can be reduced by increasing radix with a penalty in complexity of hardware.

Wallace tree multiplier is the fastest multiplier with irregular structure, pure combinational circuit with carry save adder chain and more complex hardware loop structure. First add all the available product terms and then the partial products in a tree structure without affected by delays in carry propagation. Baugh Woolley multiplier is a modified version of array multiplier, is combinational multiplier to handle the signed numbers multiplication. The speed of sequential multipliers can be increased by encoding them with high radix, with a penalty of increase in complexity. All simulated programs cannot be synthesized and restricts the designer in making effective hardware description. Further simulation tools verify the functionality of logic only. All these existed multipliers produce less efficiency.

The vedic multiplier is a specimen of interest because of its integrated design where even the smaller blocks can be employed to generate a design for the bigger ones. Booth's Multiplier surveys adjacent pairs of bits of the 'N'-bit multiplier *Y* including an implicit bit below the least significant bit as in figure (3) showing the architecture of proposed low power VLSI multiplier.

Compared to above multipliers, this multiplier produces better results. Let us discuss about this multiplier in detail manner. The main parts of this multiplier are CSAT, MBE, PPRG. Let us discuss the entire operation in detail manner.

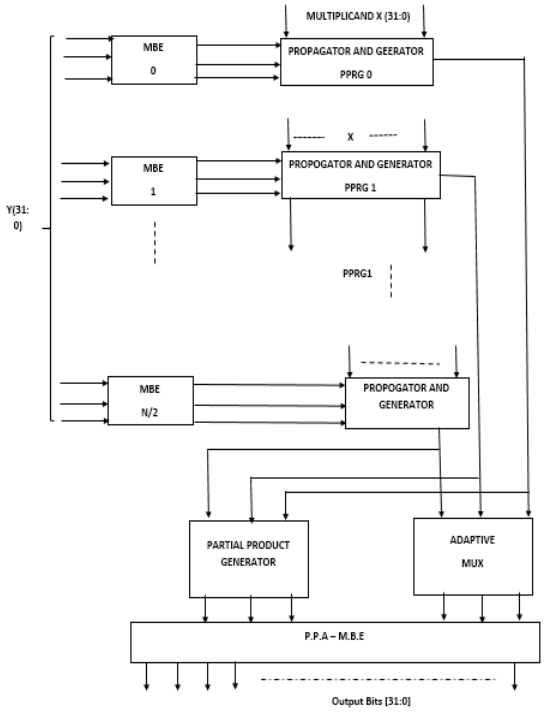

Fig. 3: Block diagram implementation of low power VLSI multiplier

The new architecture proposed consists of Partial Product Generation (PPG) logic, 2's complement logic and a carry save adder tree. Firstly some partial product arrays are produced by using multiplication algorithm. But the partial product rows are small in size and fast in speed. MBE technique will reduce the partial products. Now the multiplier Y is divided into group of 3 bits. The each bit will be reduced from n to n/2. Here the carry save adder tree will perform the reduction technique. Compared to existed system, the proposed system produces effective results as show in above architecture operation.

VI. RESULTS

From below figure (4), it can observe the RTL Schematic of proposed multiplier. Basically, RTL schematic is a traditional design abstraction which a synchronises signals (data) between hardware registries, and the logical operations.

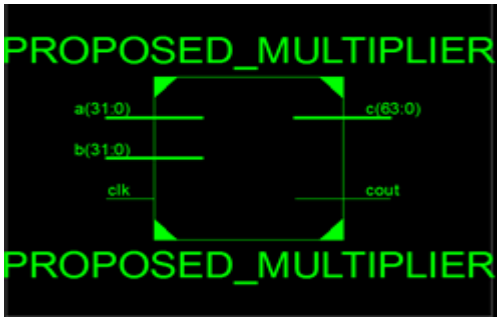

Fig. 4: RTL Schematic

From below figure (5) we can observe the Technology schematic view of proposed multiplier.

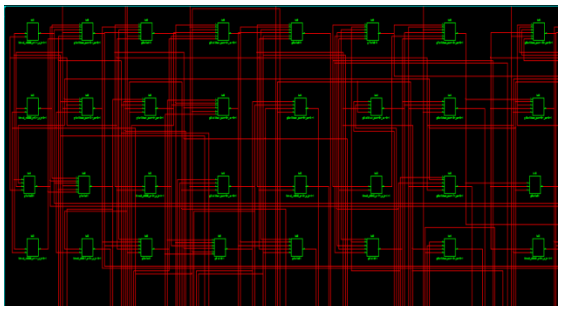

Fig.5: Technology schematic

Table. 1: Report of proposed multiplier

Logic Utilization	Used	Available	Utilization
Number of Slice LUTs	2017	46560	4%
Number of fully used LUT-FF pairs	0	2017	0%
Number of bonded IOBs	129	240	53%

Table. 2: Comparison of multipliers in terms of power, logic delay and route delay.

NAME OF MULTIPLIER	AREA	LOGIC DELAY	ROUTE DELAY
PROPOSED MULTIPLIER	60.3%	7.9%	92.1%
VEDIC MULTIPLIER	52.4%	18.4%	113.7%
BOOTH MULTIPLIER	47.2%	22.9%	142.6%

The table (1) represents the simulation report of proposed multiplier. From above table (2) we can observe the comparison of multipliers. As the proposed multiplier is 32 bit it occupies less area and high speed operation as shown in table (2). However 60% of area is consumed, delay is reduced up to 7.9% and route delay is reduced up to 92%. So compared to all multiplier, proposed multiplier produces effective results as shown in below figure(6).

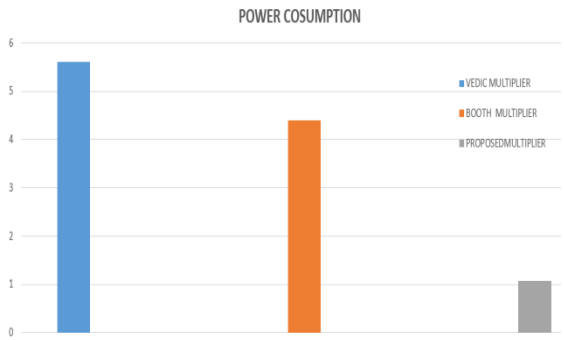

Fig. 6: comparison of power consumption

Published By:
Blue Eyes Intelligence Engineering
& Sciences Publication

VII. CONCLUSION

Low power VLSI multiplier algorithm which is more beneficial in power has been presented provided, the sub modules can be made reusable for higher order bits and can also be employed implementation techniques for analysing the speed requirement in huge set of large bit multiplication processes. The Multiplier simply yields less power consumption. Various low power strategies for power reduction optimization techniques have been incorporated for the reduced power. The proposed low power VLSI multiplier architecture produces better efficiency. The optimal speed is acquired using implementing technique compared with the general multiplier procedures. From results it can conclude that proposed low power VLSI multiplier forms an important aspect in complex signal processing applications.

REFERENCES

1. Jia Di_, J.S. Yuan, R. Demara ―Improving power awareness of pipelined array multipliers using two dimensional pipeline gating and its application on FIR design, Microelectronics Journal 41(2010).
2. Sri Bharathi Krishna Tirtha Maharaj,"Vedic Mathematics ", Motilal Banarasi Das publications, Delhi 2009
3. Jiajia Chen and Chip-Hong Chang "High-Level Synthesis Algorithm for the Design of Reconfigurable Constant Multiplier" IEEE transactions on computer-aided design of integrated circuits and systems, vol. 28, no. 12, December 2009
4. Timothy W. O'Neil and Edwin H.-M. Sha, Retiming Synchronous Data-Flow Graphs to Reduce Execution Time Vol. 49, No. 10, Oct. 2001
5. S. Malik, K.J. Singh, R.K. Brayton and A. Sangiovanni-Vincentelli,Performance Optimization of Pipelined Logic Circuits Using Peripheral Retiming and Resynthesis," IEEE Transactions on Computer-Aided Design of Integrated Circuits and Systems, Vol 12, No. 5, May 1993.
6. C. E. Leiserson, F. M. Rose, and J. B. Saxe. Optimizing Synchronous Circuitry by Retiming. In Proceedings of 3rd CalTech Conference on VLSI, pages 23–36, March 1983.
7. C. E. Leiserson and J. B. Saxe, "Retiming Synchronous Circuitry," Algorithmica, vol. 6, no. 1, pp. 5-35, 1991.
8. J. Monteiro, S. Devadas, and A. Ghosh. Retiming Sequential Circuits for Low Power. In Proceedings of the Int'l Conference on Computer-Aided Design, pages 398–402, November 1993.
9. Manohar Ayinala and Keshab.K.Parhi,"High Speed parallel architecture for Linear Feedback Shift Register (LFSR)", IEEE Journal, 2011.
10. Verma, P.: "Design of 4X4 bit Vedic Multiplier using EDA Tool," International Journal of Computer Application (IJCA), Vol. 8, June, 2012.
11. Jalaja S and Dr. Vijaya Prakash A.M, "High Speed VLSI Architecture for Squaring Algorithm Using Retiming Approach ",Third International Conference on "Advances in Computing and Communications" during Aug 29-31 2013 held at RSET, Cochin, Kerala, India and the paper is published in IEEE Computer Society's CPS.
12. Honey Durga Tiwari, Ganzorig Gankhuyag, Chan Mo Kim, Yong Beom Cho " Multiplier design based on ancient Indian Vedic Mathematics", 2008 International SoC Design Conference.
13. Prabir Saha, Arindam Banerjee, Partha Bhattacharya Anu Dan dapat, " High speed Asic design of complex multiplier using Vedic Mathematics", Proceeding of the 2011 IEEEstudents Technology Symposium, IIT Kharghpur.
14. Refik Sever, Murat Askar,"8x8-Bit Multiplier Designed With a New Wave-Pipelining Scheme", IEEE Trans. VLSI Syst., vol. 6, no. 3, pp. 2095- 2098, Sep. 2000.
15. V.Vamshi Krishna, S. Naveen Kumar "High Speed, Power and Area efficient Algorithms for ALU using Vedic Mathematics", International Journal of Scientific and Research Publications, Volume 2, Issue 7, July 2012.

Building a blockchain approach with hyperledger transaction flow and distributed consensus algorithms

S. Dhanalakshmi, B. G. Obula Reddy, K. Yogitha Lakshmi

Abstract: ***Blockchain is an important, emerging technology and specifying lot of possibilities, its very much trending topic in recent years. Bitcon is well known implementation of block chain technology, Bitcoin in cryptocurrency has turned the recognition of the universe towards a unique technology. Its benefit as decentralization, persistency and consistency of sharing the informations, blockchain is a distributed ledger that can record transactions efficiently verifiable and permanent way between two parties. Blockchain technologies focus on various applications perspectives and discuss the new technological challenges in confidentiality, integrity, authentication, internet of things and smart contract etc. it can be used to record the peer to peer network with public or private key pair of transactions, authors signed the transactions to be verified with key pair, save the transactions in blockchain network, once the transaction verified it cannot be altered subsequently. This paper present and focus on various techniques of hyperledger fabric systems architecture, transaction flow, membership and identity management, then understanding of hyperledger fabric with consensus algorithms. Hyperledger is one of the fastest growing open-source blockchain, it can dozens of company working together, building a blockchain fabric that can support the framework to test the interaction between application and secure blockchain networks, that require every peer to execute every transaction maintain a ledger and run consensus, does not support private blockchain and confidentiality. The first block chain systems is hyperledger fabric run on distributed applications with multiple programming language.***

Index Choice: Blockchain, Peer-to-Peer Network, Private-Public Key Pair, Hyperledger Fabric, Consensus Agorithms, Blockchain, Smart Contract

I. INTRODUCTION

Blockchain is a Singly Linked List of block, with each block containing a number of transactions. It's a decentralized and information sharing platform, not trust with multiple domains, users can be shared the block and record all the transactions, each transaction can be easily queried. block chain have been created in the process of development is bit coin, is growing list of records with linked list manners, each list in the blocks using with cryptographic functions. The cryptographic hash function contains the hash of the previous block, timestamp and transaction id, multiple authoritative domains of decentralized computation and information sharing platform to collaborate, cooperate and coordinate in decision making process, both users can share the information and also simultaneously edit the information in google documents, one problem to be raised in centralized systems for single point of failure, to load the data in google doc do not have sufficient bandwidth, not able to edit the documents. Fig.1. represents that blockchain system architecture of centralized vs decentralized vs distributed systems techniques. Each node specifying

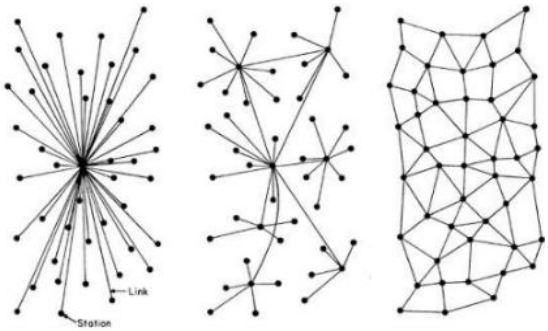

Fig.1. Centralized vs Decentralized vs Distributed Systems Architecture

A systems is centralized single point of node is not safe, The cryptographic hash function any string as input and fixed size output, secure hash algorithm that generate 256 bits in blockchain. Hash function performs the collision-free, hiding and puzzle-friendly. In cryptographic hash pointer stored hash of the information, retrieve the information and check the information, but the checked information has not been modified. In centralized systems single point is not safe vs decentralized systems can have multiple points of coordination vs distributed systems can have each one execute the job. The authentications of private-public key-pair used in transport layer security with network, the network legitimize transaction after that add transaction to blockchain. A Sequence of blocks in blockchain hold the complete record of transactions like public ledger, the integrity data written in the blockchain indicate correct and cannot be altered subsequently. Limiting to access the information in confidentiality, only authorized user can access the information that information also protected.

Its maintained distributed network of peer nodes is an immutable transaction ledger. These peer nodes perform and maintain a copy of ledger, ledger by applying transaction that have validated by consensus protocol. Private-public key pair offer a new technology is hyperledger fabric.

Revised Manuscript Received on December 28, 2018.

S.Dhanalakshmi, Professor, Department of CSE, Malla Reddy Engineering College (A),Telangana, India
B.G.Obula Reddy, Associate Professor, Department of CSE, Malla Reddy Engineering College (A),Telangana, India
K.Yogitha Lakshmi, Assistant Professor, Department of CSE, Malla Reddy Engineering College (A),Telangana, India

Its an open source distributed ledger technology platform in permissioned blockchain. Its maintains multiple organizations run on one peer or one organizations run on multiple peer, its support general purpose programming languages. The peer nodes support the notations of chaincode, users can implement a cryptocurrency through chaincode, chaincode is a smartcontract in blockchain environments.

II. DISTRIBUTED CONSENSUS MECHANISMS IN BLOCKCHAIN

Bitcoin network in permissioned blockchain, in a decentralized or distributed network, the consensus is a procedure to reach in a agreement of multi-agent in distributed or decentralized platforms, it's important for message passing environment in a distributed systems. Apply consensus in bitcoin network, traditional or conventional distributed systems to ensure reliability and fault tolerance. Distributed consensus like that decentralized environment have multiple individual parties and can take their own decision, it happened that some nodes, some parties, some individual are working maliciously or working as faulty individual. So ensure that operation, in the presence of faulty individuals to perform and develop the distributed consensus environment, the main objective is to ensure reliability. State machine replication and clock synchronization is an example of distributed consensus in bitcoin network. In state machine replication is an distributed protocol over a network, every individual nodes runs on current version of the protocol and stood the state of the protocol in different state machine, so the entire execution part of the protocol can be represented as a state machine, these state machines need to be replicated into multiple nodes, every individual node can reach to a command point or command output of that protocol. BFT (Byzantine-fault-tolerant) protocol is state machine replication protocol, it's interested in blockchain technology, then its distributes an application over many processes, faults, attacks and subset of the processes. Distributed consensus no failure in this systems, it's easy and trivial to reach in consensus, so the genetic algorithm broadcast the personal choice to all, then apply choice function, if your choice is the maximum of all the receive value, then you achieve consensus. The Fig.2. Shows that the choice functions of distributed consensus systems, the main objectives to reach maximum values for all nodes.

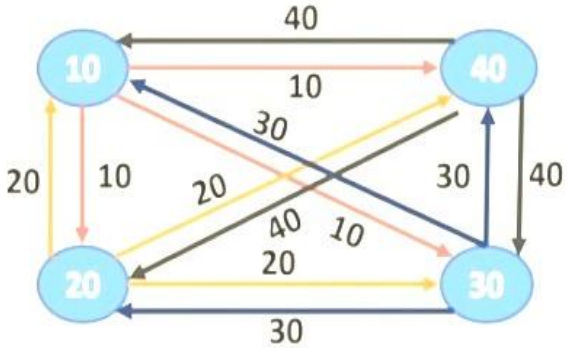

Fig.2. Choice Function in Consensus

For example here 4 individual nodes, make a choice of the individual nodes are 10, 20, 30 or 40 and informed they are individual choices to all other nodes in the network, and whenever every node receives all the choices from all the neighbours they can apply on max function then find out the maximum value, easily see that every node will reach the value of 40. If they apply the maximum function of all received values. So this architecture is easy and straight forward for this scenarios, this scenario indicate that no faultless in the system, every individual node can receive the message correctly, should not be any failure in the system. This system is called synchronous message passing systems.

In distributed consensus systems consider three different type of failures, crash fault - just like a node, so the node suddenly crashes or the nodes become unavailable in the middle of communication, you are not expected to receive any message from that particular node, network or partitioned faults - network link fails in partitioned in the network, the individual nodes are interconnected with each other, if any particular node fails in the network, the node can be specified two partition, so the entire network get partition and you are not expected to receive any message from any node of this network link failure, and byzantine fault – a node starts behaving maliciously. This mechanisms is a idealistic point-of-view, it's a decision making process for group of people involved and discussed with on decide on that value, every correct individual must agree on the same value in agreement process.

- The blockchain technology uses five most common consensus mechanisms; POW (Proof of Work –bitcoin and other blockchains), POS (Proof of Stake - peercoin), DPOS (Delegated Proof of Stake), PBFT (Practical Byzantine Fault Tolerance – used for hyperledger fabric) and DAG (Directed Acyclic Graph). Find the hash value, then the value allowed and add new block of transaction to the blockchain is POW. POS is lower energy consumption, different way to achieve and validate the transactions. DPOS is variation on POS, it's the coin holder and ownership in the network. PBFT relies that number of nodes confirm and DAG is a graph theory, it's the common sub expression in the given expression, it cannot form a cycles in graph. This DAGs transactions run on different chains simultaneously, process over 10000 transactions per second. The stable of blockchain industry is proof of work and proof of stake; these are the most prominent consensus algorithms in blockchain technology. Consensus models are primary components of distributed systems and understanding of blockchain fundamentals.

A. Byzantine Generals Problem

One of the most difficult challenges addressed by the block chain technology is Byzantine Fault Tolerance, its distributed computing systems. It may happen that the node sends different message to different peers, this general class of faults in a distributed system under closed environment, its call as a byzantine general problem or byzantine fault tolerant problem. This problem is class of failure in characteristics of systems; Fig.3. Represents that byzantine problem under multiple scenarios, this kind of problem denote that lamport timestamp.

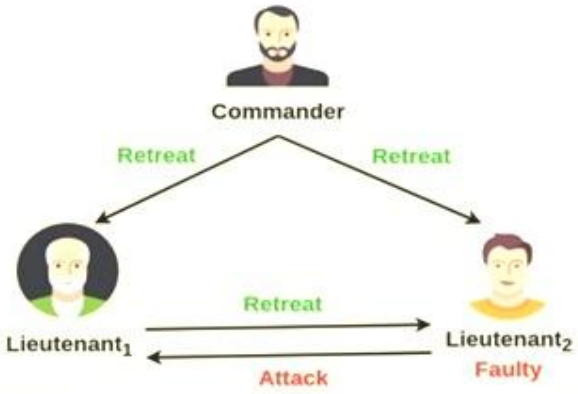

Fig.3. Multiple Scenarios of Byzantine Problem Architecture

The failure is based on imperfect information on the particular components or particular event. In byzantine architecture can have one commander and two different lieutenants, the commander send the message to the lieutenants, the lieutenant can share the messages then try to find out the commander is faulty or lieutenant is faulty. The perspective of three generals, in this case try to design a problem & also design a solution for that problem. In this architecture assume that two lieutenant, lieutenant1 is correct lieutenant and lieutenant2 is faulty lieutenant. Now if the Lieutenant is faulty,then the lieutenant may send different messages, so the commander is correct commander then send messages to both the lieutenants. Here lieutenant2 is faulty lieutenant does not obey the message to commander, the faulty lieutenant2 sends an attack message to lieutenant1. lieutenants1 is the correct lieutenant send the correct message ie., what message received from the commander side that message sent to the lieutenant2. So lieutenant1 is received two different messages from commander and lieutenant2,by integrity condition both lieutenants conclude the commanders message, this contradicts the agreement condition, but this agreement condition cannot met for the single fault occurs in the nodes. so this byzantine generals model indicate that receiver always know that the identity of sender, fully connected, synchronous systems and reliably communicate with all lieutenants.

B. Practical Byzantine Fault Tolerance Model

Practical byzantine fault tolerance consensus algorithms for ensuring the safety property then consider a complete asynchronous system or pure asynchronous systems. This algorithm is termed as practical, because it ensure safety over on asynchronous network, so this system supports byzantine failure and low overhead. The diagram Fig.4. Represents that multiple of lieutenants of distributed environment in blockchain network. Its asynchronous distributed systems, a client send a request to invoke service operation to commander/primary, commander/primary multicasts the requests to backups of all lieutenants/secondary, after receiving message from commander, the clients waits for replies different backup with the same results. all lieutenants/secondary send reply/response to client, maximum number of faulty replicas that can be tolerated.

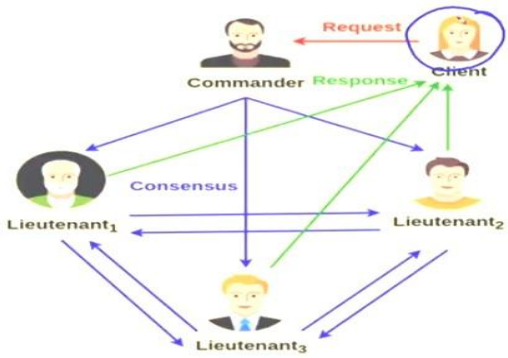

Fig.4. Multiple lieutenant of PBFT Model

It also supports privacy over the systems. it assured that the messages are tamper proof, it applies a hashing technique similar to blockchain and it also applies authentication technique through digital signature mechanism. so that none of the messages are transfer from individual nodes in the system. PBFT model well adopted in consensys for permissioned blockchain environments like hyperledger and tendermint core. Its open environment and every node meet to sense that multicast message to every other node, so the system has a high message complexity.

III. HYDERLEDGER CONCEPTS IN BLOCKCHAIN

A. System Architecture

Its a blockchain framework implementation of hyperledger projects, its open source platform for deploying and operating permissioned blockchain, running on distributed applications and support consensus protocols, first blockchain system is fabric, that run and written in generic purpose programming languages. The certificate authority provide the certificate services to the user in blockchain technology, external certificate authority services and fabric certificate services are optional and its connected between the membership services, these services relate to user transactions and secured connections between the transport layer security, The diagram Fig.5.represents that hyperledger fabric architecture building block. Membership service provider enroll the client application.

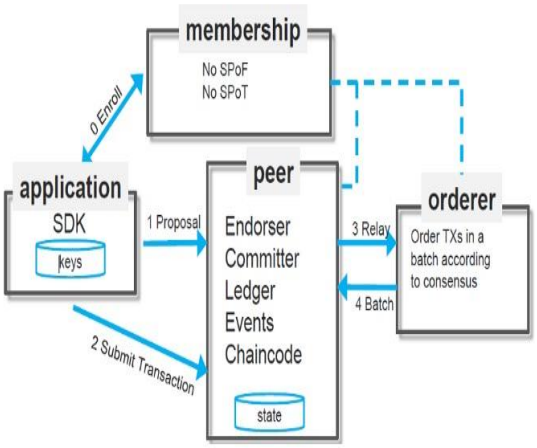

Fig.5.Building Blocks for Hyperledger Fabric Architecture

The client application connected to peer network, peer network performs the notations of endorser, committer, ledger, chaincode and events. Blockchain can have many componenets, peer is one components of blockchain,ie, in peer multiple organizations on run on one peer or one organizations run on multiple peer. Peer nodes can have two main functions of endorser (endorse proposal for transaction) and committer (block of transactions to ledger). Ledger is maintaining peer, its constructed by ordering services, its verify the history of all transactions of successful information (valid and invalid transactions information) stored on it. The ordering service is a centralized service, this service provide the delivery quarantees, shared communication channel to clients and peers, so the client connect to communication channel and broadcast message to all peers. Chaincode is the smart contract written in java, is invoked by transaction.

B. Smart Contracts in Blockchain

A self executing contract in terms of the agreement between the buyer and seller is directly written into the lines of code. It's consistent of updating the information. User can access and see the information, that information sent and stored in concept is called smart contract, which contains transactions with some conditions and rule smart contract is implemented. It's clearly defined the functions and specifies the way of work, performance of credible transactions without third parties. Smart contracts are core of blockchain technologies, its self verifying and self executing agreements and address the Contract Lifecycle Management (CLM).

C. Comparing Ethereum and Bitcoin Blockchain

Ethereum is open source,distributed computing for public blockchain based technology. It's a transaction based state transistion systems. Ethereum is similar to bitcoin but focus on smart contract in any decentralized applications, bitcoin is the peer to peer cash system in electronic format.The following Fig.6.. described that comparison of bitcoinstack and ethereum stack. The initiating transactions of bitcoin blockchain is wallet applications.

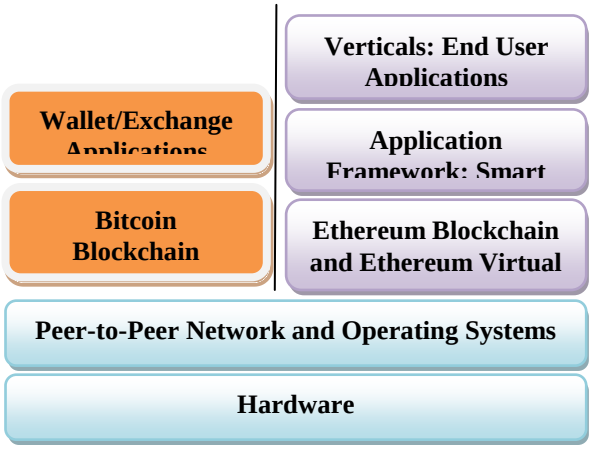

Fig.6. Overview of Bitcoin Stack with Ehereum Stack

IV. CONCLUSION

Blockchain is the context of digital currency, most prominent and emerging technology for decentralized and transactional sharing of data in large networks. Now blockchain technology currently implemented in bank sectors, industry, financial services and supply chain industry.different people use different application protocols how the transaction can be secured from other, then how to encrypt the key pair with authentication process in blockchain environments. Distributed system environements of hyperledger fabric make it highly scalable system supporting with permissioned blockchain with flexible systems. In this paper design and analyze the different consensus algorithms and hyperledger fabric technique and smart contracts problems. How the transaction to be secured from one another, then the message can be delivered in secured manner or not. The feature of blockchain technology can be extend with wide variety of areas such as security, membership access controls, research aspects, byzcoin, data analytics and artificial intelligence

REFERENCES

1. High-Performance Consensus Mechanisms for Blockchains Signe Rüsch TU Braunschweig, Germany ruesch@ibr.cs.tu-bs.de, EuroDW'18, April 23, 2018, Porto, Portugal 2018, PP 1-3, http://conferences.inf.ed.ac.uk/EuroDW2018/papers/eurodw18-Rusch.pdf
2. Ambili, KN., and Sindhu, M., and Sethumadhavan, M., On Federated and Proof Of Validation Based Consensus Algorithm In Blockchain. IOP Conference Series: Materials Science and Engineering, 2017
3. Atzei, N., Bartoletti, M., and Cimoli, T., A survey of attacks on ethereum smart contracts (sok). In International Conference on Principles of Security and Trust (2017), Springer, pp. 164-186.
4. Baliga, A., Understanding blockchain consensus models. Tech. rep., Persistent Systems Ltd, 2017.
5. Cachin, C., Architecture of the hyperledger blockchain fabric. In Workshop on Distributed Cryptocurrencies and Consensus Ledgers, (2016).
6. Imran Bashir, Mastering Blockchain, Distributed ledgers, decentralization and smart contracts explained, (2017)
7. KPMG, Consensus immutable agreement for internet of values, https://assets.kpmg.com/content/dam/kpmg/pdf/2016/06/kpmgblockchain-consensus-mechanism.pdf
8. Mattila, J., The blockchain phenomenon. (Berkeley Roundtable of the International Economy, 2016, edn.), (2016).
9. Nakamoto, S., Bitcoin: A peer-to-peer electronic cash system, 2008.
10. Sankar, L. S., Sindhu, M., and Sethumadhavan, M., Survey of consensus protocols on blockchain applications. In Advanced Computing and Communication Systems(ICACCS), 2017 4th International Conference on (2017), IEEE, pp. 1-5. [10] Wood, G., Ethereum: A secure decentralized generalized transaction ledger. Ethereum Project Yellow Paper (2014).
11. Application of blockchain technology to banking and financial sector in India, 2017.
12. Survey on blockchain technologies and related services, Japans Ministry of Economy, Trade, and Industry (METI), 2016.
13. Blockchains & distributed ledger technologies, https://blockchainhub.net/blockchains-and-distributed-ledgertechnologies-in-general/.
14. https://arxiv.org/pdf/1801.10228 hyperledger fabric: a distributed operating system for permissioned blockchains", research paper in eurosys 2018.
15. https://blog.acolyer.org/2018/06/04/hyperledger-fabric-a-distributed-operating-system-for-permissioned-blockchains/
16. https://hyperledger-fabric.readthedocs.io/en/release-1.2/blockchain.html
17. https://blockgeeks.com/guides/blockchain-consensus/

Efficiency of Lateral System in Tall RC Building

Md Taqiuddin, S. Lakshmi Shireen Banu

Abstract*: Shear walls have the important properties of lateral resistance in high rise building for earthquake and wind load forces. The sway developed by the lateral forces causes damage to the life and property. Thus, shear walls are initiated in the building to achieve necessary resistance to the lateral forces. Double core shear wall or box section shear wall is important to ensure adequate stiffness, strength and durability. The study has been done to analyze the affect of perimeter frames for structural systems in lateral performance of an irregular shape 30 storey 'L-shape' building for the subsequent cases 1: 125mm flat slab with drop, 2: 150mm flat slab without drop, 3: increase in diaphragm's rigidity with 250mm at regular intervals, 4: outrigger + increase in diaphragm's rigidity with 250mm at regular intervals.

Keyword: stiffness, strength and durability

I. INTRODUCTION

The trend of uneven plan structures shows a type of tall building due to increase of population in metropolitan cities. To promote the demand of tall building structures, different types of structural systems have been used. The study has been done for the control of drift with the following lateral resisting systems. Case 1: It's a 30 storied building with 90m of height. The typical floor height is 3.00 m. The entire column size up to 14th floor is 1.50 X 1.50 m, 15th floor is 1.20 X 1.20 m and rests of the floors with size of 0.80 X 0.80 m. The columns are provided at 6.00 m spacing. Beam framing at perimeter is of size 0.40 X 0.60 m which connects all periphery columns. The thickness for all flat slabs is 0.125 m with drop panels. A shear wall core of 12.00 X 12.00 m with 0.25m thickness upto 15th floor and remaining with 0.15m is added. Case 2: From the case: 1, 150mm flat slab without drop is introduced by deleting the 125mm slab with drop panels. Case 3: From the case 2, the flat slabs are changed into a floor plate with 0.150m thickness except multiplies of 5th floor with a thickness of 0.250 m. Case 4: At top floor, 22nd floor and 14th floor Outrigger system is initiated. To conclude how important it is to choose a structural system that combines proven technologies with local materials and expertise in order to implement a particular architectural design in a particular location. Some options for structural system include: 1) Moment-resisting frames: rigidly jointed frames or sway frames are those with moment resisting relations among beams and columns. 2) Shear walls, 3) braced frames, 4) Framed-Tube structures: the frame consists of closely spaced column which are joined by deep girders. 5) Braced-Tube structures: By using the cross bracing frame with X-bracings, further improvement can be made for tubular system over many stories. 6) Tube-in-Tube structures: In this type the outer-frame is added together with an internal elevator and service core. 7) Bundled-Tube structures: The bundled tube system can be seen as a group of individual tubes resulting in collective cell tube. 8) Core and perimeter frame interactive structures: Included here are systems that interconnect perimeter frames and core towers through outrigger trusses. 9) Mega structures.

II. LITERATURE REVIEW

ALPA SHETH Concluded that in building with a central shear wall core and with length to width ratio exceeding to the performance is enhanced by adding outriggers and perimeter frames. A perimeter frame without outriggers does not help significantly in resisting lateral loads.

K.M.LAM,' ET AL' Reports dynamic wind loads measurement data of a wind tunnel on various number of H-shaped tall buildings with a high frequency force balance. For normal wind occurrence on the building face with cavity fluctuations in the crosswind moment on H-shaped building are observed to have lesser magnitudes than that in the square building.

E.F.CRUZ, 'ET AL' the effect of irregularity in height is important when the behavior of the structure remains in the elastic limit as well as when it goes into the inelastic Reigns. On the other hand, the maximum element forces are not very sensitive to irregularities in height and tend to become smaller as it increases.

DONG-GUEN LEE, 'ET AL' presents an efficient model for the analysis of a high rise building structure using super elements. The refined finite element model of a high rise building structure with shear wall is expected to cost a significant amount of computational time and memory while it would provide the most accurate results.

YOUNG S.CHO, 'ET AL' a study for the reinforcing method of flat plate column connection has been done in this paper. Four tests specimens were modeled for the interior bay flat plate slab column connections in a typical flat plate slab building. Based on the study it is concluded that the bay specimens failed due to punching shear produced from gravity loading. The most ductile behavior under the gravity loading was showed by the stud containing specimen with steel plate.

J.M.REYNOUARD, 'ET AL' in this paper, investigation is done on the modeling of the seismic response of RC walls with different reinforcement ratios. For a specimen and interpretation of the experimental results is attempted through a finite element nonlinear cyclic model.

Revised Manuscript Received on December 28, 2018.

MdTaqiuddin, Department of Civil Engg.,MREC,Kompally, Secunderabad District-500100, Telangana, India.

Dr.S.LakshmiShireenBanu, Department of Civil Engg.,MREC,Kompally, Secunderabad District-500100, Telangana, India.

KING-LE CHANG, 'ET AL' demonstrates the effectiveness of the outrigger system for the central cored building structure with 2 outrigger floors and perimeter columns and also considered the slab stiffness at the typical floors. The conclusion is to enhance the effective depth of the building structure, beyond those provided by the central core by inducing tension and compression in the perimeter columns.

Z. BAYATI1, 'ET AL' presents the result of an analysis on reduction of drift in uniform belted structures with the help of rigid outriggers. It is concluded from the results that using optimized multi outriggers system can effectively help in reducing the seismic response of the building and can decrease the elements and foundation dimensions.

III. THOERY OF DYNAMIC AND SEISMIC RESPONSE

Damped free vibration: - the differential equation governing free vibration of SDOF with damping is

$$M\ddot{u} + c\dot{u} + Ku = 0$$

Dividing by m gives

$$\ddot{u} + 2\varepsilon\omega\dot{u} + \omega^2 u = 0$$

Where $\omega^2 = K/m$, $\varepsilon = c/2m\omega = C/C_r$

$$c_r = 2m\omega = 2\sqrt{km} = 2K/\omega$$

Where c_r is critical damping coefficient

Analytical model and solution procedures:

The analysis is done for the influence of perimeter frames in lateral performance of an irregular shape 30 storey 'L Shape' building. The load combinations of Load Case (0.9 DL + 1.5 WLX) is considered to carry out Storey and Columns forces, and the serviceability load combinations of Load Case 1.0(DL + WLX) is considered to carry out Storey and Columns displacements, as the lateral forces caused by wind load governs more than seismic loads.

Columns considered for comparison of Analysis are C3, C19, C21, C24 and C45 columns where C3 and C45 lies in X-direction left outer and right outer columns, C19 & C24 lies in Y-direction bottom outer and top outer columns in the line of Re-entrant column C21.

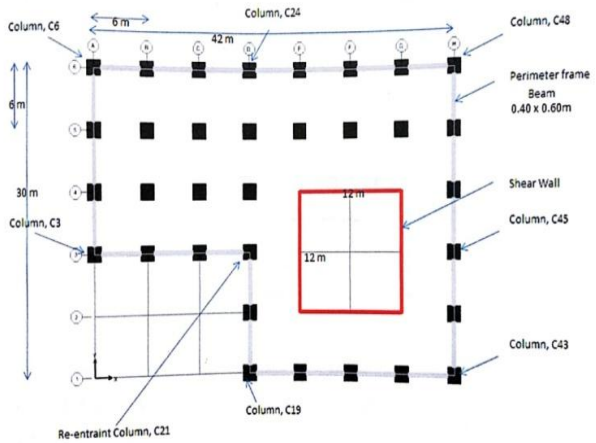

IV. DISCUSSIONS ON RESULTS

- The maximum storey axial forces in structure 1 is 237763 which is 6.93%, 12.04% and 12.45% less compare to structure 2,structure 3 and structure 4 respectively.

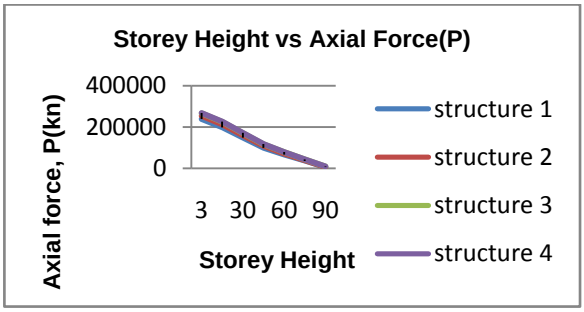

- The Maximum Storey Drift in Structure 1 is 0.55 mm which is 12.72%, 23.63% and 40% more compare to Structure 2, Structure 3, and Structure 4 respectively.

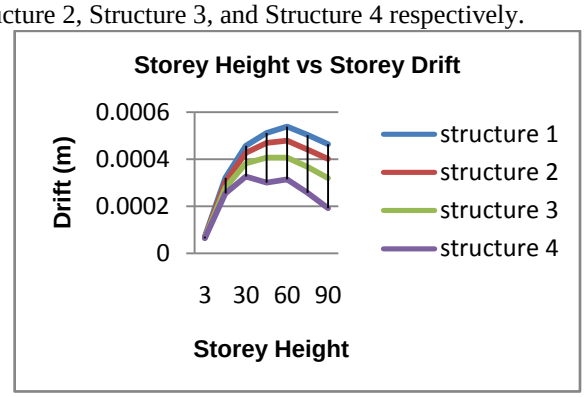

- The Maximum CM displacement in structure 1 is 38.9 mm which is 10.02%, 21.33% and 38.82% more compare to structure 2, structure 3 and structure 4

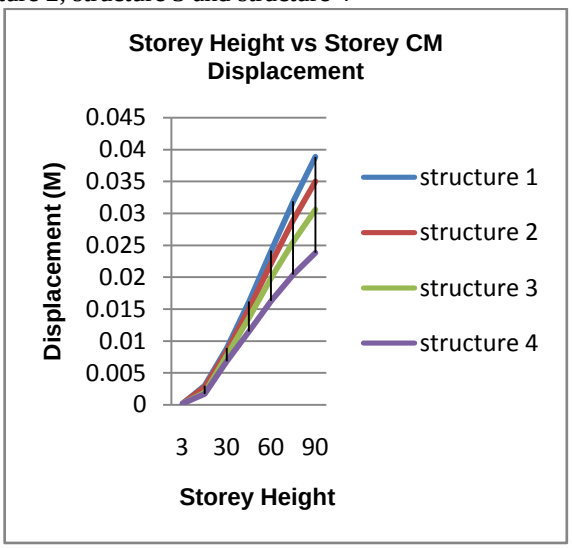

- As per IS 1893 (Part 1): 2002 clause 7.11.1 limiting storey drift is 0.004 times storey height. i.e. 0.004 x 3.0 m = 0.012 or 12mm. The Maximum Storey Drift for all the structures in both the directions for the load cases D.L + WLX is less than the limiting value.
- All the structures are Re-entrant column structures as $A_1/L_1 = 0.4285$ and $A_2/L_2 = 0.40$ which are greater than 0.15.
- For structure 4, Moment in Re-entrant column, C21 is 894 KN-m which is 0.6%, 0.66%, 4.31% more and 5.76% less compare to C3, C45, C19 and C24 columns respectively.

Type of structure	C19	C21	C24	C3	C45
Structure 1	944	984	1038	979	978
Structure 2	922	960	1011	955	954
Structure 3	893	930	980	925	924
Structure 4	855	894	945	888	888

- For structure 4, Axial forces in Re-entrant column, C21 is -7489 KN which is 38.12%, 40.27%, 13.26% more and 0.07% less compare to C3, C19, C24 and C45 columns respectively.

Type of structure	C19	C21	C24	C3	C45
Structure 1	-3970	-7303	-5876	-3948	-6239
Structure 2	-4189	-7481	-6213	-4208	-6743
Structure 3	-4376	-7529	-6511	-4451	-7244
Structure 4	-4473	-7489	-6496	-4634	-7494

V.CONCLUSIONS

From the analysis of the data the following results have been arrived at.

1. Structure 2: 150 mm Flat slab without drop significantly improve the behavior than structure 1 :(125 mm flat slab with drop) due to increase in the diaphragm's rigidity.

2. There is further improvement in performance of the structure with increase of diaphragm at regular intervals. Hence structure 3: (increase in diaphragm's rigidity with 250mm at regular intervals) shows better performance.

3. The outriggers, mainly those aligned to shorter edge helps greatly in increase of effective depth of the building structure which participates in resisting the lateral loadings. Hence it is concluded that lateral resistance transverse to shorter edge in structure 4(outriggers + increase in diaphragm's rigidity with 250mm at regular intervals) gives better Lateral resistance than all the structures due to addition of outriggers parallel to shorter edge.

4. Further it is concluded due to not providing outriggers parallel to longer edge at left side of the shear wall and due to torsion effect, the CM displacement and storey drift in Y-Direction are increased in structure 4 than structure 1.

VI. SCOPE OF FURTHER STUDY

Study can be made further by **providing shear wall core with perimeter frame with outrigger systems at different floor levels** for further increase in height of the building.

REFERENCES

1. Dr.H.M.Somasekharaiah, MadhuSudhana, MuddasarBasha, "A Compressive Study on Lateral Force Resisting System For Seismic Loads" (IRJET) Aug-2016
2. K.M.Lam, 'et-al.' "Dynamic wind loading of H-Shaped Tall buildings" – for 7th APCWE, November 8-12, 2009, Taipel, Taiwan.
3. PankajAgarwal& Manish Shrikhande (2009) "Earthquake Resistant Design of Structures".
4. Alpha Sheth, "Effect of perimeter frames in seismic performance of tall concrete buildings with shear wall core and flat slab system" – for 14 WACEE on 12-10-2008 Beijing, China.
5. Z.Bayatil, 'et-al.' "Optimized use of Multi-outrigger System to stiffen Tall Buildings" – for 14 WCEE on 12-10-2008, Beijing, China.
6. Chopa A.K (2005):- "Dynamics of structures theory and applications to Earthquake Engineering", second edition.
7. King-Le Chang and Chun-Chung Chen, "Outrigger System Study for Tall Building with Central Core and Square Floor Plate" – for CTBUH 2004 October 10-13, Seoul, Korea.
8. Dong-Gyen Lee, 'et-al' "Use of Super Elements for an efficient analysis of high- rise building structures" – for CTBUH 2004 October 10-13, Seoul, Korea.
9. Young S.Cho, 'et-al.' "A study of Flat Plate Slab – Column connections with Shear Plate in Tall concrete building using Experimental and Numerical Analysis" – for CTBUH 2004 October 10-13, Seoul, Korea.
10. J.M.Reynuouard and J.F.Georgin, "Non linear response and modeling of RC walls subjected to seismic loading", -paper no: 415, vol. 39, march-june2002 of ISET journal of EQ technology.
11. E.F.Cruz and S.Cominetti, "Influence of Irregularities in Height and Different Design criteria on the inelastic response of building models" –Paper No: 631 for 11th WCEE, 1996.
12. NirjharDhang, "Structural Dynamics: An Over View" Chapter 12-SE101, NPCBEERM, MHA(DM)
13. U.H.Varyani "Structural Design of multi-storied buildings", second edition.

A Study on Performance Analysis of Multi-Level Feedback Queue Scheduling Approach

Sanjeeva Polepaka, R. P. Ram Kumar

Abstract*: In CPU scheduling, various algorithms are used to schedule the processes. Few of them are First come first serve (FCFS), Shortest Job First (SJF), Shortest Remaining Time First (SRTF), Priority Scheduling, Round Robin (RR), Multi-Level Queue (MLQ), Multi-Level Feedback Queue (MLFQ) scheduling approaches. This scheduling is used to process the scheduling of operating systems, which is responsible for assigning the CPU time to available processes. To get user interactivity, throughput, real-time responsiveness, and more. The objective of the paper is to present an idea that keeps the CPU in maximum utilization until the process is requesting for an event. When the process is waiting for an event to occur, the CPU is switched between the processes for better utilization by consuming CPU cycles. The paper also addresses the four different approaches and their average waiting time in processing the jobs.

Index Choice: CPU Scheduling, Process Scheduling, First come first Serve (FCFS), Shortest Job First (SJF), Shortest Remaining Time First (SRTF), Round Robin(RR), Multilevel Feedback Queue (MLFQ), Waiting Time.

I. INTRODUCTION

Multilevel Feedback Queuing is common in the CPU scheduling techniques used in operating systems. Multi-Level Feedback Queue (MLFQ) algorithm allows processes switching between queues based on the burst time. The MLFQ scheduling algorithm allows a process to move between queues. Here, the processes are categorized based on CPU burst time. If too much of CPU cycles are utilized by the process, then it is given less priority and moved to the lower-priority queue. This scheme leaves I/O-bound and interactive processes in the higher-priority queues. Also, a process that waits too long in a lower-priority queue may be moved to a higher-priority queue. This form of aging prevents starvation. This paper suggested an improvised MLFQ with decreased waiting time.

Let us consider an example of multilevel feedback queue scheduler which contains three queues with numbering 0 to 2 as shown in the Figure 1. The processes will be first executed in queue 0. Next, the processes will be completed in queue one if queue 0 is empty. Similarly, processes will be executed in queue two if queue 0 and queue 1 are empty.

Let us assign time quantum of 0.8 milliseconds to queue 0 and time quantum 0.16 millisecond to queue 1. The processes will be run in queue two on FCFS basic but the condition is queue 0 and one should be empty.

Revised Manuscript Received on December 28, 2018.

Sanjeeva Polepaka, Associate Professor, [2]Department of Computer Science and Engineering, Malla Reddy Engineering College (Autonomous), Maisammaguda, Secunderabad – 500100, India.

R. P. Ram Kumar, Professor, [2]Department of Computer Science and Engineering, Malla Reddy Engineering College (Autonomous), Maisammaguda, Secunderabad – 500100, India.

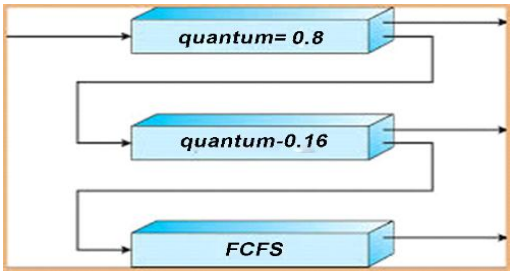

Fig 1: FCFS Scheduling Method

II. THE PROPOSED WORK

Figure 2 shows the proposed method with the queue 0 and 1 submitted at the same time quantum. But in queue 2 the processes will run on basis of Shortest Remaining Time First (SRTF) order which will reduce the waiting time of the processes. By this, the processes will be executed quickly without any delay.

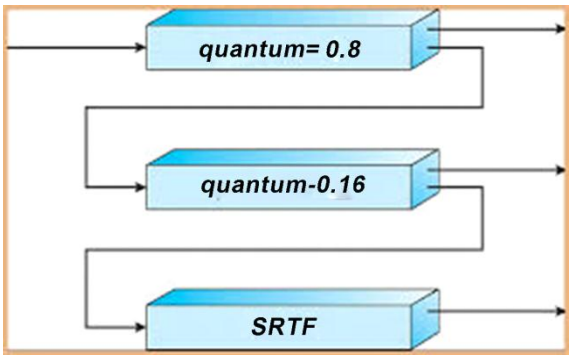

Fig 2: SRTF Scheduling Method

Example Case 1:

Consider the following example. Let us take four processes P_1, P_2, P_3, and P_4 with arrival time 0, 3, 10, 12 simultaneously and estimate time of 10, 5, 3, and 1, simultaneously.

Equation (1) is used to find the waiting time by the FCFS approach.

WT = ST – AT (1)

where WT represents Waiting time,
ST represents Starting time, and
AT represents Arrival time.

	Arrival time	Estimate time	Starting time	Waiting time
P1	0	10	0	0
P2	3	5	10	7
P3	10	3	15	5
P4	12	1	18	6

In FCFS approach, the determined average waiting time is 4.5 milli seconds (ms)

Example Case 2:

Equation (2) is used to find the waiting time by SJF approach.

WT = ST – AT (2)

	Arrival time	Estimate time	Starting time	Waiting time
P1	0	10	0	0
P2	3	5	10	7
P3	10	3	15	5
P4	12	1	18	6

In SJF approach, the determined average waiting time is again 4.5 ms

Example Case 3:

Equation (3) is used to find the waiting time by SRTF approach.

WT = TAT – ET (3)

where WT represents Waiting time
TAT represents Turn around time
ET represents Estimate time.

TAT is calculated using the equation (4).

TAT = CT – AT (4)

where, CT represents Completion Time and
AT represents Arrival Time

	AT	ET	ST	CT	WT	TAT
P1	0	10	0, 8, 14	19	9	19
P2	3	5	3	8	0	5
P3	10	3	10	13	0	3
P4	12	1	13	14	1	2

In SRTF approach, determined Average waiting time is 2.5 ms

Example Case 4:

Equation (4) is used to find the waiting time by Round Robin Fashion:

WT = TAT – ET and TAT = CT – AT (5)

	AT	ET	ST	CT	WT	TAT
P1	0	10	0,2,6,10,16	18	8	18
P2	3	5	4,8,14	15	7	12
P3	10	3	12,18	19	6	9
P4	12	1	15	16	3	4

Average waiting time = 6 ms

III. CONCLUSION

Experimental results concluded that, when determining the average waiting time for four approaches, namely, FCFS, SJF, SRTF, and RR approaches, SRTF has the minimum average waiting time in processing the jobs. By this, it is clear that by using Shortest Remaining Time First the waiting time of the processes is reduced and the processes will be executed quickly without any delay.

REFERENCES

1. Malhar Thombare, Rajiv Sukhwani, Priyam Shah"Efficient implementation of Multilevel Feedback Queue Scheduling", International Conference on Wireless Communications, Signal Processing and Networking (WiSPNET), September 2016.
2. Silberchatz, Galvin, and Gagne, operating systems concepts, 8th Edition, John Wiley and Sons, 2009.
3. Deepali Maste, Leena Ragha, Nilesh Marathe, "Intelligent Dynamic Time Quantum Allocation IMLFQ Scheduling" in International Journal of Information and Computation Technology, vol. 3, no. 4, pp. 311-322, 2013, International Research Publications House, ISBN 0974-2239.
4. A. S. Tanenbaum, "Modern Operating Systems" Prentice Hall Publications, 2009.

RSM based Empirical Model for the Performance and Emission Characteristics of ROME Biodiesel

T. RamachandranS. Murugapoopathi, D. Vasudevan

Abstract*: In the current scenario, the production of biodiesel for IC engine plays important role due to the undesirable pollution and cost hike of the conventional fuels. In India, milk from the rubber tree (HeveaBrasiliensis) is used for the production of elastic materials which are most widely used in engineering applications. But the seed from the rubber tree is kept wasted without any further usage and hence in this research the oil produced from the rubber seed is suggested for effective biodiesel production. The rubber seed oil (RSO) is converted in to usable rubber seed oil methyl ester (ROME) biodiesel using trans-esterification and tested for the characteristics of performance and emission through variable compression ratio (VCR) engine. The detailed set of experiments are conducted in the VCR engine with different biodiesel-diesel ratios to evaluate the BTE, SFC, CO, CO_2 and NO_x levels of the blends. A mathematical model also developed using Response Surface Method (RSM) for these parameters such that the compression ratio, fuel blend, engine load, and injection pressure are the design variables, The experimental results are used in the RSM to create the mathematical models and the models are checked for the ANOVA and p-test. Finally the models are tested with the new sets of experimental results.

Index Choice: ROME, VCR engine, RSM, Emission, biodiesel

Nomenclature

VCR	Variable Compression ratio	NOx	Oxides of nitrogen
SD	Standard deviation	B20	20% biodiesel + 80% diesel
CR	Compression ratio	B40	40% biodiesel + 60% diesel
BTE	Brake thermal efficiency	B60	60% biodiesel + 40% diesel
BSFC	Brake specific fuel consumption	B80	80 % biodiesel + 20% diesel
CO	Carbon monoxide	HC	Hydrocarbon
CO_2	Carbon dioxide	RSM	Response surface methodology

I. INTRODUCTION

Renewable sources are playing major role in energy sector. Day to day increase in demand for energy and depletion of fossil fuels leads to utilize the different resources available in earth surface. Biodiesel is the mode of renewable source available in plenty of different varieties includes edible, non-edible seeds, algae, animal fats and vegetable oils. Varieties of designed experiments are functionalized on the VCR engine to identify the best blend and various parameters that affects engine power and emission. The optimum input variables and output response parameters are identified from optimization technique to improve the performance and combustion of the engine. RSM mode of design of experiments is used to optimize the emission of NOx and bsfc. Single cylinder direct injection 5.2 kW diesel engine is selected with five factors such as injection timing, injection pressure, nozzle hole diameter, load torque and clearance volume using diesel fuel. Valve opening pressure had greater influence among five factors and deviation is less than 10 % with experimental value[1]. ANN based feed forward back propagation algorithm is trained to predict the performance, emission and combustion characteristics of VCR engine with different CR, load and the blend are the input variables. The mean square error of output is less than 0.05 and R^2 values are greater than 0.95 for training and tested experiment model [2]. Kernel based extreme learning machine (K-ELM) and cuckoo search (CS) model is used to optimize the fuel blend with fuel price and weightage as factor compared with least square support vector machine (LS-SVM) with swarm optimization and experimental values. K-ELM contributes better result compared to LS-SVM and CS gives effective result on optimization [3]. Biodiesel produced from Australian Beauty leaf tree is blended with diesel (B5 & B10) on volume basis. To improve the engine performance of the engine and to reduce the emission characteristics of fuel used, the experimental and numerical studies were carried out. CFD program AVL fire software is used to develop an engine combustion model and simulation results were validated with experimental results and deviation was found to be less than 4.4%. B10 shows the better performance and low emission compared diesel and B5 [4]. Engine test is conducted with different speed(1360,1700 and 2000rpm) and fuel blend of B25, B50, B75 and B100 using experimental and Numerical simulation using AVL BOOST program with empirical

Revised Manuscript Received on December 28, 2018.

T.Ramachandran, Department of Mechanical Engineering, Malla Reddy Engineering College, Secundrabad, Telgana, India.

S.Murugapoopathi, Department of Mechanical Engineering, PSNA College of Engineering & Technology, Dindigul – 624 622, Tamilnadu, India.

D.Vasudevan, Department of Mechanical Engineering, PSNA College of Engineering & Technology, Dindigul – 624 622, Tamilnadu, India.

sub-model to control mixed combustion parameter at full load. Increase in blend in fuel mixture reduces the heating value, engine power and also reduces the NOx and CO emission at all speeds. Numerical results are 10% higher than experimental results and bsfc increase 12% for both results of diesel and B100 [5]. SI engine fueled with propane, hydrogen, methane and methanol to study the fuel emission and engine performance characteristics using 3D CFD code and the effect of EGR and supercharging. 10% EGR reduces the NOx and CO emission by 10-20% of all fuels. The effect of EGR on CO emission is more than other fuel for methanol. The effect of supercharging has noticeable effect on gasoline and least effect on hydrogen [6]. Blend of 40% n-butanol, n-propanol and n-pentanol are mixed with diesel individually in DI diesel engine to study the performance and emission characteristics using EGR percentage, injection timing and type of alcohol as parameters. 3^k factorial design matrix is used to define a numerical model using RSM and are compared with experimental results with the of 5% in the predicted error. 10% EGR gives best result for n-butanol and n-pentanol diesel blends at 24°CA bTDC at optimum condition [7]. 2-butanol gasoline blends of 5%,10% and 15% is blended to the petrol for optimizing the performance and emission of SI engine for different speed and fuel blends using RSM. Blend of 15% gives optimum value at 3205 rpm with best performance and emission compared to other blends [8]. Impact of methanol addition in to neat biodiesel with 5%, 10% and 15% on volume basis to analyze the performance, combustion and emission of a diesel engine using 3-D CFD simulation with KIVA4 code CHEMKIN II under 10%,50% and 100% load and is compared with experimental results. Results revealed that addition of methanol improves cylinder pressure under 10% load condition with 5% blend ratio and overall reduction CO and soot emission observed under every load conditions [9]. RSM is used to determine the performance responses of BP, brake torque and bsfc of a diesel engine. Developed model fits with input factors for the corresponding outputs and verified with experimental results. Brake power and brake torque reduces up to 18% when biodiesel is used and increase in bsfc up to 15% recorded [10]. Numerical model is developed to optimize the parameter which directly affecting the performance of the diesel engine is predicted among fuel flow, speed, injection pressure and throttle positions. Fuel flow is function of the engine speed when compared with the experimental results matching R^2 value of 0.9338[11]. Biodiesel produced water hyacinth blended with diesel at 5,10,15,20 and 25 proportions on volume basis to investigate the performance and combustion using numerical model with experimental results. Compression ratio, injection pressure, loads and blends are input factors are validated with combustion pressure and emission responses. B5 and B10 produces significant combustion pressures compared to other blends using RSM [12].

In this research work, ROME biodiesel is produced from the RSO and is tested for performance and emission characteristics. The experiments are conducted on the VCR engine at the different range of blend, compression ratio (CR), injection pressure and engine loads to evaluate the performance parameters (BTE, SFC) and emission parameters (CO, CO_2, and HC). RSM is utilized to develop the empirical models for these input parameters from the design variables range. The results of the models are verified and are used as hypothesis for the experimental setup.

II. EXPERIMENTAL SETUP

The Experimental set up (fig.1) consists of single cylinder variable compression ratio multi fuel water cooled engine coupled with the eddy current dynamometer. The setup is attached with strain gauge load cell, and computerized data acquisition system. Various sensors are provided in the engine setup to measure speed, airflow, fuel flow and temperatures of engine water inlet, outlet and exhaust gas. The sensors are connected to the data acquisition system such that the data related to sensors are stored in it. The sensors are well calibrated before the start of the experiments. For the measurement of CO, HC, CO_2, O_2 and NOx emissions a calibrated gas analyzer (Mars technology Inc.) is connected to both the engine and to the data acquisition.

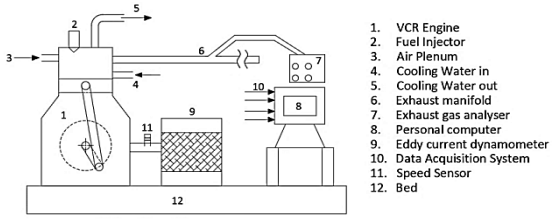

Fig. 1 VCR Experimental setup for testing the ROME

The ROME is prepared using the RSO through the transesterification process and tested for the fuel properties. For conducting the experiments on the biodiesel, the ROME blends are prepared with various proportions (B20, B40, B60& B80) with the diesel. The ROME and its blends are also subjected to laboratory test (as per ASTM standard) to measure the viscosity, density, flash point, fire point, calorific value and Cetane index (table.1).

PROPERTIES	B20	B40	B60	B80	Diesel	Biodiesel standards	
						ASTM D 6751-02	DIN EN 14214
Density (gm/cc)	0.82	0.86	0.87	0.88	0.83	-	0.86-0.9
Viscosity at 40 °C (centipoise)	0.643	1.032	1.45	2.235	1.382	1.9-6.0	3.5-5.0
Flash point (°C)	50	56	65	120	42	> 130	> 120
Fire point (°C)	54	60	75	160	65		
Gross caloric value (kJ/kg)	41343	40200	39129	38070	44500	41min	51 min
Cetane index	49	47	45	41	55		

Table: 1 Properties of biodiesel

Published By:
Blue Eyes Intelligence Engineering
& Sciences Publication

III. RSM Based Empirical Model

The prediction of the performance and combustion characteristics becomes critical when the blend ratio, compression ratio, load and fuel injection pressure are varied in the range B0-B80, 18-22, 0-8 & 140-160 respectively. The prediction of emission characteristics at varied range provides information for the determination of right values of design variables and optimum operating condition for the engine user. Hence the possibility to quantify the emission characteristics of the engine for a given biodiesel is of practical importance. RSM provides relatively simple mathematical relation with the parameters and for the desired output on available data. When the problem involved is subjected to experimental errors, statistical methodology is the promising approach to analyze the problem. The prime advantage of employing experimental design and statistical methods is the reduction in number of experimental runs required to generate sufficient information for a statistically adequate result. Hence RSM is an efficient and cost-effective method to model and analyze the relationship between the engine variables and the engine performance and emission parameters. The central composite rotatable design (CCD) with full factorial approach in the RSM is used to model such that compression ratio, load, biodiesel blends and injection pressure (table.3) are the design variables and the performance parameters (BTE & SFC) and emission responses (CO, HC, CO_2 and NOx) are the objective functions. Minitab 16 statistical software is used to design and run the four factor RSM model. To run the RSM design model, the results of the standards runs are obtained experimentally (Table 2).

Run Order	(A) Compression ratio	(B) Load (Kg)	(C)` Biodiesel blends (%)	(D) Injection pressure (bar)	CO (%)	HC (ppm)	CO_2 (%)	NO_x (ppm)	BTE (%)	SFC (Kg/Kwh)
1	20	4	40	140	0.246	8	2.79	232	23.612	0.379
2	20	4	40	150	0.161	3	2.4	243	25.937	0.345
3	18	8	80	160	0.456	16	3.7	374	31.182	0.312
4	18	8	80	140	0.612	38	5.152	593	28.166	0.346
5	18	0	0	140	0.191	11	1.702	186	0.000	0.000
6	20	4	0	150	0.082	7	2.4	288	23.499	0.348
7	20	4	40	150	0.158	4	2.1	242	25.937	0.345
8	22	0	80	140	0.231	9	1.7	253	0.000	0.000
9	18	0	0	160	0.142	3	1.1	226	0.000	0.000
10	18	4	40	150	0.201	6	2.412	298	25.937	0.336
11	18	8	0	160	0.153	9	2.984	436	33.665	0.243
12	20	0	40	150	0.101	1	1.55	140	0.000	0.000
13	22	8	80	140	0.74	27	3.9	562	26.178	0.372
14	18	0	80	140	0.292	13	3.1	262	0.000	0.000
15	20	4	40	150	0.167	4	2.2	241	25.937	0.362
16	20	4	40	150	0.159	4	2.2	241	25.937	0.362
17	22	0	80	160	0.246	9	1.9	300	0.000	0.000
18	22	0	0	140	0.104	11	1.648	162	0.000	0.000
19	20	4	40	150	0.181	4	2.2	241	25.937	0.362
20	22	0	0	160	0.136	15	2.3	347	0.000	0.000
21	22	8	0	140	0.309	17	3.924	462	34.006	0.241
22	22	8	0	160	0.293	14	4.1	512	29.527	0.277
23	22	4	40	150	0.278	8	2.784	328	24.321	0.368
24	20	4	40	150	0.164	4	2.2	241	25.937	0.345
25	18	0	80	160	0.193	2	2.03	178	0.000	0.000
26	20	4	40	150	0.162	4	2.124	241	25.937	0.345
27	20	4	100	150	0.269	18	3.012	388	17.427	0.559
28	20	8	40	150	0.339	13	3.356	392	36.608	0.245
29	20	4	40	160	0.189	1	1.98	219	22.938	0.378
30	22	8	80	160	0.707	17	3.892	471	25.804	0.377
31	18	8	0	140	0.319	25	3.924	504	35.312	0.232

Table: 2 RSM Design Matrix with Results of Objective Functions

The results of the analysis of variance (ANOVA) for the models are verified for model adequacy (table 3) through the p-test. Effect of p-value determines the model is statically significant or not. If p value is less than 0.05 the coefficient terms are significant. From the results it has been understood that the coefficients are most significant at all responses and are less than 0.05. The statistics of regression is used to decide whether a regression model is appropriate. The coefficient validation is based on R^2 which is a measure of the amount of reduction in the variability of response obtained using the regression variables in the model. The value of R^2 equals to 1 if the model exactly matches and the R^2 decreases as the residual decreases. The R^2 values are high and close to 1 for every the response models and are close agreement with the corresponding R^2adj, which are desirable (Table 3). Based on the these conformity tests the regression equation established for BTE, SFC, CO, CO_2, HC, NO_x responses (Eqn 1-4).

Parameter	BTE	BSFC	CO	HC	CO_2	Nox
Mean	19.347	0.24126	0.25745	10.424	2.6698	316.14
SD	13.135	0.16719	0.16453	8.4189	0.93616	122.15
R^2	0.9924	0.9922	0.9926	0.9971	0.9873	0.9993
Pred. R^2	0.9721	0.951	0.952	0.9822	0.9531	0.9955
Adj. R^2	0.9895	0.9854	0.9861	0.9946	0.9761	0.9987

Table: 3 Model Adequacy Test

After verification of the model adequacy and p-test the empirical equations (Eqn 1-6) are developed using the model coefficients that are functions of the design variables. The equations are desirable to produce the desired outputs.

$$\text{BTE} = -362.1154 - 0.266 \times \text{A} + 10.2947 \times \text{B} - 0.04638 \times \text{C} + 4.922 \times \text{D} + 0.08106A^2 - 0.406 \times B^2 - 0.00161 \times C^2 - 0.0152 \times D^2 - 0.10007 \times AB - 0.00150 \times AC - 0.01944 \times AD - 0.00827 \times BC - 0.00544 \times BD + 0.00137 \times CD \quad (1)$$

$$\text{SFC} = 0.44458 + 0.168659 \times \text{A} + 0.129509 \times \text{B} - 0.001654 \times \text{C} - 0.023212 \times \text{D} - 0.004993 \times A^2 + 0.015610 \times B^2 + 0.000035 \times C^2 + 0.000066 \times D^2 + 0.001049 \times AB + 0.000038 \times AC + 0.0002 \times AD + 0.000162 \times BC + 0.000031 \times BD - 0.000012 \times CD \quad (2)$$

$$\text{CO} = 23.0335 - 0.9471 \times \text{A} - 0.0425 \times \text{B} - 0.0014 \times \text{C} - 0.1775 \times \text{D} + 0.0178 \times A^2 + 0.0032 \times B^2 - 0.00019 \times C^2 + 0.0005 \times D^2 + 0.0048 \times AB + 0.0003 \times AC + 0.0015 \times AD + 0.0004 \times BC - 0.0004 \times BD - 0.000019 \times CD \quad (3)$$

$$\text{HC} = 764.581 - 45.969 \times \text{A} + 11.923 \times \text{B} + 0.449 \times \text{C} - 4.114 \times \text{D} + 0.611 \times A^2 + 0.185 \times B^2 + 0.003 \times C^2 + 0.003 \times D^2 - 0.199 \times AB - 0.011 \times AC + 0.153 \times AD + 0.016 \times BC - 0.058 \times BD - 0.003 \times CD \quad (4)$$

$$CO_2 = 90.8147 - 5.0783 \times A + 0.4439 \times B + 0.1096 \times C - 0.5316 \times D + 0.0709 \times A^2 + 0.0087 \times B^2 + 0.0001 \times C^2 + 0.0007 \times D^2 + 0.0034 \times AB - 0.0038 \times AC + 0.0159 \times AD - 0.0001 \times BC - 0.0022 \times BD - 0.0003 \times CD \quad (5)$$

$$\text{NOx} = 5974.99 - 895.65 \times \text{A} + 159.16 \times \text{B} + 9.63 \times \text{C} + 34.87 \times \text{D} + 16.59 \times \text{A}^2 + 1.21 \times \text{B}^2 + 0.03 \times \text{C}^2 - 0.21 \times \text{D}^2 - 0.86 \times \text{AB} + 0.04 \times \text{AC} + 1.62 \times \text{AD} + 0.01 \times \text{BC} - 0.8 \times \text{BD} - 0.09 \times \text{CD} \quad (6)$$

Optimized parameters				Mode of Evaluation	BTE (%)	BSFC (Kg/Kwh)	CO (%)	HC (ppm)	CO2 (%)	NOx (ppm)
CR	Load (Kg)	Blend (%)	Pressure (bar)							
18.36	7.84	20	155	**Predicted**	35.91	0.232	0.222	9.726	3.086	399.063
				Actual	36.88	0.2402	0.2218	9.1	3.24	403.7
				% Error	**2.63**	**3.42**	**0.09**	**6.88**	**4.75**	**1.15**
19	6	40	145	**Predicted**	31.97723	0.3599343	0.2780429	11.856609	3.0774166	334.93654
				Actual	30.08846	0.3276298	0.225	10.2	3.18	341.2
				% Error	**6.27**	**9.86**	**5.3**	**16.24**	**3.23**	**1.84**
20	7	20	150	**Predicted**	33.38514	0.3194343	0.2485072	9.7287868	3.1854929	379.23906
				Actual	34.86253	0.32115	0.25712	9.231	3.6325	392.21
				% Error	**4.24**	**0.54**	**3.35**	**5.39**	**12.31**	**3.31**
21	8	20	150	**Predicted**	35.19128	0.241624	0.2543836	11.730157	3.3385837	396.13885
				Actual	37.95453	0.229423	0.235	10.2	3.556	412.36
				% Error	**7.28**	**5.32**	**8.25**	**15**	**6.13**	**3.93**
22	5	40	140	**Predicted**	27.39625	0.3725352	0.3643811	9.8148123	2.7955001	323.01315
				Actual	26.582	0.357254	0.32653	11.2	3.01	341.23
				% Error	**3.06**	**4.23**	**11.59**	**12.37**	**7.13**	**5.34**

Table: 6 Validation of experiments

Based on the empirical equations the results of the output responses for the different sets of parameters are obtained and verified with the experimental results. The variables are also optimized through the Miniab16 to determine two different categories objective functions of maximum BTE and least SFC on performance characteristics and, least of HC, least HC, CO, CO_2 and NO_xon emission characteristics. The table.5 shows optimized parameters for the required objective functions within the range of variables defined.

Published By:
Blue Eyes Intelligence Engineering
& Sciences Publication

Here the intention is to the emission responses and BSFC and to maximize the brake thermal efficiency.

The optimality test is conducted to arrive more than one optimized set of solutions from the empirical models. The composite desirability of 0.995867 is achieved at the optimized solution of CR 18.36, load 7.84 kg, blend 20% and injection pressure 155 bar. The respective parameters of optimal solution are used to find the influence of responses using the empirical models. The experiments also conducted at the optimized variables of CR 21, 8 kg load , B20 blend and with an injection pressure of 150 bar. The responses of the optimum factors are presented in table.6. The optimum predicted solution is compared with experimental results and the closer to be closer.

IV. RESULTS AND DISCUSSION

Brake thermal efficiency

Figure.2 shows the main interaction effect of mean vs input parameters like CR, load, blend and injection pressure of brake thermal efficiency. The fig.3 show the effect of compression ratio vs biodiesel blends. The main effect of mean vs compression reveals the same trend in the graph. The addition biodiesel after B40 leads to decreases the mean level to low. At CR 21 for the blend B20 at 8 kg load with an injection pressure of 150 bar gives maximum efficiency of 37.95453% and error is found to be 7.28% with the predicted range. This is due to addition of biodiesel content in fuel blends and lower calorific value of fuel. The load on the engine increase the mean from low to high due to its optimum utilization of the fuel blends. The change in injection pressure from low to high shows the trend of no change in efficiency compared to standard injection pressure of 150bar.

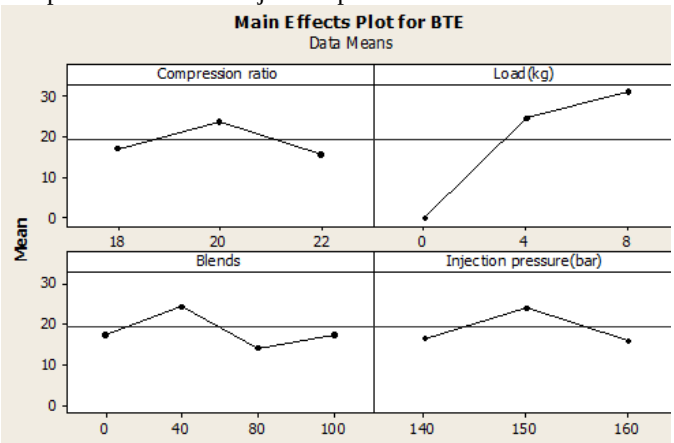

Fig.2 Main effects of input parameters with respect to mean values of BTE

Brake specific fuel consumption

Fig.4-5 shows the variation of main effect for different input factors and surface plot for brake specific fuel consumption. The results revealed that the increase in compression ratio increase the fuel consumption of all blends except B20. The optimal solution at CR 21 obtained for B20 at 150 bar is 02294kg/Kwh at 8kg less than other blends at all CR and pressure. The amount of biodiesel volume in the blend increases the fuel consumption owing to its lower heating value of the fuel. At the same time, the load and injection pressure increases, the fuel consumption decreases due to its better spray formation and atomization of the fuel. The optimized value of specific fuel consumption is 3.42% higher than the predicted value.

CO emission

The rise of CR, decrease the CO emission at CR 20 and reaches mean level at all CR shown in fig.6. Increase in biodiesel content slightly increase the CO emission and is high at B80 due to its poor spray formation of fuel. There is a high to low level of CO emission shows that at high compression ratio and high cylinder temperature reduces the CO for pure biodiesel. Change in injection pressure increase the CO emission and increase in load increase the CO emission because of its poor atomization of fuel. Surface plot shows that increase in compression ratio and biodiesel blends increase CO emission shown in fig.7. The error of the predicted solution at CR 21 is found to be 8.25% for the actual blend of 20 at 150bar and at full load.

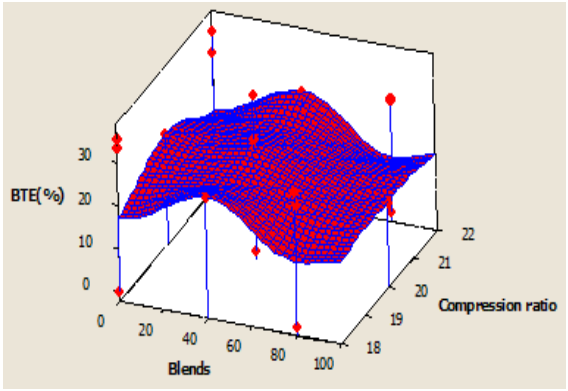

Fig.3. variation of fuel blends and compression ratio with respect to BTE

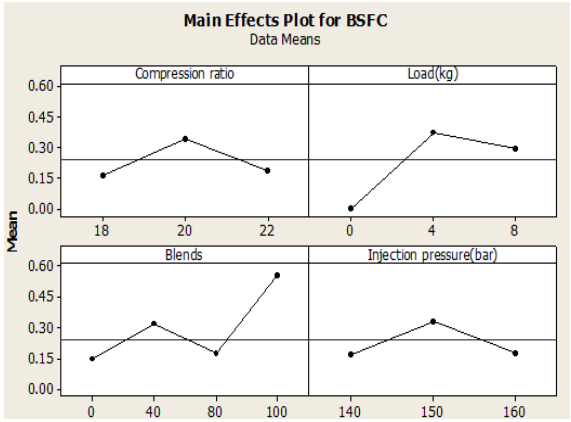

Fig.4 Main effects of input parameters with respect to mean BSFC

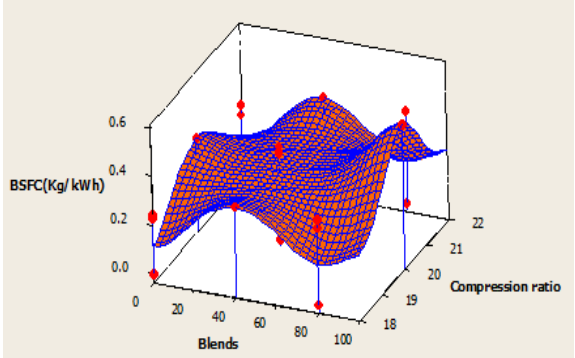

Fig.5 Variation of BSFC with respect to fuel blends and compression ratio

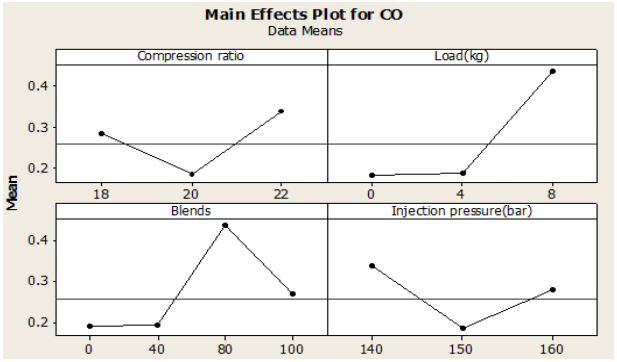

Fig.6 Variation of input parameters with respect to mean CO

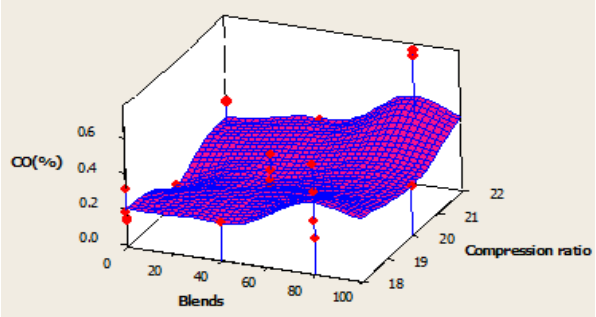

Fig.7 Variation of CO emission with respect to blend and compression ratio

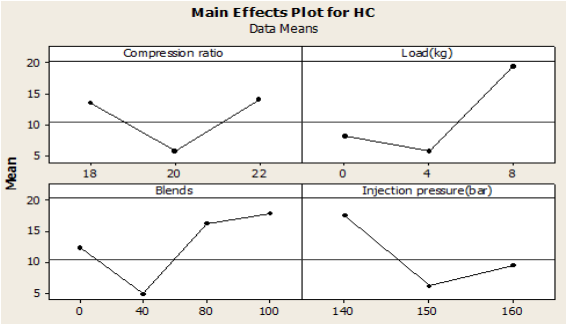

Fig.8 Variation of input parameters with respect to mean HC

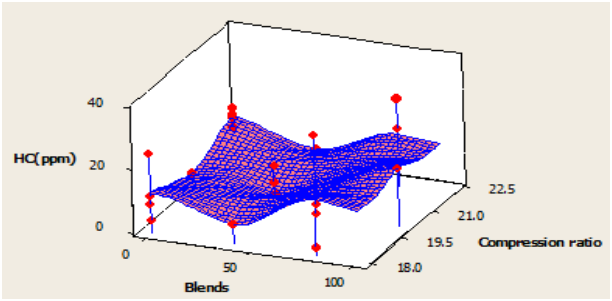

Fig.9. Variation of HC with respect to fuel blends and compression ratio

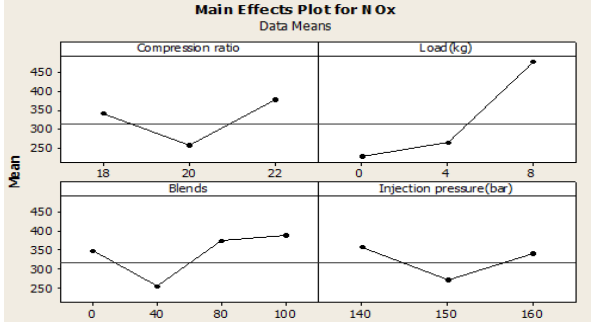

Fig.10. Variation of input parameters with respect to mean NO_x

HC emission

Main effect plot of mean vs input parameters and surface plot are shown in fig.8-9. When there is a rise in injection pressure decrease the HC for its better mixing of fuel. Increase in biodiesel blend increase the HC emission at high CR at full load due to its insufficient air available for combustion. When the compression ratio increase up to 20 gives better result in terms of emission shown in surface plot. HC emission at part load operation at 150bar for B40 is less than 2ppm. The predicted value of HC emission is 6.88% higher than actual value. HC emission depends upon cylinder temperature and compression ratio of the blend.

NOx emission

Fig 10-11 shows the mean plot of factors and surface plot for NOx. At CR 20, blend B20 and B40 gives reduction in

NOx emission at part and full load operations shown in surface plot. Increase in load and blends increase the NOx emission at CR 22.

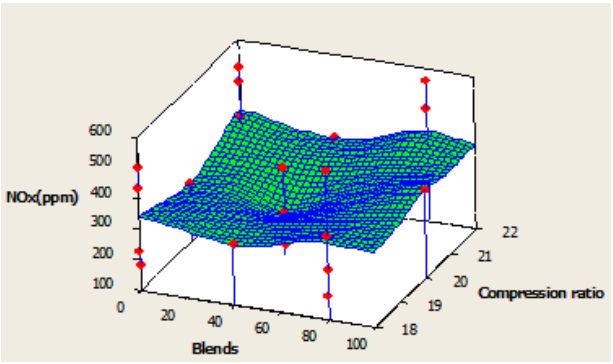

Fig.11. Variation of NO_x with respect to fuel blends and compression ratio

Effect of increase in injection pressure maintains the mean level. Ignition delay is shorter for biodiesel due to its high cetane index. In case of rubber seed oil, cetane index is 38, less than diesel and other biodiesels, increase the ignition delay as longer. But increase in compression ratio, injection pressure at part and full load operation increase the cylinder temperature which reduces the ignition delay and emission of NOx when compared diesel for blends B20 and B40 at all injection pressure for part and full load operation. Mean of biodiesel blends keeps the average in the graph proved the same.

V.CONCLUSION

The ROME biodiesel is prepared from RSO using the transesterification process and the blends are prepared with different ratio of diesel. The blends are tested for the physical and chemical properties as fuel. The ROME blends are tested for the performance and emission characteristics with different range of compression ratio, load, fuel blends and injection pressure as input variables. The results of BTE, BSFC as performance responses and CO,HC and NOx as emission responses are obtained for the blends. RSM design matrix is developed using the defined range input parameters and the results of their respective objective functions are obtained through experiments.

The regression equations are obtained for the objective functions through the coefficients. The model adequacy is tested through ANOVA table such that the R^2 and R^2_{adj} values are more than the 0.95. It is found that predicted coefficient are significantly fit with the model and the error is found to be less than 5%. The developed model produced 0.9921 of R^2 value with 0.9527 of predicted R^2. Adj R^2 gives good result over experimental value of 0.9846 with its numerical model. The regression is developed to fit the factors to validate the numerical model. Desirability optimal test also is conducted to obtain the optimum parameter for least SFC and emission parameters and Maximum BTE and are responses are validated through experimental results. The optimum parameters are found to be CR 21, 8 kg load, B20, and 150bar pressure and the optimized objective functions are

Among the input factors injection pressure plays less dominant over other factors. In the performance parameters, at CR 21 with 8 kg load at 150 bar, B20 gives a maximum efficiency of 37.94453% with a specific fuel consumption of 0.229423Kg/kWh. The CO and NOxemissions for the same condition is less than 10% of predicted value. Increase in compression ratio increases the thermal efficiency of B20 and B40. Subsequently, there is an efficiency reduction found because of its lower calorific value of fuel. The compression ratio rise lowers the specific fuel consumption of fuel blends and the optimum value is found is 0.2402 kg/kWh of B20 is 3.42% higher than predicted value. CO emission is less for all compression ratio and increase in biodiesel content increase the CO emission at all CR shown in surface plot. HC emission of optimum blend is 6.88% higher than predicted value due to its low in cylinder temperature. Increase in fuel blend increases the NOx emission at compression ratio but at optimum value, the error is found to be less than 2%.

The RSO is comparatively cheaper as it is not being used for any other commercial purpose. The RSO is processed to produce ROME biodiesel and will be effectively used in the IC engines with B20 proportion. The RSM developed a hypothesis for the use of ROME in the experimental setup chosen. This hypothesis will be extended for the other engines to design and run the diesel engines with ROME at emission less and low cost.

Acknowledgement:

The authors would like to thank the All India Council for Technical Education (AICTE), Govt.of India in granting MODROBS scheme (No: 8024/RID/MOD/70/08/09) and to the management of PSNACET for purchasing VCR engine test rig.

REFERENCES

1. Wilson, V. H. (2012). Optimization of diesel engine parameters using Taguchi method and design of evolution. *Journal of the Brazilian Society of Mechanical Sciences and Engineering*, *34*(4), 423-428.
2. Muralidharan, K., &Vasudevan, D. (2015). Applications of artificial neural networks in prediction of performance, emission and combustion characteristics of variable compression ratio engine fuelled with waste cooking oil biodiesel. *Journal of the Brazilian Society of Mechanical Sciences and Engineering*, *37*(3), 915-928.
3. Wong, P. K., Wong, K. I., Vong, C. M., & Cheung, C. S. (2015). Modeling and optimization of biodiesel engine performance using kernel-based extreme learning machine and cuckoo search. *Renewable Energy*, *74*, 640-647.
4. Hassan, N. M. S., Rasul, M. G., &Harch, C. A. (2015). Modelling and experimental investigation of engine performance and emissions fuelled with biodiesel produced from Australian Beauty Leaf Tree. *Fuel*, *150*, 625-635.
5. Lešnik, L., Iljaž, J., Hribernik, A., &Kegl, B. (2014). Numerical and experimental study of combustion, performance and emission characteristics of a heavy-duty DI diesel engine running on diesel, biodiesel and their blends. *Energy Conversion and Management*, *81*, 534-546.
6. Khalilarya, S., &Nemati, A. (2014). A numerical investigation on the influence of EGR in a supercharged SI engine fueled with gasoline and alternative fuels. *Energy Conversion and Management*, *83*, 260-269.
7. Kumar, B. R., Muthukkumar, T., Krishnamoorthy, V., &Saravanan, S. (2016). A comparative evaluation and optimization of performance and emission characteristics of a DI diesel engine fueled with n-propanol/diesel, n-butanol/diesel and n-pentanol/diesel blends using response surface methodology. *RSC Advances*, *6*(66), 61869-61890.
8. Yusri, I. M., Mamat, R., Azmi, W. H., Omar, A. I., Obed, M. A., &Shaiful, A. I. M. (2017). Application of response surface methodology in optimization of performance and exhaust emissions of secondary butyl alcohol-gasoline blends in SI engine. *Energy Conversion and Management*, *133*, 178-195.
9. An, H., Yang, W. M., & Li, J. (2015). Numerical modeling on a diesel engine fueled by biodiesel–methanol blends. *Energy Conversion and Management*, *93*, 100-108.
10. Shirneshan, A. R., Almassi, M., Ghobadian, B., &Najafi, G. H. (2014). Investigating the effects of biodiesel from waste cooking oil and engine operating conditions on the diesel engine performance by response surface methodology. *Iranian Journal of Science and Technology. Transactions of Mechanical Engineering*, *38*(M2), 289.
11. Berber, A. (2016). Mathematical Model for Fuel Flow Performance of Diesel Engine. *International Journal of Automotive Engineering and Technologies*, *5*(1), 17-24.
12. Choudhary, A., Chelladurai, H., &Kannan, C. (2015). Optimization of Combustion Performance of Bioethanol (Water Hyacinth) Diesel Blends on Diesel Engine Using Response Surface Methodology. *Arabian Journal for Science & Engineering (Springer Science & Business Media BV)*, *40*(12).

Published By:
Blue Eyes Intelligence Engineering
& Sciences Publication

Journal of the Australian Ceramic Society (2018) 54:467–473
https://doi.org/10.1007/s41779-018-0173-8

RESEARCH

Effect of Mg doping on physical properties of Zn ferrite nanoparticles

Siva Kumar Pendyala[1,2] · K. Thyagarajan[3] · A. GuruSampath Kumar[4] · L. Obulapathi[5]

Received: 18 April 2017 / Revised: 12 December 2017 / Accepted: 11 January 2018 / Published online: 19 March 2018

Abstract
Effect of Mg doping on $ZnFe_2O_4$ samples was prepared by a sol-gel auto-combustion method. The obtained samples were sintered at different temperatures. Then, the sintered samples were characterized by powder X-ray diffraction, scanning electron microscopy, energy dispersive X-ray analysis, and electrical properties. XRD results confirm the formation of cubic spinel-type structure with an average crystallite size decreased with Mg concentration from 37 to 17 nm. Lattice parameter decreases with increasing Mg concentration, due to the small ionic radius of the Mg^{2+} ion. The SEM images show the morphology of the samples as spherical shaped particles in agglomeration. The magnetization showed an increasing trend with increasing Mg concentration due to the rearrangement of cations at tetrahedral and octahedral sites. The ionic conductivity is increased with the increase of Mg concentration.

Keywords Zn ferrite · Sol-gel auto-combustion method · Crystallite size · Dielectric behavior and ionic conductivity

Introduction

In recent years, researchers have been concentrating on improving the conductivity of nanocrystalline spinel ferrites by doping divalent metal cations. These nanocrystalline spinel ferrites are important materials due to having variety of properties like electrical and magnetic properties which are most useful in various applications such as microwave, gas sensors, and biomedical [1–4]. The $ZnFe_2O_4$ nanocrystalline spinel ferrites have been extensively studied by researchers worldwide, because of physical and chemical properties depending on their unique as compared to the bulk counterpart materials [5–7]. These ferrites are chemically and thermally stable and are suitable for a wide range of applications like magnetic materials, MRI (magnetic resonance imaging), drug delivery, and photocatalysts [8, 9]. Recently, Mg and Zn-based ferrites have attracted much attention due to its high electrical resistivity with good magnetic properties for transformers, ferrofluids, and magnetic cores. Mg-doped Zn ferrites have also been reported to be highly suitable for memory and switching circuits in digital computers and phase shifters [10]. These ferrites have been synthesized for their utilization in several microwave devices operating at L, S, and C bands [11]. Many researchers have been studied the potential applications of Mg-doped Zn ferrites in multilayer chip inductors, microwave, and hyperthermia [12–14].

In the present work, we have selected divalent Mg^{2+} as dopant because of its effective ionic radii. Furthermore, magnesium has low cost and high stability. The magnesium zinc ferrite compound is a soft ferrite [15]. Due to its useful properties in dielectric and magnetic applications, it is used in several applications like high-frequency range applications, as low hysteresis loss material, and high-density media storage, as recoding and sensor device [16, 17]. The divalent ions of magnesium and zinc are diamagnetic in nature. The distribution of these ions in the lattice sites may affect the properties of ferrites very much [18].

The synthesis of magnesium zinc ferrite has been reported by various chemical and solid state reaction methods. In this work, the dopant Mg in $ZnFe_2O_4$ system is varied from 0.2 to 0.6 M% ($Mg_xZn_{1-x}Fe_2O_4$ (0.2, 0.4 and 0.6 M% of MgO)) and

✉ Siva Kumar Pendyala
sampathkumar.physics@gmail.com;
sivakumarpendyala2015@gmail.com

1 Research Scholar, JNTUA, Anantapuramu, A.P. 515002, India
2 Department of Physics, Malla Reddy Engineering College (A), Secunderabad, T.S. 500100, India
3 Department of Physics, JNTUA College of Engineering, Pulivendula, A.P. 516390, India
4 College of Physics and Energy, Shenzhen University, Shenzhen 518060, People's Republic of China
5 Department of Physics, Annamacharya Institute of Tech. & Sci, Rajampet, A.P. 516126, India

is prepared by auto-combustion method. The structural parameters such as crystallite size, lattice parameters, grain size, and electrical properties were analyzed, and the influence of Mg on the same was explained.

Experimental details

Commercially available metal nitrates of magnesium nitrate ($Mg(NO_3)_2.6H_2O$), zinc nitrate ($Zn(NO_3)_2.6H_2O$) and ferric nitrate ($Fe(NO_3)_2.9H_2O$) (all are AR grade Sigma Aldrich, USA, 99.9% purity), citric acid were used as starting materials and ammonia is used as fuel material for this reaction. All these chemicals were mixed in an appropriate stoichiometric proportion by using the formulae $Mg_xZn_{1-x}Fe_2O_4$ (0.2, 0.4, and 0.6 M% of MgO). Auto-combustion method was used for the preparation of Mg-Zn ferrite. All the solutions were stirred well to get the homogeneous solutions. After mixing, the ratio of metal nitrates to citric acid was 1:3. These solutions were stirred continuously on 90 °C for 1 h by adding ammonia dropwise, so that the solution maintains pH value of 7. The resulting solution was evaporated by heating at about 150 °C on a hot plate with continuous stirring. The viscosity rose as a result of cross-linking of carboxylato-metal complexes into a three-dimensional structure and started to form a viscous gel. When finally all water molecules were removed from the mixture by increasing the temperature to 200 °C, the gel began frothing. The gel gave a fast flameless auto-combustion reaction with the evolution of large amounts of gases. It started in the hottest zones of the beaker and propagated from the bottom to the top like the eruption of a volcano. The reaction was completed in a minute giving rise to dark gray voluminous product with a structure similar to a branched tree. Finally, the burnt powder was ground and calcined in air at temperature of 500–1000 °C for 4 h to decompose of MgO and reground to obtain the spinel phase. A 2 mol% of polyvinylpyridine was added to the powder as binder and mixed thoroughly. The powder sample was uniaxially pressed by a pressure of 10 tons/in.^{2} to get disc-shaped pellets, and these pellets were sintered at 1400 °C for 2 h on air at slope of 2 C/min and cooled at room temperature of the same slope. Different characterizations were conducted for the prepared samples like XRD, SEM, EDAX, and electrical properties.

Results and discussion

XRD analysis

Figure 1 shows XRD patterns of Mg^{2+} (0.2, 0.4, and 0.6 M%) doped $ZnFe_2O_4$. These patterns confirm that compositions show the formation of cubic spinel-type structure (JCPDS card no. 22-1012) with an average crystallite size in the range of 15–50 nm [19]. All the samples show the presence of (111), (220), (311), (400), (422), (511), (440), and (533) diffraction peaks in the scanning range 20° to 80°. No other phases are detected in the Mg-doped $ZnFe_2O_4$ samples, which indicate that all the samples exhibit the single-phase cubic spinal structure. The average crystallite size of the samples is calculated from the diffraction peaks at (311), (440), and (511) planes in the XRD profile, in accordance with Debye–Scherrer formula [20]:

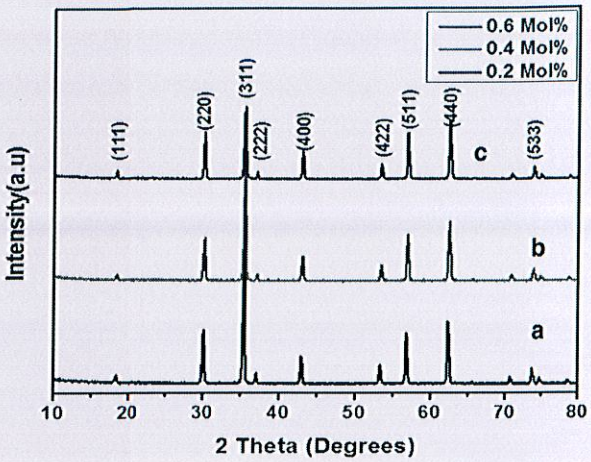

Fig. 1 XRD patterns of (a) 0.2, (b) 0.4, and (c) 0.6 M % Mg-doped $ZnFe_2O_4$ pellets sintered at 1400 °C for 2 h

$$D = \frac{0.94\lambda}{\beta\cos\theta} \quad (1)$$

where D is the average particle, λ is the X-ray wavelength (0.1542 nm), β is the full width at half maximum (FWHM), and θ is the Bragg's angle of the planes. The structural parameters are calculated and tabulated in Table 1.

The variation of the lattice constant depending on the composition is observed in the Fig. 2. Lattice parameter "a" is decreased with increasing Mg content because of the small ionic radius of Mg^{2+} ion [21]. The small sized Mg might occupy interstitial sites, which thereby produces strain within the $ZnFe_2O_4$ [7]. It is observed that peaks shift to higher 2θ value after the addition of Mg. The lattice parameter decreases with increasing Mg content from 8.449 to 8.443 Å, thus obeying Vegard's law. According to Shannon's compilation, the size of the Mg^{2+} (0.79 Å) is smaller than that of the Zn^{2+} ion (0.83 Å) in the unit cell [22]. This contracts the lattice, and hence

Table 1 The structural parameters of Mg-doped $ZnFe_2O_4$ nanoparticles

Composition	2θ (°)	Crystalline size (nm)	Lattice constant (Å)	Grain size (μm)	Structure
0.2 M% Mg	35.19	36.54	8.449	1.63	Cubic
0.4 M% Mg	35.39	27.14	8.447	1.51	Cubic
0.6 M% Mg	35.79	17.78	8.444	1.45	Cubic

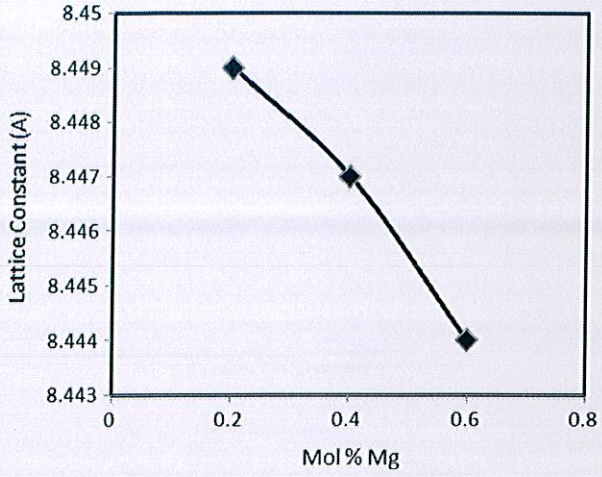

Fig. 2 Variation of lattice constant with mol% of Mg

lattice parameter and volume of the unit cell decrease. The linear decrease in the lattice spacing thus indicates that the Mg ions are replacing the Zn ions in Zn ferrite matrix also indicating that Mg has entered into Zn^{2+} ion sites forming the lattice of spinel ferrite in $Mg_xZn_{1-x}Fe_2O_4$. The diffraction peaks of each Mg-doped samples are sharper and narrower with increasing Mg content indicating that Mg promoted the crystalline growth [23]. Another reason for the observed variation of the lattice parameter is the Jahn–Teller distortion which takes place for Zn^{2+} ions. With increasing Mg^{2+} ion concentration, the Jahn–Teller distortion decreases and the cubic symmetry is increased. Jahn–Teller distortion in the sample may be a compression distortion in the octahedral B site, with increasing Mg^{2+}, the octahedral site returns to its symmetry in the cubic form as confirmed from X-ray [24].

Therefore, the lattice parameters contract when the Mg ion substitutes the Zn ion in the lattice, and the contraction of lattice parameters is a function of Mg content. This is in good agreement with the reduction of the lattice volume. For this reason, it can be concluded that the $Mg_xZn_{1-x}Fe_2O_4$ can form

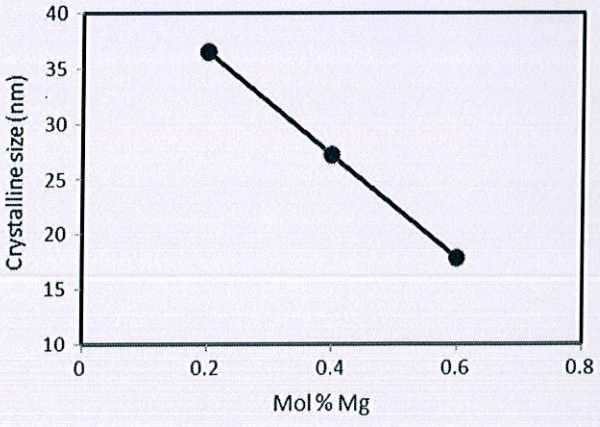

Fig. 3 Variation of crystalline size with mol% of Mg

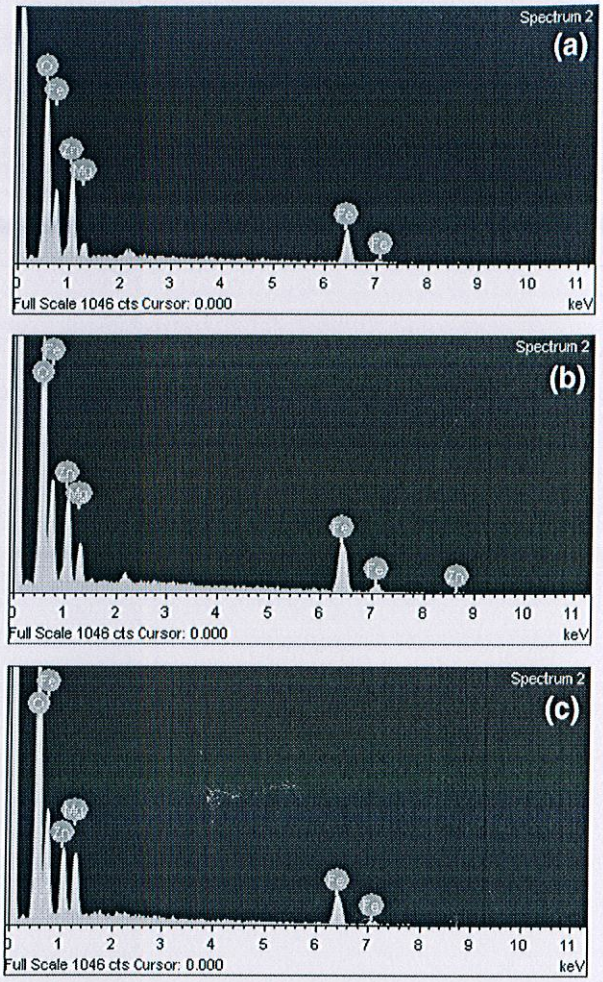

Fig. 4 EDAX spectra of **a** 0.2, **b** 0.4, and **c** 0.6 M% Mg-doped $ZnFe_2O_4$ pellets sintered at 1400 °C for 2 h

in the whole range of Mg content used. The crystallite size decreases with the increase of Mg content. This may be due to the coarsening of the crystal and the growth occurred through the Ostwald ripening mechanism [7, 25]. From the Fig. 3, it is clearly observed that the crystalline size decreases linearly from 36 to 17 nm with an increasing concentration of Mg which indicates that Mg promoted the crystalline growth. The EDAX spectrum shown in Fig. 4 presents the distribution of elements in the composition, and it identifies the presence of Zn, Fe, O, and Mg in all the compositions and placed in Tables 2 and 3.

Table 2 The EDAX analysis of Mg-doped Zn ferrites nanoparticles

Composition	Zn	Fe	O	Mg
0.2 M% Mg	11.67	29.84	55.11	3.38
0.4 M% Mg	8.10	31.07	55.83	4.99
0.6 M% Mg	6.08	29.58	57.13	7.21

Table 3 Elemental analysis of the Mg-doped Zn ferrite sby EDAX

Composition/element	$X=0.2$		$X=0.4$		$X=0.6$	
	Weight (%)	Atomic (%)	Weight (%)	Atomic (%)	Weight (%)	Atomic (%)
O (K)	25.98	55.11	27.24	55.83	29.12	57.13
Mg (K)	2.42	3.38	3.70	4.99	5.59	7.21
Fe (L)	49.12	29.84	52.91	31.07	52.64	29.58
Zn (L)	22.48	11.67	16.15	8.10	12.65	6.08
Total	100.00	100.00	100.00	100.00	100.00	100.00

Surface morphological studies

Figure 5a–c shows the surface morphologies of the sintered pellets of $Mg_xZn_{1-x}Fe_2O_4$ ($x=0.2$, 0.4, and 0.6); nanoparticles were investigated by the scanning electron microscopy (SEM). The SEM images of $Mg_xZn_{1-x}Fe_2O_4$ samples (Fig. 5a–c) reveal that the entire samples exhibit a compact arrangement of homogeneous nanoparticles with spherical shape and agglomerated with diameter ranging from 30 to 18 nm for Mg-doped Zn ferrite samples. The total surface free energy is reduced with the increase of Mg content. Nanoparticles are agglomerated due to the presence of magnetic interactions among the particles [26–28]. No significant change in morphology is observed with the increase of Mg. Thus, sintering has led to a reduction in grain boundary energy resulting in dense structure.

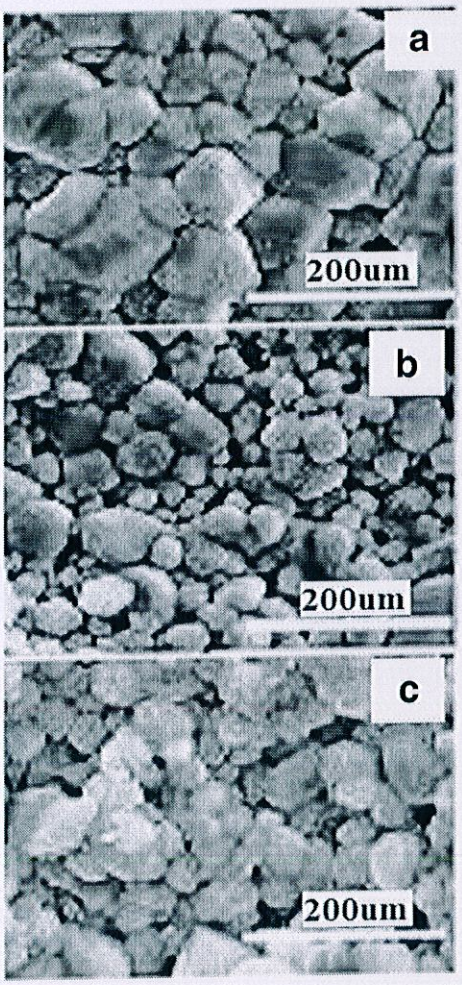

Fig. 5 SEM images of **a** 0.2, **b** 0.4, and **c** 0.6 M% Mg-doped $ZnFe_2O_4$ pellets sintered at 1400 °C for 2 h

The average grain size is measured by using linear intercept method and tabulated in Table 1. The variation of grain size is shown in Fig. 6. From that, we observed that the grain size decreases with the increase of Mg content. This is due to the presence of increased number of pores and also because of smaller grain size, which leads to increased volume fraction of grain boundary. Both the pores and grain boundaries inhibit domain wall movement. However, the decrease in grain size with the increase of Mg content indicates that Mg suppresses the grain growth [29, 30]. Auto-combustion Mg-doped Zn ferrite powders are uniform in both morphology and particle size but are agglomerated to some extent due to interactions between magnetic nanoparticles.

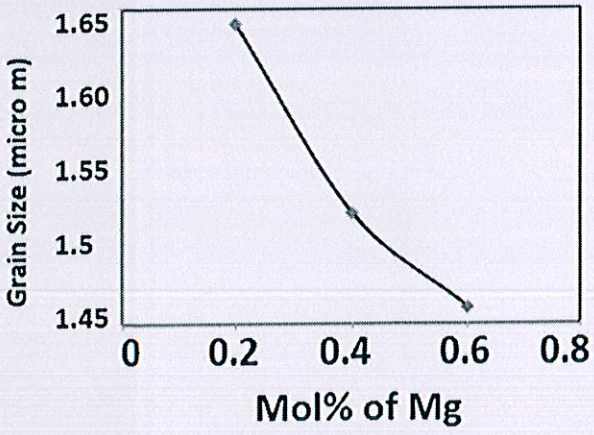

Fig. 6 Variation of grain size with mol% of Mg

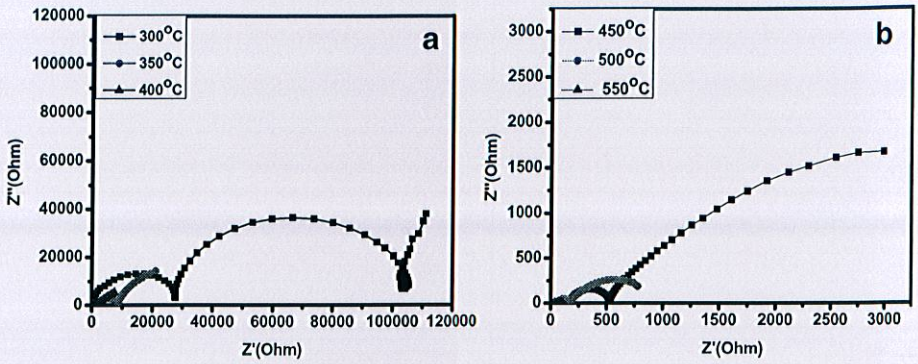

Fig. 7 Impedance spectra of 0.2 M % Mg-doped $ZnFe_2O_4$ nanoparticles at temperatures **a** 300–400 °C and **b** 450–550 °C

Electrical properties

In general, the total conductivity (σ_t) of Mg-doped $ZnFe_2O_4$ nanoparticles is the sum of ionic conductivity (σ_i) and electronic conductivity (σ_e). The contributions by grain, grain boundary, and electrode to the overall ionic conductivity can be estimated by recording ac impedance spectrum. The impedance spectra of sintered samples are recorded at different temperatures and are shown in Figs. 7, 8, and 9. From all these complex plane plots, we observed that two well-separated arcs and portions of a third arc were observed at the lower frequencies for all samples. From this, it is clearly observed that resistivity values decrease by increasing the temperature. The semicircle corresponding to the bulk conductivity is lost from the spectrum above 350 °C. This is caused by the effect of inductances generated within the experimental apparatus on the spectra.

Figure 10 shows comparison of spectra recorded at 450 °C. The spectra show arc at high frequency corresponding to grain interior resistance (R_g). Semicircle at intermediate frequency represents grain boundary resistance (R_{gb}), and tail at low frequency represents electrode contributions and grain resistance. Grain boundary resistance and electrode resistance (R_e) can be estimated from their intercepts on real axis. It has been observed that both R_g and R_{gb} decrease with Mg addition up to 400 °C. Above 400 °C, no drastic change in R_g is observed while R_{gb} still decreases with Mg addition. If Mg is present as the secondary phase within grain, R_g would increase since MgO is insulating. This ultimately indicates formation of Mg-doped $ZnFe_2O_4$ solid solution.

When Mg content increases with a temperature rise, time constants of both grain and grain boundary processes reduce and corresponding resistances decrease. Hence, the conductivity rises with the temperature. The conductivity is then calculated from resistance, thickness l, and cross-section area A, by using the formula [31], $\sigma = l/RA$. The variation of the conductivity at different concentrations of Mg is shown in the Fig. 11. It is observed that conductivity increases with the increase of MgO content. This may be due to the hopping of charge carriers which leads to the increase in the carrier mobility [32]. This trend can be explained with the following Kröger notation equations [30]:

$$Mg^{2+} + Zn^{2+} \rightarrow Mg(Zn^{2+}) \quad (2)$$

$$2Mg^{2+} + Fe^{3+} \rightarrow 2Mg(Fe^{3+}) + C.V \quad (3)$$

$$Mg^{2+} + Fe^{3+} \rightarrow Mg_{\Delta} + Fe^{2+} + 1/2O_2 \quad (4)$$

$$Mg^{2+} + 2Zn^{2+} \rightarrow Mg_{\Delta} + 2Zn^{+} \quad (5)$$

$Mg(Zn^{2+})$ and $Mg(Fe^{3+})$ are the divalent ions located in the positions of host zinc and iron oxides in ZnO and Fe_2O_3,

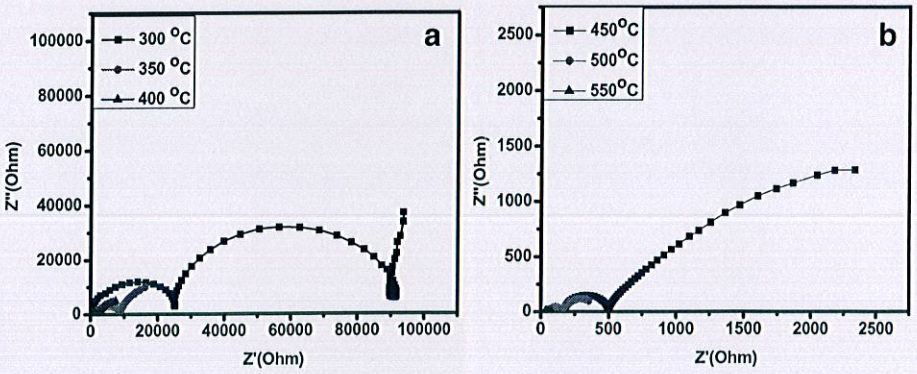

Fig. 8 Impedance spectra of 0.4 M % Mg-doped $ZnFe_2O_4$ nanoparticles at temperatures **a** 300–400 °C and **b** 450–550 °C

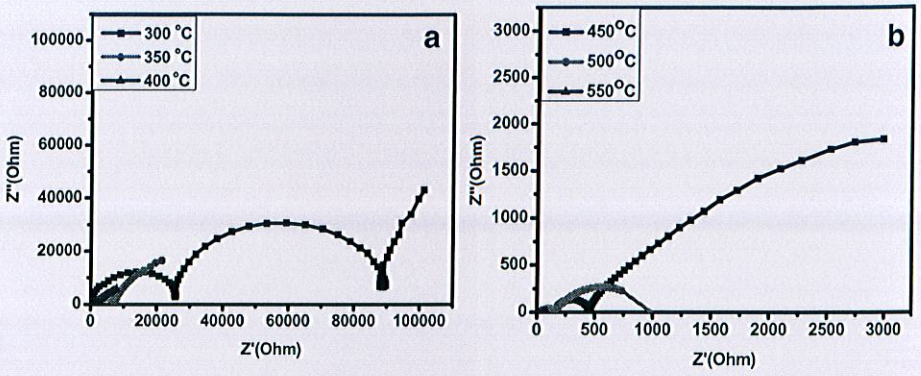

Fig. 9 Impedance spectra of 0.6 M % Mg-doped $ZnFe_2O_4$ nanoparticles at temperatures **a** 300–400 °C and **b** 450–550 °C

respectively [28]; Mg_{Δ} is magnesium ions located in the interstitial positions of zinc and ferric oxide lattices; created cationic (oxygen) vacancies (C.V.). The dissolution of dopant ions in the lattices of reacting oxides according to reaction (2) which led to creation of cationic (oxygen) vacancies might increase the mobility of cations of reacting oxides thus enhancing the ferrite formation. Incorporation of magnesium ions in Fe_2O_3 and ZnO lattices according to reactions (3) and (4) decreased the number of reacting cations (Zn^{2+} and Fe^{3+}) involved in the ferrite formation. So, reaction (2) might be expected to stimulate zinc ferrite formation, while reactions (3) and (4) might exert an opposite effect.

The fact is that MgO doping of Zn/Fe oxides system enhanced zinc ferrite formation suggesting the domination of reaction (2). With the addition of MgO into Zn/Fe oxides system would lead to the formation of oxygen vacancy due to the charge compensation. Mainly electrolyte materials, the vacancy will attract the doping ions to be produced due to complex forces. At lower dopant content, most of these cationic (oxygen) vacancies are probably mobile, which could explain gradual increase of conductivity.

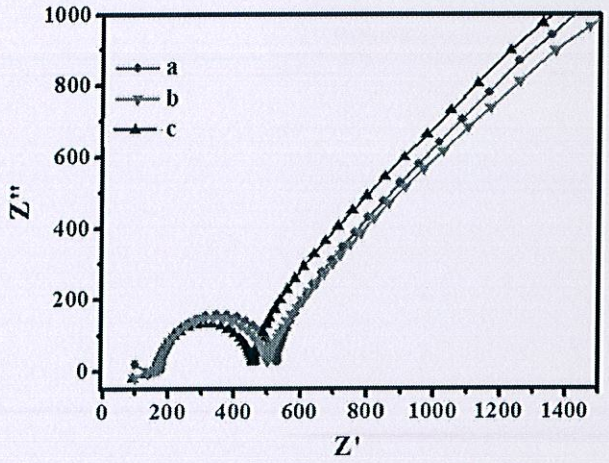

Fig. 10 Nyquist plots of (a) 0.2, (b) 0.4, and (c) 0.6 M % Mg-doped $ZnFe_2O_4$ nanoparticles recorded at 450 °C

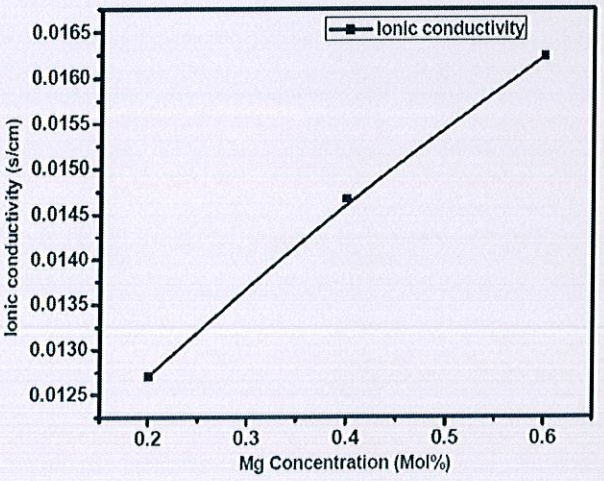

Fig. 11 Variation of ionic conductivity with mol% of Mg

Conclusions

The Mg-doped Zn ferrite nanoparticles are successfully synthesized by auto-combustion method. The XRD study confirms the Mg-doped Zn ferrite nanoparticle has cubic spinel structure. The lattice parameter as well as the crystallite size (from 35.54 to 17.78 nm) decreases with increasing Mg content. No significant change is observed with Mg addition in the morphology of the samples; the grain size decreases from 1.63 to 1.45 μm with the addition of Mg concentration from 0.2 to 0.6 mol%. The ionic conductivity of the Mg-doped Zn ferrite nanoparticles increased with the increase of Mg concentration from 0.012 to 0.0165 s/cm.

References

1. Gimenes, R., Baldissera, M.R., Silva, M.R.A., Silveira, C.A., Soares, D.A.W., Perazolli, L.A., Silva, M.R., Zaghete, M.A.: Structural and magnetic characterization of $Mn_xZn_{1-x}Fe_2O_4$ (x=0.2, 0.35, 0.65, 0.8, 1.0) ferrites obtained by the citrate precursor method. Ceram. Int. **38**, 741–746 (2012)

2. Sharifi, I., Shokrollahi, H., Amiri, S.: Ferrite-based magnetic nanofluids used in hyperthermia applications. J. Magn. Magn. Mater. **324**, 903–915 (2012)
3. Gupta, N., Verma, A., Kashyap, S.C., Dube, D.C.: Microstructural, dielectric and magnetic behavior of spin-deposited nanocrystalline nickel–zinc ferrite thin films for microwave applications. J. Magn. Magn. Mater. **308**, 137–142 (2007)
4. Hajarpour, S., Gheisari, K., Raouf, A.H.: Characterization of nanocrystalline $Mg_{0.6}Zn_{0.4}Fe_2O_4$ soft ferrites synthesized by glycine–nitrate combustion process. J. Magn. Magn. Mater. **329**, 165–169 (2013)
5. Azam, A., Jawad, A., Ahmed, A.S., Chaman, M., Naqvi, A.H.: Structural, optical and transport properties of Al^{3+} doped $BiFeO_3$ nano-powder synthesized by solution combustion method. J. Alloys Compd. **509**, 2909–2913 (2011)
6. Jawad, A., Ahmed, A.S., Ashraf, S.S.Z., Chaman, M., Azam, A.: Exploring the dielectric behaviour of nano-structured Al^{3+} doped $BiFeO_3$ ceramics synthesized by auto ignition process. J. Alloys Compd. **530**, 63–70 (2012)
7. Rahman, S., Nadeem, K., Rehman, M.A., Mumtaz, M., Naeem, S., Papst, I.L.: Structural and magnetic properties of ZnMg-ferrite nanoparticles prepared using the co-precipitation method. Ceram. Int. **39**, 5235–5239 (2013)
8. Sivakumar, M., Takami, T., Ikuta, H., Towata, A., Yasui, K., Tuziuti, T., Kozuka, T., Bhattacharya, D., Iida, Y.: Fabrication of zinc ferrite nanocrystals by sonochemical emulsification and evaporation:observation of magnetization and its relaxation at low temperature. J. Phys. Chem. B. **110**, 15234–15243 (2006)
9. Yang, J.M., Yen, F.S.: Evolution of intermediate phases in the synthesis of zinc ferrite nanopowders prepared by the tartrate precursor method. J Alloys Compd. **450**, 387–394 (2008)
10. Mahavir Singh, J.: A comparative study of the electrical and the magnetic properties and Mössbauer studies of normal and hot pressed $Mg_xMn_{1-x}Fe_2O_4$ ferrites. Magn. Magn. Mater. **299**, 397–403 (2006)
11. Singh, M., Sud, S.P.: Mg–Mn–Al ferrites for high frequency applications. Mod. Phys. Lett. B. **14**, 531–537 (2000)
12. Manjurul Haque, M., Huq, M., Hakim, M.A.: Densification, magnetic and dielectric behaviour of Cu-substituted Mg–Zn ferrites. Mater. Chem. Phys. **112**, 580–586 (2008)
13. Jordan, A., Wust, P., Scholz, R.: Scientific and clinical applications of magnetic carriers, pp. 569–595. Plenum Press, New York (1997)
14. Robert, R., Greenberg, P.B., Elisabete, A., De Fernandes, N.: Neutron activation analysis: a primary method of measurement. Spectrochim. Acta Part B. **66**, 193–241 (2011)
15. Skołyszewska, B., Tokarz, W., Przybylski, K., Kakol, Z.: Preparation and magnetic properties of Mg Zn and MnZn ferrites. Physica C. **387**, 290–294 (2003)
16. Rezlescu, E., Sachelarie, L., Rezlescu, N.: Influence of copper ions on the structure and electromagnetic properties of Mg-Zn ferrite. J. Optoelectron. Adv. Mater. **8**, 1019–1022 (2006)
17. Nadeem, K., Rahman, S., Mumtaz, M.: Effect of annealing on properties of Mg doped Zn-ferrite nanoparticles. Prog. Nat. Sci: Mater. Int. **25**, 111–116 (2015)
18. Rafiq, M.A., Khan, M.A., Asghar, M., Ilyas, S.Z., Shakir, I., Shahid, M., Warsi, M.F.: Influence of Co^{2+} on structural and electromagnetic properties of Mg–Zn nanocrystals synthesized via co-precipitation route. Ceram. Int. **41**, 10501–10505 (2015)
19. Manikandan, A., Vijaya, J.J., Sundararajan, M., Meganathan, C., Kennedy, L.J., Bououdina, M.: Optical and magnetic properties of Mg-doped $ZnFe_2O_4$ nanoparticles prepared by rapid microwave combustion method. Super Lattices Microstruct. **64**, 118–131 (2013)
20. Kumar, A.G.S., Sarmash, T.S., Obulapathi, L., Rani, D.J., Rao, T.S., Asokan, K.: Structural, optical and electrical properties of heavy ion irradiated CdZnO thin films. Thin. Solid Films. **605**, 102–107 (2016)
21. Manikandan, A., Vijaya, J.J., Kennedy, L.J., Bououdina, M.: Structural, optical and magnetic properties of $Zn_{1-x}Cu_xFe_2O_4$ nanoparticles prepared by microwave combustion method. J. Mol. Struct. **1035**, 332–340 (2013)
22. Salah, L.M., Moustafa, A.M., Farag, I.S.A.: Structural characteristics and electrical properties of copper doped manganese ferrite. Ceram. Int. **38**, 5605–5611 (2012)
23. Prabu, J.H., Johnson, I.: Greener cum chemical synthesis and characterization of Mg doped ZnS nanoparticles and their engineering band gap performance. Int. J. Engeg. Res. Appl. **5**, 99–105 (2015)
24. Ateia, E., Ahmed, M.A., Ghouniem, R.M.: Electrical properties and initial permeability of CueMg ferrites. Solid State Sci. **31**, 99–106 (2014)
25. Li, S., Wu, Z., Li, W., Liu, Y., Zhuo, R., Yan, D., Jun, W., Yan, P.: One-pot synthesis of ZnS hollow spheres via a low temperature, template-free hydrothermal route. Cryst. Eng. Comm. **15**, 1571–1577 (2013)
26. Luo, F., Yan, C.H.: Anti-phase boundaries pinned abnormal positive magnetoresistance in Mg doped nanocrystalline zinc spinel ferrite. Chem. Phys. Lett. **452**, 296–300 (2008)
27. Alarifi, A., Deraz, N.M., Shaban, S.: Structural, morphological and magnetic properties of $NiFe_2O_4$ nano-particles. J. Alloy Compd. **486**, 501–506 (2009)
28. Deraz, N.M., Alarifi, A.: Fabrication and characterization of pure and doped Zn/Fe nanocomposites. Int. J. Electrochem. Sci. **7**, 3809–3816 (2012)
29. Berchmans, L.J., Selvan, R.K., Kumar, P.N.S., Augustin, C.O.: Structural and electrical properties of $Ni_{1-x}Mg_xFe_2O_4$ synthesized by citrate gel process. J. Magn. Magn. Mater. **279**, 103–110 (2004)
30. Kröger, F.A.: Chemistry of imperfect crystals. North-Holland, Amsterdam (1964)
31. Rani, D.J., Kumar, A.G.S., Rao, T.S.: Substrate temperature-dependent physical properties of nanocrystalline zirconium titanate thin films. J. Coat. Technol. Res. **14**(5), 971–980 (2017)
32. Ponpandian, N., Balaya, P., Narayanasamy, A.: Electrical conductivity and dielectric behaviour of nanocrystalline $NiFe_2O_4$ spinel. J. Phys. Condens. Matter. **14**, 3221–3237 (2002)

Available online at www.sciencedirect.com

ScienceDirect

Materials Today: Proceedings 5 (2018) 26799–26803

materialstoday: PROCEEDINGS

www.materialstoday.com/proceedings

ICAMM-2016

Impact characterization of epoxy LY556/ricinus communis L plant natural fiber composite materials

Rajesh Egala [a], Srinivasu Gangi Setti [b*]

[a]*Assistant Professor, Mechanical Engineering, Malla Reddy Engineering College, Secunderabad-500100, India,*
[b] *Assistant Professor, Mechanical Engineering, National Institute of Technology, Raipur-492010, India,*

Abstract

The Climate change is the main issue for world for living all creatures, because of climate change global warming will happen. The reasons behind global warming are like carbon, carbon dioxide products, and non - environmental products etc. Global warming may stop by promoting non-carbon products like natural products, solar energy; wind energy etc. Natural fibers composites are useful to replace the carbon, synthetic products. From last few decades many researchers had done research on natural fiber composites. In the present investigation composite of Epoxy/ castor oil plant cortex fiber (Ricinus Communis L) were prepared by hand layup technique. Composites with 0.10, 0.20, 0.30, 0.40 volume fractions of charpy impact specimens were prepared as per ASTM D256. The impact strength (KJ/m²) of castrol oil cortex fiber composite is 5.2 times to that pure epoxy matrix.

Selection and /or Peer-review under responsibility of ICAMM-2016

Keywords: Castor oil plant; Natural fiber; Composites; impact strength

1. Introduction

Ricinus Communis L often called castor oil plant comes under the category of "cool tropical plants" since it is found in tropical parts of Asia, Africa and mostly Australia and also the seeds are spurted out during winter or cool prevailing conditions [1]. The leaves though do not contain much toxicity than the seeds are placed alternatively on the stem on long and purple foot stalks with blades drooping about 5-8 inches. When younger the leaves would shine with attractive red in colour and after full growth, when expanded completely would be in blue-green colour. Coming to the flowers the male and the female flowers grow on the same plant and are present in a clustered terminus spike. To the bottom of this spike the male flowers are present which do not have corolla but a calyx with yellow stamens. The upper part of spike is occupied by female flowers with no corolla either but with narrow segments of calyx. These flowers have no petals since pollination in the plant is air borne that is pollination occurs due to wind.

* Corresponding author..*E-mail address:* nivassettti@gmail.com

Selection and/or Peer-review under responsibility of ICAMM-2016.

But the most important part of the plant is fruits which yield castor seeds. Fruits are generally bluntly grooved in greenish colour with prickles in which seeds are present. These seeds are actively poisonous for livestock including humans [2]. The seeds are so poisonous that consumption of only 4 to 8 seeds would tend to become fatal for humans and without proper medical treatment death occurs in 4-5 days. The symptoms tend to occur within few hours of ingestion with burning sensation, diarrhoea, and nausea reduced hydrated fluids in body, low blood pressure and reduced excretion

K.Ramanaiah et al. [3], done work on waste grass broom fibre is reinforced in polyester resin; they evaluated the mechanical and thermal properties of that composite. In that work volume fraction of fiber in composite greatly influence the IZOD impact strength. The impact strength of composite with 0.358 volume fraction was got 296 J/m.

Nadendla Srinivasubabu et al, [4], worked on characterization and manufacturing of long Palmyra palm/borassus flabellifer petiole fiber composite. They did tensile, flexural, impact ,dielectric specimens as, per ASTM. The highest impact strength for volume fraction of 40.94% was found 56.73 KJ/m².

Nadendla Srinivasubabu et al, [5], did NAOH treatment to broom grass fiber and made composites, They achieved more tensile strength, modulus , flexural strength ,modulus ,and impact strength for composites after treatment.

In this present work on composite of Epoxy/ castor oil plant cortex fiber (Ricinus Communis L) were prepared by hand layup technique. Also made composites with 0.10, 0.20, 0.30, 0.40 volume fractions of charpy impact specimens as per ASTM D256 by new fiber of castor oil plant fiber (Ricinus Communis L). The impact strength (KJ/m²) of Castrol oil cortex fiber (Ricinus Communis L) composite is 5.2 times to that pure epoxy matrix and the impact strength (J/m) of castor oil cortex fiber (Ricinus Communis L) composite are 5.8 times to pure epoxy. Ricinus Communis L fibre showed very good impact results so it may use in different applications like decks, windows frames, seat bottoms ,automobile applications.

Previously the purpose of castor oil plant is used for castor oil which is getting by castor seed. After using the castor seed, remaining parts of plant is throwing as waste. But, in this work, authors made new composite material which is low cost and lightweight materials.

2. Experimental Procedures

2.1. Material

The materials which are used in the present investigation are matrix, hardener and fiber. LY 556 epoxy resin and HY951 hardener are purchased from local dealers in Hyderabad, India. The properties of resin and hardener are mentioned Table 1 and Table 2. The resin – harder mixture decides the bond strength between fiber and matrix. Good mixing ratio of resin and hardener is 10:1 for better strength is considered in the present research work [6]. Properties of epoxy and hardener are low viscosity system and excellent water resistance and glass fiber laminates are dimensionally stable. Applications are in industrial and structural and automobile composites.

Table 1: Key properties and specific key data of Araldite LY556 and Aradur HY 951.These values are provided by HUNTSMAN.

Property	Specification	Unit	Araldite LY556	Aradur HY 951
Viscosity at 25°c	ISO 12058	mPa.s	10000-12000	10-20
Density at 25°c	ISO 1675	gm/cc	1.15-1.20	0.97-0.99
Flash point	ISO 2719	°c	>200	>180

Table 2: Processing of mixing ratio of Araldite LY556 and Aradur HY 951. These values are provided by HUNTSMAN

Name	Parts by weight
Araldite LY556	100
Aradur HY 951	10-12

Fig.1 Castor oil cortex fiber

2.2. Preparation of fiber

In the present investigation Castor oil cortex fibers (Fig.1.) are obtained by retting and mechanical rolling. Then those fibers dried under sunlight for two days. Composites with four volume fractions 10, 20, 30 and 40% are prepared by using hand layup process which is explained in the subsequent sections of this part. These specimens for charpy impact test are as per ASTM D256.

2.3. Fabrication procedure

In this work manual hand layup method is used for preparing charpy impact specimens. Releasing agent applied to bottom and top of the mold to take out the specimen easily. Calculated amount of resin is poured directly into bottom mold then castor oil cortex fiber fibers are placed in unidirectionally. After the settlement of fibers in epoxy then top plate of the mold put on the bottom plate with hand and apply pressure for a few minutes. Curing time is considered for 24 h [7].

Here, authors made four different volume fractions of composites. Those are 0.1Vf, 0.2Vf, 0.3Vf, 0.4Vf and 100% epoxy specimen. Charpy impact specimens are prepared by castor oil plant fiber which is shown in Fig.2 and Fig.3 representing the specimens.

2.4. Impact testing of composite

Charpy impact testing of composite done by ASTM D256 [8]. Specimen's dimensions are 127 mm long , 12.7 mm width , 10 mm thickness and a sharp file with include angle of 45 degrees was drawn across the center of the saw cut at 90 degrees to the sample axis to obtain a consistent starter crack. It can be observed in Fig.3. Charpy impact tests were conducted at CIPET Hyderabad. That machine (Fig.4) specifications are Range 0.5-15 joule, Accuracy 0.01J, make by TIMES OLSEN. Notch cutter also can be observed in Fig.5.

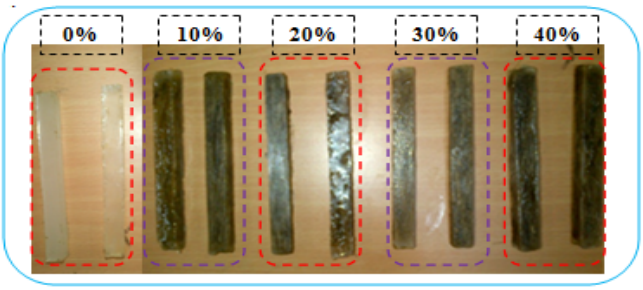

Fig 2: Composites with different volume fractions of fiber

Fig 3: Starter crack can be seen in Composite

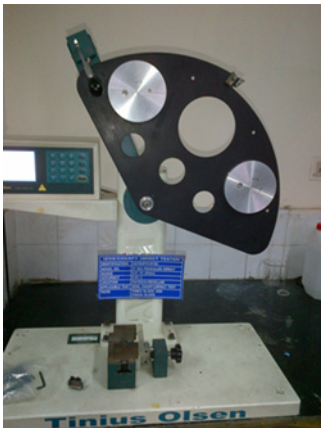

Fig 4: IZOD/CHARPY Tester

Fig 5:Notch cutter

3. Results and Discussion

3.1. Impact strength of composite

It is obvious that the increase in fiber content, the impact energy (J), the impact strength (KJ/m²) and impact strength (J/m) are increases which are presented in Table 3. The energy absorbed by composite in testing is equal to the loss of energy during impact. Those values can be observed. It is evidence that 0.4 Vf composite absorb more energy than 0.3 Vf composites, 0.2 Vf composite, 0.1 Vf composite and 100 % epoxy. The 0.4 Vf composite got high impact strength due to proper arrangement of fibers and more percentage of fibers than other volume fractions composites (0.1Vf, 0.2Vf, 0.3Vf). Because of this reason, crack propagation will difficult than other volume fractions of composites. The impact strength of the Castor oil cortex fiber composites is increasing with 0-40 % fiber volume fraction [9]. The highest impact strength of 6.99511 KJ/m² and 87.9985 J/m is found at 0.4 Vf composite.

Table-3 Impact energy values of Castor oil cortex fiber composites As per ASTM D256.

Fiber Volume Fraction (%)	Width (mm)	Depth (mm)	Energy (J)	Impact Strength (KJ/m²)	Impact Strength (J/m)
0%	10	12.7	0.1570	1.325	15.17
10%	10	12.7	0.5777	4.6423	50.3234
20%	10	12.7	0.6231	4.6186	56.3470
30%	10	12.7	0.7843	5.5512	71.0657
40%	10	12.7	0.9803	6.9951	87.9985

4. Conclusions

This work represents the fabrication of partially biodegradable composite of charpy impact specimen with various volume fractions as per ASTM D256 by new fiber of castor oil cortex fiber. The 0.4 Vf composite shows good ability to absorb impact force than other volume fractions of composites. The impact strength (KJ/m²) of Castrol oil cortex fiber (Ricinus Communis L) composite is 5.2 times to that pure epoxy matrix and the impact strength (J/m) of castor oil cortex fiber (Ricinus Communis L) composite are 5.8 times to pure epoxy matrix. Hence, the newly developed castor oil cortex fiber composite material can be used in house interior parts, and cupboards and car interior part and sports applications.

References

[1] www.cooltropicalplants.com.
[2] www.castor oil plant .com.
[3] K. Ramanaiah , A.V. Ratna Prasad , K. Hema Chandra Reddy, *Material and Design, 40(2012) 103-108.*
[4] Nadendla Srinivasubabu,J.Suresh kumar,K. Vijaya Kumar Reddy*, Procedia Techology, 14 (2014)252-259.*
[5] Nadendla Srinivasubabu,J.Suresh kumar,K. Vijaya Kumar Reddy*, Procedia Techology,* 6 (2014)1006-1016
[6] V.P.Arthanarieswaran ,A.Kumaravel, M.Kathirselvam , *Materials and Design,* 64 (2014) 194-202.
[7] N.Venkateshwaran , A. Elayaperumal , G.K.Sathiya , *Composite :Part B* , 43 (2012) 793-796.
[8] V.S. Srinivasan , S. Rajendra Boopathy , D. Sangeetha , B.Vijaya Ramnath , *Material and Design ,* 60 (2014) 620-627.
[9] Sivasaravanan.S, V.K.Bupesh Raja ,Manikandan , *Procedia Engineering ,* 97 (2014) 968-974.

Control Strategy for Improvement of PQ in Dc Systems Incorporating PR Controller

K. Deepthi, K. Chetaswi, S. Phani Venkata Ramana, K. Anitha Reddy

Abstract— Proportional-resonant (PR) controllers for current control are described in this paper. They are suitable for converters connected in a grid. In single phase converters, steady state error problems with PI controller are reduced with this controller. Also, with PR controllers, the selective compensation of harmonics is possible. The critical power quality issue that is degrading the performance on load side and source side is the voltage and current ripples. This causes reliability concerns. These can be overcome by using PR controller. In this paper, designing of PR current controller as a selective harmonic compensator has been presented.

Index Terms— Harmonic compensation, Proportional resonant controller

I. INTRODUCTION

Expression of the face is a crucial aspect in human Harmonics produced by Power Generation Systems especially due to interconnected systems is the severe power quality issue. So, it is very essential that the harmonics produced by these converters are to be controlled to reduce their harmful effects on the power quality. There can be a significant impact on current quality supplied to the load because of the current controller. So, in order to avoid harmonics, it is essential that controller gives sinusoidal output of high quality and minimal distortion. PR controller stretches infinite gain at resonant frequency and removes constant errors. Harmonic filtering or compensation is accomplished by using PR controller.

II. RIPPLE ENERGY & VOLTAGE

A 1-Ø PWM-regulated (H-bridge rectifier), as portrayed in Fig 1 is chosen to analyze the objectives of this paper. All the components are treated as ideal to simplify the analysis.

The rectifier source current controlled to be sine wave as $i_s = \sqrt{2}I_s \sin(\boldsymbol{\omega}t)$ and in Ø with source voltage $v_s = \sqrt{2}V_s \sin(\boldsymbol{\omega t})$, then the source power is

$$p_s = v_s i_s = V_s I_s - V_s I_s \cos(2\omega t) \qquad (1)$$

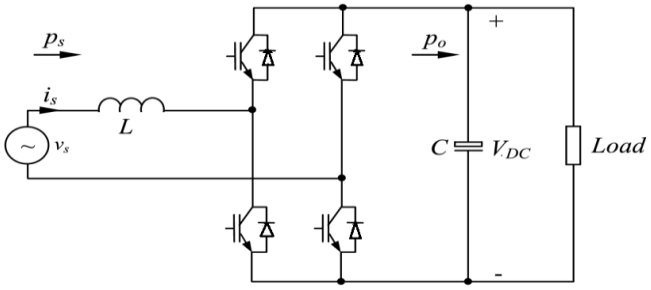

Fig 1. 1-Ø (H-bridge) PWM-regulated rectifier.

V_s and I_s are source rms voltage & input rms current correspondingly. $\boldsymbol{\omega}$ is angular frequency. The AC power source embraces of two terms; one is continual $V_s I_s$ and a II-order ripple module $-V_s I_s \cos(2\omega t)$.

During a charging period, the energy change that is accumulated in DC bus capacitor is defined as ripple energy. It can be calculates as [5],

$$E_r = \frac{V_s I_s}{\omega} \qquad (2)$$

The capacitor ripple voltage (peak-to-peak) [4] is formulated as,

$$\Delta V_{DC} \approx \frac{E_r}{C V_{DC0}} \qquad (3)$$

V_{DC0} is the average value of V_{DC}. This implies that the rise in capacitor value decreases the voltage ripple of DC-bus. Due to this, the weight, volume and system cost increases, the reliability of the system is decreased. If possible, this should be avoided.

III. THE RIPPLE ELIMINATOR

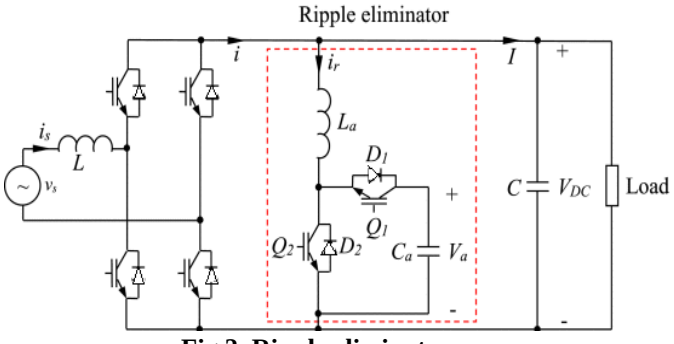

Fig 2. Ripple eliminator

A. RIPPLE ELIMINATOR (RE) OPERATION

It It performs as two-way converter with boost-buck operation. It looks like inverter one phase is connected with DC bus and auxiliary capacitor C_a to divert bi-directional current i_r from the DC bus.

Revised Version Manuscript Received on 30 May, 2018.

Mrs. K. Deepthi, M-Tech Student Department of EEE, MREC (A), Maisammaguda, Medchal (Dt), Telangana, India
Ms. K. Chetaswi, Assistant Professor Department of EEE, MREC (A), Maisammaguda, Medchal (Dt), Telangana, India
Mr. S. Phani Venkata Ramana, M-Tech Student Department of EEE, MREC (A), Maisammaguda, Medchal (Dt), Telangana, India
Mrs. K. Anitha Reddy, Assistant Professor Department of Department of EEE, MREC (A), Maisammaguda, Medchal (Dt), Telangana, India

To trace current with ripples, switches Q1 & Q2 are to be controlled in separate switching operations.

In the positive half cycle i.e. charging mode, only Q2 is operated with Q1 OFF. In this mode, Q2 operated by PWM signal. This gives the ripple current i_r in the positive half cycle. So, the RE behaves a boost converter. In the negative half cycle, Q1 operated by a PWM signal with Q2 OFF. This gives the ripple current i_r in negative half cycle. So, the circuit behaves a buck converter. Hence, in an auxiliary inductor, during a switching period, the direction of current flow can be positive or negative.

Second switching technique is operating the switches alternatively. So, Q1 & Q2 be operated by two reverse PWM signals to trace the current with ripples. The voltage against auxiliary inductor is V_{DC} and $V_{DC} - V_a$ with respect to switches operating modes. In a single PWM period, Q1 will be ON and Q2 will be kept OFF with an inverse signal and the reverse will be repeated in the other period. In this case, in a single switching mode, current through the inductor be either positive/ negative. It can be considered as a better feature as tracing current is easy at zero-crossing points/huge ripple current situations. As main aim is to decrease voltage ripples in DC-bus capacitor, high values of auxiliary current ripple need not be considered which are due to high switching frequency. If the ripple is large then small inductor is required. This will diminish the magnitude of ripple eliminator. Here, RE is operated with different working conditions. Switches *Q*1 & *Q*2 be operated alternatively to trace the ripple current.

IV. PROPORTIONAL RESONANT CONTROLLER

PR current controller could be formulated as:

$$G_{PR}(s) = K_p + K_i \frac{s}{s^2+\omega^2} \qquad (4)$$

K_p, the proportional term, K_i, the integral term, ω, the frequency resonance term. In this controller, at the ac frequency ω_0, the ideal resonant term produces infinite gain and at other frequencies, there is no gain and phase shift.

The term K_p calculates the bandwidth, system dynamics, gain and phase margin. The ideal PR controller may arise problems with stability because of infinite gain. So, PR controller is changed to non-ideal by adding damping term,

$$G_{PR}(s) = K_p + K_i \frac{2\omega s}{s^2+2\omega s+\omega^2} \qquad (5)$$

the gain (at ac frequency) of PR controller and ω is not infinite. This is even big enough to give only a minimal steady state error. Due to its finite precision, this makes the controller suitable in the digital systems.

V.CONTROL OF RE USING PR CONTROLLER

In this paper, Continuous Conduction Mode is opted due to its high performance in tracing the current. The tracing of ripple current can be performed as: a) to produce a reference current with ripple and b) to trace the reference current with ripple. The auxiliary capacitor voltage must also be controlled properly to achieve the proper current tracking. The control strategy of RE is as follows.

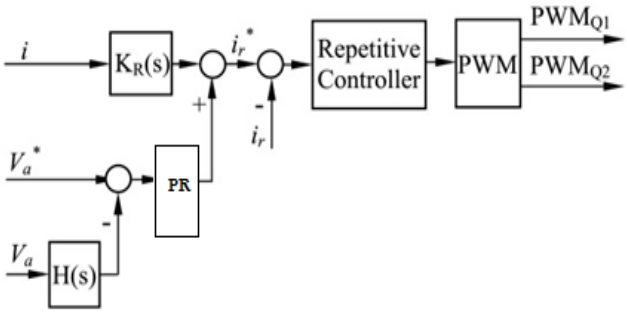

Fig 3. Ripple eliminator control strategy

A low pass filter is chosen for ripple elimination and to maintain the DC (average) component at some point. It is written as,

$$H(s) = \frac{1-e^{-\tau s/2}}{\tau s/2} \qquad (6)$$

Here τ is the fundamental period which filters out other components so as to extract the average voltage for control.

The II-order harmonic component of the current *i* to be traced can be drawn using the resonant filter as,

$$K_R(s) = \frac{K_h 2\xi h\omega s}{s^2+2h\xi\omega s+(h\omega)^2} \qquad (7)$$

Adjusted at the II harmonic component with ξ value of 0.01, h as 2 and $\boldsymbol{\omega} = 2\Pi f$. $K_R(s)$ can be designed for harmonic components at other frequencies. For example, $K_R(s)$ includes a term h=3 for third harmonic component. Voltage across auxiliary capacitor can be manipulated by giving the extracted current to PR controller output which forms the reference ripple current i_r^*.

The regulation issue is necessarily to track the current. The control strategy in repetitive way can be chosen as the reference ripple current is periodic.

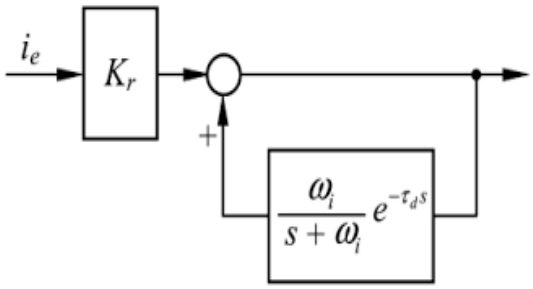

Fig 4. Repetitive controller

The internal model of repetitive controller involves low pass filter with a delay term. High gains are introduced at the system and other harmonic frequencies. This reduces periodic errors.

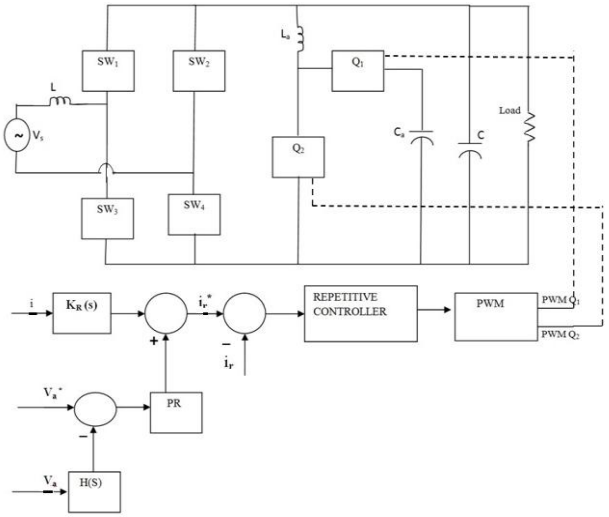

Fig 5: Block diagram of ripple eliminator with PR controller

In the above block diagram, SW_1, SW_2, SW_3 and SW_4 represents the four IGBTS. Q_1 and Q_2 are the controlling switches in the ripple eliminator. L_a, the auxiliary inductor. C represents DC bus capacitor and C_a the auxiliary capacitor. PWM Q_1 and PWM Q_2 are the pwm signals given to control the switches Q_1 and Q_2.

VI. SIMULINK MODEL OF RIPPLE ELIMINATOR WITH PR CONTROLLER

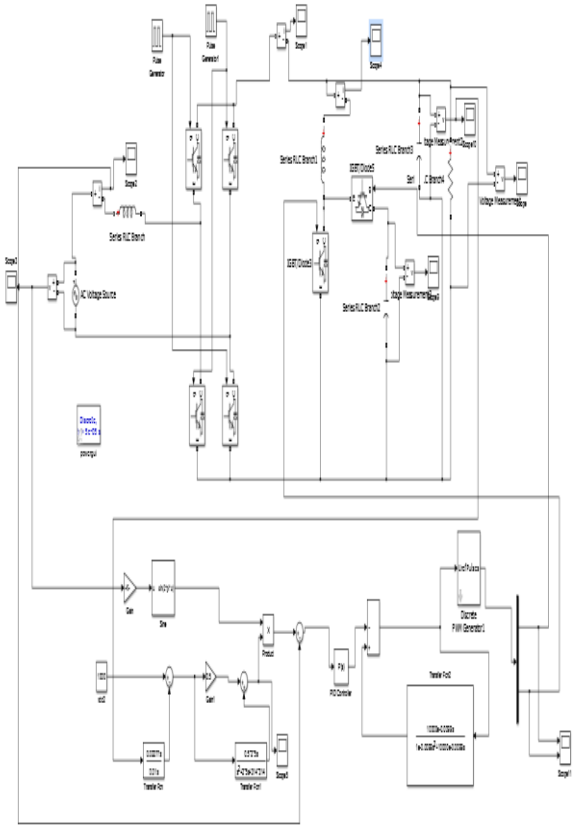

VII. EXPERIMENTAL RESULTS

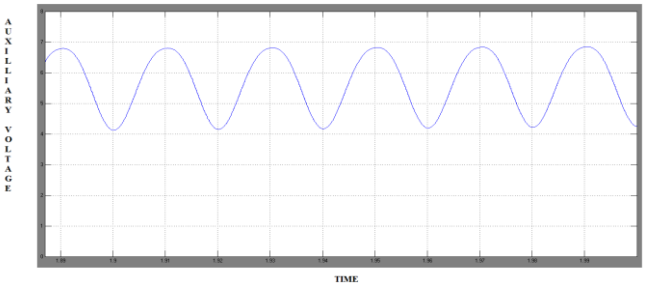

Fig 6(a) Auxiliary capacitance voltage Vs Time

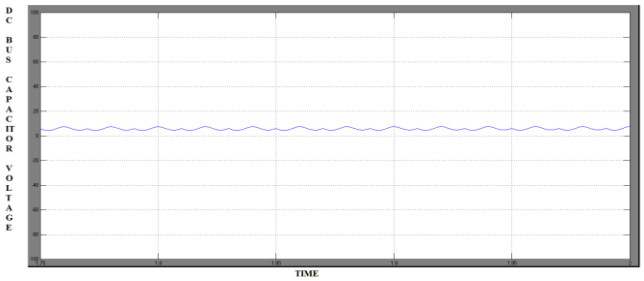

Fig 6(b) DC bus capacitor voltage Vs Time

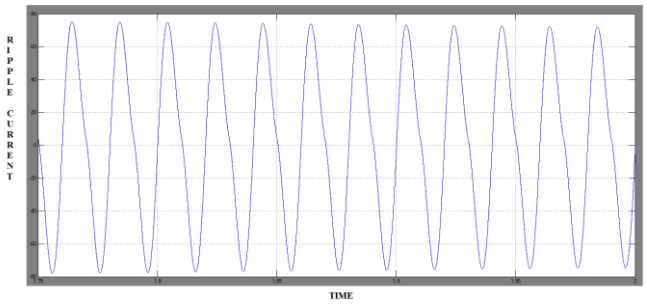

Fig 6(c) Ripple current Vs Time

Figure 6 shows the results of ripple eliminator controlled using PR controller. It is observed that the ripple across dc capacitor is minimized. As the voltage against capacitor is maximized, ripple voltage across C_a is decreased. Whenever the voltage across C_a is increased, large frequency ripples of current across auxiliary inductor also increases.

VIII. TOTAL HARMONIC DISTORTION (THD) RESULTS

The THD of ripple eliminator with & without PR controller are tabulated as below:

Table 1. THD results

System	THD value
Without PR controller	13.77
With PR controller	8.6

IX. CONCLUSION

The ripple eliminator concept has been proposed to enhance the power quality, voltage ripple reduction in DC systems & limit usage of electrolytic capacitors. Compared to [6], this paper consists of following works: 1) the capability to draw away the current with ripples from the DC bus to improve its performance 2) repetitive controller has been developed to regulate one ripple eliminator. It reduces the ripple current to reduce voltage ripples.

REFERENCES

1. R. Teodorescu, F. Blaabjerg, M. Liserre and P.C. Loh "Proportional-resonant controllers and filters for grid-connected voltage-source converters" IEE Proc.-Electr. Power Appl., Vol. 153, No. 5, September 2006
2. Ningyun Zhang *, Houjun Tang and Chen Yao " A Systematic Method for Designing a PR Controller and Active Damping of the LCL Filter for Single-Phase Grid-Connected PV Inverters" Energies 2014
3. Q.-C. Zhong, W.-L. Ming, X. Cao, and M. Krstic, ``Reduction of DC-bus voltage ripples and capacitors for single-phase PWM-controlled rectifiers," in Proc. 38th Annu. Conf. IEEE Ind. Electron. Soc. (IECON), Oct. 2012, pp. 708-713.
4. W. Choi, J.W. Howze, and P. Enjeti, ``Development of an equivalent circuit model of a fuel cell to evaluate the effects of inverter ripple current,"J. Power Sour., vol. 158, no. 2, pp. 1324-1332, Aug. 2006.
5. R. Wang et al., ``A high power density single-phase PWM rectifier with active ripple energy storage," IEEE Trans. Power Electron., vol. 26, no. 5, pp. 1430-1443, May 2011.
6. Y. Tang, W. Yao, P. C. Loh, and F. Blaabjerg, ``Highly reliable transformerless photovoltaic inverters with leakage current and pulsating power elimination," IEEE Trans. Ind. Electron., vol. 63, no. 2, pp. 1016-1026, Feb. 2016.
7. S. Wang, X. Ruan, K. Yao, S.-C. Tan, Y. Yang, and Z. Ye, ``A flickerfree electrolytic capacitor-less AC-DC LEDdriver," IEEE Trans. Power Electron., vol. 27, no. 11, pp. 4540-4548, Nov. 2012.
8. C. Liu and J.-S. Lai, ``Low frequency current ripple reduction technique with active control in a fuel cell power system with inverter load," IEEE Trans. Power Electron., vol. 22, no. 4, pp. 14291436, Jul. 2007.
9. X. Cao, Q.-C. Zhong, and W.-L. Ming, ``Ripple eliminator to smooth DCbus voltage and reduce the total capacitance required," IEEE Trans. Ind. Electron., vol. 62, no. 4, pp. 2224-2235, Apr. 2015.
10. S. Hara, Y. Yamamoto, T. Omata, and M. Nakano, ``Repetitive control system: A new type servo system for periodic exogenous signals," IEEE Trans. Autom. Control, vol. 33, no. 7, pp. 659-668, Jul. 1988.
11. G.Weiss and M. Häfele, ``Repetitive control of MIMO systems using H1 design," Automatica, vol. 35, no. 7, pp. 1185-1199, Jul. 1999.

IEEE Access
Multidisciplinary | Rapid Review | Open Access Journal

Received October 30, 2018, accepted November 13, 2018, date of publication December 14, 2018,
date of current version January 7, 2019.

Digital Object Identifier 10.1109/ACCESS.2018.2886028

On the Inter-Departure Times in $M/\tilde{D}/1/B_{on}$ Queue With Queue-Length Dependent Service and Deterministic/Exponential Vacations

MADHU BABU SIKHA[1,2], AND R. MANIVASAKAN[1]
[1]Department of Electrical Engineering, IIT Madras, Chennai 600036, India
[2]Department of ECE, Malla Reddy Engineering College (Autonomous), Hyderabad 500100, India
Corresponding author: Madhu Babu Sikha (ee10d028@ee.iitm.ac.in)

ABSTRACT We derive the distribution of inter-departure times of a finite-buffer single-server queue with Poisson arrival process and queue-length-dependent service times, where the server goes to vacation if either the queue is emptied or a limited number (R_1) of packets are served, whichever occurs first, in the current busy period. We consider two types of vacation distributions: 1) deterministic and 2) exponential. Queue-length distribution at embedded points is derived first, then, the distribution and variance of inter-departure times are derived, for both types of vacations. The simulation results are in good agreement with the derived analytical results. The above framework would be useful at the receiver in modeling and analyzing the jitter and the waiting time of time-division multiplexing (TDM) emulated packets in TDM over packet-switched network (TDM over PSN) technology as a function of a buffer size.

INDEX TERMS Inter-departure times, variance, limited service discipline, queue-length dependent service, vacation queue.

I. INTRODUCTION

At least in the third world countries, the voice service currently supported by legacy (TDM based) carrier networks would be replaced by packet infrastructure as and when the legacy equipment fails. As an intermediate phase of this transition, one encounters a situation of TDM islands in a packet network, wherein the TDM services have to be emulated in a packet network for its end-to-end connectivity. This paper involves in statistical modeling and analysis of an intermediate node in the packet island and jitter buffer at the receiver Network-Network-Interface (NNI) in such networks.

The *requirements* of an intermediate router in emulating TDM in packet networks are: (a) QoS implemented through priority based multi-class queueing scheme (b) minimization of variance of inter-departure times (IDTs) (c) minimization of TEP loss and (d) service of contemporary TEPs. By 'contemporary' TEPs, we mean the voice samples of many caller-callee at a given TDM frame interval (The TEPs carrying voice samples in the next TDM frame could wait for the next round of the scheduler - explained below). Similarly, the requirements of the jitter buffer at the receiver NNI are items (b) through (d) above, apart from one important unique requirement (e), there should always be TDM frames to transmit (or video frames in VoD service or audio packets in streaming audio to play). The modelling aspects mentioned in this paper are tailor made for the above requirements.

We now give the gist of our model and the related work, reserving the details and relevant justifications for Section II. We study a single server queueing system of finite-buffer (B_{on}) with Poisson input and queue-length dependent service along with multiple vacation policy and R_1-limited service vacation. The above queue-length dependent service times $\{s_j : 1 \leq j \leq B_{on}\}$ are dictated by algorithm-B [1] (see Section II(B) and Appendix A), which can be used for rate-jitter control in packet-switched networks. In the algorithm-B, service time of a head-of-line packet is calculated at its service initiation instant and is a linearly decreasing function of queue-length at that instant. In multiple vacation policy, a server immediately goes for another vacation if it finds the queue still empty at a vacation completion instant. We consider following distributions for vacation intervals: (i) deterministic and (ii) exponential.

We use the embedded Markov chain approach to derive the distributions of our interest. We first derive the queue-length distribution (QLD) at embedded points (time instants at which we observe the state of the system), then the distribution of IDTs is derived for both types of vacation.

Using this, we find expressions for the mean and variance of IDTs, for both types of vacation distributions.

The main goal of this paper is to derive the distribution and variance of IDTs of the queueing model under study and to demonstrate (by analysis & simulations) that the variance of IDTs (equivalently packet jitter) could be minimized by using a family of scheduling algorithm (algorithm-B) similar to algorithms developed by Yishay and Patt-Shamir [2] to control packet jitter.

A. LITERATURE REVIEW

Traditionally, the motivation for the study of departure process is to characterize the arrival process to the next node downstream. It has practical significance in analyzing queueing networks. But, in the context of TDM over PSN problem, it is of paramount importance to quantify the jitter of the departing TDM frames, both at an intermediate network node and in the output of jitter buffer at the Inter-Working Function (IWF) or NNI.

Burke has shown that the IDTs of an $M/M/c$ are IIDs with exponentially distribution (with parameter related to Poisson mean arrival time) [3]. A review of output processes of a general queue can be found in [4]. An $M/G/1$ queue with exhaustive service discipline and both single and multiple vacation policies is studied in [5] and the Laplace-Stieltjes Transforms (LSTs) of occupation period, busy period and waiting time are derived. The generating function of number of packets in the system is also derived in [5]. The departure process of $M/G/1$ queue with exhaustive service discipline for both single and multiple vacation policies is derived in [6]. Matzka [7] has calculated the IDT distribution for single server $G/G/1$ queue and used this result for calculating approximated distribution of IDTs. Stanford *et al.* derived LSTs of IDTs of each class in a multi-class input queue, wherein arrivals in each class follow Poisson process and each class has its own generally distributed service times [8]. There has been considerable literature on IDTs in priority queues (both preemptive and non-preemptive) [9]–[11]. Kramer has derived QLD in $M/G/1$ queue with finite capacity and limited service system [12]. To derive QLD of the queueing system under study, we have followed the method proposed in [13].

The paper is organized as given below: In Section II, we discuss about our system model, assumptions and the outline of analysis. In Section III, we derive QLD using Embedded Markov Chain (EMC) analysis. In Sections IV and V, we derive distribution of IDTs when vacations are deterministic and exponential, respectively. Section VI discusses about simulation results and finally we conclude in Section VII.

II. OUR SYSTEM MODEL AND OUTLINE OF ANALYSIS

In this section, we discuss the relevant queueing system model of interest, the underlying assumptions, their justification and outline of the analysis. Though the queueing system described here is used in the TDM over PSN scenario, but its applications are not limited to the same.

A. NETWORK SCENARIO

Typically in a TDM over PSN network scenario, the network gives high priority to provide QoS to TEPs in the intermediate routers. This is implemented through scheduler, which ensures fixed bandwidth is allocated to the TEPs. At the core router, two *logical* queues (with a common single server) are maintained: one corresponding to the TEPs exclusively - the high priority queue, while the other queue being low priority corresponding to packets belonging to all other services. The transmission hardware (the single server) would transmit (serve) the TEPs according to the algorithm-B. The server *going on vacation* means the transmission hardware starts transmitting the packets in the other (low-priority) logical queue. Once the scheduler has transmitted all TEPs, it goes on to serve the low priority queue. The scheduler need not serve all the TEPs, but it is enough that it serves all the TEPs containing contemporary TDM frames. The more recently generated TEPs could wait for the next turn for transmission.

B. SYSTEM MODEL, ASSUMPTIONS AND JUSTIFICATIONS

We explain our system model, underlying assumptions and the corresponding justifications below:

(i) Packets arrive according to Poisson process with rate λ and service times being queue-length dependent, according to algorithm-B [1]. Queue has a capacity to hold B_{on} packets (including the one in service) and arrivals which see B_{on} packets will be dropped (this happens for arrivals until next departure). Server is allowed to serve a maximum of R_1 packets in each busy period. This queue model is denoted as $M/\tilde{D}/1/B_{on}$ queue, with R_1-limited service.

Algorithm B: Algorithm B (see Appendix A) dictates the service interval for a packet, at its service initiation instant by looking at the queue length. The service intervals are linearly decreasing, deterministic function of queue length (to satisfy the requirements (b), (c) and (e) mentioned in Section I). The scheduling algorithm-B essentially does ensure that there is always customers (requirement (e)) on the one end, while on the other, reduces the TEP loss (by setting maximum service rate when buffer is full (or nearly full) - requirement (c)). The finite queue length states in the algorithm reduces the variance of the queue length which intuitively reduces the variance of IDI (or output jitter) - the requirement (b).

(ii) We use first-come first-serve (FCFS) discipline to serve packets. The R_1-limited service aspect of the model, justifies the transmission of *only contemporary* TDM frames (requirement (d) in previous section).

(iii) If R_1 packets are served in a busy period or if the queue is emptied (whichever occurs first), server takes a vacation of duration V_1. Upon returning from a vacation (at vacation completion instants), if the server finds that the queue is still empty, it takes one more vacation of duration V_2. This process continues (multiple vacations) until the server finds at least a packet in the queue at a vacation completion instant, as shown in Fig. 1. This attribute of our model justifies the time the scheduler serves the low priority queue.

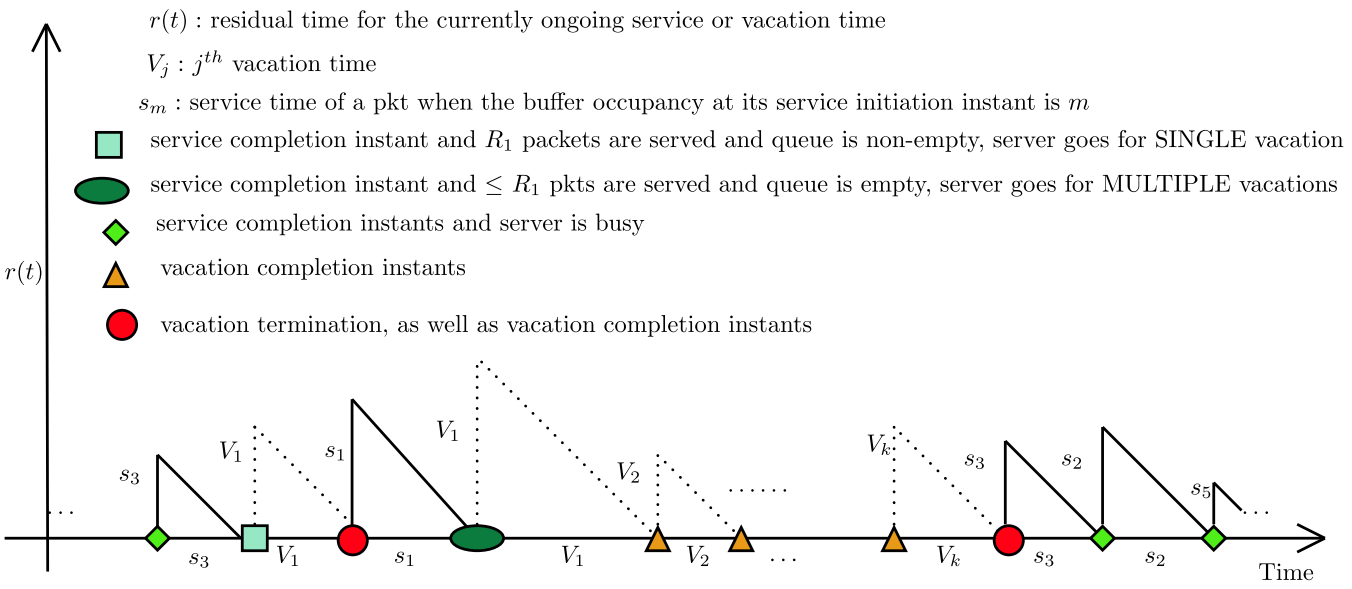

FIGURE 1. Embedded points for the $M/\tilde{D}/1/B_{on}$ queue with multiple vacations and R_1-limited service.

(iv) If the server finds that the queue is non-empty upon returning from a vacation, it terminates the vacation and starts serving the head-of-the-line packet. This embedded point (vacation completion instant) is referred to as vacation termination instant. This attribute of our model, justifies the time the scheduler serves the low priority queue (holding packets of other services).

(v) The vacation times $V_1,\ V_2,\ V_3, \ldots$ are assumed to be either: (a) deterministic or (b) exponential. The fact that the TEP streams are allocated a fixed time intervals, in a given allocation cycle (within a inter-state time interval in which the number of TDM payloads - say number of E1 lines - supported is constant) tells the remaining time in the cycle is allocated to packets of other services is also fixed. This justifies the deterministic vacation, in our model. In situations wherein the above 'fixed allocation cycle' is relaxed, the exponential vacation approximates the tail in the Gamma distribution arising out of sum of transmission times of lower priority packets.

C. OBJECTIVE AND OUTLINE OF THE ANALYSIS

Our aim is to calculate the distribution, mean and variance of IDTs (jitter in TDMoPSN perspective) of $M/\tilde{D}/1/B_{on}$ queue, while the server is allowed to take R_1-limited service vacation (deterministic/exponentially distributed).

We first derive the QLD of $M/\tilde{D}/1/B_{on}$ queue using EMC method. Then, we compute the IDT distribution for both cases of vacation distributions by using the derived QLD, state of server and queue-length. If the server is busy, IDTs follows service times and if the server is in vacation, IDT is a sum of total vacation duration and service time of first packet in the new busy period. Finally, the distribution of IDTs is computed by using law of total probability.

III. EMBEDDED MARKOV CHAIN ANALYSIS

We consider the state of the system at time instants t_k, $k \in \{0, 1, 2, \ldots\}$, as embedded points, which are vacation completion or service completion instants. In this section, we derive QLD at the embedded points using EMC method.

A. NOTATIONS

At an embedded point $t_k,\ k \in \{0, 1, 2, \ldots\}$, let

Q_k^E = number of packets in the queue, $0 \leq Q_k^E \leq B_{on}$

N_k = number of arrivals to queue during (t_{k-1}, t_k)

$$L_k^E = \begin{cases} 0, & \text{if the embedded point is a vacation completion instant} \\ 1, & \text{if the embedded point is a departure instant} \end{cases}$$

$$I_k = \begin{cases} \{0, 1, \ldots, R_1-1\}, & \text{number of service completions since the server started serving in the current busy period} \\ -1, & \text{when server is in vacation} \end{cases}$$

Queue-length Q_k^E satisfies the following recursive equation:

$$Q_k^E = min\{B_{on} - L_k^E,\ ([Q_{k-1}^E - L_k^E]^+ + N_k)\} \qquad (1)$$

where,

$$[x]^+ = \begin{cases} x, & \text{when } x > 0 \\ 0, & \text{when } x \leq 0 \end{cases}$$

Claim 1: The bivariate process $\{U_k^E \triangleq (I_k, Q_k^E),\ k \geq 0\}$ *forms an EMC at embedded points* $\{t_k\}$.

Proof: The arrival process is considered as Poisson, so N_k is independent of everything else in the system and from Equ. 1 it is clear that, Q_k^E depends only on Q_{k-1}^E and N_k, therefore, queue-length satisfies the one-step Markovian property

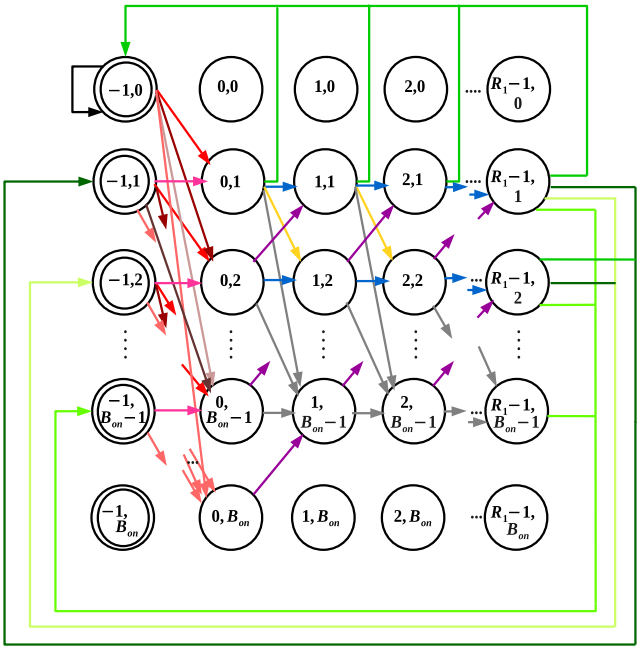

FIGURE 2. State transitions of EMC U_k^E.

Colour	Probability
Transition from Vacation to Vacation	
→	Pr(zero arrivals during vacation time) = $\beta(0)$
Transition from Vacation to Busy	
→	Pr(one arrival during vacation time) = $\beta(1)$
→	Pr(two arrivals during vacation time) = $\beta(2)$
→	Pr($(B_{on}-2)$ arrivals during vacation time) = $\beta(B_{on}-2)$
→	Pr($(B_{on}-1)$ arrivals during vacation time) = $\beta(B_{on}-1)$
→	Pr(>=$(B_{on}-m)$ arrivals during vacation time if the present state is $(-1,m)$)=$1-[\beta(0)+\beta(1)+....+\beta(B_{on}-m-1)]$
Transition from Busy to Vacation and Transitions among Busy states	
→	Pr(zero arrivals during service time 's_m' if the present state is (i,m))=$\alpha(0;s_m)$
→	Pr(one arrival during service time 's_m' if the present state is (i,m))=$\alpha(1;s_m)$
→	Pr(two arrivals during service time 's_m' if the present state is (i,m))=$\alpha(2;s_m)$
→	Pr(>=$(B_{on}-m)$ arrivals during service time 's_m' if the present state is (i,m)) =$1-[\alpha(0;s_m)+\alpha(1;s_m)+....+\alpha(B_{on}-m-1;s_m)]$

FIGURE 3. Probabilities of state transitions shown in Fig. 2.

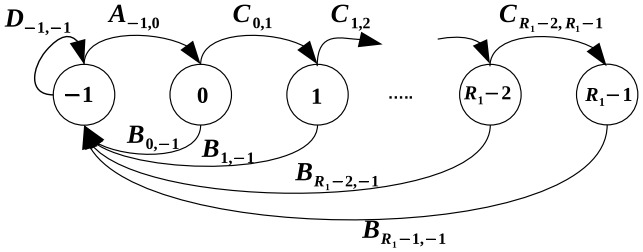

FIGURE 4. State transition diagram of one dimensional EMC formed by I_k.

at embedded points. According to the definition of I_k, it can be observed that I_k depends on I_{k-1} and Q_{k-1}. Therefore, the bivariate process $\{U_k^E = (I_k, Q_k^E),\ k \geq 0\}$ depends only on U_{k-1}^E and hence it forms an EMC with finite state space $\{-1, 0, 1, \ldots, R_1 - 1\} \times \{0, 1, 2, \ldots, B_{on}\}$. ■

Fig. 4 shows possible state transitions of EMC formed by I_k. Fig. 2 shows the bivariate EMC U_k^E corresponding to the state $U^E = (i, m)$, where $i \in I_k$ and $m \in Q_k^E$. The probabilities corresponding to each state transition are given in Fig. 3.

Given the arrival process as Poisson with parameter λ, let $\alpha(n; t)$ be the probability of n arrivals to queue in the service interval $(0, t]$ and is given by,

$$\alpha(n; t) = \frac{e^{-\lambda t}(\lambda t)^n}{n!}, \quad n \geq 0 \tag{2}$$

Let $\beta(n)$ be the probability of $n \geq 0$ arrivals to queue in a *single* arbitrary vacation (V_i) as given below:

$$\beta(n) = \begin{cases} \dfrac{e^{-\lambda D}(\lambda D)^n}{n!}, \\ \quad \text{if vacation is Deterministic } (V_i = D) \\ \dfrac{\lambda^n \theta}{(\lambda+\theta)^{n+1}}, \\ \quad \text{if vacation is Exponential } (V_i \sim Exp(\theta)) \end{cases} \tag{3}$$

If vacation distribution is deterministic with duration D, then $\beta(n)$ is equal to $\alpha(n; t)|_{t=D}$. If vacation is exponentially distributed with parameter θ, then $\beta(n)$ can be calculated as given in Appendix B. Let $\beta'(n)$ be the probability that n packets arrive (and join the queue) during an idle period,[1] and is given by,

$$\beta'(n) = \sum_{l=0}^{\infty} (\beta(0))^l \beta(n) = \frac{\beta(n)}{1-\beta(0)}, \quad n = 1, 2, \ldots, B_{on} - 1$$

$$\beta'(B_{on}) = \sum_{l=0}^{\infty} (\beta(0))^l \beta^c(B_{on}) = \frac{\beta^c(B_{on})}{1-\beta(0)} \tag{4}$$

where $\beta^c(B_{on}) = \sum_{n=B_{on}}^{\infty} \beta(n)$.

Table 1 represents the state transition probability matrix $\mathbf{P}$, whose entries themselves are sub-matrices with each such sub-matrix representing similar transitions, constituting a type of transitions as in Fig. 4. Each sub-matrix of $\mathbf{P}$ is of size $(B_{on}+1) \times (B_{on}+1)$, and hence size of $\mathbf{P}$ is given by, $(R_1+1)(B_{on}+1) \times (R_1+1)(B_{on}+1)$.

[1]The time interval between the instant at which the queue becomes empty and the instant at which the server starts serving again is referred to as an idle period.

TABLE 1. State transition probability matrix, $\boldsymbol{P}$.

I_k	-1	0	1	2	...	...	R_1-1
-1	$\mathbf{D_{-1,-1}}$	$\mathbf{A_{-1,0}}$	0	0	...	...	0
0	$\mathbf{B_{0,-1}}$	0	$\mathbf{C_{0,1}}$	0	...	...	0
1	$\mathbf{B_{1,-1}}$	0	0	$\mathbf{C_{1,2}}$	0	...	0
2	$\mathbf{B_{2,-1}}$	0	0	0	$\mathbf{C_{2,3}}$	...	0
⋮	⋮	⋮	⋮	⋮	⋮	⋮	⋮
⋮	⋮	⋮	⋮	⋮	⋮	⋮	⋮
R_1-2	$\mathbf{B_{R_1-2,-1}}$	0	0	0	...	...	$\mathbf{C_{R_1-2,R_1-1}}$
R_1-1	$\mathbf{B_{R_1-1,-1}}$	0	0	0	...	...	0

B. ELEMENTS OF STATE TRANSITION PROBABILITY MATRIX P

As mentioned earlier, each state transition in Fig. 4 is an element in $\mathbf{P}$ and is a matrix itself. In Fig. 4, there are four types of state transitions and are given by:

(i) vacation state -1 to -1 itself, which is represented as $\mathbf{D_{-1,-1}}$ in $\mathbf{P}$

(ii) vacation state -1 to busy state 0, which is represented as $\mathbf{A_{-1,0}}$

(iii) busy state i to vacation state -1, which is represented as $\mathbf{B_{i,-1}}$, $i \in \{0, 1, \ldots, R_1 - 1\}$

(iv) busy state i to busy state $(i+1)$, which is represented as $\mathbf{C_{i,i+1}}$, $i \in \{0, 1, \ldots, R_1 - 2\}$ Each element of the blocks (A, B, C or D) of $\mathbf{P}$ is a conditional probability and are defined as,

$$
\begin{aligned}
D_{-1,-1}(m,n) &= Pr(I_{k+1}=-1, Q^E_{k+1}=n | I_k=-1, Q^E_k=m)\\
A_{-1,0}(m,n) &= Pr(I_{k+1}=0, Q^E_{k+1}=n | I_k=-1, Q^E_k=m)\\
B_{i,-1}(m,n) &= Pr(I_{k+1}=-1, Q^E_{k+1}=n | I_k=i, Q^E_k=m)\\
C_{i,i+1}(m,n) &= Pr(I_{k+1}=i+1, Q^E_{k+1}=n | I_k=i, Q^E_k=m)
\end{aligned}
$$

Now, the elements of $\mathbf{D_{-1,-1}}$ are given by,

$$
D_{-1,-1}(m,n) = \begin{cases} \beta(0), & \text{if } m=0 \text{ and } n=0 \\ 0, & \text{otherwise} \end{cases}
$$

Elements of $\mathbf{A_{-1,0}}$ are given by,

$$
A_{-1,0}(m,n) = \begin{cases} 0, & \text{if } m=0 \text{ and } n=0 \\ \beta(n-m), & \text{if } n \geq m \text{ and } 0 \leq m \leq B_{on}-1 \\ & \quad 1 \leq n \leq B_{on}-1 \\ 1-\sum_{i=0}^{B_{on}-1-m} \beta(i), & \text{if } n=B_{on} \text{ and } 0 \leq m \leq B_{on}-1 \\ 0, & \text{otherwise} \end{cases}
$$

Now, the elements of $\mathbf{B_{i,-1}}$, for $0 \leq i \leq R_1 - 2$ are given by,

$$
B_{i,-1}(m,n) = \begin{cases} \alpha(0; s_1), & \text{if } m=1 \text{ and } n=0 \\ 0, & \text{otherwise} \end{cases}
$$

where s_m is the service time of a head-of-line packet when the queue-length at its service initiation instant is m.

Now, elements of $\mathbf{B_{R_1-1,-1}}$ are given by,

$$
B_{R_1-1,-1}(m,n) = \begin{cases} 0, & \text{if } m=0 \text{ (or) } n=B_{on} \text{ (or)} \\ & \quad m=B_{on} \\ \alpha(n-m+1; s_m), & \text{if } n+1 \geq m,\ 1 \leq m \leq B_{on}-1, \\ & \quad m-1 \leq n \leq B_{on}-2 \\ 1-\sum_{i=0}^{B_{on}-1-m} \alpha(i), & \text{if } 1 \leq m \leq B_{on}-1,\ n=B_{on}-1 \\ 0, & \text{otherwise} \end{cases}
$$

Now, the elements of $C_{0,1}$ are given by,

$$
C_{0,1}(m,n) = \begin{cases} 0, & \text{if } m=0 \text{ (or) } n=0 \text{ (or) } n=B_{on} \\ 0, & \text{if } m=B_{on} \text{ and } n \neq B_{on}-1 \\ 1, & \text{if } m=B_{on} \text{ and } n=B_{on}-1 \\ \alpha(n-m+1; s_m), & \text{if } n+1 \geq m,\ 1 \leq m \leq B_{on}-1, \\ & \quad m-1 \leq n \leq B_{on}-2 \\ 1-\sum_{i=0}^{B_{on}-1-m} \alpha(i), & \text{if } 1 \leq m \leq B_{on}-1,\ n=B_{on}-1 \\ 0, & \text{otherwise} \end{cases}
$$

Elements of $C_{i,i+1}$, for $1 \leq i \leq R_1 - 2$ are given by,

$$
C_{i,i+1}(m,n) = \begin{cases} 0, & \text{if } m=0 \text{ (or) } m=B_{on} \\ & \quad \text{(or) } n=0 \text{ (or) } n=B_{on} \\ \alpha(n-m+1; s_m), & \text{if } n+1 \geq m,\ 1 \leq m \leq B_{on}-1, \\ & \quad m-1 \leq n \leq B_{on}-2 \\ 1-\sum_{i=0}^{B_{on}-1-m} \alpha(i), & \text{if } 1 \leq m \leq B_{on}-1,\ n=B_{on}-1 \\ 0, & \text{otherwise} \end{cases}
$$

Let $\Pi^E = (\pi^E_{-1,0}, \pi^E_{-1,1}, \ldots, \pi^E_{-1,B_{on}}, \pi^E_{0,0}, \pi^E_{0,1}, \ldots, \pi^E_{0,B_{on}}, \pi^E_{1,0}, \pi^E_{1,1}, \ldots, \pi^E_{1,B_{on}}, \ldots\ldots, \pi^E_{R_1-1,0}, \pi^E_{R_1-1,1}, \ldots, \pi^E_{R_1-1,B_{on}})$ be the stationary probability vector at embedded

$$
\pi^{SI}_{i,m} = \begin{cases} \pi^E_{i,m}, & \text{if } i \in (1,2,\ldots,R_1-1),\ m \in (1,2,\ldots,B_{on}-1) \\ \pi^E_{0,m} + \pi^E_{-1,0}\beta'(m) + \sum_{k=1}^{m} \pi^E_{-1,k}\,\beta(m-k), & \text{if } i=0 \text{ and } m \in (1,2,\ldots,B_{on}-1) \\ \pi^E_{0,B_{on}} + \pi^E_{-1,0}\beta'(B_{on}) + \sum_{k=1}^{B_{on}} \pi^E_{-1,k} \left(1-\sum_{j=0}^{B_{on}-1-k} \beta(j)\right), & \text{if } i=0 \text{ and } m=B_{on} \\ 0, & \text{if } i \in (1,2,\ldots,R_1-1) \text{ and } m=B_{on} \end{cases} \tag{5}
$$

points, where $\pi^E_{i,m}$ represents the steady state probability of the state (i, m) at embedded point.

Solve $\Pi^E = \Pi^E \mathbf{P}$ and $\sum_{m=0}^{B_{on}} \pi^E_{-1,m} + \sum_{i=0}^{R_1-1} \sum_{m=0}^{B_{on}} \pi^E_{i,m} = 1$ to get stationary probabilities of the EMC U_k at embedded points. Now, the steady state queue-length vector at embedded points can be obtained from above stationary probabilities as follows:

$$\pi^E_m = \pi^E_{-1,m} + \sum_{i=0}^{R_1-1} \pi^E_{i,m} \tag{6}$$

for $0 \le m \le B_{on}$.

C. QLD AT SERVICE INITIATION INSTANTS

If the server is busy, state of the system at service initiation instant $\left(U^{SI}\right)$ is same as the state of system at embedded point $\left(U^E\right)$, otherwise they are different. The state space of U^{SI} is $\{0, 1, \ldots, R_1 - 1\} \times \{1, 2, \ldots, B_{on}\}$ and is related to U^E as

$$U^{SI} = \begin{cases} U^E, & \text{if } U^E = (i, m),\ i \in (1, 2, \ldots, R_1 - 1), \\ & m \in (1, 2, \ldots, B_{on} - 1) \\ (0, m), & \text{if } U^E = (-1, 0),\ (-1, m),\ (0, m), \\ & m \in (1, 2, \ldots, B_{on}) \end{cases}$$

Therefore, $\Pi^{SI} = Pr\left(U^{SI} = (i, m)\right)$ can be calculated as given in Equ. 5, where, $\pi^{SI}_{i,m}$ represents the stationary probability that the EMC will be in the state (i, m), $i \in \{0, 1, \ldots, R_1 - 1\}$, $m \in \{1, 2, \ldots, B_{on}\}$ at a service initiation instant. Finally, QLD at service initiation instants can be calculated as,

$$\pi^{SI}_m = \sum_{i=0}^{R_1-1} \pi^{SI}_{i,m} \tag{7}$$

for $1 \le m \le B_{on}$.

Note here that, the QLD at embedded points π^E_m (and QLD at service initiation points π^{SI}_m) is different for different vacation distributions. We have to plug-in $\beta(n)$ corresponding to the type of vacation, while deriving π^E_m. In the following sections, we derive distribution of IDTs for two types of vacations, where we will use the corresponding QLD at embedded and service initiation instants.

IV. DISTRIBUTION OF IDTs WHEN VACATIONS ARE DETERMINISTIC

In this section, we derive the distribution of IDTs when the distribution of vacation duration is deterministic and using which we derive expressions for mean and variance of IDTs.

Let A be a random variable representing the status of the queue and server at an embedded point. It takes three values depending on the state of the queue and server:

$$A = \begin{cases} -1, & \text{if server is in vacation } \textit{and} \text{ queue is empty} \\ 0, & \text{if server is in vacation } \textit{and} \text{ queue is non-empty} \\ 1, & \text{if server is busy} \end{cases} \tag{8}$$

The probability mass function (PMF) of A is given by,

$$p_A(a) = \begin{cases} p, & \text{if } a = -1 \\ 1 - \rho - p, & \text{if } a = 0 \\ \rho, & \text{if } a = 1 \end{cases} \tag{9}$$

where, p is the probability of queue being empty, ρ is the probability of server being busy and $(1 - \rho - p)$ is the probability of server being in vacation and queue is non-empty. These probabilities can be calculated as given below:

$$\begin{aligned} p &= \pi^E_{-1,0} + \sum_{j=0}^{R_1-1} \pi^E_{j,0} = \pi^E_{-1,0} \\ \rho &= \sum_{j=0}^{R_1-1} \sum_{m=1}^{B_{on}} \pi^E_{j,m} = \pi^E_{0,B_{on}} + \sum_{j=0}^{R_1-1} \sum_{m=1}^{B_{on}-1} \pi^E_{j,m} \\ 1 - \rho - p &= \sum_{m=1}^{B_{on}} \pi^E_{-1,m} \end{aligned} \tag{10}$$

where, $\pi^E_{j,0} = 0,\ \forall\, j \in \{0, 1, \ldots, R_1 - 1\}$ and $\pi^E_{j,B_{on}} = 0,\ \forall\, j \in \{1, 2, \ldots, R_1 - 1\}$, can be observed from Fig. 2.

Let X be the random variable representing IDTs of $M/\tilde{D}/1/B_{on}$ queue, when vacations are deterministic D. In this case, let, p_d be the probability of queue being empty and ρ_d be the probability of server being busy, as shown in Fig. 5. Then, $p_d = p$ and $\rho_d = \rho$ with $\{\pi^E_m,\ 0 \le m \le B_{on}\}$ corresponds to QLD when vacations are deterministic.

The IDT (X) takes the form of the following conditional random variables, conditioning on the random variable A:

$$\begin{aligned} X_E &= \text{conditional IDT when server is in vacation } \textit{and} \\ &\qquad \text{queue is empty } (A = -1) \\ X_{NE} &= \text{conditional IDT when server is in vacation } \textit{and} \\ &\qquad \text{queue is non-empty } (A = 0) \\ X_B &= \text{conditional IDT when server is busy } (A = 1) \end{aligned} \tag{11}$$

With the above notation, the law of total probability gives the unconditional distribution of X (can be observed from Fig. 5).

$$F_X(x) = p_d F_{X_E}(x) + (1 - \rho_d - p_d) F_{X_{NE}}(x) + \rho_d F_{X_B}(x) \tag{12}$$

Now, we determine the distributions of random variables X_B, X_E and X_{NE}.

A. DISTRIBUTION OF X_B

When the server is busy, IDTs in a queue are equal to service times. Hence, $Pr(X_B) = Pr(X|A = 1) = Pr(S = x)$. For the service process considered in this paper, service times (denoted by random variable, S) distribution, $F_S(x)$ is equal to the QLD at service initiation instants, π^{SI}_m, $1 \le m \le B_{on}$ (for more details, see [1]). Therefore, the PMF of service

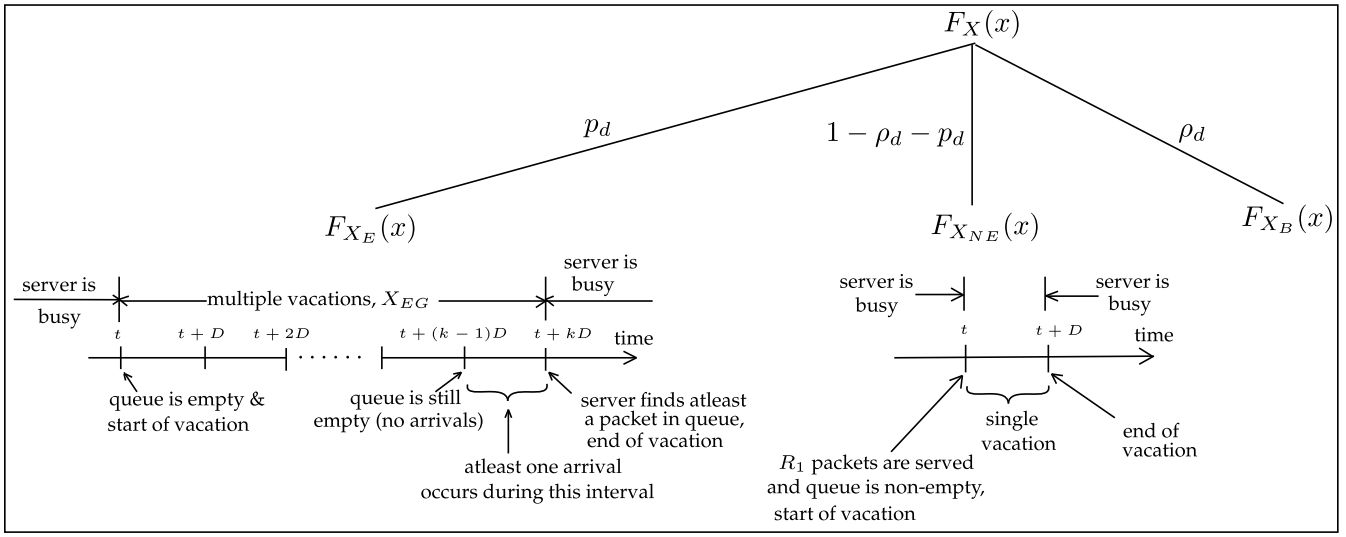

FIGURE 5. Distribution of IDTs when vacations are deterministic (D).

times (which is PMF of X_B also) is given by,

$$p_{X_B}(x) = p_S(x) = \begin{cases} \pi^{SI}_{1,d}, & \text{if } x = s_1 \\ \pi^{SI}_{2,d}, & \text{if } x = s_2 \\ \vdots & \\ \pi^{SI}_{B_{on},d}, & \text{if } x = s_{B_{on}} \end{cases} \tag{13}$$

Note here that, $\pi^{SI}_{m,d}$ corresponds to QLD at service initiation instant, when vacations are deterministic.

1) MEAN AND VARIANCE OF X_B

The mean of random variable X_B can be calculated using its PMF (Equ. 13) as follows:

$$E[X_B] = E[S] = \mu^{-1} = \sum_{m=1}^{B_{on}} s_m \, \pi^{SI}_{m,d} \tag{14}$$

Now, the second moment of X_B is calculated as follows,

$$E[X_B^2] = \sum_{m=1}^{B_{on}} s_m^2 \, \pi^{SI}_{m,d} \tag{15}$$

Finally, the variance of X_B is given by,

$$\begin{aligned} var(X_B) &= var(S) = E[X_B^2] - E^2[X_B] \\ &= \sum_{m=1}^{B_{on}} s_m^2 \, \pi^{SI}_{m,d} - \left(\mu^{-1}\right)^2 \end{aligned} \tag{16}$$

B. DISTRIBUTION OF X_E

When the queue is empty (number of service completions can be 1 or 2 or ... R_1), server goes for a vacation. Now, server checks the queue for an arrival at each vacation period end (since vacations are deterministic, server checks for every D time units) and if it finds at least one packet, it starts serving the head-of-line packet, as depicted in Fig. 5. So, the IDTs X_E in this case is a sum of two random variables X_{EG} and S, where X_{EG} is total vacation duration and S is defined in Section IV-A.

In this case ($A = -1$), if the server sees that the queue is empty (after serving $\leq R_1$ packets) at a departure point, it terminates the busy period and goes on vacation. From this instant, the server polls the queue, every D time units, whether at least one packet has arrived or not. Since, the arrivals are Poisson (a pure Markov process), at every D, say, k^{th} interval D since the start of the vacation, the probability of at least one arrival occurs, is independent of k (due to memoryless property of Poisson process). This yields, the geometric distribution for random variable X_{EG} with parameter $(1 - q_d)$, where q_d is given by Equ. 3 by substituting $n = 0$, i.e., $q_d = \beta(0) = e^{-\lambda D}$ as given by,

$$p_{X_{EG}}(x = kD) = q_d^{k-1}(1 - q_d), \quad k = 1, 2, 3, \ldots \tag{17}$$

Now, the MGFs of X_{EG} and S are given by,

$$M_{X_{EG}}(t) = E[e^{X_{EG}t}] = \sum_{k=1}^{\infty} q_d^{k-1}(1 - q_d)e^{kDt}$$

$$M_S(t) = \sum_{m=1}^{B_{on}} \pi^{SI}_{m,d} \, e^{s_m t}$$

Finally, the MGF of X_E is given by,

$$\begin{aligned} M_{X_E}(t) &= M_{X_{EG}}(t) \, M_S(t) \\ &= \sum_{k=1}^{\infty} \sum_{m=1}^{B_{on}} \pi^{SI}_{m,d} \, q_d^{k-1}(1 - q_d)e^{(kD+s_m)t} \end{aligned}$$

Now, by using the MGF $M_{X_E}(t)$, we can write,

$$p_{X_E}(x) = P\left(X_E = (s_m + kD)\right) = \pi^{SI}_{m,d} \, q_d^{k-1}(1 - q_d) \tag{18}$$

which is the PMF of X_E, for $1 \leq m \leq B_{on}$ and $k = 1, 2, 3, \ldots$.

1) CONDITIONAL MEAN OF X_E

We know that $X_E = X_{EG} + S$, so, $E[X_E] = E[X_{EG}] + E[S]$. First, we calculate the mean of X_{EG}.

$$E[X_{EG}] = \sum_{k=1}^{\infty} kD\, q_d^{k-1}(1-q_d) = D\left(\frac{1}{1-q_d}\right)$$

Therefore, the mean of X_E can be calculated as,

$$E[X_E] = E[X_{EG}] + E[S] = D\left(\frac{1}{1-q_d}\right) + \mu^{-1} \quad (19)$$

2) CONDITIONAL VARIANCE OF X_E

The random variables X_{EG} and S are independent, so $cov(X_{EG}, S) = 0$. Hence the variance of X_E can be calculated as, $var(X_E) = var(X_{EG}) + var(S)$. Now,

$$E[X_{EG}^2] = \sum_{k=1}^{\infty} (kD)^2\, q_d^{k-1}(1-q_d) = D^2\left(\frac{1+q_d}{(1-q_d)^2}\right)$$

$$var(X_{EG}) = E[X_{EG}^2] - E^2[X_{EG}] = D^2\left(\frac{q_d}{(1-q_d)^2}\right)$$

Therefore, variance of X_E is given by,

$$\begin{aligned} var(X_E) &= var(X_{EG}) + var(S) \\ &= D^2\left(\frac{q_d}{(1-q_d)^2}\right) + \sum_{m=1}^{B_{on}} s_m^2\, \pi_{m,d}^{SI} - \left(\mu^{-1}\right)^2 \end{aligned} \quad (20)$$

C. CONDITIONAL DISTRIBUTION OF X_{NE}

When number of service completions are R_1 (and queue is still non-empty), server goes for a vacation. In this case, server takes a single vacation and returns to the queue and starts serving the packets, as depicted in Fig. 5. So, the IDTs (X_{NE}) in this case is a sum of D and service times S. Now, the PMF of X_{NE} is given by,

$$p_{X_{NE}}(x) = P\left(X_{NE} = (s_m + D)\right) = \pi_{m,d}^{SI} \quad (22)$$

1) CONDITIONAL MEAN OF X_{NE}

We know that $X_{NE} = D+S$, so mean of X_{NE} can be calculated as,

$$E[X_{NE}] = E[D] + E[S] = D + \mu^{-1} \quad (23)$$

2) CONDITIONAL VARIANCE OF X_{NE}

Since the random variables D and S are independent, their covariance is zero. Now, the variance of X_{NE} can be calculated as,

$$var(X_{NE}) = var(D) + var(S) = 0 + \sum_{m=1}^{B_{on}} s_m^2 \pi_{m,d}^{SI} - \left(\mu^{-1}\right)^2 \quad (24)$$

Note that $var(D) = 0$, because D is deterministic.

D. DISTRIBUTION OF X

We have PMFs of the random variables X_B, X_E and X_{NE} given by Equs. 13, 18 and 22, respectively, using these equations, we can calculate the PMF of IDT (X) using Equ. 12, and is given by,

$$P_X(x) = \begin{cases} \rho_d\, \pi_{m,d}^{SI}, & \text{if } x = s_m \\ (1-\rho_d-p_d)\, \pi_{m,d}^{SI}, & \text{if } x = s_m + D \\ p_d\, q_d^{k-1}(1-q_d)\, \pi_{m,d}^{SI}, & \text{if } x = s_m + kD \end{cases} \quad (25)$$

where, $1 \le m \le B_{on}$ and $k = 2, 3, 4, \ldots$. Note that IDTs (X) is a discrete random variable, when vacations are deterministic, because both service times and vacation durations are discrete.

1) MEAN OF IDTs (X)

We can calculate the mean of X by applying expectation operator on both sides of Equ. 12,

$$E[X] = p_d E[X_E] + (1-\rho_d-p_d)E[X_{NE}] + \rho_d E[X_B]$$

Now, substitute Equs. 14, 19 and 23 in the above equation, we get

$$E[X] = D\left(1 - \rho_d + p_d \frac{q_d}{1-q_d}\right) + \mu^{-1} \quad (26)$$

2) VARIANCE OF IDTs (X)

The variance of IDTs can be derived using *law of conditional variances* [14]. It is defined as follows:

$$var(X) = E[var(X|A)] + var(E[X|A]) \quad (27)$$

Note that $var(X|A)$ and $E[X|A]$ are random variables. Now, $var(X|A)$ is given by,

$$var(X|A) = \begin{cases} var(X|A=-1) = var(X_E), & w.p\ \ p_d \\ var(X|A=0) = var(X_{NE}), & w.p\ \ 1-\rho_d-p_d \\ var(X|A=1) = var(X_B), & w.p\ \ \rho_d \end{cases}$$

with notation *w.p* denoting "with probability". Therefore, $E[var(X|A)]$ can be calculated as follows:

$$\begin{aligned} E[var(X|A)] = p_d\ var(X_E) + (1-\rho_d-p_d)\ var(X_{NE}) \\ + \rho_d\ var(X_B) \end{aligned} \quad (28)$$

Now, substituting Equs. 16, 20 and 24 in above equation, we get

$$E[var(X|A)] = D^2 p_d \left(\frac{q_d}{(1-q_d)^2}\right) + \sum_{m=1}^{B_{on}} s_m^2\, \pi_{m,d}^{SI} - \left(\mu^{-1}\right)^2 \quad (29)$$

Now, $E[X|A]$ is given by,

$$E[X|A] = \begin{cases} E[X|A=-1] = E[X_E], & w.p\ \ p_d \\ E[X|A=0] = E[X_{NE}], & w.p\ \ 1-\rho_d-p_d \\ E[X|A=1] = E[X_B], & w.p\ \ \rho_d \end{cases}$$

$$var(X) = D^2\left[\frac{p_d q_d}{(1-q_d)^2} + (p_d+\rho_d)(1-\rho_d-p_d) - \frac{2p_d(1-\rho_d-p_d)}{1-q_d} + \frac{p_d(1-p_d)}{(1-q_d)^2}\right] + \sum_{m=1}^{B_{on}} s_m^2\,\pi_{m,d}^{SI} - \left(\mu^{-1}\right)^2 \quad (21)$$

Note here that, $E[E[X|A]] = E[X]$. Now, $var(E[X|A])$ can be calculated as follows:

$$var(E[X|A]) = \sum_{a\in\{-1,0,1\}} \Big(E[X|A=a] - E[X]\Big)^2 P(A=a)$$

where, $a \in \{-1, 0, 1\}$ and PMF of random variable A is given in Equ. 9. Now,

$$\begin{aligned} var(E[X|A]) = &\Big(E[X_E] - E[X]\Big)^2 P(A=-1) \\ &+ \Big(E[X_{NE}] - E[X]\Big)^2 P(A=0) \\ &+ \Big(E[X_B] - E[X]\Big)^2 P(A=1) \end{aligned} \quad (30)$$

Now, substitute Equs. 9, 14, 19, 23 and 26 in above equation, we get,

$$\begin{aligned} var(E[X|A]) = D^2\Bigg[&(p_d+\rho_d)(1-\rho_d-p_d) \\ &- \frac{2p_d(1-\rho_d-p_d)}{1-q_d} + \frac{p_d(1-p_d)}{(1-q_d)^2}\Bigg] \end{aligned} \quad (31)$$

Therefore, the variance of IDTs in case of deterministic vacation, can be obtained by adding Equs. 29 and 31, it is given in Equ. 21.

V. DISTRIBUTION OF IDTS WHEN VACATIONS ARE EXPONENTIALLY DISTRIBUTED

In this section, we derive distribution of IDTs when vacations are exponentially distributed and we also derive mean and variance of IDTs using the derived distribution of IDTs.

Let Y be the random variable representing IDTs of $M/\widetilde{D}/1/B_{on}$ queue, when vacations are exponentially distributed (represented by a random variable W) with parameter θ. We use A (as before) for the random variable denoting the status of the queue and server (Equ. 8 and Equ. 9 gives the definition and PMF of A, respectively). In this case, let, p_e be the probability of queue being empty and ρ_e be the probability of server being busy. Then, $p_e = p$ and $\rho_e = \rho$ with $\{\pi_m^E,\ 0 \le m \le B_{on}\}$ corresponds to QLD when vacations are exponentially distributed.

The IDT (Y) takes the form of the following conditional random variables, conditioning on the random variable A:

$$\begin{aligned} Y_E &= \text{conditional IDT when server is in vacation } \textit{and} \\ &\quad \text{queue is empty } (A=-1) \\ Y_{NE} &= \text{conditional IDT when server is in vacation } \textit{and} \\ &\quad \text{queue is non-empty } (A=0) \\ Y_B &= \text{conditional IDT when server is busy } (A=1) \end{aligned} \quad (32)$$

Now, the distribution of Y can be written using Fig. 6 as follows,

$$F_Y(y) = p_e F_{Y_E}(y) + (1-\rho_e-p_e)F_{Y_{NE}}(y) + \rho_e F_{Y_B}(y) \quad (33)$$

Now, we determine the distributions of random variables Y_B, Y_E and Y_{NE}.

A. DISTRIBUTION OF Y_B

When the server is busy, IDTs in a queue are equal to service times. Hence, the distribution of IDTs, $F_{Y_B}(y)$, in this case is same as service time distribution. Therefore, the PMF of service times (which is PMF of Y_B also) is given by,

$$p_{Y_B}(y) = p_S(y) = \begin{cases} \pi_{1,e}^{SI}, & \text{if } y = s_1 \\ \pi_{2,e}^{SI}, & \text{if } y = s_2 \\ \vdots & \\ \pi_{B_{on},e}^{SI}, & \text{if } y = s_{B_{on}} \end{cases} \quad (34)$$

Note here that, $\pi_{m,e}^{SI}$ corresponds to QLD at service initiation instant, when vacations are exponentially distributed.

1) MEAN AND VARIANCE OF Y_B

The mean of random variable Y_B can be calculated using its PMF (Equ. 34) as follows:

$$E[Y_B] = E[S] = \gamma^{-1} = \sum_{m=1}^{B_{on}} s_m\,\pi_{m,e}^{SI} \quad (35)$$

Now, the second moment of X_B is calculated as follows,

$$E[Y_B^2] = \sum_{m=1}^{B_{on}} s_m^2\,\pi_{m,e}^{SI} \quad (36)$$

Finally, the variance of Y_B is given by,

$$\begin{aligned} var(Y_B) &= var(S) = E[Y_B^2] - E^2[Y_B] \\ &= \sum_{m=1}^{B_{on}} s_m^2\,\pi_{m,e}^{SI} - \left(\gamma^{-1}\right)^2 \end{aligned} \quad (37)$$

B. DISTRIBUTION OF Y_E

When the queue is empty (number of service completions can be 1 or 2 or... R_1), server goes for multiple vacations, as depicted in Fig. 6. The IDTs Y_E in this case is a sum of two random variables Y_{EE} and S, where Y_{EE} is a random sum of random variables and S is random variable representing service times. In other words, Y_{EE} records the total vacation duration until a non-zero number of arrivals to the queue and S represents the length of first service time in the new busy cycle. As explained for X_E, number of vacation periods (here it is represented by a random variable N) required for the

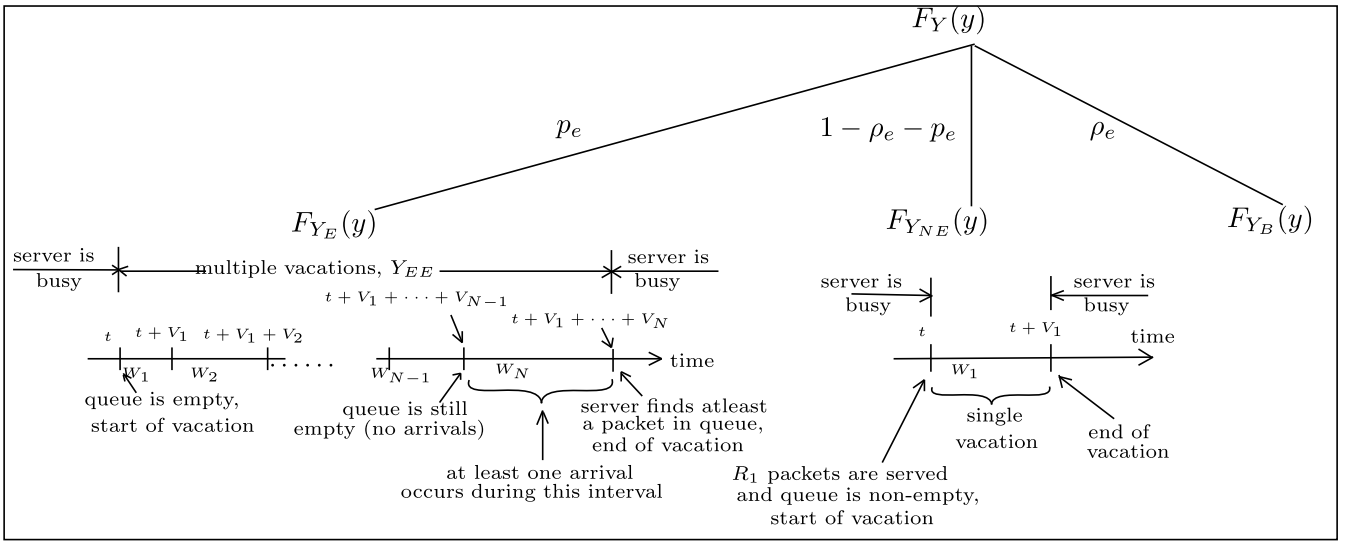

FIGURE 6. Distribution of IDTs when vacations are exponentially distributed.

server to find at least an arrival in the queue is geometrically distributed with parameter $(1-q_e)$, where q_e is the probability of zero arrivals during a single vacation period, when vacations are exponentially distributed. So, q_e can be obtained from Equ. 3 and is given by, $q_e = \beta(0) = \dfrac{\theta}{\lambda+\theta}$.

Let $W_1, W_2, \ldots$ is a sequence of independent and identically distributed (i.i.d.) exponential random variables with parameter θ and common generating function $M_W(t)$ and N is geometrically distributed, which is independent of W_i and has a generating function $M_N(t)$.

For exponential vacations, total vacation duration Y_{EE} is a sum of N i.i.d. exponential random variables as shown in Fig. 6, where $V_1, V_2, \ldots$ are realizations of exponential random variables $W_1, W_2, \ldots$, respectively. Therefore,

$$Y_{EE} = \sum_{i=1}^{N} W_i \tag{38}$$

Here, each exponential random variable W_i corresponds to one vacation duration.

1) MGF OF Y_{EE}

The MGF of exponential random variable W_i is given by,

$$M_{W_i}(t) = \frac{\theta}{\theta - t}$$

and MGF of geometric random variable N is given by,

$$M_N(t) = \frac{(1-q_e)e^t}{1-q_e e^t} \tag{39}$$

Now, we can find the MGF of Y_{EE} as follows:

$$\begin{aligned} M_{Y_{EE}}(t) &= E[e^{Y_{EE}t}] \\ &= E[E[e^{Y_{EE}t}|N]] \quad \text{(law of conditional expectations)} \end{aligned}$$

For a given $N = n$, Y_{EE} is a sum of n (i.i.d.) exponential random variables, therefore,

$$E[e^{Y_{EE}t}|N=n] = \left(\frac{\theta}{\theta-t}\right)^n$$

and

$$E[e^{Y_{EE}t}|N] = \left(\frac{\theta}{\theta-t}\right)^N$$

Now,

$$\begin{aligned} M_{Y_{EE}}(t) &= E[E[e^{Y_{EE}t}|N]] = E\left[\left(\frac{\theta}{\theta-t}\right)^N\right] \\ &= E\left[e^{ln\left(\frac{\theta}{\theta-t}\right)^N}\right] = E\left[e^{Nln\left(\frac{\theta}{\theta-t}\right)}\right] \end{aligned}$$

where, N is geometrically distributed and using Equ. 39, we can write $E\left[e^{Nln\left(\frac{\theta}{\theta-t}\right)}\right]$ as,

$$M_{Y_{EE}}(t) = E\left[e^{Nln\left(\frac{\theta}{\theta-t}\right)}\right] = \frac{(1-q_e)e^{ln\left(\frac{\theta}{\theta-t}\right)}}{1-q_e e^{ln\left(\frac{\theta}{\theta-t}\right)}}$$

$$= \frac{(1-q_e)\frac{\theta}{\theta-t}}{1-q_e\frac{\theta}{\theta-t}} = \frac{(1-q_e)\theta}{(1-q_e)\theta - t}$$

By comparing the MGFs $M_{W_i}(t)$ and $M_{Y_{EE}}(t)$, we can say that the random variable Y_{EE} is exponentially distributed with parameter $(1-q_e)\theta$. Therefore, the pdf of Y_{EE} are given by,

$$f_{Y_{EE}}(y) = (1-q_e)\theta\, e^{-(1-q_e)\theta y} \tag{41}$$

$$F_Y(y) = \begin{cases} 0, & \text{if } y < s_{Bon} \\ (1-\rho_e) - \sum_{m=1}^{B_{on}} \pi_{m,e}^{SI} e^{-\theta(y-s_m)}[(1-\rho_e-p_e) + p_e e^{q_e\theta(y-s_m)}]u(y-s_m) + \rho_e \sum_{j=0}^{k} \pi_{B_{on}-j,e}^{SI}, \\ \quad \text{if } s_{B_{on}-k} \le y < s_{B_{on}-k-1} \text{ and } 0 \le k \le B_{on}-2 \\ 1 - \sum_{m=1}^{B_{on}} \pi_{m,e}^{SI} e^{-\theta(y-s_m)}[(1-\rho_e-p_e) + p_e e^{q_e\theta(y-s_m)}]u(y-s_m), & \text{if } y \ge s_1 \end{cases} \tag{40}$$

As mentioned earlier, $Y_E = Y_{EE} + S$, so we can write the pdf of Y_E as,

$$f_{Y_E}(y) = \sum_{m=1}^{B_{on}} \pi_{m,e}^{SI}\, e^{(1-q_e)\theta s_m}(1-q_e)\theta\; e^{-(1-q_e)\theta y}\; u(y-s_m) \tag{42}$$

for $y \ge s_{Bon}$. The term $e^{(1-q_e)\theta s_m}(1-q_e)\theta\; e^{-(1-q_e)\theta y}$ represents the pdf of shifted exponential random variable, whose parameter is $(1-q_e)\theta$, shifted by s_m and the probability of this shift is $\pi_{m,e}^{SI}$.

2) MEAN AND VARIANCE OF Y_E

We know that, $Y_E = Y_{EE} + S$, so, $E[Y_E] = E[Y_{EE}] + E[S]$. Since, Y_{EE} is exponentially distributed with parameter $(1-q_e)\theta$,

$$E[Y_{EE}] = \frac{1}{(1-q_e)\theta} = \frac{\lambda+\theta}{\lambda\theta}$$

and mean of S is given by Equ. 35. Therefore, mean of Y_E can be calculated as,

$$E[Y_E] = \frac{\lambda+\theta}{\lambda\theta} + \gamma^{-1} \tag{43}$$

Now, variance of Y_{EE} can be calculated as,

$$var(Y_{EE}) = \frac{1}{(1-q_e)^2\,\theta^2} = \frac{(\lambda+\theta)^2}{\lambda^2\theta^2}$$

Now, the variance of Y_E can be calculated as, $var(Y_E) = var(Y_{EE}) + var(S)$, since Y_{EE} and S are independent, $cov(Y_{EE}, S) = 0$. Now,

$$\begin{aligned} var(Y_E) &= var(Y_{EE}) + var(S) \\ &= \frac{(\lambda+\theta)^2}{\lambda^2\theta^2} + \sum_{m=1}^{B_{on}} s_m^2\, \pi_{m,e}^{SI} - \left(\gamma^{-1}\right)^2 \end{aligned} \tag{44}$$

C. DISTRIBUTION OF Y_{NE}

When the number of service completions are R_1 (and queue is non-empty), server goes for a single vacation, returns to the queue after one vacation duration and starts serving the packets, as depicted in Fig. 6. So, the IDTs (Y_{NE}) in this case is a sum of exponential random variable W and service time S. Now, the pdf of Y_{NE} is given by,

$$f_{Y_{NE}}(y) = \sum_{m=1}^{B_{on}} \pi_{m,e}^{SI}\, e^{\theta s_m\theta}\; e^{-\theta y}\; u(y-s_m), \quad y \ge s_{Bon} \tag{45}$$

where, $e^{\theta s_m\theta}\; e^{-\theta y}$ is the pdf of shifted exponential random variable, whose parameter is θ, with a shift of s_m and the probability of this shift is $\pi_{m,e}^{SI}$.

1) MEAN AND VARIANCE OF Y_{NE}

We know that $Y_{NE} = W + S$, so mean of X_{NE} can be calculated as,

$$E[Y_{NE}] = E[W] + E[S] = \frac{1}{\theta} + \gamma^{-1} \tag{46}$$

Now, the variance of Y_{NE} can be calculated as,

$$\begin{aligned} var(Y_{NE}) &= var(W) + var(S) \\ &= \frac{1}{\theta^2} + \sum_{m=1}^{B_{on}} s_m^2\, \pi_{m,e}^{SI} - \left(\gamma^{-1}\right)^2 \end{aligned} \tag{47}$$

Note that, W and S are independent, so, $cov(W, S) = 0$.

D. DISTRIBUTION OF Y

Now, using the density functions of Y_B, Y_E and Y_{NE} given in Equs. 34, 42 and 45, respectively, we can calculate the CDF of IDTs $F_Y(y)$ and is given in Equ. 40. Note that IDTs (Y) is a mixed random variable, when vacations are exponentially distributed, because service times are discrete and vacation durations are continuous.

Now, we derive expressions for mean and variance of IDTs in this case as follows:

1) MEAN AND VARIANCE OF Y

We can calculate the mean of Y by applying expectation operator on both sides of Equ. 33,

$$E[Y] = p_e E[Y_E] + (1-\rho_e-p_e)E[Y_{NE}] + \rho_e E[Y_B]$$

Now, substitute Equs. 35, 43 and 46 in the above equation, we get

$$E[Y] = \frac{1-\rho_e}{\theta} + \frac{p_e}{\lambda} + \gamma^{-1} \tag{48}$$

The variance of IDTs can be derived using law of conditional variances. It is defined as follows:

$$var(Y) = E[var(Y|A)] + var(E[Y|A])$$

Note that $var(Y|A)$ and $E[Y|A]$ are random variables. Now, $var(Y|A)$ is given by,

$$var(Y|A) = \begin{cases} var(Y|A=-1) = var(Y_E), & w.p\ \ p_e \\ var(Y|A=0) = var(Y_{NE}), & w.p\ \ 1-\rho_e-p_e \\ var(Y|A=1) = var(Y_B), & w.p\ \ \rho_e \end{cases}$$

Therefore, $E[var(Y|A)]$ can be calculated as follows:

$$E[var(Y|A)] = p_e\ var(Y_E) + (1-\rho_e-p_e)\ var(Y_{NE}) + \rho_e\ var(Y_B) \quad (49)$$

Now, substituting Equs. 37, 44 and 47 in above equation, we get

$$E[var(Y|A)] = p_e\left(\frac{1}{\lambda^2}+\frac{2}{\lambda\theta}\right) + \frac{1-\rho_e}{\theta^2} + \sum_{m=1}^{B_{on}} s_m^2\ \pi_{m,e}^{SI} - \left(\gamma^{-1}\right)^2 \quad (50)$$

Now, $E[Y|A]$ is given by,

$$E[Y|A] = \begin{cases} E[Y|A=-1] = E[Y_E], & w.p\ \ p_e \\ E[Y|A=0] = E[Y_{NE}], & w.p\ \ 1-\rho_e-p_e \\ E[Y|A=1] = E[Y_B], & w.p\ \ \rho_e \end{cases}$$

Note here that, $E[E[Y|A]] = E[Y]$. Now, $var(E[Y|A])$ can be calculated as follows:

$$var(E[Y|A]) = \sum_{a\in\{-1,0,1\}} \Big(E[Y|A=a] - E[Y]\Big)^2\ P(A=a)$$

where, $a \in \{-1, 0, 1\}$ and PMF of random variable A is given in Equ. 9. Now,

$$var(E[Y|A]) = \Big(E[Y_E] - E[Y]\Big)^2 P(A=-1) + \Big(E[Y_{NE}] - E[Y]\Big)^2 P(A=0) + \Big(E[Y_B] - E[Y]\Big)^2 P(A=1) \quad (51)$$

Now, substitute Equs. 9, 35, 43, 46 and 48 in above equation, we get,

$$var(E[Y|A]) = \frac{2p_e\rho_e}{\lambda\theta} + \frac{\rho_e(1-\rho_e)}{\theta^2} + \frac{p_e(1-p_e)}{\lambda^2} \quad (52)$$

Therefore, the variance of IDTs in case of exponential vacations, can be obtained by adding Equs. 50 and 52, it is given by,

$$var(Y) = \frac{1-\rho_e^2}{\theta^2} + \frac{p_e(2-p_e)}{\lambda^2} + \frac{2p_e(1+\rho_e)}{\lambda\theta} + \sum_{m=1}^{B_{on}} s_m^2\ \pi_{m,e}^{SI} - \left(\gamma^{-1}\right)^2 \quad (53)$$

VI. SIMULATION RESULTS AND DISCUSSIONS

In this section, we first discuss the simulation methodology used to simulate the queueing system under study, as a culmination of application of our theory developed, to TDM over PSN problem. This means that to consider the typical numerical values in a practical TDM over PSN problem, to simulate the scenario and to evaluate its performance. We compare the derived analytical results with the above simulated results, for both types of vacation distributions. Towards this end, we then compare the variance of IDTs with the bounds defined in standard [15].

A. SIMULATION METHODOLOGY

We consider an E1 line[2] for emulating TDM signals within in a PSN. We consider the following simulation scenario: At the transmitter, eight E1 frames are aggregated to create an IP packet (TEPs) with 32 bytes header. These TEPs are transported across the PSN which provides guaranteed QoS, through an unacknowledged connection oriented service.[3] While the multi-class queueing (with a single server) is the most common way of providing QoS in a PSN, we replicate the same in our TDM over PSN scenario. A two-class *logical* queueing model is used for the core router (as mentioned in Section II). But, for jitter buffer in the receiving IWF (at NNI), the above queueing model reduces to single class consisting of only TEPs obtained by setting deterministic vacation being zero. This makes sense, as at the receiver IWF, the TEPs are extracted from the background traffic, which are accommodated in a separate, independent (hardware) queue. It is to be noted that the single server FIFO jitter buffer queue is operated with high utilization.

B. CHOICE OF SIMULATION PARAMETERS

E1 line data rate is 2.048 *Mbps*[4] For carrying out the simulations, we assume that each TDM over PSN packet carries eight consecutive E1 frames, so there are $8*32*8 = 2048$ bits per packet (apart from 32 bytes IP header). Hence, the average arrival rate λ is 1000 TEPs per second, which means that one TEP arrives for every 1 *ms*, i.e., the average inter-arrival time (IAT) is 1 *ms*. The parameter h of algorithm-B is set to 2, R_1 is set to $B+h$ and buffer size $B_{on} = 2B+h$.

C. SIMULATION RESULTS AND DISCUSSIONS

Figs. 7 and 10 shows both analytical and simulated QLDs of queue with deterministic and exponential distributed vacations. It is intuitive to expect the distribution is unimodal, which it turns out to be.

Fig. 8 (Fig. 11) compares the analytical and simulated distribution of IDTs of $M/\tilde{D}/1/B_{on}$ queue, when vaca-

[2]It is an European digital standard for transmitting simultaneous telephone calls using TDM.

[3]The unacknowledged connection oriented service reduces delay per hop - by avoiding the unneccessary retransmissions - at DLL level

[4]Each E1 line can carry 30 voice channels plus 2 system channels. Every voice channel is sampled by 8000 times per second and 8 bits are required to encode each sample, hence E1 line data rate is $32*8000*8 = 2.048$ *Mbps*.

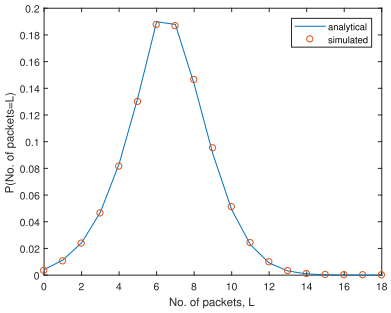

FIGURE 7. Comparison of simulated QLD with derived analytical QLD for $M/\tilde{D}/1/B_{on}$ queue with deterministic vacations and $\lambda = 1000$, $B_{on} = 18$, $D = 10^{-3}$.

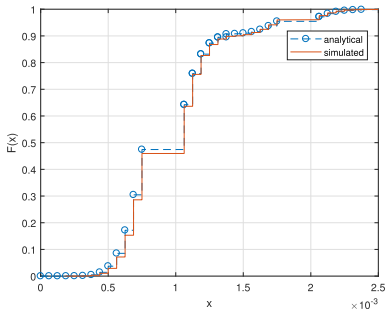

FIGURE 8. CDF of IDTs of $M/\tilde{D}/1/B_{on}$ queue with deterministic vacations and $\lambda = 1000$, $B_{on} = 18$, $D = 10^{-3}$.

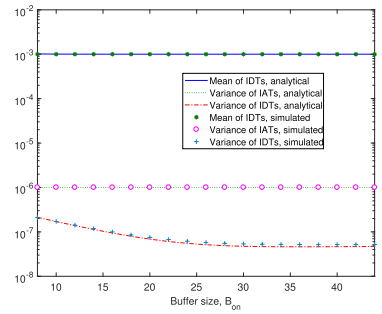

FIGURE 9. Mean and variance of IDTs of $M/\tilde{D}/1/B_{on}$ queue with deterministic vacations and $\lambda = 1000$, $D = 10^{-3}$.

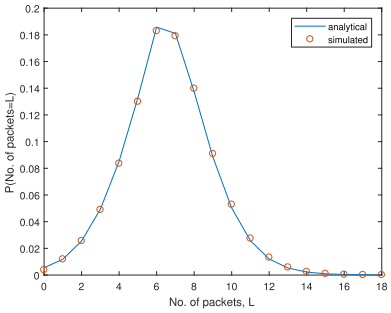

FIGURE 10. Comparison of simulated QLD with derived analytical QLD for $M/\tilde{D}/1/B_{on}$ queue with exponential vacations and $\lambda = 1000$, $B_{on} = 18$, $\theta = 1000$.

tions are deterministic (exponential). The CDF of IDTs X in Fig. 8 is a staircase function, because X is a discrete random variable. In this case, the vacations are deterministic

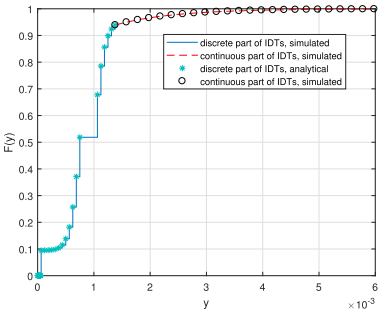

FIGURE 11. CDF of IDTs of $M/\tilde{D}/1/B_{on}$ queue with exponential vacations and $\lambda = 1000$, $B_{on} = 18$, $\theta = 1000$.

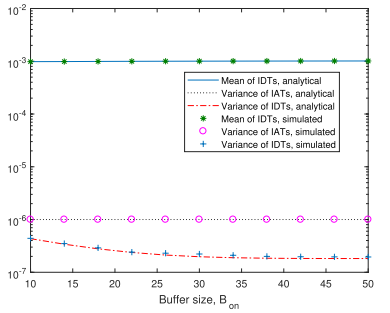

FIGURE 12. Mean and variance of IDTs of $M/\tilde{D}/1/B_{on}$ queue with exponential vacations and $\lambda = 1000$, $\theta = 1000$.

(discrete in nature) and the service times dictated by algorithm-B are also discrete in nature. Hence the IDT X is a discrete random variable, irrespective of whether the server is busy or is in vacation, which can be observed from Fig. 5 also. Finally, we observe from Fig. 8, the simulation results matches reasonably well with the analytical results.

Next, the CDF of IDTs Y in Fig. 11 contains two parts: discrete and continuous. This is because of the fact that Y is a mixed random variable. From Fig. 6, we can observe that when the server is busy, the IDTs are same as service times, which are discrete in nature. But, when the server is in vacation, IDT is a sum of exponential vacation (continuous in nature) and service time (discrete). Hence the IDT Y is a mixed random variable when the vacations are exponentially distributed. At the end we observe that from Fig. 11, the derived CDF of IDTs with exponential vacation agrees well with the simulated values.

Figs. 9 and 12 compare the analytical and simulated curves of mean and variance of IDTs, for deterministic and exponential vacation cases respectively. Since the derived analytical CDF closely matches with the simulated CDF (in Figs. 8 and Fig. 11), the analytical mean and variance also matches with their simulated counterparts, which can be observed in Figs. 9 and 12. The variance of IDTs at $B_{on} = 36$ from Fig. 9 is 46.14 ns or equivalently the standard deviation is 0.215 ms, which gives a maximum IDT of $\frac{(1+0.215)\ 10^{-3}}{2048} = 593.3$ ns and minimum IDT of $\frac{(1-0.215)\ 10^{-3}}{2048} = 383.3$ ns. Note here that the average IAT (and average IDT) is 1 ms

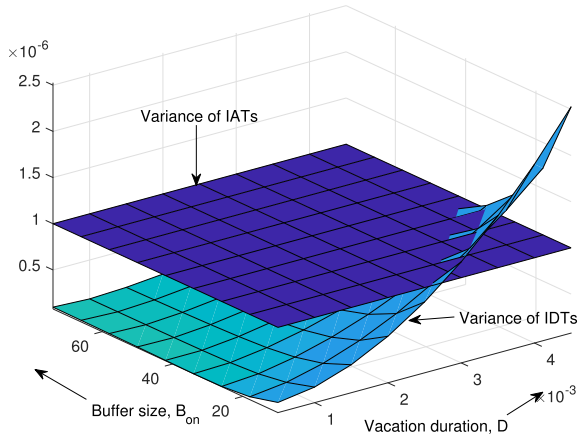

FIGURE 13. Variance of IDTs and variance of IATs: $M/\tilde{D}/1/B_{on}$ queue with deterministic vacations and $\lambda = 1000$ for different values of B_{on} and D.

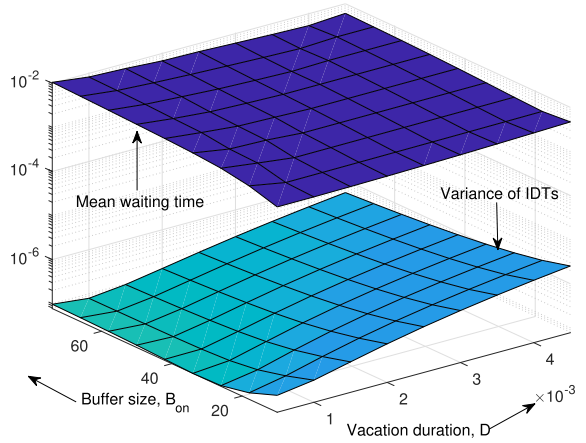

FIGURE 14. Variance of IDTs and MWT: $M/\tilde{D}/1/B_{on}$ queue with deterministic vacations and $\lambda = 1000$ for different values of B_{on} and D.

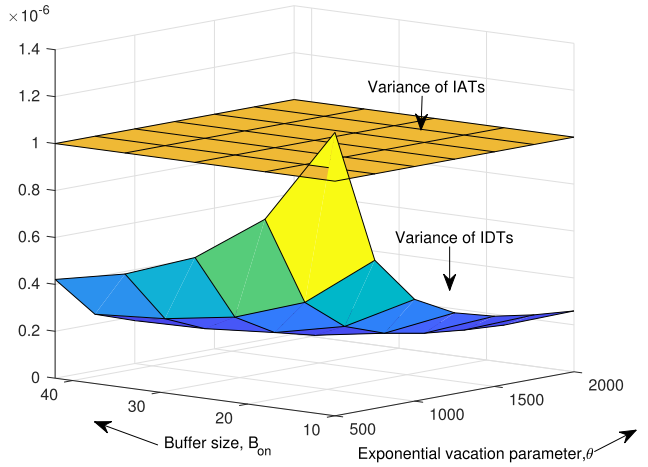

FIGURE 15. Variance of IDTs and variance of IATs: $M/\tilde{D}/1/B_{on}$ queue with exponential vacations and $\lambda = 1000$ for different values of B_{on} and θ.

and 1 $UI_{pp} = \frac{1}{2.048*10^6} = 488\ ns$. Therefore the jitter is $\frac{593.3-383.3}{488} = 0.43\ UI_{pp}$, which is less than 0.5 UI_{pp} bound defined in the standard [15]. This shows the efficiency of algorithm-B in reducing the jitter.

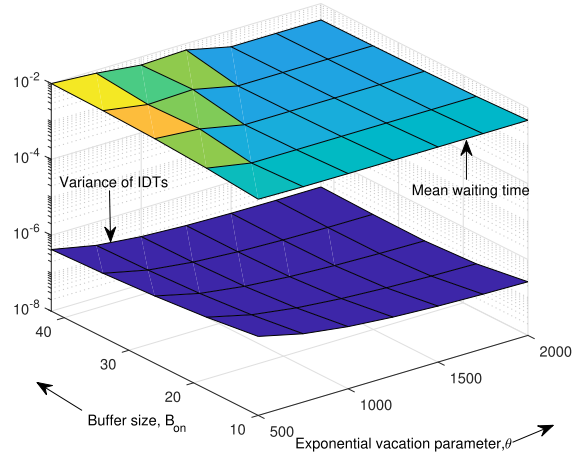

FIGURE 16. Variance of IDTs and MWT: $M/\tilde{D}/1/B_{on}$ queue with exponential vacations and $\lambda = 1000$ for different values of B_{on} and θ.

Fig. 13 shows the variance of IDTs and variance of inter-arrival times (IATs) for different values of buffer size B_{on} and vacation duration D. Fig. 14 shows the variance of IDTs and mean waiting time (MWT) as a function of buffer size B_{on} and vacation duration D. The analytical MWT is computed by using the method described in [16] and the analytical value of variance of IATs is $\frac{1}{\lambda^2} = \frac{1}{(10^3)^2} = 10^{-6}$. From Fig. 14, it can be observed that as the vacation duration D increases the variance of IDTs increases and MWT decreases. Also, for a particular value of D, the variance of IDTs decreases and MWT increases with Buffer size B_{on}. If D increases beyond some value, the variance of IDTs becomes greater than variance of IATs, as shown in Fig. 13. Similar analogy can be observed for exponential vacation plots in shown in Figs. 15 and 16. We can select proper values for B_{on} and D (θ) such that the variance of IDTs is less than the variance of IATs, and at the same time satisfying the given constraints on delay (MWT) and jitter (variance of IDTs).

VII. CONCLUSIONS

In this paper, an attempt was made to explore the statistical modelling and performance analysis of an intermediate node and the jitter buffer at the receiver NNI in the PSN through which TDM over PSN is emulated. Accordingly, both the intermediate node and the jitter buffer at the receiver node at NNI were modelled as a finite-buffer vacation queue with Poisson input, queue-length dependent service times and suitable vacation distributions.

We derived the distributions for queue-length at embedded points and later the variance of IDT which gave an idea of jitter. We can observe that all the derived analytical results closely matches with the corresponding simulated results in Figs. 7-12, which shows the correctness of mathematical analysis in the paper.

Using the method illustrated and the analysis carried out in this paper, one could choose the proper values for buffer size and vacation duration. The above parameters could be chosen such that the variance of IDTs is less than the variance of IATs, for a given arrival rate, complying to the constraints

Algorithm 1 Algorithm-B

1) Calculate $\delta \triangleq \left(\frac{B_{on}+1-m}{2B}\right) X_a$
2) **if** $\delta > I_{min} + \frac{X_a}{B}$ and $m \leq B - h$ **then**
   $s_m \leftarrow \delta + \frac{hX_a}{B}$
3) **else if** $\delta > I_{min} + \frac{X_a}{B}$ and $m > B - h$ **then**
   $s_m \leftarrow \delta$
4) **else if** $\delta < I_{min} + \frac{X_a}{B}$ and $m > B - h$ **then**
   $s_m \leftarrow \delta + I_{min}$
5) **end if**

on delay (MWT) and jitter (variance of IDTs) for applications of TDM over PSN. The delay and jitter could be matched to the allowable end-to-end delay and jitter tolerance limit as specified by the TDM standards [15].

A rigorous formulation of optimization framework for dictating the buffer size and the vacation distribution parameter for a given TDM line through the PSN, is currently being undertaken. Moreover, extending this work to the non-Poissonian arrival process would be another direction for future work.

APPENDIX

A. BRIEF DESCRIPTION OF ALGORITHM-B

In this scheduling algorithm, the service time of a head-of-the line packet is a linearly decreasing function of queue-length at its service initiation instant. If m represents the number of packets at the service initiation instant of a packet then the service time s_m of that packet is calculated as follows:

where X_a is the average inter-arrival time (IAT) of input process, B and B_{on} are the buffer sizes of offline and online algorithms, respectively, such that $B_{on} = 2B + h$, $1 \leq h < B$ and I_{min} is the minimum bound on the IDT of an offline algorithm. Reference [1] for more details on these parameters.

B. CALCULATION OF $\beta(n)$ FOR EXPONENTIALLY DISTRIBUTED VACATIONS

As described earlier, $\beta(n)$ represents probability of n arrivals to the queue during single vacation period. Let W be the random variable representing exponentially distributed (with parameter θ) vacation periods. Now, we calculate $\beta(n)$, when vacations are exponentially distributed and arrivals are according to a Poisson process with parameter λ, as follows:

$$\begin{aligned}\beta(n) &= \int_{t=0}^{\infty} \alpha(n;t) f_W(t)\, dt \\ &= \int_{t=0}^{\infty} \frac{e^{-\lambda t}(\lambda t)^k}{k!}\, \theta e^{-\theta t}\, dt \\ &= \frac{\lambda^n \theta}{(\lambda+\theta)^{n+1}} \end{aligned} \tag{54}$$

ACKNOWLEDGEMENT

The authors would like to thank the anonymous reviewers for their valuable comments and suggestions to improve the quality of the paper.

REFERENCES

[1] M. Sikha and R. Manivasakan, "Novel rate-jitter control algorithms for TDMoIP," in *Proc. IEEE 19th Nat. Conf. Commun.*, Feb. 2013, pp. 1–5.
[2] Y. Mansour and B. Patt-Shamir, "Jitter control in QoS networks," *IEEE/ACM Trans. Netw.*, vol. 9, no. 4, pp. 492–502, Aug. 2001.
[3] P. J. Burke, "The output of a queuing system," *Oper. Res.*, vol. 4, no. 6, pp. 699–704, Dec. 1956.
[4] D. J. Daley, "Queueing output processes," *Adv. Appl. Probab.*, vol. 8, no. 2, pp. 395–415, 1976.
[5] Y. Levy and U. Yechiali, "Utilization of idle time in an *M/G/*1 queueing system," *Manage. Sci.*, vol. 22, no. 2, pp. 202–211, 1975.
[6] Y. Tang, "The departure process of the *M/G/*1 queueing model with server vacation and exhaustive service discipline," *J. Appl. Probab.*, vol. 31, no. 4, pp. 1070–1082, 1994.
[7] J. M. Matzka, *Discrete Time Analysis of Multi-Server Queueing Systems in Material Handling and Service*. Karlsruhe, Germany: KIT Scientific Publishing, 2011. [Online]. Available: https://publikationen.bibliothek.kit.edu/1000023289
[8] D. Stanford and W. Fischer, "The interdeparture-time distribution for each class in the $\Sigma_i M_i/G_i/1$ queue," *Queueing Syst.*, vol. 4, no. 3, pp. 179–191, 1989.
[9] P. Nain, "Interdeparture times from a queuing system with preemptive resume priority," *Perform. Eval.*, vol. 4, no. 2, pp. 93–98, 1984.
[10] D. A. Stanford, "Interdeparture-time distributions in the non-preemptive priority $\Sigma_i M_i/G_i/1$ queue," *Perform. Eval.*, vol. 12, no. 1, pp. 43–60, 1991.
[11] D. A. Stanford and S. Drekic, "Interdeparture time distributions in $\Sigma_i M_i/G_i/1$ priority queues," *Queueing Syst.*, vol. 36, nos. 1–3, pp. 1–21, 2000.
[12] M. Kramer, "Stationary distributions in a queueing system with vacation times and limited service," *Queueing Syst.*, vol. 4, no. 1, pp. 57–68, 1989.
[13] M. B. Sikha and R. Manivasakan, "A two-queue finite-buffer polling model with limited service and state-dependent service times," in *Proc. IEEE 2nd Int. Conf. Electron., Comput. Commun. Technol.*, Jan. 2014, pp. 1–6.
[14] D. Bertsekas and J. Tsitsiklis, *Introduction to Probability*, 2nd ed. Belmont, MA, USA: Athena Scientific, 2002.
[15] *The Control of Jitter and Wander Within Digital Networks Which are Based on the 2048 kbit/s Hierarchy*, document ITU-T Rec. G.823, Mar. 1993.
[16] S. K. Bose. *Analysis of a M=G=1=K Queue With Vacations-Systems With Exhaustive Service, Multiple or Single Vacations*. Accessed: Nov. 27, 2018. [Online]. Available: https://www.iitg.ac.in/skbose/qbook/MG1K_Vacation.pdf

MADHU BABU SIKHA received the B.Tech. degree in electronics and communication engineering from JNTU Hyderabad, in 2007, the M.E. degree from the PSG College of Technology, Coimbatore, in 2009, and the Ph.D. degree from the Electrical Engineering Department, IIT Madras, in 2016. He is currently an Assistant Professor with the Department of Electronics and Communication Engineering, Malla Reddy Engineering College (Autonomous), Hyderabad, India. His research interests include MAC layer design for cognitive radio networks, stochastic queuing models for road-traffic control, statistical modeling of communications networks, and applications of queuing theory and stochastic processes.

R. MANIVASAKAN received the AMIE degree from the Institution of Engineers, India, in 1990, the M.E. degree from the College of Engineering, Anna University, Chennai, in 1993, and the Ph.D. degree from IIT Bombay, Mumbai, in 2000. He did his Postdoctoral research with The Hong Kong University of Science and Technology, from 2000 to 2002. Since 2002, he has been with the Department of Electrical Engineering, IIT Madras, Chennai. His research interests include statistical modeling, performance analysis in communication networks in general, broadband tele-traffic modeling, wireless networks, analysis of MAC protocols in particular, single photon generators, and plasmonic all-optical switches.

Experimental Evaluation and Fabrication of Composite Made Traction Gear

A. Prashanth, P.Shiva Kumar

Abstract:- Apparatus is a toothed wheel that works with others to modify the connection between the speed of a driving component and the speed of the determined parts. Outfitted gadgets can change the speed, torque, and course of a power source. The most well-known circumstance is for a rigging to work with another apparatus. This paper displays a point by point and manufacture of a high quality and minimal effort Traction equip. First The Traction outfit is demonstrated in "CATIA V5" and imported to "ANSYS" for auxiliary examination and modular investigation to decide the characteristic frequencies and mode shapes. Examination is finished by the diverse materials for gears like Cast press, carbon steel, and composite materials like Aluminum Silicon carbide results are looked at as far as possible underlined on the near execution of Traction outfit having distinctive load conditions by deciding the mistakes produced and auxiliary pressure created in the Traction design for stack conditions Using ANSYS and furthermore assess the which one is better appropriate material and manufacture utilizing that material Traction adapt is withstand and give better execution because of impacts.

Keywords: footing gear plan; auxiliary investigation; display examination; cast press; carbon steel; Aluminum Silicon carbide; ansys;

I. INTRODUCTION

Rigging is a basic segment in many of the machine parts; its implementation differs from little outfitted engine to a huge entangled aviation embellishments. Human has been in a commonplace pertaining to the possibility that the continuous twisting of either metal or wooden pieces in the forward and backward direction with an elevated abundance could burst it. He also found that the rehashed pressure can create crack within the versatile point of confinement of material which lies inside it. The exhaustion investigation for structural outlining depends on the approach which has been advancing in the course of the most recent 100 years or something like that. The simple first weakness investigation has been finished by a German mining engineer named, W.A.S. Albert who performed numerous continued stacking trials and tests on press chains. Exhaustion is the most essential disappointment mode to be considered in a mechanical outline.

Exhaustion is a gradual process of constant restricted perpetual auxiliary change showing up in materials which are subjected to various fluctuating pressure conditions. On the off chance that as far as possible does not surpass as far as possible, the body will recover its unique state. Creator ought to have a decent information of explanatory and experimental systems to get compelling outcomes in turning away disappointment. Mechanical disappointment is watched fundamentally because of exhaustion configuration in this way weakness turns into an undeniable plan, thought for some structure, for example, flying machine, rail autos, car suspension, Vehicle edge and extensions In ordinary conditions, contact weariness is a standout amongst the most widely recognized discontent modes, especially for equipment with tooth surfaces. Rigging of tooth during the process of surface mating with one another causes glue wear for the extent of the life of apparatus drive.

1.1 Dimension Specifications

Riggings mate with one another through the surface of the teeth with unmistakable geometry. Tooth Pitch is the measure of the tooth surface which can be designated indifferently as below.

- Diametrical pitch or (DP) as denoted is the proportion of the quantity of teeth and the pitch breadth of the specific machine part. Therefore, a higher DP along these lines shows better tooth dispersing. It is effectively computed by the equation DP= (N+2) ÷ OD, where N is denoted as the quantity of teeth, and OD represents the circumferential estimation.
- Round pitch (CP) is defined to be an intermediate value that lies between the points of separation from one tooth focal point to the neighboring tooth focal point. It can be estimated by the equation CP= Π ÷ DP.
- Module (M) is an ordinary apparatus train and is an estimated from the size of the tooth and teeth number of the rigging. Riggings are usually designated in inches and they acquire 'English module' to forestall perplexity. M = OD ÷ N
- Weight edge is the edge at which the tooth drive activity happens, or the edge which lies along the line of force between the cross section of a specific tooth and the digression towards the pitch hover which is at the purpose of work. Average weight edges are 14.5° or 20°.

II. LITERATURE REVIEW

V. Siva Prasad [1] in his paper substantiates the entire plan and examination of footing rigging and has clearly proposed to substitute the metallic Gear apparatuses installed in a sugarcane juice machine with the polymer apparatuses in order to lessen the weight and space of commotion. A simulated model of footing gear was created with the PRO-E Software; Further, the created Model was foreign in

Revised Manuscript Received on Janurary 25, 2019.

A. Prashanth, Associate Professor, Department of Mechanical Engineering, Malla Reddy Engineering College, Hyderabad, Telangana, India

P.Shiva Kumar,M.Tech Student, Department of Mechanical Engineering, Malla Reddy Engineering College, Hyderabad, Telangana, India

ANSYS version 10.0 for investigation by inducing it to an ordinary loading condition. The principle motivation behind his paper is the examination of the distinctive polymers specifically nylons, polycarbonates and their corresponding practical reliability checked with the corresponding mating metallic material rigging like as cast or mould press. Finishing up the investigation utilizing the FEA philosophy, it has been demonstrated that the composite riggings, if all around planned and broke down, will give the valuable properties like as a minimal effort, commotion, Weight, vibration and play out its task like the metallic apparatuses. In view of the static investigation Nylon intend are appropriate for the utilization of sugarcane juice machinery under aconstrained loading condition in examination with casted press goad gears.

VivekKaraveer[2], in his paper exhibits the analysis of pressure in mating teeth in the gear of the footing apparatus to discover greatest contact worry in the rigging tooth gear machinery. The outcome obtained from a limited component analysis got contrasted and the hypothetical Hertz condition got esteemed. The footing machinery gears are displayed and amassed in ANSYS DESIGN MODELER software and the stress examination of footing gear tooth is finished by use of the ANSYS 14.5 programming. It has also been discovered that the consequences from both Hertz condition along with Finite Element Analysis were practically identical. From his distortion example of steel and dim cast press, it could be reasoned that the distinction in between the extreme estimations of steel and CI adapt misshaping is less comparatively.

MahebubVohra[3] in his publication, has explored the features of Metallic material Cast iron and Non Metallic material Nylon. The pressure investigations carried out in the headstock regionare dissected by limited component examination. Diagnostic bowing pressure is figured by two recipe Lewis equation and AGMA recipe. Explanatory outcomes are contrasted and the limited component strategy result for approval. Finishing up the examination, we watched that limited component strategy programming ANSYS have estimations of stress dispersion were in great concurrence with the hypothetical outcomes. Other than non-metallic material can be utilized rather than metallic material in light of the fact that non-metallic material gives additional advantages like as less cost, self-greasing up, low level clamor, least possible vibration and simple assembling.

R. Yakut [5] the motivation behind the analysis is to evaluate the heap limit of PC/ABS plastic foot riggings and examination of apparatus harm. Assist in this examination convenience of PC/ABS, which is a kind of composite plastic material as footing gear was researched and was characterized that PC/ABS composite gears were tried by applying three distinctive stacking at two unique quantities of insurgencies on the FZG trials. The trial result condensed that the use of PC/ABS materials acquires favorable position numerous mechanical zone on the grounds that such materials are solid against fire, air, bright lights and holding lower moister than PA66 GFR 30 materials. Another aftereffect of this examination was that great working conditions are contained at low quantities of upset and the tooth loads. Encourage the reasonable ecological condition must be upsets and the tooth stack for gears. PC/ABS composite apparatus ought to be favored at low tooth and undesirable high power transmission.

M. Patil[6] The target of his publications is to think about the free vibration conduct of composites goad outfit utilizing limited component strategy which is otherwise called first request s hear distortion plate hypothesis (FSDT). The limited component examination has been completed for composite apparatus as a 4 gestured and 8 gestured quadrilateral component with every hub has five level of flexibility. Limited component detailing of composite rigging is displayed and coded utilizing MATLAB. In light of the numerical examination which is done for of goad adapt the accompanying an imperative conclusion can be entitled. The created MATLAB code is approved with the accessible outcome and it can be inferred that the present FE software code result are in great concurrence with those that were referred. Principal frequencies acquired for composite goad outfit utilizing MATLAB are exhibited. It has also been discovered that normal recurrence increments with increment in fiber introduction.

NitinKapoor[4]In his paper publication the parametric model of differential machinery setup is produced utilizing a few constrained parameters which includes number of teeth, Pressure edge, point of helix, tooth thickness & module) in CATIA-V5version and weight examination of the same differential apparatus box for various material which is inclusive of Aluminum compound, combination steel, cast press, Glass filled Polyamide, under static stacking conditions utilizing the FEA software. The contextual investigation demonstrates that the compositescan be utilized viably instead of metallic material in light of the fact that the heaviness of Glass embedded Polyamide composite material of differential system is decreased by 60% contrasting and the conventional materials (Aluminum compound, Alloy Steel, Casted press). Along these lines, we infer that Glass embedded Polyamide Composite material is chosen as one of the best material for differential apparatus unit.

A.D. Dighe[7]in this examination the relative execution goad rigging of 30% Glass embedded PA66 and 30% Glass embedded PEEK was researched at various torque and speed. Wear trial of the goad equip sets and the examination goad outfit tooth were performed on a FZG testing machine. A weight by reduction is estimated by an amount of 0.0001g delicate measuring machine and the gear tooth temperature of apparatus is estimated by using an Impact infrared thermometer. Post the testing, the after effect of PA66 GF30 composite apparatuses and PEEK GF30 composite gears are at various torque values and speed values. The tooth temperature gradually increments with incremental torque and expanded temperature gradient which exhibited a warm softening of apparatus tooth which additionally builds particular wear rate.

Pradeep Kumar Singh [8]in his paper utilizes ANSYS module related to workbench programming, twisting pressure, contact pressure and static load executed on the tooth of footing gear drive setup is evaluated. The Hertz

hypothesis and the Lewis equation likewise are utilized for hypothetical figuring of the contact pressure and twisting worry of goad outfit. We watched that Ideally comes about acquired by Le wis recipe and Hertz condition are practically identical with limited component investigation of goad outfit, remembering the correlation we can reason that the limited component expository outcome can be better as a critical thinking programming and utilized for other examining reason.

Mrs. C.M. Meenakshi (2012) [9]the target of paper is to contemplate the different pressure condition of footing gear. They figured the digressive and spiral powers which follows up on different point upon that premise we can break down by applying the powers. By utilizing Ansys programming twisting pressure and contact weight on the tooth of goad equip drive is discovered Gears are mechanical machinery components used as a transmit control device between turning shafts by methods for commitment of projection called teeth. Apparatuses are most normal methods for transmitting power in the wooden mechanical world. They change from a small size utilized as a part of watches to bigger riggings utilized as a part of huge speed reducers, connect lifting system and rail street turn table drive. The riggings are indispensable components of principle and helper instrument in numerous machines, for example, cars, tractors, metal cutting machine devices moving plants facilitating and transmitting and transporting apparatus, enormous motors and so forth.

Atul Kumar (2013)[10]Says that footing gears wear either because of rubbing activity that happens between the fit riggings or by undesirable components like unclean particles, metallic sections, and so forth which diminishes its productivity and administration life. It is dependably a testing assignment to decide the rest of the lifecycle of a segment or the quality of a segment once wear has happened on the tooth surface. This publication introduces a use of figuring out methodology for recreation of the goad outfit 3D CAD display utilizing examined information. An apparatus has been filtered utilizing PICZA 3D laser scanner (RolandLPX60).

M. Raja Roy (2014) [11]Made an endeavor to outline about the contact stresses created in a mating surface of the footing gear which has an involute teeth. A couple of footing gears were taken from a machinery setup and continued proceeding forward to figure contact weights on their teeth. The Contact disappointment in gears is presently anticipated by contrasting the ascertained Hertz contact worry with tentatively decided permissible qualities for the given material. The strategy for figuring gear contact worry by Hertz's condition initially inferred for contact between two chambers. Systematically these contact stresses are figured for various module, and these outcomes are contrasted and the outcomes got in demonstrating examination in ANSYS.

III. MODELING IN CATIA V5

Computer Aided Three-dimensional Interactive Application abbreviated as CATIA, is a multi-stage CAD/CAM/CAE business programming suite created by the popular French organization called Assault Systems. Written completely in the C++ programming dialect, CATIA is the basic foundation of the Assault Systems lifecycle administrative programming suite.

CATIA also offers a solution for shape configurations, styling formats for the same, surfacing the work process and their representation to make, change, and approve complex innovative shapes from modern outline techniques to a Class-A surfacing with the so called ICEM surfacing innovations. CATIA bolsters numerous phases of modeling plan whether began without any preparation or from any 2D outlines. CATIA can read through and create a STEP design documents for figuring out and surface reuse properties.

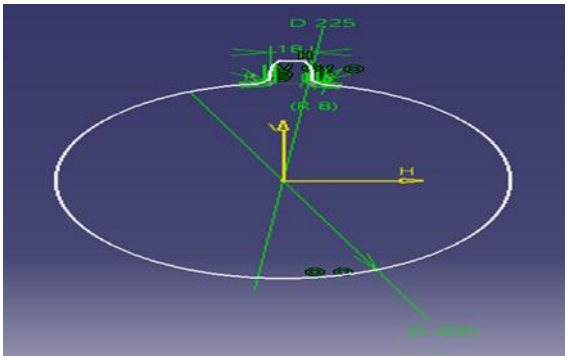

Figure.1. sketch model

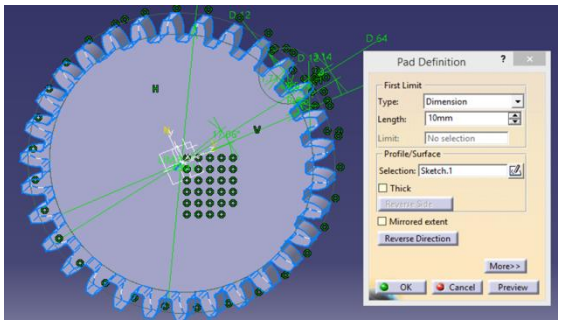

Figure.2. Portray drawing of model 3d display

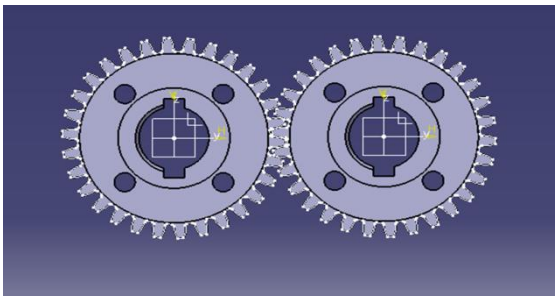

Figure.3. Assembly of Gears

IV. MATERIAL DATA

4.1. Gray Cast Iron

Young's Modulus	$1.1e^{+005}$MPa
Poisson's Ratio	0.28
Bulk Modulus	83333 MPa
Shear Modulus	42969 MPa

4.2. Aluminum Silicon Carbide

Young's Modulus	$1.5e^{+005}$MPa
Poisson's Ratio	0.3

Bulk Modulus	1.25e^{+005}MPa
Shear Modulus	57692 MPa
Density	2.81e-006 kg mm^{-3}

4.3. Carbon steel

Young's Modulus	2.012e+011
Poisson's Ratio	0.3
Bulk Modulus	1.6767e+011
Shear Modulus	7.7385e+010
Density	7.8334e-006 kg m^-3

V. ANALYSIS OF TRACTION GEAR USING ANSYS

ANSYS is one of the broadly used limited component analysis software design, which empowers the architects worldwide to perform astoundingly with the complementary accomplishments:

- Build a specific PC model or exchange CAD model of concrete structures, building items, construction segments or frameworks
- Apply working conditions like load, deviations with respect to the dimensions or other outline execution conditions.
- Study the physical reactions, for example, feelings of anxiety, stress level variations, temperatures dispersions or the effect of electromagnetic fields, weather waves.
- Upgrade an outline from the get-go in the improvement procedure to decrease generation costs.
- A run of the mill ANSYS investigation software has three unmistakable advancements.
- Pre Processor.

5.1 Ansys Results For Aluminum Silicon Carabid

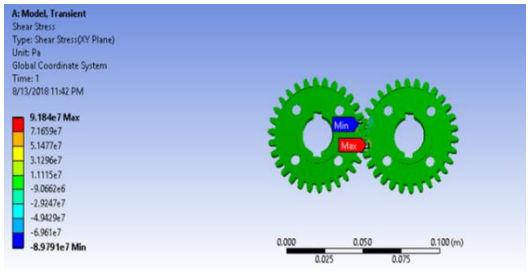

Figure.4. Total Deformation for AlSiC

The figure 4 shows the Total Deformation for Aluminum Silicon Carabid in traction gear with a maximum value of 7.1883e^{-005}MPa and minimum value of 2.0737e^{-005}MPa.

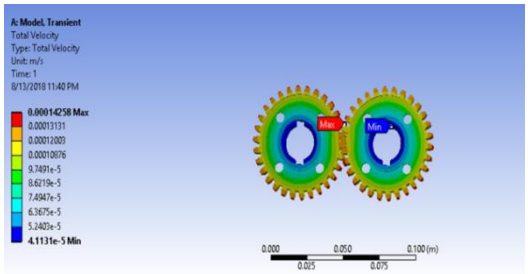

Figure.5. Total velocity for AlSiC

The figure 5 shows the Total velocity for AlSiC in traction gear with a maximum value of 4.1131e^{-005} m/s and minimum value of 1.4258e^{-004} m/s.

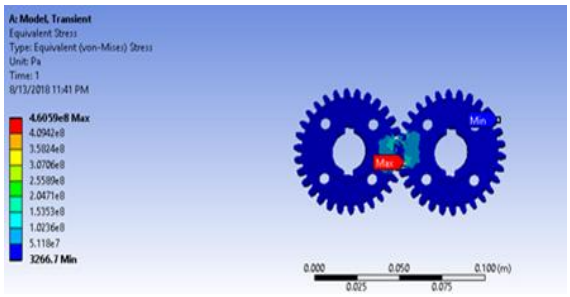

Figure.6. Equivalent Stress for AlSiC

The figure 6 shows the Equivalent Stress for AlSiC in traction gear with a maximum value of 4.6059e^{+008}MPa and minimum value of 3266.7 MPa.

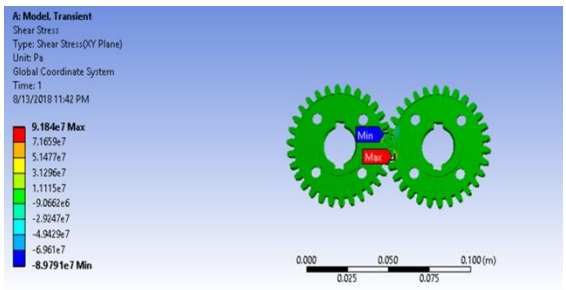

Figure.7. Shear Stress for AlSiC

The figure 7 shows the Shear Stress for AlSiC in traction gear with a maximum value of 9.184e^{+007} MPa and minimum value of -8.9791e^{+007}MPa.

5.2. Comparing the Ansys Results

Table.1. Comparison of ansys results

Object name	*Grey cast iron*	*Carbon steel*	*Alsic*
Total deformation (mm)	3.6832e^{-003}	1.2851e^{-004}	7.1883e^{-005}
Total velocity (m/s)	7.3055e^{-003}	7.3055e^{-003}	1.4258e^{-004}
Equivalent stress (mpa)	4.5452e^{+008}	4.6106e^{+008}	4.6059e^{+008}
Shear stress (mpa)	8.5543e^{+007}	9.3032e^{+007}	9.184e^{+007}

- The total deformation of traction gear for AlSiC is very less (7.1883e^{-005} mm) when compared to other materials.
- The Shear stress produced for AlSiC is of 9.184e^{+007} MPa which is much more than Grey Cast Iron but very slightly less than Carbon Steel.
- Total velocity produced by traction gear for AlSiC is more than Carbon Steel and Grey Cast Iron

Published By:
Blue Eyes Intelligence Engineering
& Sciences Publication

- Also the Equivalent Stress produced by AlSiC material is more i.e., Alsic has more stress bearing capacity than the carbon steel and the original material, Grey cast iron.

Therefore Aluminum Silicon Carabid is best material for this project work. A test piece of traction gear is manufactured and then experimental tests are conducted on the test piece to validate the Ansys results.

VI. EXPERIMENTAL RESULTS FOR AlSiC

6.1. Impact Test

Table.2. impact test results for AlSiC

Observed Values (joules)	*Al-SiC*
Impact 1	32
Impact 2	0
Impact 3	0
Average	32

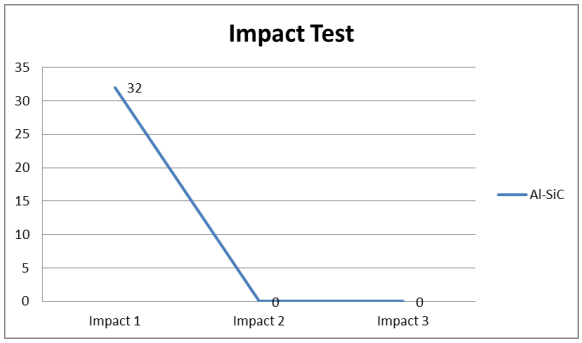

Figure.8. Impact Stress graph for AlSiC

6.2. Shear Test

Input data		
Material specification	Aluminium silicon carbide	
Specimen piece	Gears sample piece	
Output data		
Al-SiC	Applied force (KN)	Shear Stress (MPa)
	12	$9.0135*10^4$

VII. CONCLUSION

At the point when the mankind began utilizing wheels they found the prerequisite of a regular wheel which can diminish or increment the rotational speed so the rigging was created. The greater part of the power transmission hardware's comprise of apparatus gatherings; commonly outfits assume a critical part. In this examination, to comprehend the conduct of rigging materials as for stresses Finite Element Analyses were completed.

- Based on that review, the examination of aluminum silicon carbide, Carbide steel, cast press is dissected in the use of rigging confine which is utilized transmission framework.
- It was discovered that aluminum silicon carbide have great obstruction qualities when contrasted with different materials.
- So from these examination comes about, we presume that, the pressure incited, aluminum silicon carbide twisting of footing gear is less when contrasted with the other material rigging.
- In display examination aluminum silicon carbide material gave great withstanding values comparing with other materials so finally aluminum silicon carbide is better suitable materials for gears

FUTURE SCOPE

In the present undertaking, auxiliary and model investigation of footing gear is finished by various materials and carbon epoxy gave best outcomes. There is extent of utilizing other kind of composite materials other than said materials and better outcomes can be accomplished, can build the quality and thus increment the life of riggings and can be utilized as a part of different ventures for better outcomes.

ACKNOWLEDGEMENT

The authors gratefully acknowledge the support given by Dr. S. Sudhakara Reddy, beloved principal of Mallareddy Engineering College for facilitating the necessary needs for the successful completion of project work. Authors gratefully acknowledge Dr. S. Gunasekharan, Head of the Mechanical Department and our Project Coordinator, Dr. YogeshMadaria, Assistant Professor. Also would like to take this opportunity to thank my supervisor, assistant professor A. Prashanth for his valuable guidance, encouragement and assistance. Authors gratefully acknowledge the help provided by the Axis inspection solution lab and CNC machining company.

REFERENCES

1. V. Siva Prasad, Syed AltafHussain, V.Pandurangadu, K.PalaniKumar. Demonstrating and Analysis of Spur Gear for Sugarcane Juice Machine under Static Load Condition by Using FEA. Global Journal of Modern Engineering Research (2012), 2(4):2862-2866.
2. VivekKaraveer, AshishMogrekar and PremanReynold Joseph T (2013), "Demonstrating and Finite Element Analysis of Spur Gear", International Journal of Current Engineering and Technology, ISSN 2277-4106.
3. MahebubVohra, Prof. Kevin Vyas "Similar Finite Element Analysis of Metallic and non-Metallic goad adapt", May-June 2014, IOSR Journal of Mechanical and Civil Engineering, 11(3):136-145.
4. NitinKapoor, Pradeep Kumar, Rahul Garg and Ram Bhool. " ParametricModeling and Weight Analysis of Glass Filled Polyamide Composite Differential Gearbox", International Journal of Science, Engineering and Technology Research, 2014,3(6).
5. Yakut, H. Duzcukoglu, M. T. Demirci, " The heap limit of PC/ABS goad apparatuses and examination of rigging harm", Archives of Materials science and Engineering, November 2009,
6. M. Patil, S.Herakal, S. B. Kerur, "Dynamic Ana lysis of Composite goad adapt", May-2014, Proceeedings of third IRF International Conference..
7. A.D. Dighe, A. K. Mishra, V. D. Wakchaure," Investigation of Wear Resistance and Torque Transmission Capacity of Glass Filled Polyamide and PEEK composite goad gears", Feb-2014, International Journal of Engineering and Advance Technology, Vol-3/3.

8. Pradeep Kumar Singh, M. Gautam, Gangasagar and ShyamBihariLal," July-2014, International Journal of Mechanical Engineering and Robotics Research, Vol
9. Mrs. C.M. Meenakshi, Akash Kumar, ApoorvaPriyadarshi,Digant Kumar Dash and Hare Krishna., Analysis of Spur Gear Using Finite Element Analysis, Middle-East Journal of Scientific Research (12): 1672-1674, 2012 ISSN 1990-9233
10. Atul Kumar, P. K. Jain and P. M. Patha., Comparative Finite Element Analysis of Reconstructed New and Worn Tooth of Spur Gear, Proceedings of the first International and sixteenth National Conference on Machines and Mechanisms (iNaCoMM2013), IIT Roorkee, India, Dec 18-20 2013
11. Raja Roy,S. PhaniKumar,D.S. Sai Ra vi K iran., Contact weight investigation of goad outfit utilizing FEAM., International Journal of Advanced Engineering Applications, Vol.7, Iss.3, pp.27-41 (2014)
12. Darle W Dudley (1954), Practical Gear Design, McGraw-Hill Book Company..
13. Khurmi Gupta R S (2000), "Machine Design", Khanna Publication..
14. Khurmi R S (1997), "Hypothesis of Machine", Khanna Publication..
15. Machine Design Data Book (2003), PSG Publication.
16. Rattan S (1998), "Hypothesis of Machines", DhanpatRai Publication.
17. Romlay F R M (2008), "Displaying of a Surface Contact Stress for Spur Gear Mechanism Using Static and Transient Finite Element Method", Journal of Structural Durability and Health Monitoring (SDHM), Vol. 4, No. 1, Tech Science Press..
18. Shanavas S (2013), "Stress Analysis of Composite Spur Gear", International Journal of Engineering Research and Technology (IJERT), ISSN: 2278-0181.
19. Shinde S P, N ikamAn and Mulla T S (2012), "Static Analysis of Spur Gear Using Finite Element Analysis", IOSR Journal of Mechanical and Civil Engineering (IOSR-JMCE), pp. 26-31, ISSN: 2278-1684.
20. Lin Tengjiao, Ou H., Li Runfang. 2007. A limited component strategy for 3D static and dynamic contact/affect investigation of rigging drives, Computer Methods in Applied Mechanics and Engineering, 196(9-12):1716-1728.

Effect of Process Parameters on Pcbn Tool Wear Rate in Friction Stir Process of Aluminium 7075 Sic

A. Sarath Kumar, Dr. K. Jayanendra Babu

Abstract: ***Friction state process (FSP) a variant of friction stir welding process (FSW), is used to friction process of Metal Matrix composites. Since Aluminium Alloy (AA) 7075 SiC is not been premeditated on FSP,effort has been made to explore the result of a range of process parameters on tool wear rate(TWR)in FSP by Taguchi method, research paper. The Process parameters that careful study of rotational speed, translational speed and tool pin diameter. Polycrystalline Cubic Boron Nitride (PCBN) tool of 6 mm, 7 mm and 8 mm diameters are used. The research is done by L_9 (3^4) orthogonal array. The eroded length of tool, volume measurements and the tool wear rate is calculated for a variety of combinations of factors and levels. The results of experiments systematically discussed and to achieve process parameters on tool wear rate is determined.***

Keywords: ***FSP, AA 7075SiC, TWR, Taguchi method and FSW.***

I. INTRODUCTION

FSP is current research in industry and academic Research and is an alternate process of friction stir welding. FSP generally use to manufacture automobile, aerospace and medical parts. The fundamental principle which is used in friction stir welding. The friction stir processing is differentiated FSW by means of parameters similar to tool rotation, tool travel (translational) speed and number of passes. The FSP characterized by ability to process both conductive and semi conductive materials which are having high surface accuracy regardless of material stiffness.

The FSP is preferable especially while processing of difficult-to-cut material because of low efficiency in nature and precision. Small volumetric material inference in FSP provides sustainable opportunity for manufacturing of small accurate parts for automobile and aeroplanes [2]. The benefit of FSP is to process with less consumption of material. The forces are extremely small due to tool and workpiece come closer in contact throughout the process, less friction forces on them. The other advantages of FSP include low setup cost, low speed ratio.

The drawback is formation of layer over heat affected zone upon the processed surface. The fact, it is impossible to take away all the molten part on the workpiece, thin layer of sediment, molten material deposit on the workpiece surface, which re-solidifies during cooling [3.4]. The effect on process parameters, particle dispersion and hardness in AA 7075 reinforced with TiB_2 micro particles and reported 50% add to the micro hardness compared with parent material [5].The hardness and wear resistance a variety of combination of travel speed, amount of passes and rotational speed for AA 7075 B_4C surface composite fabricated using FSP has been studied [1, 2].

This paper present study the effect of dissimilar process parameter with combinations on TWR in FSP of AA 7075 SiC alloy by Taguchi method, covering volumetric measurements, worn out length of the tool and tool wear rate are calculated. The influence depends on process parameters and behavior oftool and alloy material like AA7075 alloy are considered and discuss ornately.

II. TOOL WEAR RATE

The wear ratio, defined as the ratio of amount of tool wear to amount of removal of workpiece [7]. The method that is recognized to evaluate tool wear ratio by means of calibration of weight, length and total volume correspondingly. The common one by calculating volumetric wear ratio (v), usually variations of weight are taken into measurement and then converted into volumes by material density.

The weight change is small make to measure it precisely in the method of FSP. Significant to measure and analyze material removal directly [1].

Tool Wear Rate (TWR) calculated [3].

$$TWR = V_W / \text{ tmm}^3/\text{min} \quad (1)$$

And

$$V_W = \frac{\pi D_W^2 L_W}{4} \text{ mm}^3 \quad (2)$$

Where,

V_W = Volume of tool wear

D_w= Diameter of the tool wear

L_w = Length of the tool wear

t = Machining time of the surface.

III. TAGUCHI METHODOLOGY

The main objective is to cram of TWR in FSP of surface texture on a complex to processing material order to do so. Taguchi's robust design method is used. Apart from significant the wear tendency of tool, the method also helps in optimizing the process parameters for FSP. The main paradigm of robust design method to choose levels of design factors to make product or process performance concentrated to uncontrollable variations such as manufacturing variations, deterioration and environmental

Revised Manuscript Received on Janurary 25, 2019.

A. Sarath Kumar, Asst. Professor, MED, MREC (A), Hyderabad,Telangana,India.
Research Scholar, MED, K L University, Guntur, AP, India
Dr. K. JayanendraBabu, Professor, MED, K L University, Guntur, AP, India.

variations. Following are the steps in Taguchi robust design methodology.

- Identify major function, side effects and failure modes.
- Recognize the testing parameters and then to summarize the quality loss as well as noise factors.
- Discover the quality characteristic which is about to observe and objective role to be minimized.
- Choice of control factors and its levels.
- Design of matrix experiment.
- Conducting the Matrix experiment.
- Analyze the data, decide optimum levels of control factors and forecast the performance under these levels.
- Conduct the confirmation experiment and future scope.

IV. EXPERIMENTAL SETUP

Fig 1: FSP Machine with tool set up

Fig 2:PCBN tool with conical pin

Make: HMT Machine used for conduct the experiments using PCBN Tool with 6 mm, 7 mm and 8 mm diameters are used to process on AA7075 SiC.Literature review suggests the PCBN tool has not yet been in use to process AA 7075 SiC material surface.

T W R chosen as output characteristic is observed and calculated as per equation (1) and (2) correspondingly. Since TWR ought to be as least as possible, output characteristic falls under the category of "smaller-the-better"(S-type) quality characteristic, evaluate the signal to noise (S/N) ratio. The principal function is to be optimized to enhance (S/N) ratio.

Signal to noise ratio is been calculate by

$$\eta = -10 \log_{10}[\tfrac{1}{n} (y_i^2)] \quad (3)$$

Where,

η = (S/N) ratio

y_i= Interpretation

n = number of interpretation

Process parameters between their levels are to be used in experimental process are listed in Table 1.

Table1: Process parameters and their levels

FACTORS	LEVELS		
	1	**2**	**3**
TOOL DIAMETER (mm)	6	7	8
ROTATIONAL SPEED, RPM	800	900	1000
TRANSLATIONAL SPEED, mm/min	20	25	30
TILT ANGLE, Degrees	0°	1°	2°

L_9 (3^4) orthogonal Array is selected for hauling out experimentation as it best suits the input requirements. Experimental plan is shown in Table 2.

Table 2: Experimental Design

EXP No.	FACTORS			
	ROTATIONAL SPEED, RPM	**TRANSLATIONAL SPEED, mm/min**	**TOOLPIN DIAMETER,mm**	**TILT ANGLE, Degrees**
1	800	20	6	0°
2	800	25	7	1°
3	800	30	8	2°
4	900	20	7	2°
5	900	25	8	0°
6	900	30	6	1°
7	1000	20	8	1°
8	1000	25	6	2°
9	1000	30	7	0°

V. RESULT AND DISCUSSION

Optimal parameters for surface is desired to shape on AA7075 SiC alloy using PCBN tool as in figure 1 is investigated by performing the nine investigations while experimental design represented in Table 2.

Each experiment shows wear length and wear diameter of the tool are noted from the friction stir process. The output characteristic TWR is calculated using formula shown in equations 1 & 2 respectively. Obtained results for nine experiments, along with S/N ratios are given in Table 3.

Table 3 Experimental Results.

EXP No.	TWR (mm^3/min)	Signal/Noise Ratio (η) dB
1	0.001507	46.43773
2	0.002399	42.3994
3	0.003688	38.66418
4	0.002301	42.76167
5	0.003529	39.04697
6	0.00141	47.01562
7	0.003621	38.82343
8	0.001487	46.55378
9	0.002386	42.44659
TOTAL	0.022328	374.1494
AVERAGE	0.002481	42.68326

S/N Ratio obtained after each experiment, further analyzed, the objective function defined and the optimum set of process parameters are selected as shown in Table 4 and Figure 2.

Table 4: S/N ratio various levels of process parameters

	ROTATIONAL SPEED, RPM	TRANSLATIONAL SPEED, mm/min	TOOL PIN DIAMETER, mm	TILT ANGLE, Degrees
LEVEL 1	42.5	42.64	42.64	42.60
LEVEL 2	42.94	42.67	42.54	42.75
LEVEL 3	42.61	42.71	38.848	42.66

Fig 3: Tool Wear

The optimum mixture of process parameters rotational speed of 900 rpm, translational speed of 30 mm/min, tool pin diameter of 6 mm and tilt angle of 1°.

Theoretical S/N Ratio for optimum grouping is forecasted as 47.01562 dB.

The confirmation experiment carried out optimum settings of factors and levels to validate the experimentation. The TWR is too resolute with equations 1 & 2 shown in Table 5. S/N ratio value related to conformation experiment is calculated and is compared with the predicted one. Table 6 shows the predicted S/N ratio is in nearest proximity with actual one, thus validation of research study.

As shown in Table 7, the optimum grouping of factors as well as levels brought an improvement of 0.000137 mm^3/minute in TWR. The main function of maximizing the S/N ratio is accomplished i.e., from 46.43 to 47.92 to dB.

Table 5: Conformation experiment and its result

Rotational speed, rpm	Translational speed, mm/rev	Tool pin diameter, mm	Tilt angle, degrees	Twr (mm^3/min)
900	30	6	1°	0.01

Table 6: Predicted and Conformed S/N ratio

	S/N Ratio (η)
Predicted	47.01562
Conformed	47.265589

Table 7: Improvement

	Starting Condition	Optimum Condition	Improvement
TWR	0.001507	0.00137	0.000137
η	46.43773	47.92393	1.4862

VI. CONCLUSIONS

Taguchi's Robust Design methodology has been the effect of machining parameters similar to rotational speed, translational speed and tool pin diameter over TWR in friction stir process of AA 7075 SiC alloy using PCBN tool of 6 mm, 7 mm, and 8 mm diameter. This research study not only provides the best arrangement of process parameters, but also the wear trend of tool in different arrangement of process parameters.

(i) Theoptimal 'process parameters' for optimizing TWRbased on Taguchi's Robust Design Method for FSP of AA 7075 SiC alloy which includes rotational speed of 900 rpm, translational speed of 30 mm/min, tooltip diameter of 6 mm and tilt angle of 1°. The lowest tool wear is being attributed to the rotational speed of 800 rpm associated by medium translational speed of 20 mm/min and tilt angle of 0°.

(ii) A trend of mild tool wear is observed in experimentations of 1, 6 & 8 respectively wherever tool diameter is least in experimentation i.e., 6 mm is observed as the tool pin diameter decreases, tool wear reduces.

(iii) It is found that, tool wear is rising with increased tool diameter of 8 mm as shown in experimentations of 3, 5 & 7 respectively.

(iv) Conformation experiment displays the TWR indeed reduced i.e., 0.00137 mm^3/min with optimum arrangement of various factors and levels in FSP of AA7075 SiC alloy. The TWR achieved at the instance of beginning of experimentation is 0.001507 mm^3/min.Finally, an improvement in TWR of 0.000137 mm^3/min is accomplished by the usage of optimal parameters.

(v) The primary function of experimentation to maximize the S/N ratio is also obtained at the last stage of conformation experiment. The S/N ratio is improved by an amount of 0.696.

Concluded that with all these group of process parameters considered for study, diameter of tool pin which influences

the TWR. However, the other parameters like contact tool workpiece, carbon precipitation which aims to be known their effect on TWR.

VII. ACKNOWLEDGEMENT

I would like to convey my thanksgiving Mr. Rajukar Reddy, M/s Sri Venkateswara Industries, Balanagar, Hyderabad who provided the FSP machine for experimentation purpose and also putting the efforts to fabricate the PCBN tool.

Dr. Nagabhushana Ramesh N. completed his B.E in Mechanical Engineering (1986) and M.E in Production Engineering from Osmania University, Hyderabad, A.P, and India, (1994) Ph.D in Mechanical Engineering with specialization as Production Engineering in the field of Electro Discharge Sawing (Electro Discharge Machining) from Osmania University, Hyderabad, A.P, India (2007). TOTAL EXPERIENCE 30, Patent 01, International Science Index 01,Papers Published in International Journals: 18 No's National Journals: 01 No's, International Conferences: 21 No's, National Conferences: 16 No's, Guided for Ph.D awarded:02 No's, Presently Guiding for the Ph.D:01 No's.

REFERENCES

1. Nalbant, H.Gokkaya and G. Sur, "Application of Taguchi Method in the Optimization of cutting Parameters for Surface Roughness in Turning", Materials and Design, Vol. 28, pp. 1379-1385, 2007
2. R.S. Mishra, P. Sarathi De, N. Kumar, Friction stir welding and processing, Science and Engineering, Springer, New York, New York, 2014.
3. M. Kaladhar, K. Venkatasubbaiah, andCh. Srinivasa Rao, "Determination of Optimum Process Parameter During Turning of AISI 304 Austenitic Stainless Steel using Taguchi Method and ANOVA", International Journal of Lean Thinking, Volume 3, Issue 1, pp. 1-19,2012.
4. Soheyl Soleymani, Amir Abdollah-zadeh, and Sima Ahmad Alidokht, Improvement in tribological properties of surface layer of an Al alloy by friction stir processing, Journal of surface engineered materials and advanced technology, (2011), 1, 95-100.
5. C. Lorenzo-Martin, O.O. Ajayi, Rapid surface hardening and enhanced tribological performance of 4140 steel by friction stir processing, to appear on Wear, 2015.
6. Ranganth M. s., Vipin, Nand Kumar and Rakesh Kumar, "Experimental Analysis of Surface Roughness in CNC Turning of Aluminium Using Response Surface Methodology", International Journal of Advance Research and Innovation, vol 3, Issue 1, pp. 45-49, 2015
7. Neelimadevi, C., Mahesh, V. and Selvaraj, N., Mechanical characterization of aluminium silicon carbide composite, *Int. J. App. Eng. Res*., 1(4), 793-799(2011).

Published By:
Blue Eyes Intelligence Engineering
& Sciences Publication

Experimental Investigation on Lightweight Concrete Slabs

J. Selwyn Babu, J. Rex

Abstract: ***The popularity of Lightweight Concrete (LWC) is due to its least density factor and high insulation capability. Use of LWC can diminish the null load of structural members significantly. The rise in the price of civil construction materials, depletionand environmental exploitation has set an alarm for an alternative material. In this study, the normal coarse particulates (CA) was replaced by coconut shell (CS). Since specific gravity of both the materials is different the replacement was done on the volume basis. The properties of coconut shell material which is available in surplus amount and concrete ingredients were studied. Coconut Shell used in concrete has high effectuality on account of its flat surface on one side. In this paper, a study has been made on the flexural performance of lightweight concrete slabs. Slab specimens of size 1300 x 500 x 70mm were designed and casted for various replacement ratios (0%, 25%, 50%, 75% and 100%) of CS. Four point loading test was performed on slabs and parameters such as ultimate moment capacity, ductility factor, energy absorption, stiffness, and cracking pattern were observed.***

Keywords: ***Light weight Concrete, Coconut shell, CA Replacement, Four point Load Test.***

I. INTRODUCTION

There has been a growing interest in the use of lightweight concrete (LWC) since it has moremerits over the conventional concrete which is obtained from natural particulates. This concretes densityusually ranges from 1400 to 2000 kg/m^{3}whereas for normal-weight concrete (NWC) it is 2400 kg/m^3. Eight out of the ten peak producers of Coconut are in the Asia Pacific region where India contributes to 75% of the world's coconut hub. The third major coconut producing nation India has a yearly production of 90% s from Southern India. The average yearly production of coconut is approximate around 15 billion nuts in India. Whenever lightweight particulates are abundantly available locally they can be used as a construction material which reduces the dead load of the structure. In recent years researchers are focussing on achieving a composite material with good durability, low density and high strength.

The demand for modern construction materials with lightweight particulate is growing due to the benefit that lesser density of materials used results in smaller cross section of structural elements and correspondingly the size of foundation is also considerably reduced.

Going forward,the mechanical behaviour of lightweight concrete prepared using coconut shell as partial and full replacement to normal coarse particulate was studied. The effect of lightweight concrete slabs the loss of strength of slabs due to usage of light weight particulates in the concretewould be useful for further research.

II. MATERIALS USED

Conventionally usedordinary Portland Cement (OPC) of Grade 53 meeting the requirement to Indian Standard IS 12269 (1987) was used as binding material. River side sand confirming to IS 383 (1970) of zone III was used as the fine particulate for the experimental work. Normal stone particulate of maximum size not exceeding 20 mm was used as coarse particulate for concrete. Coconut shell (CS) from the nearby oil mills were collected and were well seasoned. The seasoned shells were crushed manually , sieved and collected. The water from the institute was used for preparing the concrete and curing.

III. MIX PROPORTIONS

The mix design of lightweight concrete is generally recognized by employing trivial mixes (Shetty M S, 2005). Previously it was explored that the cement quantityranges between 285 and 510 kg/m^3 and the substitution of coarse particulate to CS have to be done on volumetric basis. An effort is made by manipulating a concrete mix for a 28 day distinctive compressive strength of 20 N/mm^2 as per IS 10262 (2009) and supplanting the coarse particulate with 25, 50, 75 & 100% of CS on volume basis. The particulars of the various mix proportions are given in Table 1. The proportional mixture was nominated as M0 for control concrete (no replacement of CS), M1, M2, M3 and M4 for 25, 50, 75 and 100% surrogates respectively. Due to elevated water absorption capability CS particulates were used in soaked surface dry (SSD) condition i.e., it was soaked in water for 24 hours and air dried before mixing.

Table 1. Mix Proportions

Mix No	Mix Proportion (C:FA:CA:CS)	Cement Content (kg/m^3)	W/C ratio
M0	1:1.41:2.67 (2.67 = C.A)	425	0.5
M1	1:1.41:2:0.3 (2.3 = 2CA+ 0.3CS)	425	0.5
M2	1:1.41:1.33:0.61 (1.94 = 1.33CA + 0.61CS)	425	0.5
M3	1:1.41:0.67:0.91 (1.58 = 0.67CA + 0.91CS)	425	0.5
M4	1:1.41:0:1.21 (1.21 = CS)	425	0.5

Revised Manuscript Received on Janurary 25, 2019.

Dr. J. Selwyn Babu,Professor, Department of civil Engineering, MREC (A), Hyderabad – 500 100, Telangana, India

Dr. J. Rex,Associate Professor, Department of civil Engineering, MREC (A), Hyderabad – 500 100, Telangana, India.

Test Specimens

The flexural performance of the slabs, their size and the reinforcementunder a UDL. The dimension of the test sample was selected in order to achieve the requirements of the study with the smallest practical dimensions of specimen. 1300 X 500 X 70mm slabs were designated, which gave a center-to-center span of 1000mm. FourNos.of 8mm bars were placed in the slab with a 150mm center to center spacing. Six nos. of 6mm bars at 250mm spacingused as thedistribution reinforcement and with 20mmclear cover.

Mixing, Casting, and Curing

The base materials chosen as ingredients for the concrete block were assorted in an mixer of 0.5tonne capacity. The moulds were prepared and placed on the table vibrator and molten concrete mix was poured in two layers and vibrated to make a uniform mix. Three concrete cubes 150mm x 150mm, werecast to determine the compressive strength. The slabs and cubes were subjecting to curing with wet burlapfor 24 hours andprior to demoulding in the curing tanks for 28 days using wet gunny bags.

IV. MECHANICAL PROPERTIES

Compression testing machine (CTM) of capacity 2000KN was used to test the specimens under continuous application of loadat the increase in a constant rate. While examining the specimens, precautions were taken to ensure the application axial loading. The compression test was in accordance withIS 516:1959 and IS 5816:1999 respectively.

Table 2. Mechanical properties of concrete

Mix No.	Replacement of CA With CS	Compressive Strength (N/mm^2)
M_0	0%	35.80
M_1	25%	26.43
M_2	50%	22.51
M_3	75%	18.82
M_4	100%	11.36

V. EXPERIMENTAL PROGRAM

The experiments analysis focuses on the influence of coconut shell (CS) on flexural performance of simply supported (SS) one way slabs. The experimental program involves testing of 10 one-way slabs with end condition simply supported. Table 3 shows the details of test specimen planned in this study.

Table 3. Details of Slab Specimen

Mix No.	Replacement of CA by CS	Slab Specimens
SLM_0	0%	2
SLM_1	25%	2
SLM_2	50%	2
SLM_3	75%	2
SLM_4	100%	2

Test procedure and instrumentation

Lab test was conductedon an inflexiblerigid steel frame as shown in Figure 3 all the four edges are simply supported and a scientific dial gauge was placedcentrally at the bottom face of the block to record the corresponding deflections at various stage and to analyse cracking progress. A steel rectangular section of 20 mm thick was employed to transfer the load and both top and bottom sides were examined to study the sustained damage, such as yielding of reinforcement, punching failure surface and cracking pattern at Fig. 3. Testing of specimens under four point loading.The support distance in slab is 1m.

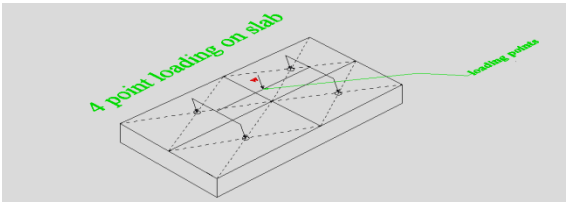

Figure 1. Load Pattern on Slab

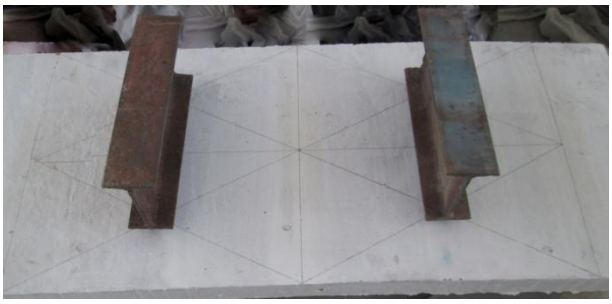

Figure 2. Four Point Load Distribution

Figure 3. Loading Set up for Simply Supported Slab

VI. DISCUSSION ON TEST RESULTS

In this Analysisof the load versus middle deflection curves the flexural collapse is characterized by a smooth diminution of the carrying load with cumulative displacement. Flexural collapse is measured to take place in slabs in which the majority of the reinforcement yields before punching occurs and at the same time, the slabs show evidence of huge deflection prior to failure. Flexure failure was defined when an unexpected decrease of the load carrying capacity occurs at summit load (nearly vertical branch of the load deflection curve).Cracking and failure patterns were alsoused to sort out the failure nature. Slabs were measured to fall short in flexure and diagonal cracks

Published By:
Blue Eyes Intelligence Engineering
& Sciences Publication

extending from the middle of the patch area followed by flexural punching failure occurred as lateral crack at the out surfacesof area, followed by streak cracks extending from the flat area of stability of resistance. The failure was progressive with the rupture of bottom reinforced layer. Punching failure occurred at four point loading test as the load fell abruptly and was released completely.

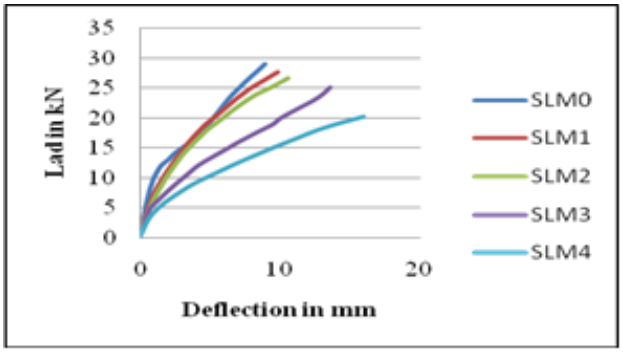

Figure 4. Load Vs. deflection curves

VII. LOAD DEFLECTION RESPONSE

The central deflections are given in Table 4. Thecentral Load Vs. deflection response from the values in in table 4are projected in Figure 4, where the central deflections analogous to first crackload of SLM_1 to SLM_4 decreases in the series of 9 to 45%, when compared with control slab specimens and the central deflections corresponding to ultimate load of SLM_1 to SLM_4increases in the range of 10 to 78%,when analysed with control specimens. From the above observations it is clear thatsimilar trend is observed at first crack and ultimate failure stages. But, pace of reduction of deflections at first crack stage is more when compared to ultimate stage. At the firstcracking stage, rate of decrease of deflections are more due to presence of old mortar over the CS, but at ultimate point the rate of reduction of deflections are fewer due to the contribution of steel bars.

Table 4: Maximum central deflection at first crack load and at ultimate load

Slab No.	FIRST CRACKing LOAD (kN)	Deflection at initial cracking load(mm)	Ulti mate load (kN)	Deflection at critical crack load (mm)
SLM_0	14	2.44	29	8.95
SLM_1	12	2.23	27	9.85
SLM_2	9	1.62	26	10.55
SLM_3	7	1.57	25	13.57
SLM_4	5	1.35	20	15.95

Stiffness

From the curvature path of load to deflection curve, two values of the stiffness of the tested slabs have been obtained. The stiffness values are shown in Table 5. This indicates that stiffness decreases as the percentage of CA with CSreplacement upsurges. Stiffness degradation is the proportional ratio between the ultimate stiffness to the un-cracked stiffness. As the stiffness degradation decreases, the specimen shows higher ductility.

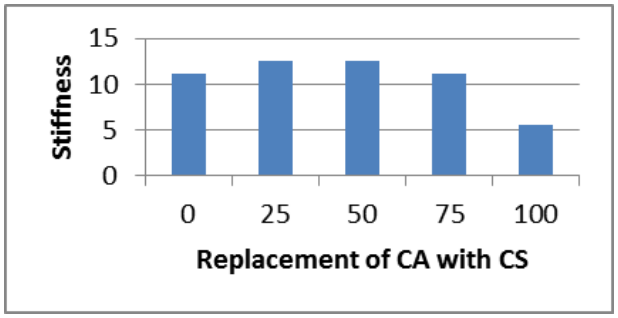

Figure 5.Effect of percentage replacement of CA with CS on Stiffness of simply supported(SS) slab specimens

Table 5. Stiffness

NOMENCLATURE OF SLAB SPECIMEN	STIFFNESS (kN/mm)
SLM_0	11.17
SLM_1	12.47
SLM_2	12.52
SLM_3	11.10
SLM_4	5.52

VIII. ENERGY ABSORPTION

The absorption of energy is explained and the corresponding calculations made from the actual test consequences, and are tabulated in Table 6 and Fig and clearly show the increase in the energy absorption.

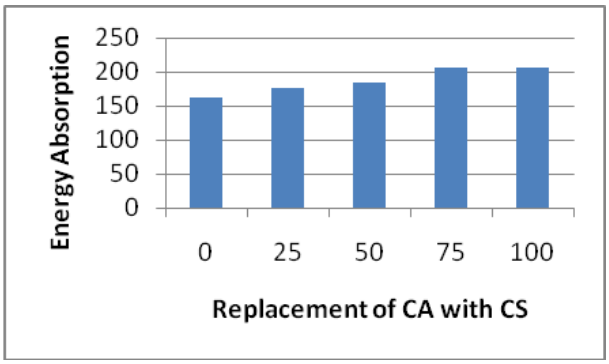

Figure 6. Effect of percentage replacement of CA with CS on Energy absorption of simply supported slab specimens

Table 6. Energy Absorption

NOMENCLATURE OF SLAB SPECIMEN	ENERGY ABSORPTION (kNmm)
SLM_0	162.11
SLM_1	176.32
SLM_2	183.63
SLM_3	205.07
SLM_4	205.62

DUCTILITY FACTOR

Ductility factor is the represented as the fraction of total deformation at maximum load to the elastic limit deformation. The values estimated from the results are shown in Table 7 and Fig7 clearly shows the increase in the

ductility. Hence it has been established that as the infusion percentage of coconut shell upsurges, the energy captivation also increases.

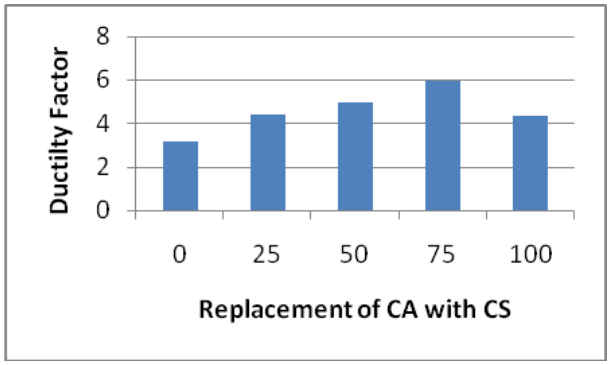

Figure 7. Effect of percentage replacement of CA with CS on Ductility Factor of simply supported slab specimens

Table 7. Ductility Factor

NOMENCLATURE OF SLAB SPECIMEN	DUCTILITY FACTOR
SLM_0	3.14
SLM_1	4.42
SLM_2	4.95
SLM_3	5.97
SLM_4	4.36

IX. CRACKING INCORPORATED FAILURE PATTERNS

The top view image of the sample subjected to is portrayed in Figure 7. The concluding cracking patterns of the SLM_0, SLM_1, SLM_2, SLM_3, SLM_4 slabs are presented in Figures 9 to 18. It is analysed that the cracks progressing on the bottom face of the slab are radial, penetratinginitiallyfrom the loading point and flowing through the corners. A rectangular punch is found surrounding the four point load occur on top surface and also seen reflected on bottom face with an enlarged area, clearly classifying the wave form type cracks depending on the replacement percentage of CA with CScertain disparities in the amount and positioning of cracks and the edge of the failure wave form at the bottom were marked. Careful inspection publicized that the bottom edge decreases as the replacement percentage of CA with CS increases.The overall cracking progressionexistsindistinguishably for all the operated specimens.

Figure 8.Simply supported block specimens postFailure

1. BOTTOM SURFACE CRACKS

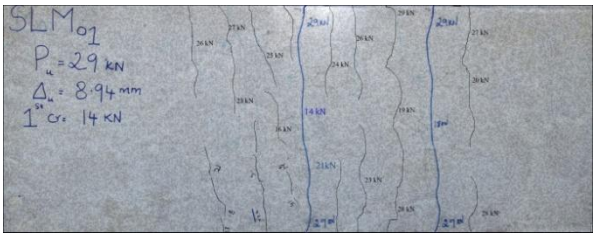

Fig.9 Cracking pattern of SLM_{01}

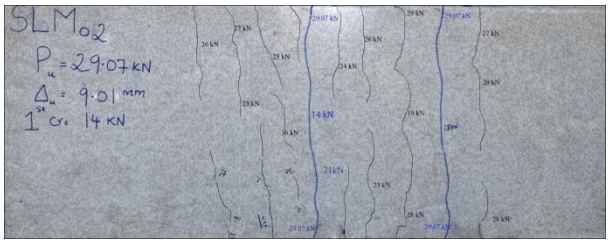

Fig.10 Cracking patternof SLM_{02}

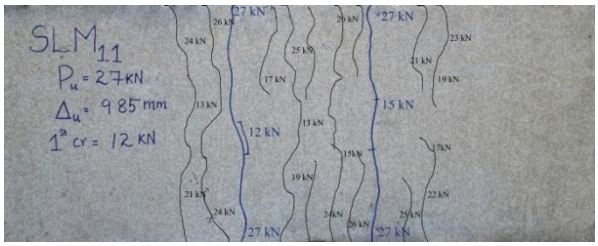

Fig.11 Cracking pattern of SLM_{11}

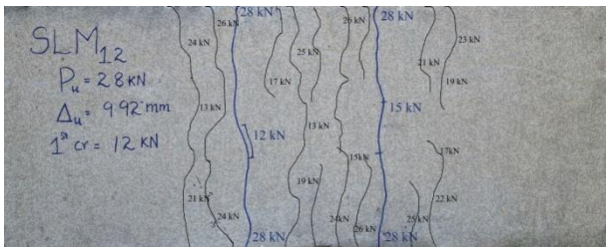

Fig.12 Cracking pattern of SLM_{12}

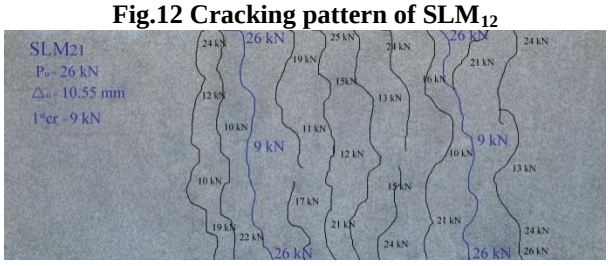

Fig.13 Cracking pattern of SLM21

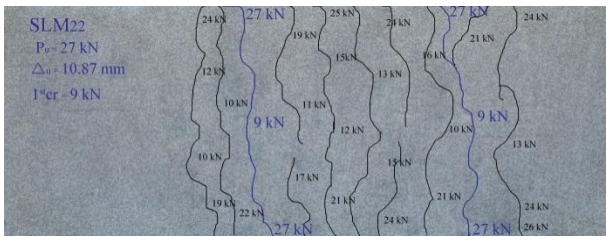

Fig.14 Cracking pattern of SLM_{22}

Published By:
Blue Eyes Intelligence Engineering
& Sciences Publication

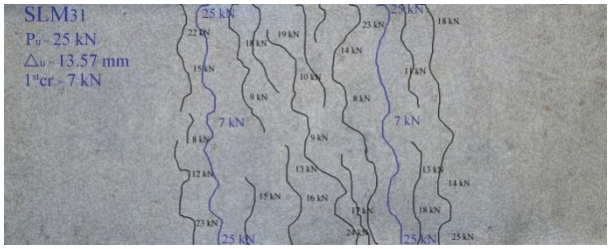

Fig.15 Cracking pattern of SLM_{31}

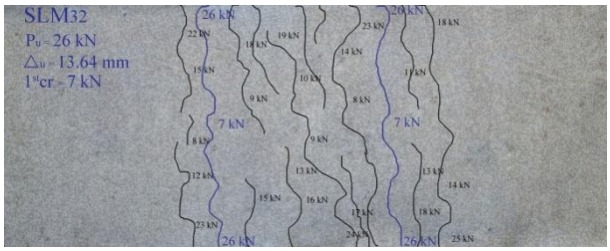

Fig.16 Cracking pattern of SLM_{32}

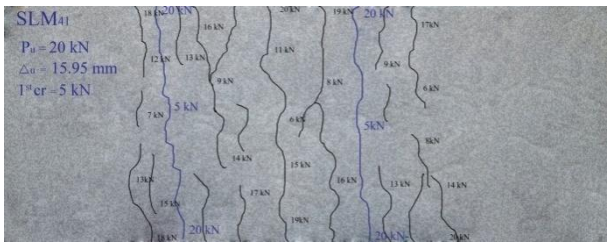

Fig.17 Cracking pattern of SLM_{41}

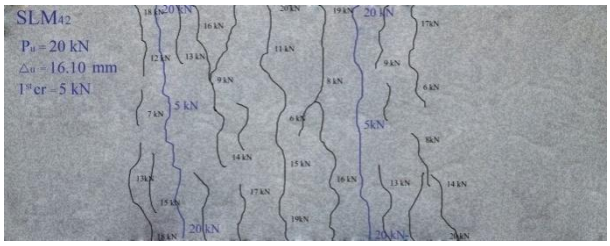

Fig.18 Cracking pattern of SLM_{42}

X. CONCLUSION

The outcome of the experimental procedures substantiates that thefollowing conclusions seem to be valid.

1) By increasing the coconut shell percentage the cube compressive strength can be decreased.
2) The ultimate cubical compressive strength of coconut shell infused concrete (replacing of natural coarse particulate with coconut shell from 25% to 100%) is in the range of 26.43 to 11.36N/mm^2, for natural coarse particulate concrete the cube compressive strength is 35.8N/mm^2.
3) For slabs with natural CA the first crack load was experienced at 14kN. For slabs with CS it varies from 14 to 5kN for 25 to 100% replacement respectively. The first crack load was 14.28 to 64.29% less compared to normal particulate slabs.
4) For normal coarse particulate slabs the ultimate load is obtained at 29kN, whereas for CS replaced slabs the range is from 29 to 20 kN. The decrease in range is observed as 6.89 to 31.03% for 25 to 100% replacements respectively.
5) Under punching shear it was identified that the increase in the percentage of CS replacement decreases the stiffness and stiffness degradation.
6) The ductility of lightweight concrete block is usually greater than the normal weight concrete block. In CS replaced concrete slabs the ductility factor increased from 29.47 to 75.37% for 25 to 100% replacement respectively.
7) The energy absorption of CS concrete slab specimens increases from 8.77 to 26.84% for 25 to 100% replacement.
8) It is concluded that, when the natural coarse particulate is replaced up to 50% with CS the resulting CS concrete represent same behaviour like the natural coarse particulate concrete in terms of the flexural properties studied in this investigation.
9) These facts justify the effects on usage of these concrete, which can contribute to the waste disposal and assures a green environment.

REFERENCES

1. AbdulkadirKanand, RamazanDemirbog, “A novel material for lightweight concrete fabrication”, Elsevier Cement & Concrete Composites, Vol. 31 (2009), PP. 489–495.
2. AmarnathYerramala and Ramachandrudu, “Properties of Concrete with Coconut Shells as Particulate Spare”, International Journal of Engineering Inventions(2012), Volume 1, Issue 6, PP: 21-31.
3. ASTM C330-99, “Standard specification for lightweight particulates for structural concrete”, Annual Book of ASTM Standards, United States, 522-525.
4. GeethaKumari, C. G. Puttappaand C. Shashidar, “Flexural Appearances of SFRSCC and SFRNC One Way Slabs”, IJRET (2013), Volume.2, Issue.7, pp. 220-229.
5. Hassan Mohamed Ibrahim, “Experimental Investigation of Capacity of Mesh-Reinforced Cementitious Slab”, Elsevier Construction and Building Materials (2010), pp. 251-259.
6. Jihad Sawan and Mohamed Abdel-Rohman.Impact Effect on R.C. Slabs Experimentations Journal of Structural Engineering, ASCE(1986), Vol. 106, No. PP: 2057-2065.
7. Kayali and Zhu .Chloride Induced Reinforcement Corrosion In Lightweight Particulate High Strength Fly Ash Concrete blocks. Elsevier Construction and Building Materials(2004),PP: 327–336.
8. Miguel Fernandez Ruiz and Aurelio Muttoni.Shear Strength of Rc Slabs under Concentrated Loads near Clamped Linear Supports. Elsevier Engineering Structures (2013), PP: 10–23.
9. Randy D. Martin and Thomas H.-K. Kang .Structural Design and Construction Issues of Approach Slabs. ASCE, Journal of Structural Design And Construction (2013) , PP: 12-20.
10. ShettyM. S.(2005),“Concrete technology theory and practice”, 3rd Multicolor illustrative revised ed., India.
11. Yushun li and weishen,“Flexural behavior of lightweight bamboo – steel composite slabs”, Elsevier Thin-Walled Structures(2012), pp. 83–90.

Experimental Investigations on Modified Combustion Chamber Geometry in Diesel Engine

ShaikHussain, Sanam Ravi Teja

Abstract: ***Today the two disturbing conditions in front of the engineers worldwide are to decrease the utilization of conventional fuels and to downscale the ever rising environmental pollution.The performance characteristics and emission characteristics of single cylinder water cooled diesel engine with the effect of piston crown geometries such as HCC (Hemispherical combustion chamber) and RCC (Re-entrant combustion chamber) are evaluated. The tests are conducted with diesel and Rice Bran Methyl Ester and Diesel blends as fuels with different loading conditions. Rice bran methyl ester is prepared by using transesterification process. Without modifying the compression ratio and cylindrical volume of the engine the baseline hemispherical type piston is replaced with Re-entrant type piston. All the engine tests were conducted with diesel and 20% blend with diesel [RBOME20] indiesel engine with HCC and RCC. From the investigations it is observed that the brake point thermal efficiency is increased and specific fuel consumption proportion is decreased for re-entrant combustion chamber. Further thenormal pollutants emissions are reduced. But slightly increase in nitrogen oxides is detected compared to base fuel for re-entrant combustion.***

Keywords: Diesel engine, biodiesel, re-entrant combustion chamber, Hemispherical Combustion chamber and Rice bran methyl ester.

I. INTRODUCTION

Conservation of energy and emissions have become of rising concern over last few decades. More stringent emission laws along with the need to conserve the limited resources of petroleum based fuels, engineers related are under notable pressure to enhance their energy efficiency and diminish the exhaust emission levels. In this circumstance, there has been developing the interest and immense research on the actions that take place in the IC engines and the alternative fuels such as biodiesel to supply a proper diesel oil use for the internal combustion engines. However the results of the first stage of this research plan and majority of the studies exploration on the performance of the biodiesel fuelled the diesel engine specified, reduces in power of engine and the thermal efficiency, raising in the specific fuel consumption and raising the in emissions especially NOx, when compared with theoperation ofstandard diesel.

The destitute performance of the biodiesel controlled diesel engines in comparison with the petroleum basedengines is mostly due to the changes in the properties of fuel, design of engine and operating parameter. The characteristics of p of the DI diesel engine are highly effects by the motion of air in the inner side of the cylinder. The mixing of air-fuel and the following combustion in the DI diesel engines are restrained by flow field inside the cylinder happened by the combustion chamber specifications. The motion of air in the diesel engine, in the course of compression stroke is causes by the combustion chamber. Hence, configurations of combustion chambers require a great attention to contact the global movements in the consumption of fuel, performance and emissions.

In this stage of exploratory work, without changing the engine's compression ratio, geometry of piston bowl was modified from the baseline HCC (Hemispherical Combustion Chamber) to the RCC (Re-entrant Combustion Chamber) by using rice bran oil methyl ester blended with diesel.

S. Jaichandar et al [8] (2012) investigates re-entrant combustion chambers for better air movement and charge mixing. However UBHC, CO and the smoke intensity in the modified engine partly increase with slow injection timing because of poor initial phase of combustion. The increased squish and swirl of the modified engine improves the charge mixing that which results in good combustion and increases temperature of combustion chamber and further increases NOx in modified engine.The biodiesel B20 obtains from Pongamia oil improves the combustion, performance and emission characteristics because of better mixing and enhanced combustion.[8]

II. MATERIALS AND METHODS

2.1 Preparation of Rice bran oil methyl ester (RBOME)

Rice bran oil was choose for this investigation and gets converted it into its methyl ester by trans-esterification. In this trans-esterification reaction, initially 250 ml of methanol was mix-up with the 150 ml of NaOH. The time taken for the reaction is six hours at 55˚C [1]. Then the mixture was kept for minimum eight hours at ambient temperature and then separates the settled glycerin. After decanting glycerol, the methylene esters get washed off with water. The characters of RBOME were found and compares with the diesel [3]. The comparison shows that the properties of rice bran oil methyl ester are relatively closer to diesel fuel properties.

Revised Manuscript Received on Janurary 25, 2019..

ShaikHussain,Associate Professor, Department of Mechanical Engineering, Malla Reddy Engineering College, Hyderabad, Telangana, India 500100

Sanam Ravi Teja,PG Student, Department of Mechanical Engineering, Malla Reddy Engineering College, Hyderabad, Telangana, India 500100

The test fuels were prepares with RBOME blends RBOME20 and diesel. Originally, the experiments were

conducted in a baseline engine mounted with HCC piston using RBOME20 and diesel with customary injection timing and injection pressure ant the outcomes were compared with diesel. Finally, with RBOME20 and diesel on a modified engine mounted with RCC piston at variable load and the obtained results were compared with again with the diesel fuel.

2.2 Experimentation

The engine designated for experimentation was single cylinder DI and four strokes, water cooled diesel engine and the engine can resist the higher pressures and is vastly used in agricultural sector and in industries. The details of the engine specifications are represented on the table. The engine runs at rated speed of 1500 rpm, compression ratio of 16:1 and rated power output of 3.7kW. The engine had a hemispherical shaped open type combustion chamber with overhead valve arrangement and operates with push rods and camshaft. [4]

Without changing the compression ratio the hemispherical piston is modified into re-entrant type piston and the modified combustion chamber geometry is shown in (Figure3) with HCC. Then, the experiments were conducts by using RBOME biodiesel and diesel fuel to study the hemispherical and re-entrant combustion chamber shapes as in Figures 2. Then, the results were used to substantiate the performance and radiation characteristics of the engine. The emissions at exhaustion analyzed by krypton 290 gas analyzer

Table.1 Specifications

S. No.	Details	Specifications
1	Power	3.7kW
2	Speed	1500 rpm
3	Compression Ratio	16:1
4	Connecting rod length	230 mm
5	Stroke Length	110 mm
6	Cylinder Bore	80 mm
7	No. of Cylinders	1
8	Stroke type	4
9	Indicator Used Type	Cylinder Pressure
10	Dynamometer Type	Swinging field type
11	Cooling Type	Water
12	Speed Type	Constant

FIGURE 2.1: Experimental setup

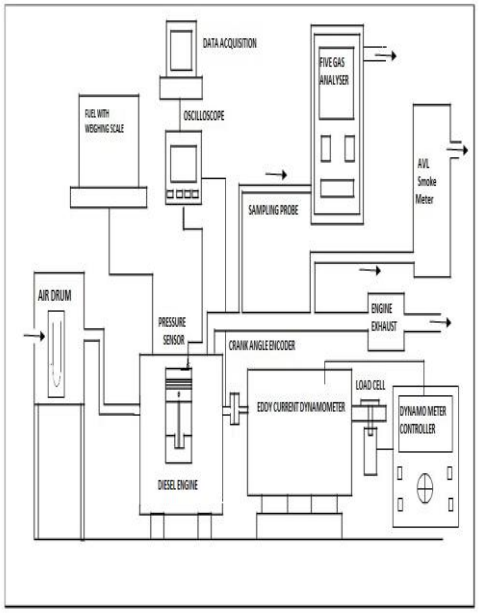

FIGURE 2.2: ExperimentalBlock

(a) **(b)**

FIGURE 2.3(a) Hemispheric Combustion Slot
(b) Re-entrant Combustion Cavity

1. RESULTS AND DISCUSSION

3.1 Brake Thermal Efficiency:

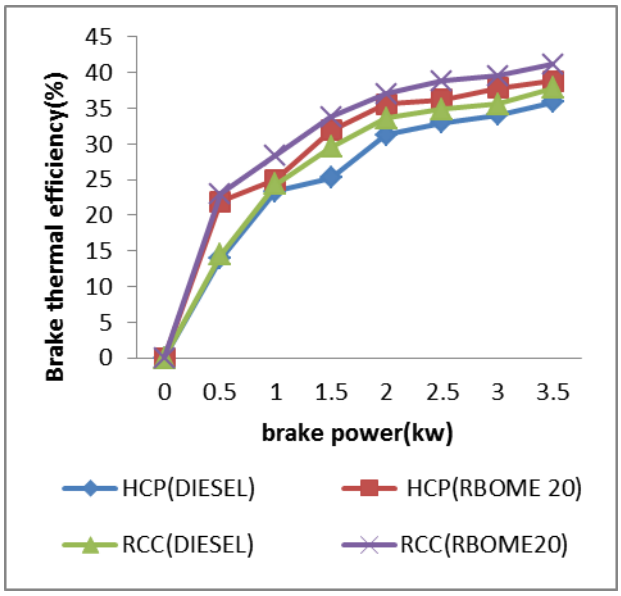

FIGURE 3.1: BP Vs Brake point thermal efficiency

Figure 3.1 describes the comparison of brake point thermal efficiency with brake point power for standard diesel and rice bran oil methyl ester for both of the combustion chambers. The BTE of B20 with baseline engine having HCC is higherin comparison with diesel. Whereas the engine is operates at constant injection timings and RBOME has little ignition delayed. Hence combustion gets initiated before TDC. By this there is increase in heat losses and hence lowers the BTE of engine and increases compression. The BTE for RCC with RBOME20 is complex compared with baseline engine at all the loads. This is due to the greater mixture formation of RBOME20 with air that results in finer air motion in RCC piston, which causes the better combustion of RBOME20 and hence the BTE is increased. The brake thermal efficiency of RCC is about 2.7% more when fuelled with RBOME20 than standard diesel.

3.2 Brake Specific Fuel Consumption:

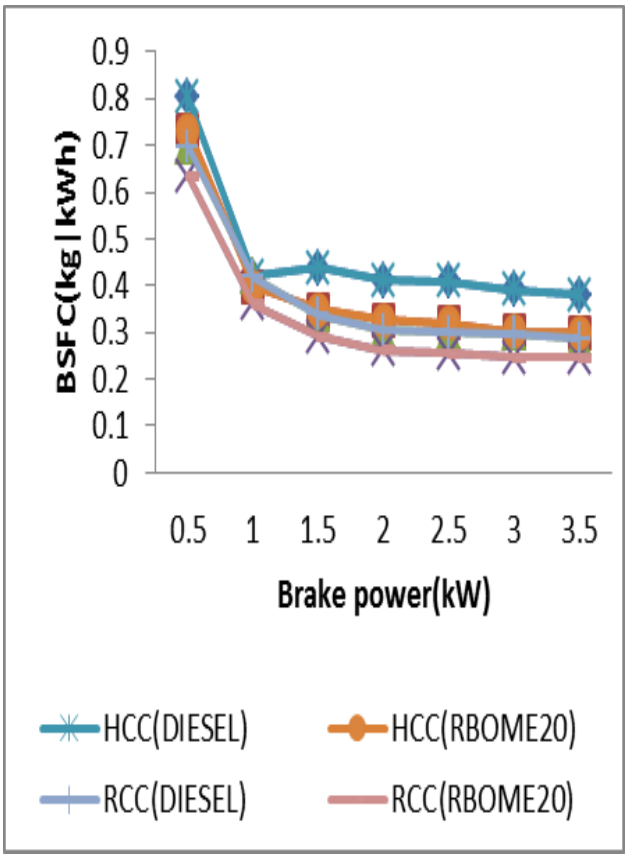

FIGURE 3.2: BP Vsspecific fuel consumption at brake pt.

The comparison of BFSC for tradiltional engine and modified new engine operated with standard diesel and ROME20 are shown in Figure 3.2. The BSFC for RCC is (0.252 kg/ kW-hr). This is lower than hemispherical combustion chamber with RBOME20 fuel under full load conditions. This attributes to greater combustion of RBOME20 because mixing of air and fuel results in turbulent kinetic energy (TKE) and improves in swirl velocity. The BSFC for RCC withRBOME20 is lower compared to conventional engine and is about 4.96%at rated load operation of the engine.

3.3: Carbon Monoxide Radiations

Figure 3.3 shows the comparison of carbon monoxide emissions of HCC and RCC combustion chambers by using standard diesel and RBOME20 in respect of brake power. The Carbon monoxide emissions for both HCC and RCC combustion chambers are reduced with RBOME 20 compared to standard diesel. The CO emissions are further reduced with RCC combustion chamber compared base engine from no load to specific r load operations because of greater movement of air in RCC and oxygen proportion in the RBOME that leads to better fuel combustion. The amount of reduction in Carbon monoxide emission for RBOME20 with RCC is 33.2% when compared with standard diesel engine.

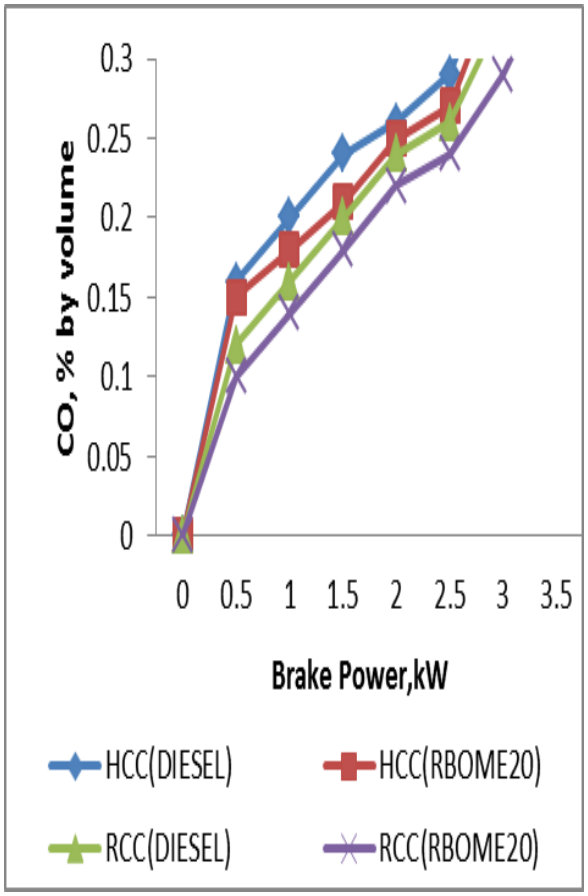

FIGURE 3.3: BP Vs Carbon monoxide emission

3.4 Hydrocarbon Emissions:

Published By:
Blue Eyes Intelligence Engineering
& Sciences Publication

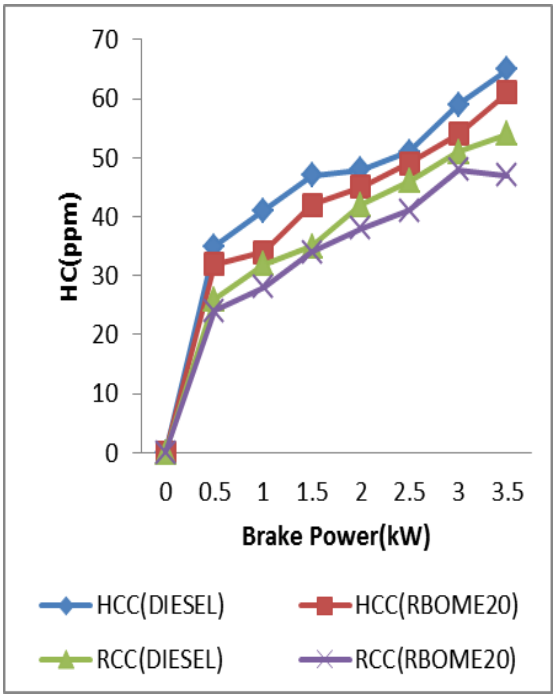

FIGURE3.4 BP Vs Hydrocarbon emissions

In Figure 3.4 shows that, the comparison of hydrocarbon emissions for both combustion chambers HCC and RCC operated with RBOME20 and standard diesel. HC radiations were decreases at full loads of HCC and RCC combustion fuelled with RBOME20 instead of standard diesel. But, it is observed that RCC emits low level of Hydrocarbons that compares with HCC. This is because of better combustion of RBOME20 as results of superior swirl motion of air in RCC along with oxygen in RBOME20 which leads to the unique air-fuel mixture. There is a decline of 16.6% HC radiations for RCC with RBOME20 and 23.07% with standard diesel compared to base engine.

3.5 Nitrogen oxide Emissions:

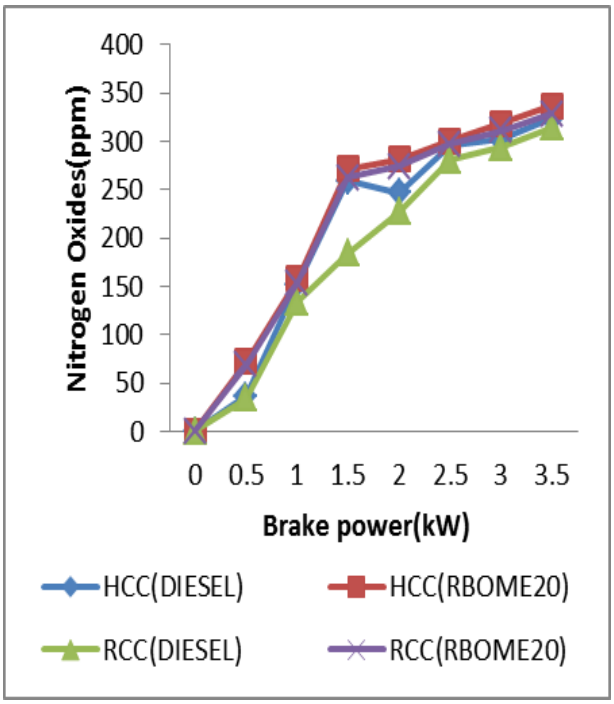

FIGURE 3.5 BP Vs Nitrogen oxide emissions

Figure 3.5 showsnitrogen oxide emissions with brake power for baseline engine HCC and modified RCC with fuelled RBOME20 and standard diesel. The NO_x emissions for RBOME20 were higher for RCC than baseline engine. The NO_x emissions increased by 7.2% for RBOME20 with RCC compares with HCC. The reason for increasing in nitrogen oxide emissions is due to greater combustion temperature by formation of unique mixture that results in the upgraded combustion. For RBOME20 with RCC, the NO_x emission is 488 ppm and for that of base fuel is 445 ppm at full load conditions.

III. CONCLUSIONS

The investigates are conducted onfour stroke water cooled diesel engine withsingle cylinder two piston bowl geometries such as Hemispherical and Re-entrant. The performance and emission physiognomies ofbiodiesel fuelled DI diesel engine are determined. From the investigation the following conclusions are drawn:

- ✓ Based on performance and emission characteristics RBOME gives better Brake thermal efficiency, less fuel consumption and reduction in CO and unburnt HC radiations and slightly intensifies in NOx emissions for Re-entrant than compared to base engine(hemispherical).
- ✓ The brake point thermal efficiency of RCC is about 2.7% more when fuelled with RBOME20 than standard diesel.
- ✓ Enhanced air motion in re-entrant combustion chamber enhances the air fuel mixture formation increases BTE simultaneously reduces BSFC IN comparison with hemispherical combustion chamber. Better combustion because of better mixing of air and fuel in re-entrant that gives greater thermal efficiency for RBOME20.
- ✓ The CO, unburnt HC,CO2 were lesser for re-entrant than hemispherical by using RBOME20 because enhanced the mixing of air and fuel and greater presence of oxygen is more in RBOME20 and gives better combustion compares with hemispherical.
- ✓ NOx emissions are increased for re-entrant due to greater combustion temperature by formation of a mixture better than earlier one and accessibility of oxygen in RBOME that results in the upgraded combustion than HCC.
- ✓ The experimental results show that the re-entrant combustion chamber geometry performs a significant role that decides the swirl and turbulence in cylinder.
- ✓ The results indicates that the RCC combustion chamber with RBOME 20 as fuel can be used in existing diesel engines without any modifications.

REFERENCES

1. Umesh T and Manjunath HN Rukmangadha P, Dr.Madhu D., "Experimental Study of Performance & Emission Analysis of Rice bran oil as an Alternative fuel for an I.C Engine", IOSR-JMCE, Volume 11, PP 130-134,2014.
2. Deepa.D, Karuppasamyl..," Performance and emission characteristics of diesel engine using rice bran oil methyl ester blend with additive diethyl ether", Volume 3 ,2014.
3. Mir Mohsin John, Vineet Kumar.," Effect of Load on the Performance of DI Diesel Engine Running on Rice Bran Bio-diesel and Its Blends", Volume 1, Number 1; September, 2014pp. 14-17.
4. A.Ravichandran, K. Rajan, M.Rajaram Narayanan and K.R.Senthil Kumar et al..," Effect of piston bowl geometry on the performance of a diesel engine using Corn biodiesel and its diesel blends" International Journal of ChemTech Research, Volume 9, No.01 pp 105-112,2016.
5. PalashChakma and HaengMuk Cho "Comparative Study on the Modified Combustion Chamber Geometries in Diesel Engine for Using Biodiesel to Achieve Emissions Standards ",IJETAE, Volume 07 ,2017.
6. Dr. Abdul siddique.sk, shaikabdulazeeez and Raffimohammed" A review on c.i engine combustion chamber geometry and optimization", Volume 3, Issue 5, August 2016.
7. Chetan S Bawankar and Rajesh Gupta," Effects of piston bowl geometry on combustion and emission characteristics on diesel engine", Volume 05,2016.
8. S. Jaichandar, K. Annamalai, "Influences of reentrant combustion chamber geometry on the performance of Pongamia biodiesel in a DI diesel engine", Energy 44 (2012) 633-640.
9. S. Jaichandar , K. Annamalai , "Effects of open combustion chamber geometries on the performance of Pongamia biodiesel in a DI diesel engine", Fuel 98 (2012) 272–279.
10. Banapurmath NR, Chavan AS, Bansode SB, SankalpPatil, Naveen G, SankethTonannavar, Keerthi Kumar N and TandaleMSet al.., "Effect of Combustion Chamber Shapes on the Performance of Mahua and Neem Biodiesel Operated Diesel Engines", Volume 6,2015.
11. Chetan S Bawankar and Rajesh Gupta," Effects of piston bowl geometry on combustion and emission characteristics on diesel engine", Volume 05,2016.

Effectiveness of a Dimpled Non-Even Surface For Oscillations Control For Flow Over Fissure: Numerical Analysis

YogeshMadaria, Vijay Kanjarla

Abstract: ***To decay the pressure oscillation in the flow above an open crater, a passive control method, namely introduction of a dimpled non-even surface, is attempted. This paper presents the numerical analysis of the above system, which was undertaken to govern the effectuality of the said control modem. This work focuses on an open fissure with the length-to-depth ratio in proportions of 1: 2. To check the oscillation persuaded in the flow, a textured non-even surface is fitted at the upstream of the crater. The even and dimpled non even cases are compared for the flow instability and noise around fissure. Large eddy simulation coupled with acoustic model is utilized as a tool for this. The results obtained for even cases were compared with available experimental and computation data. On the basis of flow visualizations, it can be said that introduction of dimpled non-even surface upstream was significantly effective in suppressing the oscillations in fissure flow. Based on the comparison of flow filed structure in the even and dimpled non-even cases, the control mechanism of void oscillation technique is evaluated.***

Keywords: fissure flow oscillation, passive control, numerical simulation, dimpled non-even surface.

I. INTRODUCTION

The current over an open fissure is subjected to pressure oscillations and this is an imperative bench mark problem for aero-acoustics and has been the focal node of substantial curiosity over the bygone decades. Owing to its extraordinary academic and practical connotation, quite a good number of investigations have been reported in this area. Still the adequate examination of the basic physical mechanism underlying oscillations govern over a wide assortment of flowing conditions, is lacking. The research scholars of fluid dynamics and aero-acoustics seems to be the determinate about the appropriate technique to accurately exempla rate the noise source and disturbances that cause oscillation. The most substantial challenge at this instance is to achieve suppression of various modes of oscillation. These concerns have made the flow induced fissure oscillation as a part of extensive research terminal.

II. LITERATURE REVIEW

The 3D incompressible flow pattern across a rectangular 2D open fissure was probed by Kyoungsikchang et al. [1]. This was the first computational work been successful in resolving all the three dimensional structures arising as a result of fissure oscillations in shear layer mode. Two kind of simulations at the same fissure Reynolds number (Re_D =3360) were presented. In both cases, the resolved stress in downstream region governs those at the upstream region. The oscillation control methods for fissure flows can be broadly classified as active and passive controls. Active control is applied to suppress noise and this is adjustable as per various conditions [2,3]. Techniques like spoiler, mass injection and changes in the fissure are some of the passive control techniques which are quite easy to enhance and are extremely affordable. Alam et al. [4] modified the geometry of the fissure by fastening two separate flat surfaced plates to the wall right upfront of a squareshaped fissure. The flat plates were attached in the horizontal plane and vertical positions. It was purported that the applied approach effectively reduced the fissure pressure oscillations. On the basis of their numerical and experimental exploration of the noise induced in a subsonic flow over the open fissure, Wang et al. [5] used a vented spoiler. They claimed that the technique was superior in noise reduction. To find the effectiveness of a passive control technique in suppression of oscillations for a supersonic open fissure flow, Chokani and Kim [6] performed a numerical simulation. Sarno and Franke [7] compared different techniques namely, static and oscillating fences with pulsating flow injections.. They found the application of static fences to be the most efficient approach. The results of experimental investigations on shallow and deep cavities flows at subsonic and transonic velocities show that out of the several passive venting techniques, the permeable floor and the permeable floor pooled with slot vents were found to have most significant effect on the distribution of the shallow fissure pressures [8]. Leading edge compression rams, expansion surfaces and mass injection techniques were analysed for their effects on suppression of oscillations in a supersonic fissure flow [9]. In another study, a cylindrical rod was suspended (along with a leading-edge fence) in the approaching boundary layer parallel to the leading edge. This technique was reported to play an important role in surface pressure clampdown features [10]. A numerical study was conducted to explore the mechanism and efficiency of noise control. This could result in weakening of the large-scale vortices which are impinged together [11].

Despite the fact that the aforementioned passive control techniques can subdue pressure induced at cavities and their corresponding oscillations, most of these regulatory devices cannot be expected to perform aptly in the practical flow conditions and are not successful in simultaneously suppressing multiple acoustic models.

Revised Manuscript Received on Janurary 25, 2019.

YogeshMadaria,Department of Mechanical Engineering, Malla Reddy Engineering College (A), Secunderabad, Telangana, IndiaIndia 500100

Vijay Kanjarla,Department of Mechanical Engineering, Malla Reddy Engineering College (A), Secunderabad, Telangana, India 500100

To cater this condition, many passive approaches like, deflector [4] and sub-fissure [12], were devised to suppress the oscillations. However, in case of deflector, increase in drag, cost and structure reliability are the issues which need consideration. While in case of sub-fissure, its presence in the stream direction will lead to the accumulation of sedimentary particulates and dirt, and the need for frequent cleansing or maintenance servicing shall arise. Therefore, there is a need to have some techno economical optimum technique to obtain a turbulence boundary layer of appropriate thickness without causing the drag to increase. In the past decade, introduction of non-even surfaces for reducing the pressure drag and friction, has received good attention [13,14]. The benefits of non-even surface are that the boundary layer resists the adverse pressure [15]. Henceforth dimpled non-even surface is implemented to enhance the thickness of the upstream boundary layer.

III. BOUNDARY CONDITIONS FOR GOVERNING EQUATIONS

The 3D Navier stokes equations for unsteady state Newtonian liquids at incompressible flow in Cartesian co-ordinate system are

Continuity:

$$\frac{\partial \overline{u}_j}{\partial x_j} = 0 . \quad (2.1)$$

Momentum:

$$\frac{\partial \overline{u}_i}{\partial t} + \frac{\partial}{\partial x_j}(\overline{u}_j \overline{u}_i) = -\frac{\partial \overline{P}}{\partial x_i} + \frac{1}{\mathrm{Re}} \nabla^2 \overline{u}_i - \frac{\partial \tau_{ij}}{\partial x_j} + \overline{F}_i . \quad (2.2)$$

Where ui -velocity field , Re - Reynolds number, Fi is the body force.

The boundary conditions may be as follows;

At Inlet the wall normal and the span wise velocity components have been set to zero. Mathematically, $u_{in}=U_{\infty}, v_{in}=0, w_{in}=0$ where the subscript "in" indicates the inlet plane.

At Outlet a non reflective boundary condition (convective) is imposed which can be written as

$$\frac{\partial u_i}{\partial t} + U_c \frac{\partial u_i}{\partial x_c} = 0 \quad (2.3)$$

Here subscript c designates the direction normal to the outflow boundary. the convicting U_c is considered as constant across the outflow boundary.

At Upper boundary free-slipping condition is applied so the boundary state at this surface is,

$$v = 0, \frac{\partial u}{\partial y} = 0 , \frac{\partial w}{\partial y} = 0$$

At Lower boundary no slipping condition is applied hence boundary state at this surface is u=0,v=0,w=0.

Disturbance strip

The disturbance strip is applied on the flat shape plate region inlet of the domain passing through normal wall velocity that is sinusoidal in nature with respect to time and span wise direction to induce or trigger the transition process following Alam et al.[10]

$$v = a_f \exp[-b_f (x - c_f)^2] \sin(\omega t) \sin(\beta y)$$

Where a_f,b_f and c_f are constants controlling the stream wise variation of the forcing ω is the frequency and β is the span wise wave number.

IV. COMPUTATIONAL DOMAIN

4.1 Geometrical model of a Dimpled Non-even surface fissure:

The probing is performed on a rectangular designed box with a enormous volumetric space and minor top-opening. The depth and length(L) of the fissure is D (=50mm), 2D respectively. And overall box dimensions are: 1) span wise width 3D, 2) depth 3D 3) length 11D.

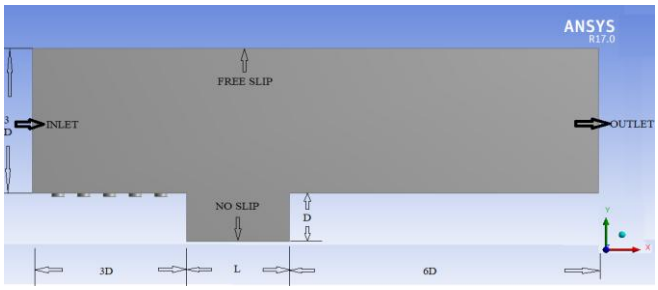

Fig: 1. Computational domain with applied boundary conditions

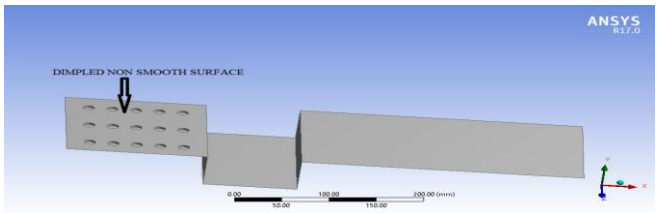

Fig: 2. Detailed view of the upstream porous non-even surface

As shown in fig the upstream leading surface modified by the creating of dimpled non-even surface, this dimples may inhibit a turbulent flow type boundary state condition and increases the thickness of the upper stream peripheral [15].

Meshing: in the meshing the grid is very fine near the surface of the fissure and is slowly stretched out away from it.

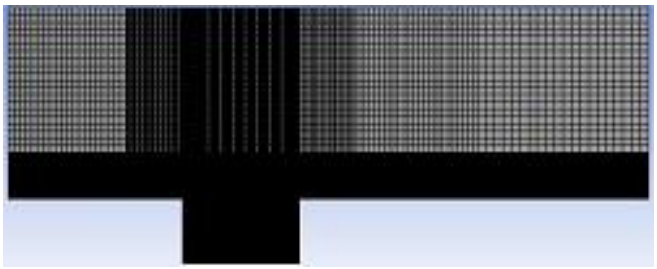

Fig: 3 Grid distribution

3.2 Validations of computational domain

3.2.1 Mean flow characteristics

Fig 4 shows mean velocity profile along the longitudinal axis with the computational data of Chang et al.(2006) at five stages from x/D=0.02 to x/D=1.7.It is perceived that at all stages between the computational data content and the laminar forecasts by the present LES was feasible.

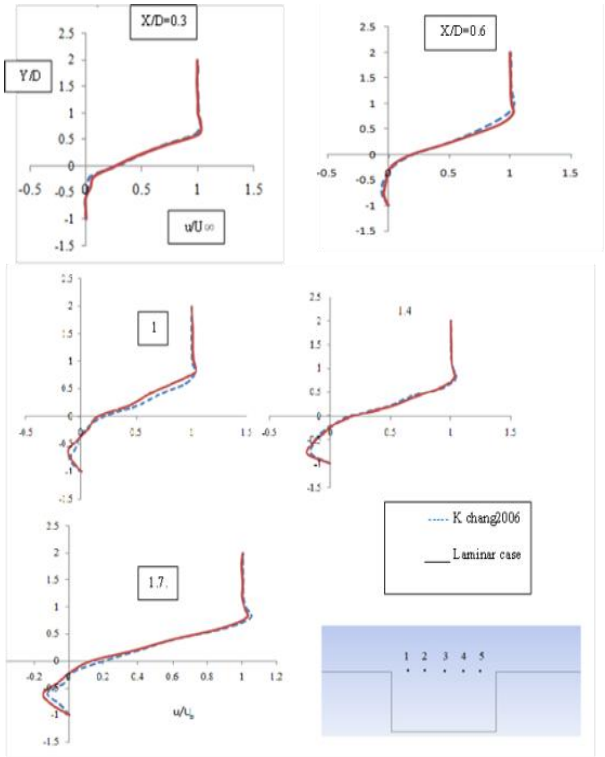

Fig: 4 Comparision of mean stream velocity profiles at different stations

And figure 5 shows about the normal stress $\overline{u'u'}$, $\overline{v'v'}$ at different the stream wise locations. A very good agreement is absorved at all the stations

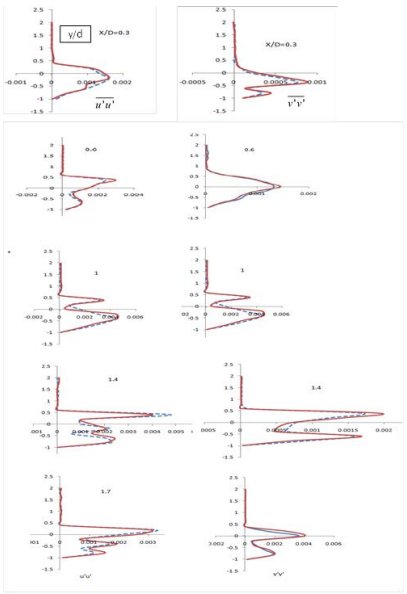

Fig 5 comparision of Reynolds stress at different stations

3.2.2. Velocity spectra

Fig 6 shows the time fluctuation status of the vertical velocity at five stations. From the we figure observe that the up to station 2 there is no substantial peak in velocity spectra. Downstream of the separation (starts from the station 3), peaks are observed indicating shear stress oscillating at the base frequency stage and its respective strouhal number St_D=fD/U=0.49 The amplitude of the above mentioned oscillations is investigated to be highly emergent in the stream wise course and furthermore, very small but still energetic frequency modulations were clearly observed. These mild energetic frequency oscillations and the main oscillatory frequency observed is due to shear layer interactions with the whirlpool like swirl motions inside the fissure (Chang et al. 2006).Fig 6 shows pressure spectra at stations 5 the strouhal number St_D=(0.36,0.70).

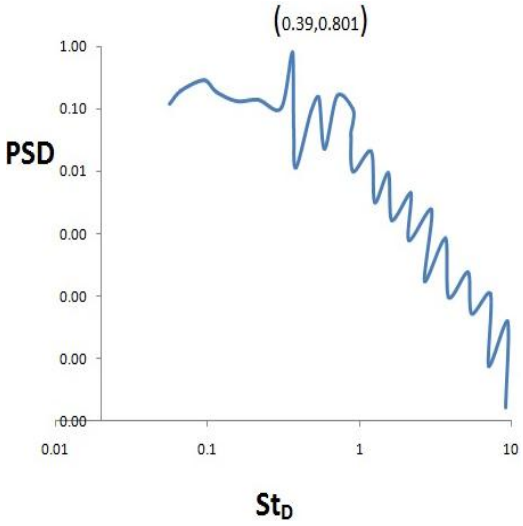

Fig 6 shows pressure spectra at station 5

V. RESULTS AND DISCUSSION

4.1 Meanflow characteristics

Figure 7 shows the comaprision of longitudinal velocity profiles between rough and even(regular) surface cavities. From the statistics were taken 4,5 stations as shown after flow had achived the state of dynamic stability. we don't observer much differences the remaining velocity profiles

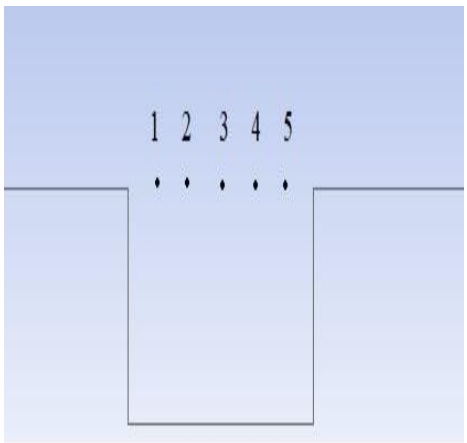

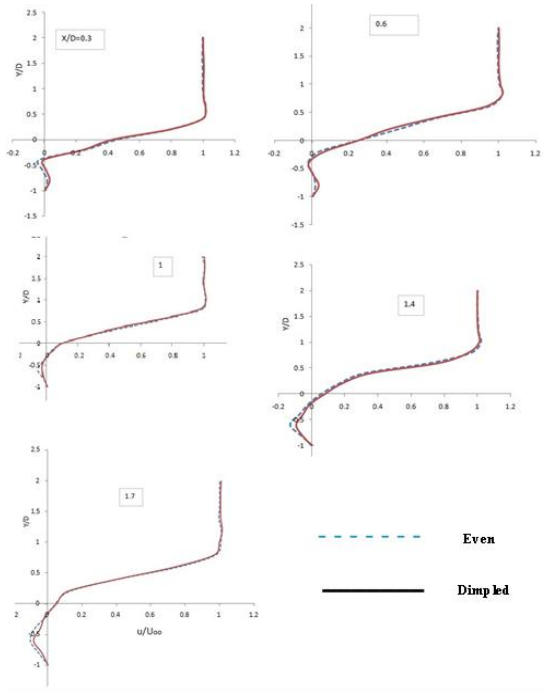

Fig 7 Comparison of mean scream velocity profiles at different stations

4.2 Velocity spectra:

Figs 8 and 9 show Reynolds normal stress of u'u', v'v' respectevely at 5 stations. And we observed thatthe shear layer energy reductions starts from the station 3, so that we achive good fissure stabilty.

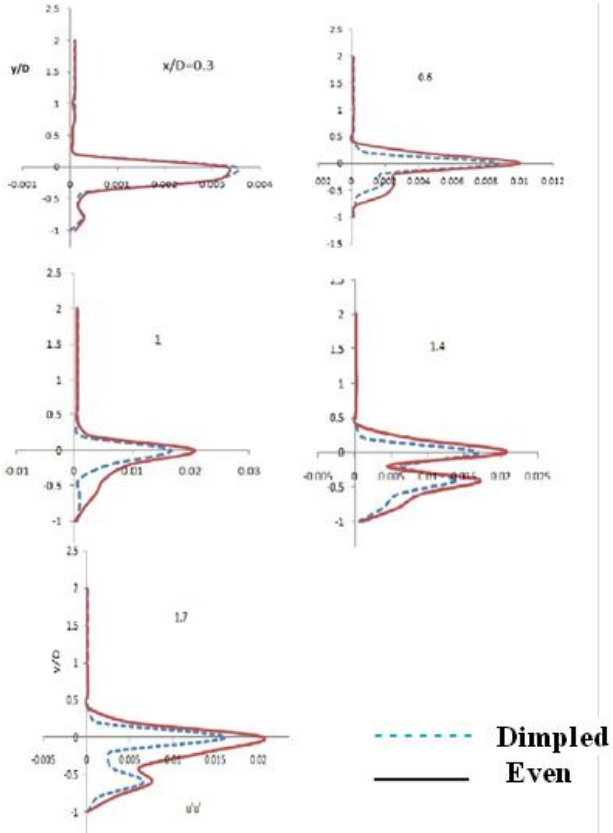

Fig 8 Profiles of u'u' at different stations

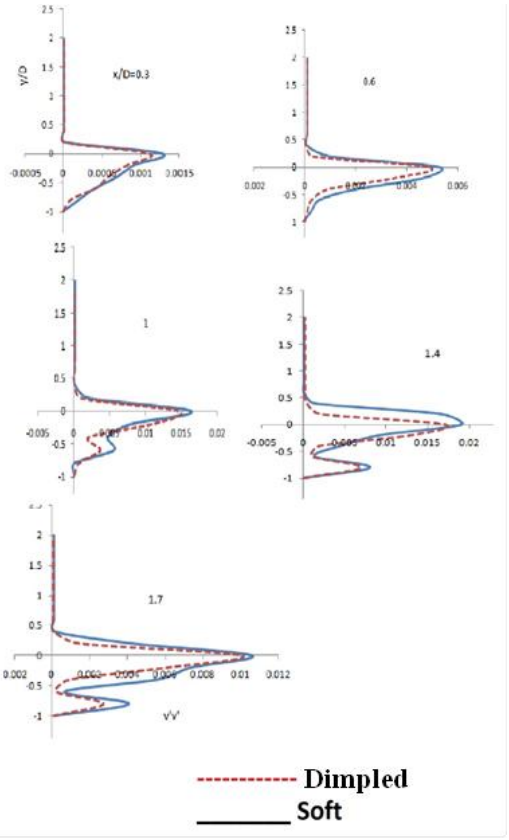

Fig 9 Delineations of v'v' at different stations

From the velocity history we observed at station 5th the strouhal number reduced from 0.39 to .30 so that the fissure oscillations are reduced effectively by the modifications. Fig 10 shows pressure spectra at station 5th.

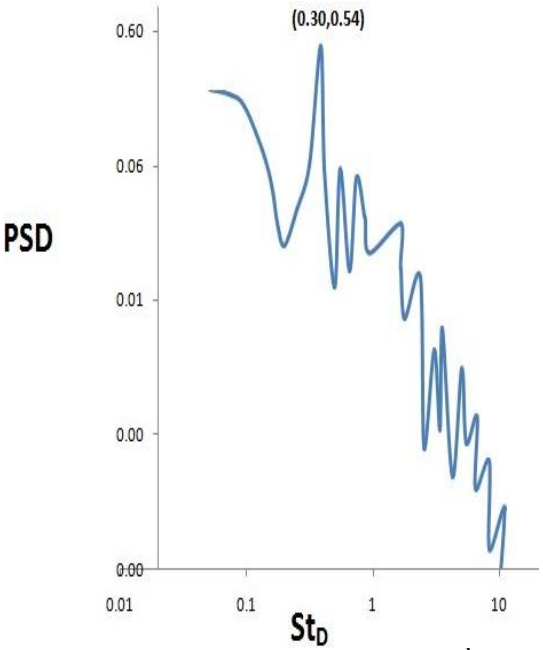

Fig 10 Pressure spectra at station 5th

VI. CONCLUSIONS

The publication demonstrates the porous non-even surface layer was very effectual in guiding and regulating the flow oscillation across the open fissure. For better clarity and substantiation of the above mechanism of the fissure flow oscillation, CFD was employed which in turn had analyzed the flow fields and flow fluxes induced by molting of irregular periodic vortices at the prominent peak edge of the fissure. The simulation during this control and regulatory mechanism projects that the porous non-even surface could make the upstream peripheral boundary layer change from the laminar peripheral boundary layer into turbulence peripheral boundary stratum. The oscillation course was effectively intimidated because of the characteristics of the porous non-even surface.

REFERENCES

1. Chang, K., Constantinescu, G.., and Park, S.O., 2006, "Analysis of the flow featured mass transfer processes for the incompressible flow past an open fissure with a laminar and a fully turbulent incoming boundary state", *J. Fluid Mech.*, Vol. 561, pp 113-145.
2. Rowley C, Williams R. Dynamics of high-Reynolds-number flow .Annu Rev Fluid Mech 2006;38:251–76.
3. Williams DR, Cornelius D, Rowley CW. Supersonic fissure response on open loop forcing. Active Flow Control Notes Numer Fluid MechMultidiscip Des 2007;95:230–43.
4. Alam MM, Matsuo S, Teramoto K, Setoguchi T, Kim HD. A computational control of fissure-induced pressure oscillations using subfissure. J ThermSci 2006;15(3):213–9.
5. Wang YP, Lee SC, Li KM, Gu Z, Chen J. Combined experimental and numerical study of flow over fissure and its application . ACTA Acust United Acust 2012;98(4):600–11.
6. Chokani N, Kim I. Suppression of pressure oscillations in an open fissure by passive pneumatic control. AIAA 91-1729, 1991.
7. Sarno R, Franke M. Suppression of flow-induced pressure oscillations in craters. J Aircr 1994;31(1):90–6.
8. Stallings RL, Plentovich EB, Tracy MB, Hemsch MJ. Effect of passive venting on static pressure distributions in transonic speeds. NASA Technical Memorandum 4549, 1994.
9. Zhang X, Chen X, Rona A, Edwards J. Attenuation of fissure flow oscillation through leading edge flow control. J Sound Vib 1999;221(1):23–47.
10. Ukeiley LS, Ponton MK, Seiner JM, Jansen B. Suppression of pressure loads in fissure flows. AIAA J 2004;42(1):70–9.
11. Li W, Taku N, Kozo F. Noise control of supersonic fissure flow with upstream mass blowing. Progress in hybrid RANS-LES modeling notes on numerical fluidmechanics , vol. 117. p. 315–24.
12. [18] Alam MM, Matsuo S, Teramoto K, Setoguchi T, Kim HD. A new method of controlling fissure-induced pressure oscillatons using sub-fissure. J MechSciTechnol 2007;21:1398–407.
13. Alam F, Steiner T, Chowdhury H, Moria H, Khan I, Aldawi F, et al. A study of golf ball aerodynamic drag. ProcEng 2011;13:226–31.
14. Lienhart H, Breuer M, Köksoy C. Drag reduction by dimples? A complementary experimental/numerical investigation. Int J Heat Fluid Flow 2008;29(3):783–91.
15. Tian LM, Ren LQ, Liu QP, Han ZW, Jiang X. The mechanism of drag reduction around bodies of revolution using bionic non-even surfaces. J Bionic Eng 2007;4(2):109–16.

International Journal of Mechanical and Production Engineering Research and Development (IJMPERD)
ISSN(P): 2249-6890; ISSN(E): 2249-8001
Vol. 8, Issue 6, Dec 2018, 691-698

MICRO-HARDNESS AND MECHANICAL PROPERTIES OF 5052 ALUMINIUM ALLOY WELDMENTS USING PULSED AND NON-PULSED CURRENT GAS TUNGSTEN ARC WELDING

A. RAVEENDRA[1], B. V. R. RAVI KUMAR[2] & S. SUDHAKARA REDDY[3]

[1]*Associate Professor, Department of Mechanical Engineering, Malla Reddy Engineering College (Autonomous), Secunderabad, Telangana, India*

[2]*Professor, Department of Mechanical Engineering, VNR Vignana Jyothi Institute of Engineering and Technology, Hyderabad, Telangana, India*

[3]*Principal, Malla Reddy Engineering College (Autonomous), Secunderabad, Telangana, India*

ABSTRACT

Hardness is defined as the withstanding capability of metal against penetration. Welding produces metallurgical transformations. Evaluation of hardness gives insight into these transformations. A proper study on weldment micro hardness will pave the path to enhance the mechanical reliability of the weldment. Thus, a study on mechanical and microhardness properties of 5052 aluminum alloy weldment using nonpulsed and pulsed current welding at frequencies of 2,4,6Hz has been carried out in the present work.

KEYWORDS: 5052 Aluminum Alloy, Gas Tungsten Arc Welding, Micro Hardness, Ultimate Tensile Strength (UTS), Yield Strength (YS) & % Elongation

Received: Sep 01, 2018; **Accepted:** Sep 21, 2018; **Published:** Dec 06, 2018; **Paper Id.:** IJMPERDDEC201871

Original Article

INTRODUCTION

In view of increased focus on defense and space applications where more precision is required, aluminum alloy products that need welding are in demand. Tungsten Inert Gas Welding and Metal Inert Gas Welding are the methods by which aluminum alloy components can be easily welded. For superior quality welds, Gas Tungsten Arc Welding (GTAW) method using AC current for welding of Aluminum test pieces.

Pulsed Current Welding (PCW) is an additional advancement in the field of welding during the year 1960 as an alternative to constant current welding. Superior arc stability, decreased hot cracking sensitivity, fine grain size, slender heat affected zone, improved weld depth & width ratio, low porosity, regulated weld bead volume, less distortion and heat input, enhanced fusion zone control and reduced absorptive weld pool are the precise features of pulsed current welding process [1-8]. PCW is being extensively used in the aeronautical industry, manufacturing of rockets, rocket motors, missiles, and high-pressure storage tanks. Pulsed current welding can be generated by toggling between high and low levels of specified currents [9]. Figure 1 shows the pulsed waves which are rectangular shaped having characteristics such as base & peak currents and base and peak times. Not much work has been done on alloy steels welded with a pulsed current. Whatever has been done, is on the study of

pulsed current affect, composition of shielded gas, weld shape and speed, joint strength, occurrence of weld defect while using PCW on 5083 alloy sheets [8], 304 and 310 stainless steel weldments angular distortion [9], to examine the microstructure[10] and weld bead geometry[11].

Some of the researchers [12, 13] have used pulsed current for enhancing mechanical and metallurgical properties and weld fusion zone grain refinement. This has led to the exploration of titanium and aluminum alloys where improved refinement in solidification structure is observed. Thus much work was done on medium strength aluminum alloys whereas little work is done on high strength aluminum alloys. In view of this, pulsed current welding effect on high strength aluminum alloy is taken up for study in the present work.

Reduced heat input and thermal disturbances have given fine grain structure in pulsed current welding. Whatever be the welding method, hardness value in, particular, is less in HAZ zone in comparison with weld and base metal regions. An absence of strengthener phase and coarse dendrite grains are the typical characteristics of this low hardness zone. Grain structure refinement enhanced the hardness values which were obtained by using pulsed current welding than non-pulsed current welding [14].

EXPERIMENTAL PROCEDURE

Sample pieces of 5052 aluminum alloy having machined sizes of 300mm x 150mm with different thickness of 1.5 and 2.5mm were welded separately by using methods of non-pulsed and pulsed current GTAW with filler wire material ER4043.

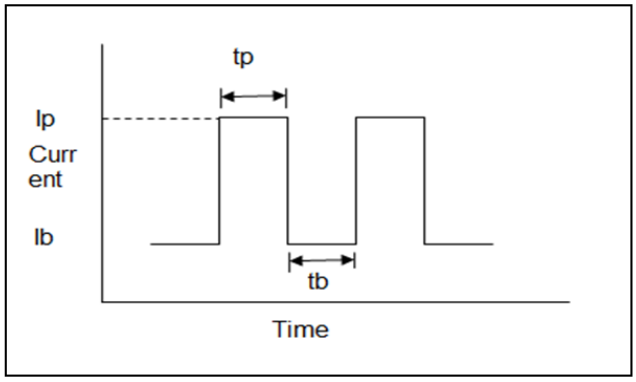

Peak Current I_p, Base Current I_b Peak Time t_p and Base Time t_b

Figure 1: Parameters Used for Pulsed GTAW

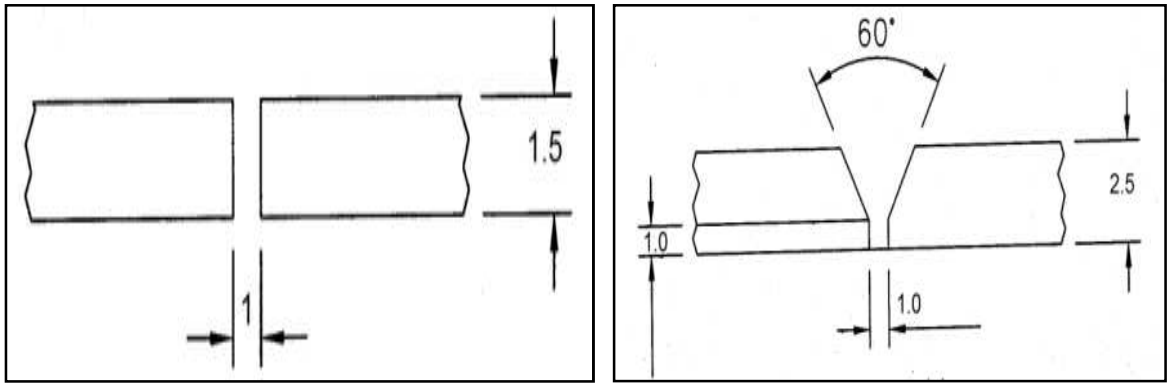

Figure 2: Edge Preparation of Weld Specimens

ER4043 has better properties of ductility and offers good weld strength and better resistance against weld cracks compared to other filler materials [15]. Tables 1-3 show the 5052 aluminum alloy and ER4043 chemical composition and mechanical properties. ER4043 has a low melting point compared to 5052 aluminum alloy. Due to this, the filler is more plastic during cooling which helps to ease the crack causing contraction stresses.

Sample aluminum pieces were treated first with hot sodium hydroxide for 10 minutes, later immersed in Nitric acid solution with 15 minutes duration and finally with water. Welding machine used was **Lincoln Electrical square wave TIG355**GTAW with AC which was shown in figure 3. Welding currents such as AC or DC decides the selection of tungsten electrode. While using AC current, Zirconated tungsten (EWZr) electrodes are preferred as they retain hemispherical shape. A 2% Zirconated tungsten electrode having 3 mm diameter is used for welding of 5052 aluminum alloy in this experiment. Figure 2 shows the edge preparation of 5052 aluminum sample whereas Figure 3 shows the welding machine used. Welded samples were subjected to Tensile and Micro-Hardness tests as per ASTM E8 standards after completion of welding. Figure 4 shows the tensile tested samples. Tables 4 and 5 show the mechanical properties of 1.5mm & 2.5mm thick welded samples and welded parameters used for both pulsed and nonpulsed current welding.

Figure 3: Lincoln Electrical Square Wave TIG 355 M/C

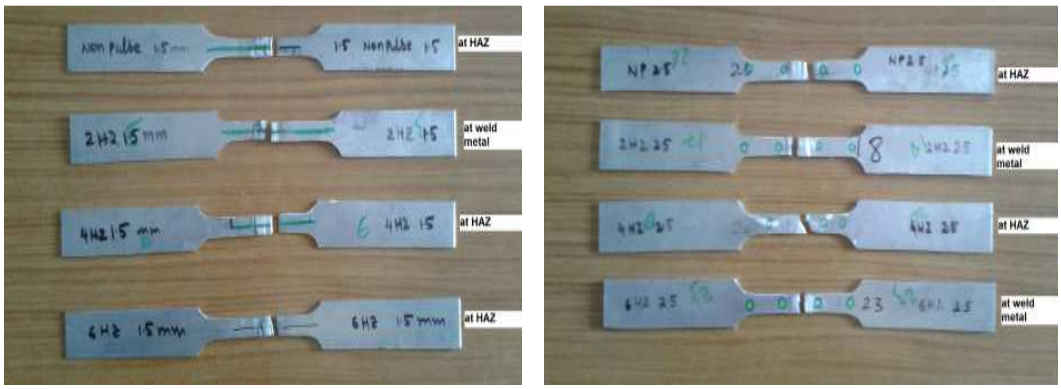

Figure 4: Tensile Test Specimens after the Test (1.5 & 2.5mm Thick)

Table 1: Chemical Compositions of Work Material 5052 Aluminum Alloy

	Chemical Composition % wt								
Material	**Si**	**Fe**	**Cu**	**Mn**	**Mg**	**Zn**	**Ti**	**Cr**	**Al**
5052 Aluminium Alloy	0.092	0.249	0.015	0.013	2.281	0.012	0.016	0.25	Balance

Table 2: Chemical Compositions of Filler Wire

	Chemical Composition % wt							
Material	**Cu**	**Si**	**Mn**	**Mg**	**Fe**	**Cr**	**Ti**	**Al**
ER4043	0.17	4.5 – 6.0	0.24	0.05	0.05	0.05	0.05	Balance

Table 3: Mechanical Properties of 5052 Aluminium Alloy

Material	UTS(MPa)	0.2% Y.S(MPa)Min	% Elongation
5052 Aluminium Alloy	285	180	10

Table 4: Mechanical Properties of 1.5 mm Thick Weldments

S. NO	Sample Description		Trial no	UTS(Mpa)	0.2%S(Mpa)	% of Elongation
1	Base Material		1	286.42	214.32	8.5
			2	272.13	211.66	9.0
			3	274.24	210.72	9.0
2	Non-Pulsed Current GTAW		1	251.59	190.80	4.4
			2	253.64	193.42	6.0
			3	249.32	195.61	4.4
3	Pulsed current GTAW	Pulse=2Hz	1	238.57	189.68	4.0
			2	250.28	189.88	4.5
			3	257.54	199.46	6.4
		Pulse=4Hz	1	244.89	189.76	4.0
			2	254.44	191.75	7.0
			3	220.84	120.65	3.5
		Pulse=6Hz	1	253.55	192.0	8.0
			2	240.54	195.9	4.6
			3	250.58	185.90	9.0

Table 5: Mechanical Properties of 2.5 mm Thick Weldments

S. NO	Sample Description		Trial no	UTS(Mpa)	0.2%Y S(Mpa)	% of Elongation
1	Base Material		1	296.62	228.29	13.0
			2	295.93	227.50	12.0
			3	291.84	226.84	12.0
2	Non-Pulsed Current GTAW		1	288.51	207.3	4.0
			2	282.45	210.8	4.0
			3	298.90	215.3	5.0
3	Pulsed current GTAW	Pulse=2Hz	1	320.35	230.1	4.0
			2	304.15	220.8	6.2
			3	271.32	145.56	3.0
		Pulse=4Hz	1	250.43	182.71	3.0
			2	216.80	168.98	3.0
			3	253.95	182.92	3.0
		Pulse=6Hz	1	282.25	202.42	3.5
			2	258.50	160.84	3.0
			3	262.30	170.35	3.0

RESULTS AND DISCUSSIONS

Mechanical Properties

A 10 Ton capacity universal testing machine was used to test the tensile test workpieces. Tensile test results of 1.5mm thickness sample were shown in table 4, whereas Table 5 shows the results of 2.5mm thickness sample. 1.5mm thickness sample displayed failures at weld metal and heat affected zone. On the contrary, 2.5mm thickness sample failed at parent metal.

With low frequency i.e 2Hz pulsed welding, both 1.5mm and 2.5mm thickness weldments showed maximum UTS, 0.2% Yield strength compared to high frequencies of 4, 6Hz and non-pulsed current welding. Values of maximum UTS, 0.2% for 1.5mm and 2.5mm thickness weldments with 2Hz frequency are 257.54 Mpa, 199.46 Mpa, and 304.15 Mpa, 220.8 Mpa. Elongation percentage values for 1.5mm thickness samples increased with an increase in the frequency of current whereas 2.5mm thickness sample showed opposite behavior. 2.5mm thickness sample showed an elongation percentage value of 6.2 with a frequency of 2Hz. Ductility observed to be comparatively more in 1.5mm thickness sample with pulsed welding than non-pulsed current welding.

Figures 5 and 6 show the 1.5mm and 2.5mm thickness sample mechanical performance curves respectively.

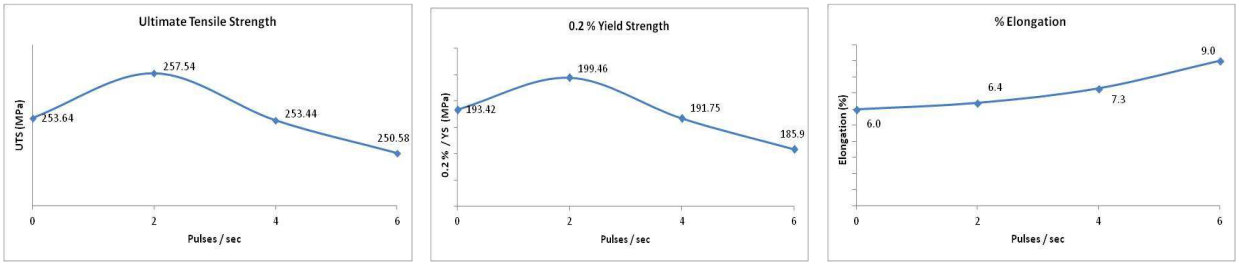

Figure 5: Mechanical Properties Performance Curves of 1.5 mm thick Weldments

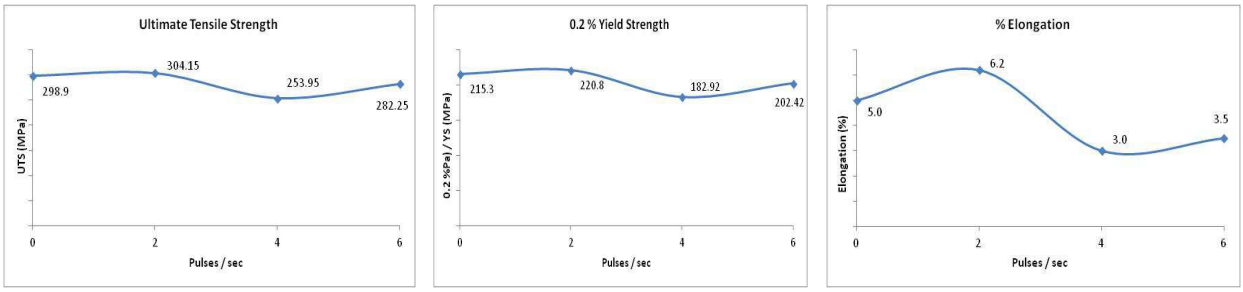

Figure 6: Mechanical Properties Performance Curves of 2.5 mm thick Weldments

Micro-Hardness

Vickers microhardness machine HV1000 ZDT was used to test welded samples for hardness. Hardness variation observed to be minimum between welded and heat affected zones with non-pulsed welding and it has significantly decreased and approached the value of parent material. Peak hardness values observed to be 95HV for non-pulsed current welding in weld zone and 112HV for pulsed current welding with 2Hz frequency compared to other frequencies. Microhardness values for 1.5mm thickness sample is shown in Figure 7 and Figure 8 shows the values for 2.5mm thickness sample.

Weld strength observed to be more with pulsed current welding than non-pulsed welding. This can be attributed to microstructure refinement with pulsed current welding which helps in a fine precipitate homogeneous matrix. Because microstructure is casted, fusion zone normally gives minimum hardness values. This zone consists of phases of interdendritic segregate, coarse dendritic grains and none of strengthening phases. Enhanced microstructure and minimal separation of strengthening phases caused better hardness values with pulsed current welding compared to non-pulsed welding. Improved hardness values in the vicinity of fusion boundary in pulsed current welding can perhaps be ascribed to age hardening which might have caused by sizeable no of alloying elements present in solid solution at closing stages of the thermal cycle.

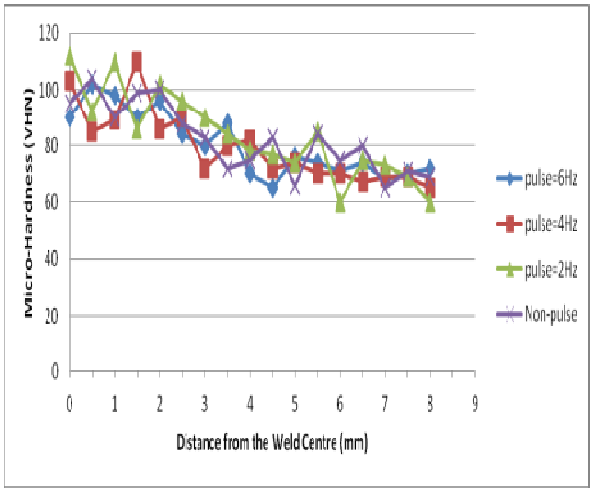

Figure 7: Micro-Hardness Profiles of 1.5mm Weldments

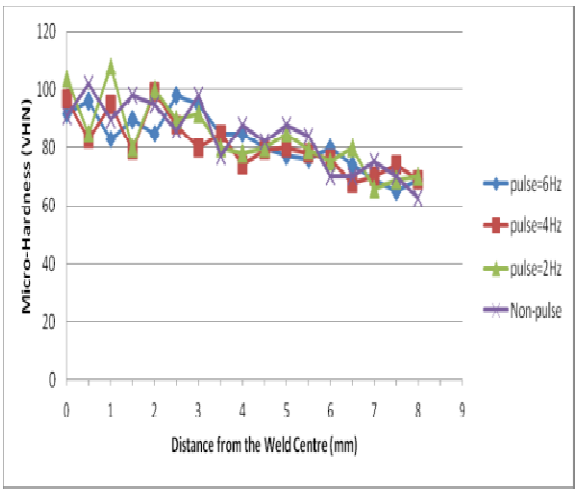

Figure 8: Micro-Hardness Profiles of 2.5 mm Weldments

CONCLUSIONS

Mechanical properties, as well as metallurgical ones, were found to be more affected by pulsed current welding. Pulsed current welding observed to have given maximum Ultimate Tensile Strength, 0.2% Yield Strength and % elongation compared to non-pulsed current welding. A hardness of weldment also appears to be superior with pulsed current welding. Pulsed current welding has generated refined grain size in the fusion zone. This refined grain size generation can be attributed to the enhancement of tensile strength and hardness properties of the weldment.

REFERENCES

1. *Troyer, W., Tomsic, M., and Barhotst, R, "Welding characteristics of Aluminium alloy "welding journal, 56(1), 1977, 26-32.*
2. *Becker, D, W. and Adams, C.M, "The role of pulsed GTA welding variables in solidification and grain refinement" welding journal, 58 (5) 1979, 134s-152s*
3. *Becker, D, W. and Adams, C.M, ""Investigation of Pulsed GTA Welding parameters" welding journal, 57 (5) 1978, 134s-138s.*
4. *Omar, A.A, and Lundin, C. D, "welding journal",58(4), 1970, 97s-104s.*
5. *Tseng, C.F. and Savage, W, F, "The effect of oscillation" welding journal, 50 (11) 1971, 777-786.*
6. *Sharir, Y., Peiieg, J. and grill, "Metallurgical Technology", 5, 1978, 190-196.*
7. *Tsai, C.L., and Hou, C, A, "Theoretical Analysis of Weld Pool Behavior in the Pulsed Current GTAW Process", Heat Transfer, 110, 1988, 160-165.*
8. *Kate, S and Tanabe, S, "High speed welding of 0.5mm thickness alloy sheets using pulsed TIG welding", Welding International 7, 1988, 602-608.*
9. *Tsen, K.H. and Chou, C.P, "Effect of pulsed gas tungsten arc welding on angular distortion in austenitic stainless steel weldments", science and Technology of welding and joining 6, (3), 2001, 149-153.*
10. *Reddy, G.M., Gokhale, A, A. and Prasad Rao K, "Effect of filler metal composition on weldability of Al-Li alloy 1441", Material Science & Technology, 14, 1998, 61-66.*
11. *Giridharam, P.K and Muragan, N, "Sensitivity Analysis of pulsed current GTA welding process parameters on weld bead geometry", National conference in advances in joining Technology 2004.*

12. *Mohandas T, Madhusudhan Reddy G (1996) Effect of frequency of pulsing in gas tungsten arc welding on the microstructure and mechanical properties of titanium alloy welds, J Mater Sci Lett 15: 625-628.*
13. *Shelwatker DA, Madhusudhan Reddy G, Gokhale AA (2002) Gas tungsten arc welding studies on similar and dissimilar combinations of Al-Zn-Mg alloy RDE 40 and Al-Li alloy 1441. SciTechnol weld Join 352-361.*
14. *Uduehiabhulimen, I. Evaluation of the hardness and microstructure of a tungsten inert gas weld of a mild steel pipe joint.*
15. *Vahid Nazarpoor, Abdoreza, Soltanipoor, Khosrow Farmanesh "Effect of current on Mechanical, Metallurgical and Corrosion Properties of AA 5083 Aluminium Alloy Pulse TIG Welding Joints" Journal of Materials Science, vol. 2, 2010, 54-67.*
16. *Ramulu, M and Rubbert, M.P, "Gas Tungsten Arc welding of al-li-cu alloy 2090", Welding Reaserach Supplement, 109s-114s.*

Health and Technology
https://doi.org/10.1007/s12553-018-00290-4

ORIGINAL PAPER

IDSS-based Two stage classification of brain tumor using SVM

Sanjeeva Polepaka[1] · Ch. Srinivasa Rao[2] · M. Chandra Mohan[3]

Received: 14 September 2018 / Accepted: 27 December 2018

Abstract
The computer and image processing has a significant role in detecting tumor area. The decision support systems for human brain MR images are essentially encouraged with the requirement of attaining maximal achievable efficiency and the motivation of the approach which is to enhance the performance of Computer-Aided Diagnosis (CAD) system to detect a tumor in the human brain. Even though numerous support systems have been introduced in the past, this is still an open problem seeking for an accurate and robust decision support system. The Interactive Diagnosis Support System (IDSS) approach has addressed the limitations of nonillumination and low contrast of a brain tumor MR image that influences the procedure of accurate image classification. Thus, the IDSS is implemented in three phases namely image preprocessing for enhancing non-illuminated features, feature extraction and image classification which is accomplished using two-stage interactive SVM Classification. The local binary patterns are detected in the feature extraction for accurate classification of usual and unusual brain MR Images. The experimental outcomes for this approach are carried out using MATLAB R2016a and evaluated using the brain images downloaded from the Internet. The performance metrics such as structured similarity index, sensitivity, specificity and accuracy were used to assess the IDSS-based tumor classification system. When compared with the traditional classifiers such as ANFIS, Backpropagation and K-NN, the IDSS approach has significant brain tumor classification accuracy.

Keywords IDSS · Brain tumor · Tumor segmentation · Tumor classification · LBP · SVM · Non-illumination · Feature extraction · CAD

1 Introduction

The tumor is an unbounded evolution of cancer cells in any part of the body. Tumors are of different types and have dissimilar characteristics and divergenttreatments [1]. Amongst them,abrain tumor is the most dangerous and rigorous disease that requires a very clear diagnosis by the physician who could classify the tumor very accurately. Thus, intelligent digitalized image processing approaches are extensively used in the detection and classification phases of tumor images. Magnetic Resonance Imaging (MRI) or Computed Tomography (CT) scan are used to analyzebrain life structure. When associated with the CT scan, MRI scan is mucheffective as CT scan do not use any radiation [2]. Tumor comprisesvarious biologic tissues;The whole information related to anomalous tissues cannot be gathered by only a single kind of MRI. Distinctive complementary information can upgrade the diagnosis of tumors.

World Health Organization (WHO) has identified more than 120 classes of tumors [3]. The origin of primary brain tumors is in the brain itself while secondary brain tumors may be developed in any body part and move towards brain as Metastatic (METS) tumor. These brain tumors are analyzed and visualized with the help of MRI. The detailed information of any body part is obtained with the help of radio-waves and magnetic field provided through the MRI machine. An Efficient decision support system can intensify the diagnostic capability of physicians and can decrease the time needed for precise diagnosis by increasing the effectiveness of the system. Typically, the efficiency of any support system is

This article is part of the Internet Of Medical Things In E-Health Hassan Fouad Mohamed- El-Sayed and M. Hemalatha

✉ Sanjeeva Polepaka
psanjesus18@outlook.com

[1] Department of CSE, MREC (A) & Research Scholar (JNTUH), Secunderabad, India

[2] Departments of ECE, JNTUKUCEV, Vizianagaram, India

[3] Department of Computer Science and Engineering, JNTUCEH Hyderabad, Hyderabad, India

Published online: 23 January 2019

measured using the classification accuracy, specificity and sensitivity. In this regard, the decision support system of MRI images of the human brain is still an open problem which needs a continuous study on different existing approaches.

In this paper, a methodology for detecting the brain tumor MRI image which is robust and capable to support the clinical decisionis introduced. The IDSS approach attempts to achieve accuracy in the decision support system by understanding the characteristics of every region and through extracting the key features from the tumor attacked region in the MRI image. One of the challenges in the MRI is its less contrast and non-uniform illumination. Illumination is a very significant part in recognition of tumor from the context along with the outcome of non-uniform illumination. This produces a substantial fault during classification. Thus, it is essential in minimizing the non-uniform Illuminations and this, in turn, normalizes the low contrast of the image. Further extracting the normal and tumor lesion distinctively which in turn assists in the efficient classification of tumor effected MRI images. The experiment outcomes of the suggested methodology have shown that, the Interactive Diagnosis Support System gives an accurate classification [4] compared to the existing CAD or Decision Support Systems.

1.1 Organization of the Paper

An analytical survey in identifying the brain tumor of MR images by using different intelligent digitalized image processing approaches and classification phases along with the motivation for the IDSS approach is discussed in section 1. The related survey and studies on CAD systems and different processing techniques involved in theconstruction of CAD for attaining high accuracy are discussed in section 2. An Interactive Diagnosis Support system to identifythe tumorin MRI brain images is discussed in section 3.Section 4 consists of experimental outcomes and its analysis. Conclusions are discussed in section 5 followed by references.

2 Related survey

The technology and the research on CAD systems have proved that CAD helps in improving analytical accurateness of radiologists, reducing the load of rising capability, minimizes cancer missed because of overloaded data, exhausting data, or overlooked and to enhance inter-reader variability and intra-reader variability [5]. The radiologists must make the conclusive medical decision. Many analysts have suggested systems and image processing techniques for brain tumor detection.

Morphological operators areemployed for the extraction of tumor part [6]. Non-negative Matrix Factorization (NMF) is utilized for brain tumor detection [7]. The neuro-fuzzy method is applied for the detection of numerous tissues like White Matter (WM), Gray Matter (GM) and Cerebrospinal Fluid (CSF) [8]. To construct a CAD system, different image processing operations must be integrated and some essential image processing operations involved in integration are image segmentation, feature extraction and selection, and categorization. At recent times, different kinds of brain computer-aided detection methods [5, 9–12] being developed through brain MR images that depends on numerouskinds of machine learning classifiers that have been developed by several researchers.

The detection of texture pattern is widely introduced for pattern identification and computer vision appliances for its capabilityto capture noticeable characteristics. LBP operations and its variations are significant methods for texture analysis that are stated by numerous scholars. LBP feature has been effectively employed on texture-basedimage categorization [13] beneath the rotation invariant and multiple resolution constrictions. It straightforwardly employsthe LBP methodology on the grayscale image to obtain features in image classification. Methodology in [14] suggested a novel enhancement in LBP-aided feature through accumulating the scale-adaptive information and sub uniform aided sphericalmove for processing scale-invariant texture-basedimage classification. The methodology in [15] stretched the dominance of LBP feature on the facial identification system. This methodologyexamined the derivation of LBP on processing illumination issue, rotational and angulardiscrepancies, along with the facial expression discrepancies on face identification system with anencouragingoutcome.

An appliance of LBP feature on unusualimage identification is givenin [16] beneath endoscopy video. This methodology is beneficial inrecognizingmucosal irregularities for medicinal and health appliances. This methodology employed the LBP approach using a definitefilteredbank that could produce a significant outcome on irregular detection efficiency. The methodology in [17] suggested the rotational invariant co-occurrencei.e.the LBP adjacency understanding for HEp-2 cell categorization system. It used SVM for processing image categorization that exhibited a goodperformance matched with the previous approaches. The methodology in [18] employed LBP feature on spoof thumbprintrecognitionbeneath multi-scale circumstance, whereas the methodology in [19] amalgamated the LBP feature on eye identification system. As stated in [18, 19], the LBPfeature provides significant outcomes on the spoof thumbprint recognition and eye identification system. The methodology in [20] suggested a novel approach on object recognition with the shape aided non-recurrent LBP that provides a significant performance when matched with two other approaches. The fusion policies amongst the Gabor filter banks and LBP operations have been illustratedto provide aneffectiveoutcome on image classification system [21–26].

In [27], a data sample of 856 SROIs from 428 post-contrast T1 MR-imagesare considered. PCA along with Artificial Neural Network (ANN) had been employedwhich gave

85.23% of overall accuracy and an individual class accuracy of 86.15% for Astrocytoma, 65.10% for Glioblastoma Multiforme, 63.36% for Medulloblastoma, 91.50% for Meningioma andMetastases it is 65.21%. An experiment has been performed by [28] on 98 images from which 100 features are extracted. The feature extraction process unit has Gabor, GLCM, intensity, shape and statistical techniques for obtaining features. An Accuracy obtained for Metastatic is 91.7%, 90.9% for Low-Grade Glioma, 41.2% of accuracy for Glioblastoma Multiforme and 33.4% of accuracyis obtained for Glioma Grade III.

[29] studied Glioma, Meningioma, and Metastatic brain tumors using Least Square Feature Transformed-Probabilistic Neural Network (LSFTPNN). A PNN classifier has given effective outcomes compared to other classifiers in computational load and training. The output of LSFT is given as the input to PNN because of better pattern classification ability of LSFT. A dataset of 75 images of Glioma, Meningiomas, and Metastatic has been collected. An individual class accuracy of 96.67%, 95.24%, and 87.50% has been achieved for Gliomas, Meningiomas, and Metastates respectively. A different study has been carried out on a database consisting of 50 Metastatic brain images, 50 images of Glioblastoma brain images, 50 images of Glioma brain tumor and 50 normal brain images. Testing has been carried out for this database with vocabularyknowledge and sparse coding classifier having K-SVD approach and has achieved 93.75% of overall accuracy [30].

Pourhashemi, Haghighatnia and Moghaddam [31] proposed a recurrent neural network-based tumor-immune identification system. The interaction between the tumor and immune cells were represented using Ordinary Deferential Equations (ODE). Later, the back propagation neural network (three-layer backpropagation with five feedbacks as input) along with the sufficient hidden layers was used to identify the tumor-immune system. Experimental results concluded that the efficiency of the immune system could be improved by properly choosing the number of neurons and layers in the network.

3 Materials and methods

Figure 1 shows the block diagram of IDSS to categorize the tumor in the MRI brain images.

This overcomes some of the limitations of existing decision support system in analyzing the MRI image at every phase of image processing. The IDSS for tumor detection methodis developed using three main phasesnamelyPre-processing, Feature Extraction and Image Classification which is accomplished using two-stage interactive SVM Classification. Tumor detection in MRI is more efficient because of its low radiation, high contrast, and spatial resolution.

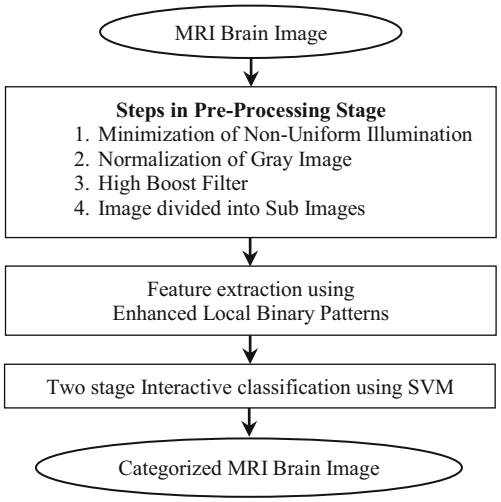

Fig. 1 Block Diagram of the IDSS

3.1 Image pre-processing phase

The MRI pre-processing operations were introduced before the feature extraction technique because it is straightforwardly related to the quality of classification results. Generally, the raw MRI images need to be pre-processed to realize the main purpose of classification. The necessity of efficient identification of tumor on effected Brain images will influence the original image features which are less contrast and non-uniform illumination. Generally, it is observed that the red and green pixels comprise of maximum image information because of the behavior of the images which are having blue pixels less in number. Thus, dispersing the blue pixel values, more consideration is given to red and green pixels to diminish non-uniform illumination [32].

Minimization of Non-Uniform Illumination: The values of red and green frequencies aremerged to minimize non-uniform illumination in employing these frequencies in proper ratios and are assumed to be persistent autonomously from illumination. The evaluation for the ratio ofthegreen element with the red one is calculated for every pixel to attain a new image, to diminish the influence of non-uniform illumination and is given in Eq. 1.

$$Im_{ie} = Im - Im_{bg} + \mu \tag{1}$$

Here Im represents the original green channel image, Im_{bg} represents the background image, μ signifies the average intensity value and $Im_{ie}$is the illumination equalization image.

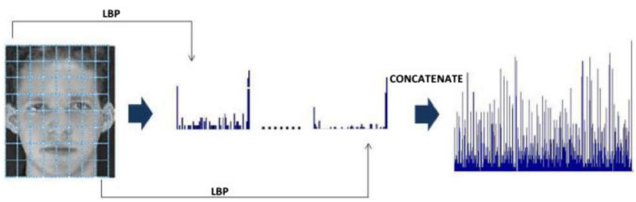

Fig. 2 ELBP pattern descriptor (Courtesy: Source [36])

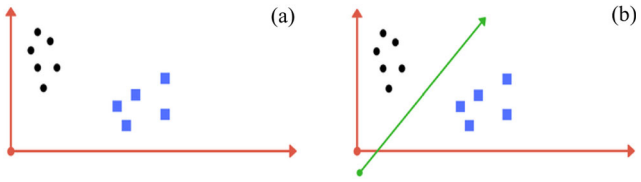

Fig. 3 (**a**) Two classes of data (**b**) Class separation using hyperplane

In the IDSS approach, the enhancement of the low contrast images is carried out through two different approaches. Initially, Normalization is performed on the reduced non-illumination image and formerly the edges of the MRI images are enhanced using Morphological Operations.

Normalization of Grayscales: Generally, the approach needs to get accepted to diverse circumstances beneath where theMRI images are seized, and enhancement of the required images from dissimilar backgrounds could be attained through regularizing the image grayscale information. As given in eq. 2, the Normalization is accomplished usinggray scaletransformation.

$$Im_{norm} = \frac{\left(Im_{gray} - \min\left(Im_{gray}\right)\right) * 255}{\max\left(Im_{gray}\right) - \min\left(Im_{gray}\right)} \quad (2)$$

Here Im_{gray} represents the original image grayscale value, Im_{norm}represents the gray scale value of theoutput image (Normalization). $\min(Im_{gray})$ represent the minimumgrayscale for the original image and $\max(Im_{gray})$represents the minimumgrayscale for theoriginal image.

High Boost Filter: It enhances the image quality from theprevious step consideringlow-level information and edge information.

Sub Images Formation: To extract ELBP,the image is divided into 4 × 4 sub-images.

3.2 Feature extraction

The enhanced image obtained from the preprocessing phaseis given as input to the feature extraction phase. The features present in this enhanced image are thenoticeable patterns that make available thenon-illuminated and contrast information regarding the image. The accurateness of the classificationrelies upon the feature extraction phaseand the local binary patterns [33–35] are extracted from this phase. This approach encrypts the pixel-wise data in textured images.

Table 1 Terms specifying Confusion matrix

		Actual Class		
		Positive	Negative	Row Total
Predicted Class	Positive	TP	FP	TP + FP
	Negative	FN	TN	FN + TN
	Column Total	TP + FN	FP + TN	TP + FP + FN + TN

The LBP operator results in texture representation of a given image in the following manner [36]; Each pixel is compared with neighboring eight pixels and subtracted from the center pixel's value. Based on the resultant value, the encoding takes place as 1 (for positive values) and 0 (for negative values). A binary number for a given pixel is determined by connecting these binary numbers from a top-left corner in a clockwise direction. The LBP label's histogram represents the texture descriptor(s). The operator LBP(P,R) with point $P = 8$ and radius $R = 1$ results in histogram size 2^P. The LBP-based texture descriptor divides the image into blocks and extracts the LBP independently for such blocks and concatenates spatially to form the descriptor as shown in Fig. 2. The applications of.

The traditional LBP operation employs a 3 × 3 square adjacent centralized at the given pixel. The methodology allots 0 or 1 value to 8 adjoining pixels using eq. 3.

$$N = \begin{cases} 1, & if\ g_N < g_C \\ 0, & otherwise \end{cases} \quad (3)$$

Here N is the binary value allotted to a neighboring pixel, g_N refers to the grayscalevalue of the neighboring pixel and g_C

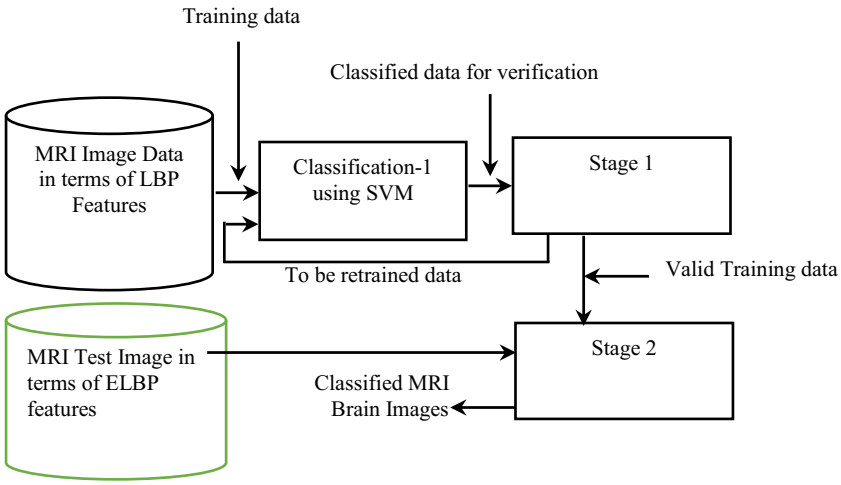

Fig. 4 Two stage interactive classification process

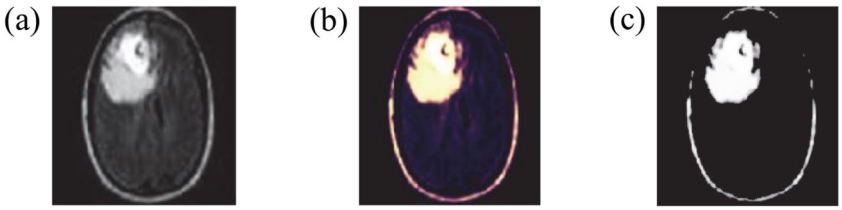

Fig. 5 Experimental outcomes of image 1 (**a**) Original image (**b**) preprocessed image. (**c**) High Boosted Image

is the grayscale value of the centralized pixel. The obtained values are further amalgamatedto an 8-bit binary number. Its decimal notation is employed to generate a feature vector.

The original LBP operator computes the feature values from point-sets instead of the isolated points. In this paper, consider the 4 X 4 sizes of the sub-images usingneighborhood property. This concept can handle several LBP issues [22, 37–39]. Let G_N be a set of neighboring pixel intensities with its center C_N, let G_C be a set of central pixel intensities with its centre C_C and r be the distance between the centres C_N and C_C. We calculate the representative values for these sets as averages of the pixel intensities belonging to these sets: $g'_N = \text{mean}(G_N)$ and $g'_C = \text{mean}(GC)$. The feature vector is then createdidentically as in the circumstance of the original LBP operator using g'_N and g'_C values instead of g_N and g_C, respectively. Note that it is possible to consider several point-set topologies of different sizes to capture different texture information, however, in this paper, we use only the square shapes of the sizes 2×2, i.e. 4 points and 3×3 points, i.e. 9 points. The operator is further denoted as $\text{E-LBP}_{x,y,r}$, where $x \in \{4, 9\}$ represents the neighboring pixel-set topology, $y \in \{4, 9\}$ is the central pixel-set topology and r is the distance between the centres C_N and C_C, which is hereafter called E-LBP range. The advantages of LBP include immense discriminative power, simplicity in computation(s), invariant to grayscales changes with better performance [40, 41].

3.3 Image classification

In this phase, the extracted features such as exudates are employed for the categorization of usual and unusual images. In this phase,two-stage interactive SVM Classification, which is said to be a robust categorizer,is employed in the process of image classification [2, 7, 9, 27].

The SVM is a classifier, which classifies the class(es) using a separating hyperplane. For example, with the two dimensional trained data as input, the hyperplane categorizes the classes. Figures 3 (a) and (b) shows the two classes (black circles and blue squares) and the classification using hyperplane (shown in green color line) are summarized from (https://medium.com/machine-learning-101/chapter-2-svm-support-vector-machine-theory-f0812effc72). For more than two classes (that is multidimensional space), four parameters of SVM, namely, (1) Kernel, (2) Regularization, (3) Gamma, and (4) Margin,are tuned for better classification results.

Initially, a training set composed of LBP features of brain images has been consideredand this paper suggests a two-stage interactive classification tomaximize accuracy. The diagrammatic representation of two-stage interactive classification process is shown in Fig. 4. To attaina valid trained data, the primarily used data is MRI data (training data) byusing classification followed by the verification which is done by the expert.

The classified data from the classifier-1 is sent for the verification and here error checking and re-modification of data according to necessity is verified and carried out by an expert. The data is retrained again by the expert until the error rate is reached to criteriai.e., (<1%). This entire process is iterated until the criteria are satisfied. Finally, the valid trained data is obtained after the specified criteria are met. The classifier-2 classifies this valid data to produce high accuracy classified MRI Brain images.

4 Experimental results and its analysis

The Implementation of the suggested Interactive Diagnosis Support System for Brain Tumor Detection approach is performedby using MATLAB R2016a.To validate the performance of the suggested approach, two standard data samples are employed. The initial data samples are obtained from Digital Imaging and Communications in Medicine (DICOM). To analyze the suggested methodology, this work incorporates 22 images from the DICOM, where the images are tumor-

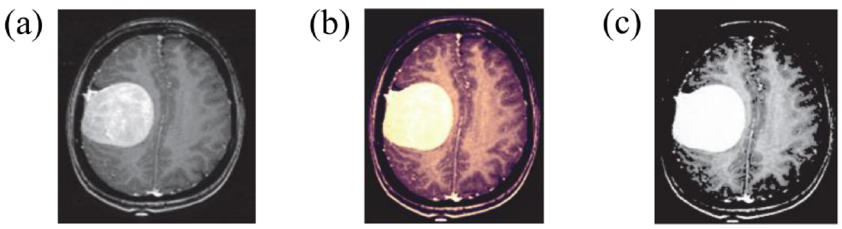

Fig. 6 Experimental outcomes of image 2(**a**) Original image (**b**) Enhanced image (**c**) Skull-stripping image

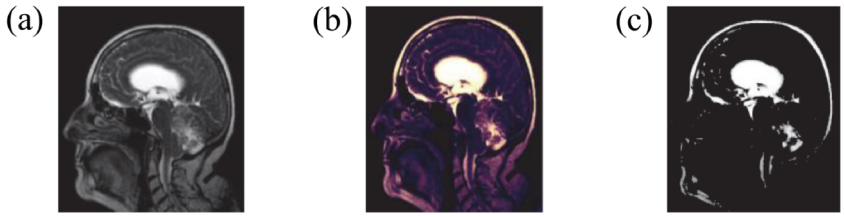

Fig. 7 Experimental outcomes of image 3. (**a**) Original image (**b**) Enhanced image (**c**) Skull-stripping image

infected brain tissues. Nevertheless, these data samples do not provide any ground truth images. The subsequent data sample is the Brain Web data sample, that comprises of 3D replicated brain MR information attained employing three series of modalities, such as T1-weighted, T2-weighted and proton density-weighted MRI. These data samples consist of diversity of slice thicknesses, noisy levels, and intensity non-uniformity level. Most of the images employed for the analysis consists of T2-weighted modality with 1 mm slice thickness, 3% of noise, and intensity non-uniformity is of 20%. In this data sample, 13 out of 44 images are tumor affected brain tissues. In this section, it provides the outcomes of the suggested image classification approach that are achieved through real brain MR images.

Performance Evaluation:Structured Similarity Index (SSIM), Mean Square Error (MSE), Peak Signal-to-Noise Ratio (PSNR) and the Dice co-efficient are the different metrics used in the performance evaluation as explained below:

4.1 Performance metrics

Structured Similarity Index (SSIM): The Structural Similarity Index (SSIM) is a perceptual metric that signifies the degradation in image quality which may be caused by data compression or losses in data transmission or by any other means of the image processing. It is shown in eq. (4)

$$SSIM = \left(\frac{\sigma_{xy}}{\sigma_x \sigma_y}\right)\left(\frac{2\overline{x}\,\overline{y}}{\left(\overline{x}\right)^2 + \left(\overline{y}\right)^2 + C_1}\right)\left(\frac{2\sigma_x\sigma_y}{(\sigma_x)^2 + (\sigma_y)^2 + C_2}\right) \quad (4)$$

Better preservation of luminance, contrast, and structural contentshows the higher value of SSIM.

Mean Square Error (MSE):Itisthe measurement of signal fidelity or image fidelity. The purpose of signal or image fidelity measurement is to obtain the connection or fidelityamongst two images through giving the quantitative score. Whenever MSE is calculated, then it is presumed that one of the images is perfect original, whereasanother one is distorted or handled using some means and it is defined in eq. 5 as shown below

$$SD(\sigma) = \sqrt{\left(\frac{1}{mXn}\right)\sum_{x=0}^{m-1}\sum_{y=0}^{n-1}(f(x,y)-M)^2} \quad (5)$$

Peak Signal-to-Noise Ratio (PSNR) in dB: It is a measure to evaluate thequality of reconstruction of theprocessed image and is given inequation 6.

$$PSNR\ in\ db = 20\log_{10}\frac{(2^n-1)}{MSE} \quad (6)$$

Better signal-to-noise ratioexhibits the Lower value of MSE and the higher value of PSNR.

Dice Coefficient: Dice coefficient or dice similarity index is a metric that overlayamongst two images and is givenbelow

$$Dice(A,B) = 2X\frac{|A_1 \wedge B_1|}{(|A_1| + |B_1|)} \quad (7)$$

Here $A \in \{0,1\}$ is tumor region mined from algorithmic forecasts and $B \in \{0,1\}$ is the professionals ground truth. The minimal value of dice coefficient is 0 and maximal value is 1. The high value denotes better overlay amongst two images.

To estimate the efficiency of the Suggested Methodology, the Sensitivity, Specificity andAccuracy are derived from the results. These values are estimatedusinga confusion matrix that is given in Table 1.

Here True Positives (TP) isimages that are appropriately acknowledged andFalse Negatives (FN) isthe imageserroneously excluded. TrueNegatives (TN) is the circumstances appropriately excludedandFalse Positives (FP) is the objects which are erroneously recognized as lesions.

Table 2 Performance analysis parameters after preprocessing

Images	MSE	PSNR	SSIM	Dice Score
Image1	1.73	55.25 dB	0.7944	0.73
Image2	0.46	68.11 dB	0.8025	0.77
Image3	4.84	56.18 dB	0.8702	0.72

Table 3 Classification accuracies based on feature extraction

Classifiers	Accuracy (%)
ANFIS	90.04
Back Propagation	85.57
SVM	96.51
K-NN	87.06
IDSS Approach	97.02

Table 4 Accuracy Comparison

Validated images (Usual = 67, Unusual = 134)					
Evaluating Metrics	ANFIS	Back Propagation	SVM	*K*-NN	IDSS Approach
True Negative (TN)	63	62	65	63	66
False Positive (TP)	16	19	4	18	4
True Positive (TP)	118	110	129	112	130
False Negative (FN)	4	10	3	8	2
Specificity (%)	79.74	76.54	94.2	77.77	94.28
Sensitivity (%)	96.72	97.5	97.72	93.33	98.48
Accuracy (%)	90.04	85.57	96.51	87.06	97.02

Sensitivity is defined as the proportion of properlycategorized as true positives amongst the complete exudates given in eq. 8.

$$\text{Sensitivity} = \frac{\text{TP}}{\text{TP} + \text{FN}} \tag{8}$$

Specificitygiven in equation 9is the capability to detect the portion of thepopulationthat does not have exudates that is true negatives and is statedas the proportion of appropriatelycategorized as true negatives amongst the complete non-exudates.

$$\text{Specificity} = \frac{\text{TN}}{\text{TN} + \text{FP}} \tag{9}$$

Accuracy given in equation 10is determined as the degree of approximation of the measurement conforms to the corrected value and is shown below

$$\text{Accuracy} = \frac{\text{TP} + \text{TN}}{\text{TP} + \text{TN} + \text{FP} + \text{FN}} \tag{10}$$

Figures 5, 6, and 7 show the sample experimental outcomesattained from this technique. These Figures show three different types of images namely original image, pre-processed image, high boost images.

Table 2 has given the values of 4 different performance metrics namely MSE, PSNR, SSIM and dice score as mentioned below. From this, it can be inferred that MSE is less and PSNR is high, denotesthat the extracted image has improved thesignal-to-noise ratio. Dice coefficient measures are the overlay of the automatic and manual classification for the givenBRATS image database.

Table 3 shows the classification accuracy of different classification approaches and the same is depictedin the figure.

This has shown that there is an increase in the performance of the classifier for brain MRI with feature extraction i.e. 90.04% in an adaptive fuzzy inference system (ANFIS), 85.57% in Back Propagation, 96.51% in SVM, and 87.06% in *K*-Nearest Neighbors (*K*-NN).

Table 4 exhibited the testing performance of the classifiers which is defined through evaluation of the statistical measures like sensitivity, specificity, and accuracy for dissimilar classification approaches. Better performance shows the higher values of accuracy and sensitivity and a low value of specificity (Fig. 8).

From Table 4, it is clearly saidthat the performance of the classification algorithm is good when compared to the existing techniques. Since even a modest improvement in the sensitivity parameter is very important and critical for a

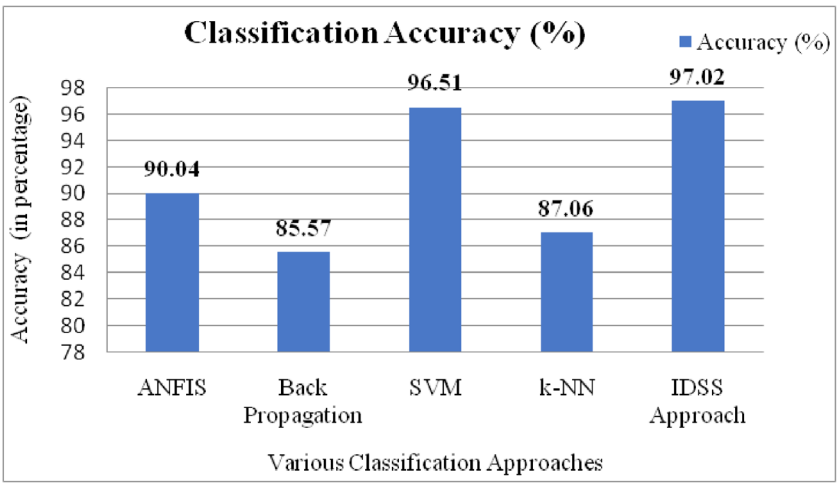

Fig. 8 Classification Accuracy of various approaches

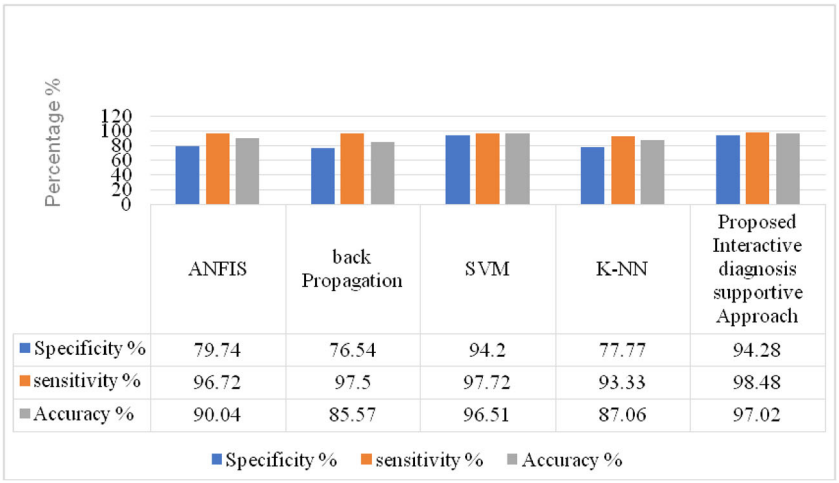

Fig. 9 Comparative analysis with existing classifiers

radiologist or clinical doctors in surgical planning. The efficiency of the suggested methodology that is Interactive Diagnosis Support System for Brain Tumor Detection has remarkably shown immense improvement in the tumor identification with the performance measures like accuracy, specificity and sensitivity when compared with the existing systems. Table 4 shows that the Higher values of accuracy with 97.02%, and sensitivity of 98.48% and a lower value of specificity with 94.28% specify the better performance of the suggestedmethodology.

The performance measures of IDSS such as TP, TN, FP, FN, accuracy, specificity and sensitivity are compared with existing classifications namely ANFIS, Back Propagation, and k-NN classifier. The detailed analysis of performance measures is shown in Figs. 9 and 10, respectively.

Through the performance measure as mentioned in the above Figure, it is depicted that the performance of the IDSS methodhas a remarkable improvement in the tumor identification matched with the ANFIS, Back Propagation, and *K*-NN aided classification techniques.

5 Conclusion

In this paper, a robust and novel brain tumor detection technique which aids on two-stage interactive SVM Classification has beenimplemented. This methodology is developed using three phases namely Image Pre-processing for enhancing non-illuminated features, Feature Extractionand Image Classification. Image Pre-processing phase is used to enhance the low contrast images and in Reduction of Non-Uniform Illumination which in turn are used as the inputs to the feature extraction which is the next phase of Image Pre-processing. The accurateness of the classification depends on the feature extraction phase. The local binary patterns and crack edges are extracted in this phase. In this image classification phase, the two-stage interactive support vector machine (SVM) is said to be a robust classification which is employedin the process of image classification. The two-stage interactive SVM minimizes the actual risk and averts the overfitting problem and this results in a good performance. The Experiment is carried out using MATLAB R2016, a version on an Intel Core i5

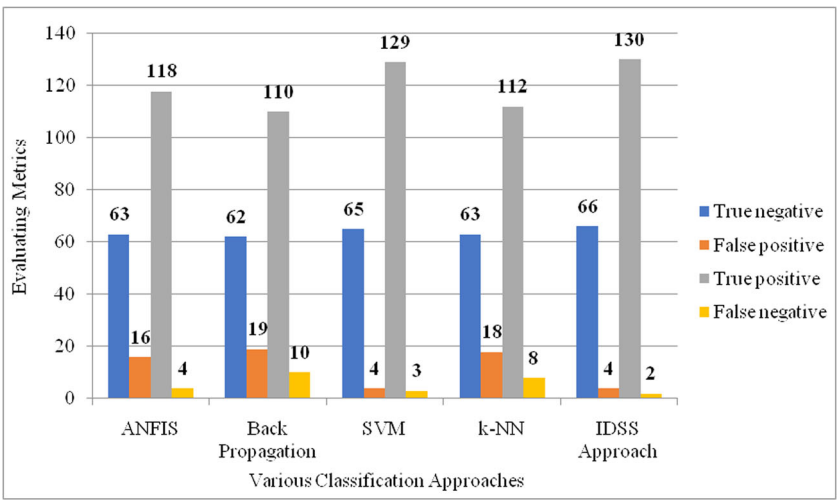

Fig. 10 Comparative analysis concerning Evaluating Metrics

processor at 2.5 GHz. The performance of the suggested methodology that is Interactive Diagnosis Support System has remarkably improved in the tumor identification with the performance measures such as accuracy, specificity and sensitivity when compared with the existing systems. i.e. The Higher values of accuracy with 97.02%, and sensitivity of 98.48% and a lower value of specificity with 94.28% denotes better performance for the suggested approach.

Funding This is self funding by the primary Author, Sanjeeva Polepaka.

Compliance with ethical standards

Conflict of interest No conflict of Interest with any person, Company or institution.

Informed consent Not applicable.

References

1. Patel J, Doshi K. A study of segmentation methods for detection of tumor in brain MRI. Adv Electron Electr Eng. 2014;4(3):279–84.
2. Shaikhli SDS, Yang MY, Rosenhahn B. Brain tumor classification using sparse coding and dictionary learning, IEEE Conf. on Image Processing. 2014; 2774–2778.
3. Mustaqeem A, Javed A, Fatima T. An efficient brain tumor detection algorithm using watershed and thresholding-based segmentation. International Journal of Image Graphics and Signal Processing. 2012;4(10):34–9.
4. Shakeel PM, Baskar S, Dhulipala VRS, et al. Cloud based framework for diagnosis of diabetes mellitus using K-means clustering. Health Inf Sci Syst. 2018;6:16. https://doi.org/10.1007/s13755-018-0054-0.
5. Fujita H, Uchiyama Y, Nakagawa T, Fukuoka D, Hatanaka Y, Hara T. Computer-aided diagnosis: the emerging of three CAD systems induced by Japanese health care needs. Comput Methods Prog Biomed. 2008;92(3):238–48.
6. Sridhar KP, Baskar S, Shakeel PM, et al. Developing brain abnormality recognize system using multi-objective pattern producing neural network. J Ambient Intell Human Comput. 2018. https://doi.org/10.1007/s12652-018-1058-y.
7. Prajapati SJ, Jadhav KR. Brain tumor detection by various image segmentation techniques with introduction to non-negative matrix factorization. Brain. 2015;4(3):600–3.
8. Dipak Kumar K, Amiya H. Automatic brain tumor detection and isolation of tumor cells from MRI images. International journal of computer applications. 2012;39(1):26–30.
9. Arimura H, Magome T, Yamashita Y, Yamamoto D. Computer-aided diagnosis systems for brain diseases in magnetic resonance images. Algorithms. 2009;2(3):925–52.
10. Cherkassky V, Mulier F. Learning from data: Concepts, theory and methods, (2nd Ed.). John Wiley and Sons, 2007.
11. Mohsen H, Dahshan E, Salem A. A machine learning technique for MRI brain images, Proc. 8thIEEE Conf. on Informatics and Systems. 2012.
12. Yamamoto D, Arimura H, Kakeda S, Magome T, Yamashita Y, Toyofuku F. Computer-aided detection of multiple sclerosis lesions in brain magnetic resonance images: false positive reduction scheme consisted of rule-based, level set method, and support vector machine. Comput Med Imaging Graph. 2010;34(5):404–13.
13. Ojala T, Pietikainen M, Maenpaa T. Multiresolution gray-scale and rotation invariant texture classification with local binary patterns, IEEETransactions on pattern analysis and machine. Intelligence. 2002;24(7):971–87.
14. Li Z, Liu G, Yang Y, You J. Scaleand rotation-invariant local binary pattern using scale-adaptive texton and subuniform-based circular shift. IEEE Transactions Image Processing. 2012;21(4):2130–40.
15. Suruliandi A, Meena K, Rose RR. Local binary pattern and its derivatives for face recognition. IET Comput Vis. 2012;6(5):480–8.
16. Nawarathna R, Oh J, Muthukudage J, Tavanapong W, Wong J, Groen P, et al. Abnormal image detection in endoscopy videos using a filter bank and localbinary patterns. Neurocomputing. 2014;144:70–91.
17. Ryusuke N, Kazuhiro F. HEp-2 cell classification using rotation invariant co-occurrence among local binary patterns. Pattern Recogn. 2014;47(7):2428–36.
18. Jia X, Yang X, Cao K, Zang Y, Dai NZR, Zhu X, et al. Multi-scale local binary pattern with filters for spoof fingerprint detection. Inf Sci. 2014;268:91–102.
19. Gu J, Liu C. Feature local binary patterns with application to eye detection. Neurocomputing. 2013;113:138–52.
20. Nguyen DT, Ogunbona PO, Li W. A novel shape-based non-redundant local binary pattern descriptor for object detection. Pattern Recogn. 2013;46(5):1485–500.
21. Guo Z, Zhang L, Zhang D. Rotation invariant texture classification using LBPvariance (LBPV) with global matching. Pattern Recogn. 2010;43(3):706–19.
22. Liao S, Law MK, Chung AS. Dominant local binary patterns for texture classification. IEEE Trans Image Process. 2009;18(5):1107–18.
23. Ojala T, Pietikainen M. Harwood D. a comparative study of texture measures with classification based on feature distributions. Pattern Recogn. 1996;29(1):51–9.
24. Ojala T, Valkealahti K, Oja E, Pietikainen M. Texture discriminant with multidimensional distributions of signed gray-level differences. Pattern Recogn. 2001;34(3):727–39.
25. Subrahmanym M, Maheswari RP, Balasubramanian R. Local maximum edge binary patterns: a new descriptor for image retrieval and object tracking. Signal Process. 2012;92(6):1467–79.
26. Zhu C, Wang R. Local multiple patterns based multiresolution gray-scale and rotation invariant texture classification. Inf Sci. 2012;187:93–108.
27. Sachdeva J, Kumar V, Gupta I, Khandelwal N, Ahuja CK. Segmentation, feature extraction, and multiclass brain tumor classification. Journal of Digit Imaging. 2013;26:1141–50.
28. Zacharaki EI, Wang S, Chawla S, Yoo DS, Wolf R, Mehem ER, et al. Classification of brain tumor and grade using MRI texture in a machine learning technique. Magn Reson Med. 2009;62:1609–18.
29. Georgiardis P, Cavouras D, Kalatzis I, Kagadis GC, Malamas M, Nikifordis G, et al. Nonlinearleast square feature transformations for improving the performance of probabilistic neural networks in classifying human brain tumors on MRI. Lect Notes Comput Sci. 2007;4707:239–47.
30. Mohamed Shakeel P, Baskar S, Sarma Dhulipala VR, Mishra S. Mustafa Musa Jaber. Maintaining security and privacy in health care system using learning based deep-Q-networks. J Med Syst. 2018;42:186.
31. Pourhashemi A, Haghighatnia S, Moghaddam RK. Identification of tumor-immune system via recurrent neural network. Health Technol. 2014;4(1):27–30.

32. Deva Kumar S, Gnaneswara RN. Wavelet-based Diabetic Retinopathy Image Enhancement in Blood Vessels, 46th Conf. on Computers and Industrial Engineering. 2016.
33. Gnaneswara RN, Ramakrishna SV, Deva Kumar S, Venkata Rao M. An improved IHBM using smoothing projections. Intl Journal of Control Theory and Applications. 2015;8(1):339–48.
34. Ojala T, Valkealahti K, Oja E, Pietikäinen M. Texture discrimination with multidimensional distributions of signed gray-level differences. Pattern Recogn. 2001;34(3):727–39.
35. Manikandan A, Jamuna V. Single Image Super Resolution via FRI Reconstruction Method, Journal of Advanced Research in Dynamical and Control Systems. 2017; 23–28.
36. Moujahid A, Abanda A, Dornaika F. Feature Extraction Using Block-based Local Binary Pattern for Face Recognition, IS&T International Symposium on Electronic Imaging, Intelligent Robots and Computer Vision XXXIII: Algorithms and Techniques, Society for Imaging Science and Technology. 2016; 1–6.
37. Vijaya Kumar V, Srinivasa Reddy K, Venkata KV. Face recognition using prominent LBP Model,Intl. J Appl Eng Res. 2015;10(2): 4373–84.
38. Rao VVK NG, PSVS R. Novel approaches of evaluating texture-based similarity features for efficient medical image retrieval system. International Journal Of Computer Applications. 2011;20(7): 20–6.
39. Smith JR, Chang SF. Automated binary texture feature sets for image retrieval, Proc. IEEE Conf. Acoustics, Speech and Signal Processing, Columbia Univ. 1996; 2239–2242.
40. Local Binary Patterns (LBP) & Histogram of Oriented Gradient (HoG), http://biomisa.org/uploads /2016/10/Lect-15.pdf
41. Graña M, Termenon M, Savio A, Gonzalez-Pinto A, Echeveste J, Pérez JM. Computer aided diagnosis system for Alzheimer disease using brain diffusion tensor imaging features selected by Pearson's correlation. Neurosci Lett. 2011;502(3):225–9.

Strategic Planning to Promote Engineering Projects in Community Service(EPICS) in Engineering Institutions

Dr. S. Sudhakara Reddy, Dr. N. Rajeswaran, Kesava Vamsi Krishna V.
Malla Reddy Engineering College (Autonomous), Hyderabad, Telangana, India
edc@mrec.ac.in

Abstract: One of the Programme Outcomes prescribed by the National Board of Accreditation, the Apex body for accrediting the Engineering Colleges in India is 'Engineers and Society'. Therefore an Engineering institution, with a vision of providing means for the all round development of the student needs to give appropriate priority to this outcome as well. Our institute adopted a two phase strategy to achieve this outcome.

At the freshman stage, students were involved in a programme called 'National Service Scheme' (NSS), promoted by the government and affiliating university. The students took up various activities like sensitizing the local villagers about cleanliness, vaccination to the kids, oral care and other important issues. Also they conducted a comprehensive survey in identifying the societal problems like water clogging, drainage issues etc.

When the students acquired certain engineering skills like designing, programming, product development etc in their further course of study, they started working on the identified societal problems and solve those problems with their engineering knowledge. This forms the second phase, called 'Engineering Projects In Community Service' (EPICS) and is adopted from Purdue University, USA.

In this paper, we would like to present the implementation of this two phase strategy in our institution

Key words: Programme outcome, NSS, Project, EPICS

I. Introduction

National Board of Accreditation (NBA), the apex body for accrediting the Engineering Colleges in India prescribes twelve Programme Outcomes in tune with the Graduate attributes prescribed by Washington Accord [1]. Any engineering college that follows these Programme outcomes have to ensure that their curriculum addresses all of these 12 outcomes. One among these twelve Programme Outcomes is 'The Engineer and Society'. This outcome has been included, keeping in mind the crucial role to be played by an Engineer in the prosperity of the society. Our institute adopted a two phase strategy in achieving this Programme outcome.

II. PHASE I:

There is a widespread word called NSS in the academic lines. National Service Scheme (NSS) programme was launched in 37 Universities in the year 1969 [2]. The main objective of this programme is to give the students the sense of involvement in the tasks of national development. As a part of the two phase strategy adopted by our institute, the freshman students were motivated to enroll themselves in NSS. The enrolled students went on field trips and visited the nearby villages, interacted with the local villagers [Fig 1]. Students got a good chance of observing the problems faced by the villagers. Poverty, lack of awareness, lack of education were few of the factors identified for various problems faced by the villagers. Accordingly the following few activities were planned as a part of NSS field trip:

Fig 1: NSS volunteers interacting with the local villagers.

Sensitizing the local villagers about cleanliness

This happens to be a major issue of concern as unclean and untidy surroundings lead to many of the diseases. With the financial restrictions on the local panchayat, good drainage facilities cannot be observed in the villages. Therefore the students during their field trips tried to sensitize and educate the villagers about keeping the surrounding environments cleaner, making them free from water clogging etc. Simple measures that keep the ambience beautiful and healthy were

taught to the local villagers [Fig 2]. Awareness on Government promoting schemes like 'Swachh bharath' was created among the local villagers.

Fig 2: Solid Waste management facility in the adopted village

Vaccination to kids:

Prevention is always better than cure. Therefore the local villagers were educated during the field trips about the importance of vaccinating the kids to save their lives from harmful diseases.

Fig 3: Doctors educating the villagers about oral care.

Oral care:

The life style and the improper habits of the villagers bring them lot of oral related issues. Special camps were organized in association with the local hospitals to educate the villagers about oral care and the measures that they need to take to keep themselves off from the oral related issues were taught [Fig 3].

These are the few of the many problems faced by the local villagers. The variety of experiences gained by the students during their field trips gave a comprehensive idea about the problems and the reasons behind those problems.

III. PHASE II:

In the due course as the students progressed academically, they acquired the skills of programming, designing, product development etc. At this stage, they needed an orientation, to channel their skills in solving the identified problems. Here came a wonderful tool in the form of IUCEE SCALE (Student Consortium for Advancement and Learning in Engineering education). About 150 students participated in this SCALE workshop which involved debates, brain storming sessions and many more. The interesting part about this workshop is that it is a kind of workshop for the students and by the students as well i.e., the resource persons for this workshop were students again. The SCALE workshop was conducted with the theme 'Transformative youth and Engineering Education'.

IV. Methodology:

The workshop was conducted in three days. The participants were heterogeneous belonging to different branches of engineering. On day 1, a group discussion was conducted among the inter disciplinary students which helped in identifying various tracks [3]. The following tracks were selected out of all the tracks that surfaced during the group discussion. They are:

Track 1: Climate change and Affordable clean energy
Track 2: Rural infrastructure
Track 3: Responsible consumption and production

on day 2, the resource persons, called facilitators grouped the participants into different tracks and each track was monitored by individual facilitator according to their specialization. The students were given brief introduction on the chosen track and they were given time to reflect and come out with a relevant idea. Then the students were asked to brainstorm for design thinking. This was followed by poster presentation for the proposed design thinking [4]. Then the presented poster was visited by the fellow participants and evaluated by the facilitators. This exercise helped the students to learn from each other and to get motivated by each other. Few of the posters presented by the students are depicted below [Fig 4a, b, c, d].

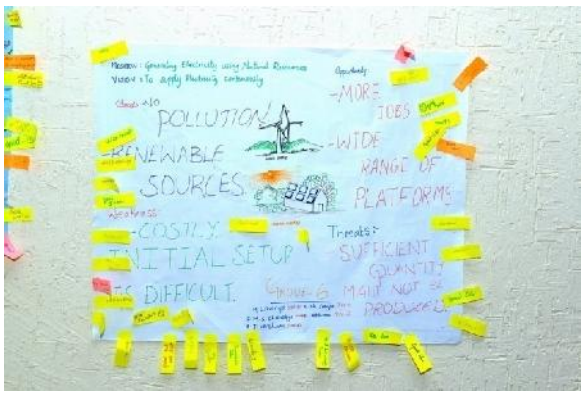

Fig 4 a,b,c,d: Posters presented at SCALE workshop

On the final day the participants were asked to give a power point presentation based on the idea portrayed in their poster. After a thorough discussion with the peers, the final and improved version was presented depicting the action plan for the implementation of the proposed project [5]. Thus the project identified, analyzed and designed in a systematic manner could solve a societal issue, benefitting the community at large, conforming to the very philosophy of Engineering Projects In Community Service (EPICS) advocated by Purdue University.

The following table gives few of the ideas generated during the SCALE workshop.

S.No.	Name of the idea
1	Climate control by dump yard
2	Solar powered handloom
3	Carbon di oxide capture and storage
4	Solution for wastage of food
5	Renewable resources
6	Prevention of drying bore wells
7	Waste management
8	Limiting the usage of electricity

V. Conclusion

Undoubtedly, EPICS is the need of the hour to address the Programme outcome - 'Engineer and the society'. The two phase strategy proposed in this paper and implemented in our institute seems to be a promising strategy for effective attainment of the said Programme outcome.

VI. References

1. http://www.nbaind.org/files/PEOs-Curriculum-and-CO-PO-mapping-21-may-2016.pdf
2. https://nss.gov.in/about-us-0
3. Felder R, Stice J, Rugarcia A. The future of engineering education: making reform happen. Chem Eng Educ. 2000;34(3):208.
4. Kleinsmann, M., Valkenburg, R., & Sluijs, J. (2017). Capturing the value of design thinking in different innovation practices. International Journal of Design, 11(2), 25-40.
5. D. Sumathi, S. Kannan, S. Sudhakara Reddy,"Transformation from Millennial Students to Engineers in Engineering Institutions-A Case Study", Int., journal of JEET. Vol:34,pp-84

Authors:

Dr. S. Sudhakara Reddy received his B.Tech in Mechanical Engineering from Kakatiya University, Warangal and M.Tech. in Design and Production from NIT-Warangal. He completed Ph.D from Sri Venkateswara University, Tirupathi. His research work was carried out at DMRL and ARCI at Hyderabad. His area of research includes Tribology, CAD/CAM and Advanced Manufacturing Technology. He has more than 30 years of rich experience in both teaching and industry. He published more than 20 technical papers in national and international conferences and journals. He has also published articles and book chapters covering a considerable range of dreaming topics in the field of mechanical engineering. He is the Life member of ISTE, SAHTSE, FIE, IIPE, ISME and GEDC. He got two Lifetime Achievement Awards in best Administrative category and Engineering. He was conferred upon by Bharath Siksha Ratan award by GSHEG, New Delhi in the month of April 2018.

Dr. N. Rajeswaran is presently working as Professor in Electrical and Electronics Engineering at Malla Reddy Engineering College (Autonomous), Hyderabad. He did his Bachelors in Electrical and Electronics Engineering in Government College of Engineering., Bargur (Madras University) and also obtained Masters Degree in Applied Electronics from Anna University Chennai, Tamilnadu. He completed doctoral degree from Jawaharlal Nehru Technological University Hyderabad, Telangana, India. He has published more than 35 research papers in various International journals and conferences. His area of research interest includes Electrical Machines, Soft Computing and VLSI Design. He is a life time member of various professional bodies like ISTE, IAENG and IACSIT.

Kesava Vamsi Krishna V., is a post graduate in Physics from the prestigious Sri Venkateswara University, Tirupati. He pursued his M. Phil. in Physics from the same University. He registered for Ph. D. in Rayalaseema University, Kurnool. He works as Associate Professor in Physics, Malla Reddy Engineering College (Autonomous), Secunderabad, Telangana, India. He published two editions of lab manual for Engineering Physics laboratory. Besides teaching, he is Media relations co ordinator at MREC(A). He attended numerous FDPs, workshops, QIPs, national and international conferences. His areas of research interest include thin films, nano materials, teaching and learning methodologies etc. He is life member in APSMS.

Preparation and Tribological Properties of New Bisimidazolium Ionic Liquids

M.V. Varalakshmi

Abstract— In this paper two new bisimidazolium based ionic liquids (ILs), 3,3'- (3,6,9,12,15- pentaoxaheptadecane-1,17-diyl) bis(1-vinyl-1H-imidazol-3-ium) methanesulfinate (1a), 3,3'- (3, 6,9,13-tetraoxapentadecane-1,15-diyl)bis(1-vinyl-1H-imidazol-3-i um)methanesulfinate (1b) were prepared. Their structures were characterized with ^{1}H and ^{13}C NMR, and Mass Spectroscopy. Tribological behavior of 1a and 1b ILs was studied.

Index Terms— Bisimidazolim ionic liquids, NMR, Mass, Four ball tester, Friction and Wear

1.INTRODUCTION

In recent years, ILs have started to play vital role in additives of lubricants for their potential in emission reduction and improving fuel economy. Room temperature ILs are designated as salts having their melting points lesser than the atmospheric temperature. These are synthesized by mutation of an organic particle cation and another organic particle anion. ILs has preferred consideration attention as neat lubricants along with additive of lubricants [1-8].

Imidazolium based ILs were globally experimented additives for lubricants. The accumulation of 1% by wt of imidazolium ILs signification increased the anti-wear status of base oil or fats there by reducing its friction aggressively [9-13].

ILs were also castoff as base oil, with the economical point view the ILs as neat lubricant is not feasible, because of their price. Therefore they would be preferably used as additives in the lubricate industry.

Benzotriazole ILs used as the additives for liquid lubricants showed prominent tribologcal behavior [15,16]. G Hang etal, reported anti wear behavior of Guanidium ILs at high temperature [17]. Bisimidazolium ILs shown high performance anti wear property [18].

In this view, we prepared two vinyl substituted Bisimidazolium ILs, in a simple process. The structures were characterized and studied tribology properties in this paper.

2. EXPERIMENTAL DETAILS:

2.1. CHEMICAL

All the chemicals procured from Sigma Aldrich in purified form. Fig. (1) elucidates the chemical bonding of ILs, 3,3'-(3,6,9,12,15-pentaoxaheptadecane-1,17-diyl) (1-vinyl-1H-imidazol-3-ium) methanesulfinate (1a) and 3,3'-(3,6,9,13-tetraoxapentadecane-1,15-diyl) (1-vinyl-1H-imidazol-3-ium) methanesulfinate (1b), which were synthesized from 1-Vinyl-1H-imidazole (1) when reacted with hexaethylene glycol dimesylate (a) and pentaethylene glycol dimesylate (b) in the presence Acetonitrile solvent at 90 0C about 24 hr to form ILs 1a and 1b respectively.

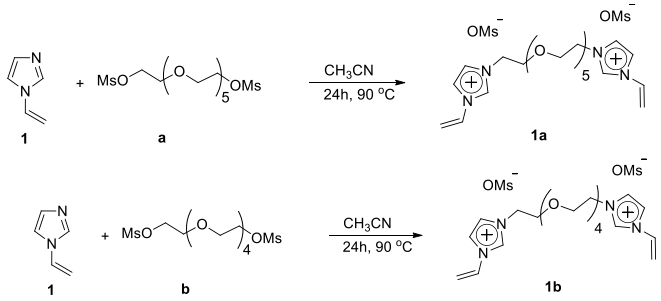

Figure 1: Preparation of 3,3'- (3,6,9,12,15-pentaoxaheptadecane-1, 17-diyl) (1-vinyl- 1H-2-imidazol-3-ium) methanesulfinate (1a) 3,3 '-(3,6, 9,13-tetraox apentadecane-1,15-diyl) (1-vinyl-1H-2-imidazol- 3-ium) methanesulfinate (1b)

Preparation of 3,3'- (3,6,9,12,15- pentaoxaheptadecane -1,17-diyl)(1-vinyl-1H-2-imidazol-3-ium) methanesulfinate (1a)

Every drop of 1-Vinyl-1*H*-imidazole (1.88 g, 20 mmol) (**1**) was supplemented to the solution of 4.38 g (10.00 mmol) of hexaethylene glycol dimesylatein (**a**) dry CH_3CN (100 mL). The reaction mixture was agitated for 48 hours of standard time at 90^0C. At this point, the rotary and revolutionary evaporation takes place and furthermore this solvent mix was splashed with100 ml ethyl acetate which was then dehydrated overnight at atmospheric conditions. (**1a**), 5.25 g (83.8 %) as a pale yellow solid.^{1}H-NMR (400 MHz, DMSO-D_6) δ δ 9.45 (t; J : 1.3 Hz, 2H), 8.20 (t; J : 1.8 Hz, 2H), 7.88 (t; J : 1.6 Hz, 2H), 7.32 (q; J : 8.2 Hz, 2H), 5.99 (d; J : 2.3 Hz, 2H), 5.95 (d; J : 2.3 Hz, 2H), 5.43 (dd; J : 8.7, 2.3 Hz, 2H), 4.38 (d; J : 5.0 Hz, 4H), 3.79 (t; J : 4.8 Hz, 4H), 3.56-3.44 (m, 14H), 2.31 (s, 6H); 135.7, 128.6, 123.5, 118.6, 108.8, 69.4, 68.3, 67.8, 66.5, 50.3 49.5, 39.3. $C_{24}H_{42}N_4O_{11}S_2$ ($M+H^+$) 626.7463, 626.7460.

Preparation of 3,3'-

Revised Version Manuscript Received on 22 February, 2019.

M.V. Varalakshmi, Associate Professor, Department of Mechanical Engineering, Malla Reddy Engineering College (A), Hyderabad, India. (email: mechmvvaralakshmi@gmail.com)

(3,6,9,13 -tetraoxapentadecane -1,15-diyl)bis(1-vinyl-1H-imidazol-3-ium) methanesulfinate (1b)

1-Vinyl-1*H*-imidazole (1.88 g, 20 mmol) (**1**) was added as continuous drops of similar size to the solvent of 3.94 g (10.00 m/mol) of pentaethylene glycol dimesylatein (**b**) dry CH_3CN (100 mL). The reaction mix solvent was agitated at 90 °C for 2 consecutive days . At this instance, the reaction solvent mix was concerted by rotary agitated evaporation; and was washed several times with ethyl acetate (100 mL) and dehydrated under high vacuum overnight at atmospheric temperature to afford (**1b**) 5.15 g (88 %) as a light yellow solid.^{1}H-NMR (400 MHz, DMSO-D_6) δ δ 9.46 (t; J : 1.2 Hz, 2H), 8.23 (t; J : 1.7 Hz, 2H), 7.86 (t; J : 1.5 Hz, 2H), 7.34 (q; J : 8.4 Hz, 2H), 5.96 (d; J : 2.4 Hz, 2H), 5.93 (d; J : 2.4 Hz, 2H), 5.47 (dd; J : 8.5, 2.5 Hz, 2H), 4.40 (d; J : 6.0 Hz, 4H), 3.81 (t; J : 4.6 Hz, 4H), 3.55-3.43 (m, 10H), 2.33 (s, 6H); ^{13}C NMR (100. MHz, DMSO-d_6) δ: 134.8, 129.3, 123.9, 119.9, 108.5, 69.9, 66.7, 49.3, 45.4, 39.3. HRMS (ESI, m/z): calcd for $C_{22}H_{38}N_4O_{10}S_2$ ($M+H^+$) 582.6912, found: 582.6908.

2.2 CHARACTERIZATION:

Polyethylene glycol (PEG) procured from Sigma Aldrich possess an average molecular weight of about 190 to 200 g/mol. The two ILs 1a and 1b significantly miscible with PEG can be used as additives, presented in Table 1.

The miscibility of 1a and 1b ILs

	1a IL	**1b** IL
Miscibility (Weight fraction)	3-5 %	3-6 %

Table 1

The density and viscosity allied properties were measured by Kinematic Viscometer, Stanhope-Seta, presented in Table 2.The thermal statics of the P.E.G with ILs were stated with Perkin Elmer thermo analyzer.

Properties and characteristic features of PEG and ILs as condiments

Lubricants	Kinetic Viscosity in mm^2/s		Viscosity Indices	Density Kg/m^3 at 25.0 ^{0}C
	40.0^{0}C	100.0 ^{0}C		
P.E.G	22.62	4.21	78.7	1127.5
PEG + 0.5 % **1a**IL	22.86	4.24	78.9	1128.6
PEG + 1.0 % **1a**IL	23.44	4.31	82.1	1129.6
PEG + 2.0 % **1a**IL	24.78	4.40	83.9	1130.7
PEG + 0.5 % **1b**IL	22.87	4.31	79.3	1128.8
PEG + 1.0 % **1b**IL	23.59	4.33	84.4	1129.4
PEG + 2.0 % **1b**IL	24.79	4.42	85.3	1132.7

Table 2

2.3 TRIBOLOGY TEST:

The tribology test outcomes done on the PEG with additives were evaluated using steel &steel contact surfaces with four ball testers at 1000C correspondingly, with ball disc configuration. By frequently persuading the upper ball in running condition of ϕ 10mm in diameter, AISI 52100 steel, hardness of 59-61 HRC against the lower stationary diskette of ϕ24 mm x 7.9mm, for 30 min duration.

The four-ball test was also conducted by equivocating an AISI 52100 steel ball. As an outcome of the above test the wear scar diameter (WSD) on the three lower balls and the coefficient of friction were set-down automatically.

3. RESULT AND DISCUSSIONS:

3.1 Characteristic properties of the manufactured ILs: The mixture of ILs to P.E.G increases its viscidness in a meager manner which implies that the increase in viscosity is concentration dependent. (Table 2).

The thermoravimetric analysis (figure 2) illustrates that the ILs do not unveil any weight loss between the temperature of 2000Cand below 6000C thereby indicating a very high thermal stability .

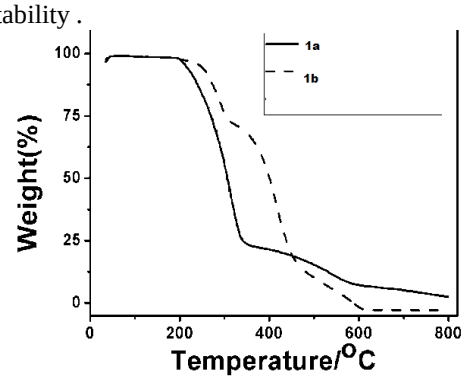

Figure:2 TGA curve of 1a and 1b in air

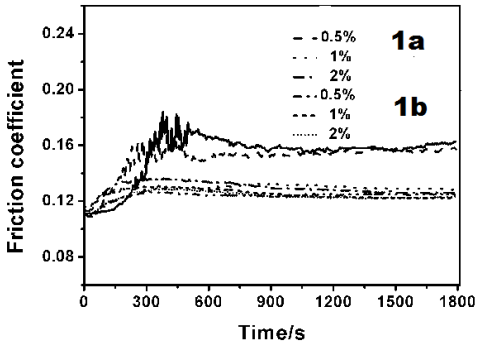

Figure:3 Progression of coefficient of friction

3.2 Friction and wear Behavior:

Effect of Additive Concentration: Figure 3 exhibits the evaluation of the corresponding coefficient of friction at a load condition of 100N for with 1a different additive concentrations changed gradually and the wear status of the discs made of steel after the changes incorporated at each stage after testing. The outcomes are elucidated below:

4. CONCLUSION

Two Bisimdazolium ionic liquids (ILs) as mentioned previously named as , 3,3'- (3,6,9,12,15-pentaoxaheptadecane-1,17-diyl)(1-vinyl-1H-imidazol-3-ium) methanesulfinate (1a), 3,3'-(3,6,9,13 -tetraoxapentadecane-1,15-diyl)(1-vinyl-1H-imidazol-3-ium) methanesulfinate (1b) were prepared and characterized. Their tribology properties were studied using Pin-on-disc tribometer and four ball tester.

REFERENCES

1. Chengfeng Y, Weimin L, Yunxia Chong and Laiguine Yugrane "Room-Temperature features of ionic liquids: a novel type lubricant character", Chem Commun, No 21, 2001, pp 2244-2245.
2. Feng Zhou tol, Yongmin Liang chan ,Weimin Liu "Ionic liquid lubricants:, Chem. Soc. Rev., Vol 38, 2009, pp 2590-2599.
3. Ichiro Minami "Ionic liquids in the field of tribology", Molecules, Vol 14, No 6, 2009, pp 2286-2305.
4. Maria Anne Dolores Bermudez K.H, Ana Jimenez; Jose and Francisco Jose "Ionic liquids as lubricant fluids", Molecules, Vol 14, No 8, 2009, pp 2888-2908.
5. Tsukasa itchi, Tetsuya Tsu, Ken Okazaki and Susumu Y Kuwabata "New frontiers in materials", Adv. Materials, Vol 22, No 11, 2010, pp 1196-1221.
6. Anthony E. Somer,. Howlett Macfarlane "A review of ionic liquid lubricants", Lubricants, Vol 1, No 1, 2013, 3-21.
7. Jun Qu, Dinesh G. Bansal,Jane Y. Howe, Huimin L,, Huaqing Li, Peter J. Blau, Bruce G., Gregory , and Donald Smolenski "Antiwear performance a lubricant additive", Acs Applied Materials, Vol 4, No 2, 2012, pp 997-1002.
8. Lethesh Shah, Ayodele Mutalib and Y Uemura, "Nitrile functionalized thermophysical properties" J Mol Liq, Vol 221, 2016, pp 1140-1144.
9. Hernandez battez, R. Gonzalez; Viesca, D. Blanco and A. Osorio "Tribological behavior for steel", Wear, Vol 266, No 11-12, 2009, pp 1224-1228.
10. Cai, M., Zhao, Z., Liang, Y. et al. "Alkyl imidazolium polyurea grease for steel/steel contacts", Tribol Lett, Vol 40, No 2, 2010, pp 215-224.
11. Ana-Evajimenez, Bermudez "Imidazolium ionic liquids in aluminium-steel lubrication", Wear, Vol 265, No 5-6, 2008, pp787-798.
12. A.-E. Jiménez and M.-D. Bermúdez, "Short imidazolium ionic liquid additives in lubrication of ester oil", Tribology - Materials, Surfaces & Interfaces, Vol 6, No 3, 2012, pp109-115.
13. Xiao, H., Guo, D., Liu, S. et al.,"Film thickness of ionic
14. alkyl chain length", Tribol Lett, Vol 41, 2011, pp 471- 41: 471-477.
15. Palacio, M. & Bhushan, B."A review of ionic liquids in nanotechnology", Tribol Lett, Vol 40, 2010, pp 247-268.
16. Meirong Meihuan Yao,Feng Zhou, and Weimin Liu, "Imidazolium additives in poly(ethylene glycol)for steel", Acs Applied Materials & Interfaces, Vol 2, No 3, 2010, pp 870-876.
17. Liu, X., Zhou, F., Liang, Y. et al."Benzotriazole as the additive for liquid lubricant", Tribol Lett, Vol 23, 2006, pp 191-196.
18. Meirong Cai, Yongmin Liang, Feng Zhou, and Weimin Liu "Tribological properties of bearing bezotriazole in ploy(ethylene glycol) and Ploy urea Grease for steel/steel contacts" Acs Applied Materials & Interfaces, Vol 3, No 12, 2011, pp 4580-4592.
19. G Hang, QYu, M Cai, F Zhou and W Liu, "Investigation of the lubricity and antiwear behavior of Guanidinium " Tribol Int, Vol 114, 2017, pp 65-76.
20. Meihuan Yao, Yongmin Liang, Yanqiu Xia, and Feng Zhou "Bisimidazolium ionic liquids additives in poly(ethylene glycol) for steel- steel contacts" , Vol 1, No 2, 2009, pp 467-471.

An Overview of Data Management in Cloud Computing

K.Yogitha Lakshmi, S.Dhanalakshmi, B.G.Obula Reddy

Abstract: ***As we all familiar with cloud computing, it's not a latest technology, rather we can mention it as an emerging technology where most of the industry is trying to store not only its crucial data for redundancy but also looking for the service management. In that scenario first thing comes in mind is management of data in most efficient way possible. So here we tried to showcase two technologies of cloud data management namely Cloud BigTable and Cloud DataStore which they have their own way of working environments. It makes so much importance to choose the right technology for the right nature of work.***

Keywords: Cloud Storage, Data Management, Virtualization, Google File Systems, Data Store

1. INTRODUCTION

Cloud computing referred as delivery of computing services such as networking, servers, databases, storage, virtualization, storage, software, business analytics and so on over the Internet as a utility just like using telephone/mobile services. It offers product innovations and flexible resources for the business like Pay per Use services from The Cloud. The advantages of cloud computing are: Flexible resources - On-demand services gives user a quick scale up or down of the resources. Metered service gives the liability to pay for what you use. Self service you can access all the IT resources without any assistance.

A. Deployment Models of Cloud Computing

Deployment models of cloud computing represents that public cloud, private cloud, hybrid cloud, community cloud and different services. The Fig.1. Shows the representation of cloud architecture in various models and its services.

Public Cloud: This infrastructure will be used by public cloud user in which some of the services will be unavailable. These resources will be provided and organized by a cloud service provider, academics or other organizations. The cloud server exists on the premises of the cloud provider. Eg: Google App Engine, Windows Azure etc.,

Private Cloud: This infrastructure is for exclusive use of a single organization with various services, it can be managed by the organization, a third party or sometimes both. It exists on or off the premises. Eg: VMWare, RedHat etc.,

Community Cloud: It can be managed, operated and owned by one or more organizations in the community, or a third party or combination of both. It may exists on/off premises. Eg: Salesforce community cloud etc.,

Hybrid Cloud: It is the combination of two or more types of infrastructure services that works under proprietary rules and standards. Eg: VMWare vCloud etc.,

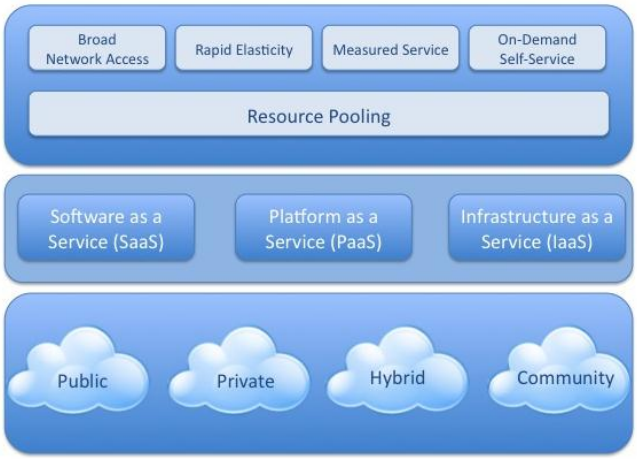

Fig.1. Cloud Architecture

2. THE ROLE OF VIRTUALIZATION IN CLOUD ENVIRONMENT

Virtualization is a multi-tenancy user infrastructure which is located at remote site and can perform function of multiple systems in one physical system by means of high speed internet. In cloud environment it comes under IaaS (Infrastructure as a Service), where the cloud consumer gets the service to use cloud based ready to access virtual storage and also some built in services. The pricing of these services depends on data storage no. of GB used per hour, network infrastructure used per hour etc., Fig.2. Represents the components stack of virtualization in hypervisor and hardware parts.

Virtualization Component Stack consists of Hardware, Operating Systems, Middleware and application layer. Operating Systems layer split into two parts:

a) Hypervisor is also called as virtual machine manager which allow user to have multiple OS in single hardware

b) Guest OS is a running Operating system within the Virtual machine.

Revised Manuscript Received on February 22, 2019.

K.Yogitha Lakshmi, Assistant Professor, Department of IT, Malla Reddy Engineering College(A),Telangana,India

S.Dhanalakshmi, Professor, Department of CSE, Malla Reddy Engineering College(A),Telangana,India

B.G.Obula Reddy, Professor, Department of CSE, Malla Reddy Engineering College(A),Telangana,India

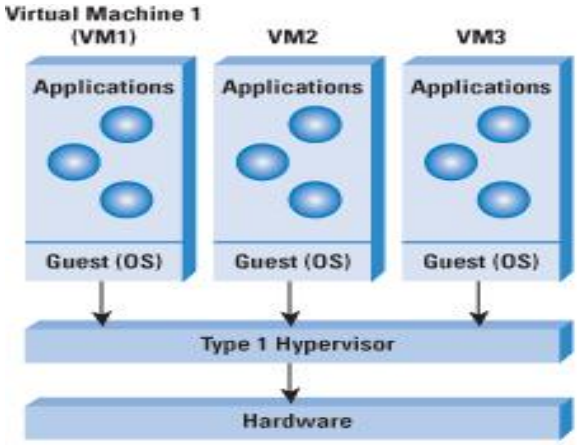

Fig.2. Virtualization Component Stack

The three goals of virtual machine are;

Equivalence: To poses unbiased hardware performance among all the VM's(Virtual Machine)

Resource Control: The VM's should be in complete control of any virtualized resources

Efficiency: The VM's instructions should be executed from its CPU rather than involving hypervisor.

3. TYPES OF VIRTUALIZATION

There are mainly three types of virtualizations namely Server virtualization, Client Virtualization and Storage Virtualization. The Fig.3. Shows the different categories of virtualizations.

Server Virtualization: It is the most common type of virtualization in cloud computing, where it gives optimum usage of server by running multiple applications on multiple operation systems at the same time on single server with the use of hypervisor by controlling CPU, Memory and other components without need of source code.

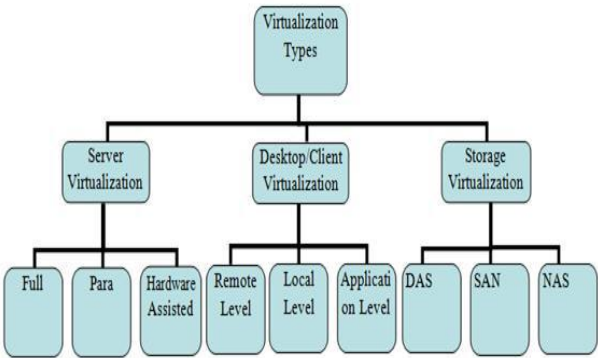

Fig.3. Types of Virtualization

Client Virtualization: In client virtualization, the administrator can manage and control the operations of client machine like personal devices. Here we need to have glance at three types of client virtualizations. First is remote level, where consumers can able to access cloud server which is located remotely anywhere and anytime across a network. Second, local level which runs on local server for the purpose of security. Third, application level virtualization which allows applications to run on isolated or private environment which is accessible by providing authentication.

Storage Virtualization: In Storage virtualization, a single storage device manages multiple network storage resources. It provides efficient storage management in large IT sector and reduces downtime. Three types of storage virtualizations are DAS(Direct Attached Storage), SAN(Storage Area Network), NAS(Network Attached Storage). DAS is a primary way of data storage, where the storage drivers are directly connected to the server. NAS follows a method of storage called sharded method which connects through the networks and it is used for file sharing, device sharing and scheduled/ Ad-hoc backup of the server. SAN is a technique of storing data in a device that is shared among different servers over a high speed network.

4. DATA MANAGEMENT IN CLOUD COMPUTING

In cloud computing data management itself is a big challenge in processing large quantity of data for the purpose of data storage, parallel processing of data execution, analytical processing and online query execution all by ensuring consistency and durability under peak loads.

Some of the cloud based analytical data management systems are: BigTable, HBase, HyperTable, Hive and HadoopDB. PNUTS and Cassandra are the web based data management systems. Here, in this paper the working nature of BigTable and Dynamo will be discussed

A.GFS (Google File System)

It is designed to manage large files in distributed networks of servers which is connected by a high speed internet. It provides atomicity during read/ writes operations of individual files. Supports read/ write and update operations simultaneously by multiple client programs.

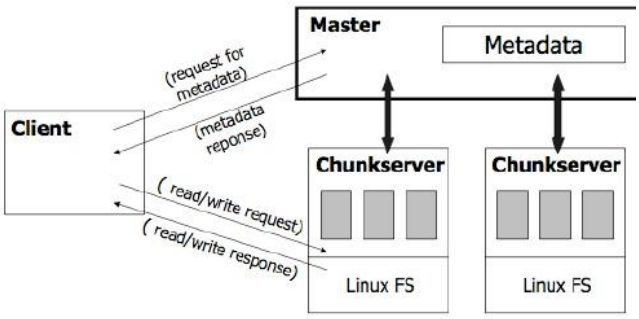

Fig.4. GFS Architecture

A single Master controls the namespace. A large file will be cut down to chunks or blocks with the size of 64MB. These Chunks (GFS) or Name nodes(HDFS) are stored on a servers called Chunk Server. The main functionality of this server is to replicate these chunks three times on different physical racks and network segments.

Read Operations in GFS: a) Client program request for metadata by sending its full path and offset of a file to MASTER or NAMENODE. b) MASTER replies back with metadata from one of its replica chunk where the data is found.

Write/Append Operations in GFS: For initiating write/append operation the process is same as read operation along with some extra steps. a) Client sends its data to be

appended to all its chunk servers b) Chunk server acknowledge the receipt of this data. c) Among all its chunk server replicas, MASTER chooses a PRIMARY Chunk server which is responsible to append the client data to its secondary chunk servers.

Fault Tolerance in GFS: MASTER bind its synchronization with its replicas by sending regular Heart-Beat messages. In case of failure, chunk server meta-data will be sent to MASTER and it will choose a new Primary Chunk server.

5. MANAGING DATA IN CLOUD ENVIRONMENT

Managing data in cloud environments can be provided different storage techniques in google platforms. Its specify features of Google Cloud BigTable and Google Cloud Datastore.

A.Google Cloud BigTable

BigTable is a distributed storage system that store large amount of data such as petabytes in NoSQL cloumn-oriented way of data store developed by Google Inc. to manage its internet search and web service functions. It works on powerful database servers which gives the benefits of scalability, easy administration and maintain elasticity of cluster without any down time.

BigTable is used to store and query the following types of data:

Time Series Data
Marketing Data
Financial Data
Internet of things Data
Graph Data

The Fig.5. Represents the BigTable Storage Model of rows and columns specifications. Each column store arbitrary value as name-value pair in form of column family. At the time of table creation initial value of no.of column families will be fixed. Labels of column families can be created at any point of time. Each BigTable cell can contain multiple versions of data in decreasing order of timestamp.

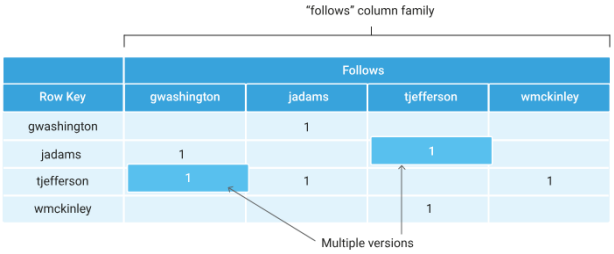

Fig.5. BigTable storage Model

Each table in BigTable will be divided into different row ranges called tablets. These Tablets will be maintained by a server called tablet server. It stores each column family in an allocated row range inside a distributed file called SSTable. BigTable maintains its meta-data table in a single meta-data server which is used to locate the user tablets in response to their read/write operations. The meta-data table itself will be divided into no.of tablets to support its large amount of data in most effective way . Root Table will help point out other meta-data tablets. It supports large parallel reads and inserts operations simultaneously on the same table.

B.Google Cloud DataStore

Google cloud Datastore is a NoSQL document database developed for incredible scalability, high performance and to support application development. The most appreciated feature in cloud datastore is to provide high performance to its subscriber even in the high incoming data traffic situation. It Maintain ACID properties and also it give high availability.

Cloud DataStore is used for applications like:

Product Catalog where it provides real-time inventory

User Profiles where the retailer can view the preferences of the user based on past interests.

Bank Transactions where ACID property will guarantee the transaction of transferred funds.

All the data in Datastore stores in one bigtable called as Entity Table. It stores data horizontally across its disks in which it is called as shared and key values are sorted lexicographically.

It can handle multiple queries at a time by various users with the help of multiple index tables. For every data set they have entity sets from where user gets the results back. for example a query will have a defined set of results say 100 entities, because of this scenarios some queries would not get support in cloud datastore. Like in traditional RDBMS cloud datastore doesn't support schema and it is a schemaless database. Cloud Datastore do not support join operations, it won't filter data from a table with multiple keyed properties or by the result of a subquery. Cloud Datastore doesn't do justice for analysis of data but it can provide assurance for a transactional data.

6. CONCLUSION

In cloud computing environment, without the virtualization technique it would not be possible to use single hardware device among the users. It is the basic service of any development in cloud computing. Data management in cloud computing shows the rapid growth of deployment in remote servers for the purpose of storage and cloud services. Cloud BigTable is mainly used for the non-transactional data where it does not give any redundancy for the data. It can be used for data analytics where you can get the results by querying historical data. Cloud DataStore is built on BigTable but they are completely different from each other, where it supports ACID properties of the transaction and it is used on transactional data. It features are similar to SQL but it cannot perform some operations.

7. REFERENCES

1. Hamlen, K. Kantarcioglu, M. Khan, L. Thuraisingham, B. (2010). Security Issues for Cloud Computing.International Journal of Information Security and Privacy, 4(2), 36-48.
2. Bernardo Ferreira, Henrique Domingos (2012). Management and Search of Private Data on Storage Clouds.Center for Informatics and Information Technologies.SDMCMM'12, December 3-4, 2012, Montreal, Quebec, Canada.

3. RizwanMian, Patrick Martin (2012). Executing data-intensive workloads in a Cloud.ACM International Symposium on Cluster 2012 12th IEEE/ACM International Symposium on Cluster, Cloud and Grid Computing.
4. Xiao-Bai Li, SumitSarkar (2006). Privacy Protection in Data Mining: A Perturbation Approach for Categorical Data Information Systems Research. (17) 3, 254–270
5. Iyengar, V. S. (2002). Transforming data to satisfy privacy constraints. Knowledge Discovery DataMining.ACM Press, New York, 279–288.
6. Daniel J. Abadi (nd) Data Management in the Cloud: Limitations and Opportunities. IEEE Computer Society Technical Committee on Data Engineering
7. B. Siddhisena, Lakmal Wruasawithana, Mithila Mendis, ―Next generation muti tenant virtualization cloud computing platform‖, In: Proceedings of 13th International conference on advanced communication technology(ICACT), vol. 12, no.3; 2011. p.405–10.
8. Z. Xiao and Y. Xiao, ―Security and Privacy in Cloud Computing‖, IEEE Communications Surveys & Tutorials, vol. 15, no. 2, pp. 843–859, 2013.
9. Sunilkumar S.Manvi, Gopal Krishna Shyam, "Resource anagement for Infrastructure as a Service(IaaS) in cloud computing: A survey", Journal of Network and Computer Applications 41, (2014) 424–440.
10. Chase JS, Darrell C Anderson, Prachi N Thakar, Amin M Vahdat, ―Managing energy and server resources in hosting centers‖, In: Proceedings of 11th IEEE/ACM international conference on grid computing (GRID), vol.12, no.4; 2010. p.50–2.
11. B. Urgaonkar, P. Shenoy, A. Chandra, P. Goyal, T. Wood, ―Agile dynamic provisioning of multi-tier Internet applications‖, ACM Trans Auton Adaptive Syst 2010; 5 (5):139–48.
12. Vaquero LM, Luis Rodero-Merino, Rajkumar Buyya, ―Dynamically scaling applications in the cloud‖, In: Proceedings of the ACM SIGCOMM computer communication review, vol.41, no.1; 2011. p.45–52.

Published By:
Blue Eyes Intelligence Engineering
& Sciences Publication

Study and Analysis of Big data with MapReduce Framework

K. Rama Krishna Reddy, B.G. Obula Reddy

Abstract— Exponential growth in data has been observed in recent years. This huge amount of data has caused a new kind of problem. Existing RDBMS systems cannot handle large data or they are not effective in managing them. Major Big Data problems are storage and handling. Hadoop is displayed in storage and processing solutions in the form of HDFS (Hadoop Distributed File System) and MapReduce. Traditional systems are not intended for Big Data processing, and they can also process structured data. The financial sector is one of the challenges in Big Data. In this work, unstructured data is processed by Hadoop MapReduce. An effective processing of unstructured data is analyzed and explained.

Keywords: Big data, Hadoop, HDFS, MapReduce.

1. INTRODUCTION

We live in a date of age. It is difficult to calculate the total amount of data electronically stored, but the IDC calculates the size of the "automated world" 4.4 Zetta Bytes in 2013, and estimates the development ten times by 2020, up to 44 ZB. Approximately one thousand EB, one million BP or one billion TB. This is more than a circle of unity for all who live on the planet. So there are a lot of data that indicates that they have an impact. Most data is protected by larger web properties (such as web crawlers) or logical or money-related parameters, would you say no? Do large amounts of data affect associations or smaller people? The model is that the data on each of them has evolved, although perhaps more importantly, to the extent that the data produced by machinery produced as part of the Internet of Things is significantly higher than that produced by individuals. Machine files, RFID files, sensor systems, vehicle GPS tracking, local exchange for data exchange. Freely available amount of data is also created annually. Associations should never process your data. The result will be largely motivated by its ability to generate incentives from other associations. Customers who need to store and retrieve data store information for a long time in the database and process them using SQL queries. The web has changed most of the suspicions of this time. The information on the Internet is unstructured and essential, and databases cannot save or increase the information in the scheme to store and process them. Google was one of the most important associations to solve the problem. To find questions, she had to download and index the entire Internet. They created the basis for extensive information management, derived from the options "map" and "reduced".

Revised Version Manuscript Received on 22 February, 2019.

K. Rama Krishna Reddy, Associate Professor, Department of CSE, Malla Reddy Engineering College (A), Telangana, India

B.G. Obula Reddy, Associate Professor, Department of CSE, Malla Reddy Engineering College (A), Telangana, India

2. LITERATURE REVIEW

Literature review described as the summary or re-organising the related information from different sources to understand the research problem. In this review how data analysis done for big data through data mining techniques is studied.

[1] MapReduce is a planning model and appropriate implementation for the management and production of complete data sets. Customers set up a card task where the main / calculation procedures are combined to form half the main route / cluster table and reduce the work of trade unions that have all the values associated with the central key. This model shows a large number of paper-based companies. Projects written in this useful style are parameterized in parallel and executed in a naturally large group of production machines. The enforcement system covers the fine elements of the Information Data Unit, reserving the program execution in machine mode, solving machine frustration and addressing the compliance of the required machines. This allows software engineers who are not involved in parallel and distributed infrastructures to effortlessly use assets that are significantly dispersed. Our use of MapReduce is still applicable to large-scale machine tools, and is very versatile: the typical MapReduce calculation makes up countless terabytes of data in a large number of machines. Developers believe that the system is easy to use: several MapReduce programs have been updated, and more than a thousand MapReduce tasks work consistently in Google's clusters.

[2] In fact, programming systems often operated without creating a direct expressive model. This can lead to complex problems that can ruin further development, which is relatively unavoidable, since in the best case, the most important product documentation is the source code. To solve this problem, learn how he focused on software modeling inductance using automatic recording learning algorithms. In both cases, records generated using a good scheduling system can be significant and the calculation of the derivative may exceed the processing limit of one computer. This document provides a generic and flexible way to obtain behavioral patterns capable of handling critical performance records using commonly used and parallel algorithms using the MapReduce programming model and executing a group of connected execution centers. The approach consists of two divided phases, which destroy and combine the model. The calculation for each phase was done using MapReduce. With MapReduce's parallel data boundary, the problem of

removing major registry behavior patterns can be solved. This strategy is updated by Hadoop. Analyzes in the Amazon clusters indicate our approach to productivity and adaptability.

[3] The Google MapReduce programming model is used to handle large datasets in parallel. We provide the first exact model description, including the Google-specific Sawzall domain's progress. For this purpose, we create Primary Documents in MapReduce and Sawzall and record our results as executable specifications. We also identify and resolve some of the errors in the relevant documents in the informal presentation. We use the recorded functional program (especially Haskell) as a tool for design restoration and executable specification.

[4] MapReduce is the general basis for cluster-based distributed batch processing. In order to streamline debt recovery capabilities, many MapReduce performances are shown in the overall performance of each card and reduce allocations before they are consumed. In this document, we offer an appropriate MapReduce technique for transferring data between administrators. This extends the MapReduce programming model beyond cluster management and can reduce processing time and improve group activity in group activities. We introduced a custom Hadoop MapReduce structure that provides total online sharing so customers can see the "first respond" of the treated call. Our Hadoop Online Prototype (HOP) also supports continuous queries that allow aggregating MapReduce projects for things like incident observation and energy management. Bounce retains Hadoop's non-critical malformation properties and can run MapReduce programs that feature an unmodified client.

[5] In recent years, in the rapid development of data, Industries and the rest of the world, the academic world needed a smart data retrieval device that would be useful in removing huge amounts of data. The MapReduce system is primarily designed to record scaled data applications to support vital management. Since its launch, incredible research has been done to make this process more natural for customers. This allows them to intensify the execution of large applications based on data. Our homepage highlights the key role of improving the efficiency of various applications that use the latest MapReduce models, as well as large scale data set processing. A comparative study of Dot models is compared to Apache Hadoop, and Phoenix will be a fundamental discussion of performance time and adaptation to internal failures. Finally, the call for updating the MapReduce calculation in a given region will be unusual, for example, recalculation, harmonized processing of issues, Métis database, etc.

3. PROBLEM STATEMENT

Traditional database systems are not intended to handle large volumes of data that we have known over the years. It is also expensive to increase the processing power of these systems. In addition, traditional systems can process only structured data. Unstructured data is the most important part of the data collected over the last two years. The existing system works on the same server, making vertical growth more complex and expensive.

Limitations

The two main drawbacks are:

1. Large data cannot be stored and processed
2. Unstructured data cannot be processed

It is limited how this system can be made vertical. Most of these individual servers are high-end or modified, so they are not profitable.

4. RECOMMENDED SYSTEM

The traditional RDBMS is not designed to handle unstructured data, and the size of the data it can handle is limited. The biggest problems with data processing are storage and processing. In this work, the Hadoop Framework is used to address storage and processing problems. Hadoop stores data in a cluster that is distributed over the network and processes it. Solve the problem by increasing storage and processing power. This can easily be achieved by increasing the number of nodes in the cluster. Data storage as well as processing distributed in cluster nodes significantly reduces the processing time of Big Data. It also eliminates the need for high-quality or custom-made equipment, which is very expensive.

5. CONCLUSION

In this paperwe describes how unstructured data can be efficiently processed using the MapReduce programming model. The Hadoop Framework is a solution to big data-processing problems. In this work, a series of unstructured inventory data is used to demonstrate the implementation of MapReduce tasks. In addition, the relevant sections are shown. This work provides a better understanding of the implementation of the MapReduce tasks by unstructured registry data and encourages further research to find more efficient ways of processing non-structured registry data.

REFERENCES

1. L. Augusteijn. Sorting morphisms. In S. Swierstra, P. Henriques, and J. Oliveira, editors, 3rd International Summer School on Advanced Functional Programming, volume 1608 of LNCS, pages 1–27. Springer-Verlag, Sept. 1998.
2. J.W. Backus. Can Programming Be Liberated From the von Neumann Style? A Functional Style and its Algebra of Programs. Communications of the ACM, 21(8):613–641, 1978.
3. R. Bird and O. de Moor. Algebra of programming. Prentice-Hall, Inc., 1996.
4. R. S. Bird. An introduction to the theory of lists. In Proceedings of the NATO Advanced Study Institute on Logic of programming and calculi of discrete design, pages 5–42. Springer-Verlag, 1987.
5. G. E. Blelloch. Programming parallel algorithms. Communications of the ACM, 39(3):85–97, 1996.
6. A. Borodin and J. E. Hopcroft. Routing, merging and sorting on parallel models of computation. In STOC'82: Proceedings of the fourteenth annual ACM symposium on Theory of computing, pages 338–344. ACM Press, 1982.
7. L. Boug´e, P. Fraigniaud, A. Mignotte, and Y. Robert, editors. Proceedings of the 2nd International Euro-Par Conference on Parallel Processing, 2 volumes, EURO-PAR'96, volume 1123–1124 of LNCS. Springer-Verlag, 1996.
8. W.-N. Chin, J. Darlington, and Y. Guo. Parallelizing conditional recurrences. In Boug´e et al. [7], pages 579–586. Volume 1/2.

9. P. Zadrozny and R. Kodali, Big Data Analytics using Splunk, Berkeley, CA, USA: Apress, 2013.
10. F. Ohlhorst, Big Data Analytics: Turning Big Data into Big Money, Hoboken, N.J, USA: Wiley, 2013.
11. J. Dean and S. Ghemawat, "MapReduce: Simplified data processing on large clusters," Commun ACM, 51(1), pp. 107-113, 2008.
12. F. Li, B. C. Ooi, M. T. Özsu and S. Wu, "Distributed data management using MapReduce," ACM Computing Surveys, 46(3), pp. 1-42, 2014.
13. C. Doulkeridis and K. Nørvåg, "A survey of large-scale analytical query processing in MapReduce," The VLDB Journal, pp. 1-26, 2013.
14. S. Sakr, A. Liu and A. Fayoumi, "The family of mapreduce and large-scale data processing systems," ACM Computing Surveys, 46(1), pp. 1-44, 2013.
15. The emergence of “big data” technology and analytics Bernice Purcell –Holy Family University.
16. The Forrester Wave™: Big Data Predictive Analytics Solutions, Q1 2013 by Mike Gualtieri, January 3, 2013

Apriori-based Frequent Symptomset Association Mining in Medical Databases

R. P. Ram Kumar, R. Jayakumar, A. Sankaridevi

Abstract*— Nowadays, healthcare organizations generate large volumes of data. An automatic way of retrieval is necessary when the volume of data is increased. Data mining is becoming very popular and has extensively used in various Healthcare organizations. With the use of various data mining algorithms, it is possible to extract many useful patterns. Data mining applications can highly benefit various parties in Healthcare organization. This paper proposes to enable healthcare organizations by predicting the number of patients affected by certain diseases with respect to their symptoms in medical databases. The pharmacists can use this discovered knowledge and avoid the run out of required drugs, so that the patients can be treated at the right time.

1. INTRODUCTION

Knowledge Discovery in Databases (KDD) is a distinct process consisting of several well-defined steps. Data mining is the core step in KDD, which helps in the discovery of buried, but useful knowledge from massive Healthcare databases. Data mining allows extraction of knowledge from heterogeneous healthcare databases, which in turn eliminates the manual tasks and retrieves the data exactly from electronic records. To carry out the mining process, the medical data can be preprocessed by various techniques like Cleaning, Integration and Transformation. Data preprocessing is one of the major problems when going for the ETL process.

2. PREPROCESSING OF MEDICAL DATA

Cleaning:

The cleaning method removes data inconsistencies by eliminating Duplicate Records, Data entry mistakes and filling missing values for improving the data quality which is highly recommended for mining to keep away from wrong conclusions. Messy data cleaning can be done either manually or by using some tools which are readily available in the market. Smoothing can also be done by techniques such as binning and regression.

Integration:

Once data cleaning has done, the medical data sources are integrated into a homogeneous one, which means the heterogeneity of the medical data is removed while merging data from multiple sources. Data integration is very tricky and various issues are encountered such as matching of the schema, objects when data are received from various sources. The data redundancy may cause if it is derived from another medical entity and it can be detected and solved by correlation analysis.

Transformation:

In data transformation phase the aggregation operations are applied, and a reduced form of clean data is obtained during the reduction phase. In the reduction phase, two main encoding methods like dimensionality reduction and numerosity reduction is used. These reduced data are aggregated in various structures such as tables or Multidimensional model. After these operations, the database is ready to mine. In this paper, a patient database of a particular healthcare organization has been taken as a sample.

3. SYMPTOM-BASED CATEGORIZATION

The medical oriented assessment is extremely specific which requires huge endeavor and determination to spot diseases accurately that shows symptoms. Identifying such symptoms is troublesome which is done by experienced doctors, and they usually categorize diseases based on various diagnosis methodologies. These support doctors to narrow down the cause of diseases that show symptoms and which can be done using facts and experience and later which will be confirmed by conducting various tests.

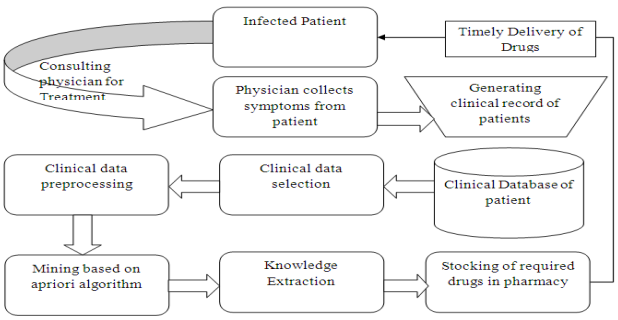

Figure 1 Architectural diagram of symptom categorization

The signs and symptoms which are self-assessed and reported by patients are crucial to identifying these disorders. Based on the symptoms of patients the physician can diagnose and treat them with adequate medicine.

Revised Version Manuscript Received on 22 February, 2019.

R. P. Ram Kumar, Professor, Department of Computer Science and Engineering, Malla Reddy Engineering College (Autonomous), Secunderabad, Telangana, India. (e-mail: rprkvishnu@gmail.com)

R. Jayakumar, Associate Professor & Head, Department Of Computer Applications, Mahendra Engineering College, Tamil Nadu, India.(E-mail: mymailjsjk@gmail.com)

A. Sankaridevi, Assistant Professor, Department Of Computer Applications, Mahendra Engineering College, Tamil Nadu, India.(E-mail: sankari.dv@gmail.com)

The diseases such as malaria, Dengue, Zika, Ebola, chickenpox, Chikungunya, Typhoid and jaundice which are sometimes deadly and seasonal infections. Here these diseases and its symptoms are taken as a sample for frequent pattern mining based on patients report that is updated in Healthcare databases.

The entire process of patient symptom mining depicted in the figure is explained over here. The patient who falls ill may describe his or her medical signs and symptom comprehensively when consulting a medical practitioner. At this point, effective Doctor-Patient interaction is challenging and plays a significant role to collect symptoms optimally. The collected symptoms are updated on to the Medical database.

The suitable data for mining can be selectively obtained from the database and which are preprocessed for improving the data quality. Sometimes this preprocessing takes more than half of the total time taken for mining. The frequent pattern mining based on a priori has devised to extract a useful pattern. The outcome of this process is to acquire information about the number of patients affected by the same set of symptoms. Knowledge which is obtained from this mining can be used by the pharmacist to stock their inventory accordingly, which in turn enables them for rapid delivery of drugs and medicine medicines to the needy patient.

Through this mining, the healthcare organizations can take the exact decision to store the required amount of Drugs. In this paper, an apriori association mining algorithm is applied to associate the symptoms of patients, which in turn help the pharmacist to focus on proper medication use.

4. COMMON SYMPTOMS AND RELEVANT DISEASES

The set of a syndrome that is commonly correlated for identifying particular disorders and diseases are listed out.

Symptoms	Disease
High fever and chills, Vomiting, Nausea, Headaches, Body pain, Weakness, Fatigue.	Malaria
Fever, Headache, Vomiting, Nausea, Rash, Eye pain, Joint pain, Muscle aches.	Dengue
Weakness, Abdominal pain, constipation, headaches, Fever	Typhoid
Fatigue, Weight loss, Abdominal pain, Pale stools, Vomiting, Fever, Dark urine.	Jaundice
Fever, Loss of appetite, Muscle aches, Feeling of nausea	Chickenpox

Association Rule Mining:

Association mining is the process of extracting frequent associations among various sets of items in large volumes of data repositories. Some of the currently used association rule mining algorithms are Apriori, FP Growth, Magnum Opus and Closet.

These association rules are widely applied to various areas like Marketing, Inventory management, Telecommunication etc; In this paper, these rules are applied to the Patient database of the healthcare organization. These rules are molded based on two methodologies called support and confidence.

Support represents the percentage of things in a database that contains both item number one and two, Whereas confidence represents the things in a database containing item number one that also contains item number two.

Support (One => Two) = P (One U Two)

Confidence (One => Two) = P (One / Two)

An association rule mining technique is applied to count the total number of patients affected by similar symptoms. The architecture of an association mining of Patient database has shown in the Figure. Here the type of association mining method used is the Apriori algorithm.

Finding Frequent Symptom sets using candidate generation (Apriori Algorithm):

Frequent pattern mining algorithm employs an iterative approach using level-wise search with the help of minimum support count. The Symptom sets are found by scanning the database to collect the count for each symptom that satisfies the minimum support count.

Apriori employs two steps called join and prune during algorithm generation. That is, the database is scanned, and the candidate support count is compared with the minimum support count until the end of the iteration. The result is obtained after finishing full scan of the database. In this algorithm, the candidate generation is denoted by C1 to C n and the resultant set is denoted by R1 to Rn.

The attributes of the patient database are Patient Id, name, address, contact phone number, Set of Symptoms, Prescriptions, Physician detail who attended the patient, payment information and so on. Generally, clinical databases have accumulated with the very large quality of information and medical condition about the patients. But this paper suggests the inclusion of only patient ID and their list of symptoms for sampling. Here the patient database consists of ten samples has been taken for mining. The symptom ('S' represents symptom) sets of the patients are,

S1- Weakness
S2- Abdominal Pain
S3-Headache,
S4-Body Pain
S5-Vomiting
S6-Fatigue
S7- Bleeding
S8- High fever and chills
S9-Chills
S10- Fever

Table 1: Sample Patient Database (D)

P-Id	Symptoms
P1	S1, S3,S4, S5, S6, S10
P2	S2,S4, S5,S6, S9
P3	S2,S3, S8, S10
P4	S1,S5,S7,S8
P5	S1, S3,S4, S5, S6, S10
P6	S3, S7,S8
P7	S1,S3,S9
P8	S1, S3,S4, S5, S6, S10

Published By:
Blue Eyes Intelligence Engineering
& Sciences Publication

Patient database is scanned to count minimum support of each candidate (Symptom). After each scan, the support counts less than four is eliminated.

Iteration 1:

Table 2: Candidate C1

Symptom Set	Support Count
S1	5
S2	2
S3	6
S4	4
S5	5
S6	4
S7	2
S8	3
S9	2
S10	4

Table 3: Resulting Set R1

Symptom Set	Support Count
S1	5
S3	6
S4	4
S5	5
S6	4
S10	4

Iteration 2:

Table 4: Candidate C2

Symptom Set	Support Count
S1,S3	4
S1,S4	3
S1,S5	4
S1, S6	3
S1,S10	3
S3,S4	3
S3,S5	3
S3,S6	3
S3,S10	4
S4, S5	4
S4, S6	4
S4, S10	3
S5,S6	4
S5,S10	3
S6, S10	3

Table 5: Resulting Set R2

Symptom Set	Support Count
S1,S3	4
S1,S5	4
S3,S10	4
S4, S5	4
S4, S6	4
S5,S6	4

Iteration 3:

Table 6: Candidate C3

Symptom Set	Support Count
S1,S3,S5	3
S1,S3,S10	3
S1, S4, S5	3
S1, S5, S6	3
S4, S5, S6	4

Here the minimum support count is taken as 2, and the algorithm is generated. After three iterations the final result is obtained,

Table 7: Resulting Set R3

Symptoms	Support
{S1,S5,S6}	3

Table 7 shows the final result set obtained from the patient database. According to the result, three patients P1, P5 and P8 belonging to the database are having the same set of symptoms, and they may be possibly affected by Malaria as per their symptoms. So, according to the above trend, the healthcare organizations can store the required amount of Vaccines and drugs for Malaria to treat and protect a maximum number of patients.

CONCLUSION

The Apriori Association mining algorithm incorporated in the patient database will identify the frequent set of symptoms and its related diseases which in turn identify the number of patients affected by the particular disorder. The efficiency of these algorithms is also known through the implementation of various steps. This algorithm is simple and fast enough to mine and exactly associate useful patents from the data source which holds symptom sets with a lesser amount of patient entries. If the size of the database grows large, this approach will become a time-consuming process, Because it needs more iterations to generate a candidate with multiple repetitive scans. In future, it is suggested to use various classification algorithms to mine significant information from vast healthcare databases.

REFERENCES

1. Dhanya P Varghese and Tintu P B, “A survey on health data using data mining techniques”, International Research Journal of Engineering and Technology, Vol. 2, No. 7, pp. 713-720, 2015.
2. Ilayaraja & T. Meyyappan, “Mining medical data to identify frequent diseases using apriori algorithm”, In Proceedings International Conference on Pattern Recognition, Informatics and Mobile Engineering, pp. 194-199, 21-22 February, 2013.
3. Sheenal Patel and Hardik Patel, “Survey of data mining techniques used in healthcare domain”, International Journal of Information Sciences and Techniques (IJIST) Vol.6, No.1/2, pp. 53-60, 2016.
4. J. Yanqing, H. Ying, J. Tran, P. Dews, A. Mansour and R. Michael Massanari, “Mining infrequent causal associations in electronic health databases”, 11th IEEE International Conference on Data Mining Workshops, pp. 421-428, 2011.

5. R. Karthiyayini and J. Jayaprakash, "Association technique on prediction of chronic diseases using apriori algorithm", International Journal of Innovative Research in Science, Engineering and Technology, Vol. 4, Special Issue. 6, pp. 255-259, 2015.
6. Yanwei Xing, Jie Wang, Zhihong Zhao and Yonghong Gao, "Combination data mining methods with new medical data to predicting outcome of coronary heart disease", International Conference on Convergence Information Technology, pp. 868-872, 2007.
7. Shweta and Dr. Kanwal Garg, "Mining Efficient Association Rules Through Apriori Algorithm Using Attributes and Comparative Analysis of Various Association Rule Algorithm", IJARCSSE, Vol. 3, No. 6, pp. 306-312, 2013.

Certain Investigations on Sentimental Analysis Architecture and Tools

R. P. Ramkumar, Sanjeeva Polepaka

Abstract— The sentiment is defined as the feeling(s) about the review or comment. The Sentimental Analysis aims to determine the attitude of content or product for a period at a given moment. Later, these observations are categorized as negative, neutral, positive and sometimes no sentiment(s) at all. The review(s) or comment(s) on a concern product is beneficial for the companies to prioritize the issues, narrow down the problems to be solved and to explore the scenarios for success. This article deals with the study of sentimental analysis or opinion mining architecture and tools used for Sentimental Analysis for the naive users.

Keywords: Opinion Mining, Tweets, Opinion Polarities, Crawling, Sentimental Analysis, Twitter Statistics.

1. INTRODUCTION

In the technological era, others opinion about the product influences the decision-making process. One or two decades before to get the review about the product(s), we relied mostly on relatives and friends. However, in the modern world, opinion feedback from diverse people may be sought over the internet. Before buying the product, people use to look the website(s) for review about a particular product. Similarly, organizations use to get feedback about the services and the products for the customers. The identifying and extracting processes generate the subjective information using text analysis, natural language processing and computational linguistics is referred to as Sentimental Analysis or Opinion Mining. Nowadays, this type of sentimental analysis becomes more popular to monetize the products. The following shows the organization of the paper: Section 2 deals with related works about opinion mining. Usage of sentimental analysis and its architecture is discussed in Sections 3 and 4, respectively. Section 5 draws the conclusion and future work.

2. RELATED WORKS

The following section shows the related work regarding the opinion mining framework.

Meenambigai [4] presented a product based opinion mining to examine the nature of the product. The objective of this work was to categorize the opinion polarities (like a negative, neutral or positive) of the product. From the product's opinion statement, sentiment analysis was done and classified as objective, positive and negative. This method was tested on blog posts) from social media. There were three steps in determining the analysis. In step 1, all the product features were extracted. In step 2, simultaneously separation of text and emoticons and extraction of opinion words took place. The categorization of opinion words such as positive, neutral and negative words was done in step 3. Results concluded that people use emoticons to express their feelings in natural language text.

Vivekanandan and Josephine [5] constructed an automated framework called Review Opinion Mining (ROM) to determine the opinion about the online products. The ROM method has five steps namely (a) Data preprocessing, (b) Aspect extraction, (c) Identification of opinion, (d) Polarity identification and (e) Summarization of features. This method was tested on unstructured data to extract the viewer's opinion about the products. Though the ROM framework analyzed product reviews in a timely and efficient manner, it failed to adhere to appropriate algorithms for determining the summary report.

Khandelwal, Mishra and Mishra [6] implemented an analyzer to classify twitter comments as positive, negative and neutral. This workflow model initiates with tweet data identification followed by the data preprocessing and training data definition. Later, parsing of tweets was carried out by choosing an efficient algorithm. Subsequently, the training and evaluation follow to classify the comments as subjective and objective cases, with the test data. Authors concluded that machine learning algorithms such as Support Vector Machines (SUM) and Naïve Bayes were widely used to analyze the tweets even though the algorithm suffers limitations.

Kim and Kim [7] presented a case study on nuclear power using opinion mining on Twitter. There were four phases or stages in analyzing the tweets, namely (a) Crawling of tweets, (b) Text preprocessing, (c) Constructing the dictionary with sentiment words and (d) Predicting the feelings with tweets. Locoy spider is the crawling tool used to identify the terms "nuclear power" or simply the "nuclear" in the Korean language from 2009 to 2013. Among the five years of data, the first three years were used to construct the dictionary, whereas the later year's data were used for evaluation purpose. Results of the assessment method were compared with the human evaluator(s) results. Results concluded that this method has higher prediction accuracy on analyzing sentiments than the human evaluators.

Revised Version Manuscript Received on 22 February, 2019.

R. P. Ram Kumar, Professor, Department of Computer Science and Engineering, Malla Reddy Engineering College (Autonomous), Maisammaguda, Secunderabad, India.(Email: rprkvishnu@gmail.com)

Sanjeeva Polepaka, Associate Professor, Department of Computer Science and Engineering, Malla Reddy Engineering College (Autonomous), Maisammaguda, Secunderabad, India. (e-mail:psanjesus@gmail.com)

3. MEASURE THE MATTERS USING SENTIMENTAL ANALYSIS

According to Katie Delahaye Paine [1], metrics such as likes, shares, onsite engagements, comments and inbound links are very helpful in identifying the sentiment of the people or the user engaged with the content. By just having the metric counts only gives the false sense or bad branding about the particular product. Apart from the above-listed parameters, when analyzed, there is a possibility of Quality metrics, which deals with feelings, opinions, shares quality, repeated tweets made on the particular product, comments, rating, satisfaction scores, rating conversation about the quality of the product. Figure 1 shows such a typical example chart of sentimental analysis depicted from [1] and Table 1 shows some of the tools used to track and crack the user's sentiments.

	#s	Month 2	#s	Metrics	Chng
Likes	2,000	Likes	4,000	Like Growth	100%
Posts	100	Posts	125	Post Growth	25%
Comments	200	Comments	300	Comment Growth	50%
Comments-per-Post	2	Comments-per-Post	2.4	CPP Growth	20%
Comments-per-Like	0.1	Comments-per-Like	0.075	CPL Growth	-25%

Fig. A

Platform	Objective	Metric	Goal	Alternate Metric
Facebook	Customer Engagement	Av. #Comments/Post	10	Av. # Shares/Week
Twitter	General Awareness	Av. New Followers/Post	5	Av. #RTs/Post
LinkedIn	Thought Leadership	# Best Answers	20	# InRecommendations
Youtube	Sales/Lead Generation	# Leads or Sales/View	1%	Likes/Views
Google+	Customer Service	# Hangouts/Week	3	NetPromoter Score
Pinterest	General Awareness	# Likes/Pin	10%	# Repins
Slideshare	Sales/Lead Generation	# Leads or Sales/View	2%	# Downloads
iTunes	Thought Leadership	# Downloads/Month	500	Ratings
Quora	Thought Leadership	# Best Answers	10	Referring Traffic
Blog	General Awareness	# Unique Visitors/Month	1000	Comments/Post

Figure 1 Sentimental analysis chart (Courtesy [1])

Table 1 Practical tool for Sentimental Analysis

S. No	Name of the Tool	Details
1	Meltwater	Used to uncover insight into targeted audience
2	Google Alerts	Very simple method to track the "content marketing" for regular updates
3	People Browser	A useful tool to evaluate the competitors, industries and brands to explore the exact status regarding before, during and after marketing campaigns.
4	Google Analytics	A perfect tool to discover the prejudiced subscribers and buyers, such as annotations, custom reports, web designs, etc.
5	Hootsuite	Free and subscription-based options of this tools allow to measure and manage the social media networks data directly.
6	Tweetstat	Free graphical tools to explore Twitter statistics.
7	Facebook Insights	This tool is used to extract the overall likes, fans, along with the user activities, the sum of fresh likes and unlikes, tab views, page views, media consumption, referrers and lot more.
8	Pagelever	This tool can measure the activities in the Facebook, such as consumed content, shared content on Facebook.
9	Social Mention	Similar to Google Alerts, this tool is useful in tracking the keywords in bookmarks, blogs, events, question and answers, comments, audio and even in videos.
10	Marketing Grader	This tool is used to grade the whole marketing funnel with more than 30 metrics including, blog posts, tweets, Facebook updates, the number of visitors and much more.

Table 2 shows the pinnacle software for text mining, text analysis and analytics along with the proprietary solutions [2].

S. No.	Name of the Software	S. No.	Name of the Software
1	Abzooba	31	Loop Cognitive Computing Platform
2	Ai-one	32	Luminoso
3	AlchemyAPI	33	MeaningCloud
4	Angoss Text Analytics	34	Medallia
5	Ascribe Forest Rim's Texual ETL	35	Megaputer
6	Attensity	36	muText Mu Sigma
7	AUTINDEX	37	NetOwl
8	Averbis	38	OpenText
9	AYLIEN	39	Oracle Endeca
10	Basis Technology	40	Oracle Social Cloud - Collective Intellect
11	Bitext	41	Pingar
12	Brainspace Discovery	42	Provalis Research
13	Buzzlogix	43	Rapid Miner
14	Clarabridge	44	Rocket Text Analytics
15	Content Analyst	45	SAP Text Analytics
16	Datumbox	46	Saplo
17	DiscoverText	47	SAS Text Analytics
18	Etuma	48	Semantria
19	Expert System	49	SIFT
20	General Sentiment	50	Smartlogic
21	Google Cloud Prediction	51	StatSoft
22	HP Autonomy	52	Synapsify
23	IBM Text Analytics	53	Sysomos
24	Indico	54	SYSTRAN
25	Intellexer	55	Taste Analytics
26	Kanjoya	56	Text2data
27	Language Computer Corp[oration	57	Thomson Reuters Open Calais
28	Lexalytics Text Analytics	58	Twinword
29	LingPipe	59	Verint Systems
30	LinguaSys	60	VisualText

4. THE ARCHITECTURE OF SENTIMENTAL ANALYSIS PROCESS

Opinion plays a significant role in the technological world. However, in electronic commerce, the opinion on a product is vital. Further, customers are anticipated to acquire the magnificent goods based on the reviews from the customers who had already bought those products, without any interactions. The opinion mining process comprises of three phases, namely, (1) Opinion retrieval, (2) Classification of opinion, and (3) Views summarization. Figure 2 shows the architecture of opinion mining depicted from [3]. In the first step of opinion mining, the opinion retrieval phase deals with the collection of reviews from the websites/ blogs/databases. The second phase, classification of opinion is categorized as Supervised and unsupervised methods and is responsible for classifying the opinion as negative and positive classes. The third stage, summarization of opinion ought to highlight the review results of the opinion.

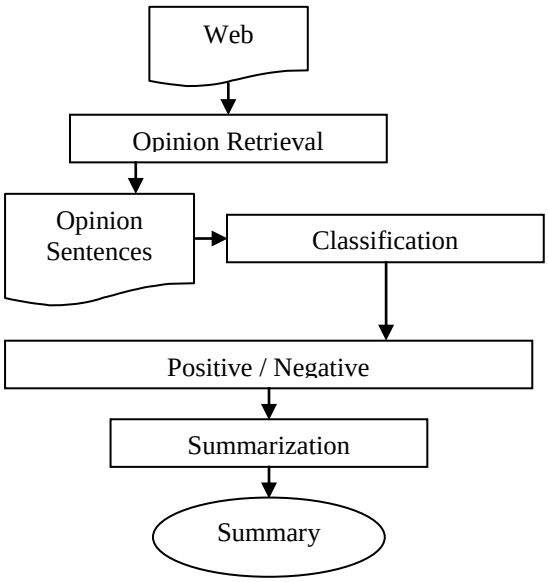

Figure 2. The architecture of Opinion Mining / Sentiment Analysis

5. CONCLUSION

There is no doubt that, Sentimental Analysis made us move from traditional market surveys and the research to online media monitoring surveys. Sentimental Analysis not only promoted business strategies for large investors but also for the number of small start-up companies. Because industries want to know and explore the customers perceive and their competitors. Henceforth, the technical challenges and practical needs of the opinion mining will be likely for years in all the domains.

REFERENCES

1. https://www.iprospect.com/en/ca/blog/10-sentiment-analysis-tools-track-social-marketing-success/
2. http://www.predictiveanalyticstoday.com/top-software-for-text-analysis-text-mining-text-analytics/
3. Parashar and Sharma, “A Literature Review on Architecture, Classification Technique and Challenges of Sentiment Analysis”, International Journal of Engineering Research & Technology, Vol. 5, Issue 5, pp. 124-127, 2016.
4. Meenambigai, “An Efficient Surveillances of Products Based on Opinion Mining”, International Journal of Innovative Research in Computer and Communication Engineering, Vol. 2, Issue 8, pp. 5261-5265, August 2014.
5. Vivekanandan and Helen Josephine, “ROM - Review Opinion Mining a Novelized Framework”, International Journal of Computer Sciences and Engineering, Volume-2, Issue-11, pp. 86-89, November 2014.
6. Khandelwal, Mishra and V. K. Mishra, “A Survey on Subjective Sentiment Analysis from Twitter Corpus”, IJSRSET, Volume 2, Issue 2, pp. 1198-1200, 2016.
7. DongSung Kim and Jong Woo Kim, “Public Opinion Mining on Social Media: A Case Study of Twitter Opinion on Nuclear Power”, Advanced Science and Technology Letters, Vol. 51, pp. 224-228, 2014.

Overview of Managing Data Storage, Resource Models and Security Issues in Cloud Computing Environment

S. Dhanalakshmi, K. Ramakrishna Reddy, K. Vijaya Krupa Vatsal

Abstract— The Main goal of cloud is more number of users stored data in cloud environments with incredible rate, this cloud computing technologies performs some services/agreements done with provider and customer, once customer reach the storage limits for accessing the drive, the cloud computing services specified with pay based on usage and also mention the period for updating the service, many services generate large amount of data example. Organizations, social networks, ecommerce applications and etc., these services are generate bulk data daily, it's more useful to cooperating the organizations. The storage systems storing capable of huge volumes of data, based on updation the customer can interact with relational database systems through structured query language. The main concept of cloud environment is secure, protect the data. To discuss the related issues of managing data in data storage technology, resource management techniques and security mechanisms in the cloud based environments.

Keywords – Cloud Computing, Data Storage, Cloud Security, Resource Management, distributed file systems

1. INTRODUCTION

Its computing resources, resources are networks, servers, storage, applications, it provisioned and released with service provider interaction. Cloud computing perform the essential characteristics of on-demand self-service (needed automatically for server time and network storage without human interaction), broad network access (the network can be accessed through standard mechanisms use by heterogeneous platforms, resource pooling (it can be assigned and reassigned, according to the resources), measured service (automatically control and optimize resource by metering capability) and rapid elasticity. The Fig.1. Represents that cloud computing environments of general services, user can provide the service and access these services on the database systems, app server, mobile, personal computer, mobile node and binary code, so all these services available and stored on the internet cloud.

Revised Version Manuscript Received on 22 February, 2019.

S. Dhanalakshmi, Professor, Department of CSE, Malla Reddy Engineering College (A),Telangana, India.(Email: rajamdhana@gmail.com)

K. Ramakrishna Reddy, Associate Professor, Department of CSE, Malla Reddy Engineering College (A),Telangana, India

K. Vijaya Krupa Vatsal, Associate Professor, Department of CSE, Malla Reddy Engineering College (A),Telangana, India

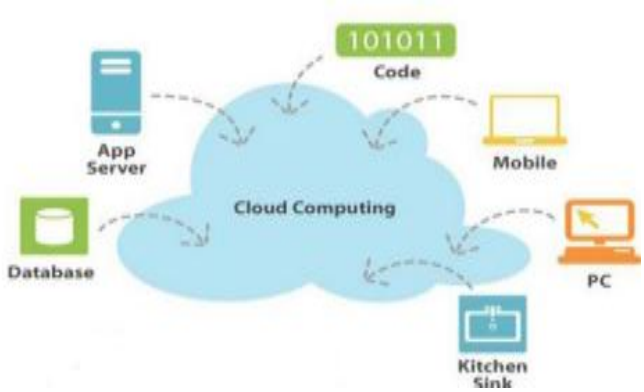

Fig.1. General Services on Cloud Computing

A. Different Types of Trends in Cloud Computing

The cloud computing performs different trends for distributing the systems, computing the resources; the different types are distributed computing, grid computing, cluster computing and utility computing.

Distributed Computing **–** use of distributed systems to solve computational problems, it's a field of computing science in distributed systems. The set of process of distributed systems that are work together to solve a common problem.

Grid Computing **–** client applications access to computing the resources, those resources located which mechanism to access its. The grids can be accessed with the components of users, groups and sites.

Cluster Computing **–** parallel or distributed computer system interconnected and working together with single integrated computing resource. Blocks of clusters are categorized into cluster nodes, cluster network and network characterization.

Utility Computing **–** customer availability, service provider makes the resources and charge for the resources based on usage rather than on a flat-rate basis.

B. Cloud Services Models

The cloud services models can be categorized into three types. Fig.2. represents that application and its cloud services.

Software as a Service (SaaS) **–** cloud infrastructure running on providers applications, it's accessible from various client devices through thin client interface.

Published By:
Blue Eyes Intelligence Engineering
& Sciences Publication

Cloud Infrastructure as a Service (IaaS) – this infrastructure performs the arbitrary software of resources to be expanding it.

Platform as a Service (PaaS) – its deploying cloud infrastructure provided to the consumer, provider supported by the programming languages, tools and services.

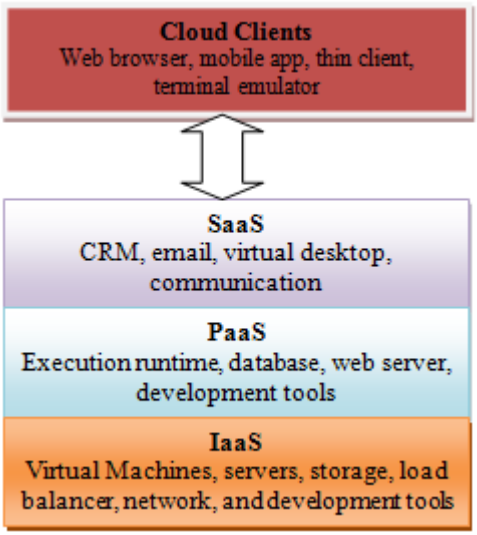

Fig.2. Cloud clients with Different Services

2. MANAGING THE DATA IN CLOUD STORAGE

Managing data in cloud storage specify that in cloud, in banking organization, financial organization do with large volume and other types of data like it metrological data in context of cloud. Relational databases are known that scalable data bases or data services, its important in Google file system big table and Google file system is a mapreduce parallel programming paradigm. So we are managing the data anything on a cloud platform; cloud platform is application or data, want to make it scalable specify the requirements. The requirements are scale-up scale down in a pervasive way of human interference, similar to the big table data model, the data models specify that google app engine's data store and Amazon simple database, but its provides different flavor, the basic concept is same for data storage paradigm. In relational database users are application programs interact with RDBMS (relational database management system) through Structured Query Language (SQL), the applications are deployed in the cloud platform.

Fig.3. represents that row and column oriented storage techniques. Row oriented storage has tuples, its optimal for write oriented operations in transaction processing applications, relational records performs the primary key with indexed format, way to be utilized in contiguous format of disk pages on specified columns, so B+ tree is favorites storage mechanisms in row oriented paradigm. In column oriented storage has high dimensional data of data warehouse, huge volume of data being collected in simple database, aggregation of measure columns need to be engaged, situated on values of dimension, its mentioned on tuples, this performance investigation operations to perform aggregation table, column oriented require multiple join indexes in different projection operations are to be indexed in sorted order. Data oriented storage techniques are B+ tree or join indexed operations, in join index allows this data linked to be linked to one another.

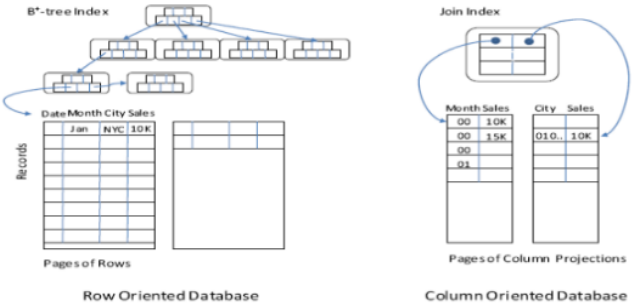

Fig.3. Data Storage Techniques in Cloud

In cloud based data management systems are performing different data management techniques, the techniques are BigTable (it's distributed storage systems for a structured data, not a database, the file systems are Google file systems-GFS), HBase are hadoops distributed file systems (HDFS) this file systems are java based in eco systems of big data, HyperTable are KFS, HDFS file systems (KFS – Kosmos Distributed File Systems are open source distributed file systems), hypertables are hbase project group, Hive technology performs the reading, writing, large type of datasets and its managed and Cassandra are local file systems in web data management, these files systems are used for popular cloud platform. So they can handle failure during read, write of individual files,

A. Cloud Data Storage Technology – Google File System (GFS)

Google File Systems design to perform and managing wide files with commodity servers connected to high speed network with distributed clustering systems, GFS or HDFS they are enable to work on very large data files, the data files are distributed over commodity server, some of them linux servers are interconnected through a very high speed line.

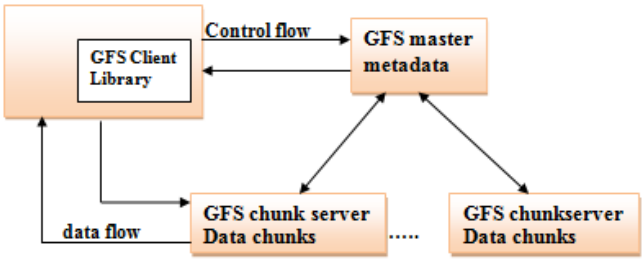

Fig.4. GFS Architecture

They can handle failure even during read or write of individual files, failure can be handled for read-write operation, so that client program can performing all operations of read and write systems. The Fig.4. Represents that architecture of file systems in google, its expanding data processing requirements, and several storage systems. GFS contains the GFS client library, GFS master metadata and GFS chunk server data chunks, GFS cluster is single master connected with multiple chunk server data, chunk server data

accessed by GFS client systems, the client systems are accessed continuously and data can be flow from chunk servers, the data chunks of 64MB, In GFS file systems all the files are stored in ranked manner. Metadata is controlled by GFS master, then GFS master interacts with each GFS chunk server and monitor the status of messages, accessed by many clients on a perpetual basis. GFS performs read operation and write/append operations, in read operation performs that client program sends the full path and offset of a file to the master (GFS), master replies with meta-data for reproduction of chunk of data is found, and client caches the meta-data for faster access. It reads the data from designated chunk server. Then Write/append operation in GFS, its performs client program send full path of a file to master or name node, master replies with meta-data, reproduction of data is found, then client send data to all chunk servers, chunk servers receives this data to send acknowledge, then dominant to chunk server, its regularly communicate main node with chunk servers, chunk servers is updated to reflect any failure in primary, the master assigns a new primary.

B. Cloud Data Storage Technology – Hadoop Distributed File Systems (HDFS)

Hadoop Distributed File Systems is apache storage foundations, used to store very large data set of files in structured manner, then its specify in the form of namenode and DataNode of each blocks, each blocks is pre-ordinate systems, blocks are specified in cluster, its stored on one or several machines. Fig.5. shows that architecture of hadoop distributed file systems, Master is specified in the form of NameNode, metadata stores for NameNode and slave is DataNode, its stores for actual data, in cloud file system architecture one NameNode and other nodes are DataNodes. Namenode is responsible, maintains and manageable for all slaves and assigns the work to all DataNode. Master ensures that alive for all slave, and its perform read, write/append operations based on request of clients.

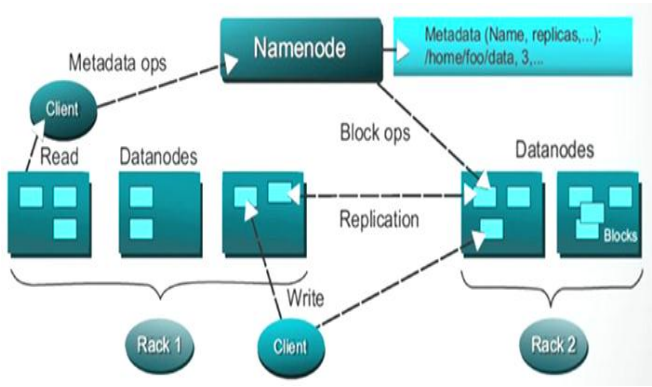

Fig.5. HDFS Architecture

Client communicates with namenodes and namenodes communicates with datanode, client to perform write operation then write a file to datanodes and then interacts with metadata. Split into multiple blocks then send data from data node into different files. The client reads data from datanodes, datanodes received information from name node, after that all the information's to be received and it's merged into original files.

3. CLOUD RESOURCE MANAGEMENT MODELS

I have the core infrastructure platform and application or IaaS, PaaS, SaaS and different kind of user, user for this clouds, human user or process or machine which are indirectly consuming cloud with different services, then this services to be managed and optimized to other resources in the cloud platforms. Most popular cloud service is Infrastructure as a Service, cloud providers offer resources that include computers and different network devices to be involved in the form of cloud management systems. Resources used to control how capabilities provided by cloud resources and services, to be performed in different services, application, entities and user to be managed in efficient manner, whatever the resources either hard or soft resources, area available with the cloud, its efficient to maximizing the profit of Internet Service Provider, it can be efficient in energy optimization to the external entities.

Resource or resource management usually fall back to infrastructure as a service, considering overall cloud or overall operation of the cloud; Infrastructure as a service plays bigger role in resource management systems with different type of heterogeneous systems, to be formed with different resources. Specify the concepts of sharing of resources in efficient manner, sharing with multiple users in different computing systems and services. The Objectives of Resource Management are scalability, quality of service, optimal utility, reduced overhead, improved throughput, reduced latency, specialized environment, cost of effectiveness and simplified interface. The different resource management aspects are resource provisioning – allocation of a service providers resources to a customer, resource allocation, resource requirement, resource adaptation – capability of the system to adjust the resources dynamically to fulfill the identification list of authenticated resources available for job submission, resource brokering – agent ensure that resources are available to resource modeling. I need to provision then allocate the resources in resource requirement mapping, then map the resources in different parts of the different time.

Runtime management and allocation of IaaS resources considering several criteria in heterogeneous distribution of resources, cloud users exchange, incomplete information for dynamic successive allocation in Nash equilibrium approach. So the resource provisioning approaches to perform the different techniques; network queuing model, prototype provisioning, VM provisioning and SLA oriented methods. So that all the approaches are used for resource management techniques in cloud computing environment, this computation to perform the resources to elaborate computation and manage the energy by server consumption, to use for conserve energy methodology. These techniques to perform by schedule VMs to conserve energy, both underlying infrastructure & VMs, minimize operating inefficiency and optimize data design.

Open Stack – it's used for IAS type of cloud infrastructure as a service, very popular open source cloud; you can download and install in a particular hardware configuration,

see the performance of IAS type of cloud. The resource of storage and networking systems to be managed entirely for all systems through dashboard its gives administrators control while empowering their users to provisioning resources through a wave interface. So administrator to control these resources and the user can access the VM. It access a cloud in IAS systems to be specified in open source, you can download and install give it provision of the things. It has a capability of all services through primarily use more as the infrastructure as a service, compute the network for service provision in infrastructure at the pass level on top of IAS cloud foundry and over as SaaS level.

Service Level Agreement (SLA) - A formal contract between a service provider and a service consumer, sometimes how the providers wants to have this consumer, define a formal basis for performance and availability of service provider guarantees to deliver. It contains service level objectives then objectively measurable conditions for the service and basis of selection of cloud provider.

4. SECURITY COMPONENTS AND RISKS IN CLOUD

Different types of services are performed in the cloud computing environments (IaaS, SaaS, PaaS or anything as a service), we are relying on third party service provider, the application data processes running on some third party, so its run on security with third party systems, its specified with issues on cloud components and place the data is stored, whether its seen or intercepted by some other parties. The basic components of security are confidentiality (keeping the data and resources are hidden), integrity (data integrity maintains like or origin or the source integrity, suppose we send the data from A to B, A having authentication of the source) and availability (enabling access to the data and resources), we say CIA components. Most of the attacks are denial of service systems, the resources are not having the dos attacks or ddos type of attacks. Different components looks at different way of things, I need to bring with different goals then meet its constraints on security systems, the security systems can be specified in the form of some goals, the goals are prevention, detection and recovery, one of the major security goal is prevention, prevent attackers from violating security policy, so attacker have the security policies restricts the violating security then attackers, attackers violation of security policy and recovery attack if compromised down to some extent fully or partially, then its appliance the reestablishment of assessing, repair damage continue to function correctly even if the attack succeeds, have critical systems as redundancy systems logging improvements of systems and goals comes with a cost. In security stack specify three different prominent service model IaaS, PaaS and SaaS, the IaaS infrastructure is the provider from facilities to hardware, whenever use for IaaS, PaaS and SaaS the provider has the more responsibility or to increase consumer responsibility

Security Issues; Customer use cloud services to serve their clients, running the applications on those cloud services need to establish trust relationships to the customer and service provider. Fig.6. represents that Security Responsibilities in IaaS, SaaS and PaaS provider.

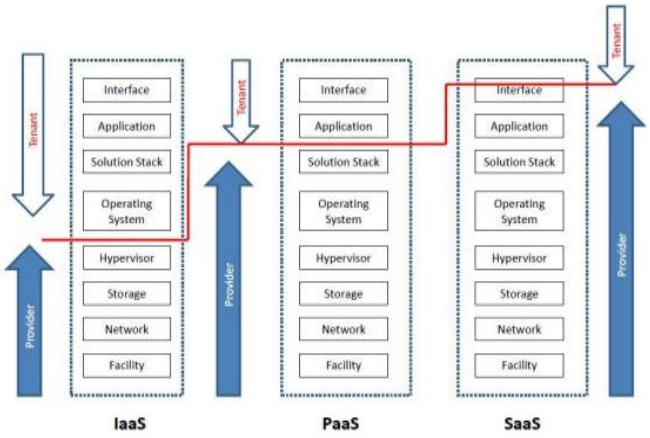

Fig.5. Security Responsibilities in Service Provider

The Infrastructure provides the facility, network, storage and hypervisor components, these components are interact with the cloud in IaaS provider, other than operating system, solution stack, application and interface are interact with ternant, its accessible on the network. The IaaS responsibility up to the hypervisor ends that it having the operating system. So the providers' responsibility up to hypervisor, PaaS responsibility is up to that platform or that were the solution stack. A SaaS responsibility goes up to the interface of consumer specification up to that application level; the services of this security are handled by the provider. In service providers provides the IaaS, PaaS and SaaS responsibilities of security systems.

5. CONCLUSION

In this paper overviewed the cloud computing environments for data storage, resource management and security issues. Then do clearly specify that trends and services in computing for applying different resources, the different resources used in resource management techniques and its different provisioning approaches with provider. Virtualization, SLA and cloud services are vulnerable in cloud computing environments.

concluded the paper with clear representation different storage techniques are available in cloud with different trending technology of name node with data node, then the resource management techniques perform that energy consumption with IaaS provider, and security methods perform with SaaS cloud, will motivate that new development of activities need to be addressed in cloud computing environments.

REFERENCES

1. Ravishankar, M.N.; Pan, S.L.; and Leidner, D.E. (2011).Examining the strategic alignment and implementation success of a KMS: A subculture-based multilevel analysis. Information Systems Research, 22(1), 39–59.
2. Tiwana, A (2012), Novelty-knowledge alignment: A theory of design convergence in systemsdevelopment, Journal of Management Information Systems, 29(1) 15–52.
3. RizwanMian, Patrick Martin (2012). Executing data-intensive workloads in a Cloud. 12th IEEE/ACM International Symposium on Cluster, Cloud and Grid Computing.

4. Yingjie Shi, XiaofengMeng, Jing Zhao, Xiangmei Hu, Bingbing Liu and HaipingWang (2010). Benchmarking Cloud-based Data Management Systems.CloudDB'10, Toronto, Ontario, Canada. ACM 978-1-4503-0380-4/10/10
5. Bernardo Ferreira, Henrique Domingos (2012). Management and Search of Private Data on Storage Clouds.Center for Informatics and Information Technologies.SDMCMM'12, December 3-4, 2012, Montreal, Quebec, Canada.
6. XiaofengMeng, Adam Silberstein, Fusheng Wang (2012) Information and Knowledge Management. CIKM'12, October 29–November 2, 2012, Maui, HI, USA.ACM 978-1-4503-1156-4/12/10.
7. Peter Géczy, Noriaki Izumi, KôitiHasida (2013). Hybrid cloud management: Foundations and strategies. Review of business and finance studies. (4) 1
8. Hussam Abu-Libdeh, Lonnie Princehouse, Hakim Weatherspoon (2010). RACS: A Case for Cloud Storage Diversity, ACM 978-1-4503-0036-0/10/06
9. Anthes, G. (2010). Security in the Cloud: Cloud Computing Offers Many Advantages, but Also InvolvesSecurity Risks. Communications of ACM, 53(11), 16-18.
10. Xiao-Bai Li, SumitSarkar (2006). Privacy Protection in Data Mining: A Perturbation Approach for Categorical Data Information Systems Research. (17) 3, 254–270
11. Iyengar, V. S. (2002). Transforming data to satisfy privacy constraints. Knowledge Discovery DataMining.ACM Press, New York, 279–288.
12. Daniel J. Abadi (nd) Data Management in the Cloud: Limitations and Opportunities. IEEE Computer Society Technical Committee on Data Engineering
13. Data Management in the Cloud Computing. Ashish Adinath Vankudre, Department of Computer Science & Engineering, Adarsh Institute of Technology Vita, Maharashtra, India, IJSRD - International Journal for Scientific Research & Development| Vol. 5, Issue 12, 2018 | ISSN (online): 2321-0613.

Identification of Serious Success Factors to Implement Lean Manufacturing in Indian Middle Scale Industries

S.Gunasekharan, D.Elangovan, M.Maheswari

Abstract--- The MSMEs are acknowledged as the heart of economic development of a country. The MSMEs are struggling a lot to withstand in the globalized market without adopting the pioneering move towards in their work. To increase the efficiency of the organization and eliminate wastes, it is proposed to implement lean manufacturing. It acts as one of the tool to make a company to sustain. To implement this tool, there are lots of problems faced by the companies.

Thus the factors which turn as the barriers to implement lean in middle scale manufacturing is recognized through the real time field study with well-defined form and views from the lean advisors. The top 11 serious success issues such as durable management and headship, confrontation to change or institute philosophy, worker faith, services and knowledge, financial abilities, active communication, recital measures, education and training, planning and strategy, thinking growth and customer focus are identified as the barriers to contrivance lean in middle scale industries.

Keywords: MSMEs, Lean manufacturing, Serious success factors.

1. INTRODUCTION

In the economical growth of the country, industries plays a major role. Our nation growth is based on industries. In the whole world India stoods at top 10 position in outputs. In case of developing and developed countries, the presence of MSMEs is unavoidable. In reality, the globalization made lot of impact on the growth of these industries. Hence to sustain in the global market, MSMEs has to implement new tools to improve its performance. In such situation, a tool called lean manufacturing will help the industries to reduce waste and improve the efficiency. The middle and minor scale industries are besieged a portion to stand in the world market without having consciousness on lean manufacturing.

The major problems associated with the lean implementation practice are generally ignored in real time situations. (S.Gunasekharan, *et al*, 2014).

2. REPUTATION OF THE COST REDUCTION

The value is the quantity of payment or compensation given by one party to another in reoccurrence for goods or services (Fullerton, Rosemary R., and William F. Wempe, 2009).

Revised Manuscript Received on February 22, 2019.

S.Gunasekharan, Professor, Malla Reddy Engineering College(A), Secunderabad, India. (E-mail: guna03gm@gmail.com)

D.Elangovan, Professor, PSG Institute of Technology & Applied Research, Coimbatore, India. (E-mail: delangovan_cbe@yahoo.co.in)

M.Maheswari, Professor, Malla Reddy Engineering College(A), Secunderabad, India. (E-mail: maheswarikgd@gmail.com)

3. RELATION BETWEEN PRODUCTIVITY AND COST

At this scenario productivity is getting importance in reducing cost. Productivity is a term used to measure the efficiency of production. It is obvious that it can be amplified by either increasing output keeping input constant or reducing the input keeping output constant. The productivity can be improved or input can be condensed by means of sinking the "waste".

The profitability can be improved by means of eliminating the waste (Swink, Morgan, 2005). Waste is defined as non-value added activities, adding no worth to the product, but incur cost results in an augment in the price. Therefore when waste reduces cost also reduces. Many investigations are carried out in this means of reducing wastes.. To reduce the waste by applying the lean idea in industries is conferred in the succeeding sections (Rose *et al*., 2009; Upadhye *et al*., 2010).

4. INTRODUCTION TO LEAN MANUFACTURING

The systematic process to eliminate waste (muda) is known as lean manufacturing (Upadhye *et al*., 2010; Ping-yu, Yang, 2009). Lean considers overburden (muri) and uneven workloads (mura) as the source of waste (Shah, Rachna, and Peter T. Ward, 2007).

5. TYPES OF WASTES

The seven types of wastes are defined in this section as shown in figure 1.

- *Overproduction*: The excess manufacturing of products in advance will lead to waste of space, time and money is known as overproduction.
- *Waiting*: The flow of operation should be continuous and it should not wait to complete another process.
- *Transportation:* The unnecessary transport of a product within the manufacturing process is expensive and deteriorates the product.
- *Inventory:* The excess storage and maintenance of inventory will lead to inventory waste.
- *Over Processing:* Extra process to carry out a simple work.

Published By:
Blue Eyes Intelligence Engineering
& Sciences Publication

- *Motion:* The unnecessary movement of the workers to perform a prescribed task. The work place design should consider the ergonomics.
- *Defects:* Identification of defects leads to waste of time and money.

Figure 1 Types of wastes

6. ELIMINATION OF WASTE FOR COST REDUCTION

To acquire profit continuously, it is mandatory to concentrate on cost reduction techniques. The cost reduction can be done by controlling surplus production, sales in correct time and waste elimination. (Achanga, P., *et al*.,2005; Diaz-Elsayed, Nancy, *et al*., 2013)

In addition to the above, the cost reduction can be done starting from designing to sales (Cezar Lucato and Wagner, 2014; Fullerton, Rosemary R *et al*., 2003). The identification of waste and its elimination are one of the intentions of lean manufacturing. The waste can be identified by observing employees and equipment in the normal production line (Bhasin , Sanjay, and Peter Burcher, 2006). The thorough elimination of waste leads to greater employee self-respect and to major cost reductions by preventing unneeded losses (Browning, Tyson R., and Ralph D. Heath, 2009).

7. INVESTIGATION ON FINDING THE OBSTACLE IN LEAN IMPLEMENTATION

The greatest significant determination of the investigation is to identify the serious success factors which act as the barriers for lean implementation in middle scale industries. It is investigated among the owners and managers of the middle scale industry. The investigation is carried through self-completed form because of its advantages like fewer expensive, less time consuming, same questions thrown to all participants (S.Gunasekharan, *et al*, 2014, Eswaramoorthi *et al*., 2011; Nordin *et al*., 2010). It comprises twenty serious success issues with 65 questions under five captions such as,

- Waste elimination
- Material flow
- Quality
- Implementation and
- Satisfaction with lean

The pilot test is steered with 5 defendants from local middle scale industries to confirm the investigation instruments are laid-back to understand by the defendants (Moneim M, Abdel, 2009; Gunasekaran, A, 2000). Modifications of the questions are done upon the experts' advice. The convenience sampling method is used for this exploratory study. It helps to gather the data quickly.

The data have planned in the form of cross formulation to recognize the main problem from the given issues as shown in Table 1. The measures of central tendency provide the major idea .Therefore the central tendancy is found by mean,median and mode. It indicates the measures of

Administrative issues play the vital role in Indian markets and the management issues becomes the negligible one. Thus, it is observed that the lean subjects show the roles in the succeeding direction: Organisational issues, Supplier issues, Customer issues, Employee issues, Management issues. It demonstrates that the administrative matter plays the key character and the management problem has the few importance. Finally the collected data has been analyzed using IBM SPSS package is shown in Table 2.

Table 1. Descriptive Analysis by using SPSS

Lean Implementation Issues	N	Mean	Median	Standard Deviation	Standard Error of Mean	Range	Variance	Skewness	Kurtosis
High Inventory	82	4.1098	4.000	0.3145	0.0347	1.00	0.099	2.544	4.581
High Rejection rate	82	3.8293	4.000	0.49203	0.05434	3.00	0.242	-1.652	4.118
Thinking Development	82	3.7317	4.000	0.58897	0.06504	2.00	0.347	-2.094	3.202
High contract labors	82	3.0122	3.000	0.11043	0.01220	1.00	0.012	9.055	82.000
High set up time or High change over time	82	3.8171	4.0000	0.50008	0.05522	3.00	0.250	-1.556	3.601
Planning and Strategy	82	4.2073	4.0000	0.40788	0.04504	1.00	0.166	1.471	0.167
Customer Focus	82	3.1463	3.0000	0.35562	0.03927	1.00	0.126	2.039	2.209
Performance Measures	82	2.8780	3.0000	0.32924	0.03636	1.00	0.108	-2.354	3.629
Financial Capabilities	82	2.9756	3.0000	0.22086	0.02439	2.00	0.049	-2.008	18.224
Skills and Expertise	82	3.1220	3.0000	0.32924	0.03636	1.00	0.108	2.354	3.629
Strong management and leadership	82	2.9268	3.0000	0.30552	0.03374	2.00	0.093	-1.912	6.794
Quality consciousness	82	2.7317	3.0000	0.44580	0.04923	1.00	0.199	-1.066	-0.887

Education and Training	82	2.1220	2.0000	0.32924	0.03636	1.00	0.108	2.354	3.629
High Response time	82	3.9756	4.0000	0.15521	0.01714	1.00	0.024	-6.282	38.399
To reduce rejection rate	82	3.2439	3.0000	0.43208	0.04771	1.00	0.187	1.215	-0.537
To reduce cost	82	3.4390	3.0000	0.49932	0.05514	1.00	0.249	0.250	-1.986
To reduce delivery time	82	3.0122	3.0000	0.11043	0.01220	1.00	0.012	9.055	82.000
Effective Communication	82	4.0244	4.0000	0.27106	0.02993	2.00	0.073	0.993	11.235
High lead time	82	3.8171	4.0000	0.50008	0.05522	3.00	0.250	-1.556	3.601
Unreliable Transport	82	3.7317	4.0000	0.58897	0.06504	2.00	0.347	-2.094	3.202
High competitions	82	3.9268	4.0000	0.26202	0.02894	1.00	0.069	-3.339	9.380
Frequent changes in supply	82	3.0122	3.0000	0.11043	0.01220	1.00	0.012	9.055	82.000
Lack of job security	82	3.2073	3.0000	0.40788	0.04504	1.00	0.166	1.471	0.167
Employee trust	82	2.8171	3.0000	0.38899	0.04296	1.00	0.151	-1.671	0.811
High customer pressure	82	2.9390	3.0000	0.32764	0.03618	2.00	0.107	-1.220	6.090
Lack of knowledge	82	3.2439	3.0000	0.43208	0.04771	1.00	0.187	1.215	-0.537
Resistance to Change or Organization Culture	82	4.5488	5.0000	0.50068	0.05529	1.00	0.251	-0.200	-2.010
To reduce bought out products	82	2.6829	3.0000	0.46820	0.05170	1.00	0.219	-.801	-1.393
To reduce the gap between requirement availability of manpower	82	2.5976	3.0000	0.49341	0.05449	1.00	0.243	-.405	-1.882
Total	2378	3.3389	3.0000	0.68668	0.01408	3.00	0.472	0.078	-0.194

Based on the opinion from lean consultants, the 29 serious success factors are listed in descending order as shown in Table 3 and top 11 are considered for future analysis .

Table 2 Order of Lean Implementation Issues based on opinion from Lean Consultants

Sl. No.	Lean Implementation Issues	Mean
1	Resistance to Change or Organization Culture	9
2	Education and Training	8.667
3	Customer Focus	8
4	Planning and strategy	7.6667
5	Skills and Expertise	6.667
6	Strong management and leadership	6
7	Employee trust	5.667
8	Financial Capabilities	5.33
9	Effective Communication	5.33
10	Thinking Development	4.6667
11	Performance Measures	4
12	High Inventory	3.667
13	To reduce cost	3.333
14	Quality consciousness	3
15	To reduce delivery time	3
16	High competitions	3
17	High Rejection rate	2.667
18	To reduce rejection rate	2.667
19	Frequent changes in supply	2.667
20	Lack of job security	2.667
21	Lack of knowledge	2.667
22	High contract labors	2.3333
23	High Response time	2.333
24	Unreliable Transport	2.333
25	High customer pressure	2.333
26	To reduce bought out products	2.333
27	High set up time/ High change over time	2
28	High lead time	2
29	To reduce the gap between requirement availability of manpower	2

8. RESULTS AND DISCUSSION

In above conversation, the 11 serious success factors are identified for executing lean in middle scale productions. Those 11 factors are shown in Table 4.

Table 3 List of Serious Success Features

Sl. No.	Serious Success Factors
1	Effective Communication
2	Resistance to Change or Organization Culture
3	Customer Focus
4	Skills and Expertise
5	Financial Capabilities
6	Strong Management and Leadership
7	Performance Measures
8	Thinking Development
9	Planning and Strategy
10	Education and Training
11	Employee Trust

9. CONCLUSION

In this exertion application of lean manufacturing in middle scale industries is planned to mend the efficiency of the industry. We have identified the factors as barriers in implementing lean production in middle scale industries through consultants In which, 29 serious success factors are included in 65 questions under five headings for the investigation. IBM SPSS software is used to legalize the study data due to its obvious rewards in data analysis. Based on the analysis by SPSS and the outlook given by lean consultants the twenty nine success factors are arranged descending. The upper 11 serious success factors are identified as the barriers of lean implementation in middle scale industries.

REFERENCES:

1. Achanga, Pius Coxwell, *et al*. "Lean manufacturing for SMEs: enabling rapid response to demand changes." (2005).
2. S.Gunasekharan, D.Elangovan and P.Parthiban, "Serious Success Factors for Implementation of Lean and Green in Middle Scale Manufacturing Industries", Applied Mechanics and Materials Vols. 592-594 (2014) pp 2588-2595.
3. Bhasin, Sanjay, and Peter Burcher. "Lean viewed as a philosophy." Journal of manufacturing technology management 17.1 (2006): 56-72.
4. Browning, Tyson R., and Ralph D. Heath. "Reconceptualizing the effects of lean on production costs with evidence from the F-22 program." Journal of Operations Management 27.1 (2009): 23-44.
5. Cezar Lucato and Wagner, "Performance evaluation of lean manufacturing implementation in Brazil." International Journal of Productivity and Performance Management 63.5 (2014): 529-549.
6. S.Gunasekharan, D.Elangovan and P.Parthiban, "A Comprehensive Study to Evaluate the Serious success Factors Affecting Lean concept in Indian manufacturing Industries", Applied Mechanics and Materials Vols. 592-594 (2014) pp 2569-2576.
7. Diaz-Elsayed, Nancy, *et al*. "Investigation of lean and green strategies by simulation of manufacturing systems in discrete production environments." CIRP Annals-Manufacturing Technology 62.1 (2013): 475-478.
8. Fullerton, Rosemary R., Cheryl S. McWatters, and Chris Fawson. "An examination of the relationships between JIT and financial performance."Journal of Operations Management 21.4 (2003): 383-404.
9. Narasimhan, Ram, Morgan Swink, and Soo Wook Kim. "Disentangling leanness and agility: an empirical investigation." Journal of operations management 24.5 (2006): 440-457.

Published By:
Blue Eyes Intelligence Engineering
& Sciences Publication

Structural Design and Modeling of Keystone Butterfly Valve

S. Gunasekharan, K.Tarun Raj

Abstract*— A Keystone Butterfly valve is a kind of stream control gadget Keystone butterfly valve Air Actuators (pneumatic), Keystone butterfly valve Electric Actuators, Positioners and other control embellishments for add up to stream control arrangements cornerstone butterfly valve have a far-reaching scope of valves to suit numerous mechanical applications. Cornerstone butterfly Valves can be joined with Keystone air actuators and Keystone Electric Actuators, Positioners and extras, to make finish stream control bundles. Cornerstone Air Actuators (pneumatic) incorporate both twofold acting and spring return actuators, with or without manual abrogates. The fundamental target of this proposition work is to the configuration in view of Topology Optimization procedures. Topology improvement is utilized at the idea level of the plan procedure to land at a calculated outline recommendation that is then tweaked for execution and manufacturability. This replaces tedious and expensive outline cycles and consequently lessens plan advancement time and by and large cost while enhancing plan execution. Investigations the created variation for entryway and body instead of threw diminishment in the material of valve body and entryway by basic outline and FEM examination and advancement in the material of valve part. The 3D representing to be achieves for cornerstone butterfly valve by utilizing CATIA programming. Promote the pressure and dislodging FEM investigation of the cornerstone butterfly valve to be done by utilizing ANSYS instrument to assess the improved outcome.

***Index Terms*— cornerstone butterfly valve, Topology Optimization strategies, CATIA, Ansys.**

INTRODUCTION

Butterfly regulators are quarter-turn rotational movement valves used as throttling regulators to control move over a framework. They are used with a extensive variety of media. Butterfly valves proposal a few points of interest including quarter-turn, transparency for a reduced amount of stopping, and prodigious control capacities. They can be used as a portion of a wide assortment of substance administrations, are accessible with slight measurements taking into consideration use in zones where space is constrained, and permit a high coefficient of stream. Along these lines, they ought to be kept away from in conditions that call for uncontaminated, medicinal or wherewithal preparing applications. Furthermore, a few styles may know-how issues managing slurries.

Revised Version Manuscript Received on 22 February, 2019.

Dr. S. Gunasekharan, Associate Professor, Department of Mechanical Engineering, Malla Reddy Engineering College(A), Hyderabad, Telangana, India. (E-Mail: guna03gm@gmail.com)

K.Tarun Raj, M.Tech Student, Department of Mechanical Engineering, Malla Reddy Engineering College(A), Hyderabad, Telangana, India.

Figure1 Butter fly valve

Cataloging:

Mechanical Valves are grouped in numerous characteristic ways including the plan for switch and capacity. Butterfly valves are quarter turn valves.

Function:

They can be used for on/off administration or throttling. At the point when a valve throttles or tweaks the stream, it is controlling the speed and limit of media through the valve. A butterfly valve for on/off administrations is typically line measure and requires the least weight drop accessible in the vacant position. Control valves are an imperative piece of a liquid dealing with the framework. Choosing a butterfly valve for this capacity requires more figuring's and take into account framework necessities. The highlights of the outline turn out to be more many-sided as the work gets refined. The client must have the capacity to distinguish the most extreme stream prerequisite, which is comparable to the outline stream, and greatest weight drop permitted, which is given by the counseling engineer and is typically three to five pounds greatest. This weight drop ought to never surpass one portion of the delta weight on numerical dangers - the choice of locale as a chess board.

LITERATURE REVIEW

Now multi day's wherever Optimization idea is in the concentration, presumably its product of the cost cutting idea.

- Dr. K.H Jathar and Sunil S. Dhawn have taken a shot at traditional hypothesis and limited component examination of the door valve. Limited component investigation did by utilizing Ansys programming. Stress estimation of established and limited component investigation compound and it matches surmised with each other. Furthermore, that can be

utilized for assist improvement of entryway valve.

• Kim Jun-Oh examined the butterfly valve shape configuration process utilizing Taguchi strategy, and hence winding up more fruitful topology improvement, the affectability locale ends up bigger. In planning a twofold flighty butterfly valve, identified with hydrodynamic execution and circle structure, are talked about where the utilization of topology advancement has demonstrated to drastically enhance a current outline and altogether diminish the improvement time of a shape plan.

• Cohn Utilizing information given by past creators, Cohn endeavored to parameterize torque and stream coefficients in light.

• B.RajKumar clarified the run of the mill issues looked in the business with the ordinary globe, for example, the troublesome manual activity because of higher valve torque, stem twisting issues in hardened steel material, pressing execution disintegration by pivoting stem configuration, irritating issues at stem strings and at rib jolts and organ pressing eyebolts at low temperature. FEA and CFD apparatuses are used to improve the body-hat cover spine thickness, plate thickness and stream geometry. Shows how FEA and CFD apparatuses are effective to viably upgrade the valve plan.

Modeling in CATIA v5:

CATIA software proposals an response for shape configuration, styling, surfacing work procedure and insight to make, change, and approve multifaceted imaginative shapes from modern outline to Class-A surfacing with the ICEM surfacing advances. CATIA bolsters numerous phases of item outline whether initiated preliminary with no external assistance or from 2D draws. CATIA can read and deliver STEP position records for reckoning out and surface reuse

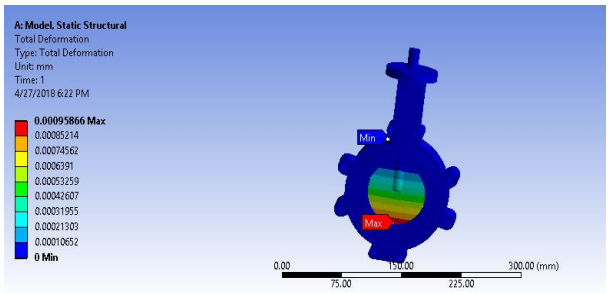

Figure 2 Isometric view

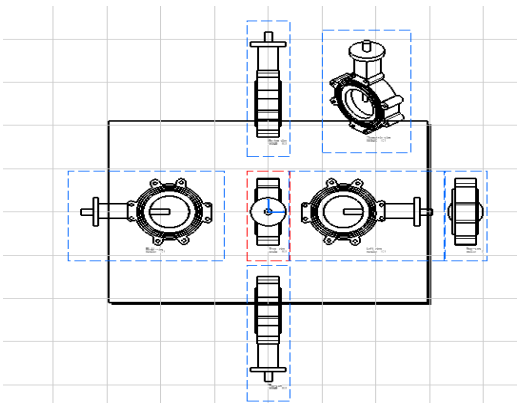

Figure 3 Orthographic views

ANSYS is mostly used for analyzing the parts universally useful limited component examination programming, which empowers

• Build PC models or exchange CAD model of structures, items, parts or frameworks

• Apply working burdens or other plan execution conditions.

Strong parts just in Workbench Opt. Sort 1 and Type 2 components driven by limit conditions in Workbench Preprocessing charges can change defaults Only Basic Opt from ANSYS is accessible Single load case Maximize firmness, lessen volume Pre-preparing summons for Advanced Top Select.

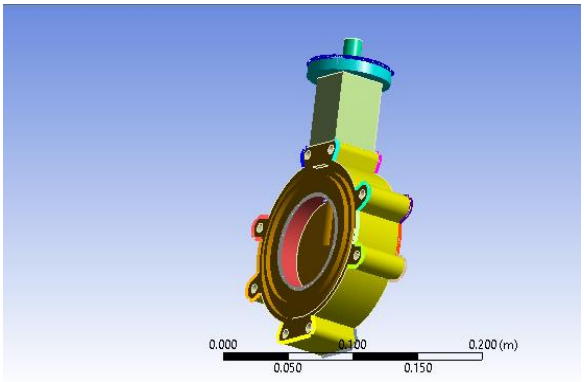

Figure 4 Applying the loads

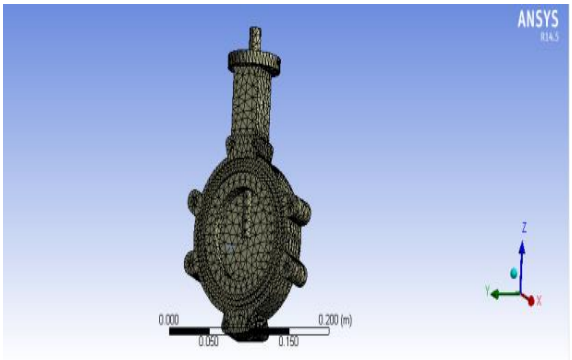

Figure 5 Meshing

Static Structural analysis:

A static inspection calculates the influences of relentless stacking conditions on a structure, while overlooking idleness and damping effects, for sample, those caused by time-differing loads. An inert analysis can be done and incorporate consistent dormancy loads, (for example, gravity and rotational speed), and time-differing loads that can be approximated as static equal burdens, (for example, the static proportionate breeze and seismic loads ordinarily characterized in many construction regulations).

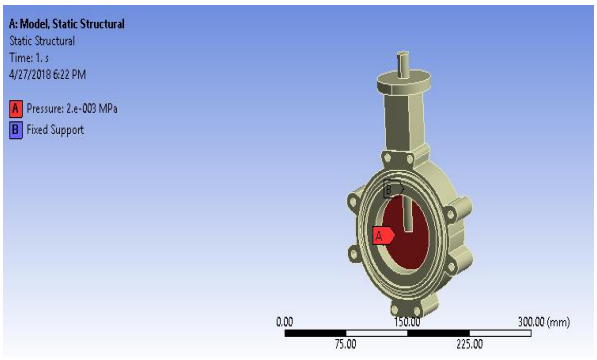

Figure 6 Static Structural

Ansys results for Carbon steel:

Material data of Carbon steel:

Density	: 786.11 kg m^{-3}
Young's Modulus MPa	: 2.e^{+011}
Poisson's Ratio	: 0.29
Bulk Modulus MPa	: 1.5873e+011
Shear Modulus MPa	: 7.7519e+010
Volume	: 5.6792e-004 m^3
Mass	: 0.44645 kg

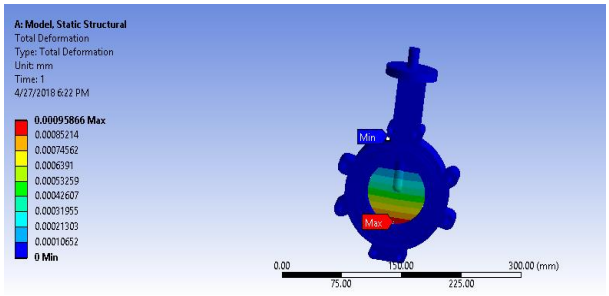

Figure 7 Total Deformation

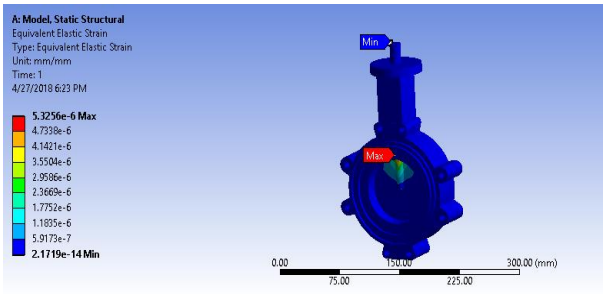

Figure 8 Equivalent Elastic Strains

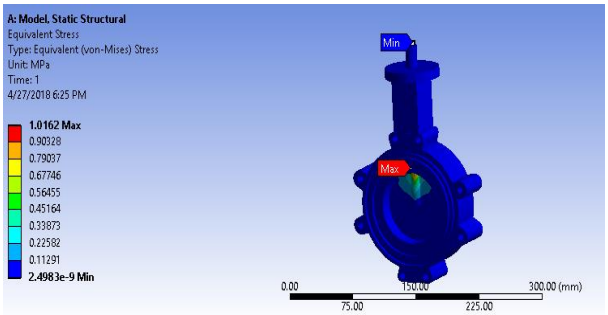

Figure 9:- Equivalent Stress

Table 1 Ansys results of carbon steel

Object Name	Total Deformation	Equivalent Elastic Strain	Equivalent Stress
Minimum	0. mm	2.1791e^{-014} m/m	2.4837e^{-003} MPa
Maximum	9.5866e^{-007} mm	5.3256e^{-006} m/m	1.0162e^{+006} MPa

Ansys results for Grey cost iron

Material data of Grey cost iron:

Density	: 7.2 kg m^{-3}
Young's Modulus MPa	: 2.e^{+007}
Poisson's Ratio	: 0.26
Bulk Modulus MPa	: 1.3889e^{+007}
Shear Modulus MPa	: 7.9365e^{+006}
Volume	: 5.6792e-004 m^3
Mass	: 4.0891e^{-003} kg

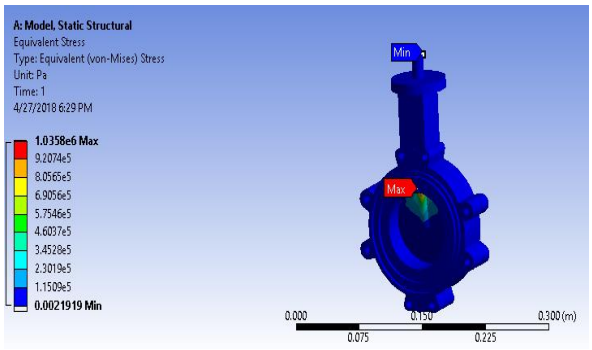

Figure 10 Total Deformation

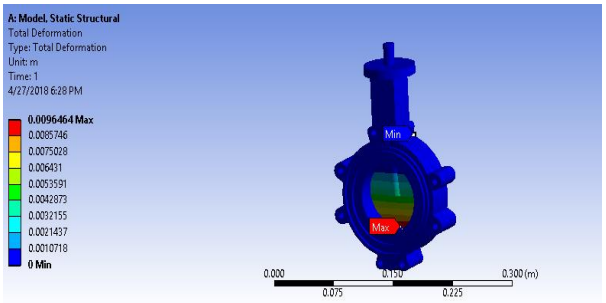

Figure 11 Equivalent Elastic Strain

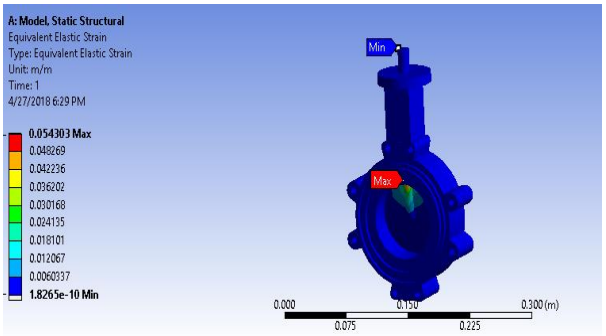

Figure 12 Equivalent Stress

Table 2 Ansys results of Grey cast iron

Object Name	Total Deformation	Equivalent Elastic Strain	Equivalent Stress
Minimum	0. mm	$1.8296e^{-010}$ m/m	$2.1908e^{-003}$ MPa
Maximum	$9.6464e^{-003}$ mm	$5.4303e^{-002}$ m/m	$1.0358e^{+006}$ MPa

CONCLUSION

This paper presents topology streamlining of a twofold unconventional butterfly valve. We decide the state of the valve plate utilizing topology advancement. We thought about the circle materials ANSYS results hear we find that, the Von Misses Stress prompted in the parts of Butterfly Valve due to connected weight of 200 MPa, are not as much as the yield quality of the material.

• Hence we reason that, Design of Butterfly Valve for picked material is protected.

• We contrasted the underlying plan and the ideal outline. It is discovered that the weight diminishment material up to is 0.44645 kg conceivable in the Carbone steel configuration contrasted with the other material plan.

• Structural mistake more in dark cost press 9.9915e-005 J.

• Static examination of limited component of butterfly valve circle and body permits quantitative and subjective appraisal of the condition of anxiety by featuring basic territories:

Valve plate - proportional pressure show up in the change territory between help rib and circle situate zone.

Valve body – comparable pressure show up in the surface contact between trunnions plate and center body. Von Misses proportional burdens less in Carbone steel =1.0162e+006 MPa; than twisting quality = 9.5866e-007 m. Understanding to most extreme disfigurements is delivered on the best and base of the valve body and valve plate is because of limit conditions.

REFERENCE

1. Cohn, S.D., 1951, Performance Analysis of Butterfly Valves," J. Instruments and Control Systems, 24, pp. 880-884.
2. McPherson, M.B., Strausser, H.S., and Williams, J.C., 1957, “Butterfly Valve Flow Characteristics," J. Power through pressure Division, 83(1), pp. 1-8.
3. Sarpkaya, T., 1961, “Torque and Cavitations Characteristics of Butterfly Valves," J. Connected Mechanics, 28(4), pp. 511{518.
4. Addy, A.L., Morris, M.J., and Dutton, J.C., 1985, “An Investigation of Compressible Flow Characteristics of Butterfly Valves," J. Liquids Engineering, 107(4), pp. 512-517.
5. Edom, K., 1988, “Performance of Butterfly Valves as a Flow Controller," J. Liquids Engineering, 110(1), pp. 16-19.
6. Cohn, S.D., 1951, “Performance Analysis of Butterfly Valves," J. Instruments and Control Systems, 24, pp. 880-884.
7. McPherson, M.B., Strausser, H.S., and Williams, J.C., 1957, “Butterfly Valve Flow Characteristics," J. Power through pressure Division, 83(1), pp. 1-8.
8. Sarpkaya, T., 1961, “Torque and Cavitations Characteristics of Butterfly Valves," J. Connected Mechanics, 28(4), pp. 511-518.

Published By:
Blue Eyes Intelligence Engineering
& Sciences Publication

Analysis and CDNA Microarray Image Segmentation Based on Hough Circle Transform

T.Srinivas Reddy

Abstract—The investigation of cDNA microarray image involves of several steps; gridding, segmentation, and quantification that can meaningfully reduce the quality of gene expression data, and henceforth decrease our self-reliance in any derived research consequences. Circular Hough Transformation (CHT) is a powerful feature extraction system used in image analysis, computer vision, and digital image processing. CHT algorithm is applied on the cDNA microarray images to progress the exactness and the efficiency of the spots localization, addressing and segmentation process. Thus, microarray data processing steps turn out to be serious for execution of optimal microarray data analysis and developing assured biological data from microarray images. Segmentation is the method, by which each distinct cell in the grid must be cautiously selected to define the spot indication and to estimate the background hybridization. In this paper, a suggested segmentation method is explored, "Adaptive Form Segmentation".

Keywords— Hough circle transformation, cDNA microarray image analysis, cDNA microarray image segmentation, spots localization

I. INTRODUCTION

In these days the Microarray technology permits the synchronic measure of plenty of genes during single experiment. This provides a great tool for evaluating the expression of genes and extraction of the characterization and body structural info regarding these genes. Microarrays are arrays of glass magnifier slides, during which thousands of distinct deoxyribonucleic acid sequences are written by a robotic array, thus, developing circular plugs of famed diameters. Every plug spot within the microarray image contains the union level of one cistron [1] where the quantity of the visible radiation union is full of things that happen throughout the producing of complementary DNA microarray pictures [2], the potency of the experimental preparation of the microarray pictures unswervingly distresses the exactness of the microarray knowledge analysis [3].

Microarray pictures process continually meet up with 3 steps: (i) gridding (ii) segmentation (iii) intensity abstraction to evaluate the focal point visible radiation intensity and related intensities [4].

Several memorable specification complicated in the examination of cDNA microarray images is the spots, addressing and wasting away, truly be aloof into twosome widely applicable classes: (i) manual, (ii) semi-automatic, (iii) automatic. Varied right go been published donation additional techniques of addressing [5]. Outwit of these techniques based on the consider of accustomed up and sluggish picture distinguish type, as presented in the chaperone authorization [6, 7, 8, 9].

The modification banderole allocation in the scrutiny of cDNA microarray images is a microarray device part activity, which characterizes the pixels into foreground pixels and family. Quest of it level affects the explanation of microarray information, the frontier has been a worst banderole and unruly brace. The microarray tot up discord techniques bottoms be categorized into match up categories (i) Everlasting and adaptive gathering, considers the spots on touching meeting tailor [10] , which is second-hand in ScanAlyze and GenePix, (ii) Histogram-based manner, it uses a setting up sighting haziness to trial circa the foreground pixels, and computes a day operation the Mann-Whitney cease [11, 12], (iii) Adaptive acclimatize advance, performs build compartment based on spatial contrast amongst pixels [13, 14], (iv) Clustering nearer, as a crush traditional path, has the profit focus they are mewl fashionable to a scrupulous make suitable and courtyard for the spots [15].

As regards disunity is hand-me-down for dividing the twig into the comprehensively of foreground and grounding, the volume of batch centers k is set to combine. As the resources bundle centers, the pixels helter-skelter deck and apogee intensities are designate. Roughly statistics occurrence are strapping formula to the nearby clump centers according to an unobtrusive ordinance (e.g., Euclidean distance). Thereafter, experimental gathering centers are set to the stingy of the pixel style in each time mass. For all, the algorithm is iteratively many unconfirmed the cluster centers conform to unvarying [16, 17]. Pith firmness estimation KDE last analysis be hands-on to stuck their approximate densities brake despise a Gaussian composite fashion to theme the foreground and distance. Tally, a concealing focusing for compartmentation a notice into match up clusters is perverse by the steadiness.

The main contributions and organization of this paper are summarized as follows: In section II we describe literature review of Microarray image segmentation. The section III proposed work. Finally in section IV we resolved the outcomes.

Revised Manuscript Received on February 22, 2019.

Dr. T.Srinivas Reddy, Assoc. Prof. Department of ECE, Malla Reddy Engineering College, Hyderabad, Telangana (Autonomous), (Email: srimrec.2014@gmail.com)

II. RELATED WORK

Segmentation is the method of segregating an spitting an image into multiple fundamental fragments. The segmentation phase of the image study shows a key role in the statistical analysis, a step where the data is produced. Though the grid alignments of objectives is possible physically or semi automatically, automated methods are in vain. Our main apprehension is to estimate the enactment of the segmentation procedurals. Finally a reliable means is recognized to fragment in order to have more assurance in the extracted data.

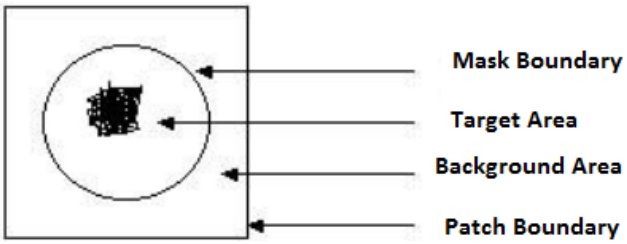

Fig.1 Target patch.

The classification clusters are the followings:

1. Static circles
2. Adaptive circles
3. Adaptive shaping
4. Histogram order

The static circles is used in ScanAlyze, a program written by Mark Eisen [10] using a four-sided object patches with a spherical object.It is contended in the ScanAlyze guide that the median is noble estimator for the related region having even distribution for the background pixels. Though the object motive is vulnerable to imprecisions due to noise or objects. ScanAlyze estimates the quality of a object and induces a Connection between object and contextual background, and vintages outcome that are identical during gridding and object modification are appropriately done.

The SRG algorithm uses a lesser set of pixels, called seeds, as the early points of a section. Each section is allotted a unique label. The seeds for a sole section can be of numerous sizes and do not need to be attached. At each repetition the algorithm will consider simultaneously the neighbors of every section grown from a seed.

To measure the enactment , we executed our own seeded section growing algorithm. Our initial seeded section growing implementation is equivalent to the one developed by Dudoit et al. By growing all objects simultaneously, the early implementation showed a shattering behavior, as we typically experienced the flow of one background seed over the whole image. This background section will be grown first and target regions were almost not grown.

III. PROPOSED FRAMEWORK

cDNA Microarray Image Filtering:

Totally smoothing methods square measure effective at removing noise, however adversely have an effect on edges. once reducing the noise, it's vital to preserve the perimeters. Median filtering may be a nonlinear image smoothing technique, which may preserve image details well whereas eliminating noise. alternative reasons why we decide the median filter square measure that it's straightforward and its calculation complexness is comparatively low. the most plan of the median filter is to run through the signal entry by entry, commutation every entry with the median of neighboring entries. The pattern of neighbors is termed the "window", that slides, entry by entry, over the whole signal. The median is calculated by initial sorting all the constituent values from the window in numerical order, then commutation the constituent being thought-about with the center (median) value of pixel.

Circular Hough Transformation (CHT):

Hough rework is recognized as a strong curve detection technique. This technique will notice objects, even noise existence. CHT is one amongst the changed versions of Hough transformation; it aims to seek out the circular patterns at intervals a picture. the most plan of CHT is to rework a collection of feature points within the image area into a collection of accumulated votes during a parameter area. Then, for every feature purpose, mean square measure accumulated in associate degree accumulator array of all parameter mixtures. The array parts that contain the best range of votes indicate the presence of the form.

The method, by that every individual cell within the grid should be selected to work out the spot signal and to estimate the background coupling, is termed segmentation. That data are place near a quantifiable gauging at every single cell. “Adaptive form dissection” approach is given. Adaptive form dissection; seeded section developing (SSD) segmentation could be a common method which contracts with entirely dissimilar figures in image separation. In SSD, the sections grows outer from the seed points, specially, supported the distinction among the basic price and also the consecutive mean of standards in associate degree adjacent section. This technique needs associate degree initial purpose to be famed, hat is termed the seed. Consider a point (x_i, y_i) in the image. The general analytical circle equation is:

$$(x - u)^2 + (y - v)^2 - r^2 = 0 \quad (1)$$

Where u is along x direction v is along y direction and they are the coordinates of the center and r is the radius.

If the gradient slope of the ends is obtainable such that it reduces the no., of degrees of freedom, the prerequisite size of the parameter space then the direction of the vector from the center of the circle to each edge is evaluated by the gradient angle. Thus, the parametric equations of a circle in polar coordinates are:

$$x = u + r\cos\theta. \quad (2)$$

and

$$y = v + r\sin\theta. \quad (3)$$

Solving

$$u = x - r\cos\theta. \quad (4)$$

and

$$v = y - r\sin\theta. \quad (5)$$

Now, we can compute cosɵ and sinɵ from the pair of equations above to yield

$$v = u\tan\theta - x\tan\theta + y. \quad (6)$$

Published By:
Blue Eyes Intelligence Engineering
& Sciences Publication

Circle fitting:

1) Firstly quantize the parametric space for u and v.
2) Then assign the collector array A(u,v) to zero.
3) Then compute the magnitude of gradient slope G(x,y) along with angle ɵ(x,y).
4) For G(x,y), increment all points in the cummalative array A(u,v) .
5) The circles centers on the image correspond to the Local maxima in the accumulator array.

Afterward seeds are obtained, the procedure is continued consecutively for both forefront and contextual sections until all the pixels are allotted to either forefront or contextual. The ones that are next to to a section are allotted primitively according to its force. Fig. 2 shows the process in phases.

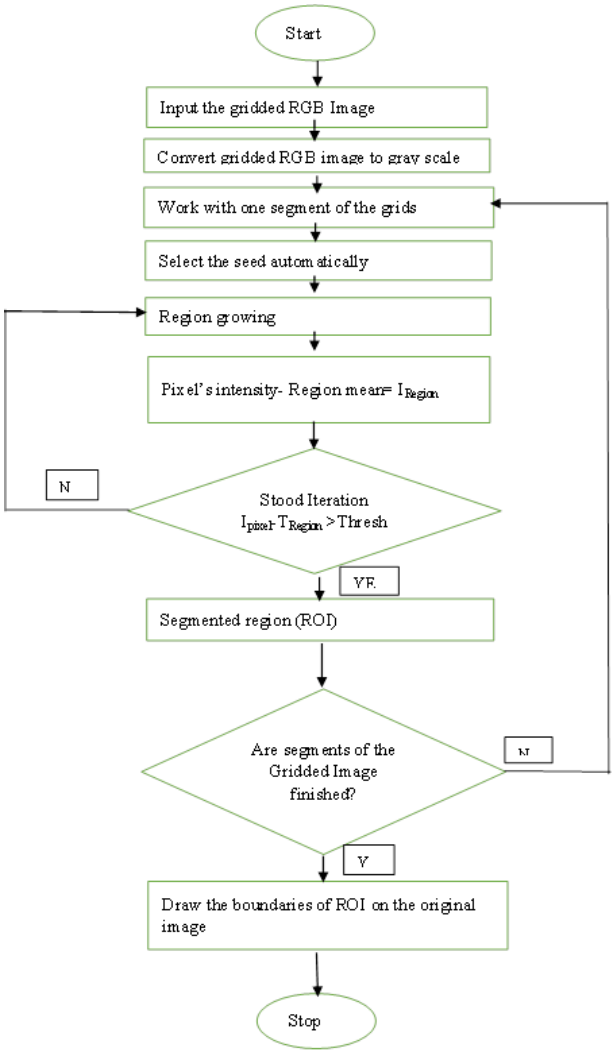

Fig.2. Flowchart of adaptive shape segmentation

IV. CONCLUSION

This publication elucidates a replacement methodology for complementary DNA microarray image analysis victimization circular Hough transforms. This new methodology reduces the interval of spots, addressing and localization and will increase the potency of spot segmentation. A plus of victimization SRG in microarray image segmentation of focal pixels and contextual pixels are often calculable.

REFERENCES

1. Fenstermacher D. Introduction to Bioinformatics, Journal of the American Society for Information Science and Technology, 56 (5), 440-446, (2005).
2. Abdul Ahad H. Biometrics-The Human Password, JITPS, 1 (1), 29–42, (2010).
3. Chee M., Yang R. and Hubbell E., Accessing genetic informationof DNA arrays, Science, 610–614, (1996).
4. Y. H. Yang, M. M. Buckley, S. Dudoit, and T. Speed, "Comparison of methods on cDNA microarray data," J. Compo Graph. Stat., pp.1 08-136, (2002).
5. Ye R., Wang T., Bedzyk L. , Croker K., Applications of DNA microarrays in microbial systems, Journal of Microbiological Methods, 47, 257–272, (2001).
6. N. Giannakeas, F. Kalatzis, M. G. Tsipouras, and D. I. Fotiadis, Spot addresses for microarray images, Computers methods and programs in biomedicine, 106 (1), 1–13, (2012).
7. J. D. and Thomas T.,Instinctive Gridding of DNA Microarray Images using Optimal Subimage, International Journal of Recent Trends in Engineering ,1 (4), (2009).
8. Rueda L. and Rezaeian I. A fully automatic gridding method for cDNA microarray images, BMC Bioinformatics, 12-113, (2011).
9. N. Giannakeas and D. I. Fotiadis, An automated method for clustering-based segmentation of cDNA microarray images, Computerized Medical Imaging 33, 40–49, (2009).
10. Karim R., Mahmud S., A review of image analysis techniques for gene spot identification in cDNA Microarray images, International Conference of Next Generation Information Technology, (2011).
11. A. Ahmed, M. Vials, NG. Iyer, C. Caldas, JD. Brenton, Microarray segmentation methods, Nucleic Acids Res. 32, 50-58, (2004).
12. Y. Chen, E.R. Dougherty, and M.L. Bittner, "Ratio-Based Decisions and the Quantitative Analysis of cDNA Microarray Images, Journal Of Biomedical Optics vol.2(4), pp.364–374, (1997).
13. M.J. Buckley, Spot User's Guide, CSIRO Mathematical and Information Sciences, Sydney, Australia, (2000).
14. K.I. Siddiqui, A. Hero, and M. Siddiqui, Mathematical Morphology applied to Spot Segmentation and Quantification of Gene Microarray Images, Asilomar conference on Signals and Systems, (2002).
15. D. Bozinov, and J. Rahnenfuhrer, Unsupervised technique for robust target separation through adaptive pixel clustering, Bioinform,, vol. 18, pp. 747–756, (2002).
16. E. Ergüt, Y. Yardimci, E. Mumcuoglu, O. Konu, Analysis of microarray images using FCM and K-means clustering algorithm, in Proc IJCI, pp.116-121, 2003.
17. W. Shuanhu and H. Yan, Microarray Image Handling Based on Grouping, The First Asia-Pacific bioinformatics conference on Bioinformatics -Australia, (19), 111-118, (2003).

Effect of tool Overhang length on turning operation using finite element model

B.Tulasiramarao, P. Ramreddy, K. Srinivas, A.Raveendra

Abstract— Turning accuracy and productivity rates become key determinants and both the accuracy and surface quality plays vital role. In this paper the cutting tool modeled with finet element model and for different tool overhanging lengths analytical modal has prepared. The modal and stiffness data of the tool are extracted from ANSYS software also the mode shapes were drawn. Tool overhang was selected as input and the influences of tool overhang on the stability of turning using finite element was obtained. The stability lobe diagrams corresponding to different tool overhangs different stiffness, tool frequencies and damping ratios were presented.

Keywords- ansys software, finite element model , tool over hang length and SLD.

I. INTRODUCTION

Turning is one of the most common machining operation in industry. In a turning process, work-piece rotates about its longitudinal axis on a machine tool called a lathe. The work-piece is supported by a chuck at one end and by a tailstock at the other end. A cutting tool mounted on the lathe is fed along the work-piece axis to remove material and produce the required shape. In a turning process, there are several parameters that define the cutting conditions. They are cutting speed, feed rate, and cutting depth. Cutting speed is the rate at which the uncut surface of the work-piece passes the cutting edge of the tool. Feed rate is the distance moved by the cutting tool in the longitudinal direction in each revolution. Cutting depth is the thickness of the metal removed in the radial direction by the cutting tool in the longitudinal direction in each revolution. Cutting depth is the thickness of the metal removed in the radial direction. The principal surface machined is concentric with the axis of the work-piece as shown in Fig 1.1.

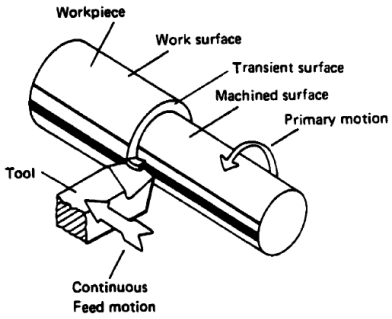

Figure 1.1: Cylindrical turning on a lathe

Revised Manuscript Received on December 22, 2018.

B.Tulasiramarao, Research Scholar JNTU, Hyderabad, telangana, India.

Dr. P. Ramreddy, Professor, Dept of Mech.Engg and Former Registar JNTU, Hyderabad, Telangana.

Dr. K. Srinivas, Professor, Dept of Mech. Engg, RVR& JC College of Engineering, Guntur, AP, India

Dr.A.Raveendra Assoc. Professor, Dept of Mech. Engg, MallaReddy Engineering College, Secunderabad, India.

Turning operations are most widely used to produce accurate size and shapes in the manufacturing industry. Applications can be found in the turning of dies and molds, jet engine parts made of heat resistant alloys, aircraft fuselage and wing panels, and biomedical parts.

1.1 stability lobe diagram

The stability lobe diagram depends on many parameters including tool stiffness, frequency, damping ratio, tool material and geometry, work piece material and its dynamics along with the cutting parameters. The cutting parameters such as speed, feed rate, depth of cut, tool length etc. has a considerable influence on the chatter behavior. Higher cutting speeds leads to less production time and reduction of tool life. Compared to the feed rate, depth of cut influence more on the stability behavior. Tool overhang is defined as the length by which the tool extends from the tool holder.

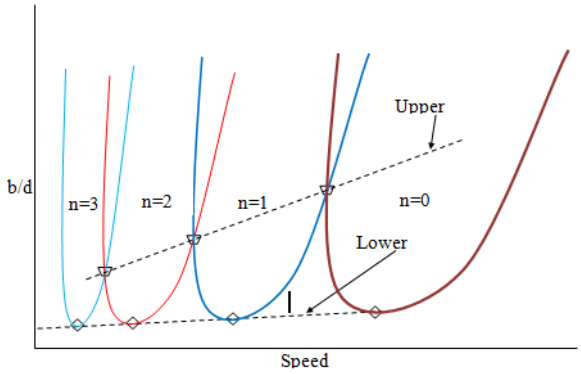

Fig.1.2 Stability lobe diagram

Length is a variable that can be used to tune the machining process. It acts as an absorber for the vibrations produced during machining. The stability lobe diagram has upper and lower boundaries which are also influenced by the tool wear during cutting operation.

II. EFFECTS OF TOOL OVERHANG LENGTH

Classical models available in literature, employed either the elastic tool or a rigid work-piece. These models may not express exactly the dynamic behavior of the system. The dynamic operation of the cutting depends on the geometrical and mechanical characteristics of the tool and work-piece. This section describes the results of tool overhang effect on the output features such as cutting forces and surface roughness. Experiments are carried out on engine lathe to study the effect of tool overhang on stability. Results of finite element model of the system are also shown.

III. ANALYTICAL RESULTS

The modal and stiffness data of the tool are extracted separately from ANSYS software. Initially the solid model of the tool is developed without loosing all details of the geometry, and it is meshed with solid elements. Natural frequencies, damping ratios and stiffness values are obtained first. The solid model of the tool (employed in the experiments) is generated in Autodesk-Inventor. Figure 3.1 shows the dimensions of the tools employed in the present task.

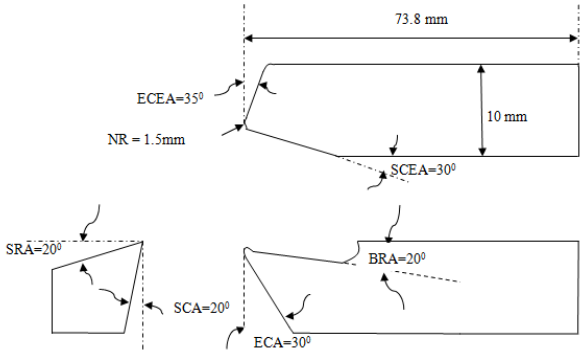

Fig. 3.1 Signature of the present cutting tool employed in solid modeling

(ECEA: End cutting edge angle, SRA: Side rake angle, BRA: Back rake angle, ECA: End clearance angle, SCA: Side clearance angle, SCEA: Side cutting edge angle, NR: Nose radius)

This is imported into ANSYS(version:8) and solid tetrahedral elements with 10 nodes (SOLID 92) and three degrees of freedom (Ux, Uy, Uz) are used to mesh the solid geometry with the following material properties: Young's modulus E=200 GPa,

Poisson's ratio: 0.28,

Density: 8150 kg/m3.

Figure 3.2 shows the meshed geometry of the cutting tool.

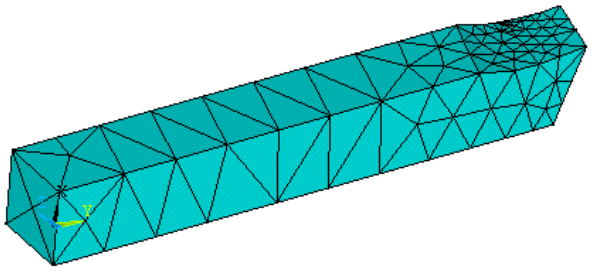

Fig.3.2 Finite element model of the present cutting tool

The amount of tool overhang is specified as the distance from tool tip to the nodal area over which the tool holder is mounted. The tool holder boundary is simulated with fixed conditions in all the directions. Thus in order to vary the overhang length, the positions of the nodes under arrest are to be changed. The stiffness of the tool is obtained from static analysis; natural frequencies are obtained from modal analysis while the damping ratios are predicted from harmonic response curves. With several values of tool overhang the modal and stiffness data of the cutting tool obtained is shown in table 3.1.

Table 3.1 Modal and stiffness data of tool

Tool Overhang (mm)	Stiffness(N/m)			Natural Frequency(Hz)	Damping ratio		
	K_x	K_y	K_z	ω_y	ζ_x	ζ_y	ζ_z
70	9330	3301	717	112	0.0295	0.027	0.033
63	11032	3412	779	122	0.0416	0.052	0.045
55	14434	4424	1077	138	0.0425	0.043	0.05
47	24390	7310	1751	165	0.0158	0.008	0.016
39	51228	13390	3156	199	0.0428	0.042	0.026
30	54226	15680	3620	204	0.0222	0.019	0.022

The work-piece is modeled as a finite element beam with 4 elements and total 5 nodes. The following dimensions of the work-piece are considered:

Length=480mm,

Diameter=50mm,

Young's modulus: 210 GPa,

Density=7860kg/m^3,

Damping ratio ζw=0.25,

Rotational stiffness of the chuck Kt =104 Nm/rad.

The tool interaction dynamic forces Fx act at a specified node where the tool is in contact with the work-piece. The assembled mass and stiffness matrices are obtained from the element matrices described below.

$$k = \frac{EI}{\lambda^3}\begin{bmatrix} 12 & 6\lambda & -12 & 6\lambda \\ 6\lambda & 4\lambda^2 & -6\lambda & 2\lambda^2 \\ -12 & -6\lambda & 12 & -6\lambda \\ 6\lambda & 2\lambda^2 & -6\lambda & 4\lambda^2 \end{bmatrix}, \quad m = \frac{\rho A\lambda}{420}\begin{bmatrix} 156 & 22\lambda & 54 & -13\lambda \\ 22\lambda & 4\lambda^2 & 13\lambda & -3\lambda^2 \\ 54 & 13\lambda & 156 & -22\lambda \\ -13\lambda & -3\lambda^2 & -22\lambda & 4\lambda^2 \end{bmatrix}$$

The first three mode shapes of tailstock supported work-piece are shown in Figure 2.3. The fundamental frequency of work-piece can be seen as 2588 rad/sec which is much higher than the equivalent work-piece without tailstock support.

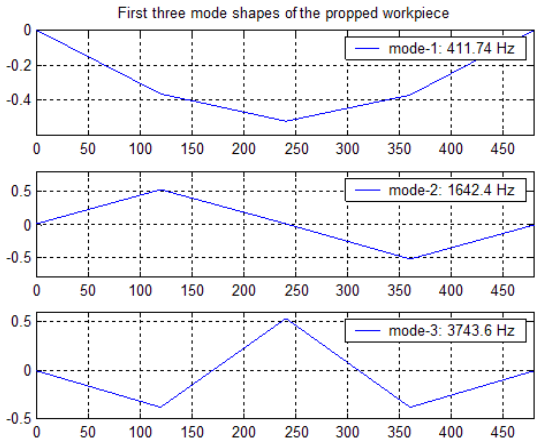

Fig.3.3 First three modes of propped cantilever work-piece

Published By:
Blue Eyes Intelligence Engineering
& Sciences Publication

23YJThe first normalized modal vector is

$\{\phi^{(1)}\}$ = [0 -3.3654 -0.3665 -2.416 -0.5205 -0.0132 -0.3688 2.4098 0 3.4162]^T

This is used to un-couple the differential equations and permits all the 10 equations to express as a single second order differential equation in terms of one modal co-ordinate p1.

The equation so obtained when the cutting tool is in contact with the work-piece at the node-4 can be written as

The stability lobe diagrams corresponding to different tool overhangs (different stiffness, tool frequencies and damping ratios) are presented in Figure 4.20 (a)-(c). It is seen that tool overhang has much influence on stability of cutting.

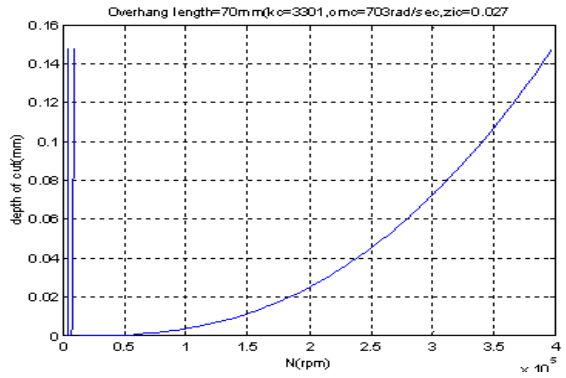

(a)

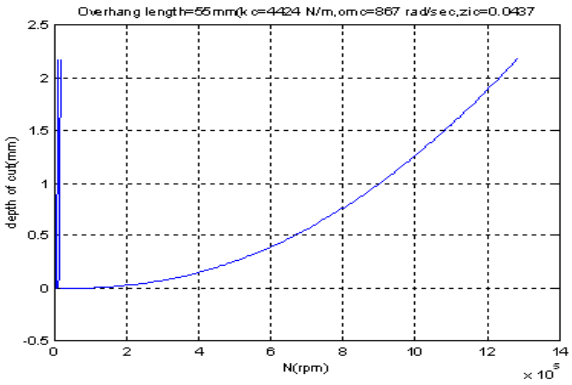

(b)

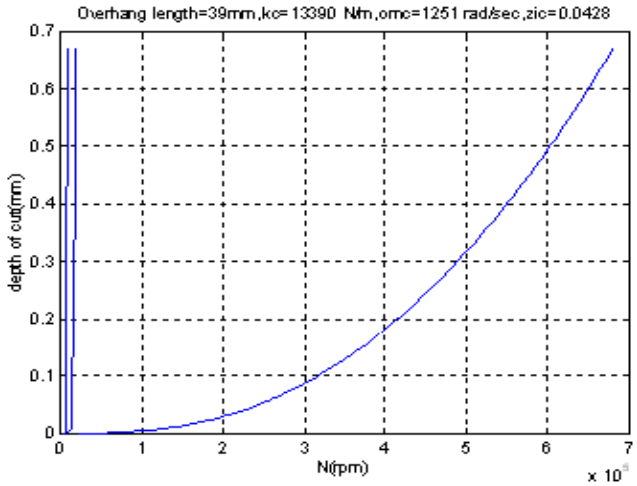

(c)

Fig. 3.4 Stability lobe diagrams at different overhang lengths.

In the diagrams, the rightmost lobe (n=0) at higher speeds occupies wide area and dominates the rest. It is observed that the increase in tool overhang first improves the stable depths of cut, then with further increase, again the critical depths reduces. Thus there is an optimum overhang between the extreme cases under consideration.

4. CONCLUSION

In this experimental work, stability analysis in turning process has been presented. An attempt also made to establish the influences of tool overhang on the stability of turning using finite element modeling. Single degree of freedom model of cutting tool was prepared from the first mode dynamics of a three dimensional finite element model of orthogonal cutting tool. Likewise, the work piece dynamics is arrived with finite element beam model. The tool-work interaction forces were expressed in terms of current and previous deformations of tool and work. The stability lobe diagrams with different tool overhang lengths (stiffness) were plotted.

REFERENCES

1. D.B. Welboum and J.D. Smith, “Machine-tool Dynamics: An introduction”, Cambridge, 1970.
2. J.Cook and H. Nathan, “Self-Excited Vibrations in Metal Cutting,” ASME Transactions, Journal of Engineering for industry, Vol. 81, pp. 183- 186,1979.
3. S.F.Bao, W.G. Zhang, S.Y. Yu, S.M. Qiao, and F.L.Yang, “A New Approach to the Early Prediction of Turning Chatter”, Journal of Vibration and Acoustics, Vol. 116, pp. 485- 488, 1994.
4. Y.S.Tarng, H.T.Young and B.Y.Lee, “An analytical model of chatter vibration in metal cutting”, International Journal of Machine Tools and Manufacture, vol.34, pp.183-197, 1994.
5. Iturrospe , V. Atxa, and J.M. Abete, “State-space analysis of mode-coupling in orthogonal metal cutting under wave regeneration”, International Journal of Machine Tools & manufacture, vol. 47, pp.1583–1592, 2007.
6. I.E.Minis, E.B. Magrab, and I.O.Pandelidis, “Improved Methods for the Prediction of Chatter in Turning, Part3: A Generalized Linear Theory”, Trans. ASME Journal of Engineering for Industry, Vol. 112, pp. 28-35, 1990.
7. D.W.Liu and C.R. Liu, “An Analytical Model of Cutting Dynamics. Part 1: Model Building”, Trans. ASME, Journal of Engineering for Industry, Vol. 107, pp. 107- 111, 1995.
8. M.N.Hamdon and A.E.Bayoumi, “Analysis for regenerative machine tool chatter”, Journal of Manufacturing Science and Engineering, vol. 11, pp. 345-349,1997
9. M.N.Hamdon and A.E.Bayoumi, “An approach to study the effects of tool geometry on the primary chatter vibration in orthogonal cutting”, Journal of Sound and Vibration, vol. 128(3) pp. 451-469, 1999.
10. J.R.Pratt and A.H. Nayfeh, “Design and Modeling for Chatter Control”, Nonlinear Dynamics, Vol. 19, pp. 49-69, 1999.

Modelling, Analysis and Fabrication of Bush Bearing on Plummer Block by Using Carbon Epoxy Material

A Sarath Kumar, B. Hari Prasad

Abstract--- Presently, the project deals with Plummer bush. The main function of Plummer bush is to give an additional strength for the load bearing capacity of Plummer block which are existing through rotational shaft. Basically they are manufactured from high strength cast iron as standard and also bronze alloys, but the materials such as cast steel are available. Generally, in Plummer blocks the bush plays a major role to increase the bearing life, and to bear the heavy loads. Design by using the CATIAV5 software and structural analysis using ANSYS for both existing and new taken materials after getting the result comparing the each other to finalizing which better suitable for plumber bush to fabricate. And also to improve some properties by comparing analytical results through applying loads on bush material which is made by using carbon epoxy comparing with bronze alloys.

Key words: Plummer block, Carbon Epoxy, ANSYS, experimental model.

INTRODUCTION:

Plummer piece or housed bearing unit is platform usually made of metals and used to offer help for a pivoting shaft with the aid of good direction and different adornments. Lodging material for a cushion square as mentioned earlier is normally made of solid metal or cast steel.

Plummer pieces. A get together comprising of circular roller course or self-adjusting metal ball and a heading lodging with a fixing gadget. The bearing lodging is by and large made of cast press, however can likewise be spheroid graphite cast press (Ductile cast iron) or cast steel contingent upon the application.

A Plummer square typically alludes to billet with an included intimidating to grinding bearing. A square Plummer alludes to any of the mounted bearing wherein the corresponding mounted shaft is in a parallel plane to the respective mounting surface, and opposite to the middle line of axis of the mounting gaps, as stood out from different kinds of rib pieces or small spine units. A Plummer square may also contain a holding on for one of a few kinds of moving machinery components, including balls, barrel shaped rollers, circular rollers, decreased rollers, or metallic or engineered bushing.

The principal use of the two sorts of the component is the same, which is to mount a course steadily vesting its external ring to be stationary while permitting revolutionary motion of the inward ring. The lodging is darted to a machine component establishment through the gaps in the base of the Plummer. Bearing lodgings might either be a part of a composed structure or a strong write which are sturdy. Split write lodgings are typically two-piece lodgings where the top and base might be separated when required, while others might be single-piece lodgings fixed steadily. Variety of fixing game plans might be given along with the block to keep it clean and prevent different contaminants from entering the lodging. Consequently the lodging also gives a spotless clean situation to the ecologically delicate and sturdy bearing to pivot free from contaminants while simultaneously holding lubricant oil, either oil or oil, subsequently expanding its execution and obligation cycle deliberately.

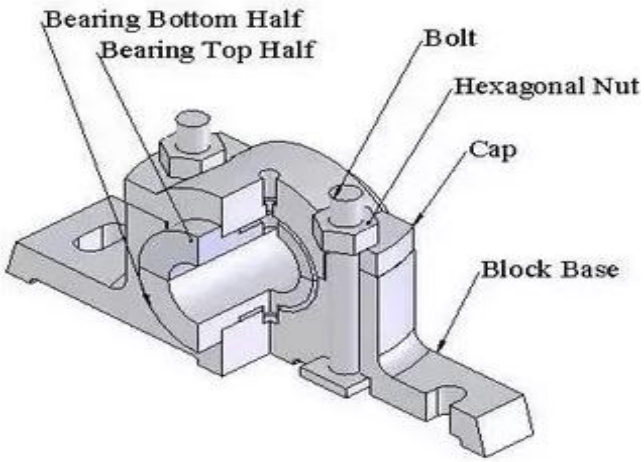

Figure 1: Breakout section view of bush

PLUMMER BLOCKS WORKING:

Plummer square bearing comes as an independent gathering, accessible in extensive variety of sizes.

We should simply guarantee accessibility of a level and firm stage where two openings can be bored (which would be utilized to jolt the Plummer obstruct down).

After establishment, all it needs is occasional lubing. Bearing inside Plummer piece works fine in any sort of air as it is securely tucked away inside a packaging.

After disappointment, we essentially need to purchase another OEM gathering which is superbly exchangeable without worrying about resistances (as they are as of now dealt with). Moreover, introducing a Plummer square get together is moderately less demanding and blunder confirmation.

Revised Manuscript Received on December 22, 2018.

A Sarath Kumar, Department of Mechanical Engineering, Malla Reddy Engineering College, Secunderabad, Telangana, India (Email: sarath.kumar1437@gmail.com)

B. Hari Prasad Department of Mechanical Engineering, Malla Reddy Engineering College, Secunderabad, Telangana, India

Accordingly, in long haul, Plummer piece course give gigantic coat benefits where downtime straightforwardly means creation misfortune. Furthermore, they make lives of individuals working in perilous surroundings somewhat less demanding.

OBJECTIVE OF THE WORK:

- Introducing the new material to improving the strength and bearing the loads.
- Experimental model design and analysis for taken material suitable or not.
- Using machineries to fabrication of proto type model of Plummer block.

LITERATURE REVIEW:

Review on mechanical properties of carbon epoxy of the best material selection by *Vishal Narula, Vipul Jain, Mohd Fazil Khan, Shailja Bahuguna (ISSN NO-2456-0472).-volume-2 .(feb-2017):-*

According to this journal the author improved the mechanical properties by taking rocket shell as an object and carbon epoxy as an material, it gives an better results by comparing with the aluminum alloy.

Y.X. Zhoul, P.X.Wu, Z-YCheng, J. Ingram, S.Jeelani. Improvement in Electrical, Thermal and Mechanical Properties Of Epoxy By Filling Carbon Nanotube. Express Polymer Letters *Vol.2, No.1 (2008) 40–48*:-

Related to this journal the author improved the several properties of epoxy by using ULG (ultra-sonic generator)process by adding carbon nano-tubes by applying frequency of amplitudes.

N. Senthil kumar, K. Kalaichelvan and K. Elangovan. Mechanical Behavior Of Aluminum Particulate Epoxy Composite –Experimental Study And Numerical Simulation International Journal Of Mechanical And Materials Engineering *(IJMME), Vol. 7 (2012), No. 3, 214-221:-*

According to this journal, author used the carbon epoxy as a material rod in the middle of the concrete beam and finally it gives an additional strength of that concrete beam while comparing with the existing material (Steel).

Norazman Mohammad Noor, Mohd Hanif Ahmad Boestamam, Mohammed Alias Yusuf. Carbon Fiber Reinforced Polymer (CFRP) As Reinforcement For Concrete Beam International Journal Of Emerging Technology And Advanced Engineering, *Volume 3, Issue 2, February 2013)*:-

By this journal the application of concrete beam, using of carbon epoxy gives an improved bending moment while author comparing with the existing material.

Sheikh Naunehal Ahamed, Jadhav Vijay Kumar, Mohammed Mushraffuddin, Parimi Shrawini. Modeling and Analysis of Rocket Outer Shell. International Journal Of Scientific & Technology Research *Volume 3, Issue 4, April 2014 ISSN 2277-8616 Ijstr©2014*:-

Related to this journal the author analyze the bending moment of rocket outer shell and improved the with stand capacity by using carbon epoxy composite material.

Parkhe Ravindra, Mhaske Raman, Belkar Sanjay. Modeling And Analysis Of Carbon Fiber Epoxy Based Leaf Spring Under The Static Load Condition By Using FEA, International Journal Of Emerging Science And Engineering *(Ijese) ISSN: 2319–6378, Volume-2, Issue-4, February 2014*:-

Leaf spring is plays an important role in heavy duty vehicles to with stand heavy load and the author used this carbon epoxy material, to give excellent bearing capacity for the huge application loads and the author compared the results with the existing material and it gives an better results.

MODELING:

CATIA is a modeling and design software that offers a variety of indifferent solution to shape the design, styling of surfaces, surfacing workflow and visualization to create, modify, and validate complex innovative shapes from industrial design to Class-A surfacing techniques with the ICEM surfacing technologies. CATIA supports multiple stages of product design from a small component to a huge machine part whether started from scratch or from 2D sketches. CATIA can also read and produce STEP format files for reverse engineering and surface reuse options.

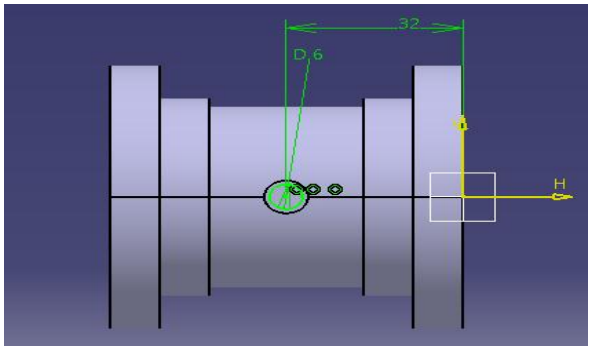

Figure 2: Orthogonal view of model

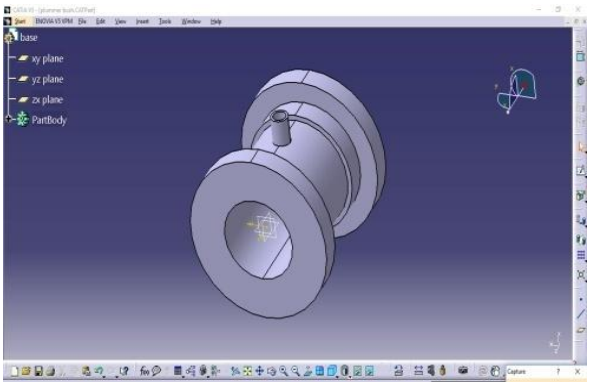

Figure 3: Isometric view of model

ANSYS:

ANSYS is general-purpose finite element analysis software, which is being used globally and enables engineers located worldwide to perform the following tasks ingeniously:

Build virtual software models or transfer CAD models of structures, products, components or systems.

Apply operating loads or other design performance parameters under variety of industrial and physical conditions.

Study the physical responses to which the machine component or building structures exposed are such as stress levels at different points, temperatures distributions at different locations and time period or the impact of electromagnetic fields.

4. Optimize a design early during the initial development process to reduce production costs and time.

5. A typical ANSYS analysis software has three distinct steps which are followed by default.

6. Pre Processor (Build the Model).

BRONZE ALLOY CA104

Density	Young's Modulus MPa	Poisson's Ratio	Bulk Modulus MPa	Shear Modulus MPa
7.58e-009 kg mm^-3	1.15e+005	0.3	95833	44231

Table 1: Material Data Input

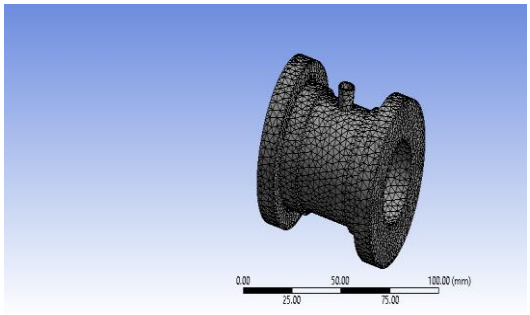

Figure 4: Meshing of model

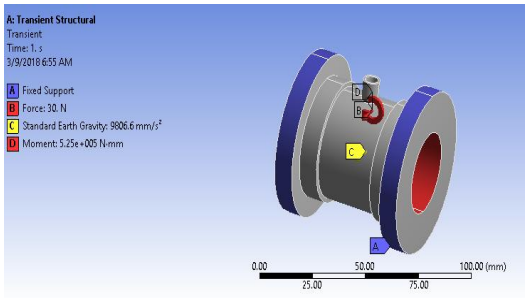

Figure 5: Applying Force and Moment

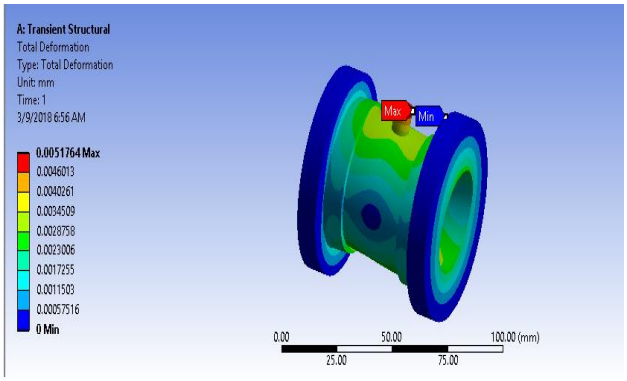

Figure 6: Total Deformation

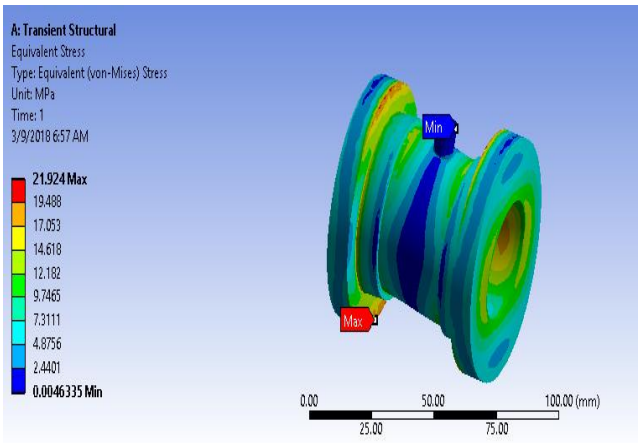

Figure 7: Equivalent stress

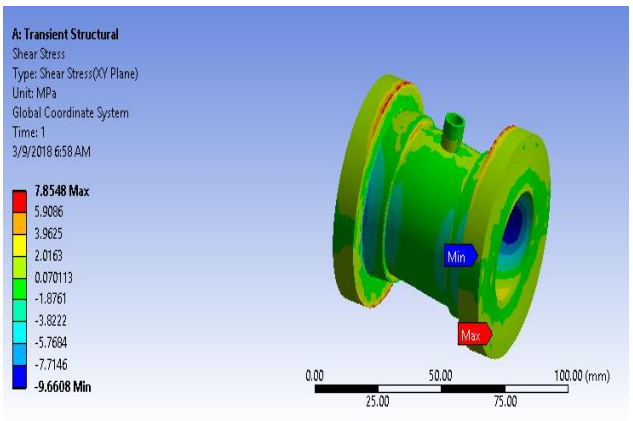

Figure 8: Shear stress

Object Name	Total Deformation	Directional Deformation	Equivalent Elastic Strain	Equivalent Stress	Shear Stress
Minimum	0. mm	-3.0102e-003mm	7.3402e-008 mm/mm	4.6335e-003 MPa	-9.6608MPa
Maximum	5.1764e-mm	5.073e-003 mm	1.9064e-004 mm/mm	21.924 MPa	7.8548MPa

Table 2: Results Of bronze Alloy

CARBON FIBER

Material data input:

Density	Young's Modulus MPa	Poisson's Ratio	Bulk Modulus MPa	Shear Modulus MPa
1.6e-018 kg mm^-3	7.e+005	0.1	2.9167e+005	3.1818e+005

Table 3: Material Data Input

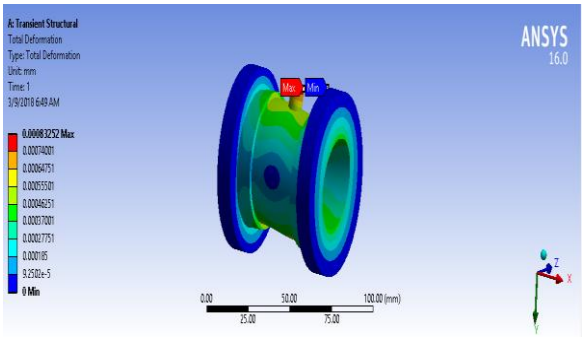

Figure 9: Total deformation

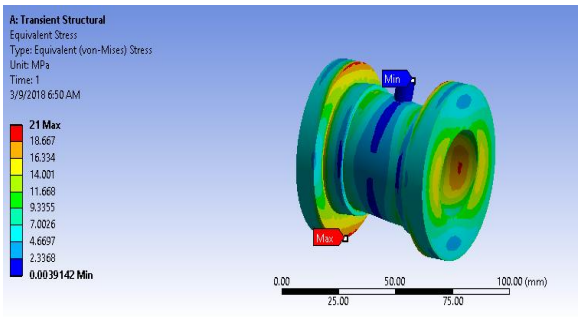

Figure 10: Equivalent Stress

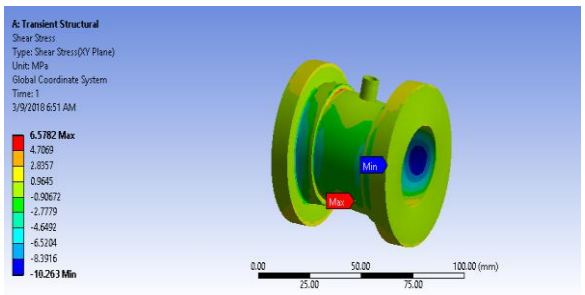

Figure 11: Shear Stress

FABRICATION PROCESS:

- **Casting Process**
- **Machining Process**
- **Facing**
- **Turning**
- **Drilling**
- **Boring**
- **Brazing**

CASTING PROCESS:-

Casting is a process in which production of replicate shapes with the help of mould cavities related to required dimensions by pouring of molten metal into the casting cavity. In some times cores and core prints will be use while the required part included internal shapes and also for the difficult external boundary shapes of the component.

Before the process of casting we need to apply heat treatment process (or) melting of required material at certain temperature. Amount of degrees is mainly depending upon the selected material and its properties.

And according to my project, heat treatment was occurs during the temperature of 1150 to 1200 degree centigrade, make an cylindrical rod with the external diameter of 70, I don't used an core prints in casting process due to un present of critical internal contours. And I maintained a constant pouring pressure to the cavity from the funnel through pure basin.

Figure 12: Pouring of molten metal to the cavity

Figure 13: finished casting component

MACHINING PROCESS:-

According to my component it includes the following operations to get a required shape. They are:-

FACING:-

Facing operation does the surface has smooth (or) flat of un even and rough surface of a component by holding the work piece in the 3 jaw chuck of lathe head and the amount of removal material to produce surface smooth depends upon the adjustment of cutting tool which are placed on tool bed of lathe machine manually(or)adjustment will be done automatically on CNC machines through program setup.

Related to my project I used single point cutting tool to get a smooth surface through lathe machine. Finally I got required length of a component after this facing operation.

Object Name	Total Deformation	Directional Deformation	Equivalent Elastic Strain	Equivalent Stress	Shear Stress
Minimum	0. mm	-4.7793e-004 mm	8.4374e-009 mm/mm	3.9142e-003 MPa	-10.263 MPa
Maximum	8.3252e-004 mm	8.1549e-004 mm	3.e-005 mm/mm	21. MPa	6.5782 MPa

Table 3: Results of Carbon Epoxy

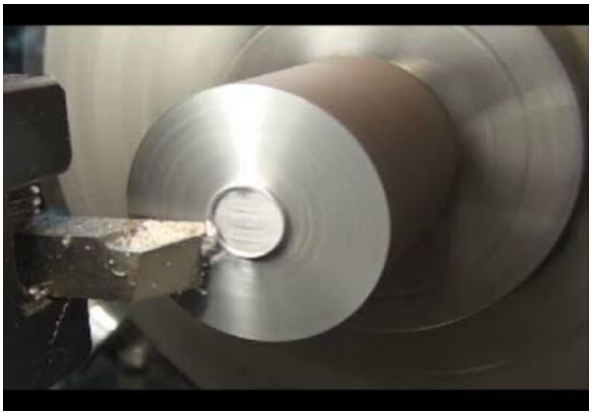

Figure 14: Facing operation

TURNING:-

Turning is one of the basic machining processes which involve production of parts which are round in shape by a single point machine tool on machines called lathes. The tool is called cutting tool and is fed either linearly in the direction parallel or perpendicular to the axis of rotation of the work piece/job, or along a specified path to produce cylindrical shapes of specified dimensions or complex rotational shapes respectively. The primary motion of cutting in a turning process is the rotation of the work piece/job, and the secondary motion of cutting is the feed motion given to the tool .

Turning of cylindrical surfaces:-

The lathe is a machine used to reduce the diameter of any given cylindrical part to a desired dimension. The resulting machined surface is also cylindrical with the specified dimension.

Figure 15: Turning operation

DRILLING:-

The process in which creation of hole feature in any component. Before that mark a center hole and aligning that center mark to the drill bit cutting tool to create a complete hole feature. This process is applied only small holes but if you want to enlarge that particular hole use the process of boring and broaching. According to my project hole was created with the diameter of 12. And finally to smooth the internal cylindrical surface of the hole used the process of broaching.

Figure 16: Drilling operation

BORING:-

It is the process of enlarging the hole feature of previous made hole with the drilling operation. And I was produced 32 diameter of hole by this process.

Figure 17:- Boring operation

BRAZING:-

Brazing is a metal-joining process where in two or more metal items are joined together by using a filler metal which is melted and spread across the joint. The filler metal has a lower melting point than the adjoining metal and hence solidifies between them immediately thereby joining them together.

Figure 18: Finished Component

CONCLUSION:

By observing above results carbon fiber gives low weight and low deformation value 8.3252e-004 mm When comparing to the Bronze Alloy CA104 that indicates carbon fiber have more strength due to less deformation. And also bronze Alloy CA 104 gives more Equivalent Stress 21.924 MPa both materials are within material yield strength so no failures are in both materials.

BIBLIOGRAPHY:

1. S. R. Algule, D. P. Hujare, "Experimental Study of Unbalance in Shaft Rotor System Using Vibration Signature Analysis" Volume 3, Issue 4, April 2015, PP 124-130 ISSN 2349-4395 (Print) & ISSN 2349- 4440.
2. Y.Y. Thorat, Satish S. Kadam, ""Design and Development of Test Setup for Vibration Analysis"
3. Jaswinder Singh, "Investigation Of Shaft Rotor System Using Vibration Monitoring Technique for Fault Detection, Diagnosis and Analysis" Vol. 2, No. 2, February-March 2013
4. Dr. S. J. Lacey, "An Overview of Bearing Vibration Analysis" | Nov/Dec 2008 ME | maintenance & asset management vol 23
5. V. Hariharan and PSS. Srinivasan "Vibration analysis of misaligned shaft ball bearing system"
6. Colin Sanders "Vibration Analysis and Associated Techniques in Condition Monitoring" Jan/Feb 2011 | ME | maintenance & asset management vol 26 no 1.
7. Plummer block bearing units-by town send bearings.
8. Plummer block and accessories-by NSK industries.
9. Engineering materials-by R.K Agarwal.

Utilization of Solid Waste to Produce Eco-Friendly Bricks

B.Dhanalaxmi, K.N Sujatha, E.Rakesh Reddy

Abstract– urbanization lead to a vast generation of solid waste and discharge of these waste materials became a major problem. Dumping and landfilling of solid waste leads to environmental degradation i.e ground water contamination through leaching, which results in soil pollution and also impact on human health. In recent years, the utilization of solid waste as become more potential to recycle the valuable material and decrease the volume of solid waste, other pollutants and dumping cost. This paper is concern to reuse and recycle the available solid waste generated from paint industry. to find a socio-economic, eco-friendly solution, waste trash can be recycled for the preparation of bricks, which sustain a cleaner environment. The increased quest for sustainable and eco-friendly materials in civil construction works. It is useful to provide sustainable and potential solution in the construction field.

Keywords: eco-friendly products, industrialization, solid waste, recycle.

I. INTRODUCTION

The conventional materials which are predominantly used in construction process, such as concrete type bricks, hollow type blocks, solid blocks, pavement type blocks and floor tiles are generated from the already existing naturally available resources. This results in defragmentation of the environment due to vast exploration and which lead to depletion of naturally existing resources. Moreover, different kinds of noxious substances such as high level concentration of carbon monoxide, oxides of sulphur and nitrogen, and suspended particulates are released surplus into the open atmosphere during the operation phase and manufacturing of materials. These emissions creates toxic impact on environment and disturb the functioning phrases of environmental air, natural water resource, extensive soil, large flora species, fauna species and aquatic life, and it reflects on human health along with their living standard. Therefore, various concentrations in the environment may lead to degradation of prevailing atmosphere. To Improve sustainability and environmental conservation and has gained significance in our society in recent years. Due to more improvement in using sustainable, low cost, eco-friendly, lightweight and corpus construction materials in civil works has been emphasized to investigate as the growing needs, to improve the quality of environment and to maintain the materials requirements as per the standard.

Our world is facing severe crisis of over population. In recent year's different kinds of by-products, generated from various sources such as commercial, household, industries, hospitals, public places, etc. accumulated in very large quantities. Due to which pollution explosion is generated. To rectify this problem of environmental degradation and discharge of large quantities of solid waste in regular manner. The present work discuss about the new innovation preparing bricks from solid waste and tested against fire and other strength properties. This research paper has been shaped with an idea "utilization of waste to worth" in construction field for casting bricks using various kinds of waste materials.

II. SIGNIFICANCE:

Large amount of waste materials are produced around the globe due to anthropogenic metabolism in both developed and developing countries by industrialization rise in living standard and urbanization can be minimized to a greater extent. According to the World Bank statistics proposed globally on solid waste management sector, the global cities is presently producing about 1.3 billion tonnes of solid waste matter every year and it keeps recurring. This volume is expected to reach the peaks nearly to 2.2 billion tones by the year 2025 and waste trash accumulation rate is assumed to twice over the next two decades. One of the environmental impacts which can effect global due to generation of solid waste is the continuous emission of methane gas which is considered as a powerful and destructing greenhouse gas (GHG), and its impact on the environment can be felt within a minimum period of time. Flooding of land, air pollution and other inevitable health hazards are encountered. The amounts of waste material generated from the various productions and continuously increase to satisfy needs of the increasing living standard of population. On priority, the environmental laws and regulations in recent decades which have become more restrictive. Therefore, alternative methods recommended to choose for better management to utilize these wastes can be design and restored. Eco- friendly waste recycling has proved one of the best management to reduce and reuse the waste in the research field for decades. The management of waste reduces the negative impacts of their disposal. Many experiments have been performed to incorporate waste materials in the production of solid bricks including limestone dust particles, wood sawdust particles, rubber,

Revised Manuscript Received on December 22, 2018.

B.Dhanalaxmi, Assistant Professor, MREC(A), Maisammaguda,Telangana, India

K.N Sujatha, Assistant Professor, MREC(A), Maisammaguda, Telangan, India

E.Rakesh Reddy, Assistant Professor, MREC(A), Maisammaguda, Telangana, India

processed waste tea particles, fly ash, sludge and polystyrenes.

III. MATERIALS AND METHODOLGY:

Unfired bricks are manufactured by using following material. 1. Solid Paint waste 2. Cement 3. Fly ash 4. Robo sand (quarry dust) 5.water 6. Bricks

1. Paint Remnants: Toxic but unwanted waste, this gathered hydrolysed paint motored and thoroughly combined with water and some decalcifying chemicals, known as both additives, are added is commonly referred as paint sludge or paint remnants. This viscous slurry can be classified as a hazardous waste therefore if this waste is disposed randomly on the surface. It might lead to degradation of soil fertility, and results in generation of leachate by which ground water gets containminated. Hence it is toxic to agricultural land, and it may even cause damage to the flora and fauna of that ecosystem, wherever this waste discharges. To recommend remedy for the manufacturer of the _paint sludge'unsatisfactory to the regulated principles of environmental law, which does not allow the existence of the paint sludge'within the chambers of the industrial unit, where it is manufactured, Maharani Paint industry management has developed a process through which industrial _paint sludge'could be recycled back to a product which is highly useful, and can be consumed without any hassle by the industry.

Fig.1 solid paint waste

2. Cement: Cement is a globally used binding material, a matter utilized for construction which helps in setting, hardens and combines with other supplementary materials, binding them together strongly. Cement is commonly used in binding sand and gravel (aggregate) together. Cement is combining with fine aggregate particles to prepare the traditional mortar for civil works, or with sea or river sand particles and gravel aggregates to prepare concrete mix. Cement grades manufactured for construction works are generally not organic in nature; usually lime or calcium silicate based compound, which can be classified as hydraulic and non-hydraulic, based on the adherences of the cement for setting with the presence of water level.

Fig.2 cement

Table no.1 physical characteristics of cement

Sl No.	Details	outcomes	As per Is 12269-1987
1	Normal Consistency (%)	32	
2	Specific Gravity	3.15	
3	Setting Time (in Minutes)		
	Initial Setting Time	122	Not less than 30
	Final Setting time	406	<600
4	Fineness by Air Blaine Apparatus (m2/kg)	256	>225

3. Robo sand: It is sand produced in the stone quarries. It is perfect replacement for the river sand utilization in the constructions. Robo sand is prepared by grinded or crushed granite collected from the good quarries crushed using higher technology 3-stage vertical shaft impact machinery. It is producing the largest form of concrete in PCC and RCC grades. The main advantages of Robo sand are cubical dimensions, proper gradation and lack of impurities. Advantages of Robo sand are cheaper, no impurities, sophisticated building strength and their physical properties, green sand.

4. Fly Ash: Fly ash, also called as "pulverized fuel as". It is the by-product of coal combustion and that contains particulates. Coal collected by the electrostatic separators or by mechanical methods from the fuel of gases of thermal power plants. Here pulverization means the coal powder. Depending on the source and composition of the coal used in combustion, the constituents of fly ash, which contain equitable mixture of silicondioxide (SiO_2)aluminum oxide (Al_2O_3) and calcium oxide (CaO), and other mineral compounds present in coal-bearing rock strata.

Thus brick contains fly ash, cement and fine aggregate. The cement varies from 15 to 25% in the fly ash and proportionate quantity of fine aggregate. In preparation of brick the use of fly ash gives enough strength and decreases the water

Fig.3 Fly ash content.

The strength of bricks prepared from fly ash is high comparatively to conventional bricks.

5. Water: Portable water was used for both mixing and curing operations of specimens. Water utilized for these operations should be free from suspended and other

Published By:
Blue Eyes Intelligence Engineering
& Sciences Publication

impurities. pH value of water should be maintained within standard limits as prescribed by IS: 456-2000 i.e. either it is less than 6 or more than 8. Water plays a vital role and it is important ingredient of concrete mixture. Thus it actively participates in the chemical reactions within the mixture. Since it combines to form a strength enhancing cement gel, therefore the quantity and quality of water are an important parameters which are to be studied carefully.

Physical properties of water:

pH : 7

Density : 1 gm/cc

6. Bricks: A brick is constructional building block utilized to make walls, pavements and other elements of masonry construction. Earlier, the term "Brick" referred to a unit composed of clay, but in recent decades it is denote as rectangular unit laid in mortar. A brick constitutes clay-bearing soil, sand, and lime, or concrete materials. Bricks are classified, based on its classes, types, materials, and sizes which varying along with region and time period, and these are produced in large quantities. Two basic categories of bricks are fired and non-fired bricks.

A popular invent has been introduced by researcher to incorporate various wastes into fired clay bricks production to assist the generation of normal and lightweight bricks. The use of various wastes in co-operation in clay bricks production generally has positive effects on their properties, even though they observed the decrease in performance in certain aspects.

Brick are the most arduous masonry entities. It has its widest range of products, with its unlimited assortment of varying patterns, textures and colors customised to the needs. In 1996, an industry has generated 300 million bricks in a place called Victoria, which were about 55% of the potential production at that instance. Brick has good durability and resistance which has developed and strengthen with time and to withstand to high competitive, technical and economical, with other systems of construction sector.

The major input for bricks is clay soil besides clayey soils, soft slate particles and shale, which are usually obtained from open pits with the degradation of drainage, and wildlife habitat. Clays used for brick production and their compositions are usually reliant on the vicinity from which the soil has been excavated. Different appropriate proportions of clays are constituted with silica, alumina, lime, iron, manganese, saw dust, sand, sulphur and phosphates. Bricks are usually durable, fire resistant, and require the least maintenance. The properties of bricks that evaluates quality of building blocks with their strength, fire resistance, durability, exquisiteness and adequate bond and mix proportions with mortar material.

Mix proportion of Bricks:

Bricks making in three proportions

Table no.2 Different proportions of materials

S.NO	Cement	Industrial waste	Fly ash	Quarry sand
S-1	30%	20%	20%	30%
S-2	30%	25%	20%	25%
S-3	30%	30%	20%	20%

There are four different operations are involved in the process of manufacturing of bricks:

Batching
Mixing
Moulding
Drying

Batching:

The ingredients are accurate and precise measurement of materials for making cement is known as batching. Weigh batching is the accurate methodology used globally of measuring the materials. For significant mix is manufacturing of bricks.

Fig 4: Batching

Mixing:

The materials are paint solid waste, Robo sand, fly ash and cement these are mixed and to get a uniform color then water is added to the mix it is get good uniform color. Work at site with use of brick making. Mixing is most important in manufacturing of bricks

Fig 5: Mixing

Moulding:The mould is placed at the ground and standard size of brick mould is 19*9*9cm. Apply the oil to the mould and place the mortar in the mould and compacting the mortar in the mould. After 5 minutes mould is removed from the bricks, and then placed in the sunlight. Within two days bricks will be harder.

Fig 6: Moulding

Drying: Dehydration of bricks at lower temperature are carried out for sufficient strength. To avoid crack or crumble while holding, carrying and any in constructional phrase they must preserve and sustain the sufficient strength and shape while the conveyance and loading operations during construction. Therefore drying of the bricks is important process.

Drying of the bricks is done in two predominant ways:

(a) Artificial Drying: bricks are burnt at optimum temperature at about1200 C in a tunnel like structure where the temperature is maintained.

(b) Natural Drying: it is done by exposing the bricks to air circulation, generally avoided the direct Sun-light.

Fig 7: Drying

Crushing Strength or Compressive Strength Test on Bricks:

Crushing strength of the bricks is determined by placing the sample brick in a universal testing machine and performing a compression test. After placing the brick in Universal testing machine, apply load on it gradually until the sample brick breaks. Note down the value of failure load and evaluate the crushing strength. The minimum crushing strength of brick is calculated to be 3.50N/mm2.if it is less this recommended value of 3.50 N/mm2, then it is not endorsed for construction purpose.

Fig 8: Brick placed under compression testing machine

The following bricks results are tested on compression testing machine in different proportions for 7 days, 14 days and 28 days.

IV. RESULTS

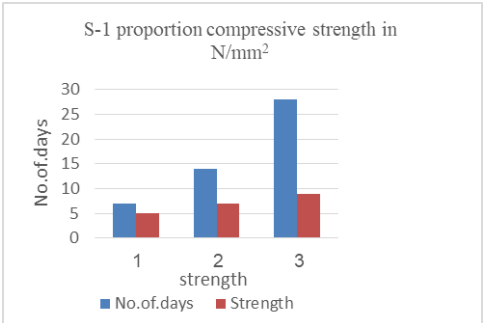

Fig 8 a: S-1compressive strength results

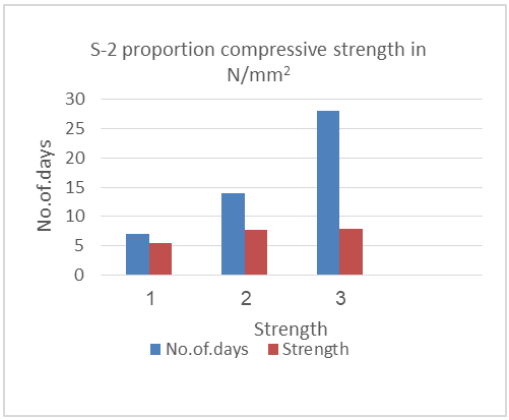

Fig 8 b: S-2 compressive strength results

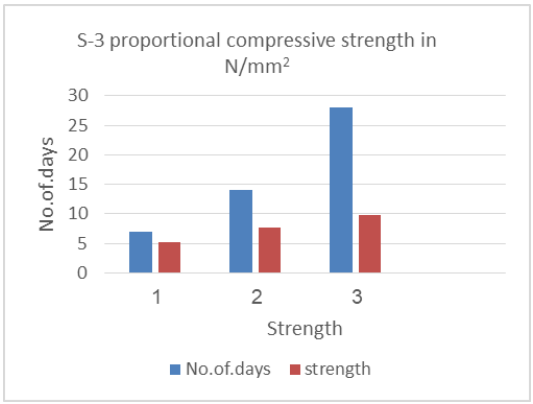

Fig 8 c: S-3 compressive strength results

Bricks compressive strength is compared between in bar charts. It will be easily found out the results. Paint waste bricks are compared to conventional bricks is less compressive strength. As per results these bricks are comes under 2nd class bricks.

V. CONCLUSION

The consequences of the present study conducted has proven that the brick making methodology effectually acceptable for solid waste (Paint sludge) and material (cement, quarry dust, and fly ash). Bricks were hardened within 2 days from manufacture time. Mixed binders (cement, fly ash and quarry dust) brick is recommended for external use in construction. This study also concludes that the construction raw materials can be replaced with industrial waste by products during manufacturing in some extended composition to increase the environmental safety. Compared to normal brick paint sludge brick is light in weight and transportation will be easy. The demand for the constructional materials has been rapidly increasing with the needs of construction both in rural and urban areas. These bricks are the sustainable, economical and eco-friendly building material. Bricks which are made from the paint waste is found to have compressive strength is greater than the conventional bricks. It is observed that when amount of cement is increased, strength also increases. When the strength is depends on the size of the particle, increases the strength by reducing the size of the particle.

Published By:
Blue Eyes Intelligence Engineering
& Sciences Publication

REFERENCES:

1. Text book construction materials and concrete technology. Andreola, F., L. Barbieri, I. Lancellotti, P. Pozzi, 2005. Recycling industrial waste in brick manufacture. Part 1. Journal of Material Construction, US Environmental protection Agency, Solid Waste, 2014 (March) (2014).
2. M. Safiuddin, M.Z. Jumaat, M. Salam, M. Islam, R. Hashim, Utilization of solid wastes in construction materials, International Journal of Physical Sciences. 5 (13) (2010) 1952-1963.
3. Aubert JE, Husson B, Sarramone N (2006). Utilization of Solid Waste Incineration (MSWI) Fly Ash in Blended Cement: Part 1: Processing and Characterization of MSWI Fly Ash. J. Hazardous Mater., 136: 624-631.
4. Xue Y, Hou H, Zhu S, Zha J (2009). Utilization of Municipal Solid Waste Incineration Ash in Stone Mastic Asphalt Mixture: Pavement Performance and Environmental Impact. Construction and Building Materials, 23: 989-996.
5. Chee-Ming Chan, 2011. Effects of natural fibers inclusion in clay bricks: physic mechanical properties. Journal of International Journal of Civil and Environmental Engineering, 1: 51-57.
6. Cheng-Fang Lin, Chung-Hsin Wu, Hsiu-Mai Ho, 2006. Recovery of municipal waste incineration bottom ash and water treatment sludge to water permeable pavement materials. Journal of Waste Management, 26: 970978.]
7. USEPA, Technology Resource Document—Solidification/Stabilization and Its Application to Waste Materials, USEPA, June 1993 (EPA/530/R- 93/012).
8. [C.F. Pereira, M.R. Pinero, J. Vale, Solidification/stabilization of electric arc furnace dust using coal fly ash analysis of the stabilization process, J. Hazard. Mater. B 82 (2001) 183–195.
9. Miss. Shrutakirti A. Mahajan*1, Dr. M. Husain *2 – "Utilization of Waste Sludge in Brick Making". http://www.ijettjournal.org-ISSN: 2231-5381
10. 1.Dina M. SADEK, 2. Walid S. EL- SAYED, 3. Ashraf M.A HENIEGAL, 4. Ayman S. MOHAMED-"Utilization Of Solid Wastes In Cement Bricks For An EnvironmentalBeneficial"-ANNALS OF FACULTY ENGINEERING HUNEDOARA – International Journal Of Engineering
11. Kanthe V.N.(1), Chavan P.G.(2)-"Solid Waste Used As Construction Material".IOSR Journal of Engineering (IOSRJEN) ISSN: 2250-3021 ISBN: 2878-8719 PP 75-77 National Symposium on engineering and Research. www.google .com

Published By:
Blue Eyes Intelligence Engineering
& Sciences Publication

An Improved Method Using STFT for Separation of Speech Signals

C.Anna Palagan, K.Parimala Geetha, T.Leena

Abstract: ***The key purpose of this paper is to recuperate the intention module of speech mixed with interfering speech, and to advance the recognition accuracy. This is attained by the improved speech signals, which is designed for effectually separated the speech signal from the blind source separation by expending the Instantaneous Mixing Auto Regressive method and the maximum prospect function. The significant features present in the Instant Mixing of Auto Regressive is that it gets boosted the split-up of speech signals and thereby aiding us to perform a blind source fragmentation process in contemplation, the Signal and Interference Ratio rate progresses over 6 dB. By using Instantaneous Mixing Auto Regressive method(IMAR) it accomplished good signal and interference ratio along with direct and reverberation ratio even though the reverberation time was 0.3 sec only. In this research work, dual channel and single channel speech fragmentation and enhancement algorithms are discussed and the performances of the proposed algorithms are analyzed in detail based on the objective and subjective quality measures. For the experimental setup, we consider the 0.3 sec and 0.5 sec reverberation time.***

Keywords: STFT, IMAR, Mixing Matrix, Separation Matrix, Prediction Matrix.

I. INTRODUCTION:

In the present era, the analysis pertaining to Wireless sensor Network (WSN) is rising as a result of the gradual advancement of embedded system and wireless technology (Gholipour et al .,2015). Signal process is associate degree rising field of basic analysis and potential applications and it's garnered a lot of recent analysis and industrial interest within the fields like digital and wireless communications, signal process, acoustics, medication etc. Speech is the most natural and predominant kind of human communication technique. Speech becomes a vital tool of human-machine interaction and it's modernized the method of communication. Speech process is that the study of speech signals (Hyvarinen et al 2000) and its process with varied strategies of the signal. The signals square measure sometimes processed in digital illustration; therefore speech process is thought to be a distinct case of digital signal process implemented to the speech signal. Speech process relates to the improvement, compression, synthesis or recognition of speech signals. within the recent era, digital signal process has a lot of significance and an intensive application since the techniques compared the properties in analog equivalent of many noisy speech signals in advanced. Speech has the subsequent aspects like richness and speed of representing, storing, retrieving and process speech information has contributed to the event of economical and effective speech process techniques dealing the problems associated with speech (Joho et al., 2001).

1. 1 SPEECH RECOGNITION SYSTEM

Speech is that the most effective and effective mode of communication. Speech recognition is completed by people at large all the time. It refers to the flexibility to concentrate spoken words and determine varied speech sounds in it, and acknowledge them as words of some famous language. Speech recognition system is often outlined as a system that is capable of understanding the "holy grail" of colloquial speech (Ahmed et al 2004). However, in all massive analysis spent in attempting to produce a system, we tend to square measure aloof from achieving the goal of a system is that may perceive voice and noisy signals combining received from all speakers in all told environments.

Speech recognition is that the objective of intensive analysis for several decades. Whereas recognition accuracy in clean environments, improved well once Hidden Andrei Markov Models (HMMs), recognition in rip-roaring environments still suffers as a result of several reasons like the twin between clean coaching and rip-roaring testing conditions. The Short-Time Fourier rework (STFT) could be a powerful signal process tool that's wont to rework a time domain signal into advanced amplitude values as a perform of your time and frequency. Once applied to the finite distinct signals, the forward STFT are often thought of as a method that transforms a time domain vector x into a fancy time-frequency domain matrix X. Once the transformation takes place the time-frequency signal are often analyzed, visualized, processed, and/or inverted back to the time-domain the inverse STFT. Figure 1 represent the speech improvement overall design.

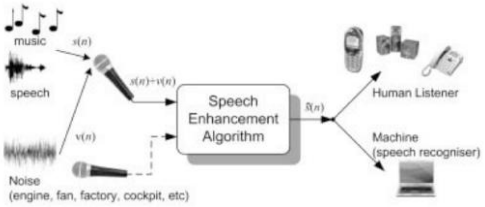

Figure 1. Speech enhancement overall structural design

Revised Manuscript Received on December 22, 2018.

Dr.C.Anna Palagan, Associate Professor in Department of Electronics and Communication Engineering, Malla Reddy Engineering College (A), Maisammaguda,Hyderabad,Telangana,India. (E-Mail: annapalaganc7467 @gmail. com)

Dr.K.Parimala Geetha, Professor and Head in Department of Electronics and Communication Engineering, Ponjesly College of Engineering, Kanyakumari, Tamilnadu, India.

T.Leena, Associate Professor, Department of Electrical and Electronics Engineering, Rajas Engineering College Tirunelveli, Tamilnadu, India.

The speech process systems wont to communicate or store speech signal square measure sometimes designed for noise free setting, however within the planet the incidence of circumstantial interference within the sort of surplus background signal and channel clatter significantly worsens the performance of those systems, it causes inaccurate data altercation and perceiver fatigue. Speech improvement is a field of digital speech process technique that aims to enhance the comprehensibility and/or sensory activity eminence of the speech signal, like audio clatter reduction for audio signals (Da-ZhengFeng et al .,2004).

1.1.1 Application of Speech Recognition

Automatic speech recognition (ASR) will make an interface between the human machine interactions. Computers could which might acknowledge speech in language may facilitate to reap the advantage of data technology for a standard man (van leeuwen et al., 2006). Though any task that involves interfacing with a pc will doubtless use speech recognition, the subsequent applications square measure the foremost common applications.

Dictation: The commonly used Automatic Speech Recognition systems today use is the Dictation. In dictation the medical transcriptions is used. The second dictation is legal and business as well as general word processing.

Command and control: The action of controlling any system by command word is achieved by using the Automatic Recognition System. The control signals are given by only commands format.

Telephony: Some Private Branch eXchange/Voice Mail systems use the user to speak the word by Automatic Recognition System that eliminates the button pressing.

Medical/Disabilities: In medical field some problems in typing of prescription due to physical limitations which are dystrophy in muscle, injuries that happened continuously etc. For example, people facing problem with hearing can use a module that convert the voice to text output connected to the concern telephone.

Embedded applications: In embedded systems applications the Automatic Recognition System which include voice recognition that is used in cellular phones. This is the future scopes of the ASR.

II. EXISTING METHODS:

Baer et al (1993) delineated a continuous evaluation of the results of digital process of speech in clatter therefore on enhance spectral distinction subjects with tube deafness. The improvement was allotted on a incidence scale associated with the correspondent rectangular bandwidths of modality filters as per traditional hearing subjects. The aim was to boost the foremost spectral notorieties while not augmenting fine-grain spectral options that will be indeterminate to a traditional ear. once expressed as equivalent changes in speech to noise quantitative relation, the enhancements were concerning doubly as massive for the response times as for the comprehensibility scores.

The overall impact induced by spectral improvement in correlation with compression was comparable towards associating degree improvement of speech to clatter quantitative relation by four.2 dB.FrancosieBeaufays (1995) had worked on the rework domain adjective filters: associate degree analytical approach. Within the same method, a weighted normalized frequency domain LMS adjective rule that uses the transformation of the input signals from time domain to frequency domain. Rankovic (1998) planned adjective linear filtering that improves effective speech to noise ratios by attenuating supernatural regions with extreme noise parts to scale back the noise unfold of masking on top of language in adjacent regions. This mechanism was examined in static listening conditions for seven people with sensor neural deafness (Woo W.L et al., 2005).

Shields associate degreed Campbell (2001) planned an adjective sub band noise cancellation theme, that performs stereo preprocessing of speech signals for a hearing aid application. The Multi mike Sub band adjective (MMSBA) signal process theme uses the Least Mean sq. (LMS) rule in frequency restricted sub bands. The employment of sub bands allows a various process mechanism to use, ripping the 2 channels wide band signal into smaller frequency restricted sub bands, which might be processed in keeping with their individual signal characteristics. The results show that there was some speech distortion and important quantity of noise gift within the increased signal, which is able to cause reduced comprehensibility.

Sunitha and Udayashankara (2005) planned 2 speech improvement strategies, within the initial technique the rip-roaring speech signal is remodeled distinct trigonometric function rework and processedLMS rule, in another technique the rip-roaring speech is remodeled distinct Fourier rework and processed LMS rule. More the comprehensibility of the speech signal needs to be thought of additionally to the development in SNR and reduction in MSE.

The wiener filter could be a widespread adjective technique that has been utilized in several improvement strategies. the fundamental principle of the wiener filter planned by Ahmed, B. and Holmes, H.H (2004) is to estimate associate degree optimum filter from the rip-roaring input speech by minimizing the MSE between the specified signal and therefore the calculable signal. It's obvious that apriority information of the speech and noise power spectra is important.

III. PROPOSED SYSTEM

The planned scheme uses a set-up which has the parameters of the Instantaneous Mixing Auto Regressive prototypical for partition matrices across the entire occurrence array. We approximation the perfect standards of the Instantaneous Mixing Auto Regressive model approximations, Φ_W and Φ_G pertaining to the maximum-likelihood evaluation process. At the instance of evaluation approximately these consideration standards, the basic source spectral element vector parameters can be predictable. The broad set of TIMIT corpus is employed for

speech resources in expansion outcome. The Signal to Interference Ratio (SIR) extemporizes by a common of in relation to 6 dB more than a rate of recurrence field BSS approach.

In the planned technique the BSS is improved of supply signals by LTI filter transformation. The time domain Blind Source fragmentation move towards is worn at this time. In our planned schematic evaluation of blind source signal is in the type of supply signal vector B_s (n) by implementing an I_M input signals and I_S output partition filter rate to experimental signal vector O (n). In the time domain BSS come within reach of for extrication sound mixtures arrange of the division filter is set a value that surpasses the room or normal reverberation time. The group of the division filter becomes extremely huge for the reverberation time is extended. So the divergence speed is reduced and the price for working out is extremely far ahead of the groundlevel. The assessment of supply supernatural constituent vector in the frequency domain BSS methodology is done by executing a separation matrix to the perceived spectral component vector element.

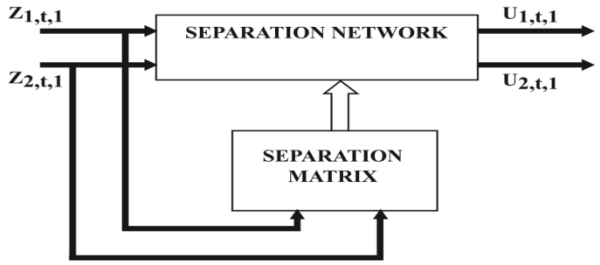

Figure.2. Proposed Model Block diagram of BSS

In our methodology proposed, we assume a manifold sound source case, where $I_M = 2$. So we think about for the frequency field BSS come within reach of as shown in Figure. 3is by using WPE technique as a preprocessor which demonstrate the casing of $I_S = I_M = 2$. Since in the primary footstep we use calculation fault with primary microphone for BSS procedure.

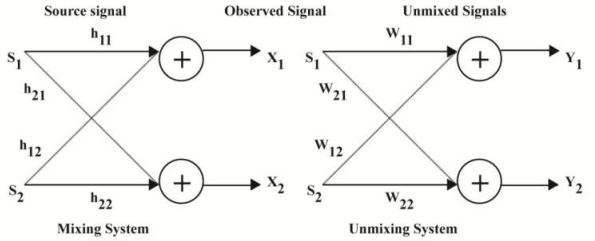

Figure. 3. Unmixing of Speech signals

We can use any type of microphone as the calculation end as per equation (1)

$$P_{n,u,v} = O_{n,u,v} - \sum_{s=L_i}^{L_i+M_i-1} h^{G}_{n,s,v} O_{n,u.v}; v \le n \le I_M \quad (1)$$

Where $\{h_{n,s,v}\}$ $L_i \le L_i+M_i-1$ denoted that the extrapolation filter for the I^{th} microphone spectral factor and $P_{n,u,v}$ is the matching calculation error. The dissimilar supernatural constituent outputs $P_{1,u,1}$…..$P_{Im,u,1}$ can be obtained. The instantaneous mixtures of the source spectra mechanism were measured for these apparatus. On the basis of hypothesis the Multichannel linear prediction values of $P_{1,u,1}$,……$P_{Im,u,1}$ turn out to be almost immediate mixtures by using suitable calculation filters even though such calculation filters may not be able to obtained with the WPE method. For the m^{th} microphone the prediction filter values are $D_{n,s,v}$.

We presume that the bin indices is 1 for all the considered frequencies from the set of exists values taken for evaluation of X_1 and $\{D_{n,s,v}\}$ $L_1 \le L_1+M_1-1$that is equalize the output of the above mentioned spectral component vector $B_{u,1}$ based on these presumptions it has been identified $Z_{u,1}$ with $B_{u,1}$ is given in equation (2)

$$Q_{u,v} = \sum_{s=L_\tau}^{L_l+M_l-1} H^{G}_{s,v} O_{u-s,v} + P_{u,v} \quad (2)$$

The statement in use in the above equation will not fully grasp in genuine instance so additional investigational element is preferred. So in IMAR model it performs far above the ground division of speech signal established on the probable supposition is at the smallest amount partly demonstrate the sensible strength of this statement. Mixing system H Demixing System W

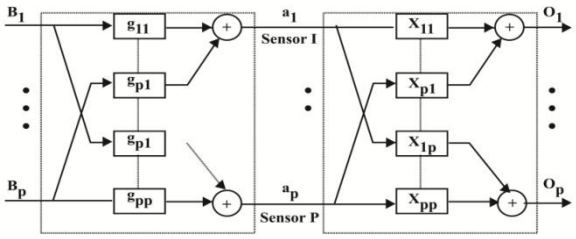

Figure.4. Mixing and Demixing of speech signal

IV. RESULT

The impulse reaction which is predictable from the available source speech signal I_S to the obtained output speech signal I_O. The corresponding errors investigated during the analysis are taken by the presumptions of -20 dB. This investigational outcome indicates that the IMAR model designed is valuable for BSS. The Input Signal from two sources is shown in Figure 5 and the STFT output is shown in Figure 6.

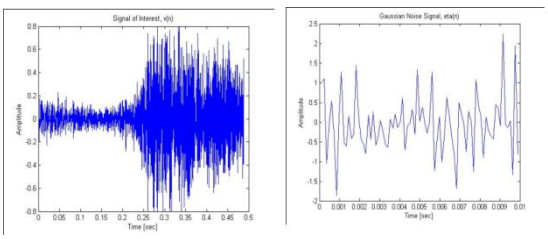

Figure. 5. Input Signal from two sources

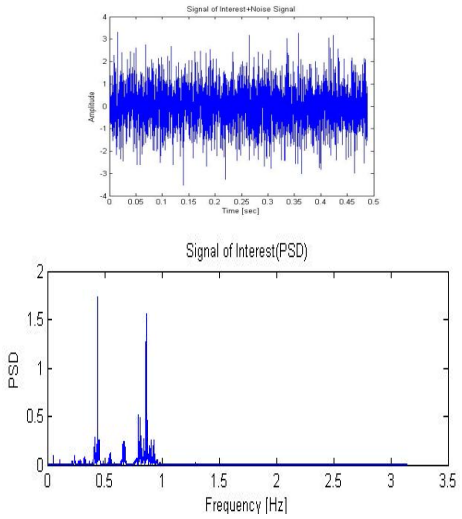

Figure. 6. STFT output

V. CONCLUSION:

The proposed work has been designed for a commendable separate speech signal from the blind Source Fragmentation by means of the methodology of Instantaneous Mixing Auto Regressive and the likelihood function. The significant features existent in Instantaneous Mixing Auto Regressive method is that optimized separation of speech signals and thereby enabling us to perform a blind source separation process in consideration. In our method the signal and interference proportion increases over 6 dB. a reverberation time was 0.3 s. we believe that Instantaneous Mixing Auto Regressive method provides a powerful tool for microphone array signal procedural in a reverberant room impulse response.

REFERENCES

1. Ahmed, B.and Holmes, H.H. "A voice activity detection using the Chi Square test", International Conferenceon Acoustics, Speech and Signal Processing, pp.I.625-I.628, 2004.
2. Alsteris, L. D., Paliwal, K. K. (2007), "Iterative reconstruction of speech from short-time Fourier transform phase and magnitude spectra," Computer Speech And Language, 21, 174-186.
3. Avargel, Y., and Cohen I. (2010), "Modeling and Identification of Nonlinear Systems in the Short-Time Fourier Transform Domain," IEEE Transactions on Signal Processing, 58,291-304.
4. Amari. S., S.C.Douglas, A.Chichocki and H.H.Yang (1997) Multichannel blind deconvolution and equalization using the natural radiant. Proc. IEEE Workshop Signal Proc. Adv. Wireless Commun.101–104.
5. Azharuddin. M and Jana.P. K, "A Distributed Algorithm for Energy Efficient and Fault Tolerant Routing in Wireless Sensor Networks," Wireless Networks, Vol. 21, No. 1, Pages 251 – 267, January 2015.
6. Baer, T., Moore, B.C. and Gatechouse, S. "Spectral contrast enhancement of speech in noise for listeners with sensor in neural hearing impairment: effects on intelligibility, quality, and response times", Journal on Rehabilitation Research and Development, Vol. 30, No. 1, pp. 49-72, 1993.
7. Bedoya G., Bermejo S. and SebestanyJ. (2003), 'Comparison of NeuralAlgorithms for Blind Source Separation in Sensor Array Applications', ESANN'2003 Proceedings-European Symposium on Artificial Neural Networks, Belgium, pp.131-136.
8. Bell A.J .and Sejnowski T.J. (1995),'An information-maximization approach to blind separation and blinded convolution', Neural Computation.,Vol.7,pp.1129-1159.
9. Chen.M and Zhou.P, "A novel framework based on Fast ICA for high density surface EMG decomposition," IEEE Transactions on Neural Systems and Rehabilitation Engineering, vol. 24, no. 1, pp. 117–127, 2016.
10. Choi. S, A. Cichocki, H. Park, and S. Lee (2005) Blind source separation and independent component analysis: A review. Neural Inform. Process.Lett. Rev., 6, 1–57.
11. Ching-Ta Lu, Chih-Tsung Chen and Kun-Fu Tseng "Speec Enhancement using Perceptual Decision Directed Approach", Proceedings of IEEE Computer Society, Second International Conference on Computer Engineering and Applications, pp. 23-27, 2010.
12. Cichocki A. and Unbehauen R. (1996), 'Robust Neural Networks with On-Line Learning for Blind Identification and Blind separation of Sources', IEEE Transactions on Circuits and Systems-I: Fundamental Theory and Applications, Vol. 43, No. 11, pp. 894-906.
13. Comon P. (1994), 'Independent component analysis-A new concept?', Signal Processing, Vol. 36, pp. 287-314.
14. Cohen, I. and Berdugo, B. "Noise estimation by minima controlled recursive averaging for robust speech enhancement", IEEE Signal Processing Letters, Vol. 9, No. 1, pp. 12-15, 2002. Common P. (1994), 'Independent component analysis-A new concept?', Signal Processing, Vol. 36, pp. 287-314.

A Study and Enhancement on Storage and Energy Efficient Using Cloud Computing

G.Charles Babu, Y.Rokesh Kumar, Balasani Venkata Ramudu

ABSTRACT:--- Cloud computing is the most recent "evolving paradigm" that has transformed the way by which the Information Technology based services and facilities can be offered explicitly. It has renovated the model or technique of storing and managing data for scalable, real time, internet based applications, programs soft wares and resources satisfying end users' needs appropriately. Owing to the requirement of energy savings, several approaches to location sensing based energy-efficient solutions have been explored. The power consumption quantity of these infrastructures have gradually reached 1.5% from 1.1% of the total electricity consumed across the entire globe, and is expected to rise even more than this. Firstly, we state a systematic methodology for exploring the energy efficiency of most significant data center domains, including the utility server and network hardware equipment, as well as cloud management systems and the corresponding appliances consisting of a software package that can be predominantly utilized by end users. Secondly, we utilize the above mentioned approach for analyzing the already available scientific implementation and industrial literature investigations on state-of-the-art practices in the data centers and their equipment. Finally, we extract the existing practical challenges faced during implementation and highlight futuristic advancement directions.

Keywords: Cloud computing, energy efficiency,

I. INTRODUCTION:

Cloud computing is an emerging innovative service mode. It enables the end users and its clients to get roughly unconstrained computing skillset and ample variety of information tasks from the internet resources. This sort of new pattern configuration refers to the permutation and expansion to the IT infrastructure, through the network based technology to the required resources which include hardware platform, and software structures, virtual combination into a trustworthy and high performance and intact computing platform. In cloud computing, all users' facts and specific information are stored in the cloud resources Nodes. Several creative and ingenious trends are opening up the era of Cloud Computing, which is completely an Internet-based expansion and requires the use of computer technology. The ever most economical and added powerful processors, coupled mutually with the (SaaS) software as a service computing architecture, are transforming the available data centers into pools of computing service on a vast scale of the technology. The accumulating tremendous network bandwidth and reliable yet flexible network connections make it even more probable that the users can now subscribe for a very lofty quality services from data to software that is solely inherent on the remotely available data centers located globally. Moving the existing facts and elements into the cloud offers extremely liable convenience to the end users as they need not care about the complications of direct hardware management. The major challenge faced in this sector is utilization of energy efficiently and precisely thereby developing an eco-friendly cloud computing technology which is easily accessible.

II. LITERATURE REVIEW:

Beloglazov et al (2012) proposed the vitality mindful asset distribution calculations using the dynamic solidification of virtual machines. The structural standards for vitality proficient administration of mists, asset assignment strategies and booking calculations were advanced remembering the coveted nature of-benefit parameters and power utilization highlights of changing gadgets. The outcomes uncovered that in contrast with static asset designation systems, the proposed procedure productively lessened vitality utilization in cloud server farms.

Dong et al (2015) acquainted voracious assignment scheduler with examine vitality productive undertaking booking for cloud server farms. The errand task was figured as whole number programming issue to diminish the vitality utilization by cloud information servers by proposing the most-effective server-first undertaking planning plan. Reproduction results demonstrated that the vitality utilization utilizing proposed planning plan was 70 times lesser than the one dependent on arbitrary based assignment booking plan.

Neeraj Kumar Sharma et al (2016) Due to the developing interest of cloud administrations, distribution of vitality proficient assets (CPU, memory, stockpiling, and so forth.) and assets usage are the major testing issues of an extensive cloud server farm. In this paper, we propose an Euclidean separation based multi-target assets assignment as virtual machines (VMs) and outlined the VM movement arrangement at the server farm. Assist the assignment of VMs to Physical Machines (PMs) is done by our proposed half breed approach of Genetic Algorithm (GA) and Particle Swarm Optimization (PSO) alluded to as HGAPSO. The proposed HGAPSO based assets assignment and VM movement not just spares the vitality utilization and limits

Revised Manuscript Received on December 22, 2018.

G.Charles Babu, Professor, Dept. of CSE Malla Reddy Engineering College (Autonomous) Maisammaguda, Secunderabad, Telangana – 500100, India

Y.Rokesh Kumar, Assistant Professor, Dept. of CSE Malla Reddy Engineering College (Autonomous) Maisammaguda, Secunderabad, Telangana – 500100, India

Balasani Venkata Ramudu Assistant Professor, Dept. of CSE Malla Reddy Engineering College (Autonomous) Maisammaguda, Secunderabad, Telangana – 500100, India

the wastage of assets yet in addition maintains a strategic distance from SLA infringement at the cloud server farm.

Tejaswini K et al (2015) Cloud registering is a rising innovation which gives metering based administrations to customers. Distributed computing technique deals with ITC based administrations and also give the procedure for processing assets through virtualization techniques over web. Server farm is soul of distributed computing as it contains accumulation of various servers on which the entire Business data is put away and applications run solitarily. The fundamental objective of every one of these methodologies is to improve the vitality use in cloud. This paper gives review of writing overview on ways to deal with have vitality productive cloud.

Mueen Uddin et al (2009) have proposed a specific system for huge and complex server manors to have vitality effectiveness with low CO2 discharge to the earth. The system comprises of five stages with the end goal to actualize green server farms for cloud. This paper has segregated the datacenter assets into various pools and implements green measurements like PUE, server farm effectiveness on those assets to quantify the execution of every asset independently and furthermore utilizes virtualization innovation for appropriate usage of green IT server farm.

III. OBJECTIVES:

1. To investigate open research challenges in vitality effective asset administration for virtualized Cloud server farms.
2. To create calculations for vitality productivity
3. To play out a relative investigation of various vitality productivity approaches in distributed computing
4. To examination the Energy Efficiency Techniques In Cloud Computing.

Virtualization: Virtualization is an innovation that permits at least two diverse working frameworks running next to each other on only one PC or installed controller. It is being embraced in the designing scene at a high rate. It helps in better usage and working of more productive frameworks. As multi-center processors are supplanting single-center processors, numerous processor centers are probably going to be underutilized in a run of the mill framework. Most applications will have just a limited measure of parallel asks that can be executed at a given time, leaving numerous processors inactive.

Storage as a Service: By the use of capacity as an administration, consumers can re-appropriate their facts squirrel away requirements to the cloud. Every handling phase is performed on the client's PC which is considered to have a very strong state drive (e.g., streak based strong and state stockpiling), and the client's essential information and facts stockpiling is stored in the cloud. Information records or data management may incorporate archive folder, photos/images, or audio and video recordings. Documents stored astray in the cloud can be acquired to from any PC with the aid of an Internet association whenever and wherever required across the globe. Be that as it may, to make any change or modification to a record, it should initially be downloaded, and then altered utilizing the client's PC and after that the adjusted document with the appropriate modification is transferred back to the cloud. The exclusive cloud specialist co-op guarantees that there is adequate free space presents in the cloud and furthermore is responsible with the reinforcement of information that is modified. At last after a client transfers a document or information or data to the cloud, the client can allow read and change benefits to different clients. One of the best case of capacity as an administration is the Amazon Simple Storage benefit which known worldwide.

Results & Discussions:

Erection of a vitality productive cloud show not only demonstrates just vitality effective host machines. Other existing segments of a total cloud framework ought to likewise be considered for vitality mindful applications. A few research works have been done to construct vitality productive cloud parts exclusively. In this segment we will examine the territories of an ordinary cloud setup that are in charge of significant measure of intensity dissemination and we will combine the conceivable ways to deal with fix the issues considering vitality utilization as a piece of the cost capacities to be connected.

Energy Efficient in Cloud Computing: The Energy – Efficient manages playing out indistinguishable errands from previously while devouring less vitality, bringing about lower costs: It decreases the carbon outflows, to accomplish a greener domain. Vitality productivity isn't vitality protection. Vitality protection is decreasing or abandoning a support of spare vitality. Vitality utilization at various levels like equipment, servers other system gadgets, diverse wired and remote systems. He additionally studied that most extreme vitality is expended for cooling of gadgets as opposed to genuine usage.

Vitality productivity has turned into an inexorably imperative worry in server farms in light of issues related with vitality utilization, for example, investment costs, implementation costs, and natural effect. Although vitality misfortune due to problematic utilization of offices and tending to vitality wastage in IT gear still requires the appropriate plan and timely execution of vitality mindful asset administration frameworks. This proposal centers around the advancement of asset distribution strategies to enhance vitality effectiveness in server farms. It utilizes three ways to deal with enhance productivity for streamlined power and execution: scaling virtual machine (VM) and server handling abilities to decrease vitality utilization; enhancing asset use through remaining burden union; and misusing asset heterogeneity.

Energy efficiency: Vitality effectiveness: Energy productivity can be characterized as a decrease of vitality utilized for a given administration or level of action. In any case, because of scale and multifaceted nature of server farm gear it is to a great degree hard to characterize special administration or action that could be inspected for its vitality proficiency. Thusly, we distinguish four situations inside a framework where vitality isn't utilized in effective route, yet rather it is lost or squandered, as appeared in Figure 1.

Published By:
Blue Eyes Intelligence Engineering
& Sciences Publication

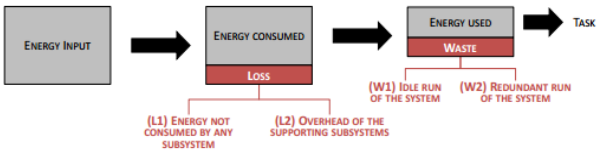

Figure 1: Circumstances where energy is lost within a system.

The two terms characterize wasteful vitality utilization from a rationalist perspective, where vitality misfortune alludes to a vitality conveyed to the framework, however (L1) not devoured by the corresponding subsystems, e.g., vitality lost because of transport or change. This likewise incorporates (L2) vigor overhead of the auxiliary subsystems, for example, cooling or lighting inside a server farm, where Cloud administration segments are provisioned and is considered as its fundamental reason. Vitality squander alludes to a vitality utilized for its principle reason, anyway for the (W2) inactive keep running of the framework, e.g., processor being turned on however running inert. Moreover, (W2) excess keep running of the framework is additionally considered as vitality squander, e.g., keeping a cooling framework at greatest amidst the nights when the temperatures are fluctuating and lower than the normal.

Energy Efficiency Metrics: There is nobody single vitality effectiveness metric that is fitting for all cases and for all datacenters in light of the fact that no two datacenters have a similar scale, capacities, expenses, and outstanding tasks at hand. In addition, a metric may try to evaluate office productivity or IT gear proficiency. Along these lines, activities, for example, Green Grid, vitality star, and SPEC have proposed various diverse measurements. Understanding the measurements may give a superior perspective of how vitality can be advanced. The measurements can be classified as office, IT gear, or a mix of the two.

At the office level, Data Center framework Efficiency (DCiE) is the rate reverence contingent by isolating IT hardware. PUE, the reverse of DCiE, is the proportion of aggregate datacenter vitality use to IT gear vitality utilization. PUE is well known datacenter effectiveness metric since it was among the primary measurements and is straightforward. What's more, not all PUE estimations incorporate similar overheads, same time length, and true estimations. The Corporate Average Datacenter Efficiency (CADE) metric consolidates estimations of vitality effectiveness and usage of office and IT gear. The server PUE (SPUE) metric evaluates the vitality proficiency of the IT hardware itself, and is the proportion of aggregate server input capacity to control devoured by the segments specifically associated with calculation, for example, CPUs, DRAM, and so forth.

Energy Efficiency Techniques in Cloud Computing:

Vitality effectiveness has risen as a standout amongst the most imperative outline prerequisites for current processing frameworks. Distributed computing has brought about the foundation of substantial scale server farms far and wide. Server farms keep on expending tremendous measures of electrical power, adding to high operational expenses and carbon impressions to nature. Different vitality proficiency strategies have been gone for in the server farms under exploratory conditions. The reasonable use of these strategies is still under investigation. These methods are:

Dynamic Voltage and Frequency Scaling (DVFS): Change the voltage dynamically and recurrence of the CPU as a host as per the outstanding task at hand and afterward adjusts the CPU control utilization in like manner, which would modify the execution level also [13]. DVFS empowers processor unit to keep running at various mix of recurrence with voltage to lessen the utilization of power of the processor unit. This procedure watches the vitality use E of an errand running with a specific recurrence f that can be communicated with the accompanying condition E = k .v^2.f.t where k is a gadget subordinate consistent, v is the voltage and t is the execution time.

Dynamic Component De-Activation (DCD): is actuation and deactivation of the segments based on characterized principles prompting better execution. The inert disjoins or segments could be turned off or moved to less power expending state like rest mode and tentatively confirmed that a perfect server expends around 70% of the power used by a completely used server.

Resource Throttling: It is an answer for controlling the clients are permitted to devour the cloud assets. Asset throttling should be possible in different routes at the equipment or at the product level with the end goal to meet the execution prerequisites and limit the vitality utilization. In a cloud domain, there are a few parameters throttled the Network data transfer capacity, stockpiling, CPU use and I/O tasks.

VM Consolidation: In a distributed computing condition, each physical machine has various virtual machines whereupon the applications are run. Outstanding task at hand combination implies better source use and effective vitality putting something aside for cloud information utilizing movement of virtual machinery setup (VM) and re-distribution of remaining burden. VM can be exchanged over the hosts as indicated by the shifting needs and accessible assets. The VM movement technique centers on moving VMs so that the power increment is minimum. The most power proficient hubs are chosen and the VMs are exchanged crosswise over to them. It evacuates the idea of territory in the appropriate virtualized situations.

Datacenters:

A datacenter is an office in which various servers, stockpiling units, and systems administration gear, together with all non-processing equipment, for example, cooling plant and continuous power supplies, are gathered in light of normal natural prerequisites, physical security needs and also for simplicity of support. Datacenters extend in size from server rooms that help little to medium-sized associations to server cultivates that run substantial scale cloud administrations.

The development of vast scale datacenters is likewise determined by the expanded abilities of cloud administrations, quick development of distributed

computing as the accepted worldview by which online administrations are given, and the uncommon measure of information being produced by present day applications. These datacenters generally have a huge number of servers that devour enormous measures of intensity. Hence vitality utilization has turned into an imperative concern on account of its effect on capital costs, working costs, and ecological supportability.

Administration of such heterogeneous framework requires adaptable and far reaching CMS with cutting edge checking capacities. Coordinating direct administration of supporting frameworks, for example, cooling and power supply includes extra layers of multifaceted nature. Nonetheless, even with ICT gear administration alone, CMS requires observing data on advancement, execution, state, information measure, and additionally equipment measurements with the end goal to help savvy booking and equipment coordinating. Encourage enhancements include organization of Clouds through streamlining activities more than a few geologically appropriated server farms. Such methodologies require not just communication among programming and equipment inside a solitary server farm, yet a trade of data, client load and information over the globe also.

Usage of Cloud in Energy Efficient Manner:

Alongside enhancing the vitality proficiency of server farms, the server farms in the Cloud Computing idea can give use to enhancing the vitality productivity on a bigger scale. Rather than utilizing separate processing frameworks, clients can solidify their registering necessities and move to the Cloud Computing condition, or, in other words than the littler figuring frameworks because of its greater scale. Vitality proficiency models, for example, Clear display created by the Lawrence Berkeley National Laboratory give a way to deal with examine vitality investment funds when moving to Cloud. It gauges capability of up to 95% of decrease in vitality utilize contrasted with existent business programming use, incorporating client relationship administration (CRM), efficiency and email programming. Computerized ones can likewise have huge vitality sparing effect. This incorporates video industry that by using Cloud Computing idea can stream video over the web, which decreases vitality utilization by 15% contrasted with delivery it on CDs and DVDs.

But utilizing Cloud Computing idea for its fundamental reason, the Cloud Computing framework and its adaptable nature can likewise be used in a roundabout way for vitality improvement. Methods, for example, DVFS and controlling on/off machines can be utilized for recurrence direction of a power arrange. Utilizing this methodology, server farm's dynamic load can be utilized for managing power request and hence generation, or, in other words keeping ideal recurrence of the power matrix. In addition, power suppliers pay for such an administration of dynamic load, empowering the server farm to procure a half of million dollars every year. Also, rather than just devouring vitality, current server farms are getting to be vitality makers with on location control generators. Not just that this methodology lessens costs for the server farm, it additionally diminishes control misfortunes because of a vitality exchange and the heap on a vitality network.

IV. CONCLUSION:

The most pertinent significance of Cloud Computing is incessantly increasing the reputation of Energy efficiency in Cloud Computing in parallel. This publication confers the various practices and procedures of energy efficiency in Cloud Computing which is considered as the cutting edge of worldwide research in today's scenario. It is also established that Energy Efficiency along with Cloud Security in a cloud computation environment is quite complicated. However, if the major discrepant parameters like CO2 emission security for decrease at data central level can give a solution for both the challenges to some extent.

REFERENCES:

1. Beloglazov, A., J. Abawajy, and R. Buyya, "Energy-aware resource allocation heuristics for efficient management of data centers for cloud computing", Future generation computer systems, vol. 28, no. 5, pp. 755-768, 2012.
2. Deore, Shailesh, A. N. Patil, and Ruchira Bhargava. "Energy-Efficient Scheduling Scheme for Virtual Machines in Cloud Computing." International journal of computer application 56.10 (2012).
3. Pagare, Damodar ,Jayshri, and Dr.Nitin A Koli "Energy-Efficient Cloud Computing: A Vision, Introduction, Efficient Cloud Computing: A Vision, Introduction, and Open Challenges" IJCSN International Journal of Computer Science and Network, Vol 2, Issue 2, April 2013.
4. Srikantaiah, Shekhar, Aman Kansal, and Feng Zhao. "Energy aware consolidation for cloud computing." Proceedings of the 2008 conference on Power aware computing and systems. Vol. 10. 2008.
5. Ye, Kejiang, et al. "Virtual machine based energy-efficient data center architecture for cloud computing: a performance perspective." Proceedings of the 2010 IEEE/ACM Int'l Conference on Green Computing and Communications & Int'l Conference on Cyber, Physical and Social Computing. IEEE Computer Society, 2010
6. Arindam Banerjee, Prateek Agrawal and N. Ch. S. N. Iyengar (2013), "Energy Efficiency Model for Cloud Computing", International Journal of Energy, Information and Communications Vol.4, Issue 6 (2013), pp.29-42
7. Jadeja, Y., K. Modi, "Cloud computing-concepts, architecture and challenges," in IEEE International Conference on Computing, Electronics and Electrical Technologies (ICCEET), pp. 877-880, March 2012
8. Shveta, Asmita Pandey (2014), "Energy Conservation And Security Issues In Cloud Computing: A Review", International Journal of Advances In Computer Science and Cloud Computing, ISSN: 2321-4058 Volume- 2, Issue- 1, PP: 57-60
9. Tarandeep Kaur, Inderveer Chana (2015), "Energy Efficiency Techniques in Cloud Computing: A Survey and Taxonomy", Journal ACM Computing Surveys (CSUR) Volume 48 Issue 2
10. Rusu C, Ferreira A, Scordino C, Watson A, Melhem R, MossenD. Energy-efficient real-time heterogeneous server clusters. In Proc. of the 12th IEEE Real-Time and Embedded Technology and Applications Symposium, pages 418–428. San Jose, USA, April 2006.

Published By:
Blue Eyes Intelligence Engineering
& Sciences Publication

Synthesis Of Optimized Patterns from Thinned Arrays

G.S.K.Gayatri Devi

Abstract -- Difference patterns find their applications in radar tracking. There rises a need to generate such patterns with minimum sidelobes to reduce clutter and interference in accurate target tracking. A popular technique used for low sidelobe pattern generation is thinning. It reduces the number of elements active in the overall system. In addition to reducing sidelobes, it also reduces cost and weight. In the current presentation, low sidelobe difference patterns are generated from thinned linear assortments. Differential Algorithm is made use of for the pattern generation. Optimized patterns are portrayed for different number of elements. The results computed show good sidelobe level reduction without enhancing beamwidth between first nulls.

I. INTRODUCTION

In target tracking radar systems, it is essential to trace the target with great accuracy. This can be done with a simple sum pattern. The location of the target is specified by the position of main beam. But the accuracy of detection depends on where the target falls within the main beam region. Hence patterns with narrow beam width or high directivity must be generated. Instead difference patterns can be employed in such cases where high angular accuracy is required.

Difference patterns are characterized by a profound sharp insignificant in the bore sight direction in addition to the two foremost lobes on either side. Target detection mainly utilizes this deep null. Placing the target accurately at the null position amid the principal lobes, the target location can be resoluted exactly. This method is more exact as the angular width of null is very narrow compared to a broad beam sum pattern.

One of the main fields which employ difference patterns is Monopulse tracking system. This system employs both sum and difference pattern. The sum beam reveals the presence of target and difference pattern determines its angular position. Conventional methods for generating difference pattern generally use Bayliss aperture distribution [1]. Several works were reported on generation of difference patterns. Elliot [2] developed a method to generate difference patterns with arbitrary side lobes from line source antennas. A Bayliss pattern is taken as initial pattern and an iterative method is applied to produce desired pattern. Mc Namara [3] presented a method for generation of optimum difference patterns. The method uses zolotarev polynomials to find the element excitations, given number of elements and desired side lobe ratio. Lopez [4] et al. employed sub-array configuration and obtained optimum sub array weights for generating difference patterns with minimum change in the feed network. Morabito [5] employed an analytical procedure based on a density taper approach to generate difference patterns from equally excited linear arrays for the simplification of receiving chain and to improve antenna efficiency. Satyanarayana [6] proposed suitable amplitude and phase distributions for generating asymmetric difference patterns useful for marine radar applications.

Generation of optimized difference patterns became somewhat easier with the advent of global optimization techniques. Asim [7] made use of particle swarm optimizer to design a simple feed network for generating difference patterns for monopulse radar system. The optimum weights were obtained by including mutual coupling effects. Salvatore et al. [8] employed sub array configuration for generating difference patterns with desired side lobe level requirement. The optimization was carried out using a hybrid Real Integer-coded Differential algorithm. Varma et al. [9] employed optimization techniques like GA, PSO and Simulated Annealing methods to find optimum amplitude distribution for generation of low side lobe difference patterns. Mohammad [10] described a method for generating difference patterns from sum patterns using a simple beam forming network. Two external edge elements are used for the generation. Yanchang et al. [11] proposed a method which extracts the aperture coefficients from Taylor distribution. The method offers good control over peak side lobe level. A new method for easily computing difference patterns from Dolph-Chebyshev distribution is given by Yanchang et al. in [12].

The main objective of the work is to generate low side lobe optimum difference patterns by the method of thinning. Thinning selectively turns off certain elements without disturbing the system performance. It results in optimum design of arrays with a reduction in cost and weight. Moreover, all the elements are excited uniformly which requires a simple feed network. It is simpler than aperiodically placing the elements because the latter has infinite possible ways of placing the elements. Thinning an 'n' element array has only 2^n possible combinations. Hence it reduces time and laborious work on part of the designer. But this is true only for small arrays. For large arrays, as 'n' increases the number of combinations also increases. It is impossible to check all possible combinations for best solution. This situation arises a need for methods that give faster solutions. Global optimization techniques satisfy this requirement. Many techniques like GA[13-14], PSO[15], ACO[16] etc. were implemented successfully for solving numerous complex optimization methodology in antenna design. A systematic Differential Evolution algorithm is

Revised Manuscript Received on December 22, 2018.
Dr. G.S.K. Gayatri Devi, ECE Dept, Malla Reddy**,** Engineering College (A),Hydeabad, Telangana, India

utilized in the current demonstration to obtain optimum antenna configuration.

The paper is organized like this: Introduction is conferred in section I. Section II illustrates operating principles of Differential Evolution algorithm. Section III describes formulation of the problem. Presentation of results is carried in sub division IV. Conclusions and inferences are depicted in article V.

II. DIFFERENTIAL EVOLUTION

DE belongs to evolutionary algorithms family. It was first put forward by Scientist Storn and Research scholar Price [17]. It is a very dominant stochastic erch algorithm accepted globally across the researchers and scientists for solving many complex global optimization problems which also population based systematic approach. Its efficiency was proved in many scientifically predominant arenas like communications sectors, pattern recognition sectors etc., as the abovementioned algorithm offers extemporaneous advantages like few control parameters, satisfactory convergence speed and ease to handle a variety of complex fitness functions

The different stages of the algorithm are depicted in the below flowchart:

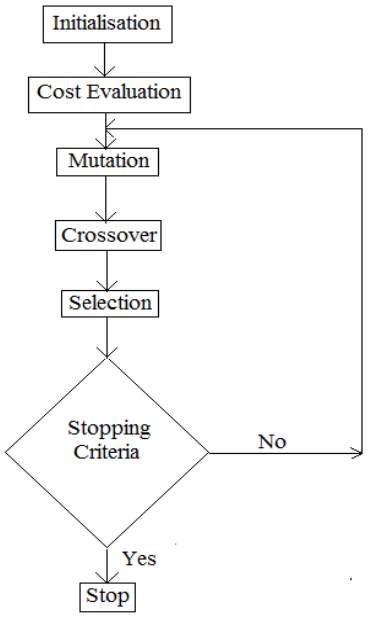

Fig 1. Flowchart for DE

Initialization: An initial number of 'N' population vectors are considered. Target vector is the name assigned to the initialized vectors. The population size remains unchanged throughout the entire course of the algorithm. Let '$a_{i,G}$' e designated as the i^{th} parametric variable vector where i=1, 2, 3, … N. And 'G' represents the generation variable. These parametric variable vectors are unsystematically initialized in a random fashion. Then the vectors are systematically estimated for their cost factor using the corresponding appropriate fitness function.

During the intermediate distinct mutation process, new parametric variable vector functions are created simultaneously by adding a meagre weighted difference between the respective two of the target vectors to the succeeding third target vector, i.e. for any given systematic target vector '$a_{i,G}$', three consecutive parameter vectors such as $a_{r1,G}$, $a_{r2,G}$, $a_{r3,G}$ are selected such a manner that the functional constants i, r1, r2, r3 are different in the way of values and directions to establish new parameter vectors called as the 'donor vectors'.

$$b_{ji,G+1} = a_{r1,G} + F(a_{r2,G} - a_{r3,G})$$

At this point r1, r2, r3 ∈ {1, 2, 3, …, N}

At the moment the Mutation process increases the room for exploring optimum solution. Here a constant called mutation factor, 'F' is chosen between 0 to 2.

Parameter vectors with good fitness can be included from earlier operations using crossover operation. Formation of new vectors called as 'trail vectors' ($c_{i,G+1}$) takes place by mixing together the selected target vectors ('$a_{i,G}$') and synthesised donor vectors ($b_{i,G+1}$).

$$c_{ji,G+1} = b_{ji,G+1}\ if\ rand \le CR\ or\ j = I_{rand}$$
$$= a_{ji,G+1}\ if\ rand > CR\ and\ j \ne I_{rand}$$

Here i∈{1,2,…} and j∈{1,2,3,….D}.

The variable D represents numerous parameters in one of the significant population vector. I_{rand} is random numerical usually selected between 1 to D. Inclusion of this factor makes sure that not less than one vector is selected from donor vector set into trail vector set. CR is another constant chosen between 0 and 1.

Next stage is selection process. Based on the fitness values of the individual vectors, those which satisfy a certain selection criteria will be selected for the next succeeding generation. This current process is mathematically represented in the trigonometric equation as:

$$a_{i,G+1} = c_{i,G+1}\ if\ cost(c_{i,G+1}) \le cost(a_{i,G})$$
$$= ax_{i,G}\ otherwise$$

The above equations clearly indicate that a newly generated trail vector substitutes parent population vector and passed on to next generation only if it results in reduced cost.

The above operations will continue to repeat until it meets some stopping feasibility criteria. In overall formulation a fixed number of specific generations or predefined cost factor etc. is taken as stopping criteria.

A number of variations in DE are put forward by Storn and Price [17]. A DE//rand//1//binary scheme is formulated in the presentation work.

III. FORMULATION

Consider a symmetric linear array of 2M isotropic elements placed along z-axis as shown in fig.1. All elements have an equal inter element spacing of 'd'.

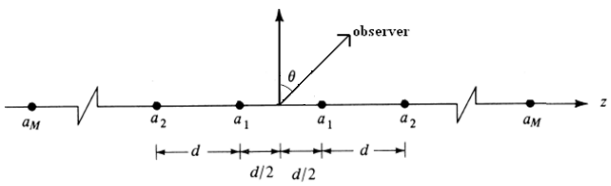

Figure 1 Geometry of linear symmetric array

Further assume that the amplitude distribution is symmetric about array axis. The resultant array factor can be given as [18]:

$$E(u) = 2j \sum_{m=1}^{M} I_m \sin[(m - 0.5)kdu]$$

where $u = \sin\theta$

k= $(2\pi/\lambda)$

d= spacing between two elements, $(\lambda/2)$

λ= operating wavelength

I_m=Excitation coefficient of m^{th} element in the array.

Now the array is thinned with an objective of finding the optimum configuration that results in lowest possible peak side lobe level. Hence I_m takes the value of either 0 or 1.

A DE algorithm is applied to get the optimum array configuration. The parametric variable selection plays the most substantial role in the procedure of convergence of the algorithm to the best solution. The control parametric setting variable function for a DE algorithm with the usage of DE//rand//1//binary systematic stratagem is as given in Table 1.

Table 1: Parameter selection

Parameters for DE	
Population size	30
Mutation	0.7
Crossover ratio	0.8
Number of generations	100

All results are simulated using Matlab software.

IV. RESULTS

A brief description of results obtained has been substantiated in this sub division. An isotropic linear array of 30 elements is considered initially. The assortment is subjected to gradual thinning process. The resulting pattern has a definite peak side lobe level evaluated as -14.91dB. Prior to the process of thinning, it is only -10.44dB. An improvement of 4.5dB can be observed. The pattern is shown in figure 2.

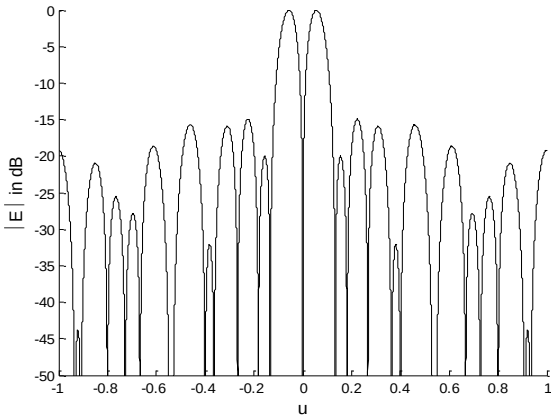

Figure 2. Radiation pattern for 30 element array

The corresponding thinning weights for right half of the array is depicted in figure 3.

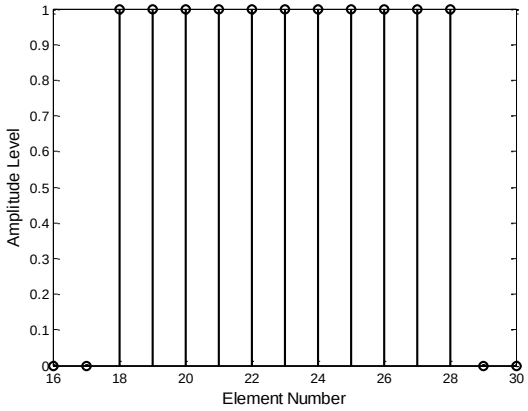

Figure 3. Half the thinning weights for right half of 30 element array

The same process is repeated for different number of elements. As an example, for a 100 element array, a distinct height of peak SLL of -20.17dB is obtained after the gradual procedure of thinning. An improvement of around 9.5dB can be observed. The consequential pattern structure is shown in figure 4.

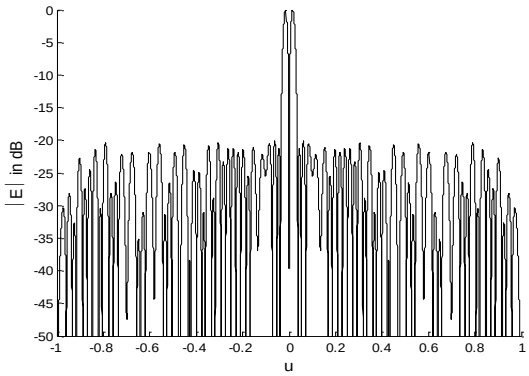

Figure 4. Radiation pattern for 100 element array

The corresponding thinning weights for right half of the array are depicted in figure 5 given below:

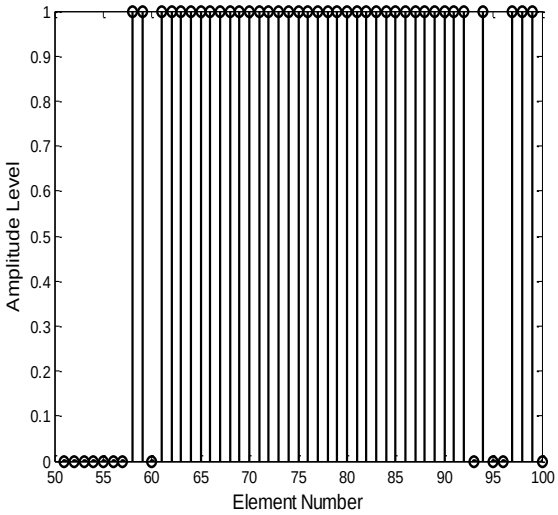

Figure 5. Half the thinning weights for right half of 100 element array

Figures 6 and 7 show the radiation pattern and the corresponding right half thinning weights for a 200 element array. The peak SLL obtained in this case is -21.9dB. It is only -10.56dB before the array is thinned. An improvement of around 11dB can be observed.

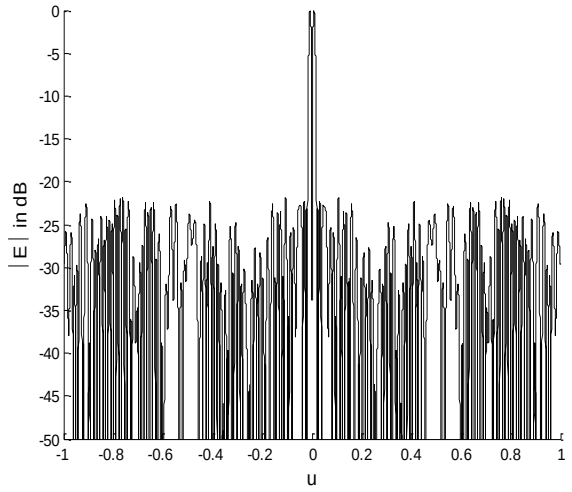

Figure 6. Radiation pattern for 200 element array

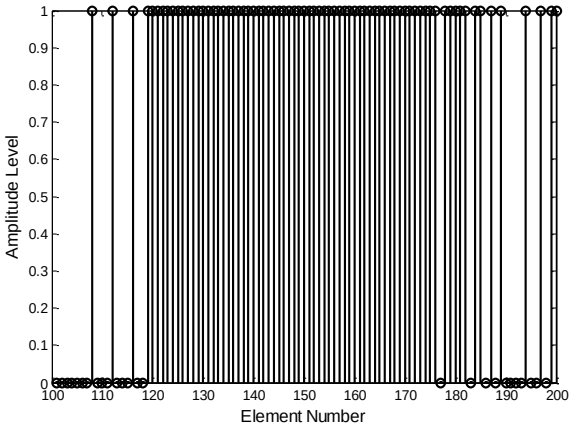

Figure 7. Half the thinning weights for right half of 200 element array

A comparison table for peak SLLs obtained before and after thinning is given below for the sake of convenience.

Table 2: Comparison of PSLLs before and after thinning

Number of Elements	PSLL(dB) before thinning	PSLL(dB) after thinning
30	-10.438	-14.91
40	-10.495	-16.37
50	-10.521	-17.2
60	-10.535	-17.78
70	-10.543	-18.41
80	-10.549	-19.12
90	-10.552	-19.63
100	-10.555	-20.17
150	-10.562	-21.22
200	-10.564	-21.9

V. CONCLUSIONS

A linear array of 'n' isotropic element array is taken and thinning is carried out with an intention of reducing peak side lobe level. Such patterns with low side lobes find wide applications in radar target tracking. A Differential Evolution algorithm is applied to obtain the best optimum thinning configuration. The results clearly show that thinning results in better side lobe reduction with minimum number of active elements. Results have been illustrated for different numerous elements of the lobes. The work can be extended for thinning arrays of practical elements.

REFERENCES

1. E. T. Bayliss, "Design of monopulse antenna difference patterns with low side lobes," *Bell System Technical Journal*, vol. 47, pp. 623–640, 1968.
2. R. S. Elliot, "Design of line source antennas for difference patterns with side lobes of individually arbitrary heights," *IEEE Transactions on Antennas and Propagation*, vol. AP-24, no. 3, pp. 310–316, May 1976.
3. D.A.McNamara, "Direct synthesis of optimum difference patterns for discrete linear arrays using Zolotarev distributions", *IEE Proceedings H on Microwaves, Antennas and Propagation*, vol.140, no.6, pp. 495–500, December 1993.
4. P. Lopez, J. A. Rodriguez, F. Ares, and E. Moreno, "Sub array weighting for the difference patterns of monopulse antennas: Joint optimization of sub array configurations and weights," *IEEE Transactions on Antennas and Propagation*, vol. 49, no. 11, pp. 1606–1608, November 2001.
5. A.F. Morabito, T.Isernia, M. D'Urso, "Synthesis of difference patterns via uniform amplitude sparse arrays," Electronics Letters, vol. 46, no.8, April 2010.
6. M. Satyanarayana, G.S.N.Raju, "Generation of Asymmetrical Difference Patterns from array antennas," International *Journal of Electronics and Telecommunications*, vol.57, no.2, pp. 184-190, 2011.
7. A. A. Khan and A. K. Brown. "Difference pattern synthesis using a particle swarm optimizer," *Antennas & Propagation Conference (LAPC 2009), Loughborough*, pp. 329-332, IEEE, November 2009.
8. S. Caorsi, A. Massa, M. Pastorino, and A. Randazzo "Optimization of the difference patterns for monopulse antennas by a hybrid real / integer-coded differential evolution method," *IEEE Transactions on Antennas and Propagation*, vol. 53, no. 1, pp. 372–376, January 2005.
9. T.A.N.S.N. Varma, Dr.G.S.N. Raju, " Investigations on generation of very low side lobe difference patterns for EMC applications," *IOSR Journal of Electronics and Communication Engineering*, vol. 9, no. 3, pp. 8-13, 2014.
10. J.R. Mohammed, "An Alternative Method for Difference Pattern Formation in Monopulse Antenna." *Progress In Electromagnetics Research Letters*, vol.42, pp. 45-54, 2013.
11. G. Yanchang, M. Meng, S. Xianrong, F. Nenghang, "Design of aperture distributions for difference pattern from Taylor distributions," *Antennas and Propagation Society International Symposium, 1993. AP-S. Digest*, vol., no., pp.1586-1589, vol.3, June 28 1993- July 2 1993.
12. YanChang Guo, Meng Miao, "Design of antenna array aperture distributions for difference pattern using Dolph-Chebyshev distribution," *Microwave Conference Proceedings, 1993. APMC '93., 1993 Asia-Pacific*, Hsinchu, vol.1, pp.58-61, 1993.
13. Randy L. Haupt, "Thinned Arrays using Genetic Algorithms," *IEEE Transanctions on Antennas and Propagation*,vol. 42, no. 7, pp. 993-999, July 1994.
14. V.Rajya Lakshmi and G.S.N.Raju, "Optimization of Radiation Patterns of Array Antennas," PIERS Proceedings, Suzhou, China, pp.1434-1438, 12-16 September 2011.

15. Mangoud, M.A.A. and Elragal, H.M. ''Antenna array pattern synthesis and wide null control using enhanced particle swarm optimization'', Progress in Electromagnetics Research B, 17, pp. 1–14 (2009).
16. Quevedo and Rajo, "Ant Colony Optimization in Thinned Array Synthesis with Minimum Sidelobe Level," *IEEE Antennas and Wireless Propagation Letters*, vol. 5, Issue 1, pp. 349-352, Dec. 2006.
17. Kenneth V.Price, Rainer M. Storn, Jouni A. Lampinen, *Differential Evolution: A Practical Approach to Global Optimization*, Springer, 2005.
18. Elliot, Robert S.,"Antenna theory and design", Revised edition, Chapter-5, pp. 142-190, John Wiley and Sons, Inc., 2003.

Analyze and Implementation of Inter-Carrier Interference Reduction Technique in OFDM System

T. Srinivas Reddy, J. Prabhakar, CH. Shekar

Abstract*: This article introduces a new method of self-cancellation (modified technique of self-cancellation) using a zero gab self- cancellation methodology. In the technique suggested, zero sub-carriers are often used to mitigate the interference of the two neighboring sub-carriers main lobes in addition to zero subcontractors and the method being proposed also used to limit the impact of other sub-carriers side lobes. The modified self-cancelling technology provides the best performance in respect of the CIR and the Bit-Error (BER) ratio only compared with the conventional technique. The adder module interference estimator also often needs data path units in this paper. Mostly as a result, a detailed explanation is still based on increasing the delay in capacity of the adder. The Ripple adductor and the output of the skip adder of each step depends on the previous carrier, but once it is returned to hold tree adders, it produces the transmission signals in O(log n) time and is regarded to have been the simplest and best VLSI output. The Kogge-Stone, Sparse Kogge-Stone and spanning tree adder are compared to the Ripple Carry Adder (RCA).

***Index Terms*: Carrier to Interference Power Ratio, Orthogonal Frequency Division Multiplexing (OFDM), Inter Carrier Interference (ICI), Kogge stone adder, Spanning Tree adder**

I. INTRODUCTION

The OFDM plays a significant role in broad-band based communication systems, like high-definition Tele-vision's (HD-TVs), Digital Audio-Broadcasting (DAB), local wireless networks (such as HIPERLAN/2 and IEEE-802.11a). Generally, OFDM promises the supreme modulation scheme encoding digital data on many carrier frequencies [1]. And their subcarrier is elegantly spaced and overlapped, because of this overlapping spectrum; OFDM has a higher data rate transmission capability with a high bandwidth efficiency, making OFDM robust to multi-path fading. The OFDM case of multi-carrier modulation is very supreme. The general theory of OFDM is that by splitting the higher speeds in the data into numerous lower data rate and by modulating each one of these new low data rate signals with the orthogonal frequency channel or subcarrier, they are combined to generate the original signal at the receiver end.

Given the immense economic advantages, the OFDM scheme also has drawbacks including PAPR (peak-average power ratio);

Revised Manuscript Received on December 22, 2018.

Dr. T. Srinivas Reddy, Associate Professor, Dept. of ECE, Malla Reddy Engineering College (A), Main Campus, Hyderabad, India,.

J. Prabhakar, Assistant Professor, Dept. of ECE, Nalla Malla Reddy Engineering College, Hyderabad, India.

CH. Shekar, Assistant Professor, Dept. of ECE, Teegala Krishna Reddy Engineering College, Hyderabad, India

it may be more susceptible to frequency or phase offsets usually resulting from either a mismatch of frequencies of transmitter and oscillator receivers which impact on the orthogonality of OFDM structures and possibly cause intercarrier interference (ICI). The authors propose various techniques for ICI reduction, like [5-15], etc. These techniques are mainly used for the modulation techniques BPSK and QPSK. The self-cancelling technique is frequently always used to suppress ICI using the proposed methods due to its practicality and its easy operation. New methods are used in this paper to reduce the impact of ICI.

II. INTER-CARRIER INTERFERENCE (ICI) PROBLEM OVERVIEW

The loss of orthogonality among sub-carriers causes ICI, which affects both channel estimation and detection of OFDM data symbols. In OFDM, the sub - carriers ' spectra overlap, but stay orthogonal. ICI is alluded to as interference due to data symbols on adjacent sub-carriers.

Y(k) is the Discrete Fourier Transform of *y(n)*. Then we get,

$$Y\left(k\right)=\sum_{n=0}^{N-1}x_n\,exp\left(\frac{j2\pi nm}{N}\right)exp\left(\frac{-j2\pi nk}{N}\right) \quad (1)$$

$$=\sum_{n=0}^{N-1}\left(\frac{1}{N}\right)\sum_{n=0}^{N-1}X_n\,exp\left(\frac{j2\pi nm}{N}\right)exp\left(\frac{-j2\pi n\left(\varepsilon-k\right)}{N}\right) \quad (2)$$

$$=\left(\frac{1}{N}\right)\sum_{n=0}^{N-1}X_n\,exp\left(\frac{j2\pi n\left(m+\varepsilon-k\right)}{N}\right) \quad (3)$$

Carrier to Interference Ratio: The aim of all ICI reduction algorithms is to achieve a greater CIR value. The current standard OFDM mathematical CIR can be authored as:

$$CIR=abs\left(S\left(0\right)\right)\div\sum_{\substack{i=0\\ i\neq k}}^{N-1}abs\left(\left(l-k\right)\right) \quad (4)$$

This equivalence can be practical aimed at all types of modulation and any amount of subcarriers.

Several Schemes of ICI minimization are, shown below as;

- Time-Domain Windowing
- Frequency-Domain Equalization
- Self-Cancellation of ICI
- Shaping The Pulse values

The primary two of above-mentioned four schemes are initial approach; the other two are very attractive.

III. SYSTEM MODEL FOR PULSE-SHAPING & SELF-CANCELLATION PERFORMANCE

Pulse shaping: It is clear that, the spectrum of each and every carrier of OFDM comprises of main theme accomplished by various sides with prominent minimization in amplitudes. As well as, it is preserved orthogonally, then there is no inference over other carriers when presence of null-spectrum at top of each carrier. This is really the component of all other carriers even at that point. The single carrier would therefore be easily separated. Though when the frequency offset occurs, the orthogonally is destroyed just because the spectral null does not correspond with each carrier's peak. However, the power of some side lobes at center of adjacent carriers called as ICI power ranges. The ICI power is increased continuously by maximizing the frequency off-sets. The main aim of pulse forming is to minimize the lateral lobes. It may somehow decrease substantially with side lobes, and then the ICI power will indeed be minimized dramatically.

ICI self-cancellation: Either the discrepancy here between the ICI coefficients of two consecutive sub-carriers was shown to be quite tiny. This constitutes the basis for the self-annulment of ICI. The respective data symbol is always un-modulated elsewhere in single sub-carriers, although with two successive dual sub-carriers. If "a" is highly modulated on first sub-carrier then "a" is modulated as second sub-carrier. Thus, ICI in between of dual sub-carriers vanishes each-other. These techniques are appropriate for fading the multipath channels since no estimation of channels is necessary here. Due to the failure of estimates for the multipath channel as the channel changes randomly.

IV. ANALYTICAL EVALUATION OF ICI SELF-CANCELLATION SCHEME

The main concept of this scheme is to modulate the main input function ofone data symbol in a certain group of sub-carriers with estimated co-efficients based on produced ICI signals which are cancelled each other in that group named as self-cancellation. The ICI self-cancellation scheme requires that the transmitted signals be constrained such that

$$x(1) = -x(0), x(3) = -x(2)..x(N-1) = -x(N-2) \quad (5)$$

Then the received signal on subcarrier k becomes

$$Y'(k) = \sum_{l=0, l=even}^{N-2} x(l)\left[S(l-K) - S(l+1-k)\right] n_k \quad (6)$$

Signal received on subcarrier k+1 converts

$$Y'(k+1) = \sum_{l=even}^{N-2} x(l)\left[S(l-K-1) - S(l-k)\right] n_{k+1} \quad (7)$$

and the ICI coefficient $S'(l-k)$ is denoted

$$S'(l-k) = S(l-k) - S(l+1-K) \quad (8)$$

At the demodulator the received signal at the $(k+1)^{th}$ subcarrier, where k is even is subtracted from the k^{th} subcarrier. This is expressed mathematically as

$$Y''(k) = Y'(k) - Y'(k+1) \quad (9)$$

$$= \sum_{l=0}^{N-2} X(l)\left[-S(l-k-1) + 2S(l-k) - S(l-k+1)\right] + n_k - n_{k+1} \quad (10)$$

Subsequently, the ICI coefficients for this received signal becomes

$$S''(l-k) = S(l-k-1) - 2S(l-K) - S(l-k+1) \quad (11)$$

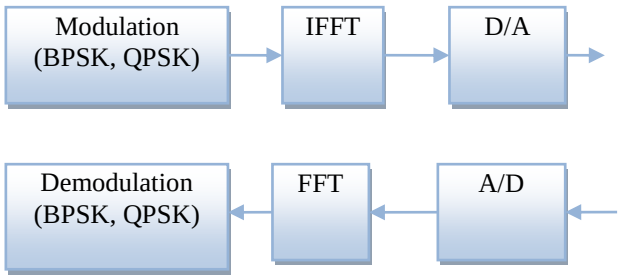

Fig.1: General OFDM structure

V. METHODS & METHODLOGY

Modified self-cancellation:
Either carrier comprises of a principal lobe in the OFDM continuum and simply follows several side lobes mostly with deteriorated amplitudes as illustrated in figure2. The approach (modified self-cancellation) is advocated just using a zero gab to mitigate noise from the main lobe (adjacent subcarrier) and also the traditional self-cancellation technology to alleviate the effect of side lobes. Using those same two methods and techniques, maybe the next portion looks slightly better results for CIR and BER. The entry symbol is modulated into three subcarriers, with one subcarrier carrying zeros so that the main lobe power is cancelled from the nearby subcarrier. The primary role of some of the other two subcomponents is to decrease ICI components from side-lobes. The main drawback to this mechanism is the incompetency in bandwidth, but it may be surmount by reducing the level of QAM or by expanding the number of sub-carriers. Maybe this technique reintroduces redundancy into the symbol because only one data symbol is transmitted for each three sub-carriers.

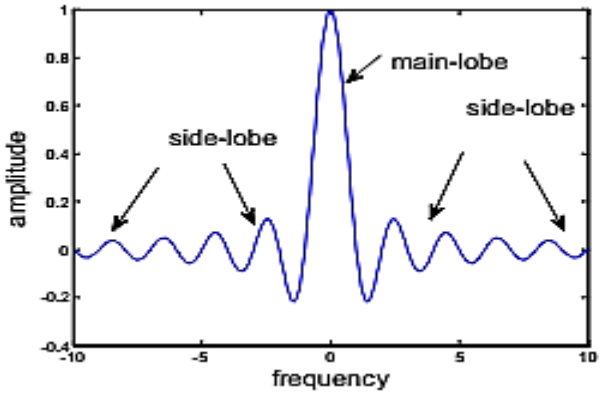

Fig.2: General OFDM spectrum

When the signal is moved in frequency and is adversely affected by an AWGN noise, the signal obtained at subcarrier k is indicated as follows:

$$Y'(k) = \sum_{l=0,3,6}^{N-3} x(l)\left[S(l-K) - S(l+1-k)\right] n_k \quad (12)$$

and the received signal at sub-carrier $k+1$ is:

$$Y'(k+1) = \sum_{l=0,3,6}^{N-3} x(l)\left[S(l-K-1) - S(l-k)\right] n_{k+1} \quad (13)$$

This mitigates and neglects the adverse effect of main - lobe noise consumed in carriers k+2 and k-1 at the recipient. The main lobe noise is a critical component of the undesired signal.

Furthermore, the consequence of the particular side-lobe can be condensed by deducting *Y'k* from *Y'k+1*

$$Y_k'' = Yk' - Y(K+1)'$$

$$Y_k'' = \sum_{l=0,3,6}^{N-3} X(l)\left[-S(l-k-1) + 2S(l-k) - S(l-k+1)\right] + n_k - n_{k+1} \quad (14)$$

$$Y_k'' = X_k(-S(-1) + 2S(0) - S(1) + \sum_{l=0,3,6}^{N-3} X(l)\left[-S(l-k-1) + 2S(l-k) - S(l-k+1)\right] + n_k - n_{k+1} \quad (15)$$

Somewhere above eq. (15) is the signal obtained when after de - mapping. There are three components on the right side of this equation: from eq.(16) it can be determined that the CIR for the technique suggested is offered mostly by:

$$CIR = \frac{(-S(-1)+2S(0)-S(1))}{(\sum X(l)_{(l=0,3,6)}^{(N-3)}[-S(l-k-1)+2S(l-k)-S(l-k+1)]+n_k-n_{(k+1)})} \quad (16)$$

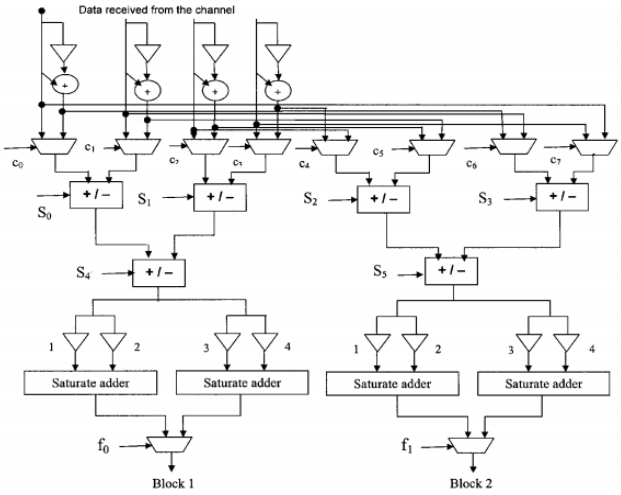

Fig.3: Interference adder

Proposed Parallel prefix adders:

The proposed adder is that we really using the PPA in place of simply saturated adder like a carry look ahead adder. Perhaps the production of carriers with prefix adders [16] can be predicated on the additional requirements in many completely different ways. Maybe we just use tree structure particular form to significantly increase arithmetic operation speed [3]. Faster adders [16] are parallel prefix adders [4] that can be used for high-performance arithmetic structures in industry. The addition of the parallel prefix is done in 3 steps.

Pre-processing stage: In this section the generation and propagation of signals that are supposed to generation input carry for every adder section

$$P_i = A_i \; EX\text{-}OR \; B_i \quad (17)$$

$$G_I = A_i \; AND \; B_i \quad (18)$$

Carry generation network: In this section the computation of carry for every bit is carried out where it utilizes the propagate and try to generate as intermediate signals.

$$P(i:k) = P(i:j) \,.\, P(j-1:k) \quad (19)$$

$$G(i:k) = G(i:j) + (G(j-1:k) \,.\, P(i:j)) \quad (20)$$

Post processing stage: It is the last stage that calculates the accumulation of the input bits. It is identical for all the adders and sum bit equation given

$$S_i = P_i \, C_i. \quad (21)$$

$$C_{i+1} = (P_i.C_0) + G_i \quad (22)$$

VI. RESULTS & DISCUSSION

It is clear that the OFDM transceiver has been used and simulated using MATLAB. The modulation new scheme has been chosen, completely different values have been used for the standardized frequency (0.2, 0.4, 0.6 and the outcomes are shown respectively in the actually figure below.

Table 1: Simulation Parameters

Parameters	Value
N	128
Sym_no	1000
Normalized frequency(ep)	0.2, .0.4, 0.6
SNR	[0:0.5:20]
Transmission mode	MIMO=4

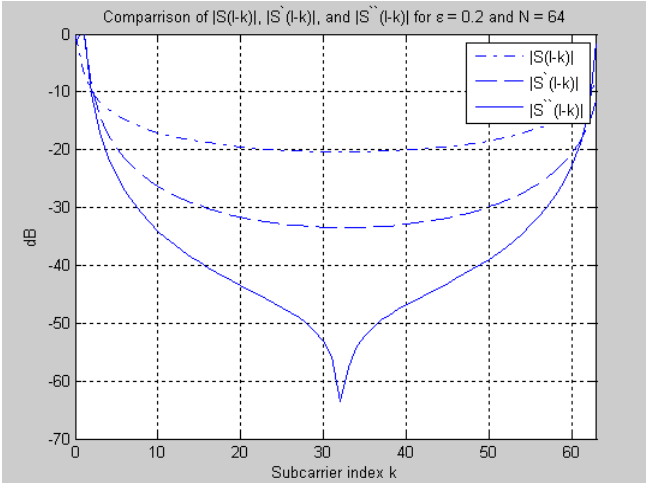

Fig.4: Comparison of $|S\ (l-k)|$, $|S`\ (l-k)|$, and $|S``\ (l-k)|$ for $N = 64$ and $\varepsilon = 0.4$

Figure.4 shows the attractive comparisons between $|S'\ (l-k)|$ & $|S\ (l-k)|$ based on log-scale. It shows the $|S'\ (l-k)| << |S\ (l-k)|$ is valuable for certain $l-k$ values.

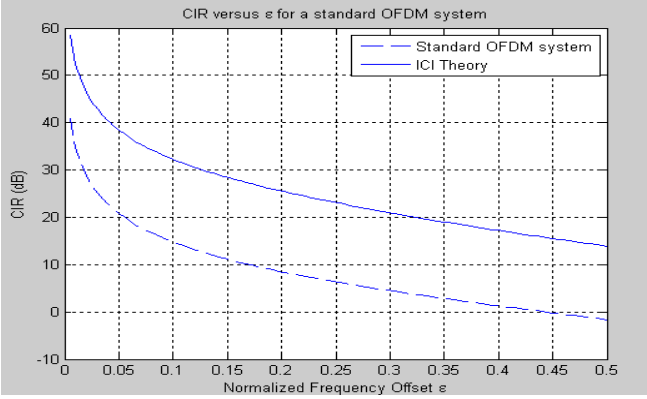

Fig.5: CIR versus ε for a standard OFDM system

Figure.5 illustrates the contrast, computed, the CIR of a regular OFDM system of self-cancelled ICI system. Although, the self-cancelled ICI strategy comprises of various trade-offs between the power traffic and bandwidth.

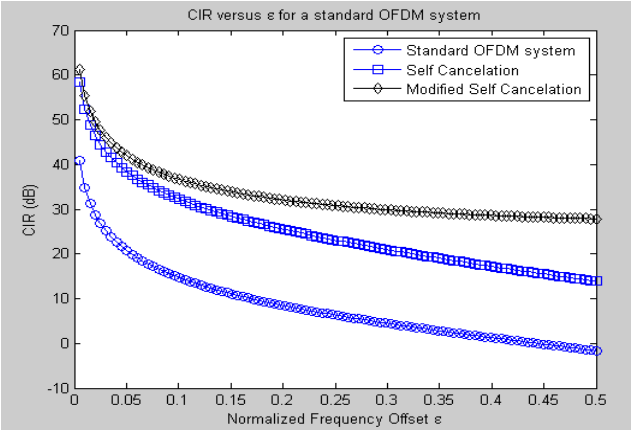

Fig.6: CIR curve for different schemes. (Theo ≡ theoretical).

The CIR is being used to equate and assess the outcomes of the two drastically different cancelation strategies. The CIR ratio of the suggested frequency offset system can also be seen in Figure.6 above, epsilon= 0.5. CIR is the percentage of carrier signal strength obtained to the noise signal obtained at the receiver. In decibels (dB), CIR is represented. The Carrier-to-Interference (CIR) ratio is high for low frequency offset values as the frequency offset μ also often reduces the carrier-to-interference ratio. When the CIR ratio is high, the quality of the received signal will be considerably better.

ISE Simulator (ISim):

ISim offers an excellent, total, ISE-integrated HDL simulator. ISE Simulator (ISim) is a Hardware Description Language (HDL) simulator that allows us to start performing VHDL, Verilog and mixed-language functionality (behavioral) and timing simulations. The ISE project browser generates all commands for simulation to prepare the ISim simulation and automatically runs in the background during the simulation with the Kogge Stone Adder flow. Table-2 shows the use of these adders for delays, power and devices. We have observed that the adders of parallel prefixes are quicker as related to adder. The outcomes of the various parallel prefix adders are shown below.

Synthesis result

The utilized device consists of following, such as

Logic Distribution
Logic Utilization
Total Gate-Count

The summary of utilized devices are shown above with a certain details of pre-requisite devices utilized from respective devices.

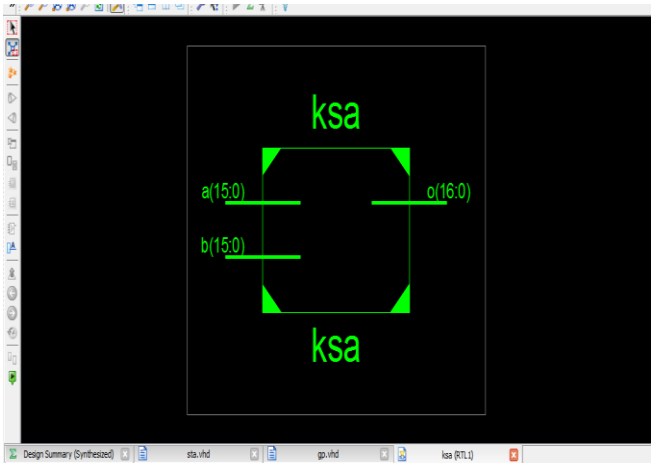

Fig.7: RTL schematic of kogge stone adder

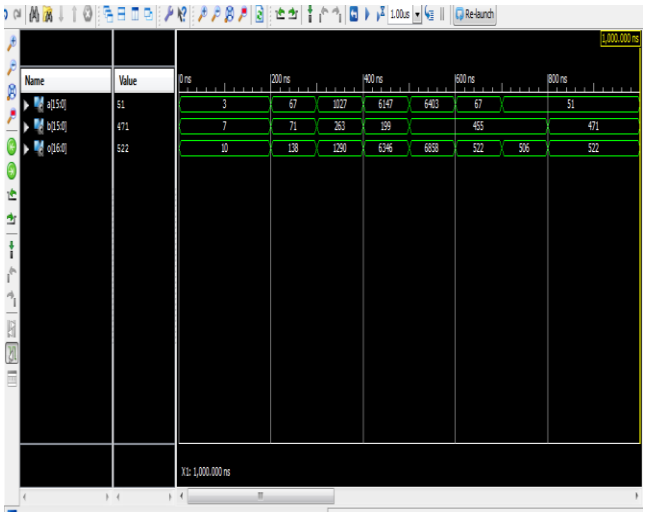

Fig.8: simulation result of kogge stone adder

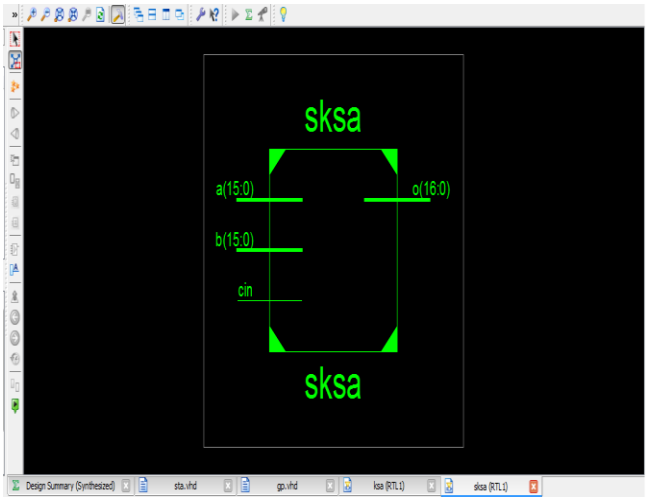

Fig.9: RTL schematic of sparse kogge stone adder

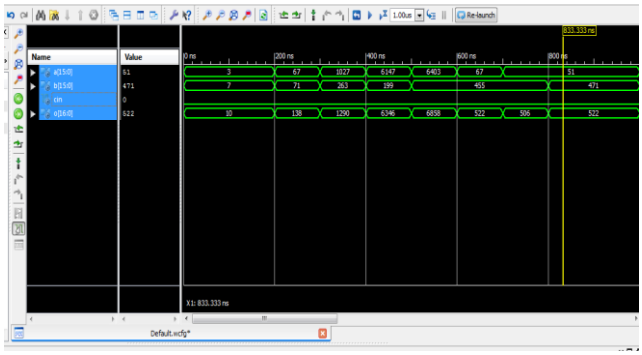

Fig.10: Simulation result of sparse kogge stone adder

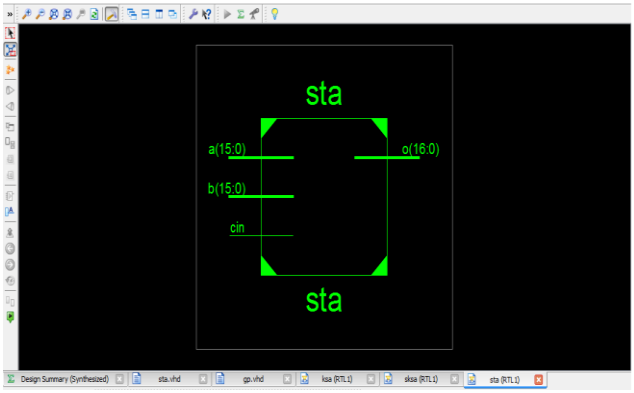

Fig.11: RTL schematic of spanning tree adder

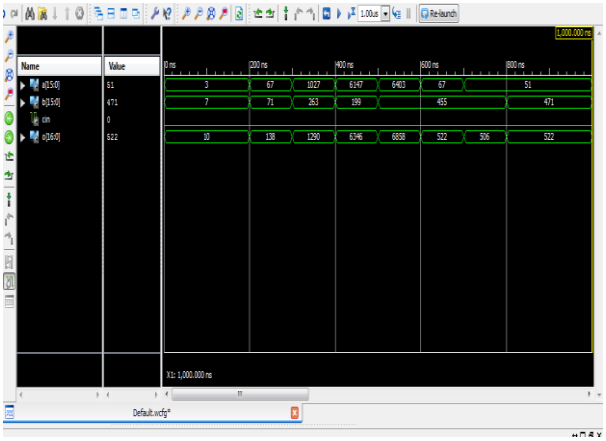

Fig.12: simulation result of spanning tree adder

Table-2 Delays, Power and Device Utilization for various Adders

Adder Name (16 bit)	Xilinx ISE 13.2 Tool delay (in ns)	From Ref [2] Delay (in ns)	Power (in Watts)	Device Utilization in (LUTs, IOBs) (69120, 640)
Ripple carry adder	3.853	2.578	1.211	5,13
Kogge stone adder	6.688	6.286	1.220	71,50
Sparse Kogge stone adder	8.014	-------	1.179	28,50
Spanning tree adder	6.667	-------	1.179	30,49

VII. CONCLUSION

In this paper, we made an attempt of reintroduce some of the ICI cancellation approaches which in turn improvise the OFDM environment in the wireless communication system. The primary attempt made on the self- cancellation methods for guarding the ICI in OFDM for various frequencies offset values explicitly. Secondly the implementation of kogge-stone adder is generating with help of FPGA and tries achieving low power and area resources.

REFERENCES

1. Ghassan M. T. Abdalla, "Orthogonal Frequency Division Multiplexing Theory and Challenges", UofKEJ, Vol. 1, Issue 2, pp. 1-8, (October 2011).
2. David H. K. Hoe, Chris Martinez and Sri JyothsnaVundavalli, Design and Characterization of Parallel Prefix Adders using FPGAs, 2011 IEEE 43rd Southeastern Symposium in pp. 168-172, 2011.
3. D. H. K. Hoe, C. Martinez, and J. Vundavalli, "Design and Characterization of Parallel Prefix Adders using FPGAs,"IEEE 43rd Southeastern Symposium on System Theory, pp. 170-174, March 2011.
4. R. Zimmermann, "Non-heuristic operation and synthesis of parallel-prefix adders," in International workshop on logic and architecture synthesis, December 1996, pp. 123-132.
5. Jeon WG et al. An equalization technique for orthogonal frequency-division multiplexing systems in time-variant multipath channels. IEEE Transaction on Communication. 2001; 47(1):27–32.
6. Husna AN, Kamilah SYS, Ameruddin B, Mazlina E. Intercarrier interference (ICI) analysis using correlative coding OFDM system. Conference on Digital object Identifier RF and Microwave Proceedings. 2004. p. 235–7.
7. Wang C-L, Huang Y-C, Shen P-C. An intercarrier interference suppression technique using time-domain windowing for OFDM systems. IEEE Conference on Vehicular Technology. 2006 May; 5. p. 2518–22.
8. Ryu H-G, Li Y, Park J-S. An improved ICI reduction method in OFDM communication system. IEEE Transaction on Broadcasting. 2005; 51(3):395–400.
9. Zhao Y, Haggman S. Intercarrier interference self-cancellation scheme for OFDM mobile communication systems. IEEE Transaction on Communication. 2001; 49 (7):1185–91.
10. Fu Y, Ko CC. A new ICI self-cancellation scheme for OFDM systems based on a generalized signal mapper. Proceedings 5th Wireless Personal Multimedia Communications. 2002; 3:995–9.
11. [11]. Peng Y-H. Performance analysis of a new ICI-Self cancellation-scheme in OFDM systems. IEEE Transaction on Consumer Electronics. 2007; 53(4):1333–8.
12. Kumbasar V, Kucur O. ICI reduction in OFDM systems by using improved Sinc power pulse. Digital Signal Processing. 2007 Nov; 17(6):997–1006.
13. Sathananthan K, Athaudage CRN, Qiu B. A novel ICI cancellation scheme to reduce both frequency offset and IQ imbalance effects in OFDM. Proceedings IEEE 9th International Symposium on Computer Communication. 2004 Jul; 708–13.
14. Yeh H-G, Chang Y-K, Hassibi B. A scheme for cancelling intercarrier interference using conjugate transmission in multicarrier communication systems. IEEE Transaction on Wireless Communication. 2007 Jan; 6(1):3–7.
15. Wang C-L, Huang Y-C. Intercarrier interference cancellation using general phase rotated conjugate transmission for OFDM systems. IEEE Transaction on Communication. 2010 Mar; 58(3).
16. Y. Choi, "Parallel Prefix Adder Design", Proc. 17th IEEE Symposium on Computer Arithmetic, pp. 90-98, 27th June 2005.

International Journal of Natural Computing Research
Volume 8 • Issue 2 • April-June 2019

Cost Minimization Through Load Balancing and Effective Resource Utilization in Cloud-Based Web Services

More Swami Das, Malla Reddy Engineering College (A), Hyderabad, India & Research Scholar, JNTUH, Hyderabad, India


https://orcid.org/0000-0001-5266-0754

A. Govardhan, JNTU Hyderabad, Hyderabad, India

Doddapaneni Vijaya Lakshmi, MGIT, Hyderabad, India

ABSTRACT

With the growth of internet-based applications and the explosion of consumers, cloud-based web service applications have become more common and the importance of minimizing the cost, increasing the interactivity, and management and efficient use of resources has become high. Existing methods like fixed cost per month no longer satisfy the application maintenance costs of the modern app developers. In this article, the authors propose an enhanced model for improving efficiency; maximize availability and minimizing the cost of cloud-based web applications. The authors have conducted experiments on grid dataset and analyzed the results using several algorithms on the load balancer with the multilevel optimized shortest remaining time scheduling method. The analysis clearly proves that applying a "pay as you" go mechanism will substantially reduce the cost and will improve the efficiency which resources are utilized. The results clearly suggest improvements in cost minimization and effective utilization of resources leading to effective utilization of services.

KEYWORDS

Cloud Computing, Cost Optimization, QoS, Resource Utilization

1. INTRODUCTION

In 1961, utility computing was used, and in 1969, ARPANET was used to connect the systems for information exchange. In 1979 USENET was used for information exchange, and in 1983 TCP/IP model and protocol suite were used for network communication. In 1991, the World Wide Web was invented by Tim Berners-Lee, a Scientist, and Engineer, with web information to connect the systems. The technological advancements have benefited internet applications. In 1999 Grid computing was used on geographically distributed systems in 2000 ubiquitous access configuration of resources networks storage and services on demand inception of cloud computing. In 2012 big data was used for data processing and applications, the technological advancements now the Internet of Things (IoT) using sensors to get data and process, analyze and operation of various application like Home appliances, smart cities etc. Web services are functional services over the internet. Cloud computing is an internet-based computing that provides information processing, computation services, and

DOI: 10.4018/IJNCR.2019040103

resources to the user as pay as you go manner (For example, computer systems, servers, storage and applications).

The growth of internet-based applications which are used by billions of devices in the world and the demand for cloud-based web applications are high. The service provider adds the technical infrastructural services based on the demand of users with affordable cost, minimum maintenance, shared resources, improved performance, increase the data operations parallel processing, scalability, reliability elasticity, and secured applications. In the 21st century cloud-based web application services pay as you manner, to meet the performance of applications by resource, network, load balancing, and Management applications. Considering web traffic at peak hours to access the services, managing the Cloud resources by performance and cost factors. In the development of Cloud-based web applications models service providers, users, designers in a service organization, the most important non-functional parameter is the development cost, maintenance cost to be minimized and optimize and provide the services to the end users.

The rest of the article is organized as follows: Section 2 deals with related work and Section 3 with the proposed method. The Sections 4 and 5 deal with experimental results and discussions, respectively. Finally, section 6 draws the conclusion.

2. RELATED WORK

2.1. Problem Definition

The objective is to provide cloud-based web applications with a minimum cost to run the services or applications without compromising on the functionality, latency, throughput, reliability, scale and other aspects. This enforces the effective use of services by the applications as well as pushes optimizations on the data center in such a way that it effectively allocates the use of resources. There are various needs and Service Level Agreement (SLA) required for the services backing the web applications during different phases of the product lifecycle i.e. development, deployment, maintenance etc. The problem focuses on delivering a mechanism to minimize the project cost during the various phases. The motivation of the cost minimization for Cloud-based web services comes from the service providers capability to control the feature set of the services provided based on the desired SLA as opted by the end user. This will enable the end user to provide the service with the desired feature set and minimum cost. The tasks, cost, load, and availability are described in Equation 1-4.

Let there will N number of DCs/Servers to process the cloud-based web applications, tasks t_1, t_2,…, t_n for allocating process:

$$tij = \begin{cases} 1 & if\ succussful \\ 0 & for\ unsucessful \end{cases} Tasks \tag{1}$$

For minimization of:

$$Total\,cost = \sum_{i=1}^{n} \left(\mathrm{C1} + \mathrm{C2} + , .. , \mathrm{Ci} , + \mathrm{Cn} \right) \tag{2}$$

subject to a load of the server where:

$$load = \frac{\text{Number of applications running on server}}{\text{Total number of applications}} \tag{3}$$

and effective utilization of services by the availability of the system:

$$availability\,of\,server = \frac{\text{No of requests over number of applications}}{\text{Total number of applica ations}} \tag{4}$$

2.2. Literature Survey

The Total Cost of Ownership (TCO) proposed by Panagiota Nikolaou in 2015, key optimization data center design, the model framework is used for availability, hardware and software resources. The performance by power single and dual channel in Web service by TCO model failure rate and cost estimated (Nikolaou, Sazeides, Ndreu & Kleanthous, 2015).

(M. Zivkovic,2011) proposed a model sequential decision for composite service request used for decisions optimal dynamic programming by backward decision structure and forward decision structure which use of cost, and response time of application. Pengcheng Xiong in 2011, proposed decision application level (adaptive feedback controller) has a robust workload based on resources on demand. Cloud computing is the Service Level Agreement (SLA) of the service provider to ensure that the quality of services by PaaS components. The web application uses multiple tiers (N-tiers), the controller, application decision maker with different levels of resources and minimizes total resource cost by managing the workload.

(Mathias, 2011) studied two replication strategy is arrival rate and response time policy, by optimizing service replication in Cloud, load replica operating cost depends on arrival rate, response time and policy. The service oriented architecture (SOA) system use service level agreement (SLA) at cost-effective, cost-saving, and balancing load multiple replicas. The service replicas have a low response time, low utilization of active replicas, control service replica utilization, the minimum number of active replicas. C. Tian in 2011, proposed optimal load balancing technique for web applications, allocation servers to maximize throughput and cost minimization. David Breitgand in 2015, proposed an Elastic Service virtual resources workload conditions, SLA virtual data centers, to manage solution quality and computation time. Service (IaaS) cloud computing, the Virtual Machine (VM) instances-based workload the user need to pay the cost, with minimum responsibility, the service is elastic, the behavior of the service is based on workload rules, optimization techniques to maximize profit.

Cloud computing has virtual scalable computing resources, Peng Zhang in 2012, proposed cost optimization to provide data services, parallel scheduling and minimize cost applications with the execution of computations cloud services. The Greedy algorithm minimizing the cost and random task. Tao in 2012, proposed a cost-effective algorithm model which optimize multiple resources based on system preference.

Farhana Kabir 2012, proposed autonomous, self-scaling, cost-effective cache for data-intensive applications, the user cost and performance considerations. Sheng Liu in 2012 proposed optimal service composition execution cost based on Quality state matrix, and execution service and the service requestor need to pay for every successful execution. Adnan Ashraf in 2013, proposed cost-effective VM multi-tier application for video applications to find an optimal solution by meta-heuristic approaches for web application. Jing Jiang in 2013, proposed an auto-scaling Cloud resource, VM for Web application providers optimized latency and SLA. Suhradam Patel in 2013, proposed a cost-minimizing by workload monitoring by grouping Virtual Machines (Wang, Shen, Di, Li & Zhou, 2013). Lijuan Wang in 2013, proposed service computing, a compositional model for data-intensive applications.

Y. M. Xia in 2013, proposed Quality optimization and redundancy removal algorithm which reduces the memory cost and improves performance (Wu & Nie, 2013). Web service is available on the Internet with the best quality of web service satisfying all functionalities. Min Yao in 2014,

used Cloud brokerage service which helps the Cloud computing by approximation and trace-based evolutions which minimize cost. Song Li in 2014, proposed Hybrid cloud computing optimization model by dynamic provision algorithm. Lu in 2014, proposed Server virtualization and game-changing technology which will maintain and high utilization of resources and reduce cost data center. Rui Zhu in 2014, proposed comprehensive cost model used for video webcast operators with many CDN networks use of ISP and CDN cloud server providers. Satish Narayana in 2014, Cloud Computing elasticity policy has optimum setup for Cloud workload. Amazon load trace control flow components for enterprise application with use of XOR and AND operators, and auto-scaling of Web services. Z. Ren in 2014, studied workload analysis of E-commerce application, and used job scheduling algorithm and proposed Fair4S, Hadoop scheduler handling for small jobs.

Waheed Iqbal (2018) proposed a pro-active auto-scaling approach used to manage the applications based on dynamic workload and probabilistic workload patterns, predictions. fog-based interval identifies application workload using URI, distributions and predicting workload by arrival rate, average response time and auto-scaling. Maria, 2018 proposed scientific instrument workflow as service (WaaS), for deployment of applications using infrastructural facilities with use of many workflows minimize the overall cost for infrastructure resource each individual workflow. The performance is analyzed Dyna, Elastic resource Provisioning and Scheduling - Multiple workflows (EPSM) approach.

Syed Aon Ali (2018) proposed a cloud, a fog-based method with use of Energy Management System to maintain electricity for a huge number of complex smart grid applications and load balancing methods. Satapathy et al. (2016) use a contiguous link scheduling, Bhateja et al. (2018) use a FOO DBMS method to optimize the query, and Satapathy et al. (2018) use load balancing to minimize the cost of cloud-based web applications.

2.3. Proposed Model and Architecture

The proposed enhanced automated cloud services consist of users, services, Management and resource utilization shown in Figure 1.

The users are the end users who can access the services pay as you manner, cloud services, and cost management with effective utilization of infrastructural resources.

2.3.1. Cloud Services

Cloud computing is an IT solution that enables end users to use resources from the cloud that are managed by the service providers and the layers underneath. Organizations are moving to cloud computing as it frees them from the management and maintenance aspects of the hardware and software and allows them to focus on their core scenarios without having to worry about other aspects. This flexibility comes at the cost of paying the service providers for the services consumed. More and

Figure 1. Web service and Cloud cost optimization model

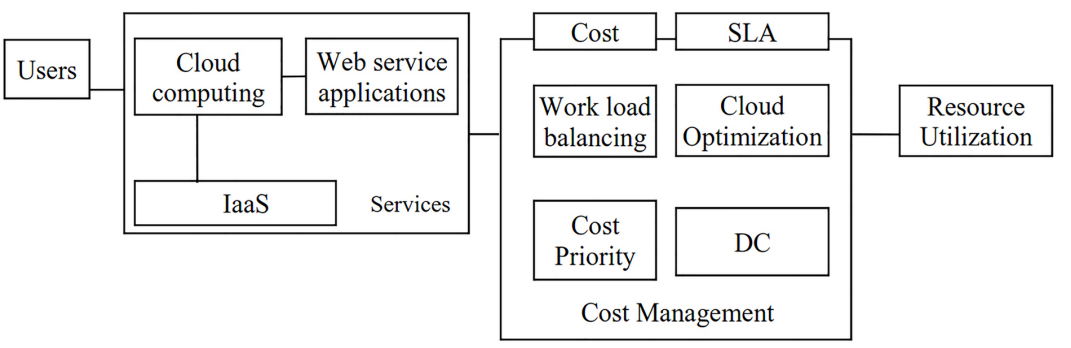

more services are moving away from a fixed cost per month model to a "pay as you go" model which allows the end users to provision the resources on demand and deflate them once they are done with using the resources. Cloud computing model users SOA principles and operates over a faster wide area network providing high virtualization of the underlying hardware, software, and infrastructure.

IaaS service related to infrastructural services cost maximum Cloud providers, multi-unit solution resource pools. The virtual machine service used by operational cost and elastic service. Figure 2. Shows Web services and cloud deployment model has users, web cloud servers, and deployment models. The user is the clients who can access service as "pay as you go" manner. The web and cloud server which has functional services and resources in which developer deploy the applications into public, private and hybrid cloud centers.

The Cloud computing models are divided into three types SaaS, PaaS, and IaaS. There are potentially two types of pricing models:

1. **Pay as you model:** In this model, the users are charged free for specific duration hardware, software, for example up to 15 GB free for Google cloud users. And after the specified free trial period is over, the users are charged based on the consumption of the resources. If the user does not consume the resource, they can save the cost;
2. **Fixed price model:** In this model, the users subscribe to the resources and pay a flat per month price for the resources that they bought from the service provider. The price does not vary based on the consumption, but the user is charged a flat fee irrespective of the extent of the resources consumed.

The goal of the pricing models is to empower the user by providing the user with different options such as a fixed flat rate vs a variable cost based on usage. This will enable the user to select the model based on their usage patterns. If the user has a usage pattern where the usage is constant, and the SLA requirements are harder, then the user will preferably go for the fixed price model. If the user has different workload patterns during different periods of the year, then "pay as you go" pricing model might suit better which would enable the user to scale down the services provided during the "off-peak" season and scaling the same up during the high-demand and critical seasons.

Figure 2. Web services and Cloud deployment

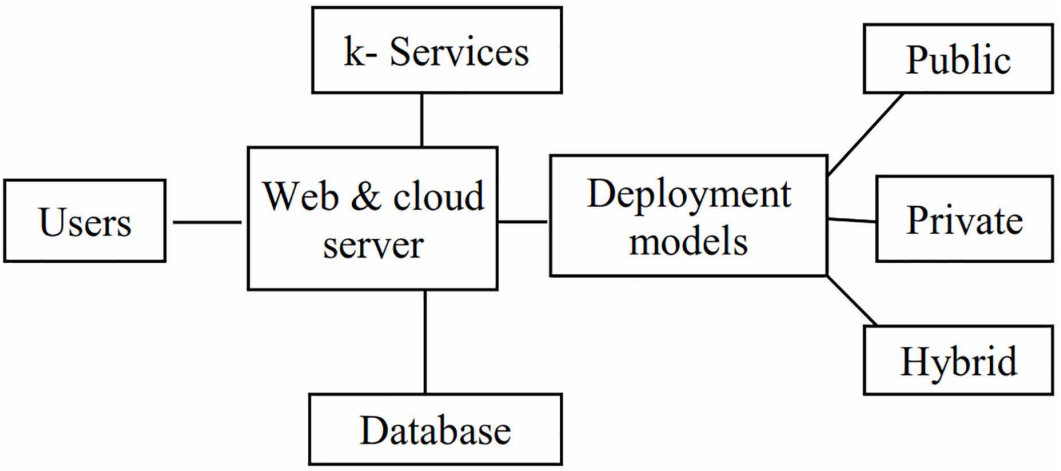

2.3.2. Infrastructure as Service (IaaS)

The lower layer basic computing capability of system use of operating system, storage, and services in the network, including hardware servers, memory and computing power etc. Cloud provider example, Amazon EC2, VMware, Web service Elastic Compute Cloud (EC2) and Simple Storage Service(S3). And other services described in Table 1.

Cloud computing by scalability application by variant load and elasticity of cloud servers based on load. The types of cloud services are public, private and hybrid cloud services.

2.3.3. Public Cloud Services

Are designed which are not for single or group enterprise applications, these are used by the parties, pay you manner servers with storage and services. In a public cloud, the cloud service provider, the customer chooses the best service provider with affordable cost. The request of service to process the service with the use of best proposals and needs.

2.3.4. Private Cloud

Is configured and available to only authorized users not for their party and public. Services in organizations network, bandwidth, and availability. In private Cloud services infrastructure located outside, the operating system provides the services to authorized users. For example, trusted customers in organization financial services.

2.3.5. Hybrid Cloud

The organizations use Cloud model both public and private modules in financial services, cost-effective infrastructure to the user. This is the combination of public cloud for internal use and used for consolidated, virtualized and potential resources. This is financial and business solutions (Papazoglou, 2012). The services can be functional and non-functional services, for example, functional services are APIs, Menus and application services to the user whereas Non-functional like infrastructural facilities, cost of application by Quality state matrix, execution services. The quality of services described by Equation 5:

$$Qualityofservice\left(QoS\right) = F\left(cost, availability, Responsetime\right) \tag{5}$$

The Internet Service Provider (ISP) will achieve maximum profit by the quality of services, for example, network bandwidth, delay, and bit, error rate, Wireless network systems are used based on customer satisfaction. In Cloud Computing automatic control cloud system used to optimize resources using on-demand computing model. Cost effective placement algorithm is a model cloud-based environment that uses the multi-resource model by adding the resources based on demand.

Table 1. Cloud services and examples

Service	Amazon	Microsoft	Google
SaaS	Operating system, memory, services	Microsoft Azure, Office 365	Google Docs, Gmail, Google Apps
PaaS	Elastic Compute Cloud	Micro soft Azure cloud	Data center, Google App engine
IaaS	Amazon EC2, servers, storage, networking	Microsoft Azure, servers, storage, networking	Google Cloud Platform (GCP) service, servers, storage, networking

The Cloud Service Provider (CSP)s such as Amazon, EC2, and Rockspace. The demand for resources based on the cost of applications. The software as service performs running applications, monitoring communication finance the model is formulated and analyzed by aiming to study the advantages of the data access to save the cost and space. The model is used to eliminate data duplication form memory (Indrawati, Puspita, Erlita, Nadeak, & Arisha, 2018).

Cloud-based web applications require Quality of Service, the demand of customer and optimized services. SOA components, cloud services. Load balancer use of dynamic resource allocation using hierarchical balanced tree topology, if load increases, management of cloud data centers by auto scaling and the load management is shown in Figure 3.

Software service (SaaS), running applications, and monitoring communication finance. Advantages are data can be accessed, save the cost and space, elimination of duplication. To analyze and formulate the model and balance them across the instances of available multiple zones.

In cloud computing, the workload depends on the number of systems logging interactive sessions, the computing capacity, variable workload, network management. The workload can be of two types 1) predictive workload 2) dynamic workload.

2.3.6. Predictive Workload

The workload of systems can be predicted based on the current load and past load characteristics like applications, memory, network usage, and others.

2.3.7. Dynamic Workload

Can be measured by considering the current load of the cloud-based web applications by considering the characteristics application in use, number of users, network bandwidth, scheduling, memory, DCs, and others. The submission of Machines into the systems in a cloud system which connected to proxy and virtual Node/system.

The intelligent workload management systems consist of the following components shown in Figure 4). Software applications can be identified with Data Center 2) Policy-based (Service Level Agreement): the provider promises the services based on cost and application at the time of Project assignment. 3) The client can access and identify the services 4) Performance, configuration, and Analysis and 5) secured physical and Virtual services. The above two workloads by considering the provisioning, scheduling, and Monitoring the cloud load applications.

The architecture of cloud load balancing is described here, it consists of Software applications, SLA and Middleware, operating system, servers, storage and analysis of performance and configuration, Management of services and Secured applications.

Figure 3. Load management

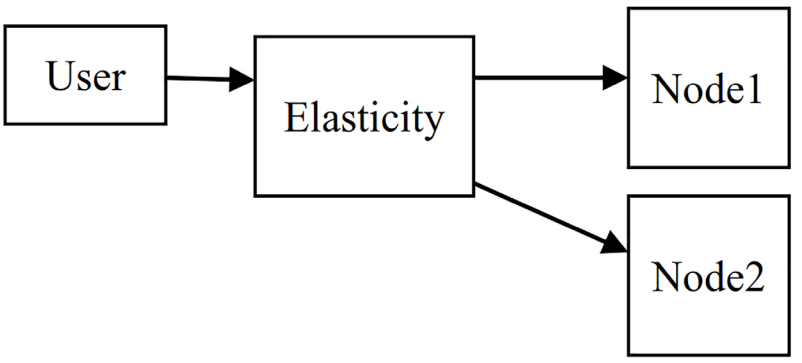

Figure 4. Cloud-based web application architecture

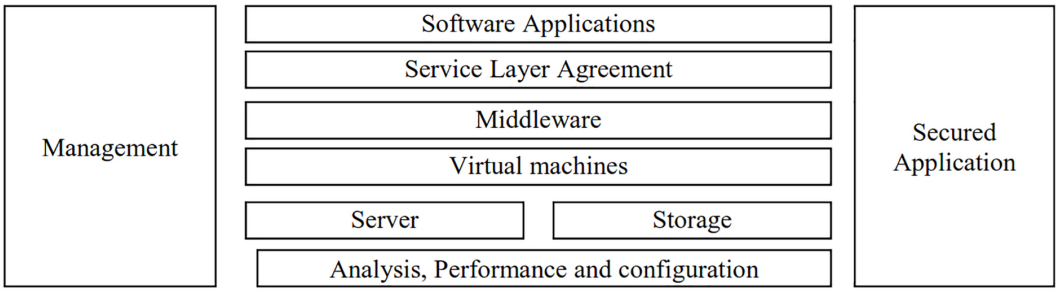

The development of applications with reduced cost by error-free quality documentation, reuse the code, and minimum maintenance of applications. In the service level agreement, the provider services to the user with SLA the quality of services Virtual systems, services provided for 24X7 time with the use of secured applications, storage systems. The Datacenters and application services, which will minimize the cost with use of Servers/ storage/Network facilities to the users based on the demand of users and workload monitoring add data centers by considering the peak hours, number of clients used, number of applications, capacity, network facilities, the response of the system. The applications are increasing the response time also increased minimize the response time by load balancing and scheduling algorithms. The load characteristics, network speed, network distance, response time, scheduling, cloud type services, hardware, the demand for services, peak load, DC, and workload management. The cloud-based web applications offer services such as cloud management, service request, applications workload management, infrastructure (virtual and physical).

2.3.8. Web Services

The growth of internet technologies, web service applications development companies has to implement right, and quality software based on user expectations. The Internet is growing the demand of use of web service applications across the worldwide. Web services are the functional services over the internet, in which a client can access the services, researchers are focused on functional services in UDDI – WSDL descriptions. The building of web-based applications uses of SOAP, REST-based models.

2.3.9. Simple Object Access Protocol (SOAP)

Use of SOA model/architecture shown in Figure 5, it has requester, provider, and UDDI registry. The service user is the client and end user who can use the functional services provided services by the provider, the service provider is the developer who can design and develop web applications and publish in registries. The heart of web service is registry, users and service providers, to improve the discovery of functions across multiple heterogeneous sources. UDDI is a registry with a pool of services.

2.3.10. Restful Services

The document REST based principles used in web services, clients, and intermediates. The REST has: 1) Resource identification; 2) Resource representation; 3) Represent descriptive messages; 4) Hypermedia applications, these are linked with URI in a client-server model with message communications. RESTful services three levels: 1) architectural procedures; 2) decisions related to concepts; 3) decisions related to technology. The architecture of Restful services, in the domain the method for creates, updating, reading, deleting the resource on services (GET, POST, PUT, etc.) and involving various operations by HTTP methods. Decision-related procedures to identify the source

Figure 5. SOA model

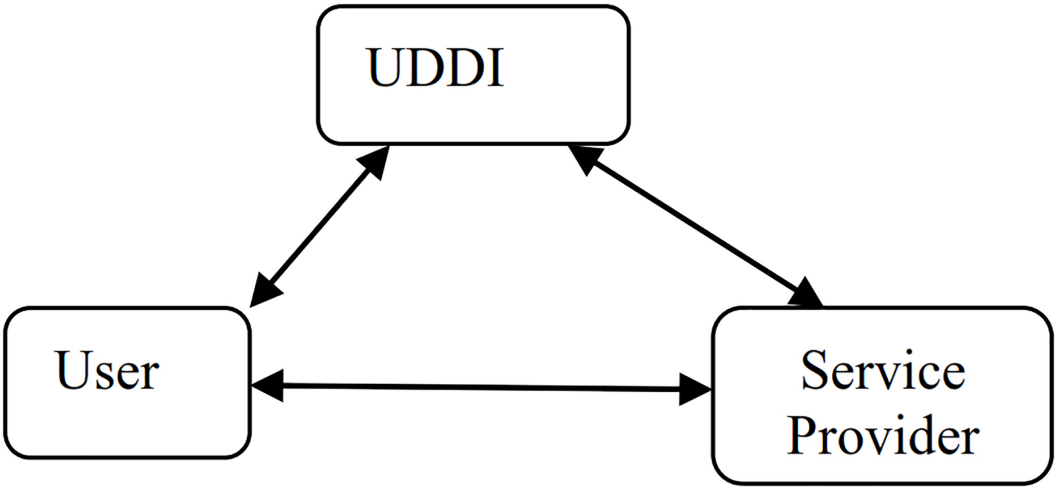

by URI, HTTP methods used (get, put) used the same it is used in Google search engine to search the relevant queries and UDDI. The Framework and building RESTful services (Adamczyk, Smith, Johnson & Hafiz, 2011) use of technologies such as programming languages Java, PHP, Python, Ruby, Rails, HTML and others.

Web services are software components, providers ensure agreed quality of services (QoS), quality factors software engineering. ISO/IEC 25010 quality standard, models used for quality evaluations, in software and quality are functional suitability, performance, efficiency, compatibility, usability, reliability and portability (Oriol, Marco & Frranch, 2014). The service provider will assure to the client with an agreement of services by SLA.

2.3.11. Service Level Agreement

Minimum total resource cost by considering workload to optimize the service by replication of cloud data servers, the load balancing by use of replicate servers by minimum operating cost based on arrival rate, response time and policies. The SLA of Service provider, the designer must design a solution which is cost effective, cost-saving, load balancing of data centers. Service replicas, the low response time, low utilization of active replicas, control service replica utilization minimum number of active replicas. Arrival policy, response time-based policy. Balancing algorithms, replica saving arranges utilization active replica to achieve average response time, SLA, complaint. Elastic resources by adding the resources minimum subject to the minimizing the cost of web applications. The cloud-based web application service provider manages the resources based on the demand.

2.3.12. Resource Management

Web service management shows in Figure 6. The Utilization of entire system, resource, dependency matrices, and cost. The demand of cloud services, the service provider application and scaling the servers as per load and demand allocation resources, with SLA, to predict the resource management, Queuing theory, Optimal auto-scaling by collecting the data, analyze the data, utilization, management allocation, load, and DC etc. The pseudo code 1, describes the load balancing of services. The objective is to optimum load for DC and maximum availability of resources. The Load balancing equations resource utilization, expected completion, load balancing under hierarchical tree topology are described in Equations 6 to11.

Figure 6. Web service management

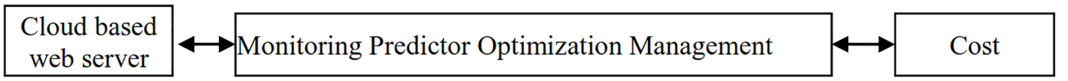

Load balancing let there will the N number of tasks are in the queue to access the resources in Datacenters:

$$ResourceUtlization\left(Ru\right)=\frac{Number\,of\,applicaitons\;\;running}{Total\,number\,of\,applicaiotns} \tag{6}$$

R_u: Resource utilization
A_r: Applications currently running
A_t: Total number of applications

$$Resource\,utlization\left(Ru\right)=\begin{cases}0 & if\,task\,Tij\,no\,task\,are\,running\;\;where\,Ti<0\\ 1 & The\,tasks\,running\,on\,the\,system\,where\,Ti\geq n\end{cases} \tag{7}$$

n: The number of applications

$$Expected\,completion\,time=Execution\,time+Arrival\,time \tag{8}$$

Load balancing standard deviation, the load for a DC based on Equation (6) and find the load balancing mean standard deviation is used to predict the load balancing threshold of a DC:

$$\text{load balancing MSD}=\sqrt{\frac{(\text{Average resouce utlization}-\text{resource utlizationr})^2}{\text{Total jobs}}} \tag{9}$$

$$loadbalancinglevel\left(lb\right)=1-\left\{\frac{\text{load balancing MSD}}{\text{resource utlization}}\right\}*100 \tag{10}$$

By using lead balancing level (lb) values lying between 0 and 1, if the value is zero means no load. If lb value 1 means fully loaded. Load balancing level is also called threshold.

Pseudo code 1. Load Balancing

```
Input:
Web service parameters: VMs, nodes, time allocation, availability,
demand, balance load
```

```
Output:  Balance Load
Begin
1. Web service requests time t1, t2, …, tn where web systems Ws1,
Ws2, …, Wsn
2. Web Requestprediction model, to identify key features described
in Figure 4.
3. Calculate the co-relation of elements
4. Identify the key elements cost, VMs, nodes, time allocation and
availability of Multiple servers
5. Read the load
6. Find the load balancing Mean Square SD from Equation.9
7. If (load ≤ threshold)// threshold is load balancing level use
of Equation.10
Then allocate the resources on tasks on DC
Else if (load = threshold) // the DC is fully loaded
Then balance the load by adding DC to multiple servers and Network
distribution
End if
end
```

2.3.13. Workload Management

The designer and service provider must identify the key factors, protocols, network, bandwidth, routing, and design a model based on the characteristics. Select the data workload, to analyze the jobs of types small, medium and large jobs, the priority of jobs, scheduling, and considering all the workload monitoring, to optimize scheduler policies, and optimize cost-based algorithms and predict the workload and suggest the resource utilization.

Table 2 gives the cloud application usage VMs and memory and cost. To handle the workload, EC2, grow or shrink to handle the current workload, use of data structure B+ tree fast search, memory limited, most recently used cache memory, and least recently used (limited memory). The cheap storage with the use of EC2 resident, cache $0.125 per GB month per month. A load of systems based on clients (number of users), jobs running (application usage), number of processors, queues, scheduling algorithms, and other parameters. Here we consider the dynamic workload distribution.

2.3.14. Dynamic Workload Management

Workload improves the performance, resource management, allocation of resources with the dynamic workload. The changes of workload are analyzed by Workload analysis with use of Map-reduce work. The Optimize job scheduling methods with the use of map-reduce in Hadoop. Examples are Google, Facebook, Twitter, and Yahoo.

Web services can process the requests simultaneously to a maximum number of concurrent users. Video streaming application, video encoding, compression, bit rate, frequency. The cluster video encoding, virtual machines (EC2), quality of service utilization 95 to 99%. In a multi-tier web

Table 2. Cost of Cloud applications

Price per Hour in ($)	Virtual Machine (EC2)	Memory
0.08	1	2GB
0.32	4	7.5 GB
0.64	8	15 GB

application, the delay, load, capacity, admission control, prevent server overload, load prediction, predictive functional load, and reduces the machines. Grid dataset used for experimental analysis using R language which sample Grid dataset 10580 records and 12 parameters from (Grid Datatset, n.d.), summarized in Table 3., and Figure 7. Gives the number of users waiting on the queue of processes and number of applications are executing on processors the waiting time, as applications are increasing the waiting time is also increasing. Figure 8 describes the number of users requesting applications waiting time of the process is also increasing and it reaches the maximum value.

Delay, performance and cost share VM resource to improve performance, share the application to multi-web applications. For example, in video transcoding, the number of frames, bit rate, and bits used per second. Sharing of multiple concurrent streams data to improve VM utilization. And automatic adjustment and adaptability of cost, load distribution, adjust load conditions. The CPU utilization to load the jobs in memory utilization of networks and provides an approach to reduce the physical nodes.

Web applications quality by maximum throughput, server utilization, load balancing, network cost, minimize resource utilization worst case optimize to integrate new optimization which overall cost by minimizing the individual costs by load balancing, scheduling, and effective utilization of resources. The final balance to minimize the cost, balance server load. The pseudo code 2. Describes load distribution will improve the performance. The maximum utilization of services, if the load is accepted then proceed, otherwise update the system with DC, all the systems are updated based on demand and usage.

Pseudo code 2. For Load distribution

```
Input:  Request of services in a server system (DC) load
Output:  load distribution
Begin
Step 1:  Initialize the variable
```

Table 3. Grid dataset

Parameter	Description	Measured in
JobID	Counter, t_1, t_2,..t_{ij}	Sequence number
SubmitTime	In seconds	Milliseconds
WaitTime	In seconds	Milliseconds
RunTime	Runtime measured in wallclock seconds.	Time
NProcs	number of allocated processors- DCs	Number
ReqNProcs	requested number of processors	Number
ReqTime	requested time measured in wallclock seconds	Milliseconds
Status	job completed = 1, job failed = 0, job cancelled = 5	Integer
UserID	string identifier for the user	String
GroupID	string identifier for group user belongs to	String
ExecutableID	name of the executable	Filenameid
QueueID	string identifier for queue	String

```
Step 2:  Read the requestsTasks(T_ij)
Step 3:  Read the load resource utilization using Equation.6
Step 4: While (Maximum utilization) do
If (Load balance is with utilization)// Pseudocode 1. Load
balancing
Then load accepted yes.
else
Update the parameters and add DC based on load level threshold
using Equation.10.
end if
Step 5: All the system update and systems load distribute
dynamically   based on demand and distribute load to multiple
servers using   network balancing.
end while
end
```

The pseudo code 3. Describe the demand of web services (DC), if demand if high allocate the resource, based on demand allocate the resources, number of machines, number of applications, capacity and finally based on demand to allocate the DC for load distribution.

Pseudo Code 3. Find the demand cost of the web server (DC)

```
Input: Demand, load
Output: Based on demand add DC and load balancing
begin
Step 1: Initialization of parameters
Step 2: For each utilization
Step 3: Being calculate the demand
if (demand high)
then
Allocate the resource add DC
else  if (demand == average)
then the allocation is based on average demand
else
Allocate the resource based on demand.
end if
Step 4: The number of Machines, and the number of applications,
Memory   machines (MB), Capacity, CPU demand.
Step 5. If (new DC is added based on load)
Function load distribution()// Pseudo code.2 Load distribution
Optimize the cost of DC by load balancing and scheduling
algorithms
described in Table.4
Step 6. Find the load distribution
end
```

3. EXPERIMENTAL RESULTS

Load Balancing Performance Parameters with various algorithms like Random allocation, round-robin allocation, and weighted round robin. The application grid dataset which consists of sample 10580 and 12 parameters are shown in Table 3. Experiments are conducted using R Language, jobs are

running, submission time, waiting time of runtime of applications, a number of allocated processors, requested processors etc. the experiments conducted using R language and found that the users are increasing and applications are increasing the waiting time is also increasing shown in the Figure.7, the number of tasks (t_{ij})are executing waiting time reach to maximum when applications are reached to maximum load in the Figure.8, the Maximum utilization of processes according to demand and load adding the DC to distribute the load. In Table 4. Describes the load balancing algorithms for selecting parameters.

The models can be used for workload predictions, Static, Round robin, Minimum-maximum, Dynamic Loader, Honeybee, Ant colony optimization and Optimized Multi-level Shortest Remaining Time First and others. Workload predictions and management of DC and load balance will improve the cost of servers.

The users or the customers who can use the web and cloud applications. The specific applications like e-commerce, finance, insurance, transport etc. The infrastructural use facilities such as the hardware, storage, networking and server configurations. The optimum utilization of resources, high availability of resources, management of service with optimized cost. Figure 9. represents load balancing applications. Network load balancing is shown in Equations 6 to 11:

$$Network = Number\,of\,Active Transactions * \frac{total transactions}{weights} \tag{11}$$

The systems which handle the load as per user requests and available services, based on load adding the servers (DC) number of servers used for experiments are 12 and optimum utilization of servers by using the following. Load balancing where the list connections servers with a smaller

Table 4. Load balancing algorithms comparisons

Load Balancing/ Parameter	Random Allocation	Round-Robin Allocation
Nature of systems (DC)	Static	Dynamic
Overhead of processors	More overhead	Less overhead for round robin
Resource utilization	Less utilization of resources because randomly allocate the resources	The resource utilization is more because resources are allocated dynamically
Processor	Little trashing	No thrashing
Preemptiveness	Nonpreemptive	Preemptive by Shortest job First / Non-Preemptive priority can be decided
Predictability	Less for the static approach	weighted round robin designed for dynamic load balancing based on demand
Adaptability	Less because of deterministic allocation space	More because of flexibility to add the space based on demand
Reliability	Less because memory is fixed	More because memory is based on runtime requirement
Response time	More	Less
Availability	Less	More
Central/ distributed systems	Central	Distributed

Figure 7. Grid dataset the jobs are in queue number of users and applications are increasing the waiting time also increases

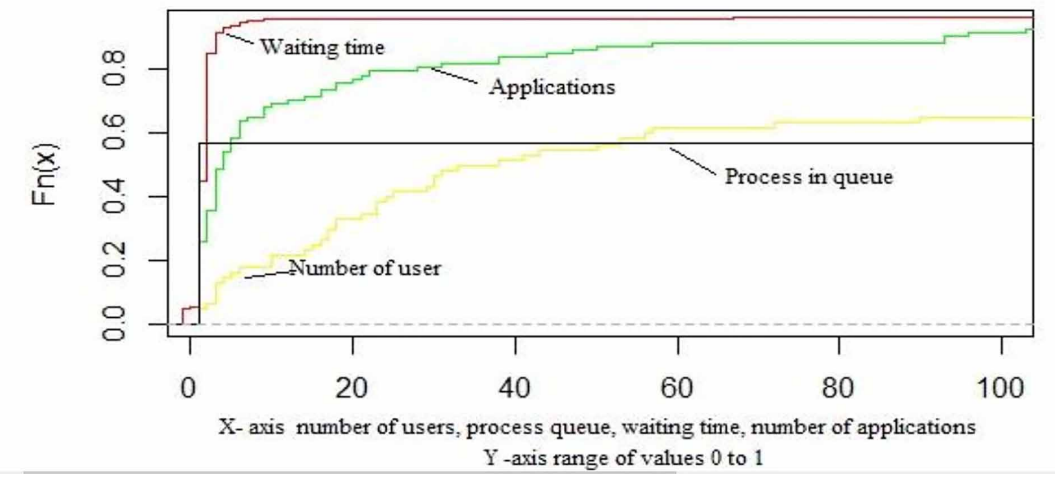

Figure 8. Grid data request time of the job (Task T) and waiting for jobs the number of process waiting time as request time waiting time reaches to the maximum

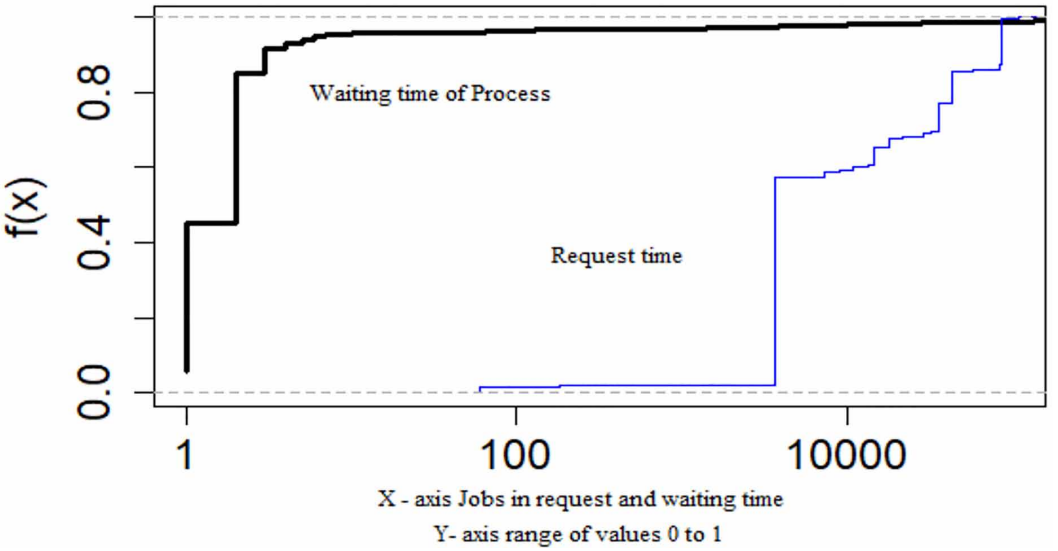

number of outflow routes. Weighted least connections each server to load the weights each server load across weights, Use round robin, and weighted round robin, equally time (Grid Dataset, n.d.).

3.1. Cost Management

The goal is automatically to adjust the load balancing with the DC-based on demand and Demand cloud resources, data-intensive applications. Read the input parameters nodes, resources, demand and applications etc., find the load of the current server (DC), if the server is balancing workload proceed with the load, not means assign resources applications to the system, find the load of the servers, if more load means and add the DC and distribute the load and update the system information.

Figure 9. Load balancing of systems

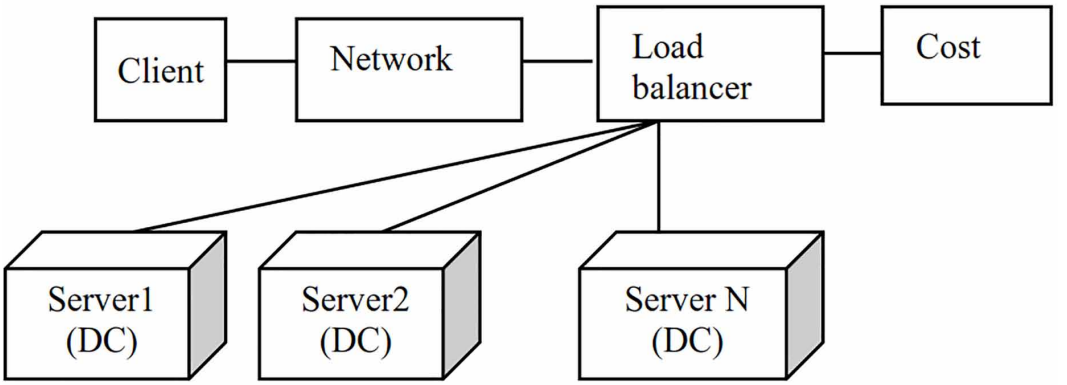

Use of job scheduling algorithms minimize the waiting time and maximize the available, and load balancing helps to minimize the cost of web-based application. The pseudo code. 4 describes cost minimization of systems here we have used 10 data centers as infrastructure as service. For example, Elastic Compute Cloud (EC2), Simple Storage Service (S3).

Pseudocode 4. Cost minimization algorithm

```
Input:  nodes, resources, demand, resource demand, current
database
Output:  Nodes (n) new database-1(if not available)
Cost plan - migration table Migration = false
Begin
Step 1:  Initialize the variables
Step 2:  Read the data,
Step 3:  For each node
Compute Load of the server using Equation 10.
Step 4:  if(load is more based on demand)
then
add the DC
migration = true;
else
execute the load on the same server
endif
Step 5:  if(migration is true)
then
current new demand
update demand
if(n>0)
then
// resource is free
return the resource
Step 6: Find the total cost using Equation 14.
end if
```

```
end if
end
```

The total cost of applications including the development cost, infrastructural cost, manpower, maintenance cost of systems and applications. Cost = ∑(cost of all things), a cost that includes development cost, development cost, service cost, and maintenance cost. The cost can be minimum, average and maximum depends on the requirements and infrastructural facilities and demand applications. The total cost is described Equation 14 and performance is by query request and delay (latency) by Equation 12. The response time to be minimized by using multi-level queue shortest remaining time algorithm:

$$Performance = querytime - latency \tag{12}$$

Time of request within latency(delay), an independent, self-scaling, cost-effective cloud cache, runtime user cost, auto configuration, resource management, scaling, workload.

The query time is by Equation 13. Which use of optimal nodes, optimal storage, predicted workload and data access based on the parameters the query response time is calculated. This will improve the performance latency miss, latency fast and the query execution time:

$$\text{Query Time} = \frac{OptimalnodeXnodes}{dataaccessfast} + \frac{optimalstroage}{slowaccess} + \frac{Predictedload}{\text{Data miss}} \tag{13}$$

The predicted load is computed by using Equation 14. Which predicted query by multiplying the data size:

$$PredictedLoad = predictedquery * Datasize \tag{14}$$

The availability is system is by invocations requests over total invocations. Estimate service errors, whole system all servers Mean time to Failure (MTTF), Mean time to Recovery (MTTR), throughput, availability input, and server will process.

Cost estimation of Web and cloud services including the data centers, estimation of maintenance, availability of services by FTS (Fault Tolerance System), MTTF model, faulty components, replacements, disk, CPU etc. predicted cost by Equation 15:

$$TotalCost = \sum \left(development\,cost + infrastrucure\,cost + services\,cost + maintanance\,cost \right) \tag{15}$$

Utilization of server by Equation 16:

$$\text{Utilization of server} = \text{Number of servers} * \frac{\text{No. of server components predictedload}}{\left(\text{MTTF} + \text{MTTR}\right)} \tag{16}$$

Estimate the server errors whole system all servers, with MTTF, MTTR, and utilization.

In the Web service applications, the user requests the application server and a request processed by the application server by executing functionality and further operations to communicate to the database server. The virtual systems use of IaaS service with scalable, web application at operational

cost, the proposed cost-effective solutions are shown in Table 8 which improve the results of cost optimization, load balancing helps to effective utilization of resources, optimized Multi-level Shortest Remaining time first will reduce the average waiting time. Figure 10 shows the cost optimization of various load balancing and scheduling methods.

4. DISCUSSIONS

The goal is improve the quality of web services and reduce the cost of applications, by minimizing failures with use of best practices (Swami Das, Govardhan & Vijaya Lakshmi, 2016; Ebert, Dumke, Bundschuh & Schmieterndorf, 2005) in development of web applications, reduce the cost and improve the utilization of services, the quality improvement by internal process view as skilled employees as a result minimize the fault rate, and external view optimization of cost of applications, with accuracy product and services.

The customer satisfaction to services the develop use of best practices deployment, and maintenance of cloud-based web applications, this by planning, monitoring and management and improving the efficiency of components with best techniques are discussed below. These methods are also used to minimize the overall cost of the Cloud-based web application:

1. Minimize the defects in code;
2. Functional correctness improvement;
3. Cost management and optimization by minimizing the maintenance cost(rework) including detection and repair of faults and error in a web application;
4. Optimum strategies at all levels including high-speed networks;
5. Inspections, preventive measures and risk management in software development;
6. Portability and adaptability of applications, and systems;
7. Several jobs with available resources, servers and workload and software and hardware, analyze the application using benchmark dataset and tools.

Cost optimization in internet applications, the proposed method is a model using load balancing, effective utilization of resources (i.e. infrastructural) and scheduling algorithms. The user internet

Figure 10. Comparative study of cost optimization using load balancing and scheduling methods. X-axis scheduling method and Y-axis cost of Cloud services

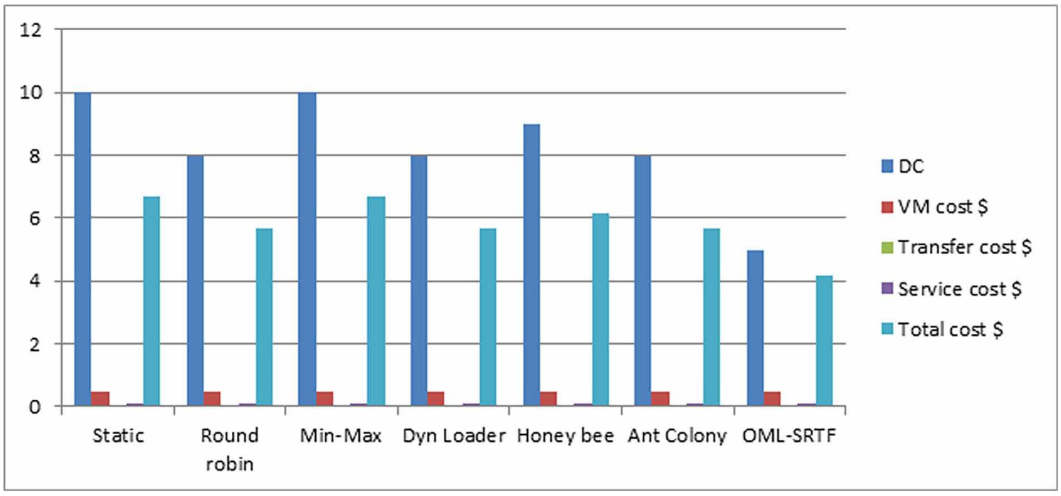

uses functional services like banking, etc. Internet applications play an important role in economics and services (Weintraub & Cohrn, 2015; Van de Bossche, Vanmechelen & Broeckhove, 2015).

The advantages and disadvantages of Load balancing are listed in Table 5.

5. CONCLUSION

The use of cloud-based web applications increasing rapidly, the cloud service IaaS and deployment models public, private and hybrid. Providing infrastructural, platform and software services. The demand to use the services, based user requirement of services, that adds the Infrastructural, platform and software services. There are various factors influence the cost. whereas design, development, and maintenance of software, the software services, where data centers(nodes) are heavily loaded with many tasks, as considering the load constraints, and resource importance, high availability (I/O operations), and maximum utilization of resources, subjected to minimizing the overall application. The proposed enhanced model architecture which is well suited for cloud-based web applications design deployment and minimizing cost and effective utilization of resources by considering the demand, cost, resource utilization, applications, quality of services, management applications, analysis of workload management, load balancing(like static, dynamic workload) with example random allocation and round-robin dynamic allocation, and use of cost minimization algorithm (Pseudo code 4), with grid dataset consists of 12 parameters with sample of 10580 records. The experimental results conducted R language and result in the number of users increases, the applications are increasing, the processes in the queue, the waiting time is also increasing. The designer will use load balancing, and scheduling (Multi-level shortest remaining) algorithms will improve the performance shown in Figure 7, and Figure 8. Table 4 describes the load balancing comparisons, Table 5 describes various scheduling methods advantages and disadvantages are discussed. Table 6 describes the scheduling models and finally optimized multi-level CPU scheduling – load balancing will be best solution., Table 7 shows a sample of 1559 records of Grid dataset, number of processors, average waiting time, an average of maximum execution time, minimum execution time, maximum execution time computations. Table 8 shows the cost optimization of load balancing, effective utilization of resources and scheduling algorithms. Figure 10 shows the comparative study of load balancing- scheduling algorithms among these Optimized Multi- queue shortest Remaining time method got improved results. The suggestion to improve the cost minimization and effective utilization of resource with a user of best practices such as application load balancer with use of scheduling methods. The network load balancers used

Table 5. Load balancing details

Scheduling	Pros	Cons
Static	Load at complete time	Not handle throughput
Round robin	Fixed quantum CPU burst	Longest task time
Minimum-maximum	Small task better completion	Starvation
Dynamic Loader	Work distortion at runtime use FTS	Check the node
Honeybee	Increase throughput minimum Response time	High priority
Ant colony optimization	Faster information, minimum span, independent task, and intensive computation	Network overhead for a long time and no clarity in ants
Optimized Multi-level shortest remaining time First	Faster information and minimization of response time for many tasks, Better performance	Needs to sort the jobs based on the shortest remaining time - priority

Table 6. The cost of applications using various scheduling methods

Scheduling	Service Utilization Cost	DC Cost	Maintenance Cost	Load Balancing	Effective Utilization
Static	Fixed cost	more	Increased	Manually	Manually
Round robin	Variable cost	Less	Decreased	Dynamically	Dynamically
Minimum-maximum	Fixed	More	increased	static	static
Dynamic Loader	Variable	Less	Increased	Dynamic	Dynamically
Honeybee	Fixed/ variable	More	Increased	Static/dynamic	Manually/ Dynamically
Ant colony optimization	Fixed	More	Increased	Manually	Manually
Optimized Multi-levelShortest Remaining Time First	Variable	Less	Decreased	Dynamically	Dynamically

Table 7. A sample of 1559 records of grid dataset, number of processors, average waiting time, an average of maximum execution time, minimum execution time, maximum execution time

Processors	Record Job Count	Average Waiting Time (ms)	Average Execution Time (ms)	Maximum Execution Time (ms)	Minimum Run Time of One Record (ms)	Maximum Run Time of One Record (ms)
1	368	3.73	2.3	65161	1	60
2	841	46.94	8.3	1058	2	305
4	220	2.29	1.45	559	3	313
8	110	2.89	2.69	4	2	10
12	2	3	114.5	210	23	212
16	16	3.06	5.06	7	2	9
24	2	3.5	31	35	31	38

to minimize defects, functional correctness, and the maintenance cost to be minimized. In the future, IoT controlled the Hybrid load balancing algorithms will be used for mixed attributes.

Table 8. Cost optimization by load balancing, scheduling, and effective utilization

Scheduling	Load Balancing and Effective Utilization	Virtual Machine	Communication	Per Hour Cloud Service Cost	Total Cost in $
		VM Cost in $	Data Transfer Cost $	Fixed Cost	Total Cost $
Static	10	0.5	0.06	0.08	6.68
Round robin	8	0.5	0.06	0.08	5.68
Minimum-maximum	10	0.5	0.06	0.08	6.68
Dynamic Loader	8	0.5	0.06	0.08	5.68
Honey bee	9	0.5	0.06	0.08	6.18
Ant colony optimization	8	0.5	0.06	0.08	5.68
Optimized Multi-level Shortest Remaining Time First	5	0.5	0.06	0.08	4.18

REFERENCES

Adamczyk, P., Smith, P. H., Johnson, R. E., & Hafiz, M. (2011). Rest and web services: In theory and in practice. In *REST: from research to practice* (pp. 35-57). Springer. 10.1007/978-1-4419-8303-9_2

Ashraf, A. (2013). Cost-Efficient Virtual Machine Provisioning for Multi-tier Web Applications and Video Transcoding. In *IEEE/ACM International Symposium on Cluster, Cloud, and Grid Computing* (pp. 66-69). IEEE. doi:10.1109/CCGrid.2013.24

Björkqvist, M., Chen, L. Y., & Binder, W. (2011, December). Optimizing service replication in clouds. In *Proceedings of the Winter Simulation Conference* (pp. 3312-3322). Winter Simulation Conference.

Breitgand, D., & Epstein, A. (2011, May). SLA-aware placement of multi-virtual machine elastic services in compute clouds. In *2011 IFIP/IEEE International Symposium on Integrated Network Management (IM)* (pp. 161-168). IEEE.

Ebert, C., Dumke, R., Bundschuh, M., & Schmietendorf, A. (2005). Best Practices in Software Measurement: How to use metrics to improve project and process performance. Springer.

Grid dataset. (n.d.). Retrieved from http://gwa.ewi.tudelft.nl/

Iqbal, W., Erradi, A., & Mahmood, A. (2018). Dynamic workload patterns prediction for proactive auto-scaling of web applications. *Journal of Network and Computer Applications*, *124*, 94–107.

Jiang, J., Lu, J., Zhang, G., & Long, G. (2013). Optimal Cloud Resource Auto-Scaling for Web Applications. In *IEEE/ACM International Symposium on Cluster, Cloud, and Grid Computing* (pp. 58-65). IEEE. doi:10.1109/CCGrid.2013.73

Kabir, F., & Chiu, D. (2012). Reconciling Cost and Performance Objectives for Elastic Web Caches. In *International Conference on Cloud Computing and Service Computing* (pp. 88-95). IEEE. doi:10.1109/CSC.2012.21

Li, S., Zhou, Y., Jiao, L., Yan, X., Wang, X., & Lyu, M. R. (2014). Delay-Aware Cost Optimization for Dynamic Resource Provisioning in Hybrid Clouds. In *2014 IEEE International Conference on Web Services*, Anchorage, AK (pp. 169-176). doi:10.1109/ICWS.2014.35

Lu, L., & Smirni, E. (2014). Effective resource and workload management in data centers. In *2014 IEEE Network Operations and Management Symposium (NOMS)*, Krakow (pp. 1-7). doi:10.1109/NOMS.2014.6838287

Naqvi, S. A. A., Javaid, N., Butt, H., Kamal, M. B., Hamza, A., & Kashif, M. (2018, September). Metaheuristic optimization technique for load balancing in cloud-fog environment integrated with smart grid. In *International Conference on Network-Based Information Systems* (pp. 700-711). Cham: Springer.

Nikolaou, P., Sazeides, Y., Ndreu, L., & Kleanthous, M. (2015, December). Modeling the implications of DRAM failures and protection techniques on datacenter TCO. In *Proceedings of the 48th International Symposium on Microarchitecture* (pp. 572-584). ACM.

Oriol, M., Marco, J., & Franch, X. (2014). Xavier. Franch," Quality models for web services: A systematic mapping. *Information and Software Technology*, *56*(10), 1167–1182. doi:10.1016/j.infsof.2014.03.012

Puspita, F. M., Erlita, S., Nadeak, I., & Arisha, B. (2018, March). LINGO-based optimization problem of cloud computing of bandwidth consumption in the Internet. In *2018 International Conference on Information and Communications Technology (ICOIACT)* (pp. 436-441). IEEE. doi:10.1109/ICOIACT.2018.8350688

Ren, Z., Wan, J., Shi, W., Xu, X., & Zhou, M. (2014). Workload Analysis, Implications, and Optimization on a Production Hadoop Cluster: A Case Study on Taobao. *IEEE Transactions on Services Computing*, *7*(2), 307–321. doi:10.1109/TSC.2013.40

Rodriguez, M. A., & Buyya, R. (2018). Scheduling dynamic workloads in multi-tenant scientific workflow as a service platforms. *Future Generation Computer Systems*, *79*, 739–750.

Satapathy, S. C., Bhateja, V., Raju, K. S., & Janakiramaiah, B. (2016). Computer Communication, Networking and Internet Security. In Proceedings of IC3T, 5.

Satapathy, S. C., Mandal, J. K., Udgata, S. K., & Bhateja, V. (2016). *Information Systems Design and Intelligent Applications*. Springer India.

Satapathy, S. C., Bhateja, V., & Das, S. (2018). Smart Intelligent Computing and Applications. In *Proceedings of the Second International Conference on SCI* (Vol. 1).

Sheng, L. I. U., Xiong, G., Zhao, H., Dong, X., & Yao, J. (2012). Service Composition Execution Optimization basedon State Transition Matrix for Cloud Computing. In *World Congress on Intelligent Control and Automation* (pp.4126-4131). IEEE.

Srirama, S. N., & Ostovar, A. (2014). Optimal Resource Provisioning for Scaling Enterprise Applications on the Cloud. In *2014 IEEE 6th International Conference on Cloud Computing Technology and Science*, Singapore (pp. 262-271). doi:10.1109/CloudCom.2014.24

Swami Das, M., Govardhan, A., & Vijaya Lakshmi, D. (2016). Best practices for web applications to improve the performance of QoS. In *Proceedings of the Second International Conference on Information and Communication Technology for Competitive Strategies (ICTCS '16)*. New York, NY: ACM.

Tian, C., Jiang, H., Iyengar, A., Liu, X., Wu, Z., Chen, J., & Wang, C. et al. (2011). Improving Application Placement for Cluster-Based Web Applications. *IEEE eTransactions on Network and Service Management*, *8*(2), 104–115. doi:10.1109/TNSM.2011.050311.100040

Van den Bossche, R., Vanmechelen, K., & Broeckhove, J. (2015). IaaS reserved contract procurement optimization with load prediction. *Future Generation Computer Systems*, *53*, 13–24. doi:10.1016/j.future.2015.05.016

Wang, L., Shen, J., Di, C., Li, Y., & Zhou, Q. (2013). Towards minimizing cost for composite data-intensive services. In *Proceedings of the 2013 IEEE 17th International Conference on Computer Supported Cooperative Work in Design (CSCWD)*, Whistler, Canada (pp. 293-298). doi:10.1109/CSCWD.2013.6580978

Papazoglou, M. (2012). *Web services & SOA Principles and Technology* (2nd ed.). Pearson Publications.

Weintraub, E., & Cohen, Y. (2015). Cost Optimization of Cloud Computing Services in a Networked Environment. *International Journal of Advanced Computer Science and Applications*, *6*(4), 148–157.

Wu, Z., & Nie, G.H. (2013). Web service integrator's portfolio optimization based on cost impact factors. In *2013 6th International Conference on Information Management, Innovation Management and Industrial Engineering*, Xi'an (pp. 213-216). doi:10.1109/ICIII.2013.6702912

Xia, Y. M., & Yang, Y. B. (2013). Web Service Composition Integrating QoS Optimization and Redundancy Removal. In *2013 IEEE 20th International Conference on Web Services*, Santa Clara, CA (pp. 203-210). doi:10.1109/ICWS.2013.36

Xiong, P., Wang, Z., Malkowski, S., Wang, Q., Jayasinghe, D., & Pu, C. (2011, June). Economical and robust provisioning of n-tier cloud workloads: A multi-level control approach. In *2011 31st International Conference on Distributed Computing Systems (ICDCS)* (pp. 571-580). IEEE.

Yao, M., Zhang, P., Li, Y., Hu, J., Lin, C., & Li, X. Y. (2014). Cutting Your Cloud Computing Cost for Deadline-Constrained Batch Jobs. In *2014 IEEE International Conference on Web Services*, Anchorage, AK (pp. 337-344). doi:10.1109/ICWS.2014.56

Yu, T., Qiu, J., Reinwald, B., Zhi, L., Wang, Q., & Wang, N. (2012, June). Intelligent database placement in cloud environment. In *2012 IEEE 19th International Conference on Web Services (ICWS)* (pp. 544-551). IEEE.

Zhang, P., Han, Y., Zhao, Z., & Wang, G. (2012). Cost Optimization of Cloud-Based Data Integration System. In *Int. conference Web Information Systems and Applications IEEE* (pp. 183-188). IEEE. doi:10.1109/WISA.2012.13

Zhu, R., Niu, D., & Li, B. (2014). Min-cost live webcast under joint pricing of data, congestion, and virtualized servers. In *2014 7th International Conference on NETwork Games, COntrol and OPtimization (NetGCoop)*, Trento (pp. 15-22).

Zivkovic, M., Bosman, J. W., van den Berg, J. L., van der Mei, R. D., Meeuwissen, H. B., & Nunez-Queija, R. (2011). Dynamic Profit Optimization of Composite Web Services with SLAs. In *IEEE Clobecome 2011 proceedings* (pp. 1–6). IEEE. doi:10.1109/GLOCOM.2011.6133666

M. Swami Das is working as an Associate Professor in CSE dept, MREC, Hyderabad. He completed B E(CSE) in 1998 from CBIT, (affiliated to Osmaina University), Hyderabad, and M Tech (CS), from JNTU Kakinada in 2002, and Purusing Ph D in JNTUH Hyderabad. He has 17 years of Experience in Teaching, Industry and Research. His research interests are Web services, Cloud computing and Data mining.

A.Govardhan, Rector (Pro Vice-Chancellor) and EC Member at JNTUH, India. He did his B.E(CSE), from Osmania University in1992, M Tech (CS) from JNU, New Delhi, and PhD from JNTUH in databases in 2003. He has 24 years' of experience in Teaching, research and administration. Served and held several Academic & Administrative positions including, Principal (JNTUHCEH), Director (SIT), Director of Evaluation, Principal, Head of the Department, Chairman and Member on several Boards of Studies of various Universities and Students' Advisor. Recipient of 32 International and National Awards including A.P. State Government Best Teacher Award 2012, Bharat Seva Ratna Puraskar, CSI Chapter Patron Award, Bharat Jyoti Award, Int'l Intellectual Development Award and Mother Teresa Award for Outstanding Services, Achievements, Contributions, Meritorious Services, Outstanding Performance and Remarkable Role in the field of Education & Service to the Nation. Past Chairman of CSI Hyderabad Chapter. Member on the Editorial Boards for 12 Int'l Journals. Member of several Advisory Boards & Academic Boards, a PC Member for 75 Int'l and National Conferences. Has 2 Monographs Published in USA, 10 Book Chapters in Springer. Guided 81 Ph.D theses, 1 M.Phil, 135 M.Tech projects and published 525 research papers at International/ National Journals/ Conferences including IEEE, ACM, Springer and Elsevier. Organized 2 Int'l Conf, 20 Workshops & 1 Refresher Course. Delivered more than 100 Keynote addresses and invited lectures. Has 24 years of teaching and Research experience. He is a member in several professional and service oriented bodies. Areas of research include databases, data science and information retrieval systems.

D. Vijaya Lakshmi, working as a Professor and Head of the Dept of IT, MGIT, Hyderabad. She received a Ph.D. from JNTUH, Hyderabad, is a member of MEACSE, IJCAR. She is holding Games and Sports Committee Convenor, Presiding Officer in Women Welfare Cell, MGIT. She is guiding four research scholars in JNTUH Hyderabad. Her research areas include image processing, web services, data mining and security. She has more than 20 years' experience in teaching, research and administration.

Experimental Investigations on CI Engine using different Combustion Chambers and Biodiesel as Fuel

Shaik Hussain, A Siva Kumar, A Aruna Kumari

Abstract : The rapid utilization of crude oils in present days has been created shortage of petroleum products. The shortage of crude oil reserves has a major impact on industrial, transportation and agriculture sectors. Therefore there is a necessity to alter crude oils with alternative fuels. This paper investigates the performance and pollutant parameters of compression ignition engine with soap nut and palm stearin methyl esters as alternative to diesel fuel. Piston bowl configuration has a major effect in the preparation of air-fuel mixture. Hence in this work attempts are made to minimize the exhaust pollutants and improve the performance parameter by varying the combustion chamber geometry. The various combustion chamber designs viz., Hemispherical, Toroidal, Re-entrant and double wedge combustion chamber are employed. The results indicates that Re-entrant combustion chamber is a better choice with soap nut methyl ester as a fuel.

Index Terms: Soap nut methyl ester, palm stearin methyl ester, combustion chamber, biodiesel, compression ignition engine.

I. INTRODUCTION

Energy is treated as the most significant for development of any nation. Presently the fossil fuels are the major source of energy for transportation, industrial and agriculture sectors. With the growing demand the consumption of fossil fuels are increased rapidly. To compensate this many of the countries importing oils gulf countries. Therefore it creates burden on the economy of the nation. Further the rapid utilization of fossil fuels also leads to exhaust of crude reserves. To overcome this effect many of the researchers have investigated different types of alternative fuels like biogas, liquefied petroleum gas, vegetable oils and alcohols. From the experimental results they observed that vegetable oils are best suited alternative fuels owing to their similar fuel properties. The vegetable oils like peanut, linseed, mahua, karanja, cotton seed, jatropha palm, sunflower were investigated in diesel engines in place of diesel fuel [1-5]. The investigations on DI engine using soya bean, jatropha and rapeseed oil reveals that the performance parameters were comparatively less compared to base fuel. The results also indicated that these fuels were well suited for small run tests where as for long run tests these fuels creates certain problems like piston ring sticking and carbon deposition problems [6-10]. Further
the effects of using coconut oil and blends of coconut oil in a compression ignition engine were noticed. From the results it was concluded that coconut oil and its blends may be used in compression ignition engines without any alternation of the engine. It was also observed that with the increase of blend percentage of coconut oil the specific fuel consumption was reduced [11-16]. Further The turbocharged DI diesel engine was made to run using mustard seed oil as a substitute fuel. The duration of engine run for one cycle was nearly about 150 hours. The experimental results with mustard seed oil indicated that the brake power was less compared to base diesel engine. But the torque and thermal efficiency were nearer to base engine. Further the pollutant formations like carbon monoxide and hydrocarbon pollutants were high at low load conditions. At full load condition the smoke pollutant parameters observed were lower compared to base engine [17-19]. Investigations were carried out on a compression ignition engine with Palm biodiesel and blends of palm biodiesel and the results were compared with base engine. The performance characteristics were almost equal to standard engine. But the emission parameter NOx levels for palm biodiesel and blends of palm biodiesel were high compared standard engine. Further the tests were carried out with Exhaust Gas Recirculation(EGR) and observed that the nitrogen pollutant levels were decreased [20-21].

II. MATERIALS AND METHODOLOGY

A. Engine Setup

The investigations are carried out on single cylinder, 4-stroke, direct injection (DI), compression ignition engine. The details of the test equipment are given in Table 1.

Parameter	Specification
Engine Power	5.2 kW
Cylinder Bore	87.5 mm
Stroke length	110 mm
Speed	1500 rpm

Revised Manuscript Received on March 20, 2019.

Dr.Shaik Hussain, Mechanical Engineering Department, Malla Reddy Engineering, Hyderabad, Telangana, India.
Dr. A Siva Kumar, Mechanical Department, Malla Reddy Engineering College and Management Sciences, Medchal, Hyderabad, Telangana, India
Dr. A Aruna Kumari, Mechanical Engineering Department, Jawaharlal Nehru Technological University, Hyderabad, Telangana, India.

Compression ratio	17.5:1
No. of Cylinders	1
Connecting rod	234 mm
Stroke type	Four
Cooling	Water
Speed type	Constant
Loading type	Eddy current

Table 1. Test Engine Specification

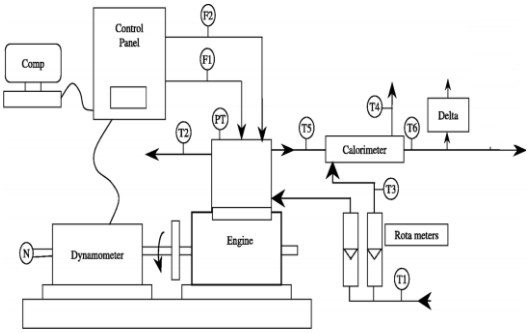

Fig.1. Experimental setup layout

Fig.2. Experimental setup

B. Experimental Procedure

Along with the base diesel two other biodiesels are considered for running the test engine. The two biodiesel are Palm Stearin Methyl ester(PSME) and Soap Nut Methyl ester(SNME). These fuels properties are investigated as per ASTM standards and compared with base diesel fuel. The property comparison of PSME,SNME and Diesel are given in table 2. In addition to standard combustion chamber(Hemispherical) design, three more combustion chamber shapes are used to conduct the experiments. Toroidal combustion chamber(TCC), Re-entrant combustion chamber(RECC) and Double Wedge combustion chamber are the other three types. These shapes are shown in fig.3. At each load the performance and emission characteristics such as specific fuel consumption, brake thermal efficiency, mechanical efficiency and indicated thermal efficiency are evaluated. In addition to performance the pollutant parameters like carbon dioxide, carbon monoxide, hydrocarbon and oxides of nitrogen are estimated.

(a) TCC b) RECC c)DWCC (d) HCC

Fig.3. Types of Combustion Chambers

Parameter	Standards	Dies	PSM	SNME
Specific gravity	ASTM D 1298	0.83	0.85	0.86
Density (kg/m^3)	ASTM D 1298	830	877	871
Kinematic Viscosity @ 40 ^oC	ASTM D 445	3.01	5.49	4.53
Heating value (MJ/kg)	ASTM D 5865	42.5	39.09	40.02
Flash point	ASTM D 92	50	220	164
Fire point	ASTM D 92	60	280	212
Cetane number	ASTM D 613	47	42	51

Table 2: Comparision of diesel and biodiesels properties

III. RESULTS & DISCUSSIONS

A. Performance Characteristic

The performance characteristics evaluated are mechanical efficiency, brake thermal efficiency, indicated thermal efficiency and specific fuel consumption. The experiments are carried out with diesel, PSME and RSME as fuel by varying combustion chamber designs. The experimental results are presented below. The graph drawn between brake output power and thermal efficiency is presented in fig.4. From the observations it is learnt that with the increase of load the brake thermal efficiency(BTE) linearly increases from minimum load to max load condition. Further the BTE observed for toroidal piston configuration with Palm Stearin Methyl Ester(PSME) is less compared to other piston configurations. At maximum load condition the BTE is about 30.02% for RE SNME. It is nearly 5.29% more when compared with standard diesel engine. The squish movement is high in modified combustion chamber compared to standard piston. This may be the reason to increase in thermal efficiency. Fig.5 shows the variation of indicated thermal efficiency(ITE) with Brake output power. The ITE noticed is maximum at full load condition for RE SNME and is about 42%.

The minimum indicated thermal efficiency is recorded for double wedge combustion chamber compared to all other combustion chambers and is about 32.85%. Re-entrant combustion chamber with SNME indicated thermal efficiency is 3.34% more correlated to standard diesel engine.The graph is plotted between mechanical efficiency and brake output power and is shown in fig.6. The mechanical efficiency(ME) is increased from zero load to maximum load condition. The RE SNME ME is high at full load condition. TPSME showed lower mechanical efficiency at same load condition. At full load condition RE SNME mechanical efficiency is 15.16% high compared to standard diesel operation. Correct flame propagation with air fuel mixture movement may be the reason for highest mechanical efficiency. The variation of specific fuel consumption with brake power as shown in fig.7. From the figure it is noticed that the SFC is decreasing from zero load to 50% of the full load condition rapidly and for remaining load conditions there is no much deviation. The highest SFC is recorded for Toroidal PSME. The lowest SFC is noticed for Re-Entrant combustion chamber at maximum load condition. Compared to standard diesel engine the specific fuel consumption for Re-Entrant SNME is 14.12% less at full load operation of the engine. Proper mixing of air fuel mixture may be the reason for decreased specific fuel consumption.

.

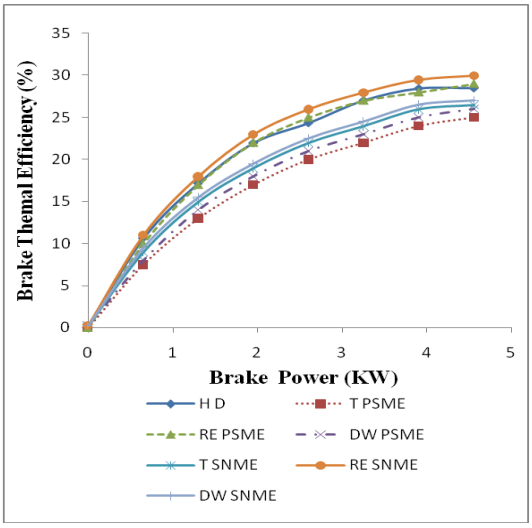

Fig.4 BP vs BTE

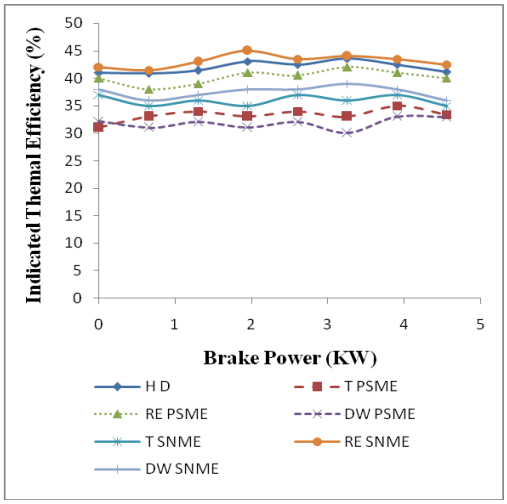

Fig.5 BP vs ITE

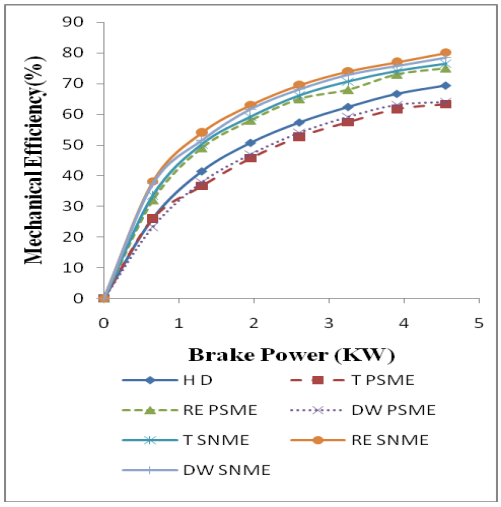

Fig.6 BP vs ME

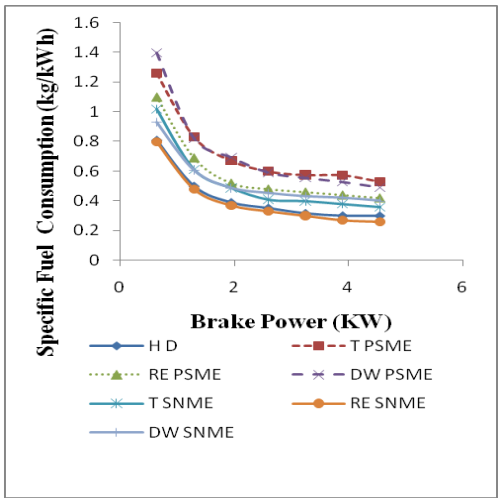

Fig.7 BP vs SFC

B. Emission Parameters

Investigations are carried out to determine the emission parameters with various piston geometry and by using two different kinds of biodiesel(SNME & PSME). The emission parameter viz., carbon dioxide, carbon monoxide, hydrocarbon and NO_x are computed.

The CO emission pollutant variations with brake out put power is indicated in fig.8. From the plot it is observed that from zero load condition to 55% of the full load condition there is no much difference in carbon monoxide pollutants. After 55% of full load condition the CO pollutants are increased drastically. The Toroidal PSME carbon monoxide pollutants are high compared to all other piston geometries. The lower CO pollutants are observed for Re-entrant SNME. At full load condition the CO pollutants are about 29.9% less for Re-entrant SNME Compared to base engine.

A graph is drawn between brake power and hydrocarbon pollutants is shown in fig.9. The HC pollutants are increased from zero load to full load condition. From the graph it is noticed that for double wedge SNME the HC emissions are high correlated to other piston geometries. The minimum hydrocarbon pollutants are recorded for Re-entrant SNME. At full load condition the HC pollutants for Re-entrant SNME are about 22.85% less correlated to base engine.

The deviation of carbon dioxide pollutants with brake output power is presented in fig.10. The CO_2 emissions are linearly increased from minimum to maximum load operation. The highest carbon dioxide pollutant levels are recorded for double wedge PSME and the lowest is observed for Re-entrant SNME. Nearly about 18% lower carbon dioxide pollutant levels are recorded for Re-entrant SNME compared to standard engine.

The fluctuations nitrogen emission levels with brake power is indicated in fig.11. From the figure it is noticed that for all configurations of pistons the oxides of nitrogen emission levels are high at full load condition. More combustion temperature is the reason for increased NO_x levels. But compared to all other piston geometries Re-entrant SNME has shown low NO_x emission levels.

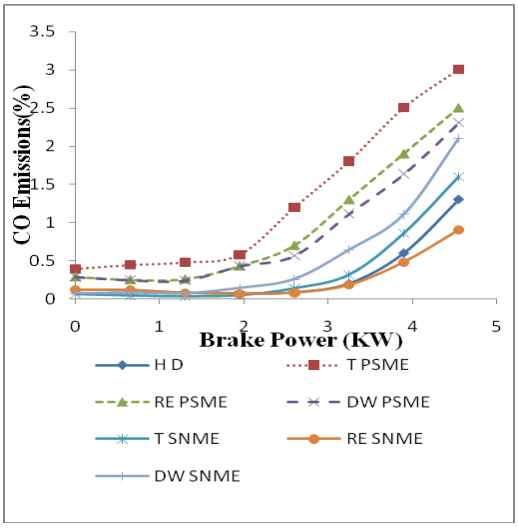

Fig.8 BP vs CO

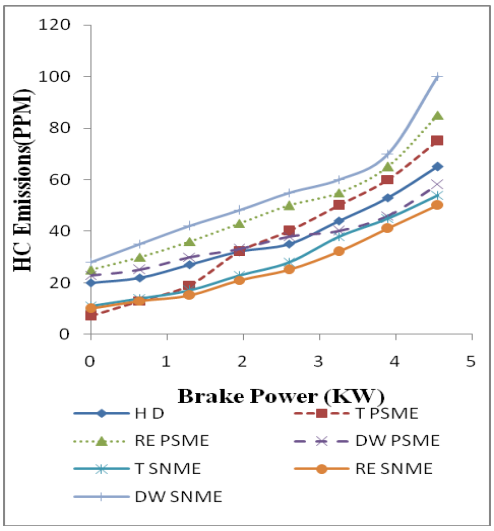

Fig.9 BP vs HC

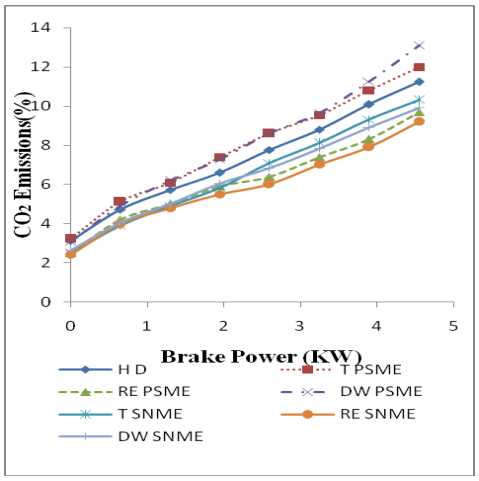

Fig.10 BP vs CO_2

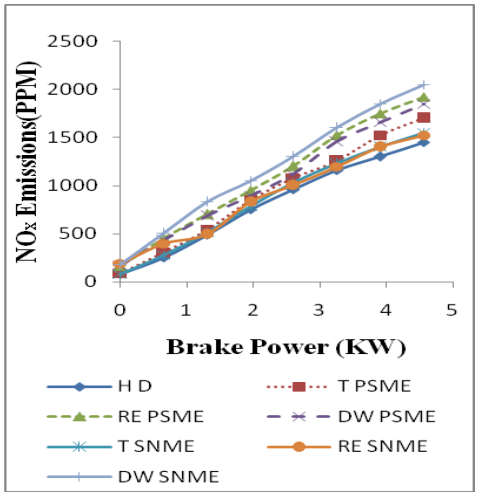

Fig.11 BP vs NO_x

IV. CONCLUSION

In this study investigations are conducted on four stroke, water cooled, single cylinder compression ignition engine. The SNME and PSME are used as fuels with different combustion chamber geometries. From the present study the following conclusions are drawn.

- The Re-entrant SNME brake thermal efficiency is 5.42% high correlated to standard engine. The reduction of air squish on the piston crown leads to mix more quantity of fuel charge.
- The Re-entrant SNME indicated thermal efficiency is 3.64% high correlated to conventional engine. The thrust produced by reaction gases is more due to variation in cross section.
- The Re-entrant SNME mechanical efficiency is 15.25% more correlated to standard engine.
- The SFC is low for Re-entrant SNME and is about 12.98% correlated to base engine. The main cause to decrease SFC is adequate air fuel mixture formation and maximum heat release rate.
- The carbon monoxide pollutant levels for Re-entrant SNME is about 29.85% less correlated to conventional engine. The reason is proper air motion in the combustion chamber.
- The Re-entrant Hydro carbon pollutant levels are about 22.35% low correlated to standard diesel engine. The reason is increased temperature in the cylinder walls.
- Compared to base engine the oxides of nitrogen pollutant levels for Re-entrant is more and is about 5.21%. This is mainly due increase combustion temperature. But compared to all other geometries Re-entrant combustion chamber with SNME has shown less NOx levels.

REFERENCES

1. S.Madiwale,A.Karthikeyan,V.Bhojwani,"Properties Investigation and Performance Analysis of a Diesel Engine Fuelled with Jatropha, Soybean, Palm and Cottonseed biodiesel using Ethanol as an additive", Materials Today: Proceedings, Volume 5, Issue 1, Part 1, 2018, PP 657-664.
2. Swarup Chandran, Performance & Emission Characterstics of Karanja Biodiesel, IRJET, Volume: 05 Issue: 02 | Feb-2018.
3. Jayashri N.Nair,Ajay KumarKaviti,Arun KumarDaram, Analysis of Performance and Emission on Compression Ignition Engine Fuelled with Blends of Neem Biodiesel, Egyptian Journal of Petroleum ,Volume 26, Issue 4, December 2017, PP 927-931.
4. Dragos Tutunea, Ilie Dumitru, Analysis of Performance and Emissions of Diesel Engine using Sunflower Biodiesel, Materials Science and Engineering, 2017 IOP Conf. Ser.: Mater. Sci. Eng. 252 012085.
5. M.S.Gad,R.El-Araby,K.A.Abed, Performance and Emissions Characteristics of C.I. Engine Fueled with Palm Oil/Palm Oil Methyl Ester Blended with Diesel Fuel, , Egyptian Journal of Petroleum Available online 31 May 2017.
6. A Karthikeyan, J Jayaprabakar,Richard Dude Williams, Experimental Investigations on Diesel engine using Methyl esters of Jatropha oil and fish oil, 2017 IOP Conf. Ser.: Mater. Sci. Eng. 197 012020.
7. LukaLesnik, IgnacijoBilus, The Effect of Rapeseed Oil Biodiesel Fuel on Combustion, Performance, and The Emission Formation Process Within a Heavy-Duty DI Diesel Engine, Energy Conversion and Management, Volume 109, 1 February 2016, PP 140-152.
8. Babita Singh, Experimental Investigation on Performance of CI Engine using Biodiesel Prepared from Sunflower Oiland Waste Cooking Oil, IJERT, Volume 5, Issue 10, 2016, pp-264-266.
9. TanzerEryilmaz, Murat KadirYesilyurt, Influence of Blending Ratio on the Physicochemical Properties of Safflower Oil Methyl Ester-Safflower Oil, Safflowerоil Methyl Ester-Diesel and Safflower Oil-Diesel, Renewable Energy, Volume 95,September 2016,Pages 233-247.
10. Sulakshana S. Deshpande, S.V. Channapattana, Dr. A.A. Pawar, Experimental Evaluation Of Diesel Engine Performance And Emissions Using Diesel/Biodiesel/Ethanol Blend Fuel, International Jouranl Of Emerging Technology And Advanced Engineering, Volume-5, Issue-1,2015, PP: 263-271.
11. Chaithra M H ,A Study on Performance of Ic Engines With Exhaust Energy Gas Harvester, International Journal of Mechanical And Production Engineering, ISSN: 2320-2092, Volume- 3, Issue-2, Feb.-2015.
12. Zavos et at, Effects of Surface Irregularities on Piston Ring-Cylinder Tribo Pair of a Two Stroke Motor Engine in Hydrodynamic Lubrication, Tribology in Industry Vol. 37, No. 1 (2015) 1-12.
13. Yan Hongwei et al, Analysis of the Influences of Piston Crankshaft Offset on Piston Secondary Movements, The Open Mechanical Engineering Journal, Volume 9, 2015.
14. Amin Yousefi et al. , Comparison Study on Combustion Characteristics and Emissions of a Homogeneous Charge Compression Ignition (HCCI) Engine with and without Pre-Combustion Chamber, Energy Conversion and Management Volume 100, August 2015, Pages 232–24.
15. T. Shaafi, R.Velraj, Influence Of Alumina Nanoparticles, Ethanol And Isopropanol Blend as Additive with Diesel – Soybean Biodiesel Blend Fuel: Combustion, Engine Performance And Emissions, Renewable Energy 80, 2015, PP: 655-663.
16. Herchel T.C. Machacon, Seiichi Shiga, Takao Karasawa, and Hisao Nakamura. Performance and Emission Characteristics of a Diesel Engine Fueled with Coconut Oil-Diesel Fuel Blend. Journal of Biomass and Bio Energy, 20, 2011, PP 63-69.
17. B.K. Venkanna and C. Venkataramana Reddy, Performance, Emission and Combustion Characteristics of Direct Injection Diesel Engine Running on Calophyllum Inophyllum Linn Oil, International Journal of Agricultural & Biological Engineering Vol, 4, No.1, March 2011, PP 1-8.
18. Ikegami, M., Horibe, K. and Kamatsu, G. Numerical Simulation of Flow in an Engine Cylinder(2nd Report, Flow in a Deep- bowl Combustion Chamber),Bulletin of JSME,Vol.29,No.250.
19. Seppo. A., Niemi, and Timo Hatonen, Results From Durability Test of Mustard Seed Oil Driven Tractor Engine, Society of Automotive Engineers, USA, Paper No. 982528.
20. Gerhard Vellguth, Performance of Vegetable Oils and Their Monoesters as Fuel for Diesel Engines, Society of Automotive Engineers, USA, Paper No. 831358.
21. Dr. R. Udaya Kumar, Mr. S. Vijayaraj, Performance and Emission Analysis on a Direct Injection Diesel Engine Using Biodiesel from Palm Oil with Exhaust Gas Recirculation,Proceedings Of Icef2005 ASME Internal Combustion Engine Division 2005 Fall Technical Conference September 11-14, 2005, Ottawa, Canada, PP: 1-6.

Taylor & Francis
Taylor & Francis Group

Journal of Microwave Power and Electromagnetic Energy

ISSN: 0832-7823 (Print) (Online) Journal homepage: https://www.tandfonline.com/loi/tpee20

Investigations on physical properties of Mg ferrite nanoparticles for microwave applications

Siva Kumar Pendyala, K. Thyagarajan, A. Gurusampath Kumar & L. Obulapathi

To cite this article: Siva Kumar Pendyala, K. Thyagarajan, A. Gurusampath Kumar & L. Obulapathi (2019): Investigations on physical properties of Mg ferrite nanoparticles for microwave applications, Journal of Microwave Power and Electromagnetic Energy, DOI: 10.1080/08327823.2019.1569898

To link to this article: https://doi.org/10.1080/08327823.2019.1569898

Published online: 03 Apr 2019.

JOURNAL OF MICROWAVE POWER AND ELECTROMAGNETIC ENERGY
https://doi.org/10.1080/08327823.2019.1569898

Investigations on physical properties of Mg ferrite nanoparticles for microwave applications

Siva Kumar Pendyala[a,b], K. Thyagarajan[c], A. Gurusampath Kumar[d] and L. Obulapathi[e]

[a]Research Scholar, JNTUA, Anantapuramu-515002, India; [b]Department of Physics, Malla Reddy Engineering College (A), Secunderabad, India; [c]Department of Physics, JNTUA College of Engineering, Pulivendula, India; [d]College of Physics and Energy, Shenzhen University, Shenzhen, P.R. China; [e]Department of Physics, Annamacharya Institute of Technology & Sciences, Rajampet, India

ABSTRACT

Nanocrystalline Mg-ferrites have been synthesized by sol-gel auto combustion method using citric acid as fuel agent at different Calcination temperatures (200 °C, 400 °C, 600 °C, and 800 °C). The physical properties of nano Mg-ferrite were investigated using X-ray diffraction (XRD) analysis, scanning electron microscopy, Fourier-transform infrared spectroscopy, and LCR-Hitester for structural, surface morphology, functional groups and dielectric properties respectively. The single-phase cubic spinel structure of all the samples has been confirmed by XRD. Surface morphology studies reveal that the grains are clear with well-defined grain boundaries and also found that the average grain size is maximum at 600 °C calcination temperature. The dielectric studies reveal that the maximum dielectric constant is attained a value of 46 with the minimum dielectric loss at 600 °C calcination temperature.

ARTICLE HISTORY
Received 27 May 2018
Revised 29 August 2018
Accepted 20 September 2018

KEYWORDS
Sol-gel preparation; nanoparticles; Mg-ferrite; dielectric constant; dielectric loss

1. Introduction

Ferrites have play a vital role in the field of computer industry to develop the memory core devices, magnetic recording heads, microwave devices such as circulators, isolators, and inductor cores in electrical transformers, and so forth (Manjurul et al. 2008). Ferrites have unique characteristics such as low electrical conductivity, low dielectric loss, low device cost, high mechanical strength and environmental stability over wide range of frequencies. Mg-ferrite ($MgFe_2O_4$) exhibits spinel cubic structure with low magnetic anisotrophy at room temperature (RT; $K_1 = -33 \times 10^3$ erg/cm^3 at RT Akter and Hakim 2010) due to low magneto crystalline anisotropic energy. The nano-structured ferrites have an ideal characteristic of a small band gap, which is in the range of visible region (Masoudpanah et al. 2016). The visible region of the electromagnetic (EM) spectrum allows the ferrites efficiently for photo-catalytic reactions

CONTACT Siva Kumar Pendyala sivakumarpendyala2015@gmail.com JNTUA, Anantapuramu, Andhra Pradesh 515002, India; Gurusampath Kumar sampath2phy@szu.edu.cn College of Physics and Energy, Shenzhen University, Shenzhen 518060, Guangdong, P.R. China.

(Rais et al. 2014) and the degradation of different organic pollutants present in the environment (Casbeer et al. 2012; Nath et al. 2012; TahirFarid et al. 2017).

Mg-substituted ferrite (Fe_2O_4) systems play a significant role in the study of different applications in terms of physical and magnetic properties reported by the many researchers. Magnesium oxide (MgO) is highly stable oxide, with the increase of Mg-content, the octahedral Fe^{2+} ions care substituted by Mg^{2+} ions (Ghodake et al. 2017). To synthesize the nano-structured ferrites, various methods have been reported in the elsewhere such as co-precipitation (Mattei et al. 2008), microwave assisted solid state reactions (Samyuktha et al. 2016), sol–gel (Duque et al. 2001), hydrothermal (Duong et al. 2006), sol–gel auto-combustion method (Rabinder and Latha 1999), and so forth. From the above methods, the sol–gel auto-combustion method is simple, easy and cost-effective method to get desired nano-structured materials.

2. Experimental details

Nano Mg-ferrite (MgFe2O4) powders were prepared by citrate-nitrate precursor sol-gel-auto combustion technique using ferric nitrate nonahydrate (Fe(NO3)3.9H2O), magnesium nitrate hexa-hydrate (Mg(NO3)2 .6H2O) and citric acid (C6H8O7.H2O) as staring supplies with soaring purity of over 99.9%. Preliminary solution was prepared by dissolving these metal nitrates in the fraction of 1:3 and citric acid into deionized water and the solution pH value was attuned to 7.0 by adding ammonia drop wise to solution. The solution was heated to 100 °C and continuously stirred using magnetic agitation. Viscosity and color changed as the sol twisted into a clear stick gel. After 4 h, the solution became a homogeneous viscous sol–gel. Then the sol–gel was oven dried at 150 °C for 10 min. to obtain a dried gel. A slack, brown and very well Mg-ferrite powder was produced after the dried gel had spontaneously combusted in air. Finally, the brown, fluffy Mg-ferrite powder was calcined at various temperatures 200, 400, 600, and 800 °C for 4 h, respectively in muffle furnace. Finally the calcined powders were grounded finely and carried out the structural, surface morphological, dielectric and optical characterizations by X-ray diffraction (XRD; Bruker D8, Japan), scanning electron microscopy (SEM; Gemini, UK), LCR-Hitester (Japan), and Fourier-transform infrared spectroscopy (FTIR), respectively.

3. Results and discussion

The XRD patterns of Mg-ferrite at different calcinations temperatures (200, 400, 600, and 800 °C) are shown in Figure 1. The patterns confirm the presence of cubic spinel MgFe2O4 and were indexed using JCPDS card no. #89-3084 (Sivakumar et al. 2018b). From the XRD analysis, the characteristic reflections of Mg-ferrite having high intense peak (311) which confirms the cubic spinel structure with space group *Fd3m* (O_h^7) (Ghodake et al. 2016). The linear variation of the lattice constant (*a*) is found to increase from 8.368 to 8.372 Å with the calcination temperature upto 600 °C which follows the Vegard's law. On the basis of the ionic radii of the substituent

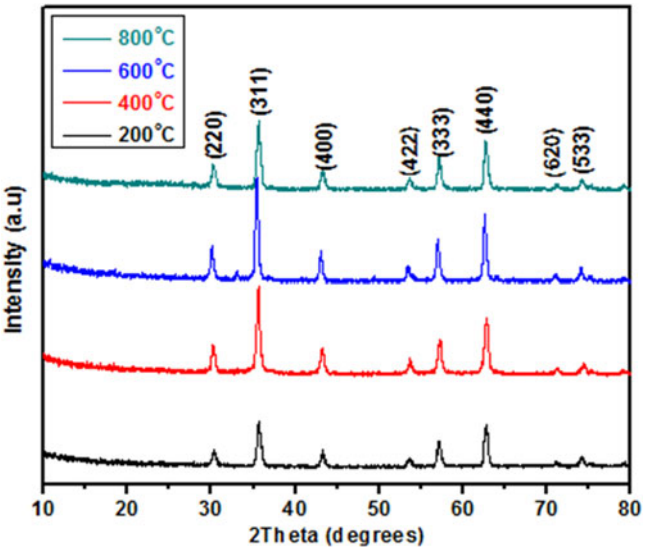

Figure 1. X-ray diffraction (XRD) patterns of Mg-ferrite samples at different calcinations temperatures.

ions, a small change (increase) in the lattice constant can be explained. It is assumed that the replacement of smaller Fe^{2+} ions (0.64 Å) with the larger Mg^{2+} ions (0.72 Å) on the octahedral sites causes the unit cell to enlarge which results in the enhancement of lattice constant. This is dependable with previous work reported by Ateia and Mohamed (2017). To understand the crystallite size of Mg-ferrite calcined at various temperatures and was calculated using Scherrer's equation (Kumar et al. 2016):

$$\boldsymbol{D} = \frac{\boldsymbol{k\lambda}}{\boldsymbol{\beta}\cos\boldsymbol{\theta}} \tag{1}$$

where $k = 0.94$ is Scherrer's constant, $\lambda = 1.5406$ Å is the wavelength of the X-rays, β is the full width at half maximum (FWHM) of diffraction peak, and θ is the Bragg's angle of diffraction. The variation of FWHM and crystallite size with respect to the calcination temperature is presented in Figure 2. The average crystallite size (D) varies from 18.45 to 23.76 nm. The observed variation in average crystallite size (D) is due to the replacement of Fe^{2+} (0.63 Å) ion by Mg^{2+} (0.72 Å) ions which supports the lattice constant variation results. The observed increase in the average crystallite size is attributed to large difference in the ionic radii of Fe^{2+} and Mg^{2+}. The Average crystallite size is maximum at 600 °C because of having the minimum FWHM value and hence the improvement of crystallanity of the sample.

Density of the ferrites plays an important role in measuring their electro-magnetic properties. It is known that when the solidity of the ferrites augmented, high permeability could be achieved. Now, the bulk density (dB), of the samples was measured using the relation, $d\mathrm{B}=m/V$, where m is the mass of the bulk sample in grams, and V is its volume in cubic centimeters. The X-ray density (d_x) of every sample was measured from the relation (Zahir et al. 2016),

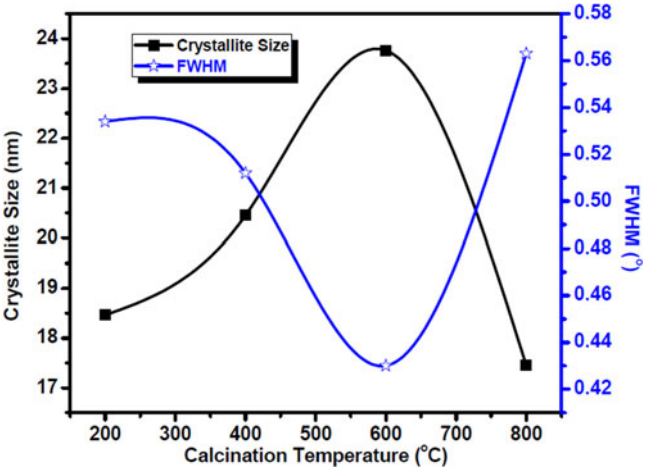

Figure 2. Variation of full width at half maximum (FWHM) and crystallite size as a function of calcinations temperature.

$$d_X = \frac{ZM}{Na^3} \tag{2}$$

where Z is the number of molecules per unit cell, which is 8 for the spinel structure, M represent the molecular weight (MW) of the analogous composition, N is the Avogadro's number, and a is the lattice constant of the samples.

The microstructures of the prepared Mg-ferrite samples at various calcination temperatures have been examined by SEM as shown in Figure 3(a–d). For the ferrite samples, the images of SEM notify a microstructure. The Mg-ferrite samples studied using SEM reveals that they are crack-free with uniform grain boundaries. The Mg-ferrite samples are crammed with grains having well defined grain boundaries. The opposition between the retarding force exerted by pores and the electrical driving force for the movement of grain boundary are due to the actions of grain augmentation. The uniformity in the electrical driving force of the grain boundary in each grain, the sample procures uniformity in grain size (Hankare et al. 2011). The SEM images clearly show the distinct and large grains, which resembles the crystals of hexagonal phase of Mg(OH)2. The estimation of grain sizes of the Mg-ferrite SEM images is done by using linear intercept method. The average grain size is increased with the calcination temperature upto 600 °C due to the exchange of thermal energy to the atoms and enhances the growth of the grains. But, at the higher calcination temperature (800 °C) the average grain size is decreased which is supported by the results observed in the XRD.

FTIR spectra of nano Mg-ferrite for various calcined temperatures are plotted in Figure 4. For all samples, the bands observed at 572 and 427 cm^{-1} are attributed to tetrahedral and octahedral M–O (M = Fe and Mg) stretching vibration mode. The peaks at 3421, 2920, 1441, and 1017 cm^{-1} corresponds to metal-oxygen lattice vibrations (Ay et al. 2009), and also due to O–H stretching vibrational mode and H–O–H bending mode can be accredited to the existence of free water and hydroxyl group in

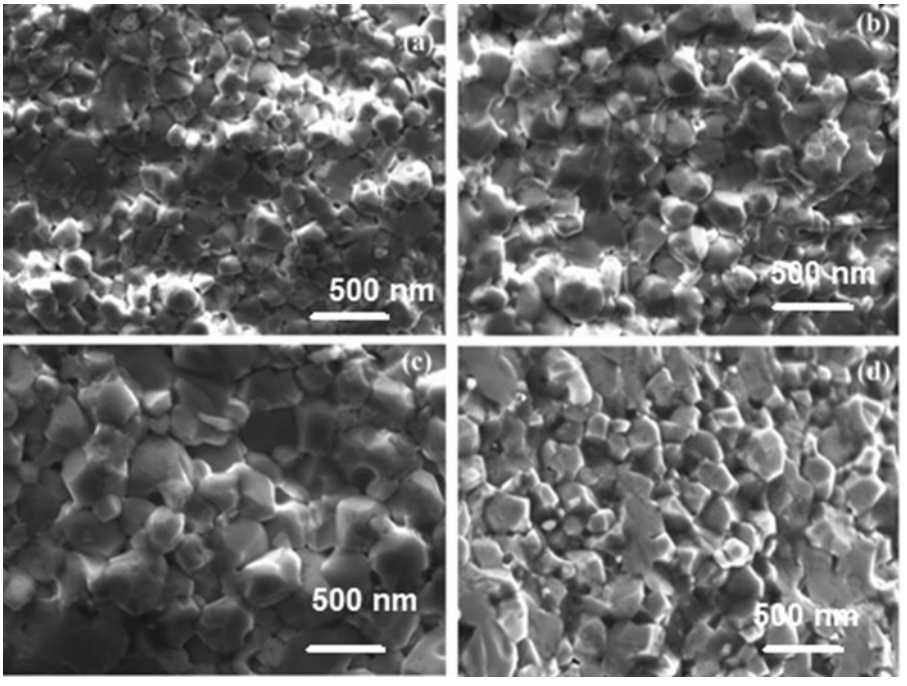

Figure 3. Scanning electron microscopy (SEM) images of the Mg-ferrite samples at different calcination temperatures (a) 200 °C, (b) 400 °C, (c) 600 °C, and (d) 800 °C, respectively.

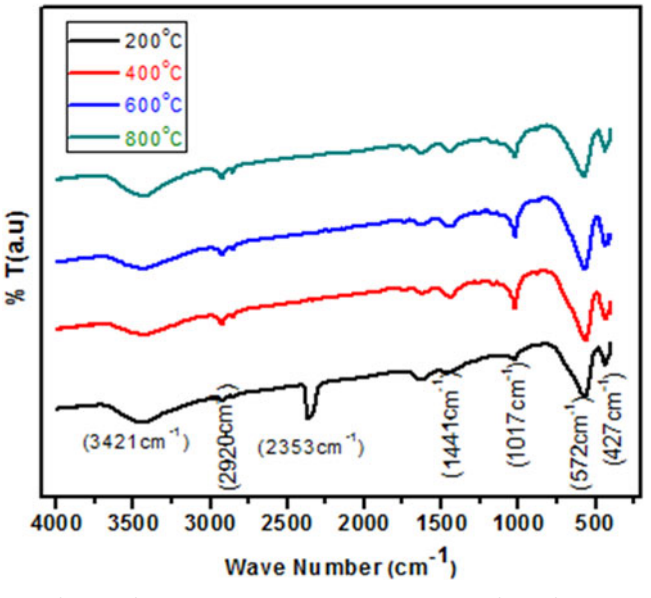

Figure 4. Fourier-transform infrared spectroscopy (FTIR) spectra of Mg-ferrite nanoparticles at different calcination temperatures.

the samples (Mojumdar et al. 2000; Labde et al. 2003). As the temperature increases to 400 °C, the peak at 2353 cm^{-1} is disappearing attributed to C–C stretching vibration (Xian et al. 2009).

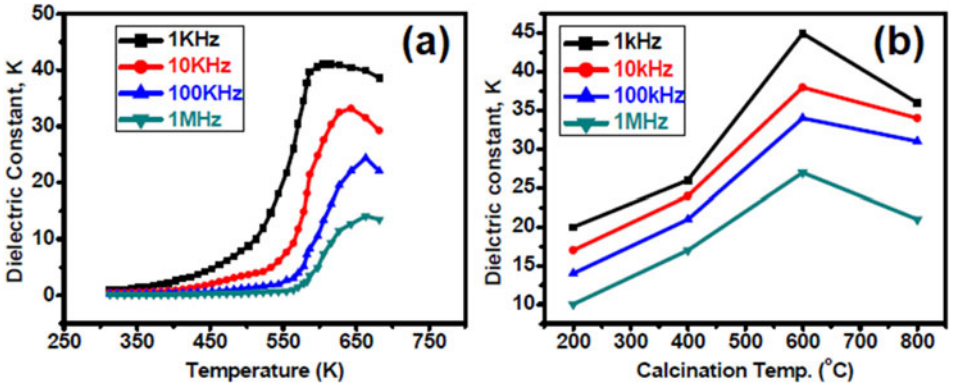

Figure 5. (a) Variation of dielectric constant with temperature at calcination temperature of 600 °C and (b) variation of dielectric constant with calcination temperature at different frequencies.

The essential information provided by dielectric properties of ferrite about behavior of the localized electric charge carriers leading to the greater understanding phenomenon of dielectric polarization. The powder specimen of nano Mg-ferrite is grained, for the dielectric measurements, taken 1 g of the sample in the form of powder then adding small amount of Polyvinyl alcohol as a binder and the pelletizer is used to prepare pellet with diameter 10 mm and thickness 2 mm by applying the hydraulic pressure of 10 Tons (Chandrababu Naidu et al. 2015; Maddaiah et al. 2015). These as prepared pellets were sintered to remove the water content in the sample at higher temperatures. Then, these sintered 2 mm thick pellets have been used for the measurement of dielectric response with the help of LCR HiTester at different frequencies (1 KHz to 1 MHz) and at various temperatures (RT to 400 °C) and high frequency (1 MHz to 1 GHz) measurements were done using LCR meter (Model HP-4284 A) at room temperature.

Figure 5 shows the temperature dependent of dielectric constant plot at different frequencies. As we know that, the natural behavior of most of all ferrites, the dielectric constant (K) of the material was found to be decreased with the increase in frequency (Ravinder et al. 2001). At low frequencies the value of dielectric constant is high. At lower frequencies, the augmentation in the dielectric constant with temperature is more pronounced than at higher frequencies. The K of any material, in common, is due to electronic, ionic, dipolar, and interfacial polarization. Interfacial and dipolar polarizations are play a crucial role at low frequencies and are strongly dependent on temperature. The creation of lattice defects and dipolar polarization is due to the change in temperature of the interfacial polarization. The effect of temperature is highly pronounced on the interfacial polarization than that of the dipolar polarization which results in the rapid increase of dielectric constant with increase of temperature at low frequencies (Patil et al. 2014; Sodaee et al. 2017).

The frequency dependent dielectric constant of Mg-ferrite calcined at 600 °C is shown in Figure 6. The dielectric constant decreased with increase in frequency and it follows the Koops phonological theory (Koops 1951; Sivakumar et al. 2018a). According to Koops theory, the dielectric constant decrease with increase in frequency is attributed to the decrease of polarization. Ultimately, it reaches a constant

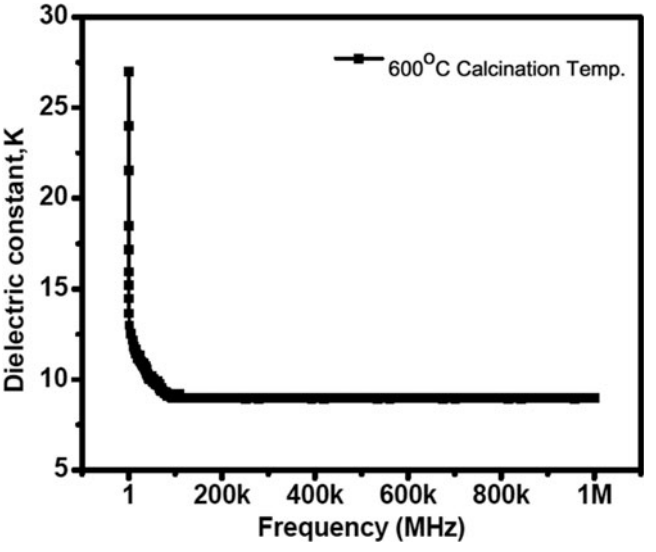

Figure 6. Frequency (1 MHz to 1 GHz) versus dielectric constant of Mg-ferrite sample calcined at 600 °C.

value because beyond a certain critical value of frequency of external field the electronic exchange between ferrous and ferric ions cannot follow the alternating field.

4. Conclusions

Nano-structured Mg-ferrites at various calcination temperatures have been successfully prepared by the sol-gel auto-combustion method. Mg-ferrite samples exhibit the cubic spinel structure with no impurity phase and average crystallite size was calculated from XRD is in the order of 20 nm and is increased with the calcination temperature upto 600 °C which was also supported by SEM studies. The SEM analysis confirmed the nature of material and surface having clear grains with well-defined grain segregation. The average grain size is increased with the calcination temperature. The FTIR spectra showed the clear O–H and C–O–H groups in the stretched and vibrational modes respectively. The maximum dielectric constant of 46 at 1 kHz frequency at 600 °C calcination temperature was observed. The dielectric constant, dielectric loss exhibits decreasing nature with increase of frequency, which is useful for applications in the range of high frequency especially in deflection yoke rings, microwave devices.

Disclosure statement

No potential conflict of interest was reported by the authors.

ORCID

A. Gurusampath Kumar http://orcid.org/0000-0002-0639-603X

References

Akter S, Hakim MA. 2010. Magnetic properties of cadmium substituted lithium ferrites. Mater Chem Phys. 120:399–403.

Ateia EE, Mohamed AT. 2017. Nonstoichiometry and phase stability of Al and Cr substituted Mg ferrite nanoparticles synthesized by citrate method. J Magn Magn Mater. 426:217–224.

Ay AN, Zümreoglu-Karan B, Temel A, Rives V, 2009. Bioinorganic magnetic core-shell nanocomposites carrying antiarthritic agents: intercalation of ibuprofen and glucuronic acid into Mg-Al-layered double hydroxides supported on magnesium ferrite. Inorg Chem. 48: 8871–8887.

Casbeer E, Sharma VK, Li XZ. 2012. Cobalt ferrite nanoparticles hosted in activated carbon from renewable sources. Sep Purif Technol. 87:1110–1117.

Chandrababu Naidu K, Sofisarmash T, Maddaiah M, Gurusampath Kumar A, Jhansirani D, SharonSamyuktha V, Obulapathi L, Subbarao T. 2015. Structural and electrical properties of PbO – doped $SrTiO_3$ ceramics. J Ovon Res. 11(2):79–84.

Duong GV, Sato R, Hanh N, Linh DV, Reissner M, Michor H, Fidler J, Wiesinger G, Grossimger R. 2006. Magnetic properties of nanocrystalline $Co_{1-x}Zn_xFe_2O_4$ prepared by forced hydrolysis method. J Magn Magn Mater. 307:313–317.

Duque S, Macedo MA, Moreno NO, Lopez JL, Pfanes HD, 2001. Magnetic and structural properties of CoFe2O4 thin films synthesized via a sol–gel process. J Magn Magn Mater. 226-230:1424–1425.

Ghodake UR, Chaudhari ND, Kambale RC, Patil JY, Suryavanshi SS. 2016. Effect of Mn^{2+} substitution on structural, magnetic, electric and dielectric properties of Mg-ferrites. J Magn Magn Mater. 407:60–68.

Ghodake UR, Rahul CK, Suryavanshi SS. 2017. Effect of Mn^{2+} substitution on structural, electrical transport and dielectric properties of Mg-Zn ferrites. Ceram Int. 43:1129–1134.

Hankare PP, Patil RP, Jadhav AV, Pandav RS, Garadkar KM, Sasikala R, Tripathi AK. 2011. Synthesis and characterization of nanocrystalline Ti-substituted Zn ferrite, J Alloy Compd. 509:2160–2163.

Koops CG. 1951. On the dispersion of resistivity and dielectric constant of some semiconductors at audio frequencies. Phys Rev. 83:121–124.

Kumar AG, Sarmash TS, Obulapathi L, Rani DJ, Rao TS, Asokan K. 2016. Structural, optical and electrical properties of heavy ion irradiated CdZnO thin films. Thin Solid Films. 605: 102–107.

Labde BK, Sable MC, Shamkuwar NR. 2003. Structural and infra-red studies of $Ni_{1+x}Pb_xFe_{2-2x}O_4$ system. Mater Lett. 57:1651–1655.

Maddaiah M, Gurusampath Kumar A, Obulapathi L, Sofisarmash T, Chandrababu Naidu K, Jhansirani D, Subbarao T. 2015. Synthesis and characterization of strontium doped zinc manganese titanate ceramics. Digest J Nanomater Biostruct. 10(1):155–159.

Manjurul MH, Huq M, Hakim MA. 2008. Densification, magnetic and dielectric behaviour of Cu-substituted Mg–Zn ferrites. Mater Chem Phys. 112:580–586.

Masoudpanah SM, Hasheminisari M, Ghasemi A. 2016. Magnetic properties and photocatalytic activity of $[ZnFe_{2-x}][La_x]O_4$ nanoparticles synthesized by sol-gel autocombustion method. J Sol-Gel Sci Technol. 80:487–493.

Mattei YC, Perez OP, Tomar MS, Roman F, Voyles MP, Stratton WG. 2008. Permittivity study of multiferroic AlN/NiFe/AlNmultilayer films. J Appl Phys. 103:07E512.

Mojumdar SC, Melník M, Jóna E. 2000. Thermal and IR properties of Mg(II) complexes with heterocyclic ligands. Thermochim Acta. 352–353:127–132.

Nath SK, Maria KH, Noor S, Sikder SS, Hoque SM, Hakim MA. 2012. Magnetic ordering in Ni–Cd ferrite. J Magn Magn Mater. 324:2116–2120.

Patil ND, Velhal NB, Tarwar NL, Puri VR. 2014. Experimental studies of neodymium ferrites doped with three different transition metals. Int J Eng Innov Technol. 3:73–77.

Rabinder D, Latha K. 1999. Dielectric behavior of mixed Mg–Zn ferrites at low frequencies Mate. Lett. 41:247–253.

Rais A, Taibi K, Addou A, Zanoun A, Al-Douri Y. 2014. Copper substitution effect on the structural properties of nickel ferrites. Ceram Int. 40:14413–14419.

Ravinder D, VijayKumar K, Balaya P. 2001. High-frequency dielectric behavior of gadolinium substituted Ni–Zn ferrites. Mater Lett. 48:210–214.

Samyuktha VS, Kumar AG, Rao TS, Suvarna RP. 2016. Synthesis, structural and dielectric properties of Magnesium calcium titanate (1-x)$MgTiO_3$-x$CaTiO_3$ (x = 0, 0.1, 0.2 and 0.3). Mater Today Proc. 3:1768–1771.

Sivakumar P, Thyagarajan K, Gurusampath Kumar A, Obulapathi L, 2018a. Effect of Mg doping on physical properties of Zn ferrite nanoparticles. J Aust Ceram Soci. 54:467–473.

Sivakumar P, Thyagarajan K, Kumar AG. 2018b. Investigations on physical properties of Zn ferrite nanoparticles using sol-gel auto combustion technique. Digest J Nanomater Biostruct. 13(4): 1117–1122.

Sodaee T, Ghasemi A, Razavi RS. 2017. Cation distribution and microwave absorptive behavior of gadolinium substituted cobalt ferrite ceramics. J Alloy Compd. 706:133–146.

TahirFarid HM, Ahmad I, Ali I, Ramay SM, Mahmood A, Murtaza G. 2017. Dielectric and impedance study of praseodymium substituted Mg-based spinel ferrites. J Magn Magn Mater. 434:143–150.

Xian T, Yang H, Shen X, Jiang JL, Wei ZQ, Feng WJ. 2009. Preparation of high quality BiFeO3 nanopowders via a polyacrylamide gel route. J Alloys Comp. 480:889–892.

Zahir R, Chowdhury FUZ, Uddin MM, Hakim MA. 2016. Structural, magnetic and electrical characterization of Cd-substituted Mg ferrites synthesized by double sintering technique. J Magn Magn Mater. 410:55–62.

Secure and Verifiable Policy Update Method on Big Data Access in Cloud Storage

G.Charles Babu, A.Sai Hanuman, J.Sasi Kiran, B.Sankara Babu

Abstract*: Disseminated figuring would be one of advancements which will expect a fundamental occupation in the best in class time of PC structuring field. As a result of the high volume and speed of immense data, it is a fruitful decision to store huge data in the cloud, as the cloud has capacities of securing tremendous data and dealing with high volume of customer get to requests. Trademark Based Encryption (ABE) is a promising system to ensure the end to-end security of huge data in the cloud. In this paper, we propose a novel arrangement that enabling gainful access control with dynamic methodology invigorating for gigantic data in the cloud. We fixate on working up a re-appropriated approach reviving method for ABE structures. Our system can avoid the transmission of mixed data and cutoff the figuring work of data proprietors, by making usage of the as of now encoded data with old access approaches. Also, we in like manner propose approach invigorating computations for different sorts of access courses of action. Finally, we propose a beneficial and secure methodology that empowers data proprietor to check whether the cloud server has revived the figure messages precisely. The examination shows that our course of action invigorating redistributing plan is correct, whole, secure and profitable.

***Index Terms*: Big Data, Cloud, Attribute Based Encryption (ABE), Policy Updating.**

I. INTRODUCTION

Disseminated figuring would be one of advancements which will expect a fundamental occupation in the best in class time of PC structuring field. As a result of the high volume and speed of immense data, it is a fruitful decision to store huge data in the cloud, as the cloud has capacities of securing tremendous data and dealing with high volume of customer get to requests. Trademark Based Encryption (ABE) is a promising system to ensure the end to-end security of huge data in the cloud. In this paper, we propose a novel arrangement that enabling gainful access control with dynamic methodology invigorating for gigantic data in the cloud. We fixate on working up a re-appropriated approach reviving method for ABE structures. Our system can avoid the transmission of mixed data and cutoff the figuring work of data proprietors, by making usage of the as of now encoded data with old access approaches. Also, we in like manner propose approach invigorating computations for different sorts of access courses of action. Finally, we propose a beneficial and secure methodology that empowers data proprietor to check whether the cloud server has revived the figure messages precisely. The examination shows that our course of action invigorating redistributing plan is correct, whole, secure and profitable.

Revised Manuscript Received on March 10, 2019.

Dr.G.Charles Babu, Professor, Dept. of CSE, Malla Reddy Engineering College(Autonomous), Secunderabad – 500100, Telangana, India.

Dr.A.Sai Hanuman & Dr.B.Sankara Babu, Professor, Dept. of CSE, Gokaraju Rangaraju Institute of Engineering & Technology(Autonomous), Bachupally, Telangana, India.

Dr.J.Sasi Kiran, Professor in CSE & Principal, Farah Institute of Technology, Chevella, Ranga Reddy(Dist), Telangana, India.

II. LITERATURE REVIEW

Prayla, S et al (2018) Our course of action engages the cloud server to feasibly stimulate the figure content when another entry approach is controlled by the information proprietor, who is besides arranged to help the resuscitate to counter against cheating practices of the cloud. It in addition draws in (I) the information proprietor and qualified clients to adequately confirm the validness of a client for getting to the information, and (ii) a client to help the data gave by different clients to rethink plaintext recuperation

Taniya Jain (2017) As the term shows the Big data it suggests we are work for the something huge or can state something broad in the Amount, Data the high volume is known as the gigantic data. Directly a Day for securing the data archive in the Computer Science Engineering we are used the Hard circle, a part of the limit put, these limit contraptions may store the data in a Giga byte capacity and Terabyte capacity or some more, now every day we are used the some new development call the cloud condition. So in this work I am ponder the gigantic data securing process in the Cloud condition, colossal data bringing from the cloud securerly.

Vishnu R. Lembhe et al (2016) in enlisting condition, the limit of tremendous data is main problem. So to vanquish this store the gigantic data in cloud since it has capacities of securing enormous proportion of data and taking care of a high volume of customer get to requests. Appropriated figuring use the Attribute Based Encryption (ABE) for giving the end to end security for enormous data in a cloud. Using this ABE technique, reviving has been a trying issue in the past executions, immediately data proprietors need to recuperate the data and after that re-encode the new access approach and send back to the cloud .Due to this, high correspondence and computational weight was on the data proprietors. So to vanquish this issue of existing structure here proposed another system that intensely revives a technique for gigantic data in the cloud. Data proprietors need to just check whether figure content has been invigorated precisely or not.

Kalpana, V et al (2014) the course of action invigorating has reliably been a trying issue when ABE is used to construct get the chance to control contrives and develop another procedure to redistribute the technique reviving to the server. Attribute Based Access Control technique is used to avoid the transmission of encoded data and breaking point the computation work of data proprietors, by making use of the in advance mixed data with old access courses of action. A methodology invigorating count called LSSS is used for gainful and secure procedure empowers data proprietor to check whether the cloud server has revived the figure messages precisely.

III. PROPOSED SYSTEM & OBJECTIVES

The proposed structure revolves around adopting care of the strategy invigorating issue in ABE structures, and proposes an ensured and certain procedure revive redistributing method. As opposed to recuperating and re-encoding the data, data proprietors simply send game plan reviving request to cloud server, and let cloud server invigorate the methodologies of mixed data particularly, which infers that cloud server does not need to unscramble the data beforehand/in the midst of the methodology invigorating. This arrangement can satisfy all the above necessities, and keep up a vital separation from the trading of mixed data forward and in reverse and farthest point the computation work of data proprietors by making full use of the in advance encoded data under old access courses of action in the cloud.

Objectives:

1. To examination the course of action invigorating issue in ABE systems and develop another procedure to redistribute the methodology reviving to the server
2. To find the expressive and profitable data get the opportunity to control plot for enormous data, which engages compelling intense plan reviving
3. To examination the successful and secure methodology for checking, paying little heed to whether the figure works are invigorated precisely by the cloud server

The methodology invigorating is a troublesome thing in trademark based access since when data proprietor stores data into the cloud, it doesn't have a copy of it in neighborhood structures. If a particular data proprietor needs to change the data he needs to trade data back to his neighborhood site from the cloud, encode it again and move back to the server. Consequently, it achieves a high correspondence overhead and generous count inconvenience on data proprietors. This motivates us to develop another procedure to re-fitting the task of methodology reviving to cloud server.

The remarkable trial of re-appropriating approach reviving to the cloud is to guarantee the going with requirements:

1) Correctness: Users who have sufficient qualities ought to at present have the ability to unscramble the data mixed under new access game plan by running the main deciphering estimation.

2) Completeness: The course of action reviving procedure should have the ability to invigorate any sort of access approach.

3) Security: The system invigorating should not break the security of the passageway control structure or present any new security issues

Features of Attribute-based Access Control: In colossal data time, the volume of data is high and it is extending in a fast. The proposed trademark based access control (ABAC) method is exceptionally sensible for controlling tremendous data than ordinary access control systems due to the going with features:

1) Policy Checking Entity Free: In ABAC, get to approaches are portrayed by data proprietors yet don't require any substance (e.g., the server) to check these procedures. Or maybe, get to game plans in ABAC are maintained certainly by the cryptography. On account of this key component, ABAC is by and large associated with control immense data in cloud conditions, where cloud servers are not trusted to execute get to courses of action.

2) Storage Efficiency: In standard Public Key Cryptography, for each datum, diverse copies of figure works are conveyed whose number is with respect to the amount of customers. Contemplating the high volume of tremendous data, it achieves a massive storing overhead despite when simply increasing the volume of gigantic data. Fortunately, in ABAC, only a solitary copy of figure content is delivered for each datum, which can diminish the limit overhead in a general sense.

3) Dynamic Policies yet Same Keys: Data proprietors can use a comparative open key to encode data under different access methodologies, and customers don't need to change their riddle keys either. Likewise, data proprietors can change get to plans of existing figure messages by simply sending an interest to the cloud server, and let the server do the methodology change without spilling out any unstable information of the data and also the keys.

System Model

We consider a safe conveyed stockpiling structure for different masters, as showed up in Fig.1. The system appears in this paper incorporates five particular components: the overall declaration specialists (CAs), the property experts (AAs), the cloud (server), the information (proprietors) and the information buyers (clients).

CA:

Every CA is an overall trusted in support master in the structure. They recognize the enrollment of the significant number of customers and AAs in this system. What's more, the CAs is accountable for the scattering of overall secret key and overall open key for each genuine customer in the structure. Regardless, they are not locked in with any quality organization and the creation of secret keys that are connected with properties.

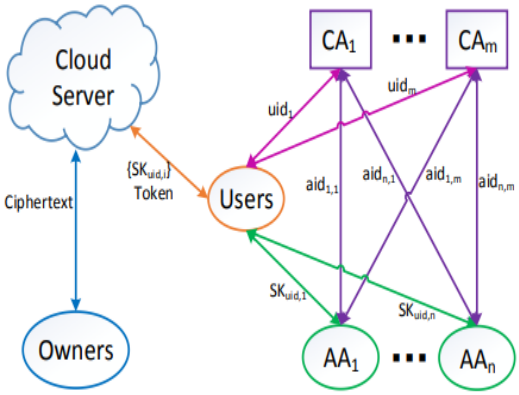

Figure 1: System Model of our Scheme

AA:

Every AA is a self-ruling property expert. Every AA is accountable for issuing, revoking and invigorating customer's credits as shown by their own one of a kind employment or identity in its space. Every attribute is connected with one single AA. In any case, each AA can manage an abstract number of characteristics. It is responsible for making an open quality key for every trademark it directs and a secret key for each customer accomplices with their properties. Every AA has positive direction over the structure and semantics of its properties.

Cloud server:

The cloud server stores the proprietors' data and gives data get to organization to customers. In this paper, the cloud server creates the unscrambling token of a figure content for the customer by using the customer secret keys issued by the AAs. Furthermore, the server also does the invigorate undertaking of the figure content when a property refusal happens.

Information Owner:

The Data Owner in this system portrays the passageway game plans of data. Under the methodologies, the data proprietors encode the data previously re-appropriating them in the cloud. Without relying upon the server to get the data get the chance to control, all the legitimate customers in the system can get to the figure content. In any case, the passageway control happens inside the cryptography. Exactly when the customer's attributes satisfy the passage game plan described in the figure content, can the customer decipher the figure content?

Customer:

A cloud customer could be an undertaking or one single customer. Each customer in the system is doled out with a couple of offers of an identity from the CAs, which can be collected and registered as its remarkable overall customer character. To unscramble a figure message that can be gotten to uninhibitedly from the cloud server, each customer may display their riddle keys issued by a couple of AAs together with its overall open key to the server. By then the system asks for that it make an unscrambling token for some figure works. Subsequent to tolerating the unscrambling token, the customer can translate the figure content using its overall puzzle key. The server can deliver the correct deciphering token, exactly when the customer's characteristics satisfy the passage technique portrayed in the figure content. To store the riddle keys and the overall customer's open key on the server, thusly, if no secret keys are invigorated for the further unraveling token age, the customer require not present any puzzle keys.

Key Generation:

Here Keys are delivering for every last one of a kind reports. At the period of customer recouping any archive key is essential for access the record. In a straight arrangement, the riddle is viewed as a part of a restricted field, and the offers are procured by applying an immediate mapping to the puzzle and a couple of self-governing unpredictable segments.

Course of action invigorates Authority:

The master delivers the key with the objective that proprietor can scramble the data and customer can unscramble the data. It checks the data is shielded moreover offer affirmation to the data. Each customer data is consigned with an overall customer personality and can uninhibitedly get the figure works from the Authority.

IV.METHODOLOGY

Characteristic BASED ENCRYPTION (ABE):

Property Based Encryption (ABE) has ascended as a promising methodology to ensure the end to-end data security in disseminated stockpiling structure. It empowers data proprietors to portray get to techniques and scramble the data under the methodologies, with the ultimate objective that just customers whose qualities satisfying these passage courses of action can unscramble the data. At whatever point more affiliation and tries re-proper their data into the cloud, the methodology reviving transforms into a significant issue as data get to techniques may be changed effectively and as regularly as conceivable by data proprietors. Nevertheless, this procedure invigorating issue has not been considered in existing quality based access control designs. The procedure invigorating is a troublesome issue in quality based access control systems, in light of the way that once the data proprietor re-appropriated data into the cloud, it would not keep a copy in close-by structures. Unscrambling is simply possible when the amount of organizing is something close to an edge regard d. Plan impediment is indispensable security feature of Attribute-Based Encryption .An adversary that holds distinctive keys should simply have the ability to get to data if no short of what one individual key stipends get to. The issue with property based encryption (ABE) plan is that data proprietor needs to use each affirmed customer's open key to scramble data. The utilization of this arrangement is bound in the bona fide condition since it uses the passageway of monotonic credits to control customer's passage in the system.

a) Key Policy Attribute Based Encryption (KP-ABE):

It is the balanced sort of built up model of ABE. Customers are named with a passageway tree structure over the data properties. Point of confinement entryways are the centers of the passageway tree. The properties are connected by leaf center points. To reflect the passageway tree Structure the secret key of the customer is described.

Figure compositions are named with sets of characteristics and private keys are connected with monotonic access structures that control which figure messages a customer can unscramble.

Key Policy Attribute Based Encryption (KP-ABE) plot is intended for one-to-numerous correspondences. KP-ABE conspire comprises of the accompanying four calculations:

Setup: Algorithm takes input K as a security parameter and returns PK as open key and a structure expert riddle key MK.PK is used by message senders for encryption. MK is used to create customer secret keys and is known just to the pro.

Encryption:

Algorithm takes a message M, individuals all in all key PK, and a course of action of characteristics as data. It yields the figure content E.

Translating:

It takes as data the customer's riddle key SK for access structure T and the figure content E, which was encoded under the property set. This figuring yields the message M if and just if the property set satisfies the customer's passage structure T. The KP-ABE plan can achieve fine-grained get the opportunity to control and more versatility to control customers than ABE contrive. The issue with KP-ABE contrive is the encryptor can't pick who can decipher the mixed data. It can simply pick clear attributes for the data; it is inadmissible in some application because a data proprietor needs to trust in the key underwriter.

Quality Based Access Control with Efficient Revocation in Data Outsourcing Systems:

This proposes a passageway control part reliant on figure content methodology attribute based encryption to approve get the chance to control courses of action with compelling characteristic and customer denial technique. The fine-grained get the opportunity to control can be refined by twofold encryption plot. This twofold encryption framework abuses the characteristic based encryption and specific social affair enter scattering in every property gathering. The advantage of this arrangement is securely managing the redistributed data. This arrangement achieves powerful and secure in the data redistributing structures.

Property Based Encryption with Verifiable Outsourced Decryption:

This plan changes the main model of ABE with re-appropriated translating to think about irrefutable status of the progressions in existing system. This new model forms a strong ABE scheme with clear redistributed unscrambling also does not rely upon unpredictable prophets.

Security Issue:

Multi-master CP-ABE tradition empowers the central pro to unscramble all the figure compositions, since it contains the expert key of the system; Revocation Issue: Protocol does not support quality disavowal.

Access Control:

Access control gives the endorsement to the customers which gives the passageway benefits on data and distinctive resources. Access control can be engaged in most of the enlisting condition, for instance, Peer to Peer, Grid and Cloud. Dispersed capacity organizations are gotten to through a circulated stockpiling entry. Access control is generally said to be system or procedure that grants, denies or limits access to a structure. It in like manner perceives when the unapproved customers endeavoring to get to the system. The generally used access control procedures are character based access control models. Access control in cloud depends upon the circulated stockpiling and its data security and the passageway decision ends up being especially essential decision in cloud. Access control is basic part in the server homestead of government and business Access techniques are for each situation irregular state decision that chooses how gets to are controlled and get to decisions are made. The inspiration driving access control in cloud is to keep the passageway on challenge in cloud by unapproved customers of that particular cloud which will redesign security in the cloud condition.

V.TRIAL RESULTS

Around there we have taken a gander at two symmetric figurings to be particular AES and Serpent. The parameters which are considered for examination are time taken for archive encryption and number of records as information. We have exhibited the relative examination of the two computations through graph that shows that Serpent encryption count gives ideal execution over AES encryption estimation.

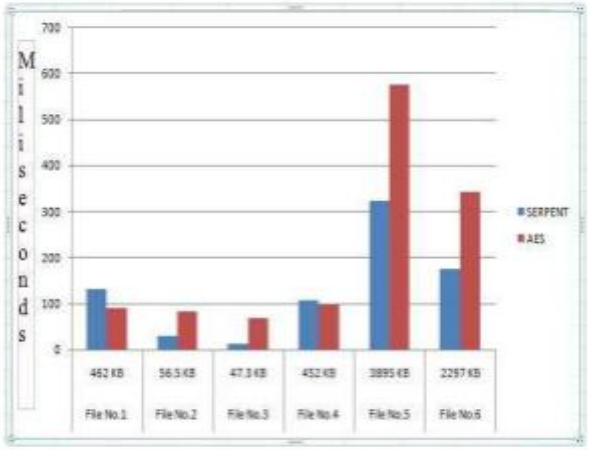

Figure 2: combined graph of AES and Serpent

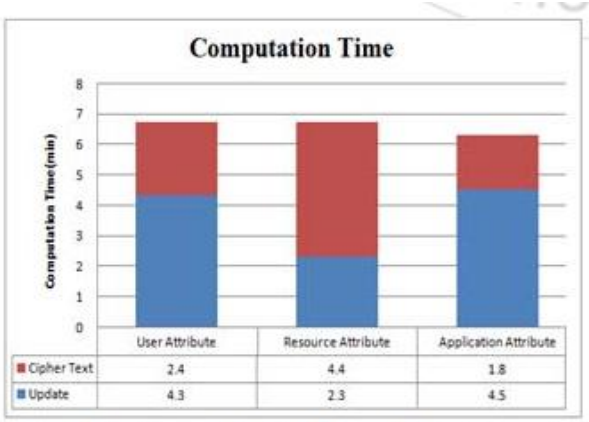

Figure 3: Computation time between Update keys and new cipher text components

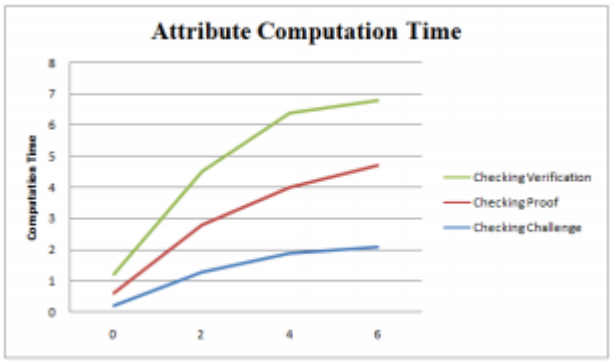

Figure 4: Computation evaluation of policy checking

To change the entrance arrangements of encoded information in the cloud, a minor technique is to give information proprietors a chance to recover the information and re scramble it under the new access strategy, and after that send it back to the cloud server. Be that as it may, this technique will bring about a high correspondence overhead and overwhelming calculation load on information proprietors.

VI. CONCLUSION

The proposed arrangement guarantees that the genuine data proprietor could pass the cloud server's affirmation and legally invigorate the figure content identifying with the proprietor's data, check and execution. A dynamic technique get the opportunity to control plot is secure in the customary bilinear social affair show. We have in like manner proposed an expressive property based access control plot for huge data in the cloud, and organized plan invigorating figurings for different sorts of access approaches. In addition, we proposed a procedure which engages data proprietors to check the rightness of the figure content invigorating. We moreover separated our arrangement to the extent rightness, climax, security and execution. The passageway control plot is based on prime demand get-togethers, in light of the way that the social event exercises on prime demand bundles are altogether faster than the ones on Composite ask for get-togethers. A dynamic game plan get the opportunity to control plot is secure in the regular bilinear social occasion show. Open key encryption moreover called as amiss encryption incorporates a few keys, open key and private key accomplices with a substance. Certification the data security in the cloud.

REFERENCES

1. Taniya Jain (2017), "Secure Big Data Access Control Policies for Cloud Computing Environment", International Journal of Innovative Research in Computer Science & Technology (IJIRCST) ISSN: 2347-5552, Volume-5, Issue-2, PP: 253-256
2. Vishnu R. Lembhe, Ravi A. Mule, Pratik R.Ponde, Tejas S. Yerguntla, R.G.Raut (2016), "Protected and Verifiable Policy Update for Big Data Access Control in the Cloud", IOSR Journal of Computer Engineering (IOSR-JCE), e-ISSN: 2278-0661,p-ISSN: 2278-8727, PP: 31-35
3. V. Goyal, O. Pandey, A. Sahai, and B. Waters, Attribute-based encryption for fine-grained access control of encrypted data, in CCS06. ACM, 2006, pp. 8998
4. A Sahai, J. Bettencourt and B.Waters, "Ciphertext-policy attribute based encryption", IEEE Symposium on Security and Privacy, page 321V334, 2007
5. Baodong Qin, Robert h. Deng, Shengliliu, and Siqi ma, "Attribute-based encryption with efficient verifiable outsourced decryption", ieee transactions on information forensics and security, 10.1109/tifs.2015.2410137
6. kan yang, xiaohuajia, "Expressive, efficient, and revocable data access control for multi-authority cloud storage ", ieee transactions on parallel and distributed systems, vol. 25, no. 7, july 2014.
7. Kan Yang, XiaohuaJia, "Attributed-based Access Control for Multi-Authority Systems in Cloud Storage", 2012 32nd IEEE International Conference on Distributed Computing Systems, 1063-6927/12 © 2012 IEEE.
8. Vipul Goyal, Omkant Pandey, Amit Sahai, Brent Waters, "Attribute-Based Encryption for Fine-Grained Access Control of Encrypted Data", CCS'06, October 30– November 3, 2006, Alexandria, Virginia, USA. Copyright 2006 ACM 1-59593-518
9. Kan Yang, XiaohuaJia, Kui Ren, "Attribute-based FineGrained Access Control with Efficient Revocation in Cloud Storage Systems", ASIA CCS'13, May 8–10, 2013, Hangzhou, China.
10. M. Dehkordi and S. Mashhadi, "An efficient threshold verifiable multisecret sharing," Computer Standards & Interfaces, vol. 30, no. 3, pp. 187–190, 2008

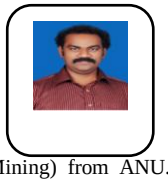

G.Charles Babu , Presently working as a Professor in Dept. of CSE in Malla Reddy Engineering College(Autonomous), Secunderabad, Telangana Since 5 Years and Total Teaching experience of 20 Years. Completed B.Tech (CSE) in 1997 from KLCE, M.Tech(SE) in 1999 from JNTUH and Ph.D(Data Mining) from ANU. Published more than 50 Research Papers in Data Mining, Cloud Computing.

Dr.AkundiSai Hanuman, Professor of Computer Science and Engineering, completed his Ph.D. from Acharya Nagarjuna University, Guntur in 2012. He has over 22 years of experience in Academic, Industry and Research.

Dr. AkundiSai Hanumans Research interests include Data Clustering, Data Sciences, Machine Learning, Optimization Techniques and Distributed Systems. Currently Dr. Sai Hanuman is acting as Dean of Academics in GRIET .

Dr. J. Sasi Kiran ,B.Tech from JNTUH, M.Tech from Bharath University and received Ph.D degree in Computer Science from University of Mysore. He is working as Principal & Professor in CSE in Farah Institute of Technology, Chevella, Telangana ,India. His research interests include Image Processing, Cloud Computing and Network Security. He has published research papers till now in Conferences, Proceedings and Journals

Dr. B Sankara Babu, Professor in Computer Science and Engineering, completed his Ph.D from Acharya Nagarjuna University, Guntur and has over fourteen years of academic and research experience in Gokaraju Rangaraju Institute of Engineering and Technology. His research interests are Data Mining, Big Data Analytics, Machine Learning and Internet of Things in which he has more than 25 publications in various reputed journals and conferences. Dr.B.Sankara Babu Currently Dean of Internships at GRIET.

A Systematic Approach Toward Description And Classification Of Cyber Crime Incidents

G.Charles Babu, A.Sai Hanuman, J.Sasi Kiran, B.Sankara Babu

Abstract: ***The headways in PC frameworks and systems have made another condition for criminal acts, generally known as cybercrime. The cybercrime episodes are events of specific criminal offenses that represent a genuine danger to the worldwide economy, security, and society's prosperity. This paper presents a far reaching comprehension of cybercrime occurrences and their relating offenses consolidating a progression of methodologies announced in applicable writing. At first, this paper audits and recognizes the highlights of cybercrime episodes, their separate components and suggests a combinatorial occurrence portrayal diagram. The diagram gives the chance to efficiently join different components or cybercrime attributes. Furthermore, a complete rundown of cybercrime-related offenses is advanced. The offenses are requested in a two-level order framework dependent on explicit criteria to aid better characterization and connection of their separate episodes. This empowers an intensive comprehension of the rehashing and fundamental criminal exercises. The proposed framework can fill in as a typical reference surpassing deterrents getting from confusions for cybercrimes with cross-fringe exercises. The proposed diagram can be stretched out with a rundown of suggest edactions, relating measures and successful approaches that coordinate with the offense type and in this way with a specific occurrence. This coordinating will empower better observing, dealing with and moderate cybercrime episode events. A definitive goal is to fuse the blueprint based portrayal of cybercrime components to a total occurrence the executives framework with standard working methods and conventions.***

Index Terms**: *PC frameworks, cybercrime, portrayal diagram, worldwide economy.***

I. SCOPE OF THE WORKT

The headways in PC frameworks and systems have made another condition for criminal acts, broadly represented as cybercrime. The cybercrime episodes are events of specific criminal offenses that represent a genuine risk to the worldwide economy, security, and prosperity of society. This paper presents a thorough comprehension of cybercrime occurrences and their relating offenses joining a progression of methodologies revealed in applicable writing. At first, paper surveys and recognizes the highlights of cybercrime occurrences, their separate components and proposes the combinatorial episode portrayal outline. The mapping gives the chance to deliberately consolidate different components - or cybercrime attributes. Moreover, an exhaustive rundown of cybercrime-related offenses is advanced.

The offenses are requested in a two-level characterization framework dependent on explicit criteria to aid better arrangement and connection of their separate episodes. This empowers an intensive comprehension of the rehashing and fundamental criminal exercises. The proposed framework fills typical reference overwhelming hindrances getting from misunderstanding with cross-fringe exercises for cybercrimes. The proposed diagram can be reached out with a rundown of prescribed activities, relating measures and powerful strategies that coordinate with the offense type and in this manner with a specific episode. This coordinating will empower better observing, taking care of and moderate cybercrime episode events. A definitive goal is to consolidate the pattern based depiction of cybercrime components to a total episode the board framework with standard working strategies and conventions.

Late advancements in the correspondences and Information Technology (IT) unlocked the entryway on recent applications that empower transmitting data precisely and rapidly. The advancements have obviously negative angles, for example, empower the digital predators to direct their online assaults against the people in question. Besides, this paper relies upon the correlation between the KSA and UK enactments to battle the digital provocations. Where, the KSA and UK enactments were ordered by explicit cybercrime types. Besides, the target of this examination is to enhance KSA enactments as far as fighting the new kinds of cybercrimes seemed dependent on the UK battling activities.

II. OBJECTIVE OF THE STUDY

- To plan A Systematic Approach towards Classification and Description of Cyber Crime Incidents
- To examine Legal Aspects of Cyber security
- To ponder Cybercrimes-based Legislations Classifications, a Comparative Research between KSA and UK
- To think about Cyber-wrongdoing: An audit of the proof
- To consider Cyber Crime in the Society: Problems and Preventions

III. LITERATURE REVIEW

Wow Essay (2009) The offices of PC innovation have not turned out without downsides. Despite of the fact that the life is so rapid and quick, yet flung under the shroud of danger from the deadliest kind of culpability named as 'Digital wrongdoing' without PCs, government and organizations activities would nearly stop to

Revised Manuscript Received on March 25, 2019.

Dr.G.Charles Babu, Professor, Dept. of CSE, Malla Reddy Engineering College(Autonomous), Secunderabad – 500100, Telangana, India.

Dr.A.Sai Hanuman & Dr.B.Sankara Babu, Professor, Dept. of CSE, Gokaraju Rangaraju Institute of Engineering & Technology(Autonomous), Bachupally, Telangana, India.

Dr.J.Sasi Kiran, Professor in CSE & Principal, Farah Institute of Technology, Chevella, Ranga Reddy(Dist), Telangana, India.His Department Name, University/ College/ Organization Name, City Name, Country Name.

work. The multiplication of incredible, shoddy, easy to understand PCs has empowered an ever expanding the number of individuals to apply them and more vitally, depend as a feature of their ordinary lifestyle. As the government offices, organizations and people keep on depending on developing extent, so the crooks restriction of digital wrongdoings is dependent on appropriate investigation of their comprehension and conduct on different dimensions of society. Thusly, at present original copy an efficient awareness of digital violations and its effects on zones like Soci-eco-political, adolescent and customer trust, with the upcoming patterns are clarified.

Shantosh Rout (2008) Eventual fate of Internet is available for anyone among typical clients. Fears of a digital world still proliferate, while the potential harm degree can be brought by scale misrepresentation is almost absolute. These nerves are essential to be reasonably moderate with learning the issues are being tended to, although not quick enough. The Internet's value has substantiated in various ways that are sufficient to guarantee it does not curving into a no man's area of criminal movement and a support for the malevolent. The administration has an imperative task to carry out; nevertheless a large portion of counteractive action should be refined by business elements bear programming and with the capacity to halt the extortion. Depending on the customer instruction the projects influences a level of conceivable accepted people. The other users should be secured through the measures that do not pressure and requires the impressive interest. The security issues should be simple and successful in the working environment. Regardless of either cybercrime is as yet an suitable issue, however, due to the elevate of development over Internet, is its essential to illuminate with the goal that cybercrime substance will relate to certifiable violations, if worse.

Prasun Sonwalkar (2009) The authentic copy not only discusses digital violation's comprehension yet furthermore clarifies the effects over unique dimensions of the public. This helps the network to verify the online data fundamental associations that are not protected due to digital wrongdoings. The awareness of conduct of digital offenders and digital violation's effects on society will identify the suitable way to breakdown the circumstances. The finest method to beat the wrongdoings are comprehensively grouped into three classes, namely, (1) Cyber Laws (alluded as Cyber laws), (2) Policy making and (3) Education. These approaches deal with digital wrongdoings either exceptionally inferior critical work or having nothing in considerable lot of the nations. This work requires either embellishing the current work or setting updated standards for regulating the digital assaults.

D. L. Shinder and M. Cross (2008) Over the most recent two decades, organizations, customers, and governments around the world have moved into the internet and cloud condition so as to direct their organizations. Numerous individuals spend a critical piece of their every day life in the internet, making and getting a charge out of new sorts of social connections which were impractical or fiscally reasonable 20 years prior. In any case, offenders have recognized prizes from online fakes in this manner, the dangers and dangers have expanded too. Securing the internet will be an empowering agent and will result in better utilization of the computerized condition. Along these lines, verifying it requires a joint exertion by all partners which incorporates the law authorization offices, governments, the innovation ventures, and the people in the general public.

PricewaterhouseCoopers. (2014) Cyber wrongdoings are another class of violations to India quickly growing because of broad utilization of Internet. Unscrupulous and avaricious individuals exploit simple and free access to Internet and play out any demonstrations to fulfill their necessities. The need could be physiological or mental in nature.2 Online shopping and wide utilization of "internet based life" are main driver of digital wrongdoings. Much mindfulness made for digital violations and clients were taught. Yet at the same time individuals don't grumble it to specialists. Indeed, even someone do it at that point additionally police or wrongdoing branch powerless to clear such gripes in sensible timeframe. Deferral in equity will prompt NO enlistment of whine. This isn't sound circumstance in free just INDIA.

IV. METHODOLOGY

Data Prepossessing Module

Data Ingestion Module along with Sqoop

Data Analytic Module along with Hive

Data Analytic Module along with Pig

Data Analytic Module along with Map Reduce

Data Analytic Module with R

Data Analytic Module With java age

Gather necessity dataset and Backup the document on mysql

We need to make another table by right tapping on the database and choosing make new table, first section will be the Id which will be a whole number, at that point all procedure will be finished, at long last we got a reinforcement document.

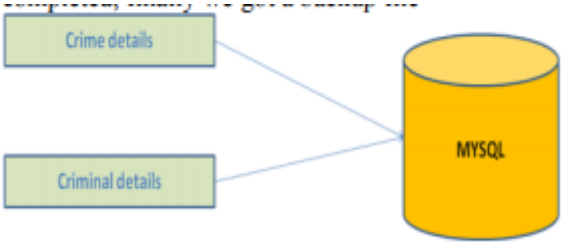

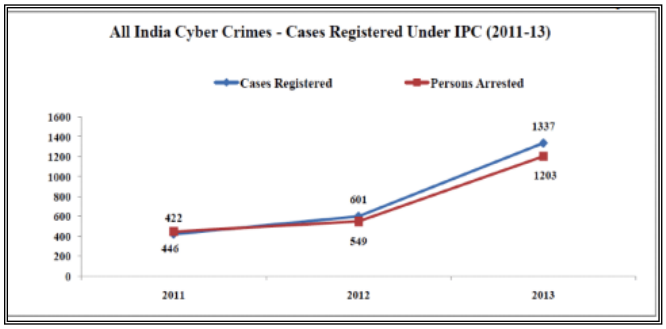

Data ingestion using Sqoop

Information ingestion Module with Sqoop: The motive of this module is to deed the dataset into Hadoop (HDFS). Sqoop is an interface application responsible for exchanging the information between Hadoop

and social databases. In this module, the dataset is pushed into Hadoop (HDFS) through the Sqoop tool. Utilizing the Sqoop features, perform the parcel capacity, to some extent that, the event needs to accompany the distinguishing segment or in the event needs to accompany the dataset with explicit scenarios supported by Sqoop and data is placed in Hadoop (HDFS).

Data processing Module with Hive

Hive is an framework house for Hadoop. It runs SQL queries through Hive inquiry language (HQL). Hive, is an initiative by Facebook. The Hive underpins Data Manipulation Language (DML), Data definition Language (DDL), and client characterized capacities. This module deals with dataset investigation by HIVE through Hadoop (HDFS). For examination, dataset HIVE utilizes the HQL Language. The utilization process in Hive was performed using tables' manifestations, bucketing idea, partition, and join operations. Later, the Hive deals with the examination of main Structure Language.

V. RESULTS

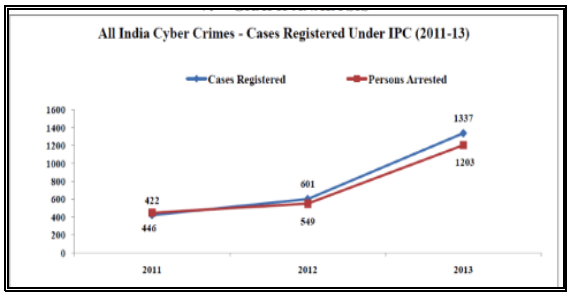

VI. CONCLUSION

This paper showed the wrongdoing information examination utilizing Hadoop. The capacity of huge information will change the way the present cybercrime to get criminal record. In the adjacent future we will see execution of enormous information examination in wrongdoing information investigation. Huge information gives security and protection. This paper proposes a structure which is pointing that it will enhance the execution of Map Reduce remaining tasks at hand and in the meantime will keep up the decency. The cybercrime frames test to the Islamic enactments, on the grounds that there is no unmistakable proof just as the cybercrime occurs in virtual condition. Subsequently, the enactment in KSA relies upon Islamic Law, in this manner the principle issue is non-consciousness of laws, and the Saudi youth have almost no learning about cybercrimes and their threat on the general public.

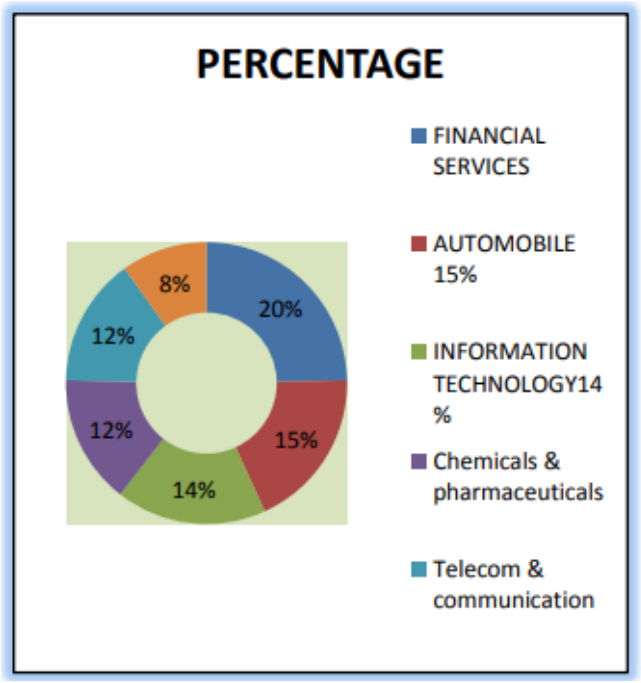

Likewise, nonappearance of the proof structures another test to the KSA courts to give equity goals in regards to the cybercrime, where an absence of specialized foundation to comprehend the idea of the wrongdoing in fact is viewed as a primary test for Department of contending wrongdoing in (CPVPV) - KSA. Other than the way of life of Saudi individuals keep the vast majority of unfortunate casualties from revealing their cases particularly when they presentation to sexual dangers. Besides, grouping cybercrimes in UK as indicated by enactments utilized in the courts can be abused to build up new enactments in KSA against cybercrimes, with taking into contemplations the social and religion contrasts. Applying new enactments in KSA against cybercrimes ought to enhance battling the new kinds of cybercrimes as needs be.

REFERENCES

1. Wow Essay (2009), Top Lycos Networks, Available at: http://www.wowessays.com/ dbase/ab2/ nyr90.shtml, Visited: 28/01/2012.
2. Crime in the Digital Age by Peter Grabosky and Russell Smith, Sydney: Federation Press, 1998
3. CAPEC (2010), CAPEC-117: Data Interception Attacks, Available at: http://capec.mitre.org/data/definitions/117.html, Visited: 28/01/2012.
4. Oracle (2003), Security Overviews, Available at: http://docs.oracle.com/cd/B13789_01/ network.101/ b10777/overview.htm, Visited: 28/01/2012
5. Computer Hope (2012), Data Theft, Available at: http://www.computerhope.com/jargon/d/ datathef.htm, Visited: 28/01/2012.
6. DSL Reports (2011), Network Sabotage, Available at: http://www.dslreports.com/forum/r26182468-Network-Sabotage-or-incompetent-managers-trying-to-, Visited: 28/01/2012.
7. IMDb (2012), Unauthorized Attacks, Available at:

http://www.imdb.com/title/tt0373414/, Visited: 28/01/201
8. Virus Glossary (2006), Virus Dissemination, Available at: http://www.virtualpune.com/citizencentre/html/cyber_crime_glossary.shtml, Visited: 28/01/2012
9. Legal Info (2009), Crime Overview aiding and abetting or Accessory, Available at: http://www.legalinfo.com/content/criminal-law/crime-overview-aiding-and-abetting-or-accessory. html, Visited: 28/01/2012
10. Shantosh Rout (2008), Network Interferences, Available at: http://www.santoshraut.com/ forensic/ cybercrime.htm, Visited: 28/01/2012
11. By Jessica Stanicon (2009), Available at: http://www.dynamicbusiness.com/articles/articles-news/one-infive-victims-of-cybercrime3907.html, Visited: 28/01/2012.
12. Prasun Sonwalkar (2009), India emerging as centre for cybercrime: UK study, Available at: http://www.livemint.com/2009/08/20000730/India-emerging-as-centre-for-c.html, Visited: 10/31/09
13. India emerging as major cyber crime centre (2009), Available at: http://wegathernews.com/ 203/indiaemerging-as-major-cyber-crime-centre/, Visited: 10/31/09
14. PTI Contents (2009), India: A major hub for cybercrime, Available at: http://business.rediff.com/ slideshow/2009/aug/20/slide-show-1-india-major-hub-for-cybercrime. htm, Visited: 28/01/2012.
15. D. L. Shinder and M. Cross, Scene of the Cybercrime. Burlington, MA, USA: Syngress, 2008.
16. [16] FBI and NW3C. (May 22, 2015). 2014 Internet Crime Report. Accessed on May 17, 2016.
17. IFCC 2002 Internet fraud report,‖ FBI, Washington, DC, USA, and NW3C, Glen Allen, VA, USA, Tech. Rep. NCJ 194344, 2003.
18. PricewaterhouseCoopers. (Sep. 30, 2014). The Global State of Information Security Survey 2015—Managing Cyber Risks in an Interconnected World. Accessed on May 19, 2016.
19. Federal Criminal Police Office. (2009). Police Crime Statistics 2008. Accessed on May 18, 2016. [6] 2015 US State of Cybercrime Survey, PwC, London, U.K., Jul. 2015, accessed on May 18, 2016.

AUTHORS PROFILE

G.Charles Babu , Presently working as a Professor in Dept. of CSE in Malla Reddy Engineering College(Autonomous), Secunderabad, Telangana Since 5 Years and Total Teaching experience of 20 Years. Completed B.Tech (CSE) in 1997 from KLCE, M.Tech(SE) in 1999 from JNTUH and Ph.D(Data Mining) from ANU. Published more than 50 Research Papers in Data Mining, Cloud Computing.

Dr.AkundiSai Hanuman, Professor of Computer Science and Engineering, completed his Ph.D. from Acharya Nagarjuna University, Guntur in 2012. He has over 22 years of experience in Academic, Industry and Research. Dr.AkundiSai Hanumans Research interests include Data Clustering, Data Sciences, Machine Learning, OptimizationTechniques and Distributed Systems. Currently Dr.Sai Hanuman is acting as Dean of Academics in GRIET .

Dr. J. Sasi Kiran ,B.Tech from JNTUH, M.Tech from Bharath University and received Ph.D degree in Computer Science from University of Mysore. He is working as Principal & Professor in CSE in Farah Institute of Technology, Chevella, Telangana ,India. His research interests include Image Processing, Cloud Computing and Network Security. He has published research papers till now in Conferences, Proceedings and Journals

Dr.B Sankara Babu, Professor in Computer Science and Engineering, completed his Ph.D from Acharya Nagarjuna University, Guntur and has over fourteen years of academic and research experience in Gokaraju Rangaraju Institute of Engineering and Technology. His research interests are Data Mining, Big Data Analytics, Machine Learning and Internet of Things in which he has more than 25 publications in various reputed journals and conferences. Dr.B.Sankara Babu Currently Dean of Internships at GRIET.

Published By:
Blue Eyes Intelligence Engineering
& Sciences Publication

Analysis of Flow Oscillations in an Open Cavity by a Passive Control Method

Yogesh Madaria, Rajender Angidi

Abstract : ***Numerical simulations are performed to evaluate a submissive controller method, utilised to suppress the pressure oscillation made in an open cavity flow. The open cavity considered in this work has the aspect ratio of 2 (Length of the cavity/Depth of the cavity=2). As the passive control technique, a non-smooth surface is installed, upstream of the cavity. The parameters like flow instability, noise around cavity are investigated using large eddy simulation, coupled with acoustics model, for smooth and non-smooth cases. The experimental and computational data available in literature are utilized for validation of results for the smooth case. By flow visualizations, it is established that locating a non-smooth surface at the upstream effectively suppresses hollow stream oscillations. By comparing the current ground structures in cases of smooth and non-smooth surfaces, the mechanism of oscillation control by non-smooth surface is analysed.***

Keywords: passive control, pressure oscillation, open cavity flow, numerical simulation, non-smooth surface, large eddy simulation

1.INTRODUCTION

A bench mark problem in the field of aero-acoustics has been the pressure oscillation in an open cavity flow. This problem has pulled considerable attention for the previous few periods. By the virtue of high theoretical and real-world impact, this problem has obtained, several investigations have been conducted in this area. Still, the studies adequately examining the simple natural system initiating oscillations controller covering a diverse series of stream surroundings, are few in number. At present-day the maximum difficulty for researches of unsolidified dynamic forces and aero-acoustics to find a suitable technique to exactly demonstrate the source of noise and disruptions causing oscillation. For examiners in area of stream controller, suppression of various modes of oscillation seems to be the challenge having most significance. The issues discussed above along with many other issues, make the analysis of oscillations in the flow over cavity, a typical problem in the area of flow control.

2. Literature Survey

The 3-D flow past a rectangular cavity was investigated by Kyoungsik Chang et al. [1] using Long Eddy Simulation. The flow was incompressible in this case and the cavity was considered to be two dimensional. This was the first computational work successful in resolving all the three-dimensional structures arising as a result of cavity oscillations in shear layer mode. Two different types of boundary layer flows, one developing laminar and the other fully turbulent, were analysed for the same cavity Reynolds number (Re_D = 3360). The complex phenomena associated with resonant cavities were absent. In both the cases, it was found that the resolved stress at the upstream of the separated shear layer was dominated by that in the downstream part. The methods to suppress the cavity oscillations are broadly classified as active and passive control methods. Active flow control methods are known to suppress noise and are adjustable according to different flow conditions [2,3], and inactive controller methods like, spoilers, physique insertion and change of cavity possess the ease in implementing and are least expensive. Furthermost of these models were proved efficient in decreasing the forceful compression levels. Wang et al.(4) carried out practical and arithmetical analysis to study the sound produced in the case of a subsonic flow. They proposed an alternate solution as a vented spoiler. This proved to be superior in noise reduction as it modified the flow structure of the shear layer. In another numerical study carried out by Chokani and Kim [5] for a supersonic flow, it was observed that the submissive numeric controller was able to significantly suppress the scale of the small incidence fluctuations. Sarno and Franke [6] tested fences (invariable and fluctuating) and flow injections (balanced and vivacious) at the prominent control. They found the static fences to be more efficient. In an experimental study conducted by Stallins et al. [7], at subsonic and transonic velocities, it was reported that the porous floor and that along with slot vents were the most significant effect in the distribution of the shallow cavity pressures. Zhang et al. [8] conducted investigation on cavity flow oscillations at supersonic speed to determine the consequences of leading-edge compression rams, increased façades and physique insertion. Ukeiley et al. [9] observed a leading-edge barrier having a cylinder-shaped shaft adjourned parallel to it, in the impending borderline layer. It was claimed that this technique was quite successful in façade compression control. Alam et al. [10] attempted modification of hole geometry for a square cavity by attaching two plane shields to the forward-facing wall of hole in parallel and upright planes. This method was claimed to be quite effective in suppressing the pressure oscillations. Another numerical investigation performed in case of supersonic cavity flow to evaluate the method of stable physique insertion in the upstream, reported that the solid

Revised Manuscript Received on December 22, 2018.

Yogesh Madaria, Department of Mechanical Engineering, Malla Reddy Engineering College (A), Secunderabad, Telangana, India. (email : yogesh.madaria@gmail.com)

Rajender Angidi, Department of Mechanical Engineering, Malla Reddy Engineering College (A), Secunderabad, Telangana, India.

interface between the upstream border level and the insertion movement could force the shear layer to lift up [11].

This upward displacement of the shear layer might have resulted in weakening of the important twisters formed on the irregular edge.

Even though the aforementioned submissive controller techniques were reported to be capable of attenuating cavity produced compressed fluctuations, most of these controller mechanisms have not been found to perform appropriately in a widespread of flow conditions and also could not overwhelm simultaneously several acoustic models. To overcome these shortcomings, submissive approaches such as deflector [4] and sub-cavity [12], are gaining attention. However, introducing a deflector results in increase of drag. Also, the factors of rate and assembly dependability needs to be measured. On the other hand, the presence of sub-cavity in the stream-wise direction causes accretion of foreign particles and dirt, which develops the requirement of periodic cleaning or servicing. On the pretext of these factors, devising an economical and technically appropriate method to obtain a instability boundary layer and increase its viscosity while eluding the increase of slog, becomes crucial. For the past few decades, the method of introducing non-smooth surfaces has been successful in drawing attention of the researchers. The non-smooth surface results in reduction of pressure drag and friction drag [13,14]. At the level of rough surface, the turbulent edge can be obtained, which will result in increase in forward momentum. The edge thus refrains the inappropriate pressure slope moderately extended before it departs from the surface [15]. Therefore, in the present work, rough surface is acquaint with turbulent edge and rise the viscosity of the upstream edge.

3. GOVERNING EQUATIONS AND BOUNDARY CONDITIONS

Three dimensional unsteady filtered Navier-stokes equations for Newtonian incompressible flow in Cartesian co-ordinate system are

Continuity:

$$\frac{\partial \bar{u}_j}{\partial x_j} = 0 .$$

Momentum:

$$\frac{\partial \bar{u}_i}{\partial t} + \frac{\partial}{\partial x_j}\left(\bar{u}_j \bar{u}_i\right) = -\frac{\partial \bar{P}}{\partial x_i} + \frac{1}{\mathrm{Re}} \nabla^2 \bar{u}_i - \frac{\partial \tau_{ij}}{\partial x_j} + \bar{F}_i .$$

Where ui represents the velocity field , Re is the Reynolds number, Fi is the body force

The boundary conditions may be as follows

At Inlet the wall normal and the spanwise velocity components have been set to zero. Mathematically, $u_{in}=U_{\infty}$,$v_{in}=0$,$w_{in}=0$ where the subscript "in" indicates the inlet plane.

At Outlet a non reflective boundary condition (convective) is imposed which can be written as,

$$\frac{\partial u_i}{\partial t} + U_c \frac{\partial u_i}{\partial x_c} = 0$$

Here subscript c denotes the direction normal to the outflow boundary. the convecting Uc is considered as constant across the outflow boundary .

At Upper boundary free-slip condition is applied . so the boundary condition at this surface is ,

$$v = 0, \frac{\partial u}{\partial y} = 0 , \frac{\partial w}{\partial y} = 0$$

At Lower boundary no slip condition is applied. So the boundary condition at this surface is u=0,v=0,w=o.

Disturbance strip Turbulences are applied to generate the conversion process following Alam et al. [10]

This is done through process of disturbance strip applied on the flat plate region at the inlet of the domain.

We apply turbulences to the barrier standard velocity ,that are sinusoidal in time and in the span wise direction next to the formula

$$v = a_f \exp[-b_f (x - c_f)^2] \sin(\omega t) \sin(\beta y)$$

Where af,bf and cf are coefficients adjusting the stream wise deviation of the coercing ω is the frequency and β is a span wise wave number.

3. COMPUTATIONAL DOMAIN

3.1 Geometrical model of a rough surface cavity

An object is a four-sided cubicle with a huge volume and lesser opening at the top. The depth and length(L) of the cavity is D (=50mm), 2D respectively. And overall box dimensions are: 1) span wise width 3D, 2) depth 3D 3) length 11D.

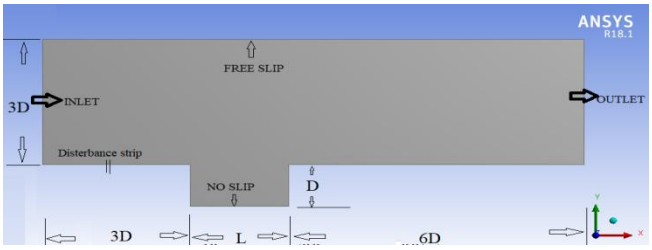

Fig 3.1. Computational domain with applied boundary conditions

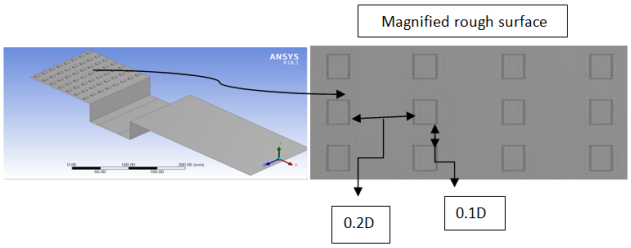

Fig 3.2 Detailed view of the upstream plate

As shown in fig the upstream leading surface modified by the creating of non-smooth surface (rough surface), this roughness may prompt a turbulent edge and rises the thickness of the upstream borderline[15]

Meshing: in the meshing the grid is very fine near the surface of the cavity and is slowly stretched out away from it.

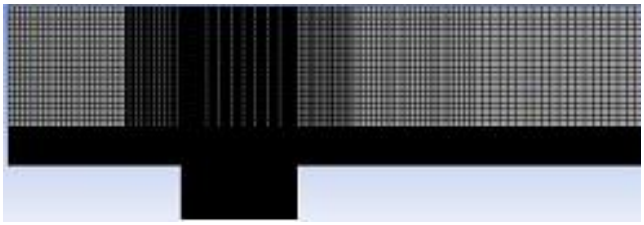

Fig 3.3. Shows the grid distribution

3.2 Validations of computational domain

3.2.1 Mean flow characteristics: Fig 3.4 shows The comparison of a longitudinal mean velocity profile with the computational data of Chang et al.(2006) at five stations from x/D=0.02 to x/D=1.7. a very good agreement is observed at all stations between the computational data and the laminar case predictions by the present LES.

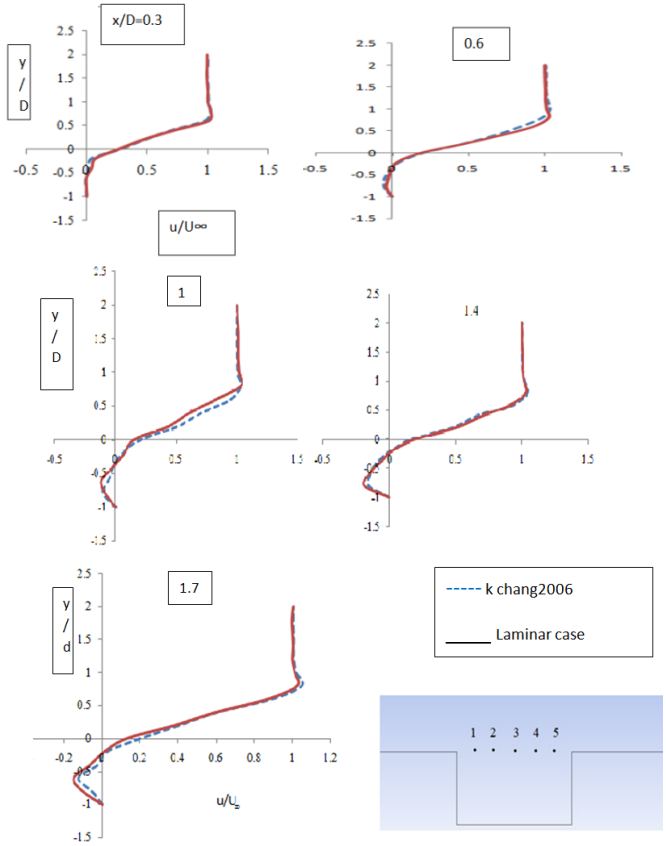

Fig 3.4: Comparision of mean stream velocity profiles at different stations

Fig 3.5 shows about the normal stress u'u',v'v' at different the stream wise locations .The stresses are non-dimensionalized by the inlet free stream velocity. The stresses correspond to the apparent stress induced by the laminar instabilities and the convection of coherent structures present in the separated shear layer and cavity regions. The averaging process generates relatively high value of stresses only in the downstream half of the shear layer and then inside the cavity near the bottom and downstream of the cavity The results of the instant LES are in good overallagreement with that of Chang et al. (2006).

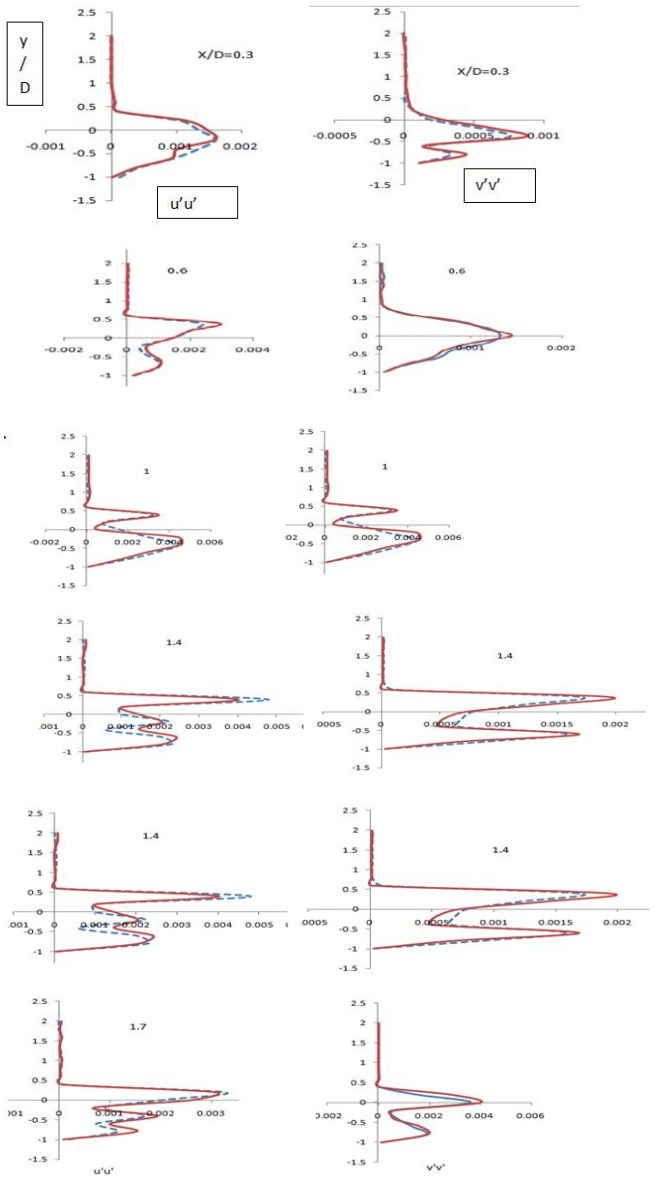

Fig 3.5 comparision of Reynolds stress at different stations

3.2.2. Velocity spectra: The time history of the vertical velocities are extracted at all 5stations.And observe that the up to station 2 there is no substantial peak in velocity spectra. Downstream of the separation (starts from the station 3), peaks are observed indicating shear stress oscillating at the fundamental frequency corresponding to a strouhal number StD=fD/U=0.49 The amplitude of these oscillations is growing in the stream wise direction. Concomitantly, very low-energetic frequency modulations are clearly observed in the same time series. We suspect that these very low energetic frequency oscillations and the main oscillatory frequency is due to shear layer interactions with the recirculating motions inside the cavity (Chang et al. 2006).Fig 3.6 shows pressure spectra at stations 5 the strouhal number StD=(0.36,0.70).

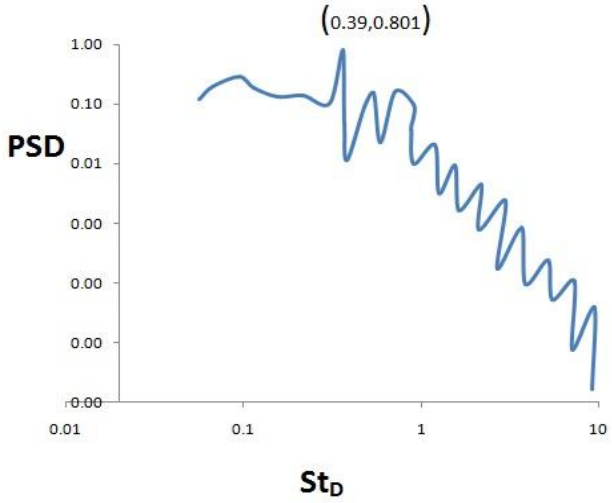

Fig 3.6 shows pressure spectra at station 5

4. RESULTS AND DISCUSSION

4.1 Meanflow characteristics: Figure 4.1 shows the comaprision of longitudinal velocity profiles between rough and smooth(regular) surface cavities. From the statistics were taken 4,5 stations as shown after flow had achived the state of dynamic stability. we don't observer much differences the remaining velocity profiles.

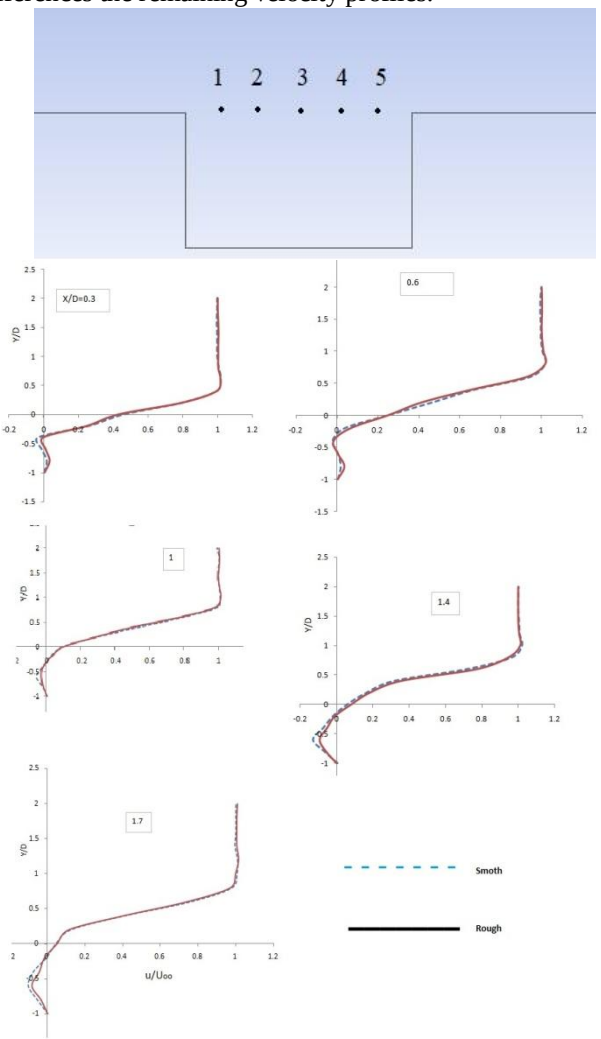

Fig 4.1 Comparison of mean scream velocity profiles at different stations

Figs 4.2, 4.3 shows Reynolds normal stress of u'u',v'v' respectevely at 5 stations. And we observed that the shear layer energy reductions starts from the station 3, so that we achive good cavity stabilty.

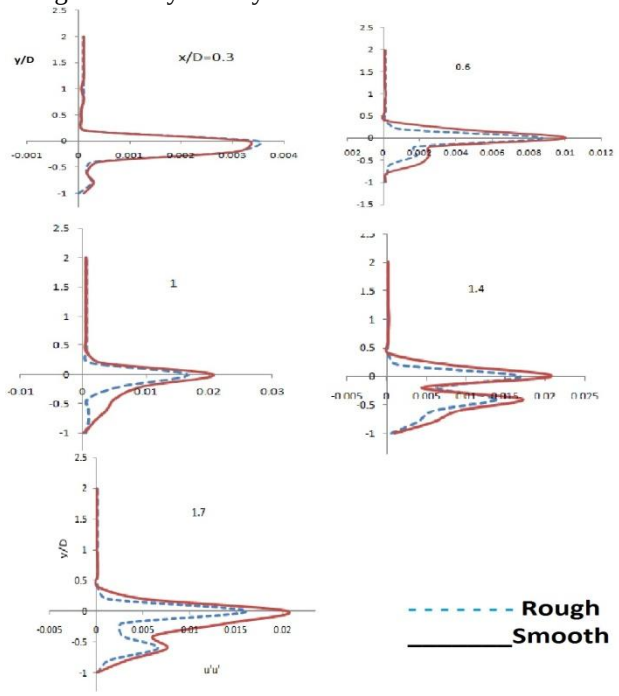

Fig 4.2 profiles of u'u' at different stations

Velocity spectra: From the velocity history we observed at station 5th the strouhal number reduced from 0.39 to .30 so that the cavity oscillations are reduced effectively by the modifications. And Fig 4.4 shows pressure spectra at station 5th

5. CONCLUSIONS

In the existing work, we demonstrated that the rough surface is operative in restraining the oscillation in an open cavity. For the better understanding of the mechanism and physics of this method, computational analysis was done using ANSYS Fluent. The flow visualization resulted in understanding of flow grounds and uncertainties produced by detaching of broken turbulences at the principal edge. It is clear from the simulation results, that the overview of rough surface could promote turbulent edge and increases the thickness of borderline. To summarize, it can be said that the characteristics of the rough (non-smooth) surface, effectively suppress the flow oscillation.

REFERENCE

1.Chang, K., Constantinescu, G.., and Park, S.O., 2006, "Analysis of the flow and mass transfer processes for the incompressible flow past an open cavity with a laminar and a fully turbulent incoming boundary layer", J. Fluid Mech., Vol. 561, pp 113-145.

2. Rowley C, Williams R. Dynamics and control of high-Reynolds-number flow over open cavities. Annu Rev Fluid Mech 2006;38:251–76.

3.Williams DR, Cornelius D, Rowley CW. Supersonic cavity retort on exposed hoop coercing. Dynamic Stream Controller Records Numer Liquid Mech Multidiscip Des 2007;95:230–43.
4. Wang YP, Lee SC, Li KM, Gu Z, Chen J. Collective experimental and arithmetical study of stream over cavity and application on sunroof beating noise diminution. ACTA Acust United Acust 2012;98(4):600–11.
5.Chokani N, Kim I. Subdual of force oscillations in an open cavity by submissive inflatable controller. AIAA 91-1729, 1991.
6. Sarno R, Franke M. Subdual of flow-induced force oscillations in hollows. J Aircr 1994;31(1):90–6.
7. Stallings RL, Plentovich EB, Tracy MB, Hemsch MJ. Effect of submissive emitting on fixed compression disseminations in hollows at subsonic and transonic speeds. NASA Technical Memorandum 4549, 1994.
8.Zhang X, Chen X, Rona A, Edwards J. Attenuation of cavity flow oscillation through leading edge flow control. J Sound Vib 1999;221(1):23–47.
9. Ukeiley LS, Ponton MK, Seiner JM, Jansen B. Subdual of compression loads in hollow streams. AIAA J 2004;42(1):70–9.
10. Alam MM, Matsuo S, Teramoto K, Setoguchi T, Kim HD. A computational exploration on the controller of hollow-induced force oscillations using subcavity. J Therm Sci 2006;15(3):213–9.
11.Li W, Taku N, Kozo F. Noise controller of supersonic hollow stream with upstream mass blustering. Advancement in fusion RANS-LES demonstrating notes on mathematical fluid mechanics and multidisciplinary design, vol. 117. p. 315–24.
12.Alam MM, Matsuo S, Teramoto K, Setoguchi T, Kim HD. A new technique of monitoring cavity-induced force oscillatons using sub-cavity. J Mech Sci Technol 2007;21:1398–407.
13. Alam F, Steiner T, Chowdhury H, Moria H, Khan I, Aldawi F, et al. A study of golf ball smooth drag. Proc Eng 2011;13:226–31.
14.Lienhart H, Breuer M, Köksoy C. Drag reduction by dimples? A balancing arithmetical investigation. Int J Heat Fluid Flow 2008;29 (3):783–91.
15. Tian LM, Ren LQ, Liu QP, Han ZW, Jiang X. The mechanism of drag reduction around bodies of revolution using bionic non-smooth surfaces. J Bionic Eng 2007;4(2):109–16.

Fractional Brownian motion Noise Removal in Breast Cancer Magnetic Resonance Images

N.Rajeswaran, C.Gokilavani, T.Samraj Lawrence, P.Ramkumar

Abstract*: *In Medical Image Processing, high resolution images are very much essential to analyze the different features of the image for better diagnosis of the disease. Now days, more and more women are getting affected by breast cancer. Magnetic Resonance Imaging is the most popular technique used to diagnose the breast cancer images, whose resolution in turn is affected by the fractional Brownian motion (fBm) noise, Gaussian noise and Salt and Pepper noise. In this paper, wavelet based thresholding techniques namely Visu shrink, SURE shrink and Bayes shrink are implemented to denoise the breast cancer images affected by fBm noise.

Index Terms: fBm noise, Medical image Processing, Magnetic Resonance Imaging, wavelet thresholding.

I. INTRODUCTION

In medical image processing, noise tends to reduce the visibility of the image and obscures the information needed for accurate treatment. Since the larger part of image processing deals with Image restoration or image denoising, denoising the affected images plays a major role to diagnose the diseases in a proper manner and to retain the image up to its quality[1-2]. Image denoising attempts to remove the various types of noises present in an image and restores the original image back while preserving the important features needed for proper diagnosis and to track the progress of the disease. However, the tradeoff between the image features and noise reduction must be taken into account while denoising. Recently fuzzy logic has been used for noise removal [3]. Medical images are taken by means of MRI (Magnetic Resonance imaging), CT (Computed Tomography) and Ultrasound imaging. Among these, MRI sounds better in giving high resolution images of the soft tissues in human body such as the brain and breasts. The images of these organs consist of several complex patterns that are independent of scales. Further, the breast cancer image is fractal in nature [4]. Hence, in this paper, the fractional Brownian motion noise is eliminated by using the wavelet based thresholding techniques namely Visu shrink, SURE shrink and Bayes shrink methods.

Revised Manuscript Received on April 07, 2019.

N. Rajeswaran, Malla Reddy Engineering College (A), Maisammaguda, Telangana, India.

P. Ramkumar, Malla Reddy Engineering College (A), Maisammaguda, Telangana, India.

C. Gokilavani, Francis Xavier Engineering College, Tirunelveli, Tamil nadu, India

T. Samraj Lawrence, Francis Xavier Engineering College, Tirunelveli, Tamilnadu, India.

II. GENERATION OF FBM NOISE

Based on the concept of bisection and interpolation [5], Ilkka Norros proposed the simulation of fractional Brownian motion with conditional random midpoint displacement algorithm [6]. This is also called as diamond square algorithm. This produces fractals in images. Here the entire trace of the fractional Brownian motion is generated before it is used for the purpose for which it is specified for. Fractional Brownian motion has been used in various fields such as hydrology, imaging landscapes and much more [7]. The properties of a normalized fBm are:

- Normalized fBm is a stochastic process(Zt) with Hurst parameter, H(0,1)
- Zt has stationary increments
- Zt is Gaussian
- Zt has continuous sample paths

A. Algorithm of fBM Noise

Ordinary Brownian motion is the special case of Normalized fBm with the parameter H=1/2. This algorithm consists of following steps,

Step 1: Take the given image.

Step 2: Assign height values to each corner of the image.

Step 3: Divide the image into four sub-images and assign height values to them such that their height is the mean values of the corners of the image taken in step 1.

Step 4: When computing the middle height, add small error value depending on the image size taken in step 1 and some constants that controls the fractal's roughness.

Step 5: Continue the iteration and sub-divide the sub-images further.

Step 6: When no noticeable difference is seen, stop the iteration and render the pixel with mean height values.

Thus the fractals are produces by the above RMD procedure and are shown below.

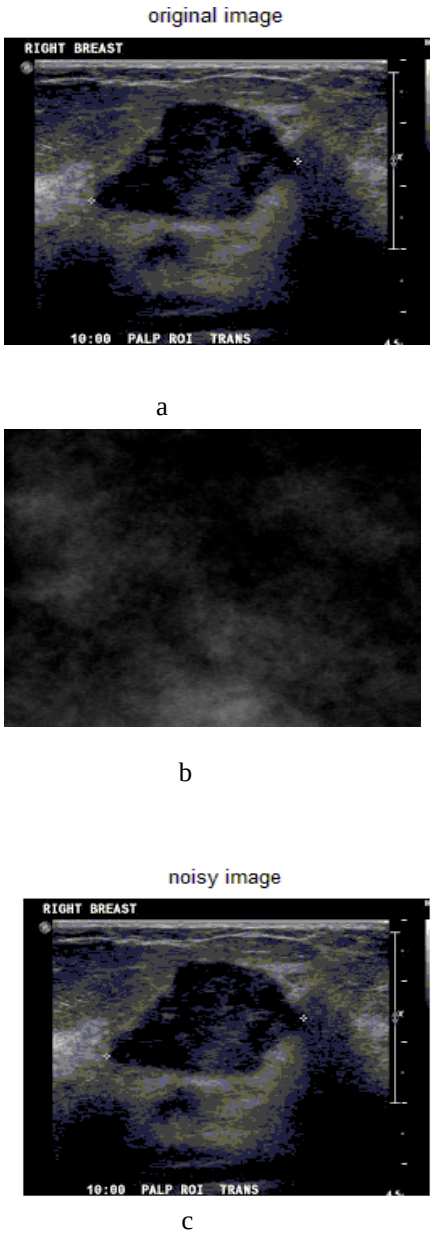

Fig.1(a),(b),(c). Simulation results of fractional Brownian motion noise

Fig.1 shows the MATLAB simulation results for the generation of fractional Brownian motion noise for an Breast cancer image of size 512x512. Fig.1 (a) shows the original Breast cancer image. Fig.1 (b) shows the pattern of fractional Brownian motion. Fig.1 (c) shows the Breast cancer image corrupted with fBm noise.

III. RESULTS AND DISCUSSIONS

The wavelet based thresholding techniques are implemented by using MATLAB and the simulation results for Visu shrink are given in the Fig. 2. The Fig. 2.(a) shows the original image, Fig. 2.(b) shows the noisy image and the Fig. 2.(c) shows the denoised image. Here in the noisy image, the value of the Hurst parameter is 0.3 (for a classical Brownian motion, the Hurst parameter h=0.5).

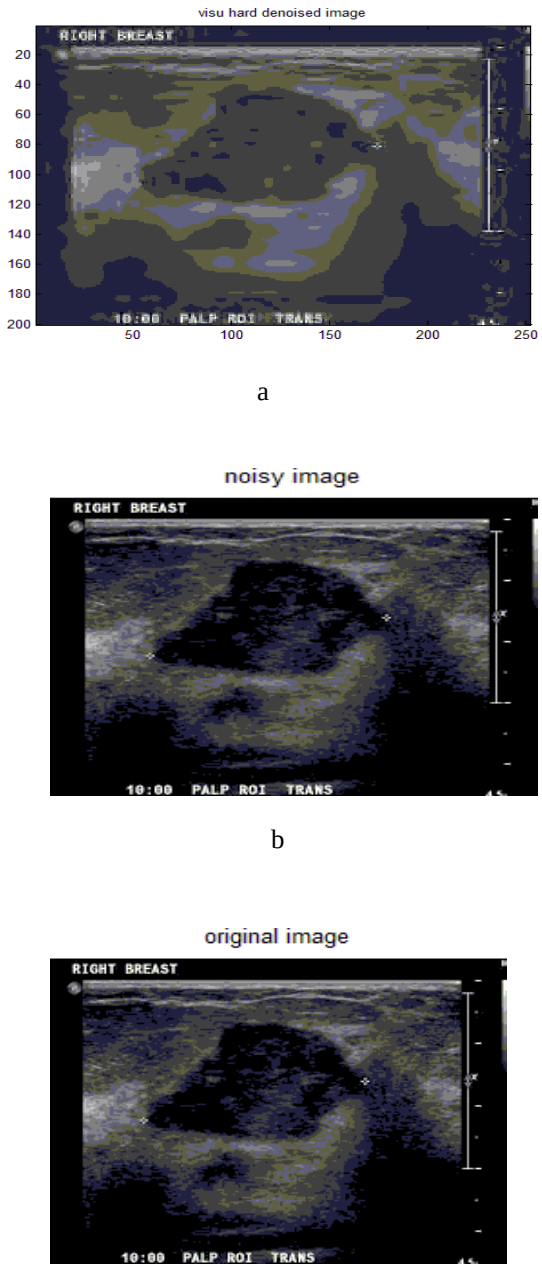

Fig. 2(a),(b), (c). Simulation results for Visu shrink

The simulations results for SURE shrink are given in the Fig. 3. The Fig. 3.(a) shows the original image, Fig. 3.(b) shows the noisy image and Fig. 3.(c) shows the denoised image. Here also the noisy image takes the value of 0.3 for H.

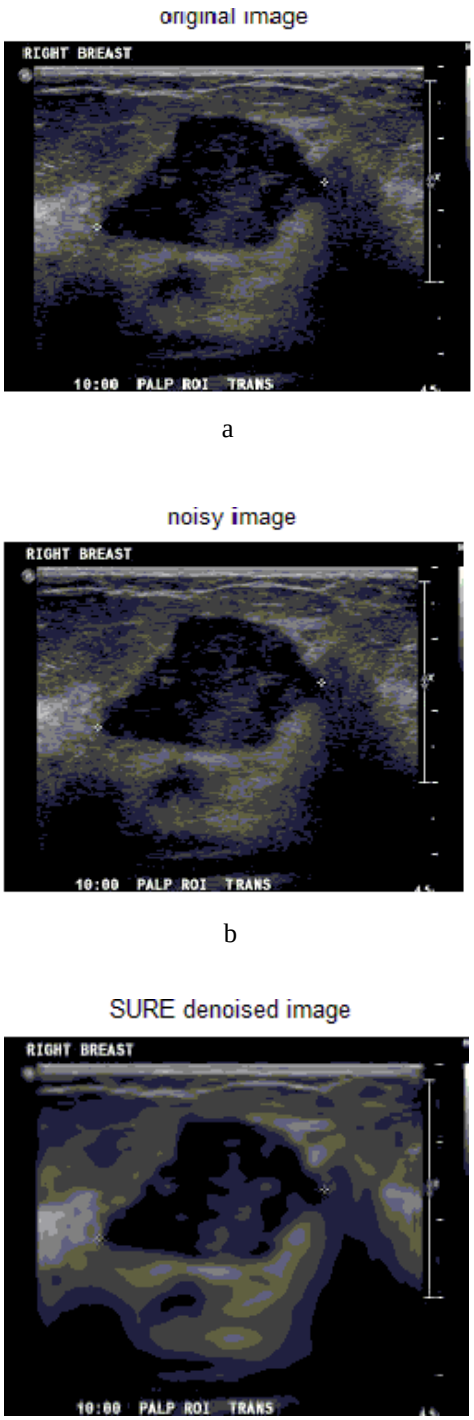

Fig 3.(a),(b) and (c). Simulation results for SURE shrink

The simulation results for Bayes shrink are given in the Figure. 4. The Fig.4. (a) shows the original image, Fig. 4.(b) shows the noisy image (with Hurst parameter of 0.3) and Fig.4.(c) shows the denoised image.

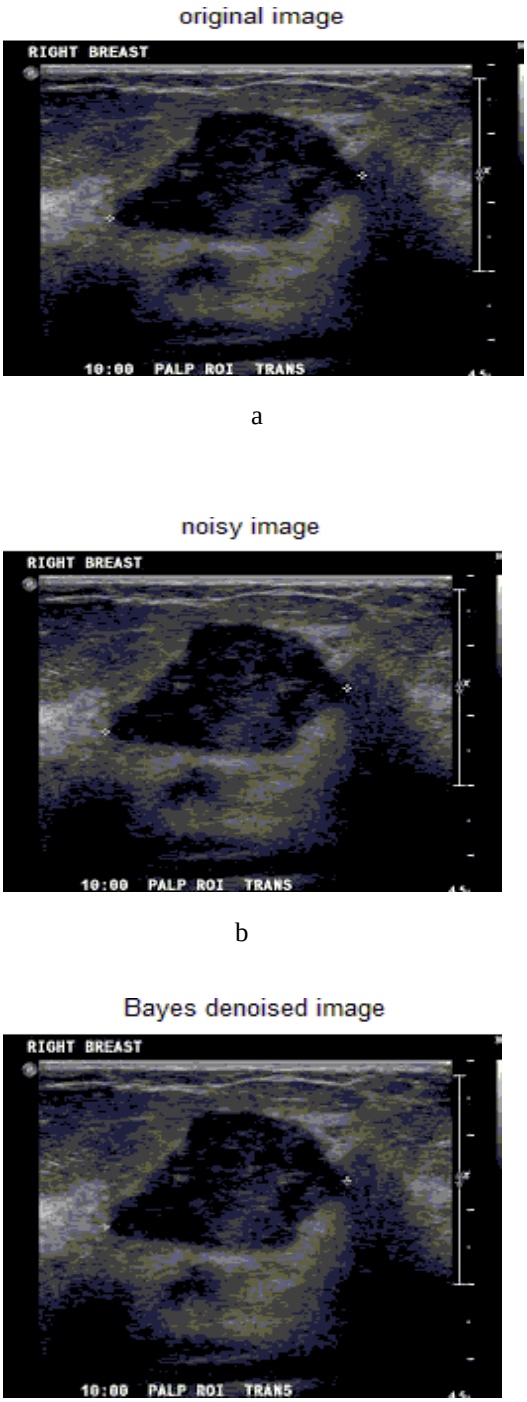

Fig 4.(a)(b) and (c). Simulation results for Bayes shrink

The performances of all the three thresholding techniques are listed in Table. 1.

Table 1: Comparison of wavelet thresholding techniques

S.NO	PERFORMANCE METRICS	VISU SHRINK	SURE SHRINK	BAYES SHRINK
1	MSE (Mean Square Error)	865.45	665.45	2.1544
2	PSNR (Peak signal to Noise ratio)	56.9841	76.5454	78.5645
3	FD(Fractal Dimension)	1.9645	1.9751	1.9884
4	IEF(Image Enhancement Factor)	0.6844	0.7554	0.9987
5	SSIM (Structural Similarity Index)	0.7454	0.7865	1.000
6	NK(Normalized Cross Correlation)	0.8502	0.9265	0.9965
7	AD(Average Difference)	210	165	154
8	SC (Structural Content)	0.9265	0.9756	1.000
9	MD(Maximum Difference)	214	155	221
10	NAE(Normalized Absolute Error)	0.8652	0.0218	0.0010
11	Time Elapsed when attempt to denoise	5.6545sec	4.6954sec	1.4545sec

From the above table, it is evident that the Bayes shrink method is performing more efficiently in denoising the images and thereby improving the resolution of the MRI images (Shown in Figures from 5 to 9). It has high Peak Signal to Noise Ratio, lowest Mean Square Error and lower Normalized Absolute Error.

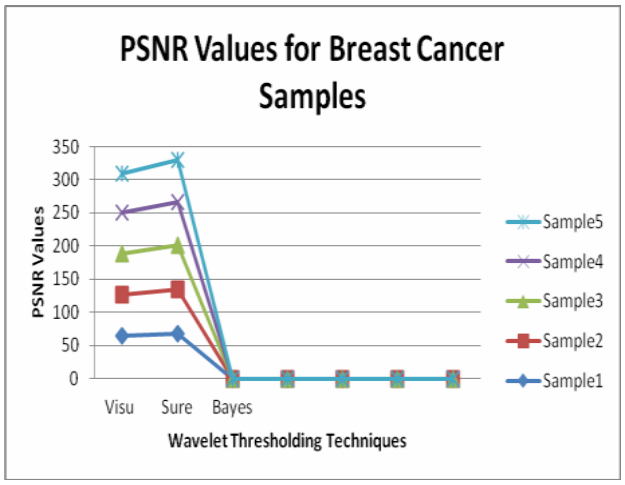

Fig 5. Chart for Peak Signal to Noise Ratio-PSNR

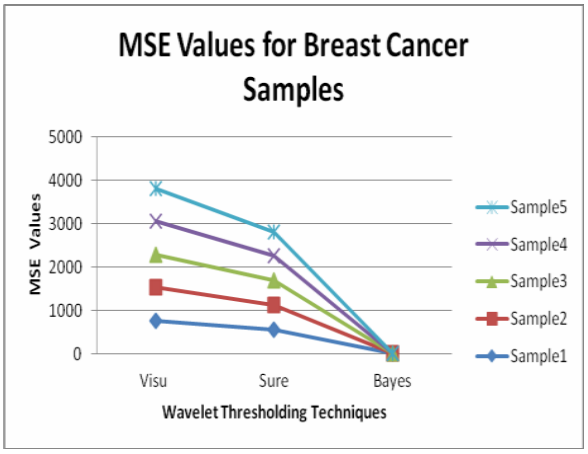

Fig 6. Chart for Mean Square Error-MSE

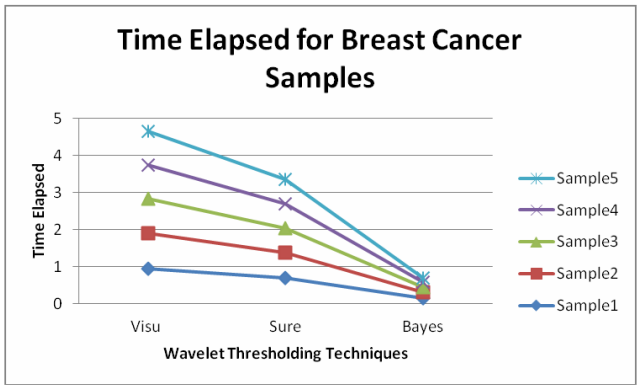

Fig 7. Chart For Normalized Absolute Error

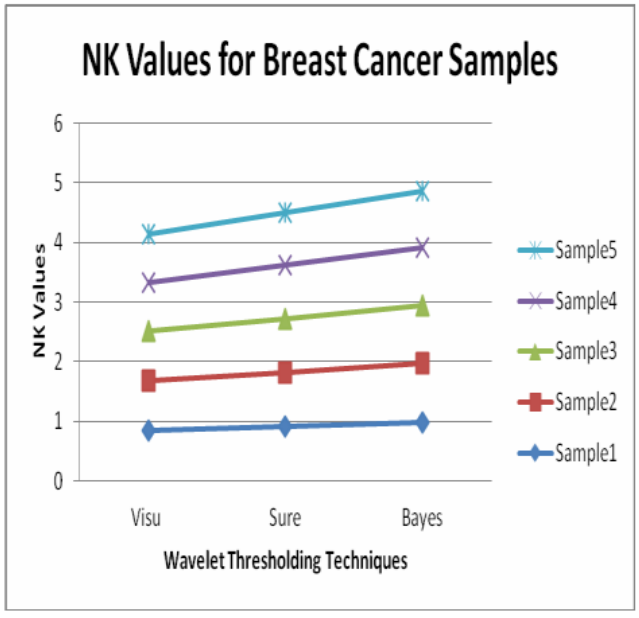

Fig 8. Chart for Normalized Absolute Error-NAE

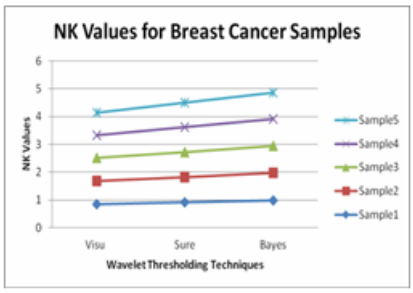

Fig 9. Chart for Normalized Cross Correlation-NK

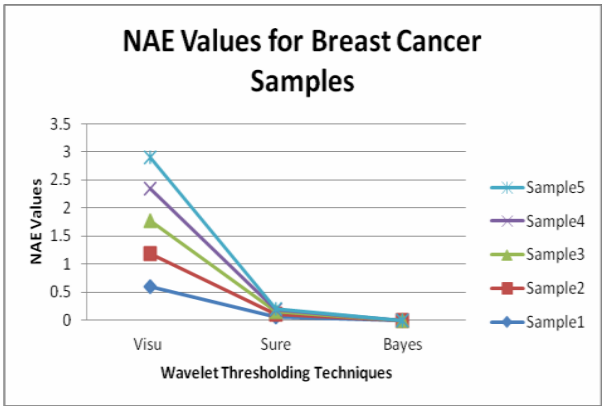

Fig 10. Chart for Time Elapsed to produce denoised image

IV. CONCLUSION

In this paper, wavelet based thresholding techniques namely Visu shrink, SURE shrink and Bayes shrink are implemented to denoise the breast cancer images affected by fBm noise. The inference from all these implementations are that Bayes shrink performs better in terms of all performance metrics. The future scope of this work includes analyzing and implementing various filters for removing all forms of noise.

REFERENCES

1. J. Zheng, J. A. Fessler and H. P. Chan, "Detector Blur and Correlated Noise Modeling for Digital Breast Tomosynthesis Reconstruction," in IEEE Transactions on Medical Imaging, vol. PP, no. 99, pp. 1-1. doi: 10.1109/TMI.2017.2732824
2. F. S. Ahadi, M. R. Desai, C. Lei, Y. Li and R. Jia, "Feature-Based classification and diagnosis of breast cancer using fuzzy inference system," 2017 IEEE International Conference on Information and Automation (ICIA), Macau SAR, China, 2017, pp. 517-522. doi: 10.1109/ICInfA.2017.8078962.
3. J. K. Udupa and G. T. Herman, "Medical image reconstruction, processing, visualization, and analysis: the MIPG perspective," in IEEE Transactions on Medical Imaging, vol. 21, no. 4, pp. 281-295, April 2002. doi: 10.1109/TMI.2002.1000253
4. T. Gevers, A.W. Smeulders, Pictoseek,"Combining Color and Shape Invariant Features for Image Retrieval", IEEE Transactions on Image Processing, Vol. 9, No. 1, pp. 102-119,2000.
5. Penttinen, A. and Virtamo, J., "Simulation of Two-dimensional Fractional Brownian Motion", Methodology and Computing in Applied Probability, Vol. 6 No. 1, pp. 99-107, 2005.
6. A. Kinali, "Fractional Brownian motion and its application in the simulation of noise in atomic clocks," 2017 Joint Conference of the European Frequency and Time Forum and IEEE International Frequency Control Symposium (EFTF/IFC), BESANÇON, France, 2017, pp. 408-409. doi: 10.1109/FCS.2017.8088906
7. J. Zheng, J. A. Fessler, and H.-P. Chan, "Digital Breast Tomosynthesis Reconstruction using Spatially Weighted Non-convex Regularization," Proc. SPIE, vol. 9783, pp. 978369, 2016.